37

The Astrophysical Journal

THE UNIVERSITY OF CHICAGO PRESS
CHICAGO, ILLINOIS

THE CAMBRIDGE UNIVERSITY PRESS
LONDON

THE MARUZEN-KABUSHIKI-KAISHA
TOKYO, OSAKA, KYOTO, FUKUOKA, SENDAI

THE MISSION BOOK COMPANY
SHANGHAI

THE
ASTROPHYSICAL JOURNAL

An International Review of Spectroscopy and Astronomical Physics

EDITORS

GEORGE E. HALE
Mount Wilson Observatory of the Carnegie Institution of Washington

EDWIN B. FROST
Yerkes Observatory of the University of Chicago

HENRY G. GALE
Ryerson Physical Laboratory of the University of Chicago

COLLABORATORS

JOSEPH S. AMES, *Johns Hopkins University;* ARISTARCH BELOPOLSKY, *Observatoire de Poulkova;* WILLIAM W. CAMPBELL, *Lick Observatory;* HENRY CREW, *Northwestern University;* CHARLES FABRY, *Université de Marseille;* ALFRED FOWLER, *Imperial College, London;* CHARLES S. HASTINGS, *Yale University;* HEINRICH KAYSER, *Universität Bonn;* ALBERT A. MICHELSON, *University of Chicago;* HUGH F. NEWALL, *Cambridge University;* ERNEST F. NICHOLS, *Massachusetts Institute of Technology;* ALFRED PEROT, *Paris;* CARL RUNGE, *Universität Göttingen;* HENRY N. RUSSELL, *Princeton University;* SIR ARTHUR SCHUSTER, *The University, Manchester;* FRANK SCHLESINGER, *Yale Observatory*

VOLUME LIII

JANUARY–JUNE, 1921



THE UNIVERSITY OF CHICAGO PRESS
CHICAGO, ILLINOIS

QB
1
A9
1.53-54
Cop.2

Published
January, March, April, May, June, 1921

Composed and Printed By
The University of Chicago Press
Chicago, Illinois, U.S.A.

CONTENTS

NUMBER I

PAGE

Radiation Pressure and Celestial Motions. Henry Norris Russell 1

The Parallaxes of 1646 Stars Derived by the Spectroscopic Method. W. S. Adams, A. H. Joy, G. Strömberg, and Cora G. Burwell 13

The Spectroscopic Orbit of the Cepheid Variable X Cygni. John C. Duncan 95

Provisional Elements of the Eclipsing System RS Canum Venaticorum. Bancroft Walker Sitterly 99

NUMBER II

A Photo-Electric Study of Algol. Joel Stebbins 105

An Examination of the Infra-Red Spectrum of the Sun, λ 8900–λ 9900. Frederick S. Brackett 121

The Variation with Temperature of the Electric Furnace Spectrum of Manganese. Arthur S. King 133

The Orbit of the Short-Period Spectroscopic Binary 65 τ Cygni. J. S. Paraskévopoulos 144

The Vacuum-Spark Spectra in the Extreme Ultra-Violet of Carbon, Iron, and Nickel. R. A. Millikan, I. S. Bowen, and R. A. Sawyer 150

Intensity Differences in Furnace and Arc among the Component Series in Band Spectra. Arthur S. King 161

Elements of the Eclipsing System SX Cassiopeiae. Mary Fowler . 165

Notice to Contributors 168

NUMBER III

On the Passage of a Star through a Nebula. Ernest W. Brown . 169

On the Geometrical Classification of Long-Period Variables. J. G. Hagen 179

Characteristic Behavior of the Bright Lines in Stellar Spectra of Class Md. Paul W. Merrill 185

The Orbits of Seven Spectroscopic Binaries. R. F. Sanford . . 201

Pressure-Shifts in a Calcium Arc. L. F. Miller 224

Preparation of Abstracts 231

NUMBER IV

PAGE

Sir Norman Lockyer, 1836–1920. A. L. Cortie, S. J. 233

Measurement of the Diameter of α Orionis with the Interferometer. A. A. Michelson and F. G. Pease 249

Wave-Lengths of Lines in the Iron Arc from Grating and Interferometer Measures λ 3370–λ 6750. Charles E. St. John and Harold D. Babcock 260

On the Absorption Spectrum of Hydrogen Chloride. Walter F. Colby and Charles F. Meyer 300

The Exceptionally High Solar Prominence of October 8, 1920. Oliver J. Lee 310

Suspected Variable, Bond 624, in Trapezium of Orion. J. A. Parkhurst 317

Minor Contributions and Notes: Use of a Lime Cathode of Carbon in Spectroscopy, Y. Sugiura and T. Matoba, 323; A Modification of the Electron Theory of Dispersion, to Account for the Change of Refractive Index with Temperature, G. Szivessy, 326; On the Pressure in the Atmospheres of the Stars, P. Salet, 327.

NUMBER V

On the Measurement of Pole-Effect and Its Connection with Magnetic Separation. H. Nagaoka 329

The Structure of the Bismuth Lines. H. Nagaoka and Y. Sugiura 339

The Mutual Action of Adjacent Photographic Images. Frank E. Ross 349

Observations of the Nebular Lines in the Spectrum of the Long-Period Variable Star R Aquarii. Paul W. Merrill 375

On Systematic Displacements of Lines in Spectra of Venus. Charles E. St. John and Seth B. Nicholson 380

Bright and Dark Nebulae near ζ Orionis Photographed with the 100-Inch Hooker Telescope. John C. Duncan 392

Index 397

THE
ASTROPHYSICAL JOURNAL
AN INTERNATIONAL REVIEW OF SPECTROSCOPY
AND ASTRONOMICAL PHYSICS

VOLUME LIII JANUARY 1921 NUMBER 1

RADIATION PRESSURE AND CELESTIAL MOTIONS

By HENRY NORRIS RUSSELL

ABSTRACT

Radial velocities of nebulae.—Various suggested explanations are shown to be inadequate. (1) The maximum *radiation pressure due to the Galaxy* as a whole is probably less than 2×10^{-13} dynes/cm^2. After deriving an expression for the acceleration which this could produce in a spiral nebula of a given apparent diameter, parallax and spectroscopic rotation, it is shown that even on the most favorable assumptions the acceleration of the Andromeda nebula cannot exceed 1.1×10^{-10} cm/sec^2., or that of N.G.C. 4594, 1.5×10^{-13} cm/sec^2. (2) The *gravitational attraction of the Galaxy* upon these nebulae is probably much greater than the repulsion due to radiation, but it is nevertheless too small to account for their observed radial velocities. (3) And *electrostatic repulsion*, if sufficient to neutralize gravitational attraction, would cause the disruption of the bodies. In fact pressure of any sort could not sensibly alter the motion of a spiral nebula without seriously deforming it.

Radiation pressure between binary stars must even in extreme cases be less than one ten-thousandth of the gravitational attraction, and is probably much smaller.

The radial velocities of those spiral nebulae which have so far been observed show a strong preponderance of motions of recession. It has been suggested[1] that this indicates that these nebulae are repelled by the galactic system, and that radiation pressure may be the effective force involved. This hypothesis may easily be tested by quantitative calculations, and the result is found to be decisively against it.

1. *Magnitude of the radiation pressure.*—We are here concerned with the radiation of the galactic system as a whole rather than

[1] H. Shapley, *Astrophysical Journal*, 50, 133, 1919.

that of individual stars. According to the recent determination by van Rhijn[1] the light which the earth receives from one square degree of the sky (after correction for sources internal to the solar system) varies from 0.010 of that of a first magnitude star, for regions near the galactic pole, to 0.080 at the galactic equator, the average for the whole sky being 0.035. From a point well outside the galactic plane the surface brightness of the Galaxy, viewed normally to its plane, should be twice that of our sky near the galactic pole, or 0.020. We shall probably overestimate the total radiation at such a point if we assume that half the celestial sphere has the average brightness of our sky, 0.035, while the other half is quite dark. The whole radiation from the bright hemisphere will equal that of 720 stars of the first magnitude; but the flux of radiation perpendicular to the diametral plane will be half as great, or equal to 360 stars of the first magnitude, or one star of magnitude -5.4. The sun as seen from the earth is of visual magnitude -26.7, and the pressure of its radiation upon a black surface normal to it is 4.5×10^{-5} dynes per square centimeter. If the average character of starlight is assumed to be similar to that of sunlight, the radiation pressure due to the galactic hemisphere works out as 1.33×10^{-13} dynes/cm^2. Since the luminous efficiency of sunlight is near the maximum, this estimate may be somewhat low. We will therefore adopt 2.0×10^{-13} dynes/cm^2 as the radiation pressure due to the light of the Galaxy at an external point not far from it. For points at distances comparable with the diameter of the galactic system, the luminous part of the sky will be less than a hemisphere, and the pressure smaller, and at great distances it will be inversely proportional to the square of the distance.

2. *Assumptions regarding radiation pressure on nebulae.*—The conditions under which radiation pressure may produce the greatest effect in setting a nebula into bodily motion may be summarized as follows:

a) The plane of the nebula is perpendicular to the direction of the pressure.

[1] H. Shapley, *Astrophysical Journal*, 50, 373, 1919.

b) The nebula intercepts as much radiation as an opaque circular disk equal in diameter to its own maximum diameter.

c) The mass of the nebula is as small as is consistent with known data.

These assumptions will give a superior limit for the influence of radiation pressure. To estimate the mass, we may use the spectroscopic observations, which show that the central portions of some nebulae are rotating substantially like rigid bodies, and assume that the centrifugal force at the periphery of this region is equal to the gravitational attraction of the whole mass. On account of the shape of the nebula, the latter attraction will be somewhat greater than if the mass was concentrated at the center; but this factor will probably be more than balanced by the neglect of radiation pressure inside the nebula, which, in so great a mass, is likely to be important.[1]

Let us now suppose that the radius of this central portion of the nebula is r, its extreme outer radius R, and its parallax π (all in seconds of arc), and that the peripheral velocity at the distance r is V kilometers per second. The true radius of the nebula is then R/π astronomical units, or $1.5\times10^{13}\ R/\pi$ cm and its area $7.04\times10^{26}\ R^2/\pi^2$ cm^2, so that the whole force of radiation pressure upon it will at most be $F=1.4\times10^{14}R^2/\pi^2$ dynes. The radius of the central region is $1.5\times10^{13}r/\pi$ cm and the velocity at this distance 10^5V cm/sec. The mass is $M=\frac{v^2r}{G}$, where v and r are expressed in C.G.S. units, and G is the gravitational constant, 6.66×10^{-8}. Hence

$$M=2.25\times10^{30}\frac{V^2r}{\pi}\ \text{gm.} \qquad (1)$$

The acceleration produced in this mass by radiation pressure is therefore

$$A=6.3\times10^{-17}\ R^2/V^2r\pi\ \text{cm/sec}^2. \qquad (2)$$

All the quantities which appear in the second member of this equation are approximately known except π. The smaller the parallax, the greater will be the effect of radiation pressure.

[1] Jeans, *Monthly Notices of the Royal Astronomical Society*, **79**, 328, 1919.

3. *Numerical examples.*—We will now apply these formulae to the two nebulae for which sufficient data exist.

a) The great nebula in Andromeda: Pease's spectrograms[1] indicate that the radial velocity along the major axis of this nebula changes by 0.48 km per second of arc from the nucleus, up to a distance of at least 160″. The velocities in the plane of the nebula are probably 1.03 times the radial velocities. We assume therefore $r = 180''$, $V = 90$ km/sec. (which may be too small). For the maximum radius Lundmark[2] gives $R = 3600''$. The parallax is very uncertain. To get a maximum effect we will take Lundmark's value,[3] the smallest that has ever been suggested, $5'' \times 10^{-6}$. We thus obtain the acceleration,

$$A = 1.12 \times 10^{-10} \text{ cm/sec}^2.$$

b) N.G.C. 4594.—The radial velocity changes by 2.78 km per second of arc up to a distance of at least 140″.[4] The radial velocities are practically in the plane of the nebula. We therefore let $r = 150''$, $V = 415$ km/sec. From Lundmark's list we have $R = 210''$; $\pi = 7'' \times 10^{-7}$ (the mean of two very discordant estimates). These data give

$$A = 1.53 \times 10^{-13} \text{ cm/sec.}^2$$

The greater of these two accelerations, acting continuously for 100 million years, would produce a velocity of 3.5 km/sec. At the present radial velocity of −316 km/sec., the Andromeda nebula would require 6.5×10^4 years to traverse the enormous assumed distance of 200,000 parsecs, and radiation pressure during this interval would reduce its velocity by 23 km/sec. For N.G.C. 4594 the corresponding effects are very much smaller. These estimates are probably very much exaggerated. The nebulae in question are by no means as large as the circles which circumscribe them; it is far from certain that they absorb all the radiation that falls upon them; and, above all, their actual parallaxes may be much greater than the assumed values. Moreover, the assumed

[1] *Proceedings of the National Academy of Sciences*, 4, 24, 1918.

[2] *Kgl. Sv. Vet. Akad. Handlingar*, 60, 8, 61, 1919.

[3] *Ibid.*, p. 62.

[4] Pease, *Proceedings of the National Academy of Sciences*, 2, 520, 1916.

distances are so great that it is probable that, seen from such distances, the Galaxy would cover but a small portion of a hemisphere and that its radiation would be correspondingly smaller. It appears therefore safe to conclude that radiation pressure cannot have modified the radial velocities of these nebulae, during the time when they were in the vicinity of the Galaxy, by any important fraction of their present amounts. Though only two nebulae are at present available for discussion, the results are so conclusive as to settle the question.

4. *Comparison with gravitational attraction.*—It must not be forgotten that the stars composing the Galaxy exert a gravitational attraction on the nebulae, as well as a radiation pressure. For any given star the ratio of these two forces is independent of the distance, but varies with the mass and area of the body on which they act. The same will evidently be true of the radiation and gravitation of the galactic system as a whole. At the earth's distance from the sun, the gravitational force is $g = 0.592$ dynes per gram, and the radiation pressure $p = 4.49 \times 10^{-5}$ dynes/cm^2. For a body of mass m grams, which presents an effective surface s cm^2 to the sun's rays, the ratio

$$\frac{g}{p} = 1.32 \times 10^4 \frac{m}{s} \qquad (3)$$

so that radiation pressure becomes important only for very small particles, as is well known. The corresponding ratio for the Galaxy as a whole will be greater or less than this according as the average emission of radiation per unit mass of galactic matter is greater or less than in the case of the sun. This average value would be hard to estimate; but we may set a superior limit to it by taking the corresponding quantity for the giant stars, which are known to be the brightest in proportion to their mass.

In an investigation by the writer[1] 169 slow binaries of all spectral types from B to M, which gave evidence of being giant stars, were found to have mean absolute magnitude -0.8, corresponding to 180 times the sun's light, and an average mass 8.1 times that of the sun, so that the ratio of light to mass is 22 times that for the sun.

[1] For an abstract of some of the results, see *Publications of the American Astronomical Society*, 3, 327, 1918.

In view of the great numbers of dwarf stars, which give out far less light in proportion to their masses, and the existence of unknown quantities of dark matter, it is probable that the radiation per unit mass for the Galaxy as a whole is much less than this; but, assuming this exorbitant value, we find $g/p = 600\ m/s$.

On the assumptions of section 2, we find for a spiral nebula as a whole $m/s = 3.2 \times 10^3\ V^2 r\pi/R^2$. Introducing the numerical data of section 3, we find for the Andromeda nebula $m/s = 1.8 \times 10^{-3}$ gm/cm², $g = 1.1p$, while, for N.G.C. 4594, $m/s = 1.3$ gm/cm²; $g = 800\ p$. The computed surface density for the Andromeda nebula is much the smaller of the two, because the "central region" has been assumed to be much smaller in comparison to the whole nebula.

Since all the data have been deliberately chosen so as to exaggerate the importance of radiation pressure, it may be concluded that, in all probability, the gravitation of the galactic system is much more important, in its influence upon the nebulae, than the pressure of its radiation.

5. *Magnitude of the attraction.*—To get a rough idea of this, let us suppose that the mass of the galactic system is equal to 10^{10} suns, or 2×10^{43} grams (which is four times larger than Jeans's estimate[1]), and that this acts as if concentrated at a point from which distances are measured.

For the Andromeda nebula we have, from (1), $M = \frac{3.3 \times 10^{36}}{\pi}$ gms and for N.G.C. 4594 $M = \frac{5.8 \times 10^{37}}{\pi}$ gms. The parabolic velocity, U, for two bodies of masses M and m', at a distance r, is given by the equation $U = \frac{G(m+m')}{r}$. For a nebula of parallax π, $r = \frac{3.08 \times 10^{18}}{\pi}$ cm. Introducing $m' = 2 \times 10^{43}$, and the values of M given above for the two nebulae, we find, for the Andromeda nebula, in kilometers per second,

$$U = 6600\ (\pi + 1.6 \times 10^{-7})^{\frac{1}{2}}.$$

Similarly, for N.G.C. 4594, we find $U = 6600\ (\pi + 2.9 \times 10^{-6})^{\frac{1}{2}}$. The parabolic velocity would equal the observed radial velocity of

[1] *Problems of Cosmogony*, p. 222 (1919).

the Andromeda nebula, -316 km/sec., if $\pi = 0''.0023$. For N.G.C. 4594, with a radial velocity of $+1180$ km/sec., the corresponding value of π is $0''.032$.

There can be no reasonable doubt that the distances of these two nebulae are greater than the limits thus assigned, and it follows that, on the assumptions made, the gravitational attraction of the whole Galaxy is insufficient to produce the observed radial velocities by a fall from infinity, or to prevent the nebulae from receding to an infinite distance. As a large value was purposely taken for the assumed mass of the Galaxy, the conclusion appears trustworthy.

6. *Radiation pressure on stars.*—It has been recently suggested[1] that radiation pressure may nearly neutralize the attraction of the components of certain spectroscopic binaries for one another, or of such a nebula as that in Orion upon the neighboring stars.

For a pair of stars similar to the sun, we have from (3) (introducing $s = 1.52 \times 10^{22}$, $m = 1.98 \times 10^{33}$) $p/g = 5.8 \times 10^{-16}$. Taking now the sun's mass, radius, cross-section, etc., as units, and considering the influence of a star of mass M_1, area S_1, and surface-brightness J_1, upon a companion of mass M_2 and area S_2, we have

$$p/g = 5.8 \times 10^{-16} J_1 \frac{S_1 S_2}{M_1 M_2}. \qquad (4)$$

Let a be the mean distance of M_1 from the center of gravity, e the eccentricity of the orbit, and y the ratio M_1/M_2. The periastron distance is $a\,(1+y)\,(1-e)$. The sum of the radii of the stars must be less than this; whence $S_1 S_2 < \frac{1}{16} a^4 (1+y)^4 (1-e)^4$. If P is the period in days, we have (remembering that a is measured in solar radii)

$$M_1 + M_2 = 0.013 \frac{a^3 (1+y)^3}{P^2},$$

whence, from (4)

$$p/g < 2.14 \times 10^{-13} \frac{J_1 P^4 (1-e)^4}{a^2 y}.$$

[1] Henroteau, *Journal of the Royal Astronomical Society of Canada*, 14, 93, 1920.

Let K be the semi-amplitude of variation of radial velocity of the bright star (in km/sec.). Then, in our units

$$a \sin i = 0.0198\, KP(1-e^2)^{\frac{1}{2}}$$

and

$$p/g < 5.5\times 10^{-10} \frac{J_1}{y} \frac{P^2}{K^2} \frac{(1-e)^3}{1+e} \sin^2 i\,. \qquad (5)$$

The last two factors are always less than unity; and y is greater than unity in all spectroscopic binaries for which it can be determined.

Applying (5) to those spectroscopic binaries for which p/g comes out greatest, and introducing plausible (and, on the whole, high) values of J_1, we find:

Star	P	e	K	Spectrum	J	Limit of p/g
	days		km			
ζ Tauri	138	0.18	14.95	B3	30.	6.6×10^{-7}
δ Canis Majoris	270		1.5	F8	2.	3.6×10^{-5}
η Boötis	489	0.18	8.46	G	1.	8.5×10^{-7}
ϵ Ursae Majoris	1510	0.31	3.5	A	10.	2.5×10^{-4}
γ Geminorum	2175	0.30	6.12	A	10.	1.8×10^{-4}
α Scorpii	2120	0.20	2.12	Ma	0.1	2.4×10^{-5}
α Orionis	2220	0.24	2.45	Ma	0.1	2.0×10^{-5}
ϵ Hydrae	5588	0.65	8.45	F8	2.	1.3×10^{-5}

The quantities in the last column have still to be multiplied by the factor $\frac{\sin^2 i}{y}$ and also by another (and usually very small) factor arising from the fact that the stars are probably very far from being in contact at periastron. It is therefore evident that radiation pressure between the components of a binary system must in all cases be utterly negligible, in comparison with gravitation.

The whole luminous radiation of the Orion nebula is probably less than that of δ Canis Majoris (which is at a comparable distance). Unless the mass of the whole nebula is less than that of the star, its gravitational attraction must enormously exceed the pressure of its radiation upon any body of stellar dimensions and mass.

Radiation pressure is doubtless effective on comets' tails, on account of their excessively low mean density, and is also of funda-

mental importance in the interior of giant stars, where the intensity of the radiation is exceedingly great; but it appears to be almost impotent under other circumstances. Eddington[1] has recently shown that it is doubtful whether it is competent to support even so tenuous a structure as a solar prominence.

7. *Deformation of nebulae by pressure.*—It may be shown, more generally, that it is very improbable that any uniform pressure whatever could sensibly affect the motions of spiral nebulae without seriously deforming them.

It is probable that most of the mass is concentrated in the central parts of the nebula, while the pressure will influence mainly the extensive outlying regions. It follows that, under the action of a lateral pressure, the nebula will assume a dished form, convex to the direction from which the pressure comes, so that the gravitational attraction of the central mass upon any outlying portion will have a component perpendicular to the general plane of the nebula, and opposite in direction to the pressure, which balances the difference in the acceleration of the two masses by the pressure itself. These gravitational forces will transfer the momentum imparted by the pressure from the outer regions to the nucleus and cause the whole nebula to move as one mass.

Pressure acting parallel to the plane of the nebula would distort the arms, in this plane, in a similar fashion.

No such distortions are apparent upon the photographs of spiral nebulae; and it appears safe to conclude that, even at the outer edge, the gravitational attraction is fully ten times as great as the effects of any lateral pressure which may be present.

From the data of section 3, the gravitational acceleration at the outer edge of the nebula is found to be $g = 6.66 \times 10^{-4} \frac{V^2 r\pi}{R^2}$ cm/sec.^{2}. Suppose now that the lateral pressure is q dynes per cm. The acceleration which this will produce upon the nebula as a whole is $A = 3.1 \times 10^{-4} \frac{R^2 q}{V^2 r\pi}$ cm/sec^2. If K is the ratio of the effective surface density (gm/cm^2) for any part of the nebula to the mean surface density for the whole nebula, the acceleration of this part alone under the action of the pressure would be A/K. Let K_1 be

[1] *Monthly Notices of the Royal Astronomical Society*, **80**, 723, 1920.

the corresponding value for the central region and K_2 for the outer edge; then the relative acceleration of the two is $A\left(\frac{1}{K_2}-\frac{1}{K_1}\right)$. This must not exceed one-tenth of g, which gives

$$A<6.7\times10^{-5}\frac{V^2r\pi}{R^2}\frac{K_1K_2}{K_1-K_2}.$$

The value of the last factor can hardly be estimated, but it is likely to be small, since K_1 is probably considerably greater, and K_2 much less, than unity. We have, therefore,

$$A<6.7\times10^{-5}\frac{V^2r\pi}{R^2}.$$

Introducing the numerical values of section 3, we find, for the Andromeda nebula,

$$A<3.5\times10^{-12}\text{ cm/sec}^2.$$

and, for N.G.C. 4594,

$$A<2.5\times10^{-9}\text{ cm/sec}^2.$$

The latter acceleration would require 1.5×10^9 years to produce the observed radial velocity of the nebula, and during this time would drive it to a distance of 9×10^5 parsecs, which is comparable with the distance assumed above. It might therefore be claimed that the motion of this nebula could be accounted for by a repulsive pressure of some sort; but it should be remembered that several factors, all tending to diminish the pressure effect, have been ignored in the foregoing discussion. The magnitude of the necessary pressure, 3×10^{-9} dynes/cm^2, is improbably great, being equivalent to that of radiation of the quality of sunlight, and thirty times as bright as that of the full moon.

For the Andromeda nebula, the greatest permissible pressure is much less than that assumed in section 3, which shows only that the choice among uncertain data, there made with the purpose of exaggerating the influence of radiation pressure, went too far.

The argument of this section assumes that the outer parts of a spiral nebula are permanently associated with the nucleus and in some sort of equilibrium. This is more than dubious; but, if the

arms of the spiral are in process of relatively rapid dissipation into space, the influence of pressure upon the motion of the nucleus must be much less than that calculated above.

8. *Electrical forces.*—Finally, a brief examination may be made of the suggestion that electrical repulsive forces are concerned in the motions of the nebulae.

In view of the distances and velocities concerned, only electrostatic forces need be considered. Here a serious difficulty immediately appears. If the galactic system as a whole and the nebula as a whole are similarly charged, and the electrostatic repulsion between them exceeds the gravitational attraction, then the same should be true of the forces acting between the separate parts of either system, and both should disintegrate. Moreover, the magnitude of the charges and potentials involved is extraordinary. To realize the order of the quantities concerned, suppose that the charge on any body is proportional to its mass, and just sufficient to neutralize the gravitational attraction. The necessary quantity of electricity is $C^{\frac{1}{2}}$ or 2.58×10^{-4} electrostatic units per gram. Consider a spherical mass of radius r and mean density ρ. Its total charge will be $\frac{4}{3}\pi\rho r^3C^{\frac{1}{2}}$ e.s.u. Since all bodies of astronomical size behave as conductors, this charge will be concentrated on the surface, with a surface density $\sigma=\frac{1}{3}\rho rC^{\frac{1}{2}}$. The capacity of the sphere is r in electrostatic units, and the potential at the surface will be

$$V=\tfrac{4}{3}\pi\rho r^2G^{\frac{1}{2}} \text{ e.s.u.}$$

At the surface of the sphere there will be an outward pressure p, due to the mutual repulsion of the elements of the charge, given by the equation $p=2\pi\sigma^2=\frac{2}{9}\pi\rho^2r^2G$. It is easily verified that this is one-third of the gravitational pressure at the center of the mass, if the latter is homogeneous.

For the earth we have $\rho=5.5$, $r=6.37\times10^8$ cm, whence $V=2.4\times10^{15}$ e.s.u. $=7.2\times10^{17}$ volts! The electrical pressure at the surface comes out 5.75×10^{11} dynes/cm^2 or 570,000 atmospheres—which would suffice to tear the surface material loose and blow it away into the depths of space. For bodies of stellar dimensions the results are still more extravagant.

It appears therefore that, even if it were possible to charge bodies of planetary, and much more of stellar, dimensions to such potentials that their electrostatic repulsion equaled their gravitational attraction, they could not retain these charges.

9. The results of this summary survey of the problem indicate that radiation pressure between individual stars is wholly negligible; that such pressures, even under the most favorable assumptions, cannot account for any considerable portion of the observed velocities of the spiral nebulae; or even counteract the gravitational attraction of the Galaxy; that it is extremely improbable that pressure of any sort could set the nebulae in such rapid motion without deforming them to a degree inconsistent with observation; and that electrostatic repulsions appear also to be excluded.

Even the gravitational attraction of the Galaxy appears to be insufficient to account for the magnitude of these velocities—to say nothing of their signs. Two known explanations, at least, remain—the gravitation of a hypothetical huge system of which all the nebulae, and our Galaxy, are but parts, and a relativity effect, depending perhaps on the "curvature" of space as a whole, as discussed by de Sitter.[1] In the writer's opinion, it is more important at present to increase the volume of data available than to postulate the existence of unknown forces to explain the small amount of evidence which we now possess.

PRINCETON UNIVERSITY OBSERVATORY
September 30, 1920

[1] *Monthly Notices of the Royal Astronomical Society*, 78, 28, 1917.

THE PARALLAXES OF 1646 STARS DERIVED BY THE SPECTROSCOPIC METHOD[1]

By W. S. ADAMS, A. H. JOY, G. STRÖMBERG, and CORA G. BURWELL

ABSTRACT

Spectroscopic method of determining absolute magnitude and parallax.—Some years ago it was discovered that there is a correlation between the relative intensities of certain spectral lines and absolute magnitude for stars of the more advanced spectral types. In the past three years a large number of new trigonometric parallaxes has become available and has enabled this correlation to be established more accurately. For the stars for which trigonometric parallaxes have been determined the absolute magnitudes have been computed directly, but for the Cepheid variables the parallactic motion has been used, and in the case of the giant M stars a combination of results derived from peculiar motion and trigonometric parallaxes. The formulae employed are shown in the text. The absolute magnitudes obtained in this way have been plotted against the relative intensities of certain pairs of lines and from the resulting curves reduction tables have been constructed for each observer. These curves are continuous except in the case of stars of the late K and M types where the division into giants and dwarfs introduces a marked discontinuity. The absolute magnitudes and parallaxes derived by means of these tables are found to have probable errors of ±0.4 magnitude and ± 20 per cent, respectively. The method used in classifying the spectra and in estimating the intensities of the spectral lines is described.

Absolute magnitudes and spectroscopic parallaxes of 1646 stars, including revised values for 495 stars contained in the 1917 list.—An extensive table gives the Boss or Cincinnati number, the name and position of each star, the Harvard visual magnitude, total proper motion, spectral type, absolute magnitude, and spectroscopic parallax. The trigonometric parallax is given, if known.

The determination of the absolute magnitudes of stars from the intensities of certain spectral lines has formed a regular part of the stellar spectroscopic work of the Mount Wilson Observatory during the past five years. Photographs of the spectra obtained for measurements of radial velocity have also been utilized for the calculation of absolute magnitudes, and the lists of stars under observation have been selected with both of these purposes in view.

Since the last publication in 1917, of absolute magnitudes and parallaxes for any considerable number of stars, numerous

[1] *Contributions from the Mount Wilson Observatory*, No. 199.

developments and changes have taken place in the methods used for particular groups of stars and in the material upon which the spectroscopic reductions are based. The rapid increase in the number of parallaxes determined trigonometrically by the photographic method has in particular added greatly to the accuracy of the fundamental values used as the basis of the spectroscopic reductions. They have also made it possible to divide the stars into groups of comparatively small range in spectral type, and thus to secure a continuity in the reduction tables which was not possible when the material was more scanty. With the aid of this large amount of valuable trigonometric parallax material, and the results furnished by computations based on the parallactic and peculiar motions in the case of stars having very small parallaxes, we now feel reasonably certain that a reduction scale has been established which will not require very serious modification in the future. Such corrections as may become necessary when our knowledge of systematic errors in trigonometric parallaxes and of mean parallax relationships is more advanced than at present can probably be applied in the form of tabular modifications of the results given here.

The main purpose of this communication is to place in the hands of astronomers the results in the form of absolute magnitudes and parallaxes so far obtained by the use of the spectroscopic method. For this reason no attempt is made in this place to discuss the bearing of the material on a number of stellar problems. We expect, however, at an early date to supplement this article with a consideration of the evidence afforded by the results on such questions as the giant and dwarf divisions among the stars of the several spectral types, the relationship of parallax to proper motion, the probable systematic errors in parallax determinations, and the motion in space of the stars in the list.

DERIVATION OF THE REDUCTION TABLES

The general principle employed in the derivation of the reduction tables has been to group the stars according to spectral type and absolute magnitude, using provisional tables for computing the latter, and then to derive systematic corrections to the pro-

visional absolute magnitudes on the assumption that the corrections are constant for the groups in question.

The relative accuracy of the three methods used in computing mean absolute magnitudes—from trigonometric parallaxes, parallactic motions, and peculiar motions—is quite different for the near and the distant stars. For the nearer stars the trigonometric parallaxes give by far the most reliable results, while for stars among which there are no large parallaxes the parallactic motion gives the best result, provided the peculiar motions are small, no selection based upon proper motion has been made, and the group of stars as a whole is at rest relative to the stars in general. For this reason the parallactic motion has been used to compute the mean absolute magnitudes only for very large groups of stars. The result in such cases has been found to agree closely with that derived from trigonometric parallaxes and hence has been used merely as a check upon the latter. Exceptions are the Cepheids and the stars of similar spectral type for which the parallactic motion has been used exclusively.

A peculiar feature is that the parallactic motion for the dwarf stars gives very much larger mean parallaxes than those derived directly from measured parallaxes, probably indicating that these stars as a whole have a velocity differing from that of the stars in general.

The peculiar motion can give accurate results only if the peculiar velocities are large as compared with the solar motion. The results from the peculiar motion are in good agreement with the results from trigonometric parallaxes for all stars fainter than about absolute magnitude $+2$. For such stars, however, the measured parallaxes are large enough to provide good determinations of the mean absolute magnitudes, and consequently the only case in which the results from the peculiar velocities have been used is that of the giant M stars, for which a combination of the results from trigonometric parallaxes and from peculiar motions has been employed.

The formulae used for computing mean absolute magnitudes from trigonometric parallaxes, parallactic motions, and peculiar motions will now be deduced.

a) Trigonometric parallaxes.—The following notation has been used:

π = true parallax
π_0 = trigonometric parallax
ϵ_0 = true error of the trigonometric parallax
M_t = true absolute magnitude defined as the apparent magnitude at a distance corresponding to a parallax of 0".1 (10 parsecs)
M = most probable absolute magnitude
M_1 = absolute magnitude as given by the provisional reduction tables
S = systematic correction to M_1 for reducing it to M
T = accidental error of M_1+S
m = apparent magnitude
π_1 = spectroscopic parallax based on M_1 as the absolute magnitude

We then have:

$$M_t = M_1 + S + T = m + 5 + 5 \log (\pi_0 + \epsilon_0)$$

and

$$M_1 = m + 5 + 5 \log \pi_1$$

Hence

$$S + T = 5 \log \frac{\pi_0 + \epsilon_0}{\pi_1}$$

or

$$\left.\begin{aligned} &\pi = \pi_0 + \epsilon_0 = \pi_1 \, 10^{0.2(S+T)} = \pi_1 \sigma \tau \\ &\text{where} \quad \sigma = 10^{0.2S} \text{ and } \tau = 10^{0.2T} \end{aligned}\right\} \quad (1)$$

Further

$$\left.\begin{aligned} &\tau = 10^{0.2T} = 1 + E + \tfrac{1}{2}E^2 + \ldots \\ &\text{where} \quad E = \frac{0.2\,T}{\text{Mod}} = 0.4605\,T \end{aligned}\right\} \quad (2)$$

We shall limit ourselves in the following to the second order of the error T.

From equations (1) and (2) we may deduce an expression for the mean of a number of parallaxes. We shall then make use of the well-known approximate formula

$$\overline{ab} = \bar{a}\,\bar{b}$$

which is valid if the two variables a and b vary *independently* of one another. Since π_1 is dependent upon T and thus also upon τ and

E, we must separate π_1 from τ before taking the arithmetical mean. From equation (1) we obtain

$$\pi_1\sigma=\frac{\pi_0+\epsilon_0}{\tau}=(\pi_0+\epsilon_0)(1-E+\tfrac{1}{2}E^2)$$

From this equation we deduce

$$\pi_1\sigma-\pi_0 A=\epsilon_0-\pi E \tag{3}$$

where

$$A=1+\tfrac{1}{2}E^2 \tag{4}$$

In the following we shall assume that the errors ϵ_0 and T, and hence also E, have a normal error-distribution.

Taking the arithmetical mean of a number of equations of form (3) we obtain

$$\overline{\pi_1\sigma}-\bar{\pi}_0\bar{A}=0 \text{ or } \frac{\overline{\pi_1\sigma}}{\bar{A}}=\bar{\pi}_0=\bar{\pi} \tag{5}$$

where

$$\bar{A}=1+\tfrac{1}{2}\bar{E}^2>1 \tag{6}$$

The quantity $\pi_1\sigma$ is the parallax corresponding to the most probable absolute magnitude $M=M_1+S$. The mean of a series of these parallaxes is not exactly equal to the mean of the corresponding trigonometric parallaxes, but is systematically larger. This fact depends upon the unequal effects produced in the spectroscopic parallax by a positive and a negative error of the same size in the estimation of the absolute magnitude.

In order to make the spectroscopic parallaxes directly comparable with the trigonometrical ones, we shall define the quantity $\frac{\pi_1\sigma}{\bar{A}}$ as the spectroscopic parallax π', and in the first instance determine the quantity $\frac{\sigma}{\bar{A}}$. The absolute magnitudes corresponding to these spectroscopic parallaxes have been denoted by M' and are those given in the catalogue.

We then have

$$M'=m+5+5\log\pi_1\sigma-5\log\bar{A}$$

$$M'=m+5+5\log\pi'$$

The most probable absolute magnitude M defined in such a way that a positive and a negative error T have the same probability is related to M' by the equation

$$M = M' + 5 \log \bar{A} \tag{7}$$

and

$$\bar{A} = 1 + \frac{0.02\,\theta^2}{\mathrm{Mod}^2} \tag{8}$$

where θ is the mean error in an estimate of the absolute magnitudes.

In the determination of $\frac{\sigma}{\bar{A}}$ we start from the equations of condition (3)

$$\pi_1 \sigma - \pi_0 A = \epsilon_0 - \pi E$$

If the range in the values of π_1 is small, we may find $\frac{\sigma}{\bar{A}}$ by taking arithmetical means of equations (3) multiplied by the relative weights p of the trigonometric parallaxes:

$$\frac{\sigma}{\bar{A}} = \frac{\Sigma p \pi_0}{\Sigma p \pi_1} \tag{9}$$

If the range in π is considerable, we do not utilize to their full extent the higher weights of the larger parallaxes by using equation (9). An ordinary least-squares solution might give erroneous results on account of the effect of large values in the errors E and ϵ_0. For this reason we have in general used a compromise between the direct mean of the equations of condition as given by (9) and the ordinary least-squares solution based upon the weighting of the errors ϵ_0. Dividing the results into three or four groups according to the size of π_1, we have as in (9)

$$\left.\begin{aligned} &\frac{\sigma}{\bar{A}} \Sigma p \pi_1 - \Sigma p \pi_0 = 0 \\ &\text{Weight} = \frac{1}{k^2 \Sigma p + \dfrac{\eta^2 (\Sigma p \pi_0)^2}{n}} \end{aligned}\right\} \tag{10}$$

where k is the mean error of the trigonometric parallaxes corresponding to unit weight, n is the number of stars, and

$$\eta^2 = \bar{E}^2 = \frac{0.04\,\theta^2}{\mathrm{Mod}^2}$$

If we assume definite values of k and η we can make an ordinary least-squares solution of equations (10). The values of k and η used are

$k = \pm 0''.015$, corresponding to a probable error in π_0 of $\pm 0''.010$

$\eta = \pm 0.205$, corresponding to a probable error in $M_1 + S$ of ± 0.3

In order to secure a grouping independent of the errors in the estimates of the absolute magnitudes, a solution was made using the proper motions reduced to zero apparent magnitude as a basis of the grouping. In this case there is less danger of a systematic effect upon the sums ΣT and ΣE which we have to suppose to be equal to zero.

In the first computation of the systematic correction to the provisional reduction tables all available trigonometric parallaxes for stars in the list were used. The reductions to absolute parallaxes were generally computed from the apparent magnitudes of the comparison stars, using the table given by Kapteyn in *Groningen Publications*, No. 24, page 15. For the parallaxes determined at the Allegheny, McCormick, and Sproul observatories a constant reduction of $+0''.005$ and for the Mount Wilson parallaxes one of $+0''.002$ has been applied throughout. The weights of the different determinations based upon the size of the probable errors are as follows:

Mount Wilson	1.5	Vôute	0.5
Greenwich	1.5	Abetti	0.4
Allegheny	1.0	Russell	0.3
McCormick	1.0	Peter	0.3
Sproul	1.0	Jost	0.3
Yerkes	1.0	Kapteyn	0.4
Yale	0.5	Flint I	0.05
Fox	1.0	Flint II	0.2

A second approximation was made using only the parallaxes determined at the Allegheny, McCormick, Yerkes, and Mount Wilson observatories, all being given the same weights. Slight corrections based on this latter computation were then applied to the tables resulting from the first approximation. In the final analysis the reduction tables are thus based almost exclusively on

the four series of trigonometric parallaxes mentioned above. The differences between the two solutions are, however, very small.

b) *Parallactic motion.*—The co-ordinates of a star in space relative to the sun and referred to the equatorial system of co-ordinates are

$$\left.\begin{aligned} X &= r\cos\alpha\cos\delta \\ Y &= r\sin\alpha\cos\delta \\ Z &= r\sin\delta \end{aligned}\right\} \tag{11}$$

where r is the distance from the sun and α and δ are the right ascension and declination of the star. Differentiating these equations with respect to the time, we obtain the velocity components x, y, and z, in km per second relative to the sun.

$$\left.\begin{aligned} x &= V\cos\alpha\cos\delta - \frac{k}{\pi}(\mu_1\sin\alpha + \mu_2\cos\alpha\sin\delta) \\ y &= V\sin\alpha\cos\delta + \frac{k}{\pi}(\mu_1\cos\alpha - \mu_2\sin\alpha\sin\delta) \\ z &= V\sin\delta + \frac{k}{\pi}\mu_2\cos\delta \end{aligned}\right\} \tag{12}$$

where

V = radial velocity

π = parallax

$\mu_1 = \mu_\alpha\cos\delta$

$\mu_2 = \mu_\delta$

μ_α and μ_δ = annual proper motion in α and δ in seconds of arc

$$k = \frac{\text{astronomical unit of length in km}}{\text{number of seconds in a year}} = 4{\cdot}737$$

Introducing the velocity components x_0, y_0, and z_0 of the sun relative to the geometrical centroid of a large number of stars, we have

$$x + x_0 = \epsilon_1, \qquad y + y_0 = \epsilon_2, \qquad z + z_0 = \epsilon_3$$

where ϵ_1, ϵ_2, and ϵ_3 are the peculiar velocity components of the star referred to this centroid.

If we use the same co-ordinates for the sun's apex for all spectral types and absolute magnitudes and adopt the values computed

for the stars of later type given in *Mount Wilson Contributions*, No. 144, page 14,

$$\alpha_0 = 270^\circ.9, \qquad \delta_0 = +29^\circ.2, \qquad V_0 = 21.48 \text{ km/sec.}$$

we find

$$x_0 = +0.28, \quad y_0 = -18.75, \quad z_0 = +10.48$$

The following auxiliary quantities have been tabulated:

$$\left.\begin{aligned} A_0 &= x_0 \sin\alpha - y_0 \cos\alpha \\ B_0 &= x_0 \cos\alpha \sin\delta + y_0 \sin\alpha \sin\delta - z_0 \cos\delta \end{aligned}\right\} \tag{13}$$

We can then derive

$$\left.\begin{aligned} \frac{k\mu_1}{\pi} - A_0 &= \epsilon' \\ \frac{k\mu_2}{\pi} - B_0 &= \epsilon'' \end{aligned}\right\} \tag{14}$$

The quantities ϵ' and ϵ'' are the components of the peculiar velocities of the stars on two axes perpendicular to the line of sight in the direction of increasing right ascension and declination.

In order to obtain the mean absolute magnitude we may proceed in the following way, the notation being the same as in the discussion of the trigonometric parallaxes:

$$\pi = 10^{0.2(M_1+S+T-m)-1} = \frac{0.1\,\sigma\tau}{\rho}$$

where

$$\sigma = 10^{0.2S}$$
$$\tau = 10^{0.2T}$$
$$\rho = 10^{0.2\,(m-M_1)}$$

Equations (14) may then be written

$$\frac{10k\mu_1\rho}{\sigma\tau} - A_0 = \epsilon', \qquad \frac{10k\mu_2\rho}{\sigma\tau} - B_0 = \epsilon'' \tag{15}$$

The components of the proper motions μ_1 and μ_2, however, are affected by systematic and accidental errors. The systematic corrections given by Boss in his *Catalogue*, page xxviii, have been

applied.[1] Denoting the accidental errors in μ_1 and μ_2 by η_1 and η_2 we can write equations (15) in the following form:

$$\left.\begin{aligned} \frac{A_0\sigma\tau}{10k}-\mu_1\rho&=\rho\eta_1-\frac{\sigma\tau\epsilon'}{10k}\\ \frac{B_0\sigma\tau}{10k}-\mu_2\rho&=\rho\eta_2-\frac{\sigma\tau\epsilon''}{10k}\end{aligned}\right\} \tag{16}$$

As in the case of the trigonometric parallaxes, we shall write τ in the form

$$\tau=1+E+\tfrac{1}{2}E^2=A+E$$

The equations of conditions are then

$$\left.\begin{aligned} A_0x-\mu_1\rho&=\rho\eta_1-\frac{\sigma\epsilon'}{10k}-\frac{\sigma A_0E}{10k}\\ B_0x-\mu_2\rho&=\rho\eta_2-\frac{\sigma\epsilon''}{10k}-\frac{\sigma A_0E}{10k}\end{aligned}\right\} \tag{17}$$

where

$$x=\frac{A\sigma}{10k}=\frac{(1+\frac{1}{2}E^2)\sigma}{10k}$$

The first terms on the right-hand side of these equations increase with the apparent magnitude. The second terms are usually the largest, while the existence of the third terms tends to decrease the weights for stars farthest from the apex and antapex. In order to make the weights more uniform we have in the case of the distant stars limited ourselves to those brighter than apparent magnitude 5.5. At the same time this limitation decreases the effect of a selection among these stars according to proper motion, since nearly all can be assumed to be selected on account of brightness alone. In order to reduce the effect of large peculiar motions and large accidental errors in the absolute magnitudes, we have collected the equations of condition (17) into a few groups according to the size of A_0 and B_0, formed means, and given each of these new equations of condition a weight according to the number of stars.

The new equations of condition are then

$$\left.\begin{aligned} \overline{A_0}x-\overline{\mu_1\rho}&=0\\ \overline{B_0}x-\overline{\mu_2\rho}&=0\end{aligned}\right\} \quad \text{Weight } N \tag{18}$$

[1] The *Catalogue*, however, gives the total proper motion without these corrections.

When x has been found from the solution of equations (18) we have

$$\sigma\bar{A} = 10kx$$

and

$$\frac{\sigma}{\bar{A}} = \frac{10kx}{\bar{A}^2} \tag{19}$$

The mean absolute magnitude M' used for computing the most probable parallaxes can then be obtained by adding the quantity

$$5 \log \frac{\sigma}{\bar{A}} = 5 \log x + 5 \log k + 5 - 10 \log \bar{A}$$

to the mean of the provisional magnitudes $\overline{M_1}$, a provisional value of $\bar{A}$ being used.

This method of deriving mean absolute magnitudes from the components of the parallactic motions requires less computation than that based upon the total parallactic motion. It is similar to that used by Charlier in his study of the B stars.[1] The systematic correction to the absolute magnitudes due to the errors in the estimates of the latter that must be applied in order to obtain the most probable parallaxes ($-10 \log \bar{A}$) has a tendency to make the parallaxes smaller. This would probably account for the difference found in the mean parallax of the B stars when based on the one hand upon the assumption of equality of the absolute magnitudes, and on the other directly upon the proper motions (Kapteyn, Plummer, Bergstrand, and others).

c) *Peculiar motion.*—From equations (16), limiting ourselves to terms of the first order in the errors, we derive

$$\left.\begin{aligned} \xi\mu_1\rho - A_0 &= \epsilon' - \xi\eta_1\rho + A_0 E \\ \xi\mu_2\rho - B_0 &= \epsilon'' - \xi\eta_2\rho + B_0 E \end{aligned}\right\} \tag{20}$$

where

$$\xi = \frac{10k}{\sigma}$$

From the radial velocities corrected for the sun's motion we can compute for definite groups of stars the average radial velocity

[1] *Meddelanden från Lunds Astronomiska Observatorium*, Ser. II, No. 14.

$\frac{\Sigma|V'|}{n}$. This quantity can be supposed to be nearly identical with $\frac{\Sigma|\epsilon'|}{n}$ or $\frac{\Sigma|\epsilon''|}{n}$.

Assuming the dispersion in ϵ' and ϵ'' to be considerably larger than in the other terms on the right-hand sides of equations (20), we derive

$$\left.\begin{aligned}\Sigma|\xi\mu_1\rho - A_0| &= \Sigma|\epsilon'| + \frac{\xi^2\eta_1^2\bar{\rho}^2 + A_m^2\bar{E}^2}{2\Sigma|\epsilon'|}n^2 \\ \Sigma|\xi\mu_2\rho - B_0| &= \Sigma|\epsilon''| + \frac{\xi^2\eta_2^2\bar{\rho}^2 + B_m^2\bar{E}^2}{2\Sigma|\epsilon''|}n^2\end{aligned}\right\} \qquad (21)$$

where A_m and B_m denote the average numerical values of A_0 and B_0, η_1^2 and η_2^2 are the squares of the mean errors in the measurements of the component of proper motion, $\mu_\alpha \cos\delta$ and μ_δ, and n is the number of stars. Since the results from the peculiar motions were used only for the giant M stars where the peculiar velocities are large, it was found that the second terms in the right-hand members could be neglected. Equations (21) then reduce to the more simple form

$$\left.\begin{aligned}\Sigma|\xi\mu_1\rho - A_0| &= \Sigma|\epsilon'| \\ \Sigma|\xi\mu_2\rho - B_0| &= \Sigma|\epsilon''|\end{aligned}\right\} \qquad (22)$$

The average radial velocities corrected for the solar motion, for the K term, and for the effect of stream motion were then computed and the values of $\Sigma|\epsilon'|$ and $\Sigma|\epsilon''|$ obtained from them. Equations (22) were then solved by assuming approximate values of ξ and computing the corrections to these values. The results thus obtained were nearly the same as those found from computing geometrical mean parallaxes from the τ and v components according to the method devised in *Mount Wilson Contributions*, No. 144, page 7.

REDUCTION CURVES

The values of $\Delta M_1 = 5 \log \frac{\sigma}{A}$ having been computed for groups of stars of different spectral types and absolute magnitudes, according to formulae (10), (18), and (22), the sums $M_1 + \Delta M_1 = M'$ were

properly weighted and plotted against the mean intensities of the several spectral lines used in the determination. When the correlation curves were computed, a continuous change of absolute magnitude with line-intensity and with spectral type was found

TABLE I

$\frac{4077}{4072}$	Fo	F8	$\frac{4215}{4250}$	F8	G4	Ko	K4	K8	M
.....			+5.0.....	−2.9	−2.4	−1.7	−0.6	−2.9	
+3.0.....	−0.5	−0.3	+4.0.....	−1.4	−0.8	+0.4	−0.2	−1.6	
+2.0.....	+1.1	+1.5	+3.0.....	+0.1	+0.6	+2.7	+0.3	−0.4	
+1.0.....	+2.3	+2.4	+2.0.....	+1.7	+2.0	+3.7	+1.2	+0.5	
0.0.....	+3.0	+3.3	+1.0.....	+3.2	+3.8	+4.4	+6.0		
−1.0.....	+3.8	+4.3	0.0.....	+4.8	+5.1	+5.2	+6.5	+7.2	
−2.0.....	+4.3	+5.0	−1.0.....	+6.4	+6.1	+6.1	+7.2	+8.2	+ 9.0
.....			−2.0.....			+6.9	+7.9	+9.4	+11.4

$\frac{4290}{4271}$	Fo	F8	$\frac{4454}{4461}$	F8	G4	Ko	K4	K8	M
.....			−2.0.....			−2.7	0.0		
+2.0.....	+0.5	+0.3	−1.0.....	−1.6	−1.1	+2.8	+1.2		
+1.0.....	+2.0	+1.6	0.0.....	+3.0	+3.8	+4.9	+5.5		
0.0.....	+2.9	+2.5	+1.0.....	+5.5	+5.8	+5.9	+6.2		
−1.0.....	+4.1	+3.7	+2.0.....		+6.7	+6.5	+6.7	+7.1	+ 7.2
−2.0.....	+4.3	+4.7	+3.0.....			+6.7	+7.3	+7.7	+7.8
−3.0.....		+5.0	+4.0.....				+7.7	+8.3	+8.4
.....			+5.0.....					+8.8	+9.0
.....			+6.0.....					+9.1	+9.9
.....			+7.0.....						+10.8
.....			+8.0.....						+11.1

			$\frac{4454}{4494}$	F8	G4	Ko	K4	K8	M
.....			0.0.....		−3.0	−0.4	+0.4		
.....			+1.0.....	+1.9	+2.4	+4.0	+1.6		
.....			+2.0.....	+5.1	+5.4	+5.5	+6.0		
.....			+3.0.....		+6.5	+6.2	+6.4	+6.8	
.....			+4.0.....			+6.5	+6.8	+7.3	+ 7.3
.....			+5.0.....				+7.2	+7.8	+ 7.9
.....			+6.0.....					+8.4	+ 8.5
.....			+7.0.....					+8.8	+ 9.2
.....			+8.0.....					+9.1	+10.0
.....			+9.0.....					+9.5	+10.7
.....			+10.0.....						+11.0

except in the case of stars of the late K and M types, where the division into giants and dwarfs caused a marked discontinuity. The scale used in the estimates of the line-intensities being an arbitrary one, different reduction tables were computed for the three

observers, Adams, Joy, and Miss Burwell. An abstract of the tables for Mr. Adams' scale is given below. The differences of intensity for the pairs of lines employed are given under their wave-lengths and the corresponding absolute magnitudes under the successive spectral types.

Among the giants the rate of change of absolute magnitude with line-intensity is very large in the case of the line 4454, and for this reason the two estimates of this line whenever made have been given half-weight.

PROBABLE ERRORS OF THE ABSOLUTE MAGNITUDES

A determination of the probable errors of the absolute magnitudes has been made using the trigonometric parallaxes for this purpose.

Equation (3) can be written

$$\pi' - \pi_0 = \epsilon_0 - \pi E = v$$

where π' is the most probable spectroscopic parallax.

Calling the weights of the trigonometric parallaxes p, we find

$$\overline{E^2} = \frac{\Sigma p v^2 - nk^2}{\Sigma p \pi_0^2 - nk^2} \qquad (23)$$

where k is the mean error of a parallax of weight unity.

If a star has been measured by several observers, the error in the trigonometric parallax becomes smaller, but the error in the spectroscopic parallax is unaffected. It is, therefore, necessary in some way to equalize the weights of the trigonometric parallaxes, and we have used the method of giving all stars for which the weight is equal to 1 or larger the weight unity, omitting all parallaxes of smaller weights. As before, the unit of weight has been assumed to be such as would correspond to an external probable error of $\pm 0''.010$. Calling the mean error of the absolute magnitudes θ, we have

$$\theta^2 = 25 \text{ Mod}^2 \, \overline{E^2} = 4.715 \overline{E^2}$$

The following table gives the values of the probable errors r computed by this method:

TABLE II

Spectrum	*M*	Number	*r*	Spectrum	*M*	Number	*r*
A–F4.....	< 2.0	28	±0.30	G5–G8....	< 1.0	42	±0.51
	2.1 to 3.0	31	.58		1.1 to 5.0	30	.38
	> 3.0	25	.42		> 5.1	24	.25
F5–F8....	< 3.5	38	±0.34	G9–K4....	< 1.0	59	±0.32
	> 3.6	48	.38		1.1 to 3.0	27	.53
					3.1 to 6.0	33	.46
F9–G4....	< 4.0	42	±0.64		> 6.1	38	.36
	4.1 to 5.0	39	.12				
	> 5.1	18	.46	K5–K9....	< 2.0	23	±0.00
					> 7.5	25	.24
				M.....	< 3.0	33	±0.00
					> 7.0	17	.20

When the probable error is equal to 0.00, the residuals are smaller than those due exclusively to the effect of a probable error ±0″.010 in the trigonometric parallaxes.

For the sake of convenience we may assume a probable error in the absolute magnitudes of ±0.40 throughout. The corresponding value of $\bar{A}$ is then

$$\bar{A} = 1 + \frac{\overline{E^2}}{2} = 1 + \frac{0.02 r^2}{0.455 \text{ Mod}^2} = 1.0373$$

The correction which must be applied to the absolute magnitudes M' given in the table, in order to convert them into the most probable ones, is therefore (equation 7)

$$5 \log \bar{A} = +0.08$$

The probable errors r' of the spectroscopic parallaxes can be computed from the formula

$$r' = \frac{r}{5 \text{ Mod}} \pi$$

If

$$r = \pm 0.40$$

we find

$$r' = \pm 0.184\, \pi$$

In other words, the probable error of the spectroscopic parallaxes is somewhat below 20 per cent of the parallax itself.

EFFECT OF SYSTEMATIC ERRORS IN THE TRIGONOMETRIC PARALLAXES

Several studies of the systematic difference between various series of trigonometric parallaxes have been made recently. A special solution has been undertaken, applying the systematic corrections derived by van Maanen and Miss Wolfe (*Mt. Wilson Contr.*, No. 189) for reduction to a mean system. The most important of these corrections is that of +0".0027 to the Allegheny parallaxes,[1] which, on account of their large number and high weight, has a tendency to make the spectroscopic parallaxes larger. The effect upon the absolute magnitudes, if these corrections were applied to the measured parallaxes, can be seen from the following table:

TABLE III

Spectrum	A–F8	F9–G8	G8–K4	K5–K9	M
Giants.....	+0.03	+0.09	+0.06	0.00	+0.03
Dwarfs.....	+0.05	+0.04	+0.03	+0.01	+0.03

The spectroscopic parallaxes would then be increased by a quantity equal to $(10^{0.2\,\Delta M} - 1)$. It thus appears that the systematic effect arising from this source is very small.

COMPARISON WITH TRIGONOMETRIC PARALLAXES

A direct computation of the difference, spectroscopic *minus* trigonometric parallax, has been made for the stars whose parallaxes have been determined at the Allegheny, McCormick, Yerkes, and Mount Wilson observatories. The algebraic mean difference, assigning all the stars the same weight, is given in the third column of the following table, while the weighted mean difference is given in the fourth column. The weights are here based upon the facts that the errors in the spectroscopic parallaxes are proportional to the parallaxes themselves, while the errors in the trigonometric

[1] The correction given in the paper cited is +0".0042, which is a mean of two determinations. A mean reduction to absolute parallax of +0".0035 was used, while in the present system we have used +0".005, which accounts for the difference.

parallaxes are independent of this. The quantity S' is computed from the equations of condition

$$S' = \pi' - \pi_0, \quad \text{weight } \frac{1}{\epsilon_0^2 + E^2\pi^2}$$

where the errors in the trigonometric parallaxes and the absolute magnitudes are based upon the probable errors $\pm 0''.010$ and ± 0.4, respectively. We have then

$$\overline{\epsilon_0^2} = 0.00022, \; \overline{E^2} = 0.0746$$

TABLE IV

	Number	Not Weighted S	Weighted S'
Allegheny	296	$+0''.0018$	$+0''.0031 \pm 0''.0007$
McCormick	209	-0.0008	$+0.0020 \pm 0.0010$
Yerkes	98	$+0.0019$	$+0.0016 \pm 0.0015$
Mount Wilson	79	-0.0030	-0.0032 ± 0.0011
	682	$+0''.0005$	

It is to be noted that in computing the reduction tables the larger parallaxes have the highest weights, so that we cannot expect S and still less S' to become zero when all the stars are taken together.

The weighted means S' can be supposed to represent the systematic corrections to the trigonometric parallaxes, if these corrections can be regarded as constant. They agree well with those found by van Maanen and Miss Wolfe except in the case of the McCormick parallaxes. The difference between the weighted mean S' and the unweighted mean S shows a dependence upon the size of the parallax, which can hardly be due to the spectroscopic parallaxes, since for the other series of results the values of S and S' are very nearly the same. A direct comparison between parallaxes of the same stars measured at the four observatories shows that the correction to the McCormick parallaxes seemingly depends upon the apparent magnitude, so that the unweighted mean probably gives a more reliable value for the systematic correction for these stars in general.

THE CEPHEIDS AND PSEUDO-CEPHEIDS

The absolute magnitudes of the Cepheid variables and the stars with similar spectra, which for convenience we may call Pseudo-Cepheids, have been computed from the parallactic motions alone, the trigonometric parallaxes being too small to furnish reliable data for this purpose. These two classes of stars have been reduced with the same tables, as it was found that their mean absolute magnitudes were about the same.

If the absolute magnitudes of the Cepheids are plotted against $0.2m+\log \mu$, a marked correlation between these quantities can be found.

TAURUS GROUP

A comparison of the spectroscopic parallaxes of the stars belonging to the Taurus group with the parallaxes of these stars as measured by Boss[1] and Kapteyn[2] was made and the results are given in the following table:

TABLE V

Spectrum	M	Number*	$\bar{\pi}'$	$\bar{\pi}_0$	ΔM
A8–F2.....	1.6 to 2.5	7	0".017	0".025	+0".86
F5–G0.....	3.7 to 4.1	7	.020	.024	+0.45
G5–K2.....	4.5 to 5.5	4	.022	.023	+0.12
G7–G9.....	0.4 to 1.4	4	.025	.025	−0.03

* Several of the stars used here are not given in the main table, as in some cases only one spectrogram has been secured.

The large positive correction to the absolute magnitudes for the F-type stars cannot be reconciled with the great number of large trigonometric parallaxes for the stars of this type in general. Most of the F-type stars belonging to the Taurus group, however, show very hazy lines which are difficult of estimation, and for this reason these stars can probably not be regarded as representative of the F stars in general.

[1] *Astronomical Journal*, No. 604, 1908.

[2] *Groningen Publications*, No. 23, 1909.

COMPARISON WITH RESULTS FOR FIVE HUNDRED STARS

The absolute magnitudes of the stars contained in the list of 500 published in 1917[1] were subject to errors due mainly to three causes: (1) the insufficiency of the trigonometric parallax material upon which the reduction curves were based; (2) the resulting necessity for grouping into too large divisions of spectral type; (3) the uncertainty in the reduction of the Cepheid variables.

The discussion of the method of reduction used for the stars contained in this list shows how great an improvement has been effected as regards the first two of these factors. A completely different system of reduction has been used for the Cepheid variables and stars having a similar type of spectrum. These were treated under the normal spectral types in the list of 500 stars, while in the present discussion they have been reduced independently as a special class. This has resulted in a large systematic difference compared with the earlier values, the present absolute magnitudes being considerably brighter.

TABLE VI

DIFFERENCES IN *M*, 1920 SYSTEM *minus* 500 STARS

	$M<3.0$		$M=3.0-5.0$		$M>5.0$	
	Number	Difference	Number	Difference	Number	Difference
A–F8....	23	−0.46	77	−0.54	1	−0.3
F9–G8...	51	−0.30	51	−0.05	41	−0.20
G9–K4...	78	+0.08	12	+0.83	64	−0.12
K5–K9...	10	−1.01			29	−0.07
M.....	29	−1.12			15	−0.10
Cepheids.	14	−2.9				
All types except Cepheids	191	−0.32	140	−0.24	150	−0.13

The summary above gives the results of a comparison for 495 stars common to the two lists, the differences given being the corrections necessary to apply to the stars in the list of 500 in order to reduce their absolute magnitudes to the present system. As would be expected, the corrections for the fainter stars are considerably smaller than those for the brighter.

[1] *Mt. Wilson Contr.*, No. 142; *Astrophysical Journal*, 46, 313, 1917.

METHOD OF ESTIMATION OF INTENSITIES

A brief description of the method of classifying the spectra and of estimating the intensities of the spectral lines used in the determination of the absolute magnitudes will perhaps be of value.

The spectrograms are examined under a Hartmann spectrocomparator and the hydrogen lines are first compared with the neighboring lines λλ 4326, 4352, and 4405 in the case of Hγ, and λλ 4872 and 4957 in the case of Hβ. From the relative intensities of these pairs of lines, with the aid of a reduction table based upon standard spectra, the "measured" type of spectrum is determined. In the case of spectra between Fo and Go comparisons are also made with λλ 4227 and 4384, while Hβ is omitted.

Estimations of the spectral type are made from direct comparisons with typical spectra selected from the Harvard list. The spectra of three stars having the types Fo, F5, and Go have been photographed upon one standard plate, and those of three other stars with spectra G5, Ko, and K5 upon another plate. These spectra are placed under the second microscope of the spectrocomparator and are brought side by side with that of the star to be classified. Values intermediate between those of the typical stars are estimated from comparison with the stars having spectra on either side, especial consideration being given to the calcium line λ 4227 and the chromium lines λλ 4255 and 4275, which vary rapidly with spectral type and form a valuable criterion. It is probable that all three of these lines vary to some extent with absolute magnitude, but the effect seems to be slight except in extreme cases like the Cepheid variables.

The estimations of the relative intensities of the pairs of lines for determinations of absolute magnitude are made in the same way as those of the hydrogen lines. In stars of types A to F7 the lines compared are $\frac{4}{4}\frac{0}{0}\frac{7}{7}\frac{7}{2}$ and $\frac{4}{4}\frac{2}{2}\frac{9}{9}\frac{0}{1}$. In types F8 to G, the three pairs $\frac{4}{4}\frac{2}{2}\frac{1}{5}\frac{5}{0}$, $\frac{4}{4}\frac{4}{4}\frac{5}{6}\frac{5}{2}$, and $\frac{4}{4}\frac{4}{4}\frac{5}{9}\frac{5}{5}$ have been added, and these have been used exclusively for later types of spectra except the M-type giants. The latter and the Cepheid variables have been treated separately. For the M-type giants the intensities of the lines λλ 4077 and 4215 have been compared directly with those in the spectra of the stars

β Andromedae and μ Geminorum. In the case of the Cepheids the pairs of lines have been $\frac{4077}{4072}$, $\frac{4215}{4250}$, and $\frac{4290}{4271}$, a special table being used for reduction purposes.

DESCRIPTION OF CATALOGUE

In the extensive table which follows, the successive columns contain the following data for each star:

Column 1. Number in Boss *P.G.C.* or in *Cincinnati Publication*, No. 18.

2. Name of star, double stars being assigned the number in Burnham's *General Catalogue* in case they have no Greek letter or Flamsteed number.

3 and 4. Right ascension and declination for 1900.

5. The magnitudes from the revised *Draper Catalogue* are used for stars within the first twelve hours of right ascension. In the case of faint B.D. stars the B.D. magnitude has been corrected in accordance with the values given in *H.A.*, **72**, 214. In the case of double stars and spectroscopic binaries, the magnitude of the brighter component has been calculated from the combined magnitude in accordance with the relative intensities of the two components.

6. Total proper motion taken from Boss's *P.G.C.* or *Cin.* 18 when given.

7. Estimated Mount Wilson spectrum.

8. Spectrum as determined from the intensities of the hydrogen lines.

9. Absolute magnitude M' calculated from the line-intensities.

10. Parallax corresponding to M'.

11. Weighted trigonometric parallax.

12. Authority for the trigonometric parallax. The following are the principal abbreviations used: A, Allegheny; Ab, Abetti; C, Cape; D, Dearborn; F, Flint; G, Greenwich; J, Jewdokimow; Jo, Jost; K, Kapteyn; Kos, Kostinsky; M, McCormick; R, Russell; Ram, Rambaut; S, Sproul; W, Mount Wilson; Y, Yale; Ye, Yerkes.

The significance of the symbols occurring in the catalogue is as follows:

* See note at end of table.

† Magnitude corrected to the brighter component of the double star or spectroscopic binary.

‡ Unpublished proper motion by Kapteyn.

§ Cepheid or Pseudo-Cepheid reduced by special curves.

|| Unpublished proper motion by Roy.

TABLE VII

Boss	Name	α 1900	δ 1900	Harv. Vis. Mag.	μ	Spectrum Est.	Spectrum Meas.	Spect. Abs. Mag.	Spect. π	Trig. π	Auth.
C 2	Bu. 12740 S.	0h 0m4	+45°16′	8.9	0″.858	K7		8.8	0″.096	0″.102	A, Ye, Y, D
3	Bu. 12755 Br.	0 1.0	+57 53	6.4	0.266	G4	G2	5.3	0.060	0.036	S
3	Bu. 12755 Ft.	0 1.0	+57 53	7.5	0.266	G7	G7	5.3	0.036		
6		0 1.4	+28 28	6.2	0.419	G9	G7	5.8	0.083	0.150	Y
9	5 Ceti	0 3.1	− 3 0	6.3	0.006	K2	G4	1.2	0.010		
12	β Cassiop.	0 3.8	+58 36	2.4	0.559	F2	F4	1.6	0.069	0.071	A, M, Y, *et al.*
C 9	A.G. Hels. 38	0 4.0	+64 31	7.0	0.30	K0	G9	4.3	0.029		
19	22 Androm.	0 5.1	+45 31	5.1	0.004	F2	F3	1.3	0.017		
.....	A.G. Chris. 15	0 5.4	+66 35	9.2	0.138‡	G8	G7	4.1	0.010		
.....	A.G. Leiden 33	0 5.4	+32 34	7.2	0.052‡	K5	K0	0.5	0.005		
.....	SX Cassiop.*	0 5.5	+54 20	9.1†		A6p		2.2	0.004		
31	χ Pegasi	0 9.4	+19 39	4.9	0.094	Ma	K2	0.0	0.010	0.015	A
33	7 Ceti	0 9.6	−19 29	4.7	0.068	Ma	K2	1.1	0.019		
41		0 11.6	+60 59	5.8	0.002	G3	G2	− 0.9	0.004		
C 25	Groom. 34	0 12.7	+43 27	8.1	2.890	Ma		10.4	0.288	0.280	Ye, Y, R, *et al.*
53	ι Ceti	0 14.3	− 9 23	3.8	0.037	K3	K1	0.6	0.023		
56	41 Piscium	0 15.5	+ 7 38	5.6	0.015	K3	K0	0.7	0.010		
62	42 Piscium	0 17.2	+12 56	6.4	0.063	K2	K1	0.9	0.008		
63	9 Ceti	0 17.7	−12 46	6.4	0.396	G2	G2	5.7	0.072		
.....	A.G. Leiden 117	0 20.3	+33 34	8.3	0.019‡	K0	G8	1.7	0.005		
.....	A.G. Leiden 134	0 22.3	+33 29	8.0	0.075‡	K0	G7	3.3	0.012		
81	47 Piscium	0 22.8	+17 20	5.3	0.117	Mb	G6	0.1	0.009		
84	48 Piscium	0 23.0	+15 54	6.5	0.018	K5	K1	0.5	0.006		
86		0 24.5	+76 28	6.4	0.335	K0	G9	3.9	0.032		
89	28 Androm.	0 24.8	+29 12	5.3	0.066	F2	F3	2.5	0.028		

90.....	12 Ceti.....	$0^h24^m.9$	$-4°31'$	6.0	0".011	K4	K2	0.7	0".008		
96.....		0 26.2	+52 17	5.7	0.056	Ko	G9	0.3	0.008	0".008	W
106.....		0 27.5	+27 44	6.4	0.014	G6	G6	− 0.2	0.005	0.005	W
116.....	13 Ceti.....	0 30.1	− 4 9	5.7†	0.408	F7	F8	3.8	0.042	0.053	S
121.....		0 31.3	+43 56	5.4	0.035	K2	G8	1.4	0.016		
125.....		0 32.0	+34 51	5.6	0.019	Go	F7	− 0.3	0.007		
127.....	Bu. 335.....	0 32.2	−25 19	6.4†	1.390	G9	G5	5.5	0.066	0.104	M, F
128.....		0 32.4	+ 2 35	6.6	0.122	K3	Ko	1.1	0.008		
130.....	ϵ Androm.....	0 33.3	+28 46	4.5	0.336	G3	G3	0.2	0.014	0.063	A, Ye, S
131.....		0 33.6	+48 48	5.7	0.019	K5	G9	0.5	0.009		
C 80.....	Lal. 999.....	0 34.0	+ 2 35	7.4	0.819	G4	G1	5.5	0.042	0.033	Y, J
132.....	δ Androm.....	0 34.0	+30 19	3.5	0.162	K3	K3	0.8	0.029	0.020	A
133.....	54 Piscium.....	0 34.2	+20 43	6.1	0.595	K1	Ko	6.2	0.105	0.111	A, M, Y
135.....	α Cassiop.....	0 34.8	+55 59	2.5	0.060	G8	G8	− 1.0	0.020	0.023	M, F
C 86.....	Lal. 1045.....	0 35.3	+39 39	7.5	0.797	K4	K2	6.3	0.058	0.054	A, Y
C 87.....	Lal. 1065.....	0 35.5	−24 21	6.2	0.711	G2	G3	4.7	0.050		
137.....		0 35.6	− 4 54	6.1	0.023	G8	G6	1.5	0.012		
138.....	32 Androm.....	0 35.7	+38 55	5.4	0.007	G6	G5	1.1	0.013		
.....	Groom. 127.....	0 37.8	+70 17	6.9	0.035	G7	G5	1.4	0.008		
147.....	β Ceti.....	0 38.6	−18 32	2.2	0.230	G6	G6	0.3	0.042	−0.052	F
C 98.....	Lal. 1198.....	0 40.0	+ 1 15	8.1	0.591	K5	K6	6.7	0.052	0.056	M, Y
160.....		0 41.2	−23 4	5.6	0.189	G7	G6	2.5	0.024		
161.....	57 Piscium.....	0 41.3	+14 56	5.6	0.064	Mb	G8	0.4	0.009	0.014	W
164.....	ζ Androm.....	0 42.0	+23 43	4.3	0.129	G7	G4	0.8	0.020	0.031	A
165.....	60 Piscium.....	0 42.2	+ 6 12	6.2	0.016	G8	G5	1.4	0.011		
168.....	η Cassiop. Br.....	0 43.0	+57 17	3.7	1.242	F8	Go	4.3	0.132	0.186	A, M, S, *et al.*
168.....	η Cassiop. Ft.....	0 43.0	+57 17	7.4	1.242	K5	K2	8.3	0.151		
171.....		0 43.1	+ 4 46	5.8	1.366	K3	K1	6.5	0.138	0.170	Y, F
C105.....	Groom 145.....	0 43.3	+69 54	8.0	0.415	K3	K2	6.2	0.044	0.028	Y
173.....	δ Piscium.....	0 43.5	+ 7 2	4.6	0.093	K5	K1	0.9	0.018	0.017	A

TABLE VII—*Continued*

Boss	Name	α 1900	δ 1900	Harv. Vis. Mag.	μ	Spectrum		Spect. Abs. Mag.	Spect. π	Trig. π	Auth.
						Est.	Meas.				
174	64 Piscium	$0^h43^m.7$	+16°24′	5.2	0″.204	F4	F7	3.5	0″.046		
178¹	65¹ Piscium	0 44.5	+27 10	6.3	0.092	Fo	F2	0.7	0.008	0″.010	W
178²	65² Piscium	0 44.5	+27 10	6.3	0.092	Fo	F1	1.4	0.011		
181	19 Ceti	0 45.1	−11 11	5.2	0.325	F8	F7	3.9	0.055		
189		0 47.1	+60 35	4.9	0.188	F8	F7	3.6	0.055		
191	20 Ceti	0 47.9	− 1 41	4.9	0.017	K6	Ko	0.3	0.012		
193	26 Cassiop.	0 49.1	+58 26	5.0	0.053	K2	K1	0.5	0.013		
200	28 Cassiop.	0 50.7	+58 38	4.8	0.100	G5	G6	0.7	0.015	0.073	A
206	η Androm.	0 51.9	+22 53	5.0†	0.060	G6	G8	0.5	0.013	0.011	A
209	68 Piscium	0 52.4	+28 27	5.6	0.017	G7	G6	0.0:	0.008		
210		0 52.7	+13 9	6.4	0.022	G5	G4	0.1	0.005		
217		0 54.6	+ 5 57	6.3	0.023	Mb	G6	1.0	0.009	−0.001	W
218	2 Urs. Min.	0 55.0	+85 43	4.5	0.086	K3	K2	0.5	0.016		
C136	Lal. 1799	0 57.2	+ 4 31	8.4	0.438	K5	K4	7.1	0.055	0.038	M, Y
226	ϵ Piscium	0 57.8	+ 7 21	4.4	0.085	G6	G6	0.2	0.014	0.027	A, M
233	73 Piscium	0 59.7	+ 5 7	6.2	0.031	K4	Ko	0.8	0.008		
C142	A.G. Hels. 914	1 0.3	+63 24	8.7	1.55	K7	K4	8.4	0.087		
243	75 Piscium	1 1.3	+12 25	6.2	0.040	G7	G6	1.8	0.013		
244	μ Cassiop.	1 1.6	+54 26	5.3	3.760	G5	G3	5.6	0.115	0.127	A, Ye, F, *et al.*
C146	Lal. 1964	1 2.2	+22 26	8.6	0.525	K5	K4	7.5	0.060	0.097	Y
252	80 Piscium	1 3.2	+ 5 7	5.7	0.326	F1	F1	2.5	0.023		
C149	Lal. 1966	1 3.3	+61 1	7.8	0.638	F5	F5	3.5	0.014	0.022	Ye, Y
255	η Ceti	1 3.6	−10 43	3.6	0.246	K2	K1	1.2	0.033		
259	β Androm.	1 4.1	+35 5	2.4	0.216	Ma	G8	0.5	0.042	0.049	A, M, F
C150	Lal. 1985	1 4.1	+67 15	6.6	0.236	F7	F8	4.0	0.030	0.023	G

261.....	81 Piscium.....	1h 4m.5	+19° 7′	5.6	0″.004	F2	F5	0.4	0″.009		
267.....	33 Ceti.....	1 5.4	+ 1 55	6.2	0.004	K4	K0	0.7	0.008		
270.....	χ Piscium.....	1 6.1	+20 30	4.9	0.021	G5	G6	0.0	0.010	0″.013	A
271.....	τ Piscium.....	1 6.2	+29 34	4.7	0.081	K1	G9	0.5	0.014		
281.....	φ Piscium.....	1 8.3	+24 3	4.6	0.047	G7	G7	0.4	0.014		
287.....	38 Ceti.....	1 9.7	− 1 31	5.8	0.221	F4	F6	2.8	0.025		
C165.....	W.B. 1h161.....	1 13.5	− 1 23	8.1	0.489	K1	G8	6.1	0.040	−0.011	Y
C167.....	Lal. 2387.....	1 14.0	− 9 27	8.9	0.528	G1	G0	4.7	0.014	0.026	Y
C174.....	W.B. 1h262.....	1 15.8	+30 49	8.8	0.50	K2	K2	6.3	0.032		
304.....	ξ Androm.....	1 16.4	+45 0	5.0	0.41	K0	G9	1.0	0.016		
C177.....	Lal. 2450.....	1 16.9	+18 10	8.0	0.524	G1	G1	4.7	0.022	0.017	Y
305.....	43 Ceti.....	1 17.5	− 0 58	6.5	0.017	K0	G9	0.5	0.006		
310.....	ψ Cassiop.....	1 18.9	+67 36	5.0	0.086	K1	G9	0.8	0.014		
313.....	θ Ceti.....	1 19.0	− 8 42	3.8	0.228	K0	G9	0.3	0.020	0.101	F
C185.....	W.B. 1h356.....	1 19.5	+17 59	9.1	0.606	K2	K1	6.3	0.028		
318.....	ρ Piscium.....	1 20.9	+18 39	5.3	0.041	F0	F1	2.7	0.030		
321.....	ω Androm.....	1 21.7	+44 53	5.0	0.356	F1	F6	2.6	0.033	0.022	M, Ye, F, J
325.....	α Urs. Min. §.....	1 22.6	+88 46	2.1	0.044	F9	F8	− 3.0	0.010	0.041	F *et al.*
C196.....	Lal. 2682.....	1 23.6	+21 13	7.9	0.495	K3	K2	6.4	0.050	0.067	Y, D
327.....	38 Cassiop.....	1 23.8	+69 45	6.0	0.158	F4	F6	3.7	0.035	0.039	A
332.....	μ Piscium.....	1 24.9	+ 5 38	5.1	0.292	K5	K1	0.5	0.012		
335.....	η Piscium.....	1 26.1	+14 50	3.7	0.031	G5	G6	− 0.4	0.015	0.022	A, M
C204.....	Lal. 2751.....	1 27.3	+68 26	6.7	0.402	G3	G2	4.7	0.040	0.026	G
338.....	χ Cassiop.....	1 27.4	+58 43	4.9	0.038	G5	G7	−0.1	0.010	0.020	A
.....	Groom. 331.....	1 27.7	+71 56	7.8	0.037	F6	F9	1.5	0.006		
349.....	40 Cassiop.....	1 30.5	+72 32	5.5	0.008	G5	G5	−0.3	0.007		
350.....	υ Androm.....	1 30.9	+40 54	4.2	0.418	F8	F9	3.7	0.079	0.057	M
355.....		1 31.6	+57 28	5.7	0.004	K0	G6	−0.3	0.006		
357.....	υ Persei.....	1 31.9	+48 7	3.8	0.127	K4	K1	0.5	0.022	0.034	A
C226.....	Lal. 2975.....	1 32.7	+29 4	8.7	0.482	K1	G9	6.1	0.030		

TABLE VII—*Continued*

Boss	Name	α 1900	δ 1900	Harv. Vis. Mag.	μ	Spectrum Est.	Spectrum Meas.	Spect. Abs. Mag.	Spect. π	Trig. π	Auth.
C229	Lal. 3022	$1^h33^m.9$	+27°36′	7.9	0″.502	G8	G5	5.4	0″.032	0″.047	Y
C231	Lal. 2966	1 34.2	+66 25	7.6	0.753	G4	G1	5.9	0.046	0.036	Y
372		1 35.7	+42 7	5.1	0.817	G1	G0	4.8	0.087	0.098	A, M, Y, J
373		1 35.7	+25 14	6.3	0.135	F3p	F4	2.6	0.018	0.036	W
375		1 36.0	+29 32	6.0	0.013	G7	G7	0.6	0.008		
378	ν Piscium	1 36.2	+ 4 59	4.7	0.021	K4	K1	0.8	0.017	0.055	A
C238	A.Oe. 1867	1 36.8	+63 20	8.2	0.70	K5	K5	7.7	0.079		
381	Bu. 877 Br.	1 36.8	−11 49	6.1†	0.410	F2	F4	2.7	0.021		
382	107 Piscium	1 37.1	+19 47	5.3	0.734	K1	K1	5.8	0.126	0.129	Y
C240	Lal. 3153	1 37.4	−18 24	7.4	0.543	G0	G1	4.7	0.029		
387		1 37.7	− 4 12	5.3	0.028	K3	K1	0.5	0.011		
391	τ Ceti	1 39.4	−16 28	3.6	1.922	G7	G5	6.1	0.316	0.317	M, F, Sitt
393	o Piscium	1 40.1	+ 8 39	4.5	0.085	G6	G7	0.0	0.012	0.017	A
394		1 40.5	+63 22	5.7	0.634	K0	G9	5.6	0.096	0.089	Y, J
405		1 43.0	+32 11	5.8	0.354	F7	F7	3.8	0.040		
410	1 Arietis Br.	1 44.6	+21 47	6.2†	0.018	G9	K0	1.2	0.010		
414	54 Ceti	1 45.6	+10 33	5.9	0.074	F3		2.7	0.023		
420	55 Androm.	1 47.3	+40 14	5.6	0.009	K2	K0	0.5	0.010	0.006	W
421	α Trianguli	1 47.4	+29 6	3.6	0.233	F2	F4	1.2	0.033	0.050	A
426	ξ Piscium	1 48.4	+ 2 42	4.8	0.033	G7	G5	0.7	0.015		
430		1 50.0	+36 47	6.1	0.005	K3	G9p	1.0	0.009		
432	56 Androm.	1 50.2	+36 46	5.8	0.180	G9	G7	1.7	0.015		
434	7 Arietis	1 50.3	+23 5	6.0	0.011	K0	G8	0.9	0.010		
.....	B.D. +32°356	1 52.3	+32 28	8.8		F8	F7	2.6	0.006	−0.001	D
.....	A.G. Leiden 743	1 53.1	+33 51	7.6	0.033‡	G9	G6	1.9	0.008		

450.....	112 Piscium.....	1^h54^m9	+ 2°37′	5.8	0″.336	Go	F9	4.0	0″.044		
451.....	47 Cassiop.....	1 55.1	−21 19	5.7	0.014	Ma	G8	0.3	0.008		
453.....	υ Ceti.....	1 55.3	−21 34	4.2	0.130	K6	K3	0.7	0.020		
.....	Groom. 441.....	1 56.8	+54 13	7.7	0.026	F6	F6	3.0	0.012		
468.....	γ^1 Androm.....	1 57.8	+41 51	2.3	0.070	K2	G9	−0.1	0.033	0″.010	A, S, Y, F
472.....		1 58.2	+17 46	6.4	0.024	K4	K1	0.9	0.008		
477.....	α Arietis.....	2 1.5	+22 59	2.2	0.239	K2	Ko	0.7	0.050	0.044	A, F, J
C274.....	Lal. 3922.....	2 2.5	− 1 5	6.9	0.466	G1	Go	4.1	0.028	−0.042	Y
486.....		2 4.1	+73 33	6.2	0.071	G6	G5	−0.2	0.005		
493.....	16 Arietis.....	2 5.5	+25 28	6.2	0.011	K4	K2	0.9	0.008		
498.....	55 Cassiop.....	2 6.6	+66 3	6.2	0.003	F6	F7	3.2	0.025		
500.....	6 Persei.....	2 7.0	+50 36	5.4	0.386	G5	G5	0.7	0.012	0.006	A, Ye
C286.....	Lal. 3987.....	2 7.5	+67 13	7.8	0.603	K2	K2	6.1	0.046	0.071	S, Y
.....	Bu. 1144.....	2 7.6	+47 1	6.4	0.112‡	F1	F4	3.4	0.025	0.075	S
504.....	66^2 Ceti.....	2 7.7	− 2 52	5.7	0.374	F9	F8	3.3	0.033		
505.....	65 Ceti.....	2 7.7	+ 8 23	4.5	0.026	G4	G3	−1.4	0.006		
C288.....	A.Oe. 2526.....	2 9.2	+64 30	8.4	0.50	G2	G2	5.8	0.030		
C289.....	W.B. 2^h95.....	2 9.5	− 1 40	9.2	1.034	F8	F8	3.9	0.009	0.014	Y
C291.....	Lal. 4141.....	2 9.7	+23 49	6.9	0.494	G7	G4	4.7	0.036	0.036	M, Y
513.....	8 Persei.....	2 10.9	+57 26	6.1	0.073	K2	K1	0.7	0.008		
514.....	δ Trianguli.....	2 10.9	+33 46	5.1	1.182	Go	Go	4.8	0.087	0.101	A, M, Y, *et al.*
515.....	7 Persei.....	2 11.0	+57 3	6.2	0.007	G4	G3	−0.3	0.005		
.....	Groom. 489.....	2 11.4	+42 8	7.9	0.022	F1	F3	2.3	0.008		
518.....	67 Ceti.....	2 12.0	− 6 53	5.7	0.141	G8	G7	0.9	0.011		
523.....		2 12.8	+ 1 17	5.8	0.527	F7	F8	3.6	0.036	0.024	M
C298.....	A.Oe. 2618.....	2 14.0	+70 43	8.5	0.62	K2	K1	6.3	0.036		
532.....		2 14.5	−26 25	6.4	0.505	G7	G6	5.0	0.052		
C300.....	Lal. 4222.....	2 14.5	+68 18	7.4	0.13	Ko	G9	2.8	0.012		
539.....	69 Ceti.....	2 16.8	− 0 4	5.9	0.006	Ma	G7	0.2	0.007		
.....	A.G. Leiden 886.....	2 17.9	+33 24	7.6	0.056‡	K3	K1	0.9	0.005		

TABLE VII—*Continued*

Boss	Name	α 1900	δ 1900	Harv. Vis. Mag.	μ	Spectrum		Spect. Abs. Mag.	Spect. π	Trig. π	Auth.
						Est.	Meas.				
543	κ Fornacis	2h18m0	−24° 16′	5.4	0″.210	G2	G1	2.4	0″.025		
545	65 Androm.	2 19.0	+49 50	4.9	0.031	K5	K1	0.3	0.012	0″.005	A
556	25 Arietis	2 22.1	+ 9 45	6.5	0.355	F5	F6	3.8	0.029		
572		2 26.3	+ 1 49	5.4	0.013	K3	G9	1.0	0.013		
575	σ Ceti	2 27.3	−15 41	4.8	0.141	F1	F3	2.2	0.030		
577	36 H Cassiop.	2 28.5	+72 23	5.3	0.031	G4	G5	−0.6	0.007		
581		2 29.5	+36 52	5.9	0.010	K3	G9	0.9	0.010		
582	15 Trianguli	2 29.7	+34 15	5.6	0.061	Ma	G7	0.3	0.009	0.015	W
588		2 30.6	+ 6 25	5.9	2.320	K3	K4	6.5	0.132	0.131	A, M, Y, *et al.*
589	ν Ceti	2 30.6	+ 5 9	5.0	0.042	G3	G4	−0.7	0.008		
591	31 Arietis	2 31.2	+12 1	5.7	0.297	F4	F6	3.9	0.044		
592	30¹ Arietis	2 31.2	+24 13	7.4	0.152	F5	F6	3.1	0.014	0.029	W, S
593	30² Arietis	2 31.2	+24 13	6.6	0.140	F3	F4	2.9	0.018		
C340	Lal. 4855	2 32.6	+30 24	7.2	0.625	Go	F8	4.4	0.028	0.026	Y, F
605	ε Ceti	2 34.7	−12 18	5.0	0.280	F4	F4	2.7	0.035		
612	84 Ceti	2 36.1	− 1 7	5.7	0.250	F6	F7	3.5	0.036		
617	θ Persei	2 37.4	+48 48	4.2	0.351	F6	F6	3.9	0.087	0.083	A, Y
619	14 Persei §	2 37.6	+43 52	5.6	0.004	Gop	F7	−2.6	0.003		
622	γ Ceti Ft.	2 38.1	+ 2 49	6.2	0.210	F3	F6	4.1	0.038	0.049	A, M, Ye, Y
631	1 Eridani	2 40.4	−19 0	4.6	0.327	F7	F6	3.6	0.063		
634	39 Arietis	2 42.0	+28 50	4.6	0.196	K1	G9	0.0	0.012	0.027	A
637	SU Cassiop. §	2 43.0	+68 28	6.1	0.016	F4	F4	−1.4	0.003	0.010	W
639	η Persei	2 43.4	+55 29	3.9	0.030	K4	G5	0.4	0.020		
644	16 Persei	2 44.3	+37 54	4.3	0.213	A8	Fo:	1.5	0.028	0.022	A
C364	A.G. Bonn 2435	2 44.9	+45 34	9.2	0.63	G4	G3	5.7	0.020		

646	17 Persei	2^h45^m4	+34°39′	4.7	0″.077	K5	K1	0.7	0″.016	0″.010	A
650	2 Eridani	2 46.5	−21 25	4.8	0.053	G8	G5	1.2	0.019		
653	τ Persei	2 47.2	+52 21	4.1	0.008	G1	Go	−0.2	0.014		
654	20 Persei A	2 47.4	+37 56	5.8†	0.099	Fo	F3	2.5	0.022	0.013	Ye, S
660	45 Arietis	2 50.2	+17 56	5.9	0.018	Mc	G8	−0.3	0.006	0.011	W
661	ρ Arietis	2 50.8	+17 37	5.6	0.340	F5	F4	3.5	0.038		
665	η Eridani	2 51.5	− 9 18	4.0	0.229	Ko	G9	1.4	0.030		
667		2 52.4	+20 16	5.8	0.222	F4	F3	3.3	0.032		
672		2 53.0	+46 49	5.6	0.035	G3	G3	0.5	0.009	−0.007	W
C388	W.B. 2^h927	2 55.2	+ 5 36	8.2	0.667	K1	G9	5.7	0.032	0.096	Y
C392	Lal. 5490	2 56.0	+61 20	6.7	1.002	G4	G2	5.2	0.050	0.043	Y, J
691	α Ceti	2 57.1	+ 3 42	2.8	0.078	Ma	G9	−0.1	0.026	0.013	A, M
694	γ Persei	2 57.6	+53 7	3.1	0.010	F9	F9	−0.1	0.023	0.011	A, M
698	ρ Persei	2 58.8	+38 27	3.7	0.173	Mb	G7	−0.8	0.013	0.048	M, R
707		3 1.6	− 6 29	5.6	0.002	Ma	G9	0.1	0.008		
710	ι Persei	3 1.8	+49 14	4.2	1.269	G1	Go	4.4	0.110	0.104	Ye, S, Y, *et al.*
712	54 Arietis	3 2.7	+18 25	6.5	0.042	K6	K2	0.5	0.006	0.031	W
713	κ Persei	3 2.7	+44 29	4.0	0.240	Ko	G8	0.9	0.024	0.037	A
717	ω Persei	3 4.8	+39 14	4.8	0.022	K1	G9	0.5	0.013		
718	δ Arietis	3 5.9	+19 21	4.5	0.152	Ko	G8	0.7	0.017		
721	48 H Cephei	3 7.6	+77 22	5.5	0.083	A7		1.6	0.017		
722	94 Ceti	3 7.7	− 1 34	5.1	0.209	F9	F8	4.1	0.063		
723	α Fornacis Br.	3 7.8	−29 23	4.0	0.726	F6	F6	3.6	0.083		
C423	B.D. +71°190	3 8.3	+71 55	9.0	0.43	G7	G8	5.3	0.018	0.015	G
C427	W.B. 3^h113	3 9.4	+ 8 37	7.7	0.578	K1	K1	6.1	0.048	0.079	Y
746		3 12.5	+33 51	4.9	0.013	K2	G8	0.2	0.012	0.012	A
752	κ Ceti	3 14.1	+ 3 0	5.0	0.282	G5	G4	4.9	0.096		
755		3 14.3	+28 41	4.7	0.027	K4	Ko	0.3	0.013		
759	16 Eridani	3 15.1	−22 7	4.0	0.065	Mb	G8	0.0	0.016		
765		3 16.0	+64 14	5.6	0.019	K2	G5	1.3	0.013		

TABLE VII—*Continued*

Boss	Name	α 1900	δ 1900	Harv. Vis. Mag.	μ	Spectrum		Spect. Abs. Mag.	Spect. π	Trig. π	Auth.
						Est.	Meas.				
768	62 Arietis	3^h16^m2	+27° 15′	5.6	0″.020	G6	G7	0.2	0″.008		
770	63 Arietis	3 17.0	+20 23	5.2	0.050	K4	K2	0.4	0.011		
772	α Persei §	3 17.2	+49 30	1.9	0.039	F5	F8	−1.3	0.023	0″.017	Yc, M, F
778	o Tauri	3 19.4	+ 8 41	3.8	0.103	G7	G4	0.1	0.018	0.006	A
C453	Lal. 6320	3 20.1	− 5 42	8.1	0.816	K5	K5	7.2	0.066	0.062	S, Y, J
795	σ Persei	3 23.5	+47 39	4.6	0.023	K4	Ko	0.4	0.014	0.013	A
804	5 Tauri	3 25.4	+12 36	4.3	0.018	G6	G5	0.1	0.014		
814	ϵ Eridani	3 28.2	− 9 48	3.8	0.972	K1	K1	6.0	0.275	0.317	M, Y, F
	A.G. Berlin 960	3 29.6	+18 34	7.9	0.012‡	Mb	G8	0.1	0.003		
823	Bu. 1787 Br	3 31.7	+ 0 16	6.2†	0.151	G8p	G9	5.4	0.069	0.012	M
825	10 Tauri	3 31.8	+ 0 5	4.4	0.536	F9	F9	3.6	0.069	0.058	A, M, Y, J
826		3 33.5	+62 54	5.3	0.022	Ma	G7	−0.5	0.007		
831	21 Eridani	3 34.1	− 5 57	6.0	0.204	Ko	G9	3.6	0.033		
832		3 34.5	+59 39	6.0	0.002	K2	G7	2.0	0.016		
C489	W.B. 3^h617	3 35.3	− 3 32	6.7	0.745	F6	F7	3.9	0.028	0.010	M, Y
C499	A.G. Chris. 631	3 38.2	+68 21	9.2	0.30	K8	K3	9.0	0.091	0.074	G
847	ν Persei	3 38.4	+42 16	3.9	0.009	F5	F5	0.6	0.022	0.021	A, M
848	δ Eridani	3 38.5	−10 6	3.7	0.749	G9	G9	3.4	0.087	0.147	M, Y, F
862	Bu. 1854 Br	3 40.2	+41 9	8.6†	1.372	Ko	G6	6.3	0.035	0.030	M, Ye, D, *et al.*
862	Bu. 1854 Ft	3 40.2	+41 9	9.2	1.372	K2	Ko	6.7	0.032		
864		3 40.4	+65 13	4.7	0.004	Ma	G5	−0.6	0.009		
	B.D. +23°535	3 41.4	+23 25	8.0		F6	F6	3.6	0.013		
	B.D. +23°542	3 41.7	+23 18	8.3		K1	G9	2.4	0.007	0.065	Y
873	27 Eridani	3 42.5	−23 33	4.3	0.548	F3	F4	2.7	0.048	0.073	M
C513	W.B. 3^h811	3 44.4	+ 1 4	8.6	0.67	K1	Ko	5.7	0.026		

C518	B.D. +22°583	3h46m2	+22°23′	7.8	0″.388	G5	G4	5.2	0″.030	0″.039	Ye
C521	Lal. 7036	3 46.4	+60 53	7.8	0.479	K0	G8	6.1	0.046	0.060	J
889		3 46.4	+48 21	5.9	0.058	K0	G8	0.8	0.009	0.020	W
892		3 47.4	+17 2	6.0	0.147	F1	F0	2.4	0.019		
895		3 48.4	+75 53	8.3	0.646	K6	K5	8.4	0.105	0.060	Ye, Y, K
897	Bu. 1927	3 48.6	+60 49	5.3†	0.016	K4	K0	0.3	0.010		
901	32 Eridani Br	3 49.3	− 3 15	5.0	0.034	G4	G4	0.2	0.011	0.005	M
	A.G. Albany 1158	3 53.2	+ 1 10	7.9	0.008‡	K1	G9	0.8	0.004		
915	γ Eridani	3 53.4	−13 48	3.2	0.130	K5	K0	0.5	0.029	0.019	M
919		3 55.0	+17 55	5.8	0.141	A8	A9	2.2	0.019		
927		3 56.5	+35 2	8.6	2.200	K0	G8	6.1	0.032	0.040	Ye, S, Y, *et al.*
C542	Bu. 2007	3 57.4	+39 14	7.4†	0.201	G4	G3	4.7	0.029		
933	36 Tauri	3 58.4	+23 50	5.7	0.022	F4p	F7	3.5	0.036	0.014	W
936	37 Tauri	3 58.8	+21 49	4.5	0.113	K0	G9	0.8	0.018	−0.017	A
937		3 58.9	+ 2 33	5.4	0.190	F7	F8	3.2	0.036		
949	49 Persei	4 1.6	+37 28	6.2	0.214	K1	K0	2.4	0.017		
950	50 Persei	4 1.9	+37 47	5.6	0.260	F7	F8	3.9	0.046	0.048	A
C553	Fed. 635	4 2.1	+76 2	8.2	0.25	K0	G9	6.2	0.040	0.025	G
951		4 2.3	+17 4	6.1	0.024	K5	K4	0.4	0.007		
952	43 Tauri	4 3.3	+19 21	5.7	0.114	K1	K0	1.4	0.014	0.024	M
955	44 Tauri	4 4.7	+26 13	5.6	0.046	F1	F2	2.2	0.021		
960	37 Eridani	4 5.5	− 7 11	5.6	0.010	G8	G5	1.5	0.015		
961	45 Tauri	4 6.0	+ 5 16	5.7	0.143	F4	F4	3.1	0.030		
963	o Eridani	4 7.0	− 7 6	4.1	0.081	A8	A9	0.3	0.017		
972	47 Tauri A	4 8.5	+ 9 1	5.1†	0.036	G4	G4	0.2	0.010		
C560	A.G. Berlin 1366	4 8.6	+22 6	9.1	0.54	A8	F2	2.8	0.006		
977		4 9.6	+80 35	5.6	0.020	G8	G7	0.9	0.012		
980	48 Tauri	4 10.1	+15 9	6.4	0.124	F1	F1	1.9	0.013		
984	40 Eridani	4 10.7	− 7 49	4.5	4.085	K1	K0	6.2	0.219	0.196	M, J, F, C
C570		4 11.9	+16 42	8.3	0.110	G7	G6	5.5	0.028		

TABLE VII—*Continued*

Boss	Name	α 1900	δ 1900	Harv. Vis. Mag.	μ	Spectrum		Spect. Abs. Mag.	Spect. π	Trig. π	Auth.
						Est.	Meas.				
1000	γ Tauri	4^h14^m1	+15° 23′	3.9	0″.120	G7	G8	0.7	0″.023		
	55 Tauri	4 14.2	+16 17	7.1†	0.107	F7	F7	3.9	0.023		
1002	φ Tauri	4 14.2	+27 7	5.1	0.086	K1	G9	1.4	0.018		
1014	Bu. 2149	4 16.5	+20 35	6.3†	0.011	Ma	G6	0.9	0.008	0″.001	W
	Bu. 2154	4 17.1	+14 49	7.2†	0.096‡	F9	F9	4.1	0.024		
1017	δ Tauri	4 17.2	+17 18	3.9	0.115	G9	G7	0.4	0.020		
	B.D. +16°591	4 18.6	+16 50	7.8	0.102	F5	F5	3.8	0.016		
C 582	Lal. 8256	4 18.7	+16 39	8.0	0.135	Go	F9	4.0	0.016		
1025		4 19.1	+18 49	6.0	0.123	A9	A8	2.0	0.016		
C 585	Lal. 8248	4 20.1	+46 38	6.7	0.317	G4	G3	3.9	0.028	0.002	Jo
C 586	Lal. 8311	4 20.4	+15 18	7.4	0.115	F8	F8	3.9	0.020		
1044	ε Tauri	4 22.8	+18 58	3.6	0.120	G9	G8	1.0	0.030	0.028	A
1045	θ^1 Tauri	4 22.9	+15 44	4.0	0.108	G9	G8	1.4	0.030		
1055	81 Tauri	4 24.9	+15 28	5.5	0.110	F2	F1	1.6	0.017		
1058	85 Tauri	4 26.1	+15 38	6.0	0.109	Fo	Fo	2.5	0.020		
C 593	Lal. 8610	4 29.2	+16 47	7.4	0.11	K3	K2	1.0	0.005	−0.036	K
1071	47 Eridani	4 29.4	− 8 26	5.4	0.035	Ma	G7	0.7	0.011		
	A.G. Berlin 1228	4 29.6	+19 46	7.2	0.033‡	F8	F7	3.2	0.016		
1074	58 Persei §	4 29.8	+41 4	4.5	0.025	G4p	F8	−4.2:	0.002	0.103	Ye, D
C 594	A.Oe. 4961	4 29.8	+52 42	8.5	0.53	K6	K3	8.5	0.100		
1077	α Tauri	4.30.2	+16 18	1.1	0.203	K4	K2	1.0	0.096	0.055	M, Ye, Y, *et al.*
	SZ Tauri §	4 31.4	+18 20	7.1	0.016‖	F8p	F6	−2.1	0.001		
1086	89 Tauri	4 32.4	+15 50	5.8	0.094	A8	A7	+2.1	0.018		
	B.D. +66°343	4 32.8	+66 32	8.9	0.375‡	G4	G6	5.0	0.017	0.022	G
1091	53 Eridani	4 33.6	−14 30	4.0	0.179	K1	G8	1.9	0.038		

C 602	Groom. 864	4^h34^m5	+41°56′	7.3	0″.690	G2	G1	5.6	0″.046	0″.027	A, Y, Jo, F
1098		4 34.7	−14 33	5.6	0.186	Ko	G9	3.1	0.032		
1100		4 35.4	+75 46	6.0	0.138	A8		2.0	0.016		
1105	54 Eridani	4 36.1	−19 52	4.5	0.094	Ma	G9	0.1	0.013		
1120		4 40.5	+18 33	6.1	0.091	K3	K3	0.5	0.008		
1128		4 42.7	+63 20	5.8	0.111	Mb	G9	0.5	0.009	0.002	M
1131		4 42.8	+18 33	6.8	0.440	Go	Go	5.0	0.044		
1136	96 Tauri	4 44.0	+15 44	6.3	0.017	K2	G8	0.9	0.008		
C 619	Groom. 884	4 44.4	+45 41	7.1	0.676	F9	F9	5.7	0.052	0.086	S, Y, R, J
1140	π^3 Orionis	4 44.4	+ 6 47	3.3	0.471	F5	F6	3.7	0.120	0.156	M
.....	Bu. 2381	4 45.7	+10 54	7.7†		Go	F8	4.6	0.024	0.024	A, S, F
.....	Bu. 2383	4 46.2	+13 29	6.8†		F9	F6	4.0	0.028	0.007	F
1149	4 Orionis	4 46.9	+14 5	5.2	0.059	Ma	G7	0.7	0.012		
1154	5 Orionis	4 48.2	+ 2 21	5.7	0.034	Ma	Ko	0.5	0.009	0.009	W
1164		4 49.6	+74 7	6.2	0.050	K3	K1	0.7	0.008		
.....	SU Aurigae §	4 49.6	+30 24	8.7		F7p	F8	−1.1	0.001		
1167	ι Aurigae	4 50.5	+33 0	2.9	0.028	K3	Ko	0.0	0.026	−0.011	F
1168		4 50.6	−16 54	5.8	0.001	G8	G6	1.2:	0.012		
C 634	A.G. Leiden 1812	4 51.3	+34 7	8.0	0.60	G9	G6	6.4	0.048		
1175	99 Tauri	4 51.7	+23 48	6.0	0.025	Ko	G8	1.5	0.012		
1176	8 Camelop.	4 51.8	+53 0	6.4	0.012	K3	Ko	0.7	0.008		
1179		4 52.7	+66 41	6.3	0.355	F7	F6	3.9	0.033	0.000	Jo
1181	10 Orionis	4 53.4	+ 1 34	4.7	0.006	K2	G9	0.2	0.012		
1182	5 Aurigae	4 53.4	+39 15	6.0	0.013	Fo	F3	2.5	0.020	0.002	W
1185	β Camelop. §	4 54.5	+60 18	4.2	0.013	F7p	F8	−2.9	0.004		
.....	RX Aurigae §	4 54.5	+39 49	7.6		F9p	F7	−1.7	0.001		
1187	ϵ Aurigae §	4 54.8	+43 41	3.4	0.014	F5p	F9	−2.0	0.008	0.060	J
1190	ζ Aurigae	4 55.5	+40 56	3.9	0.032	G8p	G1	1.6	0.035	−0.007	A, Ab
C 648	W.B. 4^h1189	4 55.9	− 5 52	6.5	1.247	K5	K6	6.9	0.120	0.119	M, S, W, *et al.*
1196	12 Camelop.	4 57.5	+58 53	6.4	0.039	G5	G2	0.2	0.006		

TABLE VII—*Continued*

Boss	Name	α 1900	δ 1900	Harv. Vis. Mag.	μ	Spectrum		Spect. Abs. Mag.	Spect. π	Trig. π	Auth.
						Est.	Meas.				
1202	9 Aurigae	4^h58^m8	+51° 28′	5.0	0″.178	F4	F1	2.3	0″.029		
C 654	Lal. 9428	5 0.0	+64 48	6.4	0.190	F2	F4	2.8	0.019	0″.022	G
1211	ϵ Leporis	5 1.2	−22 30	3.3	0.072	K4	K1	0.7	0.030	0.022	M
1212	104 Tauri	5 1.5	+18 31	5.0	0.540	G0	G1	4.4	0.076	0.045	A, Y
1217	13 Orionis	5 2.2	+ 9 21	6.3	0.381	G0	G0	5.1	0.058		
1219	14 Orionis	5 2.5	+ 8 22	5.9†	0.066	F2	F2	2.0	0.017	0.022	S
1221	107 Tauri	5 2.9	+19 44	6.6	0.018	G5	G3	0.6	0.006		
1222		5 3.3	+46 50	5.6	0.170	F3	F3	2.3	0.022	0.032	Jo
1234		5 5.9	+15 55	5.4	0.004	K6	K1	0.5	0.010		
1235	19 H Camelop	5 6.1	+79 7	5.2	0.174	F5	F6	3.0	0.036		
C 674	W.B. 5^h87	5 7.1	− 9 13	8.0	0.57	K0	G9	5.8	0.036	0.049	D
1246	α Aurigae	5 9.3	+45 54	0.7†	0.437	G1	G1	0.1	0.076	0.067	A, Y, Jo, *et al.*
1247		5 9.4	+ 5 2	5.8	0.017	K3	K0	0.7	0.010		
1259	λ Aurigae	5 12.1	+40 1	4.8	0.843	G1	G0	4.3	0.079	0.081	A, M, S, *et al.*
1267		5 13.3	+20 2	6.2	0.048	K0	G7	1.4	0.011	0.021	W
C 683	Lal. 9960	5 14.1	− 3 11	8.6	0.722	K5	K4	7.1	0.050	0.074	Y
1309	17 Camelop	5 20.7	+62 59	5.8	0.005	Ma	G8	0.7	0.010		
C 698	Bu. 2745 Br	5 23.3	+54 35	7.6	0.409	G1	G1	5.5	0.038	0.024	Ye
C 699	Lal. 10299	5 23.5	− 3 34	8.6	0.841	K6	K6	8.4	0.091	0.058	Y, D
1323	β Leporis	5 24.0	−20 50	3.0	0.094	G2	G2	−0.7	0.018	0.004	M
1334		5 26.3	+74 59	6.4	0.019	K5	K1	0.4	0.006	0.011	A, Jo
C 705	W.B. 5^h592	5 26.4	− 3 42	8.8	2.222	Ma		9.7	0.151	0.165	M, S, Ye, *et al.*
C 706	B.D. −0°981	5 26.6	+ 0 2	8.4	0.507	G6	G6	5.3	0.024		
1347	α Leporis §	5 28.3	−17 54	2.7	0.003	F4p	F4	−0.7	0.021	0.014	M
1348		5 28.4	+54 22	6.0	0.007	K6	K0	0.4	0.008		

1360		$5^h 29^m.9$	+85° 9′	6.4	0″.020	K4	K1	0.7	0″.008	
C 709	Groom. 990	5 30.4	+51 23	7.9	0.563	K2	K0	6.3	0.048	0″.036 A, M, Y, Jo
1373	40 Orionis	5 31.4	+ 9 14	4.4	0.321	G7	G6	1.6	0.028	0.029 A, S, Ye
	A.G. Bonn 4626	5 32.3	+42 37	7.4	0.038‡	K4	K1	0.6	0.004	
1380		5 32.4	+65 39	5.8	0.024	K4	K1	0.7	0.010	
1385		5 33.2	+53 26	6.4	0.510	K0	G9	5.7	0.072	0.100 A, Y, Jo, Ab
C 714	Groom. 986	5 33.3	+74 34	7.3	0.240	G4	G3	3.7	0.019	0.021 G
1393	24 Camelop.	5 34.5	+56 32	6.2	0.037	K0	G8	2.3	0.017	
1394	23 Camelop.	5 34.9	+61 26	6.4	0.002	G5	G5	0.2	0.006	
	A.G. Bonn 4686	5 37.0	+43 31	7.7	0.033*	K0	G6	2.8	0.010	
	A.G. Bonn 4698	5 38.4	+42 49	8.0		K2	K1	0.0	0.003	
C 725	Lal. 10797	5 39.2	+37 15	7.3	0.706	K1	K0	5.7	0.048	0.086 A, D, Y, J
1419	γ Leporis Ft.	5 40.3	−22 27	6.4	0.461	K5	K3	6.9	0.126	0.149 M
1420	γ Leporis Br.	5 40.3	−22 29	3.8	0.468	F6	F5	3.8	0.100	
1424	130 Tauri	5 41.6	+17 41	5.5	0.010	F4	F2	1.8	0.018	
1429	τ Aurigae	5 42.2	+39 9	4.6	0.035	G5	G7	0.3	0.014	0.014 A
1434	132 Tauri	5 42.9	+24 32	5.0	0.036	K0	G7	2.3	0.029	
1439	υ Aurigae	5 44.2	+37 17	5.0	0.052	Ma	K0	0.0	0.010	
1441		5 44.5	+ 9 50	5.9	0.014	G6	G6	0.8	0.009	
1442	ν Aurigae	5 44.6	+39 7	4.2	0.008	K0	K0	0.2	0.016	0.022 A
1444		5 44.7	+27 56	5.6	0.009	G7	G7	0.1	0.008	
1456	δ Leporis	5 47.0	−20 53	3.9	0.696	G7	G6	1.5	0.033	0.024 M
1461	χ Orionis	5 48.5	+20 15	4.6	0.208	G1	G1	4.4	0.091	0.105 A, M
1468	α Orionis	5 49.8	+ 7 23	0.9	0.029	Ma	G3	−3.8	0.012	0.021 A, Y
C 739	Lal. 11196	5 50.3	+13 55	6.5	0.629	G5	G1	5.7	0.069	0.078 A, Y
1472	δ Aurigae	5 51.3	+54 17	3.9	0.153	G7	G8	0.7	0.023	0.029 A, M, Ye, *et al.*
1476	η Leporis	5 51.9	−14 11	3.8	0.138	F3	F4	2.6	0.058	0.036 M
1479	π Aurigae	5 52.5	+45 56	4.6	0.011	Mb	G6	−0.8	0.008	
1483		5 53.0	+44 35	6.4	0.051	K2	K1	1.1	0.009	
1494		5 55.1	− 3 5	4.7	0.084	K1	G8	2.1	0.030	

TABLE VII—*Continued*

Boss	Name	α 1900	δ 1900	Harv. Vis. Mag.	μ	Spectrum		Spect. Abs. Mag.	Spect. π	Trig. π	Auth
						Est.	Meas.				
C 756	A.G. Berlin 1866	5^h57^m3	+19°23′	9.0	0″93	F9	F9	4.9	0″015		
1508	1 Gemin	5 58.0	+23 16	4.3	0.108	G4	G3	2.1	0.036	0″025	A
1511		5 59.2	−26 17	5.2	0.104	K2	G8	1.4	0.017		
C 760	Lal. 11471	5 59.5	+35 24	6.1	0.332	G1	G0	4.8	0.055	0.048	A
1513	63 Orionis	5 59.6	+ 5 26	5.8	0.007	G6	G5	0.4	0.008		
1514	66 Orionis	5 59.7	+ 4 10	5.7	0.012	G4	G1	−1.1	0.004		
C 761	B.D. +26°1067	5 59.7	+26 34	8.9	0.42	K4	K2	6.6	0.035	0.021	Ye
	Groom. 1059	6 0.6	+76 31	8.0†	0.004	F5	F7	2.5	0.008		
1549	6 Gemin	6 6.3	+22 56	6.3	0.027	Ma	G4	0.8	0.008	0.003	W
1560	1 Lyncis	6 8.7	+61 33	5.3	0.005	Mb	G5	0.6	0.011		
1561	η Gemin	6 8.8	+22 32	3.7	0.065	Ma	G6	−0.5	0.014	0.016	A, M, R
1504	71 Orionis	6 9.0	+19 11	5.2	0.224	F6	F5	2.9	0.035	0.039	A
1565	κ Aurigae	6 9.0	+29 32	4.4	0.274	G8	G7	0.5	0.017	0.026	A, Jo
C 780	W.B. 6^h128	6 9.6	+44 45	8.6	0.41	G9	G8	6.4	0.036	0.102	Ram
1573	8 Gemin	6 10.2	+24 0	6.1	0.029	G5	G5	0.7	0.008		
1576	43 Aurigae	6 10.8	+46 24	6.5	0.133	K1	K0	0.7	0.007	0.036	Jo
1577	74 Orionis	6 10.8	+12 18	5.1	0.212	F5	F4	3.4	0.046		
1582		6 12.0	+ 5 8	5.8	0.282	G0	F9	3.8	0.040	0.051	A
1596		6 14.4	+14 42	6.0	0.019	K6	K1	0.6	0.008		
1599		6 15.0	− 2 54	5.2	0.009	Ma	K0	0.0	0.009	−0.004	M
1604	μ Gemin	6 16.9	+22 34	3.2	0.128	Ma	G6	−0.8	0.016	0.026	A, M
1606	46 Aurigae §	6 17.2	+49 20	5.1	0.014	K2p	G5	−3.6	0.002		
1608	5 Lyncis	6 18.1	+58 28	5.5	0.011	K6	K2	0.6	0.011		
	T Monocer. §	6 19.8	+ 7 8	6.2	0.029‖	G1p	G0	−2.0	0.003		
1622	α Argus*	6 21.7	−52 38	−0.9	0.018			−3:	0.038	0.007	C

1627.....	6 Lyncis.....	6^h22^m1	+58° 14′	6.0	0.″330	G8	G7	2.9	0.″024	0.″004	A, Ab, Jo
1629.....	RT Aurigae §	6 22.1	+30 33	5.3	0.024	F8p	F5	−1.9	0.003	0.031	W, S
1632.....	47 Aurigae.....	6 22.6	+46 45	6.0	0.007	K5	K1	0.5	0.008	0.017	M
1643.....		6 24.9	+78 5	5.9	0.019	K5	K1	0.7	0.009	0.017	W
1646.....	WW Aurigae	6 25.9	+32 32	6.6†	0.035	A7p		1.9	0.012		
1653.....	12 Monocer.....	6 27.0	+ 4 56	6.0	0.027	G8	G7	0.9	0.009		
1665.....	8 Lyncis.....	6 28.6	+61 34	6.0	0.341	G8	G6	2.9	0.024	0.035	A, Jo
1673.....	23 H Camelop.....	6 29.2	+79 40	5.6	0.620	F7	F8	4.2	0.052	0.037	Y
.....	W Gemin. §.....	6 29.2	+15 24	7.1	0.009‖	Gop	F6	−2.6	0.001		
.....	Bu. 3474.....	6 30.2	+27 22	7.0†	0.061*	Go	Go	4.3	0.029	0.040	A, S
1687.....	51 Aurigae.....	6 31.7	+39 29	5.7	0.119	K3	K1	1.1	0.012		
.....	W.B. 6^h886.....	6 32.0	+12 14	8.3		F1	A9	1.8	0.005	−0.021	Ye
1704.....	25 Gemin.....	6 35.0	+28 17	6.5	0.017	G5	Go	−1.2	0.003		
1707.....	55 Aurigae.....	6 35.8	+44 37	5.2	0.055	K5	K2	0.8	0.013		
C 824.....	Lal. 12831.....	6 37.3	+40 44	6.9	0.171	Mb	G7	0.4	0.005	−0.004	Jo
1717.....	ϵ Gemin.....	6 37.8	+25 14	3.2	0.020	G8	G2	−1.4	0.012	0.009	A, M
1721.....	30 Gemin.....	6 38.3	+13 20	4.6	0.076	K2	Ko	1.0	0.019		
1724.....	56 Aurigae.....	6 39.5	+43 41	5.3	0.158	F9	F9	4.3	0.063	0.077	A, Jo
1725.....	ξ Gemin.....	6 39.7	+13 0	3.4	0.231	F3	F6	2.0	0.052	0.051	A, M
1732.....	α Can. Maj.....	6 40.7	−16 35	−1.58	1.316	A3		1.3:	0.376	0.376	F, C
1740.....	18 Monocer.....	6 42.6	+ 2 31	4.7	0.026	Ko	G9	0.2	0.013	0.024	A
1756.....	35 Gemin.....	6 44.8	+13 32	5.9	0.013	K3	Ko	0.8	0.010		
1758.....	24 H Camelop.....	6 45.5	+77 6	4.8	0.085	K5	K5	0.3	0.013		
C 834.....	Lal. 13284.....	6 47.4	− 5 3	6.8	0.582	K5	K4	7.1	0.115	0.121	Y
1776.....	Bu. 3678.....	6 48.6	+58 33	4.9	0.134	G4	G4	0.1	0.011	0.029	S
1778.....	38 Gemin.....	6 49.0	+13 18	4.7	0.112	A8	A8	2.4	0.035	0.049	A
1783.....	θ Can. Maj.....	6 49.5	−11 55	4.2	0.138	K4	K1	0.8	0.021	0.017	Ye
C 837.....	A.G. Bonn 5621.....	6 49.5	+40 13	8.3	0.43	K5	K4	7.3	0.063		
C 841.....	W.B. 6^h1500.....	6 51.4	+ 1 18	7.7	0.570	G6	G3	5.6	0.038	0.006	Y
.....	Groom. 1239.....	6 51.9	+69 21	7.5	0.005	Ma	G8	0.7	0.004		

TABLE VII—*Continued*

Boss	Name	α 1900	δ 1900	Harv. Vis. Mag.	μ	Spectrum Est.	Spectrum Meas.	Spect. Abs. Mag.	Spect. π	Trig. π	Auth.
1801	51 H Cephei	6^h53^m7	+87°12′	5.3	0″.051	Ma	G9	0.4	0″.011		
C 847	Lal. 13427	6 54.0	+48 32	8.2	0.697	K4	K2	6.6	0.048	0″.032	M, Ye, Y
1809		6 57.2	+29 30	6.0	0.838	G2	G1	5.1	0.066	0.061	A, Y, F
1815	ζ Gemin, §	6 58.2	+20 43	4.0	0.009	Gop	F9	−3.4	0.003	0.015	A, S, Ab
1818		6 59.2	− 5 11	5.9	0.006	K2	G6	0.5	0.008		
1822		6 59.6	+34 38	5.6	0.087	G4	G4	0.1	0.008	0.036	W
C 859	Lal. 13792	7 3.5	+25 54	7.0	0.225	G5	G4	4.8	0.036	0.031	A
C 861	Lal. 13849	7 4.2	+21 25	6.5	0.510	G9	G7	4.6	0.042	0.042	A, S, Y
1839	δ Can. Maj. §	7 4.3	−26 14	2.0	0.005	G2p	G0	−2.9	0.010	−0.059	F
1840	τ Gemin	7 4.8	+30 25	4.5	0.053	K3	K2	0.5	0.016	0.010	A
1841	63 Aurigae	7 4.8	+39 29	5.1	0.048	K3	K1	1.0	0.015		
1846		7 5.6	+51 36	5.7	0.019	Mb	G9	0.1	0.008	0.002	M, W
1854	18 Lyncis	7 7.2	+59 49	5.3	0.272	K2	K0	1.3	0.016	0.036	A
1856	51 Gemin	7 7.6	+16 20	5.3	0.051	Mb	G7	0.1	0.009		
1860		7 8.4	+47 25	5.6	0.184	F9	F9	5.0	0.076	0.069	Jo
1861	52 Gemin	7 8.6	+25 4	6.0	0.105	K7	K4	0.4	0.008		
1868	53 Gemin	7 9.7	+28 4	5.9	0.020	Ma	K2	−0.2	0.006	0.008	W
1873	24 Monocer	7 10.2	+ 0 1	6.5	0.019	G5	G5	−0.2	0.005		
C 873	Lal. 14146	7 11.3	−12 53	7.7	0.513	F9	F9	3.9	0.017	0.051	M, Y
1898	δ Gemin	7 14.2	+22 10	3.5	0.025	A7		1.1	0.033	0.062	A, M
1909	R Can. Maj	7 14.9	−16 12	6.0†	0.212	A9	F0	1.7	0.014		
1912	65 Aurigae	7 15.4	+36 57	5.2	0.089	K1	G9	1.2	0.016		
1919	66 Aurigae	7 17.2	+40 52	5.3	0.024	K0	G8	−0.3	0.008	−0.061	Ab
1926	59 Gemin	7 18.3	+27 50	5.7	0.020	F0	F2	1.3	0.013		
1931	ι Gemin	7 19.5	+28 0	3.9	0.145	G8	G8	0.5	0.021	0.026	A, M

1937.....		7^h20^m5	+68°40′	5.8	0″044	Ko	G7	1.8	0″016	
1940.....		7 20.9	+21 44	6.4	0.309	F5	F6	3.9	0.032	0″040 A
1945.....	63 Gemin.....	7 21.8	+21 39	5.3	0.133	F3	F5	2.8	0.032	
1952.....	ρ Gemin.....	7 22.7	+31 59	4.2	0.236	A9	F1	1.5	0.029	0.055 M, Jo
1962.....	6 Can. Min.....	7 24.2	+12 13	4.8	0.019	K3	Ko	0.4	0.013	0.024 A
1963.....		7 24.3	− 1 42	5.8	0.011	K3	G8	0.8	0.010	
1971.....		7 26.0	+17 18	5.6	0.089	K1	Ko	0.7	0.011	0.000 W
.....	Groom. 1324.....	7 26.3	+66 41	7.5	0.017	Mb	G9	0.6	0.004	
.....	Comp. α Gemin.*.....	7 28.2	+32 8	9.4†	0.203	Mdp		9.2	0.091	0.079 A, M, Ye, *et al.*
1987.....	υ Gemin.....	7 29.8	+27 7	4.2	0.119	K6	K2	0.5	0.018	0.015 A
1999.....	25 Monocer.....	7 32.3	− 3 53	5.2	0.072	F4	F5	1.3	0.017	
2000.....	23 Lyncis.....	7 32.6	+57 19	6.2	0.018	K4	Ko	0.4	0.007	
2001.....	o Gemin.....	7 32.6	+34 49	4.9	0.125	Fo	F1	0.8	0.015	0.023 A, Ab
2005.....	74 Gemin.....	7 33.7	+17 54	5.2	0.004	K8	Ko	−0.3	0.008	
2006.....		7 33.8	+48 22	5.8	0.144	G7	G8	0.2	0.008	0.011 A
2008.....	α Can. Min.....	7 34.1	+ 5 29	0.5	1.242	F3	F5	3.2	0.347	0.309 M, S, Ye, *et al.*
2020.....		7 36.4	+14 27	5.8	0.015	Ma	G6	−0.4	0.006	0.006 W
2021.....	γ Monocer.....	7 36.5	− 9 19	4.1	0.079	Ko	G9	0.4	0.018	0.005 M
2023.....	σ Gemin.....	7 37.1	+29 8	4.3	0.247	K1p	G7	2.6	0.046	0.027 A, Ye, Jo
2024.....	51 Camelop.....	7 37.1	+65 42	6.0	0.046	K2	K1	0.8	0.009	
C 922.....	W.B. 7^h1029.....	7 38.1	+39 49	6.8	0.68	F6	F8	3.8	0.025	0.025 Ye
2029.....	κ Gemin.....	7 38.4	+24 38	3.7	0.066	G7	G6	0.9	0.028	0.024 A, M
2031.....	β Gemin.....	7 39.2	+28 16	1.2	0.625	G9	G8	1.7	0.126	0.064 Y
2034.....		7 39.8	+80 31	6.5	0.478	G9	G6	4.8	0.046	0.049 G, Y
2049.....	π Gemin.....	7 41.1	+33 40	5.3	0.040	Ma	Ko	0.3	0.010	0.028 Ab
2051.....	4 Puppis.....	7 41.3	−14 19	5.1	0.017	A8		1.6	0.020	
2065.....	ξ Puppis §.....	7 45.1	−24 37	3.5	0.007	G6p	G1	−4.2:	0.003	
2075.....	Bu. 4310.....	7 47.1	−13 38	5.7	0.344	Go	Go	5.2	0.079	0.079 M, S, F
2076.....	25 Lyncis.....	7 47.2	+47 39	6.4	0.017	K1	G8	0.4:	0.006	
C 935.....	Lal. 15290.....	7 47.2	+30 55	8.2	1.962	F9	F8	4.7	0.020	0.055 A, Y, M, *et al.*

TABLE VII—*Continued*

Boss	Name	α 1900	δ 1900	Harv. Vis. Mag.	μ	Spectrum Est.	Spectrum Meas.	Spect. Abs. Mag.	Spect. π	Trig. π	Auth.
2079	26 Lyncis	7^h47^m4	+47° 49′	5.7	0″.043	K4	K1	0.4	0″.009		
	Lal. 15389	7 47.8	−13 36	6.9	0.101*	K0	G9	2.0	0.011		
2084		7 48.2	+74 11	5.6	0.034	K3	K1	0.8	0.011		
C 940	Lal. 15394	7 49.1	+19 31	7.9	0.471	K4	K3	6.5	0.052	0″.075	D
2098	1 Cancri	7 51.3	+16 3	6.0	0.056	K3	K3	0.8	0.009		
C 947	Lal. 15547	7 53.7	+21 8	8.6	0.573	G9	K0	5.6	0.025	0.089	Y
C 949	Lal. 15565	7 54.3	+29 31	6.9	1.170	G7	G4	5.9	0.063	0.066	A, Ye, Y
2117	2 Cancri	7 54.9	+25 40	5.9	0.014	G8	G7	−0.6	0.005		
2118	3 Cancri	7 55.1	+17 35	5.8	0.015	K4	K0	0.4	0.008		
2130		7 57.1	+ 2 37	4.5	0.106	K2	G9	1.1	0.021	0.030	A, S
C 952	Fed. 1221	7 57.2	+72 13	8.0	0.496	G0	G2	5.7	0.035		
2131	χ Gemin	7 57.4	+28 4	5.0	0.056	K3	K1	0.3	0.012		
C 955	Bu. 4414	7 58.8	+12 35	8.6†	0.141	K0	G9	3.2	0.008	0.088	S
2144	9 Cancri	8 0.4	+22 55	6.2	0.024	Mb	G7	0.4	0.007		
2146	μ Cancri	8 1.9	+21 52	5.4	0.085	G3	G1	3.7	0.046		
2148		8 2.5	+42 43	6.4	0.073	K3	K2	0.8	0.008	−0.030	Ab
2150	55 Camelop	8 2.9	+68 46	5.5	0.006	G4	G4	−0.7	0.006		
2153	ρ Puppis §	8 3.3	−24 1	2.9	0.100	F7p	F6	−2.1	0.010	0.031	M
2155	29 Monocer. §	8 3.6	− 2 42	4.4	0.025	G3p	F9	−4.2:	0.002		
2157	14 Cancri	8 4.4	+25 49	5.8	0.361	G5	G5	3.2	0.030	0.036	A
2161		8 5.4	+32 46	7.0	0.807	G6	G2	5.8	0.058	0.046	M, Y, Jo
2168	ζ Cancri A	8 6.5	+17 57	5.6	0.155	F9	F9	3.5	0.038	0.038	Ye, S, F
2169	ζ Cancri C	8 6.5	+17 57	6.0	0.155	G0	F9	4.4	0.048		
2174		8 7.0	+76 4	5.7	0.027	G6	G7	0.3	0.008		
2183	20 Puppis	8 8.7	−15 29	5.0	0.015	G3	G1	−2.0	0.004		

2193.....	57 Camelop.....	8^h10^m6	+62°49′	5.8	0″.018	G6	G5	0.9	0″.010		
2195.....	β Cancri.....	8 11.1	+ 9 30	3.8	0.075	K4	K1	0.4	0.021	0″.003	A, M
C 977.....	W.B. 8^h181.....	8 12.0	+30 56	8.6	0.873	K5	K5	7.2	0.052	0.014	Y, F
2199.....		8 13.7	−12 18	6.0	1.030	Ko	G7	6.2	0.110	0.081	M, S, Y, F
2202.....	χ Cancri.....	8 14.0	+27 32	5.2	0.388	F7	F7	3.6	0.048	0.066	A, S
2203.....		8 14.3	+ 60 57	6.5	0.011	Ko	G8	2.4	0.015		
2208.....	31 Lyncis.....	8 16.0	+43 31	4.4	0.107	K5	K1	0.7	0.018	0.009	A, Ab
C 982.....	A.Oc. 8869.....	8 16.3	+66 48	8.9	0.52	K4	K3	6.4	0.032		
2218.....	20 Cancri.....	8 17.6	+18 39	5.9	0.064	F1		1.9	0.016		
2220.....		8 17.9	+42 20	6.2	0.011	K6	G8	0.5	0.008		
2223.....	21 Cancri	8 18.5	+10 57	6.3	0.021	Ma	G8	0.4	0.007		
2224	298 G Puppis §.....	8 18.6	−26 2	5.9	0.017	F5p	F2	−2.0	0.003		
2227.....	1 Hydrae.....	8 19.6	− 3 26	5.7	0.216	F1	F3	3.6	0.038		
2229.....	25 Cancri.....	8 20.2	+17 23	6.2	0.246	F4	F4	2.8	0.021		
2231.....		8 20.3	+67 38	6.0	0.056	G7	G7	1.4	0.012		
2234.....		8 20.5	+ 7 53	5.2	0.043	G5	G4	−0.4	0.008		
2230.....		8 20.6	+45 59	6.3	0.362	G6	Go	4.9	0.052		
2245.....	27 Cancri.....	8 21.2	+12 59	5.8	0.116	Mb	G4	0.3	0.008	0.029	W
2247.....	o Urs. Maj.....	8 22.0	+61 3	3.5	0.166	G2	G2	−0.8	0.014	0.002	A, F
2268.....		8 26.4	+38 22	6.0	0.204	K3	K2	0.7	0.009		
2272.....	32 Lyncis.....	8 26.9	+36 47	6.1	0.139	F3	F4	3.1:	0.025	0.088	Jo
2275.....	32 Cancri.....	8 27.1	+24 25	6.4	0.091	G9	G7	0.7	0.008		
.....	A.G. Cam. 3181.....	8 28.2	+54 4	8.7		G8	G7	2.9	0.007		
2278.....		8 28.6	+73 59	6.3	0.106	G8	G8	1.6	0.011		
C1000.....	W.B. 8^h596.....	8 28 8	+42 6	8.6	0.66	K4	K2	6.7	0.042	0.022	Ye
2282.....	35 Cancri.....	8 29.6	+19 56	6.6	0.045	F5	F7	1.7	0.011		
2285.....	Bu. 4677 Br.....	8 30.5	+ 6 58	6.0	0.195	F8	F7	4.0	0.040	0.024	W
2286.....	Bu. 4677 Ft.....	8 30.5	+ 6 58	7.2	0.201	G4	G4	5.5	0.046		
2289.....		8 30.9	+53 45	5.7	0.072	G4	G4	0.7	0.010		
2290.....	π Urs. Maj.....	8 31.5	+64 41	4.8	0.052	K2	G9	1.0	0.017	0.018	A

TABLE VII—*Continued*

Boss	Name	α 1900	δ 1900	Harv. Vis. Mag.	μ	Spectrum		Spect. Abs. Mag.	Spect. π	Trig. π	Auth.
						Est.	Meas.				
2293		$8^h31^m.9$	+53° 4′	6.0	0″.040	K2	K1	1.2	0″.011	−0″.028	A
2294		8 32.1	+33 9	6.1	0.023	K2	G9	0.7	0.008		
C1008	Lal. 16933	8 32.2	+26 24	7.6	0.237	G1	G1	4.5	0.024	0.027	A
C1012	Lal. 16904	8 33.1	+56 2	8.1	0.470	G5	G2	5.4	0.029	−0.042	Y
2302	σ Hydrae	8 33.5	+ 3 42	4.5	0.027	K2	Ko	−0.1	0.012	0.019	A
C1014	Lal. 17046	8 34.4	+11 53	7.9	0.531	K2	Ko	6.3	0.048	0.031	M
2312	Bu. 4714 Br.	8 34.8	−22 19	5.4	0.478	G6	G5	3.1	0.035	−0.042	F
	A.G. Leiden 3622	8 35.8	+33 44	8.5		K2	K1	1.3	0.004		
2321	9 Hydrae	8 37.1	−15 35	5.0	0.099	Ko	Ko	2.4:	0.030		
2333		8 38.6	+42 3	8.2	0.702	K4	K3	7.1	0.060	0.049	S, Y
2335	31 Monocer.	8 38.8	− 6 52	4.7	0.007	G2	F7	1.1	0.019		
2336	δ Cancri.	8 39.0	+18 31	4.2	0.240	G9	G9	0.8	0.021	0.018	A, M
2338	46 Cancri.	8 39.2	+31 4	6.1	0.020	G3	G3	−1.0	0.004	0.007	W
	A.G. Leiden 3648	8 39.3	+33 36	8.0	0.011‡	K2	G8	1.1	0.004		
2348	ι Cancri	8 40.6	+29 8	4.2	0.054	G5	G5	−1.3	0.008	0.028	A, M
2354 Br.	ϵ Hydrae AB	8 41.5	+ 6 47	3.5†	0.196	F9	G0	2.1	0.052	0.017	A, M, S, Ait
2354 Ft.	ϵ Hydrae C	8 41.5	+ 6 47	7.5	0.196	F5	F7	3.5	0.016		
C1040	Bu. 4815 S.	8 46.0	+71 11	8.7	1.390	K6	K5	8.7	0.100	0.086	G, F
	Bu. 4815 N.	8 46.0	+71 11	9.1	1.390	K9	K5	9.2	0.105		
2378	53 Cancri.	8 46.5	+28 38	6.3	0.022	Mb	G7	0.8	0.008	0.000	M
2380	55 Cancri.	8 46.6	+28 43	6.1	0.541	K2	K1	5.7	0.083	0.080	A, M, Y, Jo
2384	Bu. 4839 Ft.	8 48.1	+30 57	6.6	0.051	Ko	G9	0.9	0.007		
2384	Bu. 4839 Br.	8 48.1	+30 57	6.1	0.051	G9	G8	0.0	0.006		
C1050	W.B. 8^h1147	8 49.0	+26 35	6.7	0.44	G1	G1	4.2	0.032	0.018	Ye
2393	ξ Hydrae	8 50.1	+ 6 20	3.3	0.104	G5	G7	−0.9	0.014	0.017	A, M

2394.....	60 Cancri.....	$8^h50^m.5$	+12° 0′	5.7	0″.021	K4	K0	0.6	0″.010		
2404.....	ι Urs. Maj.....	8 52.4	+48 26	3.1	0.502	A5		1.9	0.058	0″.090	Y, Ab, F
2410.....		8 53.5	+18 31	6.6	0.089	Mc	G9	0.2	0.005		
2411.....	ρ Urs. Maj.....	8 53.5	+68 1	5.0	0.021	Ma	K1	−0.1	0.009		
2412.....		8 54.0	−15 45	5.9	0.324	F5	F5	3.9	0.040		
2413.....	10 Urs. Maj.....	8 54.2	+42 11	4.1	0.504	F3	F6	3.2	0.066	0.066	A, S, Y, F
2437.....		9 0.2	+38 51	4.7	0.043	G3	G3	−2.7	0.003	0.007	A
2441.....	13 Urs. Maj.....	9 1.6	+67 32	4.9	0.070	F5	F6	3.8	0.060		
2442.....	Bu. 4929 Br.....	9 1.7	+23 23	7.3	0.161	F3	F5	3.5	0.017	0.019	W
2442.....	Bu. 4929 Ft.....	9 1.7	+23 23	7.7	0.161	F4	F4	3.5	0.014		
2447.....	75 Cancri.....	9 2.9	+27 3	6.0	0.404	G2	G2	4.1	0.042		
2449.....	ξ Cancri.....	9 3.6	+22 27	5.2	0.008	K0	G8	0.8	0.013		
2450.....	κ Pyxidis.....	9 3.7	−25 27	4.8	0.040	K3	G9	1.1:	0.018		
C1083.....	Lal. 18067.....	9 3.8	−14 44	7.3	0.557	G0	G0	4.9	0.033		
2455.....	79 Cancri.....	9 4.6	+22 24	6.1	0.010	G8	G6	2.1	0.016		
2464.....	81 Cancri.....	9 6.8	+15 24	6.4	0.576	G9	G6	5.5	0.066	0.044	A, Y
.....	Bu. 4968 Br.....	9 6.9	+47 24	7.8†	0.038	F7	F6	3.3	0.013		
2469.....	Bu. 4972[1].....	9 7.6	+53 7	7.9	1.677	K8	K7	8.7	0.145	0.152	Ye, F, Ab, *et al.*
2470.....	Bu. 4972[2].....	9 7.6	+53 7	8.0	1.686	K6	K5	8.6	0.132		
2478.....		9 9.1	+35 3	6.0	0.149	G1	G1	1.5	0.013		
2490.....	23 Hydrae.....	9 11.7	− 5 56	5.4	0.004	K2	K0	0.2	0.009		
C1096.....	Bu. 5005.....	9 12.0	+29 0	7.9†	0.517	K3	K3	6.5	0.052	0.067	S, Y, F
2501.....	83 Cancri.....	9 13.4	+18 8	6.6	0.180	F6	F7	3.5	0.024		
2507.....	α Lyncis.....	9 15.0	+34 49	3.3	0.216	K5	K2	0.6	0.029	−0.057	Jo
2516.....	θ Pyxidis.....	9 17.1	−25 32	4.9	0.022	Ma	G9	0.8	0.015		
2524.....	κ Leonis	9 18.8	+26 37	4.6	0.061	K2	K0	1.3	0.022	−0.004	A
.....	A.G. Leiden 3861.....	9 19.7	+33 12	7.9	0.037‡	G9	G7	2.3	0.008		
2528.....		9 20.0	+17 1	6.3	0.079	K0	G8	2.2	0.015	0.015	W
2529.....	28 Hydrae.....	9 20.4	− 4 41	5.8	0.023	K4	G9	0.6	0.009		
2533.....	α Hydrae.....	9 22.7	− 8 14	2.2	0.035	K5	K0	0.1	0.038	0.004	Y, F

TABLE VII—*Continued*

Boss	Name	α 1900	δ 1900	Harv. Vis. Mag.	μ	Spectrum Est.	Spectrum Meas.	Spect. Abs. Mag.	Spect. π	Trig. π	Auth.
2536	1 H Draco	9^h22^m9	+81°46′	4.6	0″.027	K4	K1	0.5	0″.015		
2540	23 Urs. Maj.	9 23.7	+63 30	3.8	0.117	A6		1.3	0.032		
C1126	Lal. 18672	9 24.7	+ 6 5	7.6	0.533	K4	K2	6.6	0.063		
2540	24 Urs. Maj.	9 25.6	+70 16	4.6	0.090	G3	G2	2.0	0.030	0″.048	Y
2550	λ Leonis	9 26.0	+23 25	4.5	0.056	K6	K2	0.5	0.016	0.039	M
2552	θ Urs. Maj.	9 26.2	+52 8	3.3	1.092	F5	F6	3.0	0.087	0.073	A, M, Ab, *et al.*
2555	ξ Leonis	9 26.6	+11 45	5.1	0.130	G9	G7	−0.1	0.009		
2556	6 Leonis	9 26.6	+10 9	5.3	0.024	K3	K0	0.5	0.011		
C1131	Lal. 18721	9 26.9	+27 26	7.1	0.279	G8	G8	5.2	0.042	0.055	A
.....	S Antliae*	9 27.9	−28 11	6.5		A8p		0.7	0.007		
2566	10 Leo. Min.	9 28.1	+36 50	4.6	0.030	G4	G4	0.7	0.016		
2573	11 Leo. Min.	9 29.7	+36 16	5.5	0.753	K1	G6	5.4	0.096	0.140	A, S, Y, Jo
2580	8 Leonis	9 31.5	+16 53	5.9	0.021	K1	G7	0.6	0.009		
C1143	A.Oc. 10038	9 31.5	+72 12	7.8	0.26	F6	F6	3.9	0.017	−0.002	G
2589	2 Sextantis	9 33.2	+ 5 6	4.8	0.176	K2	G9	1.5	0.022		
2595	ι Hydrae	9 34.7	− 0 41	4.1	0.085	K3	K1	0.8	0.022		
2602	o Leonis §	9 35.8	+10 21	3.8	0.150	F5p	F6	−1.4	0.009	0.032	A, M
2603	13 Leonis	9 35.9	+26 22	6.4	0.049	K2	G8	0.7	0.008	0.012	W
.....	W Urs. Maj.*	9 36.7	+56 25	8.6†		F8p		3.5	0.010	0.012	Ye
C1153	Lal. 19022	9 37.1	+43 10	8.1	0.819	K5	K6	7.2	0.066	0.086	Ye, K, F
2609		9 37.7	−23 28	5.0	0.474	F8	F7	4.2	0.069		
2612	ψ Leonis	9 38.3	+14 29	5.6	0.014	Ma	G7	0.6	0.010		
2614		9 39.4	+57 35	5.4	0.025	Mb	G6	0.2	0.009		
2618	ε Leonis	9 40.2	+24 14	3.1	0.048	Go	Go	−0.9	0.016		
2621		9 40.9	+ 7 10	6.0	0.040	Ma	G8	0.9	0.009		

2622.....	18 Leonis.....	$9^h41^m.0$	+12° 16′	5.9	0″.016	K5	G9	0.6	0″.008		
2632.....	υ Urs. Maj.....	9 43.9	+59 31	3.9	0.330	A8	A8	1.5	0.033		
2639.....	23 Leonis.....	9 45.6	+13 32	6.7	0.037	K7	Ko	0.2	0.005		
2648.....	μ Leonis.....	9 47.1	+26 29	4.1	0.227	K3	K2	0.6	0.020	0″.025	A
2656.....		9 49.5	+73 21	6.0	0.079	K2	K1	0.4	0.008	0.001	Ab
2660.....		9 50.3	+57 54	6.0	0.068	G4	G4	0.3	0.008	0.006	W
2663.....		9 51.1	+ 9 24	5.9	0.090	K1	G9	0.3	0.008	0.010	W
2671.....		9 52.8	+ 8 47	6.3	0.035	K4	K1	0.6	0.007		
2680.....	π Leonis.....	9 54.9	+ 8 31	4.9	0.043	Ma	K1	−0.9	0.007		
C1189.....	Groom. 1596.....	9 54.9	+56 5	8.3	0.498	G7	G5	5.7	0.030	0.069	Y
2681.....	20 Leo. Min.....	9 55.2	+32 25	5.6	0.681	G7	G3	5.3	0.087	0.064	A, K, Jo, F
C1192.....	A.Oe. 10427.....	9 56.1	+71 21	8.3	0.24	G1	G2	3.9	0.013	0.027	G
C1197.....	Groom. 1603.....	9 57.9	+38 30	6.8	0.170	F6	F7	3.7	0.024	0.032	A
2696.....	31 Leonis	10 2.6	+10 29	4.6	0.117	K5	K3	0.4	0.014		
.....	Comp. α Leonis.....	10 2.9	+12 29	7.6	0.247	K2	Ko	6.2	0.052	0.033	Y
C1211.....	Lal. 19780.....	10 3.6	−19 15	7.2	0.355	G2	Go	5.1	0.038	0.057	F
2701.....		10 5.0	+41 9	6.5	0.017	K2	G8	0.6	0.007		
C1218.....	Groom. 1618.....	10 5.3	+49 58	6.8	1.451	K6	K6	8.3	0.200	0.177	K, F, P
2706.....	λ Hydrae.....	10 5.7	−11 52	3.8	0.221	Ko	G9	−0.7	0.013		
C1222.....	Lal. 19821.....	10 6.3	+24 15	8.6	0.414	G4	G2	5.7	0.026	0.049	Y
C1225.....	A.Oe. 10640.....	10 7.5	+53 1	9.2	0.74	K3	K3	7.0	0.036	0.073	Ye
.....	A.Oe. 10642.....	10 7.5	+50 48	9.0		G6	G4	1.0	0.003		
C1229.....	Lal. 19896.....	10 8.9	+ 3 39	7.7	0.464	G1	Go	4.5	0.023	−0.048	Y
2728.....	35 Leonis.....	10 11.0	+24 0	5.9	0.209	G1	G1	3.3	0.030	0.026	A, M
2730.....	ζ Leonis.....	10 11.1	+23 55	3.6	0.027	Fo	F3	−0.1	0.018	0.010	M
2734.....	39 Leonis.....	10 11.7	+23 36	5.8	0.423	F8	F7	3.7	0.038	0.092	Y
2740.....		10 14.1	+54 43	6.2	0.023	Ko	G9	1.3	0.010		
C1244.....	W.B. 10^h234.....	10 14.2	+20 22	9.2	0.490	Mdp		10.5	0.182	0.196	D
2741.....	40 Leonis.....	10 14.3	+19 59	5.0	0.329	F5	F5	3.2	0.044	0.052	M
2742.....	γ Leonis Br.....	10 14.5	+20 21	2.6	0.338	G8	G8	0.8	0.044	0.000	M, Y, F
2743.....	γ Leonis Ft.....	10 14.5	+20 21	3.8	0.353	G5	G5	−0.2	0.016		

TABLE VII—*Continued*

Boss	Name	α 1900	δ 1900	Harv. Vis. Mag.	μ	Spectrum		Spect. Abs. Mag.	Spect. π	Trig. π	Auth.
						Est.	Meas.				
C1246	Mün. 5178	$10^h15^m.7$	−0°58′	8.9	0″.679	K5	K3	7.4	0″.050		
2750		10 16.2	+41 44	5.9	0.194	F9	F8	3.5	0.033	0″.090	M, Jo
2751	μ Urs. Maj.	10 16.4	+42 0	3.2	0.084	K5	G8	0.7	0.032	0.051	Y
2757	43 Leonis	10 17.8	+ 7 3	6.3	0.108	K2	K0	0.7	0.008		
2762	30 H Camelop.	10 18.9	+83 4	5.3	0.084	F0	F3	2.3	0.025		
2771	μ Hydrae	10 21.3	−16 20	4.1	0.153	K5	K2	0.8	0.022		
2775		10 21.9	+49 19	6.5	0.898	G2	G1	5.6	0.066	0.078	K, R, F
2776	β Leo. Min.	10 22.1	+37 13	4.4	0.161	G6	G7	1.2	0.023	0.013	M, Ab
2780	35 Urs. Maj.	10 22.8	+66 8	6.4	0.045	K2	K1	1.0	0.008		
C1264	W.B. 10^h 366	10 23.2	− 6 5	8.1	0.478	G9	G8	5.2	0.026		
2785	36 Urs. Maj.	10 24.2	+56 30	4.8	0.182	F8	F7	3.6	0.058	0.091	A, S
2795		10 25.7	+81 1	6.6	0.016	G6	G7	0.2	0.005		
2799	9 H Draco	10 26.6	+76 14	5.0	0.030	G7	G7	0.2	0.011		
2800	46 Leonis	10 26.9	+14 39	5.7	0.041	Ma	G7	1.0	0.012	0.005	W
2806		10 27.7	+49 42	7.6	0.292	F8	F6	4.3	0.022	0.045	K
2822		10 31.6	−11 42	5.8	0.734	F7	F6	3.9	0.042	0.007	Y, F
2830	p Velorum*	10 33.1	−47 42	5.1†	0.167	Fop		2.2	0.026		
2831	38 Leo. Min.	10 33.4	+38 26	5.8	0.227	F9	F8	2.2	0.019	0.029	Ab
2836	φ Hydrae	10 33.7	−16 21	5.1	0.111	G7	G5	1.0	0.015		
2844	35 H Urs. Maj.	10 35.9	+69 36	5.2	0.023	K4	G9	0.7	0.013		
2846	33 Sextantis	10 36.3	− 1 13	6.4	0.191	K0	G8	3.5	0.026		
	A.G. Albany 4102	10 37.2	+ 1 23	7.6	0.008‡	K0	G8	1.9	0.007		
2853		10 37.7	+46 44	5.3	0.289	A9	A9	1.6	0.018	0.031	Jo
2857		10 38.1	+46 44	8.1	0.280	F9	F9	4.4	0.018	−0.004	K

.....	A.G. Leiden 4263.....	10h38m8	+33° 9′	7.6	0.″033‡	A9		2.5:	0.″010		
2865.....	41 Urs. Maj.....	10 40.1	+57 54	6.5	0.081	Ma	K1	1.0	0.008		
2868.....	37 Sextantis.....	10 40.9	+ 6 54	6.3	0.039	K1	K0	0.8	0.008		
2881.....	43 Leo. Min.....	10 43.4	+29 57	6.3	0.103	G9	G9	1.3	0.010	0.″036	W
2888.....	ν Hydrae.....	10 44.7	−15 40	3.3	0.214	K1	K0	1.0	0.035		
C1307.....	Lal. 20881.....	10 46.1	+20 49	8.1	0.502	F1	F0	3.6	0.013	0.007	Y
2897.....		10 46.7	+70 23	6.1	0.403	K0	K1	4.3	0.044	−0.011	Y
.....	A.G. Leiden 4299.....	10 47.1	+33 31	7.6	0.049‡	G9	G8	2.3	0.009		
2899.....	46 Leo. Min.....	10 47.7	+34 45	3.9	0.304	K1	G9	1.4	0.032	0.058	M, Ab
2910.....		10 50.2	+34 2	5.2	0.113	K1	G9	0.7	0.013	0.014	Ab
2912.....		10 50.5	+42 33	6.1	0.101	K1	G9	3.0	0.024		
2915.....	56 Leonis.....	10 50.8	+ 6 43	6.0	0.023	Mc	G5	−0.6	0.005	−0.004	W
C1325.....	Lal. 21008.....	10 50.9	+28 17	8.6	0.472	G6	G5	5.2	0.021	0.050	Y
2918.....		10 52.0	+78 18	6.3	0.081	G7	G7	0.5	0.007		
2920.....	47 Urs. Maj.....	10 53.9	+40 58	5.1	0.320	G2	G1	4.1	0.063	0.080	A
2921.....		10 54.0	+36 38	6.2	0.095	Ma	G8	1.0	0.009		
2922.....		10 54.5	+46 4	5.7	0.016	K5	K0	0.5	0.009		
2925.....	α Crateris.....	10 54.9	−17 46	4.2	0.481	K0	G9	−0.1	0.014		
2927.....	58 Leonis.....	10 55.4	+ 4 9	5.0	0.023	K1	G9	0.5	0.013		
2931.....	61 Leonis.....	10 56.7	− 1 57	5.0	0.041	K6	K1	0.3	0.012		
2933.....	α Urs. Maj.....	10 57.6	+62 17	2.0	0.139	G8	G8	0.4	0.048	0.037	F
2935.....	22 H Camelop.....	10 57.9	+36 38	7.6	4.779	Ma		10.5	0.380	0.411	Ye, S, Y, *et al.*
2938.....	62 Leonis.....	10 58.5	+ 0 32	6.2	0.066	K3	K2	0.6	0.008		
2942.....	χ Leonis.....	10 59.9	+ 7 53	4.7	0.350	F5	F4	0.8	0.017	0.012	M
2943.....	51 Leo. Min.....	10 59.9	+25 45	7.5	0.409	F7	F7	4.7	0.028	0.039	Y
C1349.....	Lal. 21258.....	11 0.5	+44 2	8.9	4.519	Ma		10.1	0.174	0.190	M, R, K, *et al.*
2950.....	65 Leonis.....	11 1.8	+ 2 30	5.7	0.386	G9	G7	2.6	0.024		
2958.....	ψ Urs. Maj.....	11 4.0	+45 2	3.2	0.069	K0	G9	1.3	0.042		
.....	Bu. 5695 B.....	11 5.5	+31 0	9.8	0.623	Ma		8.8	0.063	0.048	Y
C1361.....	Bu. 5695 A.....	11 5.6	+31 0	8.8	0.623	K7	K3	8.4	0.083		

TABLE VII—*Continued*

Boss	Name	α 1900	δ 1900	Harv. Vis. Mag.	μ	Spectrum		Spect. Abs. Mag.	Spect. π	Trig. π	Auth.
						Est.	Meas.				
2984.....	Bu. 5695 C.....	11h 5m6	+31° 2′	9.0		G6	G6	3.8	0″.009		
2971.....	Bu. 5706 A.....	11 8.6	+74 1	7.8†	0″.405	K5	K4	7.2	0.076	0″.088	F, Bgs
2976.....	72 Leonis	11 9.9	+23 38	4.9	0.018	Ma	G5	−0.5	0.008		
2978.....	73 Leonis.....	11 10.6	+13 51	5.5	0.028	K2	K1	1.0	0.013		
2980.....		11 11.1	+50 1	6.0	0.092	G6	G9	1.4	0.012	−0.081	Y
2983.....	75 Leonis.....	11 12.1	+ 2 34	5.4	0.159	Ma	K2	0.7	0.012		
2984.....	ξ Urs. Maj. Br.....	11 12.9	+32 6	4.4	0.732	F9	F9	4.9	0.126	0.158	Y, Ab, F
2984.....	ξ Urs. Maj. Ft.....	11 12.9	+32 6	4.9	0.732	G2	G2	5.3	0.120		
2985.....	ν Urs. Maj.....	11 13.1	+33 38	3.7	0.027	K4	G9	0.4	0.022		
2986.....		11 13.2	− 4 31	7.3	0.808	G8	G6	6.1	0.058	0.034	M, Y
2989.....	δ Crateris.....	11 14.3	−14 14	3.8	0.230	G9	G7	0.7	0.024		
C1383.....	A.Oe. 11677.....	11 14.8	+66 23	9.2	2.986	Ma		10.9	0.219	0.198	F, Bgs
2995.....	56 Urs. Maj.....	11 17.3	+44 2	5.1	0.038	G6	G7	−0.1	0.009		
2997.....	λ Crateris.....	11 18.4	−18 14	5.2	0.314	F3	F4	1.2	0.016		
2999.....	ι Leonis Br.....	11 18.7	+11 5	4.0	0.176	F4	F4	2.8	0.058		
3014.....	83 Leonis Br.....	11 21.7	+ 3 33	6.5	0.743	G9	G7	5.3	0.058	0.023	Y, R
3015.....	83 Leonis Ft.....	11 21.7	+ 3 33	7.6	0.736	K4	K5	6.4	0.058		
3021.....	τ Leonis.....	11 22.8	+ 3 24	5.2	0.028	G7	G6	0.1	0.010		
3022.....		11 23.4	+62 19	5.9	0.267	F3	F3	3.1	0.028		
3025.....	85 Leonis.....	11 24.5	+15 58	6.0	0.066	K3	K2	1.1	0.011		
3029	87 Leonis.....	11 25.2	− 2 27	5.1	0.026	K4	G9	1.1	0.016		
3030	86 Leonis.....	11 25.3	+18 58	5.7	0.078	Ko	G8	1.1	0.012	0.009	W
.....	Bu. 5805.....	11 25.4	+41 51	7.6†	0.130‡	F2	F4	2.9	0.012		
3031.....	λ Draconis.....	11 25.5	+69 53	4.1	0.045	K5	Ko	0.2	0.017	0.018	M
3032.....	88 Leonis Br.....	11 26.6	+14 55	6.3†	0.387	F9	F9	3.6	0.029		

3033.....	Bu. 5811	11h26m7	+61°38′	5.8†	0.″079	F4	F6	4.0	0.″044	0.″057	S
C1426.....	Lal. 21927.....	11 28.4	+65 48	7.2	0.204	F5	F7	3.7	0.020	0.027	G
3047.....		11 29.6	−32 18	6.1	1.058	K2	Ko	6.2	0.105	0.235	F
3050.....	2 Draconis.....	11 30.2	+69 53	5.4	0.176	G5	G7	−0.4	0.007		
3058.....	υ Leonis.....	11 31.8	− 0 16	4.5	0.035	G8	G7	1.0	0.020		
.....	SU Draconis §.....	11 32.2	+67 53	9.2		A5		0.9:	0.002		
3069.....	Bu. 5858 Br.....	11 33.5	+45 40	6.3	0.583	F8	F9	4.1	0.036	0.038	K
3069.....	Bu. 5858 Ft.....	11 33.5	+45 40	8.6	0.583	K4	K2	6.7	0.042		
3075.....	61 Urs. Maj.....	11 35.8	+34 46	5.5	0.390	G5	G4	4.8	0.072		
3078.....	62 Urs. Maj.....	11 36.4	+32 18	5.7	0.347	F2	F4	3.8	0.042	0.042	W
3081.....	3 Draconis.....	11 36.9	+67 18	5.5	0.058	K2	Ko	0.6	0.010		
3087.....	ξ Crateris.....	11 39.7	−17 48	4.9	0.052	G7	G5	1.1	0.017		
C1452.....	Groom. 1822.....	11 40.3	+48 14	8.0	0.644	F9	Go	4.1	0.017	0.024	K
3089.....	ν Virginis.....	11 40.7	+ 7 5	4.2	0.188	Ma	G6	0.2	0.016		
3090.....	χ Urs. Maj.....	11 40.8	+48 20	3.8	0.137	Ko	G8	1.3	0.032		
3098.....	93 Leonis.....	11 42.8	+20 46	4.5	0.155	F4	F7	3.1	0.052	0.029	M
3100.....		11 43.7	−26 12	5.4	0.028	Mc	G7	0.2	0.009		
3105.....	β Virginis.....	11 45.5	+ 2 20	3.8	0.793	F7	F7	3.5	0.087	0.104	A, M, Y
3112.....	Groom. 1830.....	11 47.2	+38 26	6.5	7.047	G8	G5	6.0	0.079	0.106	M, Y, K, *et al.*
.....	A.G. Leip. 4431.....	11 48.7	+14 35	8.1	0.032‡	F1		2.7	0.008		
C1475.....	Bu. 5960 S	11 49.4	+19 58	8.4	0.445	G4	G5	5.9	0.032		
C1476.....	Bu. 5960 N.....	11 49.5	+19 59	8.4	0.436	G6	G6	5.3	0.024		
3125.....	66 Urs. Maj.....	11 50.8	+57 9	5.9	0.012	K1	G9	0.4	0.008		
C1487.....	Lac. 4055.....	11 53.0	−27 8	7.2	1.243	K5	K3	7.0	0.091	0.039	F
3137.....		11 55.6	− 9 53	5.6	0.491	G9	G7	4.8	0.069	0.101	Y, M
3141.....		11 56.5	+36 36	5.6	0.136	G9	G8	0.9	0.012	0.036	W
3145.....		11 57.4	+43 39	6.8	0.629	G7	G5	3.6	0.023	0.017	K, F
3155.....	ο Virginis.....	12 0.1	+ 9 17	4.2	0.221	G6	G6	0.4	0.017	0.039	A
C1497.....	Lal. 22701.....	12 0.1	− 0 57	8.4	0.531	G8	G6	6.4	0.040	0.110	Y
3157.....		12 0.6	+63 30	6.2	0.087	K1	K1	2.0	0.014		

TABLE VII—*Continued*

Boss	Name	α 1900	δ 1900	Harv. Vis. Mag.	μ	Spectrum Est.	Spectrum Meas.	Spect. Abs. Mag.	Spect. π	Trig. π	Auth.
3166	α Corvi	12h 3m3	−24° 10′	4.2	0.″093	F1	F1	2.8	0.″052		
C1511	Groom. 1855	12 4.6	+40 49	7.4	0.325	K0	G6	5.7	0.046	0.″064	K
3169	10 Virginis	12 4.6	+ 2 28	6.1	0.190	K2	K1	1.6	0.013	0.028	W
3172	ε Corvi	12 5.0	−22 4	3.2	0.065	K3	K1	0.5	0.029	0.026	M
3177		12 6.5	+82 16	6.3	0.019	K3	G9	0.8	0.008		
3179	68 Urs. Maj.	12 6.8	+57 37	6.5	0.020	K4	K0	0.8	0.007		
C1522	W.B. 12h69	12 7.4	− 2 32	7.4	0.732	G6	G2	5.0	0.033	0.011	Y, F
C1523	Lal. 22901	12 7.8	+10 36	8.0	0.430	K0	G9	5.1	0.026		
C1524	Lal. 22908	12 8.1	+11 24	7.9	0.589	G4	G2	5.5	0.033	0.049	A, Y
3186	1 Can. Ven.	12 9.8	+53 59	6.3	0.023	G9	G7	0.5	0.007		
C1533	Lal. 22954	12 10.0	− 9 44	6.1	1.024	F3	F6	3.7	0.033	0.026	Y, F
3193	2 Can. Ven.	12 11.1	+41 13	5.8	0.051	K6	K2	0.6	0.009		
3194	7 Comae	12 11.3	+24 30	5.1	0.028	G8	G7	1.3	0.017		
	SW Draconis §	12 12.8	+70 4	10.0		F4		0.6:	0.001		
	A.G. Berlin 4636	12 13.0	+19 0	7.5	0.026	F6	F6	2.6	0.011		
C1542	Pi. 12h40	12 14.1	+17 6	7.0	0.237	G2	G2	4.4	0.030	0.024	A
3208	6 B Urs. Min.	12 14.4	+88 15	6.3	0.067	F0		2.0	0.014		
3209	9 Comae	12 14.5	+28 43	6.3	0.245	F8	F7	3.4	0.026	0.054	S
3213	16 Virginis	12 15.3	+ 3 52	5.1	0.307	K0	G7	1.6	0.020	−0.006	A
3216	11 Comae	12 15.7	+18 21	4.9	0.139	G6	G6	0.7	0.014		
3217		12 15.8	−13 1	5.4	0.002	K1	G9	1.3	0.015		
C1551	W.B. 12h309	12 16.9	+42 42	9.1	0.57	Ma		8.5	0.076		
C1557	A.Oe. 12584	12 17.9	+73 48	8.2	0.49	G6	G6	5.4	0.028		
3230	5 Can. Ven.	12 19.2	+52 7	5.0	0.011	G6	G5	0.1	0.011		
	Bu. 6158	12 19.4	+26 9	6.6†		A8		2.1	0.013	−0.022	S

C1563	Lal. 23223	12h19m9	− 3° 40′	8.0	0″.258	G2	G2	5.4	0″.030	0″.055	Ye
C1564	Lal. 23231	12 19.9	+38 52	8.1	0.62	F6	F7	4.3	0.017		
3233		12 20.2	+24 29	6.1	0.072	G9	G9	0.6	0.008	0.005	W
3234	71 Urs. Maj.	12 20.3	+57 20	6.0	0.028	Mb	G8	0.5	0.008		
3242	γ Comae	12 22.0	+28 49	4.6	0.122	K2	K1	0.7	0.017	0.002	A
3248	73 Urs. Maj.	12 22.8	+56 16	5.8	0.031	Ma	Ko	0.5	0.009		
3254	18 Comae	12 24.4	+24 40	5.5	0.025	F2	F3	0.9	0.012		
C1579	Lal. 23361	12 24.6	− 2 46	8.6	0.721	G3	G3	6.1	0.032	0.095	Y
3258		12 24.9	−12 50	6.4	0.251	Go	F9	3.9	0.032		
3261	7 Can. Ven.	12 25.3	+52 5	6.2	0.275	F6	F6	3.0	0.023		
3265	4 Draconis	12 25.7	+69 45	5.2	0.084	Mb	G7	−0.8	0.006		
	A.G. Berlin 4695	12 26.1	+17 10	7.5	0.025‡	K1	Ko	2.0	0.008		
3272	η Corvi	12 26.9	−15 39	4.4	0.444	F2		2.5	0.042		
3274	20 Virginis	12 28.0	+10 51	6.5	0.063	G8	G8	0.4	0.006		
3279	β Can. Ven.	12 29.0	+41 54	4.3	0.758	Go	Go	4.4	0.105	0.107	A, M, Y, F
3280	β Corvi	12 29.1	−22 51	2.8	0.061	G5	G4	0.0	0.028		
3285	24² Comae	12 30.1	+18 56	5.2	0.016	K1	Ko	0.3	0.011		
3294		12 33.3	+ 2 24	6.0	0.090	Mb	G9	0.7	0.009		
3298	χ Virginis	12 34.1	− 7 27	4.8	0.085	K3	K2	0.6	0.014		
C1604	B.D. +69° 671	12 36.0	+69 21	8.2	0.46	G1	G2	4.9	0.022	0.036	G
3307	γ Virginis S	12 36.6	− 0 54	3.7	0.564	Fo		2.2	0.050	0.068	R, F, Bel
3307	γ Virginis N	12 36.6	− 0 54	3.7	0.564	F1		2.4	0.055		
	Groom. 1923	12 37.8	+84 12	7.2	0.232	F7	F9	3.2	0.016	0.000	G
3321	10 Can. Ven.	12 40.3	+39 49	6.0	0.375	F6	F8	3.9	0.038	0.063	A
3326	33 Virginis	12 41.3	+10 6	5.9	0.531	Ko	G9	4.2	0.046	−0.008	S, Y
3327	27 Comae	12 41.7	+17 7	5.3	0.008	K3	K1	0.4	0.010		
3336	7 Draconis	12 43.5	+67 20	5.7	0.008	K3	G8	0.7:	0.010		
C1627	Lal. 23900	12 43.9	+25 23	6.4	0.367	G6	G5	5.3	0.060	0.026	A
C1630	Lal. 23917	12 44.6	+ 1 45	8.1	0.665	G8	G4	6.1	0.040	0.029	A, Y
3344		12 46.2	− 9 48	6.5	0.021	G8	G7	0.9	0.008		

TABLE VII—*Continued*

Boss	Name	α 1900	δ 1900	Harv. Vis. Mag.	μ	Spectrum		Spect. Abs. Mag.	Spect. π	Trig. π	Auth.
						Est.	Meas.				
3346	37 Virginis	12h40m5	+ 3° 36′	6.1	0.″035	K3	K1	0.6	0.″008		
3347	31 Comae	12 46.8	+28 5	5.1	0.031	F6	F7	2.1	0.025		
3348	32 Comae	12 47.2	+17 37	6.5	0.023	K4	G9	0.6	0.007		
C1640	Lal. 23995	12 47.9	−17 57	8.3	0.877	F3	F7	3.4	0.011		
3353	38 Virginis	12 48.1	− 3 1	6.2	0.262	F6	F6	3.3	0.026		
3362	ψ Virginis	12 49.2	− 9 0	4.9	0.032	Ma	G6	−0.3	0.009		
3367	δ Virginis	12 50.6	+ 3 56	3.7	0.479	Mb	G7	0.3	0.021	0.″002	A, Y
C1657	Lal. 24168	12 53.9	− 9 18	7.7	0.850	K2	K0	6.4	0.055	−0.015	Y
3374	36 Comae	12 54.0	+17 57	5.0	0.036	K6	K1	0.9	0.015		
C1664	Pi. 12h243	12 55.7	+18 55	6.1	0.245	F5	F5	3.4	0.029	0.022	A
C1666	A.Oe. 12585	12 56.1	−26 50	8.2	0.545	F4	F6	3.8	0.013		
C1667	W.B. 12h920	12 56.2	− 7 54	8.7	0.493	G6	G5	5.7	0.025	0.010	Y
3381	38 Comae	12 56.2	+17 40	6.0	0.033	G8	G7	0.8	0.009		
3383	ϵ Virginis	12 57.2	+11 30	3.0	0.273	G6	G6	0.0	0.025	0.034	F
3398	40 Comae	13 1.5	+23 9	5.9	0.066	Mc	G8	0.2	0.007	0.043	W
3401	41 Comae	13 2.4	+28 10	4.9	0.089	K4	K2	0.4	0.013		
3402		13 2.4	+62 35	6.3	0.045	G8	G7	2.6	0.018		
C1687	Lal. 24414	13 3.8	+ 5 46	6.9	0.682	G4	G2	4.1	0.028	0.029	A, Y
3406		13 4.2	+10 33	6.0	0.020	K0	G8	1.2	0.011		
3408	50 Virginis	13 4.5	− 9 48	6.2	0.023	K4	K1	0.5	0.007		
	B.D. +18° 2696	13 4.6	+18 0	8.1		K3	K1	1.0	0.004	−0.002	Ye
3412	α Comae	13 5.1	+18 3	5.2†	0.450	F4	F5	3.9	0.055	0.070	A, Ye, F
C1692	Lal. 24504	13 6.4	+10 9	8.5	0.559	G2	G2	4.7	0.017	0.028	Y
3422	53 Virginis	13 6.7	−15 40	5.1	0.314	F6	F6	3.2	0.042		
C1693	A.Oe. 13407	13 7.0	+68 2	8.8	0.75	K2	K0	5.6	0.023	0.010	G

3424	β Comae	13h 7m2	+38° 23′	4.3	1″184	G1	G0	4.7	0″120	0″131	M, Y, F, P
C1695	A.G. Berlin 4855	13 7.5	+18 3	7.8	0.578	F6	F9	4.4	0.021		
3438	57 Virginis	13 10.6	−19 25	5.3	0.322	K1	K0	2.2	0.024		
3442		13 11.5	+81 0	6.3	0.008	G8	G7	0.3:	0.006		
3443	59 Virginis	13 11.8	+ 9 57	5.2	0.382	G0	F9	4.4	0.069	0.075	A
C1712	Bu. 6442 Br.	13 11.9	+17 33	6.6†	0.691	K3	K1	6.4	0.091	0.076	S
3446	σ Virginis	13 12.6	+ 6 0	5.0	0.016	Ma	G6	0.3	0.012		
3447	20 Can. Ven.	13 13.1	+41 6	4.7	0.125	F4	F3	−1.4	0.006		
3448	61 Virginis	13 13.2	−17 45	4.8	1.529	G8	G5	4.9	0.105	0.136	M, F
3449	γ Hydrae	13 13.5	−22 39	3.3	0.083	G7	G5	0.3	0.025	−0.012	M
C1719	W.B. 13h241	13 14.9	+35 39	9.6	0.884	Ma	K5	9.6	0.100	0.080	Y
C1722	W.B. 13h216	13 15.7	+ 4 39	8.8	0.575	K3	K3	6.4	0.033	−0.021	Y
C1723	Lal. 24774	13 16.1	+43 38	8.2	0.438	K1	K0	6.1	0.038	0.179	Y
3475	ξ^2 Urs. Maj.	13 19.9	+55 27	4.0	0.028	A7		1.9	0.038	0.022	M
3483		13 22.6	+63 46	6.5	0.444	G7	G5	5.1	0.052		
3485		13 23.2	− 0 19	7.5	0.462	G2	G2	4.2	0.022		
3487	70 Virginis	13 23.5	+14 19	5.2	0.634	G3	G4	3.9	0.055	0.065	A, M, Y
3488		13 23.6	+72 55	6.1	0.030	K4	G9	0.3	0.007		
.....	Groom. 2004	13 24.4	+70 50	7.5	0.040	F1		2.7	0.011		
.....	Groom. 2005	13 25.3	+70 39	7.5	0.039	K0	G8	2.2	0.009		
C1748	Lal. 25012	13 26.6	− 1 49	7.3	0.887	G9	G7	5.9	0.052	0.053	Y
3499	74 Virginis	13 26.8	− 5 44	4.8	0.112	Ma	G8	0.6	0.014		
3500		13 26.9	+42 37	6.2	0.094	K1	K0	1.6	0.012		
3511		13 30.3	+37 42	5.0	0.085	F5	F5	2.4	0.030		
3526	Bu. 6578	13 34.6	+11 15	6.3†	0.112	A9p		1.5	0.011	0.015	A, Ye, M, *et al.*
.....	B.D. +76° 493	13 34.9	+76 25	8.0		G4	G3	4.9	0.024	0.022	G
.....	Groom. 2026	13 35.1	+48 24	7.9	0.026	F3		2.2	0.007		
.....	A.G. Leiden 4974	13 36.0	+33 21	7.8	0.059‡	F8	F7	3.0	0.011		
3534	82 Virginis	13 36.4	− 8 12	5.2	0.108	Ma	G9	0.3	0.011		
3537	84 Virginis	13 38.0	+ 4 3	5.7†	0.302	K3	K1	0.4	0.009		

TABLE VII—*Continued*

Boss	Name	α 1900	δ 1900	Harv. Vis. Mag.	μ	Spectrum Est.	Spectrum Meas.	Spect. Abs. Mag.	Spect. π	Trig. π	Auth.
3541		13^h39^m0	$+23°12'$	6.4	0″.072	K5	K2	0.7	0″.007		
3542	83 Virginis	13 39.1	−15 41	5.7	0.009	G3p	F7	−0.6	0.006		
C1784	A.G. Berlin 4999	13 40.2	+18 20	9.6	1.86	Ma		10.1	0.126	0″.090	D, Ye, R
C1786	Lal. 25372	13 40.7	+15 26	8.5	2.298	Mb	K4	10.2	0.219	0.200	M, Ye, Y, *et al.*
C1789	Pi. 13^h200	13 41.5	+56 23	6.4	0.372	F6	F7	3.5	0.026	0.027	A
3551		13 41.9	− 9 13	6.2	0.042	K4	K3	0.6	0.008		
3554		13 42.0	+ 6 51	6.3	0.499	F9	G0	4.3	0.040	0.028	A
3558	τ Boötis	13 42.5	+17 57	4.5	0.487	F7	F6	3.0	0.050	0.046	A, Y
3571	89 Virginis	13 44.4	−17 38	5.1	0.108	K0	G9	1.1	0.016		
C1800	Bu. 6641 Br	13 44.5	+27 29	7.9	0.455	K6	K4	7.1	0.069		
C1800	Bu. 6641 Ft	13 44.5	+27 29	8.2	0.455	K6	K4	7.4	0.069		
C1804	Lal. 25484	13 45.8	−23 53	6.5	0.058	G2	G1	5.6	0.066		
3581		13 46.7	+35 10	6.0	0.072	Ma	K0	0.7	0.009	0.012	W
3584		13 47.4	+34 56	5.0	0.044	Ma	G8	0.4	0.012		
3589	10 Draconis	13 48.5	+65 13	4.8	0.004	Mb	G7	−0.5	0.009		
3594	90 Virginis	13 49.6	− 1 1	5.3	0.091	K1	K0	0.4	0.011		
3595	Bu. 6668 Br	13 49.7	− 7 34	6.5†	0.167	F8	F8	4.1	0.033		
3596	η Boötis	13 49.9	+18 54	2.8	0.373	F9	G0	2.8	0.100		
3605		13 53.8	+15 8	6.0	0.087	K4	K2	0.5	0.008		
3616		13 59.0	−14 29	6.4	0.048	K1	K0	2.1	0.014		
3623	θ Centauri	14 0.8	−35 53	2.3	0.750	K1	G8	1.0	0.055	−0.062	F
3629	96 Virginis	14 3.7	− 9 52	6.5	0.016	G8	G7	−0.1	0.005		
3630		14 3.9	+44 20	5.4	0.037	Mb	G6	−0.8	0.006		
3631	13 Boötis	14 4.6	+49 56	5.4	0.068	Ma	G6	−0.2	0.008		
3635	12 Boötis	14 5.8	+25 34	4.8	0.076	F6	F7	1.9	0.026		

3641		14h 7m.5	−26° 9′	6.3	0″.004	G8	G6	0.9	0″.008		
3642	κ Virginis	14 7.6	− 9 49	4.3	0.130	K2	G9	1.0	0.022		
3644		14 8.5	− 0 22	5.8	0.241	F5	F5	2.6	0.023		
3647		14 9.1	− 5 29	6.3	0.317	F8	F8	3.7	0.030		
3649	4 Urs. Min.	14 9.2	+78 1	5.0	0.038	K3	Ko	0.7	0.014		
3650	14 Boötis	14 9.3	+13 26	5.5	0.267	F7	F6	4.1	0.052	0″.097	W
3656		14 10.2	+69 54	5.4	0.068	Ma	K1	0.3	0.010		
3658		14 10.4	+41 59	6.2	0.122	K3	K2	0.7	0.008	0.025	W
3660	ι Virginis	14 10.8	− 5 31	4.2	0.427	F6	F6	2.4	0.044		
3662	α Boötis	14 11.1	+19 42	0.2	2.282	Ko	G9	1.2	0.158	0.075	Y, F
3671		14 13.3	−25 22	5.9	0.538	F5	F7	3.7	0.036		
3673		14 13.8	+35 58	4.8	0.016	Ko	G9	2.1	0.029		
C1882	Lal. 26196	14 14.4	− 4 41	7.6	0.664	K2	K1	6.3	0.055	0.116	Y, F
C1885	Lal. 26294	14 17.6	+30 6	8.6	0.727	K6	K5	8.4	0.091		
3691	2 Librae	14 18.0	−11 15	6.3	0.066	G8	G7	1.7	0.012		
C1886	Lal. 26289	14 18.1	+ 1 43	6.3	0.525	G2	G2	5.7	0.076	0.070	Y, F
3692	Bu. 6842 BC	14 18.5	+ 8 54	7.4†	0.072	Fo	F3	2.2	0.009	0.018	Ye, S
C1894	A.G. Berlin 5072	14 21.1	+24 6	9.5	1.39	Ma	K5	9.5	0.100	0.062	Ye, R
3703		14 21.4	+38 51	6.3	0.019	K1	Ko	1.0	0.009		
3704	θ Boötis	14 21.8	+52 19	4.1	0.471	F6	F7	3.0	0.060	0.067	A
3715	24 Boötis	14 25.2	+50 18	5.6	0.312	G3	G2	1.8	0.017	0.023	A
C1908	Lal. 26481 Br.	14 25.8	−15 11	8.2†	0.433	G2	G2	5.3	0.026	0.238	F
3717	ρ Boötis	14 27.5	+30 49	3.8	0.149	K3	K1	0.8	0.025	0.036	A
3718	5 Urs. Min.	14 27.7	+76 8	4.4	0.021	K4	K1	0.9	0.020		
3722	γ Boötis	14 28.1	+38 45	3.0	0.182	A7		1.8	0.058		
C1913	B.D. +10° 2703	14 28.7	+ 9 47	8.9	0.55	K3	K1	6.2	0.029		
3729	σ Boötis	14 30.3	+30 11	4.5	0.228	Fo		2.9	0.048		
3734		14 31.7	−11 53	6.2	0.946	F4	F5	3.2	0.025	0.049	Y
3735	α Centauri Br.*	14 32.8	−60 25	0.3	3.680	G6	G5	4.8	0.794	0.759	C, Wr
3735	α Centauri Ft.*	14 32.8	−60 25	1.7	3.680	K4	K3	6.2	0.794		

TABLE VII—*Continued*

Boss	Name	α 1900	δ 1900	Harv. Vis. Mag.	μ	Spectrum		Spect. Abs. Mag.	Spect. π	Trig. π	Auth.
						Est.	Meas.				
3736		14^h33^m6	+18°44′	6.0	0″.096	Ko	G9	1.9	0″.015	0″.057	W
3754	32 Boötis	14 36.9	+12 5	5.6	0.205	G5	G5	1.0	0.012		
3758	μ Virginis	14 37.8	− 5 13	4.0	0.339	F1	F3	2.4	0.048	0.048	M
C1939	Bu. 6977	14 38.2	+58 23	7.4†	0.244	Ko	G9	4.6	0.028		
3771	ϵ Boötis Br.	14 40.6	+27 30	2.7	0.049	G8	G7	−0.9	0.019	0.015	A, F
	A.G. Leiden 5276	14 41.1	+34 48	7.8	0.044‡	Ma	G8	0.8	0.004		
C1947	Bu. 6999	14 41.4	+10 4	7.5†	0.272	G3	G2	5.2	0.035		
	Bu. 7001	14 41.7	+42 48	7.8†	0.129*	F5	F7	3.2	0.012	−0.022	S
	A.G. Berlin 5351	14 44.2	+18 37	7.4	0.026‡	Ko	G8	2.2	0.009		
3785		14 45.2	+38 13	6.0	0.276	F2	F2	2.4	0.019	0.015	A
	RY Boötis §	14 45.2	+23 27	7.2	0.051‖	F2	F4	0.5:	0.005		
3790	11 Librae	14 45.8	− 1 53	5.0	0.160	G6	G4	0.8	0.014		
C1962	Lal. 27026	14 46.0	−23 53	7.6	1.022	K5	K5	6.9	0.072	0.041	F
3798	ξ Boötis Br.	14 46.8	+19 31	4.8	0.168	G6	G6	5.8	0.158	0.178	A, M
3798	ξ Boötis Ft.	14 46.8	+19 31	6.8	0.168	K4	K3	6.9	0.105		
	Groom. 2165	14 48.6	+66 3	7.2	0.007	Ma	G8	0.4	0.004		
C1972	Lal. 27137	14 48.9	+19 33	6.0	0.485	K1	Ko	5.9	0.095	0.086	A
C1973	Lal. 27155	14 49.3	+23 45	8.7	0.817	K4	K3	6.9	0.044		
3809	β Urs. Min.	14 51.0	+74 34	2.2	0.030	K4	Ko	0.5	0.046	0.014	F
3810	15 Librae	14 51.3	−11 0	5.6	0.002	K2	Ko	1.2	0.013		
3812	Bu. 7060 Ft.	14 51.6	−20 58	8.9	1.916	Ma		9.9	0.158	0.194	M, F, Sitt
3813	Bu. 7060 Br.	14 51.6	−20 58	5.8	2.039	K3	K6	6.7	0.151		
C1980	Lal. 27298	14 52.3	+54 4	7.9	1.086	K1	G8	6.3	0.048	0.056	Ye, Y, P, F
3816	1 Serpentis	14 52.4	+ 0 14	5.7	0.069	K1	K1	1.8	0.017	0.044	W
C1986	Pi. 14^h229	14 53.7	− 4 35	6.0	0.384	F8	F8	4.0	0.040		

C1988	Lal. 27274	14^h54^m2	$-21°36'$	8.5	0″.785	F4	F6	3.3	0″.009		
3827		14 56.0	+66 20	4.9	0.082	Mb	G8	−0.6	0.008		
3833		14 57.1	+82 55	5.7	0.294	F8	F9	3.6	0.038	0″.010	G
3836	β Boötis	14 58.2	+40 47	3.6	0.063	G4	G5	−0.7	0.014	0.030	A, M
3837	σ Librae	14 58.2	−24 53	3.4	0.094	Mb	G7	0.7	0.029		
3842	ψ Boötis	15 0.2	+27 20	4.7	0.178	K2	Ko	0.9	0.017		
3843	9 Urs. Min	15 0.3	+72 9	6.7	0.398	F9	Go	4.3	0.033	0.043	G
3846	44 Boötis Ft.*	15 0.5	+48 3	6.1		G2p	G4	5.2	0.066		
3847	44 Boötis Br.	15 0.5	+48 3	5.3	0.387	Go	Go	4.6	0.072		
3855	45 Boötis	15 2.9	+25 16	5.0	0.262	F4	F4	3.3	0.046	0.059	A
C2010	Lal. 27531	15 2.9	− 7 31	8.1	0.484	F9	Go	3.9	0.014		
C2011	Lal. 27558	15 3.0	+ 9 16	8.7	0.534	F6	F9	4.2	0.013		
C2019	A.Oe. 14320	15 4.7	−15 54	9.4	3.680	G9	G5	5.7	0.018	0.039	Ye, R, V
3867		15 7.5	+19 21	6.0	0.004	Mb	G7	0.2	0.007	0.005	W
C2024	Lal. 27742	15 8.3	+19 39	6.8	0.668	G6	G2	4.2	0.030	0.004	Y, R
C2025	Lal. 27743	15 8.3	+19 40	7.6	0.654	G7	G5	5.2	0.033		
C2027	Lal. 27744	15 8.8	− 0 58	7.2†	1.376	Ko	G7	5.8	0.052	0.070	Ye, Y, F
3882	3 Serpentis	15 10.2	+ 5 19	5.4	0.023	G9	G7	0.8	0.012		
3887	δ Boötis	15 11.5	+33 41	3.5	0.155	G5	G5	−0.6	0.015	0.031	A
3895	5 Serpentis	15 14.2	+ 2 9	5.2	0.644	F6	F7	3.5	0.046	0.055	A, Y
C2043	Lal. 27922	15 14.6	− 8 18	7.9	0.211	F9	F9	3.5	0.013	−0.005	A
C2044	Lal. 27958	15 14.7	+26 4	8.1	0.568	G9	G5	5.4	0.029	0.031	Y
3900	28 Librae	15 15.2	−17 48	6.2	0.069	G8	G6	0.9	0.009		
3907	6 Serpentis	15 15.9	+ 1 5	5.5	0.125	K2	K2	1.8	0.018	0.133	F
.....	A.G. Leiden 5456	15 16.1	+31 3	9.9		F5	F6	3.5	0.005		
C2055	W.B. 15^h 268	15 17.7	+ 1 47	8.7	0.507	K4	K3	6.7	0.040	0.118	Y
3923	η Cor. Bor.	15 19.1	+30 39	5.6†	0.237	Go	Go	4.3	0.055	0.084	S, Ye
3926	μ^1 Boötis	15 20.7	+37 44	4.5	0.169	Fo		2.2	0.035	0.046	M, S, F
3927	μ^2 Boötis	15 20.7	+37 42	7.2†	0.172	Go	Go	4.7	0.032		
3931	9 Serpentis	15 21.2	+15 47	5.5	0.033	K6	Ko	0.2	0.009		

TABLE VII—*Continued*

Boss	Name	α 1900	δ 1900	Harv. Vis. Mag.	μ	Spectrum		Spect. Abs. Mag.	Spect. π	Trig. π	Auth
						Est.	Meas.				
.....	A.G. Berlin 5543.....	15^h21^m6	+18°31′	8.3†	0″023‡	F7	F7	2.8	0″008		
3936.....	ι Draconis.....	15 22.7	+59 19	3.5	0.010	K3	K1	0.1	0.021	0″025	A
C2064....	Bu. 7268 Br.....	15 22.7	− 8 59	6.8	0.349	G8	G7	5.5	0.055		
..... ...	Bu. 7268 Ft.....	15 22.7	− 8 59	8.1	0.349	K2	K2	6.0	0.038		
C2067.. ...	B.D. +67° 887.....	15 23.1	+66 54	9.0	0.28	G8	G7	5.1	0.017	0.017	G
3938.....		15 23.3	+25 27	6.3	0.039	Ma	G9	−0.1	0.005		
3940.....	β Cor. Bor.....	15 23.7	+29 27	3.7	0.190	F2	F4	−0.3	0.016		
3942.....	34 Librae.....	15 25.0	−16 16	5.9	0.019	G9	G8	1.2:	0.012		
C2071.....	Lal. 28358.....	15 26.6	+57 47	6.9	0.209	F5	F6	4.2	0.029	0.029	F
3952.....	37 Librae.....	15 28.7	− 9 43	4.8	0.389	K1	K0	2.9	0.042		
3959.....	γ Librae.....	15 29.9	−14 27	4.0	0.065	G9	G8	0.5	0.020		
3960.....	δ Serpentis Br.....	15 30.0	+10 52	4.2	0.068	A7		1.4	0.028	0.013	Ye
3960.....	δ Serpentis Ft.....	15 30.0	+10 52	5.2	0.068	A8		1.5	0.018		
3963.....	15 Serpentis.....	15 31.0	+17 59	6.1	0.081	G7	G6	1.0	0.010		
3968.....	16 Serpentis.....	15 31.7	+10 21	5.4	0.139	G4	G6	0.1	0.009		
C2086.....	W.B. 15^h716.....	15 32.4	+40 10	7.9	0.455	K4	K5	6.6	0.055	0.046	R
C2087.....	W.B. 15^h720.....	15 32.5	+40 8	7.4†	0.456	K3	K2	6.1	0.055		
3983.....	Bu. 7362 Br.....	15 35.0	+80 47	6.9	0.246	G3	G3	5.7	0.058	0.022	W
4001.....	α Serpentis.....	15 39.3	+ 6 44	2.8	0.139	K2	K1	−0.2	0.025	0.056	A, M, F
4010.....	λ Serpentis.....	15 41.6	+ 7 40	4.4	0.244	G0	G0	4.4	0.100	0.086	A
C2112.....	Groom. 2273.....	15 41.7	+53 18	7.3	0.261	G2	G3	4.8	0.032	0.015	A
4015.....	κ Serpentis.....	15 44.2	+18 27	4.3	0.110	Ma	K0	0.0	0.014		
4024.....	δ Cor. Bor.....	15 45.4	+26 22	4.7	0.110	G4	G3	1.7	0.025	0.013	A
4029.....		15 46.1	−13 50	6.2	0.044	G5	G3	0.3	0.007		
4031.....	ρ Serpentis.....	15 46.9	+21 17	4.9	0.049	K5	K2	0.7	0.014		

4032	κ Cor. Bor.	15h47m5	+35°58′	4.8	0″.364	K1	K0	1.6	0″.023	0″.030	A
4040	39 Serpentis	15 48.5	+13 31	6.2	0.586	G1	G1	5.1	0.060	0.031	A, Y
4042	χ Herculis	15 49.2	+42 44	4.6	0.760	F7	F9	4.2	0.083	0.099	Y
4048		15 50.2	+20 36	5.8	0.083	K4	G8	0.8	0.010	0.040	W
4054	2 Herculis	15 51.3	+43 26	5.5	0.075	Ma	G8	0.6	0.011		
4055	γ Serpentis	15 51.8	+15 59	3.9	1.332	F5	F6	4 3	0.120	0.063	A, M, Y, *et al.*
4063	ε Cor. Bor.	15 53.4	+27 10	4.2	0.109	K2	K1	0.9	0.022		
C2134	W.B. 15h1323	15 54.5	+28 1	8.1	0.85	G8	G8	6.0	0.038		
4067	49 Librae	15 54.7	−16 14	5.5	0.750	F6	F6	3.6	0.042		
4075	5 Herculis	15 56.7	+18 6	5.3	0.153	G7	G7	0.7	0.012		
4077	ρ Cor. Bor.	15 57.2	+33 36	5.4	0.810	F9	G0	3.6	0.044	0.035	A, M, Y
4082	ξ¹ Scorpii	15 58.9	−11 6	4.8†	0.071	F5	F6	3.0	0.044	0.046	M, Ye
4083	ξ² Scorpii	15 58.9	−11 6	7.2	0.080	G7	G6	5.0	0.036		
C2149	Lal. 29307	15 59.9	+25 31	7.1	0.862	K0	G7	5.7	0.052	0.058	Ye
4090	θ Draconis	16 0.0	+58 50	4.1	0.459	F7	F8	3.2	0.066	0.066	Kos
C2152	Lal. 29330	16 1.2	+10 57	8.5	0.491	K0	G9	6.0	0.032		
C2154	Groom. 2305	16 1.5	+39 26	6.8	0.571	G9	G5	6.1	0.072	0.069	Y
4096		16 2.0	−26 4	5.6	0.122	Ma	G8	0.6	0.010		
C2160	Lal. 29439	16 2.9	+38 55	8.6	0.591	K5	K2	7.1	0.050	0.014	Y, K
	Groom. 2312	16 3.3	+70 23	8.2	0.020	Mb	G9	1.0	0.004		
4101	κ Herculis Br.	16 3.6	+17 19	5.3	0.046	G5	G4	−0.2	0.008	−0.011	Ye
4102	κ Herculis Ft.	16 3.6	+17 19	6.5	0.048	K2	K1	1.1	0.008		
4103	47 Serpentis	16 3.6	+ 8 48	5.9	0.024	Mb	G6	0.4	0.008		
C2163	Lal. 29437	16 4.3	+ 6 40	6.0	0.760	K0	K2	4.4	0.048	0.014	A, Y
4106		16 4.6	− 3 12	5.4	0.016	K5	K2	0.3	0.010		
4108	τ Cor. Bor.	16 5.3	+36 45	4.9	0.325	K0	K0	2.8	0.038	0.044	A
4125	10 Herculis	16 7.4	+23 45	6.0	0.028	Mc	G7	0.0	0.006		
4130	9 Herculis	16 8.3	+ 5 17	5.6	0.046	K4	K2	0.8	0.011	0.008	W
4131	χ Scorpii	16 8.3	−11 35	5.5	0.020	K2	K0	1.1	0.013		
4132	Bu. 7551 S	16 8.6	+13 48	7.6	0.459	G9	G7	5.3	0.035	0.078	M
4132	Bu. 7551 N	16 8.6	+13 48	7.6	0.459	G9	G8	4.7	0.026		

TABLE VII—*Continued*

Boss	Name	α 1900	δ 1900	Harv. Vis. Mag.	μ	Spectrum		Spect. Abs. Mag.	Spect. π	Trig. π	Auth.
						Est.	Meas.				
.....	A.G. Leiden 5723.....	16h 9m0	+32°51′	7.9	0.″027‡	K1	K0	1.0	0.″004		
4134.....	δ Ophiuchi.....	16 9.1	− 3 26	3.0	0.161	K8	G8	0.3	0.029	0.″045	M
4137.....	18 Scorpii.....	16 10.2	− 8 6	5.6	0.563	G2	G1	4.7	0.066	0.039	Y
4138.....	σ^1 Cor. Bor. Ft.....	16 10.9	+34 7	6.7	0.302	F9	F9	4.2	0.032	0.044	A, F
4138.....	σ^2 Cor. Bor. Br.....	16 10.9	+34 7	5.8	0.302	F8	G0	3.7	0.038		
.....	A.G. Leiden 5734.....	16 11.4	+32 24	8.5	0.035‡	K4	G8	1.0	0.003		
.....	A.G. Berlin 5827.....	16 12.5	+19 6	7.6	0.034‡	K2	K0	1.7:	0.006		
4147.....	ε Ophiuchi.....	16 13.0	− 4 27	3.3	0.086	G6	G6	0.0	0.022	0.051	M
.....	A.G. Lund 6686.....	16 13.2	+38 53	8.0	0.026‡	K3	G9	0.9	0.004		
4150.....		16 13.3	−19 58	6.4	0.026	G5	G5	0.3	0.006		
4152.....		16 14.0	+66 37	8.2	0.011	K2	G8	1.2	0.004		
4157.....	20 Urs. Min.....	16 15.0	+75 28	6.5	0.041	K2	K1	0.7	0.007		
4159.....		16 15.6	+60 0	5.6	0.022	Mb	G6	−0.3	0.007		
C2184.....	Lal. 29917.....	16 16.5	+67 29	8.9	0.505	K0	K4	8.0	0.066	0.117	D, Y
4163.....	σ Serpentis.....	16 17.0	+ 1 16	4.8	0.172	A9		1.5	0.022	0.031	A
4165.....	γ Herculis.....	16 17.5	+19 23	3.8	0.062	A7		1.4	0.033	0.017	A
4169.....	ξ Cor. Bor.....	16 18.2	+31 7	4.7	0.132	G9	G9	0.7	0.016	0.014	A
4173.....	ν^1 Cor. Bor.....	16 18.6	+34 2	5.4	0.049	Ma	G9	0.3	0.010		
4175.....	ν^2 Cor. Bor.....	16 18.7	+33 56	5.3	0.055	K0	K2	0.6	0.012		
.....	A.G. Leiden 5784.....	16 19.2	+32 52	7.9	0.011‡	K4	K0	0.7	0.004		
4181.....	η Urs. Min.....	16 20.4	+75 59	5.0	0.261	A8		1.7	0.022		
.....	A.G. Leiden 5792.....	16 20.7	+32 42	8.1	0.038‡	K4	K1	0.7	0.003		
.....	A.G. Berlin 5877.....	16 21.0	+17 32	7.9	0.019‡	G0	F9	3.2	0.012		
4188.....		16 22.3	− 7 22	5.4	0.176	Mb	G8	−0.5	0.007		

4192	η Draconis	$16^h22^m.6$	$+61°44'$	2.9	0".062	G6	G5	0.7	0".036	0".019	M, F
4193	α Scorpii	16 23.3	−26 13	1.2	0.034	Ma	G2	−2.7	0.017	0.029	C
4195		16 23.5	+ 0 53	5.5	0.076	K5	K3	0.5	0.010	0.016	W
C2199	Bu. 7642	16 24.5	+18 37	7.8†	0.508	K3	K2	6.6	0.058	0.088	Y
4202	ϕ Ophiuchi	16 25.4	−16 24	4.4	0.066	G5	G6	−0.3	0.012		
C2201	Lal. 30044	16 25.6	+ 4 26	7.4	1.450	F7	F6	4.0	0.021	0.025	A, Y, F
4204	β Herculis	16 25.9	+21 42	2.8	0.107	G5	G6	−1.0	0.017	0.020	F
4206	ω Ophiuchi	16 26.2	−21 15	4.6	0.033	A7		1.7	0.026		
C2202	Groom. 2354	16 27.4	+48 11	7.0	0.301	F7	F8	3.8	0.023	0.001	A
4211	31 Herculis	16 27.8	+33 44	6.7	0.039	K4	K1	0.5	0.006		
4212	29 Herculis	16 27.9	+11 42	4.9	0.204	K6	K2	0.5	0.013	−0.012	A
4222	12 Ophiuchi	16 31.1	− 2 7	5.9	0.546	Ko	G9	5.6	0.087	0.088	A
C2214	Lal. 30271	16 32.6	+31 9	7.3	0.482	F7	F6	4.1	0.023	0.054	A, D, Y
4228		16 33.3	+46 49	6.0	0.020	G6	G6	−0.3	0.007		
.....	B.D. $+51°$ 2121	16 34.2	+51 45	9.6	0.119	G3	G2	4.8	0.011	0.017	K
4234		16 34.9	+77 39	6.4	0.286	G8	G6	2.4	0.016		
4239	24 Scorpii	16 35.8	−17 33	5.0	0.025	G5	G5	−0.4:	0.008		
4242	42 Herculis	16 36.0	+49 7	5.1	0.044	Ma	G9	−0.3	0.008		
4246	ζ Herculis Br.	16 37.5	+31 47	3.0	0.604	G1	G1	2.4	0.076	0.114	A, Ye, S, *et al.*
4255	η Herculis	16 39.5	+39 7	3.6	0.101	G5	G5	0.9	0.029	0.056	A, M, R, F
4257	41 Herculis	16 40.1	+ 6 17	6.7	0.352	G8	G8	4.7	0.040	0.024	A, Ye
4259	18 Draconis	16 40.2	+64 47	5.0	0.017	K1	G8	1.4	0.019		
4262		16 40.8	+15 56	5.8	0.054	Mb	G9	0.8	0.010	0.022	W
4264	43 Herculis	16 41.0	+ 8 46	5.4	0.016	K5	K3	0.8	0.012		
C2238	W.B. 16^h1259	16 41.4	+33 41	8.6	0.37	K8	K5	9.0	0.120	0.190	D
C2242	Lal. 30699	16 42.9	+68 16	7.6	0.509	G9	G6	5.4	0.036	0.047	Y
4270		16 43.4	+56 58	4.9	0.062	Fo	F1	2.3	0.030		
4273	20 Ophiuchi	16 44.3	−10 36	4.7	0.133	F5	F5	2.7	0.040		
.....	Bu. 7778	16 46.4	+ 9 34	7.0†		F6	F6	3.1	0.017	0.001	A
.....	Bu. 7783	16 47.9	+28 49	6.7†		F4	F6	3.4	0.022	0.024	A, Ye, S

TABLE VII—*Continued*

Boss	Name	α 1900	δ 1900	Harv. Vis. Mag.	μ	Spectrum		Spect. Abs. Mag.	Spect. π	Trig. π	Auth.
						Est.	Meas.				
C2248	Lal. 30694	16^h47^m9	+ 0°11′	6.8	1.″664	Ko	G6	5.8	0.″063	0.″099	A, Y, F
C2251	W.B. 16^h906	16 50.1	− 8 9	9.2	1.234	Md		10.1	0.151	0.150	Ye, Y
4303		16 50.3	−16 39	6.5	0.089	Ko	Ko	4.1	0.033		
4305		16 50.4	+43 0	6.7	0.349	F9	G0	4.0	0.029	0.031	A
4307		16 50.6	+21 7	5.5	0.059	G7	G6	0.9	0.012	0.001	W
4311	54 Herculis	16 51.0	+18 36	5.6	0.106	K0	K3	0.3	0.009	0.008	A
4315	κ Ophiuchi	16 52.9	+ 9 32	3.4	0.295	K2	K0	0.6	0.028		
4316	57 Herculis	16 53.4	+25 30	6.7	0.008	G5	G5	0.8	0.007		
4318		16 53.8	−24 56	5.9	0.022	Ma	K1	0.2	0.007		
4322	19 Draconis	16 55.5	+65 17	4.8	0.252	F7	F8	3.6	0.058	0.087	A
4323	30 Ophiuchi	16 55.8	− 4 4	5.0	0.103	K5	K3	0.2	0.011		
4326	29 Ophiuchi	16 56.0	−18 44	6.4	0.052	K0	G8	2.1	0.014		
4327	ε Urs. Min	16 56.2	+82 12	4.4	0.015	G2	G2	−1.4	0.007		
4330	32 Ophiuchi	16 58.5	+14 14	5.1	0.070	Mb	K0	−0.1	0.009		
C2277	Lal. 31132	16 59.8	+47 12	6.7	0.856	K0	G4	6.0	0.072	0.090	A, Y
4342		16 59.8	− 4 54	7.9	1.464	K5	K5	7.9	0.100	0.060	Ye, Y, F
4343		16 59.9	+35 33	6.8	0.058	Mb	G7	0.1	0.005	0.009	W
C2279	Lal. 31065	17 0.2	+ 0 51	5.9	0.321	G0	F9	4.1	0.044	0.039	A
4354	μ Draconis S.	17 3.3	+54 36	5.8	0.108	F5	F5	3.0	0.028		
4354	μ Draconis N.	17 3.3	+54 36	5.8	0.108	F5	F6	2.9	0.026		
.....	Groom. 2420	17 3.4	+73 27	7.7	0.007	K5	K0	0.7	0.004		
4364		17 6.3	+40 54	5.1	0.053	K3	K2	0.8	0.014		
4370	36 Ophiuchi S.	17 9.2	−26 27	5.3	1.235	K1	K1	6.3	0.158		
4371	36 Ophiuchi N.	17 9.2	−26 27	5.3	1.224	K2	K0	6.3	0.158	0.140	F
4372		17 10.1	−26 24	6.7	1.223	K4	K3	7.3	0.132		

4373.....	α^1 Herculis.....	17h10m1	+14°30′	3.5	0″.030	Mb	G5	−2.3	0″.007	−0″.004	A, M
4374.....	α^2 Herculis.....	17 10.1	+14 30	5.4	0.032	F9	G0	1.7	0.018		
4379.....	41 Ophiuchi.....	17 11.5	− 0 20	4.8	0.065	K2	K1	1.2	0.019		
4381.....	π Herculis	17 11.6	+36 55	3.4	0.025	K4	K1	0.4	0.025	0.017	A
4393.....		17 14.9	+28 56	5.8	0.045	G8	G8	0.6	0.009	0.015	W
C2310.....	Lal. 31528.....	17 15.4	+ 9 34	8.2	0.313	G0	G1	4.3	0.017	−0.017	A
4403.....	72 Herculis.....	17 16.9	+32 36	5.4	1.060	F8	G1	5.5	0.105	0.087	A, S, Y, F
4413.....		17 18.7	−21 21	6.0	0.045	G8	G5	1.7	0.014		
4414.....		17 19.0	−24 9	6.3	0.004	K1	G8	1.3	0.010		
4420.....	44 Ophiuchi.....	17 20.3	−24 5	4.3	0.132	A9	F0	1.6	0.029		
C2322.....	W.B. 17h322.....	17 20.8	+ 2 14	7.9	1.315	K5	K6	8.0	0.105	0.132	Ye, R, Y, F
4423.....		17 21.3	− 5 0	5.0†	0.104	F1	F3	2.1	0.026		
4424.....		17 21.4	−12 25	6.3	0.075	F6	F6	3.1	0.023		
4425.....	σ Ophiuchi.....	17 21.6	+ 4 14	4.4	0.004	K1	G8	0.7	0.018		
4433.....	Bu. 8038.....	17 25.2	− 0 59	6.0†	0.215	G6	G5	5.0	0.063	0.065	Ye, S
C2333.....	Lal. 32047.....	17 25.3	+67 23	6.3	0.536	K0	G8	5.9	0.083	0.071	A, G, Y
.....	Lal. 31905.....	17 26.5	+ 1 45	7.2		K2	K3	2.1	0.010	0.039	Y
4438.....	λ Herculis.....	17 26.7	+26 11	4.5	0.021	K2	K1	0.4	0.015		
4443.....	β Draconis §.....	17 28.2	+52 23	3.0	0.016	Gop	F8	−3.5	0.005	0.005	A, M
4447.....		17 29.2	+16 23	5.7	0.058	G9	G8	1.8	0.017		
C2341.....	Bu. 8068 C.....	17 29.9	+ 6 4	8.6	0.623	F6	F8	3.8	0.011	−0.004	Y
.....	Bu. 8068 A.....	17 30.0	+ 6 6	7.9	0.070*	F8	F7	3.8	0.015		
4464.....	27 Draconis.....	17 32.4	+68 12	5.2	0.138	G9	G9	1.1	0.015		
C2347.....		17 33.4	+18 37	9.1	1.39	K0	K5	9.7	0.132	0.128	Ye
4470.....	26 Draconis.....	17 34.0	+61 57	5.3	0.563	G0	G0	4.0	0.055	0.084	A, Ye, M, Y
.....	B.D. +18° 3424.....	17 34.3	+18 37	9.4		K2	K0	6.1	0.022	0.008	Ye
.....	7: 1917 Serpentis*.....	17 34.3	−11 53	10.5		A8p		2.9	0.003		
C2351.....	A.G. Chris. 2703.....	17 35.8	+68 52	8.5	0.150	K0	G0	3.3	0.009		
C2353.....	Lal. 32322.....	17 36.3	+37 16	8.5	0.945	F7	F9	4.1	0.013		
C2354.....	A.Oe. 17415.....	17 37.0	+68 26	9.5	1.334	Mb		10.5	0.158	0.254	Ye, G, F, *et al.*

TABLE VII—*Continued*

Boss	Name	α 1900	δ 1900	Harv. Vis. Mag.	μ	Spectrum Est.	Spectrum Meas.	Spect. Abs. Mag.	Spect. π	Trig. π	Auth.
4480	Bu. 8114 Br.	17h37m0	+24°34′	6.5	0″.052	K2	K1	0.8	0″.007	0″.022	W
	Bu. 8114 Ft.	17 37.0	+24 34	8.6	0.052	F0	F1	2.5	0.006		
	B.D. +68° 947	17 37.2	+68 27	8.0		F2	F4	2.4	0.008	0.011	Ye
4483	ω Draconis	17 37.5	+68 48	4.9	0.327	F2	F3	2.8	0.038	0.045	A
4487	β Ophiuchi	17 38.5	+ 4 37	2.9	0.158	K2	K1	0.6	0.035	0.025	A, M
C2358	Lal. 32390	17 39.0	+21 40	7.4	0.623	G8	G7	5.8	0.048		
4488	84 Herculis	17 39.3	+24 22	5.7	0.132	G2	G2	3.3	0.033	0.006	A
4493	X Sagittarii §	17 41.3	−27 48	4.7	0.023	F0p	F8	−1.3	0.006		
4497	μ Herculis A	17 42.5	+27 47	3.5	0.817	G5	G5	3.7	0.110	0.105	A, M, Y, *et al.*
4504	ψ Draconis Br.	17 43.7	+72 12	4.9	0.267	F3	F6	3.1	0.044	0.030	A
4505	ψ Draconis Ft.	17 43.7	+72 12	6.1	0.279	F7	F9	3.7	0.033		
4508	87 Herculis	17 44.8	+25 39	5.3	0.046	K1	G9	1.6	0.018		
	Groom. 2485	17 50.9	+42 40	7.6	0.004	K0	G7	2.4	0.009		
4530		17 51.6	+22 29	5.7	0.002	K2	K0	0.3	0.008		
4531	ξ Draconis	17 51.8	+56 53	3.9	0.123	K3	K1	0.7	0.023	0.026	A
4535	θ Herculis	17 52.8	+37 16	4.0	0.006	G9	G7	−0.3	0.014	0.000	A
4536	ν Ophiuchi	17 53.5	− 9 46	3.5	0.118	G7	G8	−0.2	0.018	0.029	M
	Z Herculis	17 53.6	+15 9	7.6		F2p	F5	2.7	0.011	0.033	Ye
4538	ξ Herculis	17 53.9	+29 16	3.8	0.090	G7	G5	0.9	0.026	0.025	A
4539	35 Draconis	17 53.9	+76 59	5.0	0.244	F5	F6	3.2	0.044	0.012	A, G
4541	γ Draconis	17 54.3	+51 30	2.4	0.027	K5	K1	0.6	0.044	0.012	A, M, F, *et al.*
4542	ν Herculis §	17 54.7	+30 12	4.5	0.004	F2p	F3	−0.2	0.012		
4544	ρ Serpentis	17 55.2	− 3 41	4.6	0.153	F0	F3	1.9	0.029		
4546	6 Sagittarii	17 55.6	−17 9	6.3	0.012	K1	G7	0.2	0.006		
4547	93 Herculis	17 55.6	+16 45	4.7	0.012	K2	G8	−0.3	0.010		

4554	34 Draconis	17^h56^m9	+72° 1′	5.5	0″.009	F4	F5	1.7	0″.017		
4555		17 57.1	+45 30	5.9	0.044	K6	K3	0.6	0.009	0″.026	W
4556	95[1] Herculis	17 57.3	+21 36	5.2	0.030	G1	G2	−0.3	0.008		
C2388	W.B. 17^h1805	17 58.4	+26 20	7.1	0.72	K1	K0	6.0	0.060	0.040	A
4564	W Sagittarii §	17 58.6	−29 35	4.7	0.015	G0p	F5	−2.0	0.004		
4571	70 Ophiuchi Br	18 0.4	+ 2 31	4.3	1.131	K0	G9	5.8	0.200	0.187	A, M, Ye, *et al.*
4571	70 Ophiuchi Ft	18 0.4	+ 2 31	6.0	1.131	K4	K7	7.2	0.174		
C2392	W.B. 17^h1236	18 0.7	+ 4 39	6.8	0.296	G1	G0	5.4	0.052	0.053	A
	Groom. 2506	18 1.4	+42 51	7.5	0.035	K2	G8	1.1	0.005		
C2396	Pi. 17^h368	18 2.1	+ 8 52	7.7	0.152	F7	F7	3.2	0.013	0.009	A
4580	71 Ophiuchi	18 2.5	+ 8 43	4.7	0.025	G6	G7	−0.1	0.011		
4582	99 Herculis	18 3.2	+30 33	5.2	0.113	F5	F7	4.4	0.069	0.045	M, S, Ye, *et al.*
	W Serpentis §*	18 4.1	−15 34	9.0		F9p	G0	−0.6	0.001		
4593		18 4.6	+36 23	5.7	0.213	K3	K1	0.6	0.010		
4595		18 4.9	+ 3 6	5.7	0.205	F4	F5	2.8	0.026	0.085	A
	Groom. 2521	18 5.9	+43 33	8.1	0.017	K1	G8	1.3	0.004		
C2403	Lal. 33439	18 6.3	+38 27	6.4	0.58	K3	K2	6.5	0.105	0.082	A, Y
4601		18 6.5	+36 27	5.9	0.009	G7	G6	1.0	0.011		
4606	104 Herculis	18 8.1	+31 23	5.0	0.018	Ma	K0	−0.1	0.010		
4609		18 8.5	+54 15	5.9	0.274	G9	G9	2.8	0.024	0.012	A
	A.G. Leiden 6547	18 8.5	+33 16	7.1	0.020‡	K6	K1	0.5	0.005		
4618		18 11.6	− 3 2	6.1	0.274	G2	G2	−0.3	0.005		
4623	36 Draconis	18 13.3	+64 22	5.0	0.346	F2	F4	3.5	0.050		
4629	105 Herculis	18 15.1	+24 24	5.5	0.016	K2	K0	0.2	0.009	0.002	W
4630		18 15.4	−24 58	6.4	0.011	Mc	G5	0.8	0.007		
4632	Y Sagittarii §	18 15.5	−18 54	5.8	0.013	G2p	F8	−1.6	0.003		
4635	74 Ophiuchi	18 15.9	+ 3 20	4.9	0.015	G5	G7	−0.5	0.008		
4636	106 Herculis	18 16.1	+21 55	5.0	0.062	K6	K3	0.2	0.011		
4638	η Serpentis	18 16.1	− 2 55	3.4	0.898	G8	G7	2.5	0.066	0.057	Y, J
4647		18 17.6	+51 18	6.2	0.062	K1	K0	0.7	0.008	0.036	W

TABLE VII—*Continued*

Boss	Name	α 1900	δ 1900	Harv. Vis. Mag.	μ	Spectrum		Spect. Abs. Mag.	Spect. π	Trig. π	Auth.
						Est.	Meas.				
.....	A.G. Leip. 8449.....	$18^h18^m.0$	+ 7° 9′	7.6	0″.012‡	K2	K1	0.8	0″.004		
4650.....	ζ Scuti.....	18 18.2	− 8 59	4.8	0.062	G8	G8	0.4	0.013		
4656.....	109 Herculis.....	18 19.4	+21 43	3.9	0.324	K1	K0	1.5	0.033	0″.015	A, Jo
.....	Groom. 2557.....	18 19.9	+43 53	8.2	0.001	G8	G7	1.1	0.004		
.....	A.G. Leip. 8478.....	18 20.3	+ 9 41	7.9	0.016‡	K3	G8	0.8	0.004		
4660.....		18 20.8	+ 7 59	5.7	0.004	G0	G0	−0.8	0.005		
C2420.....	B.D. +8° 3689.....	18 21.4	+ 8 44	7.9	0.55	G5	G4	5.5	0.033	0.033	A, K
C2421.....	B.D. +8° 3692.....	18 21.6	+ 8 34	8.5	0.47	G9	G6	5.2	0.022	0.041	A, K
4665.....	λ Sagittarii.....	18 21.8	−25 29	2.9	0.197	K0	G0	3.2	0.115	0.069	F
.....	A.G. Leip. 8507.....	18 22.0	+ 8 3	8.9	0.151	G2	G1	5.7	0.023	0.015	K
4672.....	χ Draconis.....	18 22.9	+72 41	3.7	0.638	F5	F6	4.1	0.120	0.105	M, G, Y
C2423.....	Groom. 2571.....	18 23.7	+46 1	8.3	0.398	G0	F9	4.5	0.017	0.006	A
4678.....	60 Serpentis.....	18 24.5	− 2 3	5.4	0.038	G9	G9	1.7	0.018		
.....	Groom. 2577.....	18 25.3	+44 11	7.7	0.014	K3	K0	1.0	0.005		
4686.....	42 Draconis.....	18 25.7	+65 30	5.0	0.104	K1	G9	1.3	0.018		
.....	U Sagittarii §.....	18 26.0	−19 12	6.9	0.012‖	G0p	F7	−1.4	0.002		
.....	A.G. Leip. 8585.....	18 26.1	+ 8 1	7.6	0.029‡	Ma	K0	1.5	0.006		
4688.....		18 26.3	+59 29	6.5	0.061	G8	G7	2.8	0.018		
4701.....		18 28.6	+23 33	6.0	0.011	K4	K1	0.4	0.008		
4705.....	1 Aquilae.....	18 29.8	− 8 19	4.1	0.318	K4	K1	0.6	0.020		
.....	Groom. 2622.....	18 31.6	+65 18	8.7	0.023	F0		2.4	0.006		
4711.....		18 31.7	+52 16	5.4	0.008	G7	G7	−0.4	0.007		
4713.....		18 31.8	+ 6 36	5.4	0.146	F0	F1	1.6	0.017	0.024	A
.....	Bu. 8679.....	18 33.2	− 3 17	7.1†		G0	F8	4.6	0.032	0.035	Ye
4723.....		18 34.5	+63 37	8.1	0.254	F7	F7	4.0	0.015	0.028	A

4724		18h34m6	+77°28′	5.8	0″.006	K2	G8	0.6	0″.009		
4731	2 Aquilae	18 36.8	− 9 9	4.7	0.014	F5	F3	1.3	0.021		
C2450	W.B. 18h1064	18 37.1	+31 28	8.8	0.82	K3	K2	6.6	0.036	0″.033	A
4750		18 41.2	−10 14	5.8	0.005	F6	F3	1.1	0.012		
4753	110 Herculis	18 41.4	+20 27	4.3	0.345	F4	F6	3.3	0.063	0.057	A, M, Jo
C2456	Bu. 8798 Br	18 41.7	+59 29	8.8	2.307	Mb		10.7	0.240	0.289	Ye, D, R, *et al.*
4758		18 42.0	+26 33	4.9	0.029	K1	G9	1.5	0.021		
4763	Bu. 8825	18 43.1	+60 57	6.3†	0.010	K0	G7	1.6	0.012		
.....	YZ Sagittarii §	18 43.7	−16 50	7.4		G1p	F9	−2.7	0.001		
C2462	Lal. 34986	18 43.8	+10 39	8.0	0.463	K4	K4	6.8	0.058	0.062	A, Y
.....	Lal. 34958	18 44.1	−10 29	7.9		K2	K1	4.9	0.025		
.....	Bu. 8849	18 44.9	+49 20	7.8†.		F2	F3	1.4	0.005	0.017	Ye
4780	33 Sagittarii	18 48.0	−21 29	5.8	0.012	G0	G5	0.2	0.008		
4787		18 49.3	+52 51	5.6	0.288	G8	G8	3.2	0.033	0.048	A
4790	o Draconis	18 49.7	+59 16	4.8	0.086	G8	G4	−0.5	0.009		
4797	113 Herculis	18 50.5	+22 31	4.6	0.005	F9	G0	1.7	0.026		
4800	12 Lyrae	18 51.0	+36 46	4.5	0.010	Mb	G4	−1.2	0.007		
4805		18 51.7	+41 28	5.6	0.007	G8	G9	0.0	0.008		
4809	37 Sagittarii	18 51.8	−21 14	3.6	0.037	K0	K0	0.7	0.026		
4814	R Lyrae	18 52.3	+43 49	4.3	0.077	Mc	G8	−1.4	0.007	0.028	Ab
C2475	Mün. 18180	18 53.1	+ 5 48	9.8	1.247	Ma	K6	9.7	0.095	0.069	A, R
4815		18 53.3	+32 46	5.2	0.235	G0	F9	4.8	0.083	0.095	A, S, F, J
4817		18 53.8	+17 14	5.4	0.009	F8	F7	0.3	0.010	0.001	W
4823	ε Aquilae	18 55.1	+14 56	4.2	0.100	K1	K0	1.0	0.023		
.....	A.G. Berlin 7148	18 56.2	+18 20	8.0	0.017	G7	G4	1.7	0.006		
4834	12 Aquilae	18 56.3	− 5 53	4.2	0.048	K1	K0	2.0	0.036		
4847	o Sagittarii	18 58.7	−21 53	3.9	0.098	G8	G9	1.3	0.030		
4852	15 Aquilae Ft	18 59.7	− 4 11	7.2	0.037	K5	K4	0.8	0.005		
4860		19 1.2	+31 36	5.8	0.085	K5	K1	0.7	0.010	0.026	W
C2492	B.D. +7° 3967	19 2.2	+ 7 29	9.5	0.812	K5	K3	7.8	0.046	0.040	Ye

TABLE VII—*Continued*

Boss	Name	α 1900	δ 1900	Harv. Vis. Mag.	μ	Spectrum		Spect. Abs. Mag.	Spect. π	Trig. π	Auth
						Est.	Meas.				
.....	TT Aquilae §.....	$19^h\ 3^m.2$	+ 1° 0′	7.6		G2p	F0	−1.4	0″.002		
C2495.....	Lal. 35851.....	19 3.5	+16 42	6.0	0″.308	G4	G4	3.7	0.035	0″.063	A
4874.....	π Sagittarii §.....	19 3.8	−21 11	3.0	0.040	F4p	F3	−0.8	0.017	0.017	M
4880.....		19 6.5	−21 49	6.4	0.032	K0	K0	1.4	0.010		
C2507.....	Bu. 9114 A.....	19 7.7	+38 37	8.2	0.267	G4	G6	5.5	0.029	0.023	M, S
C2507.....	Bu. 9114 BC.....	19 7.7	+38 37	8.7†	0.267	K0	G0	5.8	0.026		
C2508.....	Bu. 9116 C.....	19 8.0	+16 41	7.6	0.243	G6	G7	5.0	0.030	0.021	M
4892.....	Bu. 9137 Ft.....	19 9.5	+49 40	6.8	0.630	G4	G2	5.5	0.055	0.045	M, W, R, *et al.*
4893.....	Bu. 9137 Br.....	19 9.5	+49 40	6.6	0.654	G6	G3	5.7	0.066		
.....	Bu. 9136.....	19 10.0	+18 54	7.7†	0.031‡	F7	F7	3.3	0.013		
4898.....		19 10.8	+14 55	5.7	0.020	G8	G7	−1.4	0.004		
4903.....	43 Sagittarii.....	19 11.8	−19 8	5.0	0.023	G7	G6	0.5	0.013		
4909.....	δ Draconis.....	19 12.5	+67 29	3.2	0.133	G8	G7	0.8	0.033	0.035	A
4910.....		19 12.7	+49 54	6.3	0.014	G8	G6	1.5	0.011		
4912.....	θ Lyrae.....	19 12.9	+37 57	4.5	0.010	K0	G7	0.2	0.014		
4915.....		19 13.3	−15 43	6.3	0.285	K3	G9	0.9	0.008		
4919.....	24 Aquilae.....	19 13.7	+ 0 9	6.5	0.009	G9	G7	1.2	0.009		
4920.....		19 14.0	+46 49	6.0	0.285	F4	F6	2.8	0.023	0.018	A
4923.....	κ Cygni.....	19 14.8	+53 11	4.0	0.133	G7	G7	1.1	0.026	0.040	A, Ab
4926.....	26 Aquilae.....	19 15.2	− 5 36	5.1	0.110	G7	G7	2.6	0.032		
4932.....	44 Sagittarii.....	19 15.9	−18 2	4.0	0.031	A8		1.7	0.035	0.049	M
4940.....	τ Draconis.....	19 17.5	+73 10	4.6	0.176	K4	K3	0.5	0.015		
4950.....	31 Aquilae.....	19 20.2	+11 44	5.2	0.961	G8	G6	5.1	0.095	0.067	A, M, Ye, *et al.*
4953.....	δ Aquilae.....	19 20.5	+ 2 55	3.4	0.265	A9		1.8	0.048	0.057	A, M
4961.....		19 21.3	+24 44	6.2	0.658	F6	F4	3.9	0.035	0.060	Y, Jo, F

.....	RR Lyrae §	19h22m3	+42°35′	7.3	0″.221‖	Fop	F3	0.3	0″.004		
.....	U Aquilae §	19 24.0	− 7 15	6.6	0.017‖	Gop	F7	−2.3	0.002		
4976	α Vulpeculae	19 24.5	+24 28	4.6	0.170	Ma	Ko	0.1	0.013		
4978	8 Vulpeculae	19 24.8	+24 34	6.0	0.012	G9	G8	0.7	0.009		
4985		19 26.4	−28 13	7.0	0.741	G6	G4	5.8	0.058		
4986	β^1 Cygni	19 26.7	+27 45	3.2	0.009	Ko	G6	0.8	0.033	0″.000	A, M, Y
.....	Bu. 9401 Br	19 29.0	+20 11	7.4†	0.057*	A7		1.1	0.006	−0.018	A
4995	μ Aquilae	19 29.2	+ 7 10	4.6	0.262	K3	K2	0.7	0.017	0.021	A
C2554	Groom. 2875	19 29.5	+58 23	6.7	0.664	K4	K2	6.7	0.100	0.030	A, Y
C2558	Lal. 37120	19 29.7	+32 59	6.6	0.517	G1	F9	4.4	0.036	0.043	A, M, Y
5005		19 31.7	+51 1	5.8	0.205	F6	F6	3.3	0.032		
.....	U Vulpeculae §	19 32.3	+20 7	7.0	0.031‖	Gop	F9	−2.0	0.002		
5009	σ Draconis	19 32.6	+69 29	4.8	1.840	G9	G7	5.8	0.158	0.192	M, Y, P, *et al.*
5014	θ Cygni	19 33.8	+49 59	4.6	0.249	F2	F5	3.4	0.058	0.070	A, M, Y, *et al.*
5019	54 Sagittarii	19 35.0	−16 31	5.4	0.085	K1	Ko	1.7	0.018		
5021	ϕ Cygni	19 35.4	+29 55	4.8	0.035	G8	G8	0.9	0.017		
5023	α Sagittae	19 35.6	+17 47	4.4	0.036	F9	F8	−0.9	0.009	−0.004	M
5027	β Sagittae	19 36.6	+17 15	4.4	0.038	G8	G7	0.0	0.013		
5031		19 37.8	+45 17	5.0	0.142	F4	F4	1.5	0.020	−0.003	Y
5033	χ Aquilae	19 37.9	+11 35	5.6†	0.013	F5	F7	2.4	0.023		
5037	16^1 Cygni	19 39.2	+50 18	6.3	0.217	G2	G1	5.1	0.058	0.038	A, M, S, Ye
5038	16^2 Cygni	19 39.2	+50 17	6.4	0.204	G3	G3	4.6	0.044		
.....	Bu. 9569	19 39.8	+26 53	6.6	0.062	Go	F9	1.8	0.011	−0.010	A
5043		19 40.4	+41 32	6.0	0.017*	K6	K2	0.4	0.008	0.006	W
5044	56 Sagittarii	19 40.5	−20 0	5.1	0.165	Ko	G9	1.7	0.021		
5045	15 Cygni	19 40.7	+37 7	5.0	0.076	G7	G7	0.1	0.011	0.020	A
.....	SU Cygni §	19 40.8	+29 1	6.6		F7p	F5	−1.1	0.003		
5047	γ Aquilae	19 41.5	+10 22	2.8	0.014	K3	G9	0.3	0.032	0.034	M
C2579	Bu. 9602	19 41.8	+33 22	9.2†	0.433	K4	K2	6.7	0.032	0.041	M
5051	17 Cygni Br	19 42.6	+33 30	5.0	0.452	F6	F5	2.9	0.038	0.045	A, M, Y
5051	17 Cygni Ft	19 42.6	+33 30	8.1	0.452	K4	K2	6.5	0.048		

TABLE VII—*Continued*

Boss	Name	α 1900	δ 1900	Harv. Vis. Mag.	μ	Spectrum		Spect. Abs. Mag.	Spect. π	Trig. π	Auth.
						Est.	Meas.				
5052	δ Sagittae	19h42m9	+18°17′	3.8	0″.009	Ma	G1	0.2	0″.019		
C2585	Bu. 9650	19 45.0	+35 4	6.9†	0.119	F4	F4	3.1	0.017	0″.021	S
5063		19 45.9	+38 27	6.2	0.016	G3	G3	−0.5	0.005		
5071	η Aquilae §	19 47.4	+ 0 45	4.1	0.012	F9p	F9	−2.7	0.004	0.004	M
5075	20 Cygni	19 48.1	+52 44	5.2	0.072	K5	K3	0.2	0.010	0.020	Ab
5079	ϵ Draconis	19 48.5	+70 1	4.0	0.087	G2	G5	0.7	0.022		
5082	56 Aquilae	19 48.7	− 8 50	6.0	0.022	K4	K2	0.9	0.010		
5089	ξ Aquilae	19 49.4	+ 8 12	4.9	0.126	G9	G9	0.8	0.015	0.039	M
5093	β Aquilae	19 50.4	+ 6 9	3.9	0.484	G8	G7	3.9	0.100	0.076	A, M, S
5096		19 51.2	+36 44	5.8	0.008	F6	F6	0.9	0.011		
5098	S Sagittae §	19 51.5	+16 22	5.8	0.004	G1p	F8	−2.5	0.002		
5103	η Cygni	19 52.6	+34 49	4.0	0.052	K0	G9	1.8	0.036		
5116		19 54.0	+58 35	5.1	0.025	K5	K1	0.4	0.012		
5118	γ Sagittae	19 54.3	+19 13	3.7	0.062	K0	K2	0.5	0.023	0.005	A
5119		19 54.4	−10 13	5.9	0.488	F8	F8	4.2	0.046	−0.004	Y
C2607	Lal. 38139	19 55.5	−12 31	7.6	0.504	F6	F6	4.5	0.024		
5125	13 Sagittae	19 55.6	+17 15	5.6	0.015	Mc	G6	0.5	0.010		
5129	62 Sagittarii	19 56.5	−27 59	4.6	0.037	Mb	G7	0.3	0.014		
C2616	Lal. 38287	19 58.0	+15 20	7.2	0.608	G8	G5	5.6	0.048	0.085	M, Y
5142	62 Aquilae	19 59.2	− 0 59	5.8	0.119	K1	G7	1.7	0.015		
5143	τ Aquilae	19 59.3	+ 7 0	5.6	0.025	G8	G7	0.0	0.008		
5144		19 59.5	+29 38	5.7	0.853	G7	G7	4.8	0.066	0.049	A, Y, F
5146	15 Sagittae	19 59.6	+16 48	5.9	0.578	G1	G0	5.0	0.066	0.104	Y, Jo
C2620	Lal. 38383	19 59.7	+23 5	7.2	1.369	K2	K0	6.6	0.076	0.059	A, M, Y, *et al.*

5149.....	64 Draconis.....	20h 0m.4	+64° 32′	5.4	0″.015	Ma	G8	−0.1	0″.008		
5153.....	ρ Draconis.....	20 2.4	+67 35	4.7	0.051	K2	K1	0.7	0.016		
5157.....	27 Cygni.....	20 2.6	+35 42	5.5	0.496	G8	G6	4.1	0.052	0″.050	Ye
5163.....		20 3.6	+52 52	5.7	0.334	F4	F4	3.9	0.044	0.066	Ab, Y
.....	B.D. +36° 3883.....	20 3.7	+36 17	7.1		Ma	G7	1.0	0.006	−0.004	M
5166.....		20 4.6	−36 21	5.3	1.626	K3	Ko	6.7	0.190		
5167.....	17 Sagittae C.....	20 5.5	+20 36	7.3	0.011	K1	Ko	2.9	0.013	0.028	S
5169.....	17 Sagittae A.....	20 5.5	+20 37	6.3	0.111	F2	F2	3.0	0.022	0.019	S
C2634.....	Pi. 20h23.....	20 6.6	+15 53	7.3	0.578	K2	K1	6.0	0.055	0.065	Y, M
5176.....	2 Capricorni.....	20 6.9	−12 55	5.9	0.269	F4	F4	3.8	0.038		
.....	Bu. 9979.....	20 7.1	+43 39	7.7†		G5	G3	5.1	0.030	0.049	S
5177.....	19 Vulpeculae.....	20 7.6	+26 31	5.8	0.020	K3	G8	0.5	0.009		
.....	A.G. Berlin 8022.....	20 8.2	+15 47	7.6	0.016	F6	F7	3.4	0.014		
5180.....		20 9.1	−27 20	5.7	1.256	K2	K2	5.9	0.110	0.042	F, V
5184.....	68 Draconis.....	20 9.9	+61 47	5.7	0.155	F6	F5	3.0	0.029	0.037	W
5187.....	o^2 Cygni.....	20 10.5	+46 26	4.0	0.002	G9p	G1	−2.0	0.006	−0.002	A, M
C2645.....	Bu. 10044 A.....	20 11.0	+52 49	7.2†	0.179	F5	F7	3.4	0.017	0.016	A
5197.....	α^1 Capricorni §.....	20 12.1	−12 49	4.6	0.015	Gop	F7	−3.9	0.002	−0.012	M
5201.....	24 Vulpeculae.....	20 12.5	+24 22	5.4	0.027	G7	G5	0.5	0.011	−0.027	A
5202.....	α^2 Capricorni.....	20 12.5	−12 51	3.8	0.058	G8	G6	1.2	0.030	−0.012	M
5206.....	σ Capricorni.....	20 13.6	−19 26	5.5	0.011	K2	Ko	1.3	0.014		
5216.....	β Capricorni.....	20 15.4	−15 6	3.2	0.035	F8	F7	0.3	0.026	0.007	M
.....	Bu. 10135 Ft.....	20 15.9	+55 5	7.4	0.021	F3	F3	2.8	0.012		
5219.....		20 16.5	+66 32	6.1	0.557	G2	G1	5.2	0.066	0.120	Y, J
C2654.....	A.Oe. 20452.....	20 17.7	−21 40	8.2	1.182	F6	F7	3.7	0.013	0.044	F, V
5229.....	γ Cygni §.....	20 18.6	+39 56	2.3	0.003	Gop	Go	−3.0	0.009	0.014	A, M, Y, F
5231.....		20 19.2	+40 42	6.1	0.054	K6	Ko	0.2	0.007		
5235.....	39 Cygni.....	20 19.9	+31 52	4.6	0.041	K5	K2	0.5	0.015		
5244.....	ρ Capricorni A §.....	20 23.2	−18 9	5.1	0.026	A9	Fo	−1.0	0.010	0.024	M
5255.....	41 Cygni §.....	20 25.3	+30 2	4.1	0.010	F6	F4	−1.1	0.009	−0.018	M

TABLE VII—*Continued*

Boss	Name	α 1900	δ 1900	Harv. Vis. Mag.	μ	Spectrum Est.	Spectrum Meas.	Spect. Abs. Mag.	Spect. π	Trig. π	Auth
5256		20^h25^m5	−15°23′	6.2	0″.073	G2	G2	−0.2	0″.005		
5263		20 26.9	−10 12	5.8	0.317	G3	G2	4.9	0.066	0″.035	F
5267	44 Cygni	20 27.2	+36 36	6.3	0.013	F6	F6	0.8	0.008		
5276		20 29.5	+56 26	6.3	0.021	K4	K0	0.8	0.008		
C2667	Groom. 3215	20 29.3	+41 33	7.0	0.475	K0	G7	6.0	0.063	0.017	A, Y, Jo
5280		20 30.4	+72 12	6.4	0.025	K4	K2	0.8	0.008		
5284	70 Aquilae	20 31.5	− 2 54	5.2	0.011	K4	G8	1.0	0.014		
	V Vulpeculae §	20 32.3	+26 11	8.6		G7p	G9	−0.8	0.001		
5291	β Delphini	20 32.9	+14 15	4.0†	0.113	F3	F5	2.3	0.046	0.027	M, S, Ye, F
C2672	Lal. 39816	20 34.2	−24 8	6.3	0.658	G8	G7	6.2	0.095		
5304	κ Delphini	20 34.3	+ 9 44	5.2	0.315	G2	G1	3.4	0.044		
5305	1 Aquarii	20 34.3	+ 0 8	5.4	0.094	G9	G9	1.6	0.017		
C2673	Groom. 3243	20 34.4	+42 29	7.1	0.197	F6	F6	3.2	0.017	0.000	A
5306	υ Capricorni	20 34.4	−18 29	5.3	0.035	Ma	G7	0.2	0.010		
C2676	Lal. 39866	20 34.6	+ 4 37	8.4	0.844	K5	K4	8.0	0.083	0.061	A, Ye, Y
5317	10 Delphini	20 36.6	+14 14	6.2	0.012	K3	K0	1.0	0.009		
5319	49 Cygni	20 37.0	+31 57	5.9†	0.018	G8	G4	0.0	0.007		
	A.G. Berlin 8332	20 37.6	+19 30	7.5	0.009	K1	G8	2.0	0.008		
5321		20 38.2	+60 9	6.0	0.186	F5	F6	3.6	0.033	0.049	Y, Ab
	X Cygni §	20 39.5	+35 14	6.5	0.018	G3p	G0	−2.1	0.002	0.006	S
	A.G. Leiden 8454	20 41.1	+31 25	8.0	0.015	K1	G9	1.5	0.005		
5331	52 Cygni	20 41.5	+30 21	4.3	0.027	G8	G7	1.2	0.024	0.014	M
	Bu. 10504 Br.	20 41.5	+15 32	7.5	0.121*	G8	G6	5.5	0.040	0.016	A
	Bu. 10504 Ft.	20 41.5	+15 32	8.2	0.100*	G6	G7	5.3	0.026		
5334	γ^1 Delphini Ft.	20 42.0	+15 46	5.5	0.195	F6	F7	3.0	0.032	0.026	M, S
5335	γ^2 Delphini Br.	20 42.0	+15 46	4.5	0.207	K1	K1	1.1	0.021		

5336	ϵ Cygni	$20^h42^m.2$	$+33°36'$	2.6	0".483	G7	G7	0.8	0".044	0".036	A, M, F, J
5338	3 Aquarii	20 42.5	− 5 24	4.6	0.039	Ma	Ko	0.4	0.014		
5344		20 42.9	+57 13	4.6	0.241	F8	F8	3.5	0.060	0.032	A, Y
5346	η Cephei	20 43.3	+61 27	3.6	0.826	G8	G8	3.2	0.083	0.092	A, M, Ye, *et al.*
5370	T Vulpeculae §	20 47.2	+27 53	5.8	0.015	F9	F7	−1.7	0.003		
5373	31 Vulpeculae	20 47.8	+26 43	4.8	0.103	G2	G3	−1.6	0.005		
5379	32 Vulpeculae	20 50.3	+27 41	5.2	0.009	K5	K3	0.5	0.012		
5385	17 Delphini	20 50.9	+13 20	5.4	0.023	Ko	G7	0.4	0.010		
C2707	A.Oc. 21338	20 51.3	+61 48	8.6	0.77	Ma	K5	9.4	0.144	0.139	A
5388		20 52.1	+80 11	5.6	0.040	Ko	G9	1.6	0.016		
C2709	Fed. 3638	20 52.4	+74 23	7.9	0.691	G6	G4	5.3	0.030	0.015	A Y, F
	Groom. 3359	20 53.6	+69 34	7.8	0.020	G9	G5	1.7	0.006		
5397	33 Vulpeculae	20 53.8	+21 56	5.6	0.005	K4	Ko	1.0	0.012		
5399	ϵ Equulei AB	20 54.1	+ 3 55	6.0†	0.191	F1	F4	2.4	0.019	0.019	M, S
5399	ϵ Equulei C	20 54.1	+ 3 55	7.4		F2	F2	3.3	0.015		
5409	Bu. 10659	20 55.9	+18 56	6.2†	0.075	Ma	K1	0.5	0.007	0.009	W
C2718	Groom. 3357	20 56.1	+39 52	6.6	0.314	F7	F8	3.9	0.039	0.040	Ye, Jo
	A.G. Leiden 8661	20 58.8	+31 57	7.2	0.014‡	K4	G9	0.5	0.005		
C2728	W.B. 20^h1454	20 59.1	+ 2 36	8.1	0.485	F6	F7	3.9	0.014	−0.015	M, Y
5420		20 59.2	+38 16	6.2	0.012	G8	G6	1.5	0.012		
5422	3 Equulei	20 59.6	+ 5 6	5.9	0.019	K3	Ko	1.0	0.011		
C2732	Lal. 40844	21 0.4	+ 6 41	8.9	0.553	K7	K5	8.7	0.091	0.081	Ye, Y
5430	24 Capricorni	21 1.3	−25 24	4.6	0.059	K4	K1	0.7	0.017		
5431	ξ Cygni §	21 1.3	+43 32	3.9	0.007	K2p	G5	−2.9	0.004	−0.003	A
5432		21 2.3	+30 47	5.9	0.010	F7	F6	0.7	0.009		
5433	61^1 Cygni	21 2.4	+38 15	5.6	5.267	K7	K7	8.3	0.347	0.307	A, M, W, *et al*
5434	61^2 Cygni	21 2.4	+38 15	6.3	5.153	K8	K7	8.7	0.302		
5441	ν Aquarii	21 4.1	−11 47	4.5	0.094	G8	G8	2.0	0.032		
	A.G. Leiden 8741	21 4.9	+32 22	8.1	0.023‡	Ko	G6	2.4	0.007		

TABLE VII—*Continued*

Boss	Name	α 1900	δ 1900	Harv. Vis. Mag.	μ	Spectrum		Spect. Abs. Mag.	Spect. π	Trig. π	Auth
						Est.	Meas.				
.....	B.D. +38° 4362.....	21h 5m.2	+38°19′	7.8		K2	G9	1.7	0″.006	−0″.031	R
5443.....	γ Equulei.....	21 5.5	+ 9 44	4.8	0″.169	Fo	Fo	−0.4	0.009		
C2749.....	W.B. 21h97.....	21 7.4	+17 21	7.3	0.915	F4	F3	4.0	0.022	0.032	A, Y, F, J
5452.....	ζ Cygni.....	21 8.7	+29 49	3.4	0.059	G6	G7	−1.1	0.013	0.026	A, M
C2753.....	Fed. 3738.....	21 8.8	+73 18	8.6	0.518	Ko	K1	6.1	0.032		
5455.....	δ Equulei AB.....	21 9.6	+ 9 36	5.1†	0.306	F6	F7	4.0	0.060	0.053	M, F, Hus
5456.....	φ Capricorni.....	21 9.9	−21 4	5.4	0.007	K2	G8	1.1	0.014		
5457.....	29 Capricorni.....	21 10.2	−15 35	5.5	0.019	Mb	G9	0.4	0.010		
5460.....	τ Cygni.....	21 10.8	+37 37	3.8	0.455	F1	F3	1.9	0.042	0.042	A, M, S, *et al.*
5461.....	α Equulei.....	21 10.8	+ 4 50	4.1	0.104	F6	F7	1.9	0.036	0.034	A
C2763.....	Lal. 41348.....	21 12.9	− 0 15	8.6	0.476	K5	K3	7.0	0.048		
.....	A.G. Berlin 8683.....	21 13.8	+17 18	7.6	0.022‡	K1	G9	1.5	0.006		
.....	A.G. Berlin 8684.....	21 13.9	+17 34	7.2	0.016‡	F4	F3	3.5	0.018		
C2769.....	Bu. 10881 Br.....	21 14.0	−26 46	6.6†	0.665	G8	G5	5.6	0.063	−0.100	F
5476.....	16 Aquarii.....	21 15.8	− 4 59	6.0	0.026	G7	G6	1.6	0.013		
5481.....		21 16.5	+58 12	5.8	0.014	F3	F7	1.7	0.015		
5482.....	34 Vulpeculae.....	21 16.6	+23 26	5.8	0.253	G9	G9	0.6	0.009		
5486.....		21 16.8	+76 35	6.2	0.020	K4	K1	0.5	0.007		
5489.....	1 Pegasi.....	21 17.5	+19 23	4.2	0.118	Ko	Ko	1.4	0.028	0.020	A, Ye
5490.....	17 Aquarii.....	21 17.6	− 9 45	6.2	0.050	K4	K2	0.8	0.008		
.....	A.G. Berlin 8723.....	21 18.4	+16 4	7.6	0.022‡	K4	Ko	1.1	0.005		
.....	A.G. Bonn 15400.....	21 18.6	+41 26	9.1		K3	K1	1.2	0.003		
5507.....	ζ Capricorni §.....	21 21.0	−22 51	3.9	0.023	G1p	F9	−3.9	0.003		
5519.....		21 23.9	+31 47	5.7	0.134	Fo	F1	2.9	0.028	0.032	W
C2790.....	W.B. 21h502.....	21 24.5	−12 56	9.4	1.052	K6	K6	8.5	0.066		

5522	2 Pegasi	21h25m4	+23°12′	4.8	0″017	K4	K2	0.6	0″014		
5523	71 Cygni	21 25.8	+46 6	5.3	0.114	G9	G8	1.5	0.017	0″036	A, S, Ye, Ab
C2797	W.B. 21h594	21 26.0	+45 27	7.9	0.056	G8	G7	5.6	0.035	0.025	A
5527	β Aquarii §	21 26.3	− 6 1	3.1	0.017	F9	F8	−2.1	0.009	−0.016	M, F
	B.D. +45° 3566	21 26.8	+46 6	8.3		Fo	Fo	2.0	0.006		
	Groom. 3502	21 30.0	+67 56	8.7	0.027	K2	Ko	2.1	0.005		
5542		21 30.1	− 4 26	5.8	0.021	Ko	G8	−0.1:	0.007		
5543	ρ Cygni	21 30.2	+45 9	4.2	0.099	G5	G4	1.3	0.026	0.013	A, Ab, Y
5546	72 Cygni	21 30.7	+38 5	5.0	0.148	G9	Ko	0.6	0.013	0.003	A, Y
	A.G. Leiden 9045	21 33.8	+32 41	7.6	0.045‡	G8	G7	1.2	0.005		
5559	24 Aquarii	21 34.4	− 0 30	7.4†	0.236	F8	F7	4.0	0.021	0.017	F, J
5560	25 Aquarii	21 34.5	+ 1 48	5.3	0.088	Ko	G9	1.9	0.021		
5562	γ Capricorni §	21 34.6	−17 7	3.8	0.188	F4	F4	−0.7	0.013	0.018	M
	A.G. Leiden 9056	21 35.1	+31 5	8.2	0.047	F8	F8	3.0	0.009		
5566	42 Capricorni	21 36.1	−14 30	5.3	0.331	Go	G1	3.8	0.050		
5569	26 Aquarii	21 37.1	+ 0 50	5.8	0.015	K2	G9	1.0	0.011		
5570	κ Capricorni	21 37.1	−19 19	4.8	0.142	G2	G3	−1.4	0.006		
5583		21 39.1	+40 42	5.5	0.026	Ma	G9	0.3	0.009		
5584	ε Pegasi	21 39.3	+ 9 25	2.5	0.025	Ko	G4	−0.3	0.028	0.006	A, M, F
5587	μ^1 Cygni A	21 39.7	+28 18	4.7	0.370	F5	F6	3.5	0.058	0.046	M
5589	46 Capricorni	21 39.7	− 9 33	5.3	0.010	G7	G6	−0.1	0.008		
C2823	A.G. Berlin 8366	21 39.7	+24 53	9.1	0.65	Ko	G7	6.1	0.025		
5590	9 Pegasi	21 39.8	+16 53	4.5	0.029	G5	Go	−0.6	0.010		
5591		21 39.9	+28 19	7.6†	0.061	A9		2.3	0.009		
5592	κ Pegasi	21 40.1	+25 11	5.3†	0.033	F2	F5	2.7	0.030	0.038	A, M, S, *et al*
5593	μ Cephei	21 40.4	+58 19	4.5	0.002	Ma	G8	0.3	0.014	0.010	A
5594	11 Cephei	21 40.5	+70 51	4.8	0.153	K1	K1	0.6	0.014		
5595	47 Capricorni	21 40.9	− 9 44	6.2	0.016	Mb	G7	0.1	0.006		
5599	12 Pegasi	21 41.5	+22 29	5.4	0.016	Ko	G2	1.5	0.017		
5602		21 41.8	+25 6	6.5	0.148	K1	K2	1.9	0.012	0.005	W

TABLE VII—*Continued*

Boss	Name	α 1900	δ 1900	Harv. Vis. Mag.	μ	Spectrum		Spect. Abs. Mag.	Spect. π	Trig. π	Auth
						Est.	Meas.				
5614	12 Cephei	21^h44^m5	+60° 14′	5.6	0.″006	K5	K3	0.5	0.″010		
5616	13 Pegasi	21 45.4	+16 49	5.3	0.096	A8		1.4	0.015		
.....	A.G. Leiden 9158	21 46.5	+32 12	8.6		Ko	G6	3.3	0.009		
.....	Groom. 3594	21 47.2	+64 46	7.9	0.010‡	Mb	G6	0.8	0.004		
.....	A.G. Leiden 9164	21 47.3	+31 27	7.5	0.029‡	K4	K2	0.9	0.005		
5623	μ Capricorni	21 47.8	−14 1	5.2	0.308	A9	F2	1.9	0.022		
.....	Groom. 3604	21 48.7	+66 22	8.2	0.014	F2	F3	3.3	0.011		
5638		21 51.4	+53 28	6.9	0.172	F6	F7	3.2	0.018	0.″014	A
5645		21 53.2	−21 40	6.2	0.015	Mb	G7	0.7	0.008		
5650		21 53.8	+63 9	5.4	0.012	Mdp		−0.3	0.007		
5651		21 54.3	+29 21	6.8	0.540	F6	F4	4.1	0.029	0.040	S, Y, F, J
5655	28 Aquarii	21 56.0	+ 0 7	5.8	0.006	K4	K2	1.2	0.012		
5657	19 Pegasi	21 56.2	+ 7 47	5.8	0.022	K4	K1	1.0	0.011		
5658	20 Pegasi	21 56.2	+12 38	5.7	0.077	F3	F3	2.3	0.021		
5661	16 Cephei	21 57.8	+72 42	5.2	0.174	F3	F3	2.6	0.030	0.038	A
5671	32 Aquarii	21 59.6	− 1 23	5.2	0.045	A9		1.0	0.014		
5674	ν Pegasi	22 0.6	+ 4 34	4.9	0.144	K6	K3	0.3	0.012	0.016	A, M
5676	α Aquarii §	22 0.6	− 0 48	3.2	0.015	Go	F8	−2.8	0.006	0.010	M
5677	ξ^1 Cephei Ft	22 0.9	+64 8	6.5	0.226	F7	F7	3.9	0.030	0.029	A
5682	Bu. 11514 Br	22 1.8	+82 23	7.1	0.141	F6	F6	3.5	0.019	0.006	W
5683	Bu. 11514 Ft	22 1.9	+82 23	7.8†	0.142	G3	G4	4.8	0.025		
5688	ι Pegasi	22 2.4	+24 51	4.0	0.209	F4	F6	3.6	0.083	0.079	A, M, S
5691		22 2.7	+18 59	5.8	0.126	F1	F5	2.4	0.021	0.013	W
C2885	Groom. 3689	22 3.1	+52 39	7.9	0.629	K1	G7	4.8	0.024	0.051	Ye, Y, F, J
5694		22 3.8	+58 21	6.3	0.030	G6	G5	1.0	0.009		

5707		$22^h\ 5^m.3$	− 4°46′	6.1	0″.063	G9	G7	1.1	0″.010		
5709	π Pegasi	22 5.5	+32 41	4.4	0.026	A9		0.3	0.015	0″.005	A
5714	ζ Cephei	22 7.4	+57 42	3.6	0.012	K2	G4	0.5	0.024	0.026	A, M
5716	24 Cephei	22 7.9	+71 51	5.0	0.028	G2	G3	−2.0	0.004		
5721		22 8.2	+56 21	5.4	0.270	F6	F7	3.4	0.040	0.027	A
5723		22 8.4	+69 38	5.5	0.058	F2	F2	2.6	0.026	0.084	S
5724		22 8.4	+34 7	5.4	0.047	K2	K1	0.8	0.012		
5744	θ Aquarii	22 11.6	− 8 17	4.3	0.112	G5	G7	−0.7	0.010		
5745		22 11.6	− 9 32	6.1	0.053	K3	K1	0.8	0.009		
5746	1 Lacertae	22 11.6	+37 15	4.2	0.020	K3	K1	0.4	0.017	0.005	A
5749	44 Aquarii	22 11.9	− 5 53	5.8	0.020	G5	G4	−0.4	0.006		
C2903	Lal. 43492	22 12.3	+12 24	7.0	0.853	G1	G0	5.7	0.055	0.038	A, M, Y, *et al.*
5752	45 Aquarii	22 13.6	−13 48	6.1	0.074	G9	G9	1.7	0.013		
5769		22 18.3	− 7 42	6.1	0.006	G6	G6	0.6	0.008		
5772	33 Pegasi	22 18.8	+20 21	6.1	0.338	F4	F5	4.1	0.040	0.060	W
5776	β Lacertae	22 19.6	+51 44	4.6	0.190	G8	G8	2.1	0.032	0.017	A
5782	53^2 Aquarii A	22 21.1	−17 15	6.4	0.225	G1	G1	4.3	0.038		
5786	34 Pegasi	22 21.5	+ 3 53	5.8	0.295	F7	F7	3.9	0.042	0.067	F, J
5790	35 Pegasi	22 22.8	+ 4 12	4.9	0.325	K0	G9	1.8	0.024	0.033	A
.....	Groom. 3781	22 23.1	+69 23	8.0	0.019	G7	G5	2.3	0.007		
.....	A. G. Berlin 9185	22 23.4	+16 45	7.5	0.017‡	K0	G8	2.2	0.009		
5793	ξ^1 Aquarii	22 23.7	− 0 32	4.6	0.173	F2	F2	1.6	0.025	0.036	M
5794	ξ^2 Aquarii	22 23.7	− 0 32	4.4	0.212	F2	F4	1.6	0.028		
C2922	Krüger 60 A	22 24.4	+57 11	9.3†	0.87	Mb		10.8	0.200	0.261	M, Ye, R, Bar
5800	37 Pegasi	22 24.9	+ 3 55	5.7†	0.141	F1	F2	0.9	0.011		
5804	5 Lacertae §	22 25.4	+47 12	4.6	0.021	K2p	G4	−2.8	0.003	0.005	A
5807	δ Cephei §	22 25.5	+57 54	4.1	0.012	G0	F9	−2.7	0.004	0.011	A
.....	Groom. 3813	22 27.1	+75 43	7.9	0.009‡	K1	G8	1.7	0.006		
5822		22 30.1	−24 30	6.0	0.016	K0	G7	1.1	0.011		
C2937	A.G. Albany 7817	22 30.5	+ 4 52	8.4	0.45	G1	G2	4.1	0.014		

TABLE VII—*Continued*

Boss	Name	α 1900	δ 1900	Harv. Vis. Mag.	μ	Spectrum Est.	Spectrum Meas.	Spect. Abs. Mag.	Spect. π	Trig. π	Auth.
5835	κ Aquarii	22^h32^m6	$-4°45'$	5.3	0.″138	K2	K1	0.8	0.″013		
5838	31 Cephei	22 33.3	+73 7	5.2	0.171	F2	F3	0.2	0.010	−0.″034	Y
5851	Bu. 11895	22 35.9	+14 1	6.6†	0.302	G4	G5	4.5	0.038		
5852	11 Lacertae	22 36.1	+43 45	4.6	0.097	K2	K0	0.7	0.017		
5865	η Pegasi	22 38.3	+29 42	3.1	0.036	G1	G3	−0.2	0.022	−0.003	A, M, S, F
5868	Bu. 11936 A	22 39.6	+38 56	6.2†	0.016	K4	K2	0.4	0.007	0.006	W
5868	Bu. 11936 B	22 39.6	+38 56	8.3	0.016	G8	G8	1.5	0.004		
C2968	Pi. 22^h214	22 40.9	+29 56	6.5	0.461	K0	G8	4.8	0.046	0.015	Ye, Y
5874	ξ Pegasi	22 41.7	+11 40	4.3	0.545	F5	F6	3.8	0.079	0.058	A, M, Y
5875	λ Pegasi	22 41.7	+23 2	4.1	0.060	G7	G6	−0.3	0.013	0.037	A
5878	68 Aquarii	22 42.2	−20 8	5.4	0.237	G6	G6	1.4	0.016		
5884	τ Aquarii	22 44.3	−14 7	4.2	0.039	K5	K2	0.5	0.018		
5885	μ Pegasi	22 45.2	+24 4	3.7	0.154	G7	G6	1.1	0.030	0.024	A, M
5891	ι Cephei	22 46.1	+65 40	3.7	0.139	K0	G9	1.1	0.030	0.042	A, M
5892		22 46.4	+13 26	8.0	0.474	K2	K1	6.3	0.046	0.150	J
5894	σ Pegasi	22 47.3	+ 9 18	5.3	0.516	F4	F6	3.2	0.038	0.042	Ye, Y, F
5895	λ Aquarii	22 47.4	− 8 7	3.8	0.036	Ma	G9	0.3	0.020		
5899	34 H Cephei	22 47.9	+82 37	5.0	0.064	K2	K0	1.6	0.021		
5909	Bu. 12046	22 50.0	− 5 31	6.0†	0.018	G8	G6	1.7	0.014		
5914		22 52.0	+49 12	5.1	0.012	K2	K5	0.8	0.014		
5915		22 52.1	− 5 21	6.4	0.023	G6	G7	1.5	0.011		
5917	51 Pegasi	22 52.6	+20 14	5.6	0.210	G4	G3	4.6	0.063		
5920	Bu. 12090	22 53.5	+ 8 50	7.0†	0.420	G0	F9	4.2	0.028		
5923		22 54.3	−13 36	6.3	0.014	K3	K0	0.4	0.007		
C3001	Lal. 44964	22 55.0	−23 4	7.7	0.899	K4	K1	7.2	0.079		

C3002	A.G. Chris. 3703	22^h55^m1	+68° 29′	8.4	0″066	Ko	G8	5.6	0″028		
5927	36 H Cephei	22 55.2	+83 49	5.0	0.106	K5	K2	0.4	0.012		
5931	B.D. +56° 2923 §	22 55.9	+56 25	5.5	0.009	G2p	G2	−2.6	0.002		
C3007	Lal. 45028	22 56.7	− 4 23	7.6	0.478	K3	K3	6.1	0.050	0″053	M, Y
5940	β Pegasi	22 58.9	+27 32	2.6	0.234	Mb	G7	0.0	0.030	0.000	A, M, J, F
5942	3 Androm	22 59.7	+49 30	4.9	0.230	G9	G8	1.3	0.019	−0.004	A
C3019	Fed. 4371	23 1.2	+67 52	7.5	0.615	G6	G1	5.7	0.044	0.056	Y
5950	86 Aquarii	23 1.3	−24 17	4 8	0.068	G5	G6	1.2	0.019		
5952	55 Pegasi	23 2.0	+ 8 52	4.7	0.016	Ma	K4	0.3	0.013	0.005	A
5954	56 Pegasi	23 2.2	+24 56	5.0	0.038	Kop	G2	1.9	0.025		
5958	5 Androm	23 3.2	+48 45	5.8	0.194	F6	F5	3.4	0.033		
C3028	Lal. 45292	23 4.0	− 2 48	8.3	0.587	K4	K3	6.5	0.044	0.035	Y
5962	57 Pegasi	23 4.5	+ 8 8	5.4	0.004	Mb	G3	0.2	0.009		
5963	89 Aquarii §	23 4.6	−23 0	4.9	0.013	F8	F9	−0.7	0.008		
5966	π Cephei	23 4.7	+74 51	4.7†	0.028	G2	G1	−0.2	0.011	−0.014	S
5972	6 Androm	23 5.8	+43 0	5.8	0.275	F5	F4	3.7	0.038		
5975	7 Androm	23 8.0	+48 52	4.6	0.134	F0	F0	2.3	0.035	0.048	A, M
5976		23 8.5	+56 37	5.6	2.102	K5	K5	7.2	0.209	0.172	S, J, P, F
5977	Bu. 12234 Br	23 8.9	− 9 28	8.3	0.557	F5	F7	3.9	0.013	0.019	Y
.....	Bu. 12234 Ft	23 8.9	− 9 28	9.4	0.557	G2	G3	5.6	0.017		
5978	ϕ Aquarii	23 9.1	− 6 35	4.4	0.193	K9	K2	0.6	0.017		
5981	91 Aquarii	23 10.7	− 9 38	4.5	0.367	Ko	G9	1.4	0.024		
5982	61 Pegasi	23 10.9	+27 42	6.5	0.015	G3	F9	0.0	0.005		
5988	γ Piscium	23 12.0	+ 2 44	3.8	0.753	G5	G4	0.5	0.022	0.021	A, M, Y
5989		23 12.1	+52 40	5.6	0.270	F8	F8	3.9	0.046	0.049	W
5993	8 Androm	23 13.1	+48 28	5.0	0.038	Ma	G9	0.2	0.011		
C3053	Bu. 12290	23 13.8	+ 4 52	9.0†	0.492	K2	G9	6.4	0.030	0.011	M, Ye, Y, J
5998	94 Aquarii	23 13.9	−14 0	5.3	0.314	G5	G5	2.1	0.023		
5999	96 Aquarii	23 14.2	− 5 40	5.7	0.193	F1	F2	2.7	0.025		
6000	o Cephei	23 14.5	+67 34	5.0†	0.066	G7	G7	0.7	0.014	0.032	A

TABLE VII—*Continued*

Boss	Name	α 1900	δ 1900	Harv. Vis. Mag.	μ	Spectrum		Spect. Abs. Mag.	Spect. π	Trig. π	Auth.
						Est.	Meas.				
C3054	W.B. 23^h257	23^h15^m0	+28°19′	8.8	0″.66	K1	K0	6.2	0″.030	0″.061	Ye
6002		23 15.0	+47 50	6.4	0.206	K1	K0	1.0	0.008		
C3059	Lal. 45755	23 16.8	+43 33	7.6	0.671	K0	G7	6.0	0.048	0.039	Y, R
6012	98 Aquarii	23 17.7	−20 39	4.2	0.153	K0	G8	1.6	0.030		
6016		23 18.1	+59 35	5.9	0.003	K4	G8	0.5	0.008		
6020		23 18.9	+31 59	6.5	0.233	A9	F3	2.3	0.014		
6024	υ Pegasi	23 20.4	+22 51	4.6	0.191	F6	F7	1.3	0.022	0.025	A, M
	A.G. Cam. 8232	23 21.0	+52 26	6.9		Mb	G9	0.5	0.005		
	A.G. Bonn 17799	23 22.6	+43 19	8.0		K2	K1	1.5	0.005		
6040	70 Pegasi	23 24.1	+12 13	4.7	0.062	G6	G5	0.5	0.014		
6042		23 24.4	− 5 5	6.4	0.283	K5	K4	0.6	0.007		
	Groom. 4079	23 25.8	+43 25	8.1	0.009	K0	G7	2.8	0.009		
6048	d'Agelet 6348	23 26.4	− 4 38	6.5	0.247	F8	F9	3.6	0.026		
6049	14 Androm.	23 26.4	+38 41	5.3	0.294	G9	G7	1.5	0.017		
C3081	A.Oc. 25685	23 26.5	+58 37	6.8	1.06	K0	K0	5.6	0.058	0.075	Y
C3085	A.Oc. 25734	23 28.2	+62 36	7.4	0.42	G4	G3	4.0	0.021	−0.012	Y
6059	72 Pegasi	23 29.0	+30 46	6.0†	0.053	K4	K2	0.7	0.009		
	Groom. 4094	23 29.3	+73 40	8.0	0.013	G8	G5	2.0	0.006		
C3096	d'Agelet 6348	23 31.0	+17 53	8.0	0.702	G5	G5	5.7	0.035		
6071	λ Androm.	23 32.7	+45 55	4.0	0.449	G8	G5	2.5	0.050	0.028	A, Y
6077	ι Piscium	23 34.8	+ 5 5	4.3	0.574	F4	F7	3.9	0.083	0.098	M, Y, J
6078	γ Cephei	23 35.2	+77 4	3.4	0.169	K1	K1	2.3	0.060	0.070	Ye
	Groom. 4129	23 36.9	+75 2	8.0	0.028	G9	G7	2.5	0.008		
6089	77 Pegasi	23 38.3	+ 9 47	5.4	0.007	Ma	G6	−0.1	0.008		
C3115	Pi. 23^h164	23 38.5	+57 31	7.0	0.610	G2	F9	4.7	0.035	−0.062	Y, F

6094.....	78 Pegasi.....	23^h39^m0	+28°48′	5.0	0″.080	G7	G7	1.1	0″.017		
6097.....		23 39.9	+55 15	6.6	0.029	G6	G6	0.3	0.006	0″.008	W
C3117.....	W.B. 23^h819.....	23 40.0	+29 0	8.9	0.91	K1	K1	6.2	0.029		
6101.....	ψ Androm.....	23 41.1	+45 52	5.1	0.022	G5p	G0	−3.8	0.002		
6105.....	Lal. 46607.....	23 42.1	+56 54	5.8	0.021	K3	G8	0.3	0.008		
6106.....	τ Cassiop.....	23 42.2	+58 6	5.1	0.087	K0	G9	0.4	0.012		
6109.....		23 43.4	− 6 56	6.3	0.026	K1	G9	1.6	0.012		
C3124.....	Lal. 46650.....	23 44.0	+ 1 52	8.7	1.393	Ma	K4	10.1	0.190	0.182	Ye, Y, R, *et al.*
C3126.....	A.G. Albany 8170.....	23 44.9	+ 2 19	8.4	0.499	G8	G5	4.6	0.017	0.027	Ye, R
6123.....	22 Piscium.....	23 46.8	+ 2 22	5.8	0.020	K4	K0	0.7	0.010		
6124.....		23 47.2	+77 3	6.5	0.278	F2	F4	3.4	0.024		
6127.....	ϕ Pegasi.....	23 47.4	+18 34	5.2	0.047	Ma	K0	0.4	0.011	0.014	A
6129.....		23 47.5	+74 59	6.6	0.332	K3	K3	6.7	0.105	0.097	A, M, W
6135.....	ρ Cassiop. §.....	23 49.4	+56 57	4.8	0.007	G5p	G4	−3.3	0.002	0.032	A, M.
C3131.....	Lal. 4c867.....	23 49.9	+28 5	7.3	0.573	K2	K3	6.0	0.055		
.....	Grcom. 4170.....	23 51.4	+73 35	8.2	0.020	K2	K1	1.4	0.004		
6145.....		23 52.0	+42 6	6.0	0.012	F6	F4	1.7	0.014		
6150.....	ψ Pegasi.....	23 52.7	+24 35	4.8	0.056	Ma	G8	0.1	0.012		
6151.....		23 53.0	+49 53	6.8	0.245	G4	G4	5.0	0.044		
6156.....	ω Piscium.....	23 54.2	+ 6 19	4.0	0.186	F3	F4	2.3	0.046	0.013	A, M
.....	B.D. +26° 4721.....	23 54.2	+26 43	8.3		G9	G6	2.1	0.006	0.006	F
C3146.....	A.Oe. 23166.....	23 54.3	−20 35	7.4	0.608	G5	G4	5.7	0.046		
6171.....	30 Piscium.....	23 56.8	− 6 34	4.7	0.053	Mb	G7	0.0	0.012		
6172.....	85 Pegasi A.....	23 56.9	+26 33	5.8	1.291	G3	G2	5.6	0.091	0.096	A, S, Ye, *et al.*
6176.....	Bu. 12704 Br.....	23 57.5	+65 33	5.8	0.018	G8	G7	0.8	0.010		
C3162.....	Pi. 23^h267.....	23 59.7	+34 6	6.2	0.766	G1	G0	4.3	0.042	0.033	A, Y

NOTES

SX Cassiopeiae. Period 36.5 days. Enhanced line spectrum similar to α Cygni. Hydrogen lines Hβ and Hγ have bright edges.

A.G. Bonn 4686. Proper motion from Groombridge.

Boss 1622. Estimates made from plates lent by the Lick Observatory.

Bu. 3474. Proper motion by Batterman.

Comp. α Geminorum. Bu. 4122C, distant 72″. A spectroscopic binary having bright hydrogen lines.

Lal. 15389. Proper motion by Bossert.

S Antliae. Short-period variable. Period $=0^{d}.32$. Spectrum lines extremely poor, probably indicating rapid rotation. Secondary component suspected.

W Ursae Majoris. Algol variable. Period 8 hours. Both spectral components show. Lines very wide due to rapid rotation of the two stars.

Boss 2830. A close visual and spectroscopic binary. Estimates made from plates taken by Sanford at the Mills Station of the Lick Observatory.

Boss 3735. Estimates from plates lent by the Lick Observatory.

Bu. 7001. Proper motion from Greenwich.

Boss 3846. Spectrum lines very poor, resembling those of W Ursae Majoris.

Bu. 8068A. Proper motion from Porter.

7:1917 Serpentis. Peculiar variable discovered by Wolf and Barnard. Hβ bright.

W Serpentis. Spectrum shows doubly reversed bright hydrogen lines.

Bu. 9401 Br. Proper motion from A.G. Berlin.

Bu. 9569. Proper motion from Auwers.

Bu. 10504 Br. and Ft. Proper motion from A.G. Berlin.

Mount Wilson Observatory
October 1920

THE SPECTROSCOPIC ORBIT OF THE CEPHEID VARIABLE X CYGNI[1]

By JOHN C. DUNCAN

ABSTRACT

Cepheid variable X Cygni.—A brief summary of previous observations relating to this variable is given. From twenty-three spectrograms made at Mount Wilson with the 60-inch reflector and single-prism spectrograph, the *elements of the spectroscopic orbit* have been computed. The values of K (28 km/sec.), of $a \sin i$ (6, 121,000 km), and of the mass-function (0.034) are remarkably large. The probable error for a plate is large in comparison with the deviations in the measures of a single plate made by different observers; but there is no evidence of a secondary oscillation.

The variable star X Cygni ($\alpha = 20^h 39^m.5$, $\delta = +35°14'$; 1900.0) was discovered by S. C. Chandler[2] in 1886. Of a number of published determinations of its photometric elements, the best is probably that of M. Luizet,[3] which is based on observations covering 554 periods and made by eight different observers. Luizet gives as the time of maximum brightness

$$\text{J.D. } 2410190.684 \text{ (Paris M.T.)} + 16^d.38543\ E,$$

and finds that, though the maxima and minima are repeated with regularity, the amount of the change of light is not constant, the magnitude at maximum ranging from 6.5 to 6.2, and at minimum from 7.4 to 7.2. Secondary oscillations appear in both the rising and the falling branches of the curve. The duration of the increase of light is $6^d.1$.

The spectrum as classified at the Harvard Observatory is F5, peculiar. Like other Cepheids, the star is bluer and has stronger hydrogen lines at maximum brilliancy than at minimum. The variation in the radial velocity was discovered by Frost.[4]

Table I gives a list of the spectrograms of X Cygni taken at the Mount Wilson Observatory. They were made by Messrs. Adams, Joy, Strömberg, Sanford, Merrill, and Duncan, with the

[1] *Contributions from the Mount Wilson Observatory*, No. 196.

[2] *Astronomical Journal*, **7**, 32, 1886.

[3] *Astronomische Nachrichten*, **193**, 83, 1912.

[4] *Astrophysical Journal*, **25**, 60, 1907.

60-inch reflector and single-prism spectrograph, using the 18-inch camera. All were measured by Miss Brayton and Mr. Duncan, and some also by Miss Burwell and Messrs. Adams, Joy, Strömberg, and Sanford. No systematic differences in the measures were found, and the column headed "Velocity" gives the mean results, reduced to the sun. The Greenwich mean time given in Table I refers to the middle of the exposure. The phase is the number of days after maximum light according to the elements of Luizet.

TABLE I

Plate Number	Date	G.M.T.	J.D., G.M.T.	Phase	Velocity	O−C	Number of Measures
					km/sec.	km/sec.	
6353..	1917 Nov. 3	16^h03^m	242 1536.669	$7^d.273$	+16.2	−2.2	6
6358..	4	18 05	1537.754	8.358	+24.2	−0.8	5
7213..	1918 Aug. 17	22 31	1823.939	15.991	−14.8	−0.9	4
8261..	1919 June 8	22 05	2118.920	16.034	−17.4	+0.2	2
8329..	July 3	22 01	2143.918	8.261	+26.2	+2.0	2
8336..	5	21 12	2145.884	10.227	+40.4	+6.6	2
8341..	7	22 15	2147.927	12.270	+31.0	−3.0	2
8348..	8	22 49	2148.951	13.294	+27.7	+2.5	2
8357..	10	20 57	2150.858	15.201	− 6.6	−0.4	3
8363..	11	20 39	2151.861	16.302	−23.0	0.0	2
8370..	12	20 10	2152.841	0.708	−17.4	+2.6	2
8375..	13	19 46	2153.824	1.781	−16.6	+0.6	2
8387..	14	22 16	2154.928	2.885	− 7.2	+3.8	2
8400..	15	22 03	2155.919	3.876	− 6.0	−1.5	2
8412..	17	18 50	2157.868	5.825	+ 5.0	−3.9	3
8436..	19	18 13	2159.843	7.800	+20.0	−1.7	2
8478..	Aug. 6	21 14	2177.885	9.457	+34.2	+3.5	2
8482..	7	18 46	2178.782	10.354	+38.6	+4.4	2
8522..	10	19 59	2181.832	13.404	+23.7	−0.1	2
8523..	10	21 11	2181.883	13.455	+19.4	−4.5	2
8545..	11	20 50	2182.868	14.440	+14.4	+7.3	2
8689..	Sept. 10	15 55	2212.663	11.465	+33.6	−2.5	2
8692..	10	20 45	2212.865	11.667	+32.0	−3.6	2

Preliminary elements were derived by the method of Lehmann-Filhés. As no planimeter was available, the necessary areas were determined by tracing the velocity-curve on thin paper, cutting out the areas, and weighing them on a chemical balance. Luizet's photometric period was assumed as the orbital period, and there

appeared no good reason for changing it. The preliminary elements are:

$K = 28.0$ km/sec.
$\omega = 110°$
$e = 0.25$
$T = 15^d.0$ after light maximum
$\gamma = +9.5$ km/sec.

A least-squares solution was based on these elements, the observations being given equal weight and grouped to form eighteen

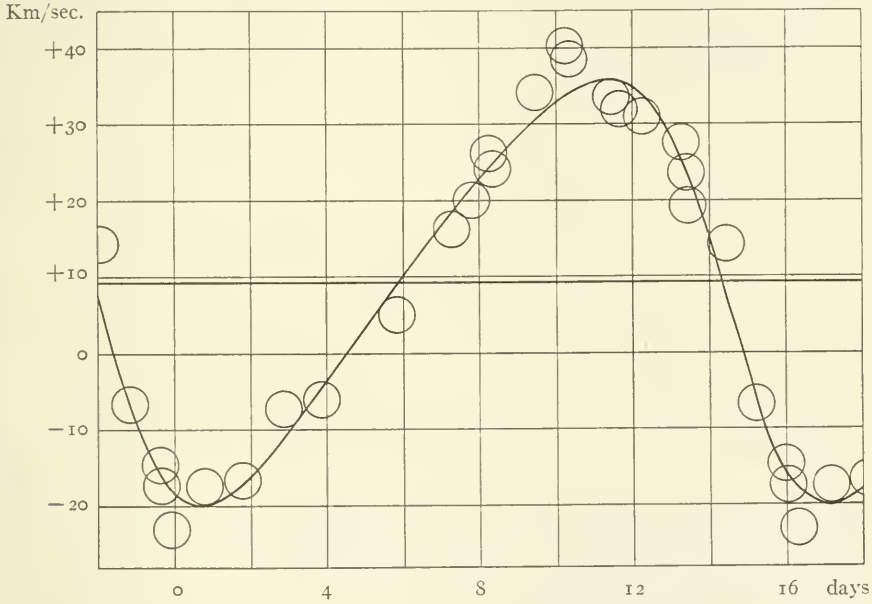


FIG. 1.—Velocity-curve of X Cygni. Abscissae are intervals after maximum light; the radius of the circles representing the observations is equal to the probable error of a single plate.

normal places. The period was not included in this solution. The following elements were thus obtained:

$K = 28.03 \pm 0.73$ km/sec.
$\omega = 98°.2 \pm 14°.9$
$e = 0.246 \pm 0.027$
$T = 14^d.557 \pm 0^d.523$
$\gamma = +9.32$ km/sec.

By the least-squares adjustment the sum of the squares of the residuals was reduced but slightly, from 78.07 to 76.24.

As ω and T were the only elements greatly changed, and as they showed the greatest probable errors, a second solution was made with these as the only variables. The results were

$$\omega = 101^{\circ}.1 \pm 4^{\circ}.3,$$
$$T = 14^{d}.685 \pm 0^{d}.169.$$

The sum of the squares of the residuals was again slightly reduced, this time to 75.22. The finally adopted elements, from which the residuals given in Table I and the velocity-curve shown in Figure 1 were computed, are:

$$P = 16^{d}.38543$$
$$K = 28.03 \text{ km/sec.}$$
$$\omega = 101^{\circ}.1$$
$$e = 0.246$$
$$T = 14^{d}.685 \text{ after light maximum}$$
$$\gamma = +9.32 \text{ km/sec.}$$
$$a \sin i = 6{,}121{,}000 \text{ kilometers}$$
$$\frac{m_1^3 \sin^3 i}{(m+m_1)^2} = 0.034$$

Maximum negative velocity occurs $0^{d}.7$ after maximum brightness
Maximum positive velocity occurs $1^{d}.1$ after minimum brightness

The values of K, $a \sin i$, and the mass function are considerably larger than in the case of any other Cepheid which has been spectroscopically investigated. The probable error of a single plate, computed from the residuals in Table I, is ± 2.44 km/sec., a value much larger than the good agreement of the different measures on each plate might have led one to expect. There seems, however, to be no good evidence of a secondary oscillation in a period commensurate with that of the principal one.

Mount Wilson Observatory
August 1920

PROVISIONAL ELEMENTS OF THE ECLIPSING SYSTEM RS CANUM VENATICORUM

By BANCROFT WALKER SITTERLY

ABSTRACT

Eclipsing binary RS Canum Venaticorum.—Provisional elements for this system, B.D.+36°2344, have been computed on the basis of a series of observations made by Maggini in 1916. The light-curve (Fig. 1) shows extremely long minima which together take four-ninths of the whole period. The two giant stars apparently touch at periastron; they are elongated toward each other; and move in an orbit with an eccentricity of 0.17. The eclipses are either total or annular. The probable distance is 1200 light-years.

This discussion is based upon a series of observations made by Maggini upon the star B.D.+36°2344 by the Argelander method, and published by him in Volume 34 of the *Publications of the Arcetri Observatory*, Florence, in 1916. Although these observations do not define the star's light-curve with sufficient exactness to warrant great confidence in the elements obtained from it, the curve's form is so unusual in some respects that it was considered worth while to attempt a solution. The methods followed were those of Russell and Shapley, described in their contributions to the *Astrophysical Journal* in 1912 and 1913.

The striking features of the curve's form are: (1) minima of extremely long duration, in proportion to the length of the period, indicating that the stars are very close together; (2) a noticeable difference in the durations of the minima, suggesting a considerable ellipticity in the orbit; (3) a sharply bowed form of the curve between eclipses, denoting that the stars are elongated toward one another. The depths of the minima are also noteworthy, especially that of the secondary; they show that the stars are not very different in size and that they eclipse one another nearly totally.

The first step in the solution was to group Maggini's observations, which were means of five Argelander estimates each, and rather unequally spaced, into convenient normals. In most cases

Maggini's observations were paired, but a few were taken by threes and a few singly. Then the curve was "rectified," removing the effect of the elliptic figure of the stars, in the usual manner. The eccentricity of figure came out more than three-tenths, a value somewhat above the average. But the "rectified" curve was still not a horizontal straight line outside eclipses, as expected, but showed a brightening of the system toward primary minimum. Since the secondary minimum, though its middle point did not seem much displaced, was seen to last five hours longer than the primary (indicating a considerably eccentric orbit with periastron near the point of primary eclipse), this brightening was considered a heating effect caused by the approach of the stars to one another at periastron, and its effect was taken out of the curve by applying a correction $\Delta m = a \cos\theta + b \sin\theta$; setting $a = 0.05$ and $b = 0$ gave a satisfactory correction.

It was now found by trial that by advancing the epoch of primary minimum by $0^d.0074$ and retarding the secondary epoch by $0^d.0223$, the curve might be improved. This gave at once a value for the transverse component of the eccentricity of the orbit: $e \cos\omega = 0.02$; the determination is not very exact, for the secondary minimum is not well defined by the observations. The line-of-sight component is given by the ratio of the durations of the minima; after several trials the value $e \sin\omega = 0.167$ appeared to fit the two curves best, but this is even less accurately determined than $e \cos\omega$. The two values combined gave $e = 0.17$, $\omega =$ nearly $85°$.

Next, an approximation to the elements, from the shape of the primary minimum and the depths of both minima, was tried in the usual manner on the hypothesis of uniformly illuminated disks. It appeared at once from the steepness of the curve that the eclipses must be total or annular; in fact, the assumption that the orbit is exactly edge-on to our line of sight, so that the stars eclipse each other centrally, gave most satisfactory results. A preliminary solution made the fainter star two-thirds as bright as the other and one-fourth larger, the primary eclipse being total and the secondary annular. But the sum of the radii of the stars came out greater than the radius of the orbit, that is, the stars were in contact —a result difficult to reconcile with the form of the curve, but

demanded by the great duration of the minima. The two minima together occupy 45 per cent of the whole period.

Here we had a curious assembly of data. If the system were really two separate stars, the sum of the radii could not be greater than the periastron distance of centers in the orbit, but it could not be much less than this and even approximately fit the curves of minima. The hypothesis of central transit was necessitated by the form of the curve at primary minimum, which also determined the ratio of radii and proportionate luminosity of the two stars within narrow limits. It was therefore decided to *assume* elements in accordance with these data and compute a light-curve to fit them; then to compare this with the observations, and if necessary to repeat the process several times. Since the stars eclipsed one another centrally, it was a simple matter directly to compute the percentage of eclipse at any instant by means of the p-functions of Russell's method, even for the combination of "darkened" disks, eccentric orbit, and elliptic stars, which combination would present considerable complication if attacked as usual from the other end. Accordingly, for various percentages of obscuration during each eclipse, the distance of the centers of the stars was computed by the formula:

$$\text{distance of centers} = a_1 (1 + pk),$$

where a_1 is the longest radius of the larger star, k the ratio of the stars' radii, and p a function of k and the percentage of obscuration, tabulated by Russell and Shapley. a_1 and k were assumed as above stated. A curve was drawn for each minimum analogous to a light-curve, but with the loss of light plotted against the distance of centers instead of against the phase. To compare the observations with this curve the distance of the centers of the stars for the time of each normal was computed by the formula: $[r \cos (v+\omega)] [1 - z \cos^2 \theta]^{-\frac{1}{3}}$, in which r, the radius vector of the orbit, and v, the true anomaly, were computed from the previously chosen values $e = 0.17$, $\omega = 85°$, while the second factor is Russell's function to remove the effect of the ellipticity of the stars. This quantity, together with the observed loss of light, having been found for each normal, the normals were plotted with the

quasi-light-curve above mentioned and residuals directly read off. A few trials in this manner gave curves on both the "uniform" and "darkened" hypotheses.

TABLE I

RESIDUALS

Normal	Weight	O−C Uniform	O−C Darkened	Normal	Weight	O−C Uniform	O−C Darkened
1	2	+0.01	−0.01	21	2	+0.04	+0.01
2	2	+0.02	+0.08	22	2	+0.07	+0.04
3	2	0.00	+0.06	23	2	+0.04	+0.04
4	2	+0.03	+0.09	24	2	+0.01	+0.01
5	2	+0.03	+0.09	25	2	−0.05	−0.05
6	2	+0.04	+0.10	26	2	+0.02	
7	2	0.00	+0.06	27	2	0.00	
8	2	−0.01	+0.04	28	3	0.00	
9	2	−0.04	+0.01	29	1	−0.05	
10	2	−0.04	−0.01	30	3	+0.02	+0.02
11	2	−0.07	−0.05	31	2	−0.04	−0.01
12	2	−0.01	−0.01	32	2	−0.11	−0.06
13	2	+0.01		33	2	−0.04	+0.02
14	2	+0.01		34	3	+0.08	+0.13
15	1	0.00		35	2	+0.07	+0.11
16	2	−0.02	−0.02	36	2	−0.03	+0.03
17	1	+0.02	+0.02	37	2	−0.08	0.00
18	2	+0.06	+0.07	38	2	−0.17	−0.14
19	3	+0.02	−0.01	39	2	−0.08	−0.11
20	2	+0.05	+0.02	40	1	+0.01	−0.03

Probable error of one normal of unit weight: { on "uniform" assumption, 0.04952 / on "darkened" assumption, 0.05577

Like the majority of eclipsing binaries, this system seems to have the brighter star the smaller, according to the "uniform" solution, but the larger by the "darkened" solution. The "uniform" curve, it may noted, fits a trifle better than the "darkened." These solutions, though each deviates considerably from the observed normals, represent them as closely as might be done without allowing the stars actually to coalesce. By the "uniform" solution, the stars just touch at periastron; by the "darkened" they are separated at that point by 0.003 of the major axis of the orbit. Neither supposition seems quite compatible with a stable system, but any diminishing of the stars'

radii leads to much increased deviation from the observational curve. More accurate observations might clear up the difficulty here, and seem very desirable, since the system appears to represent a very interesting stage in the evolution of binaries. A spectroscopic study would also shed much light on the true condition of the system, and seems perfectly feasible, since the maximum brightness is about $7^{M}.9$.

TABLE II

ELEMENTS

Element	Symbol	Value	
		Uniform	Darkened
Ratio of radii of stars	k	0.800	0.850
Semi-major axis of brighter star	a_b	0.368	0.445
Semi-major axis of fainter star	a_f	0.460	0.378
Semi-minor axis of brighter star	b_b	0.338	0.423
Semi-minor axis of fainter star	b_f	0.422	0.360
Eccentricity of meridian section of stars	$\epsilon = \sqrt{z \operatorname{cosec}^2 i}$	0.397	0.312
Inclination of orbit	i	90° 0′	90° 0′
Eccentricity of orbit	e	0.17	
Longitude of periastron	ω	85° 0′	
Primary eclipse		Total	Annular
Secondary eclipse		Annular	Total
Ratio of brightness of stars at perihelion to brightness at aphelion		1.09	
Light in terms of system of brighter star	L_b	0.600	0.722
Light in terms of system of fainter star	L_f	0.400	0.278
Ratio of surface brightness of stars	J_b/J_f	2.34	1.87
Density of brighter star in terms of sun	$\bar{\rho}_b$	0.025	0.014
Density of fainter star in terms of sun	$\bar{\rho}_f$	0.013	0.023
Semi-major axis of brighter star in terms of sun	$\bar{a}_b$	3.43	4.15
Light of brighter in terms of sun	$\bar{L}_b$	75	
Parallax	π	0″.003	
Distance in light-years		1200	
Spectral type		F8	

Assuming that each star has the mass of the sun, the actual radii and dimensions in terms of the sun were computed. The densities come out considerably less than the sun's, indicating an earlier stage of evolution. Miss Cannon gives the spectrum as F8, and a computation of the probable brightness and parallax of the brighter component by Shapley's formulas shows this as one of the "giant" stars, seventy-five times as bright as the sun and more than a thousand light-years distant. Residuals of the

observations from the two computed curves are given herewith in Table I, and elements in Table II. Figure 1 gives the light-curves.

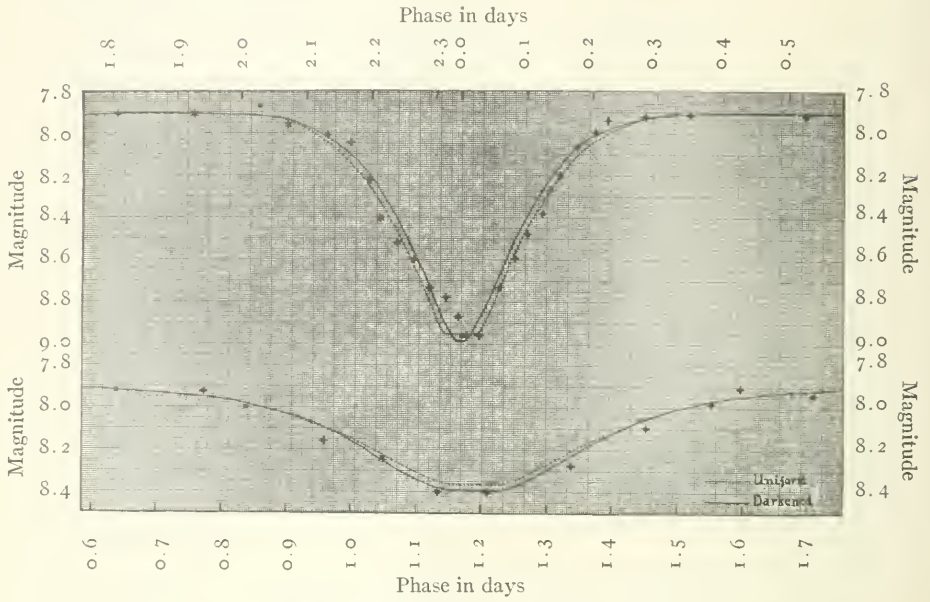


FIG. 1—Mean light-curve of RS Canum Venaticorum

In conclusion I wish to acknowledge my indebtedness to Professor Russell, of the Princeton Observatory, not only for the entire method of the solution but for his care in going over and correcting the work as it progressed.

PRINCETON UNIVERSITY OBSERVATORY
August 1920

THE
ASTROPHYSICAL JOURNAL
AN INTERNATIONAL REVIEW OF SPECTROSCOPY
AND ASTRONOMICAL PHYSICS

VOLUME LIII MARCH 1921 NUMBER 2

A PHOTO-ELECTRIC STUDY OF ALGOL

By JOEL STEBBINS

ABSTRACT

Variable star, Algol; photometric study.—Observations during 1919–1920 with a photo-electric photometer give a new *light-curve* for this star which is considerably more accurate than the curve obtained in 1909–1910 with the selenium photometer (Fig. 1, Table XII). Besides confirming the secondary minimum and the continuous variation between minima, the new results show an effect due to the ellipsoidal shape of the components of the system. The phase of the secondary minimum indicates that there can be no rapid motion of the line of apsides of an elliptical orbit; in fact all of the photometric evidence points to a circular orbit. Corrections to the ephemeris for the times of minimum are given. Neglecting the light of the third body the *elements of the eclipsing binary system* are derived (Table XI), but it is pointed out that definitive values of the elements cannot be found until measures of the spectrum and magnitude of the third component and a very accurate parallax for Algol are available. The elements found agree closely with those obtained in 1909–1910. Certain differences suggest a *color-index for the satellite* which would make it somewhat yellower than the primary.

Constancy of three comparison stars.—The star δ *Persei* is suspected of variation to the extent of $0^{M}04$ or $0^{M}05$, but *l and* π *Persei* were found to be constant within $0^{M}01$.

Photo-electric photometer for stars.—*The precision* which may be reached is indicated by the results in Tables VII and XIII.

Since the determination of the light-curve of Algol in 1909–1910 with the selenium photometer,[1] the only confirmation of the existence of the secondary minimum that has come to my attention is by M. Maggini, of Florence,[2] who worked in lights of two colors

[1] *Astrophysical Journal*, **32**, 185, 1910.

[2] *Popular Astronomy*, **26**, 380, 1918.

with a visual photometer. However, he did not find any variation of light between minima, and from his published data I am unable to determine how it was that the star was measured with no apparent change between eclipses.

Quite often in the past, variations in the photometric period of Algol have been attributed to the effect of an unseen third body, and with the spectroscopic detection of a companion to the system, with a period of 1.9 years, it is possible to take another step in the study of this star. If the relative orbit of the eclipsing satellite is elliptical and the line of apsides is in motion, we would have one explanation for the displacement of the times of primary minimum. In particular, the position of the secondary minimum with respect to the primary is a very delicate test of the correctness of the elliptical orbit, and it was to establish any change in the time of secondary minimum that after the lapse of ten years I decided to make a new determination of the light-curve.

Algol was the first star to be studied exhaustively with the selenium photometer when this instrument had been made sensitive enough to take accurate measures of second-magnitude stars, and fair measures of the third magnitude, or of Algol at greatest eclipse. In 1913 the experiments with selenium were definitely abandoned in favor of the photo-electric cells, which were being developed in our physics laboratory by Dr. Jakob Kunz. Since that time the photo-electric photometer has reached a stage of progress where, with the same 12-inch telescope, objects of photographic magnitude 6.0, or even fainter, can be measured more accurately than any stars whatever with the selenium photometer.

During the winter of 1919–1920 an entirely new series of measures of Algol has been taken with the new instrument, and the results are given in this paper. For convenience the earlier work with selenium will be designated as the series of 1910, and the new work the series of 1920.

In 1910 the comparison stars used were α Persei and δ Persei. As Algol has a spectrum of class B8 and α Persei of F5, this comparison star was not considered at all for the new work, it being our present practice to observe stars as nearly of the same spectral class as are available. δ Persei, spectrum B5, is an excellent com-

parison object, and many measures were taken of it. However, on several occasions δ was found to be unmistakably faint to the extent of $0^{M}04$ or $0^{M}05$, indicating that it is possibly an eclipsing variable of small range, though a spectroscopic orbit has not been determined. This variation of δ may have affected slightly the measures of Algol at primary minimum in 1910. but not enough to be noticed. When the trouble was detected this time, the whole series with δ was discarded for the study of Algol, but the measures will be used for the test of the light of δ. In fact, no better comparison star can be found than a thoroughly studied variable like Algol, if observed between eclipses, as its variations are known to a certain degree, whereas a so-called constant star taken at random may vary in any unknown fashion.

TABLE I

Comparison Stars

H.R.	Star	Harvard Magnitude	Photo-electric Magnitude	Spectrum
936	β Persei	2.1–3.2	(5.0)	B8
1122	δ Persei	3.10	3.02	B_5
1002	l Persei	4.98	5.02	A_2
879	π Persei	4.62	4.66	A_2

By means of neutral shade-glasses to cut down the light of bright stars, it is practicable to use fainter objects for comparison stars, and in this case the two stars l Persei and π Persei make a very good combination when Algol is measured through a shade. The stars observed in 1920 are given in Table I. The rough photo-electric magnitude is derived from the Harvard visual magnitude, the "color-equation" of the installation according to revised measures being $0^{M}70$. The same shade-glasses were used as in previous work,[1] and with shade III on Algol, which reduces the light 2.8 magnitudes, the variable at maximum is very nearly equal to l, and a quarter of a magnitude fainter than π. Near primary minimum, by changing to the lighter shade II the apparent light of Algol can still be kept about the same as the comparison stars. The positions of l and π in the sky, one on

[1] *Astrophysical Journal*, **49**, 346, 1919.

each side of Algol, give a most excellent elimination of the atmospheric extinction, as the visual differential correction between Algol and the mean of the two stars does not exceed $0^{M}.002$ from sidereal time $21^{h}.0$ to $7^{h}.0$.

There are many measures during the series of 1920 which give the difference between l and π with only a small extinction correction, and dividing these we have for the difference, π brighter than l, the results shown in Table II.

TABLE II

DIFFERENCE BETWEEN l AND π PERSEI

November 1919	$0^{M}.259$	$\pm$	$0^{M}.0009$
December 1919—January 1920	0.259	$\pm$	0.0021
October 1920	0.256	$\pm$	0.0029
Adopt	$0^{M}.259$	$\pm$	$0^{M}.0012$

There is no indication that either l or π was variable in light.

Another constant to be determined was the difference in the absorptive powers of the two shades II and III, which for Algol have approximately the values $1^{M}.66$ and $2^{M}.82$. It is only the difference that enters into the result, and not the total absorption of either shade. The various determinations are as follows:

TABLE III

DIFFERENCE BETWEEN SHADES II AND III

Other stars, average for spectrum B8	$1^{M}.146$	Neglecting dark current
Direct measures of Algol	1.147	
Direct measures of Algol	1.163	With correction for dark current
From fit of light-curve at primary minimum	1.169	
Adopt	$1^{M}.160$	

The round figure of $1^{M}.160$ was adopted more or less arbitrarily. When two stars of considerable difference in brightness are compared in rapid succession, the residual dark current from the brighter star, which lasts for one or two minutes, is added on to the light-effect from the fainter one. In regular work it is our custom to apply the same correction to both stars, because in bright moonlight the effect of the background of the sky is then

simply included as an addition to the correction for dark current. The difference between the two reductions with or without the dark current is generally of the order of a hundredth of a magnitude for one whole magnitude, or a difference in scale of say 1 per cent.

The photo-electric measures of Algol are given in Tables IV and V. The phase is computed from the final adopted epoch of minimum, and was reduced to the sun by Pannekoek's table. In Table IV, near primary minimum, each difference of magnitude is always referred to l Persei, + meaning Algol brighter than l, and is the mean of two sets of measures on the variable, taken ordinarily in the order: two readings on Algol, four on l, four on Algol, four on π, two on Algol, and so on. The only exception was on J.D. 2422281, when a number of sets were taken with l alone. In Table V each difference of magnitude is the mean of three sets, except where noted differently in the last column. Here the means for l and π have been taken separately, though the measures overlap, the observing schedule being as before. All measures in both tables have been corrected for atmospheric extinction, and the π sets have been corrected by $0^{M}259$ to reduce to l.

The present period of Algol was computed from Hellerich's elements.[1] On comparison with his elements III the photo-electric observations give, by a graphical solution for the primary minimum, a correction of $-0^{h}11 = -0^{d}0046$. Using his predicted period and the present determination of the epoch we have

$$\text{Minimum} = \text{J.D. } 2422321.5947 + 2^{d}.867301 \cdot E,.$$

from which the phases in Tables IV and V were computed.

In October 1920 Algol was observed during primary minimum on three nights as an additional check on the period and the light at minimum. The measures were taken exactly as those in Table IV, each observation being with the two comparison stars l and π, and shade II was used throughout. The results are in Table VI, where the computed phase in the fourth column is from Hellerich's elements III, uncorrected, while the observed phase in the next column is based upon the light-curve of the present series.

[1] *Astronomische Nachrichten*, **209**, 227, 1919.

TABLE IV

OBSERVATIONS OF ALGOL AT PRIMARY MINIMUM

J.D. 242	G.M.T.	Phase	Difference of Magnitude	Shade, Comparison Star	J.D. 242	G.M.T.	Phase	Difference of Magnitude	Shade, Comparison Star
2275	12^h47^m8	-4^d31	-0^M055	III	2278	19^h42^m8	$+5^d80$	$+ M001$	III
(Nov. 12 '19)	13 0.0	−4.11	− .116	III		20 12.6	+6.29	+ .003	III
	13 13.8	−3.87	− .112	III		20 24.0	+6.47	+ .003	III
	13 27.2	−3.65	− .186	III	2281	13 07.8	+2.47	−0.440	III
	13 38.4	−3.47	− .165	III		13 25.5	+2.69	− .379	III
	13 48.6	−3.29	− .180	III		13 37.0	+2.88	− .316	III
	14 01.6	−3.07	− .292	III		13 48.6	+3.07	− .254	III
	14 13.3	−2.89	− .333	III		14 00.6	+3.27	− .218	III
	14 24.0	−2.70	− .356	III		14 10.6	+3.44	− .174	III
	14 37.6	−2.47	− .427	III		14 25.8	+3.69	− .122	III
	14 50.5	−2.26	− .478	III		14 38.0	+3.89	− .088	III
	15 00.3	−2.10	− .571	III		14 50.8	+4.11	− .066	III
	15 16.4	−1.83	− .628	II		15 05.2	+4.35	− .028	III *l*
	15 27.4	−1.65	− .732	II		15 17.9	+4.57	− .012	III *l*
	15 40.8	−1.42	− .808	II		15 29.6	+4.76	+ .001	III *l*
	15 53.3	−1.22	− .881	II		15 41.6	+4.96	+ .003	III *l*
	16 05.3	−1.02	− .958	II		15 53.5	+5.16	+ .001	III *l*
	16 17.2	−0.82	−1.000	II		16 05.8	+5.37	− .006	III *l*
	16 41.2	−0.41	−1.130	II		16 19.2	+5.59	+ .006	III *l*
	16 51.4	−0.25	−1.207	II		16 31.2	+5.79	− .006	III *l*
	17 01.4	−0.08	−1.173	II		16 41.9	+5.97	+ .006	III *l*
	17 14.1	+0.13	−1.228	II		16 55.9	+6.20	+ .007	III
	17 25.1	+0.31	−1.171	II		17 08.4	+6.41	+ .002	III
	17 35.1	+0.48	−1.138	II		17 20.4	+6.61	− .006	III
	17 53.2	+0.79	−1 067	II	2321	15 17.4	+1.11	− .902	II
	18 06.0	+1.00	− .974	II		15 35.8	+1.43	− .810	II
	18 18.9	+1.21	− .932	II		15 51.8	+1.69	− .692	II
	18 48.0	+1.69	− .706	II		16 08.8	+1.97	− .590	II
	18 59.6	+1.89	− .632	II		16 24.4	+2.23	− .498	II
	19 10.8	+2.08	− .569	II		16 37.2	+2.45	− .425	II
	19 27.0	+2.35	− .456	III		17 03.6	+2.89	− .315	III
	19 38.2	+2.53	− .410	III	2341	12 03.9	−3.86	− .150	III
	19 50.0	+2.73	− .362	III		12 18.0	−3.63	− .135	III
	20 03.8	+2.96	− .282	III		13 00.1	−2.93	− .310	III
	20 14.8	+3.15	− .218	III		13 26.6	−2.49	− .432	II
	20 25.8	+3.33	− .219	III		13 42.0	−2.23	− .526	II
	20 48.5	+3.71	− .116	III		13 55.2	−2.01	− .582	II
	21 00.0	+3.90	− .096	III		14 12.4	−1.71	− .674	II
	21 10.4	+4.07	− .071	III		14 29.3	−1.43	− .807	II
2278	15 21.7	+1.44	− .768	II		14 44.6	−1.18	− .874	II
	15 31.8	+1.61	− .719	II		15 13.2	−0.71	−1.074	II
	15 42.2	+1.78	− .666	II		15 29.2	−0.43	−1.124	II
	15 54.0	+1.98	− .588	II	2381	13 27.4	−5.97	+ .016	III
	16 04.4	+2.15	− .530	II		13 42.9	−5.70	+ .032	III
	16 14.4	+2.31	− .460	II		14 00.3	−5.41	− .008	III
	16 25.9	+2.50	− .410	II		14 14.2	−5.18	− .014	III
	16 36.4	+2.69	− .352	II		14 28.7	−4.94	− .013	III
	16 46.4	+2.85	− .305	II		14 42.2	−4.71	+ .010	III
	17 07.3	+3.19	− .238	III		14 58.2	−4.45	− .028	III
	17 21.0	+3.43	− .161	III		15 13.2	−4.21	− .074	III
	17 35.2	+3.67	− .145	III		15 27.1	−3.93	− .094	III
	17 57.9	+4.04	− .087	III	2384	13 05.2	−3.15	− .260	III
	18 11.1	+4.26	− .043	III		13 18.4	−2.94	− .296	III
	18 24.1	+4.48	− .022	III		13 32.4	−2.71	− .365	III
	18 39.0	+4.73	− .017	III		13 47.6	−2.45	− .438	II
	18 52.2	+4.95	+ .010	III		13 58.4	−2.27	− .506	II
	19 05.1	+5.17	.000	III		14 10.1	−2.08	− .574	II
	19 19.4	+5.39	.000	III		14 27.8	−1.79	− .694	II
	19 31.4	+5.60	− .006	III		14 30.5	−1.59	− .764	II
						14 51.5	−1.39	− .849	II

NOTES

J.D. 2422275—Measures at first were through smoke which gradually cleared. After about two hours the conditions were good.

2341—Sky only fair.

From the means in the last column of Table VI there is found for the correction to the ephemeris from Hellerich's elements III,

$$-0^h.30 \pm 0^h.007.$$

As the correction of the previous season was $-0^h.11$, we see that the ephemeris has run off $0^h.19 = 11$ minutes in the course of 298

TABLE V

OBSERVATIONS OF ALGOL AT SECONDARY MINIMUM AND BETWEEN MINIMA

J.D. 242	G.M.T.	Phase	Difference of Magnitude	Comparison Star, Sets	J.D. 242	G.M.T.	Phase	Difference of Magnitude	Comparison Star, Sets
2265	15^h15^m	$33^h.40$	$-0^M.016$	*l*, 2	2317	13^h26^m	$40^h.89$	$+0^M.040$	*l*
2268	14 04	35.41	− .009	*l*		13 36	41.06	+ .030	π
	14 30	35.84	− .006	*l*	2319	17 16	23.83	+ .035	*l*
	15 04	36.41	− .004	*l*		17 23	24.02	+ .036	π
	15 27	36.80	+ .013	*l*	2333	15 39	14.19	+ .017	*l*
	17 06	38.44	+ .062	*l*		15 47	14.33	+ .021	π
	17 27	38.80	+ .045	*l*	2335	13 27	59.99	+ .018	*l*
	18 37	39.96	+ .031	*l*		13 37	60.15	+ .014	π
	19 01	40.36	+ .021	*l*	2337	12 18	38.07	+ .008	*l*
	20 07	41.46	+ .033	*l*		12 26	38.15	+ .017	π
2273	17 03	20.76	+ .022	*l*		13 08	38.85	+ .032	*l*
2274	15 13	42.93	+ .041	*l*		13 17	39.00	+ .038	π
2276	16 04	22.96	+ .034	*l*		14 05	39.80	+ .024	*l*
	16 09	23.05	+ .037	π		14 14	39.95	+ .041	π
2280	17 36	51.68	+ .012	*l*		14 58	40.68	+ .030	*l*
	17 42	51.78	+ .022	π		15 06	40.81	+ .024	π
2282	16 06	29.37	+ .036	*l*		16 11	41.90	+ .034	*l*
	16 12	29.47	+ .033	π		16 18	42.01	+ .025	π
	16 46	30.03	+ .057	*l*		16 44	42.45	+ .022	*l*, 2
	16 52	30.13	+ .044	π	2353	13 27	10.24	− .004	*l*
	17 31	30.78	+ .016	*l*		13 35	10.38	+ .018	π
	17 36	30.87	+ .038	π	2354	13 05	33.87	+ .021	*l*
	18 18	31.57	+ .018	*l*		13 13	34.01	− .001	π
	18 25	31.68	+ .019	π		14 07	34.91	+ .003	*l*
	18 55	32.18	+ .011	*l*		14 13	35.01	− .026	π
	19 01	32.29	− .001	π		15 10	35.96	− .013	*l*
	19 31	32.78	+ .012	*l*		15 19	36.11	− .029	π
	19 37	32.88	.000	π	2363	15 30	45.82	+ .028	*l*
2296	15 17	20.46	+ .044	*l*		15 38	45.95	+ .021	π
	15 25	20.60	+ .035	π	2366	15 07	48.62	− .003	*l*, 4
2306	17 48	56.53	+ .035	*l*		15 09	48.65	+ .022	π
	17 56	56.67	+ .026	π	2386	14 47	46.53	+ .021	π, 2
2307	17 56	11.84	+ .014	*l*		15 07	46.87	+ .055	*l*, 2
	18 02	11.94	+ .019	π	2389	14 07	49.05	+ .056	*l*, 2
2312	15 10	60.26	+ .022	*l*, 2		14 15	49.18	+ .030	π, 2
	15 11	60.28	− .014	π	2391	13 31	27.63	+ .028	*l*
	15 48	60.89	+ .016	*l*		13 38	27.74	+ .021	π
	15 58	61.06	+ .017	π		14 06	28.21	+ .045	*l*, 2
2313	14 22	14.64	+ .028	*l*		14 13	28.33	+ .023	π, 2
	14 28	14.74	+ .036	π	2392	13 55	52.02	+ .039	*l*, 1
2317	12 35	40.04	+ .047	*l*		14 05	52.19	+ .037	π, 1
	12 42	40.16	+ .031	π					

NOTES

J.D. 2422265—Further measures stopped by clouds.

2312—Sky fair.

2313—Sky thick but uniform.

2354—Sky thick but uniform.

2363—Sky fair.

2366—Sky fair, measures discordant.

days or 104 periods. The epoch from the adopted correction of the last minimum is

J.D. 2422619.7866 = $0^{d}0003$.

It will perhaps be worth while to observe one or more minima in this way each year, as the epoch can be determined with a probable error of less than one minute.

TABLE VI

OBSERVATIONS IN OCTOBER 1920

J.D. 242	G.M.T.	Difference of Magnitude	Computed Phase	Observed Phase	Correction to Ephemeris	Mean Correction
2599	$18^{h}40^{m}4$	$-0^{M}734$	$+1^{h}24$	$+1^{h}62$	$-0^{h}38$	
	18 50.3	−0.688	+1.45	+1.74	−0.29	
	19 00.0	−0.618	+1.62	+1.93	−0.31	$-0^{h}33$
2616	19 09.1	−0.334	−3.10	−2.80	−0.30	
	19 20.3	−0.377	−2.91	−2.65	−0.26	
	19 32.0	−0.430	−2.71	−2.47	−0.24	−0.27
2619	17 31.2	−0.870	−1.50	−1.26	−0.24	
	17 42.2	−0.944	−1.36	−1.07	−0.29	−0.26
	17 54.4	−1.004	−1.16	−0.89	−0.27	
	18 07.2	−1.068	−1.06	−0.73	−0.33	
	18 19.6	−1.142	−0.74	−0.47	−0.27	−0.29
	18 34.6	−1.188	−0.45			
	19 08.2	−1.170	+0.07			
	19 19.4	−1.122	+0.26	+0.55	−0.29	
	19 33.4	−1.056	+0.50	+0.77	−0.27	
	19 49.6	−0.966	+0.76	+1.02	−0.26	−0.27
	20 03.6	−0.837	+0.99	+1.34	−0.35	
	20 14.8	−0.804	+1.18	+1.43	−0.25	
	20 27.2	−0.680	+1.39	+1.76	−0.37	−0.32
	20 38.0	−0.622	+1.57	+1.92	−0.35	
	20 49.5	−0.558	+1.76	+2.09	−0.33	−0.34

As the measures of Table VI were made after the computations of this paper were finished, they were not used further. The three observations beginning with $18^{h}19^{m}6$ on J.D. 2422619 are all within a half-hour of minimum, and give residuals from the final light-curve of $+0^{M}004$, $+0^{M}003$, and $-0^{M}006$ respectively, or a mean of $0^{M}000$, which shows that as far as accidental error is concerned the lowest point of the curve is well determined.

Table VII gives the normal magnitudes formed in the usual way from the observations in Tables IV and V. The residuals were formed from the final light-curve. Except near the time of greatest eclipse at primary, the number of sets in each normal are nearly enough equal so that all normals may be given the same

weight. The number of nights in a normal is presumably more important than the number of sets. The normals of Table VII together with the light-curves of the 1920 and 1910 series are shown in Figure 1.

TABLE VII

NORMAL MAGNITUDES

Phase	Difference of Magnitude	Residual O−C	Sets	Phase	Difference of Magnitude	Residual O−C	Sets
−4h32	−0M052	−0M012	6	5d06	+0M004	+0M002	8
−3.94	−0.118	− .026	8	5.49	− .002	− .005	8
−3.51	−0.166	.000	8	5.94	+ .002	− .001	8
−3.02	−0.289	− .011	8	6.44	.000	− .005	8
−2.70	−0.372	− .009	8	10.31	+ .007	− .007	6
−2.36	−0.462	+ .004	8	11.89	+ .016	− .002	6
−2.10	−0.563	− .008	8	14.40	+ .023	.000	9
−1.74	−0.682	+ .005	8	20.61	+ .034	+ .002	9
−1.48	−0.793	− .008	6	23.00	+ .036	+ .003	6
−1.26	−0.868	+ .002	6	23.92	+ .036	+ .003	6
−0.92	−0.979	+ .023	4	27.68	+ .024	− .008	6
−0.57	−1.099	+ .019	4	28.27	+ .034	+ .002	4
−0.33	−1.168	+ .001	4	29.62	+ .042	+ .010	9
+0.02	−1.206	.000	4				
+0.40	−1.154	+ .003	4	30.59	+ .033	+ .006	9
+0.90	−1.020	− .011	4	31.81	+ .016	+ .002	9
+1.16	−0.917	− .007	4	32.65	+ .004	− .002	9
+1.49	−0.766	+ .016	6	33.76	+ .001	+ .008	7
+1.72	−0.688	+ .007	6	35.11	− .011	.000	9
+1.95	−0.603	+ .007	6	35.97	− .016	− .013	9
+2.19	−0.514	+ .009	8	36.60	+ .004	.000	6
+2.44	−0.433	+ .008	8	38.22	+ .029	+ .006	9
+2.66	−0.376	− .001	8	38.88	+ .038	+ .009	9
+2.90	−0.304	+ .005	8				
+3.17	−0.232	+ .008	8	39.90	+ .032	.000	9
+3.47	−0.175	− .001	8	40.19	+ .033	+ .001	9
+3.80	−0.106	+ .008	8	40.79	+ .031	− .001	9
+4.07	−0.075	− .001	6	41.47	+ .032	.000	9
+4.36	−0.031	+ .004	6	42.46	+ .029	− .003	8
+4.69	−0.009	− .003	6	46.10	+ .023	− .010	8
				48.05	+ .025	− .007	8
				49h97	+ .033	+ .002	7
				51.94	+ .030	+ .002	5
				56.60	+ .030	+ .012	6
				60.13	+ .018	+ .008	8
				60.74	+ .006	− .002	9
				63.12	+ .013	+ .010	6
				63.87	− .006	− .008	6

DETERMINATION OF THE ELEMENTS

After a graphical solution had been made for the time of primary minimum, so that the final phases could be computed,

the next step was to use the observations between minima for a determination of the radiation-effect and ellipticity of figure. The 1910 observations had indicated a conspicuous rise in the light from primary to secondary, but no measurable maximum at phase $\pi/2$ due to elongation of the components of the system. The more accurate new series, however, shows that it is worth while to include in the solution the ellipticity term. Using thirteen nor-

TABLE VIII

COMBINED NORMALS, PRIMARY MINIMUM

Phase	Difference of Magnitude	Rectified Light	Residual in Light	No. of Sets
0^h02	-1^M200	0.352	0.000	4
0.33	−1.168	.362	+ .001	4
0.40	−1.154	.366	+ .001	4
0.57	−1.099	.384	+ .007	4
0.91	−1.000	.417	+ .002	8
1.21	−0.892	.458	− .001	10
1.48	−0.780	.504	+ .002	12
1.73	−0.685	.547	+ .002	14
2.02	−0.583	.597	− .001	14
2.28	−0.488	.649	+ .001	16
2.55	−0.404	.699	.000	16
2.80	−0.338	.741	.000	16
3.12	−0.251	.800	.000	12
3.48	−0.172	.858	.000	12
3.94	−0.096	.918	− .003	18
4.33	−0.045	.961	− .003	9
4.77	−0.008	.991	− .007	9

mals following primary and fourteen following secondary, there was found by least-squares

$$\text{Difference of magnitude} = 0^M0285 - 0^M0164 \cos\theta - 0^M0148 \cos^2\theta, \quad (1)$$
$$\pm 15 \qquad \pm 11 \qquad \pm 27$$

where θ is the phase-angle, and the probable errors were computed in the usual way, the probable error of a single normal being $\pm 0^M0039$. The coefficient of $\cos^2\theta$ gives for the ellipticity constant $z = 0.027$.

The solution was made by Russell's method. The normals at primary minimum before and after zero phase were combined on one branch of the curve, and the resulting combined normals were rectified by adding $+0^M0148 \cos^2\theta$ to the observed magnitudes, then reducing to light and adding $0.0149\,(1+\cos\theta)$ in light units. The result and the residuals are in Table VIII. There are fewer

observations in the half-hour near zero phase, but these residuals are not unduly large.

The constants of the rectified curve are given in Table IX.

The time of secondary minimum cannot be determined with great accuracy, but nevertheless even with a variation of only

TABLE IX

RECTIFIED CURVE

	Magnitude	Range	Light	Loss of Light
Maximum	+0.045		1.000	
Primary minimum	−1.089	1.134	0.352	0.648
Secondary minimum	+0.003	0.042	0.962	0.038

$0^{M}04$ this test of the ellipticity of the orbit is more delicate than that by any other method. The phase of secondary was determined graphically, and tabulating the comparison with previous results we have:

TABLE X

PHASE OF SECONDARY MINIMUM

Light-curve, 1920	$34^{h}65$
Light-curve, 1910	34.67
Spectroscopic, $e=0.05$	36.46
Assumed, $e=0.00$	34.41

The close agreement with the previously observed time is largely accidental, but there is once more no photometric evidence of any considerable orbital eccentricity, and for the purposes of this paper the orbit may be considered circular.

In 1910 the elements of Algol were determined with no allowance for possible light of the third body, but with the known third component of long period it is evident that we have here a case similar to that of λ Tauri, and the computed elements will depend upon how much of the light of the system comes from the distant satellite. I learn from Dr. Schlesinger that he has in hand a study of the Allegheny spectrograms which show additional lines at primary minimum; if these lines are due to the third body it may be possible to determine the actual masses of the three components, and to estimate the light of the third body. For

the present it will be sufficient to determine the elements, neglecting the third body's light, $L_3=0$, for comparison with the 1910 results, and then to indicate the influence of L_3.

Using Russell's method and notation for partial eclipse of uniform disks it was found that a satisfactory light-curve is given by $C=0.0935$, $D=0.0500$, $\chi=1.870$. Carrying through the solution for the elements, and arranging the 1910 results in the same form for comparison, we have:

TABLE XI

ELEMENTS OF THE ECLIPSING SYSTEM

		1920	1910
Ratio of radii	k	0.85	0.88
Area of bright body obscured at minimum	a_0	0.700	0.711
Light of bright body	L_b	0.925	0.898
Light of bright side of faint body	Lf	0.075	0.102
Light of fainter side of faint body	$Lf-2b$	0.045	0.058
Ratio of surface brightness of bright sides of bodies	Jf/Jb	0.059	0.088
Radius of bright body, radius of orbit = 1	a_b	0.207	0.210
Radius of faint body, radius of orbit = 1	af	0.244	0.239
Cosine of inclination	$\cos i$	0.142	0.134
Ellipsoidal constant	z	0.027	0.0
Ratio of axes of ellipsoids	b/a	0.987	1.0
	c/a	0.978	1.0
Mean density of system, sun = 1	ρ_0	0.07	0.07
Duration of eclipse		9^h66	9^h80
Albedo, Lambert's law	μ_1	0.7	1.1
Albedo, Seeliger's law	μ_2	1.0	1.5

A comparison of the elements shows that there is little difference between the two series, except for the ellipticity of figure detected in 1920, and the smaller light measured for the fainter component. The selenium photometer gave practically the same color-sensitivity as visual measures, whereas the color-equation of the photo-electric installation is 0.70 magnitude. The intensity of the bright side of the companion in the new series is 0.059, whereas it was 0.088 with selenium. These two values, which correspond to the secondary minima of 0^M04 and 0^M06 respectively, show that the companion compared with the primary of spectrum B8 was measured only two-thirds as bright in photo-electric as in visual light, which would indicate a spectrum of approximately Go. If we had observations of sufficient precision, and also could allow for the light of the third component of the system, the

determinations of the light of the two sides of the fainter body with instruments of different color-sensitivity would give a rough measure of the color-index, and hence of the spectrum of each side of the faint star. In the present case, however, I doubt if we can say more than that the satellite is a yellower star than the primary.

As in the case of λ Tauri,[1] the solution for partial eclipses is given by the intersection of the two curves,

$$\chi(k, \alpha_0, \tfrac{1}{4}) = \text{constant},$$

$$\alpha_0 = \frac{1}{1-L_3}\left(1-\lambda_1+\frac{1-\lambda_2}{k^2}\right),$$

where the introduction of L_3 into the last equation takes account of the third body. The larger the value of L_3, the greater is the area of eclipse at primary minimum, and the smaller is the bright body compared with the eclipsing satellite. An upper limit of L_3 is given, however, by the fact that its light may not show even when the total light of the system is reduced 1.2 magnitudes at minimum, or to one-third of the light at maximum. It is just here, however, that the additional spectrum lines at primary minimum may give an estimate of the light of the third body. It is not probable that L_3 is much greater than 0.10, which would give it nearly one-third of the total light at minimum. This would reduce the computed relative radius k to 0.78, as compared with $k=0.85$ shown in Table XI for $L_3=0$. It is obvious that with the light of the third body undetermined only rough elements for Algol can be found, but the uncertainty for this system is no greater than for any other of the many eclipsing stars where there may happen to be unknown additional companions.

All of the computations in this paper are based upon assumed uniform intensity of the apparent disks of the components of Algol. In view of the satisfactory agreement of the observations with the computed light-curve, and the uncertain influence of the third body, it has not seemed worth while to consider the additional complication of darkening at the limb.

In Table XII is the final light-curve of 1920 computed from the elements in Table XI, together with a comparison with the

[1] *Astrophysical Journal*, 51, 211, 1920.

curve of 1910. To make the comparison, the printed difference of magnitude of 1910 have been changed in sign, and $0^{M}.174$ has then been added to make the average magnitude between eclipses the same for the two series. The average difference between the two curves in the table is $0^{M}.006$, which depends, however, upon

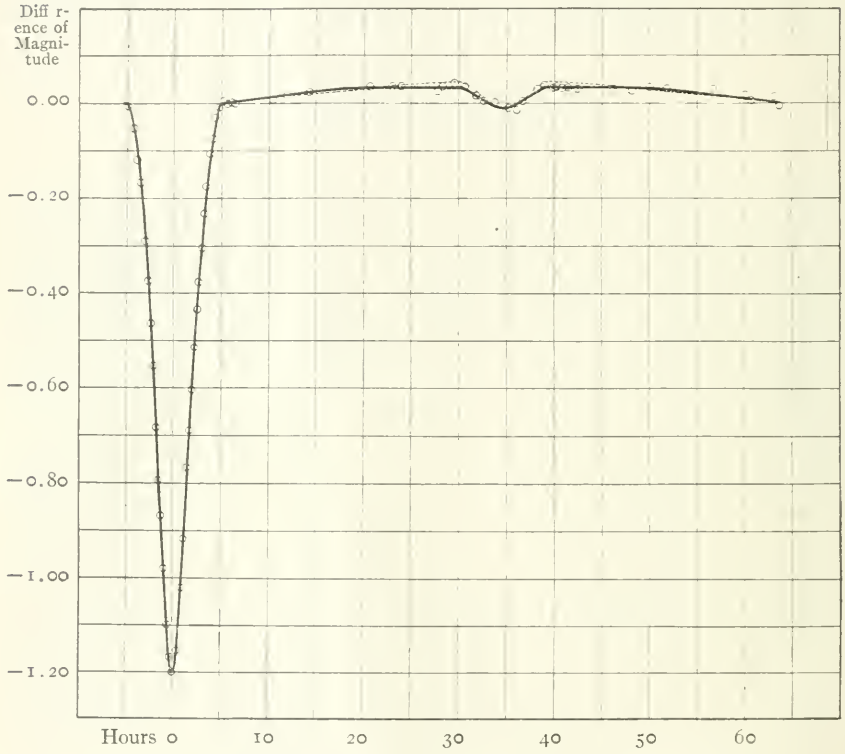


FIG. 1.—Light-curve of Algol. Heavy line, 1920; broken line, 1910

the number of points selected during and between the eclipses. With the forced agreement at maximum, the difference at greatest eclipse is $0^{M}.004$. The two curves are shown in Figure 1, where on the scale used the same line represents the two curves during primary minimum; this is rather remarkable inasmuch as the adjustment between the curves was made outside of the eclipses, and previous observers have found considerable differences in the forms of the light-curves taken in different colors. Any difference

in the epoch of minimum as derived in light of different wave-lengths would not show in this comparison of series not taken simultaneously.

TABLE XII

LIGHT-CURVES OF ALGOL

Phase	1920	1910	Difference	Phase	1920	1910	Difference
± 0^{h}0	−1^{M}200	−1^{M}196	−0^{M}004	30^{h}0	+0^{M}031	+0^{M}045	−0^{M}014
± 0.5	−1.135	−1.136	+ .001	31.0	+ .023	+ .036	− .013
± 1.0	−0.972	−0.976	+ .004	32.0	+ .012	+ .022	− .010
± 1.5	− .778	− .776	− .002	33.0	.000	+ .004	− .004
± 2.0	− .592	− .596	+ .004	34.0	− .010	− .012	+ .002
± 2.5	− .422	− .436	+ .014	34.65	− .012	− .015	+ .003
± 3.0	− .283	− .296	+ .013	35.0	− .011	− .014	+ .003
± 3.5	− .168	− .176	+ .008	36.0	− .003	− .003	.000
± 4.0	− .084	− .091	+ .007	37.0	+ .009	+ .014	− .005
± 4.5	− .021	− .026	+ .005	38.0	+ .021	+ .032	− .011
± 4.83	+ .002	.000	+ .002	39.0	+ .031	+ .043	− .012
+ 5.0	+ .002	.000	+ .002	39.48	+ .031	+ .046	− .015
10.0	+ .012	+ .008	+ .004	40.0	+ .032	+ .046	− .014
15.0	+ .024	+ .018	+ .006	45.0	+ .033	+ .038	− .005
20.0	+ .032	+ .030	+ .002	50.0	+ .031	+ .027	+ .004
25.0	+ .033	+ .040	− .007	55.0	+ .022	+ .016	+ .006
29.82	+ .031	+ .046	− .015	60.0	+ .010	+ .006	+ .004

A test of the accuracy of the present measures is given by the residuals in Table VII, from which the comparison with 1910 is made in Table XIII. The weight of the determination of a light-

TABLE XIII

PROBABLE ERRORS AND WEIGHTS

	1920	1910
Number of normals at primary minimum	30	20
Probable error of one normal	0^{M}007	0^{M}023
Relative weight of determination	16.2	1
Number of normals at secondary and between minima	36	24
Probable error of one normal	0^{M}004	0^{M}006
Relative weight of determination	3.4	1
Relative weight of complete curve	4	1

curve may be taken as proportional to n/r^2, where n is the number of normals and r the probable error of each.

It is thus seen that the photo-electric measures give a curve which, when compared with the selenium curve, has sixteen times the weight at minimum, more than three times the weight at maximum, and about four times the weight for the whole curve. Also

it is to be noted that in the new series the light of Algol was cut down with a shade-glass, fivefold at minimum and thirteen fold at maximum. The observing time was less in 1920 than in 1910, perhaps a fair estimate being that the new curve represents half the effort of the old one. The selenium measures are therefore quite superseded, and no doubt after another ten years, if not before, someone else or myself will be able to improve upon the present results.

There has been only one parallax of Algol published since 1910, that from Yerkes, $+0''.020 \pm 0''.014$, and until there are several more modern photographic determinations available, it seems scarcely worth while to recompute the total light and surface brightness of the components. Dr. Schlesinger has sent me a value of $\pi = 0''.032$ for the absolute parallax, from the results of Chase, Russell, and Yerkes. This is 10 per cent larger than the parallax, $0''.029$, quoted at the end of my previous paper, and would make the total light of Algol about two hundred times that of the sun. This with a plausible assumption as to the ratio of the masses would give the companion a surface intensity ten times that of the sun, which value is presumably rather high for the spectrum G, estimated from the secondary minimum. It is evident that we need the best parallax that can be determined by several observers.

Therefore, in spite of the increased accuracy over the former work, the present photometric measures cannot give definitive results for the system. If the spectrum of the third body can be measured, its light estimated, and also the parallax determined with a small relative error, then, as it has been said, we shall know "all about Algol."

I am indebted to Mr. C. C. Wylie for some of the observations toward the end of the 1920 series, and to Miss Iva Hamlin for many of the reductions. The present satisfactory performance of the photometer is due largely to Dr. Elmer Dershem, who rebuilt most of the instrument during the summer of 1919.

This work is a portion of that accomplished with the aid of grants from the Draper fund of the National Academy of Sciences.

University of Illinois Observatory
November 1920

AN EXAMINATION OF THE INFRA-RED SPECTRUM OF THE SUN, λ 8900–λ 9900[1]

By FREDERICK S. BRACKETT

ABSTRACT

Photography of infra-red spectra to λ 9900.—In previous work scattered light has been a serious obstacle to the extension of observations into the infra-red. By using a monochrometer with the second slit removed the author *eliminated scattered light* and obtained, on plates sensitized with dicyanin, spectrograms of even intensity which show fine structure to λ 9850. This limit seems to be fixed in astronomical work by Langley's broad atmospheric absorption band ϕ. Below λ 9400 a *water solution of malachite green* is recommended as a *screen* since it is almost opaque to wave-lengths shorter than λ 7200.

Infra-red solar spectrum λ 8900 to λ 9900.—Spectrograms made in the first order of a 15-foot concave grating mounted in the constant temperature pit of the Mount Wilson laboratory gave the *wave-lengths* of 563 lines to about 0.01 A, at least as far as λ 9650 (Table I). To determine the *origin* of the lines, solar-rotation photographs were made with the 13-foot spectrograph of the 60-foot tower telescope, and spectrograms taken under conditions of low and high humidity were compared. It was found that 45 and possibly 70 lines, including one-fifth of the fainter lines observed, are of solar origin, while 60 of the stronger diffuse telluric lines broaden remarkably as the humidity increases and hence undoubtedly form an *absorption band due to water vapor between λ 9300 and λ 9650.* Of the solar lines, 14 are attributed to *iron* and 1 or 2 to *nickel.*

The investigator is naturally attracted to the less refrangible end of the spectrum by the fact that the characteristic displacements due to some of the most interesting spectroscopic phenomena increase with increasing wave-length, among them being the Doppler effect, the Zeeman effect, pressure shift, and the possible Einstein effect. But before work of precision can be done in any region, it is desirable, if not absolutely necessary, to make some preliminary survey of the field. In the case of the infra-red spectrum of the sun the work of Dr. Meggers, which he has been kind enough to furnish the Mount Wilson Observatory in advance of publication, gives identifications and wave-lengths down to 9000 A, and it is the purpose of the present investigation to extend these results as far as can readily be done with dicyanin-bathed plates.

Since Dr. Meggers published his map of the solar spectrum from 6800 A to 9600 A,[2] frequent attempts have been made to extend

[1] *Contributions from the Mount Wilson Observatory*, No. 197.

[2] *Astrophysical Journal*, 47, 1, 1918.

the limit to still longer wave-lengths by photography with plates bathed in dicyanin, but until recently the attempts have met with little success. In March of this year Dr. K. Burns[1] published his photographs showing the more outstanding structure to almost 9900 A. On all of these plates, however, much of the finer structure beyond 9200 A appears to have been lost. That the chief cause of this lack of contrast is scattered light there can now be little doubt. When the present investigation was first undertaken, it was believed that the chief difficulty was the loss of defining power in the lenses, due to a rapid change in the properties of the glass with increasing wave-length. But the appearance of a ghost of the B group between 9600 A and 9700 A on a plate taken with the 13-foot spectrograph of the 60-foot tower telescope seemed to prove that the presence of scattered light was responsible.

In order to establish this fact with certainty, a series of tests was made in the laboratory with a one-meter concave grating. Exposures were first tried with a screen opaque to wave-lengths shorter than 6400 A. On these plates the contrast fell off rapidly beyond 9200 A, until even the strongest lines were lost at 9600 A. Exposures were then made through a water solution of malachite green. A screen more than a centimeter in thickness proved almost opaque to all wave-lengths shorter than 7200 A. Photographs taken with this screen were much superior to those previously obtained and showed lines well beyond 9750 A. For infra-red work at wave-lengths shorter than 9400 A this type of screen may be strongly recommended.

As screens opaque to still longer wave-lengths, and at the same time transparent beyond 9000 A, were not available, the only possibility of further progress lay in preliminary analysis. For this purpose a Hilger monochrometer with the second slit removed was set in collimation with the spectrograph. It was found that when the first slit of the monochrometer was open about two millimeters, light extending over several hundred angstroms was admitted to the slit of the spectrograph.

By calibrating the screw of the monochrometer, settings could be made which would admit any desired range of spectrum.

[1] *Lick Observatory Bulletins*, No. 327, 1920

PLATE I



INFRA-RED SPECTRUM OF THE SUN, λ8900–λ9900

Moreover, this adjustment could be changed during the exposures, so that the intensity could be adapted to the sensitiveness of the plate for a given wave-length. This made it possible, even in the extreme infra-red where the sensitiveness falls off rapidly, to obtain photographs of even density throughout a long range of spectrum. Plates made with this arrangement showed sharply defined lines as far as the slightest trace of continuous background could be detected.

The monochrometer was used with a 15-foot Anderson concave grating in a Rowland mounting placed vertically in a constant temperature pit, and photographs were taken which show the fine structure to 9800 A. The first order of the grating was used, giving a scale of about 3.7 A to the millimeter. Although the grating proved quite fast, the system was optically slow; the aperture ratio was $f/45$ and much of the light was lost because of the astigmatism characteristic of the Rowland mounting, when used at the large angle necessary for the infra-red, even in the first order.

The best dicyanin at hand at the time the investigation was begun was of old German stock, which proved slightly superior to that obtained from the Bureau of Chemistry of the Department of Agriculture. Exposures ranged from seven to twenty-one hours, extending over as many as three days. This is the most rigorous test to which the mounting in the constant temperature pit has been subjected and proves clearly its merit, since even these long exposures show practically no loss of definition. The longest exposure reveals lines to almost 9900 A; the portion of the spectrum between 9600 A and 9900 A shown on this photograph is reproduced in Plate I*c*.

In February of this year, however, a shipment of dicyanin labeled A VI–8 was received from the Bureau of Chemistry which proved much faster than anything previously used. Photographs on bathed Seed 23 plates were obtained in seven hours which showed lines beyond 9800 A.

In order to determine the wave-lengths of lines which could be used as a basis for the reduction of the plates, exposures were made on the same plate to the second-order iron arc and to the first-order infra-red solar spectrum. The light from the arc was

thrown directly upon the slit by two small prisms on either side of the beam from the monochrometer. Because of astigmatism, however, all the lines extend entirely across the plates. All screening arrangements near the plate were avoided on account of the danger of moving the plate-holder. The arc exposure was made in five parts, distributed symmetrically throughout the solar exposure. The illumination of the grating by both arc and sun was carefully adjusted, so that any possible displacement due to differences in illumination would presumably be small. As the grating used is one of the most perfect, the coincidence of the two orders can be subject to little question. The two plates obtained agreed perfectly. It is to be regretted, however, that lack of time prevented checking them by a different set-up. In measuring these plates all lines were avoided which showed any suggestion of blend.

The rotation plates for the separation of the solar and telluric lines were taken with the 13-foot spectrograph of the 60-foot tower telescope, which projects an image of the sun about 6.7 inches in diameter. Although lenses are used in both collimator and camera of the spectrograph, it was found that a fair focus could be obtained over the whole region. The chief difficulty in the work proved to be the many adjustments necessary for both the monochrometer and the spectrograph. The 13-foot spectrograph is a two-lens system with one reflection, and the grating is set at a considerable angle, so that the dispersion is considerably greater than normal, thus giving a scale in the infra-red of the first order of 3.3 A to the millimeter. Although the aperture ratio of the system is limited by the telescope to $f/60$, being non-astigmatic, it proved over twice as fast as the 15-foot concave grating.

Because of the already complicated optical system, the use of prisms to unite the beams from the limbs of the sun was not attempted. A simple exposing screen in front of the slit was used. The exposure for one limb was made in two parts, one before and one after the exposure for the other limb, so that any mechanical shift would not introduce a displacement.

Photographs of the spectrum of the center of the sun were also taken, in order to determine the wave-lengths of the solar lines. As these plates were taken in the middle of August, a correction of

+0.009 A had to be added because the earth was then approaching the sun. Inasmuch as the period of exposure was longer in the afternoon than in the morning, a slight correction, −0.002 A, had to be subtracted. A total correction of +0.007 A has therefore been applied to all solar wave-lengths.

Fortunately, plates were secured at times of both high and low humidity. An examination of these plates on a comparator showed beyond 9300 A a remarkable broadening of the lines on photographs taken during high humidity, which is entirely independent of exposure time, appearing alike on plates of different densities. As the mean altitude of the sun was about the same for all exposures, there can be little doubt that this effect is due to water-vapor. In the list of wave-lengths only those lines which showed the most marked effect have been attributed to water-vapor, although it is quite likely that others than those so designated are due to this source.

The reduction of the rotation plates showed roughly 10 per cent of the five hundred lines measured to be of solar origin. Of these, fourteen may be attributed to iron and possibly one or two to nickel. In the region between 9300 A and 9650 A over sixty broad diffuse lines appear which are due to water-vapor.

In measuring the plates the chief emphasis has been laid on consistency. The wave-lengths recorded represent measures made on from two to eight plates. In the region from 9000 A to 9650 A the wave-lengths should be reliable to less than ±0.01 A, except where the line is marked with an "a." Beyond 9650 A the wave-lengths are determined by extrapolation, and systematic errors may enter.

On the first plates obtained intensities were estimated between 00 and 10, but on the later plates showing both fainter and broader lines, they were classified between 000 and 12. In the case of the water-vapor lines this classification is not altogether satisfactory, since at times of high humidity some of them extend over several angstroms. These lines also present special difficulty in measurement, not only because of their broad diffuse character, but also because they do not widen symmetrically with increasing humidity. Their wave-lengths are merely approximate.

TABLE I

λ	Intensity	Source Element	λ	Intensity	Source Element
9000.45	7B		9100.60	1	*A*, *S*, Fe
9003.81	6		9105.47	3	
9007.02	0	*S*	9106.30	0	*S*, Ni
9007.03	1		9107.06	0	U
9008.57	000	*S*	9107.42	1	U
9009.09	0		9108.41	1V	
9009.88	00	*S*	9110.57	000	*S*
9010.57	000	*S*	9111.92	0	*S?*
9011.05	4		9113.04	00	
9016.80	5		9114.50	000	*S*
9018.12	0		9115.73	0	
9021.68	000	*S*	9117.08	0R	
9022.71	4		9118.09	1	
9024.53	000	*S*, Fe	9118.98	3	
9025.07	4		9124.37	0	*S*
9029.45	0		9124.93	00	
9031.47	2		9127.87	1	
9034.98	00		9128.65	1	
9040.16	0		9129.90	1	
9041.20	000		9130.70	3	
9042.32	00		9132.53	1	
9042.88	1		9134.36	1	
9047.46	0		9134.87	0	*S?*
9048.62	000		9136.07	1	
9051.18	00		9136.64	3	
9053.03	2		9137.12	1	
9060.49	1		9139.89	000	
9061.52	00	*S*	9140.55	0	
9061.87	00		9141.14	00	
9062.77	1		9142.77	00	
9064.08	1		9143.55	00	
9069.20	4		9144.22	0	
9070.43	000	*S*, Fe	9144.64	00	
9072.03	5		9145.79	000	
9073.20	00		9146.25	0	*S*, Fe
9074.36	3		9147.05	000	*S*
9078.33	00	*S*, Ni?	9148.02	00	*S*, Fe
9079.13*a*	00		9148.78	00	
9079.84*a*	1	*A*, *S*, Fe	9150.12	1	
9080.57	00		9150.88	0	
9081.37	3		9151.85	0BR	
9085.50	00	*S*, Ni?	9152.69	2	
9086.71	2		9153.24	2	
9087.08	4		9154.23	000	*S*
9088.49	0	*S*, Fe	9155.68	6BR	
9089.55	00	*S*, Fe	9156.93	0	
9089.94	0		9160.15	1	
9090.42	00		9160.97	1	
9092.58	1		9162.69	0V	
9093.85	1		9164.05	0BR	
9095.01	1	*S*	9167.38	00	
9095.38	0		9168.01	1	
9098.52	0		9168.88	0	*S?*
9099.83	2		9169.43	0	

TABLE I—*Continued*

λ	Intensity	Source Element	λ	Intensity	Source Element
9170.78	oo		9251.19	2	
9171.76	oo		9252.53	oo	*S*
9172.58	o		9253.23	oo	*S*
9172.97	oo		9253.84	oo	*S*
9173.06	o		9254.44	o	
9174.23	3		9255.29	oo	*S?*
9175.31	2		9255.87	1	*S*
9176.97	3		9257.01	oo	
9178.62	1		9258.36	o	*S*. Fe
9179.39	ooo		9259.17	o	*S?*Fe
9181.30	1		9260.45	1	
9182.15	ooo		9261.06	oo	
9183.59	oo		9261.67	oo	
9184.48	2		9262.35	o	
9185.06	2		9263.16	oo	
9186.56	oo		9263.97	ooo	*S*
9190.33	o		9266.26	1	
9191.71	oo		9267.22*a*	oo	
9192.67	2		9269.17	o	
9195.46	2		9270.14	oo	*S?*
9196.12	2		9270.88	oo	*S?*
9199.20	oo		9272.30	o	
9205.69	o		9273.14	2	
9206.03	o		9274.32	oo	
9207.90	o		9275.16	o	
9208.70	o		9275.80	oo	
9210.09	o	*S*, Fe	9276.31	ooo	
9212.92	2		9276.92	oo	
9214.74	3		9277.60	o	
9215.70	oo		9278.91	4	
9217.35	4		9279.83	1	
9218.36	oo	*S*	9280.21	o	
9222.10	o		9281.99	o	
9225.10	2		9282.78	o	
9228.19	oo	*S*	9284.22	oo	
9228.76	oo		9284.98	2	
9229.70	oo		9285.70	oo	
9230.58	oo		9286.53	1	
9232.84	1		9286.90	o	
9234.85	1		9288.00	ooo	*S*
9235.30	oo		9288.60	oo	*S?*
9235.83	oo		9288.98	oo	*S?*
9237.49	o	*S*	9289.95	o	*S?*
9238.18	1		9290.59	oo	*S*
9239.07	1		9291.43	3	
9240.03	ooo	*S*	9292.78	o	
9240.45	oo		9293.23	1	
9242.33	oo	*S*, Fe	9294.56	2	
9243.10	o U		9295.21	3	
9243.41*a*	oo		9296.50	oo	
9244.53 44.74	1 2D		9297.23	oo	
9244.93	1		9297.80	4	
9246.41	3		9298.70	o	
9249.57	o		9300.53	3	

TABLE I—*Continued*

λ	Intensity	Source Element	λ	Intensity	Source Element
9301.14	2		9357.55*a*	6–9 } U	*w*
9301.98	2		9358.93*a*	5–8 }	*w*
9302.77	oo		9360.24	ooo }	
9303.92	4		9360.60	oo }	
9304.66	1		9361.28	2	
9305.48	oo		9361.93	oo	
9306.34	oo		9362.33	o	*S*, Fe
9307.30	1		9363.39	1V	
9308.14	4		9364.95*a*	4–8 }	*w*
9308.97*a*	o		9366.46*a*	5 } 10	*w*
9309.62	5–9	*w*	9367.41	1B }	
9310.91*a*	oo		9369.60*a*	5–9	*w*
9311.80	2		9371.58*a*	7B–12B	*w*
9312.72	ooo		9373.14	2	
9314.08	1		9374.34	o	
9315.21	3		9375.28	3	
9316.11*a*	4–8 } U	*w*	9375.74	oo*	
9319.14*a*	5–9 }	*w*	9377.74*a*	7–11	*w*
9320.12	o		9379.74*a*	3–5	*w*
9320.83*a*	4–6	*w*	9381.22*a*	7–11 } U	*w*
9321.76	oo		9382.22	2 }	
9322.55	3		9383.63	2	
9323.20	3		9385.84*a*	oo	
9324.24	3– }		9386.84*a*	7–11 }	*w*
9325.06*a*	1 } –9D	*w*	9387.91	3 }	
9325.67*a*	4 }	*w*	9390.88	o	
9326.71*a*	oo		9391.84	3	
9327.82	4		9394.43	3	
9328.80	1		9396.32	2	
9329.93	oo		9400.18	2	
9330.53	1		9401.68	3BV	
9331.52	2		9402.67	1	
9333.55*a*	5–8 } U	*w*	9403.31	oo	
9334.64*a*	4–7 }	*w*	9404.51	1	
9335.69	o }		9405.30*a*	oo	
9336.13	1 }		9405.78	ooB	*A*, *S*?
9337.23	3		9406.96	3	
9337.88	o		9408.00	oo	
9338.52	2 }		9409.10	3	
9339.47*a*	5–8 }	*w*	9410.44*a*	5–8	*w*
9342.52*a*	6–8 }	*w*	9411.38	1_0	*S*?
9344.05*a*	9D–12 } U	*w*	9411.91	o	
9345.67*a*	6–8 }	*w*	9412.75	1	
9346.98	2 }		9413.55	2	*A*,*S*?
9347.70	o	*S*?	9414.10	2	*A*,*S*?Fe?
9348.46	1		9415.07	1	*S*
9349.31	oo		9416.08	oo	
9350.52	3 }		9416.87	o	*S*
9352.01	oo }		9417.72*a*	4–7	*w*
9353.06*a*	3–5 } U	*w*	9420.09	oo	
9353.65*a*	3–4 }	*w*	9420.81	o	
9354.50*a*	5–7 }	*w*	9421.90	4	
9355.26*a*	1–3 }	*w*	9424.89	o	
9356.58	1		9426.85*a*	7–11 } U	*w*
			9428.36*a*	7–10 }	*w*

TABLE I—*Continued*

λ	Intensity	Source Element	λ	Intensity	Source Element
9430.68*a*	5V–8V	*w*	9500.76*a*	6, 4 –12D	*w*
9432.03*a*	ooo	*S?*	9501.71*a*		*w*
9432.85	oo	*S*	9503.30	ooB	
9434.97	oo		9504.51	1	
9437.90*a*	7–10 Wings	*w*	9505.68	3B	
9440.89*a*	10D–14D	*w*	9506.81	oo	
9442.48	1		9507.82	oB	
9443.39*a*	3–5	*w?*	9508.86	oB, oo	
9444.47	2		9509.38		
9446.08	4		9510.83	2	
9447.13	oo		9512.69	1	
9449.22	2		9513.82	1	
9450.38	3		9514.55	1	
9452.65	oo		9516.35*a*	1, 6 –12U	
9454.12*a*	3–5	*w?*	9517.06*a*		*w*
9454.79*a*	3–5	*w?*	9518.05	1	
9456.22*a*	4–7	*w*	9519.34*a*	3–5, o	*w*
9456.98*a*	o–2	*w?*	9520.04*a*		
9459.96*a*	6–10	*w*	9520.62	oo	
9461.16*a*	7–11	*w*	9522.30*a*	7–12	*w*
9463.03	oo		9523.62	1	
9464.05	o		9525.16	4	
9464.88	1		9526.91	oo	
9465.52	2		9527.60	1	
9467.12	1		9528.53	3BR	
9467.90	1		9529.51	2	
9468.68	2		9531.30	o	
9469.50	3		9531.79	1	
9470.57	2		9533.48	1	
9471.63	ooo	*S?*	9535.00	ooB	
9472.51	oo		9536.12*a*	4–6	*w*
9473.14	ooB		9538.47	4	
9474.36	5B, 3 U		9540.98	5	
9475.27			9543.93*a*	6–11D	*w*
9476.07	2		9544.61	2	
9476.85	2		9545.92	1	
9478.99	oo		9546.63	o	
9480.23*a*	5–7	*w*	9547.15	oo	
9481.97*a*	7, 2 –11D	*w*	9548.75	3	
			9550.05	2R	*A, S*
9484.04	oo		9550.42	1	
9485.17	oo		9551.02	1	
9486.10	2		9553.48*a*	5–7, 3–5 U	*w*
9486.95	o, 1		9554.51*a*		*w*
9487.49			9556.11	2	*S*
9489.86	1		9557.33*a*	4–6	*w?*
9491.61	1		9558.49	3	
9493.41*a*	4–6, 6–8 U	*w*	9558.89	3	
9494.49*a*		*w*	9559.70*a*	ooo	*S*
9496.54	oB		9562.70	4	
9497.51*a*	5–7	*w*	9563.91	3	
9498.88	oo		9565.11	3	
9499.60*a*	3–5	*w*	9566.16*a*	4–7	*w*

TABLE I—*Continued*

λ	Intensity	Source Element	λ	Intensity	Source Element
9568.91*a*	3–5	*w*	9640.26	1	*S?*
9570.42	1B		9640.68	2	
9571.38*a*	3–5	*w*	9643.17	1	*S?*
9572.85	1		9645.06*a*	2–8D	*w*
9574.42	0		9645.59*a*	2–8D	*w*
9575.75	1		9646.50	2	
9577.10	2		9648.68*a*	1–3	*w?*
9579.36*a*	0–2	*w?*	9649.53	0V	
9580.05*a*	3–5	*w?*	9650.28	00	*S*, Fe?
9581.12*a*	3–5 U	*w*	9651.02*a*	00	
9581.84*a*	2–4 U	*w*	9651.33*a*	00	
9583.66	0		9651.97	1	
9584.82	0		9652.90	2	*A*, *S*
9585.92	2D		9653.64	000	
9587.17	3		9654.68	2	*S*, *A*, Fe?
9588.57	4		9656.17	1V	
9589.32	5		9657.37	2	
9590.28	4		9658.47	0	*S?*
9592.00	2		9659.78	2	
9592.62	3		9660.92	3	
9594.20	2		9662.36	3V	
9594.86	2		9663.26	0	
9596.46	1B		9664.04	00	
9597.84	4D		9664.68	3R	
9598.91	2		9666.59	1	
9599.60	0		9667.21	2	
9600.55	0		9668.27	0	
9601.22	2		9670.04	2V	
9603.43	1V		9670.67	3V	
9604.62	2	*S?*	9680.41	4	
9605.24	2		9681.10	0	
9606.22	2		9681.82	1	*S?*
9608.11	4B		9682.70	00	
9610.11	2		9684.25	0B	
9610.69	00		9685.81	00	
9614.13	1		9686.44	2	
9615.26	5D		9688.72	0	
9618.14	3R		9690.21	00	
9620.08	2		9691.93	3	
9621.28	3	*A*, *S?*	9693.99	00	
9622.74	3		9694.74	0B	
9624.56	2		9698.32	2	
9625.32	0		9699.68	00	
9625.83	0		9700.15	0	*S?*
9626.40	2	*A*, *S?*	9701.47	3	
9628.20	1		9705.53	00B	
9628.74	1		9708.97	1	
9629.32	000		9715.33	4	
9630.06	00		9723.18	2	
9633.58	00		9724.62	2	
9636.16*a*	4–9	*w*	9730.66	1	
9637.58*a*	4–7	*w?*	9735.07	3BV	
9638.45	1	*S*	9736.63	5BDR	

TABLE I—*Continued*

λ	Intensity	Source Element	λ	Intensity	Source Element
9737.83*a*	0		9782.35	2	
9738.54*a*	0		9787.19*a*	0	
9743.53	3B		9791.09	2	
9749.36	3		9793.38*a*	1B	
9753.90	2		9795.26*a*	00	
9757.74	2		9799.52	2	
9761.73*a*	00		9801.78	2	
9762.90	2BR		9803.27	1	
9764.14*a*	00B		9813.48*a*	0	
9765.51	2B		9817.70*a*	00	
9768.71*a*	0B		9825.57*a*	00	
9774.00	2B		9831.97*a*	0	
9776.84	1		9848.89*a*	0	
9779.46	2				

The separation of the solar and telluric lines is based chiefly upon two rotation plates. As the Doppler displacement due to solar rotation is of the order of 0.13 A, there is little doubt as to the origin of well-defined lines. But if the lines are diffuse, unsymmetrical, or blended, question arises. If noticeable displacement occurs on one plate but not on the other, a question mark has been placed after the *S*, which is used to indicate lines of solar origin. If the evidence of blending is unmistakable it has been indicated by *A*, *S*. Lines due to water-vapor have been indicated by *w*, and lines showing decided asymmetry by V or R placed after the intensity, according as the line is shaded to the violet or the red, respectively. Where lines were not completely resolved, it has been indicated by joining the intensities by brackets. Where they were practically unresolved, U has been placed after the bracket. Broad lines have been indicated by B.

In conclusion it may be stated that the monochrometer, used instead of a screen, has certain unquestionable advantages over any of the screens at present available: (1) it removes all scattered light from the background and makes it possible, by increasing the exposure sufficiently, to obtain the very faint lines, which are especially important in the region under investigation; (2) it is faster than the battery of screens found necessary to remove even the major portion of the extraneous light in the region beyond

9400 A; (3) it presents for any limited portion of the region a very convenient method of grading the exposure to suit the sensitiveness of the plate.

The results of the investigation show (1) that at least one-fifth of the lines of 0 intensity or less are of solar origin; (2) that one-third of these solar lines are due to iron; (3) that a very strong water-vapor band exists between 9300 A and 9650 A.

The fact that in the present case, as well as in the recent work by Burns and also in the early investigations of Abney, it was found impossible to photograph beyond 9900 A is probably to be explained by the presence of the strong absorption band at about 1 μ, which was designated by Langley[1] by the symbol ϕ. The rapidly falling sensitiveness of the plates renders it impossible to photograph any portion of the spectrum beyond this band.

I am indebted to Mrs. Brackett for the computation and reduction of the measures, and to Dr. St. John and Mr. Babcock for furnishing me with wave-lengths in both sun and iron arc based on the International system. It gives me great pleasure to express my appreciation to these and also to other members of the staff for their interest and help.

Mount Wilson Observatory
September 1920

[1] *Annals Smithsonian Astrophysical Observatory*, 1, 1900.

THE VARIATION WITH TEMPERATURE OF THE ELECTRIC FURNACE SPECTRUM OF MANGANESE[1]

By ARTHUR S. KING

ABSTRACT

Variation of the electric furnace spectrum of manganese with temperature to 2400°.— The spectrum produced in the tube-resistance furnace at 1700°, 2000°, and 2400° C. was examined from λ 2795 to λ 8200; but no lines were found beyond λ 6500. Table I contains the relative intensities of the lines in the arc spectrum and in the furnace spectra for the three temperatures; it also gives the *temperature classification* of these lines according to the method used in previous articles. Some lines observed at 1560° C. are given in Table II; the triplet λ 4031 to λ 4035 was still strong and well reversed at this low temperature. As with other furnace spectra, the ultra-violet wave-length limit is shorter the higher the temperature. In the discussion the interesting behavior of some of the lines is pointed out. None of the enhanced lines given by Lockyer occur in the furnace spectrum.

The following results for the furnace spectrum of manganese were obtained by the methods used in previous studies of metallic spectra.[2] Manganese metal was used in the tube furnace, the inclosing chamber being pumped to a pressure of a few millimeters. Temperatures of approximately 1700°, 2000°, and 2400° C., designated as "low," "medium," and "high," respectively, were employed in studying the range of spectrum from λ 2800 to λ 6600. The peculiarities of the spectral lines as regards the temperature at which they first appear and the rate of increase with rising temperature have been tabulated from these data.

The spectrograms were made for the most part with the first and second orders of a fifteen-foot concave grating, while the very bright spectra given by the second order of a one-meter grating were used for a few photographs.

The operation of the furnace, when the tube was charged with manganese, was without notable features other than the lack of

[1] *Contributions from the Mount Wilson Observatory*, No. 198.

[2] *Mt. Wilson Contr.*, Nos. 66, 76, 94, 108, 150, 181; *Astrophysical Journal*, **37**, 239, 1913; **39**, 139, 1914; **41**, 86, 1915; **42**, 344, 1915; **48**, 13, 1918; **51**, 179, 1920.

carbide formation, in which this metal contrasted strongly with iron. Instead of sticking to the tube and gradually eating through, the manganese vaporized and then, in diffusing from the tube, condensed in the cooler portions at the ends, leaving but little residue in the hotter region. This necessitated frequent renewal of the charge of metal during the run.

In order to hold the temperature unchanged during the rather long exposures at low and medium temperatures, direct current from a large generator was frequently used on account of the close adjustment of voltage which can be made. As in the case of the iron spectrum,[1] no difference was observed between the effect of direct and alternating currents at a given temperature.

EXPLANATION OF TABLE I

The first column of Table I gives the arc wave-lengths measured by Exner and Haschek,[2] except in a few cases for which the wave-lengths of close doublets, on the international system, were taken from the measures of Kilby.[3] Frequent references to notes at the end of the table are indicated by asterisks, while a dagger means that the line was found by Kilby to be decidedly stronger in the spark than in the arc.

As in previous papers, the remaining columns give the intensity estimates for lines in the arc and for three furnace temperatures. Nebulous lines are indicated by "n" after the value of the intensity, while "r" and "R" indicate partial and complete self-reversal. Lines of Class I and Class II are strong at low temperature, those of Class II strengthening more rapidly as the temperature rises. Lines of Class III are absent or faint at low temperature, but appear at medium temperature, and are usually considerably stronger at high temperature. Class IV appears at the highest furnace temperatures, while Class V is usually absent in the furnace. "A" after the class number indicates that the line in question is relatively weak in the arc—usually not more than half as strong as in the high-temperature furnace.

[1] *Mt. Wilson Contr.*, No. 193; *Astrophysical Journal*, 52, 187, 1920.

[2] *Spektren der Elemente bei normalem Druck*, Leipzig, 1911.

[3] *Astrophysical Journal*, 30, 243, 1909.

TABLE I

TEMPERATURE CLASSIFICATION OF MANGANESE LINES

λ (EXNER AND HASCHEK)	ARC INTENSITY	FURNACE INTENSITIES			CLASS
		High Temperature	Medium Temperature	Low Temperature	
2794.92	500R	500R			IV
2797.05	5	1			IV
2798.37	400R	400R			IV
2799.99	10	2			IV
2801.20	400R	400R			IV
2804.24	7	3			IV
2806.25	6	2			IV
2808.12	5	2			IV
2809.20	7	2			IV
2812.99	7	2			IV
2813.60	7	2			IV
2814.09	4				V
2818.09	8	3			IV
2818.85	6	1			IV
2821.58	5	2			IV
2822.68	6	2			IV
2823.40	2	1			IV
2824.5	8n				V
2826.8	15n				V
2830.92	6	2			IV
2836.43	3	1			IV
2858.85	6	1			IV
2872.68	5	1			IV
2892.77†	5				V
2907.32	7				V
2914.71	50	15	1		IV
2925.67*	70	8, 10	1		IV
2928.79	7				V
2930.35	5	2			IV
2933.19†	25	tr			V
2934.13	6				V
2938.00	8n				V
2939.40†	30	tr			V
2940.01	5				V
2940.330*	10	8	1		IV
2940.512*	10n	5			IV
2941.15	7	1			IV
2949.31†	30	2			IV
3007.80	6	1			IV
3008.35	4				V
3011.30	5	tr			IV
3011.52	7	1			IV
3014.82	5				V
3016.60	8	1			IV
3022.90	10	2			IV
3040.76	12	4			IV
3041.35	4				V
3042.87	4				V
3043.46	9	3			IV

TABLE I—*Continued*

λ (Exner and Haschek)	Arc Intensity	Furnace Intensities			Class
		High Temperature	Medium Temperature	Low Temperature	
3044.69	50	7	4		III
3045.70	12	4			IV
3045.90	5				V
3047.14	15	5	1		IV
3048.95	5	1			IV
3054.53	40	8	5		III
3062.30	20	5	2		III
3066.19	20	5	2		III
3070.40	20	6	3		III
3073.33	20	7	2		III
3079.80	15	6	1		IV
3081.52	10	5			IV
3097.18*	8	1			IV
3100.43	5	2			IV
3101.67*	5	4?	3?		III?
3110.86	6	1			IV
3115.60	6				V
3120.54	4				V
3142.80	4				V
3148.36	15	5	1		IV
3161.19	15	6	1		IV
3178.61	15	7	1		IV
3207.00	5	3			IV
3212.98	15	9	5	1	III
3217.04*	8	?	?	2	II
3224.90*	10	?	?	2	II
3226.15	6	5	1		IV
3228.20	30	20	12	6	II
3230.81	12	10	7	2	III
3234.0	15n	2			IV
3235.1	10n	2			IV
	15n	3			IV
3236.90	20	15	10	5	II
3237.4	20n	5			IV
3240.53	7	10	2		III
3240.75	5	6	1		IV
3243.93	12	12	6	1	III
3248.64	15	15	8	3	III
3251.27	5	6	1		IV
3253.09	12	12	7	2	III
3254.14	5	4			IV
3256.25	12	12	7	2	III
3258.52	10	12	5	1	III
3260.40	10	12	3	1	III
3264.83	10	15	5	1	III
3267.90	4				V
3268.83	3				V
3270.49	3				V
3273.15	3				V
3278.65	5	6			IV
3280.90	5	6			IV
3296.16	4	2			IV

TABLE I—*Continued*

λ (Exner and Haschek)	Arc Intensity	Furnace Intensities			Class
		High Temperature	Medium Temperature	Low Temperature	
3297.01	6	8	1		IV
3298.35	5	2			IV
3303.40	3				V
3312.05	6	3			IV
3313.41	5n	2			IV
3313.70	4	1			IV
	4	1			IV
3314.59	6n	3			IV
3315.07	6n	3			IV
3316.47	4	2			IV
3316.61	5n	1			IV
3317.47	10n	5			IV
3320.82	6	5			IV
3330.80	8	8	1		IV
3343.85	4	2			IV
3345.47	4	2			IV
3420.95	4				V
3439.13	6				V
3442.13†	30				V
3460.45†	25				V
3474.20†	12				V
3474.27†	10				V
3483.22†	20				V
3488.80†	20				V
3495.99†	10				V
3496.96	6				V
3497.66†	8				V
3531.94†	30	10	6	1	III
3532.14†*	50	15	10	3	III
3532.27†*	50	15	10	3	III
3547.91†	50	20	12	4	III
3548.18†	40	20	12	3	III
3548.33†	30	10	6	2	III
3569.61†	60	30	15	6	III
3569.95†	40	20	10	2	III
3570.17†	20	8	3		III
3577.99*	40	?	15	8	II
3586.69*	30	?	7	3	II
3595.29	20	12	4	1	III
3607.69	20	10	10	4	II
3608.66	20	10	10	4	II
3610.49	20	10	8	2	III
3619.42	15	10	8	1	III
3623.96	15	8	6	1	III
3629.89	12	5	4	tr	III
3660.58	5				V
3670.00	4	2	1		III
3670.67	5	3	2		III
3677.13	4				V
3682.23	4				V
3693.83	6				V
3696.70*	8				V

TABLE I—*Continued*

λ (Exner and Hascheк)	Arc Intensity	Furnace Intensities			Class
		High Temperature	Medium Temperature	Low Temperature	
3701.88*	4	?	2		III
3706.23	5				V
3719.06	5				V
3732.05	5				V
3790.38	10	8	8	2	III
3799.40*	4	?	2		III
3800.70	4				V
3802.05	4				V
3806.90	20r	15	15	15	I
3809.75*	10	?	10	5	II
3816.90	5	3	3	1	III
3823.64	20r	15	15	10	II
3824.03*	10	?	10	4	II
3829.80*	5	?	4	1	III
3834.01*	8	?	8	5	II
3834.50	12	12	12	8	II
3839.90*	8	?	6	3	II
3841.23	10	8	8	4	II
3844.12*	7	?	6	3	II
3918.46	3				V
3921.94*	3n	?	tr		IV
3924.23*	3	?	tr		IV
3926.63	10				V
3929.41	2	2			IV
3953.00	3				V
3985.40	3				V
3986.98	3				V
4018.28	20	20	20	15	I
4026.58	4				V
4030.92	200R	200R	200R	200R	I
4033.21	150R	150R	150R	150R	I
4034.62	100R	100R	100R	100R	I
4035.88	15	15	15	12	I
4041.53	50r	35	30	25	I
4045.31*	4				V
4048.90	15	15	12	10	I
4055.70	20	20	18	15	I
4058.10	4				V
4059.09	10	12	10	8	I
4059.54*	5	?	tr		IV
4061.90	5				V
4063.70*	8	8?	8?	6?	I
4070.48	5	6	5	3	II
4079.38	12	15	12	10	I
4079.61	10	12	10	8	I
4083.11	12	15	15	12	I
4083.82	12	15	15	12	I
4235.125*	6	2	2	1	II
4235.306*	8	6	6	4	I
4239.90	5	2	2	1	II
4257.83	5	2	2	1	II
4266.10	6	2	2	1	II

TABLE I—*Continued*

λ (Exner and Haschek)	Arc Intensity	Furnace Intensities			Class
		High Temperature	Medium Temperature	Low Temperature	
4281.30.....	6	3	3	2	II
4312.71*.....	3	?	1	tr	II
4412.04.....	3	1			IV
4415.04.....	10	6	5	3	II
4436.52.....	8	6	4	1	III
4451.78.....	15	12	10	6	II
4453.19.....	6	5	3	1	III
4455.20.....	5	4	2	tr	III
4455.51*.....	6	?	3?	1?	III?
4456.02.....	6	5	2	tr	III
4457.22.....	5	3	1	tr	III
4457.76*.....	8	?	?	?	?
4458.48.....	12	8	4	2	II
4460.59*.....	3	?	?	?	?
4461.30.....	8	4	2	tr	III
4462.20.....	20	12	6	2	III
4464.88.....	8	8	5	3	II
4470.33.....	6	6	4	1	III
4472.98.....	5	5	3	1	III
4490.27.....	5	6	4	1	III
4499.09.....	7	8	6	2	III
4502.40.....	7	8	6	2	III
4605.52.....	4				V
4626.69.....	4	3	2		III
4671.89.....	3				V
4701.31.....	3				V
4709.89.....	10	6	4	1	III
4727.70*.....	10	?	4	1	III
4739.30.....	8	6	3	1	III
4754.24.....	50	50	60	40	I
4761.73.....	10	10	6	1	III
4762.60.....	30	25	20	5	III
4766.08.....	10	10	8	2	III
4766.63.....	20	20	15	4	III
4783.62.....	50	50	60	40	I
4823.71.....	50	50	60	40	I
4966.03.....	3	3	2		III
5005.03.....	2	2	1		III
5017.77.....	2				V
5074.92.....	2				V
5118.10.....	3				V
5151.10.....	3				V
5196.76.....	3	3	2		III
5197.40.....	1	1			IV
5255.48.....	4	4	3		III
5341.25*.....	20	50	25	4	IIIA
5377.86.....	6	1	tr		III
5394.89.....	10	30r	30	30	IA
5399.70.....	4	2	1		III
5407.67.....	5	10	8	2	IIIA
5413.90.....	2	1			IV
5420.61.....	10	20	15	3	IIIA

TABLE I—*Continued*

κ (Exner and Haschek)	Arc Intensity	Furnace Intensities			Class
		High Temperature	Medium Temperature	Low Temperature	
5432.75	4	35	35	35	IA
5457.64	1	2	2	1	IIA
5470.88	8	20	10	4	IIA
5481.61	4	10	5	2	IIA
5506.10*	2	?	3	1	III
5517.00	7	20	10	2	IIIA
5537.99*	5	?	5	1	III
6013.74	30	30	6	1	III
6016.90	40	40	10	2	III
6022.05	50	50	12	3	III
6384.88	4				V
6413.77	2	4	2		IIIA
6441.14	8	2			IV
6491.92	15	3			IV
6605.7	6n				V

λ	Remarks
2926	Close doublet, just resolved.
2940.3, 2940.5	Doublet measured by Kilby. Exner and Haschek give λ2940.50.
3007	Double. Arc components about equal.
3102	Furnace line may be partly Ni.
3217, 3225	Pure absorption lines at high temperature. Partial absorption at medium temperature.
3532.14, 3532.27	λ's by Hasselberg. Exner and Haschek give λ3532.20.
3578–3587	Disturbed by carbon.
3697	Close doublet.
3702	Concealed by continuous ground at high temperature.
3799–3844	Disturbed by carbon.
3922, 3924	Concealed by continuous ground at high temperature.
4045	Close doublet.
4060	Disturbed by carbon.
4064	Blend Fe. Probable intensity of Fe line subtracted.
4235	Doublet measured by Kilby. Exner and Haschek give 4235.41.
4313	Disturbed by carbon.
4455–4457–4460	Blend with impurity lines.
4728	Disturbed by carbon.
5341	Probably double.
5506, 5538	Disturbed by carbon.

DISCUSSION OF RESULTS

Several groups of lines whose behavior is of special interest may be noted. The first is the strong triplet at λλ 2795, 2798, 2801. These lines reverse widely in the high-temperature furnace. The emission wings fill up the space between the lines, but are of low density. The effect is that of three absorption lines on a weak

continuous ground. No temperature stage has been found which gives these as narrow emission lines. Presumably they will occur as such at high temperature when a trace of manganese is present, though an examination of some iron spectrograms failed to show them. At reduced temperature the lines are not narrow or indeed visible at all, because the furnace spectrum does not then extend so far into the ultra-violet. This is a peculiarity often met with in furnace spectra; lines in the ultra-violet having the characteristics of low-temperature lines require high temperatures for their production because the low-temperature spectrum ceases before this wave-length is reached. The effect is so general with different elements that there seems to be no reason to ascribe it to absorption by a vapor within the furnace.

At about λ 3000, the medium temperature begins to show some lines distinctly. The prominent lines up to this point, in addition to the λ 2800 triplet, are those of the series triplet λλ 2915, 2926, 2941, of which the last two are clearly complex and probably also the first. The components of λ 2926 are resolved in the furnace spectrum. This triplet is given by Kayser and Runge[1] as belonging to the same series as λλ 3532, 3548, 3570, lines which are also complex; but the two triplets appear in different temperature classes because the member of shorter wave-length occurs at the extreme limit of the medium-temperature spectrum.

λλ 3217 and 3225 show a peculiar behavior. At high temperature they are simple absorption lines, with no sign of emission wings. Their strength at medium temperature is uncertain, the emission being partly neutralized by absorption, while at low temperature they are sharp emission lines. No other lines of this type occur in the spectrum.

The tendency, which prevails throughout the spectrum, for lines of similar type to appear in groups is illustrated by those from λ 3442 to λ 3498. They are absent in the furnace but strong in the arc, and yet stronger in the spark. They are thus enhanced lines of intermediate type. None of the enhanced lines given by Lockyer[2] occur in the furnace spectrum.

[1] *Abhandlungen der preussischen Akademie*, 1904.

[2] Solar Physics Committee, *Tables of Wave-Lengths of Enhanced Lines*, 1906.

The series triplet λ 3532 to λ 3570, each member of which has three components, is also strengthened in the spark. In the furnace these lines appear between 1600° and 1700°, but strengthen very rapidly with increasing temperature.

The prominent low-temperature group between λλ 4000 and 4100 contains the very sensitive triplet λλ 4031, 4033, 4035. These lines are of extreme persistence, occurring very generally as impurity lines in arc spectra. Their intensity in the furnace seems to depend very largely on the vapor density, and with an ordinary charge of manganese present they are always widely reversed. This was the condition at the lowest temperature used, 1560°, when most of the low-temperature lines were barely registered on the plate. The intensities of this triplet given in the table therefore signify little relatively to the general run of the manganese lines. At low temperature, with much vapor present, they can be made much stronger than at high temperature with less vapor. The extreme sensitiveness of these three lines to anomalous dispersion, the degree of which is found to depend on the tendency of a line to reverse, was noted in a former paper.[1]

The group in the blue near λ 4450 consists of strong arc lines which are relatively weak in the furnace, being for the most part in Class III. Near λ 4800 several prominent furnace lines occur, among them the triplet of Class I, λλ 4754, 4784, 4824. These are very strong at low temperature and are placed by Kayser and Runge in the first sub-series, another member of which is the triplet at λλ 3148, 3161, 3179. The latter lines are beyond the range of the low-temperature furnace, appearing faintly at medium temperature.

Near λ 5400 is another set of prominent lines, which in general are relatively stronger in the furnace than in the arc, a class not noted in other parts of the manganese spectrum. λλ 5395 and 5433 are remarkable for their strength at low temperature. λ 5341 is stronger than either of these at high temperature, but falls off rapidly below 2000°. The temperature of the furnace, especially in the lower range, may be closely gauged by the relative intensity of λ 5341 as compared with λ 5395 or λ 5433.

[1] *Mt. Wilson Contr.*, No. 130; *Astrophysical Journal*, **45**, 254, 1917.

The red end of the manganese furnace spectrum is weak, except for the triplet at λ6014 to λ6022 and this fades rapidly with decreasing temperature. The spectrum was photographed with dicyanin-bathed plates as far as λ 8200, but no lines were found in the furnace beyond λ 6500.

Table II lists what may be regarded as the residual furnace lines. The intensity estimates were made from a spectrogram of

TABLE II

MANGANESE LINES IN FURNACE AT 1560° C.

λ	Intensity	λ	Intensity
3806.90	2	4055.70	5
3823.64	1	4059.09	1
3834.50	1	4063.70	1
4018.28	3	4079.38	3
4030.92	100R	4079.61	
4033.21	75R	4083.11	2
4034.62	50R	4083.82	2
4035.88	3	4754.24	10
4041.53	10	4783.62	10
4048.90	3	4823.71	10

long exposure taken with the one-meter concave grating. The temperature of the furnace read 1560° C. The lines of the triplet λ 4031 to λ 4035 are strong and well reversed. Evidently they are emitted at a considerably lower temperature than that used here. The other lines in Table II are the most pronounced low-temperature lines and in some cases are just strong enough to be distinctly registered. λλ 5394.89 and 5432.75 would doubtless be listed among these lines if the photograph had included the region.

MOUNT WILSON OBSERVATORY
November 1920

THE ORBIT OF THE SHORT-PERIOD SPECTROSCOPIC BINARY 65 τ CYGNI

By J. S. PARASKÉVOPOULOS[1]

ABSTRACT

Spectroscopic binary components of the triple system 65 τ Cygni.—This interesting system is a visual binary whose brighter component is a spectroscopic binary. During 1920 several continuous series of spectrograms obtained with the Bruce spectrograph of the Yerkes Observatory enabled the *elements of the orbit* to be computed. The period is only $3^h25^m.4$, the shortest yet known, and $a \sin i$ is only 14,924 km. Taking the parallax of the system as $0''.031$, the distance apart of the components comes out about 1,600,000 km. But from the brightness of the brighter component, absolute magnitude about 1.5, its diameter is probably about 9,000,000 km. Apparently, then, the separation of the components is less than the diameter of one of them. But neither the hypothesis of a pear-shaped body nor that of a pulsating star seems to explain the facts satisfactorily.

The star 65 τ Cygni ($\alpha = 21^h10^m.8$, $\delta = +37°37'$) is a triple system of great interest. Alvan G. Clark found in 1878 that this $3^M.8$ star has a companion of about 8^M. It was soon recognized that these form a visual binary system.[2] The latest elements which fairly represent the recent measures are those of Aitken:[3]

$P = 47$ years	$\omega = 105°.5$
$T = 1889.60$	$\iota = \mp 42°.7$
$e = 0.22$	$\Omega = 149°.8$
$a = 0''.91$	Angles decreasing

Professor Storrs B. Barrett,[4] of the Yerkes Observatory, detected some years ago that the spectrum of this star shows a variable radial velocity.

Spectrum.—The limiting distance for the Bruce spectrograph of the Yerkes Observatory being in practice between $2''$ and $3''$, the spectrum of the two components of the visual system cannot be studied separately. The spectrograms obtained record only a single spectrum, belonging to the brighter component: they do not show the spectrum of the fainter visual component or of the spec-

[1] Of the National Observatory at Athens. Volunteer Research Assistant at Yerkes Observatory, 1919–1921.

[2] Burnham, *General Catalogue of Double Stars.*

[3] *Publications of the Lick Observatory*, 12, 161.

[4] *Astronomische Nachrichten*, 177, 174, 1908.

troscopic companion. The spectrum of this bright component is of type Fo, according to the *Revised Harvard Photometry*.[1]

Since the discovery of the binary character of τ Cygni, a large number of spectrograms of this star have been taken at the Yerkes Observatory with the Bruce spectrograph arranged for one prism. The time usually required for a satisfactory exposure is between 25 and 40 minutes. A comparison spectrum of titanium and of iron was impressed on all the plates. All the spectrograms were measured on the Gaertner measuring machine and reduced by the author. The following are the wave-lengths for the lines that have been used chiefly:

Fe	4045.975	Hδ	4101.900	Fe	4260.640	Hγ	4340.634
Fe	4063.759	Sr	4215.703	Cr	4289.885	Cr	4351.930
Fe	4071.908	Ca	4226.904	Fe	4299.410	Ti	4395.203
Sr	4077.885	Fe	4250.945	Fe	4325.939	Fe	4404.927

Ti	4443.976		
Mg	4481.400		
Ti–Co	4549.808		
Ti	4563.939		
Ti	4572.156		

TABLE I

(For Julian Day 2, 422,522)

Plate	Date	(G.M.T.)	Exposure	V	n	V_c	O−C
			m	km		km	km
I B 5859...	1920 July 16	.597	40	−23.98	17	−26.76	+2.78
5860...		.630	40	−29.95	19	−29.12	−0.83
5861...		.659	36	−15.88	14	−14.74	−1.14
5862...		.686	33	−16.54	17	−16.50	−0.04
5863...		.713	33	−22.99	16	−21.47	−1.52
5864...		.740	32	−22.67	17	−26.90	+4.23
5865...		.766	32	−29.38	18	−30.24	+0.86
5866...		.790	25	−20.37	14	−18.96	−1.41
5867...		.819	24	−14.66	14	−15.10	+0.44
5868...		.850	40	−19.08	9	−20.40	+1.32
5869...		.881	28	−27.85	14	−26.60	−1.25

Period and elements of the orbit.—An examination of the radial velocities showed that the period must be short, but I failed to find any period that would fit them all until on July 16, 1920, I secured in one night a series of eleven plates from which the period was found equal to $0^d.1425$ (or $3^h25^m.2$). The results of the observations and measurements for this date are collected in Table I. Mr. Frank R. Sullivan, engineer in charge of the 40-inch telescope, assisted me in securing the plates. Under n are given the number

[1] *Harvard Annals*, 50, 181.

of lines measured for each plate. V_c is the computed radial velocity and O−C the difference between the observed and the computed radial velocity. With the foregoing data and the Lehmann-Filhés

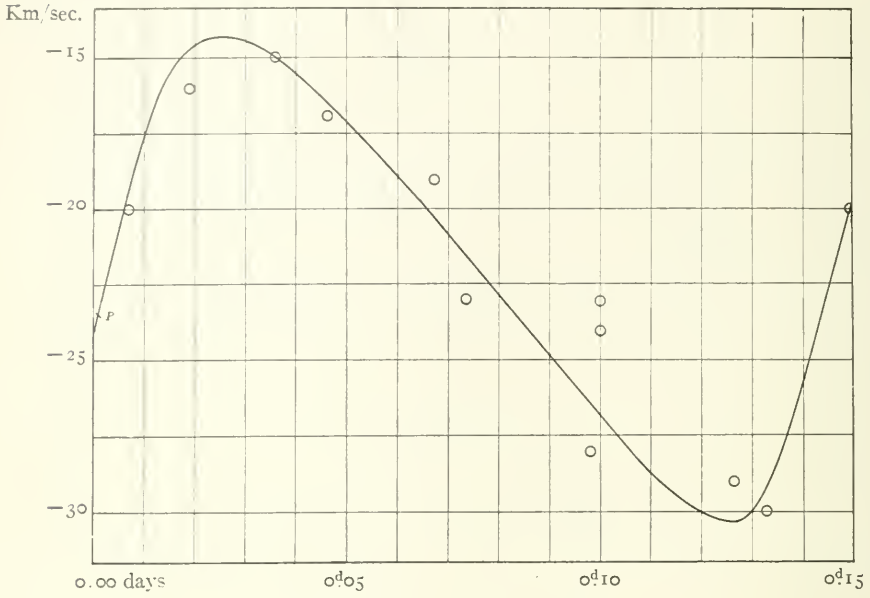


FIG. 1.—Velocity-curve of 65 τ Cygni

method, I obtained the following elements for the orbit of the spectroscopic binary,

$P=0^d.1425$	$T=$J.D. 2,422,522.641
$\omega=263°.0$	$a \sin i=14{,}924$ km
$e=0.306$	$K=8.0$ km/sec.
$\mu=(7\times360°)+6°.333$	$\gamma=-22.0$ km/sec.

Owing to the possibility of rapid changes in the amplitude and shape of the velocity-curve, similar to those found by Mr. R. K. Young[1] in the case of 12 Lacertae, I did not try to reduce to one period all the obervations obtained during this year. Nevertheless, I attempted to improve the period above, deduced from a single night's observations, by using short series of plates taken on March 29, April 5, 6, and June 18 of this year. A period of 0.14265 day seems to represent all these observations in a satisfac-

[1] *Publications of the Dominion Astrophysical Observatory*, Victoria, 1, No. 2.

tory way. This value of P corresponding to $3^h25^m.4$ is the shortest period thus far found for any spectroscopic binary.

The value of a sin i.—The value of $a \sin i$ for τ Cygni is extremely small, almost equal to the earth's diameter. This is also the case for all the spectroscopic binaries of very short period, like β Cephei, 12 Lacertae, β Canis Majoris, etc. The value of the semi-major axis a itself remains unknown as long as the inclination is not determined. But since the average value of sin i cannot be very small, this is an indication that a is also small.

The combined magnitude of the spectroscopic binary is $3^M.82$. As no lines of the spectroscopic companion are recorded, we infer that its magnitude cannot be more than 5.5. Consequently the magnitude of the bright component cannot be less than 4.0. Accepting this lowest limit, I found that the absolute magnitude of this bright component is 1.5 (by using the formula $M = m + 5 + 5 \log \pi$ and adopting a parallax of $0''.031$ given by Adams).[1] As the absolute magnitude of the sun is 5.5, it follows that the difference in brightness between those two stars is $2.5^{4.0} = 39.81$. If now we suppose that equal surfaces of the sun and of the bright component of the spectroscopic binary emit the same quantity of light,[2] we deduce that the surface of the latter is forty times the surface of the sun, and consequently the diameter of the star is about 6.3 times the diameter of the sun, i.e., equal to $6.3 \times 1{,}400{,}000 = 8{,}820{,}000$ km.

Let us now call

M = the mass of the bright component
m_1 = the mass of the spectroscopic companion
m_2 = the mass of the visual companion
x = distance between the bright component and its spectroscopic companion

Supposing the semi-major axis of the visual orbit to be 1 we get, the period being 47 years:

$$\left(\frac{47}{0.00039}\right)^2 \cdot \frac{M+m_1+m_2}{M+m_1} = \frac{1}{x^3}.$$

[1] The values of the trigonometric parallax of τ Cygni present large discrepancies. I adopted the value of $0''.031$ given by Adams and Joy in *Contributions from the Mount Wilson Observatory*, No. 142.

[2] The spectral type of 65 τ Cygni being Fo.

G. Van Biesbroeck[1] obtained as a value of the mass-ratio in the visual binary:

$$\frac{M+m_1}{M+m_1+m_2}=0.53.$$

Consequently,

$$x^3=0.53\ (0.00039/47)^2 \text{ and } x=0.000418.$$

If we adopt $\pi=0''.031$ as we did before, and $0''.91$ as the value of the semi-major axis of the visual orbit, we find

$x=0.000418\times 0.91\times 149{,}000{,}000/0.031=1{,}830{,}000$ km, or 0.0123 astronomical units, and for the mass of the spectroscopic system:

$$M+m_1=\frac{x^3}{P^2}=\frac{(0.0123)^3}{(0.00039)^2}=12.2 \text{ times the mass of the sun.}$$

All these values seem very reasonable, but we must not forget the uncertainty of the determinations of the parallax. The distance x is inversely proportional to the adopted parallax, and the total mass of the spectroscopic binary varies as the reciprocal of the cube of the parallax.

As we saw, the bright component must be larger than our sun, i.e., larger than the distance x between the former and its spectroscopic companion. In that case, we have necessarily to do with a pear-shaped body. But how could we explain the periodic shifting of the spectral lines of a pear-shaped body? Such a body would evidently give diffuse lines, but without variable displacements. In order to reconcile these conflicting conclusions, attempt was made to study the problem on the assumption of a single pulsating body. Unfortunately the deficiency of sufficient data does not enable us to get any positive result. By means of Lord Kelvin's[2] formula

$$T_n=2\pi\sqrt{\frac{2n+1}{2n(n-1)}}\cdot\sqrt{\frac{a}{g}},$$

where T_n is the period of oscillation of the harmonic of order n, a is the radius of the sun, g is the surface gravity. Professor F. R.

[1] *Astronomical Journal*, **29**, 173, 1916.

[2] *Philosophical Transactions*, **153**, 612, 1863.

Moulton[1] finds for our sun a pulsation period of 3^h8^m ($0^d.13056$), whence we see that in the case of 65 τ Cygni its period of $0^d.1425$ may just as well be explained by the pulsation hypothesis. Professor Moulton, examining the effects of oscillations of the sun upon its temperature and rate of radiation, concludes that: "If the sun were undergoing a dilatational oscillation of extreme range of $0''.1$ in diameter (i.e., 70 km), the rate of radiation at minimum radius would be 2.56 times that at maximum radius. That is, the variation would be more than one star magnitude." If we suppose 65 τ Cygni to be a pulsating star, we can find a *rough value* of the semi-amplitude of the harmonic motion of a molecule on the surface of the star by means of the known formula of the harmonic undamped motion

$$v = 2\pi A/T \cdot \cos 2\pi \cdot t/T,$$

where v is the velocity at the time t; T is the period of oscillation; A is the semi-amplitude of the oscillation. The maximun velocity of this molecule is given by the formula

$$v = 2\pi A/T$$

and it is of course equal to K, half the range of the observed radial velocities ($v = K = 8$ km/sec.). Consequently $2A = 30.730$ km, as against 70 km as the upper limit for the sun, and still the star is not known to be variable.

In any case, it seems that the results concerning the short-period spectroscopic binaries begin to open a new view as to the evolution of the stellar systems.

In closing, the author wishes to express his indebtedness to Professor Edwin B. Frost, Director of the Yerkes Observatory, and to Professor G. Van Biesbroeck, for their interest and suggestions during the progress of the present work.

YERKES OBSERVATORY
September 1920

[1] *Astrophysical Journal*, **29**, 261, 1909.

THE VACUUM-SPARK SPECTRA IN THE EXTREME ULTRA-VIOLET OF CARBON, IRON, AND NICKEL

By R. A. MILLIKAN, I. S. BOWEN, and R. A. SAWYER

ABSTRACT

Spectroscopy of the extreme ultra-violet.—(1) *A concave grating* to be suitable for work in this region must satisfy far more rigorous demands than for work in the visible and should throw most of the light into the first-order spectrum. The authors therefore had some gratings ruled with great precision and with a light touch so that about half the original surface was left between the rulings. It was not found practical to increase the number of lines to more than 1100 per mm. (2) *Measurement of the wave-lengths.* Equations for the corrections to be applied to plate measurements because of the flatness of the plate and its inclination to the axis of the grating are derived, and the use of spectrum lines of higher order to determine this angle of inclination is explained.

Vacuum-spark spectra of carbon, iron, and nickel in the extreme ultra-violet.—The intensities and wave-lengths, accurate to about 0.2 A, of about 75 lines due to carbon (λ 360–λ 1931), of about 200 lines due to iron (λ 271–λ 2153), and of about 75 lines due to nickel (λ 731–λ 1860) are given in Tables I–III.

In preceding papers[1] report has been made upon the development of a method for the extension of the study of spectra into hitherto-unexplored regions of the ultra-violet and upon some of the most important of the results which have thus far come from this study. The present paper deals: (1) with the ruling of gratings suitable for work with very short wave-lengths, (2) with the technique of the measurement of wave-lengths in this region, and (3) with a detailed tabular statement of the character of the spectra emitted by the atoms of carbon, iron, and nickel.

I. THE GRATING PROBLEM

In the ordinary process of ruling gratings for work in the visible portion of the spectrum the surface of the grating is entirely cut away by the point of the diamond and the spectrum is produced by reflections from a series of new surfaces formed by the facets of the diamond. This in general throws the major portion of the

[1] *Astrophysical Journal*, **52**, 47, 1920, and **52**, 286, 1920; *Physical Review*, **12**, 168, 1918, and *Science*, **19**, 138, 1919.

light into a spectrum of higher order than the first, an indispensable condition for the high resolution upon which the excellence of a grating ordinarily depends. For work in exploring the extreme ultra-violet, on the other hand, the overlapping of spectra renders all spectra save that of the first order well-nigh useless, so that it becomes indispensable to throw the major portion of the light into that order.

Again the ratio of grating-space to wave-length is ordinarily of the order of 4 or 5 to 1. In the case of the shortest wave-lengths which have been obtained in the present work this ratio is more than 100 to 1. This condition clearly imposes immensely greater demands upon the perfection of the reflecting surface and the exact identity of the rulings than are imposed by work in the visible region.

We therefore soon discovered that gratings which were excellent for work in the visible and of which we had high hopes for this work were altogether useless. We accordingly tried the expedient of ruling our gratings with a very "light touch" so as to leave a portion of the original surface functioning in the production of the spectra. If by such a procedure we succeed in cutting away just half of the surface, for example, the whole light will be thrown into the central image and into the odd orders in the intensity ratios 1, 0.4, 0.05, etc., the energy falling off as the inverse square of the order (always odd). The gratings with which we have succeeded in obtaining our shortest wave-lengths have been ruled as nearly as possible in this way.

On account of the necessity of leaving between the rulings a portion of the original surface no particular success has been had in increasing the number of lines to the mm. The largest number used has been 1100 per mm, and the usual number about 500.

II. THE MEASUREMENT OF WAVE-LENGTHS

Since for these short waves, incident nearly perpendicularly upon the grating, the spectra are very close to the so-called *normal* type, the first procedure in the determination of wave-length has been to find the approximate wave-length λ' of every new line by means of a grating-constant obtained by dividing the

wave-length of the standard Al lines λλ 1854.7 and 1862.7 by their measured distances from the central image. These two standard lines were in general just obtainable at one end of our photographic plates when the central image was near the other end, their distances from the central image being about 8 cm, when the focal length of the grating was 83.5 cm and the grating-constant 505 lines per mm.

To the approximate wave-length λ′ thus obtained were applied corrections to take account of the facts (1) that the photographic plate was straight instead of curved, and (2) that it might be slightly inclined to the normal to the grating. These corrections were obtained as follows (see Fig. 1):

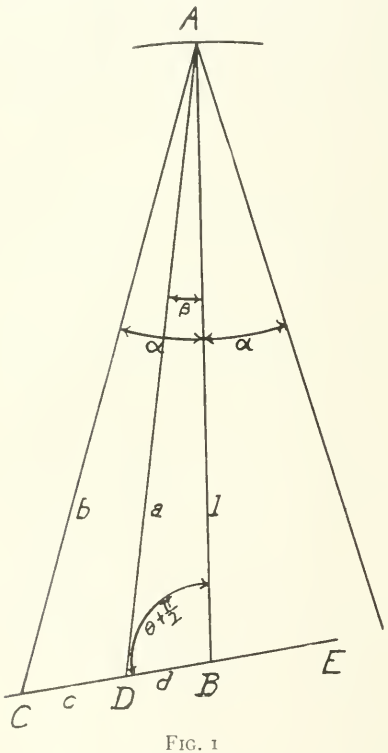


FIG. 1

Let

A be the center of the grating
CE the photographic plate
AB the axis of the grating
AC the path of a ray to the central image of the slit
AD the path of a ray to any spectral line
s = the grating-space
λ = the true wave-length of any line
λ' = the approximate wave-length of any line as given by the assumption of a normal spectrum
λ_0 = the wave-length corresponding to a line at B on the normal to the grating

And let

$AB = l$
$AD = a$
$AC = b$
$CD = c$
$DB = d$

and

$BAC = \alpha$
$BAD = \beta$
$CBA = \frac{\pi}{2} + \theta$

Then by the simple theory of the grating

$$\frac{\lambda}{s}=\sin\alpha-\sin\beta \tag{1}$$

also since λ_0 is that wave-length for which $\sin\beta=0$

$$\frac{\lambda_0}{s}=\sin\alpha \tag{2}$$

But

$$\sin\alpha=\frac{c+d}{b}\sin\left(\theta+\frac{\pi}{2}\right)$$

$$\sin\beta=\frac{d}{a}\sin\left(\theta+\frac{\pi}{2}\right)$$

$\therefore$ from (1)

$$\frac{\lambda}{s}=\left(\frac{c+d}{b}-\frac{d}{a}\right)\sin\left(\theta+\frac{\pi}{2}\right) \tag{3}$$

and from (2)

$$\frac{\lambda_0}{s}=\frac{c+d}{b}\sin\left(\theta+\frac{\pi}{2}\right) \tag{4}$$

Dividing (3) by (4)

$$\frac{\lambda}{\lambda_0}=\frac{a(c+d)-bd}{(c+d)a}$$

$$=\frac{ac+(a-b)d}{a(c+d)}$$

$$=\frac{c}{c+d}\left[1+\frac{(a-b)d}{ac}\right].$$

But by the assumption of linearity of scale

$$\frac{\lambda'}{\lambda_0}=\frac{c}{c+d}$$

$$\therefore\quad \lambda=\lambda'\left[1+\left(1-\frac{b}{a}\right)\frac{d}{c}\right] \tag{5}$$

But

$$b=\sqrt{l^2+(c+d)^2+2l(c+d)\sin\theta}$$

$$a=\sqrt{l^2+d^2+2ld\sin\theta}$$

Or, expanding and dropping terms of higher orders,

$$b = l\left[1+\tfrac{1}{2}\left(\frac{c+d}{l}\right)^2+\frac{c+d}{l}\sin\theta\right]$$

$$a = l\left[1+\tfrac{1}{2}\left(\frac{d}{l}\right)^2+\frac{d}{l}\sin\theta\right].$$

Dividing

$$\frac{b}{a}=\frac{1+\tfrac{1}{2}\left(\frac{c+d}{l}\right)^2+\frac{c+d}{l}\sin\theta}{1+\tfrac{1}{2}\left(\frac{d}{l}\right)^2+\frac{d}{l}\sin\theta}.$$

Again expanding and dropping terms of higher orders,

$$\frac{b}{a}=1+\frac{(c+d)^2-d^2}{2l^2}+\frac{c}{l}\sin\theta.$$

Substituting this value for $\frac{b}{a}$ in (5)

$$\lambda=\lambda'\left[1-\left\{\frac{(c+d)^2-d^2}{2l^2}+\frac{c}{l}\sin\theta\right\}\frac{d}{c}\right]$$

$$=\lambda'\left[1-\left\{\frac{c+2d}{2l^2}+\frac{\sin\theta}{l}\right\}d\right]$$

which gives as the correction term

$$\lambda-\lambda'=-\lambda' d\left\{\frac{c+2d}{2l^2}+\frac{\sin\theta}{l}\right\}.$$

Obviously the last part vanishes if $\theta=0$, i.e., if AB is normal to CE. Hence, the correction for a flat plate is merely

$$-\lambda' d\left\{\frac{c+2d}{2l^2}\right\} \tag{6}$$

And for an angle θ, if present, it is

$$-\frac{\lambda' d}{l}\sin\theta \tag{7}$$

In general sin θ can, if desired, be made so small that the corrections contained in (7) need not be used at all. (See, however, below.) To obtain the corrections corresponding to (6) the point B was first located by taking half the distance between the slit E and its direct image C. Then with the measured values of c and d the correction curve for (6) was plotted using $\lambda - \lambda'$ as ordinates and λ' as abscissae. This curve is shown in Figure 2. A line was then drawn from the origin to the point on the curve corresponding to

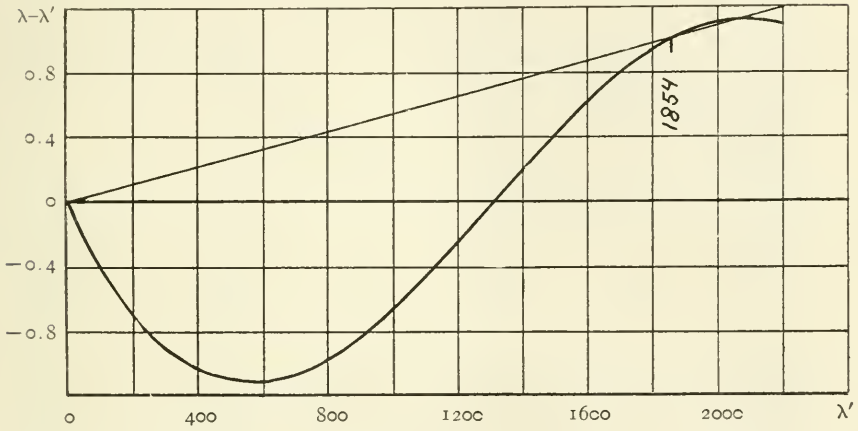


FIG. 2

the standard wave-length 1854.7. The distance between this line and the curve then represents the correction term required for any wave-length.

In practice the foregoing procedure was somewhat modified because of the appearance on the plates of second and higher orders of some of the stronger lines. With the aid of the values of λ' and the corrections obtained from Figure 2, all lines which appeared in more than one order were located with an error of not more than 0.5 A. A systematic departure from an exact multiple relationship between these measurements meant that the angle θ of equation 7 was not quite zero. To find its most probable value a curve corresponding to (7) was plotted with sin θ taken arbitrarily as 0.01. This curve is shown in Figure 3. If then the difference between a measurement on a first-order line

and one-half of the corresponding measurement on a second-order line was on the average the value found in the curve of Figure 3, the value of sin θ was considered to be 0.01. If it was

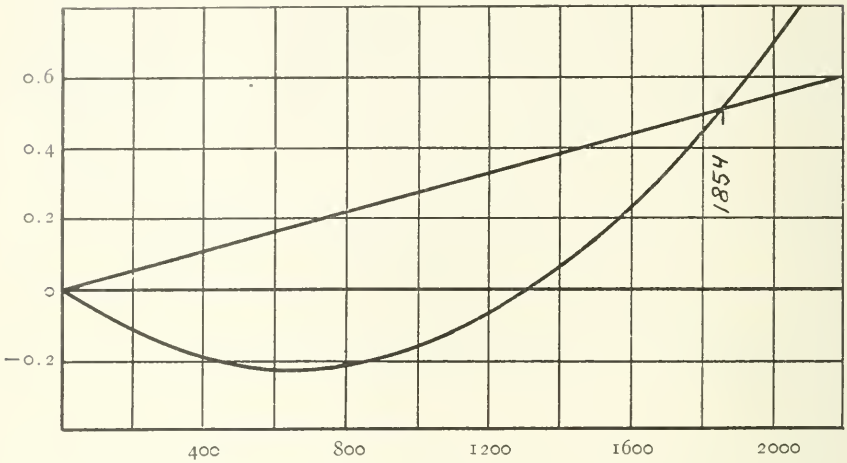


FIG. 3

twice the value found in Figure 3, sin θ was taken as 0.02, etc. The whole series of wave-lengths obtained with the aid of (6) was then corrected with the aid of (7), using the value of sin θ obtained in this way from these spectra of higher orders.

III. SPECTRA OF IRON, CARBON, AND NICKEL

TABLE I

IRON SPECTRUM

Intensity	λ	Intensity	λ	Intensity	λ
o O?	271.5	o	663.3	o	1089.4
1	290.8	4	666.9	1	1117.9
2	294.3	4	669.9	1	1125.3
2	297.3	o	680.2	2	1143.4
o	301.0	1	691.2	1 O?	1153.4
o O?	304.0	1	694.0	1	1158.0
2	308.5	o	696.8	o	1166.1
2	311.8	2	723.1	o	1169.2
1	330.5	3	729.9	o	1172.3
1	334.5	1	739.8	o	1179.1
o	357.6	o O?	749.7	1	1182.5
o	361.6	2 O?	760.8	2	1186.4
5	365.8	2 C?	808.2	1	1192.2
1	377.1	2	813.7	o C?	1194.7
4	381.1	1	816.7	1	1212.5
9 C?	385.2	1	820.1	2	1228.9
9 C?	387.7	1	823.4	o	1238.0
7	392.9	1	837.8	2	1254.1
4 O?	395.6	1	841.1	2	1260.8
3	400.8	2	845.0	1	1266.2
2	407.2	2	847.7	2	1272.2
2	411.1	2	851.8	1	1277.5
4	417.5	1	854.9	1	1285.9
3	422.0	4	859.9	o	1291.2
3	426.5	3	863.2	o C?	1297.1
1	445.5	1	869.1	o	1301.6
3	502.4	2	873.6	o	1309.5
3	506.7	2	876.3	o	1311.1
o	519.2	2	880.6	o	1315.3
1	529.4	2	884.1	1	1317.9
1	531.7	2	891.2	1	1321.1
7 C?	548.7	o O?	899.3	o	1345.9
7	552.1	2	911.5	o	1348.9
1	558.8	3	929.2	1	1358.1
1	562.1	o	934.8	2 C?	1362.0
3	565.7	o	937.7	1	1365.8
3	569.8	o	944.4	2	1373.9
1	577.3	1	950.2	1	1376.3
3 O?	580.2	o	955.3	2	1387.8
3	584.0	2	962.4	2	1409.4
1	588.2	1	967.0	1	1415.2
o	590.9	o	971.5	2	1430.6
3 C?	594.2	1	981.2	1	1440.7
4 O?	598.1	3	983.8	o	1449.2
4	602.4	2 Si?	994.0	o	1456.0
9 O?	609.1	2 Si?	997.8	1	1465.4
2	612.8	1	1000.3	o	1469.3
1	632.9	2	1006.0	o	1472.6
1 C?	636.9	6	1017.6	2	1525.5
o	639.6	2	1021.8	2	1532.3
1	646.4	1	1026.9	2	1538.3
1	654.5	4	1031.8	2	1542.5
2 C?	661.8	2	1062.1	o	1556.5

TABLE I—*Continued*

Intensity	λ	Intensity	λ	Intensity	λ
0	1563.6	1	1710.6	2 C?	1931.0
1	1568.6	2	1718.3	1	1937.9
0	1576.6	2	1724.0	1	1944.3
1	1580.3	0	1746.9	1	1950.6
0	1584.7	1	1770.2	2	1953.6
0	1591.7	0	1775.9	2	1959.5
1	1595.2	1	1786.1	1	1964.5
2	1597.7	1	1787.5	1	1983.1
1	1601.5	0	1792.8	1	1987.3
0	1609.3	1	1797.9	1	1992.1
0	1615.4	1 C?	1827.6	1	1995.0
1	1622.2	2	1843.9	1	2000.1
1	1626.8	1	1850.0	0	2035.7
2	1630.9	1	1860.0	0	2040.1
1	1639.9	2	1870.8	0	2051.1
0	1646.8	1	1877.6	1	2058.0
1 C?	1656.7	2	1881.9	1	2069.3
0	1658.8	1	1891.0	2	2079.8
1	1662.5	4	1895.6	1	2085.4
1	1673.3	0	1901.1	2	2091.0
1	1676.0	0	1907.0	2	2098.7
0	1681.3	0	1910.2	0	2104.4
1	1687.2	3	1914.2	0	2108.2
0	1690.7	1	1917.9	0	2145.4
1	1695.3	1	1922.6	0	2152.9
0	1702.2	2	1926.4		

TABLE II

CARBON SPECTRUM

Intensity	λ	Intensity	λ	Intensity	λ
0	360.5	0 O?	749.6	7	1247.5
2 Na?	372.1	1	786.5	5	1262.4
4	384.4	5	799.9	5	1278.7
4	386.4	6	806.7	2 Si?	1294.9
1	410.8	5	810.0	2	1296.8
1	450.9	0	848.4	3 Si, Ca?	1299.2
6	459.7	5	858.5	1	1310.5
1	493.7	1	884.8	2	1322.3
4	499.7	10	904.1	7	1323.7
1	511.7	1	936.4	15	1335.0
1	517.6	4	945.6	1	1356.2
2	530.3	0	954.4	5 Ca?	1362.6
2	533.3	0	960.6	4 Si, Ca?	1393.9
7	538.4	0	966.6	4 Si, Ca?	1402.9
2	543.5	12	977.1	1	1426.9
2	549.6	2 O, N?	991.1	1	1432.2
3	560.5	10	1010.2	2	1463.7
3	564.7	1	1022.8	1	1482.1
6	574.5	12	1036.7	4	1548.8
3	585.7	8 Si?	1066.0	3	1550.9
5	595.1	3 O, N?	1085.3	5	1561.3
1 O?	600.2	3	1092.6	1	1577.6
1 O?	609.5	3 Si, Ca?	1109.6	1 B?	1624.3
3	636.3	2	1111.3	5	1657.6
5	641.8	3	1137.4	2	1752.3
6	651.5	4	1141.5	1	1827.3
0	661.5	15	1175.6	0	1910.2
8	687.3	3	1194.1	7	1931.1
0	711.0	5 Ca?	1206.6		
0	743.6	2	1230.2		

TABLE III

NICKEL SPECTRUM*

Intensity	λ	Intensity	λ	Intensity	λ
0	731.0	1	1417.1	0	1662.7
0 C?	786.2	1	1420.9	1	1673.2
0	861.0	1	1429.0	1	1688.9
0 C?	944.7	0	1430.9	2	1693.4
1	1072.7	1	1435.2	2	1708.4
1	1079.0	1	1439.6	2	1710.9
1 C?	1084.0	1	1445.4	2	1716.2
0	1091.6	0	1449.5	1	1720.2
0	1100.6	1	1452.8	1	1724.0
0	1107.2	0	1455.6	0	1734.2
0	1118.0	1	1462.6	1	1739.4
0	1224.4	1	1468.9	1	1742.7
1	1234.2	1	1477.6	2	1748.2
1	1245.0	1	1483.5	2	1753.7
1	1253.0	0	1490.6	1	1765.5
1	1265.9	1	1494.0	2	1770.3
1	1277.0	2	1499.7	1 Al?	1777.0
1	1306.7	1	1513.8	0	1789.1
1	1314.6	0	1517.5	1	1792.1
1	1318.4	1	1521.6	0	1795.7
0	1346.6	2	1527.4	1	1812.3
0	1351.2	1	1535.6	0	1820.2
1	1357.3	0	1539.1	1	1824.0
0	1364.3	1	1544.3	1	1831.0
1	1372.2	1 C?	1561.5	0	1848.5
0	1382.4	1 Al?	1606.3	0	1850.7
1	1386.6	0 Al?	1613.0	1 Al?	1855.2
2	1398.5	0	1621.2	0	1859.7
2	1411.3	1	1653.8		

*The spectrum of nickel between 700 and 200 angstroms, to which point it has recently been carried, will be reported upon later.

RYERSON LABORATORY
UNIVERSITY OF CHICAGO
January 1921

INTENSITY DIFFERENCES IN FURNACE AND ARC AMONG THE COMPONENT SERIES IN BAND SPECTRA[1]

By ARTHUR S. KING

ABSTRACT

Intensity differences between band spectra emitted by electric furnace and by arc.— Large-scale photographs of the "*cyanogen*" *band at* λ *3883*, made in the third order of a 30-foot spectrograph, showed the A_1 series of lines is enhanced over the A_2 series so as to become the dominant series (Plate II). Also some new faint doublet appeared. The two series, then, seem not to belong to the same temperature class, and may be expected to be differently affected by pressure, etc. The "*cyanogen*" *band at* λ*4216* also showed similar changes. In the *Swan band* λ *5165* the triplet series is enhanced in the furnace spectrum with reference to the adjacent doublet series.

In spectrograms of moderate dispersion in which the spectrum of the electric furnace was photographed with comparison arc spectra, it was noted that the "cyanogen" band λ 3883, which frequently appeared, showed an apparent difference in structure, the component lines seeming to be more numerous in the furnace when the general intensity was about the same for both sources. Closer examination showed this to be due to an intensification in the furnace of band lines which are present but relatively faint in the arc.

Since the phenomenon indicated a variability among band lines similar to that generally observed for line spectra given by arc and furnace, the nature of the difference was investigated with higher dispersion, the third order of the 30-foot plane grating spectrograph being used. As this band is emitted more strongly at atmospheric pressure than in the vacuum furnace, and as it was desirable furthermore to avoid differences of pressure, a new furnace built to stand long exposures at high temperatures was employed. In this, the graphite tube is supported in large bronze holders, cast hollow for water-cooling, with graphite bushings around the ends of the tube. The heated portion of the tube is protected merely by a cast-iron water jacket which retards the wasting away of the

[1] *Contributions from the Mount Wilson Observatory*, No. 194.

tube by preventing active circulation of air. Large-scale photographs were thus secured for tube temperatures of approximately 2700°, 2500°, and 2350° C., a spectrum of the carbon arc being taken in each case adjacent to that of the furnace.

The portion of the band between the first and second heads, being free from the overlapping which occurs beyond the second head, was most suitable for comparison. It was clear that the different appearance in furnace and arc is due to an enhancement in the furnace of the series of lines designated by Uhler and Patterson[1] as "A_1." This is weaker in the arc than the "A_2" series, composed of doublets, up to a point not far from the head of λ3883, some lines of the A_1 series being very faint in a normally exposed arc spectrum. In the furnace, A_1 is the dominant series. At 2350°, the A_1 lines are nearly twice as strong as those of the A_2 series. At 2500°, reversals begin for both series, but a much larger proportion of the A_1 lines is reversed. At 2700°, almost all members of both series are reversed, the reversals of A_1 lines being decidedly wider.

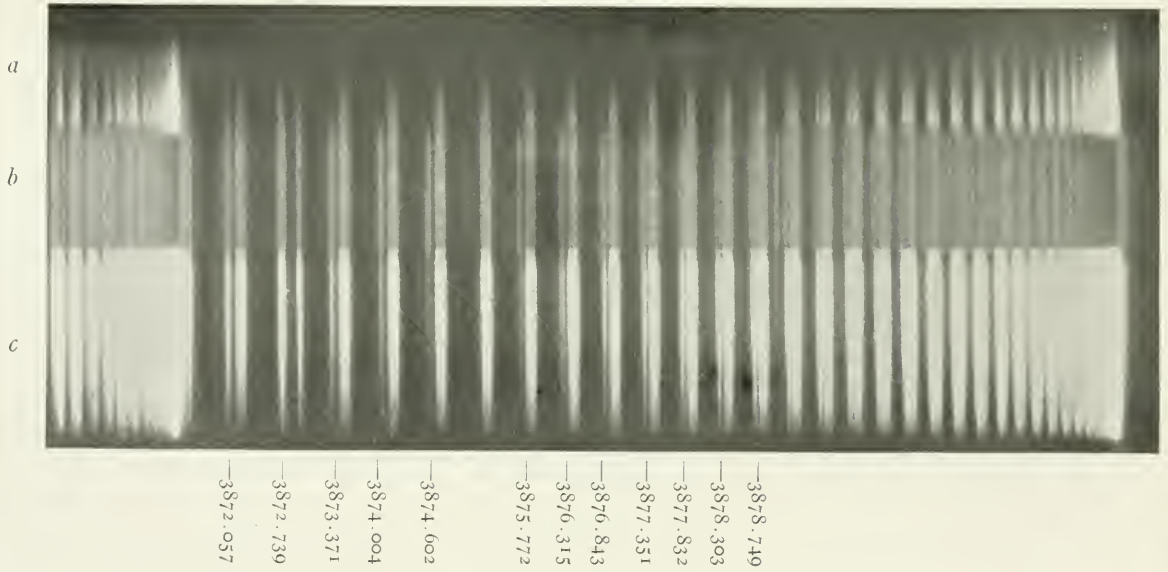
Plate II shows the section of the band most favorable for examination, with the furnace spectrum at 2500° between two arc spectra of different exposures.

In the following table a comparison is given of the band lines of arc and furnace for a portion of this region. The wave-lengths are those of Uhler and Patterson, and the series symbols and intensities for the arc lines are also taken from their paper. *F* and *f* indicate degrees of faintness, while *w*, *m*, and *i* signify weak, medium, and strong, respectively. The same gradation is adopted for the furnace spectrum and degrees of reversal are indicated by *r* and *R*. The intensity relations for the remaining lines up to the head at λ 3883 are similar to those of the last three lines in the table.

In addition to strengthening the A_1 series (and perhaps others beyond the second head), a series of faint doublets, not quite strong enough to measure, appears in the furnace band between λλ 3871 and 3875. These do not show in the arc band even when this is very strong. The furnace thus appears to be especially effective in bringing out the full structure of a band.

[1] *Astrophysical Journal*, 42, 434, 1915.

PLATE II



Section of λ 3883 band in furnace (*b*) and arc (*a*, *c*), showing high intensity of A_1 series of single lines (marked) in furnace as compared with A series of doublets.

An examination of the "cyanogen" band at λ 4216 and that at λ 5165 belonging to the Swan spectrum, the latter being photographed in furnace and arc under high dispersion, showed in each case a strengthening of certain series by the furnace. The triplet

TABLE I

INTENSITIES OF BAND LINES IN ARC AND FURNACE

λ	Series	Arc (U and P)	Furnace
3872.057	A_1	*m*	*i r*
.180	A_2	*i*	*m*
.252	A_2	*i*	*m*
.739	A_1	*i*	*i r**
.965	A_2	*m*	*m*
3873.371	A_1	*w*	*i r*
.501	A_2	*i*	*m*
.567	A_2	*i*	*m*
3874.004	A_1	*f*	*i*
.123	A_2	*i*	*m*
.190	A_2	*i*	*m*
.602	A_1	*F*	*i*
.727	A_2	*i*	*m*
.791	A_2	*i*	*m*
3875.310	A_2	*i*	*m*
.375	A_2	*i*	*m*
.772	A_1	*F*	*i*
.873	A_2	*i*	*i*
.939	A_2	*i*	*i*
3876.315	A_1	*f*	*i*
.415	A_2	*i*	*i*
.481	A_2	*i*	*i*
.843	A_1	*w*	*i r*
.938	A_2	*i*	*i*
3877.005	A_2	*i*	*i*
.351	A_1	*w*	*i r*
.446	A_2	*i*	*i*
.506	A_2	*i*	*i*
.832	A_1	*m*	*i R*
.925	A_2	*i*	*i r*
.989	A_2	*i*	*i r*
3878.303	A_1	*m*	*i R*
.389	A_2	*i*	*i r*
.448	A_2	*i*	*i r*
.749	A_1	*i*	*i R*
.828	A_2	*i*	*i r*
.891	A_2	*i*	*i r*

* Double violet component reversed in furnace.

series proceeding from the head at λ 5165 is enhanced in the furnace to about the intensity of the strongest line of the adjacent doublet series, thus doing away with the contrast which the arc shows on account of the predominance of the doublet series.

The question as to whether temperature produces the difference between furnace and arc cannot well be tested at present, on account of the great increase in vapor density, with resulting reversals, when the graphite tube is heated to high temperature. A considerable difference in temperature, such as between 2300° and 2700°, involves the uncertainty of comparing sharp and reversed lines. The difference between furnace and arc indicates, however, that the contrasted series belong in different temperature classes. If so, there should be a difference in their response to displacing agencies such as pressure or those electrical actions which affect wave-length, since, for the line-spectra of metals, lines relatively strong in the furnace are less subject to displacements.

A further feature resulting from the fact that the lines composing a band do not behave as a unit is that this dissimilarity must be taken into account in atomic models designed to explain the radiation of band spectra. A considerable degree of independence evidently exists between the centers emitting the component series of a band which itself is a member of a family of bands.

Mount Wilson Observatory
September 1920

ELEMENTS OF THE ECLIPSING SYSTEM SX CASSIOPEIAE

By MARY FOWLER[1]

ABSTRACT

Eclipsing system SX Cassiopeiae.—From the normals obtained from the later (1915) observations of Luizet, the *elements of the system* have been computed (Table II). The *light-curve* at the minima is given and also a *picture of the system.* The stars are both giants with radii about 13 and 10, and brightness about 100 and 24, respectively, in terms of the sun. The primary eclipse is annular, the secondary total.

For this star ($\alpha = 0^h 5^m 5$, $\delta = +54°20'$ for 1900.0) Shapley[2] published elements based on observations by Luizet,[3] and Luizet later[4] published further observations, upon which the present elements are based. These observations are not so numerous as

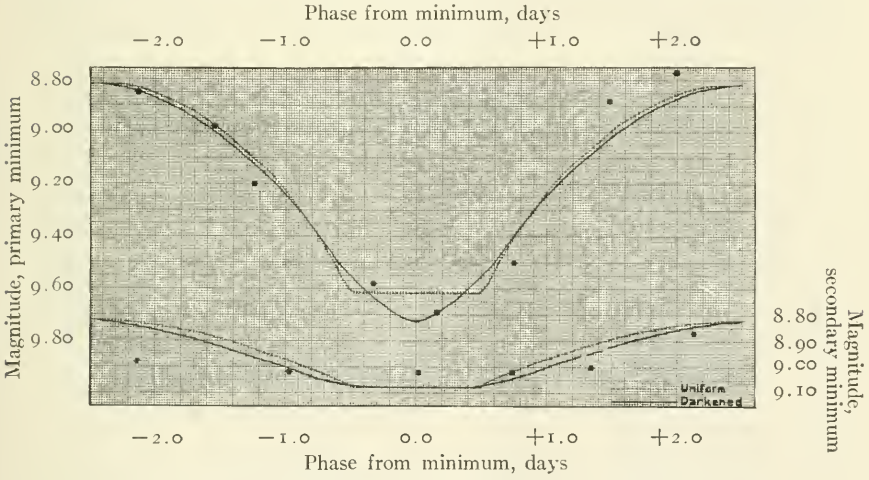


FIG. 1.—Light-curve of SX Cassiopeiae at the eclipses

those for RT Lacertae, nor do they give as smooth a curve, particularly around secondary minimum. They are reduced to the magnitude scale in the same way as those for RT Lacertae, but in this case Luizet's normals are taken singly, not in pairs.

[1] This paper was chiefly prepared by Miss Fowler before the war, and completed by me at Professor Russell's request.—Bancroft Walker Sitterly.

[2] *Contributions from the Princeton University Observatory*, No. 3.

[3] *Bulletin Astronomique*, **26**, 278, 1909. [4] *Ibid.*, **32**, 66, 1915.

Both minima are fairly deep—the combined loss of light is about 80 per cent; and the shape of the curve in its uneclipsed portion indicates a high degree of ellipticity in the figures of the spheroidal stars. After "rectifying" for this, as usual, "uniform" and "darkened" solutions were made. The first gave an orbital inclination over 87°, so, in the second, central transit was assumed in order to make the theoretical curve steep enough at the eclipses, and even this did not give a very close fit. The "darkened" assumption is just a trifle the better fit all over. Both solutions make the larger star the brighter, so that primary eclipse is annular and secondary total, a condition opposite to that of Shapley's solution.

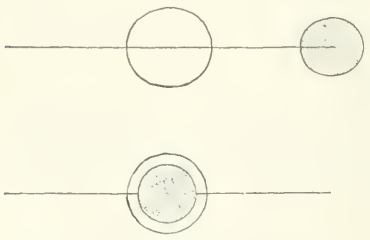


FIG. 2.—SX Cassiopeiae at elongation and at primary minimum, according to the "darkened" solution.

TABLE I

TABLE OF OBSERVATIONS, SX CASSIOPEIAE

No.	Phase	Observed Magnitude	O.-C. Uniform	O.-C. Darkened	No.	Phase	Observed Magnitude	O.-C. Uniform	O.-C. Darkened
	Days					Days			
1.....	0.158	9.69	+0^{M}06	−0^{M}01	20.....	18.303	9.02	−0^{M}05	−0^{M}05
2.....	0.746	9.50	+0.10	+0.10	21.....	19.025	9.02	0.00	−0.02
3.....	1.482	8.88	−0.12	−0.14	22.....	19.626	9.00	+0.08	+0.06
4.....	1.984	8.77	−0.09	−0.11	23.....	20.413	8.87	+0.04	+0.02
5.....	2.462	8.76	−0.06		24.....	21.360	8.84	+0.04	
6.....	3.186	8.79	−0.01		25.....	22.191	8.78	−0.01	
7.....	3.958	8.76	−0.03		26.....	22.905	8.75	−0.02	
8.....	4.962	8.74	−0.03		27.....	24.093	8.73	−0.01	
9.....	6.199	8.74	0.00		28.....	25.449	8.72	0.00	
10.....	7.639	8.73	+0.02		29.....	26.630	8.73	+0.03	
11.....	8.612	8.74	+0.03		30.....	27.820	8.71	0.00	
12.....	9.418	8.69	−0.01		31.....	29.117	8.75	+0.04	
13.....	10.246	8.71	0.00		32.....	30.647	8.76	+0.02	
14.....	11.597	8.72	−0.01		33.....	31.956	8.81	+0.04	
15.....	12.602	8.68	−0.06		34.....	33.350	8.82	+0.01	
16.....	13.849	8.74	−0.03		35.....	34.430	8.85	+0.02	0.00
17.....	15.082	8.82	+0.01		36.....	35.018	8.98	0.00	−0.03
18.....	16.156	8.98	+0.16	+0.14	37.....	35.326	9.20	+0.09	+0.08
19.....	17.320	9.03	+0.050	+0.02	38.....	36.232	9.58	−0.04	−0.04

Probable error of one normal, on "uniform" hypothesis, ±0^{M}0357; on "darkened" hypothesis, ±0^{M}0344.

Adams and Joy[1] give the spectrum of the bright component of the system as "very much like that of a Cygni." Only one spectrum was visible, confirming the present orbit's indication that the stars are very unequal in brightness. Computation by Shapley's methods[2] of the hypothetical dimensions and distance shows that these stars are emphatically "giants," as their low density would suggest.

TABLE II

TABLE OF ELEMENTS, SX CASSIOPEIAE

EPOCH AND PERIOD = J.D. 2417983.45 G.M.T. ± 0.17 + (36.5668 ± 0.0041) E

Element	Symbol	Value	
		Uniform	Darkened
Ratio of radii of stars	k	0.800	0.735
Type of eclipse:			
Primary		Annular	Annular
Secondary		Total	Total
Semi-major axis:			
Brighter star	a_b	0.232	0.260
Fainter star	a_f	0.186	0.191
Semi-minor axis:			
Brighter star	b_b	0.204	0.241
Fainter star	b_f	0.163	0.177
Eccentricity of meridian section of stars	$\epsilon = \sqrt{z \cdot \operatorname{cosec}^2 i}$	0.484	0.382
Inclination of orbit	i	87°40′	90°0′
Least apparent distance of centers	$\cos i$	0.041	0.000
Light of brighter star	L_b	0.810	0.809
Light of fainter star	L_f	0.190	0.191
Ratio of surface brightness of stars	J_b/J_f	2.73	2.29
Density of stars in terms of sun:			
Brighter star	$\bar{\rho}_b$	0.0004	0.0003
Fainter star	$\bar{\rho}_f$	0.0008	0.0007
Light of brighter star in terms of sun	$\bar{L}_b$	100	
Greatest radius of stars in terms of sun:			
Brighter star	$\bar{a}_b$	13.5	15.2
Fainter star	$\bar{a}_f$	10.9	11.2
Absolute magnitude of brighter star	$\bar{M}_b$	−3.7	
Parallax	π	0″.00029	
Distance in light-years		11000	
Spectral type		A2	

Table I gives the normals and residuals, and Table II the elements. The light-curve at the minima is shown in Figure 1, while Figure 2 pictures the system.

PRINCETON UNIVERSITY OBSERVATORY
August 1920

[1] *Publications of the Astronomical Society of the Pacific*, **31**, 308, 1919.

[2] *Contributions from the Princeton University Observatory*, No. 3, pp. 9, 117.

NOTICE TO CONTRIBUTORS

There is occasionally published in the *Astrophysical Journal* a Standing Notice (for instance, on pages 179–80 of the number for September 1917). This is principally intended to guide contributors regarding the manuscript, illustrations, and reprints. This notice contains the following paragraph:

> Where unusual expense is involved in the publication of an article, on account of length, tabular matter, or illustrations, arrangements are made whereby the expense is shared by the author or by the institution which he represents, according to a uniform system.

The present sheet has been printed for amplifying further that paragraph.

The "uniform system" according to which "arrangements are made" is as follows: The cost of composition in excess of $50, and of stock, presswork, and binding of pages in excess of 40 pages, for any one article shall be paid by the author or by the institution which he represents at the current rates of the University of Chicago Press. When four articles from one institution or author have appeared in any one volume, on which the cost of composition has amounted to $50 each, or when the total cost of composition incurred by the *Astrophysical Journal* on articles for one institution has reached the sum of $200, the entire cost of the composition, stock, presswork, and binding of any additional articles appearing in that volume shall be paid by the author or by the institution which he represents.

As to illustrations, the arrangement cannot be quite as specific, but it may be generally assumed that not more than three half-tone inserts can be allowed without payment by the author. The cost of paper, presswork, and binding for each full-page insert is about $8.00, aside from the cost of the half-tone itself. In the matter of zinc etchings, considerable latitude has to be allowed, as in many cases diagrams take the place of more expensive tables. It may be assumed, however, that it will seldom be possible for the *Journal* to bear an expense of over $25 for diagrams and text illustrations in any one article.

Contributors should notice that since January 1917 it has been impossible to supply any free reprints of articles.

Reprints of articles, with or without covers, will be supplied to authors at cost. No reprints can be furnished unless a request for them is received before the *Journal* goes to press.

THE EDITORS

THE
ASTROPHYSICAL JOURNAL
AN INTERNATIONAL REVIEW OF SPECTROSCOPY
AND ASTRONOMICAL PHYSICS

VOLUME LIII APRIL 1921 NUMBER 3

ON THE PASSAGE OF A STAR THROUGH A NEBULA

By ERNEST W. BROWN

ABSTRACT

Effect of the passage of a star through a nebula consisting of a swarm of particles; theory.—Neglecting the effects of mutual collisions between the particles when the swarm is undisturbed as well as the gravitational attraction of the swarm on its constituents, the author derives the formulae for the hyperbolic motion of the particles and shows that all those originally at a distance b from the path of the star will cross that path at the same point at a distance $b^2/2a$ behind the star, where a is the ratio of the mass of the star to the square of its speed, V^2. If we suppose that as a result of this focusing action collisions occur along the path of the star, these might produce a gaseous appendage of conical form with an angle β such that $\sin \beta$ is equal to the ratio of the mean velocity of the gas molecules to V.

Variable nebula N.G.C. 2261 (Hubble), with fan-shaped appendage.—The above theory suggests an *explanation* of the form of the appendage, and certain numerical consequences as to the mass, scale of magnitude, distance, and life of this object are deduced.

The general problem of the phenomena produced when a star encounters a nebula is one of great complexity and one which can only be properly treated by extended mathematical and physical investigations. In any case it must demand numerous assumptions concerning the physical conditions of both star and nebula. But there are certain forms of the problem which will yield to more simple treatment and which may furnish a qualitative idea of the phenomena and also some indications of the numerical magnitudes involved. It is one of them to which attention is drawn in this paper, illustrations being furnished by certain

planetary (?) nebulae and in particular by Hubble's[1] variable nebula, N.G.C. 2261 = H. IV 2 = h 399 = G.C. 1437.

I assume at the outset that the "nebula" involved is a swarm of discrete particles or small masses, the swarm being of very great extent but with such low volume density that we may neglect the effects of mutual collisions between the particles when the swarm is undisturbed, as well as the gravitational attraction of the swarm on its own constituents. The star is supposed to be passing through the interior of the swarm with constant velocity relative to the swarm: this involves the further assumption that the retardation of its motion produced by collisions is very small compared with the other velocities involved. Since the relative motion of the star and the swarm is alone involved in the investigation, I shall suppose that the star is at rest and that the particles of the swarm have a velocity V, constant in magnitude and direction at a great distance from the star, this velocity being only

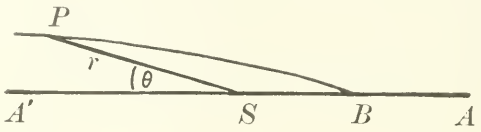


FIG. 1

changed on the approach of the particle to the star by the attraction of the latter.

Under these conditions, every particle of the swarm moves as though the rest of the swarm did not exist, except in so far as the attraction of the star may later cause collisions.

Let S be the center of the star and draw $A'SA$ parallel to the direction of motion of each particle of the swarm when at a great distance from the star. Let PB be the orbit of a particle during its passage near the star. This orbit is a hyperbola, the antecedent asymptote of which is parallel to $A'SA$; let the orbit intersect SA in B. Since we have to deal with a swarm, there will exist a ring of such orbits, all of them intersecting at B, which will therefore be a center of collision for the particles following these orbits. There will similarly be centers of collision at all points of SA,

[1] *Astrophysical Journal*, 44, 190, 1916.

starting from some point near S and extending to infinity in the direction SA.

Three classes of phenomena have to be considered. First, the orbits of particles before they intersect the line SA; second, the motions after collision along this line; third, the effects of particles which collide with the star, since we must suppose the latter to have an appreciable diameter.

Under the limitations imposed, the investigation of the first is simply that of hyperbolic motion applied to this particular case. The effect of the third may be dismissed briefly, since the supposition that the relative velocity of the star and of the main body of the swarm is not sensibly affected will be retained throughout. The second is that which presents the features of chief interest and which is assumed to be mainly responsible for the visible phenomena.

HYBERBOLIC MOTION

I now develop the formulae for hyperbolic motion which will be required.

Take S as origin and SA' the initial line for the polar co-ordinates r, θ of a particle P at time t. Let μ be the mass of the star in astronomical units and b the perpendicular distance of P from SA' at time $t=-\infty$, when it is moving parallel to $A'S$ with velocity V. Then the well-known equations of motion are

$$\left.\begin{aligned} &\frac{d^2r}{dt^2}-r\left(\frac{d\theta}{dt}\right)^2=-\frac{\mu}{r^2},\\ &r^2\frac{d\theta}{dt}=\text{moment of velocity}=\text{constant}=bV \end{aligned}\right\}. \tag{1}$$

The equation of the conic which satisfies these equations is

$$\frac{1}{r}=A\cos\theta+B\sin\theta+C, \tag{2}$$

where A, B, C are constants to be determined by the given conditions of the problem.

Differentiating (2) with respect to the time and substituting for $d\theta/dt$ from the second of equations (1) we obtain

$$\frac{dr}{dt}=(A\sin\theta-B\cos\theta)bV. \tag{3}$$

Differentiating again and substituting for d^2r/dt^2 and for $d\theta/dt$ from (1) we find

$$(A\cos\theta+B\sin\theta)\frac{b^2V^2}{r^2}-\frac{b^2V^2}{r^3}=-\frac{\mu}{r^2},$$

or

$$A\cos\theta+B\sin\theta-\frac{1}{r}=-\frac{\mu}{b^2V^2}=-\frac{a}{b^2}, \tag{4}$$

in which we have defined a by putting

$$\mu=aV^2.$$

To determine A, B, C we are given that $dr/dt=-V$ and $r=\infty$ when $\theta=0$. Substituting these values in (2), (3), (4), we obtain

$$A+C=0, \quad -V=-B\cdot bV, \quad A=-\frac{a}{b^2}.$$

Hence (2) and (3) become

$$\frac{b}{r}=(1-\cos\theta)\frac{a}{b}+\sin\theta, \tag{2a}$$

$$\frac{dr}{dt}=-V\left(\cos\theta+\frac{a}{b}\sin\theta\right), \tag{3a}$$

to which the energy equation,

$$v^2=\left(\frac{dr}{dt}\right)^2+r^2\left(\frac{d\theta}{dt}\right)^2=\frac{2\mu}{r}+V^2, \tag{5}$$

may be joined, where v is the velocity at distance r.

Let SB be denoted by c. Then $r=c$ when $\theta=\pi$ and we obtain from (2a), (3a),

$$r=c=\frac{b^2}{2a}, \quad \frac{dr}{dt}=V, \text{ when } \theta=\pi. \tag{6}$$

The point of closest approach to the star (periastron) is obtained by putting $dr/dt=0$; let $\theta=\alpha$ at this point. Then from (3a) we have $\tan\alpha=-b/a$. Thence from (2a),

$$r=\sqrt{a^2+b^2}-a \quad \text{when } dr/dt=0. \tag{7}$$

Let R be the effective radius of the star, that is, the closest distance at which any particle does not collide with any part of the star's mass. The smallest value of b for such a particle is,

from (7), given by $b^2=R^2+2aR$. Since $c=b^2/2a$, the smallest possible value of c (which will be denoted by c_0) is given by the equation

$$c_0=\frac{R^2}{2a}+R. \tag{8}$$

It is understood that when the star has a gaseous envelope any particle which is retarded by the envelope is retained by the star; this assumption can be modified later.

We now deal with the motions of the particles after the collisions have taken place along the line SA. The velocities perpendicular to SA being destroyed by the collisions, the particles, supposed inelastic, will begin to move along SA with velocity V, as shown by equation (6), whatever value c may have; this velocity will be decreased in the succeeding motion by the attraction of the star.

The ideal case in which all collisions take place on SA will be retained while the effect of the collisions is considered. I suppose that enough heat is generated by the collisions to turn all the incoming matter into a gaseous condition and that the gas immediately starts to obey the laws of an ordinary gas. Under the conditions laid down, there is no restriction on the motions of its molecules, that is, there is no external pressure. They will therefore begin to move with their proper molecular velocities relatively to the motion of the whole mass. Let the mean molecular relative velocity be U. From each point of SA will then start a spherical wave whose radius increases at the rate U while (if we neglect the retardation produced by the attraction of the star) the whole sphere moves with velocity V parallel to SA. The wave front will therefore lie along a cone of angle β such that

$$\sin\beta=\frac{U}{V}.$$

Molecular velocities are of the order of a kilometer per second while stellar velocities are of the order of twenty kilometers per second on the average so that we should expect the cone in general so have a very small angle. If, however, V be of the order of two kilometers per second, the angle rises to the order of 30°.

With a low relative velocity we cannot neglect the retardation produced by the attraction of the star. The principal effect is to diminish V as t increases and therefore to increase β. The generating lines of the cone enveloping the wave-front, instead of being straight, will be curved with convexity toward SA.

Next, the particles of the swarm are pouring into this expanding gas when the process is in full operation and the collisions no longer take place on SA; they will in general be changed into a gaseous condition by collisions with the molecules of the latter before they reach SA. In the mean, the velocities perpendicular to SA are still destroyed owing to the symmetry of the whole process with respect to this line. The velocity parallel to SA before collision at any point whose co-ordinates are r, θ, is from (1), (3a), (2a),

$$\begin{aligned}\frac{dr}{dt}\cos\theta - r\frac{d\theta}{dt}\sin\theta &= -V\left(\cos^2\theta + \frac{a}{b}\sin\theta\cos\theta\right) - \frac{bV}{r}\sin\theta \\ &= -V\left\{\cos^2\theta + \frac{a}{b}\sin\theta\cos\theta + \frac{a}{b}\sin\theta\,(1-\cos\theta) + \sin^2\theta\right\} \\ &= -V\left(1+\frac{a}{b}\sin\theta\right).\end{aligned}$$

As θ is less than π for all such cases, the actual velocity parallel to SA communicated to the expanding gas is greater than if the collisions took place on SA, but tends toward V with increasing magnitude of the periastron distance. The tendency is therefore to diminish the angle of the cone. This action, however, is also less effective near the vertex of the cone; the result is to produce a curvature of the generating lines of the wave-front surface with concavity toward SA and therefore in the opposite direction to that found in the previous paragraph. Considerable internal motion will be produced in the expanding gas, but I am chiefly considering here the outline of the wave-front.

Next consider these portions of the stream which collide with the star so as to become portions of its mass. Whatever the original condition of the star on the approach of the swarm, the collisions will heat up its surface and in time produce a gaseous envelope which will increase the effective radius of the star, the

latter being the radius within which capture of the particles of the swarm takes place. Further, although the captures take place mainly in the front portion of the envelope, the impulses as well as the gravitational attraction of the nucleus will tend to spread the envelope to the rear portions so that the envelope will probably remain approximately spherical.

There will be a number of particles which are not sufficiently retarded by the outer portions of the envelope to be captured; these will pass through with velocity diminished by this cause and so intersect SA in points which are at a less distance from S than C_0. A clear outline of the vertex of the fan cannot therefore be expected.

Before we attempt to compare these deductions with observation it is necessary to examine the light given out. Consider the mass of gas produced at any moment in the envelope of the star and in the fan before it has been cooled by expansion and radiation. The latter processes are gradual and considered alone would produce in the fan a triangular-shaped projection whose central portions are bright, with diminishing light toward the sides and rear. But the incoming stream on meeting the wave-front should be rapidly converted into heated gas and so tend to outline the latter with some approach to definiteness, and there does not seem to be any reason to expect systematic variations in the light of any part of the projection along lines perpendicular to SA; naturally, toward the rear there will be a gradual diminution of the light given out. No such definite outline is to be expected in the envelope of the star since its matter is being continually arranged in layers of increasing density with but little loss of heat due to expansion; the interior portions will have the highest temperature.

This attempt to outline the character of the phenomena produced under a speculative hypothesis must be treated with considerable reserve in the absence of any calculation. But it does not seem useful at the outset to go into details before the possibilities and probabilities of the principal features have been under discussion. With the knowledge which has been gathered of the distribution and motion of matter in space it appears that the passage of a star through widely diffused matter will be by no

means a rare phenomenon like that of the close approach of two stars. As a matter of fact this investigation was begun in order to examine the possibilities it might furnish of the evolution of a planetary system. During a visit to Mount Wilson last spring in which the idea was discussed, my attention was called to Hubble's variable nebula as possibly furnishing an example of the phenomena outlined above. As is well known, this object consists mainly of a starlike nucleus (which is known as the variable star R Monocerotis) with a fan-shaped appendage. Attention, however, had been mainly directed to the variability in the light-giving power of the fan rather than to its mode of formation.

On the hypothesis of this paper the sine of half the angle formed by the two sides of the fan should give the ratio of U to V, that is, the ratio of the molecular velocity of the expanding gas to the relative velocity of the star and swarm. In Hubble's nebula (N.G.C. 2261) this half-angle is about 30°, giving a relative velocity of the order of two kilometers per second. The equation $\mu = aV^2$ thence gives a relation between μ the mass of the star and a the "scale" of the system. Let μ_0 be the mass of the sun, V_0 the mean orbital velocity of the earth, and a_0 the mean radius of the earth's orbit. Then since V_0 is approximately 30 kilometers per second, we have

$$\frac{\mu}{\mu_0} = \frac{a}{a_0}\frac{V^2}{V_0^2} = \frac{1}{225}\frac{a}{a_0}. \tag{9}$$

By equation (8) the distance of the vertex of the cone from the center of the star is

$$c_0 = \frac{R^2}{2a} + R. \tag{8}$$

The photographs seem to show that c_0 and R are of the same order of magnitude. If $c_0 = 2R$, we have $a = \frac{1}{2}R$. It is to be noted, however, that a increases rapidly with a decrease of $c_0 - R$. It is immaterial which of these quantities we use to denote the scale of magnitude of the system. I have adopted a for convenience.

There is no direct information available as to the parallax, but from indirect evidence Hubble (*loc. cit.*) believes that it is measurable, provided suitable definition of the center of the nucleus

can be obtained photographically. The general information now available concerning the magnitudes of such objects seems to indicate the same fact. We may, in fact, expect a mass comparable with that of a star. If this is the case we should expect a corresponding scale of linear magnitude. If the mass of the nucleus of the nebula is the same as that of the sun, equations (8), (9) show that the effective radius would be 450 times that of the earth's orbit. It may be conjectured that the mass lies between 1/10 and 10 times that of the sun, giving an effective radius between 45 and 4500 times the radius of the earth's orbit. With the exposures hitherto made[1] the maximum radius of the envelope is about 5″. If this be also the effective radius, the parallax should lie between 0″.1 and 0″.001, so that there is reason to hope that a direct measure of this latter quantity may be obtainable.

The nebula has been photographed for about twenty years. In the period 1908 to 1916, there is no very noticeable change in the angle of the fan, indicating that, on the hypothesis of this paper, the change in relative velocity during this time is small. The same thing is indicated in the later photographs of Lampland. If we suppose that the velocity during 20 years has averaged 2 kilometers per second, the distance traversed in that time will be 1.3×10^9 kilometers, a small quantity in comparison with the extent of nebular clouds. There seems to be no reason why the present conditions may not continue for a considerable period.

The outstanding feature of the fan is its rapid, irregular variation in light-giving power in different parts while its outline remains approximately the same. These variations may be attributed to local variations of density in the swarm and perhaps also to cumulative effects in the interior of the fan which are released in pulses rather than continuously. It is premature to discuss hypotheses to account for the fact that one side of the projected fan is slightly concave to the interior while the other side is slightly convex. There is a small circular condensation close to the nucleus and in front of it at an angle of about 45° to the axis of the fan. Hubble (*loc. cit.*) believes that there is evidence that this object has moved

[1] I am indebted to Mr. C. O. Lampland for the opportunity to examine many of the photographs which he has taken of this nebula at the Lowell Observatory.

toward the center of the nucleus at the rate of about 0″.5 a year: if motion of this object around the nucleus can be detected, some interesting further possibilities in the development of the hypothesis of this paper will be open to consideration. It is, however, difficult to see any explanation for two faint wisps of nebulosity projected to some distance from the nucleus in front and symmetrically situated with respect to the axis of the fan, although they appear to follow the tracks of particles which later collide with the star.

In No. 81 of the *Bulletin of the Lowell Observatory* (3, 63, 1918) V. M. Slipher states that the nucleus and the fan have the same spectrum. It is necessary for the hypothesis that this should be so, for the external part of the nucleus as well as the fan must consist mainly of gas derived from the particles of the swarm after the envelope has once been formed. Slipher and Lampland also notice that the spectrum resembles that of a nova in its earlier stages, an interesting observation in view of the speculations which have been made as to the mode of formation of the latter objects.

Certain other nebulae exist in which the fan-shaped appendage is replaced by one with nearly parallel sides. Opportunity to examine photographs of these was also afforded me at Flagstaff last spring. If these nebulae are formed in a manner similar to that assumed for Hubble's nebula, we should conclude that the relative velocity of the swarm and star was much greater than 2 kilometers per second. In view of known stellar velocities these should prove to be the more common objects of this class. Further, it is to be noted that these objects must be seen in a direction nearly perpendicular to that of relative motion. For such objects viewed along or nearly along this direction, the appearance would be very different, ranging from an oval-shaped nebulosity with the star on the longer axis but away from the center, to a circular nebulosity surrounding the star. It might be hoped that relative displacements along the line of sight could be measured as a test, but the faintness of these objects is at present a serious obstacle to such measures. References to previous observations of these objects will be found in the first paper of Hubble referred to above.

YALE UNIVERSITY
December 1920

ON THE GEOMETRICAL CLASSIFICATION OF LONG-PERIOD VARIABLES

By J. G. HAGEN

ABSTRACT

Classification of long-period variables.—The writer gives a table of the *constants of the light-curves* of 66 variables as determined by harmonic analysis, and shows that on the basis of these constants the variables fall into three groups which coincide with the three main classes given in the *Harvard Annals* for 1907: (1) with uniform variation, (2) with broad minima, and (3) with a rapid increase. The first group corresponds in general to Phillips' Group I, and the last two are subdivisions of his Group II.

I

A large amount of material on long-period variable stars is contained in the *Harvard Annals*, 57, Part 1 (1907). The observations were mostly made at Harvard and the reduction was intrusted to Mr. L. Campbell. The results are there presented in very convenient form, in a statistical Table XII and on two Plates I and II.

1. Of all the seventy-five stars discussed in that volume, sixty-seven were found regular enough for showing graphically the different forms of light-curves. They are divided into five groups, two of which comprise only four stars each and might well be taken as modified forms of one or other of the larger groups. In fact the four curves of "broad maxima" and the other four of "rapid decrease" look like accidental irregularities from the large class of "uniform variation." Thus premised, the two Harvard plates exhibit three classes of light-curves with these characteristics: uniform variation, broad minima, rapid increase.

2. It is true that on page 209 it is expressly stated that these groups must not be considered as establishing different classes of long-period variables, and it may be that no further attention would have been paid to them, had not the Rev. T. E. R. Phillips subjected the very same stars to harmonic analysis and, in the main, reproduced the same classification. In his presidential

address before the British Astronomical Association, October 25, 1916, Phillips gave the results of his analysis and, from the relation between the phases of the second and third harmonics, recognized two principal groups of light-curves.

3. The writer has followed up the subject in the *Monthly Notices* (**79**, 572, 1919) and in the *Astronomische Nachrichten* (**209**, 257, 1919) and tried to show that from the same harmonics three groups of light-curves can be deduced and that these groups coincide with the three classes of the Harvard plates. The coincidence was naturally to be expected because the coefficients and phases of the harmonic formulae are deduced from the ordinates of the light-curves and cannot reveal qualities other than those contained in the drawings. Yet the writer's argument did not seem generally convincing, probably because he did not enumerate the stars of each group and did not represent the groups in a diagram. Supplying both points seems to be justified by the importance of the subject. While the short-period variables are divided into two classes distinct not only apparently by the shape of their light-curves but in their physical constitution, the long-period variables are so far from being physically understood, that at least their geometrical classification should be brought out as clearly as possible.

II

The following three tables contain all the stars whose light-curves are graphically represented on the two Harvard plates, though they do not comprise all the stars examined by Phillips. The stars are arranged by Pickering's catalogue numbers, i.e., in the order of R.A.

1. In the column $(M-m)/P$ the notation is Chandler's for the time from minimum to the next maximum divided by P, the period of variation. The fraction is readily transformed into the quantity considered by Professor Turner:

$$\alpha = \{2(M-m)-P\}/P.$$

The last three columns are taken from Tables II and III of Phillips, including also the doubtful stars, which are distinguished

by parentheses. It appears at once that Phillips examined all the Harvard stars except V Cancri.

The angles ϕ_2 and ϕ_3 are the phases of the second and third harmonics in the formulae of the light-curves; wherever necessary they have been diminished by 360° in order to make their differences

TABLE I

STARS OF UNIFORM VARIATION

Star's No.	Name	$(M-m)/P$	ϕ_2	ϕ_3	Phillips
001726	T Andromedae	0.47	+110°	+ 80°	II
001755	T Cassiopeiae	.58	− 36	191	I
011272	S Cassiopeiae	.42	+135	107	II
021024	R Arietis	.50	+ 13	197	I
050953	R Aurigae	.53	− 58	216	I
065355	R Lyncis	.46	+ 42	211	I
072708	S Canis Minoris	.48	+ 33	207	I
084803	S Hydrae	.47	− 24	189	I
085008	T Hydrae	.49	+(10)	(360)	
094211	R Leonis	.45	+114	154	I
123307	R Virginis	.48	+ 10	216	I
123961	S Ursae Majoris	.48	+ 7	263	I
124606	U Virginis	.49	− 15	197	I
132202	V Virginis	.46	+179	182	II
134440	R Canum Ven.	.49	+ 14	205	I
141954	S Boötis	.49	− 2	258	I
142584	R Camelopardalis	.50	+ 7	213	I
143227	R Boötis	.48	+126	202	I
151520	S Librae	.37	+ 37	186	I
163266	R Draconis	.44	+122	60	II
164715	S Herculis	.45	− 77	187	I
170215	R Ophiuchi	.47	+192	195	II
180531	T Herculis	.48	+ 51	160	I
191019	R Sagittarii	.44	+147	94	II
201008	R Delphini	.49	+166	171	II
201647	U Cygni	.44	+ 28	188	I
204405	T Aquarii	.50	+(171)	(242)	
205023	R Vulpeculae	.41	+ 43	153	I
210868	T Cephei	.54	− 65	205	I
213678	S Cephei	0.59	− 77	+204	I
Sum	30	14.34	1403	5693	
Mean		0.48	+ 47°	+190°	

from the mean of each group less than 180°. The angles thus reduced will give more correct figures for the "range" within which they vary for each group than the uncorrected angles.

In the last column the "group" found by Phillips is assigned to each star.

TABLE II

STARS WITH BROAD MINIMA

Star's No.	Name	$(M-m)/P$	ϕ_2	ϕ_3	Phillips
001909	S Ceti	0.46	+178°	+195°	II
012502	R Piscium	.45	154	113	II
021403	o Ceti (Mira)	.36	118	59	II
042209	R Tauri	.40	180	107	II
042309	S Tauri	.26	149	105	II
081112	R Cancri	.52	169	154	II
120905	T Virginis	.37	177	159	II
121418	R Corvi	.45	162	147	II
122803	Y Virginis	.44	(154)	(28)	
132422	R Hydrae	.43	165	181	II
132706	S Virginis	.46	159	161	II
151714	S Serpentis	.43	176	125	II
161122*b*	S Scorpii	.54	167	140	II
162119	U Herculis	.40	154	111	II
163137	W Herculis	.43	148	125	II
200357	S Cygni	.52	233	+206	I
203847	V Cygni	.38	(138)	−(26)	
230110	R Pegasi	.35	164	+133	II
233815	R Aquarii	0.43	+176	+100	II
Sum	19	8.08	3121	2383	
Mean		0.43	+164°	+125°	

TABLE III

STARS WITH RAPID INCREASE

Star's No.	Name	$(M-m)/P$	ϕ_2	ϕ_3	Phillips
001838	R Andromedae	0.38	+ 97°	+ 66°	II
022000	R Ceti	.37	80	226	I
022813	U Ceti	.31	55	241	I
054920	U Orionis	.39	126	106	II
070122*a*	R Geminorum	.42	98	35	II
081617	V Cancri	.42			
093934	R Leonis Minoris	.40	141	106	II
103769	R Ursae Majoris	.46	126	75	II
115919	R Comae Ber.	.33	122	+ 33	II
123160	T Ursae Majoris	.42	94	− 4	II
151731	S Coronae	.40	104	+ 69	II
160118	R Herculis	.44	136	102	II
161122*a*	R Scorpii	.37	136	137	II
193449	R Cygni	.36	103	93	II
194632	χ Cygni	.46	(131)	(154)	
225120	S Aquarii	.36	103	21	II
231508	S Pegasi	.43	105	93	II
235350	R Cassiopeiae	0.40	+118	+ 89	II
Sum	17 (+V Cancri)	7.12	1875	1642	
Mean		0.40	+110°	+ 97°	

2. There are some discrepancies between the two classifications. Among the thirty stars of uniform variation seven are ascribed to Group II, but three of them are near the intersection of the two straight lines in Phillips' diagram. Again there is one star of Group I among the nineteen stars with broad minima, also near the point of intersection, and two stars of Group I in the third table. A percentage of six contradictory cases among sixty-six common stars seems to be small, in view of the fact that partly different light-curves were used for the two classifications. How much the light-curves of long-period variables differ from one appearance of the star to another may be seen from the monographs of Heis, Guthnick, and Rosenberg on the typical stars *o* Ceti and χ Cygni.

TABLE IV

MEAN RESULTS

GROUPS			LIGHT-CURVE		CO-ORDINATES		RANGE	
Phillips	Harvard	Stars	$(M-m)/P$	α	ϕ_2	ϕ_3	ϕ_2	ϕ_3
I.....	Uniform variation.	30	0.48	−0.04	+ 47°	+190°	296°	300°
II*a*...	Broad minimum...	19	0.43	−0.15	+164	+125	115	212
II*b*...	Rapid increase....	17	0.40	−0.21	+110	+ 97	110	245

III

The discussion of the results is made easy by Table IV in which the mean values of the preceding tables are united, and by the accompanying diagram, where the phase-angles ϕ_2 and ϕ_3 are taken as co-ordinates of the stars, following Phillips' model except that different types are used to distinguish the stars of the three groups. It is to be noted that the diagram has eight stars less than that of Phillips.

1. The main result brought out clearly by both table and diagram consists in this, that there are three characteristic groups of light-curves and that these groups are roughly identical with the three classes of the Harvard plates: curves of uniform variation, curves with broad minima, and curves with rapid increase.

2. A secondary feature of Table IV and of the diagram is that uniform variation appears to be the general rule and that the other two types of light-curves are more like exceptions, though rather frequent ones. Indeed, several columns of Table IV show

a numerical progression from the first to the third class, e.g., in the values of $(M-m)/P$ or their equivalent values a, so also does the column of the mean co-ordinates ϕ_3. Yet on the whole the first group differs more from the other two than these differ among themselves. The first group comprises nearly one-half of all the stars examined and the range of its phase-angles is much wider than that of the other groups. For this reason the

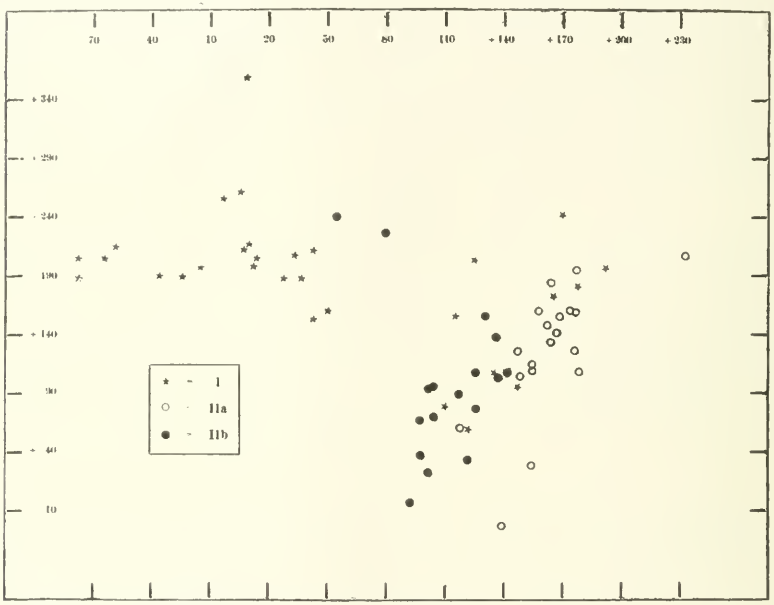


FIG. 1.—Classification of long-period variables. Ordinates, −10 to +340, represent ϕ_3; abscissae, −70 to +230, represent ϕ_2.

main division, proposed by Phillips, into Groups I and II is justified: it separates the uniform light-curves from the less regular ones; but these deviations from the regular type should be specified by the subgroups II*a* and II*b*.

By thus giving the classification of the long-period variables its precise geometrical interpretation it is hoped that a small step is made forward toward the physical explanation of these stars, a problem for which no definite solution has so far been obtained.

VATICAN OBSERVATORY, ROME
September 12, 1920

CHARACTERISTIC BEHAVIOR OF THE BRIGHT LINES IN STELLAR SPECTRA OF CLASS Md[1]

By PAUL W. MERRILL

ABSTRACT

Periodic changes in the emission lines of spectra of Class Md variables.—R Leonis, R Hydrae, R Serpentis, X Ophiuchi, χ Cygni, and T Cephei have been observed spectroscopically over a considerable part of their light periods, from two to twelve spectrograms having been made of each. The intensities of Hδ, Hγ, λ 4202 Fe, λ 4308 Fe, λ 4571 Mg, and some other bright lines at the different phases are recorded in Table IV. A compilation and discussion of past and present data referring to these lines shows that they appear after light minimum, in the order mentioned, in every long-period variable of Class Md whose spectrum has been adequately observed, and exhibit substantially the same remarkable behavior as in the type star *o* Ceti. There is strong evidence, therefore, that these spectral variations, shown in Figure 1, are characteristic of stars of this class. *The changes in relative intensity of the lines of the Balmer series of hydrogen and also of certain iron lines* are particularly interesting. A discussion of the physical interpretation of these variations is reserved until more data are available.

Although it has been known for many years, chiefly through the extensive labors of the Harvard College Observatory, that striking changes occur in the spectra of numerous long-period variable stars, practical difficulties have prevented the securing of satisfactory observations through the whole light cycle. It is therefore not yet possible to give a complete description of the spectroscopic changes which accompany the extraordinary fluctuations in brightness. Much valuable material has, however, already been gathered: the combined results of several observers have shown numerous salient features of the variations in the spectrum of *o* Ceti; some of the same phenomena have been observed in χ Cygni; and changes in other stars have been indicated by shorter series of observations.

The present discussion will be confined largely to the bright lines, as observations of the continuous spectrum and of the absorption lines and bands do not yet afford a reliable basis for a description of the characteristic changes.[2] The data for the bright lines

[1] *Contributions from the Mount Wilson Observatory*, No. 200.

[2] The available observational material bearing on the absorption spectrum is not extensive, owing to the faintness of the stars, except at maximum, and to other circumstances. It is, however, definitely known that variations do take place, but

are not so complete as might be desired, but certain features are definitely established, and the general course of the changes is indicated. Much remains to be determined, however, especially in regard to the behavior of the spectrum at minimum brightness.

The new observational material described here refers to the stars in Table I. These are among the best known of the long-period variables, and all possess spectra strongly resembling that of *o* Ceti.

TABLE I

STARS OBSERVED

Star	α 1900	δ 1900	Magnitude
R Leonis	9^h42^m2	$+11^\circ 54'$	4.6—10.5
R Hydrae	13 24.2	−22 46	4.0— 9.8
R Serpentis	15 46.1	+15 26	5.6—13
X Ophiuchi	18 33.6	+ 8 44	6.5— 9.0
χ Cygni	19 46.7	+32 40	4.0—13.5
T Cephei	21 8.2	+68 5	5.1—10.5

TABLE II

RESULTS OF HARVARD OBSERVATIONS

Star	Range	Period	$m-M$	Br.	Ft.
o Ceti	5.7 mags.	332 days	0.64	0.19	0.30
R Leonis	4.2	313	.55	.26	.28
R Hydrae	5.4	425	.57	.15	.32
R Serpentis	6.3	357	.61	.20	.28
X Ophiuchi	2.2	337	.45	.32	.44
χ Cygni	8.3	406	.54	.22	.17
T Cephei	3.9	387	0.46	0.23	0.27

Data from *Harvard Annals*, **57**, 202, showing the character of the light-variation, are given in Table II, in which *o* Ceti is included for convenient comparison. The fourth column, "$m-M$," shows

apparent discrepancies or, perhaps, real differences between different stars, make it difficult to know which variations should be considered as characteristic. For instance it is stated by Adams and Joy, *Publications of the Astronomical Society of the Pacific*, **32**, 163, 1920, and by Shane, *ibid.*, **32**, 234, 1920, in confirmation of previous observations, that in *o* Ceti the absorption bands of titanium oxide increase in strength as the star wanes, but, in the case of X Ophiuchi, observations by the writer from May to September, 1920, show that the bands grew decidedly weaker while the brightness was decreasing. Although there are several possible explanations of this apparent discrepancy their discussion will not be taken up here.

the fraction of the period during which the light decreases; the fifth, "Br.," gives the fraction of the period during which the light is more than one-half as great as at maximum, and the last column, "Ft.," that fraction during which the light is less than twice as great as at minimum.

All the observations in Table III were made with one-prism spectrographs. The column "Phase" is the only one requiring explanation. This indicates for each plate the fraction of the period before (−), or after (+), light maximum. The photometric data were kindly supplied by the Harvard College Observatory.

R LEONIS

Jan. 16, 1920. This observation was made about 110 days after minimum and 60 days before maximum. The light-curve rose gradually for 70 or 80 days after minimum, and then much more rapidly.

May 30, 1920. This last observation was about 60 days before minimum.

R HYDRAE

A minimum occurred on April 27, 1920, magnitude 9.5. The first plate, on May 31, was taken 34 days after minimum, but the star had brightened only half a magnitude. Two bright lines which are the last to appear during the decreasing phase are still in evidence. The bright hydrogen lines, which in Md stars are weak or absent at minimum, have not yet appeared. The continuous spectrum is weak but is visible from λ 4500 toward longer wave-lengths, being interrupted by wide absorption bands of titanium oxide. The second plate, taken on July 8, when the increase in magnitude since minimum had been 1.7 magnitudes, shows more continuous spectrum due to a generally more effective exposure, but the band absorption is very strong; Hδ is a distinct emission line; Hγ is not seen, although continuous spectrum is visible in its neighborhood; λ 4308 is not seen; near λ 4571 the continuous spectrum is strong and the magnesium line of that wave-length, if present at all, is so blended with the background as to be indistinguishable.

TABLE III

OBSERVATIONS

Date	Mag.	Phase	Telescope	Camera	Exposure	Remarks
			R Leonis			
1920 Jan. 16..	9.0	−0.19	100-inch	18-inch	164m	
April 8..	6.4	+ .08	100	18	30	
11..	6.5	+ .09	60	18	140	
11..	6.5	+ .09	60	18	40	
May 5..	7.4	+ .16	60	18	152	
11..	7.6	+ .18	60	18	150	Hubble observer
30..	8.3	+0.24	100	18	80	
			R Hydrae			
1920 May 31..	9.0	−0.33	100-inch	18-inch	214m	
July 8..	7.8	−0.25	100	7	50	
			R Serpentis			
1920 May 1..	7.6	+0.13	100-inch	18-inch	106m	
30..	8.8	+ .20	100	18	184	
June 1..	8.8	+ .21	100	18	184	
July 8..	10.7	+0.32	100	7	160	
			X Ophiuchi			
1919 June 9..	6.6	−0.03	60-inch	18-inch	24m	
10..	6.6	− .02	60	18	30	
1920 April 8..	7.3	− .16	100	18	(70)	Clouds
May 1..	6.9	− .09	100	18	62	
4..	6.8	− .08	60	18	52	
31..	6.6	.00	100	18	80	
July 5..	7.0	+ .10	60	18	110	
6..	7.0	+ .11	100	18	90	
31..	7.5	+ .18	100	18	66	
Sept. 2..	8.3	+ .28	100	18	110	
27..	8.8	+ .35	100	18	180	
Oct. 27..	9.0	+0.44	100	18	90	Clouds
			χ Cygni			
1920 May 30..	8.2	−0.08	100-inch	18-inch	66m	
June 1..	8.1	− .07	100	18	40	
30..	5.2	.00	60	18	125	Benioff observer
July 29..	5.8	+ .07	100	18	90	
Sept. 3..	6.5	+ .16	100	18	66	
26..	8.1	+ .21	100	18	180	
Oct. 26..	9.6	+0.29	100	18	180	

TABLE III—*Continued*

OBSERVATIONS

Date	Mag.	Phase	Telescope	Camera	Exposure	Remarks
	T Cephei					
1917 Nov. 3..	7.6	−0.19	60-inch	18-inch	50^m	Joy observer
Dec. 3..	6.8	− .11	60	18	80	Joy observer
1918 Jan. 2..	5.8	− .04	60	18	60	Joy observer
Oct. 24..	7.2	− .27	60	18	150	Joy observer
1920 June 3..	8.0	+ .20	60	18	240	
July 5..	8.9	+ .28	60	18	364	
28..	9.4	+ .34	60	18	508	
Sept. 5..	10.1	+0.44	60	7	520	

R SERPENTIS

Maximum occurred on March 16, 1920, magnitude 6.1. The facts concerning the following minimum are not available at present. It appears, however, that the minimum brightness was not above the fourteenth magnitude. The spectroscopic observations described in Table IV cover about the central third of the decreasing branch of the light curve.

X OPHIUCHI

Maximum light and the decreasing phase are well covered by the observations. The last plate, taken on October 27, was probably about 20 days before minimum. The magnitude at this time was not more than a few tenths above the minimum magnitude. On April 8, 1920, Hγ shows small contrast with the continuous spectrum; on May 1, this contrast is decidedly greater. On July 31, the titanium bands have a curious, blended appearance; the heads of the bands are not sharp, and as the absorption is less than on the preceding plates the bands are not so pronounced. The bands are still weaker in September. The decrease in intensity of Hγ from September 2 to September 27 is striking; this line is practically absent from the spectrum on the latter date. The only emission line observed on the plate of October 27 is λ 4571, just at the red edge of which there appears a well-defined and rather strong *dark* line. This has developed within a month, as no

absorption was observed in this position on the preceding plate. A somewhat similar appearance of bright and dark portions of the same line has been observed by Stebbins[1] in *o* Ceti at λ 4308 and λ 4376, and by the writer in other stars in connection with the manganese line λ 4030. This phenomenon suggests that the well-known displacement of the dark lines with respect to the bright lines may be due in part to a reinforcement by a partially developed emission line of the continuous spectrum on the violet edge of the dark lines.

X Ophiuchi is a double star, Hu 198, with a measured separation of 0".2. The small light-range and some of the spectral peculiarities may thus be due to exceptional circumstances. The motions and light-variations of the components are being investigated by Van Biesbroeck at the Yerkes Observatory.[2]

RÉSUMÉ OF OBSERVED CHANGES IN THE BRIGHT LINES

Upon combining the data of Table IV with those previously available for Md stars, it is found that certain phenomena shown by the bright lines appear in substantially the same form in several stars. We thus conclude that these phenomena are characteristic of the variation of Md stars and that they are, therefore, of great importance in the study of the problems presented by these remarkable objects.

The changes exhibited by some of the more conspicuous bright lines are outlined in the following pages. In most cases several illustrative instances are cited to indicate the character and extent of the data upon which each statement rests. This collection of references and quotations may prove useful to anyone desiring to review the observational evidence.

Hydrogen lines.—The bright hydrogen lines are such conspicuous and characteristic features of Md spectra that they have been the means in many instances of the discovery of long-period variables at the Harvard Observatory. The variations of these lines have accordingly attracted more notice than any of the other spectral modifications presented by Md stars. Notes in the

[1] *Lick Observatory Bulletins*, 2, 93, 1903.

[2] December, 1920, meeting of the American Astronomical Society.

TABLE IV

INTENSITIES OF EMISSION LINES

Date	Phase	Hη	Hζ	3905	Hε	Hδ	4202	4308	Hγ	4373	4376	4571	Hβ
R Leonis													
1920 Jan. 16...	−0.19					2							
April 8...	+ .08	1	3	1		15	3		7		tr.		
11...	+ .09	1−	3	0.5		15	4		7		0.5		
May 5...	+ .16	1.5	3.5	1+	2	15	6	3	10	2	1.5	4	
11...	+ .18	1.5	3.5	1	2	15	6	4	12	2	1	5	1
30...	+0.24					4	4	3+	6	2	1	5	tr
R Hydrae													
1920 May 31...	−0.33							1				3	
July 8...	−0.25					2							
R Serpentis													
1920 May 1...	+0.13		0.5			8			7				1
30...	+ .20		0.5			8	2+	2	7	1	0.5	2	2
June 1...	+ .21		0.5	tr		8	3	3	7	1	1	3	3
July 8...	+0.32					4+	3	4	4	0.5	1	4+	1.5
X Ophiuchi													
1919 June 9...	−0.03					6			4				
10...	− .02					7			4				
1920 April 8...	− .16					7			2				
May 1...	− .09		0.5	tr		9			4				
4...	− .08		0.5			8			4				
31...	.00	1−	2	1−		9	tr		6				
July 5...	+ .10					6	1		4				
6...	+ .11	0.5	1	0.5		7	2		6				
31...	+ .18					2	1		4				
Sept. 2...	+ .28					1	2−	1+	2	1−		2	
27...	+ .35						tr	1				2	
Oct. 27...	+0.44											1	
χ Cygni													
1920 May 30...	−0.08		2			7			2+				1
June 1...	.07		1			6			2				0.5
30...	.00		3	1−		15	tr		7				8
July 29...	+ .07	2	6	2		15	3	1	7				7
Sept. 3...	+ .16	1	3	1		15	3	3−	8	1		1	5
26...	+ .21		2	1		7	3	4	7	1		3	3
Oct. 26...	+0.29			tr		3	4	5	4	2	0.5	4	3
T Cephei													
1917 Nov. 3...	−0.19					3							
Dec. 3...	− .11		tr			15			4				
1918 Jan. 2...	− .04	2−	5	1		15	1		8				2
Oct. 24...	− .27					4			1+				
1920 June 3...	+ .20					2	2−	2+	4	0.5		4	0.5
July 5...	+ .28						2	4	2	0.5		6	0.5
28...	+ .34						1−	2				4	
Sept. 5...	+0.44						0.5	1				2	

Harvard publications show that in practically every Md star the relative intensities of Hγ and Hδ are subject to wide variations.

Although the bright hydrogen lines (referring particularly to Hγ and Hδ) are usually of very great intensity, nevertheless it appears that near the phase of minimum light they are weak or absent from the spectrum.

To avoid repetition certain references will hereafter be indicated by number as follows:

(1) Stebbins, "The Spectrum of *o* Ceti," *Lick Observatory Bulletins*, **2**, 78, 1903.
(2) Eberhard, "On the Spectrum and Radial Velocity of χ Cygni," *Astrophysical Journal*, **18**, 198, 1903.
(3) Merrill, "Spectroscopic Observations of Stars of Class Md," *Publications of the Astronomical Observatory, University of Michigan*, **2**, 45, 1916.
(4) Adams and Joy, "Note on the Identification of Certain Bright Lines in the Spectrum of *o* Ceti," *Publications of the Astronomical Society of the Pacific*, **30**, 193, 1918.
(5) Adams and Joy, "Changes in the Spectrum of Omicron Ceti," *Publications of the Astronomical Society of the Pacific*, **32**, 163, 1920.

ABSENCE OR WEAKNESS OF BRIGHT HYDROGEN LINES NEAR MINIMUM

o Ceti. 1902, Oct. 4, to 1903, Jan. 5. Phase, +0.36 to +0.64. Reference (1). Hydrogen lines weaker than other bright lines, or not observed at all. "On 584 and 594 (1903, Jan. 2 and 5) the continuous spectrum was visible in the Hγ and Hδ regions, but no trace of a bright line was seen in either case. The evidence furnished by these later plates therefore strengthens the conclusion that the bright lines disappeared at minimum."

R Hydrae. 1920, May 31. Phase, −0.33. Table IV. Hγ and Hδ not observed although other bright lines and some continuous spectrum are present.

X Ophiuchi. 1915, June 4. Phase, −0.38. Reference (3). Faint continuous spectrum; no bright lines.

1920, Sept. 27 and Oct. 27. Phase, +0.35 and +0 44. Table IV. Hγ and Hδ are very weak or absent.

T Cephei. 1920, July 28 and Sept. 5. Phase, +0.34 and +0.44. Table IV. Hγ and Hδ are not seen and are certainly much weaker than other bright lines.

Adams and Joy found that near the minimum of *o* Ceti the usual hydrogen lines were replaced by others having quite different characteristics. Whether this is typical behavior for long-period variables is not known.

HYDROGEN LINES AT MINIMUM

o Ceti. 1920, Jan. 15 to Feb. 6. Phase, +0.51 to +0.57. Reference (5). "The hydrogen lines appear very diffuse and greatly displaced toward the red. The brightest of the three hydrogen lines on this photograph is Hβ, Hγ being next and Hδ faint."

Shortly after minimum brightness the hydrogen lines Hγ and Hδ appear faintly as emission lines, Hγ being at first much the weaker, so that for a time Hδ may be seen alone. Both lines grow in intensity until maximum or after, but Hγ gains relatively to Hδ so that during the decreasing phase, before both lines disappear, Hγ may become much the stronger.

In a brief summary of the general features of the spectra of long-period variable stars[1] as photographed with objective-prism spectrographs by the Harvard Observatory, Miss Cannon says: "Changes occur in the class of spectrum during the light variation, and in the relative intensities of the bright lines. In some cases, Hδ appears first and becomes from ten to twenty times as bright as Hγ. At maximum light, Hγ often reaches equality with Hδ. The relative intensities of these two lines often vary at different maxima of the same star." The results from slit spectrograms, as noted below, are in harmony with Miss Cannon's observations.

CHANGES IN RELATIVE INTENSITIES OF Hγ AND Hδ

o Ceti. 1915, Nov. 5, 12. Phase, −0.2. Reference (3). "On Nov. 5, Hγ is so weak as not to be readily visible. It is easily seen on Nov. 12, but is not much stronger than the adjacent continuous spectrum. This is strikingly at variance with its appearance on my earlier plates and as observed by others."

1919, Autumn. Phase decreasing. Reference (5). "As the star grows fainter the relative intensity of the hydrogen lines changes, Hγ becoming stronger with reference to Hδ."

R Leonis. 1920, April 8 to May 30. Phase, +0.08 to +0.24. Table IV. Relative intensities of Hγ and Hδ changed from 7:15 to 6:4.

R Virginis. 1915, March 28 to May 7. Phase, −0.11 to +0.16. Reference (3). Relative intensities of Hγ and Hδ changed from 3:4 to 2−:1.

X Ophiuchi. 1920, April 8 to July 3. Phase, −0.16 to +0.18. Table IV. Relative intensities of Hγ and Hδ changed from 2:7 to 4:2.

[1] *Popular Astronomy*, **27**, 527, 1919.

χ Cygni. 1901, Aug. 2 to Nov. 23. Phase, -0.03 to $+0.24$. Reference (2). "From Aug. 2 until Sept. 19 Hδ was considerably brighter than Hγ; from Oct. 3 to 15 Hγ and Hδ differed little from each other; on Oct. 26 they were equal; and on Nov. 9 and 23 Hγ was brighter than Hδ."

1920, May 30 to Oct. 26. Phase, -0.08 to $+0.29$. Table IV. Relative intensities of Hγ and Hδ changed from 2+:7 to 4:3.

The foregoing are instances of considerable variation in the hydrogen lines occurring in a single light cycle. Many more examples can be found by comparing observations in different cycles, but deductions from such comparisons must be made with circumspection since it is not safe to assume that the behavior of the spectrum of a long-period variable is identically repeated in different cycles.

The relative intensities of the hydrogen lines near maximum are very different from laboratory values. The most striking discrepancies are the great strength of Hδ and of numerous ultraviolet lines, and the relative weakness of Hβ and Hϵ. Miss Maury[1] and C. D. Shane[2] have called attention to the relative weakness of Hκ, Hλ, and Hμ in *o* Ceti; the same phenomenon has been observed partially in other Md spectra through the fact that the hydrogen series appears to stop abruptly with Hι. Other peculiarities of the hydrogen series are described by Shane. By combining the results of several observers it appears that a bright Hα line may or may not be present in the spectrum of *o* Ceti. Unfortunately this line has not been observed systematically over any considerable period of time. The variation in Hβ is thought by Father Cortie[3] to be connected with the brightness of the maximum. According to him, at a bright maximum the titanium oxide bands are especially weak and Hβ especially strong. This same correlation between Hβ and the titanium bands appears also in comparing the average characteristics of different stars.[4] Hϵ (though seldom observed) may increase relatively to Hδ and Hζ during the decline in brightness.

[1] *Harvard Annals*, **28**, 45, 1897.

[2] *Publications of the Astronomical Society of the Pacific*, **32**, 234, 1920.

[3] *Scientific American Supplement*, **85**, 21, 1918.

[4] *Publications of the Astronomical Observatory, University of Michigan*, **2**, 63, 1916.

CHANGES IN RELATIVE INTENSITY OF Hε

o Ceti. 1902, June 27 to Sept. 22. Phase, +0.07 to +0.33. Reference (1).
Relative intensities of Hδ, Hε, and Hζ changed from 420:4:30 to 40:10:7.
R Leonis. 1920, April 8 to May 11. Phase, +0.08 to +0.18. Table IV.
Relative intensities of Hδ, Hε, and Hζ changed from 15:−:3 to 15:2:3.5.

Observations by Shane[1] at the Lick Observatory have revealed the interesting fact that in variables of Class N the characteristic phenomena connected with the bright hydrogen lines are much the same as in variables of Class Md. It appears, however, that in Class N the bright hydrogen lines reach their greatest intensities earlier in the light cycle, and are less persistent after maximum light than in the Md stars.

Bright lines not due to hydrogen.—Besides the hydrogen series there are other bright lines subject to very great changes in intensity during the light cycle. The available data, though rather fragmentary, make clear a certain system in these changes which is undoubtedly followed by several, and probably by many or all, Md long-period variables. Accordingly an attempt will be made in the following paragraphs to indicate some of the phenomena connected with these various bright lines as typical of Md variation.

λ 3905.—This line, thought to be due to silicon (3905.51 I.A.), is (excepting hydrogen) one of the strongest and most persistent of the emission lines during the time that the star is bright. After maximum it seems to gain relatively to the hydrogen lines, but it is possible that this increase arises from the diminution of the latter. Its behavior near the minimum phase is not known for it has usually been photographed only when the continuous spectrum and the bright hydrogen lines are strong. It appears certain, however, that λ 3905 does not grow stronger toward minimum to any such degree as do λ 4308 and λ 4571 (see below). Further observations of this line are much to be desired.

λ 4202.—This iron line (4202.033 I.A.) has very frequently been observed as an emission line in Md spectra. Appearing about the time of maximum, it grows steadily stronger during the first part of the decline until it may equal or surpass Hγ and Hδ. This increase does not continue throughout the decreasing light phase,

[1] *The Spectra of Certain Class N Stars, Lick Observatory Bulletins*, 10, 79, 1920.

as toward minimum this line is in turn exceeded in intensity by λ 4308 and λ 4571.

CHANGES IN RELATIVE INTENSITY OF λ 4202

o Ceti. 1902, June 27 to Oct. 6. Phase, +0.07 to +0.37. Reference (1). Relative intensities of Hγ, λ 4202, and Hδ varied from 420:10:420 to 13:40:13.

R Leonis. 1920, Jan. 16 to May 30. Phase, −0.19 to +0.24. Table IV. Relative intensities of Hγ, λ 4202, and Hδ varied from −:−:2 to 6:4:4.

χ Cygni. 1920, June 30 to Oct. 26. Phase, 0.00 to +0.29. Table IV. Relative intensities of Hγ, λ 4202, and Hδ varied from 7:−:15 to 4:4:3.

T Cephei. 1920, June 3 to July 28. Phase, +0.20 to +0.34. Table IV. Relative intensities of Hγ, λ 4202, and Hδ varied from 4:2−:2 through 2:2:− to −:1−:−.

λ 4308.—This line, apparently belonging to the iron spectrum (4307.909 I.A.), becomes bright at a later phase than the somewhat similar line λ 4202, and grows stronger than λ 4202 if the observations are continued a sufficient time past maximum. Near maximum λ 4308 is sometimes observed as an absorption line, usually of low intensity.

CHANGES IN RELATIVE INTENSITIES OF λ 4202 AND λ 4308

o Ceti. 1902, June 27 to Oct. 26. Phase, +0.07 to +0.43. Reference (1). Relative intensities of λ 4202, λ 4308, and Hγ varied from 10:−:420 through 19:12:190 to 40:60:13. λ 4308 appeared between July 22 and 29; phase, about +0.16.

R Leonis. 1920, April 8 to May 30. Phase, +0.08 to +0.24. Table IV. Relative intensities of λ 4202, λ 4308, and Hγ varied from 3:−:7 to 4:3+:6.

R Serpentis. 1920, May 30 to July 8. Phase, +0.20 to +0.32. Table IV. Relative intensities of λ 4202, λ 4308, and Hγ varied from 2+:2:7 to 3:4:4.

χ Cygni. 1901, Aug. 24 to Nov. 23. Phase, +0.02 to +0.17. Reference (2). "λ 4308 increased in brightness the fainter the star became." 1920, July 29 to Oct. 26. Phase, +0.07 to +0.29. Table IV. λ 4308 appeared as an emission line between June 30 and July 29. Relative intensities of λ 4202, λ 4308, and Hγ varied from 3:1:7 to 4:5:4.

T Cephei. 1920, June 3 to July 28. Phase, +0.20 to +0.34. Table IV. Relative intensities of λ 4202, λ 4308, and Hγ varied from 2−:2+:4 to 1−:2:−. Compare with plate of 1918, Jan. 2, on which the intensities were 8:−:1. Compare also with Hδ. Intensities of λ 4308 and Hδ on 1917, Dec. 3, 1918, Jan 2, were −:15 and on 1920, July 5, 4:−. The relative intensities of these two lines must have changed 250 or more times.

λ 4571.—This line, which is probably a low-temperature magnesium line (4571.114 I.A.), does not appear until a later epoch than λ 4202 and λ 4308, but gains in relative strength as minimum is approached. In several instances it has finally become the strongest line in the photographic spectrum. This is probably typical behavior. This line is usually observed near the maximum phase as a weak absorption line.

CHANGES IN RELATIVE INTENSITIES OF λ 4308, Hγ, AND λ 4571

o Ceti. 1902, July 22 to Oct. 26. Phase, +0.14 to +0.43. Reference (1). Relative intensities of λ 4308, Hγ, and λ 4571 changed from 12:190:– to 60:13:75.

1918, March 2. Phase, +0.44. Reference (4). "This line (λ 4571) is the most intense of any on the photograph with the exception of those due to hydrogen." This precise condition was not shown by any of Stebbins' photographs although it was approached on Aug. 11, Aug. 25, and Sept. 6, 1902.

R Leonis. 1920, May 5 to May 30. Phase, +0.16 to +0.24. Table IV. Relative intensities of λ 4308, Hγ, and λ 4571 changed from 3:10:4 to 3+:6:5.

R Hydrae. 1920, May 31. Phase, −0.33. Table IV. Only two bright lines are visible, λ 4308 and λ 4571. Compare with the observation of July 8, and with the Ann Arbor observations.

R Serpentis. 1920, May 30 to July 8. Phase, +0.20 to +0.32. Table IV. Relative intensities of λ 4308, Hγ, and λ 4571 changed from 2:7:2 to 4:4:4+.

χ Cygni. 1920, July 29 to Oct. 26. Phase, +0.07 to +0.29. Table IV. Relative intensities of λ 4308, Hγ, and λ 4571 varied from 1:7:– to 5:4:4.

T Cephei. 1920, June 3 to Sept. 5. Phase, +0.20 to +0.44. Table IV. Relative intensities of λ 4308, Hγ, and λ 4571 changed from 2+:4:4 to 1:–:2.

GENERAL DISCUSSION

It should not be inferred that the foregoing references represent all the known observational material bearing on each line. They have been selected as the most complete and reliable illustrations of the changes under discussion. Fragmentary observations indicate that the same course of spectral variation is followed in other stars, and in these same stars in other light cycles.

In Figure 1 an attempt has been made to display graphically the changes in the intensities of the lines Hγ, Hδ, and λ 4202, λ 4308, and λ 4571, as related to the light phase. The relationships

depicted are believed to be typical of long-period variables of Class Md. It is clear that considerable differences exist between the spectra of different stars at any given phase, but all stars of the o Ceti type which have been adequately observed have shown, with no very great variations, the changes in spectrum indicated in Figure 1. The phases at which certain lines appear or disappear may vary somewhat in different stars. Figure 1 is intended to represent the average behavior of the small group of stars observed, and may require modification when more complete data become available.

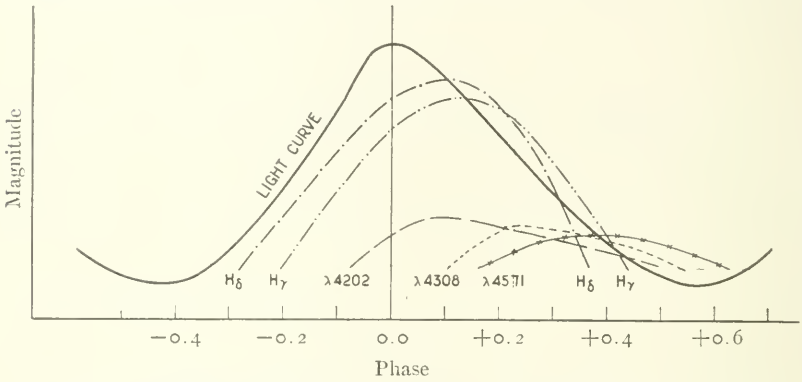


FIG. 1.—Intensities of bright lines in Md spectra in relation to the variation in total light. The light-curve, which is the mean curve for o Ceti, R Leonis, R Hydrae, χ Cygni, and T Cephei, has an amplitude of 5.3 magnitudes. The amplitudes of the other curves are not determined.

The method of comparing observations of different stars by referring them to the light phases counted from maximum to maximum is obviously but a first approximation. For an exact comparison of the behavior of different stars the light-curves cannot be assumed to be of the same shape, or to be identically repeated in different cycles. In a final discussion the circumstances of any particular cycle should be recognized either by counting the phase from maximum to *minimum* instead of from maximum to maximum, or by dropping the time relation and using instead the *magnitude* when observed, as compared with the magnitudes at the maximum and minimum of the same cycle.

In addition to the lines which have been discussed in the preceding pages a large number of other less conspicuous bright lines

have been observed in Md spectra, including λλ 3852, 3967, 4007, 4030, 4102, 4138, 4178, 4215, 4233, 4373, 4376, and 4512, all of which appear subject to variation. The intensities of λ 4373 and λ 4376 are found in Table IV. After some further observations have been secured several of these lines can probably be grouped according to their behavior and compared with the stronger lines λ 4202, λ 4308, and λ 4571. They may thus prove useful aids in interpretation. It is hoped to discuss them in a future contribution.

Adams and Joy have pointed out that "the bright lines appearing in the spectrum of *o* Ceti near minimum of light are lines which are strengthened at low temperatures."[1] This is undoubtedly correct, but it appears that some other cause in addition to low temperature must be operative to produce the observed peculiarities. The magnesium line 4571 is indeed an extreme low-temperature line and its behavior strongly suggests low temperature as the prevailing condition near minimum. With λ 4202 and λ 4308 and some other lines, however, the case is not so clear. There is no apparent reason why certain of these lines should be so strongly accentuated as compared with other lines of the same elements in the same temperature class[2] and having comparable intensities. It will probably be well to reserve discussion of temperature and other physical conditions until the fainter emission lines mentioned in the foregoing paragraph have been more extensively observed.

It is believed that the spectral changes described in this paper have such intimate connection with the light variations of Md stars that a knowledge of them is quite essential to a correct general interpretation of the phenomena exhibited by stars of this class. More complete observations of the bright lines, of the dark lines and bands, and especially of the spectrum near minimum will be required as a basis for a satisfactory discussion of the conditions prevailing in these stars and of the causes of variation. The writer is inclined to favor the "veil theory" of variation as outlined a few years ago,[3] but even if this be correct much amplification will be needed.

[1] *Publications of the Astronomical Society of the Pacific*, **30**, 193, 1918.

[2] King, *Mt. Wilson Contr.*, No. 66; *Astrophysical Journal*, **37**, 309, 1913.

[3] *Publications of the Astronomical Observatory, University of Michigan*, **2**, 70, 1916.

o Ceti, the brightest of the long-period variables and having a period which differs appreciably from a year, offers the strategic point for an observational attack on the physical problems of Md variation, provided we are justified in assuming that the remarkable spectral features of this star and their variations are not isolated peculiarities but may be accepted as typical Md phenomena. One consequence of the present discussion may be increased confidence that this is the case.

Mount Wilson Observatory
December 1920

THE ORBITS OF SEVEN SPECTROSCOPIC BINARIES[1]

By R. F. SANFORD

ABSTRACT

Seven spectroscopic binaries, Boss 373, OΣ 82, Lalande 29330, Companion to α Herculis, 205 Draconis, Boss 5591, Lalande 46867.—The elements of the orbits have been derived from 15 to 30 spectrograms of each, most of them made with an 18-inch camera and the 60-inch or 100-inch reflector. In the case of the first, fifth, and sixth binaries, both components were measured. The periods are each about 4 days except for the fourth and seventh, which are 51.6 and 6.72 days respectively. Radial-velocity diagrams are shown in Figures 1–7. The *spectroscopic parallax, proper motion, and absolute magnitude* of each, as furnished by Adams and Joy, are given in Table I. Lalande 29330 and 46867 are particularly interesting because of low luminosity, +6, and late spectral class, K. Lalande 46867 is very similar in spectroscopic peculiarities to σ Geminorum.

α Herculis and companion.—The *radial velocity* of the center of mass of the companion is −37.2 km/sec., whereas that of α Herculis is −32.2 km/sec.; and from the parallax they are separated at least 250 astronomical units. These facts indicate that they probably form merely *an optical pair.*

Probable eclipsing variable star.—The data for *205 Draconis* suggest that it would be a favorable case to examine for variability caused by eclipse. Its magnitude is 7.2 and spectral class F2.

This paper deals with the derivation of the elements of the orbits of the seven spectroscopic binary stars listed in Table I.

TABLE I

Name	Mag.	α 1900	δ 1900	Spectral Class	Abs. Mag.	μ	$\pi_{sp.}$	No. Rev.
Boss 373 = Σ 145..	6.3	1^h36^m	+25° 14′	F3–F3	+2.6	0″.135	0″.018	161
OΣ 82	7.0	4 17	+14 49	F9	+4.1	0.096	0.024	194
Lalande 29330....	8.5	16 1	+10 57	K0	+6.0	0.491	0.032	350
Comp. α Herculis-								
Boss 4374.....	5.4	17 10	+14 30	F9	+1.7	0.032	0.018	7
205 Drac. = β 971.	7.2	18 45	+49 19	F2–F2	+1.4		0.005	119
Boss 5591 = Pi. 267	6.9	21 40	+28 19	A9–A9	+2.3	0.061	0.009	103
Lalande 46867...	7.3	23 50	+28 5	K2	+6.0	0.573	0.055	179

The last four columns of the table give, respectively, the absolute magnitude, proper motion, spectroscopic parallax, and number of revolutions of the binary in its orbit between the first and last observations. Six of the stars were announced as binaries in a note by Adams and Joy,[2] who have also furnished from manuscript the data for absolute magnitude, proper motion, and spectroscopic parallax.

[1] *Contributions from the Mount Wilson Observatory*, No. 201.

[2] *Publications of the Astronomical Society of the Pacific*, **31**, 41, 1919.

The spectroscopic parallaxes for the first, fifth, and sixth binaries may be considerably in error, since blends of the spectra of the two stars may affect the relative intensities of the lines used for the determination of the absolute magnitudes. The spectral class in these three cases is indicated for both components. The elements of three of the above binaries have been previously announced by the writer.[1]

The spectrograms upon which the orbits depend were obtained with spectrographs of one-prism dispersion and an 18-inch camera, the only exceptions being a few plates of Lalande 29330, noted in Table IV, which were obtained with a 7-inch camera. Both the 60-inch and the 100-inch reflector were used: in all cases the letter prefixed to the plate number indicates the telescope—a Greek γ for the 60-inch series, and the letter *C* for the 100-inch series. Except where noted in the remarks, Seed 30 plates were used.

An effort was made in each case to determine the period as soon as possible and thereafter to secure with the minimum number of plates a reasonably good distribution over the velocity-curve. In some cases this has led to the determination of the elements from rather fewer plates than has usually been the custom. But no great increase in accuracy would have been possible without the addition of a very considerable number of observations and it was considered better to spend the time in the investigation of other orbits rather than accumulate observations on a few binaries.

The tables of observations accompanying the individual discussions are similar, each giving the plate number, date, Greenwich mean time of mid-exposure, the phase from periastron, the measured velocity, the residuals from the final elements, the weights assigned when any distinction has been made among the plates of a binary, and finally such remarks as seemed necessary. When the spectra of both components have been measured on the same plate two columns for velocities and two sets of residuals are given in the tables.

A few general remarks will make clear the procedure which has been followed and will avoid unnecessary repetition.

Since, in every case but one, at least 100 revolutions of the stars in their orbits separate the first and last observations, it seemed

[1] *Publications of the Astronomical Society of the Pacific*, **32**, 192, 1920.

justifiable to assume that the period already determined needed no correction. Except for Lalande 29330 and the companion to α Herculis, the preliminary period has, therefore, been taken as final. The freehand velocity-curves drawn through the plotted observations were used to determine preliminary elements by Russell's method.[1] When a velocity diagram included the curves of both components, the preliminary elements used were based upon both curves, excepting of course the semi-amplitude of velocity variation, K. For such binaries the elements were corrected by the method of least squares, using the equations of condition given by Harper,[2] in which a single set of normal equations is derived from the observed velocities of both primary and secondary. Assuming the period to be known and noting that the angles of periastron for primary and secondary differ by 180°, it is readily seen that there are six independent elements to be corrected, so that the normal equations involve six unknown quantities. For the binaries showing only one spectrum, the equations adapted by Schlesinger[3] were used to derive corrections to the preliminary elements.

In all cases where the elements are given for two components, those which are common to the two have not been repeated. Those which belong to the secondary alone are distinguishable by the subscript 1.

A radial velocity diagram has been drawn for each binary (Figs. 1–7). The zero for the abscissae corresponds to the epoch of periastron. The curves are based upon the elements adopted as final; the individual velocities are represented by circles with radii equal to the probable error of a velocity of unit weight; and a broken line indicates the velocity of the center of mass (γ).

The details for the individual stars are briefly as follows:

BOSS 373

This star is the brighter component of the double Σ 145. The fainter component is of the eleventh magnitude, 11″ distant, in

[1] *Astrophysical Journal*, **40**, 282, 1914.

[2] *Publications of the Dominion Observatory*, **1**, 327, 1914.

[3] *Publications of the Allegheny Observatory*, **1**, 33, 1908.

p.a. 32°. Measures separated by 35 years show no evidence of orbital motion.

Table II gives the nineteen spectrograms available for the derivation of the elements, and three others subsequently obtained. Fifteen of these gave velocities for both components and showed

TABLE II

OBSERVATIONS OF BOSS 373

PLATE NO.	DATE	G.M.T.	PHASE	VELOCITY		O−C		WT.
				Prim.	Second.	Prim.	Second.	
				km/sec.		km/sec.		
γ 7272...	1918 Aug. 27	23^h57^m	$3^d.880$	−25.2	+44.9	+ 6.1	+ 1.4	0.5
7379...	Sept. 20	22 53	1.228	+68.9	−60.5	+ 5.1	− 0.7	1.0
7412...	23	22 37	4.217	+12.8		+ 0.5	+17.8	0.5
7448...	Oct. 17	21 26	1.560	+39.8	−28.4	+ 5.5	− 0.6	0.5
7582...	Nov. 21	18 43	0.969	+76.1	−74.0	− 5.0	+ 4.7	1.0
7596...	22	17 56	1.934	+10.2		+12.9	− 0.7	0.5
7603...	Dec. 11	17 22	3.181	−76.3	+90.6	− 3.1	+ 1.5	1.0
7618...	12	18 19	4.212	+10.4		− 1.2	+14.7	0.5
7628...	13	18 16	0.775	+79.5	−83.4	− 9.1	+ 3.4	1.0
7639...	14	16 30	1.702	+10.2		− 9.5	+23.2	0.5
7646...	15	19 22	2.820	−68.4	+78.4	− 2.1	− 3.1	1.0
7662...	18	16 34	1.269	+61.2	−67.0	+ 0.8	−10.8	1.0
7739...	1919 Jan. 11	16 48	3.106	−74.5	+87.2	− 1.4	− 1.8	1.0
7769...	15	18 05	2.724	−58.6	+78.1	+ 3.3	+ 1.4	1.0
7782...	17	16 20	0.217	+72.1	−68.5	+ 3.8	− 3.8	1.0
7850...	Feb. 8	15 45	0.018	+47.3	−47.6	+ 1.6	− 7.4	1.0
8942...	1920 Jan. 6	15 50	3.851	−35.1	+47.5	− 0.6	+ 0.4	0.5
8958...	9	16 07	2.429	−50.7	+55.6	− 7.1	− 1.3	0.5
8991...	Feb. 6	15 02	3.775	−44.8	+53.5	− 2.1	− 2.4	1.0
9428...	Aug. 3	23 48	1.315	+60.8	−44.2	+ 5.3	+ 7.7	
9502...	29	21 45	0.622	+81.7	−60.2	− 6.9	+27.7	
9519...	Sept. 1	22 24	3.657	−55.4	+64.3	− 1.0	− 3.2	

that both are of spectral class F3. On the other four plates the velocities of the two components differ so little that with the dispersion employed the lines could not be separately measured. Mr. Joy had obtained 4.4 days as an approximate period, which soon led to 4.43474 days as the best value for the assembly of the observations about a single epoch.

The following preliminary elements were found:

$P = 4.43474$ days	$K = 79$ km/sec.
$e = 0.12$	$K_1 = 89$ km/sec.
$\omega = 270°$	$T =$ J.D. 2,421,940.65
$\omega_1 = 90°$	$\gamma = +5$ km/sec.

The four plates on which the lines of the two components are blended were combined into two normal places; otherwise each plate furnished a conditional equation for each component, thus giving a total of thirty-four equations. The weights depend upon the separation of the lines of the two components and refer equally to the velocities for primary and secondary. Two least-squares solutions were made with the corrections to six elements as unknowns. In the second solution the corrections were small for all except ω and T. A third solution was then made assuming all elements to be definitive except these two. This solution gave

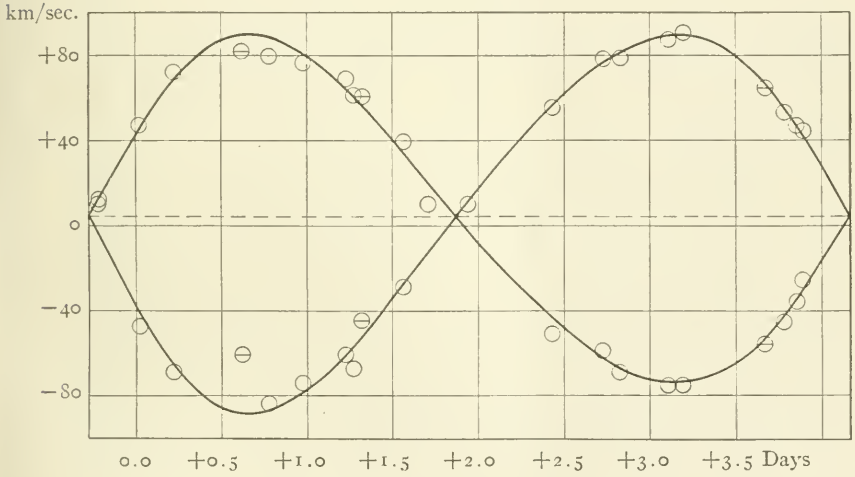


FIG. 1—Velocity-curves of Boss 373

only slight corrections. The second solution (six unknowns) and the third (two unknowns) yield elements from which nearly identical residuals result. In either case the quantity Σpv^2 is little more than 50 per cent of its value for the preliminary elements. Applying the corrections obtained by the three solutions and deriving the probable errors from the second solution we have the following final elements:

$P = 4.43474$ days	$T =$ J.D. $2{,}421{,}940.9865 \pm 0^d.0053$
$e = 0.108 \pm 0.011$	$\gamma = +4.6$ km/sec.
$\omega = 295°.58 \pm 5°.02$	$a \sin i = 4{,}942{,}100$ km
$\omega_1 = 115°.58 \pm 5°.02$	$a_1 \sin i = 5{,}371{,}800$ km
$K = 81.5 \pm 1.3$ km/sec.	$m \sin^3 i = 1.16\ \odot$
$K_1 = 88.6 \pm 1.3$ km/sec.	$m_1 \sin^3 i = 1.06\ \odot$

The probable error of a radial velocity of unit weight based upon all the residuals, including those from the four plates with blended spectra, is ± 3.5 km/sec. The three observations obtained after the elements were derived have been plotted upon the velocity diagram (Fig. 1) as barred circles. The velocity for the secondary star from γ 9502 is discordant. This plate is strongly exposed. The velocity derived from Hγ alone is -81 km/sec., which agrees fairly well with the curve.

0Σ 82

The star is a visual binary in comparatively rapid motion, the position angle having changed about 180° since discovery. The elements by different computers still differ widely, however, the periods ranging from 90 to 158 years. The last available observations of the visual pair were kindly furnished by Dr. Aitken. In 1916 the position angle was about 75° and the separation about 0″.7. During the period covered by the spectrograms it was not possible to separate the brighter star from the fainter on the slit, even with the 100-inch reflector. Consequently light from both visual components entered the slit, but in the time needed to get a good spectrogram, component *B*, two magnitudes fainter than *A*, could produce no appreciable effect upon the photographic plate. Consequently the spectroscopic binary here studied is star A.

The data of the fifteen plates available are given in Table III. The five plates taken on successive nights showed the period to be close to four days, and a subsequent adjustment of all fifteen observations was best made by using $P = 4.00000$ days.

Since the period is an exact number of days, it was impossible to observe all parts of the velocity-curve. Fortunately two of the regions that could be observed correspond to maximum and minimum radial velocity. Little would have been gained by multiplying observations of the four parts of the curve that can be represented, and it was therefore decided to derive the best elements possible from the fifteen plates available.

The curve resulting from an assembly of the observations about a single epoch gave the following provisional elements:

$P = 4.00000$ days	$K = 35.0$ km/sec.
$e = 0.15$	$T =$ J.D. 2,422,274.680
$\omega = 0°.00$	$\gamma = +37.4$ km/sec.

These were once corrected by the method of least squares applied to the equations of Schlesinger. The resulting elements and their probable errors are adopted as final for the data available:

$P = 4.00000$ days $\quad K = 36.1 \pm 0.7$ km/sec.
$e = 0.060 \pm 0.020$ $\quad T = \text{J.D. } 2{,}422{,}274.8123 \pm 0^{d}.2400$
$\omega = +12°.74 \pm 13°.56$ $\quad \gamma = +37.4$ km/sec.
$a \sin i = 1{,}980{,}000$ km

$$\frac{m_1^3 \sin^3 i}{(m+m_1)^2} = 0.0193 \odot$$

TABLE III

OBSERVATIONS OF 0Σ 82

Plate No.	Date	G.M.T.	Phase	Velocity	O−C
				km/sec.	km/sec.
γ 6511	1917 Dec. 30	$18^{h}43^{m}$	$2^{d}.968$	+45.0	+3.6
6655	1918 Jan. 30	15 44	1.844	+ 4.3	+0.9
6761	Mar. 22	15 45	0.844	+34.6	−1.5
7451	Oct. 18	0 08	2.194	+ 7.4	−0.3
8782	1919 Oct. 13	0 25	2.205	+ 7.4	−0.6
8850	Nov. 10	20 38	3.048	+43.2	−2.7
8858	11	22 13	0.114	+74.8	+2.4
8865	12	17 25	0.914	+31.5	−0.6
C 213	13	22 18	2.117	+ 1.0	−5.1
C 217	14	19 26	2.998	+42.5	−0.6
γ 8908	Dec. 9	20 57	0.061	+73.8	+0.2
γ 8922	13	16 49	3.889	+76.2	+0.7
C 244	1920 Jan. 12	19 07	1.985	+ 9.6	+5.4
C 245	13	15 30	2.833	+34.4	+0.4
C 282*	Feb. 11	15 06	3.817	+74.5	−0.9
γ 3804†	1914 Oct. 26	22 10	2.110	+11.3	+5.4

* Seed 23. † Not used for orbit.

The quantity Σpv^2 corresponding to these elements is less than 50 per cent of its value for the preliminary elements. The probable error of a velocity of unit weight is ±2.0 km/sec. The size of the probable error, the sum of the residuals, the small number of observations, and the uncertainties that enter because of the limited portions of the velocity-curve which can be observed, render further approximations inadvisable.

After the elements had been derived it was discovered that a spectrogram, listed at the end of Table III, had been taken on October 26, 1914. The velocity from this plate has been plotted

in the diagram (Fig. 2) as a barred circle. Four hundred and sixty-one revolutions of the binary separate this plate from the epoch of the velocity diagram. If the period were lengthened by 0.00050 of a day, this velocity would fall upon the curve and the distribution of the other velocities would hardly be affected; but as it stands the representation is as good as for some of the other plates, and the period has been left as previously found. After the lapse of several years it will be possible to make any slight change in the period that may be necessary.

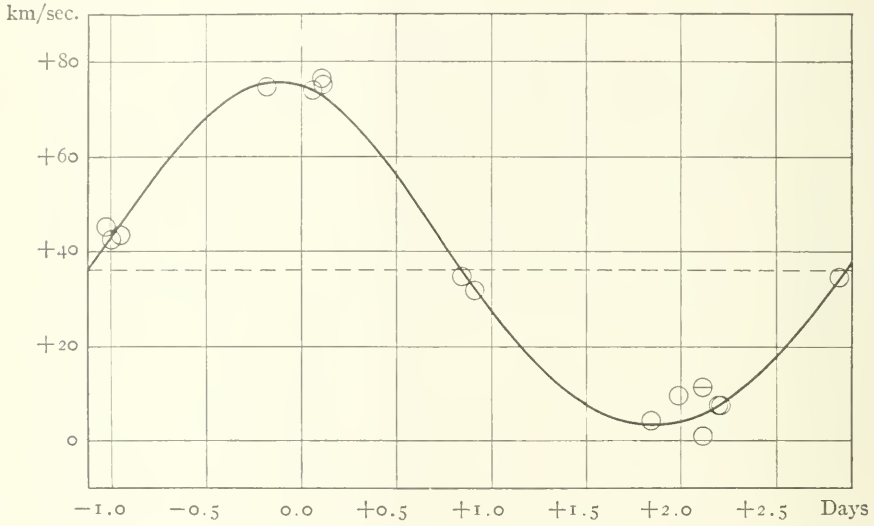


FIG. 2.—Velocity-curve of OΣ 82

From spectrograms of 19 members of the Taurus stream, Adams, Joy, and Strömberg[1] find +39 km/sec. as the mean radial velocity of the group. The velocity of the center of mass of OΣ 82 *A* found above for 1919 is +37.4 km/sec. Bearing in mind that the period of the visual binary is certainly more than 50 years and that the mass of the visual component *B* almost certainly is less than that of *A* (it is two magnitudes fainter), the radial velocity of component *A* (+37.4 km/sec.), the proper motion, and the position seem to designate the system as a member

[1] *Publications of the Astronomical Society of the Pacific*, **32**, 195, 1920.

of the Taurus stream. The mean value of the parallax for the group from the determinations of Boss and of Kapteyn, and from the spectroscopic results, giving equal weight to each, is +0″.023. If we call M_A the mass of visual component A, and M_B the mass of visual component B, we can compute the value of M_A+M_B for each of the three orbits given by Hussey.[1] Further, if we assume the velocity of the center of mass of the visual binary to be +39 km/sec., the velocity of B can be derived from the velocity of A(+37.4 km/sec.) and the parallax, +0″.023. From the velocities of A, B, and the center of mass the ratio $\frac{M_B}{M_A}$ can be calculated for each set of elements. The values (M_A+M_B) and $\frac{M_B}{M_A}$ then give M_A and M_B corresponding to each orbit. The quantity $\frac{m_1^3 \sin^3 i}{(m+m_1)^2}$, derived from the spectroscopic observations, contains $m+m_1=M_A$; hence, if we substitute successively the values of i given for each of the three visual orbits, M_A may be split up into the two parts m and m_1. The results are as follows:

	Orbit by	Glasenapp	Gore	Hussey
Unit is mass of sun	M_A m	1.94 1.17	4.45 3.44	6.19 5.04
	M_A m_1	0.77	1.01	1.15
	M_B	0.78	0.68	0.93

These values are given with the clear understanding that they are based upon the assumption that the radial velocity of the center of mass of OΣ 82 differs in nowise from the mean value for 19 other stars of the group. Furthermore no one of the three sets of visual elements is probably correct, nor does it follow that i has even approximately the same value in the spectroscopic orbit as in the visual orbit.

Note added February 17, 1921.—Exceptionally good conditions of seeing upon the night of November 23, 1920, made it possible to separate stars A and B of the visual binary OΣ 82 with the 100-inch telescope, and an attempt was made to secure the spectrum of star B separated from that of star A. As the position angle, 75°, is not favorable, guiding was difficult. The velocity derived from

[1] *Publications of the Lick Observatory*, 5, 60, 1901.

measurement of this plate is +38.6 km/sec. The velocity predicted from the elements of the spectroscopic binary, star A, is +5.0 km/sec. Hence there is no question but that the spectrum obtained is that of B. Furthermore this velocity is that of the Taurus stream which was used in the discussion of the probable masses. The spectral class of B is not greatly different from that of A, though probably slightly later.

LALANDE 29330

This binary is of particular interest because of its low luminosity (abs. mag. = +6.0) and late spectral class, K0. The twenty plates upon which its orbit is based are summarized in Table IV. Spectrograms upon five succeeding nights led to a trial of periods around four days. A smooth velocity-curve was obtained when $P = 4.28495$ days was used. This yielded the preliminary elements:

$P = 4.28495$ days	$K = 38.2$ km/sec.
$e = 0.10$	T = J.D. 2,422,418.619
$\omega = 134°$	$\gamma = -60.3$ km/sec.

TABLE IV

OBSERVATIONS OF LALANDE 29330

Plate No.	Date	G.M.T.	Phase	Velocity	O−C	Wt.
				km/sec.	km/sec.	
γ4886*....	1916 June 18	19^h09^m	4^d095	− 43.0	+0.1	0.5
4985*.....	Aug. 13	16 33	4.281	− 56.8	−1.8	0.5
5759*.....	1917 May 3	21 30	1.815	− 84.5	−4.8	0.5
5862*.....	June 9	20 54	0.225	− 67.8	+2.3	0.5
5918*.....	July 1	18 42	0.708	− 93.8	−0.2	0.5
6040*.....	Aug. 2	16 15	2.611	− 36.7	+6.8	0.5
6861*.....	1918 Apr. 25	23 26	3.240	− 20.8	+2.6	0.5
7231*.....	Aug. 21	16 18	0.962	− 94.8	+3.3	0.5
C 349.....	1920 Apr. 3	23 15	0.917	− 99.0	−1.3	1.0
354.....	4	23 42	1.936	− 75.3	−0.8	1.0
359.....	5	21 28	2.843	− 31.7	+2.4	1.0
363.....	6	22 26	3.884	− 29.9	+2.2	1.0
407.....	May 6	20 57	3.826	− 31.0	−1.3	1.0
413.....	7	21 32	0.565	− 85.1	+3.5	1.0
415.....	8	18 45	1.450	− 88.9	+3.5	1.0
433.....	26	18 57	2.317	− 59.6	−2.6	1.0
465.....	June 4	22 14	2.885	− 35.9	−3.3	1.0
468.....	5	18 30	3.729	− 26.5	0.0	1.0
471.....	6	16 10	0.337	− 80.8	−3.8	1.0
402†.....	26	21 30	3.427	− 20.6	+1.5	0.5
557.....	July 28	16 36	0.944	−101.1	−3.1	1.0

* 7-inch camera. † Underexposed.

The first eight plates were secured with a camera of 7 inches focal length instead of the usual 18-inch camera. These and one of the later plates, which was much underexposed, were given half-weight, all the others unit weight. A least-squares solution with twenty-one conditional equations was made by Schlesinger's method for the correction of all six elements. The changes for P, K, and γ were small, while those for the other three elements were of sufficient size to require a second least-squares solution for these three unknowns. The deviations from an ephemeris based on the resulting elements showed satisfactory agreement with the

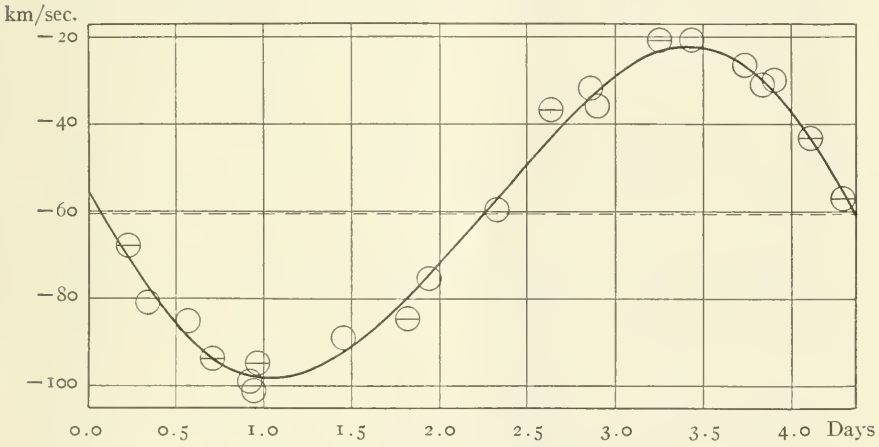


FIG. 3.—Velocity-curve of Lalande 29330

residuals given by the conditional equations. These elements were therefore adopted as final. With their probable errors they are:

$P = 4.28503 \pm 0.00016$ days $\quad K = 38.1 \pm 0.3$ km/sec.

$e = 0.089 \pm 0.024$ $\quad T = \text{J.D. } 2{,}422{,}418.0522 \pm 0^{d}0221$

$\omega = 82°.49 \pm 13°.40$ $\quad \gamma = -60.6$ km/sec.

$$a \sin i = 2{,}238{,}160 \text{ km}$$

$$\frac{m_1^3 \sin^3 i}{(m+m_1)^2} = 0.0244 \odot$$

The corresponding value of Σpv^2 is one-half that from the preliminary elements.

Reference to the table of observations shows that the first eight spectrograms obtained with low dispersion give satisfactory

residuals, whose mean is very little larger than that of the other residuals. This result tends to give one confidence in the observed velocities of faint stars of late spectral class, which must be obtained with low dispersion. In the velocity diagram (Fig. 3) barred circles represent the eight velocities derived with low dispersion.

It is noteworthy that we have here a star absolutely faint ($M = +6.0$) as the brighter member of a spectroscopic binary whose period is short and whose eccentricity is small for stars of its spectral class. Attention may also be called to the large velocity of the center of mass. The space motion derived from the radial velocity, proper motion, and parallax is 75.8 km/sec. with its apex at $A = 116°.7$, $D = -6°.8$. The rectangular components, x, y, z, where x and y are parallel to the galactic plane, are $x = -72.2$, $y = -16.7$, $z = +12.8$ km/sec.; further $L = 193°$ and $B = 10°$, where L and B are the galactic longitude and latitude of the apex. These may be compared with the mean values found by Adams and Joy[1] for 29 stars with large radial velocities: $\bar{x} = -59.5$, $\bar{y} = -44.5$, $\bar{z} = -4.4$, $\bar{v} = 74.4$ km/sec., $L = 217°$, $B = -3°$.

The agreement with the stars used by Adams and Joy is seen to even better advantage when x, y, z are plotted upon their velocity diagram.

COMPANION TO α HERCULIS

This star, hereafter referred to as B, was found from measures of the first two plates to have a variable radial velocity. It is the companion to α Herculis, hereafter designated A, whose spectral class is Mb and whose magnitude varies between 3.1 and 3.9, with a period that is uncertain if not irregular. In the visual pair no certain evidence of orbital motion has been found. Boss gives a proper motion for A of 0".030 and for B of 0".032. The magnitude of B is 5.4 and its spectral class F9, forming, with A, a striking visual pair, apparently red and blue. Their separation, 5", makes it easily possible to obtain a pure spectrum of the fainter star with either the 60-inch or 100-inch telescope, provided the seeing is good.

Table V contains the data for the twenty-eight spectrograms available for the orbit. A period of 51.6 days gave a satisfactory

[1] *Mt. Wilson Contr.*, No. 163, 1919; *Astrophysical Journal*, **49**, 179, 1919.

assemblage of the velocities about a single epoch and furnished a velocity-curve from which the following preliminary elements were derived:

$P = 51.6$ days	$K = 31.8$ km/sec.
$e = 0.08$	$T =$ J.D. 2,422,467.13
$\omega = 15^\circ.5$	$\gamma = -37.2$ km/sec.

TABLE V

OBSERVATIONS OF THE COMPANION TO α HERCULIS

Plate No.	Date	G.M.T.	Phase	Velocity	O−C
				km/sec.	km/sec.
C 60*....	1919 Sept. 10	15^h23^m	$2^d.010$	− 9.2	+5.4
66†....	19	15 58	11.034	−43.4	+2.2
114.....	Oct. 12	15 03	33.996	−36.2	+4.1
350.....	1920 Apr. 4	0 48	2.042	−18.6	−3.9
408.....	May 6	22 28	34.947	−33.3	+3.7
416.....	8	21 04	36.887	−29.0	+1.1
422.....	10	23 20	38.980	−25.0	−1.9
430.....	25	23 35	2.400	−18.5	−2.9
442*....	28	23 39	5.405	−28.3	−3.2
470‡....	June 5	23 48	13.411	−48.2	+5.0
477‡§...	7	21 10	15.301	−55.8	+2.5
508.....	July 3	15 55	41.083	−17.7	−0.9
519.....	5	19 24	43.227	−10.1	+1.5
527.....	7	16 27	45.104	−16.8	−8.3
539*....	23	15 55	9.493	−45.6	−5.5
γ9404*....	30	16 13	16.505	−64.9	−4.0
C 573.....	Aug. 2	15 27	19.473	−64.3	+0.9
γ9431*....	4	17 50	21.572	−68.0	−2.0
C 622.....	30	15 07	47.460	− 6.9	−0.1
C 627.....	31	15 08	48.460	− 0.8	+6.0
γ9514*....	Sept. 1	14 58	49.452	−11.4	−4.0
γ9531.....	3	16 15	51.506	− 3.0	+7.5
C 647.....	5	15 04	1.867	−13.7	+0.5
C 664.....	25	15 17	21.876	−65.3	+0.7
γ9573.....	26	15 07	22.870	−67.4	−1.7
γ9581.....	27	14 42	23.852	−64.2	+0.8
γ9591.....	28	14 58	24.863	−65.5	−1.6
γ9616§....	Oct. 3	14 51	29.858	−58.0	−4.5

* Overexposed.
† Focus poor.
‡ Seed 23.
§ Strongly exposed.
|| Somewhat underexposed.

Since the interval between the first and the last observation covers but seven revolutions of the binary in its orbit, it seemed best to derive a correction for the period from the least-squares solution, together with corrections to the other five elements. As the table shows, *B*, which is really a very bright star for the one-prism spectrograph and 100-inch telescope, has given in several

cases overexposed plates. It is assumed that the necessity of measuring upon such plates farther to the violet than usual has given the advantage of greater dispersion, which compensates for some falling off in focus. Hence all values of the radial velocity were given weight unity, and corrections derived from the set of six normal equations based upon the twenty-eight conditional equations. The resulting corrections proved to be moderate in size and effected a reduction of 25 per cent in the value of Σpv^2.

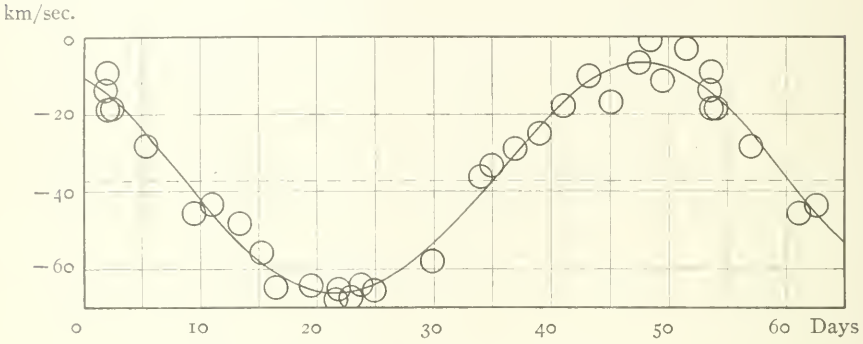


FIG. 4.—Velocity-curve of companion to α Herculis

Hence they have been adopted as final and with their probable errors are to be found below:

$P = 51.590 \pm 0.002$ days
$e = 0.028 \pm 0.026$
$\omega = 27°.89 \pm 19°.3$
$K = 29.64 \pm 0.77$ km/sec.
$T = \text{J.D. } 2{,}422{,}468.581 \pm 3^d.030$

$\gamma = -37.2$ km/sec.
$\frac{m_1^3 \sin^3 i}{(m+m_1)^2} = 0.1395\ \odot$
$a \sin i = 2{,}102{,}700$ km

The probable error derived for a determination of velocity of weight unity is ± 2.85 km/sec.

Attention is called to the fact[1] that the radial velocity of A is -32.2 km/sec., whereas that for the center of mass of B as here determined is -37.2 km/sec., showing a difference whose reality, in part at least, can hardly be doubted. Taking the distance between A and B as $5''$, the projected linear separation obtained by using the spectroscopic parallax $0''.018$ derived for B turns out to be greater than two hundred and fifty astronomical

[1] *Lick Observatory Bulletin*, No. 229, 1913.

units. The true separation cannot be less than this amount. This, with the considerable difference in the radial velocities, is evidence of a very loose or practically negligible gravitational connection between the two stars unless the masses are very large. It is not improbable that we have here an optical pair.

Coblentz'[1] radiometric measures of *B* led Burns[2] to conclude that light from *A* was probably involved in the measurement. This seems very probable in view of experience with the 100-inch and 60-inch telescopes whose focal lengths, in Cassegrain form, give a much greater linear separation of *A* and *B* in the focal plane than would be the case with the Crossley reflector used in Newtonian form. It may be pointed out, however, that the only indication of spectral class available to Coblentz, viz., the designation as a "blue" star, is not borne out by the spectrum, which is F9, hence the star is approximately "yellow." Although it is certain that the secondary member of the spectroscopic binary is photographically at least one magnitude fainter than the primary, for the spectrum is not recorded, its spectral class may be such as to help account for the discrepancy in Coblentz' measures.

205 DRACONIS

This binary is evidently the brighter component of the visual double β 971. The fainter component is of magnitude 8.5. Burnham says "it, β 971, is certainly a binary and in rapid motion. The measures indicate that the plane of the orbit is nearly in the line of sight. The period will probably be short." The last observation reported by him in which the two stars were resolved is by Aitken:

1905.29 p.a. 26°.6 dist. 0″.37.

Thirty spectrograms were obtained between August 22, 1918, and November 14, 1919. The data are in Table VI. Both spectra show lines when the difference in velocity is sufficient, but the lines are so poor that considerable uncertainty attaches to the measured velocities, a difficulty increased at times by the blending of lines of the two spectra. Observations upon successive nights considered

[1] *Lick Observatory Bulletin*, No. 266, 1914.

[2] *Publications of the Astronomical Society of the Pacific*, **27**, 110, 1915.

in connection with the results for pairs of plates upon the same night led to a trial of periods around four days. $P=3.76468$ days was found to represent the observations best and was adopted as final. When all the observations had been gathered about a single epoch with this period, the two resulting velocity-curves led to the following preliminary elements:

$P=3.76468$ days $K=96.5$ km/sec.
$e=0.10$ $K_1=102.5$ km/sec.
$\omega=166°$ $T=$J.D. 2,422,161.597
$\omega_1=346°$ $\gamma=-14.0$ km/sec.

TABLE VI

OBSERVATIONS OF 205 DRACONIS

PLATE NO.	DATE	G.M.T.	PHASE	VELOCITY		O−C		
				Primary	Secondary	Primary	Secondary	
				km/sec.		km/sec.		
γ 7239...	1918 Aug. 22	18^h37^m	$0^d.299$	+ 83.9	−112.4	+16.9	− 7.3	
7376...	Sept. 20	18 41	2.948	−23.3		(−24.7)	(+15.8)	
7385...	21	17 50	0.149	+ 87.0	−116.0	+11.1	− 1.9	
7395...	22	17 50	1.149	−15.1		(+36.9)	(−29.7)	
7404...	23	17 01	2.115	−109.2	+ 77.1	0.0	+ 4.9	
7523...	Oct. 26	15 05	1.154	−25.8		(+27.0)	(−41.2)	
8328*..	1919 July 3	20 22	2.904	+ 28.7	− 53.7	(+34.4)	(−21.7)	
8354...	9	23 17	1.495	− 83.6	+ 56.4	+13.2	− 3.3	
8374...	13	18 22	1.525	−109.1	+ 79.4	− 9.5	+16.9	
8411...	17	16 57	1.702	−111.0	+ 72.8	+ 1.1	− 2.3	
8416...	17	23 39	1.981	−122.9	+ 88.7	− 7.7	+10.5	
8417†..	18	16 50	2.697	− 68.1	+ 23.4	(−28.8)	(+21.6)	
8435...	19	16 45	3.694	+ 60.6	−111.3	−17.6	+ 5.1	
8438...	19	21 36	0.131	+ 83.9	−117.9	+ 7.3	− 3.1	
8441...	Aug. 2	16 27	2.622	−27.2		(+23.8)	(−40.8)	
8444...	2	21 22	2.827	−21.7		(− 3.5)	(− 2.3)	
8447...	3	16 14	3.615	+ 77.4	−110.4	+ 1.5	+ 3.6	
8458‡..	4	16 19	0.852	+ 15.7	− 56.0	(+20.0)	(−22.6)	
8462...	4	21 55	1.085	−14.0		(+28.0)	(− 9.4)	
8467...	5	15 55	1.835	−103.5	+ 77.1	+12.7	− 2.1	
8471...	5	21 40	2.075	−117.9	+ 76.0	− 6.4	+ 1.5	
8703...	Sept. 12	15 35	2.172	− 93.3	+ 42.7	+12.0	−25.5	
8765§..	Oct. 11	15 13	1.042	− 51.5	+ 16.7	(−16.3)	(+19.0)	
8776...	12	15 23	2.049	−111.3	+ 66.5	+ 1.4	− 9.2	
C 118...	13	15 28	3.052	+ 29.8	− 55.7	+12.2	− 0.3	
γ 8786...	14	15 18	0.281	+ 63.7	−113.3	− 4.7	− 6.8	
C 156	..	Nov. 1	15 55	3.248	+ 35.3	− 83.5	− 9.5	− 0.7
171...	4	15 44	2.476	− 91.0	+ 44.2	−18.7	+ 9.1	
210	..	13	15 10	0.158	+ 76.5	−118.0	+ 1.0	− 4.3
215¶..	14	14 35	1.134	− 50.9	+ 15.2	(− 1.2)	(+ 2.9)	

* First measured as single spectrum; vel. −10.1 km/sec.
† First measured as single spectrum; vel. −11.9 km/sec.
‡ First measured as single spectrum; vel. −22.0 km/sec.
§ First measured as single spectrum; vel. −15.6 km/sec.; Seed 23. || Seed 23.
¶ First measured as single spectrum; vel. −18.6 km/sec.; Seed 23.

In deriving the corrections to the elements by the method of least squares only those spectrograms were used, nineteen in all, upon which both spectra had been measured. These were given equal weight and combined into twelve normal places which resulted in twenty-four conditional equations of the form given by Harper.

The correction found for e reduced it to zero, thus giving a circular orbit in which of course ω and T are arbitrary. The time of maximum positive velocity for the primary was adopted for T.

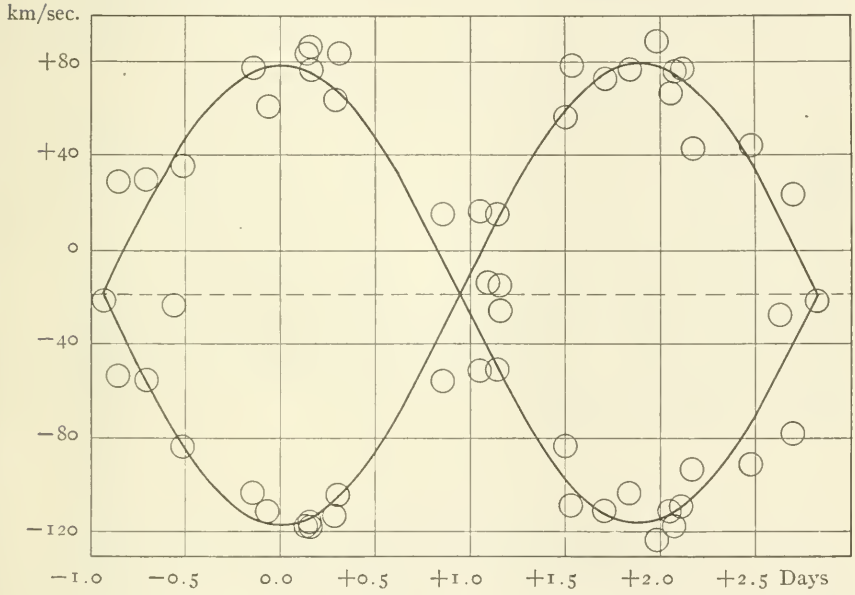


FIG. 5.—Velocity-curves of 205 Draconis

Since some of the corrections were rather large, a second least-squares solution, based upon the circular elements, was made. The quantity, Σpv^2, for the final elements is about 25 per cent of the value it had for the preliminary elements. The preliminary elements of this binary are somewhat less accurate than was the case for the others. Corrected as indicated by the two solutions they gave the following elements and probable errors:

$P = 3.76468$ days
$K = 97.7 \pm 2.0$ km/sec.
$K_1 = 98.3 \pm 2.0$ km/sec.
T = J.D. 2,422,159.7691 $\pm 0^d0178$
$\gamma = -18.8$ km/sec.

$a \sin i = 5{,}058{,}000$ km
$a_1 \sin i = 5{,}089{,}000$ km
$m \sin^3 i = 1.48 \odot$
$m_1 \sin^3 i = 1.47 \odot$

The probable error of a velocity of unit weight derived from the nineteen spectrograms whose spectra are separated is ±4.5 km/sec. In the table of observations the residuals for those plates which did not contribute to the normal places have been placed in parentheses. It will be seen from the velocities or from the remarks that in all cases they were first measured as single spectra. Later it was found that by going to the extreme violet end of the spectrum the increased dispersion gave some material for the velocities of both components, but in a region that has already departed from good focus. These measures have been given in the velocity columns, but the residuals indicate their relative inferiority.

The intensities of the absorption lines for the two components were so little different that they could not be used as a reliable criterion of phase. The results for K and K_1 and the similarity of the spectra are in accord with this lack of difference in intensity.

If Burnham's conclusion that the plane of the orbit of the visual double is nearly in the line of sight is correct, and if the inclination of the spectroscopic orbit should be nearly the same, this binary would be a favorable case to examine for variability caused by eclipse. The large amplitudes K and K_1 are likewise favorable to this possibility.

BOSS 5591

Table VII contains the data for the nineteen spectrograms which form the material for deriving the orbit. Sixteen of these gave velocities for both components. The phase could not be determined with certainty from differences in the intensities of the spectral lines of the two components, which seem to be identical in spectral class A9. As in the case of 205 Draconis, plates on successive nights, combined with pairs upon the same night (the latter to be sure that the period was not less than a day), resulted in a choice of 3.74860 days as best for grouping the observations about a single epoch. Preliminary elements were obtained as follows:

$P=3.74860$ days	$K=97.8$ km/sec.
$e=0.175$	$K_1=98.0$ km/sec.
$\omega=89°.2$	$T=$J.D. 2,422,175.243
$\omega_1=269°.2$	$\gamma=+0.3$ km/sec.

In correcting the preliminary elements only the velocities from plates showing both spectra were used, sixteen in all. The period was assumed to need no correction. Three pairs of plates, taken in each case at nearly the same time and at favorable parts of the orbit, furnished three normal places. Otherwise each plate furnished a conditional equation for both primary and secondary star. All plates used were given unit weight.

Although corrections to the preliminary elements were twice derived by the method of least squares applied to the twenty-six

TABLE VII

OBSERVATIONS OF BOSS 5591

PLATE NO.	DATE	G.M.T.	PHASE	VELOCITY		O−C	
				Second.	Prim.	Second.	Prim.
				km/sec.		km/sec.	
γ 7408.....	1918 Sept. 23	19^h11^m	$0^d.524$	− 63.4	+65.7	+12.9	−17.7
7577.....	Nov. 21	15 10	3.128	+ 94.7	−81.0	− 5.1	+ 9.1
7594.....	22	16 14	0.423	− 81.3	+81.4	−15.9	+ 8.7
7626.....	Dec. 13	15 16	2.641	+ 68.4	−77.4	− 6.4	−11.9
7636.....	14	14 55	3.627	+ 31.8	−33.9	−13.8	+ 2.8
7643.....	15	15 02	0.882	− 98.2	+97.8	−12.3	+ 4.9
8365.....	1919 July 11	23 14	3.051	+104.3	−86.4	+ 5.1	+ 3.2
8376.....	13	21 55	1.247	− 74.2	+76.0	− 8.2	+ 2.6
8413.....	17	20 38	1.445	− 50.0	+65.6	− 1.0	+ 8.9
8437.....	19	19 45	3.408	+ 94.5	−82.0	+11.9	− 8.9
8443.....	Aug. 2	19 57	2.421	+0.2			
8451.....	3	19 50	3.417	+ 87.1	−85.8	+ 5.7	−13.8
8456.....	4	0 05	3.594	+ 59.9	−52.5	+ 7.7	− 9.2
8460.....	4	20 06	0.680	− 76.3	+95.6	+ 9.1	+ 3.2
8469.....	5	18 40	1.620	+5.0			
8473.....	6	0 12	1.859	−0.4			
C 119*....	Oct. 13	16 22	3.041	+105.4	−80.0	+ 6.2	+ 9.5
123*....	14	16 56	0.326	− 50.8	+66.3	+ 0.2	+ 7.8
129*....	15	16 46	1.316	− 49.3	+60.7	+11.3	− 7.2

* Seed 23.

conditional equations, the corrections from the second solution were so small that the elements adopted as final and their probable errors are based upon the results of the first solution. These are:

$P = 3.74860$ days — $T = \text{J.D. } 2{,}422{,}175.1577 \pm 0^d.0880$

$e = 0.189 \pm 0.021$ — $\gamma = +4.2$ km/sec.

$\omega_1 = 82°.66 \pm 9°.00$ — $a_1 \sin i = 4{,}728{,}000$ km

$\omega = 262°.66 \pm 9°.00$ — $a \sin i = 4{,}662{,}000$ km

$K_1 = 93.2 \pm 2.8$ km/sec. — $m_1 \sin^3 i = 1.17\ \odot$

$K = 92.1 \pm 2.8$ km/sec. — $m \sin^3 i = 1.19\ \odot$

Attention is called to the fact that in giving the final elements, the order is the same as for the preliminary elements, but the subscripts have been changed, because the corrections to the elements have interchanged the two stars in respect to the semi-amplitudes, K and K_1, and hence to their masses.

Substitution of the unknowns derived from the first solution in the conditional equations gives residuals in substantial agreement with those derived from the final elements. Σpv^2 is 64 per

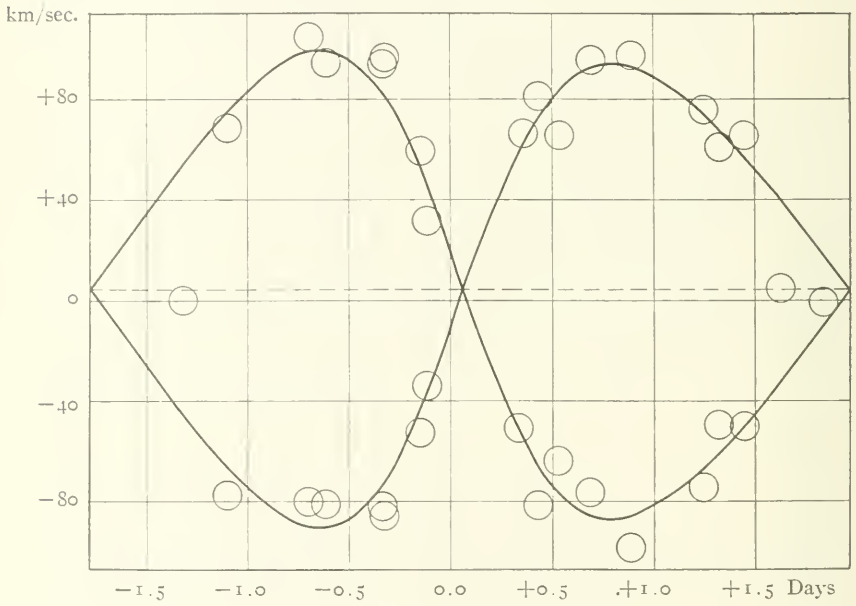


FIG. 6.—Velocity-curves of Boss 5591

cent of its value for the preliminary elements. The probable error of a velocity of unit weight for either component, on the basis of all residuals for plates with double spectra, is ± 6.4 km/sec. This is larger than that for either of the other two spectroscopic binaries showing double lines, and is to be accounted for in part by the fact that all plates were given unit weight. The spectral class is somewhat earlier than that of the others, which involves a greater uncertainty in the measures.

LALANDE 46867

This spectroscopic binary shows only the spectrum of a single star of class K2 from which the absolute magnitude derived is +6.0. The twenty-five spectrograms available are listed in Table VIII. The velocity-curve, which proved satisfactory when all observations were assembled around a single epoch with $P = 6.7217$ days, yielded the following preliminary results:

$P = 6.7217$ days	$K = +39.2$ km/sec.
$e = 0.08$	$T =$ J.D. 2,422,220.768
$\omega = 20°.5$	$\gamma = -20.2$ km/sec.

Plate γ9492, for which the preliminary elements give a residual far larger than for any other plate in the table and which was found to be in poor focus except in the region of the H and K lines, was omitted from the least-squares solution but retained in the table because the velocity derived from the emission lines H and K, to be referred to later, agrees fairly well with the velocity computed from the elements. The twenty-four remaining plates were given equal weight and the period was assumed to be known with the requisite accuracy, since the interval between the first and last spectrograms corresponds to one hundred and seventy-nine revolutions of the binary in its orbit. When the remaining five elements had been corrected by the method of least squares, the new elements were found to decrease the quantity Σpv^2 by only 3 per cent. Therefore, as so corrected, they are adopted as final and are given below with their probable errors:

$P = 6.7217$ days	$\gamma = -19.8$ km/sec.
$e = 0.059 \pm 0.019$	$\frac{m_1^3 \sin^3 i}{(m+m_1)^2} = 0.0125\odot$
$\omega = 18°.6 \pm 16°.3$	$a \sin i = 3{,}552{,}300$ km
$K = 38.5 \pm 0.76$ km/sec.	
$T =$ J.D. $2{,}422{,}220.7403 \pm 0^d.3005$	

The probable error for a single determination of velocity of weight unity is ±2.8 km/sec.

Plate γ9671, obtained by Mr. Hoge on a partly cloudy night, is very strongly exposed and was noticed by him to have two emission lines in the violet. These proved to be H and K of calcium superposed upon their usual broad absorption lines. Thereafter an effort was made to expose plates strongly enough to show this

feature of the spectrum. By using earlier plates which upon second examination showed this feature, velocities from these two emission lines were secured from twelve plates in all. They are listed in a separate column in Table VIII and placed in parentheses whenever they are derived from plates on which these lines are extremely feeble. Judging from the better-exposed plates, the

TABLE VIII

OBSERVATIONS OF LALANDE 46867

Plate No.	Date	G.M.T.	Phase	Velocity Abs. Lines	Velocity H and K	O−C Abs. Lines
				km/sec.	km/sec.	km/sec.
γ6036	1917 July 31	23h28m	0d.916	−11.1		− 3.3
6367	Nov. 23	16 38	1.401	−25.5		− 1.0
6499	Dec. 29	15 01	3.725	−46.5		+ 2.3
7214*	1918 Aug. 17	23 39	6.548	+28.5		+ 7.9
7271	27	22 47	3.067	−55.0		+ 1.0
7410	Sept. 23	21 10	3.114	−53.0		+ 2.9
8722*	1919 Sept. 14	22 40	2.927	−60.5		− 4.4
C 555	1920 July 27	20 36	3.921	−49.7		− 5.0
γ9434	Aug. 4	22 33	5.278	− 4.2		− 2.6
9492†	28	21 18	2.340	−36.7	−46.4	+14.0
9504	29	23 25	3.440	−48.6	(−62.4)	+ 4.6
C 626	31	0 13	4.463	−33.5		− 4.0
C 630	31	23 10	5.418	+ 5.9		+ 2.9
γ9518‡	Sept. 1	21 26	6.357	+15.4	+13.3	− 5.5
C 665	25	16 27	3.252	−58.1		− 3.0
γ9578	26	20 21	4.415	−27.9		+ 3.1
9587	27	21 00	5.442	+ 8.6	(+ 6.0)	+ 4.9
9595	28	19 43	6.389	+20.6	(+25.9)	− 0.3
9671	Oct. 26	19 01	0.750	+ 4.2	+ 2.1	+ 4.5
9678	27	20 15	1.802	−39.4	−29.6	− 1.5
9680	28	16 45	2.656	−55.0	−57.7	− 0.2
C 738	31	19 31	5.772	+ 9.7	+ 9.3	− 3.2
C 743	Nov. 1	17 32	6.689	+18.2	+ 7.7	− 1.1
γ9734	21	16 25	6.478	+18.8	+20.2	− 2.1
C 774	23	19 19	1.876	−35.8	(−34.6)	+ 4.2

* Underexposed.

† Best focus around H and K. Plate not used in least-squares solution. ‡ Focus poor.

H and K emission lines yield the same velocities as the lines of the absorption spectrum. No satisfactory measures of the H and K absorption lines could be made.

In general the absorption lines of Lalande 46867 seem to be less sharp than for the general run of stars of spectral class K2.

The spectroscopic binary σ Geminorum, spectral class G9, abs. mag. +1.1,[1] has been noted both by H. M. Reese,[2] who announced

[1] *Mt. Wilson Contr.*, No. 142; *Astrophysical Journal*, 46, 313, 1917.

[2] *Lick Observatory Bulletin*, No. 31, 2, 29, 1903.

its variable velocity, and by Harper,[1] who published its orbit, to have abnormally fuzzy lines. Schwarzschild[2] reports having observed H and K emission lines in objective-prism spectrograms of σ Geminorum. A plate of this star obtained by Mr. Duncan for the writer showed emission lines H and K but, relatively to the adjacent continuous spectrum, these were weaker than in Lalande 46867. The velocity derived from the emission lines was in close agreement with that for the absorption lines and agreed as well as

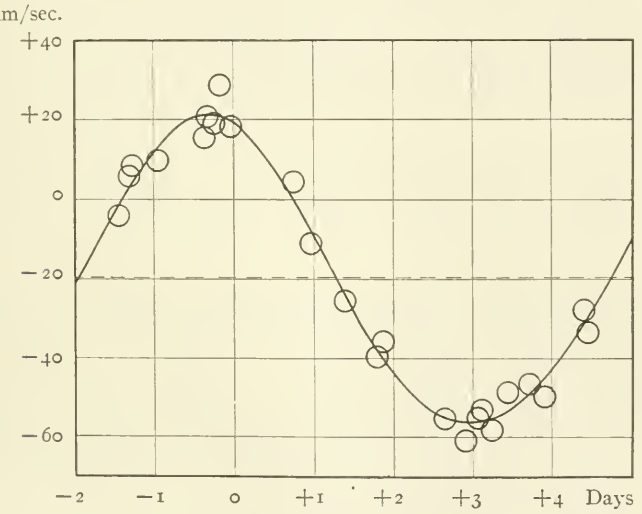


FIG. 7.—Velocity-curve of Lalande 46867

could be expected with the velocity computed from Harper's elements. Hence these stars present several points of similarity: (*a*) spectral class; (*b*) character of absorption; (*c*) presence of emission lines for H and K; and (*d*) the fact that both are spectroscopic binaries with eccentricities smaller and periods shorter than the average for binaries of this spectral class. There is a notable difference in the absolute magnitude (σ Geminorum, +1.1, Lalande 46867, +6.0), associated with emission lines which are stronger relatively to the continuous spectrum in the case of the absolutely fainter star.

MOUNT WILSON OBSERVATORY
October 1920

[1] *Publications of the Royal Astronomical Society of Canada*, **5**, 200, 1911.

[2] *Astrophysical Journal*, **38**, 292, 1913.

PRESSURE-SHIFTS IN A CALCIUM ARC

By L. F. MILLER

ABSTRACT

Pressure-shifts in calcium-arc spectrum, λ 3150 to λ 6500.—A 4-mm, 4-amp. arc between Ca electrodes, one water-cooled, the other pointed, was operated in a chamber in which the pressure was varied from 5 to 76 cm of Hg. By using the second order of a 21.5-ft. grating, shifts of 0.001 A could be detected. Table II gives the mean results for 75 lines. The H and K lines, the P and T series lines, and a few other lines show a shift of 0.001 A or less. All lines which broaden toward the violet show a shift toward the violet; all others tend to shift toward the red. The shift is the same for all lines of each term of a series, and increases with the term number, except that there is an indication that for the lower term of the T_1 series the shift is positive instead of negative as in the case of terms 4 to 6. Mechanical shifts were eliminated by comparison with iron lines of class *a* and *b*.

The present paper gives results on the measurement of pressure-shifts for all the principal lines in the photographic region of the calcium spectrum.

Apparatus.—It will not be necessary to write a detailed description of the apparatus, as conditions were kept, as far as possible, similar to those described by Gale and Whitney[1] in their study of the pole-effect.

Light source.—The arc was formed between two calcium electrodes 9 mm in diameter, arranged in a horizontal position within a closed steel chamber where the pressure could be varied by means of an ordinary oil pump. The pressure was changed from about 5 cm mercury as the lower pressure to atmospheric pressure as the higher pressure. If a greater value had been used, many of the most important lines, especially those of the first and second subordinate "triplet" series, would have become too broadened and diffuse for measurement. It was endeavored to maintain a constant length of arc of 4 mm. The positive pole was water-cooled and flat-faced, while the negative pole was rather sharply pointed. By this arrangement it was found possible to maintain a

[1] *Astrophysical Journal*, 44, 65, 1916.

fairly constant arc. Interruption would occur principally when, after operating for a time, the electrode surface became coated with a crusted formation of non-conducting oxide. This length of time depended more or less on the amount of air present and the success with which the action of the arc could be uniformly distributed over the surface of the electrode by the hand regulation of the arc. On some of the longer exposures it was necessary to open up the chamber one or more times during the course of the exposure to file off and clean the electrodes. The latter were sawed and machined out of very irregular chunks. The metal did not always seem to be of uniform consistency, and apparently this caused at times much fluctuation of the arc and rapid deterioration of the surface.

Source of current.—A 110-volt direct current was used to operate the arc. A suitable resistance was placed in the circuit to maintain a current of about 4 amperes.

Condensing system.—The quartz window in the pressure chamber and the quartz condensing lens made it possible to obtain all the desired lines between λ 6499.8 and λ 3158.9. By means of convenient regulations on the pressure chamber and condensing lens, the middle point of the arc image, enlarged four times, could be readily maintained on the slit.

Dispersing system.—The second-order spectrum of a 21.5-foot Rowland concave grating was employed. The scale was 1.32 A per mm.

Photographs.—The size of photographic plate used was 2×19 inches, a length great enough to cover about 600 A.

A large part of the work presented in this report was performed about three years ago, when it was almost impossible to get suitable materials. The war cut off completely the supply of extra-thin glass which had previously been used for these plates and which fitted so well the curvature of the plate-holder. The thinnest glass obtainable at this time was between 1/16 inch and 1/8 inch. Some of the plates could only be made to bend along the arc without breaking by slightly warming them and allowing each plate to rest on end supports with a suitable weight on the middle for a number of hours. This seemed to loosen up the glass structure

sufficiently to permit safely the necessary bending in the plate-holder. Films were used at the red end of the spectrum, but since the plate-holder was not made for films it was difficult to make them lie smoothly. If heavier celluloid could have been obtained, the films would have been very satisfactory. The occulting device described and used by Whitney[1] was employed in this work. Being mounted from the floor, it avoided any danger of mechanical shifts due to changing of the shutter. The latter was arranged so as to expose a middle strip upon the plate when in one position and a strip above and below when in the other position. The middle was generally exposed at the high pressure and the strip above and below at the low pressure.

Method of measurement.—The measurements of the shifts were obtained with a small comparator made by Wm. Gaertner & Co. A small candle-power incandescent lamp was arranged with a condensing lens to illuminate the field. This permitted a large increase of illumination of the field when necessary, with very little increase of the intensity of light about the room. A rheostat in circuit also permitted the adjustment of the intensity of illumination to any desirable degree.

It is well known by those working in this field that, because of the varying character of lines as well as incomplete and irregular photographic action, it is often necessary to study lines to a certain extent in order to determine their character, and that, on the other hand, looking at a line too long will fatigue the eye. Interposing a piece of green glass to give a green-colored field, especially with the more intense illuminations, was found of the greatest aid in reducing this fatigue.

Procedure.—In order to obtain a measure of any mechanical shift which might occur during any exposure, iron filings were imbedded in, or placed on the top edge of, the electrodes, and from the pressure-shifts of certain iron lines previously determined by Gale and Adams[2] the correction constant was determined. All mechanical shifts were measured by those iron lines which are classified by Gale and Adams[3] as class *a* lines. In a few instances

[1] *Astrophysical Journal*, **44**, 65, 1916.

[2] *Ibid.*, **35**, 10, 1912; **37**, 391, 1913.

[3] *Ibid.*

some class *b* lines were used as a double check on the mechanical shift, and in one instance a class *c* line. The measurements with these latter lines corroborated those of the *a* lines. Exposures of the whole photographic region were obtained by moving the camera to seven successive positions from the red to the violet, as will be observed in Table I. This allowed considerable overlapping of some regions, so that the correction constant from the iron lines could be applied to two adjacent regions, and afforded a double check on the mechanical shift.

TABLE I

	λ		λ
Region A	6500	to	5900
Region P	6150	to	5550
Region B	5857	to	5261
Region I	5270	to	4675
Region C	4725	to	4125
Region D	4175	to	3575
Region E	3725	to	3125

Exposures in regions A and P were made on Wratten and Wainwright "Panchromatic" films; in regions B, I, and C on Cramer "Inst. Iso"; and in regions D and E partly on Cramer "Crown" plates and partly on Seed 27 dry plates. Owing to the difficulty of obtaining sufficient quantities of plates, three or four exposures were usually made on one plate. Incomplete and irregular photographic action on many plates, even on the more intense exposures, seemed to indicate a poor grade of films. Difficulties were also experienced with faulty developers.

Results.—Table II gives the results obtained. All lines are grouped under two general divisions, the series and the non-series groups. The first column indicates the wave-lengths of the lines, and series designation, if any. The second column gives the shifts; the third, the number of plates measured; while the fourth column contains the average difference from the mean. The fifth shows the character of the broadening of the lines, as far as one could judge with a change of pressure of only one atmosphere. Unless there was a fairly definite indication of how the line broadens, it was marked "s," symmetrical. Only a few of the lines seemed

TABLE II*

	λ	Shift	Number	Average Difference	Broadening		λ	Shift	Number	Average Difference	Broadening
						Series Group					
p	6499.8.	.002	3	.001	s	$T1_4$	4456.1				
	6403.9	.001	4	.001	s		4454.9				
	6449.9.	.001	4	.001	s		4435.8	−.001	23	.001	uv
	4302.6.	.000	4	.001	s		4435.1				
	4283.1.	−.001	4	.001	s		4425.6				
SL_2	5041.0.	.015	4	.001	ur	$T1_5$	3644.8				
	4527.1.	.027	11	.002	ur		3644.5				
	4240.5†						3631.1	−.029	24	.002	uv
SL_3	4878.3.	.031	7	.003	ur		3630.8				
	4355.4.	.068	6	.010	ur		3624.1				
t_4	4586.1	.030	21	.002	ur	$T1_6$	3361.9	−.054	12	.008	uv
	4581.6						3350.2				
	4578.8						3344.4				
t_5	4098.6	.044	16	.003	ur	$T2_3$	6162.4	.012	19	.002	s
	4095.0						6122.4				
	4092.7						6102.9				
T	4318.8.	−.001	4	.001	uv	$T2_4$	3973.8	.016	18	.003	ur
	4299.1.	−.001	4	.001	uv		3957.2				
	4289.5.	.000	4	.001	uv		3949.1				
P_2	3737.1	.008	14	.001	sh	$T2_5$	3487.7	.041	11	.005	ur
	3706.1						3474.9				
							3468.6				
P_1	3181.4.	.013	5	.001	ur	$T2_6$	3286.2	.046	6	.007	ur
	3179.4.	.013	4	.001	ur		3274.8				
	3158.9.	.014	3	.001	ur		3269.3				
H	3968.6.	.001	8	.001	Rs						
K	3933.8.	.001	8	.001	Rs						
						Non-Series Group					
	6471.8.	.002	4	.001	s		5513.1..	−.023	6	.003	uv
	6462.7.	.001	4	.001	s		5349.6..	.005	7	.001	sh
	6439.3.	.001	4	.001	s		5270.4..	.004	5	.001	sh
	6169.8.	.012	4	.002	s		5265.7..	.003	9	.001	sh
	6169.3.	.013	3	.002	s		5264.4..	.010	6	.001	sh
	5857.7.	.022	5	.002	ur		5262.4..	.010	5	.001	sh
	5603.1.	.006	12	.002	s		5261.9..	.011	6	.001	sh
	5601.1.	.006	12	.001	s		5189.0..	−.003	7	.001	uv
	5598.6.	.003	4	.001	s		4685.4..	−.009	6	.001	uv
	5594.6.	.007	4	.002	s		4307.9..	−.001	4	.001	uv
	5590.3.	.005	10	.001	s		4240.5..				
	5588.9.	.005	5	.003	s		4226.9..	.018	7	.002	Rs
	5582.1.	.005	10	.001	s						

*The wave-lengths and series designations are from Kayser's *Handbuch*, for ease of comparison with Whitney's tables for pole-effect for these same lines. See Gale and Miller, *Physical Review*, **17**, 428, 1921.

†λ 4240.5 was masked by λ 4226.9.

to retain their sharpness more than the others and these are marked "sh." Unsymmetrical broadening to the red or to the violet is designated respectively by "ur" and "uv." Only three lines are reversed with increase of pressure, and they remained symmetrical. These are marked "Rs."

The results were arranged at first according to the order of the wave-lengths of the lines measured. Although there seems to be in general an increase in the magnitude of the pressure-shifts as one proceeds toward the shorter wave-lengths, there are so many exceptions that we cannot as yet see any definite law. The same thing is true in regard to the broadening of the lines.

It is only when the results are arranged according to the series grouping of the lines that the observations take on a more definite character. Royds,[1] in his discussion on the different character of spectrum lines belonging to the same series, raised the question whether calcium would act like iron in that the unsymmetrical widening and pressure-shift both take place in the same direction. It will be observed from Table II that the first subordinate "triplet" series in calcium is unsymmetrically broadened toward the violet and the pressure-shift is toward the violet. In the second subordinate "triplet" series and also in the Fowler series t_4 and t_5 the unsymmetrical broadening is toward the red and the pressure-shift is toward the red.

Royds also raised the question, as suggested by Moore,[2] whether the Fowler series would have practically zero shift because the Zeeman effect was approximately zero, or whether there would be a large shift because the lines of this series are susceptible to density effects. The latter seems to be the case.

Royds[3] also points out in his paper that lines in the same series may have entirely opposite characteristics in one part compared with the lines in another part. Thus in the first subordinate "triplet" series of barium, lines 5819, 5800, 5777, 5536, 5519, and 5424 broaden and shift to the red, while lines 4493, 4489, 4393, 4323, and 4264 broaden and shift to the violet. The same change of characteristics appears possible in the first and second

[1] *Astrophysical Journal*, 41, 154, 1915.

[2] *Ibid.*, 33, 385, 1911.

[3] *Ibid.*, 41, 154, 1915.

subordinate "triplet" series of calcium. As one proceeds from the shorter wave-lengths to the longer, the broadening and shifts decrease, and if these quantities could be measured for the lower members in the infra-red, it appears that they would be in the opposite direction. There are strong indications that this is true at least in the first subordinate series.

There are only a few lines which seem to tend to retain their sharpness more than the others as the pressure increases; they are the lines from λ 5270.4 to λ 5261.9 and the lines λ 3737.1 and λ 3706.1 (P_2 series).

Only three lines showed reversals in this work, the H and K lines and λ 4226.9. There are many lines marked "s" which would undoubtedly show unsymmetrical broadening with greater increase of pressure, but it was not perceptible within the limits here used.

I wish to express my appreciation to the members of the Department of Physics of the University of Chicago for their aid and interest, especially Dr. Gale, who suggested this problem. I am also very grateful to the Department of Physics of the University of Nebraska for the loan of their comparator, with which most of the measurements were made.

University of Chicago
September 1920

PREPARATION OF ABSTRACTS

Every article in the *Astrophysical Journal*, however short, is to be preceded by an abstract which should be submitted by the author with the manuscript. In order that the abstract may aid the reader by furnishing an index and brief summary of the contents of the article, and may also be suitable for reprinting in an abstract journal, it should be of the type of those which have been appearing in the *Astrophysical Journal* during 1920. It is requested that the abstracts be prepared in accordance with the following:

DIRECTIONS AND RULES

1. *Notes.*—Read the article carefully, taking rough notes covering all the new information reported, keeping a specially sharp lookout for new incidental results and suggestions not directly related to the main subject.

Material not new need not be described; a valuable summary of previous work, however, should be noted.

2. *Subtitles.*—Write, first, a title describing the group of results forming the main contribution of the article, including all that belong together. If there are in addition results which do not come under that title, gather them into as few groups as possible and formulate a complete and precise title for each. For examples of such subtitles see the italicized parts of the abstracts for 1920.

Each subtitle should describe the corresponding information so precisely that the chance of any investigator being misled into thinking the article contains the particular information he desires when it does not, or vice versa, may be small. "Zeeman effect for metallic furnace spectra" is too broad unless all metals have been studied, for an investigator may be interested at the time, in only one metal; but "Infra-red arc spectrum of iron to 3μ" evidently satisfies this rule.

In general a subtitle is sufficiently precise if it carries the classification of the information three stages or the equivalent, for instance if it gives (*a*) the elements and substances, (*b*) the property, and (*c*) the phase or range studied.

The subtitles should together form a complete index of the new information; that is they should include every measurement, observation, method, suggestion, and theory which is presented as new and of value in itself. They should be complete in themselves and independent of the main title of the article.

3. *Text.*—Write a paragraph summarizing the main group of results and including the corresponding subtitle either all at the beginning or with parts scattered through the text; and then do likewise for the other groups.

[1] The rules and illustrative abstracts were prepared by G. S. Fulcher, chiefly while associated with the National Research Council.

A separate paragraph should be used for each distinct subject involved, but no more than necessary. All material which can easily be grouped together under a single title should be summarized in the same paragraph. Parts of subtitles may be scattered through the text, but the subject of each paragraph must be given at the beginning. Italicize subtitles but no other words or phrases.

The text should summarize the author's conclusions and should transcribe all numerical results of general interest, including all that might be looked for in a table of astronomical and physical constants, with an indication of the accuracy of each. It should give all the information that anyone, not a specialist in the particular field involved, might care to have in his notebook.

Complete sentences should be used except in the case of subtitles. The abstract should be made as readable as the necessary brevity will permit.

4. *Final checking.*—Re-read the article so as to check the abstract and correct any omissions and mistakes; read the subtitles by themselves to see that they properly index the information; and read the abstract to see whether it cannot be condensed and its English be improved.



SIR NORMAN LOCKYER
From a photograph taken in 1903

THE
ASTROPHYSICAL JOURNAL
AN INTERNATIONAL REVIEW OF SPECTROSCOPY
AND ASTRONOMICAL PHYSICS

VOLUME LIII MAY 1921 NUMBER 4

SIR NORMAN LOCKYER, 1836–1920

By A. L. CORTIE, S.J.

Among the names of those who laid the foundations of that branch of astronomical science, which dealing mainly with the constitution of the heavenly bodies is known as astrophysics, a prominent place will always be held by that of Norman Lockyer. He was one of the pioneers in the application of the spectroscope to the study of the solar surface and envelopes, and in the detailed examination of the spectra of the stars. He made fundamental discoveries, especially in solar physics, and he developed modes and methods of research which have subsisted even to the present day. The enunciation by Kirchhoff in 1859, of the principle underlying the reversal of the Fraunhofer rays in the solar spectrum, was an opportunity and an incentive to discovery offered to all astronomers. Lockyer was one of the very few to appreciate what a vast field lay open in the domain of the physics of the heavenly bodies, and with enthusiasm and energy, with native skill and great courage, he entered into his labors. We must not forget that before he was subsidized by the government, and established as an official astronomer, Lockyer was an amateur, and as such a worthy representative of the long line of amateur astronomers who, especially in England, have done yeoman service in the advance of the science. He took to astronomy because he loved it, and because of the appeal it made to his intellectual faculties. It was in his leisure hours, when freed from the daily toil which was his lot as a

secretary in the war office, that Lockyer helped to lay the solid foundations of the science of astrophysics.

He was born at Rugby May 17, 1836, and died at the Hill Observatory, Sidmouth, August 17, 1920. He had therefore completed his eighty-fourth year. Janssen, whose name will ever be associated in the history of astrophysical science with that of Lockyer, died in 1907, and was in his eighty-fourth year. Lockyer received his first lessons in science from his father, who was one of the early workers in research with regard to the electric telegraph. He was educated at various private schools and on the Continent. This was fortunate, for had he been educated at any of the public schools, or universities, he would have been taught very little, if any, science, and had he taken up the career of an astronomer, he would doubtless have been absorbed in the rank and file of those who followed the traditional, and in those days somewhat narrow, grooves. But he possessed independence of mind, resourcefulness, adaptability, and moreover, as an amateur, was at liberty to select his own field for work. In the year 1857 he received an appointment as a clerk in the war office, and his work there was so much appreciated that in 1865 he was selected to edit the Army Regulations. In 1870 he was made secretary of the Duke of Devonshire's Royal Commission on Science. This important post he owed not only to his proved business capacity but also to the fame which he had already acquired by his great discovery of the year 1868. When this Commission had finished its labors, he was transferred to the Science and Art Department, and became definitely an official astronomer, or rather a government servant devoted to research in the domain of astrophysics. But only partially, for his official duties still included the organization of the loan collection of scientific apparatus and of the Science Museum, which was subsequently founded, as well as the inspection of training colleges.

In 1862 Lockyer was living at Wimbledon and had erected, in a garden in front of his house, a $6\frac{1}{4}$-inch equatorial by Cooke of York. With this instrument he observed the opposition of Mars of that year, and communicated an account of his observations, which seems to have been his first scientific paper, to the Royal Astronomical Society.

He was first interested in the sun by the warm controversy as to the nature of the constituents of the solar surface which Secchi and Langley rightly described as granular, but which Nasmyth had likened to willow leaves. Lockyer took part in the discussion and contributed a paper on the subject to the Royal Astronomical Society. He noticed in particular the changing forms of these elemental constituents of the solar photosphere.

Similarly, it was the publication of Faye's theory of sun-spots in the year 1865 which suggested to Lockyer that the question as to the nature of sun-spots could best be solved by the application of the spectroscope. Accordingly he purchased a direct-vision Herschel-Browning spectroscope of small dispersion, and attaching it to his equatorial threw the image of a spot on the slit. The absorption lines visible in the spectrum of the photosphere were present in that of the spot, but in some cases were widened in the spot. It followed therefore that a sun-spot was seemingly a region of increased absorption.

These preliminary spectroscopic observations of the sun-spots whetted the appetite of Lockyer to explore the solar envelopes, and in particular to determine the precise nature of the solar flames photographed by De la Rue and Secchi in the total solar eclipse of 1860. In this important matter in the history of solar spectroscopy it will be better to quote Lockyer's own words as set forth in a "Memorandum on the Solar Researches Carried on by Sir Norman Lockyer 1863–1906," which was privately printed in London, 1906. He writes:

> Talking these matters over with Balfour Stewart, we came to the conclusion that it could help us in other ways, because, if the objects photographed by De la Rue in 1860 were gases or vapors, their bright lines ought to be revealed when a large dispersion was used, although I had failed to trace them with a small one. As great dispersion was required both for the spectra of the "red flames," and for settling the question raised by the widening of lines in spots, when my paper of 1866 was sent in to the Royal Society, I made my first application to the Government Grant Committee for money to provide a solar spectroscope of large dispersion to attach to the equatorial. The grant was approved; but, in consequence of delays, the instrument did not reach me till October, 1868, by which time I had changed my residence from Wimbledon to 24 Fairfax Road, West Hampstead, where I had built an observatory, the 6¼-inch Cooke being still the instrument used.

On October 20, 1868, I saw the bright lines, as I had anticipated in 1866. On November 5 I discovered that the prominences were but higher waves in a sea which enveloped the photosphere. This new envelope I named the chromosphere.

But Lockyer had been anticipated in the observation of the bright lines of the chromosphere and prominences, independently, and unknown at the time, by Janssen, who had observed the bright-line spectrum of the prominences in the total solar eclipse of August 18 at Guntoor, in India. So vivid were these lines that they had forced Janssen to exclaim, "Je verrai ces lignes-là en dehors des éclipses!" Next day and for several days he carried out his intention and succeeded, as he had intuitively anticipated, in viewing the bright hydrogen and helium lines even on the uneclipsed sun. Janssen sent a communication on the subject to the Academy of Sciences in Paris. By a dramatic coincidence it arrived in time to be read at the same session, on October 26, as Lockyer's account of his success in viewing the spectrum of the prominences, which had also been sent to the Academy. The two names are indissolubly united in this discovery of prime importance in solar physics. The Academy of Sciences to commemorate the discovery caused a medal to be struck which bears the effigies both of Janssen and of Lockyer.

In the dedication of the papers collected together in his work *Solar Physics* Lockyer wrote:

> This book is dedicated to Balfour Stewart and to Jules Janssen. Encouraged by the first of these friends, I have undertaken the researches which have gained me the friendship of the second.

There is no sign here of petty jealousy, or of stupid claims of priority. In the year 1870, when Paris was besieged by the Germans, Lockyer by his kindly intervention obtained a safe conduct for his friend, so that he might be able to observe the total solar eclipse of that year. But Janssen spurned the idea of receiving any favors from the enemies of his country, and preferred to leave the beleaguered city in a balloon. Those of us who attended the meetings of the International Union for Co-operation in Solar Research at Meudon, in 1907, will remember the large painting of this episode which was hung in the room in which we gathered for our discussions.

This important discovery created great enthusiasm among astronomers, and undoubtedly promoted throughout the whole world the foundation of observatories devoted especially to solar research. Lockyer was quick to perceive that, in order to ascertain the origin and character of the bright lines he had observed in the prominences, it would be necessary to compare the celestial with terrestrial sources of light. He was fortunate in obtaining the co-operation of Professor Frankland, and together they made experiments upon hydrogen, sodium, iodine, under various conditions of pressure and of temperature. He soon recognized as the results of these experiments that the yellow line in the chromosphere and prominences could not be due to hydrogen or to sodium. It therefore represented an unknown element which he named "helium." It was not until twenty-seven years later that Sir William Ramsay detected helium in the mineral cleveite and in some of the gases which are given off from terrestrial waters. We also know now that it is an emanation from radium, and it plays a most important part in all questions concerning the constitution of matter.

Lockyer's activities at this period were also directed to the observation of total solar eclipses in Sicily in 1870, and in India in 1871. On the first occasion he was balked by clouds, but in 1871 he was successful and, with Respighi, employed for the first time in eclipses the prismatic camera, an instrument which had been so successful in the hands of Secchi in furnishing the various types of stellar spectra. Although the prismatic camera does not give the exact wave-length of the lines of the chromospheric spectrum, for this purpose a slit spectroscope and a reference spectrum is needed, yet it has the advantage of showing spectral images of the radiations as bright arcs, the extent of the arc in angle being a function of the height to which the metallic vapor ascends in the sun's atmosphere. It was certainly a brilliant idea to adopt the instrument for studying the bright lines in total solar eclipses.

Lockyer may also be credited with being the first to realize the necessity of combining laboratory researches with the observation of the spectra of the heavenly bodies. By the year 1872

he had accumulated a considerable number of observations of the lines in the chromosphere. He had also, by his studies of the hydrogen spectrum with Frankland, come to the conclusion that the arrow-head appearance of the F line in the chromosphere was due to pressure. He would therefore undertake a research on the spectra of the metallic elements under varying conditions of temperature and of pressure. Accordingly, aided by a government grant, he set up a laboratory in his private house and engaged the services of an assistant. In the year 1873 his instruments, astronomical and physical, were moved to South Kensington and erected in temporary wood and canvas observatories in the garden of the Royal Horticultural Society. A sapper, when not otherwise engaged, was told off as his photographic assistant. Here we have the prototype and the germ idea, which has fructified in such a magnificent modern astrophysical observatory as that of Mount Wilson.

Lockyer had been elected a Fellow of the Royal Society in the year 1869, and his contributions to its *Proceedings* and *Transactions* on his researches in spectrum analysis in connection with the sun were numerous, original, and important. In his photographs of the metallic spectra he had detected the difference between long and short lines, the thickening and thinning of lines with pressure, the variation in length, brightness, strength, and number of lines, and the change in general produced by variations in temperature. He had made a photographic map of the solar spectrum between wave-lengths 3900 and 4100 on a scale four times that of Angstrom's map, and had plotted on it the comparison with lines of iron, calcium, magnesium, nickel, and other elements. Meanwhile he had continued his systematic observation of the solar prominences, employing a seeing-slit, had discovered the metalloids carbon and silicon in the sun, and had been the first to recognize that the displacements of the spectral rays in the spectrum of the prominences were due to radial movements in the gases. This he rightly attributed to the Doppler-Fizeau principle, which was then little known. He was the first also in showing that the coronal ring at the wave-length 5303, then known as K 1474, from the position

it occupied in Kirchhoff's maps, was coterminous with the lower corona. His photographs also gave detailed knowledge of the spectrum of the lowest layers of the solar atmosphere, the so-called "flash" spectrum, which is only visible in the first two and last two seconds of totality in total solar eclipses.

It was not until the year 1879 that a Solar Physics Observatory was definitely established at South Kensington, and a committee appointed "to advise on the methods of carrying on observations on solar physics." Lockyer was of course the dominating personality of this committee, and was practically free to carry on any researches he considered to be advisable. The next year he was directed to give a course of lectures on astronomical physics to the students of the science school, and in 1882 was appointed full professor. In this capacity he inaugurated a course of practical training in the use of instruments, which eventuated in the increase of his observatory staff by the inclusion of research students. Thus Professor Fowler joined the staff in this capacity in 1885, and became Lockyer's demonstrator in 1888. The grant in aid at this time was £500 annually, which was increased in 1898 to £1,000.

It is wonderful what Lockyer effected on such an inadequate pittance. But he had inspired his staff with some of his own enthusiasm and spirit of hard work, and a series of memoirs appeared under the auspices of the Solar Physics Committee which are indispensable to all workers in astrophysics, and are models of accurate research. One of the most important of these researches was that which was concerned with the differences in the radiations given by an element according to its vaporization by the flame, the electric arc, or the electric spark. In particular he drew the important distinction between the lines which appear in the arc alone and those which are strengthened in passing from the excitation of the arc to that of the spark. The latter lines he named "enhanced" lines, and their importance in all questions of solar and stellar physics is paramount. They are for instance the characteristic lines of the "flash" and chromospheric spectra, and are prominent in the early spectral phases of new stars.

As we have seen, Lockyer's very first observations of the solar surface with the spectroscope were those of sun-spots. At South Kensington a very long series of observations, extending over many years, were undertaken under his direction on not the widest but the six most widened lines in each of the regions F–*b* and *b*–D. From the reduction of these observations he found that the lines widened in sun-spots were not common to spots and prominences, and that lines of the prominence, at least those produced in the lower strata, were precisely those which are intensified in passing from the arc to the spark. Lockyer also announced that the lines most affected in sun-spots at the times of solar maxima were the fainter lines, while those similarly most prominent at solar minima were the stronger lines. He connected this periodic variation with the prevalence of the monsoons in the Indian Ocean, and consequently with the years of plenty and of famine. But about the same time (1881) we at Stonyhurst, as a supplement to these investigations, took up the systematic observation of the most widened lines, and of all the lines in the region C–D. It was very soon evident that the sun-spot spectrum was constant, with practically no variation, though there was some evidence of stronger iron lines being found among the most widened lines at times of sun-spot minimum. In their later publications on this subject the South Kensington observers adopted the same view, and more than thirty years' observations have convinced me that the sun-spot spectrum is essentially constant. The great predominance of the fainter lines of the elements among the most widened lines, and especially of those of titanium and vanadium, were concomitantly and independently observed both at South Kensington and at Stonyhurst. Such observations were preliminary to the magnificent map of the sun-spot spectrum produced by Hale at Mount Wilson, and to the solution of the appearance of widening as due to the magnetic fields of sun-spots, as also to Fowler's identification of the spot-bands as being due to titanium oxide. With regard to sun-spots also, the areas of all such, in the period 1832–1900, from all available sources, were utilized to form curves, which were issued as one of the publications from South Kensington.

Lockyer directed no less than eight expeditions to observe total eclipses of the sun. In fact so predominant was his influence and strong personality in these expeditions that one of his friends, we think it was Clerk-Maxwell, good-naturedly lampooned him in the following humorous couplets:

> And Lockyer, and Lockyer,
> Gets cockier, and cockier;
>
> For he thinks he's the owner
> Of the solar corona.

In several of those which occurred in distant regions he had the service of a war vessel and its crew placed at his disposal by the Admiralty. He had unbounded faith, and rightly so, as we have ourselves experienced, in the adaptability and proverbial readiness of the "handy man." Accordingly he would train quite a number of officers and men to take part, under himself and his immediate assistants, not only in the astronomical observations, but in all sorts of incidental meteorological and kindred observations. He united enthusiasm with great orderliness and method. Each time he took part in an eclipse expedition he made the previous observations serve as the foundation of further researches. With the prismatic camera, for instance, he felt his way, and increased the dispersion at each succeeding eclipse. He has produced a series of most valuable memoirs of his observations, especially noteworthy being the chromospheric reductions in the Indian eclipse of 1898, when he had Fowler as his assistant. He also obtained important results of permanent value on the varying forms and on the constituents of the sun's corona.

Although observation and experiment are the sure basis and foundation of natural science, yet its chief end and function is the search for the causes of phenomena. Hence we find in the progress of all science that working hypotheses are broached which strive to co-ordinate all the knowledge so far acquired and to point the way to fresh observation and experiment. Most of these are discarded as scientific knowledge advances to be replaced by others of more far-reaching import. But not wholly discarded, for in a good hypothesis many of the root or germ ideas survive.

The various changes noticed in the spectra of the elements under varying conditions of temperature, pressure, and electrical excitation, in experiments in the laboratory, had suggested to him the idea that either the high temperatures, or the electric stresses employed, were breaking up the substances into various "molecular groupings." With regard to the sun, the hypothesis enunciated supposed that, at the high temperatures prevailing in the photosphere and the lower reaches of the overlying envelopes, the chemical elements were broken up or dissociated. Accordingly, if the elements as known to us exist at all in the sun, they are found only in the higher or relatively cooler layers of its atmosphere. Vertical currents bring down the formed material to be dissociated in the lower reaches. Hence reduced in density it reascends to become formed material again in the appropriate heat level. The hypothesis is worked out fully in his work on *The Chemistry of the Sun*. The fundamental idea, that of dissociation of the chemical elements, subsists, whatever may be thought of the details of his scheme, and at present in the electronic theory as to the constitution of the elements is of very great importance.

In his studies in solar physics Lockyer was naturally led to investigate the connections which may possibly exist between solar and terrestrial phenomena. As early as 1872 he published a paper on the relation between sun-spots and meteorology in which he endeavored to show that a relation exists between the sun-spots and the cycle of monsoons. Thirty years later, in conjunction with his son, Major J. W. S. Lockyer, he returned to the same subject. Having detected in the solar prominences a period of about 3.8 years, he showed that this period coincided with a similar periodic intensification of both high- and low-pressure means for India and Cordoba, and that pressure changes respond more quickly to solar influence than does rainfall. He next extended the investigation to the Pacific Archipelago and to Australia, and showed that the connection was substantiated. A corresponding area in America gave inverse action like Cordoba. Finally, these short-period variations of atmospheric pressure, which he assimilated to the Bombay-Cordoba "seesaw," appeared to be prevalent at numerous stations scattered all over the world.

If this oscillation of terrestrial pressure types can be connected with periodicity in the prominences, a means is afforded of long-period weather forecasting. Certainly the general law of the circulation of winds in the Southern Hemisphere, which was established by the Lockyers in this series of memoirs, has been verified, and is now admitted by many meteorologists.

Concomitantly with these researches, the solar prominence and spot circulation for the period 1872–1901 was studied by father and son. It was established that the prominences show a poleward drift, that at prominence minima there is only one zone, in contradistinction to the sun-spots which affect two zones, though the subsidiary maxima were coincident in time with two zones of prominences. This led them to investigate the relation between solar prominences and terrestrial magnetism. It was found that polar prominences follow a different law from equatorial prominences, and that while diurnal magnetic variations seemed to be in agreement with the equatorial prominences, great magnetic storms vary with polar prominences. The seasonal variation in the frequency of magnetic storms, the minima occurring near the equinoxes, was attributed to the position of the sun's axis relatively to the earth. But we think that in so far as metallic prominences are connected with sun-spots, it is only incidentally that prominences are associated with magnetic disturbance. Otherwise there does not seem to be any link between the two phenomena. It is quite true, however, that magnetic disturbances are more frequent when the heliocentric position of the earth is in the semi-equatorial solar regions.

It was not until the year 1890 that Sir Norman Lockyer extended his researches so as to include observations of the spectra of nebulae and stars. He began with the spectrum of the nebula in Orion, of which, with a two-prism spectroscope attached to the 30-inch reflector, he obtained a photograph showing twenty-eight, and later over forty, lines, some of which he noted as coincident with the chief bright lines in the star P Cygni. Comet *a* (1890) and Nova Aurigae (1892) next attracted his attention, and in the latter year he published a discussion of 443 photographs of the spectra of 171 stars taken chiefly with a 6-inch prismatic camera, furnished

with objective prisms of $7\frac{1}{2}^{\circ}$ and 45° angle. The paper contained a classification of the stars based on the extent of the absorption in the ultra-violet. It is noteworthy from the fact that he divided the stars, on a temperature basis, into two main groups of ascending and descending stars. It will not be necessary to discuss in detail his observations of the spectra of other stars, as β Lyrae, γ Cassiopeiae, α Aquilae, Nova Persei, in which he had the expert assistance of Professor Fowler and Mr. F. E. Baxandall. Several of the memoirs issued under the auspices of the Solar Physics Committee contain most valuable detailed lists of lines observed in the spectra of stars, and, what is most valuable, corresponding lists of the chemical origins of the lines. In particular we may mention the catalogue of four hundred and seventy of the brighter stars classified according to their chemistry, the memoir on some of the phenomena of new stars, and, as an associated laboratory research, the tables of wave-lengths of the enhanced lines.

For more than thirty years Lockyer's researches and studies were directed to the classification of the stars according to their spectra. Some of the last bulletins he issued from the Hill Observatory, near Sidmouth, were devoted to the same subject. The root idea of his classification as it had been in his studies of the solar spectrum, in the photosphere, spots, reversing-layer, and prominences, was that of the dissociation of the elements at high temperatures. He maintained that the process of stellar evolution is not merely a cooling process, but that there are many stars which are rising in temperature, as well as those which are cooling. The sun and the stars are mainly gaseous bodies, and in such bodies, so long as the density of the gaseous mass remains low, there must be a rise in effective temperature as condensation proceeds. The gaseous mass loses energy by radiation of light and heat at its surface. The process will go on until the condensation has reached such a stage that no longer is radiation at its surface compensated for by the contraction of the body on its center. It will then cool rapidly. This seemingly paradoxical law, that cooling bodies rise in temperature until they cease to be wholly gaseous, was first enunciated by J. Homer Lane, of Washington, in 1892, and has been developed by Ritter. Sir Norman Lockyer starts with

the assumption that a nebula is a swarm of meteorites at a low temperature. This fundamental assumption is negatived by modern spectroscopic studies, such for instance as those made at the Lick Observatory. As condensation proceeds, the temperature of the bodies formed from the nebula, says Lockyer, rises, with a corresponding change in the spectrum, until the highest temperature is reached. We thus have stars with fluted spectra, metallic stars, proto-metallic stars, when dissociation takes place, cleveite-gas stars, and proto-hydrogen stars. Then follow the changes, in reverse order, in the spectra, as the cooling bodies lose temperature by radiation at their surfaces in excess of that gained by condensation. There are therefore two arms to Lockyer's "temperature curve," the one an ascending arm and the other a descending arm. According to this theory, stars of class M are placed on the ascending arm, immediately above the nebulae, and the stars of class N, showing the carbon absorption, immediately following the sun, on the descending arm. The discrimination of stars at higher temperatures into groups of ascending temperature, and groups of cooling stars, is founded upon the appearance of arc and spark lines in the respective spectra in varying intensities. This is the criterion that is employed by W. S. Adams in his spectroscopic determinations of stellar parallaxes. In Lockyer's classification of the stars, those on the ascending branch of the curve differ from those on the descending branch at the same temperature, because the hydrogen lines are thinner and the metallic lines more intense as compared with the same lines in the spectra of stars on the descending branch.

Lockyer labeled his classes of stars by the names of representative stars in the different classes. Thus after the condensing nebula we have the Antarian, Aldebarian, Polarian, Cygnian, Rigelian, Taurian, and Crucian stars. At the summit of the curve stand the Alnitamian and Argonian classes. On the descending arm come in order Achernarian, Algolian, Markabian, Sirian, Procyonian, Arcturian, and Piscian stars. This order would correspond to M, K_5, G, F, A_2, B8, B_3, B_2 ascending; B, O, at the summit; and B_5, B8, A, F_5, G, K, N descending, on the Harvard system of classification.

The central idea of Lockyer's hypothesis has been rejuvenated and modified by Henry Norris Russell, although the data upon which his arrangement rests are derived from the absolute magnitudes, the masses, and the densities of the stars. It agrees, too, with Lockyer's system in making the B class of stars a class apart at the summit of the curve. But the discrimination of the K and M stars into "giants" and "dwarfs" is a profound modification of Lockyer's scheme, in which all the stars of the M class are in an early stage of development. In Russell's classification the "giants" are in an early stage and the "dwarfs" in a late stage. The difference in luminosity is attributed to a difference in volume or size, which means a difference in density, and also to differences in surface brightness.

Lockyer's observations, researches, and theories are summarized in two works, the *Meteoritic Hypothesis* (1890) and *Inorganic Evolution* (1900). These embody an attempt to bring all the known phenomena of the heavens under one category. Nebulae, comets, new stars, variable stars, are all supposed to be due to the clash of meteor streams, from the condensation of which come stars and suns. It was a bold and masterly piece of theorizing. Although there is no chance of its being generally accepted, it contained, as we have seen, many fundamental ideas of modern physics, it evoked much criticism, and acted as an incentive to research.

Our main theme has been the research work of Lockyer in the domain of solar and stellar physics. We can but briefly mention some of his numerous other activities. In 1869 he founded the weekly scientific journal *Nature*, which is the leading journal of the sort probably in the world, and has secured an international circulation. It is in fact indispensable to the scientific worker. For fifty years Sir Norman Lockyer was its editor, ably assisted in later years by the present editor, Sir Richard Gregory. Its form has been practically unmodified from its foundation.

In 1894, as the result of a visit to Egypt, Lockyer became interested in the orientation of temples and their astronomical significance in connection with the heliacal risings and settings of the stars. On returning to England, he extended his researches so

as to embrace the stone circle at Stonehenge. His work, *The Dawn of Astronomy*, contains the results of his measures and of the conclusions he deduces from them.

In 1903–1904, Lockyer was president of the British Association and delivered a stirring address on "The Influence of Brain Power on History." His plea was for the foundation of more national universities, and the address produced a great impression. It eventuated in the foundation of the British Science Guild, for the furtherance of scientific interests, political and social. He became president of the Guild in 1912.

Lockyer was initiated into the game of golf by Professor Tait, who had also suggested to him originally the first ideas of his meteoritic hypothesis. Tait, it is related, once worked out by rigid dynamics the maximum flight of a golf ball when driven from the tee. Next morning his son, Freddy, who was one of the greatest exponents of the game, went out to the links and drove a ball a few yards farther than the range calculated by his father. Lockyer, with his customary enthusiasm in every subject he took up, revised the rules of golf, and published his revision in book form in 1896. This revision had not a little to do with the form of the rules as subsequently adopted at St. Andrews.

Among Lockyer's closest friends was the eminent poet, Sir Alfred Tennyson. Accordingly in a book written in 1910, in conjunction with his daughter, on *Tennyson as a Student and Poet of Nature*, he collected all passages in the poems which dwelt with the scientific aspects of natural phenomena.

In 1913 it was decided to move the Solar Physics Observatory from South Kensington, as the site was required for other buildings in connection with the departments of science and art. Lockyer advocated a hill site, at Salcombe Regis, near Sidmouth, which undoubtedly possesses great advantages in suitability of climate. But the committee to which the matter was referred decided that the observatory should be transferred to Cambridge, and thus be attached to the university. Although Lockyer was an old man, this decision undoubtedly helped to break him up. But with indomitable pluck and admirable courage, he would start the Hill Observatory, as a separate establishment, under its own

corporation. This he succeeded in doing, and he leaves it in a flourishing condition.

Sir Norman Lockyer, created K.C.B. in 1897, died full of academic and scientific honors. He was LL.D. of Aberdeen, Edinburgh, and Glasgow universities, Sc.D. of Cambridge, D.Sc. of Oxford and Sheffield. In 1875 he received the Janssen Medal of the Paris Academy of Sciences, and was elected a corresponding member. From the Royal Society he received the Rumford Medal. He was also an honorary member of the American Academy of Arts and Sciences, and of numerous other foreign academies and societies. He married twice, first Winifred, daughter of Mr. William James, of Trebinshon, near Abergavenny, who died in 1879, and secondly in 1903 Mrs. Bernard E. Broadhurst, daughter of the late Mr. S. E. Browne, of Bridgewater and Clifton. He had four sons and two daughters.

Stonyhurst College
December 28, 1920

MEASUREMENT OF THE DIAMETER OF α ORIONIS WITH THE INTERFEROMETER[1]

By A. A. MICHELSON and F. G. PEASE

ABSTRACT

Twenty-foot interferometer for measuring minute angles.—Since pencils of rays at least 10 feet apart must be used to measure the diameters of even the largest stars, and because the interferometer results obtained with the 100-inch reflector were so encouraging, the construction of a 20-foot interferometer was undertaken. A very rigid beam made of structural steel was mounted on the end of the Cassegrain cage, and four 6-inch mirrors were mounted on it so as to reduce the separation of the pencils to 45 inches and enable them to be brought to accurate coincidence by the telescope. The methods of making the fine adjustments necessary are described, including the use of two thin wedges of glass to vary continuously the equivalent air-path of one pencil. Sharp fringes were obtained with this instrument in August, 1920.

Diameter of α Orionis.—Although the interferometer was not yet provided with means for continuously altering the distance between the pencils used, some observations were made on this star, which was known to be very large. On December 13, 1920, with very good seeing, no fringes could be found when the separation of the pencils was 121 inches, although tests on other stars showed the instrument to be in perfect adjustment. This separation for minimum visibility gives the angular diameter as 0″.047 within 10 per cent, assuming the disk of the star uniformly luminous. Hence, taking the parallax as 0″.018, the linear diameter comes out 240×10^6 miles.

Interferometer method of determining the distribution of luminosity on a stellar disk.—The variation of intensity of the interference fringes with the separation of the two pencils depends not only on the angular diameter of the disk but also on the distribution of luminosity. The theory is developed for the case in which $I = I_0 (R^2 - r^2)^n$, and formulae are given for determining n from observations.

Table of values of $\int_0^1 (1-x^2)^{n+\frac{1}{2}} \cos kx\, dx$, for n equal to 0, $\frac{1}{2}$, 1, and 2, and for k up to 600°, is given.

It was shown in *Contributions* Nos. 184 and 185,[2] that the application of interference methods to astronomical measurements is not seriously affected by atmospheric disturbances, and indeed observations by these methods have proved feasible even when the seeing was very poor. The explanation of this apparent paradox lies in the fact that when the whole objective is effective, the atmospheric disturbances, being irregularly distributed over the surface, simply blur the diffraction pattern; but in the case of two isolated pencils too small to be affected by such an integrated disturbance, the resulting interference fringes, though in motion,

[1] *Contributions from the Mount Wilson Observatory*, No. 203.

[2] *Astrophysical Journal*, 51, 257, 263, 1920.

are quite distinct, unless the period of the disturbances is too rapid for the eye to follow.

When it was found that the interference fringes remain at full visibility with the slits separated by the diameter of the 100-inch mirror, it was decided to build an interferometer with movable outer mirrors (Fig. 1) in order to make tests with separations as great as 20 feet.

The interferometer beam (Plate IV*a* and Fig. 2) was made of structural steel, as stiff and rigid as circumstances of weight and

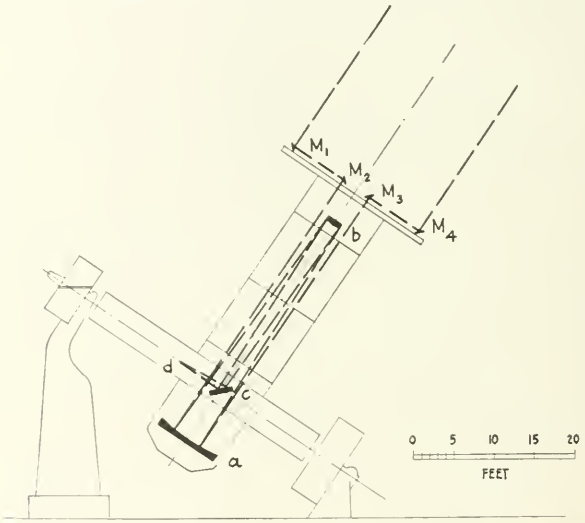


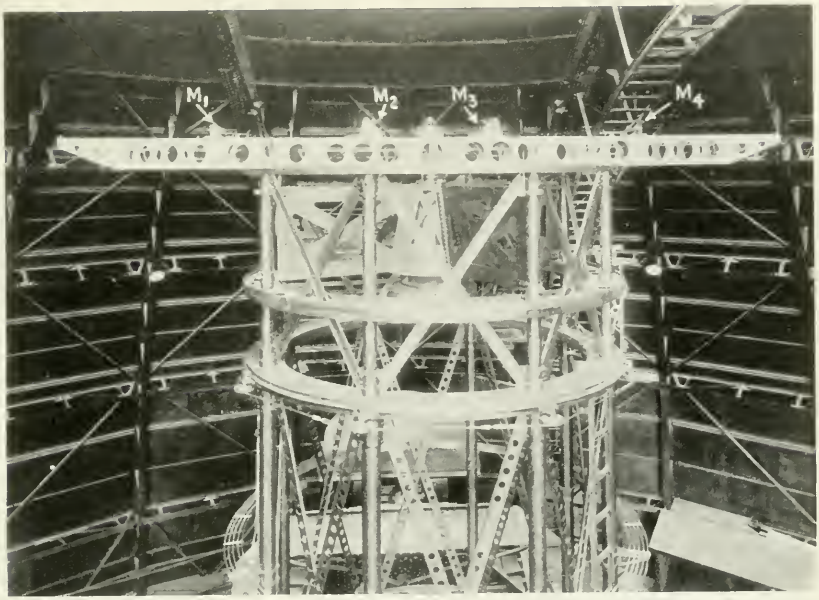
FIG. 1.—Diagram of optical path of interferometer pencils. M_1, M_2, M_3, M_4, mirrors; *a*, 100-inch paraboloid; *b*, convex mirror; *c*, coudé flat; *d*, focus.

operation would permit, for flexure causes a separation of the two pencils, and any vibration as great as one-thousandth of a millimeter blurs the fringes.

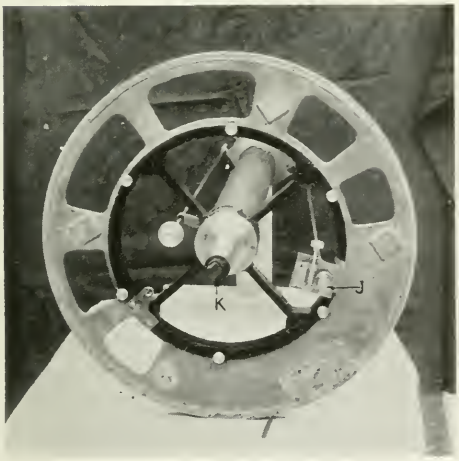
The beam is constructed of two 10-inch channels with flanges turned inward, separated by pieces of 12-inch channel and covered on the bottom with $\frac{3}{16}$-inch (4.75 mm) steel plate (*C*, Fig. 2), all riveted securely together.

To reduce the weight holes were cut wherever the removal of metal would not cause a weakening of the structure. The inner edges of the top flanges were planed true to 0.001 of an inch

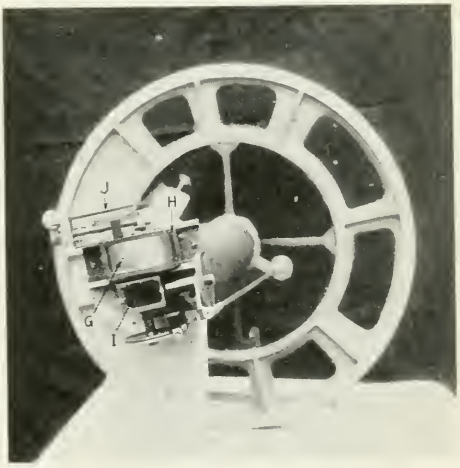
a



b



c



INTERFEROMETER USED WITH 100-INCH HOOKER REFLECTOR

a. *A*, 20-foot interferometer beam on end of telescope; M_1, M_2, M_3, M_4, mirrors; *D*, Cassegrain cage
b, *c*. Adapter at focus; *J*, rod to shift wedge; *K*, direct-vision prism; *G*, fixed wedge; *H*, movable wedge; *I*, plane-parallel compensator.

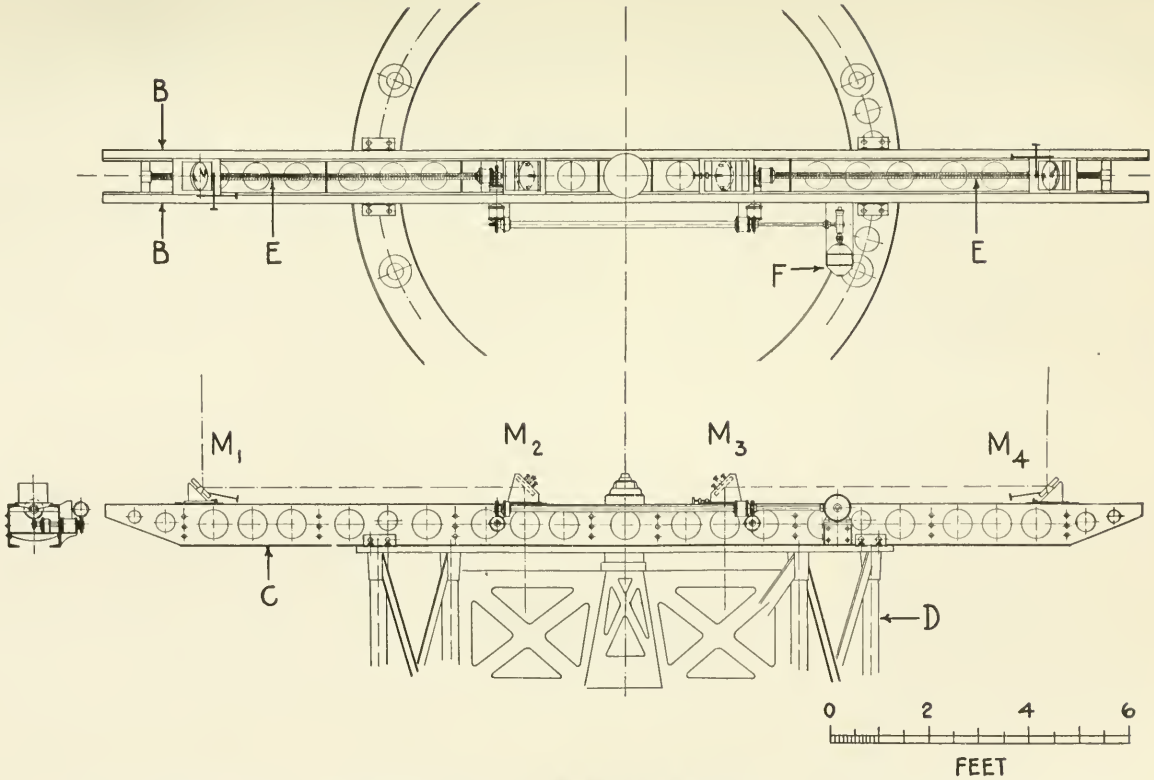


FIG. 2.—Diagram of 20-foot interferometer beam. M_1, M_2, M_3, M_4, mirrors; B, B, 10-inch channels; C, steel plate; E, E, screws to move outer mirrors; F, motor drive for screws; D, Cassegrain cage.

(0.025 mm), the beam being supported as it was to be mounted on the telescope.

Four mirrors, M_1, M_2, M_3, M_4 (Figs. 1 and 2 and Plate IV*a*), about 6 inches (152 mm) in diameter, inclined 45° to the base, are mounted on slides; M_2 and M_3 are adjusted by three screws at the back, while M_1 and M_4 are adjustable about two horizontal axes by means of fine screws at the ends of 9-inch (228 mm) lever arms. The mirrors M_2 and M_3 are permanently fixed except that M_3 has a motion of several millimeters along its slide parallel to the beam.

The nearly constant separation of the mirrors M_2 and M_3 by about 45 inches (114.2 cm) gives the fringe pattern a fixed spacing equal to 0.02 mm, easily visible with a magnification of 1600. The mirrors M_1 and M_4 can be shifted along the beam; their distances from M_2 and M_3 must be equal, a condition satisfied as closely as possible by measurement with steel scales.

The beam is mounted on the end of the Cassegrain cage (Plate IV*a* and Fig. 2), which is 11 feet (3.35 m) in diameter, and all observations are made at the Cassegrain focus corresponding to an equivalent focal length of 134 feet (40.84 m). Two pencils from the star are reflected from the outer mirrors M_1 and M_4 to mirrors M_2 and M_3, thence over the ordinary course in the telescope to the paraboloid (*a*, Fig. 1), the convex mirror (*b*, Fig. 1), the coudé flat (*c*, Fig. 1), and finally the focus (*d*, Fig. 1).

M_2 and M_3 are adjusted during the day and M_1 and M_4 on a star at night; and usually after the first setting of a run the image always appears in the field of view of the telescope.

Coincidence of the two interferometer pencils at the focus is obtained by first adjusting the mirrors M_1 and M_4 and then tilting a plane-parallel glass plate, 15 mm thick (*I*, Fig. 3, and Plate IV*c*), in the path of one of the pencils, which also serves to compensate the path of the double wedge mentioned below.

Equality of path in the two interferometer pencils is obtained by first setting the mirrors M_1 and M_4 symmetrically on the beam, as nearly as possible, and then adjusting the double wedge of glass (*G*, *H*, Fig. 3, and Plate IV*c*, 2 feet within the focus) in the path of one of the pencils, the relative motion of the wedges altering the path slowly and continuously.

One of the wedges (*H*, Fig. 3), whose angles are about 10°, can be moved 25 mm either side of its mean position, parallel to the inclined surfaces. One turn of the rod (*J*, Plate IV*b*) shifts this wedge 0.5 mm, thus introducing an equivalent air path of about 0.045 mm. Although fringes can be observed throughout one-third of a turn, corresponding to an air path of 0.015 mm, or about 26 light-waves, the finding of the fringes is notably facilitated by a direct-vision prism (*K*, Plate IV*b*) placed in front of the eyepiece, which permits observation of interference bands with a path-difference of several hundred waves.

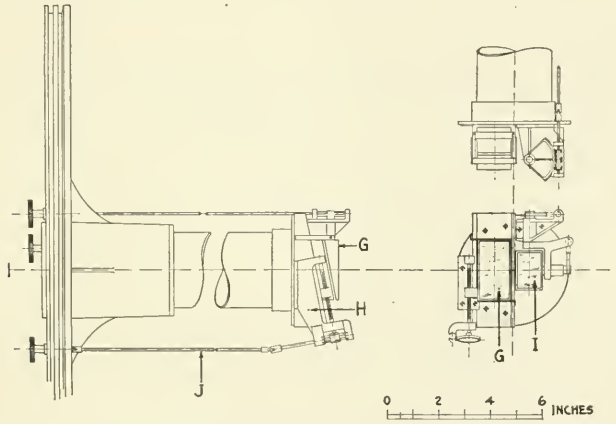


FIG. 3.—Diagram of adapter at focus. *G*, fixed wedge; *H*, movable wedge; *I*, plane-parallel compensator; *J*, rod to shift wedge.

To obtain a series of reference or "zero" fringes the end of the telescope tube is entirely covered, save for two apertures in the beam (in addition to those of mirrors M_2 and M_3), 6 inches (152 mm) in diameter. The pencils entering these apertures pass through the wedges and the compensating plate, respectively, and produce an image of the star in the field of view. When adjusted for coincidence and equality of path, these pencils interfere and produce the zero fringes which cross the reference image.

The interferometer images are next brought into the field of view of the eyepiece and made to coincide a short distance from the zero star, thus forming a second star in the field of view. Usually the adjustment of the mirrors M_1 and M_4 is sufficient to do this and the parallel plate compensator is used only for differential deflection

of the steel beam. As soon as the wedge is moved to equalize the path-difference in the interferometer pencils, the zero fringes disappear and count is made of the turns of the rod required to bring the interferometer fringes into view. The mirror M_3 is then moved a small amount to compensate for this difference, and after several trials both sets of fringes are seen in the field of view crossing their respective images.

Differential refraction between air and glass limits the amount by which the effective thickness of the wedges may differ from that of the compensator, but interferometer fringes have been found with the wedge 20 mm from its mean position, corresponding to a 2-mm difference of air path.

Fringes were obtained with this apparatus in August, 1920, with the mirrors M_1 and M_4 at various distances apart, and, as there was no appreciable deterioration in their visibility at 18 feet (5.49 m) as compared with a separation of 6 feet (1.83 m), it seems reasonable to hope that this distance can be increased to 50 feet (15.24 m) or even to 100 feet (30.48 m). Work was discontinued after this series of experiments and again resumed in December, 1920.

Although provision is only just now being made for continuous alteration of the distance between the mirrors, as is essential in making accurate measurements, it was nevertheless decided to attempt a measurement of the angular diameter of α Orionis, for the calculations of Eddington, Russell, and Shapley, based on estimates of apparent surface brightness, had indicated that this star would be a promising subject for investigation.

The possibility of measuring the angular diameter of a distant object by interference methods depends upon the following considerations.

Let the distribution of light in the disk be represented by

$$I = I_0(R^2 - r^2)^n,$$

r being the distance from the center, R the radius of the star, n the exponent of darkening at the limb. The visibility of the interference bands is

$$V = \frac{1}{P} \sqrt{C^2 + S^2},$$

where

$$C=\int F(x)\cos kx\,dx, \qquad S=\int F(x)\sin kx\,dx,$$

$$P=\int F(x)\,dx, \qquad k=\frac{2\pi b}{\lambda d},$$

in which b is the distance between two pencils entering the interferometer, λ the mean length of the light-waves of the source, and d the distance of the source. $F(x)dx$ is the total intensity of a strip of the source whose width is dx. For a symmetrical source such as a star disk,

$$V=\frac{C}{P}.$$

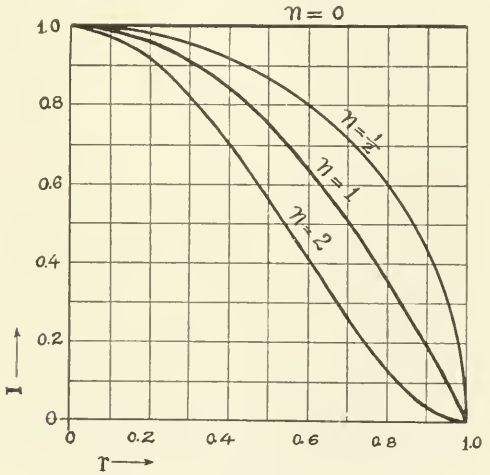


FIG. 4.—Distribution of light in various sources

If the illumination is uniform, $F(x)=1\sqrt{R^2-x^2}$, whence

$$V=\frac{\int_0^R 1\sqrt{R^2-x^2}\cos kx\,dx}{\int_0^R 1\sqrt{R^2-x^2}\,dx},$$

tables for which have been computed by Airy.

If the illumination can be represented as a function of the distance from the center, $I=(R^2-r^2)^n$, then

$$F(x)=\int_0^{\sqrt{R^2-x^2}}(R^2-x^2-y^2)^n dy$$

which, expanded in series and substituted in V, gives

$$V=\frac{\int_0^R (R^2-x^2)^{\frac{2n+1}{2}}\cos kx\,dx}{\int_0^R (R^2-x^2)^{\frac{2n+1}{2}}\,dx}.$$

This integral has been computed under the direction of Professor Moulton, the results being summarized in the accompanying

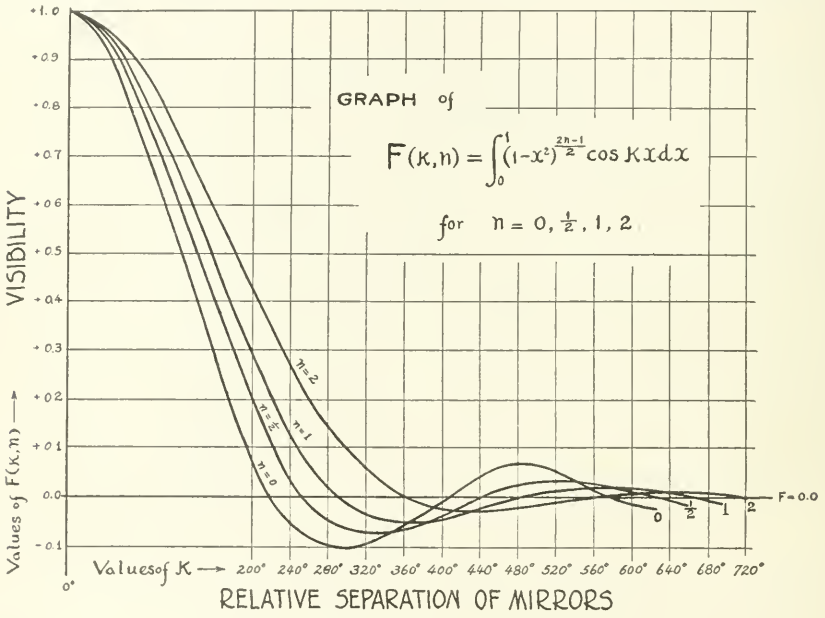


FIG. 5.—Visibility-curves for various sources

table; and in Figure 4 is shown the distribution of light in the source for the values $n=0$, $\frac{1}{2}$, 1, and 2, and in Figure 5 the resulting visibility-curves.

It will be noted that for $n=0$ the first disappearance of the fringes occurs at $k=220°$, while for $n=0.5$, the value is $k=257°$. For this value of n, the corresponding value of the diameter of Betelgeuse would be about 17 per cent greater than given below. (For the sun, the value of n is not far from 0.4.)

VALUES OF

$$F(k, n) = \int_0^1 (1-x^2)^{\frac{2n+1}{2}} \cos kx\, dx$$

$n=0$		$n=0.5$		$n=1$		$n=2$	
k	$F(k,n)$	k	$F(k,n)$	k	$F(k,n)$	k	$F(k,n)$
0°	+0.785	0°	+0.785	0°	+0.785	0°	+0.785
100	+0.507	30	+0.765	40	+0.746	40	+0.761
130	+0.378	60	+0.702	80	+0.663	80	+0.694
160	+0.243	90	+0.607	120	+0.536	120	+0.590
200	+0.065	120	+0.490	160	+0.383	160	+0.468
230	−0.024	150	+0.363	200	+0.237	200	+0.342
240	−0.050	180	+0.238	240	+0.112	240	+0.221
280	−0.100	210	+0.127	280	+0.024	280	+0.123
320	−0.095	240	+0.038	320	−0.029	320	+0.054
360	−0.053	257°27′	0.000	360	−0.045	360	+0.003
400	−0.007	270	−0.024	400	−0.039	400	−0.019
440	+0.036	300	−0.057	440	−0.020	440	−0.024
520	+0.042	330	−0.068	480	−0.001	480	−0.018
600	−0.011	360	−0.059	520	+0.012	520	−0.006
.....		390	−0.040	600	+0.013	560	0.000
.....		420	−0.016	640	+0.005	600	+0.005
.....		450	+0.005	680	−0.004	680	+0.005
.....		480	+0.019			720	+0.002
.....		510	+0.028				
.....		540	+0.026				
.....		570	+0.019				
.....		600	+0.009				
.....		630	−0.002				

While it may be too much to expect that we shall be able to deduce the actual distribution of the light in the source from observations of the visibility-curve itself, it may be worth while to point out that this is theoretically possible; and perhaps the case will not be entirely hopeless when the requisite skill in making the observations has been obtained by practice.

If b_1 and b_2 are the distances at which the fringes vanish for the first and second times, then the following formula will give a fair approximation to the value of n in the light-curve:

$$n = -1 + 75\left(\frac{b_1}{b_2} - \tfrac{1}{2}\right)^2.$$

Or again, if V_m is the visibility at the first negative maximum (that at $b=0$ being unity),

$$n = 0.22\left(\frac{1}{V_m} - 7.8\right)^{0.7}.$$

It will be seen from this discussion that the measurement sought is that value of the separation of the outer mirrors M_1 and M_4 for which the fringes vanish. This corresponds to the point where the graphs (Fig. 5) cross the horizontal axis, that is, for the value $F(k,n)=0$. A preliminary investigation by Merrill, with the apparatus used by Anderson[1] in the measurement of Capella, revealed in fact a definite decrease in visibility of the fringes of α Orionis for the maximum separation of the slits (100 inches). This was true, moreover, for all position angles, which indicated that the star is not a binary and that the decrease in visibility is to be attributed to a measurable diameter.

On December 13, 1920, after preliminary settings on β Persei with the mirrors separated 81 inches (229 cm) and on β Persei and γ Orionis with a separation of 121 inches, thus insuring that the instrument was in perfect adjustment, it was turned on α Orionis and fringes across the interferometer image were sought for some time, but could not be found. The seeing was very good, and the zero fringes could be picked up at will.

When next turned on α Canis Minoris the fringes stood out on both images with practically no adjustment of the compensating wedge, which furnishes a check on the disappearance of the fringes for α Orionis.

It is clear from these observations that the disappearance of the fringes in the case of α Orionis cannot have been due to any disturbance of the mirrors caused by changes in the position of the telescope, for changes such as those here involved require only a few turns of the rod controlling the compensating wedge to counteract differences in atmospheric path and flexure and bring the fringes again into view. There is therefore no chance that they were simply overlooked in the case of α Orionis.

To observe the recurrence of the fringes near the second maximum for α Orionis, the mirrors were next separated a distance of 13 feet and the telescope turned on α Canis Minoris, fringes appearing across both star images as soon as the component pencils were brought into coincidence. On December 14 and the nights following, the seeing was very poor, the visibility of standard check stars

[1] *Mt. Wilson Contr.*, No. 185; *Astrophysical Journal*, **51**, 263, 1920.

being decidedly less than on the night of December 13; consequently no attempt was made to observe the second maximum and minimum of α Orionis, but attention was turned to other stars, and settings were made on α Ceti, α Tauri, and β Geminorum. The zero fringes were seen in every case, although with slightly decreased visibility; but it was only at rare intervals of better seeing that the interferometer fringes could be seen at all. From this fact it is presumed that there was an actual decrease of visibility for these stars and that some estimate of their diameters can be made with the 20-foot beam. Observations on these and other objects of presumably large diameter are being continued.

Assuming that the effective wave-length for α Orionis is λ 5750, its angular diameter from the formula $\alpha = 1.22\ \lambda/b$ proves to be 0″.047; and with a parallax[1] of 0″.018 its linear diameter turns out to be 240×10^6 miles, or slightly less than that of the orbit of Mars. This value corresponds to a uniformly illuminated disk, while for one darkened at the limb, this result, as mentioned above, would be increased by about 17 per cent. The uncertainty of the measurement of the angular diameter is about 10 per cent.

Cordial acknowledgment is tendered to Director George E. Hale for placing the resources of the Observatory at our disposal and for his enthusiastic co-operation in furthering the investigation.

Mr. J. A. Anderson was present on several occasions and we wish particularly to acknowledge his valuable assistance in checking the measures on December 13.

Mount Wilson Observatory
February 1921

[1] The weighted mean of Adams' spectroscopic parallax, 0″.012, and the trigonometric values of Elkin, 0″.030, and of Schlesinger, 0″.016.

WAVE-LENGTHS OF LINES IN THE IRON ARC FROM GRATING AND INTERFEROMETER MEASURES λ 3370–λ 6750[1]

By CHARLES E. ST. JOHN and HAROLD D. BABCOCK

ABSTRACT

Wave-lengths of iron-arc lines from λ3370 to λ6750; grating and interferometer measurements.—To avoid errors due to pole-effect a 12-mm, 5-amp. Pfund arc was used. This arc has also the advantage of yielding very sharp lines. To eliminate instrumental errors, spectrograms made with two Michelson and three Anderson gratings and with four pairs of interferometer plates were compared. Table III contains the mean *results for 1026 lines*, of which 976 were measured on each of from 1 to 62 grating spectrograms and 576 on each of from 1 to 39 etalon spectrograms. The agreement shown indicates that for most of the lines the weighted mean wave-length is accurate to 0.001 A. In the case of 250 stable lines, the agreement with Bureau of Standards measurements is good. But for 46 lines of groups *c*5 and *d*, the Bureau measurements are systematically greater, the mean difference being 0.007 A, due to *pole-effect in the 6-mm, 6-amp. arc.* Of 78 *International Secondary Standards* measured with the interferometer, 62 stable lines came out as follows: 53 within ±0.001, 8 within ±0.002, 2 within ±0.003, and 1 within 0.004 A of the adopted values; while in the case of 16 lines belonging to groups *c*5 and *d*, the International values are systematically greater, the mean difference being 0.007 A, due to pole-effect in the arcs used in the original determinations. Evidently these sources had the same order of pole-effect as the 6-mm, 6-amp. arc. *Ghosts and reversals* gave the same wave-lengths as those obtained from fine lines produced in the core of a lean arc. A comparison of readings from long and short exposures of the same lines showed no *intensity effect* in the case of interferometer measurements.

Spectroscopic measurements.—(1) *Method of reduction of interferometer spectrograms.* The elimination of a gauge plate over the slit and the introduction of a plate constant, $K\lambda$, which may be determined from measurements of the ring diameters alone, greatly reduce the labor of measurement and reduction, without decreasing the precision. (2) *Comparison of grating and interferometer.* The advantages and disadvantages of each are discussed.

I. INTRODUCTION

In a previous paper[2] we discussed the influence of pole-effect in the iron arc upon the measurement of the wave-lengths of certain lines in the lists of adopted secondary and suggested tertiary standards. It was shown that the arc 6 mm in length, carrying a current of 6 amperes, adopted at the Bonn meeting of the Inter-

[1] *Contributions from the Mount Wilson Observatory*, No. 202.

[2] *Mt. Wilson Contr.*, No. 137; *Astrophysical Journal*, 46, 138, 1917.

national Union for Co-operation in Solar Research, gave a pole-effect of +0.006 A even in its central plane, and that the wave-lengths of the secondary standards belonging to groups *c*5 and *d* were affected to approximately the same amount. This has been confirmed in the present investigation.

In the *Report of the Committee on Standards of Wave-Length* adopted at the Washington meeting of the American Section of the International Astronomical Union[1] the source to be used in the determination of iron standards of wave-length is defined as "the Pfund arc operated between 110 and 250 volts, as convenient, with 5 amperes or less, at a length of 12 millimeters, and used over a central zone at right angles to the axis of the arc not to exceed $1\frac{1}{4}$ millimeters in width." Under these specifications the iron arc yields wave-lengths that appear to be free from pole-effect and is easily workable for wave-lengths shorter than 6000 A. For longer wave-lengths the time of exposure is excessive and pole-effect is not entirely eliminated.

The committee also recommended that independent measurements be made with the grating and with the interferometer, "on the ground that the errors of these two instruments are largely complementary." In the determinations carried out by us, both methods have been employed.

II. APPARATUS AND METHODS

The apparatus used for the interference observations is in the main the same as that described in a previous paper.[2] It is now permanently installed in a double-walled, wooden case with convenient arrangements for projecting the light into it. Various etalons have been used, the plates being either of fused quartz or glass, and the separators of invar or fused quartz. The thickness varied from 2.5 mm to 15 mm; most of the photographs were taken with etalons of 5, 7.5, or 10 mm. The rings were projected upon the slit by a concave mirror having a focal length of 633 mm. No thermostat was used in connection with the interference apparatus, as efficient protection from temperature changes was afforded by

[1] *Proceedings of the National Academy of Sciences*, 6, 367, 1920.

[2] *Mt. Wilson Contr.*, No. 137; *Astrophysical Journal*, 46, 138, 1917.

the housing. On the longest exposures no loss of definition can be observed, and the results from these plates show no systematic deviations from those yielded by short exposures. The interferometer plates were several times resilvered by cathodic deposition. On account of the different ratio between its reflection and transmission coefficients, gold was occasionally used for one of the reflecting surfaces. The phase-change corrections have been evaluated in the usual manner by plotting the differences between observed and known wave-lengths for the standards occurring upon each plate. The correction-curves have always been straight lines. No correction for atmospheric dispersion has been applied, since the standards are distributed throughout the extent of each region photographed.

Careful attention has been given throughout the investigation to the adjustment of each part of the apparatus, and no difficulty has been experienced from mechanical disturbances. The etalon was so located with respect to the mirror which projects the rings upon the slit as to bring an image of its diaphragm into focus upon the grating, in accordance with the remark of Buisson and Fabry in their important paper.[1] Furthermore, the size and shape of the diaphragm were so chosen that its image was much smaller than the grating, and the slit-width was so adjusted that diffraction never widened the image beyond the lateral boundaries of the ruled surface. These precautions and the use of large apertures in the projecting systems insured uniform illumination *upon the photographic plate* of several more rings for each line than were actually used for measurement.

As indicated in the paper already referred to, the method of reduction employed at Mount Wilson for interferometer plates is not the same as that described by Buisson and Fabry, Pfund,[2] Burns,[3] and others. These observers derived the fractional order of interference by means of an equation of the form

$$\epsilon = \frac{p\theta^2 D^2}{8L^2},$$

[1] *Journal de physique*, 7, 169, 1908.

[2] *Astrophysical Journal*, 28, 197, 1908.

[3] *Bulletin of the Bureau of Standards*, 12, 179, 1915.

where

ϵ = fractional order of interference for the ring whose linear diameter is D.

θ = angular distance of standard gauge marks in front of the slit, as seen from lens which projects the rings on the slit.

L = linear distance of photographed gauge marks for the same spectral line.

p = order of interference at center of ring system.

This requires, in addition to the photograph of the interference pattern, an exposure to the spectrum with the etalon removed and the gauge plate inserted in front of the slit, from which the value of L is obtained. The quantity θ has also to be determined from independent observations.

A simple transformation of this equation, however, makes possible a marked saving in labor and offers other advantages which are referred to below. If we define by m the magnification of the spectrograph for a given spectral line, and let F be the focal length of the lens or mirror which projects the rings upon the slit, it is readily seen that in the equation above θ^2/L^2 may be replaced by $1/m^2F^2$, giving

$$\epsilon = \frac{pD^2}{8F^2m^2}$$

or more generally, for the n^{th} ring, counting the innermost as the first,

$$n - 1 + \epsilon = KD_n^2 ,$$

where K is written for $p/8F^2m^2$. It is evident that both ϵ and K may be determined from this equation if two diameters are measured. For any two consecutive rings, for example the first and second, it is seen that

$$K\lambda = \frac{\lambda}{D_2^2 - D_1^2} .$$

An increase in accuracy may be obtained, however, if the condition is imposed that m be constant for all spectrum lines upon the plate. If e is the thickness of the etalon,

$$K\lambda = \frac{p\lambda}{8F^2m^2} = \frac{2e}{8F^2m^2} ,$$

which is a constant for the plate considered. The determination of this plate-constant and its application to the problem will be understood from a description of the procedure followed.

Two measurements in reverse directions are made upon the diameters of each of the first two rings for every line upon the plate, except when the fractional order of interference is judged to be less than 0.3, in which case the measures are made upon the second and third rings instead. The two observations upon each diameter are then averaged, and the rough value of the wave-length is divided by the difference of the squares. The number thus derived, in which only four significant figures are retained, is a value of the plate-constant, $K\lambda$, the accuracy of which is then increased as desired by using a sufficient number of lines. The refined value of the plate-constant, divided by the rough wave-length and multiplied by the square of a ring diameter, yields the fractional order directly. The two fractional orders thus obtained from the two rings measured are averaged to produce the final fractional order. In practice it is found that the probable error of a single determination of the plate-constant is about 0.6 per cent, from which it follows that the mean of 35 or 40 values will have a probable error of one part in one thousand, the accuracy aimed at in these measurements. It may be remarked that no systematic difference appeared in the fractional orders yielded by individual rings for the same line.

The assumption of constant magnification in the spectrograph over the field used, while not rigorously true, is found in practice to be permissible in the case of the apparatus employed for this work and also for a plane-grating spectrograph of the Littrow type having a glass lens of 18 feet focal length. An extreme case is found in a quartz spectrograph wherein the normal to the photographic plate stands at an angle of 65° with the optical axis of the camera lens. In the ultra-violet the magnification for this instrument varies as the square root of the wave-length, and the plate-constant is $K\lambda^2$ instead of $K\lambda$. In general the method can be applied without difficulty for any type of spectrograph by a slight modification of the procedure described above.

In the course of the present investigation many determinations of the plate-constants have been made. It has been found that for the same adjustments of the spectrograph, $K\lambda$ for different plates is constant within the errors of observation when the etalon is the same, and that etalons of different thickness give plate-constants in the ratio of the thicknesses, as indicated by the equation above.

Furthermore, it may be pointed out that, when the interference rings are projected by a concave mirror upon the slit of a spectrograph of the type used for this work, it is easy to derive a fundamental instrument-constant from which the plate-constant, $K\lambda$, may be obtained directly from a knowledge of the setting of the spectrograph camera. As indicated above, however, the practice followed in this investigation has been to determine $K\lambda$ from each plate, in which case the instrument-constant serves as a valuable check.

An application of the laws of propagation of errors to the two equations stated above for deriving the fractional order of interference shows that in general the probable error of ϵ is larger for the method of Buisson and Fabry than for the Mount Wilson method. This is to be expected from the fact that in the first method auxiliary quantities θ and L must be observed, the effect of whose probable errors can only be to increase the probable error of the result. A comparison of the results of our interferometer measurements with those of other observers, as well as with values derived from gratings, strengthens the conclusion that the method used by us for deriving fractional orders involves no sacrifice of accuracy as compared to the procedure usually adopted. Furthermore, the simplicity and directness which characterize the new method, the lessening of the necessary photographic and microscopic observations, and the additional numerical checks which become available through its use combine to lend it weight and emphasize its value.

In the region λ 3370–λ 5662 the interferometer plates were measured and reduced for the most part by two observers independently; the weighted means of their results are given in Table I. Over the region of longer wave-lengths most of the measuring was done by one of them, but nearly all of the lines

tabulated were measured and reduced by a third observer upon a selected list of plates. A comparison of the results shows that the various observers are in excellent agreement, no systematic differences of any significance being found between them. It is probable that effects dependent upon personal equation are too small to influence the final values.

The grating measures include only the stable lines from the list published by St. John and Ware,[1] but cover all the lines in the two new series of plates. The old series by St. John and Ware, λ 4118–λ 6500, was taken with the 30-foot Littrow spectrographs on Mount Wilson and in Pasadena, for which Michelson plane gratings with available ruled surfaces 37×114 mm were used in the second-order; scale, 0.88 A per mm. In the new laboratory series the 15-foot concave-grating spectrograph[2] was used in the third order for the region λ 3370–λ 4200. The grating, made by Anderson, has a ruled surface 50×106 mm; scale as used, 1.25 A per mm. From λ 4100 to λ 5658 the 30-foot Littrow spectrograph with an Anderson grating, ruled surface 63×72 mm, was used in the second order; scale, 0.88 A per mm. The new mountain series, λ 3600–λ 5500, was taken with the 30-foot spectrograph of the 60-foot tower telescope. The second order was employed; scale, 0.88 A per mm. The grating, ruled surface 114×160 mm, was made by Anderson and loaned by the Physical Laboratory of the Johns Hopkins University.

The comparators used were constructed in the observatory shop; the screws have been tested and found satisfactory. The standard measuring machines have screws 20 cm long; one specially designed machine with a screw 50 cm long furnished an excellent means for adjusting the reference lines, as its exceptionally long range allows the inclusion of many standards in a single run under constant conditions.

Two methods of reducing the grating data have been used. In one the interpolation between standards was made from a curve whose abscissae are the mean wave-lengths of adjacent secondary

[1] *Mt. Wilson Contr.*, No. 61; *Astrophysical Journal*, **36**, 14, 1912; *Mt. Wilson Contr.*, No. 75; *Astrophysical Journal*, **39**, 5, 1914.

[2] King, *Mt. Wilson Contr.*, No. 84; *Astrophysical Journal*, **40**, 205, 1914.

standards and whose ordinates are the scale-factors for the intervals. In the other, the wave-lengths were calculated from an empirical formula derived from three standards, of the form

$$\lambda = a + bx + cx^2.$$

A curve of corrections was obtained for the deviations of the other standards from the calculated values.

III. THE REGIONS OF THE SPECTRUM COVERED

The interferometer measures extend from λ 3370 to λ 6750. The grating series cover the regions λ 3370–λ 5658 and λ 5975–λ 6500. The gap between λ 5658 and λ 5975, owing to the dearth of suitable standards in this region, is too wide to bridge with the grating. In both the grating and interferometer series all measurable lines were observed. The new laboratory series of grating plates were greatly varied in exposure time in order to obtain a wide range of line-intensity. When feasible, measurements were made upon lines reversed and unreversed and also upon clearly determined ghosts.

IV. SOURCES

For the region λ 3370–λ 6000 the interferometer photographs were taken from a horizontal zone, $1\frac{1}{4}$ mm wide, at right angles to the axis, of a 12-mm Pfund arc carrying 5 amperes or less. For the region λ 6000–λ 6750 the integrated light of a somewhat shorter Pfund arc was used, only stable lines being measured upon the plates.

In the early series by St. John and Ware no particular attention was at first given to the character of the arc, which in general was approximately 5 mm long, or to the portion from which the light was taken. For this reason only the wave-lengths of the lines not subject to pole-effect are retained. In the new grating series the wave-lengths are those given by a 12–14-mm arc with a current of 5 amperes. In the four grating series the wave-lengths of the stable lines are in excellent agreement. The wave-lengths of the lines showing pole-effect depend only upon observations made on the arc recommended by the American committee.

V. RESULTS

The wave-lengths with related data are entered in Table I. The third column gives the group and class. When both group and class are shown the allocation is taken from the paper by Gale and Adams.[1] When no entry appears, the line is practically free from pole-effect, but data are lacking for definite classification. Groups *c*5 and *d* contain all the lines with recognized positive pole-effect; as our data are insufficient to differentiate the two groups, the lines not in the list of Gale and Adams are provisionally assigned to the major group *d*. Lines with a negative pole-effect constitute group *e*.[2] An interrogation point indicates that the evidence for grouping is contradictory. "G" and "I" relate the remarks to grating and interferometer respectively. The dependence of the wave-lengths upon direct measurements, ghosts, or reversals is indicated by "direct," "g," and "r" in the corresponding combination. The other symbols are those suggested by Burns[3] and recommended in the *Report* of the American committee.[4] "A" indicates a probable error less than 0.0007 A; "B," 0.0007 A–0.0012 A, and "C," that the determination is poor; "h" = hazy; "l" = shaded to red; "v" = shaded to violet.

While the interferometer spectrograms were under the microscope, weights 1, 2, and 3 were assigned to the various lines, corresponding to poor, average, or excellent quality. This furnished the basis for combining the observations and also for grouping the final wave-lengths into three classes according to the total weights attached to them. The classes A, B, and C, equivalent to those recommended by the committee, have in general the following limits and numbers of lines:

A = weight from 10 to 159; number of lines 352.
B = weight from 4 to 9; number of lines 111.
C = weight from 1 to 3; number of lines 113.

[1] *Mt. Wilson Contr.*, No. 58; *Astrophysical Journal*, **35**, 10, 1912.

[2] St. John and Ware, *Mt. Wilson Contr.*, No. 75, p. 4; *Astrophysical Journal*, **39**, 8, 1914.

[3] *Lick Observatory Bulletin*, **8**, 29, 1913.

[4] *Proceedings of the National Academy of Sciences*, **6**, 367, 1920.

TABLE I

WAVE-LENGTHS OF LINES IN THE IRON ARC (λ 3370–λ 6750), INTERNATIONAL SYSTEM

λ		GROUP	GRATING		INTERFEROMETER		REMARKS
Grating	Interferometer		Plates	Probable Error	Plates	Probable Error	
3370.788	.788		8	A	5	B	
3378.684			7	A			
3379.022			8	B			
3380.115			8	B			
3382.409			6	B			
3383.697			6	A			
3383.982	.987		8	A	1	C	
3392.309			7	A			
3392.656	.656		10	A	2	C	
3394.595	.590		8	B	1	C	G, h
3396.980	.982		8	A	1	C	
3399.336	.337		12	A	8	A	
3401.520	.524		8	A	2	C	
3402.262			8	B			
3404.355	.351		3	C	4	B	G, v
3406.442			6	B			
3406.805	.803		8	A	1	C	
3407.464	.462		16	C	21	A	G, direct, g
3410.171			1	C			
3411.355			6	B			
3413.134	.135		12	A	12	A	
3415.537			7	A			
3417.	.274	*e?*			2	C	
3417.845	.845		12	A	14	A	
3418.508	.510		12	A	6	A	
3422.500			6	B			
3422.658	.665		8	A	3	C	Diff. > error
3424.287	.288		12	A	4	B	
3425.013			8	A			
3426.384			8	B			G, v
3426.638			8	A			
3427.003			6	A			
3427.123	.124		18	B	5	A	G, direct, g
3428.194	.197		8	A	6	A	⊙ Fe, Co
3431.816			1	C			
3440.611	.611		16	C	3	B	
3440.993	.988		12	B	3	C	Diff. > error
3442.673			7	A			
3443.881	.879		12	A	28	A	
3445.152	.152		12	A	13	A	

TABLE I—*Continued*

λ		Group	Grating		Interferometer		Remarks
Grating	Interferometer		Plates	Probable Error	Plates	Probable Error	
3445.763		*d*	1	C			
3447.282	.281		8	B	4	B	
3450.333	.331		8	A	5	A	
3451.	.629				1	C	
3451.917	.920		8	A	2	C	
3452.278	.281		8	A	1	C	
3453.023			6	A			
3458.305			6	A			
3459.915			6	A			
3461.	.654				2	C	
3462.	.354				1	C	
3465.866	.863		12	B	27	A	
3475.455			18	A			
3475.652			8	A			
3476.707	.706		11	B	27	A	
3476.854			5	A			
3483.008	.010.		6	A	1	C	
3485.340	.345		7	A	7	A	⊙ Fe Co
3489.667	.675		6	A	1	C	
3490.575	.576		17	B	26	A	G, direct, g
3492.	.959				5	B	
3495.286	.289		8	B	5	A	
3497.110	.111		7	B	1	C	G, l
3497.843	.843		11	A	29	A	G, direct, g
3500.563			1	C			
3506.499	.501		3	C	5	A	
3508.	.495				1	C	
3513.819	.820		18	B	30	A	
3515.	.056				3	B	
3521.264	.264		12	A	31	A	
3521.834			6	B			
3524.076			4	B			
3524.240			8	B			
3526.040			12	A			
3526.168			12	A			G, l
3526.378			8	B			
3526.466			8	A			
3526.674			8	B			
3527.793	.798		8	A	3	B	G, v
3529.821	.824		8	A	3	B	⊙ Fe-Co
3530.386			6	A			
3533.009			8	B			
3533.199			10	B			
3536.559	.559		12	A	14	A	
3537.492			1	C			

TABLE I—*Continued*

λ		Group	Grating		Interferometer		Remarks
Grating	Interferometer		Plates	Probable Error	Plates	Probable Error	
3537.730....			6	A			
3537.897....			8	A			
3540.126....	.128		7	A	2	C	
3540.710....			1	C			
3541.088....	.088		12	A	20	A	
3542.080....	.080		12	A	16	A	
3543.670....			6	A			
3545.644....	.641		8	A	4	B	
3547.204....			1	C			
3549.869....			1	C			
3552.837....	.839		8	A	1	C	
3553.744....	.747		8	A	1	C	
3554.122....	.125		8	A	2	C	
3554.931....	.928		16	A	22	A	Diff.>error
3556.889....	.883		12	C	11	B	G, l, wgt very low; I, h
3558.522....	.518		17	B	33	A	G, direct, g; diff.>error
3559.507....			6	A			
3565.383....	.381		16	C	23	A	G, h, direct, g
3565.584....			8	A			
3568.978....			6	A			
3570.103....	.100		4	B	1	C	
3571.	.997		6	B	2	C	
3573.893....			7	A			G, line on violet
3575.250....			5	A			
3575.375....			7	B			
3575.983....			1	C			
3576.759....			5	B			
3581.197....	.196		6	A	18	A	G, r; I, r
3581.646....			3	C			
3582.202....	.201		7	A	1	C	
3583.338....			5	B			
3584.664....	.665		10	A	2	C	
3584.791....			6	A			
3584.961....			8	A			
3585.320....	.322		5	A	10	A	G, g
3585.709....	.710		15	B	1	C	G, direct, g
3586.114....			8	A			
3586.987....	.987		10	A	29	A	
3587.425....			6	A			
3587.753....			8	A			
3588.919....			6	A			
3589.109....	.106		10	B	2	C	
3589.455....			8	A			
3594.636....	.636		8	A	11	A	
3599.627....			6	A			

TABLE I—*Continued*

λ		Group	Grating		Interferometer		Remarks
Grating	Interferometer		Plates	Probable Error	Plates	Probable Error	
3602.	.513				1	C	
3603.206....	.207		12	A	11	A	
3603.829....			3	C			G, l
3605.466....	.460		12	C	16	B	Diff.>error; I, h
3606.682....	.682		12	A	28	A	
3608.147....			6	A			
3608.862....	.861	*b*1	13	B	24	A	G, direct, g
3610.164....	.164		12	A	18	A	
3610.704....			1	C			
3612.074....	.073		8	A	4	A	
3612.941....			1	C			
3614.562....			1	C			
3616.573....			8	A			
3617.318....			6	A			
3617.790....	.789		12	A	9	A	
3618.393....			8	A			
3618.773....	.770	*b*1	6	A	22	A	G, g; I, r, direct
3621.465....	.463		18	B	13	A	
3622.009....	.009		15	B	11	A	
3623.190....	.188		11	B	5	A	
3625.	.148				4	A	
3630.353....	.354		6	A	1	C	
3631.104....			11	C			
3631.467....	.466	*b*1	6	B	22	A	G, g; I, r
3632.043....	.043		8	B	2	B	
3632.559....			11	B			
3632.980....			3	C			
3634.336....			11	B			
3636.996....			3	C			
3637.863....			3	C			
3638.300....	.300		23	A	14	A	
3640.392....	.392		23	A	21	A	
3643.628....			11	B			
3645.823....			15	A			
3647.428....			15	B			
3647.846....	.845	*b*1	4	B	22	A	G, r; I, r, direct
3649.305....			19	A			
3649.509....	.511		15	B	11	A	
3650.032....			15	C			
3650.281....			15	A			
3651.471....	.470		26	A	20	A	
3655.468....	.463		18	A	2	C	
3659.520....	.520		21	A	10	A	
3664.541....		*d*	6	A			
3667.265....		*d*	4	C			

TABLE I—*Continued*

λ		Group	Grating		Interferometer		Remarks
Grating	Interferometer		Plates	Probable Error	Plates	Probable Error	
3669.152....			1	C			
3669.524....	.524		10	A	9	A	
3670.	.072				1	C	
3674.	.767				1	C	
3676.313....	.315		19	A	10	A	
3677.310....			9	B			
3678.863....	.865		11	A	1	C	
3679.916....	.916	*a*1	10	B	32	A	G, g, r; I, r, direct
3682.226....	.228		16	B	11	A	
3683.059....	.059		12	A	7	A	
3684.113....	.113		24	B	7	A	
3686.002....	.001	*e*	23	B	7	A	
3686.261....			1	C			
3687.101....			15	B			
3687.460....	.460	*b*1	8	B	32	A	G, g, r
3687.657....			14	B			
3689.462....	.463		18	B	11	A	
3690.731....	.731		12	B	4	A	
3693.009....	.009		19	C	14	A	
3695.055....	.056		28	B	12	A	
3697.433....	.433	*d*	16	A	6	A	
3698.613....			5	C			
3699.149....			2	C			
3701.091....	.091		6	A	15	A	
3702.033....	.037		14	A	1	C	
3702.502....		*e*	2	C			
3703.558....			9	B			
3703.699....		*d*	10	C			
3703.826....			9	C			
3704.465....	.466		30	A	9	A	
3705.568....	.568	*a*1	17	C	30	A	G, g, r; I, r, direct
3707.051....	.051		20	A	3	B	
3709.251....	.250	*b*1	26	A	30	A	
3709.537....			4	C			
3711.227....	.227		20	A	2	B	
3711.413....			11	B			
3715.917....	.914		7	B	3	B	
3716.449....	.449		29	A	11	A	
3718.408....	.410		20	A	1	C	
3719.939....	.937	*a*1	23	A	23	A	G, r; I, r, direct
3722.030....			2	B			
3722.564....	.565	*a*1	18	A	31	A	G, direct, g, r; I, r, direct
3724.380....	.380		8	A	18	A	
3725.500....			1	C			
3726.929....		*e*	18	A			

TABLE I—*Continued*

λ		Group	Grating		Interferometer		Remarks
Grating	Interferometer		Plates	Probable Error	Plates	Probable Error	
3727.098			22	A			
3727.622	.623	*b*1	10	A	30	A	G, g
3727.811			19	A			
3728.670			3	C			
3730.388	.391		19	A	1	C	
3730.947	.948		15	A	1	C	
3731.377	.375		13	A	1	C	
3732.400	.398		34	A	18	A	
3733.319	.321	*a*1	25	A	28	A	G, direct, g, r; I, r, direct
3734.870	.866	*b*1	13	A	19	A	Diff.>error; I, r, direct
3735.327			22	A			
3737.135	.134	*a*1	25	A	25	A	G, g, r; I, r, direct
3738.309	.309		20	A	9	A	
3739.122			2	B			
3739.529		*d*	15	A			
3740.248	.250	*d*	10	B	1	C	
3742.624	.622		5	B	1	C	
3743.365	.366	*b*1	41	A	32	A	G, direct, g
3743.470			3	B			
3744.108	.106	*e*	15	A	1	C	
3745.564	.562	*a*1	38	A	14	A	G, direct, g
3745.902	.904	*a*1	53	A	14	A	G, direct, g, r
3746.488			2	B			
3746.933		*e*?	18	A			
3748.264	.264	*a*1	49	A	22	A	G, direct, g, r; I, r, direct
3748.971		*e*	19	A			
3749.490	.489	*b*1	44	A	23	A	G, direct, g, r; I, r, direct
3751.061			3	C			
3751.822			2	C			
3752.422			2	B			
3753.156			2	C			
3753.615	.614		25	A	15	A	
3754.508		*e*	3	B			
3756.071			3	B			
3756.942	.941		17	A	2	B	
3757.461			6	B			
3758.238	.236	*b*1	48	A	22	A	G, direct, g, r; I, r, direct
3760.053	.054		24	A	12	A	
3760.534	.536		12	B	3	C	G, .524, h, v
3761.418			2	C			
3763.791	.791	*b*1	51	A	26	A	I, r, direct
3765.543	.543	*b*1	16	B	13	A	G, g near
3767.195	.195	*b*1	50	A	28	A	G, direct, g, r; I, r, direct
3768.	.032				1	C	
3773.701		*e*	1	C			

TABLE I—*Continued*

λ		Group	Grating		Interferometer		Remarks
Grating	Interferometer		Plates	Probable Error	Plates	Probable Error	
3774.827....	.827		30	A	6	A	
3775.862....			2	C			
3776.458....	.458		20	A	6	A	
3777.063....			1	C			
3777.450....			6	B			
3778.511....			8	A			
3778.699....			4	B			
3779.488....	.488		2	C	1	B	G, l
3781.189....	.190		4	B	1	B	
3781.940....			2	C			
3782.124....			2	C			
3782.452....			2	C			
3782.610....			1	C			
3785.708....			2	C			
3785.950....	.949		34	A	5	A	
3786.178....			11	C			
3786.679....	.680		32	A	4	A	
3787.166....			2	C			
3787.885....	.885	*b*1	33	A	31	A	G, direct, r
3789.180....			15	A			
3789.430....		*d*	2	C			
3789.572....			5	C			
3790.095....	.097		33	A	16	A	
3790.658....			3	C			
3790.758....			10	B			
3791.506....			3	C			
3792.158....			7	B			
3793.480....			9	B			
3793.874....			11	C			
3794.342....	.342		32	A	4	B	
3795.006....	.005	*b*1	57	A	27	A	G, direct, r
3795.533....			4	C			
3797.518....	.519		37	A	7	A	
3797.950....			2	C			
3798.515....	.514		62	A	29	A	G, direct, g, r
3799.551....	.551		60	A	31	A	G, direct, r
3801.683....	.682		17	A	2	C	
3801.806....			4	C			
3801.977....		*e*	4	C			
3802.285....			5	C			
3804.015....			5	C			
3805.346....	.346		36	A	18	A	
3806.205....		*d*	19	C			
3806.700....	.700		25	A	11	A	
3807.540....	.541		32	A	13	A	

TABLE I—*Continued*

λ		Group	Grating		Interferometer		Remarks
Grating	Interferometer		Plates	Probable Error	Plates	Probable Error	
3808.288			4	C			
3808.733	.733		25	A	2	B	
3810.761			25	B			
3811.894			10	C			
3812.967	.968		37	A	32	A	G, direct, r
3813.061			10	C			
3813.640			17	C			
3814.527	.529		24	A	1	C	
3815.843	.843	*b*1	24	A	23	A	G, r; I, r, direct
3816.342			24	A			
3820.430	.429		53	A	21	A	G, direct, g, r; I, r, direct
3821.181	.183		41	A	11	A	
3821.836			22	B			
3824.076			8	B			
3824.444	.446		25	A	26	A	G, r
3825.406			3	C			
3825.884	.885	*b*1	40	A	24	A	G, g, r; I, r, direct
3826.838			3	C			
3827.574			10	B			
3827.826	.826	*b*1	28	A	27	A	G, g, r
3829.127		*d*	3	B			
3830.759			3	B			
3830.852		*d*	2	C			
3833.312	.314		39	A	7	A	
3834.224	.225	*b*1	32	A	25	A	G, g, r; I, r, direct
3836.334	.334		25	A	7	A	
3837.134			4	C			
3839.260	.259		23	A	9	A	
3840.439	.439		28	A	23	A	G, g, r
3841.051	.052		50	A	23	A	G, direct, g, r
3843.260	.260		26	A	16	A	
3845.694			4	C			
4846.414			12	B			
3846.805	.804		30	A	12	A	
3849.970	.971		32	A	28	A	G, direct, r
3850.821	.821		20	A	21	A	
3852.576	.576		32	A	9	A	
3855.848		*d*	3	C			
3856.372	.374		28	A	29	A	G, g, r; I, r, direct
3859.216	.215		30	A	7	A	G, direct, g, r
3859.915	.914		29	A	22	A	I, r, direct
3861.343			15	B			
3865.529	.527		31	A	32	A	G, direct, r
3867.221	.222		23	A	8	A	
3871.752	.751		14	B	2	C	

TABLE I—*Continued*

λ		Group	Grating		Interferometer		Remarks
Grating	Interferometer		Plates	Probable Error	Plates	Probable Error	
3872.506....	.505		34	A	29	A	G,.direct, g, r
3873.764....	.765		21	A	8	A	
3876.045....			15	A			
3878.023....	.022		26	A	22	A	G, direct, r
3878.576....	.575		24	B	20	A	G, direct, g, r; I, r, direct
3883.284....	.284		11	B	1	C	
3884.363....	.358	*b*	17	B	3	C	
3885.512....	.514	*b*	24	C	4	B	
3886.286....	.285	*a*1	17	C	20	A	G, direct, r; I, r, direct
3887.052....	.055	*b*1	27	B	20	B	G, direct, g, r
3888.518....	.518	*b*1	23	B	29	A	G, direct, g, r
3890.846....		*b*	16	B			
3891.934....	.926	*b*	16	C	3	B	Diff. > error
3893.396....	.396		10	B	5	A	G, direct, g
3893.926....			6	B			
3894.007....			1	C			
3895.660....	.660	*a*1	17	B	30	A	
3897.451....			5	B			
3897.898....		*b*	10	B			
3899.039....		*e*	2	C			
3899.713....	.710	*a*1	14	B	28	A	G, direct, g
3900.521....			6	B			
3902.948....	.950	*b*1	4	A	21	A	G, g
3903.904....		*b*	16	A			
3906.486....	.484	*a*1	13	C	23	A	
3906.750....			12	A			
3907.466....			3	C			
3907.940....	.936	*b*	16	C	6	B	
3909.666....			7	B			
3909.	.832	*b*			2	B	
3910.848....	.847		8	B	2	C	
3913.637....	.637	*b*	13	A	5	A	
3916.737....		*b*	14	B			
3917.186....	.186	*a*	16	A	6	A	
3918.321....			14	B			
3918.420....			13	B			
3918.646....		*b*	14	B			
3919.071....		*b*	13	A			
3920.262....	.260	*a*1	11	B	19	A	
3920.841....		*d*	3	C			
3922.915....	.916	*a*1	11	C	17	A	
3925.648....		*b*	10	B			
3925.945....	.950	*a*1	15	B	5	C	
3927.923....	.924	*a*	18	B	16	A	
3928.087....		*d*	10	B			

TABLE I—*Continued*

λ		Group	Grating		Interferometer		Remarks
Grating	Interferometer		Plates	Probable Error	Plates	Probable Error	
3929.116			3	C			
3929.210			3	C			
3930.301	.300	*a*1	18	C	16	A	G, direct, r
3931.124			6	C			
3932.630	.631	*b*	12	A	3	B	
3932.919			2	B			
3933.608			3	C			
3935.817	.817	*b*	15	B	7	A	
3937.330	.332	*b*	5	B	2	C	
3940.883	.883	*a*	19	B	7	A	
3941.285		*d*	6	C			
3942.445	.444	*b*	10	B	8	A	
3943.341		*b*	4	B			
3944.750			2	C			
3944.892		*b*	6	B			
3945.121		*b*	7	B			
3947.004			7	B			
3947.535		*b*	12	B			
3948.107		*d*	14	B			
3948.780	.781	*b*	15	A	4	B	
3949.958	.958	*b*	15	A	4	A	
3951.168	.172	*b*	15	C	3	C	
3952.607	.607	*b*	15	A	6	A	
3953.158		*b*	9	B			
3955.354		*d*	4	C			
3955.958		*b*	2	C			
3956.463	.459	*b*	9	B	4	B	
3956.681	.682	*b*4	12	A	6	A	
3957.029		*d*	12	A			
3960.286			4	C			
3961.149			4	C			
3963.110		*d*	8	C			
3964.520	.528	*b*	8	C	1	C	
3965.513		*d*	2	C			
3966.067	.067	*b*	14	A	7	A	
3966.632		*e*	13	B			
3966.826		*e*	2	C			
3967.424	.424		4	B	2	B	
3967.966			6	A			
3969.261	.262	*b*1	27	B	11	A	G, direct, r
3969.630			5	B			
3970.264			2	C			
3970.393		*b*	3	C			
3971.327	.327	*b*	20	A	9	A	
3973.657		*b*	5	B			

TABLE I—*Continued*

λ		Group	Grating		Interferometer		Remarks
Grating	Interferometer		Plates	Probable Error	Plates	Probable Error	
3974.399			2	C			
3976.617	.617	*d*	7	B	1	C	
3976.867			6	C			
3977.745	.745	*b*4	14	A	10	A	
3981.776	.777	*b*	16	B	5	B	
3983.963	.961	*b*	15	A	10	A	
3985.395			5	C			
3986.178	.178	*b*	11	B	1	C	
3989.861			5	C			
3990.381		*b*	7	B			
3994.119		*b*	7	C			
3995.201		*d*	2	C			
3995.998		*b*	5	B			
3996.970		*b*	7	C			
3997.396	.396	*b*4	14	A	11	A	
3998.058	.059	*b*	13	A	9	A	
4000.268			2	C			
4000.468		*b*	2	C			
4001.669	.666	*b*	8	C	4	B	
4003.766		*b*	4	B			
4004.834		*b*	2	C			
4004.978		*b*	2	C			
4005.247	.247	*b*1	16	B	13	A	G, direct, r
4006.316		*b*	7	C			
4006.633		*b*	5	C			
4007.279		*b*	14	B			
4009.717	.717	*a*	14	B	11	A	
4013.643			1	C			
4013.824		*b*	5	C			
4014.536	.536	*b*	14	A	9	A	
4017.157	.158	*b*	13	B	4	B	
4018.284			2	C			
4021.871	.872	*b*	8	A	12	A	
4024.111			2	C			
4024.738	.735	*d*	3	C	2	C	
4030.501		*d*	7	B			
4040.652		*e*	2	C			
4044.618	.615	*b*	2	C	3	C	
4045.816	.817	*b*1	7	B	5	A	G, .807 g
4051.925			2	C			
4052.314			2	C			
4062.448	.447	*b*	9	B	11	A	
4063.288		*d*	7	B			
4063.596	.599	*b*1	6	C	7	A	G, .587 g
4066.983	.983	*b*	7	B	5	B	

TABLE I—*Continued*

λ		Group	Grating		Interferometer		Remarks
Grating	Interferometer		Plates	Probable Error	Plates	Probable Error	
4067.276....	.275	*b*	6	C	3	C	
4067.987....	.985	*b*	7	B	3	B	
4070.	.768				2	C	
4071.740....	.743	*b*1	6	C	10	A	G, .733 g
4074.796....			3	C			
4076.234....			2	C			
4076.638....	.638	*b*	4	B	7	A	G, 3057 4th order coincides
4076.812....			2	C			
4078.367....			2	C			
4079.850....		*b*	3	C			
4080.228....		*b*	1	C			
4082.127....			2	C			
4083.782....			2	C			
4084.501....	.500	*d*	7	B	1	C	
4085.013....		*b*	4	B			
4085.314....		*b*	7	B			
4089.227....			2	C			
4091.563....			2	C			
4092.289....			2	C			
4095.980....	.975	*b*	7	C	10	A	
4097.101....			2	C			
4098.186....	.184	*b*	6	C	7	A	
4100.750....	.744		2	C	6	A	
4101.274....		*d*	2	C			
4107.495....	.494	*b*	9	A	16	A	
4109.072....			2	C			
4109.812....	.808	*b*	8	B	13	A	Diff. > error
4112.974....		*d*	2	C			
4114.454....	.450	*b*	6	C	11	A	
4114.959....			2	C			
4118.552....	.550	*b*	18	B	19	A	
4120.215....	.211	*b*	3	C	7	A	
4121.810....	.808		14	B	7	A	
4122.524....	.525	*b*	3	B	7	B	
4123.750....			3	B			
4125.624....		*d*	1	C			
4125.886....			2	A			
4126.193....	.194	*b*	3	B	1	C	
4127.615....	.614		20	B	12	A	
4127.809....			3	B			
4132.061....	.063	*b*1	21	B	17	A	
4132.905....	.906	*b*	6	B	9	A	
4133.871....		*d*	1	C			
4134.684....	.684	*b*4	19	A	18	A	
4136.514....		*d*	6	B			

TABLE I—*Continued*

λ		Group	Grating		Interferometer		Remarks
Grating	Interferometer		Plates	Probable Error	Plates	Probable Error	
4137.006....	.003	*b*	7	B	14	A	⊙ enh Mn
4139.935....		*a*	1	C			
4143.421....	.420	*b*	17	A	10	A	
4143.872....	.874	*b*1	11	B	14	A	
4147.676....	.675	*b*	26	A	14	A	
4149.374....	.374	*e*	8	A	5	B	
4150.260....		*d*	6	C			
4152.173....	.174		8	B	3	C	
4153.907....	.909	*d*	16	A	4	B	
4154.111....			2	C			
4154.505....	.504	*b*	36	A	5	B	
4154.813....	.815	*d*	16	A	1	C	
4156.805....	.804	*b*	32	A	15	A	
4157.792....	.788	*d*	15	B	2	C	
4158.801....	.800	*d*	8	B	4	B	
4170.907....	.906	*b*	31	A	1	C	
4171.698....		*d*	1	C			
4172.128....			7	A			
4172.751....		*a*	7	B			
4173.324....		*b*	6	B			
4173.928....		*a*	6	B			
4174.919....		*a*	18	A			
4175.642....	.642	*b*	43	A	13	A	
4176.574....	.572	*e*	10	B	7	B	⊙ Fe–Mn
4177.599....	.599	*a*	17	B	8	A	
4181.760....	.760	*b*	24	A	21	A	
4182.386....		*b*	4	A			
4184.897....	.896	*b*	35	A	17	A	
4187.047....	.045	*d*	12	A	11	A	
4187.804....	.805	*d*	12	A	11	A	
4191.439....	.438	*d*	12	A	11	A	
4191.687....		*e*?	4	C			
4195.340....	.338	*d*	10	A	4	B	
4195.617....			1	C			
4196.220....		*d*	6	C			
4198.312....	.312	*d*	3	C	11	A	
4198.647....		*d*	5	C			
4199.099....	.101	*b*	31	A	18	A	
4200.932....		*e*	4	C			
4202.033....	.034	*b*1	37	A	18	A	
4203.988....	.990	*b*3	24	A	12	A	
4205.548....			2	C			
4206.704....	.703	*a*	6	B	5	A	
4207.133....	.132	*b*	7	C	5	B	
4208.612....		*b*	7	B			

TABLE I—*Continued*

λ		Group	Grating		Interferometer		Remarks
Grating	Interferometer		Plates	Probable Error	Plates	Probable Error	
4210.355....	.352	c_5	13	A	9	A	Diff.>error
4213.652....	.652	b	8	B	8	A	
4215.432....		b	4	C			
4216.188....	.188	b_3	20	A	20	A	
4217.554....	.552	d	9	B	4	B	
4219.367....	.367	b	36	A	18	A	
4220.348....	.350	b	7	B	1	C	
4222.222....	.221	d	9	B	10	A	
4224.179....	.177	e	22	B	7	B	
4225.463....	.462	d	10	B	1	C	
4225.958....		b	7	B			
4226.428....		b	7	B			
4227.437....	.436	d_5	10	A	11	A	
4229.518....			1	C			
4229.762....			1	C			
4233.142....		d?	2	C			⊙ Mn–Fe
4233.611....	.610	d_5	10	B	11	A	
4235.	.945	d_5			12	A	
4237.164....			2	C			
4238.029....		d?	6	B			
4238.818....	.819	d	10	B	4	B	
4239.849....	.849	a	1	C	1	C	
4240.374....			3	C			
4242.732....			2	C			
4245.264....	.261	b	10	C	2	B	
4246.092....		b	4	C			
4247.436....	.434	d	10	A	7	A	
4248.230....		b	7	B			
4250.128....	.126	c_5	12	C	7	A	
4250.792....	.792	b	42	A	16	A	
4254.337....	.340	d	5	A	3	B	Cr
4258.322....		a	5	B			
4258.621....			1	C			
4258.958....		e	1	C			
4260.482....	.482	c_2	8	B	15	A	
4264.211....		d	1	C			
4265.262....			1	C			
4266.970....	.971	b	7	B	3	B	
4267.831....	.832	b	6	A	3	B	
4268.	.746	b			1	C	
4271.163....	.159	d	7	C	5	C	
4271.766....	.766	b_1	33	B	11	A	
4274.	.802				2	B	Cr
4276.686....		?	1	C			
4278.236....		?	1	C			

TABLE I—*Continued*

λ		Group	Grating		Interferometer		Remarks
Grating	Interferometer		Plates	Probable Error	Plates	Probable Error	
4279.866....		?	1	C			
4282.408....	.408	*b*1	30	A	20	A	
4285.448....	.449	*b*	6	B	4	B	
4288.150....			5	C			
4290.384....			3	C			
4290.872....			2	C			
4291.465....		*a*3	7	B			
4294.130....	.130	*b*2	8	C	19	A	
4298.044....	.042		6	A	4	B	
4299.243....	.242	*d*5	8	B	11	A	
4302.	.193				1	C	
4304.554....			2	C			
4305.454....	.459	*b*	2	C	3	C	Fe, Cr?
4307.908....	.908	*b*1	48	A	7	A	
4309.038....		?	1	C			
4315.090....	.090	*b*3	45	A	19	A	
4321.803....			3	C			
4325.766....	.767	*b*1	52	A	8	A	
4327.103....	.101	*b*	6	B	1	C	
4337.052....	.052	*b*3	47	A	19	A	
4338.262....			1	C			
4343.259....		*d*	4	B			
4343.701....			5	B			
4346.560....	.560		5	B	1	B	
4348.941....		?	1	C			
4351.551....	.551	*b*	6	C	6	A	
4352.739....	.740	*b*3	20	A	20	A	
4358.508....	.506	*b*	6	B	4	B	
4367.582....	.584	*b*	17	A	5	B	
4367.908....		*a*	6	B			
4369.776....	.777	*b*3	30	A	20	A	
4373.563....	.567		5	B	1	C	
4375.934....	.934	*a*3	40	A	26	A	
4383.550....	.550	*b*1		A	8	A	
4387.898....	.900	*b*	6	B	2	C	
4388.414....	.415	*d*?	10	B	2	C	
4389.247....	.246	*a*	7	B	1	C	
4390.955....	.957	*b*	6	B	5	A	
4401.295....		*d*	6	A			
4404.755....	.755	*b*1	45	A	12	A	
4407.715....	.716	*c*4	24	A	7	A	
4408.420....	.420	*c*4	30	A	18	A	
4409.125....		?	1	C			
4415.128....	.128	*b*1	53	A	18	A	
4422.573....	.573	*b*3	40	A	32	A	

TABLE I—*Continued*

λ		Group	Grating		Interferometer		Remarks
Grating	Interferometer		Plates	Probable Error	Plates	Probable Error	
4427.314	.314	*a*3	30	A	38	A	
4430.621	.620	*c*4	35	A	34	A	
4432.574			7	B			
4433.225		*e*	12	A			
4433.795		*d*	6	C			
4435.153		*a*	11	A			
4439.885			7	B			
4442.345	.345	*c*4	11	A	34	A	
4442.837			9	B			
4443.197	.200	*b*3	31	A	32	A	Diff.>error
4446.844		*d*	9	B			
4447.136			4	A			
4447.723	.724	*c*4	32	A	37	A	
4450.323			6	C			
4454.386	.386	*b*3	12	B	28	A	
4454.658		*d*	2	C			
4455.035		?	2	C			Probably Mn
4456.334			3	C			
4459.123	.125	*c*4	27	A	39	A	
4461.656	.656	*a*3	22	A	34	A	
4461.992		*d*	1	C			
4466.556	.557	*b*4	22	A	37	A	
4469.386	.384	*d*	5	B	18	A	
4472.724		?	3	C			
4476.026	.023	*b*4	16	C	29	A	Double in vacuum. Cf. *Astrophysical Journal*, 44, 331, 1916.
4479.615			4	A			
4480.145			5	B			
4481.624			3	C			
4482.	.174	*a*			14	A	G, too close; I, meas. at orders 22250, 32890
4482.	.260	*a*			14	A	
4484.231	.229	*d*	4	B	13	A	
4485.681	.682	*e*?	5	A	4	B	I, h
4488.143			3	B			
4488.920			2	C			
4489.745	.744	*a*3	13	A	23	A	
4490.087	.087		3	B	2	C	⊙ Mn–Fe; I, fringes poor
4490.776			5	B			
4494.572	.570	*c*4	40	A	38	A	
4495.569		*d*	1	C			
4495.969			3	B			
4504.841		*d*	1	C			
4514.192	.191		8	A	2	B	
4517.533	.532		11	A	4	B	
4523.406			3	A			
4525.148	.146	*d*?	5	A	22	A	

TABLE I—*Continued*

λ		Group	Grating		Interferometer		Remarks
Grating	Interferometer		Plates	Probable Error	Plates	Probable Error	
4526.566....			1	C			
4528.622....	.620	*c*4	29	A	29	A	
4531.155....	.155	*b*3	28	A	31	A	
4531.636....		*d*	2	A			
4537.680....			1	C			
4547.025....			3	B			
4547.853....	.853	*b*	29	A	22	A	
4549.473....			5	B			
4550.788....		*d*	3	B			
4552.548....	.547		7	B	1	C	
4556.130....	.134	*e*?	24	A	22	A	⊙ Fe–Cr
4556.942....			1	C			
4558.111....			1	C			
4560.099....		*d*	1	C			
4566.523....			3	B			
4574.728....	.726		7	B	2	B	
4581.520....	.519	*d*	3	C	2	B	
4583.838....			3	B			
4587.135....			4	B			
4592.658....	.658		13	A	28	A	
4595.367....	.365		5	B	1	C	
4696.069....			5	B			
4598.125....		*d*	3	B			
4600.940....			2	C			
4602.009....	.007		5	A	4	A	
4602.947....	.947		17	A	30	A	
4607.659....	.657	*d*	5	A	7	A	
4611.289....	.288	*d*	5	A	14	A	
4613.212....	.214	*d*	3	B	2	B	
4614.219....			1	C			
4618.768....			4	A			
4619.297....	.297		5	A	10	A	
4625.057....	.055	*d*	5	B	10	A	
4630.127....	.128		5	A	10	A	
4632.917....	.918		5	A	14	A	
4635.849....			3	B			
4637.516....	.513	*d*	3	B	4	A	
4638.018....	.019	*b*	18	A	6	A	
4643.471....	.471		5	B	6	A	
4647.439....	.440	*b*	17	A	28	A	
4654.504....	.504	*b*	3	B	6	A	
4654.632....	.629	*d*	3	C	4	B	
4661.541....			1	C			
4661.978....			3	A			
4663.186....			1	C			

TABLE I—*Continued*

λ		Group	Grating		Interferometer		Remarks
Grating	Interferometer		Plates	Probable Error	Plates	Probable Error	
4667.462	.461	*b*	5	B	14	A	
4668.144	.145	*d*	5	A	10	A	I, h
4669.177	.177		5	A	2	C	I, h
4673.172	.171		18	A	4	B	
4678.856	.854				25	A	
4680.300			2	C			
4682.114			2	C			
4683.568			3	C			
4687.390			2	C			
4689.498			2	C			
4690.149			3	C			
4691.417	.417		18	A	22	A	
4700.174		*d*	1	C			
4701.055			6	C			
4704.962	.960		7	B	1	C	I, h
4705.467		?	4	C			
4707.283	.283	*d*	6	B	16	A	
4707.490			7	B			
4709.005		*d*	5	C			
4710.288	.288	*b*	22	A	16	C	
4721.000			5	C			
4727.408		*d*	6	B			
4728.	.558				6	B	
4729.031		*e*	1	C			
4731.494			6	C			
4733.598	.598	*a*	9	A	12	A	
4734.103			3	C			
4735.849			9	B			
4736.782	.782	*d*	7	B	20	A	
4737.636			4	C			
4740.346			4	B			
4741.084			3	C			
4741.534	.535	*b*	9	A	8	A	
4745.807	.809	*b*	4	B	6	A	
4757.585			7	A			
4771.705			2	C			
4772.818	.819	*b*	7	A	4	B	
4779.447			3	C			
4786.813	.812	*b*	28	A	12	A	
4788.760			6	B			
4789.656	.655	*b*	22	A	15	A	
4800.655			1	C			
4802.886			2	C			
4832.737			1	C			
4838.522			1	C			

TABLE I—*Continued*

λ		Group	Grating		Interferometer		Remarks
Grating	Interferometer		Plates	Probable Error	Plates	Probable Error	
4839.552....			2	C			
4843.158....			2	C			
4855.686....			2	C			
4859.750....	.750	*c*5	4	A	16	A	
4863.656....			2	C			
4871.327....	.327	*c*5	4	B	23	A	
4872.145....	.147	*c*5	3	A	18	A	
4878.220....	.220	*c*5	4	A	12	A	
4881.729....			2	C			
4882.154....		*d*	2	C			
4885.438....			3	B			
4886.338....			3	C			
4890.764....	.765	*c*5	3	B	23	A	
4891.503....	.501	*c*5	2	C	20	A	
4903.319....	.319	*d*	4	A	10	A	I, fringes poor
4909.390....		?	2	C			
4910.030....		?	3	C			
4910.331....		?	2	C			
4910.573....		?	2	C			
4918.998....	.001	*c*5	3	C	21	A	
4920.510....	.513	*c*5	2	B	23	A	
4924.776....	.775	*b*	16	A	2	B	
4938.820....	.823	*d*	5	B	5	B	
4939.247....		?	1	C			
4939.690....	.692	*a*	10	B	8	A	
4946.396....	.398	*d*	6	C	1	C	
4950.115....		*d*	2	C			
4957.305....		*c*5	3	C			
4957.603....	.605	*c*5	7	C	6	B	
4966.097....	.099	*d*	3	B	6	A	
4967.902....		*e*	2	C			
4969.930....		*d*	2	C			
4973.111....		*d*	2	C			
4978.609....		*d*	2	C			
4982.510....		*d*	3	B			
4983.261....		*d*	3	B			
4983.858....		*d*	3	B			
4985.264....		*d*	3	B			
4985.556....		*d*	4	C			
4988.966....		*d*	3	C			
4991.280....		*d*	2	C			
4994.135....	.136	*a*	50	A	10	A	
5001.873....	.873	*d*	8	B	6	A	
5002.802....		?	3	C			
5005.722....	.722	*d*	7	A	1	C	

TABLE I—*Continued*

λ		Group	Grating		Interferometer		Remarks
Grating	Interferometer		Plates	Probable Error	Plates	Probable Error	
5006.129....	.128	*d*	7	A	8	A	
5007.291....		*d*	4	A			
5012.074....	.074	*a*	6	A	23	A	
5014.952....	.953	*d*	7	B	3	B	
5018.440....			6	B			
5022.247....	.245	*d*	6	C	1	C	
5027.138....		*d*	4	B			
5028.131....			7	C			
5041.076....	.077	*a*	24	A	6	B	
5041.761....	.760	*a*	31	A	10	A	
5049.827....	.827	*a*	30	A	14	A	
5051.640....	.640	*a*	32	A	12	A	
5065.022....		*e*	1	C			
5068.776....	.775	*d*	4	B	5	B	
5074.759....		*e*	4	B			
5079.228....		*b*	19	A			
5079.744....		*a*	23	B			
5083.344....	.343	*a*	17	B	7	A	
5097.000....		*e*	1	C			
5098.705....	.705	*b*	42	A	3	B	
5107.454....		*a*	22	A			
5107.647....		*a*	22	A			
5110.415....	.416	*a*	18	A	7	A	
5123.727....	.725	*a*	20	B	5	B	
5125.132....	.131	*d*	4	C	1	C	
5127.367....	.365	*a*	21	B	4	B	
5131.477....		*a*	2	C			
5133.696....	.692	*e*	4	C	6	B	Pole-effect extreme; I, fringes poor
5137.390....		*d*	3	C			
5139.262....		*d*	5	C			
5139.470....		*d*	5	C			
5142.543....			3	C			
5142.935....	.933	*a*	21	A	1	C	
5150.846....	.844	*a*	30	A	5	B	
5151.918....	.916	*a*	18	B	4	B	
5162.290....	.290	*d*	5	C	2	B	Pole-effect extreme; I, fringes poor
5165.424....		*d*	1	C			
5166.289....	.288	*a*	7	B	2	B	
5167.492....	.492	*a*	25	A	26	A	
5168.904....	.902	*a*	4	C	1	C	
5171.601....	.600	*a*	31	A	18	A	
5191.461....	.463	*d*	5	A	12	A	
5192.351....	.351	*d*	5	B	12	A	
5194.946....	.946	*d*	6	A	11	A	
5195.479....		*e*	7	C			

TABLE I—*Continued*

λ		Group	Grating		Interferometer		Remarks
Grating	Interferometer		Plates	Probable Error	Plates	Probable Error	
5198.713....	.716	*a*	4	B	4	B	
5202.340....	.341	*a*	38	A	7	A	
5204.582....	.586	*a*	2	C	1	C	Fe, Cr?
5208.601....	.605	*d*	4	B	3	C	
5215.187....		*d*	4	B			
5216.280....	.280	*a*	35	A	3	B	
5217.397....		*d*	4	C			
5226.870....		*d*	4	B			
5227.192....	.194	*a*4	36	A	8	A	
5229.859....		*d*	4	C			
5232.946....	.949	*d*5	4	B	21	A	
5242.497....	.496	*a*	17	B	3	B	
5250.652....	.652		15	A	3	B	
5263.316....	.316	*d*	4	A	1	C	
5266.033....		*d*	3	A			
5266.562....	.564	*d*5	13	C	19	A	
5269.540....	.541	*a*1	54	A	14	A	
5270.360....	.362	*a*4	4	B	19	A	
5273.381....		*b*	1	C			
5281.800....	.800	*d*	4	B	7	A	
5283.627....	.629	*d*	4	B	9	A	
5302.	.308	*d*			5	A	
5307.	.367	*a*			3	B	
5324.186....	.188	*d*5	4	C	22	A	
5328.044....	.044	*a*1	4	A	15	A	
5328.537....	.535	*a*4	4	B	11	A	I, fringes poor
5329.996....		*a*	1	C			
5332.906....	.904	*a*4	15	C	3	B	
5339.938....	.939	*d*5	3	B	6	A	
5341.029....	.027	*a*4	4	B	17	A	
5364.881....		*e*	3	B			
5365.405....		*a*	3	B			
5367.475....	.475	*e*	3	C	7	B	
5369.976....	.967	*e*	3	B	8	B	Diff.>error
5371.495....	.494	*a*1	20	A	18	A	
5379.582....		*a*	1	C			
5383.378....	.376	*e*	3	C	15	B	
5393.179....	.176	*d*5	3	B	8	A	
5397.136....	.133	*a*4	4	B	31	A	
5400.512....	.510	*e*	3	C	1	C	
5404.149....	.144	*e*	3	B	15	B	Diff.>error
5405.780....	.780	*a*4	20	A	30	A	
5410.918....	.916	*e*	3	B	13	B	
5415.208....	.204	*e*	3	B	15	B	
5424.071....	.072	*e*	3	B	16	B	

TABLE I—*Continued*

λ		Group	Grating		Interferometer		Remarks
Grating	Interferometer		Plates	Probable Error	Plates	Probable Error	
5429.702....	.701	a_4	20	A	20	A	
5434.529....	.528	a_4	20	A	32	A	
5445.048....	.046	e	3	C	3	B	
5446.920....	.921	a_4	44	A	21	A	
5455.616....	.615	a_4	4	C	22	A	
5462.972....		e	3	C			
5463.284....		e	3	C			
5466.406....		d	1	C			
5473.912....	.909	d	3	C	1	C	
5476.300....		a_4	2	C			
5476.573....	.574	d_5	3	A	5	B	
5497.522....	.521	a_3	48	A	20	A	
5501.470....	.470	a_3	48	A	17	A	
5506.784....	.783	a_3	48	A	21	A	
5535.419....		a_4	24	A			
5543.930....		d	1	C			
5554.894....	.893	e	3	C	1	C	
5563.605....		d	3	C			
5565.708....	.710	e	4	B	1	C	
5569.627....	.627	d_5	3	C	20	A	
5572.849....	.851	d_5	3	C	20	A	
5576.095....	.098	d_5	3	C	12	A	
5586.765....	.765	d_5	3	C	26	A	
5598.305....	.302	e	3	C	1	C	
5602.955....	.955	d_5	3	C	9	A	
5615.653....	.653	d_5	3	C	24	A	
5624.548....	.551	d_5	3	C	17	A	
5638.269....	.269	d_5	1	C	2	C	
5658.826....	.826	d_5	3	C	8	A	
5662.	.523	d			5	B	
5701.	.553	?			2	C	
5731.	.771	?			2	C	
5752.	.043	?			1	C	
5753.	.136	d			4	B	
5775.	.090	d			2	C	
5956.	.702	b			2	C	
5975.354....	.356	b_4	35	A	3	C	
6027.059....	.058	b_4	35	A	10	A	
6042.	.092	e			4	B	
6065.492....	.491	b_4	35	A	13	A	
6127.912....	.915	b	31	A	4	B	
6136.625....	.623	b_4	40	A	22	A	
6136.999....		b	26	A			
6137.701....	.703	b_4	20	A	22	A	
6157.731....	.736	b_4	31	B	10	A	Diff. > error

TABLE I—*Continued*

λ		Group	Grating		Interferometer		Remarks
Grating	Interferometer		Plates	Probable Error	Plates	Probable Error	
6165.366....	.366	*b*	36	A	3	B	
6173.342....	.344	*b*4	38	A	10	A	
6191.568....	.568	*b*4	40	A	22	A	
6200.322....	.324	*b*4	30	A	8	A	
6213.438....	.440	*b*4	40	A	18	A	
6215.	.152	*b*4			3	B	
6219.289....	.291	*b*4	51	A	20	A	
6230.734....	.734	*b*4	40	A	20	A	
6240.	.656	?			2	C	
6252.568....	.566	*b*4	40	A	21	A	
6254.268....	.267	*b*4	40	A	20	A	
6256.	.373	*b*			17	A	
6265.145....	.145	*b*4	40	A	20	A	
6270.	.238	*b*			4	B	
6280.	.627	*a*			9	A	
6290.	.975	*e*?			3	C	
6297.801....	.807	*b*4	40	B	16	B	Diff.>error
6315.312....	.319	*b*	36	B	1	C	Diff.>error
6318.028....	.029	*b*4	40	A	22	A	
6322.694....	.698	*b*	40	B	11	B	Diff.>error
6335.341....	.344	*b*4	40	A	22	A	Diff.>error
6344.159....	.162	*b*	8	B	4	B	
6355.039....	.042	*b*	16	B	9	A	
6358.	.701	?			7	B	
6380.	.755	*b*			3	C	
6393.612....	.612	*b*4	40	A	2	A	
6421.363....	.361	*b*	30	A	21	A	
6430.859....	.859	*b*4	40	A	20	A	
6462.	.738	*b*			7	B	
6469.	.220	?			1	C	
6475.	.641	*b*			3	B	
6494.993....	.994	*b*4	40	A	23	A	
6518.	.383	*b*			3	B	
6546.	.253	*b*			22	A	
6569.	.236	?			2	C	
6575.	.030	*b*			2	C	
6592.	.927	*b*			20	A	
6609.	.125	*b*			3	B	
6663.	.457	*b*			11	A	
6678.	.003	*b*4			21	A	
6750.	.166	*b*			4	B	

VI. DISCUSSION

a) *Agreement with standards.*—Eighty-three secondary standards were measured with the interferometer, of which 64 belong to groups of stable lines and 19 to groups *c*5 and *d*. For the 64 stable lines the differences, secondary standards *minus* Mount Wilson, are as follows:

0.000A for 24 lines; ±0.001A for 29; ±0.002A for 8; ±0.003A for 2; +0.004A for λ4076.

The sum of the positive differences is +0.030 A, of the negative differences A −0.025. For the 19 standards of groups *c*5 and *d* the mean difference, secondary standards *minus* Mount Wilson, is +0.007 A, a difference due to pole-effect in the sources used in the original determinations of the secondary standards. It is unfortunate that such differences are involved in the adopted secondaries. It will lead to a series of iron standards and a series of iron wave-lengths differing from each other, unless revised values based on a source measurably free from pole-effect are soon substituted for those adopted.

b) *Questioned standards.*—Questions have been raised by different observers about the lines in the subjoined list. The difficulties encountered are in the majority of cases due to the characteristics of the 6-mm, 6-amp. arc which does not produce these lines fine and sharp enough for satisfactory measurement with the interferometer. With the exception of λ 3556 and λ 4076 for which the adverse criticism is general and apparently justified by the character of the lines or of their immediate surroundings, these lines are measurable with high precision in the 12-mm, 5-amp. arc, as they then permit the use of a satisfactory order of interference.

c) *Ghosts and reversals.*—The long exposures used in the grating series to obtain the weak lines brought out ghosts of the very strong lines. These were measured and the wave-lengths of the lines calculated from the positions of the ghosts, and when possible settings were made upon the primary line, "direct measure." The gratings were made on the Rowland ruling engine, whose spacing wheel has 750 teeth. All reversals were measured and for some

lines the wave-lengths were found in all three ways. The wave-lengths from these separate determinations have been compared with the Mount Wilson interferometer wave-lengths, obtained from

	Remarks	Authority
λ 3513.....	Not sharp in 6-mm, 6-amp. arc	Bureau of Standards
	Good in 12-mm, 5-amp. arc	Mount Wilson
	Discrepancy of 0.006 A	Viefhaus*
λ 3556.....	Little wgt., poor in 6-mm, 6-amp. arc	Bureau of Standards
	Low wgt., p.e. large, shaded to red	Mount Wilson
	Meas. difficult, weak line to violet	Viefhaus
	Companion to red and violet	Goos†
λ 3677.....	Poor in 6-mm, 6-amp. arc	Bureau of Standards
	Good in 12-mm, 5-amp. arc	Mount Wilson
λ 3850.....	Not sharp in 6-mm, 6-amp. arc	Bureau of Standards
	Good in 12-mm, 5-amp. arc	Mount Wilson
λ 3865.....	Very poor in 6-mm, 6-amp. arc	Bureau of Standards
	Broad in 6-mm, 6-amp. arc	Goos
	Good in 12-mm, 5-amp. arc	Mount Wilson
λ 3906.....	Very poor in 6-mm, 6-amp. arc	Bureau of Standards
	Very discordant in grating measures	
	Good in 12-mm, 5-amp. arc	Mount Wilson
λ 4076.....	Very poor in 6-mm, 6-amp. arc	Bureau of Standards
	Poor, λ 3057 4th order coincides in 3d	Mount Wilson
	Difficult, shaded to violet and red	Viefhaus
λ 4191.....	Very poor in 6-mm, 6-amp. arc	Bureau of Standards
	d line good in 12-mm, 5-amp. arc	Mount Wilson
λ 4233.....	Very poor in 6-mm, 6-amp. arc	Bureau of Standards
	d line good in 12-mm, 5-amp. arc	Mount Wilson
λ 4736.....	No wgt. in 6-mm, 6-amp. arc	Bureau of Standards
	d line good in 12-mm, 5-amp. arc	Mount Wilson
λ 5167.....	Poor in 6-mm, 6-amp. arc	Bureau of Standards
	Good in 12-mm, 5-amp. arc	Mount Wilson
λ 5266.....	0.003 A > international value, 6-mm, 6-amp. arc	Bureau of Standards
	d line good in 12-mm, 5-amp. arc	Mount Wilson
λ 5371.....	Not sharp in 6-mm, 6-amp. arc	Bureau of Standards
	Good in 12-mm, 5-amp. arc	Mount Wilson
λ 6678.....	No wgt. in 6-mm, 6-amp. arc	Bureau of Standards
	Good in 12-mm, 5-amp. arc	Mount Wilson

* *Zeitschrift für wissenschaftliche Photographie*, **13**, 209, 245, 1914.

† *Astronomische Nachrichten*, **199**, 33, 1914.

weaker exposures upon the center of a somewhat leaner arc giving very fine lines. The results of the comparisons for some threescore lines are: mean difference, ghosts *minus* interferometer, −0.0004 A, reversals *minus* interferometer, −0.0002 A, "direct measures" *minus* interferometer, +0.0020 A.

From the close agreement of the wave-lengths given by reversals and ghosts with those from the interferometer it is evident that the reversals and ghosts correspond to the lines when produced in the core of a lean arc and hence that the absorbing centers in the cooler outer vapor producing the reversals have the same period as the emitting centers in the core of the arc, and that the maximum of the line, to which the ghosts correspond, is not displaced by the strong exposure. The excess of 0.002 A given by the direct measures indicates a slight unsymmetrical widening for such over-exposed lines, in general toward the red. This characteristic renders them of doubtful utility as standards when unreversed, unless produced in a lean arc. As under special circumstances strong lines only may be available for reference, the reliability of the wave-lengths given by ghosts or reversals may prove useful.

VII. COMPARISONS WITH BUREAU OF STANDARDS

a) *Stable lines as a whole.*—Approximately 250 stable lines are common to the interferometer measures[1] of the Bureau of Standards and the Mount Wilson lists. For the Mount Wilson interferometer measures *minus* the Bureau of Standards, the sum of the positive differences is +0.187 A, the sum of the negative differences −0.162 A, the mean difference ±0.0014 A, the systematic difference +0.0001 A. For the Mount Wilson grating measures *minus* the Bureau of Standards, the sum of the positive differences is +0.202 A, the sum of the negative differences −0.184 A, the mean difference ±0.0015 A, and the systematic difference again +0.0001 A.

b) *Stable lines by spectral regions.*—From Table II it is seen that for the interferometer measures there is good agreement except in the region to the red of λ 6200. Here the Mount Wilson wave-lengths average 0.001 A longer than the measures of the Bureau of

[1] Burns, Meggers, and Merrill, *Bulletin of the Bureau of Standards*, 13, 245, 1916.

Standards. This lack of agreement probably arises from the paucity of standards in the orange-red region and slight variations in drawing the correction-curves.

The Mount Wilson grating wave-lengths appear to be systematically too small for the region λ 3373–λ 3500 compared with both interferometer series. This, however, is due to the inclusion of a few lines showing large negative differences; and whenever the systematic difference approximates 0.001 A, it would fall well below that limit by omitting two or three lines of low weight.

c) Unstable lines of groups c5 and d.—There are 46 lines of groups *c*5 and *d* common to the Bureau of Standards and Mount Wilson interferometer series. For these the Bureau of Standards wave-lengths obtained with the central zone of the 6-mm, 6-amp. arc adopted at Bonn[1] are systematically longer than those made with the central zone of a 12-mm, 5-amp. arc. The average difference Bureau of Standards *minus* Mount Wilson is +0.007 A. There are 34 other lines of the same groups common to the Mount Wilson interferometer series and the grating measures by Burns.[2] For these lines the average difference Burns *minus* Mount Wilson is +0.008 A. From this it appears that the source adopted at Bonn exhibits nearly the same degree of pole-effect as the arc used originally by Burns. In their paper Burns, Meggers, and Merrill say: "The region λ 3500 A to λ 4200 A was observed with both 4 and 6 amperes, but no differences in wave-length were detected as a result of the increased current strength."[3] Unfortunately for such a test, unstable lines are relatively rare in this region, and they observed only one such line, viz., λ 4191. Of this they say[4] that it could be measured only with a low order of interference and had little weight in the final results. Their wave-length for it differs by 0.003 A from the international value. In saying that interferometer observations under the conditions used by them were found to be reasonably free from the effects of pole-shifts, they seem to have had in mind not absolute effects, but

[1] *Transactions of the International Union for Co-operation in Solar Research*, 4, 59, 1914.

[2] *Lick Observatory Bulletin*, 8, 27, 1913.

[3] *Loc. cit.*, p. 247. [4] *Ibid.*, p. 261.

rather that the arc used by them did not differ greatly from the average arc with which the secondary standards were originally obtained. This agrees with the Mount Wilson observations which show that the secondary standards of groups *c*5 and *d* are contaminated by pole-effect to practically the same degree as the Bureau of Standards measurements of lines of these groups. That the measurement of these lines in the 6-mm, 6-amp. arc is difficult and relatively uncertain is shown by the Bureau of Standards measures; for 12 secondary standards belonging to groups *c*5 and *d* the mean difference, Bureau of Standards *minus* International, is

TABLE II

MOUNT WILSON *minus* BUREAU OF STANDARDS BY SPECTRAL REGIONS

REGION	INTERFEROMETER		GRATING	
	Number of Lines	Systematic Difference	Number of Lines	Systematic Difference
3370–3500	23	+0.0003 A	30	−0.0013 A
3500–3600	17	0.0000	18	+0.0006
3600–3700	16	+0.0005	15	+0.0006
3700–3800	13	+0.0001	16	+0.0003
3800–3900	12	−0.0004	12	+0.0001
3900–4000	11	−0.0005	13	−0.0003
4000–4200	18	−0.0006	19	+0.0010
4200–4400	18	−0.0006	18	−0.0003
4400–4600	22	−0.0001	23	+0.0002
4600–4800	15	−0.0003	18	−0.0003
4800–5200	19	+0.0006	22	+0.0009
5200–5700	22	0.0000	24	+0.0008
6000–6200	12	−0.0001	10	−0.0011
6200–6500	24	+0.0010	17	−0.0003
6500–6750	8	+0.0010		

+0.0012 A, while for stable standards it is 0.0000 A. and in their list of secondary standards differing by more than 0.001 A from International values, half of the lines belong to groups *c*5 and *d*, though they form only one-fifth of the total number of secondary standards.

d) *Intensity effect.*—Burns, Meggers, and Merrill were of the opinion that for lines weaker than the standards the grating gives wave-lengths different from those obtained by the interferometer, but that the wave-lengths obtained by the latter instrument are free from an intensity effect. In the present series of grating measures an effort was made to obtain as many of the weaker

lines as possible. The lines common to this series and the Bureau of Standards list have been compared in three groups, intensities 1–3, 4–5, and stronger than 6.

It is evident from results given in Table III that in the Mount Wilson grating series the wave-lengths of lines weaker than the standards show no systematic deviation from the Bureau of Standards interferometer values depending upon line-intensity. There is, moreover, no systematic difference between the Mount Wilson grating and interferometer measures for weak lines, or between the interferometer measures for strong and weak exposures.

e) *Grating and interferometer.*—As to the use of both grating and interferometer in obtaining relative wave-lengths as suggested by the American committee, we have found the practical advantage

TABLE III

BUREAU OF STANDARDS INTERFEROMETER *minus* MOUNT WILSON GRATING

	INTENSITIES					
	1–3		4–5		6 and Above	
Positive differences.....	+0.069	36 lines	+0.077	43 lines	+0.021	12 lines
Negative differences.....	−0.079	33 lines	−0.068	39 lines	−0.038	21 lines
Zero differences.....	0.000	17 lines	0.000	33 lines	0.000	12 lines
Mean differences.....	±0.0017	86 lines	±0.0013	115 lines	±0.0013	45 lines
Systematic differences...	−0.0001	86 lines	+0.0001	115 lines	−0.0004	45 lines

to be the detection of accidental errors, to which attention was directed by occasional marked disagreement between the results from the two methods, rather than the elimination of complementary errors. Even with optically perfect instruments each method has in practice both advantages and disadvantages.

For the interferometer the main points of superiority are: (1) the long range of spectrum on each plate, allowing the use of many standards or the bridging of wide gaps between standards; (2) the wide variation of resolving power without loss in extent of spectrum; (3) the moderate sensibility to instrumental disturbances; and (4) the less exacting character of the necessary microscopic measurements. The disadvantages are: (1) the integrating effect introduced by diaphragms with relatively large openings in front of the etalon; (2) the loss in separation of close lines due to coincidences

and the low auxiliary dispersion usually employed; (3) the loss of light due to absorption in the metal film; and (4) the necessity of applying the correction for phase-change.

For the grating spectrograph the advantages are: (1) the easily obtained high dispersion combined with great resolution for spectral regions rich in lines; (2) the relative ease, in practice, with which faint lines may be obtained; (3) the simplicity of the instrumental equipment; and (4) the great analyzing power in forms free from astigmatism. Its disadvantages are: (1) the extreme sensitiveness to instrumental disturbances; (2) the difficulties involved in obtaining the necessary degree of perfection in the illumination; (3) the narrow spectral range under high dispersion, limiting the number of available standards; and (4) the higher precision required in the measurement of the spectrograms.

The theoretical advantages of the two instruments are well compared by Dr. Sparrow as follows:

> The defects of the gratings are fixed. If we have a good instrument we can make measurements as good as the best; if it is defective a definite limit is set to the accuracy of all our measurements. With the interferometer a good pair of plates may become defective through rotating one of them, or through tarnish or non-uniformity of the silver film; on the other hand, we may more or less average out the errors of a defective pair by this process, since each silvering or change of position makes virtually a new pair of plates.[1]

In the present investigation we have used three pairs of glass interferometer plates by Jobin and a pair of fused quartz by Hilger. The plates were several times resilvered with films of high uniformity, and were frequently changed in relative angular position. In no case was a plate used on which there appeared any evidence of tarnish or variable thickness of metal. Five high-quality gratings, two by Michelson and three by Anderson, were used in obtaining the grating series of spectrograms. As the apparent distribution of intensity in a spectral line depends upon the peculiarities of the ruling engine and the particular conditions under which each grating is produced, it is plainly an advantage in eliminating any resultant systematic errors to use gratings ruled upon two types of engine and under different circumstances for the

[1] *Astrophysical Journal*, 49, 95, 1919.

two types. In view of the diversity of instrumental equipment employed, it is probable that defects inherent in the particular instruments, whether interferometers or gratings, play a minor rôle in both series of measures.

Moreover, the absence of systematic effects depending upon line-intensity, the precautions taken to avoid errors due to pole-effect, and the substantial agreement shown by the wave-lengths in the two series lend weight to the results. It is perhaps not too much to hope that, for lines common to our two lists and having probable errors marked A or B, the weighted mean wave-length will be found accurate to one unit in the third decimal place.

Assistance in measurement and reduction has been given by Mrs. A. H. Joy, who as Miss Burns was formerly a member of the computing division, by Miss A. M. Brayton, by Miss A. L. Miller, and by Miss L. M. Keener. For their interested co-operation and efficient work we wish to express our appreciation.

Mount Wilson Observatory
November 1920

ON THE ABSORPTION SPECTRUM OF HYDROGEN CHLORIDE

By WALTER F. COLBY and CHARLES F. MEYER

ABSTRACT

Hydrogen-chloride absorption band, 3.16 to 3.70 μ.—Because of the great theoretical interest attached to the absorption spectrum of HCl, the authors have undertaken to add experimental data. For most of the observations an absorption chamber 60 cm long which could be heated to incipient redness was used, since Paton had found that as the temperature is raised the number of observable lines is increased while there is no *shift due to temperature*. These results were confirmed. The mean *wave-numbers for 28 lines*, 20 of which have shorter wave-lengths than the center of the group, are given in Table I. The *law of spacing* is not parabolic, as has been supposed, but a cubic term is found to be necessary. The wave-numbers are given by the equation $\nu = 28{,}863.60 + 205.82\ n - 3.082\ n^2 - 0.0165\ n^3$, the mean difference between observed and calculated being 2. The cubic term cannot be due to overlapping of lines at the base. The results obtained by Paton at 250° C. have been reduced. An explanation of the deviations from Imes's results is suggested. Only slight evidence of the *existence of a satellite* on the long-wave-length side of each line was obtained. No compensation chamber was used in these experiments, as a direct test showed it to be superfluous.

The absorption of hydrogen chloride falls into two regions, one extending from 3.35 μ to 3.85 μ (see Fig. 1*b*), and the other from 1.73 μ to 1.83 μ (Fig. 1*a*). The second region falls at approximately twice the frequency of the first and is less intense, whence it has come to be known as the "harmonic," and the first as the "fundamental." In each region the absorption consists of numerous lines, regularly but not uniformly spaced. The only precise measurements which have been made upon these lines were made by Imes,[1] who worked with the absorbing gas at room temperature, as did previous investigators.[2]

Some work on the "fundamental" carried out by Mr. Paton,[3] with the absorbing gas at a temperature of 250° C., showed that as the temperature of the gas was raised, the individual lines retained

[1] *Astrophysical Journal*, **50**, 251, 1919.

[2] Brinsmade and Kemble, *Proceedings of the National Academy of Sciences*, **3**, 420, 1917, and Eva v. Bahr, *Verhandlungen der deutschen physikalischen Gesellschaft*, **15**, 1150, 1913.

[3] *Physical Review*, **15**, 541, 1920.

their position as nearly as could be measured, but that through a redistribution of intensities of absorption the number of observable lines was increased. This was to be expected on the basis of the rotational theory now commonly held for this type of absorption.

The absorption spectrum of hydrogen chloride is of great theoretical interest, and for this reason the authors have undertaken to add to experimental data existing upon it. The present paper deals with what has thus far been done upon the "fundamental." Certain points which are of interest have been established, but other points remain unestablished, and no work has yet been done upon the "harmonic." It is hoped to do something

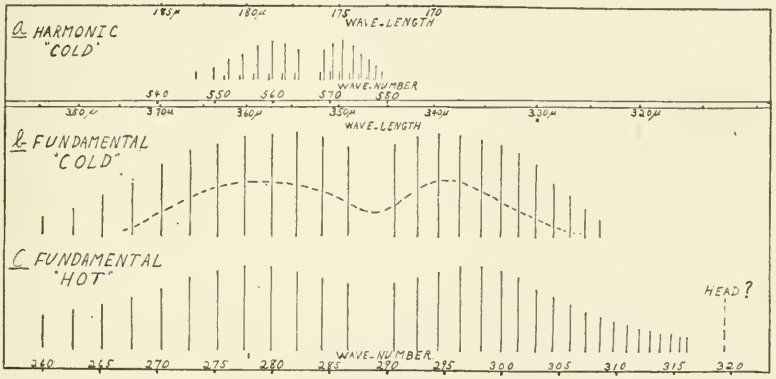


FIG. 1

more in the future with hydrogen chloride and with the other hydrogen halides.

The apparatus is similar to that used by Imes, and we have used the same 7500-line grating. The absorption chamber consists of a tube of high-temperature glass kindly furnished by the Libby Glass Company. It is 60 cm long and 8 cm in internal diameter and is provided with mica windows. Provision is made for heating electrically, and when working with the gas "hot," the tube was heated to a glow which could be just seen in a darkened room.

Some measurements have also been made with the gas "cold" (room temperature), some with the 60 cm chamber, some with

Imes's chamber 16 cm long, and some using a still shorter chamber 4 cm long.

The wave-lengths of twenty lines on the side of the center toward short wave-lengths, and eight lines on the opposite side of the center have been measured. The center is marked by the absence of one line in the otherwise regular spacing. The lines on the side of short wave-lengths were measured first, and when plotting between n, the number of the line counted from the center, and ν, the wave-number, it was possible to fit these lines so closely to a parabola that it was believed that the spacing of the entire band would be represented by a parabola. This belief

TABLE I

n	ν Measured	ν Computed	Difference	n	ν Measured	ν Computed	Difference
−8	27031.	27028.	3.	7	30148.	30148.	0.
−7	278.	277.	1.	8	309.	305.	4.
−6	520.	521.	−1.	9	453.	454.	−1.
−5	760.	760.	0.	10	597.	597.	0.
−4	991.	992.	−1.	11	732.	733.	−1.
−3	28217.	28219.	−2.	12	858.	861.	−3.
−2	437.	440.	−3.	13	984.	982.	2.
−1	652.	655.	−3.	14	31095.	31096.	−1.
1	29065.	29066.	−1.	15	198.	202.	−4.
2	265.	263.	2.	16	298.	300.	−2.
3	456.	453.	3.	17	388.	391.	−3.
4	636.	637.	−1.	18	481.	474.	7.
5	816.	814.	2.	19	554.	549.	5.
6	986.	984.	2.	20	615.	616.	−1.

was expressed in a paper given before the Physical Society at Cleveland last November. But when the eight lines on the other side were measured, it was found that these rapidly deviated from this parabola, and a little consideration made it clear that it would not be possible to fit a parabola to the entire band. The results of the measurements are given in Table I. The first column on the left gives the number of the line, which, on the side of short wave-lengths, is taken as positive and on the side of long wave-lengths is taken as negative; these will in future be referred to respectively as the positive and negative sides. The measured wave-numbers are given in the second column. The wave-numbers given throughout are "waves per decimeter." This unit is chosen

as it is convenient in this discussion, and a change of one wave per decimeter in this region means very nearly a change of one A in wave-length.

In passing out from the center on the positive side, the lines crowd more and more closely together, as can be seen in Figure 1. It was hoped that by raising the temperature of the gas sufficiently, and thus raising the absorption in the lines of higher number, it might be possible to detect a definite head to this absorption region. The existence of a head has not been established, but we hope to use still higher temperatures in the future with a view to searching for it again. The possibility of developing a head on the positive side has caused us to devote most of our attention to measurements of lines on this side. Moreover, on the negative side, after about the twelfth member, the lines fall into a region of absorption by water-vapor, and this complicates the making of measurements.

The eight lines which have been measured on the negative side, and the first eighteen of the twenty on the positive side, have been fitted to a cubic. The equation of the cubic is:

$$\nu = 28863.60 + 205.8239n - 3.081809n^2 - 0.0164817 1n^3.$$

The nineteenth and twentieth lines were not included in the computation, but they fall satisfactorily on the extrapolated curve. The values calculated according to this cubic are given in the third column of the table, and the differences between measured and calculated values are given in the fourth column.

In Figure 2, curve II, are plotted the residuals obtained after subtracting the arbitrary parabola

$$\nu' = 28880.24 + 204.271n - 3.33654n^2$$

from the cubic. The plotted points show the residuals obtained after subtracting the same parabola from the measured wave-numbers. Now if the spacing of the lines were truly parabolic, then we should still have a parabola left after subtracting a parabola, and it is evident that this is not so.

The wave-numbers given in Table I are in general not the result of a single measurement of the position of a line. On some

lines as many as six measurements were made. There were sixty-seven measurements made in all with the gas "hot," and twenty-seven made with the gas "cold." No systematic shift due to temperature has been observed and, in making up the averages of column 2 of the table, fourteen measurements with the gas "cold" were included. Something more will be said below regarding "cold" measurements.

The above-mentioned parabola has also been subtracted out of Imes's measured wave-numbers and the residuals have been plotted. Figure 2, I, is a smooth curve going through these points: the points themselves have been omitted to avoid confusion of

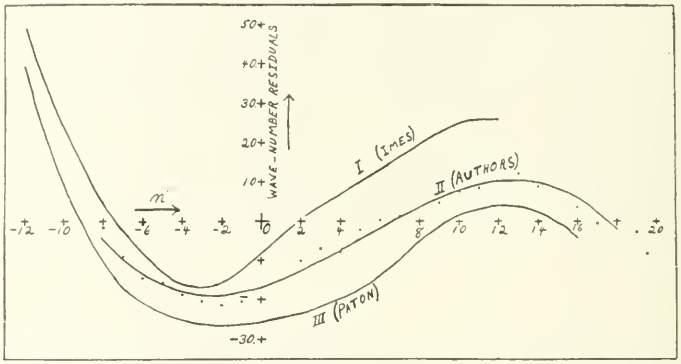


FIG. 2

the diagram. It will be noted that the differences between Imes's values and our own are rather large on the positive side, and this we measured first. We spent much time in trying to reconcile the two sets of data, and at first believed that some systematic error had crept into one set of determinations or the other. A somewhat faulty determination of the spectrometer constant may account for a portion of the differences. The spectrometer constant is determinable to about 0.007 per cent, so that two faulty determinations in opposite directions might account for four units. Again, a faulty determination of the position of the central image of the grating is to be considered. Our practice in determining the position of the central image has been to pass the central image over the thermopile slit, making settings every half-minute of arc,

and taking galvanometer readings at each setting. The intensity of the beam of infra-red radiation is cut down in this case by placing a piece of tissue paper across the beam just before it enters the first slit of the spectroscope; otherwise the galvanometer would go off the scale. The positions of the central image determined in this way have been checked by making five measurements upon absorption lines with the grating turned first to one side of the normal and then to the other. In every determination the check was quite satisfactory. On the other hand, Imes determined the position of the central image visually and did not make any very careful check upon the visual method as applied to his thermopile, and as it frequently happens that the true position of the central image differs slightly from the one visually determined, it may be that some error has crept into his results from this source. But the entire differences between his values and ours cannot be satisfactorily explained as experimental error.

There is probably a real shift in Imes's determinations as compared to ours. There are several causes which may be operative in producing shifts. In the first place, there is the slope of the continuous background which is very marked in Imes's curves. In Figure 1*b*, the waved broken line represents this continuous absorption. It is absorption between the lines due to overlapping at the base. If we consider the sixth line, then the fifth and seventh overlap with it at the base, and as the fifth is a more intense line than the seventh it will overlap more, and there will be a shift toward the fifth line. The magnitude of this shift for a given line will depend upon the numbers of molecules causing absorption in the adjacent lines, and these numbers depend upon the mass of gas in the path, and upon the temperature which affects the distribution of rotational velocities. The mass of gas in the 60 cm chamber "hot" would be about four-thirds that in the Imes chamber, since the chamber is four times as long and the absolute temperature is about three times that of the gas "cold." But the temperature distributes the rotational velocities more evenly, so that the slope of the continuous background is less steep in the 60 cm chamber.

Secondly, it may well be that the absorption lines thus far observed in the "fundamental" do not represent the ultimate structure of the absorption. In the "harmonic" a faint satellite was observed by Imes on the side of long wave-lengths of the more prominent members, Figure 1*a*. The satellite has been explained by Loomis[1] as being due to an isotope of chlorine, and if this explanation is correct it should also be present in the "fundamental." But our definition may be just insufficient to detect it, and the measurements may give the position of a composite of the strong line and this satellite. The position of maximum absorption for this composite would, on account of the exponential law of absorption, shift somewhat with varying numbers of molecules taking part in the absorption, though the ratio of the number of molecules affecting the strong line and the satellite may be supposed constant under all conditions.

Shifts due to overlapping and due to the satellite would affect the law of spacing. But consideration makes it clear that the elimination of the effect of overlapping cannot change the law into a parabola, and we have experimental evidence that it does not. It is somewhat premature to speculate upon the effect of elimination of shift due to the hypothetical satellites, as they may be spaced differently than Loomis supposes.

The accepted formula for absorption bands in this region is of a parabolic type

$$\nu = c_0 \pm c_1 n + c_2 n^2$$

either by the Bjerrum postulate or by the more recent and more satisfactory theory of Sommerfeld-Lenz. In both theories c_0 is dependent on the atomic vibration-frequency and is by far the largest contribution of the three terms. Loomis has pointed out that in the case of HCl the heavier isotope of Cl will produce a satellite with a ratio of frequency 1330/1331 to the predominant line. This ratio is the square root of the ratio of the reduced masses and affects c_0. As an extension of this idea one would likewise expect a variation of c_1: there would be not simply a series of equally spaced doublets, but the separation would grow with

[1] *Astrophysical Journal*, **52**, 248, 1920.

order on the positive side and decrease with order on the negative side. The effect on c_1 is due to a difference in the moments of inertia. The contributions of this term would therefore have a ratio of 1330/1332, the ratio of the reduced masses. The term itself, however, is of a lower order than the first and we could only hope to detect its contribution in the case of the higher values of n. The separation due to c_0 is 21.7, and that due to c_1 is 6.3 for $n = +20$. Together they produce a separation of 28.

A word should be said regarding the possibility of shift due to temperature. None is to be expected theoretically, and none has been observed, but individual measurements of a line frequently differ by eight or ten units and sometimes by larger amounts. It would be necessary to measure a given line or lines a number of times "cold" and a number of times "hot," and under conditions especially chosen to avoid all possibility of shift from the two causes mentioned above, before one could conclude that there is no shift as great as three or four units due to temperature. The measurements with the 60 cm chamber "cold" probably fulfilled these conditions approximately. They were made in the very beginning of our work as preliminary measurements. We at that time drew off gas from the chamber by means of an aspirator to prevent it from escaping into the room, and drew air from the room into the chamber so that it was by no means filled with gas.

Four lines on the negative side have been measured "cold" with Imes's chamber. The wave-numbers agree closely with Imes's values. We have not undertaken to map the entire region in this way as the labor involved would be considerable and would show nothing of great value. The measurements which were made "cold" with the 4 cm chamber agree very closely with the "hot" measurements with the 60 cm chamber.

Mr. Paton has kindly put at our disposal the full data which he obtained. These had never been worked up with care, as no reliable determination of the spectrometer constant was made, and the temperature of the grating was not recorded. The data are nevertheless valuable in several respects. Mr. Paton's "hot" curve was made at 250° C., with a chamber 6 cm long; thus the continuous spectrum in his curve is practically absent. We have

computed wave-numbers from his data, using an arbitrary spectrometer constant to throw the wave-numbers into the right region, and have then subtracted the same parabola. Figure 2, III, is a smooth curve drawn through the points, the points themselves being omitted. It is clear that the law of spacing is still not a parabola.

The absorption-curves of a number of the lines in this set of data show a slight asymmetry which is suggestive of a satellite on the side of long wave-lengths. The degree of asymmetry lies within the experimental error of the determination of the absorption percentage, so it is not surprising that some lines should show an asymmetry on the other side. Of twenty-three lines in which the absorption percentage rises above 30 per

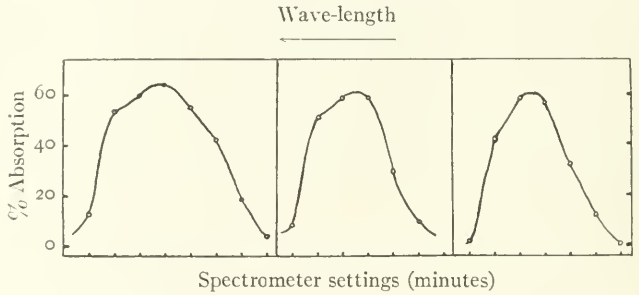


FIG. 3

cent, twelve lines show the asymmetry on the side of long wave-lengths, eight are symmetrical, two are irregular on both sides, and one shows the asymmetry on the other side. In Figure 3 are reproduced the absorption curves which show it most pronouncedly. The evidence is of course very slight. We had searched for the satellite, using a narrow slit-width, 0.25 mm, whereas most of our work has been done with a slit-width of 0.40 mm, and Imes and Paton used about 0.50 mm. We did not find the satellite. The galvanometer deflections were very small and the errors in absorption percentage correspondingly great, and it is possible, too, that the column of gas was too long and that the satellite, if it exists, was merged into the principal line.

The question has occasionally arisen whether accuracy in determinations of wave-numbers is to be gained by using a

compensating chamber; that is, by observing galvanometer deflections first with the beam passing through the absorption chamber, and then with the beam passing through a chamber of equal length containing dried air. We did not use a compensating chamber in our work, but located absorption maxima directly from the curve of deflections. By way of comparison of the two methods, we have plotted from one of Mr. Paton's sets of data first the curve of deflections and then the curve of absorption percentage obtained from the deflections through the compensating chamber. The position of every absorption maximum on the two curves is practically identical.

University of Michigan
January 1921

THE EXCEPTIONALLY HIGH SOLAR PROMINENCE OF OCTOBER 8, 1920

By OLIVER J. LEE

ABSTRACT

Solar prominence of October 8, 1920.—Fifty-seven photographs were obtained, covering the various stages of the growth and gradual breaking up and final disappearance of this prominence, which attained the record height of 831,000 km. The changes are described in detail with the help of 7 photographs and 6 plots. The superstructure rose slowly at first until coherence with the base was partly broken, when the velocity suddenly changed to a much higher value, which was maintained until a more complete break was accompanied by another sudden increase. The motion of other parts was quite complex, some material returning to the sun, while other parts seemed to be attracted to points outside the sun. Electrostatic forces may have been acting, but it is not understood how. The prominence was associated with no sun-spot and seemed to be a new eruption. The H line of calcium was used in making the spectroheliograms.

The first photograph of this prominence was taken at G.M.T. 3^h5^m, October 8, through a thick haze with scattered clouds. The topheavy appearance of the eruption suggested that it might show changes, and it was followed throughout the day in spite of the unfavorable conditions. Until local noon twenty-six photographs had been taken at various intervals, and it was evident that the top of the structure was about to be separated from the base. It was therefore followed until G.M.T. 8^h33^m, when the last vestiges of it are seen at an elevation above the solar limb of 831,000 km or more than 19 minutes of arc. A fresh breeze blew directly into the dome all day, and the resulting oscillation of the telescope is all too much in evidence on many of the photographs. At no time was the prominence strong, and it was a matter of surprise to find the faint structure of the prominence recorded as the plates were developed. Fifty-seven photographs were obtained during the day.

The eruption took place on the east limb of the sun in latitude 24° south and longitude 266°. Photographs of the disk with the H line of calcium are available for the next few days, but they give no evidence of disturbance at this point beyond a few floccular specks. The nearest spot is perhaps 40 or more degrees away. On

PLATE V

Fig. 1 Fig. 4 Fig. 5

Fig. 1

Fig. 2

Fig. 3

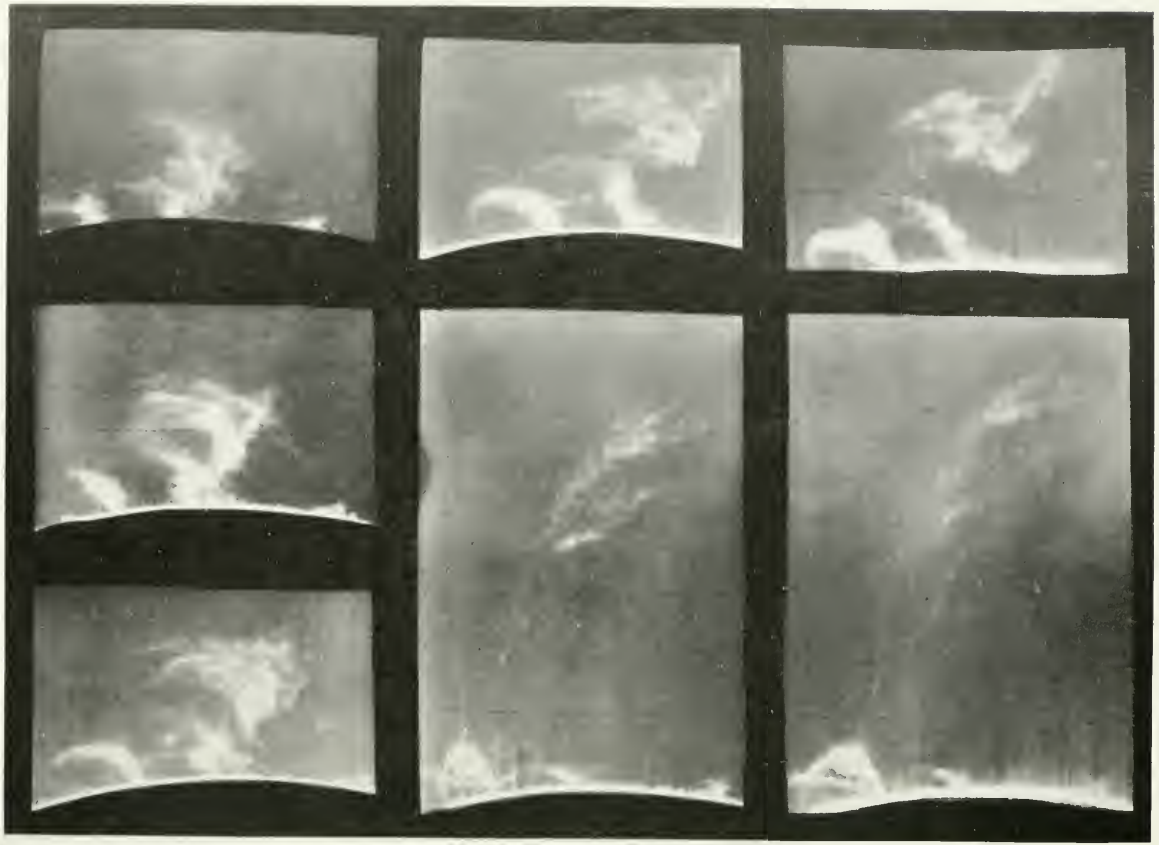


Fig. 3 Fig. 6 Fig. 7

SOLAR PROMINENCE OF OCTOBER 8, 1920

FIG. 1—3^h32^m G.M.T. FIG. 3—6^h24^m G.M.T. FIG. 5—7^h17^m G.M.T. FIG. 7—7^h54^m G.M.T.
FIG. 2—5^h43^m G.M.T. FIG. 4—6^h59^m G.M.T. FIG. 6—7^h50^m G.M.T.

the previous day a low diffuse prominence overlay this region, but its form had nothing in common with the first photographs made on October 8. This circumstance, taken with the fact that new matter was being shot up into the base of the prominence during its development, indicates that the latter was a new eruption.

In the diagram the plot *A* exhibits the vertical ascent of the crest or top of the prominence. It was not possible to derive a similar plot for the under side of the prominence, the changes in form being too radical. In the first section of plot *A* the crosses in each case represent the mean height of from two to five photographs taken in quick succession. After the changes became more rapid, as shown in the second and third parts of this plot, it became more difficult to set on the faint traces of matter forming the top of the crest. In all the plots given in the figure the numbers are the velocities in kilometers per second.

Plot *A* is made up of three straight lines. While instantaneous increases in velocity are indicated, the times of observation and the scale of the plot do not preclude the possibility that the change occupied several minutes. There can be no doubt that in each interval of time the velocity of ascent is constant. From a study of twenty-four eruptive prominences, Pettit[1] has established that the velocities of ascent in prominences receive impulsive increments of speed, and that between these moments of increase the velocities are constant.

The accompanying plate exhibits some of the most striking changes of form. No attempt has been made to reproduce the last stages photographed.

Considerable difficulty was experienced in measuring the velocities of different parts in the early forms. The masses are too irregular and diffuse. About eighty determinations of velocity were made with the "blink" comparator on thirty-seven points. The individual velocities are of course rather discordant. Directions of motion are more satisfactory and give a fairly good indication of how the main body of the prominence became detached from the base. The five smaller cuts show how this took place.

[1] *Astrophysical Journal*, 50, 206, 1919; *Publications of the Yerkes Observatory*, Vol. III, Part IV, probably will appear in 1921.

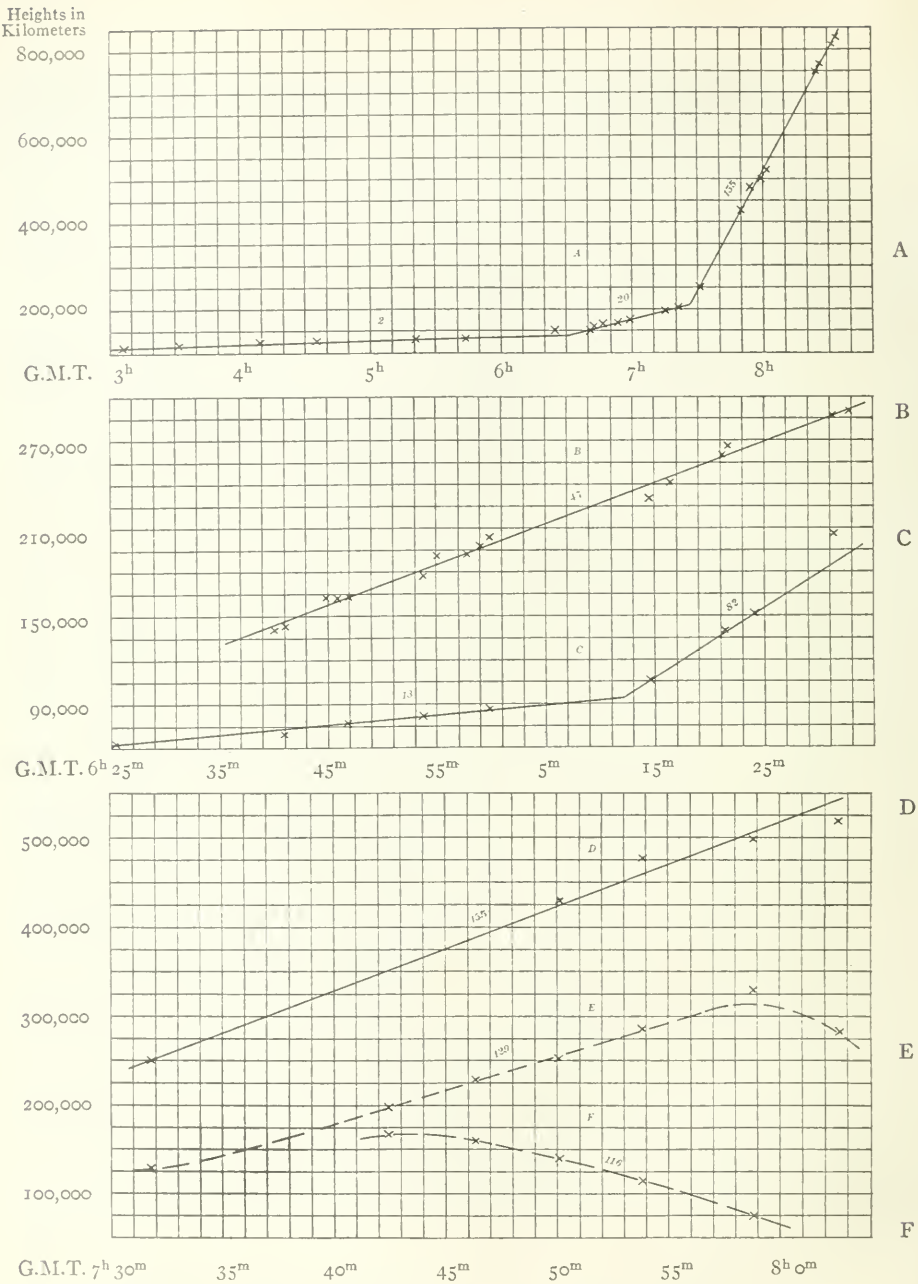


Diagram 1.—Heights and velocities of *A*, the crest; *B*, the secondary eruption from the head; *C*, the isolated cloudlet at the right; *D*, the crest for comparison with *E* and *F*; *E*, the large, dense condensation near the bottom of the ascending head; *F*, the small bright knot approaching the horn prominence.

During the first interval of observation the superstructure was slowly rising. The greatest velocities during this period were in the streamers toward the left, the largest being 77 km per second. The objective of these arms seemed to be some point of attraction outside the lower left-hand corner of the figures, as indicated in the first photograph. Then the low hornlike prominence at the left became the more powerful and grew in size and brightness with the stream of matter fed to it by the main eruption and other matter coming up into it from the limb of the sun itself. The branches projecting from time to time higher up seemed variously affected by the attraction of the horn and the point at its left and, once detached from the main mass, moved outward and up or down with velocities ranging from 14 to 26 km per second. Between the stages shown in the first two figures the straggling material between the base and head was drawn off to the left, while on the right it settled down toward the limb of the sun at the rate of a very few kilometers per second. The resulting cleavage is well shown in the photograph taken at G.M.T. 6^h24^m, although the roughly parallel lines from between which the matter was drawn are clearly seen much earlier in the series. The denser connected masses in the main head resisted this action and began ascent with increased speed. The rapid rise of the secondary eruption in the upper right-hand corner of the head is shown separately in plot *B*. The break in cohesion between this part and the rest of the head is indicated in the second figure and took place in a manner analogous to that described above. During its separation from the head it experienced for a while a slight swaying motion toward the right, southward. Then after the second large increase in velocity upward it lost its form and dissipated rapidly. The northward parts of the head proved most refractory and had swayed back toward the north several degrees of latitude when the greatest height was attained. At G.M.T. 8^h27^m the crest is still quite conspicuous. On the photographs taken at G.M.T. $8^h31^m53^s$ and $8^h33^m27^s$ the remnant is so faint that had there been but one plate no claim to an unequaled record of altitude could have been made. As it is, the last two exposures corroborate each other perfectly.

The absence of any accurate information about the component of velocity in the line of sight and of perspective in prominences makes a discussion of motions difficult, and phenomena are not always what they seem. In the stage shown in Figure 3, taken at G.M.T. 6^h24^m, a small spike projects upward from the base across the open space toward the detached mass. This body broke loose from its apparent base, traversed the open space at a velocity varying from 13 to 30 km per second, and joined the receding mass. Transfer of other material across this space is clearly seen also in the next two figures.

The small cloudlet seen widely separated toward the right was followed for nearly one hour. At G.M.T. $5^h42^m49^s$ it is a nucleus in the arm projecting downward from the right of the main head. The next figure shows it detached and strengthened by accretion. Measurement along a solar radius of nine photographs gives the points in plot *C*. The last image was indistinct and the measure of it was not given any weight in plotting. The rest indicate two periods of constant velocity connected by a short interval of change. The velocities themselves and the times of change are seen to be independent of those of the main mass. Micrometric measures in rectangular co-ordinates show that this knot at first moved away from the head at an angle of 34° with the tangent to the limb; then it changed direction to an angle of 65°, but did not get its increase in speed for another 10 to 12 minutes.

Another feature of the eruption is shown in the last group of plots. It concerns the separation of the parts of the head, the crest stubbornly resisting disruption and continuing its dash to the greatest height so far recorded, while other parts singly or in groups deserted and vanished or started back to the sun. The process continued for sometime but reached a climax when the crest had attained an altitude of 450,000 km above the limb. One small knot started back earlier and was beautifully recorded on five photographs. Two intermediate stages are shown in Figures 6 and 7. Plot *F* refers to this knot. It took a straight course with constant velocity for the top of the horn prominence, the fifth exposure showing it almost in contact. The horn itself, which had

persisted for five hours of observation with only minor changes in form, at this time exploded, shooting streamers toward the left and weakening. About fifteen minutes earlier the stump of the main prominence had discharged itself into the horn and now only an insignificant knob remained.

Plot *E* refers to the motions of a large dense mass probably coming from the lower right portion of the head. After sharing the ascending motion it finally slid into the course taken by material returning to the sun. The reversal of motion of this mass is shown. There may be later traces of it but certain identification is not possible. Plot *D* shows the altitudes of the crest during this period for comparison.

The study of this prominence elicits the following remarks:

1. Motions in this and similar prominences must be due to the interplay of many forces.

2. While this eruption took place, the parts farthest from the horn prominence and the nearby point of attraction have moved with the greater freedom.

3. So long as there was continuity of material in base and head only a very gradual rising motion took place. Once cohesion was broken, in this case by the clearing of a lane across the neck, more rapid ascent began.

4. The first increase in velocity followed the partial break shown in the third figure. The second increase came just after the more complete break seen in the fifth.

5. A center of attraction existed at some point not far to the left of the horn prominence.

6. Apparently a differentiation took place in the ascending mass so that part of it continued upward and other parts were drawn back to the sun. This is not due to the presence of different elements, since the spectroheliograph in this adjustment will record only the monochromatic radiation of the H line of calcium. Is it due to change in polarity of the crest or transfer of charge from it to its neighbor? How can this affect the motion of the appendages and not also the motion of the crest, which remains constant, as shown by its plot of altitudes? Or, can it be that breaks in the

cohesion of material amount to interrupting the paths in which transfer of charge takes place with the result of sudden change in repulsive force?

7. The base of the prominence discharged violently into the horn at the time when the crest shed its appendages. The simultaneous dissipation of widely separated parts of an eruption has been noted by Evershed.[1] Does this indicate a local field, having particular properties, surrounding this complete operation? If so, the field is not one connected with spots or a marked floccular area. It may be the field lying between sun-spot fields and having, in a fashion, complementary properties.

8. The dense part of the horn is the goal of material returning to the sun from above in a funnel-shaped path. Why should not this material rather seek the point at the left? Particularly so since the horn itself "blew up" and discharged its substance furiously toward this point only a short time later?

9. The slow development of the structure for the first hours of observation indicate a growth rather than a sudden eruption. At the rate of rise found for the first period of observation, 1.9 km per second, the prominence could have grown from the limb of the sun up to the altitude first observed in less than ten and a half hours.

10. The smaller types of jetlike ejections from the limbs of the sun are apparently real eruptions. It is more than likely that the large structures, which attain high altitudes, grow out rather leisurely and finally suffer violent disruption because of internal mechanical changes coupled with static conditions in the solar atmosphere.

YERKES OBSERVATORY
December 14, 1920

[1] *Bulletin No. LV*, Kodaikanal Observatory, 1917.

SUSPECTED VARIABLE, BOND 624, IN TRAPEZIUM OF ORION

By J. A. PARKHURST

ABSTRACT

Variability of Bond 624 in Orion.—The photo-visual magnitudes obtained from 67 plates covering the past 16 years have been arranged in order of phase according to Hartwig's elements, but no periodic variation from the mean, $8^{M}.32$, is shown and the average deviation of the normal point is only $0^{M}.06$. The comparison stars used gave excellent standards for the detection of any variation, even slight. Evidently the elements given by Hartwig cannot be correct.

Photo-visual magnitudes of seven stars in Orion, Bond 619, 628, 640, 685, 708, 734, and 741 are given and compared with Graff's values.

Hartwig has published in *Vierteljahrsschrift der Astronomischen Gesellschaft*, **55**, 220, 1920, the following elements of minimum

G. M. T.

1919 August 28, J. D. $2422199.576+6^{d}.4754$ E.

An ephemeris based on these elements also appeared in *Astronomische Nachrichten*, **212**, 231, 1920. These publications led me to arrange the plates taken with the Yerkes 40-inch refractor in order of phase according to Hartwig's elements, in search for photographic evidence of variation.

These plates were taken through a yellow filter and therefore give photo-visual magnitudes, which agree very closely with visual observations in ordinary fields. The results of a preliminary examination of 103 plates taken between 1900, September 20, and 1919, March 19, were published in *Popular Astronomy*, **27**, 578, November 1919.

Most of the plates had exposures of one to two hours and on many of them the bright stars of the trapezium with the surrounding nebulosity were too large and dense for accurate measures. Such plates were either excluded from the following list, or, if included on account of phase-value near predicted minimum, were given half weight. On plates with exposures of 5 to 50 minutes, the images of the trapezium stars were small enough to permit measurement with an artificial scale in the Hartmann microphotometer.

The system of standard magnitudes was determined by such measures of plates taken with objective-gratings, giving the following system, and the comparison with Graff's visual magnitudes.

The systematic difference, Parkhurst minus Graff, for the mean of seven stars is $+0^{M}06$. The difference for θ_2 = Bond 685, Graff's basis, is $+0^{M}02$. The individual differences are large; negative for stars in the dense nebulosity near the trapezium, and positive for stars in less nebulosity.

TABLE I

Star	Plate						Mean	Graff	Diff. P.–G.
	358	359	362	399	401	402			
Bond 619	$6^{M}86$	$6^{M}70$	$6^{M}72$	$6^{M}69$	$7^{M}04$	$6^{M}84$	$6^{M}78$	$7^{M}19$	$-0^{M}41$
628	5.22	5.16	4.92	5.23	5.14		5.18	5.42	−0.24
640	6.84	6.71	6.74	6.55	7.04	6.78	6.73	6.83	−0.10
θ_2=685	5.22	5.18	4.98	5.23	5.14		5.19	5.17	+0.02
708	6.60	6.60	6.56	6.58	6.56	6.55	6.58	6.41	+0.17
734	7.10	7.04	6.89	7.00	7.47		7.07	6.64	+0.43
741	9.09	8.67	8.39	8.53	9.01	8.20	8.52	7.97	+0.55
Means							6.58	6.52	

On such plates of exposures less than 30^{m}, taken with or without the objective grating, the nebulosity is not troublesome and the star-images can be measured with considerable precision. When the exposure was an hour or more it was only possible to estimate the magnitudes somewhat roughly, such results being marked (:) in the list and given half weight. But even on these plates a change of half a magnitude would be quite noticeable. The best of the plates used, about one-third the total number, are quite free from the uncertainties encountered in visual comparisons on the bright, shifting background of nebulosity; the photographic results should therefore have relatively greater weight.

The results of measurements of 67 plates are given in Table II, for which the headings of the columns are self-explanatory. The plates were grouped in order of phase after minimum according to Hartwig's elements. The average magnitude of Bond 624 is 8.32,

TABLE II

NORMAL POINTS

PLATE NO.	CAL. DATE	JULIAN DAY 24	PHASE	MAG.	MEAN	
					Phase	Mag.
401	1921 Jan. 27	22717.653	0^d04	8.18		
57	1909 Apr. 1	18398.583	0.1	8.25:		
65	1911 Jan. 28	19065.601	0.1	8.00		
365	1919 Dec. 3	22296.810	0.1	8.5 :		
61	1910 Feb. 19	18722.546	0.2	8.25:	0.15	8.32
18	1906 Jan. 28	17596.628	0.2	8.5 :		
339	1917 Dec. 25	21953.732	0.22	8.5 :		
22	1906 Feb. 10	17252.625	0.22	8.5 :		
72	1911 Dec. 5	19376.730	0.24	8.25:		
73	1911 Dec. 18	19389.745	0.3	8.25:		
90	1914 Feb. 15	20179.627	0.37	8.5 :		
138	1914 Nov. 1	20438.800	0.52	8.25:		
80	1912 Mar. 5	19467.552	0.58	8.5 :		
66	1911 Feb. 4	19072.623	0.6	8.5 :	0.56	8.30
26	1906 Oct. 21	17505.587	0.6	8.10		
20	1906 Feb. 4	17246.625	0.73	8.32		
70	1911 Nov. 29	19370.773	0.76	8.00:		
69	1911 Oct. 28	19338.572	0.94	8.25:		
86	1913 Jan. 23	19791.707	0.96	8.25:		
56	1909 Mar. 20	18386.595	1.0	8.25:		
143	1914 Nov. 21	20458.817	1.10	8.31	1.07	8.33
202	1916 Jan. 16	20879.713	1.13	8.5 :		
302	1917 Dec. 9	21572.754	1.28	8.4 :		
150	1914 Dec. 24	20491.724	1.64	8.25:		
67	1911 Feb. 18	19086.583	1.7	8.30		
50	1908 Feb. 20	17992.543	1.8	8.20		
304	1917 Dec. 16	21579.773	1.83	8.5 :	1.86	8.36
87	1913 Feb. 6	19805.670	1.97	8.5 :		
48	1908 Dec. 25	17966.675	2.0	8.20		
75	1912 Jan. 8	19410.740	2.06	8.5 :		
13	1905 Dec. 16	17196.691	2.49	8.5 :		
30	1907 Feb. 10	17617.568	2.5	8.5 :		
59	1909 Dec. 25	18666.712	2.6	8.5 :		
51	1908 Oct. 17	18232.906	2.7	8.30	2.67	8.36
71	1911 Dec. 1	19372.715	2.71	8.25		
23	1906 Mar. 17	17287.585	2.8	8.5 :		
198	1915 Nov. 14	20816.772	2.93	8.25:		
203	1916 Feb. 13	20907.659	3.17	8.25:		
49	1908 Feb. 2	17974.579	3.5	8.25:		
402	1921 Feb. 19	22740.576	3.57	8.02	3.56	8.23
402	1921 Feb. 19	22740.606	3.61	8.11		
336	1918 Nov. 13	21911.800	3.61	8.25		
25	1906 Mar. 31	17301.581	3.9	8.5 :		

TABLE II—*Continued*

Plate No.	Cal. Date	Julian Day 24	Phase	Mag.	Mean Phase	Mean Mag.
200	1916 Jan. 6	20869.700	4d06	8.25:		
42	1907 Dec. 1	17910.712	4.3	8.25:		
54	1909 Feb. 6	18344.566	4.3	8.5 :		
91	1914 Feb. 19	20183.585	4.33	8.25:		
355	1919 Nov. 5	22268.800	4.47	8.20		
397	1921 Jan. 12	22702.719	4.53	8.26		
159	1915 Feb. 17	20546.587	4.69	8.25:	4.57	8.28
44	1908 Jan. 2	17943.612	4.8	8.25		
68	1911 Apr. 1	19128.584	4.87	8.25		
92	1914 Feb. 26	20190.596	4.87	8.40		
358	1919 Nov. 12	22275.758	4.95	8.30		
359	1919 Nov. 12	22275.772	4.97	8.23		
360	1919 Nov. 12	22275.811	5.00	8.0 :		
246	1917 Jan. 23	21252.719	5.03	8.0 :		
311	1918 Feb. 3	21628.725	5.46	8.25:		
362	1919 Nov. 19	22282.779	5.49	8.20		
363	1919 Nov. 19	22282.821	5.54	8.25:	5.48	8.19
399	1921 Jan. 26	22716.703	5.56	8.09		
81	1912 Apr. 5	19498.573	5.70	8.25:		
338	1918 Dec. 11	21939.808	5.73	8.5 :		
234	1916 Oct. 25	21162.809	5.76	8.25:		
37	1906 Oct. 4	17853.911	5.8	8.5		
52	1908 Nov. 28	18274.774	5.8	8.5 :		
89	1914 Feb. 14	20178.609	5.82	8.5 :		
93	1914 Mar. 12	20204.580	5.89	8.25:		
64	1911 Jan. 21	19058.636	6.0	8.25:		
60	1910 Jan. 30	18702.704	6.20	8.5 :	6.09	8.44
301	1917 Nov. 18	21551.765	6.20	8.5 :		
309	1918 Jan. 9	21603.643	6.27	8.25:		
343	1919 Mar. 19	22037.579	6.37	8.5 :		
55	1909 Mar. 6	18372.576	6.47	8.5 :		

the deviations of the normal points from the mean range from $0^{M}00$ to $0^{M}13$ with an average value of $0^{M}06$.

No evidence of variation of Bond 624 can be found from these plates covering the past sixteen years. The plates taken between 1919 and 1921 indicate that the elements cannot be correct, but the possibility remains that the exposures may have avoided the minima corresponding to somewhat different elements.

Figures 1, 2, and 3, which are reproductions of photographs, will give a fair idea of the appearance of the images, and of the possibility of accurate measures. They also show that the nebulosity does not affect short exposures enough to introduce errors in the results.

Figure 1 reproduces the central part of Plate O,362 taken 1919, November 19, with grating P6 and an exposure of 10 minutes. The scale is small enough to include the trapezium and also the

FIG. 1.—Negative O, 362

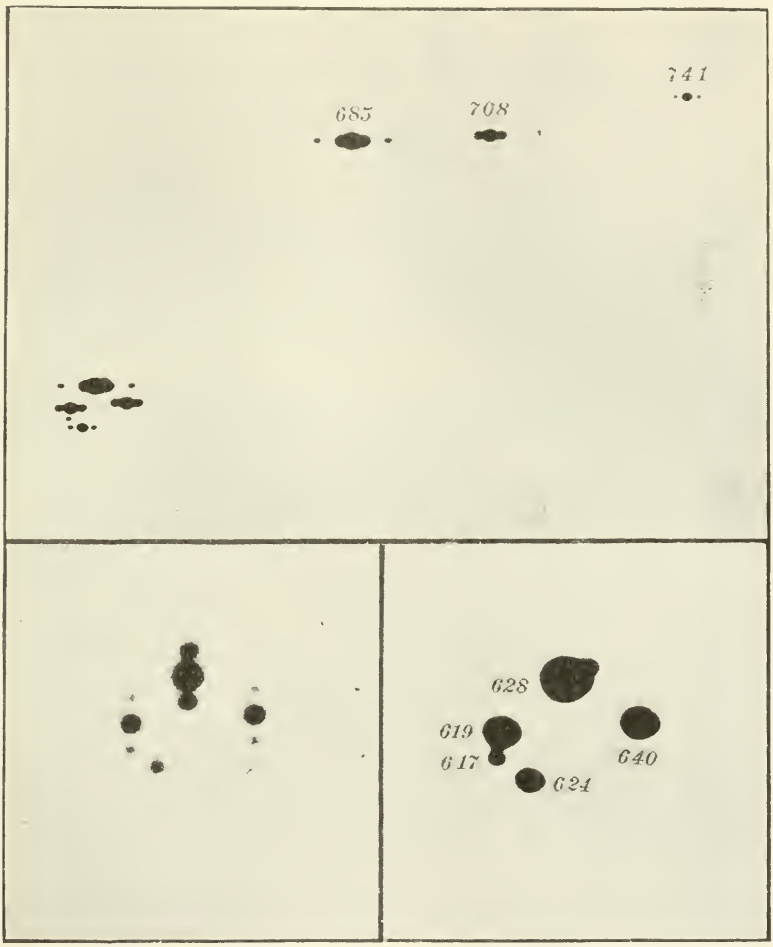


FIG. 3.—Negative O, 401

FIG. 2.—Negative O, 48

line of three stars, Bond 685, 708, and 741. Figure 2, which is a reproduction of O,48 taken 1908, January 25, with an exposure of 20 minutes, shows the trapezium on a sufficiently large scale to

hold the Bond numbers in the vicinity of the five brightest stars. Overlapping the image of 628 will be seen part of the image of Bond 633, sometimes called the sixth star in the trapezium. Figure 3 reproduces the central part of Plate O,401 taken 1921, January 27, at 15^h40^m G.M.T., with an exposure of 10 minutes, through grating P6, and is given for the purpose to be mentioned later.

Figure 1 will give an idea of the possibility of accurate measures, with an absolute scale of magnitudes on the plate, derived from the difference in apparent magnitude between the central and the spectral images of the first and third orders. These constants for the grating P6 have been carefully determined, giving the difference between central and first order spectrum as 2.38 magnitudes, and that between central and third order spectrum as 5.03 magnitudes. In Figure 1 it will be seen at a glance that the size of the central image of Bond 624 lies between the central and spectral images of the stars 619 and 640. It is also comparable with the spectral image of Bond 708 and with the central image of Bond 741. These four comparison stars therefore give us excellent standards for the detection of any variation, even slight, in Bond 624.

In *Astronomische Nachrichten*, **212**, 383, 1921, Hartwig reports a minimum for 1921, January 14, at $9^h \pm$ G.M.T. This corresponds to epoch 78. The next minimum which could be observed in this longitude was the second following, epoch 80. Plate O,401 was taken at epoch 80 with the phase value of 0.04 days. The measured magnitude of Bond 624 on this plate is 8.18, which is about 0^M1 brighter than the mean. No confirmation of the variation can be found from this plate, which shows, moreover, that the elements given by Hartwig cannot be correct.

YERKES OBSERVATORY
March 1921

Minor Contributions and Notes

USE OF A LIME CATHODE OF CARBON IN SPECTROSCOPY

ABSTRACT

Lime cathode of carbon may be prepared by soaking a thin hard carbon strip, such as may be cut from a telephone diaphragm, in a solution of calcium and barium nitrate and then drying it. By heating this cathode in a vacuum and applying a potential difference of a few hundred volts between it and a nearby anode, an electronic current of several amperes per cm² may be obtained which may be used for *melting small quantities of highly refractory substances* or for exciting intense light from the anode metal. *This new and powerful source of line spectra* is so intense that the structure of the spectrum lines of such metals as Cd, Bi, and Pb may be studied with an echelon grating or a Lummer-Gehrcke plate. The life of the strip was usually long enough, about 20 or 30 minutes, to outlast the anode material, which was placed in a small silica tube.

Structure of bismuth lines.—Photographs made with a Lummer-Gehrcke plate and a spectrograph show the structure of lines λλ 4722, 4308, 4122, 3596, 3511, and 3397. No measurements are given.

It is well known, that calcium or barium oxide coated on a strip of platinum foil and heated red hot, sends out a large number of electrons, which may be used with advantage for melting small quantities of highly refractory substances in vacuum or for exciting intense light from metals.

The so-called Wehnelt cathode was successfully employed by Janicki,[1] Wali-Mohammed,[2] Takamine,[3] King,[4] and others in spectroscopy, for obtaining sharply defined spectral lines.

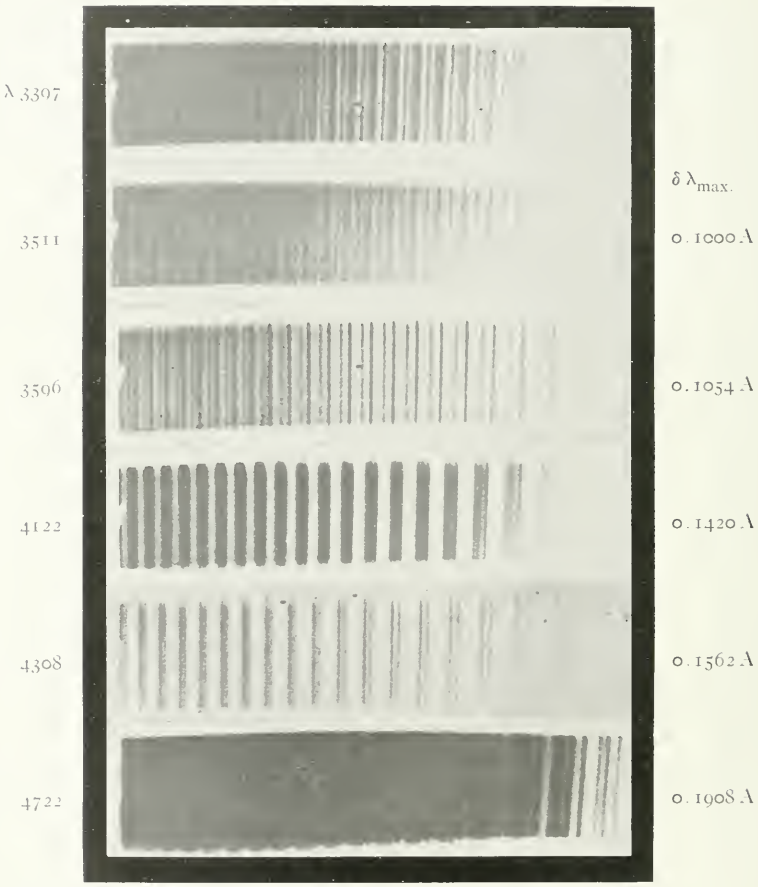
At the suggestion and under the guidance of Professor Nagaoka, the following experiment was made with the object of replacing the platinum foil of the cathode by a hard carbon strip. The carbon was previously soaked in a solution of calcium and barium nitrate, and dried; by using it as cathode, we can obtain electronic currents of several amperes per cm² in vacuum, and successfully

[1] *Annalen der Physik*, **29**, 833, 1909.
[2] *Dissertation*, Gottingen, 1912.
[3] *Jour. Coll. Sci.* (Tokyo), **8**, 51, 1915.
[4] *Astrophysical Journal*, **44**, 303, 1916.

apply this current for spectroscopic use. As a cathode, we cut a thin carbon strip from a telephone diaphragm in rectangular shape, 3×12 mm. The strip was heated red hot, and after cooling dipped in a solution of calcium and barium nitrate; before using, it was dried in a gas flame. Its ends were held by small steel clamps. Acheson graphite was pasted on the plate to make sure of good contact at the clamps. The strip was heated by an alternating current, which was led in by steel wires, sheathed in glass tubes. Currents of 8 to 16 amperes were used to heat the strip red hot, and on applying sufficient voltage between the anode and the cathode, the electronic current was established between them. Usually the heating current was taken off after reaching this stage, and no heating was necessary to maintain the current. The voltage between the electrodes was about 200 volts, but when the electronic current of several amperes was established it dropped to 30 or 40 volts. This potential difference was generally determined by the nature of the anode.

The life of the carbon strip depends on the pressure of gas in the vessel in which it is placed, the amount of the oxides coated on it, the amount of the heating current sufficient to cause emission of electrons to vaporize the metal of the anode, and the strength of the electronic current. It was necessary to keep the electrodes near each other and vaporize the metal. For Cd, Pb, and Bi, the distance was about 1 cm when the potential difference between the electrodes was about 200 volts. After 20 or 30 minutes, the carbon strip became gradually porous and broke down; but generally the anode metal was all vaporized before the carbon fell to pieces. The life of the strip was longer, the harder the carbon; generally initial over-heating was unfavorable, but when metallized with the anode material, the life was much longer. The metal was molten in a silica tube of about 2 mm internal diameter, and came in contact with the end of an iron lead-wire. With metals of high melting-point, such as copper, iron or tungsten, wires of these metals were taken. For examining salts, it was necessary to have a thin wire of a conducting substance passing through the salt. For studying powders of molybdenum or iodine, the powders were pressed into a silica tube. It was found advantageous to use different sizes of silica tube for different sub-

PLATE VI



Satellites of Lines of Bismuth

stances. The anodes and cathodes sketched above were placed in a brass tube of about 4 cm internal diameter and 27 cm long, and provided with a silica plate cover, while the other end was closed by an ebonite plug, through which the electrodes were led. Owing to excessive heating, the tube was water-jacketed and the interior of the tube protected by inserting a thin mica cylinder. The tube was evacuated by a Gaede mercury pump, and the pressure maintained nearly constant during the experiment and kept much below 1 mm of mercury. It was afterward found advantageous to use a shorter but wider tube, with which lines of bismuth were studied. On increasing the heating current, the carbon strip was surrounded by a glow, and bright spots appeared at the anode which gradually spread over the whole surface of the silica tube exposed to cathode bombardment.

The intensity of the light depends on the current. The surface of carbon cathode emits a continuous spectrum interspaced with bands, but they do not interfere with the spectroscopic investigation, as the light from the anode only is focused on the slit of the spectroscope. The anode light is very intense, so that satellites of the bismuth line λ 4722 can be distinctly photographed by an echelon grating with exposure of 30 seconds only. With metals of low melting-point, the potential difference of 200 volts is sufficient to bring out good results, but with iron and other refractory substances, it is necessary to use higher voltages.

A glance at Plate VI will show how distinctly the satellites of the bismuth lines $\lambda\lambda$ 4722, 4308, 4122, 3596, 3511, 3397 can be photographed, by means of a quartz Lummer-Gehrcke plate and spectrograph of the same material by using the extraordinary ray. All the lines were taken on a single plate with an exposure of 5 minutes. The lines are not measured, as the orders of spectra of the satellites are not definite with a single plate; only with crossed spectra can we determine the orders.

We have to thank Mr. T. Mishima, assistant in the Institute of Physical and Chemical Research, for his kind assistance during the progress of the present work.

Y. Sugiura and T. Matoba

Physical Institute
Imperial University, Tokyo
July 1920

A MODIFICATION OF THE ELECTRON THEORY OF DISPERSION, TO ACCOUNT FOR THE CHANGE OF REFRACTIVE INDEX WITH TEMPERATURE

ABSTRACT

Electron theory of dispersion.—Attention is called to the fact that W. Voigt was the first to modify the Lorentz theory in such a way as to explain the *change of refractive index with temperature.*

Under the foregoing title Mr. Hulburt published in this *Journal*[1] an article in which he modified the Lorentz electron theory, in order to explain the decrease of the refractive index with increasing temperature.

Exactly the same modification of the electron theory was developed for the same purpose by the late Professor W. Voigt in his paper, "Contributions to the Electron Theory of Light," published in the year 1901.[2]

Voigt starts from the equation of motion of the dispersion electron in the well-known form

$$m_s\frac{d^2\xi}{dt^2}+k_s\frac{d\xi}{dt}+f_s\xi=e_sE_x$$

(where the subscript s denotes the sth type of electron) and he assumed that the quantities k_s and f_s are changed by the influence of a thermal or mechanical deformation.

In case of the deformation being caused by the change of temperature, Voigt showed that the refractive index μ of transparent isotropic media is expressed by

$$\mu^2-1=\sum_s\frac{4\pi N_s(1-\Delta)\frac{e_s^2}{m_s}}{\frac{k_s}{m_s}(1+b_s\Delta)-\frac{4\pi^2c^2}{\lambda^2}},$$

where N_s is the number of electrons of the sth type per unit volume, λ the wave-length of vibration, c the velocity of light in vacuo and Δ the dilatation produced by the change of temperature; the sum is to be extended to all types of electrons of the medium.

[1] *Astrophysical Journal*, 51, 223, 1920.

[2] *Annalen der Physik* (4), 6, 459, 1901.

This formula corresponds to equation 6 of Mr. Hulburt's paper; his remark that no previous attempt has been made to explain quantitatively the change of the refractive index with temperature, on the basis of the electron theory of dispersion, is therefore erroneous.

G. SZIVESSY

MÜNSTER i/W.
November 1920

ON THE PRESSURE IN THE ATMOSPHERES OF THE STARS

ABSTRACT

Pressure in the atmospheres of Arcturus and Procyon.—A comparison of radial-velocity measurements of lines known to show large pressure-shifts with those of other lines seems to indicate pressures of, respectively, about 3 and 2 times that of the sun in the atmospheres of these two stars. However, it is not certain that the small positive shifts observed are due to pressure.

Permit me to call attention to the measures of the pressure in the atmospheres of the stars from observations of the displacements of the lines of the classes *a*, *b*, *c*, *d*, of Gale and Adams.[1] I should be interested to know if my results are confirmed with the more powerful instruments in America. With the use of Hartmann's spectrocomparator, I have compared the spectrum of Arcturus and of Procyon with that of the sun on plates obtained with the spectrograph arranged by M. Hamy in connection with the equatorial coudé. The scale of these spectrograms is 1 mm = 4A at λ 4300.

The difference in radial velocity was first determined from reference to the arc lines and from reference to the enhanced lines. When those lines only were used which appeared sufficiently isolated in Rowland's map, the difference in displacement was found to be +0.2 km/sec. for Arcturus, and +0.5 km/sec. for Procyon. This is in good agreement with the values of 0.08 and 0.58 km/sec., respectively, found by W. S. Adams[2] with a more powerful instrument.

Afterward I determined the difference between the radial velocity of the star obtained (*1*) with the lines of classes *a* and *b*, and the

[1] *Astrophysical Journal*, **35**, 31, 1912. [2] *Ibid.*, **33**, 67, 1911.

radial velocity obtained (*2*) with the iron lines of class *c* and with those lines of titanium shifting strongly under pressure. The result was +0.7 km/sec. for Arcturus, and +0.3 for Procyon, which would correspond to an average displacement of 0.010 A for Arcturus and 0.004 A for Procyon at λ 4400. If these displacements are due to pressure, it would be inferred that the pressure in the atmosphere of Arcturus is three atmospheres greater than that in the sun, while that in the atmosphere of Procyon would not exceed that of the sun by more than one or two atmospheres.

In the region between λ 4200 and λ 4700, I was able to measure only one line of class *d*, namely 4233.61 (Fe). Compared with the mean from all the other lines, the displacement of this line would be +0.006 A for Arcturus and only +0.004 A for Procyon.

If these results shall be confirmed by observations with more powerful instruments, they will tend to prove that the pressures in the atmospheres of the stars are very slightly greater than that of the sun, until type F inclusive is reached. The slight displacement of the line of class *d* would even suggest that the small displacements observed are not due to pressure.

P. Salet

Observatoire de Paris
February 9, 1921

THE
ASTROPHYSICAL JOURNAL
AN INTERNATIONAL REVIEW OF SPECTROSCOPY
AND ASTRONOMICAL PHYSICS

VOLUME LIII JUNE 1921 NUMBER 5

ON THE MEASUREMENT OF POLE-EFFECT AND ITS CONNECTION WITH MAGNETIC SEPARATION

By H. NAGAOKA

ABSTRACT

Method of measuring minute shifts of spectral lines.—By using a *displaceable slit* and by interposing an echelon or Lummer-Gehrcke plate between the source and the spectrograph, the same lines from two parts of an arc or from any two sources may be photographed side by side and shifts of one or two milli-angstroms can be determined from the displacement of the interference points, if the lines are sharp and are not interfered with by neighboring lines. The method could be used for the *comparison of spectra of isotopes* or for a study of the *pole-effect*. As a comparison source, the vacuum discharge from a lime cathode of carbon is recommended as both intense and free from pole-effect.

Relation of pole-effect to Zeeman effect for iron lines.—As Gale and Adams have found a relation between pressure-shift and magnetic separation for lines of the same type, it might be expected that the pole-effect also varies with the Zeeman effect; but a study of the available data shows that for positive shifts of pole-effect there is no correlation and for negative shifts the magnetic separation, if anything, seems to decrease as the amount of the shift increases.

The so-called "pole-effect" is evidently a complicated phenomenon, in which the shift of the spectrum lines due to pressure, the length of the arc, the velocity of electrons and of ions, the potential gradient near the electrodes, and other minor causes are involved. These various elements contributing to the pole-effect act simultaneously, and at present it seems next to impossible to separate and identify them. According to the investigations of

St. John and Babcock,[1] the Pfund arc with carbon as the negative pole is almost free from the pole-effect, and may be used for the comparison of wave-lengths; in fact it is planned to use the iron lines as secondary standards. The practical need of determining wave-lengths to a thousandth of an angstrom, makes necessary the easy measuring of pole-effect, to determine whether or not the required exactness can be obtained with the arc. By the method employed by St. John and Babcock, exact measurement can be obtained, but the apparatus requires much space; a far simpler arrangement may be applied practically for testing the presence of pole-effect.

The method which I have employed may be called that of slit-displacement. The narrow vertical slit of a spectroscope is so constructed that by means of a fine screw, the slit may be shifted smoothly by nearly the amount of its width in a horizontal direction, so that in one position of the slit the spectrum of the standard arc can be photographed, and in the shifted position that of the arc to be tested. The spectroscope must of course be of high resolution; it may be a Fabry-Perot interferometer, a Lummer-Gehrcke plate, or an echelon grating, all of which have in general resolving powers greater than a six-inch grating. For this purpose, the light from the portion of the arc to be examined is made to fall on the interferometer; and the transmitted light is received on the collimator of a spectrograph with the displaceable slit before mentioned. The spectrograph which I used was provided with a Cornu prism of quartz, the objective of the collimator and of the camera lens being made of the same material. Very good results were obtained with a Lummer-Gehrcke plate of quartz. The photographs were tolerably sharp and extended to the ultra-violet. On a single photographic plate, a spectral region extending over 1000 angstroms can be obtained with good definition.

The light to be measured is focused on the horizontal slit of an echelon spectroscope, with the edges of the plates horizontal; after passing the echelon, the light is brought to a focus and then projected, by means of a micro-planar, on to the displaceable slit of a prism spectrograph, and the spectrum photographed. The

[1] *Astrophysical Journal*, 46, 138, 1917.

spectrum consists of a series of interference points arranged in vertical lines, which in the absence of the echelon grating would correspond to continuous lines. On account of the thickness (nearly 36 cm) of the glass echelon grating used in the experiment, it was not possible to go far into the ultra-violet region. By using a photographic objective of sufficiently long focus, it was possible to obtain spectrograms with sufficiently large intervals for successive spectra to show the pole-effect. The interval for successive orders of spectra in the foregoing experiment was about 0.400 A for λ 5000, so that it was easy to observe a shift of 0.002 A. With the quartz plate, the interval was about one-half of the above amount; consequently the measurement could be pushed to about 0.001 A. In all these experiments, the great drawback was the indefiniteness of the interference points; in other words, the lines from an iron arc *in air* are broader than those from a vacuum arc; the consequence is that the position of the center of the interference points is difficult to measure, and the error of observation is thus not very small. On the contrary, the same experiment with the iron-iron arc at 110 volts, or by cathode bombardment, both in vacuum, gives extremely well-defined interference points, whose mean position can be determined with great accuracy. In this respect, the arc in air is far inferior to that in vacuum, and is also subject to various fluctuations, which cannot at present be avoided, so long as it is operated in air.

The foregoing method is open to the objection that the source under investigation and the comparison spectrum cannot be photographed simultaneously. This can, however, be in a great part eliminated by photographing the lines to be compared in successive steps in reverse order and by taking the mean. The echelon grating is more sensitive to a change of temperature than the Lummer-Gehrcke plate, but as it takes only a few minutes for each exposure, the variation arising from the change of temperature, if due precaution be taken, is generally negligibly small.

Apart from the pole-effect, the process sketched above will be of some importance in comparing the spectra of isotopes, in which the difference in wave-length, such for example as ordinary lead and radio-lead, is according to Aronberg and Merton of the order

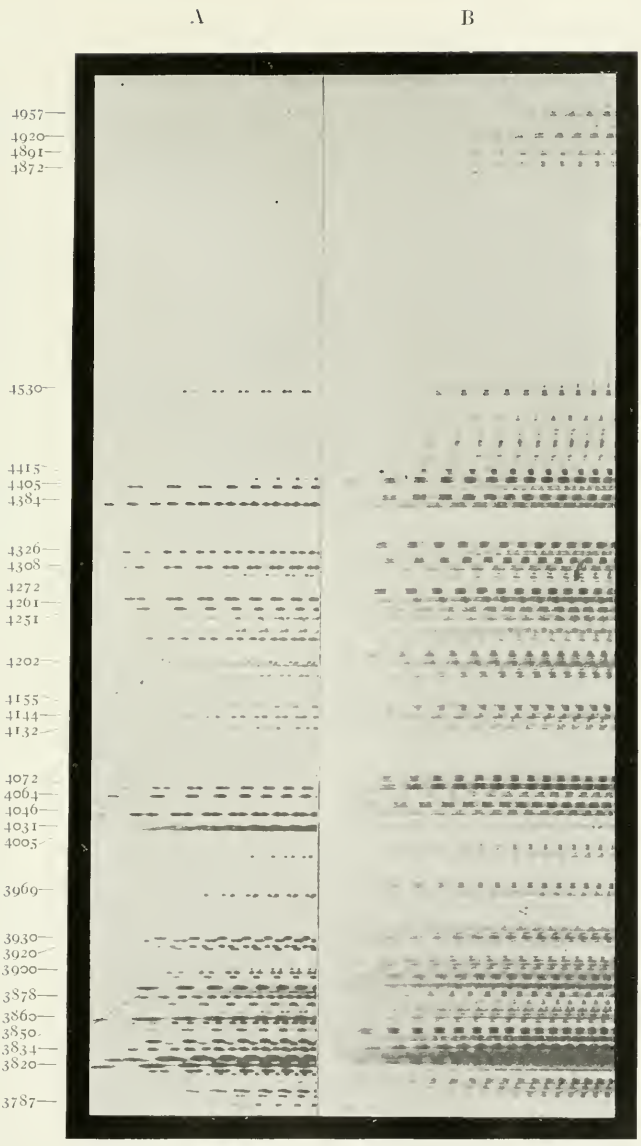
of a few milli-angstroms. For very fine measurements, the source of light obtained by cathode bombardment of the elements is strongly to be recommended, for otherwise the appearance of interference points is rather vague and ill-defined, so that the comparison is not free from errors of setting. As the question of the isotopes is at present attracting the attention of chemists and physicists, it will not be out of place to mention a method which, though originally intended for the purpose of studying pole-effect, will be useful for the spectral investigation of the isotopes, and other problems of similar nature, in which the determination of a small difference in wave-length is aimed at. The accompanying photographs (Plate VII) show a comparison of an iron arc at the center and at the negative pole, and were obtained by the above-mentioned process with a Lummer-Gehrcke plate of quartz.

In the upper figure, the left column of interference points refers to the center, and the right column to the negative pole of 6-mm arc. The shift of the lines is indicated by the inclination of the line joining the neighboring points, and the sense of the shift is also apparent from that of inclination. In the figure, the positive shift is given by a clock-wise rotation. Unfortunately the dispersion of the quartz prism is not large enough to separate lines lying close together, so that the shift is masked by the presence of neighboring lines. For applying the method successfully, higher dispersion is necessary to prevent the intrusion of other lines. The interval between successive interference points is 0.133 A for λ 4000, so that the shift can be easily determined to a few thousandths of an angstrom.

The lower figure shows an iron spectrum excited by a lime cathode. The interference points are more distinct than those given by an ordinary arc, but many lines show unsymmetrical reversals. The position of the points can however be determined with greater accuracy, so that for purposes of exact measurement of wave-length the cathode excitation will be found to give definite results, as many causes contributing to pole-effect are eliminated by placing the source of light in a high vacuum.

Let us now pass to the second part of the discussion. However complex the causes of pole-effect may be, an apparent connection

PLATE VII



Negative Pole Center of Arc

TABLE I

Wave-Length	Type	n	p	Pole-Effect
3676.88 ?	3	1.746		+ 6
3697.44	6 ?		2.522	+ 6
3703.70	3			+ 5
3721.51 ?	3	2.470		+ 5
3735.33	4 ?	3.384	1.190	+ 5
3787.60	8	1.508 0.763	0.767	+ 7
3811.01 ?	3	1.756		+10
3814.79 ?	5	? 1.250		+12
3817.65	3	1.159		+30
3830.87	3			+ 8
3920.85 ?	3	2.271		+ 8
3928.09	3	2.282		+10
3941.29 ?	3 ?	2.962		+14
3947.00	4 ?	1.560		+ 4
3948.11	3	1.585		+ 9
3957.03	3	1.807		+18
3963.11	?			+12
3965.44 ?				
3976.62	3	2.019		+ 4
4018.28	3	1.784		+ 4
4024.75	3 ?	1.290		+13
4030.51	6 ?	1.685		+11
4072.52 ?	3	1.025		+ 8
4073.76	3	2.169		+ 8
4083.78 ?				
4084.51	3 ?	1.798		+ 7
4101.27 ?	3	1.796		+ 8
4104.13 ?				+ 8
4109.07				+ 4
4118.90 ?	3	1.597		+10
4150.28 ?	3 ?	2.305		+18
4153.92	3	2.196		+12
4154.82	3	2.230		+ 4
4157.80 ?	6 ?	2.400		+18
4158.81	?	3.405		+14
4187.05	7 ?	2.253		+ 8
4187.81	3	2.292		+10
4191.44	7	3.073 1.502	0.790	+10 I.S.
4195.34	3	1.818		+ 9
4196.22	3	2.039		+11
4198.31	3	2.172		+10
4210.36	3	4.547		+ 6
4217.56	6 ?	2.259		+ 8
4222.22	3	2.665		+ 6A
4225.46	6	2.508		+ 4
4227.45	3	1.728		+14
4233.16	6 ?	1.574		+ 7
4233.61	9	4.351 3.068 1.478	0.780	+10 I.S.
4235.95	3	2.519		+ 9

TABLE I—*Continued*

Wave-Length	Type	n	p	Pole-Effect
4238.83	3	1.781		+11
4247.44	3	1.973		+11
4250.13	7 ?	2.115		+10
4260.49	3	2.330		+12
4271.17	3	2.160		+10
4299.25	3	2.197		+ 9
4407.71	3 ?	3.247		+11
4462.01 ?	3	2.185		+20
4469.39	3 ?	2.192		+ 8
4531.64	6 ?	1.939	0.506	+ 6
4611.29 ?	3	3.067		+ 6
4637.52	3 ?			+12
4654.64	3 ?	2.506		+ 7
4668.15	6 ?	1.661		+13
4707.29	3 ?	1.647		+12
4736.79	6 ?	1.898		+12
4859.76	8	1.194	1.143	+14 I.S.
4891.50	?	1.620		+12
4903.32	6 ?	3.600	0.632	+ 9 I.S.
4919.01	6 ?	2.441	1.115	+16 I.S.
4920.52	3 ?	1.845		+13
4923.94	7 ?	2.537		+46
4938.83	4 ?	3.023		+18
4946.40	3	1.968		+24
4957.31	6 ?	2.565	0.773	+14
4957.61	3 ?	2.307		+14
4966.10	3	2.134		+17 I.S.
4973.11	4 ?	1.003		+18
4978.61	unaffected			+18
4982.52	3 ?	1.890		+26
4983.27	3	2.362		+20
4985.27	3	2.337		+16
4985.56	6 ?	2.885		+19
4991.29	3 ?	2.023		+30
5001.88	3	1.660		+23
5005.73	3	1.953		+32
5006.13	6 ?	1.176	0.724	+16
5014.96	4 ?	1.488		+22
5022.25	3	1.043		+24
5027.14	3 ?	1.998		+14
5039.27	3	2.363		+26
5090.79	6 ?			+10
5099.05 ?				+20
5125.14	6 ?	1.976		+20
5137.39	6 ?	2.148		+14
5139.27	3 ?	2.713		+21
5139.48	4 ?	2.622		+20
5162.32	3 ?	2.200		+30
5191.47	7 ?	2.606		+19
5192.36	7 ?	2.780	0.790	+19 I.S.
5208.61	3 ?	2.294		+20
5215.20	3 ?	2.296		+20
5217.41	3 ?	2.259		+16
5229.86	3 ?	2.248		+15

TABLE I—*Continued*

Wave-Length	Type	n	p	Pole-Effect
5232.96	7 ?	1.851		+25 I.S.
5263.32	3	2.352		+20
5266.57	7 or 9	1.810		+17 I.S.
5273.18	3	2.343		+14
5281.80	?	1.115		+19
5283.64	3	2.232		+18
5302.32	3	2.272		+14 I.S.
5324.19	3	2.286		+15 I.S.
5339.94	3	2.329		+19
5353.38	3			+14
5393.19	3	2.314		+17
5473.91	3	2.289		+14
5476.58	3	2.157		+19
5487.78	4 ?			+36
5563.61	3	2.107		+21
5569.63	7 ?	1.080		+20 I.S.
5572.86	7 ?	1.511		+25
5576.10	unaffected			+21
5586.77	7 ?	1.634		+24 I.S.
5602.96	5	1.139	2.318	+19
5615.66	3	1.859		+22 I.S.
5624.56	6 ?	2.098	1.520	+23
5638.28	6 ?			+15

with the magnetic separations seems to have been but little noticed. Gale and Adams[1] remark that there is some relation between pressure-shift and magnetic separation for iron, when lines of the same group and of the same type of separation are compared. As pressure-shift is directly connected with pole-effect, the relation between the pole-effect and magnetic separation may be considered as a consequence of the fact noticed by Gale and Adams. In comparing the magnetic separation of iron lines made by A. S. King,[2] we at once notice that the pole-effect has some intimate connection with it. The lines of iron examined by King for the Zeeman effect and by St. John and Babcock for pole-effect are not always the same, so that a complete comparison is impossible, but there are many lines common to these investigations, which shed some light on the connection between the two.

Tables I and II give the wave-length, the types of magnetic separation, the amount of magnetic separation of the normal component as given by King, and the displacement of the lines from

[1] *Astrophysical Journal*, 35, 10, 1912.

[2] *Papers of the Mt. Wilson Solar Observatory*, 2, Part I, 1912.

the negative pole compared with the center of the arc measured in thousandths of an angstrom, taken from St. John and Babcock's[1] paper.

From the tables we notice that the types of magnetic separation are uncertain for many lines with pole-effect. There is a group of such lines extending from λ 440$_{m\mu}$ to λ 523$_{m\mu}$ showing a positive pole-effect; nearly all the lines in this interval given in the table are of doubtful types. With the negative effect, this is more strongly marked. In the latter case, the connection between the amount of separation and the pole-effect is more definite than in the former. When the mean normal separation is plotted against the negative pole-effect, the mean position of the points is nearly represented by a straight line, which is shown in Figure 1.

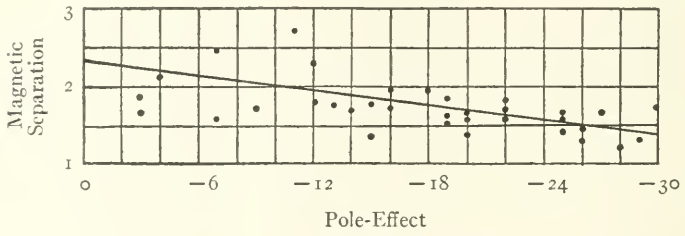


Fig. 1

It shows that the amount of separation is not at all proportional to the pole-effect, but, on the contrary, it tends to become smaller as the pole-effect increases.

Further we notice that many lines showing large pole-effect are diffuse, and are sometimes blended or fringed. Generally speaking, the Zeeman effect is characterized by the symmetry of the separated lines, with only small exceptions. The line of symmetry is generally the line in the undisturbed position, so that even if the type of separation is not exactly known, the initial position will remain unaltered. The uncertainty may arise from the unsymmetrical reversal of the lines or the widening of the lines due to the magnetizing field. Especially will the unsymmetrical widening tend to make the separation indefinite. In

[1] *Astrophysical Journal*, 42, 231, 1915.

addition to this, the length of the arc and the nature of the material will greatly affect the vapor-pressure and the potential-gradient at the poles, and consequently produce the pole-effect. A direct

TABLE II

Wave-Length	Type	n	p	Pole-Effect
3682.21	3	1.696		− 3
3689.90 ?	6 ?	2.739	0.712	−11
3694.00	?	2.235		
3701.08	?	1.723		− 9
3748.96	4 ?	1.708		−14
3773.69	0	unaffected		−12
3797.95 ?	3	1.809		−12
3845.26 ?	6 ?	1.582	1.332	− 7
3966.62 ?	6 ?	2.147		− 4
4172.64	3			−17
4200.92	3	2.482		− 7
4433.22	3 ?			− 6
5065.02	3 ?	1.329		−29
5074.75	6 ?	1.585		−22
5079.00	?	1.771		−13
5096.99	6 ?	1.974		−16
5133.67	6 ?	1.743		−45
5364.86	6 ?	1.229		−28
5367.46	3 ?	1.437		−25
5369.96	3 ?	1.581		−20
5383.37	3 ?	1.656		−25
5404.13	3 ?	1.599		−25
5410.90	3 ?	1.486		−26
5415.19	3 ?	1.739		−30
5424.06	3 ?	1.693		−27
5445.04	3 ?	1.399		−20
5554.88	6 ?	1.628		−19
5565.78	6 ?	1.542		−19
5693.64	3			− 7
5705.99	3 ?	1.858		−19
5816.36	?	1.306		−26
5862.35	3	1.990		−18
5914.16	4 ?	1.880		− 3
5930.18	3 ?	1.669		−20
5984.81	3	1.848		−22
5987.06	3 ?	1.740		−16
6020.18	3 ?	2.332		−12
6024.06	3	1.788		−15
6042.08	?			−12
6056.99	6 ?	1.361		−15
6078.48	3 ?	1.718		−22
6102.18	3			−10
6103.19	6 ?		1.565	−15

connection between magnetic separation and pole-effect does not seem to exist, but the lines of uncertain separation show a positive or a negative pole-effect, on account of their being either diffuse

or blended, of widening or displacing unsymmetrically under pressure. Other causes, as electrostatic effect, the potential fall at the poles, and the reversal of lines, will have some influence in producing the effect.

Considering the various changes to which the iron arc in air is susceptible, the wave-length of the iron lines may be somewhat different according to the experimental circumstances. If the accuracy sought for the comparison is of the order of a milli-angstrom, it is highly desirable to use the iron arc obtained by the cathode bombardment.

My thanks are due to Mr. T. Mishima and Mr. S. Sakurai, assistants in the Institute for Physical and Chemical Research, for assisting in the experiments and calculations.

Physical Institute
Imperial University, Tokyo
July 1920

THE STRUCTURE OF THE BISMUTH LINES

By H. NAGAOKA and Y. SUGIURA

ABSTRACT

Structure of the bismuth lines λλ *4722, 4308, and 4122.*—The intense light produced by bombarding bismuth with a large electronic current from a limed carbon cathode was analyzed by crossing (1) an echelon grating with a glass Lummer-Gehrcke plate and (2) the glass Lummer-Gehrcke plate with one of quartz, to eliminate ghosts. Ten photographs thus obtained are reproduced. For the line λ 4722 the five positive components found by previous observers were confirmed and in addition seven weak negative satellites were discovered, showing that the line has the same general structure as most lines of heavy metals. The principal component is probably multiple, though it has not yet been resolved. Line λ 4122 has four strong components. Line λ 4308 consists of two principal lines 0.350 A apart, each of which is a narrow doublet; in addition there are two faint satellites. The authors point out some constant frequency-differences common to the satellites of these lines and suggest that they may be interpreted in terms of the quantum theory.

Fluctuations of relative intensity of the parts of the central component of the Bi line λ *4722* were observed.

The structure of the bismuth line λ 4722, studied by Baeyer and Gehrcke,[1] Takamine,[2] Lunelund,[3] and Wali-Mohammad,[4] was investigated by L. Aronberg[5] with a ten-inch Michelson plane grating. He showed that the satellites found by Baeyer and Gehrcke and Takamine are nearly correct. The bismuth line was excited by cathode particles as in the experiments of Takamine, but Baeyer and Gehrcke used a bismuth arc, and they arrived at the same result; the discrepancy between the observations of Lunelund and Wali-Mohammad lay principally in the nature of the instrument, as the orders of the spectra observed with an echelon grating are ambiguous and may be interpreted in various ways. Another curious feature in the distribution of the satellites of this line was its one-sidedness. Most of the satellites hitherto investigated, and especially those of mercury lines, are on both sides

[1] *Annalen der Physik*, **20**, 285, 1906.

[2] *Proceedings of the Tokyo Mathematical and Physical Society*, **8**, February 1915.

[3] *Annalen der Physik*, **34**, 505, 1911.

[4] *Astrophysical Journal*, **9**, 189, 1914.

[5] *Ibid.*, **47**, 102, 1918.

of the principal line, so that the $\delta\lambda$'s are both positive and negative; with the bismuth line, they are confined to the positive side only. We have no doubt as to the order of the grating spectra, and the position is uniquely determined; the only objection is, however, the weakness of the spectra of higher orders, so that only with long exposures can we photograph all the satellites. Some doubts were expressed concerning Takamine's photographs, as faint traces of dots were visible in the immediate neighborhood of the positive satellites, which appeared as distinct interference points. This seemed to be due to some instrumental error, and no measurements were made on them. With the lime cathode of carbon, which we have recently developed for spectroscopic work, currents of 2.5 to 4.5 amperes could be maintained for some time between the cathode and the anode of the metal to be studied, so that it was interesting to test the singularity in the structure of the bismuth line with new and powerful means of excitation, and by using a Lummer-Gehrcke plate of glass and one of quartz, which can be crossed with each other to detect the presence of ghosts. By this means we found that the satellites are not confined to the positive side only, but there are many faint components on the negative side, so that the structure of the bismuth line is similar to most of the complex lines of other elements.

The instruments used were as follows, and were all made by Hilger:

An echelon grating of 35 plates, thickness of each plate 9.350 mm with steps of 1 mm; resolving power 435,000 for wave-length λ 5000.

A Lummer-Gehrcke plate of light flint glass; length 20 cm, thickness 1.09116 cm, resolving power 400,000.

A Lummer-Gehrcke plate of quartz; length 13 cm, thickness 4.724 mm, resolving power 566,000.

The spectra were photographed by means of a micro-planar of 7.5 cm focal length, after crossing the echelon grating and the glass plate, while those produced by crossing the plates of glass and quartz, using the extraordinary ray, were photographed with a large quartz spectrograph provided with a Cornu prism. The crossed spectra so obtained were examined with a micrometer

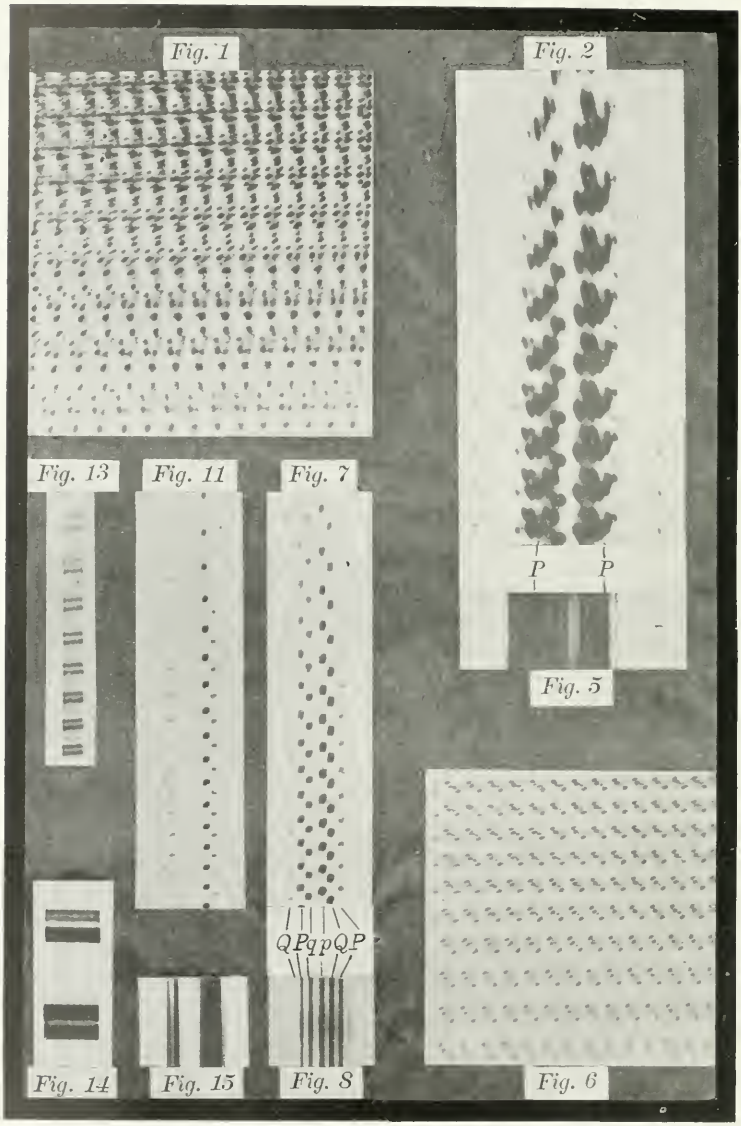


FIG. 1.—Bi λ 4722. Glass L. G. plate crossed with quartz L. G. plate
FIG. 2.—Bi λ 4722. Echelon crossed with L. G. plate
FIG. 5.—Bi λ 4722. Echelon
FIG. 6.—Bi λ 4122. Glass L. G. plate crossed with quartz L. G. plate
FIG. 7.—Bi λ 4122. Echelon crossed with glass L. G. plate
FIG. 8.—Bi λ 4122. Echelon
FIG. 11.—Bi λ 4308. Echelon crossed with glass L. G. plate
FIG. 13.—Bi λ 4308. Quartz plate
FIG. 14.—Bi λ 4308. Horizontal echelon
FIG. 15.—Bi λ 4308. Echelon

microscope and with a comparator. As we had no experience with the crossing of the quartz plate, a preliminary experiment was made on the mercury line λ 4359. The measurement of the plate showed close coincidence in the position of the satellites, as already given by one[1] of us from a combination of a Lummer-Gehrcke plate with a Fabry-Perot interferometer.

Structure of the line λ *4722.*—Crossed spectra of λ 4722, obtained by the combination of the glass and quartz plates, and by the echelon grating and the glass plate, are shown in Figures 1 and 2 (Plate VIII). The former shows at once a number of components which are more numerous than those hitherto given, while the

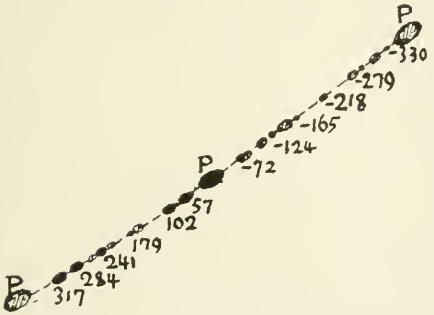


FIG. 3.—Quartz and glass plates



FIG. 4.—Glass plate and echelon

latter is almost similar to the photograph obtained by Takamine, but is marked by a number of weak interference points, very near to those whose position has been already determined by previous investigators. These weak points evidently correspond to spectra of higher order; by following the line connecting them, they are found to belong to the negative components. The existence of false lines due to certain instrumental errors, such as reflection within the echelon plates, may be suspected, but comparison with the crossed spectra of the Lummer-Gehrcke plates will at once decide the question whether or not the doubtful wave-lengths are real. On studying the points, we found that they are arranged according to the following scheme (Figs. 3 and 4). The negative

[1] *Proceedings of the London Physical Society*, **29**, 91, 1917.

components are very faint and the exact position rather difficult to make out; consequently the error of setting during the measurements is not small, and the coincidence in the position of the lines is not perfect, as with the positive components.

TABLE I

Crossed Spectra		Crossed Spectra		Mean	Intensity
Glass Plate	Quartz Plate	Glass Plate	Echelon		
0.316 A	0.314 A	0.320 A	0.318 A	0.317 A	7
281	282	285	287	284	7
241	238	243	243	243	8
179	179	?	?	179 ?	1
102	101	103	102	102	6
56	58	56	58	57	8
0	0	0	0	0	10
faint	faint	− 31	− 32	− 32	1
faint	68	− 76	− 78	− 72	1
− 122	− 124	− 109 ?	− 126	− 124	0.5
− 167	− 168	− 155	− 169	− 165	0.5
− 219	− 219	− 218	− 216	− 218	3
− 295 d*	− 293 d	− 263	− 265	− 279	1
−0.328 d	−0.330 d	−0.322	−0.321	−0.328	1

* d = diffuse

TABLE II

Gehrcke and Baeyer	Takamine	Aronberg	Nagaoka and Sugiura
0.316 A	0.320 A	0.318 A	0.317 A
289	284	284	284
242	238	240	243
104	102	102	102
57	56	56	57
0	0	0	0
.....			− 32
.....			− 72
.....			− 124
.....			− 165
.....			− 218
.....			− 279
.....			−0.328

Further comparison with the echelon spectrum alone was made, but as several components on the positive and the negative side were found to be nearly coincident, as shown in Figure 5 (Plate VIII), the question was difficult to settle with this photograph. The table gives the position of the satellites with reference to the principal line.

The coincidence between different instruments is nearly perfect for the positive components, but with weak negative components the discrepancy is tolerably large. It is certain that with intense light we can observe components on the violet side of the principal line, which lie nearly in the middle of the numerous satellites. This is the general characteristic of most complex lines, and the bismuth line λ 4722 presents no singularity, which the old determinations seemed to indicate.

It must, however, be noticed that there is a zinc line at λ 4722.164 in the neighborhood of the bismuth line. The line is apparently double or triple but, if bismuth contains zinc as an impurity, the components of the line may appear as satellites and give false structure to the bismuth line. Crossed spectra of a mixture and zinc were taken, showing that the zinc line is not in line with bismuth on the drawing, Figure 3, and can be easily eliminated. In the crossed spectra of bismuth given in Figures 1 and 2, there is no indication of the presence of zinc.

Another probability is the intrusion of the line λ 4733 belonging to bismuth into the crossed spectra of λ 4722. By placing the edge of the echelon horizontally, the position of the line relative to λ 4722 in the spectra was ascertained. It was evident that the line may appear as satellite +180 or −328; consequently there is some doubt as to whether or not the component +179 may be due to intrusion. This line was therefore eliminated from the table.

The blue line of bismuth thus consists of more than a dozen components and resembles the green line of mercury, λ 5461. It is perhaps characteristic of such heavy elements that they have a large number of lines with complex structure. The lines of bismuth, lead, and mercury, including the band spectra, seem to be of this nature.

Structure of the line λ 4122.—The bismuth line λ 4122 was studied by Kayser and Runge, Gehrcke and Baeyer, Lunelund, and Takamine. The first-mentioned physicists give the line as a doublet, the second as a triplet, the third and fourth as a quartet, but the intervals are all different.

To settle this point, crossed spectra were taken as shown in Figures 6 and 7. The interpretation of the spectra is graphically

represented in Figures 9 and 10. The principal lines are denoted by P and Q in the figures, the interval between them being 0.200 A; they are accompanied by two lines on the positive and the negative side as given in the table. Taking P as the principal line, we have the following lines.

TABLE III

	Crossed Spectra		Crossed Spectra		Mean	Intensity
	Glass Plate	Quartz Plate	Glass Plate	Echelon		
p.....	0.123 A	0.124 A	0.121 A	0.120 A	0.122 A	8
P.....	0	0	0	0	0	10
Q.....	− .201	− .199	− .202	− .198	− .200	10
q.....	−0.321	−0.321	−0.323	−0.317	−0.321	8

The next table gives the comparison of different determinations.

TABLE IV

Gehrcke and Baeyer	Takamine	Lunelund	Kayser and Runge	Nagaoka and Sugiura
0.150	57	0.050		0.122
0	4122.010	0	4122.010	0
−0.210	4121.690	− .050	4121.690	− .200
.....	− 58	−0.110		−0.321

Evidently Kayser and Runge took the mean points of the first two and of the last two lines as a doublet, whose interval is 0.32 A. In the interpretation of the crossed spectra Takamine seems to have



Fig. 9.—Echelon and glass plate

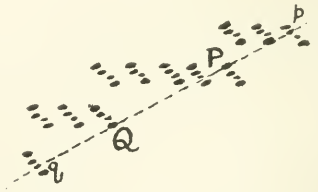


Fig. 10.—Glass and quartz plates

been misled by Kayser and Runge's value, which clearly had the above meaning, and did not refer to the interval between the doublets. It is thus seen how the results obtained with one or

two interferometers are sometimes erroneous; possibly three such instruments will be necessary to solve the problem of the distribution of the satellites without ambiguity.

Structure of the line λ 4308.—The bismuth line λ 4308 was examined with the crossed spectra of an echelon grating and a Lummer-Gehrcke plate as shown in Figure 11, but the details are not clearly made out; it will perhaps require a higher voltage to obtain good results. The principal lines form a doublet at distance of 0.350 A, and each line is a doublet at intervals of 0.024 and 0.023 A. They are accompanied by two faint satellites 0.117 and −0.106, from mean points of the doublet forming the principal lines as shown in Figure 12. The existence of the faint

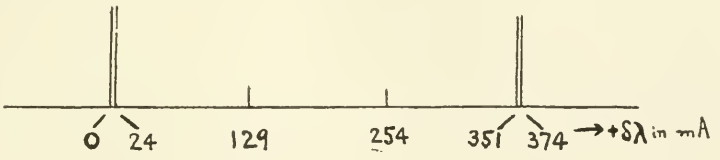


FIG. 12.—Structure of λ 4308

satellites is clear from the photograph obtained with the quartz plate, shown in Figure 13. The results obtained with the echelon grating (Figs. 14 and 15), glass and quartz plates agree tolerably well with each other. This line had not been investigated by other physicists, so that we have no other data with which to compare the measurements.

Regularity in the frequency intervals.—As one of us has already noticed, we sometimes meet with a constant difference in the frequency of the satellites. Such was found to be the case with the mercury and cadmium lines; the bismuth lines seem to show the same characteristic, which is evident in Table V, which illustrates the difference in wave-numbers $\delta\nu = -\frac{\delta\lambda}{\lambda^2}$ per cm. It is to be remarked that the differences found on page 346, Δ_1, Δ_2, Δ_3, are nearly in the ratio 5:3:2. In addition to this, some of the differences are multiples of other differences, as may be seen from the tables.

TABLE V

λ	$\delta\nu\times10^{2}$	λ	$\delta\nu\times10^{2}$
(A) 4122	188.5	(C) 4722	−142.2
	117.6		−127.3
	− 71.8		− 80.3
(B) 4308	− 63.1		− 45.8
	+ 57.1		− 25.6
	± 12.7		0
			14.4
			32.3
			55.6
			74.0
			97.8
			125.0
			147.0

From these we find:

A: 117.6− 0=117.6
B: 188.5−71.8=116.7
63.1+57.1=120.2
C: 142.2−25.6=116.6
147.0−32.3=114.7

Mean=117.1=Δ_1

A: 117.6−71.8=45.8
B: 57.1−12.7=44.4
45.8− 0=45.8
C: 127.3−80.3=47.0
97.8−55.6=42.2

Mean= 5.0=Δ_3

25.6 (C)=2×12.8 (B)
188.5 (B)=3×62.8 (B)
127.1 (C)=3×42.4=3Δ_3
71.8 (A)=5×14.4 (C)
63.1 (B)=5×12.6 (B)

A: 71.8− 0=71.8
B: 63.1+12.7=75.8
C: 147.0−74.0=73.0
125.0−55.6=69.4
74.0− 0=74.0
45.8+25.6=71.4

Mean=72.6=Δ_2

147.0 (C)=2×73.5
142.2 (C)=2×71.1

Mean 144.6 =2×72.3=2Δ_2

127.3 (C)=2×63.6
125.0 (C)=2×62.5

Mean 126.1 =2×63.1 (B)

The interpretation of the foregoing results will probably rest on quantum relations, having some connection with the electronic configuration of the atom.

With heavy elements, it is clear that the number of bound electrons about the atomic nucleus is numerous, so that the electronic configuration is not unique, but there are a great number

of stable distributions of electrons which differ slightly from one another. If the emission of light takes place by the passage of electrons from one configuration to another, the difference in frequency in a slightly varied system will be small, if the initial or the final system be but little different from the system giving rise to the principal line; thus the existence of satellites can be easily explained.

Consider that the emission of frequency ν takes place according to Bohr's scheme

$$h\nu = W_1 - W_2$$

where h is Planck's constant and W_1 and W_2 are the initial and final energy of the electron; then

$$h(\nu+\delta\nu) = W_1 - W_2 + \delta W,$$

where δW may be due either to the change in the initial or final configuration of the electrons, or in both configurations. If δW remains constant in the altered system, and the initial orbit of the radiating electron remains unchanged, it is possible to have different lines with constant difference in frequency. Thus the regularity in the frequency differences is probably to be ascribed to the small variation in the initial or final configuration of the radiating electrons.

In the experiments here described, the lines were excited by swiftly moving cathode particles; the voltage was perhaps insufficient to bring out minute details of the component satellites; but we believe that the details of $\lambda\lambda$ 4722 and 4122 were cleared up in the present experiment by using a higher voltage and a greater current-density between the electrodes than were used by previous investigators. A lime cathode of carbon can be used with advantage in such spectroscopic work, and the cost of such cathodes is negligible compared with the limed platinum cathodes, which wear out after some use.

An important observation was made by one of us during the experiment with the echelon spectrum of λ 4722. The principal line had finite breadth, and the intensity was somewhat fluctuating. It was first thought that the whole line would be subject to such

alternations of intensity, but actual observation showed that only a small portion of the line was subject to flickering, from which it appeared that what was supposed to be a single line consists of three or four lines closely packed together, as is the case with the green line of mercury, λ 5461. It is somewhat singular that all parts of the line are not simultaneously affected. Perhaps such fluctuations are caused by the minute change in the electronic configuration within the atom, and the light is excited by the intrusion of high-speed electrons from the cathode into the atomic system. The electron groups giving rise to the visible spectrum are confined to the outside boundary of the atom, and the configuration will be more susceptible to small changes than in the neighborhood of the atomic nucleus, where X-ray spectra are excited. If we can obtain some means of supplying electrons of moderate speed, we shall ultimately obtain some easy means of powerful illumination.

In conclusion, we have to thank Mr. T. Mishima and Mr. S. Sakurai, assistants in the Institute for Physical and Chemical Research, for great help rendered during the experiment and in the reduction of the results.

Physical Institute
Imperial University, Tokyo
August 1920

THE MUTUAL ACTION OF ADJACENT PHOTOGRAPHIC IMAGES[1]

By FRANK E. ROSS

ABSTRACT

Mutual action of adjacent photographic images.—(1) *Stars and bright lines.* A review of previous work shows that the results are so conflicting that general conclusions cannot be drawn. Three factors seem to control the action. The *turbidity effect* causes an attraction through optical reinforcement of adjacent sides of the images. An equation is derived from which the attraction is found to be negligible, except for very small images very close together. The *gelatine effect* causes an attraction due to the more rapid drying of the developed image. It is measured by the difference in the separation of images when wet and when dry. For normal exposures of star images less than 0.1 mm apart the attraction is equal to about 2 μ for ordinary developers excepting pyro-metol, while in the case of lines the attraction is about 5 μ. This attraction is only slightly changed by varying the amount of sulphite or by the use of a hardener. The *developer or Kostinsky effect* causes a repulsion as a result of the restraining effect of the products of the developing reaction, as in the Eberhard effect. It varies somewhat with the developer but increases with the exposure. The *variation of the total effect with exposure* is such that overexposed images show strong repulsion due to the large developer effect, whereas normally exposed images show an attraction which usually amounts to 2 or 3 μ. To minimize the error which the effect may introduce into measurements of such images, the exposure should be as short as possible. The phenomenon is so complicated that it may be impossible to eliminate it completely. (2) In the case of *absorption lines*, both the gelatine effect and the developer effect cause a repulsion, but in addition to the attraction due to the turbidity effect there is a further attraction due to a difference in the sharpness of outer and inner edges caused by turbidity and halation. In general the total effect is an attraction, about 1 μ for normal exposures but larger for overexposures. Seed 30 plates were used.

Effect of exposure on the time of drying of photographic film.—A normally exposed image dries faster than an underexposed or an overexposed region.

On account of the high degree of precision which had been reached in the determination of the positions of the stars by photography during the first decade of its application to this field, it was not unnatural to suppose that the photographic method could be employed with equal advantage in the determination of the relative positions of double stars and satellites. In both of these special fields of observational astronomy, the systematic errors in the usual visual methods are both troublesome and

[1] *Communication from the Research Laboratory of the Eastman Kodak Company*, No. 119.

important, so that it was hoped that photographic methods might be employed with profit. However, without any question being raised at the time as to the accuracy of the photographic results, it was at once found that its application to the measurement of double stars was limited to pairs of only moderate separation, the important pairs having a separation of the order of one second of arc or less being unresolvable even with the largest telescopes. A greater field of usefulness appeared in observations of satellites, in which it is important to eliminate the systematic errors known to be present in the visual observations.

The first to question the accuracy of photographic measures of double stars and satellites, as far as the writer is aware, was S. Kostinsky[1] in 1906. He observed an apparent repulsion of neighboring images and cites as a possible explanation the well-known fact that in the wet condition images lie below the surface of the surrounding gelatine. In a later paper[2] Kostinsky discusses the phenomenon at length. By photographing a wide double star for varying exposure times, he finds a progressive retrocession of centers, as the following data, taken from his measures, show:

Exposure Time	Diameter		Distance between Borders	Measured Distance between Centers
	Star	Companion		
min.	mm	mm	mm	mm
1.....	0.282	0.039	+0.086	0.2467
16.....	0.482	0.080	−0.014	0.2667

Thus for the long exposure, giving an overlap of 0.014 mm, the distance relative to that for the shorter exposure increases 0.020 mm. From all data he finds the contraction of centers, y, in microns:

$$y = 7.9\left(1 - e^{\frac{80-x}{100}}\right)$$

where x is the distance in microns between adjacent borders of the images of the stars.

[1] *Mittheilungen der Nikolai-hauptsternwarte zu Pulkowo*, Vol. I, No. 11.

[2] *Ibid.*, Vol. II, No. 14.

H. E. Lau[1] in 1912 obtained similar results from a different procedure. He exposed a plate to the Praesepe cluster for five minutes, then moved the telescope about 11″ and exposed again for five minutes. A series of double stars of equal components but of a wide range in magnitude is thus obtained, which should vary in separation if the Kostinsky effect is present. The resulting repulsion, y, as a function of the distance between borders, Δ, is shown in the following table:

Δ mm	y mm
0.034	0.0027
.051	.0019
.069	.0008
.086	.0001
.103	.0000
.120	.0000
0.138	0.0000

Kostinsky's formula gives for $\Delta = 0.034$, a contraction $y = 0.0046$ mm, which is somewhat larger than Lau's value.

H. H. Turner,[2] on the other hand, notes an apparent *attraction* between adjacent lines on a photographic plate, *réseau* lines intersecting at a small inclination being bowed inward near the point of intersection. The effect vanished when the centers of the lines were separated by $\frac{1}{3}$ mm or more. When the lines were in contact, the centers being then separated by 0.075 mm (computed), the actual separation was less by 0.006 mm. This means that two fine spectral lines, each of width 0.075 mm, and in contact, have had their true separation diminished by 8 per cent. Turner attributed the phenomenon to a displacement of the light maxima in the images, a phenomenon discussed at length below.

F. A. Bellamy,[3] from a study of the double stars of the Oxford astrographic catalogue, supports Turner's conclusions. Bellamy compares the photographic separations with the values in Burnham's *General Catalogue*. In all, 436 pairs were examined. In the case of the overlapping images (overlapping one-third of the radius) the apparent contraction was large, averaging about 8 per

[1] *Astronomische Nachrichten*, **192**, 179, 1912.

[2] *Monthly Notices*, **77**, 519, 1917.

[3] *Ibid.*, **77**, 521, 1917.

cent. With images not quite in contact, the clear space being 0.02 mm, the contraction amounted to 2 per cent. When the clear space became about 0.08 mm all trace of contraction disappeared.

Hertzsprung[1] finds both contraction and repulsion in photographic measures of double stars depending on the atmospheric conditions and on the separation of the components. He explains the attraction as arising from the addition of density to each image at its inner edge, due mutually to the light from the other. This explanation is the same as Turner has suggested. He finds the effect most pronounced on nights of bad seeing, amounting to 0.007 mm. On the other hand, repulsions occur on nights of the best definition and in the case of close pairs.

Mitchell and Olivier[2] made an extended series of photographic measurements of the triple star Krueger 60, in which the components A and B approached within 1″.84 (0.09 mm) of each other. Comparison with Barnard's visual measures shows no evidence of either attraction or repulsion.

There appears to be but little in the literature on the behavior of close spectral lines. C. E. St. John[3] has the following:

> A comparison has recently been made between the separation of close pairs as given in the Rowland tables and as measured upon plates of higher dispersion than that used by Rowland. For pairs consisting of lines of intensities 3 and 4 whose separations are 0.0 to 0.1 Å, 0.1–0.2, and 0.2–0.35, the Rowland values exceed those found at Mt. Wilson by 0.011 Å, 0.007 Å, and 0.004 Å, respectively.

From one point of view these can be considered as repulsions of the lines on the Rowland plates, the scale of which is 1 Å = 1 mm. The effect appears to be greater and effective at greater separations than found in the case of stellar images described above. However, according to another investigation by St. John,[4] there is evidence of part of the effect at least being due to psychological causes. He finds that for measures of close spectral lines made in the ordinary way and on the Koch microphotometer, the microphotometer gives the smaller separation.

[1] *Observatory*, 44, 56, 1921. [2] *Astronomical Journal*, 32, 179, 1920.

[3] *Proceedings National Academy of Sciences*, 2, 228, 1916.

[4] *Year-Book of the Carnegie Institution of Washington*, No. 15, p. 240, 1916.

On the other hand, F. Goos[1] finds that Kayser's measures of the separation of close doubles in the iron arc differ from his own in the following way:

Average separation, 0.24 Å=0.09 mm,
Separation (Goos−Kayser), −0.0042 Å=−0.0016 mm±0.0004 mm,
Scale: Kayser, 1 Å=1 mm; Goos, 1 Å=0.36 mm.

Since the scale of Kayser's plates is the greater, these results show that the lines of Goos's plates suffer an *attraction* in opposition to the repulsion shown on the Rowland plates. Thus an inconsistency in the results affecting any general conclusions is to be found in measures of spectral doubles, as well as in measures of double stars.

The writer has previously investigated the action of adjacent images on each other in the particular case of a large central image and a small neighboring image.[2] The smallest distance between adjacent borders utilized was 0.12 mm, in which case under certain conditions of development the small image was displaced toward the larger by 0.020 mm. The effect was found to be appreciable when the border separation became as great as 0.42 mm, the image displacement in this case being 0.006 mm. The effects are thus seen to be larger and operative at greater distances than in the cases noted by the writers quoted above. They agree in general with the results of Turner, Bellamy, and Goos in showing the existence of a contraction, and are apparently opposed to those of the earlier investigators and to St. John's results.

Aside from possible systematic errors of measurement, there appear to be three distinct factors controlling the deviations from normal action in the case of neighboring images, as follows:

a) A mutual light-action causing each of the images to assume an oval form, the geometrical centers being displaced inward, the result being an apparent attraction. This effect will be called the "turbidity effect."

b) Displacements of the gelatine in which the images are imbedded, which can be called the gelatine effect, measured and discussed by the writer in the paper quoted.

c) It appears necessary to assume the existence of an abnormal action of the developer in developing the latent image, such as is

[1] *Astrophysical Journal*, 35, 232, 1912. [2] *Ibid.*, 52, 101, 1920.

found in the Eberhard effect.[1] One of the main objects of the present paper is the investigation of this effect, which may be called the "Kostinsky effect." Each of the three phenomena will be considered at some length.

The turbidity effect.—Consider the case of photographing a double star or a pair of spectral lines having components of equal intensity. The distribution of light in the film due to each component is[2]

$$I = I_0 e^{-\kappa r}, \tag{1}$$

where I_0 is the intensity in the central diffraction disk, and I the intensity at a distance r from the center of star or line. κ is a parameter whose numerical value is given by

$$\kappa = \frac{2 \log 2}{\text{Mod.}} \times \frac{1}{m} = \frac{1.386}{m}, \tag{2}$$

where m is the increase, in microns, in the diameter of one of the stellar images or spectral lines for each doubling of the exposure time, or, more strictly, for doubling of the intensity. The relative distribution of light is thus fully determined.

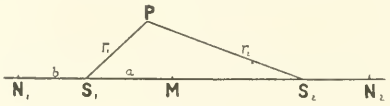


FIG. 1

Let S_1 and S_2 (Fig. 1) represent the centers of a pair of close stars of equal components. Let P be any point in the immediate neighborhood, distant r_1 and r_2 from S_1 and S_2. The total intensity of light at P is evidently

$$I_P = I(e^{-\kappa r_1} + e^{-\kappa r_2}). \tag{3}$$

The boundary line of the stellar image is determinable by the condition $I_P = \text{constant}$, which gives as the equation of its outline

$$e^{-\kappa r_1} + e^{-\kappa r_2} = \text{constant} = C. \tag{4}$$

[1] *Physikalische Zeitschrift*, 13, 288, 1912.

[2] *Astrophysical Journal*, 52, 206, 1920.

This represents a family of transcendental curves, real branches of which are a family of lemniscates. In Figure 2 a number of the curves are accurately drawn to scale. The practical case is chosen of a separation of centers of 0.1 mm. κ is chosen equal to 0.05, corresponding to $m = 28$, a value which is of the order of magnitude found for large telescopes and high-speed emulsions. In Figure 2 a pair of point images are chosen, corresponding to the case of critical definition. In Figure 3 the curves for disk-images are shown. In this case r_1 and r_2 are measured from the edge of each

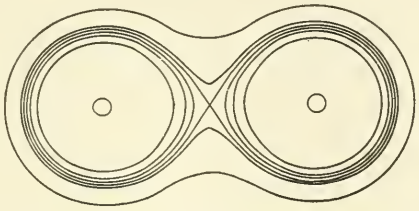


FIG. 2.—Outlines of neighboring images for point sources

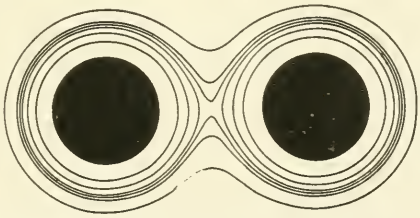


FIG. 3.—Outlines of neighboring images for equal circular sources

disk. It is seen that the character of the curves is the same in the two cases. The curves are oval in form, becoming more and more pronounced as the exposure time or intensity is increased. The center of each image is displaced toward the other, the amount of the displacement increasing with the size. In other words, double stars and close spectral lines are subject to an apparent *attraction* of an amount depending upon the separation of their adjacent borders. In the important and interesting case of *contact* the figures show that instead of the images coming together along a curve as would naturally be expected, they meet in a point, the outline of each image in the neighborhood of their intersection being

composed of two lines intersecting at an angle of considerable size in the practical cases under consideration. These oval forms should be observable, and the corresponding attraction of centers should be measurable. That they are not, in general, is due to the masking effect of the Kostinsky phenomenon, as will appear later.

It is not difficult to obtain a formula giving the attraction or displacement of centers of adjacent stellar images or spectral lines. Since the maximum effect is attained for equal components, only that case will be considered. The method is easily extended to the case of unequal components. Referring to Figure 1, putting $S_1S_2=s$, equating the illumination at M with that at N_1

$$I[e^{-\kappa a}-e^{-\kappa(s-a)}]=I[e^{-\kappa b}+e^{-\kappa(s+b)}]\,. \tag{5}$$

In all practical cases the second term on the right can be neglected. The equation is then rearranged as follows:

$$e^{\kappa(a-b)}=1+e^{-\kappa(s-2a)}\,. \tag{6}$$

Put

$\delta=$ total displacement of centers,

$r=$ separation of adjacent edges;

it is evident that

$$\delta=a-b,$$
$$r=s-2a,$$

leading to the following simple equation for the "attraction" of double stars or spectral pairs

$$e^{\kappa\delta}=1+e^{-\kappa r}\,. \tag{7}$$

For the special case of contact of images, the equation becomes

$$e^{\kappa\delta}=2,$$

or finally, since

$$\kappa=\frac{2\log 2}{\text{Mod.}}\frac{1}{m},$$

$$\delta=\tfrac{1}{2}m; \tag{8}$$

hence we have the remarkable theorem that in the case of contact of images the contraction is equal to the increase which takes place

in the radius of a stellar image for each doubling of the exposure time, and is moreover independent of the size of the image itself. The theorem applies to spectral lines as well, in this case the radius being replaced by the half-width. In practical cases m lies between 10 (very sharp) and 30 (diffuse); the corresponding maximum attraction of stellar images or spectral lines accordingly lies between 0.005 mm and 0.015 mm. Table I, computed from (7), gives the value of the attraction δ for various values of m, and of r, the separation of the adjacent edges of stellar images or spectral lines.

TABLE I

VALUES OF δ (IN MICRONS)

m	10μ	15μ	20μ	25μ	30μ
κ.....	0.139	0.093	0.070	0.056	0.046
mm					
r=0.000.....	5.0	7.5	10.0	12.5	15.0
.010.....	1.6	3.6	5.8	8.1	10.6
.020.....	0.4	1.6	3.2	5.0	7.3
.040.....	0.0	0.3	0.9	1.8	3.2
0.080.....	0.0	0.0	0.1	0.2	0.5

The gelatine effect.—As already remarked, data have been collected by the writer on the mutual action of adjacent images in the case where one of the images is large. It is necessary to measure the effect in the case of small images, as in double stars and close spectral lines. The experiments must be so arranged that the effects so far as possible can be differentiated.

It has been shown (*Astrophysical Journal*, **52**, 106, 1920) that movements of the gelatine surrounding and within adjacent images cause an apparent attraction between images which is brought into evidence by comparing measurements of the same pairs made with plate wet and plate dry. It is clear that this effect can be differentiated from the "attraction" of the latent image already discussed, and from the "repulsion" of the Kostinsky effect discussed in a later paragraph.

A test-object, A, composed of ten artificial double stars, all of equal size, was photographed on Seed 30 plates, the separations being adjusted so as to reproduce conditions obtaining in practice. It was photographed in a special precision camera reducing 20

diameters. An enlargement of one of these exposures is shown in Figure 4. The separation of the close pair (*jj'*) is 0.052 mm, and of the widest pair (*aa'*) 0.104 mm. The average diameter of the images is 0.04 mm. Five exposures were made on each plate

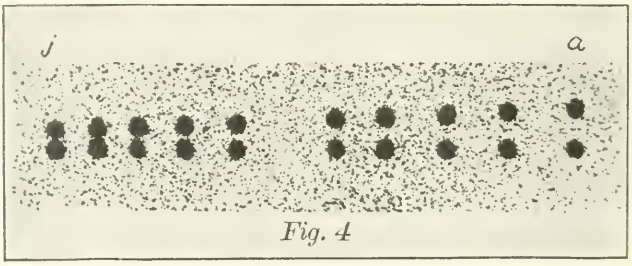


FIG. 4.—Enlarged images of double-star test object

and were measured wet and dry. The plates, ten in all, were developed in several different kinds of developer, including the staining: pyro, pyro-metol, and caustic hydroquinone; and the non-staining: hydroquinone and metol-hydroquinone. Since the differences brought out between the action of the various developers,

TABLE II

CONTRACTION IN DRYING OF IMAGES OF CLOSE DOUBLE STARS (IN MICRONS)

Pair	Mean of Ordinary Developers	Pyro-Metol	Edge Separation
	μ	μ	mm
aa'	0.9	8.4	0.080
bb'	1.4	5.6	.071
cc'	1.4	7.0	0.62
dd'	1.8	5.0	.053
ee'	1.8	5.2	0.44
ff'	2.0	3.4	.036
gg'	2.0	5.6	.027
hh'	2.3		.018
ii'	1.2		.009
jj'	0.9		0.000±
Mean	1.6	5.7	

excepting the single case of pyro-metol, were not striking, the results from all ten plates are averaged in Table II. All measurements recorded in this and in the following tables were made on a

Hilger comparator at a uniform magnification of 75. The plates in all cases were Seed 30.

The values for the pairs *i* and *j* are uncertain owing to the difficulty of accurately measuring pairs in close contact. For this reason the last three pairs were not measured on the plate developed in pyro-metol. It is seen that the very strongly staining and tanning developer, pyro-metol, stands apart from the ordinary developers in the magnitude of the contraction, confirming the results found and described in a former paper.[1] A further conclusion of importance is that the contraction is *independent* of the separation, within the limits of the experiment, which include all practical cases of interest. It can be concluded that, for the close doubles of separation 0.1 mm or less, the contraction due to the movement of the gelatine is 0.0016 mm for all ordinary developers. That different results were not obtained for the two classes of developers, staining and non-staining (with the single exception of pyro-metol), seems surprising in view of the results obtained previously. In the previous work, however, a much larger test-object was used, so that the conditions of the experiments were not similar to those just described. It is clear that much work remains to be done on this branch of the subject before general conclusions as to the action of different developers can be reached.

The series of measurements on the double-star group furnishes information on the Kostinsky effect, as well as on the gelatine effect just considered, for measurement of the separation of the double stars on the test-plate itself, assuming no distortion in the optical system, gives the relative values of the separation of the images of the test-plate. For this comparison only the pairs *aa'* and *jj'* will be considered. The results are:

	mm
Separation of centers of *aa'* in test-plate	2.000
Separation of centers of *jj'* in test-plate	1.022
Photographed *aa'* (measured wet)	0.1049
Photographed *jj'* (measured wet)	0.0532

By simple proportion from the first three quantities, *jj'* should be 0.0536 mm. This agrees with the measured value within the

[1] *Astrophysical Journal*, 52, 101, 1920.

error of measurement, leading to the conclusion that no distortion of any kind is apparent. But from Table I, assuming $m = 10$, a value close to the true one, and assuming further that the images j and j' are in contact, we find a computed turbidity contraction of 0.0050 mm. Since the gelatine effect has already been eliminated, it must be concluded that in this case the turbidity contraction and the Kostinsky repulsion are mutually destructive. This is not surprising since attractions and repulsions in equal number have been obtained by various investigators, as shown in the introduction.

The gelatine effect for spectral emission lines.—The test-object, B, in this case consisted of two pairs of parallel lines having equal components, which were photographed on Seed 30 plates in the same way as the double-star test-object. The pairs are designated *a* and *b* in Table III, which gives the results of measurement.

TABLE III

CONTRACTION OF SPECTRAL PAIRS IN DRYING

	a	*b*
Mean separation (dry)	0.149 mm	0.107 mm
Mean width of lines	0.100 mm	0.080 mm
Contraction with caustic-hydroquinone dev	5.0 μ	4.3 μ
Contraction with chlor-hydroquinone dev.	4.6 μ	4.6 μ
Contraction with pyro-soda dev	6.2 μ	6.0 μ
Contraction with pyro-metol dev	15.4 μ	14.3 μ

It is seen that the gelatine contraction for spectral pairs is twice that for double stars of equal separation. This may be in part due to the greater width of the spectral lines, as well as to their linear extent. Further experiments with narrower lines are to be made. It appears to be true that the gelatine effect is greater for the important case of spectral doubles than in that of double stars. As in the case of double stars (Table II), all developers excepting pyro-metol are seen to give nearly the same effect.

Effect of sulphite.—Since the staining and tanning action of a developer to a certain extent can be controlled by its sulphite concentration, corresponding variations in the contraction of the gelatine should occur if it is true that tanning of the gelatine is

a factor in contraction of the image. Experiments were made with pyro developer in which the amount of sulphite was altered between wide limits. It is not necessary to give details. The contraction was actually found to diminish with increasing sulphite.

Action of hardening agents.—It is found that hardener in the fixing bath reduces the contraction only slightly. In a different experiment, plates after fixing were bathed in a concentrated solution of quinone; and in another case in a 10 per cent formalin solution. In order to obtain the maximum effect, the plates were developed in pyro-metol. An average reduction of 25 per cent in the contraction was obtained. These results were expected, since hardening of the gelatine should not alter to any great extent the variation of water content of a developed image with its density.

Drying time of a developed image.—It is desirable to have direct or observational data on the drying time of a developed image, since in the explanation given by the writer of the contraction of

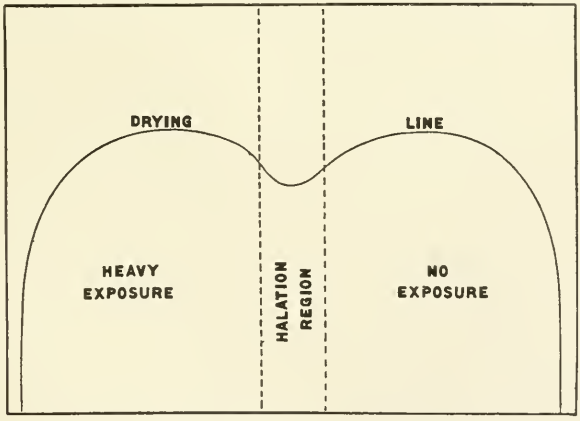


FIG. 5.—Drying line on a partially dried plate

an image due to movements of the gelatine it is assumed that a developed image dries more quickly than the clear gelatine surrounding it. The following experiments were made.

Five-by-seven plates were exposed to light over half their surface, developed in pyro-metol, and after fixing allowed to dry. The exposed portion was found to dry more quickly in all cases. Figure 5 shows the drying line of a partially dried plate, one-half

of which had been subjected to a heavy overexposure. Between the region of overexposure and the clear gelatine there is a halation strip one inch in width. The dip in the drying line in the halation region brings out the remarkable fact that a normal exposure dries more quickly than either clear gelatine or an overexposure. This difference in drying between normal and overexposure was verified by numerous experiments.

The Kostinsky effect.—The anomalous actions just discussed which affect the true distance between images of close double stars and spectral lines on a photographic plate are not competent to explain the phenomena actually observed, for, as shown, both the turbidity effect and the gelatine effect result in an apparent attraction of images. As cited in the introduction, there are many conclusive cases of apparent repulsion of images, so that we must look to a third class of anomalous actions to explain all the facts observed.

One method of studying the mutual action of adjacent images is that followed by Kostinsky, namely, of measuring the distance of centers of a series of images of a double star or close spectral pairs, real or artificial, the time of exposure being varied in such a way that the size of the images varies from threshold to one producing contact or even overlapping. When the experiment is made in this way, it must be assumed that the distribution of light in each image is perfectly symmetrical, or at least that any dissymmetry is the same for both images. However, with good modern optical instruments a lack of symmetry need not be feared, if exposures are made on close doubles and in the optical axis. In this connection it may be said that Lau's method (p. 351) of obtaining the effect is open to question on this account, since the exposures were not axial, but distributed over the plate. It is quite likely, however, that this error is negligible.

Experiments with artificial double stars.—Two pairs of artificial double stars to be used as test-objects were accurately cut from a thin plate, the dimensions being as follows:

Pair	Diameter of Circles mm	Separation of Centers mm
C	1.08	3.39
D	6.64	7.98

The double-star images to be studied were obtained by photographing test-objects C and D in a precision camera as in previous experiments. The exposure times were 1^s, 2^s, 4^s 4^m in the case of object C, giving a series of double stars, the diameter of whose components varied regularly from 0.07 mm to 0.18 mm, varying somewhat with developer and development time. Many plates were exposed in this way and developed for different lengths of time in different developers in the hope of finding a variation in the effect which would lead to an understanding of its nature. In this preliminary series of experiments no certain variation with developer and development time was disclosed. In Table IV, giving the result of these measures, the mean result from all plates and all developers is given, eleven plates in all being measured.

TABLE IV

RESULTS FROM DOUBLE-STAR TEST-OBJECT C

Exposure Time	Separation of Edges	Diameter of Images	Separation of Centers	Computed Turbidity Correction
	mm	mm	mm	mm
1.0 sec.	0.096	0.076	0.1724	
1.9	.084	.088	.1720	
3.8	.071	.101	.1720	
7.5	.060	.112	.1717	
15.0	.048	.124	.1724	0.0000
30.0	.036	.136	.1724	+ .0002
60.0	.024	.150	.1749	+ .0008
120.0	.016	.160	.1764	+ .0015
240.0	0.010	0.171	0.1813	+0.0026

The fourth column of this table shows a strong and undoubted "repulsion" of centers of such a magnitude as to completely overshadow the so-called gelatine and turbidity "attraction" effects. The turbidity effect is given in the last column, computed from formula (7) with $m = 12.5$.

Test-object D.—This test-object was designed for the purpose of finding out to what extent the repulsive effect shown in the case of test-object C depends on the *size* of the component images. The measurements of only one plate are given in Table V, as they are illustrative of the average result obtained. Development was in pyro-soda. The measurement in the case of test-object D was made in a different way from that of object C, for it can be objected

that the result obtained for C was due to psychological causes, the bisection of centers in the process of measurement being influenced in a varying systematic manner by the presence of the neighboring

TABLE V

RESULTS FROM DOUBLE-STAR TEST-OBJECT D

Exposure Time	Separation of Edges	Separation of Centers	Mean Longitudinal Diameter D_1	Mean Transverse Diameter D_2	$D_2 - D_1$
sec.	mm	mm	mm	mm	mm
1.0.....	0.068	0.413	0.346	0.350	0.004
1.9.....	.059	.413	.354	.358	.004
3.7.....	.052	.412	.360	.368	.008
7.5.....	.049	.416	.367	.376	.009
15.0.....	.044	.419	.374	.387	.013
30.0.....	.041	.422	.380	.396	.016
60.0.....	.035	.425	.389	.402	.013
120.0.....	0.032	0.428	0.396	0.411	0.015

or comparison image. Accordingly, in the case of object D, the settings of the micrometer thread were made on the edges of each star, and the separation of centers was computed. This also gives



FIG. 6.—Images of a double star in contact

the longitudinal diameter of each stellar image. As a check, the transverse diameter of each stellar image was measured, for a reason which will appear in Table V.

The repulsion is seen to be greater than in the case of test-object C, although the minimum separation of edges is greater. This

was to be expected, if the explanation of the phenomenon presently to be given is the correct one. In order to eliminate from $D_2 - D_1$ any error in perfect roundness of the holes in the test-object, an auxiliary series of exposures was made in which each hole of the test-object was covered in turn. The mean of a series of exposures made in this way gave $D_2 - D_1 = 0.004$ mm. This correction has been applied in the foregoing table. It is seen that as the images approach they become decidedly oval in form, the greater axis being transverse. An enlargement of these images is shown in Figure 6, in which the oval form is apparent to the eye.

The Kostinsky effect on spectral emission lines.—In order to investigate the Kostinsky effect on spectral emission lines, a test-object E was made having but one pair of slits of the following dimensions:

Width of slits	0.36 mm
Distance between centers of slits	2.94 mm

On account of the importance of the Kostinsky effect on spectral lines, an extensive series of experiments was made with this test-object. Five developers were used. In all twenty plates were exposed, four for each developer. The plates were measured both wet and dry. In measuring the wet plates, pointings were made through the back, in order to eliminate errors due to capillarity. The exposures on each plate were timed to include images not far from threshold size at one end to images nearly in contact at the other end of the series.

The results of Table VI are plotted in Figure 7 (p. 367). In the first place it is noticed that the gelatine effect (wet-dry) is practically the same for all developers. Since the minimum separation of edges is 0.028 mm, the maximum turbidity effect is negligible (Table I). Accordingly the curves (wet) give the true Kostinsky effect, it being assumed from previous work that the gelatine effect is not present in the wet condition of the plate. It is possible that further work on the subject may modify this assumption.

There appears from the curves to be considerable variation of the Kostinsky effect with developer. The effect is greatest for pyro developer, and smallest for metol-hydroquinone. The remarkable fact is brought out that in the case of measures on the

dry plate, one to which naturally the greatest interest is attached, there is first an attraction, followed by a repulsion as the separation becomes smaller. This may serve in part to explain the contradictory results obtained by various investigators quoted in the

TABLE VI

RESULTS FROM TEST-OBJECT E (SPECTRAL DOUBLES)

Developers: *a*, caustic hydroquinone; *b*, pyro-metol; *c*, metol-hydroquinone; *d*, pyro; *e*, ferrous oxalate.

EXPOSURE TIME	SEPARATION OF CENTERS					SEPARATION OF ADJACENT EDGES				
	a	*b*	*c*	*d*	*e*	*a*	*b*	*c*	*d*	*e*
	Measured Dry									
	mm	mm	mm	mm	mm	mm	mm	mm	mm	mm
1.0 sec.	0.1500	0.1480	0.1500	0.1498	0.1502	0.125	0.122	0.128	0.128	0.128
1.9.....	.1490	.1475	.1490	.1485	.1498	.116	.112	.120	.119	.120
3.7.....	.1482	.1472	.1492	.1478	.1483	.105	.101	.107	.110	.110
7.5.....	.1478	.1463	.1488	.1473	.1465	.094	.091	.095	.098	.099
15.0.....	.1480	.1450	.1485	.1470	.1472	.083	.076	.085	.088	.085
30.0.....	.1478	.1465	.1472	.1473	.1478	.072	.065	.072	.076	.073
60.0.....	.1470	.1445	.1490	.1458	.1458	.060	.055	.061	.068	.063
120.0.....	.1470	.1442	.1468	.1455	.1433	.047	.044	.054	.055	.052
240.0.....	.1470	.1457	.1482	.1465	.1438	.037	.033	.044	.048	.042
480.0.....	0.1490	0.1470	0.1500	0.1492	0.1470	0.030	0.028	0.035	0.038	0.036
Means..	0.1481	0.1462	0.1487	0.1475	0.1470					
	Measured Wet									
1.0 sec..	0.1510	0.1488	0.1502	0.1512	0.1512					
1.9.....	.1515	.1480	.1510	.1520	.1512					
3.7.....	.1510	.1507	.1522	.1502	.1493					
7.5.....	.1498	.1503	.1525	.1520	.1498					
15.0.....	.1512	.1500	.1522	.1510	.1505					
30.0.....	.1515	.1502	.1540	.1508	.1512					
60.0.....	.1522	.1512	.1543	.1525	.1507					
120.0.....	.1520	.1493	.1533	.1545	.1502					
240.0.....	.1555	.1528	.1545	.1552	.1515					
480.0.....	0.1560	0.1575	0.1562	0.1582	0.1538					
Mean...	0.1522	0.1509	0.1530	0.1528	0.1509					
Mean Wet-Dry	0.0041	0.0047	0.0043	0.0053	0.0039					

introduction. The explanation is simple. In the first stages the gelatine attraction is stronger than the Kostinsky repulsion, while in the latter stages, when the separation becomes less than about 0.06 mm, the Kostinsky repulsion predominates. The behavior of ferrous oxalate is curious, and needs to be checked. It is to be

noted that in the case of all developers, development was fairly complete, having been pushed to the point where fog became noticeable.

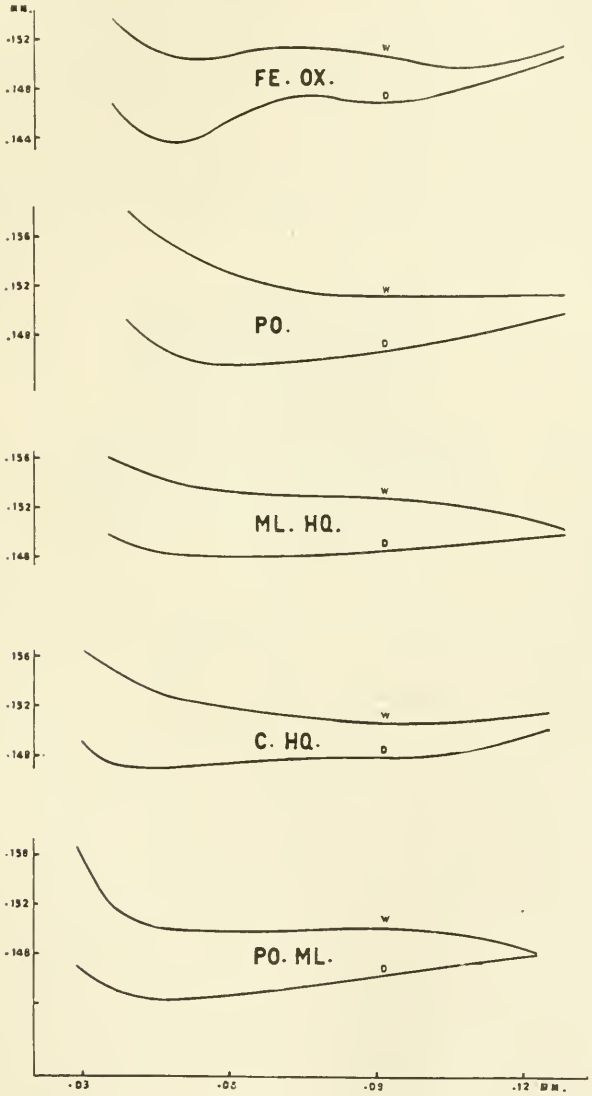


FIG. 7.—Separation of close emission-lines for various developers. Abscissa, edge separation.

Another series of experiments is planned which will allow the curves to be followed closer to the point of contact. In the present instance this could have been done simply by increasing the exposure, but the resultant lack of sharpness of the outline would have made accurate measurement difficult. It is simply a matter of choosing test-objects of suitable dimensions, to get contact simultaneously with sharpness of outline.

As to the cause of the Kostinsky effect, it seems reasonable to assume that it is a *developer* effect and but another manifestation of the Eberhard effect.[1] In the process of development, reaction products are formed which are known to have a powerful restraining

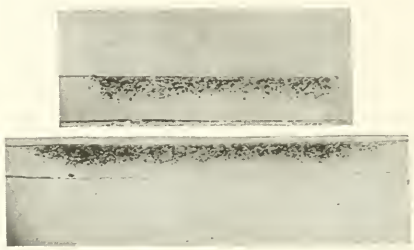


FIG. 8.—Two sections of photographic images showing Eberhard effect

action on development. The bright ring surrounding strong, sharp negative-images is one manifestation of this action. The action may be something more than a simple, restraining one, for the bright ring is very often seen around minute stellar images. The action must accordingly be a positive and permanent one, the products of development acting on the image in its immediate neighborhood as soon as formed, the effect spreading to adjacent regions as they diffuse, until their concentration becomes too low to be effective. With these assumptions, the Kostinsky "repulsion" of neighboring images is easily explained. Consider a pair of adjacent images. As development goes on, the liberated products of development pour into the intervening space from both sides, restraining or inhibiting development of the latent image in this region, as explained above. But, on the "far" sides, the concentration of the products of development is only one-half. There

[1] *Physikalische Zeitschrift*, 13, 288. 1912.

is less restraining action of the latent image in these regions, therefore. The net result of this non-symmetrical action on each image is an apparent repulsion or retrocession of centers. This action is very well illustrated in Figure 6 which is an enlargement of a pair of close images, the oval form being quite perceptible. In Figure 8 the action *downward* in the film is shown. It will be noticed that the density or amount of silver is less in the center of the image than at the edge. This is the true Eberhard effect, of dependence of *density* of image on its size. The Kostinsky and Eberhard effects are considered to be but different manifestations of a common phenomenon: in the Kostinsky effect we are concerned with the developer effect on size of image, in the Eberhard effect with the developer effect on density of image.

Up to this point a seemingly confused mass of material has been presented, the results from which appear more or less contradictory: in some cases the net result of an experiment is a repulsion, in others an attraction. It is therefore pertinent to inquire if there is any principle governing the *net* effect. It will be noticed that in general in those cases where a repulsion has been obtained, the images were formed by *overexposure;* and in those cases where an attraction was found, the exposures have been normal. This is equally true with respect to the results obtained by other investigators quoted above, and those obtained by the writer as just described. As to the cause, it is only necessary to assume that in overexposure the retarding action of the products of development is very great, or that it is directly proportional to the exposure. This is a not unreasonable assumption. Instead of the separation of images, therefore, being the only controlling factor in the Kostinsky repulsion, or development effect, as has heretofore been assumed, an equally powerful factor is the exposure value.

The conclusion is that in average work a slight *contraction* in separating distance of neighboring stellar images or bright emission lines in spectra is to be expected. But on account of variations in exposure from normal to overexposure, it is by no means certain in any given case that contraction will result: there may be no effect, or there may even be a repulsion. Summing up, if exposures are kept at a minimum, errors exceeding two or three microns need

not be feared. The importance of reducing the exposures to the lowest possible value is to be emphasized.

Behavior of close absorption lines.—Upon applying the reasoning used in the treatment of close double stars and bright-line spectra or emission lines to the case of absorption lines, important differences arise in the case of all three of the factors of turbidity, gelatine effect, and development effect. This is especially true in respect to the turbidity effect. Consider two neighboring absorption lines, separated by an illuminated strip. The intensity of illumination in this area must be less than in the regions adjacent to the "far" boundaries of the lines. This becomes clear when it is noted that in the case of a turbid medium such as a photographic emulsion the intensity of the illumination at any point within it is the resultant of the flux at the surface combined with flux from the surrounding regions, which has been bent from its normal course by diffraction and reflection. In the case in hand, the surrounding regions are the unilluminated absorption lines which lie on each side of the bright area. There is therefore a deficiency of illumination at the adjacent edges of the absorption lines leading, in the developed image, to an apparent broadening of each line asymmetrically. Owing to the factor of turbidity, therefore, but in quite a different manner from the action of turbidity on emission lines, the distribution of light leads to an apparent attraction of spectral absorption lines. While the amount of the attraction in the case of emission lines can be calculated, as shown above, any simple mathematical treatment of the corresponding problem of absorption lines does not seem possible. Only in a qualitative sense can the attraction be proved existent. It is quite evident, moreover, that the action is greater the closer the lines, so that the general law of the action in both cases appears to be the same, although explained physically in different ways.

Unlike the turbidity action, the disturbing action of the gelatine seems to be reversed in passing from emission to absorption lines. Recalling that the movement of the edge of an image in the process of drying is always toward the region of greater density, and noting further that the weak density separating the absorption lines has less of a "pull" than the stronger density adjacent to the far edges,

it follows that absorption lines are apparently repulsed owing to their asymmetric broadening in drying. It is quite likely that the action is weaker than in the case of bright-line spectra, for in order to preserve the definition and even the visibility of absorption lines the exposures given are relatively weak and the developed densities low. The writer has previously shown[1] that the gelatine effect diminishes as the density of the image becomes less. In bright-line spectra, on the contrary, the visibility is improved by long exposures, so that the central diffraction-image may be in this case very much overexposed. The chemical actions in development are accordingly more intense, leading to greater disturbance than in the case of absorption lines.

It remains to consider the development disturbance in close absorption lines. Applying the hypothesis used in the previous cases of double stars and emission lines, namely, that the edge of a silver image loses density in development by an amount proportional to the chemical activity going on in the region back of the edge, it will be seen that the far edges of absorption lines suffer to a greater extent than the near or adjacent edges, so that here again an apparent repulsion takes place. As in the case of the gelatine effect, the amount of the action should be less for absorption than for bright-line spectra, owing to the low densities concerned.

In addition to the three disturbances just considered which are present in both emission and absorption spectra, there is a fourth disturbance which is effective only in the case of absorption lines. On account of the great extent of the illuminated area of the plate back of the non-adjacent edges of the absorption lines, it is to be expected that the distribution or falling off in light-intensity at these edges is different from that at the near or contiguous edges. From general considerations the light-curve at the far edges should be flatter, or κ, in the intensity equation (1), smaller. Accordingly m, the rate of growth of these edges with exposure, is greater (equation [2]). The result is an apparent attraction of the lines. The effect is enhanced by halation.

Considering the totality of the disturbing actions concerned in the case of absorption lines, it may be predicted that errors in

[1] *Astrophysical Journal*, 52, 104, 1920.

the measurement of adjacent absorption lines are small. It is accordingly difficult to explain the difference between the Rowland and the Mount Wilson measures, found by St. John, as being due to the phenomena here considered, which strengthens the case for the "personality" explanation of the differences, or at least a portion of them. The anomalies found by Goos are more of the order that might be expected.

The writer has made a series of laboratory experiments on artificial absorption lines, the results from which will now be given. In a first experiment a series of nine pairs of lines was arranged on the test-object (called F) to be photographed, the separation of

TABLE VII

Absorption Lines, Varying Separation

Pair	Wet			Dry				Wet-Dry
	S_o	Sc	Diff.	S_o	Sc	Diff.	E	
	mm	mm	mm	mm	mm	mm	mm	mm
1.....	0.0793	(0.0793)	(0.0000)	0.0800	(0.0800)	(0.0000)	0.035	−0.0007
2.....	.0703	.0713	− .0010	.0713	.0719	− .0006	.031	− .0010
3.....	.0660	.0669	− .0009	.0673	.0675	− .0002	.029	− .0013
4.....	.0557	.0565	− .0008	.0560	.0570	− .0010	.027	− .0003
5.....	.0520	.0531	− .0011	.0527	.0536	− .0009	.024	− .0007
6.....	.0487	.0487	.0000	.0490	.0491	− .0001	.022	− .0003
7.....	.0417	.0435	− .0018	.0420	.0439	− .0019	.021	− .0003
8.....	.0410	.0427	− .0017	.0423	.0431	− .0008	.020	− .0013
9.....	0.0343	0.0374	−0.0031	0.0353	0.0378	−0.0025	0.012	−0.0010

the widest pair being 1.50 mm and of the closest 0.71 mm. The width of the lines is equal to the separating spaces. The distances on the test-object were accurately measured, so that, assuming no optical distortion, the relative correctness of the reduced separations in the photograph can be tested by simple proportion. Table VII shows the results obtained. Each measured distance given is the mean of measurement of nine separate exposures.

S_o is the measured separation of centers of the lines; S_c is the value computed as above described. E is the separation of adjacent edges. Results are given for plates measured both wet and dry. The prediction that the actions would be small is verified. The net result is an apparent *attraction* of close, spectral absorption lines. Accordingly in this case the repulsive developer action must be relatively small.

It is important to obtain data on the behavior of absorption lines for overexposures, as has already been done for double stars and emission lines. For this purpose two test-objects G and H were made, composed of parallel opaque strips about 6 mm wide. In G the strips were placed far apart, in H close together. The dimensions are as follows:

	G	H
	mm	mm
Separation of centers of strips.....	8.694	6.620
Separation of adjacent edges.....	2.414	0.400

These were photographed in the camera as before, with exposure times from 1 to 120 seconds and completely developed in Process developer. Two series of each were made and each plate measured twice, so that the numbers given below are the means of four separate values. In order to eliminate personality error, settings were made on the four edges, from which the separation of centers was computed. In the shortest exposure (1 sec.) the densities were low and of the order obtained in practical work.

TABLE VIII

Absorption Lines with Increasing Exposure

Exposure Time	G			H			Width of Lines
	S Wet	S Dry	E	S Wet	S Dry	E	
sec.	mm	mm	mm	mm	mm	mm	mm
1.....	0.453	0.457	0.125	0.347	0.350	0.008	0.34
2.....	.453	.456	.129	.346	.351	.013	.34
4.....	.449	.455	.136	.345	.349	.018	.33
7.....	.449	.458	.149	.341	.347	.024	.32
15.....	.451	.457	.161	.337	.345	.036	.31
30.....	.448	.454	.175	.333	.341	.047	.30
60.....	.449	.454	.190	.333	.341	.060	.28
120.....	0.448	0.455	0.188	0.331	0.337	0.070	0.27
Mean.	0.450	0.456					

In the case of the wide pair G, no certain variation with exposure time is apparent. But in the case of the close pair a strong attraction with increasing exposure, or else a repulsion with diminishing separations, is apparent. In order to decide which of these alternative statements is the correct one, recourse may be had to the

measured separations of the lines on the test-object itself, already given. We find in this way:

$$\text{Separation of H (wet)} = 0.453 \frac{6.620}{8.694} = 0.345 \text{ mm}$$

$$\text{Separation of H (dry)} = 0.457 \frac{6.620}{8.694} = 0.348 \text{ mm}$$

Thus, except for a slight repulsive action, which can be neglected for the moment, the separations in the case of test-object H are correctly given for the short exposures even though the edges of the lines are nearly in contact. In the case of the heavy exposures on H the lines are relatively far apart and yet a strong attraction has taken place, amounting to 13 μ. This is very readily explained as due to the fourth disturbing factor outlined above, namely, the greater turbidity on the far sides of the absorption lines combined with halation. In fact, the greater sharpness of the inside of each absorption line was apparent in the measurement. This cannot be considered an optical lack of sharpness since the field angle for the outside edge is only 6′.

A sufficient number of experiments have been described to show the great complexity of the mutual action of adjacent images. It has been the aim of the paper to cover the field only in a general way in order to disclose the factors of importance. A partial solution of the problem of eliminating mutual attractions and repulsions has been indicated. It remains for future work to make a detailed study of the action of various developers in the hope of securing one giving correct or normal development of the latent image.

Eastman Kodak Company
Rochester, N.Y.
February 3, 1921

OBSERVATIONS OF THE NEBULAR LINES IN THE SPECTRUM OF THE LONG-PERIOD VARIABLE STAR R AQUARII[1]

By PAUL W. MERRILL

ABSTRACT

Discovery of nebular lines in the spectrum of R Aquarii.—This star has a typical Md spectrum similar to that of about 85 per cent of all long-period variable stars. In October, 1919, the bright nebular lines λλ 4363, 4658, 4959 N_2, and 5007 N_1, and the helium line λ 4471, which also occurs in nebulae, were found to be superposed on the Md spectrum. Later observations have shown that these lines do not share in the changes of intensity exhibited by the light of the variable star, although they appear to emanate from the same object.

Intensities and *displacements* of the Md and nebular lines are given in Table I.

R Aquarii (R.A. 1900 = $23^h38^m.6$, Dec. 1900 = $-15°50'$) has been known as a variable star since 1811. The photometric data, according to the Harvard College Observatory, are as follows: maximum magnitude 6.2; minimum magnitude 11.0; period 385.5 days. The same authority states that R Aquarii has the broadest minimum of 75 long-period variables whose light curves were carefully studied. Its mean light-curve has a broad, flat minimum and a very rapid rise to maximum.

The Harvard objective-prism photographs have shown the spectrum to be of the same class as that of 85 per cent of the long-period variables, namely, Md. Spectra of this class are marked by bright hydrogen lines superposed upon a continuous spectrum which is notched by numerous absorption bands of titanium oxide. Variations in the relative intensities of the bright Hγ and Hδ lines are common in Md spectra, and have been found in the spectrum of R Aquarii.

So far as known, the first slit spectrogram of this object was secured on October 16, 1919, with a single-prism spectrograph attached to the 100-inch Hooker telescope. This showed, in addition to the usual Md spectrum, several bright lines characteristic of gaseous nebulae. Three such lines were conspicuous, namely,

[1] *Contributions from the Mount Wilson Observatory*, No. 206.

λ 5007 N_1, λ 4959 N_2, and λ 4363, while λ 4658 and λ 4471 He were faintly visible. Plate IX reproduces four spectrograms.

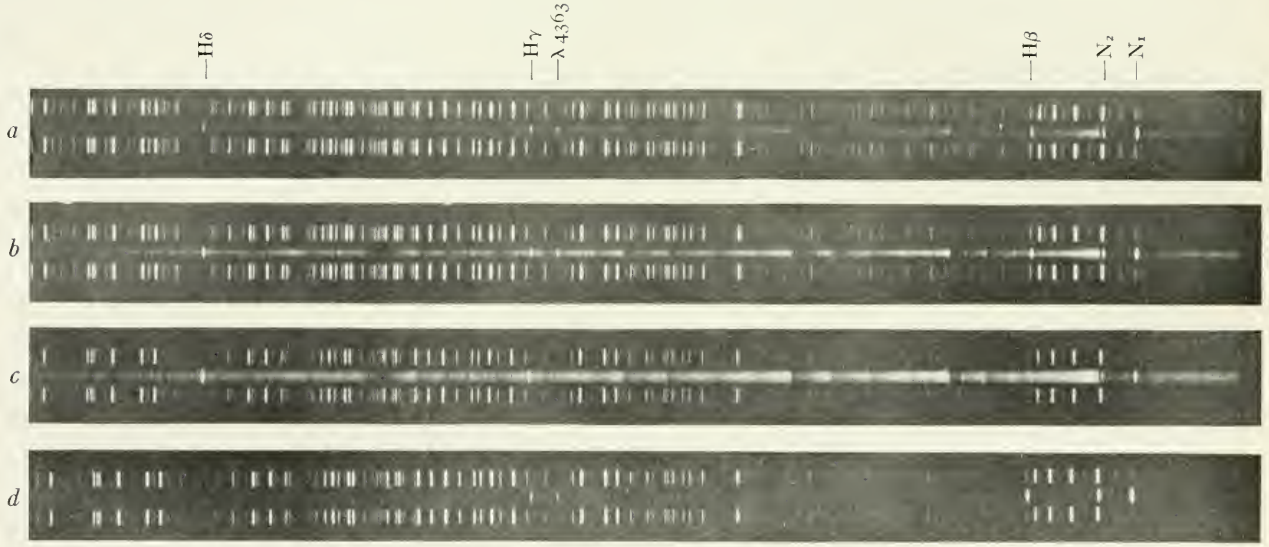
On this date the star was of magnitude 8.3; during the next fifteen days it brightened rapidly, and then remained nearly constant at magnitude 6.9 for about two months, after which a rapid decline took place.[1] This maximum appears to have been unusually broad and flat. The spectrographic observations following October 16, 1919, showed that the nebular lines did not share in the increase in intensity exhibited by the bright lines of the Md spectrum. No well-exposed plate was secured in the short interval *after* maximum before the star was lost in the evening sky, but such plates as were obtained indicated that the nebular lines had begun to regain their previous intensities with respect to the Md spectrum. By the time observations could be resumed in the morning sky in June, 1920, the star had faded to the tenth magnitude and was not much above its minimum brightness. Nevertheless, the chief nebular lines could be photographed with about the same exposure times as at maximum, although the continuous spectrum was practically absent, even with considerably longer exposures.

The approximate relative intensities of the emission lines as photographed with a single dense flint prism on Seed 30 plates are given in Table I.

The Md spectrum of R Aquarii near maximum light contains the bright hydrogen lines Hβ, Hγ, and Hδ, which are superposed upon corresponding bright lines associated with the nebular spectrum. This is made clear by a study of the manner in which the intensities and displacements of these lines vary during the light cycle. At maximum the Hγ and Hδ lines of the Md spectrum are many times as strong as the corresponding nebular Hγ and Hδ lines, but at minimum they appear to be of negligible strength compared with these nebular lines. The relative intensities of the hydrogen lines in the Md spectrum of R Aquarii at maximum and the disappearance of these lines at minimum are not at all unusual for this type of spectrum. The bright magnesium line

[1] Mr. Leon Campbell, of Harvard College Observatory, has kindly supplied the photometric data.

PLATE IX



Spectrograms of the Long-Period Variable Star R Aquarii, Showing Lines Characteristic of Gaseous Nebulae

Secured with a one-prism spectrograph of 18-inch camera-focus attached to the 100-inch Hooker telescope.

(*a*) October 16, 1919; 43 days before maximum; magnitude 8.3.

(*b*) October 19, 1919; 40 days before maximum; magnitude 8.2. Strömberg, observer.

(*c*) November 1, 1919; 27 days before maximum; magnitude 7.0. Adams, observer.

(*d*) September 4, 1920; 281 days after maximum, 47 days after minimum, and 109 days before the next maximum. Magnitude 10.2.

3767

λ 4571, which was observed in the spectrum of R Aquarii at minimum, is characteristic of Md stars at this phase.[1]

The relative intensities of the lines in the nebular spectrum do not appear to be precisely matched in any nebula observed by Wright[2] although there are several objects in his list that are similar in some particulars. The decrease in intensity in the Balmer series of hydrogen in passing from Hγ to Hδ is rapid as compared with the nebulae. Other noteworthy features are the strength of λ 4363, the presence of λ 4658, and the absence (or

TABLE I

INTENSITIES AND DISPLACEMENTS OF LINES IN THE SPECTRUM OF R AQUARII

WAVE-LENGTH IA	IDENTIFICATION	INTENSITIES		DISPLACEMENTS (km/sec.)	
		Nebular	Md (max.)	Nebular	Md
4101.74	Hδ	1	60	(− 6)	−32
4340.47	Hγ	5	30	−12	−33
4363.21*	Nebular	4		−25	
4471.48	He	1		(−10)	
4571.11	Mg				(−34)
4658.2*	Nebular	1		(−15)	
4861.33	Hβ	10	5	−10	
4958.91†	Nebular (N_2)	11		− 7	
5006.84†	Nebular (N_1)	20		− 7	
Absorption lines					−19

* Wright, *Publications of the Lick Observatory*, **13**, 183, 1918.

† Campbell and Moore, *Lick Observatory Bulletins*, **9**, 9, 1916.

relative weakness) of λ 4686. An additional nebular line, λ 3869, was observed in the spectrum of R Aquarii by Moore[3] at the Lick Observatory on November 3, 1919. Light of this wave-length is strongly absorbed by the dense flint glass of the Mount Wilson spectrographs, but faint traces of the line appear to be present on spectrograms taken here on October 17 and December 14, 1919, and September 2, 1920. Wright has made some very interesting comments[4] on the absence of the companion line λ 3967, and on some other features of this spectrum.

[1] *Mt. Wilson Contr.*, No. 200; *Astrophysical Journal*, **52**, 185, 1921.

[2] *Publications of the Lick Observatory*, **13**, 183, 1918.

[3] *Publications Astronomical Society of the Pacific*, **31**, 309, 1919.

[4] *Ibid.*

In spite of the extraordinary nature of this combination spectrum, various observations appear to show that the nebular lines and the Md spectrum both emanate from the same star. Notes on these observations have been published[1] and need not be repeated here. Radial-velocity data bear on this question, but the measurements made at Mount Wilson and given in Table I do not as yet afford conclusive evidence concerning the nature of the connection between the two spectra. The values in the table, with the exception of those in parentheses, depend upon from seven to eighteen one-prism plates, and should not be much in error. $H\beta$ and the chief nebular lines are in a part of the spectrum which is somewhat unfavorable for accurate measurement, but tests on N.G.C. 7027 and on bright-line stars show that no considerable systematic error is to be expected. All the lines associated with the nebular spectrum probably give the same displacement within errors of measurement, except λ 4363, which is shifted toward the violet by 0.2 A. It is improbable that Wright's value of the wave-length (4363.21 I A) is in error by so large an amount. The lines of the Md spectrum exhibit perfectly typical behavior, the same relative displacement of about 14 km between bright and dark lines having been found in *o* Ceti and in many other Md stars.

The principal facts concerning the line displacements in the spectrum of R Aquarii may be summarized as follows:

Md bright lines	−33 km/sec.
λ 4363, nebular	−25
Md absorption lines	−19
Nebular lines, except λ 4363	−10

The displacements are expressed in kilometers per second merely for convenience. The cause of the differences is not obvious; they may or may not be due to relative motion. One does not readily believe that the object is a long-period binary with an Md star for one component and a planetary nebula for the other.

The question as to whether in Md stars in general the bright lines, or the dark lines, or neither, yield the correct radial velocity

[1] Wright, *Publications Astronomical Society of the Pacific;* Merrill, *ibid.*, **31**, 305, 1919, and **32**, 247, 1920.

of the star is an important one. It is hoped that a statistical investigation, observations for which are now being secured, will indicate the solution. Perhaps the behavior of the nebular lines in R Aquarii will throw a side light on this puzzling phenomenon.

It would be of great interest to know whether the nebular lines have been present in the spectrum of R Aquarii for many years past, or whether they are the results of some recent outburst. The Harvard record, consisting of objective-prism spectrograms of small dispersion, dates from 1893. The fact that the nebular lines are not observable on the Harvard plates, even on those made at minimum light when the continuous spectrum would be very weak, tends to show that they have not been so strong at all times as they have been recently; but the evidence is perhaps not quite conclusive.

At present we have so little knowledge of the chemical and physical interpretation of the nebular lines that the meaning of their presence in R Aquarii cannot be stated. Since the Md spectrum probably arises under low-temperature conditions, the possibility of the production of the chief nebular lines N_1 and N_2 and of λ 4363 without intense conditions of excitation is suggested. It may be of significance in this connection that λ 4686, which in the laboratory requires high excitation for its production, has not been observed in R Aquarii. Laboratory experiments on long columns of gases under low excitation might not be amiss.

Mount Wilson Observatory
March 1921

ON SYSTEMATIC DISPLACEMENTS OF LINES IN SPECTRA OF VENUS[1]

By CHARLES E. ST. JOHN and SETH B. NICHOLSON

ABSTRACT

Systematic displacements of the solar lines in spectra of Venus.—Under certain conditions of observation there are line displacements to the violet of a few thousandths of an angstrom when comparison is made with the position of the lines in the spectrum of integrated skylight. Other conditions remaining constant, the displacements are greater at low than at high altitudes.

Atmospheric refraction.—The correlation with the altitude at the time of observation points to refraction as the controlling factor rather than to a repulsive "earth-effect" acting on the solar vapors as suggested by Evershed. The altitude correlation is represented by $\Delta\lambda 10^{-3} = 1.4 - 1.0 \cot h$. The residuals, after removing the effect depending upon altitude, correlate equally well with the semidiameter D of Venus, the phase angle i, or the angle VSE. The observations are satisfactorily represented by the relation $\Delta\lambda 10^{-3} = 1.3 - \frac{8.5 \cot h}{D}$ which is deduced from the assumption that the observed displacements are caused by unsymmetrical illumination of the slit due to the separation of the visual and photographic images by atmospheric refraction, and that the unequal illumination is a function of the diameter of the image and the width of the slit.

Superposed skylight.—Spectroscopic observations of Venus beginning at sunset or ending at sunrise are not measurably affected by superposed skylight.

I. INTRODUCTION

Evershed and Royds have proposed an interpretation of the differences between terrestrial and solar wave-lengths[2] based solely on radial velocity. They assume that the solar gases at all points on the sun are receding from the earth. This means, they say, an "earth-effect"—an actual repulsion of the solar gases by the earth, and not by other planets. Through such earth-induced movements of the solar vapors Evershed has attempted to explain displacements of the Fraunhofer lines at the center, over the disk, and at the limb of the sun, discarding interpretations involving pressure-effects, radial convection currents, anomalous dispersion, and the Einstein gravitational shift.[3] No explanation of an "earth-

[1] *Contributions from the Mount Wilson Observatory*, No. 208.

[2] *Kodaikanal Observatory Bulletin*, No. 39, 1916.

[3] *Observatory*, **43**, 153, 1920.

effect" is suggested and the arbitrary and extraordinary nature of the assumption is recognized; yet Evershed is so convinced of its reality that he says,[1] "Whether we like it or not, it seems necessary to admit that the Earth *does* affect the Sun, causing a movement of the gases analogous to that taking place in a comet." This view he believes is confirmed by his observations upon the spectrum of Venus. The idea of an apparent "earth-effect" upon solar phenomena is not new. Sykora[2] in 1897 called attention to a predominance of eastern prominences, and in 1907 Mrs. Maunder's paper "An Apparent Influence of the Earth on the Numbers and Areas of Sun-Spots in the Cycle 1889–1901" was communicated to the Royal Astronomical Society.[3]

According to Evershed's assumption, the displacements observed in the light from the earth-facing hemisphere of the sun should differ from those observed in the light from any other hemisphere; for example, from the hemisphere facing Venus.

He finds that when the angle Venus-sun-earth is small the wave-lengths in the spectrum of Venus are slightly shorter than those in direct sunlight; that this difference increases as the angle *VSE* increases; that when the angle is 90° the shortening equals the difference, sun *minus* arc, the wave-lengths from Venus and in the terrestrial source then becoming equal; and that for larger angles the displacements relative to the arc are to the violet; that is, in the light from the earth-facing hemisphere of the sun the Fraunhofer lines are displaced toward longer wave-lengths, while in the light from the opposite hemisphere the displacements are toward the violet when compared with the terrestrial source.[4] In order to obtain independent observational data bearing upon these extraordinary results, we have carried out two series of observations, the first in 1919 with Venus east of the sun, and the second in 1919–1920 with Venus west of the sun.

II. INSTRUMENTS AND METHODS

The observations were made with the Snow telescope of 60-foot focus in connection with a Littrow grating-spectrograph, focus

[1] *Observatory*, **42**, 52, 1919.

[2] *Memorie della Società degli Spettroscopisti Italiani*, **26**, 161, 1897.

[3] *Monthly Notices*, **67**, 451, 1907.

[4] *Observatory*, **43**, 156, 1920.

18 feet. The horizontal beam from the 2-foot concave mirror is directed downward by a 45° flat upon the slit of the spectrograph installed in the constant-temperature pit recently added to the equipment of the Snow telescope. The diameter of the image of Venus varied from 1.3 to 3.3 mm. The slit was 0.05 mm wide, its position being, in general, approximately normal to the terminator. The grating was ruled by Anderson and kindly loaned by Professor R. W. Wood, of the Johns Hopkins Physical Laboratory. The ruled surface is 95 mm × 170 mm; it is very bright in the first order and, as used, gives a linear dispersion of 3 A per mm. The collimating lens has an aperture of 6 inches.

Exposures were made upon the iron arc simultaneously with exposures upon Venus, the sky, or the center of the sun. In 1919 the center of an enlarged image of the arc was projected upon the slit, the intensity being controlled by a rotating sector and ray filter. In the second series a ground glass was placed in front of the arc, and the integrated light was used. Any errors in the wave-lengths of the reference lines would affect the measurements of Venus and of the sky in the same way, leaving the relative wave-lengths dependable. The iron lines in Table I were used as standards of reference.

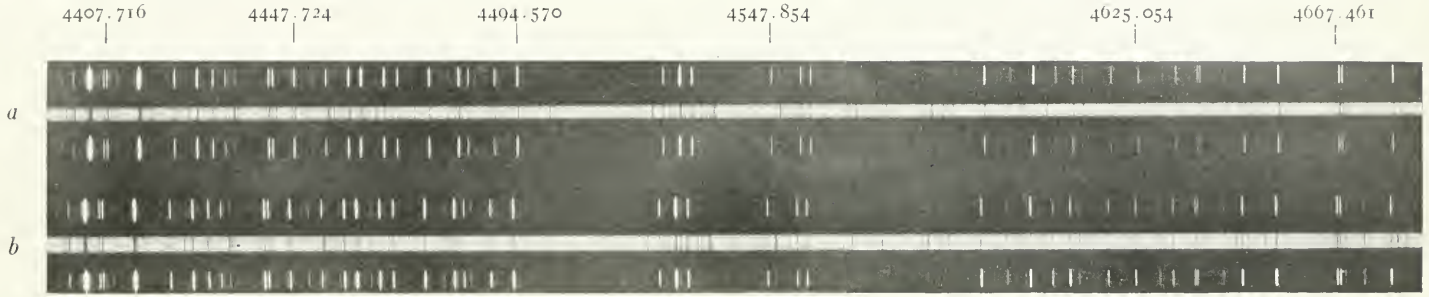
TABLE I

REFERENCE LINES—INTERNATIONAL SYSTEM

4375.934 A	4466.557 A	4592.658 A
4407.716	4494.570	4625.054
4427.314	4525.146	4647.440
4447.724	4547.854	4667.461

The wave-lengths of 30 lines were measured in the spectra of the center of the sun, of skylight, and of Venus. The spectrograms were measured red right and red left and reduced by identical methods. In all, 56 spectrograms of Venus were secured, 41 of the sky, and 9 of the sun. It early became evident that the center of the sun and the integrated skylight give the same wave-lengths, the contribution of the limb-displacements to the red being inappreciable in the integrated light. The sky *minus* center for the 30 lines is +0.0001 A. The lines measured are given in Table II.

PLATE X



PHOTOGRAPHS OF THE SPECTRA OF VENUS AND THE SKY

a. Venus, Plate V119, 1919, November 21, $17^h\ 17^m - 18^h\ 21^m$ P.S.T.
b. Sky, Plate V115, 1919, November 20, 19 45 −20 45 P.S.T.
The comparison spectra are of the iron arc. Enlargement 2.

These lines were selected irrespective of whether they are blends or not, as they were to be used for relative wave-lengths only.

The data for the individual plates are given in Tables III and IV. The time of observation has been taken as the mean of the beginning and the end of the exposure, except in a few cases where clouds interrupted. No attempt has been made to obtain the mean time of the effective exposure, which would be somewhat different from that used on account of the change in atmospheric

TABLE II

LINES MEASURED IN SPECTRA OF VENUS AND THE SKY

Rowland λ	Int.	Element	Limb-Center	Rowland λ	Int.	Element	Limb-Center
4376.107...	6	Fe	+0.005	4527.101...	3	Ca?	+0.007
4422.741...	3	Fe, Y		34.953...	4	Ti	+0.004
35.851...	4	Ca	+0.006	48.024...	3	Fe	+0.008
42.510...	6	Fe	+0.006	54.211...	8	Ba	+0.008
43.976...	5	Ti	+0.008	63.939...	4	Ti	+0.008
47.892...	6	Fe	+0.005	71.275...	5	Mg	+0.007
51.752...	3	Mn		84.018...	4	Fe—	+0.012
56.030...	5	Mn_2,Ca_3		4602.183...	3	Fe	
68.663...	5	Ti—	+0.007	03.126...	6	Fe	
76.214...	7	Fe_4, Ag_3		25.227...	5	Fe	
82.376...	8	Fe_5, Fe_3	+0.004	26.358...	5	Cr	
84.392...	4	Fe		29.521...	6	Ti-Co	
85.846...	3	Fe		30.306...	4	Fe	
94.738...	6	Fe	+0.010	51.461...	4	Cr	
4508.455...	4	Fe?,—	+0.011	52.343...	5	Cr	

absorption. The third column gives the difference between the measured wave-lengths in the spectrum of Venus and those of the same lines in the spectra of the sky, corrections for velocity having been applied in both cases. The difference between the heliocentric longitudes of Venus and the earth was used as the angle *VSE*. The quantity h is the true altitude of Venus. The phase angle of Venus is indicated by i and the semi-diameter by D.

The velocity of Venus relative to the earth was obtained from the hourly variation in the logarithm of the geocentric distance. The relative velocity of Venus and the sun was calculated in the same way from the variation in the logarithm of the radius vector of Venus. The velocity of the observer due to the diurnal rotation

TABLE III

OBSERVATIONAL DATA, VENUS EAST OF THE SUN

DATE	EXPOSURE P.S.T.	$\Delta\lambda$ V−SKY	h	D	ANGLE *VSE*	i	VELOCITY IN LINE OF SIGHT				Q	SUNSET P.S.T.	PLATE NO.	MEASURER
							V−E	Rot. E	V−S	Total				
		A					km	km	km	km				
1919 April 3..	6^h43^m–8^h3^m	−0.007	14°	6″.3	103°	46°	− 9.48	+0.37	−0.16	− 9.27	4°	6^h13^m	V19	S
7..	7 0 –8 15	−0.004	14	6.4	101	47	− 9.81	+0.36	−0.13	− 9.58	5	6 16	24	S
8..	6 20 –7 20	−0.004	24	6.4	100	48	− 9.88	+0.35	−0.13	− 9.66	5	6 17	25	S
20..	6 35 –8 5	−0.007	22	6.8	93	53	−10.80	+0.35	−0.05	−10.50	77	6 27	30	S, N
21..	6 36 –8 6	+0.003	22	6.8	92	53	−10.88	+0.35	−0.05	−10.58	78	6 27	31	S, N
May 5..	6 48 –8 18	−0.005	24	7.3	82	59	−11.90	+0.34	+0.05	−11.51	264	6 38	38	S
5..	8 30 –9 25	−0.006	8	7.3	82	59	−11.90	+0.35	+0.05	−11.50	264	6 38	39	N
6..	6 38 –8 8	−0.002	27	7.4	81	60	−11.96	+0.33	+0.05	−11.58	84	6 39	40	S
6..	8 16 –9 16	+0.002	11	7.4	81	60	−11.97	+0.35	+0.06	−11.56	84	6 39	41	S
8..	6 48 –7 48	−0.002	28	7.5	80	60	−12.10	+0.33	+0.07	−11.70	265	6 40	49	S
8..	7 51 –9 3	−0.004	15	7.5	80	60	−12.10	+0.35	+0.07	−11.68	265	6 40	50	S
11..	7 3 –7 53	−0.004	27	7.6	79	62	−12.29	+0.33	+0.09	−11.87	87	6 43	61	N
11..	7 58 –9 13	−0.004	13	7.6	79	62	−12.29	+0.35	+0.09	−11.85	87	6 43	62	N
12..	6 53 –7 43	0.000	29	7.7	78	62	−12.36	+0.33	+0.09	−11.94	87	6 43	66	S
12..	7 47 –9 8	−0.004	16	7.7	78	62	−12.36	+0.35	+0.09	−11.92	87	6 43	67	S
31..	7 6 –8 6	−0.001	29	8.8	66	72	−13.36	+0.33	+0.19	−12.84	96	6 57	68	M
31..	8 12 –9 12	−0.005	15	8.8	66	72	−13.36	+0.35	+0.19	−12.82	96	6 57	69	M
June 1..	7 5 –8 5	+0.005	29	8.8	65	72	−13.40	+0.33	+0.20	−12.87	277	6 58	70	N
1..	8 11 –9 11	0.000	15	8.8	65	72	−13.40	+0.35	+0.20	−12.85	277	6 58	71	M
2..	6 40 –7 41	+0.003	34	8.9	64	72	−13.44	+0.32	+0.20	−12.92	97	6 58	72	N
2..	7 58 –9 1	−0.001	17	8.9	64	72	−13.45	+0.35	+0.20	−12.90	97	6 58	73	M
3..	7 0 –8 0	+0.001	30	9.0	64	73	−13.48	+0.33	+0.20	−12.95	278	6 58	77	M
3..	8 10 –9 15	+0.001	15	9.0	64	73	−13.49	+0.35	+0.20	−12.94	278	6 58	78	N
4..	7 3 –7 59	−0.002	30	9.0	63	73	−13.52	+0.33	+0.21	−12.98	98	6 59	79	M
4..	8 7 –9 17	+0.005	16	9.0	63	73	−13.53	+0.35	+0.21	−12.97	98	6 59	80	N
22..	7 34 –8 20	−0.002	24	10.7	51	84	−13.99	+0.35	+0.24	−13.40	105	7 6	83	N, M
July 2..	7 36 –8 24	−0.006	21	11.9	45	90	−14.05	+0.36	+0.23	−13.46	203	7 7	87	M
3..	7 56 –8 56	−0.002	15	12.0	44	90	−14.05	+0.37	+0.23	−13.45	102	7 7	89	S, N
4..	7 36 –8 26	−0.006	21	12.1	44	91	−14.05	+0.36	+0.23	−13.46	89	7 7	90	S, M
20..	7 14 –8 16	−0.005	18	14.8	34	102	−13.61	+0.36	+0.17	−13.08	93	7 2	96	S, M
21..	7 19 –8 29	−0.003	15	15.1	33	103	−13.56	+0.36	+0.17	−13.03	273	7 2	99	S, N

TABLE IV

Observational Data, Venus West of the Sun

Date	Exposure P.S.T.	Δλ V−Sky	h	D	Angle VSE	i	Velocity in Line of Sight				Q	Sunrise P.S.T	Plate No.	Measurer
							V−E	Rot. E	V−S	Total				
		A					km	km	km	km				
1919 Nov. 3..	17^h10^m–17^h57^m	−0.003	34°	15″.8	32°	103°	+12.64	−0.29	−0.20	+12.15	270°	18^h14^m	V104	N
4..	15 56 −16 56	+0.011	21	15.6	33	102	+12.69	−0.35	−0.20	+12.14	270	18 14	107	N, M
4..	17 10 −18 12	+0.007	36	15.6	33	102	+12.69	−0.28	−0.20	+12.21	270	18 14	108	S
20..	16 21 −17 21	+0.001	24	12.8	42	90	+13.03	−0.32	−0.12	+12.59	266	18 29	113	S
20..	17 28 −18 28	−0.001	36	12.8	42	90	+13.03	−0.25	−0.12	+12.66	266	18 29	114	N
21..	16 10 −17 11	−0.001	22	12.7	43	90	+13.03	−0.33	−0.11	+12.59	270	18 30	118	S
21..	17 17 −18 21	−0.004	35	12.7	43	90	+13.03	−0.26	−0.11	+12.66	270	18 30	119	S
23..	16 55 −17 45	−0.001	30	12.4	44	89	+13.03	−0.29	−0.10	+12.64	90	18 32	124	S
23..	17 52 −18 37	0.000	39	12.4	44	89	+13.03	−0.22	−0.10	+12.71	90	18 32	125	N
Dec. 8..	17 25 −18 35	−0.001	32	10.7	54	81	+12.91	−0.24	0.00	+12.67	79	18 46	129	S
9..	16 5 −18 20	+0.010	21	10.6	54	80	+12.90	−0.32	0.00	+12.58	80	18 46	131	N
26..	16 32 −17 33	−0.010	17	9.2	64	72	+12.44	−0.31	+0.11	+12.24	88	18 56	133	S
26..	17 37 −18 39	−0.006	27	9.2	64	72	+12.43	−0.24	+0.11	+12.30	88	18 56	134	N
27..	16 45 −17 40	+0.007	18	9.1	65	71	+12.40	−0.30	+0.12	+12.22	269	18 57	137	N
27..	17 45 −18 43	+0.008	28	9.1	65	71	+12.40	−0.23	+0.12	+12.29	269	18 57	138	S
28..	16 42 −17 38	−0.005	18	9.0	65	70	+12.37	−0.30	+0.12	+12.19	269	18 57	141	S
28..	17 43 −18 47	−0.002	28	9.0	65	70	+12.37	−0.23	+0.13	+12.27	269	18 57	142	N
1920 Jan. 29..	18 0 −18 45	−0.003	19	7.2	85	57	+11.10	−0.25	+0.24	+11.09	89	18 51	151	S
31..	16 50 −17 55	−0.015	9	7.1	86	57	+11.02	−0.31	+0.24	+10.95	90	18 50	152	N, M
31..	17 56 −18 46	+0.001	18	7.1	86	57	+11.02	−0.26	+0.24	+11.00	90	18 50	153	N
Feb. 10..	17 40 −18 40	+0.001	14	6.8	92	53	+10.58	−0.28	+0.23	+10.53	96	18 42	155	N
11..	17 25 −18 35	−0.004	13	6.7	92	52	+10.52	−0.29	+0.23	+10.46	276	18 42	157	S
12..	17 20 −18 35	+0.002	12	6.7	93	52	+10.47	−0.30	+0.23	+10.40	277	18 41	159	N
13..	17 38 −18 46	−0.011	14	6.7	93	51	+10.47	−0.28	+0.23	+10.42	97	18 40	161	S
Mar. 11..	17 18 −18 14	−0.004	10	5.9	109	42	+ 9.04	−0.34	+0.12	+ 8.82	110	18 8	166	S

of the earth has been derived in the usual way. Q is the angle between the line joining the cusps and the slit of the spectrograph, measured from the north cusp in the direction of the illuminated portion of the disk to the end of the slit nearest the plate holder. In the first series the red end of the spectrum was on the right as one looked at the slit from the plate holder. In the second series the red was on the left until the end of 1919, when the grating was again reversed. The measurers are identified by the initials S, N, M, indicating St. John, Nicholson, and Miller, respectively.

We take this opportunity to express our appreciation of the assistance given us by Miss Miller in the work of measurement and reduction and by Mr. Edison Hoge in making the observations.

III. DISCUSSION

1. *Correlations.*—Evershed correlated his observations with the angle VSE and adopted an interpretation based upon the "very incredible hypothesis"[1] that an "earth-effect" is driving the solar vapors from the earth-facing hemisphere of the sun. Our observations are better correlated with the altitude of Venus at the time of observation. The natural tendency is to use as high an altitude as possible, with the result that the altitude of Venus at the time of observation varies with the angle VSE. Our observations, therefore, can apparently be correlated with the angle VSE nearly as well as with altitude, but on 18 nights spectrograms were taken at both high and low altitudes: mean high altitude 29°.2, mean low altitude 16°.1, which give $\Delta\lambda$ low $-\Delta\lambda$ high $=-0.0014$ A. Among the low altitude plates are four at mean altitude 24°.2. Pairs in which the low-altitude plates had relatively high altitudes contribute little, on the basis of the correlation with altitude, to the difference shown by the plates at low and high altitudes. On omitting these plates the difference $\Delta\lambda$ low $-\Delta\lambda$ high for the 14 remaining pairs rises to -0.0021 A. As there was no change in the angle VSE between the plates of each pair or in the instrumental adjustments, this difference between plates at low and high altitudes is definite evidence of an effect depending in some way on the altitude of the planet, which

[1] *Observatory*, 43, 156, 1920.

shortened the wave-lengths in the spectrum of Venus observed at low altitude, and indicates that the altitude of Venus is the controlling factor in our observations.

An effect depending on low altitude is naturally associated with refraction, and hence with cot h. To obtain a relation independent of the angle VSE and dependent only upon altitude the coefficient of cot h in the equation

$$\Delta\lambda_1-\Delta\lambda_2=A(\cot h_1-\cot h_2)$$

was derived from each of the 18 pairs of plates. Its value closely approximated 0.001 A. By means of this relation the influence of altitude was eliminated from the 56 original observations. The residual displacements showed a slight variation with the relative position of the earth, sun, and Venus. It should be noted, however, that the angle VSE is only one of the variables dependent upon the relative positions of the three bodies which may be used in seeking such correlations. A satisfactory correlation is made by assuming that the observed displacements are fundamentally due to conditions arising from low altitude, and that the effect is greatest when the image of Venus is smallest. This would be the case if the systematic discrepancies were attributable to unsymmetrical illumination of the slit arising from atmospheric refraction and from the small and varying diameter of the image in relation to width of slit. This is the simplest interpretation of our observations, in that it refers the entire effect to a single rational cause. A solution by least squares for this correlation gives

$$\Delta\lambda 10^{-3}=1.3-8.5\frac{\cot h}{D},$$

where D is the semidiameter of Venus in seconds of arc.

If the angle VSE is used, the observations may be represented by

$$\Delta\lambda 10^{-3}=3.0-1.0\cot h-3.0(1-\cos VSE).$$

By introducing the phase angle i, the following equation may be used:

$$\Delta\lambda 10^{-3}=2.3-1.0\cot h-3.5\cos i.$$

As far as the observations are concerned, these three equations represent them equally well, but the first offers the most reasonable and probable explanation.

In the computation of the velocity corrections the value 8".80 was used for the solar parallax, and the velocity displacements due to rotation of the planet were assumed to be negligible, as would be the case for the long rotation period shown by Slipher's observations.[1] An error in either of these assumptions would not affect the correlations, since deviations due to either of these causes would appear with opposite signs in the two series and be eliminated in the correlations which combine them both. It may be remarked that when the observations are corrected for the systematic displacements to the violet discussed above, the difference between morning and evening series, viewed in the light of the probable error of the observations, is not of an order that would indicate a divergence from the assumed parallax or a rate of rotation higher than that found by Slipher.

2. *Superposed skylight.*—Venus can be seen on the slit of the spectrograph at any time during the day, and some preliminary plates indicate that it may be possible to secure reliable observations in full daylight, provided the relative velocity of Venus and the earth is large enough to separate completely the absorption lines in the spectra of Venus and the sky. When the angle *VSE* is large, however, the displacement due to the relative velocity is less than the width of a line, and wave-lengths measured under such conditions are affected by an error depending on the brightness of the sky and the amount of displacement. This error appears as a shift to the violet when Venus is west of the sun, and to the red when Venus is east of the sun. Tests were made with superposed spectra having different exposures and a relative displacement of 0.120 A. They showed that a superposed spectrum having 5 per cent of the intensity of the primary spectrum was sufficient to produce measurable shifts.

When the angle *VSE* is large, the time available is short, and therefore it is necessary, with Venus east of the sun, to begin the exposures as early as possible and, with the planet west of the sun,

[1] *Lowell Observatory Bulletin*, 1, 9, 1903.

to continue them until the brightness of the sky reaches the permissible limit. To examine our observations for possible effects due to superposed skylight near twilight and dawn, we have selected groups of observations in which the components have approximately equal altitudes but begin at unequal intervals after sunset or end at unequal intervals before sunrise. The effect of altitude is by this arrangement of the observations the same for each group. An examination of the data in Table V reveals no measurable effect due to superposed skylight, even when the exposures were begun at sunset or ended at sunrise, as is shown by the agreement between the components of each group.

TABLE V

ABSENCE OF EFFECT OF SUPERPOSED SKYLIGHT

1919				1919–1920			
Begun after Sunset	No. Plates	h	$\Delta\lambda$	Ended before Sunrise	No. Plates	h	$\Delta\lambda$
min.				min.			
36	5	17°	−0.005	6.3	3	15°	−0.002
15	2	16.5	−0.004	− 1.5	4	14	−0.003
14	6	26	−0.002	13	6	31	−0.001
1.6	8	26	−0.001	− 1	3	37	+0.002

3. *The effects of altitude.*—The spectroscopic conditions arising from low altitude are complex, and the following considerations show that further investigation is required to determine the rôle played by the various factors in producing the observed displacements. The atmospheric dispersion at low altitude displaces the photographic image relative to the visual image very appreciably. When the guiding is done upon the visual image, as in these observations, this relative displacement may produce dissymmetry in the illumination of the slit. At 8° altitude the dispersion between λ 4500 and λ 5700 is 8″, a third of the diameter of the planet at maximum elongation. Campbell found large differences in the radial velocity of Venus when he compared the values obtained by placing the slit just inside the terminator with those obtained

when the slit was just inside the limb.[1] These differences, which he attributed to non-uniform illumination of the slit, reversed in sign when the spectrograph was rotated through 180°. In observations such as ours non-uniform illumination of the slit due to guiding on the visual image would depend not only upon the atmospheric dispersion at low altitude but also upon the diameter of the image relative to the width of the slit. This source of error we hope to eliminate in our next series of observations upon Venus by using a blue screen in the observing telescope, thus making it possible to keep the photographic image symmetrically placed on the slit. We have not yet found a satisfactory reason why rotation of the spectrograph did not reverse the sign of the displacements, as was expected if they are due entirely to non-uniform illumination of the slit.

The refraction, moreover, requires compensation in both right ascension and declination, involving systematic corrective movements of the image on the slit. We were obliged to overcome the drift in declination by a progressive tilt of the concave mirror, a faulty procedure, as the angle of incidence at the grating is very sensitive to changes in the direction of the beam from the concave mirror. This possible source of error will be eliminated from our next observations as motor controls on the second flat now enable the observer to guide by it.

4. *Kodaikanal observations.*—The following Kodaikanal observations are collected from the reports and papers by Evershed:[2]

TABLE VI

VENUS—SKY FROM KODAIKANAL OBSERVATIONS

VSE	45°	62°	67°	75°
V−Sky	+0.0026[3]	−0.0034	−0.0024	−0.0068
VSE	95°	102°	135°	140°
V−Sky	−0.0009	−0.0052	−0.014	−0.007 A

[1] *Lick Observatory Bulletin*, **9**, 30, 1916.

[2] *Kodaikanal Observatory Report*, p. 2, 1917; p. 2, 1918; p. 3, 1919; *Monthly Notices*, **78**, 278, 1918; **79**, 257, 1919; **80**, 395, 1920; *Observatory*, **43**, 156, 1920.

[3] *Kodaikanal Observatory Report*, 1918. Four excellent plates give orbital velocity 3.5 per cent low. *Monthly Notices*, **78**, 279, 1918: 0.45 km/sec. less than orbital velocity. A displacement of +.0067 A is deduced from these statements and averaged with that of the 1918 series.

Observations when the angle *VSE* is 135°–140° are necessarily made with Venus at altitudes of about 10°; near maximum elongation they would most naturally be made at high altitudes; and with *VSE* near 90°, at intermediate altitudes. The altitudes for the Kodaikanal observations are not available, but, if they are near the values suggested as probable, Evershed's observations of V−Sky may also be correlated with altitude. The question is then one of interpretation; plates at high and low altitudes with the same value of *VSE*, and at low altitude with large and small *VSE*, will eventually furnish a definite answer. As far as present observations have a bearing on the question, they indicate that the main factors producing the displacements are those depending upon the low altitude of Venus at the time of observation. When this effect is eliminated, the remaining residuals, which seem to vary with the relative position of earth, Venus, and sun, are more reasonably correlated with the varying diameter of the planet than with the angle *VSE*.

Mount Wilson Observatory
March 1921

BRIGHT AND DARK NEBULAE NEAR ζ ORIONIS PHOTOGRAPHED WITH THE 100-INCH HOOKER TELESCOPE[1]

By JOHN C. DUNCAN

ABSTRACT

Photographs made with the 100-inch Hooker telescope of the Mount Wilson Observatory are reproduced in two plates. They exhibit the following features: the *bright nebulae N.G.C. 2024* and *2023* and *I.C. 431, 432,* and *434:* the *dark cosmic cloud Barnard 33,* which indents or overlies the nebula I.C. 434; the *great disparity in the number of faint stars* on opposite sides of a line passing nearly north and south through ζ Orionis; and a *striated appearance* in the faint nebulosity west of I.C. 434.

Evidence is given of the existence of *four distinct types of extended masses* in the neighborhood, and suggestions made in explanation of the aspect of the region as presented by the photographs.

The region surrounding the star ζ, at the southeastern end of the Belt of Orion, has been studied on account of its remarkable nebulae by several observers, the first of whom was W. Herschel, who listed it as No. 25 of his fifty-two regions that contain diffuse nebulosity.[2] Six of its nebulae are included by Dreyer in the *New General Catalogue* or the first *Index Catalogue.* Photographs showing many of its interesting features have been published and discussed by W. H. Pickering,[3] Roberts,[4] Wolf,[5] Keeler,[6] Barnard,[7] and Curtis.[8]

During the past winter I have made photographs of this region at the principal focus of the 100-inch Hooker telescope, and the

[1] *Contributions from the Mount Wilson Observatory,* No. 209.

[2] *Philosophical Transactions,* **101,** 276, 1811.

[3] *Annals of Harvard College Observatory,* **32,** 66, and Plate III, Fig. 3, 1895.

[4] *Astrophysical Journal,* **17,** 74, and Plate IV, 1903; also, *Monthly Notices,* **63,** 31, and Plate 1, 1903.

[5] *Monthly Notices,* **63,** 304, and Plate 11, 1903.

[6] *Publications of the Lick Observatory,* **8,** Plate XIII, 1908.

[7] *Astrophysical Journal,* **38,** 500, and Plate XX, Fig. 1, 1913; also *Publications of the Lick Observatory,* **11,** Plate XX, 1913.

[8] *Publications of the Astronomical Society of the Pacific,* **30,** 66, and Plate IV, Fig. 1, 1918; *Publications of the Lick Observatory,* **13,** 23, and Plate II, Fig. 5, 1918.

PLATE XI

N



E W

Bright and Dark Nebulae South of ζ Orionis
Scale: 1 mm = 14″.0 (0.89 that of original negative)

PLATE XII

N

E



W

ζ Orionis and the Nebulae on the East and North
Scale: 1 mm = 12″.8 (0.81 that of original negative)

great focal length, light-gathering power, and resolving power of this instrument have brought out certain remarkable features with great distinctness. Two of these photographs are reproduced in Plates XI and XII. The original negatives are 8×10 inches in size, but in making the reproductions only the central parts were used and these were reduced in scale. The excellence of the reproductions is due largely to the skill of Mr. Ellerman, who increased the intensity of the images of faint nebulosities by successive copying on slow plates.

PLATE XI.—Center of plate (1920.0), $\alpha = 5^h37^m.0$, $\delta = -2°31'$. 1920, November 13. Exposure three hours. Seeing good, but figure of mirror somewhat imperfect. Seed 23 plate.

The bright star ζ Orionis is just off the north side of the plate, and a bright ray, produced by diffraction of its light by one of the steel supports of the secondary mirror, extends from it toward the south and east. The brightest star shown is D.M. −2°1337, 19 mm from the bottom of the plate and 42 mm from the right side. Its visual magnitude, as given by the *Durchmusterung*, is 7.5.

Almost vertically through the middle of the plate lies the nebula I.C. 434, which was discovered photographically at the Harvard Observatory in 1887.[1] It here appears as the bright fringe of a diffuse nebulosity that fills the western half of the field. This diffuse nebulosity is remarkably striated, the striae lying in a direction approximately east and west. The fringe has numerous branches and irregularities and is suggestive of the edge of a relatively thin sheet that is crumpled and turned edgewise to the observer. Earlier observers have noted the scarcity of faint stars east of the nebulous fringe as contrasted with their great abundance on the west. The effectiveness of the Hooker telescope in photographing faint stars makes this contrast very conspicuous.

In the northeastern corner of the field is the nebula N.G.C. 2023, which surrounds a star of magnitude 8.5, not shown on the plate because of overexposure of the nebula. It is terminated rather abruptly on the west side, and shows a clearly defined dark marking on the east. The existence of spiral rays, noted by the Harvard observers,[2] is not here confirmed.

[1] *Annals of Harvard College Observatory*, 18, 115, 1890. [2] *Ibid.*, 116, 1890.

By far the most interesting object shown on the plate is the dark cloud near the center, which forms a bay in the bright nebula and which has attracted attention since the earliest photographic observations of the region. It is listed by Barnard as No. 33 of his dark markings of the sky.[1] On the present plate, faint lights appear within the cloud, and a notable silver lining is shown along its western edge. On the original negative the eastern boundary can be traced on the faint background of the sky, and is seen to extend north and east nearly to N.G.C. 2023. An aid to tracing its position is found in the diffracted ray from ζ Orionis, which seems to have been too faint to affect the plate perceptibly by its own light but is plainly visible where the plate has been brought to its threshold by the nebulous background, so that the ray is interrupted where it crosses the dark cloud. A second and much smaller and paler dark bay lies about 15′ north of Barnard 33, near the 8.5 magnitude star D.M. −2°1343, and a third about 6′ still farther north.

PLATE XII.—Center of plate (1920.0). $\alpha = 5^h37^m.3$, $\delta = -1°53'$. 1920, December 8. Exposure, 5 hours, 35 minutes. Sky somewhat hazy. Seed 30 plate.

ζ Orionis is near the west side of the plate, where irradiation has spread its light into a great blot. The star may be located accurately at the intersection of the rays produced by the mirror supports. At the extreme northwest corner of the plate is the nebula I.C. 431, and 10′ east of this is I.C. 432. These nebulae surround the stars D.M. −1°1001 and −1°1005 respectively, stars of about 8.5 visual magnitude. A few of the stars that lie near the north edge of Plate XI appear also near the south edge of Plate XII. The continuation of the nebula I.C. 434 toward ζ may be seen on Plate XII, which shows also that the disparity in the number of faint stars on the east and west sides of the nebulous fringe continues some distance north of ζ, where the line of division seems to turn somewhat toward the west.

The greater part of Plate XII is occupied by the remarkable nebula N.G.C. 2024, discovered in 1786 by W. Herschel, who described it[2] as a "remarkable nebulosity, divided in 3 or 4 large

[1] *Astrophysical Journal*, 49, 14, 1919.

[2] *Philosophical Transactions*, 79, 248, 1789.

patches including a dark space." The brightest parts cover a space some 25′ in diameter, and there are faint extensions, one of which reaches as far as I.C. 432 on the northwest. Both this nebulosity and that of I.C. 434 can be traced on the original plate to within 5′ of ζ Orionis, where they are concealed in the glare about the bright star. The irregularities of the bright and dark markings of N.G.C. 2024 are such as to defy description, which fortunately is unnecessary, as they are well shown in the illustrations. The character of this nebulosity appears to be different from either that of I.C. 434 or that of the neighboring nebulous stars.

A study of the photographs of this region tends to the conviction that we have here to do with extended masses of not less than four distinct types: (1) the ropy, branching nebulosity of I.C. 434; (2) the nebulosity of N.G.C. 2024; (3) the nebulous stars N.G.C. 2023 and I.C. 431, 432, and 435;[1] (4) dark nebulosities, best exemplified by the cloud Barnard 33.

The phenomena shown suggest the following speculations: Perhaps the fringe of I.C. 434 represents the common boundary of a dense, dark mass on the east and a body of thin, luminous nebulosity on the west. These two masses may have a relative motion toward each other, which results in a concentration of the bright nebulosity along the line of contact, this concentrated nebulosity being the fringe. The faint nebulosity west of the fringe must be sufficiently transparent to transmit the light of the starry background, while the dark material on the east obscures all the stars behind it. The bright nebula N.G.C. 2024 seems to be of the nature of a bright outcropping of the dark nebula, which indeed is probably nowhere absolutely non-luminous unless it be so in the darkest part of Barnard 33. Perhaps the four stars that show nebulous burs—D.M. −1°1001, −1°1005, −2°1345, and −2°1350—are imbedded in the dark nebula and illuminate that part of it which lies immediately around them, the nebulosities of the third type being due in part to this cause and in part to the same cause as those of the second type. We may suppose the non-nebulous stars that appear east of I.C. 434 to lie between the observer and the dark nebula.

[1] The nebula I.C. 435 is some 20′ east of N.G.C. 2023 and is not shown in the illustrations. It surrounds the 8.5 magnitude star D.M. −2°1350.

Mr. E. P. Hubble has kindly loaned me a plate made by him with the Hooker telescope 1920, November 18, which shows the region immediately north of ζ Orionis. The line of cleavage between the regions of few and of many stars is clearly marked on this plate, and passes in a zigzag fashion northwest of ζ nearly to I.C. 431, where it bends toward the west and returns, forming a bay about 15′ deep, and then passes northeastward to a point near the sixth-magnitude star $-1°1004$, about 1° north of ζ and near the north edge of the plate. There is on this plate no hint of a nebulosity similar to I.C. 434, and the line of cleavage has not here the regularity that is noticeable in that part of it lying south of ζ. Long-exposure photographs of the Orion region made with the 10-inch Cooke refractor of this observatory by Mr. Hubble and Mr. Pettit indicate that the obscuring mass east of ζ Orionis is only a part of a much larger region that extends several degrees toward the northeast, enveloping the bright nebula Messier 78, and also, though less plainly, some distance toward the south. The general outlines of this dark region can be traced on the Franklin-Adams chart.

Mount Wilson Observatory
March 1921

INDEX TO VOLUME LIII

SUBJECTS

PAGE

Abstracts, Preparation of 231
Algol, a Photo-Electric Study of. *Joel Stebbins* 105
R Aquarii, Observations of the Nebular Lines in the Spectrum of the Long-Period Variable Star. *Paul W. Merrill* 375
Arc, Pressure-Shifts in a Calcium. *L. F. Miller* 224
Bismuth Lines, Structure of the. *H. Nagaoka* and *Y. Sugiura* . . . 339
Calcium Arc, Pressure-Shifts in a. *L. F. Miller* 224
RS Canum Venaticorum, Provisional Elements of the Eclipsing System. *Bancroft Walker Sitterly* 99
Carbon in Spectroscopy, Use of a Lime Cathode of. *Y. Sugiura* and *T. Matoba* 323
Carbon, Iron, and Nickel, Vacuum-Spark Spectra in the Extreme Ultra-Violet of. *R. A Millikan, I. S. Bowen*, and *R. A. Sawyer* . . . 150
SX Cassiopeiae, Elements of the Eclipsing System. *Mary Fowler* . 165
Classification of Long-Period Variables, Geometrical. *J. G. Hagen* . 179
Contributors, Notice to 168
65 τ Cygni, Orbit of the Short-Period Spectroscopic Binary. *J. S. Paraskévopoulos* 144
X Cygni, Spectroscopic Orbit of the Cepheid Variable. *John C. Duncan* 95
Diameter of α Orionis with the Interferometer, Measurement of the. *A. A. Michelson* and *F. G. Pease* 249
Dispersion, to Account for the Change of Refractive Index with Temperature, a Modification of the Electron Theory of. *G. Szivessy* . . 326
Electron Theory of Dispersion, to Account for the Change of Refractive Index with Temperature, a Modification of the. *G. Szivessy* . . 326
Grating and Interferometer Measures λ 3370–λ 6750, Wave-Lengths of Lines in the Iron Arc from. *Charles E. St. John* and *Harold D. Babcock* 260
Hydrogen Chloride, Absorption Spectrum of. *Walter F. Colby* and *Charles F. Meyer* 300
Images, Mutual Action of Adjacent Photographic. *Frank E. Ross* . 349
Infra-Red Spectrum of the Sun λ 8900–λ 9900, Examination of the. *Frederick S. Brackett* 121
Interferometer, Measurement of the Diameter of α Orionis with the. *A. A. Michelson* and *F. G. Pease* 249
Interferometer Measures λ 3370–λ 6750, Wave-Lengths of Lines in the Iron Arc from Grating and. *Charles E. St. John* and *Harold D. Babcock* 260

PAGE

Iron, and Nickel, Vacuum-Spark Spectra in the Extreme Ultra-Violet of Carbon. *R. A. Millikan, I. S. Bowen,* and *R. A. Sawyer* . . . 150
Iron Arc from Grating and Interferometer Measures λ 3370–λ 6750, Wave-Lengths of Lines in the. *Charles E. St. John* and *Harold D. Babcock* 260
Lime Cathode of Carbon in Spectroscopy, Use of a. *Y. Sugiura* and *T. Matoba* 323
Lines, Structure of the Bismuth. *H. Nagaoka* and *Y. Sugiura* . . 339
Lines in Spectra of Venus, Systematic Displacements of. *Charles E. St. John* and *Seth B. Nicholson* 380
Lockyer, Sir Norman, 1836–1920. *A. L. Cortie, S.J.* 233
Magnetic Separation, Measurement of Pole-Effect and Its Connection with. *H. Nagaoka* 329
Manganese, Variation with Temperature of the Electric Furnace Spectrum of. *Arthur S. King* 133
Motions, Radiation Pressure and Celestial. *Henry Norris Russell* . . 1
Nebula, On the Passage of a Star through a. *Ernest W. Brown.* . . 169
Nebulae near ζ Orionis Photographed with the 100-Inch Hooker Telescope, Bright and Dark. *John C. Duncan* 392
Nebular Lines in the Spectrum of the Long-Period Variable Star R Aquarii, Observations of the. *Paul W. Merrill* 375
Nickel, Vacuum-Spark Spectra in the Extreme Ultra-Violet of Carbon, Iron, and. *R. A. Millikan, I. S. Bowen,* and *R. A. Sawyer* . . . 150
Notice to Contributors 168
Orbit of the Cepheid Variable X Cygni, Spectroscopic. *John C. Duncan* 95
Orbit of the Short-Period Spectroscopic Binary 65 τ Cygni. *J. S. Paraskévopoulos* 144
Orbits of Seven Spectroscopic Binaries. *R. F. Sanford* 201
Orion, Suspected Variable, Bond 624, in Trapezium of. *J. A. Parkhurst* 317
α Orionis with the Interferometer, Measurement of the Diameter of. *A. A. Michelson* and *F. G. Pease* 249
ζ Orionis Photographed with the 100-Inch Hooker Telescope, Bright and Dark Nebulae near. *John C. Duncan* 392
Parallaxes of 1646 Stars Derived by the Spectroscopic Method. *W. S. Adams, A. H. Joy, G. Strömberg,* and *Cora G. Burwell* 13
Photo-Electric Study of Algol. *Joel Stebbins* 105
Photographic Images, Mutual Action of Adjacent. *Frank E. Ross* . . 349
Pole-Effect and Its Connection with Magnetic Separation, Measurement of. *H. Nagaoka* 329
Pressure and Celestial Motions, Radiation. *Henry Norris Russell* . 1
Pressure in the Atmospheres of the Stars. *P. Salet* 327
Pressure-Shifts in a Calcium Arc. *L. F. Miller* , 224
Prominence of October 8, 1920, Exceptionally High Solar. *Oliver J. Lee* 310
Radiation Pressure and Celestial Motions. *Henry Norris Russell* . . 1

PAGE
Refractive Index with Temperature, a Modification of the Electron Theory of Dispersion, to Account for the Change of. *G. Szivessy* . 326
Solar Prominence of October 8, 1920, Exceptionally High. *Oliver J. Lee* 310
Spectra, Intensity Differences in Furnace and Arc among the Component Series in Band. *Arthur S. King* 161
Spectra in the Extreme Ultra-Violet of Carbon, Iron, and Nickel, Vacuum-Spark. *R. A. Millikan*, *I. S. Bowen*, and *R. A. Sawyer* 150
Spectra of Class Md, Characteristic Behavior of the Bright Lines in Stellar. *Paul W. Merrill* 185
Spectra of Venus, Systematic Displacements of Lines in. *Charles E. St. John* and *Seth B. Nicholson* 380
Spectroscopic Binaries, Orbits of Seven. *R. F. Sanford* 201
Spectroscopic Binary 65 τ Cygni, Orbit of the Short-Period. *J. S. Paraskévopoulos* 144
Spectroscopy, Use of a Lime Cathode of Carbon in. *Y. Sugiura* and *T. Matoba* 323
Spectrum of Hydrogen Chloride, Absorption. *Walter F. Colby* and *Charles F. Meyer* 300
Spectrum of Manganese, Variation with Temperature of the Electric Furnace. *Arthur S. King* 133
Spectrum of the Long-Period Variable Star R Aquarii, Observations of the Nebular Lines in the. *Paul W. Merrill* 375
Spectrum of the Sun, λ 8900–λ 9900, Examination of the Infra-Red. *Frederick S. Brackett* 121
Star through a Nebula, On the Passage of a. *Ernest W. Brown* . . 169
Stars, Pressure in the Atmospheres of the. *P. Salet* 327
Sun, λ 8900–λ 9900, Examination of the Infra-Red Spectrum of the. *Frederick S. Brackett* 121
Temperature, a Modification of the Electron Theory of Dispersion, to Account for the Change of Refractive Index with. *G. Szivessy* . 326
Temperature of the Electric Furnace Spectrum of Manganese, Variation with. *Arthur S. King* 133
Ultra-Violet of Carbon, Iron, and Nickel, Vacuum-Spark Spectra in the Extreme. *R. A. Millikan*, *I. S. Bowen*, and *R. A. Sawyer* . . 150
Variable, Bond 624, in Trapezium of Orion, Suspected. *J. A. Parkhurst* 317
Variable Star R Aquarii, Observations of the Nebular Lines in the Spectrum of the Long-Period. *Paul W. Merrill* 375
Variable X Cygni, Spectroscopic Orbit of the Cepheid. *John C. Duncan* 95
Variables, Geometrical Classification of Long-Period. *J. G. Hagen* . 179
Venus, Systematic Displacements of Lines in Spectra of. *Charles E. St. John* and *Seth B. Nicholson* 380
Wave-Lengths of Lines in the Iron Arc from Grating and Interferometer Measures λ 3370–λ 6750. *Charles E. St. John* and *Harold D. Babcock* 260

INDEX TO VOLUME LIII

AUTHORS

PAGE

ADAMS, W. S., A. H. JOY, G. STRÖMBERG, and CORA G. BURWELL. Parallaxes of 1646 Stars Derived by the Spectroscopic Method . 13

BABCOCK, HAROLD D., and CHARLES E. ST. JOHN. Wave-Lengths of Lines in the Iron Arc from Grating and Interferometer Measures λ 3370–λ 6750 260

BOWEN, I. S., R. A. SAWYER, and R. A. MILLIKAN. Vacuum-Spark Spectra in the Extreme Ultra-Violet of Carbon, Iron, and Nickel 150

BRACKETT, FREDERICK S. Examination of the Infra-Red Spectrum of the Sun, λ 8900–λ 9900 121

BROWN, ERNEST W. On the Passage of a Star through a Nebula . 169

BURWELL, CORA G., W. S. ADAMS, A. H. JOY, and G. STRÖMBERG. Parallaxes of 1646 Stars Derived by the Spectroscopic Method . 13

COLBY, WALTER F., and CHARLES F. MEYER. On the Absorption Spectrum of Hydrogen Chloride. 300

CORTIE, A. L., S.J. Sir Norman Lockyer, 1836–1920 233

DUNCAN, JOHN C. Bright and Dark Nebulae near ζ Orionis Photographed with the 100-Inch Hooker Telescope 392

Spectroscopic Orbit of the Cepheid Variable X Cygni 95

FOWLER, MARY. Elements of the Eclipsing System SX Cassiopeiae . 165

HAGEN, J. G. On the Geometrical Classification of Long-Period Variables 179

JOY, A. H., G. STRÖMBERG, CORA G. BURWELL, and W. S. ADAMS. Parallaxes of 1646 Stars Derived by the Spectroscopic Method . 13

KING, ARTHUR S. Intensity Differences in Furnace and Arc among the Component Series in Band Spectra 161

The Variation with Temperature of the Electric Furnace Spectrum of Manganese 133

LEE, OLIVER J. Exceptionally High Solar Prominence of October 8, 1920 310

MATOBA, T., and Y. SUGIURA. Use of a Lime Cathode of Carbon in Spectroscopy 323

MERRILL, PAUL W. Characteristic Behavior of the Bright Lines in Stellar Spectra of Class Md 185

Observations of the Nebular Lines in the Spectrum of the Long-Period Variable Star R Aquarii 375

MEYER, CHARLES F., and WALTER F. COLBY. On the Absorption Spectrum of Hydrogen Chloride 300

PAGE

MICHELSON, A. A., and F. G. PEASE. Measurement of the Diameter of α Orionis with the Interferometer 249
MILLER, L. F. Pressure-Shifts in a Calcium Arc 224
MILLIKAN, R. A., I. S. BOWEN, and R. A. SAWYER. Vacuum-Spark Spectra in the Extreme Ultra-Violet of Carbon, Iron, and Nickel . 150
NAGAOKA, H. On the Measurement of Pole-Effect and Its Connection with Magnetic Separation 329
NAGAOKA, H., and Y. SUGIURA. Structure of the Bismuth Lines . . 339
NICHOLSON, SETH B., and CHARLES E. ST. JOHN. Systematic Displacements of Lines in Spectra of Venus 380
PARASKÉVOPOULOS, J. S. Orbit of the Short-Period Spectroscopic Binary 65 τ Cygni 144
PARKHURST, J. A. Suspected Variable, Bond 624, in Trapezium of Orion 317
PEASE, F. G., and A. A. MICHELSON. Measurement of the Diameter of α Orionis with the Interferometer 249
ROSS, FRANK E. Mutual Action of Adjacent Photographic Images . 349
RUSSELL, HENRY NORRIS. Radiation Pressure and Celestial Motions . 1
ST. JOHN, CHARLES E., and HAROLD D. BABCOCK. Wave-Lengths of Lines in the Iron Arc from Grating and Interferometer Measures λ 3370–λ 6750 260
ST. JOHN, CHARLES E., and SETH B. NICHOLSON. Systematic Displacements of Lines in Spectra of Venus 380
SALET, P. On the Pressure in the Atmospheres of the Stars . . . 327
SANFORD, R. F. Orbits of Seven Spectroscopic Binaries 201
SAWYER, R. A., R. A. MILLIKAN, and I. S. BOWEN. Vacuum-Spark Spectra in the Extreme Ultra-Violet of Carbon, Iron and Nickel . 150
SITTERLY, BANCROFT WALKER. Provisional Elements of the Eclipsing System RS Canum Venaticorum 99
STEBBINS, JOEL. A Photo-Electric Study of Algol 105
STRÖMBERG, G., CORA G. BURWELL, W. S. ADAMS, and A. H. JOY. Parallaxes of 1646 Stars Derived by the Spectroscopic Method . 13
SUGIURA, Y., and T. MATOBA. Use of a Lime Cathode of Carbon in Spectroscopy 323
SUGIURA, Y., and H. NAGAOKA. Structure of the Bismuth Lines . . 339
SZIVESSY, G. A Modification of the Electron Theory of Dispersion, to Account for the Change of Refractive Index with Temperature . 326

The Astrophysical Journal

THE UNIVERSITY OF CHICAGO PRESS
CHICAGO, ILLINOIS

THE CAMBRIDGE UNIVERSITY PRESS
LONDON

THE MARUZEN-KABUSHIKI-KAISHA
TOKYO, OSAKA, KYOTO, FUKUOKA, SENDAI

THE MISSION BOOK COMPANY
SHANGHAI

THE ASTROPHYSICAL JOURNAL

An International Review of Spectroscopy and Astronomical Physics

EDITORS

GEORGE E. HALE
Mount Wilson Observatory of the Carnegie Institution of Washington

EDWIN B. FROST
Yerkes Observatory of the University of Chicago

HENRY G. GALE
Ryerson Physical Laboratory of the University of Chicago

COLLABORATORS

JOSEPH S. AMES, *Johns Hopkins University;* ARISTARCH BELOPOLSKY, *Observatoire de Poulkova;* WILLIAM W. CAMPBELL, *Lick Observatory;* HENRY CREW, *Northwestern University;* CHARLES FABRY, *Université de Paris;* ALFRED FOWLER, *Imperial College, London;* CHARLES S. HASTINGS, *Yale University;* HEINRICH KAYSER, *Universität Bonn;* ALBERT A. MICHELSON, *University of Chicago;* HUGH F. NEWALL, *Cambridge University;* ERNEST F. NICHOLS, *Massachusetts Institute of Technology;* ALFRED PEROT, *Paris;* CARL RUNGE, *Universität Göttingen;* HENRY N. RUSSELL, *Princeton University;* SIR ARTHUR SCHUSTER, *Twyford;* FRANK SCHLESINGER, *Yale Observatory*

VOLUME LIV

JULY–DECEMBER, 1921



THE UNIVERSITY OF CHICAGO PRESS
CHICAGO, ILLINOIS

Published
July, September, October, November, December, 1921

Composed and Printed By
The University of Chicago Press
Chicago, Illinois, U.S.A.

CONTENTS

NUMBER I

PAGE

Sherburne Wesley Burnham, 1838–1921. Edwin B. Frost . . . 1

The Relationship of Absolute Magnitude to Space-Velocity. W. S. Adams, G. Strömberg, and A. H. Joy 9

The Electric Furnace Spectrum of Scandium. Arthur S. King . 28

Magnetic Rotary Dispersion in Transparent Liquids. R. A. Castleman, Jr., and E. O. Hulburt 45

A Study of Arc-Cathode Spectra. Arthur St. C. Dunstan and Benjamin A. Wooten 65

Minor Contributions and Notes: Identification of Air Lines in Spark Spectra from λ 5927 to λ 8683, Paul W. Merrill, F. L. Hopper, and Clyde R. Keith, 76; Avoidance of Atmospheric Dispersion in Measures with the Stellar Interferometer, G. Van Biesbroeck, 78; Errata, 80.

NUMBER II

The Eclipsing Variable 1 H. Cassiopeiae, with Evidence on the Darkening at the Limb of a Stellar Disk. Joel Stebbins . . 81

Mutual Influence of Fraunhofer Lines. W. H. Julius 92

Natural and Magnetic Rotatory Dispersion of Optically Active Transparent Liquids. E. O. Hulburt 116

The Orbit of 49 δ Capricorni. Clifford C. Crump 127

The Spectrum of Fluorine. William R. Smythe 133

On the Accuracy with Which Mean Parallaxes Can Be Determined from Parallactic and Peculiar Motions. Henry Norris Russell 140

Reviews: *Tables du mouvement képlérien, première partie*, F. Boquet (Frank Schlesinger) 146

NUMBER III

The Fluorescence of Mercury Vapor. J. S. Van Der Lingen and R. W. Wood 149

Wave-Lengths and Periodic Changes of Spectral Type in the Variable Star *l* Carinae. Sebastian Albrecht 161

PAGE

Excitation Stages in Open Arc-Light Spectra. Part I. B. E. Moore 191

A Photometric Study of Y Camelopardalis. Raymond Smith Dugan 217

The Spectroscopic Binary Boss 3644, Virginis. John C. Duncan . 226

NUMBER IV

The Definition of a Nova. J. G. Hagen, S.J. 229

Investigations on Proper Motion, Fourth Paper. Adriaan van Maanen 237

Excitation Stages in Open Arc-Light Spectra. Part II. B. E. Moore 246

The Low-Current Arc. Part I. V. L. Chrisler 273

The Spectrum of Radium Emanation. R. E. Nyswander, S. C. Lind, and R. B. Moore 285

Note on Cooling by Expansion in Sun-Spots. Henry Norris Russell 293

Notice to Contributors 296

NUMBER V

A Study of the Ultra-Violet End of the Solar Spectrum. Charles Fabry and H. Buisson. 297

Studies Based on Colors and Magnitudes in Stellar Clusters. XIX. Harlow Shapley and Myrtle L. Richmond 323

On Majorana's Theory of Gravitation. Henry Norris Russell . 334

Investigations on Proper Motion, Fifth Paper. Adriaan van Maanen 347

Index 357

A



SHERBURNE WESLEY BURNHAM

From a snap-shot by Dorothy Wallace in 1908

THE
ASTROPHYSICAL JOURNAL
AN INTERNATIONAL REVIEW OF SPECTROSCOPY
AND ASTRONOMICAL PHYSICS

VOLUME LIV JULY 1921 NUMBER 1

SHERBURNE WESLEY BURNHAM, 1838–1921

By EDWIN B. FROST

Sherburne Wesley Burnham, senior astronomer at the Yerkes Observatory from its opening in 1897 until his retirement in 1914, died at his home in Chicago on March 11, 1921, at the age of eighty-two years.

He leaves an imperishable memory in the history of stellar astronomy, for the great number of new double stars which he discovered, for the vast quantity of precise measurements of such objects which he made, and for his monumental work of critical compilation. His symbol β is recognized throughout the astronomical world as the synonym of scientific precision and of remarkable visual discrimination.

Mr. Burnham was a "self-made man." This term is somewhat overworked, perhaps particularly on the Continent of Europe, where it is supposed to be rather typical of successful Americans. It expresses the fact that he did not have the advantage of any studies at a college or university in mathematics or astronomy, nor did he have, during the years when he was acquiring his knowledge in this department, much direct contact with professional astronomers, from whom he could obtain advice. He had to go to such books as he could find in the libraries in Chicago and by his own

efforts acquaint himself with the methods of observing and the literature of astronomy in the field which he pursued.

After some study at the academy in the town of his birth, Thetford, Vermont, in the hill country of New England, he practiced shorthand by himself, and in 1858 went to New York, where he found employment in business. Later, during the Civil War, he was in New Orleans with the Union troops, serving as an official reporter for the military government, and subsequently he was similarly employed at several Constitutional Conventions in the southern states. After the war he came to Chicago and continued as official court reporter for more than twenty years. This labor of recording the verbal testimony before the United States courts and then writing it out in longhand was indeed arduous, and involved no small strain upon his eyes; but for a score of years he observed at night as assiduously as if he had no engagements for the day.

His interest in astronomy had been awakened by the possession of two small telescopes in succession, and he ordered from the Clarks in 1869 a 6-inch refractor, with the stipulation that it should be as good as they could make. After this telescope was delivered in 1870, his attention was directed to double stars and it appeared that he had a most extraordinary keenness of vision, particularly in this discrimination as to the character of a stellar image. The objective was a fine one, perhaps a prototype for the subsequent masterpieces of optical skill made by the Clarks.

In 1873 and 1874, the Royal Astronomical Society published in the *Monthly Notices* five lists of new double stars by Mr. Burnham. He had obtained great assistance from Webb's *Celestial Objects for Common Telescopes* and had entered into correspondence with Mr. Webb, whose encouragement was of much value to him and led to his connection with the Royal Astronomical Society, of which he became a member in 1874. With the 6-inch telescope he discovered 451 new double stars, many of which were so close as to give difficulty to other observers having much larger instruments. The forty-fourth volume of the *Memoirs* of the Royal Astronomical Society, published in 1879, contained the measures of 250 new doubles, with micrometric observations of 250 other pairs. For about six years of the period between 1877 and 1884,

Mr. Burnham had the opportunity to use the fine 18½-inch refractor of the Dearborn Observatory, then located in the city at the former Chicago University; and for part of the time he held, at least nominally, the office of director of that observatory. During part of the year 1881 he was associated with the then new Washburn Observatory of the University of Wisconsin at Madison, of which Professor E. S. Holden was the director. There he observed both with the 15½-inch telescope and his 6-inch, the latter being purchased by the University of Wisconsin as a part of its equipment.

When the Lick Observatory was opened in 1888, the position of astronomer was offered to him and was promptly accepted, although no doubt at a very considerable pecuniary sacrifice, especially for a man with a family of six children. The Lick Observatory was not unfamiliar to him, as he had been there twice before, on commissions from the Lick Trustees: once for two months in 1879, to test (with his 6-inch refractor) the conditions of observing on Mount Hamilton, which had been chosen as the site for the new observatory; and in 1881, to observe the Transit of Mercury, for which he was able to use the 12-inch telescope, then already mounted. He carried out a fruitful program of observations of double stars at the Lick Observatory, with the use of the 36-inch and 12-inch refractors for four years. This was only interrupted by an expedition to Cayenne, to observe the eclipse of December 21, 1889. Internal conditions had developed at the observatory which were not agreeable to Mr. Burnham and he resigned his position in June, 1892, and returned to Chicago, where he was offered the office of clerk of the United States Circuit Court. His duties in this position were highly responsible, but perhaps less exacting than they had been previously when he was court reporter. He discharged these duties with great accuracy and ability, and his services were highly appreciated by the judges and other officers of the federal court, and by a wide circle of men in the legal profession. He, in turn, had great respect, amounting in some cases to veneration, for many of the distinguished jurists presiding in the courts in which he served during his terms of office in both capacities. From 1897 to 1902, he also acted as receiver for the Chicago & Northern Pacific Railroad.

For a period of five years, beginning in 1892, Mr. Burnham was not directly connected with an observatory and his use of a telescope was limited to occasional visits to the Dearborn Observatory, then at Evanston under the directorship of Hough. Burnham's interest in double stars was not in the least diminished, however, and he published a dozen papers in the *Monthly Notices*, chiefly on the orbits of stars which he had previously observed. He was also occupied with his manuscript catalogue of all double stars, which he had begun many years before.

In 1892 the University of Chicago received from Mr. Yerkes the promise that he would present to it a well-equipped observatory, and the disks for the 40-inch refractor were purchased by him. There were delays in completing the plans for the observatory, however, so that the building could not be begun until 1895; but meanwhile Mr. Burnham was appointed astronomer, with the title of Professor of Practical Astronomy, in the University of Chicago. His actual work was not begun, however, until after the formal opening of the observatory, in October, 1897, when he was assigned two nights a week with the great telescope. He commonly came to the observatory on the afternoon of Saturday and observed through that night and through Sunday night, taking what rest he could in his office during the intervening day; but he was off for his duties at the court on the early train on Monday morning, carrying with him his records of observations, which were kept in a most systematic manner and were promptly reduced. His observing program was selected with great care and his methods were such that he worked very efficiently and rapidly. He greatly preferred to observe toward the east and rarely reversed the telescope to follow a star which had gotten away from him to the west. Under exceptional circumstances he measured as many as 100 pairs in a single night with the forty-inch telescope! He seldom allowed himself to be distracted by other astronomical objects, however interesting, but he occasionally measured nebulae which came within the field. He made no search for new double stars after he began work with the 40-inch telescope, rightly judging that it was more important to follow up the difficult pairs which were beyond the reach of many telescopes, but which were of the greatest interest because of the rapid motion often revealed. He soon collected his

own measures and those of some other observers of 1290 double stars which he had discovered between 1871 and 1899, and these were published in 1900, as Volume I of the *Publications of the Yerkes Observatory*.

In 1902 he resigned his position as clerk of the court, despite the fact that he could have availed himself of its life-tenure. This gave him all of his time for astronomical work, which had never been the case before except for the four years when he was at the Lick Observatory and for the six months at the Washburn Observatory. He did not move out to Williams Bay, however, preferring to maintain the family home in Chicago, where it had been so long established.

With this additional freedom he thus had further opportunity for completing his great *General Catalogue of Double Stars within 121° of the North Pole*, which was now in its third edition as a manuscript. Attempts had been made for some years to find means for publishing this, but it was not until 1906 that this could be done. The recently endowed Carnegie Institution of Washington undertook in 1905 the publication of the work, and the printing was begun at the University of Chicago Press, where Mr. Burnham personally supervised the composition. The preparation of this comprehensive work constantly brought to light objects requiring new observations before their inclusion in the catalogue; thus most of his observations at the 40-inch telescope, from 1900 to 1906, nearly 10,000 in number, found their original publication in this catalogue. The first of these two stately quarto volumes summarizes the statistical information as to 13,665 double stars, in 275 pages; the second gives in 1086 pages the detailed information as to all the important observations of these pairs, with diagrams of the orbits of many of them. Aside from its large amount of original data this is not a mere compilation, for Professor Burnham's experienced discrimination is seen throughout the work; while he gave references to the complete literature for every pair, he published in detail only the data of observers whose work was of a high standard of excellence.

Although Mr. Burnham never did any actual teaching and, so far as we know, never gave a public lecture, nevertheless by his fine example of persistent devotion to his special line of research, and

by his untiring work of observation, even at an age when most men would have availed themselves of the privilege of retiring, he led the way in America in the field of double stars and has been followed by a worthy band, who gladly recognized him as master. For many years Mr. Burnham gave freely his valuable counsel to many younger observers in making up their programs for observations of double stars.

After the publication of the great catalogue, Mr. Burnham directed his observations largely to the micrometric reference of stars, chiefly from the *General Catalogue*, to faint stars in their vicinity, with a view to determining the relative proper motion, because he fully appreciated the great superiority of such observations with a telescope having a focal length of 19 meters over those made with meridian circles. His results, which included nearly 10,000 measures, were published in 1913 in a quarto volume of 311 pages by the Carnegie Institution of Washington, with the title *Measures of Proper Motion Stars Made with the 40-Inch Refractor of the Yerkes Observatory in the Years 1907–1912*. These measures lay the foundation for a very much better knowledge of relative proper motions of these stars as they may be remeasured in future years. Such observations of stars did not require the high standard of "seeing" necessary for close double stars with a big instrument, and there is also a possibility that there was some slight falling off in the keenness of β's vision after he was seventy years of age.

Physically Mr. Burnham was slight and of moderate stature, but all his muscles were at his command. The co-ordination of his hand and eye had always been notable. Thus he was an expert shot with the rifle, unusually good at bowling, and generally a man who mastered whatever he undertook. His endurance was exceptional, whether it was shown in climbing about the cañons near the Lick Observatory, or in long rides on his bicycle, or in carrying on his work at the great telescope during thirteen or even fourteen hours of a cold winter's night. He was abstemious in his habits and took very little food during his visits to the Observatory, but he had constant comfort from his cigar. The photograph which accompanies this sketch is taken from a snap-shot made while he

was at his ease near the observatory, when he was about seventy years of age.

He was an expert with the camera and had won the prizes at exhibits in the earlier days, but there are very few portraits of himself available.

He knew nothing of bodily weakness until early in the year 1913, when he suffered from what may have been a form of influenza. He said that it was the first time in his life that he had been sick and that he was "all played out." He was then seventy-five years old. He never again fully recovered his strength, so that his visits to the observatory thereafter were fewer and his last observations with the 40-inch telescope were made on May 13, 1914. During that summer he retired, on a pension, in accordance with the statutes of the University of Chicago. He was still given the opportunity to use the telescope, but did not avail himself of it, and after 1917 he did not often leave his home. Toward the end of February, 1921, his hip was broken from a fall, and from this, in his enfeebled condition, recovery was impossible. His death occurred a fortnight later.

In 1868 Mr. Burnham was married to Mary Cleland, who survives him with their three sons and three daughters, together with eight grandchildren.

A complete bibliography of Mr. Burnham's writings need not be given here. Summaries of his observations have been published in more than one place: thus Volume II of the *Publications of the Lick Observatory* (1894) gives the place of publication of his nineteen catalogues of new double stars, which had been printed chiefly in the *Monthly Notices* of the Royal Astronomical Society or in the *Astronomische Nachrichten;* it contains the complete details of the observations of the last six catalogues, covering stars β 1026 to β 1274, which were discovered and measured at the Lick Observatory. That volume also includes some measures of nebulae with the 36-inch refractor. Again, for convenience of reference, these original sources of publication were collected in Volume I of the *Publications of the Yerkes Observatory*, covering the history of the 1290 β stars. He increased his list of new double stars but little after this; in fact, he avoided them, so that the total number of β stars is 1340.

Six extensive lists of measures were published in the *Astronomische Nachrichten* between 1907 and 1911. Many of these are also contained in the volume on proper motion stars. At Mr. Burnham's request a final collection of measures was extracted from his notebooks by Professor Philip Fox and published in the *Astronomical Journal* in 1918.

After the publication of the *General Catalogue*, Mr. Burnham still maintained his manuscript edition, keeping it up to date so as to include the great numbers of new double stars discovered by Professor Hussey and by Professor Aitken in their systematic searches for such objects. When his health began to fail, Mr. Burnham passed this valuable MS catalogue on to Professor Eric Doolittle, who was carrying it forward at the time of his premature and lamented death in 1920. In accordance with a prior arrangement, it then went to Professor Aitken, under whose careful supervision it will be maintained and a new extension published.

Professor Burnham received the Gold Medal of the Royal Astronomical Society in 1894, and the Lalande Prize of the French Academy of Sciences was awarded to him in 1904. Yale College gave him the honorary degree of A.M. in 1878, and in 1915 he received the honorary degree of Sc.D. from Northwestern University.

YERKES OBSERVATORY
June 1921

THE RELATIONSHIP OF ABSOLUTE MAGNITUDE TO SPACE-VELOCITY[1]

By W. S. ADAMS, G. STRÖMBERG, and A. H. JOY

ABSTRACT

Variation of the velocity of stars with absolute magnitude.—*A statistical study* of the radial, tangential, and space-velocities of 1350 stars, mostly of types F, G, K, and M, shows a marked correlation with absolute magnitudes. The results are given in the form of equations and tables. The increase in average space-velocity for a decrease of one magnitude in brightness varies with the type, but is of the order of 3 km/sec. The greater homogeneity of the giant stars as a class and their comparative freedom from large individual motions are indicated by the results. As would be expected for a random distribution of velocities as to direction, the average radial velocities are about half the corresponding average space-velocities.

Frequency of the space-velocities of stars cannot be represented by a distribution according to Maxwell's law, for there is a large excess of stars with high velocities, but a type of *frequency function* based upon the assumption of a normal error-distribution in the logarithms of the velocities is found to represent the observations much more closely. The function is proportional to $e^{-h^2(\log v - \log \bar{v})^2}$, where v is the geometrical mean space-velocity.

In a communication published in 1915, Kapteyn and Adams[2] showed that the radial velocities of a considerable number of stars depended upon proper motion and mean parallax in such a way as to indicate that the brighter stars intrinsically move more slowly than the fainter stars. More extensive investigations by Adams and Strömberg[3] in 1917, and by Strömberg in 1918,[4] based upon 1300 stars of spectral types F, G, K, and M, gave similar results. For this purpose the absolute magnitudes derived by the spectroscopic method were used, and not only the radial velocities but also the components at right angles to the direction of the sun's apex were included in the discussion. An average change in radial velocity of about 1.3 km for each unit of absolute magnitude was indicated by these investigations.

The subject had already been discussed by Eddington[5] on the basis of stars with parallaxes determined by the trigonometric

[1] *Contributions from the Mount Wilson Observatory*, No. 210.

[2] *Mt. Wilson Communications*, No. 1; *Proceedings of the National Academy of Sciences*, 1, 14, 1915.

[3] *Mt. Wilson Contr.*, No. 131; *Astrophysical Journal*, 45, 293, 1917.

[4] *Mt. Wilson Contr.*, No. 144; *Astrophysical Journal*, 47, 7, 1918.

[5] *Stellar Movements*, p. 52, 1914.

method, and some of the important consequences of such a relationship had been pointed out by Eddington, Russell, Halm, and others. Additional evidence will therefore be of especial value for investigations dealing with the motions of stars in our Galaxy and their connection with spectral type and mass.

Previous studies of the subject have been limited to components of the stellar motions either in the line of sight or at right angles to it. With the rapid accumulation of parallax observations, both trigonometric and spectroscopic, and a similar increase in determinations of radial velocities, we can extend the investigation to the actual motions of the stars in space. In the pages which follow we shall compute the space-motions of the stars in our list, derive the frequency-law representing their distribution, and study the relationship of these motions to absolute magnitude.

The velocity-components of a star relative to the sun are computed from the following equations:

$$x = V \cos\alpha \cos\delta - \frac{k}{\pi}(\mu_\alpha \sin\alpha \cos\delta + \mu_\delta \cos\alpha \sin\delta)$$

$$y = V \sin\alpha \cos\delta + \frac{k}{\pi}(\mu_\alpha \cos\alpha \cos\delta - \mu_\delta \sin\alpha \sin\delta)$$

$$z = V \sin\delta + \frac{k}{\pi}\mu_\delta \cos\delta$$

where x, y, and z are the velocity-components in the equatorial system, expressed in kilometers per second, V is the radial velocity relative to the sun, α and δ are right ascension and declination, μ_α and μ_δ the corresponding proper motions, π is the parallax, and k is a constant equal to 4.737 km/sec.

If x_0, y_0, and z_0 are the velocity-components of the sun referred to the centroid of a large number of stars, we can obtain the components x_1, y_1, and z_1 of the star relative to this centroid from the equations

$$x_1 = x + x_0, \qquad y_1 = y + y_0, \qquad z_1 = z + z_0.$$

The space-velocity v of the star, corrected for the sun's motion, is therefore

$$v = \sqrt{x_1^2 + y_1^2 + z_1^2}.$$

The parallaxes used in this investigation are those obtained by the spectroscopic method and published recently.[1] In a few instances where the parallaxes are large the trigonometric values have been used instead. The proper motions are from the *Catalogue* of Boss or *Cincinnati Publications*, No. 18, with the addition

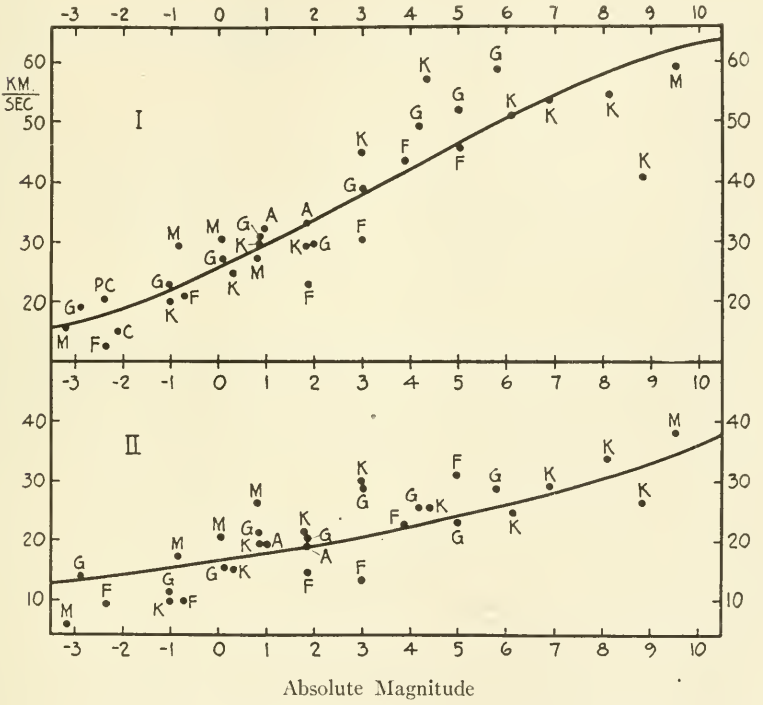


FIG. 1.—Curves showing the relationship of space-velocity to absolute magnitude for the various spectral types.

Curve I. Abscissae, average absolute magnitudes; ordinates, geometrical means of space-velocities. The continuous curve alone is shown.

Curve II. Abscissae, average absolute magnitudes; ordinates, average radial velocities.

of a few values determined by Kapteyn, Roy, and others. The radial velocities have been taken from Campbell's list in *Lick Observatory Bulletin*, No. 229, from the Mount Wilson lists published

[1] *Mt. Wilson Contr.*, No. 199; *Astrophysical Journal*, **53**, 13, 1921.

in *Contributions*, Nos. 79 and 105,[1] and from unpublished Mount Wilson results.

Since many of the stars observed at Mount Wilson were selected on the basis of small proper motion, it is evident that there may

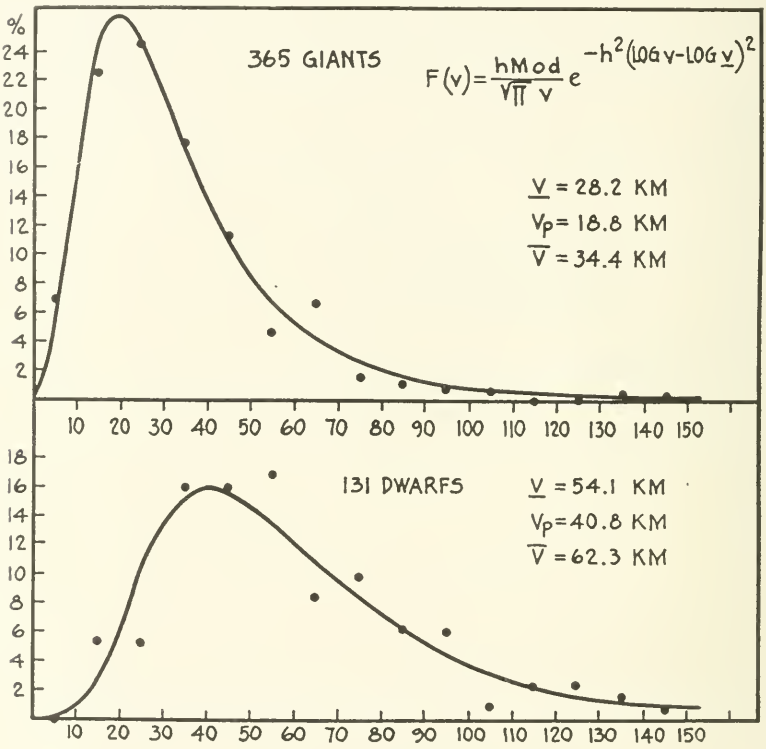


FIG. 2.—Frequency-curves for space-velocities of stars of spectral type K. Upper curve is based on 365 giant stars, lower curve on 131 dwarfs. Abscissae are space-velocities, ordinates are numbers of stars expressed in percentages of the whole within the limits of every 10 kilometers of space-velocity.

be too large a proportion of stars with velocity-components in a plane perpendicular to the line of sight, which are nearly equal in direction and amount to the sun's velocity projected on this plane. For this reason we have omitted from the discussion 101 stars,

[1] *Astrophysical Journal*, 39, 341, 1914; 42, 172, 1915.

this number being based on the distribution of proper motions given by Kapteyn in *Groningen Publications*, No. 30.

The detailed results based upon the values derived from the individual stars are given in Table I. The symbols in this table have the following meaning:

$\overline{M}$ = mean absolute magnitude
$\overline{v}$ = average space-velocity
$\overline{T}$ = average tangential velocity not corrected for the sun's motion. This is equal to $\left(\overline{\frac{\mu}{\pi}}\right)$
θ = average radial velocity
$\underline{v}$ = geometrical mean of space velocities
$\underline{T}$ = geometrical mean of tangential velocities
r_1 and r_2 = probable deviations of log v and log T for a single star from the mean values log v and log T.

All of these quantities have been computed from the individual values of v, T, log v, log T and V', the last being the radial velocity corrected for the sun's motion. The probable errors in log $\bar{v}$ and log $\underline{T}$ have been converted into corresponding errors in $\bar{v}$ and $\underline{T}$. The values used for the solar motion are those derived in 1917.[1]

$$A_0 = 270^\circ.9; \quad D_0 = +29^\circ.2; \quad V_0 = 21.48 \text{ km/sec.}$$

The use of the values $A_0 = 270^\circ$, $D_0 = +30^\circ$, $V_0 = 20.0$ km would in general affect $\bar{v}$ and $\underline{v}$ by less than 0.1 km.

The values for the A-type stars in Table I are based almost wholly upon stars of types A7 to A9, and the uncertainty in the determination of the absolute magnitudes may be larger than for stars of the succeeding types. Occasionally stars with absolute magnitudes falling on the limit between two groups are included with half-weight in each of the groups. Thus among the A-type spectra a star of absolute magnitude +1.5 is accountable for the fractional values appearing in the column giving the number of stars.

The use of the geometrical mean in this investigation has been found desirable for two reasons. In the first place it is influenced much less than the arithmetical mean by the inclusion of stars of

[1] *Mt. Wilson Contr.*, No. 144; *Astrophysical Journal*, 47, 7, 1918.

TABLE I

Absolute Magnitude and Space-Motion

M	No.	$\bar{M}$	$\bar{v}$	$\bar{T}$	θ	v	T	r_1	r_2
				Type A (A7 to A9)					
			km	km	km	km	km		
−0.1 to +1.5....	11.5	+1.0	34.2	23.2	19.3	32.2± 2.4	19.4±2.6	±0.108	±0.201
+1.5 to +2.5....	14.5	1.9	36.6	31.8	19.6	32.9± 2.6	24.7±3.6	0.129	0.244
				Type F (Fo to F9)*					
−3.5 to −1.5....	9	−2.3	16.5	20.3	9.5	12.3± 2.6	15.2± 3.0	±0.271	±0.258
−1.5 to +0.5....	21	−0.6	43.7	44.6	11.7	23.7	19.8		
	20†	−0.7	32.2	33.7	9.8	20.9± 3.7	17.4± 3.9	0.338	0.427
+0.5 to +2.5....	54.5	+1.9	28.1	26.9	14.6	22.8± 1.4	18.5± 1.7	0.198	0.286
2.5 to 3.5....	90	3.0	52.4	49.1	22.3	34.1± 1.7	30.3± 1.8	0.198	0.241
	85.5‡	3.0	34.5	33.4	13.4	30.1± 1.1	26.8± 1.4	0.150	0.205
3.5 to 4.5....	109	3.9	77.4	73.3	29.0	51.5± 2.8	47.6± 2.6	0.246	0.246
	99.5‡	3.9	54.5	51.9	22.5	43.6± 2.1	40.3± 2.0	0.208	0.211
4.5 to 5.7....	8.5	5.0	143.5	125.4	74.4	76.9±20.6	67.1±17.8	0.336	0.331
	6.5‡	5.0	54.0	47.4	31.0	45.5±10.4	39.7± 9.6	0.249	0.266
				Type G (Go to G9)					
−4.5 to −1.5....	22	−2.9	30.1	27.0	13.7	21.7± 2.9	17.9± 2.5	±0.271	±0.288
	20	−2.9	25.6	21.7	14.0	19.2± 2.5	15.4± 2.0	0.255	0.263
−1.5 to −0.5....	25.5	−1.0	27.8	25.9	11.0	22.7± 1.9	19.4± 2.0	0.187	0.222
−0.5 to +0.5....	62.5	+0.1	35.7	32.2	15.5	27.2± 1.5	22.4± 1.5	0.193	0.233
+0.5 to +1.5....	72.5	0.9	37.8	31.8	21.0	30.2± 1.5	23.6± 1.5	0.186	0.230
1.5 to 2.5....	35.5	1.9	35.9	29.0	19.8	29.6± 2.0	22.7± 1.8	0.181	0.210
2.5 to 3.5....	18	3.0	45.4	39.0	29.4	38.8± 3.2	33.2± 3.4	0.154	0.189
3.5 to 4.5....	42.5	4.2	59.7	57.2	25.6	49.4± 3.4	47.6± 3.2	0.198	0.189
4.5 to 5.5....	73.5	5.0	58.7	58.2	23.1	51.9± 2.4	48.6± 2.5	0.168	0.187
5.5 to 6.6....	51	5.8	88.3	88.0	34.0	61.9± 3.4	63.4± 3.4	0.174	0.166
	50§	5.8	70.3	70.7	28.7	58.6± 3.0	60.0± 2.9	0.157	0.148
				Type K (Ko to K9)					
−4.0 to 0.0....	14	−0.8	44.4	42.2	11.9	26.6± 5.5	21.8± 5.0	±0.333	±0.372
	12	−1.0	28.0	23.6	9.9	20.0± 3.2	15.7± 3.2	0.276	0.312
0.0 to +0.5....	74.5	+0.3	29.4	22.8	14.6	24.4± 1.2	14.8± 1.1	0.182	0.289
+0.5 to +1.5....	186.5	0.9	36.5	28.6	19.5	29.6± 1.0	20.4± 0.8	0.190	0.248
1.5 to 2.5....	47	1.9	34.6	24.6	21.1	29.4± 1.7	17.0± 1.5	0.173	0.269
2.5 to 3.5....	11.5	3.0	48.8	37.6	29.8	45.9± 3.6	29.4± 4.6	0.116	0.231
3.5 to 5.5....	12.5	4.4	62.6	53 5	25.8	57.2± 4.6	32.7± 5.1	0.125	0.242
5.5 to 6.5....	67.5	6.1	67.3	70.4	24.3	50.9± 2.5	59.8± 2.8	0.177	0.162
6.5 to 7.5....	36	6.9	59.3	56.4	29.3	53.5± 2.8	52.8± 2.2	0.136	0.105
7.5 to 8.5....	12.5	8.1	58.7	54.8	33.7	54.2± 5.0	50.9± 4.3	0.143	0.130
8.5 to 9.7....	8	8.8	47.3	41.0	26.5	40.6± 6.7	36.2± 5.4	0.202	0.182
				Type M (Ma to Md)					
−3.8 to −2.7....	2	−3.2	16.4	11.2	5.6	15.8± 3.4	11.0± 1.7	±0.131	±0.095
−1.5 to −0.5....	13.5	−0.8	36.4	33.1	17.4	29.6± 2.7	21.4± 4.8	0.142	0.350
−0.5 to +0.5....	67.5	+0.1	36.5	28.2	20.4	30.2± 1.5	19.5± 1.4	0.174	0.249
+0.5 to +1.5....	31	0.8	32.0	26.3	26.3	27.2± 1.8	21.3± 1.8	0.154	0.203
8.5 to 10.0....	7	9.5	61.3	53.9	38.3	58.8± 4.7	49.3± 6.2	0.093	0.143
10.0 to 13.4....	11	10.9	62.3	50.0	37.5	51.4± 7.6	41.2± 5.8	0.214	0.203

* *Cin.* 560 (Sp. = A8, $M = 2.8$, $v = 557$, $V' = +327$) included in F type.

† RR Lyrae ($v = 274$, $V' = -49$) omitted.

‡ Stars with $v > 180$ omitted. These appear to form a separate group.

§ *Cin.* 2019 ($v = 986$) omitted

TABLE I—*Continued*

M	No.	$\overline{M}$	$\bar{v}$	$\bar{T}$	θ	v	T	r_1	r_2
	CEPHEID VARIABLES \|\|								
			km	km	km	km	km		
−3.4 to −2.1....	7	−2.6	19.9	24.6	10.1	12.2 ± 3.5	21.2 ± 3.3	±0.327	±0.178
−2.0 to −1.1....	8	−1.8	20.5	21.9	12.4	17.8 ± 2.4	19.9 ± 2.5	0.166	0.156
Sum and means	15	−2.1	20.2	23.2	11.3	14.9 ± 2.3	20.5 ± 1.9	0.255	0.159
	PSEUDO-CEPHEIDS								
−4.2 to −2.8....	14	−3.6	28.2	24.4	9.8	21.4 ± 3.7	15.6 ± 3.2	±0.277	±0.334
−2.7 to −0.1....	14	−1.2	30.6	22.4	19.3	19.0 ± 4.1	12.9 ± 2.5	0.353	0.308
Sum and means	28	−2.4	29.4	23.4	14.6	20.1 ± 2.7	14.2 ± 2.0	0.309	0.315

\|\| RR Lyrae ($M = 0.3$, $v = 274$ km, $V' = -49$) omitted.

exceptionally high velocities. In the second place, as will be shown later, the form of frequency-function representing most closely the observed distribution of the space-velocities is one in which the logarithm of the geometrical mean of the velocities is one of the fundamental constants. The conversion of the geometrical into the arithmetical mean may be made readily through multiplication by a factor dependent upon the dispersion in the logarithms of the space-velocity around the mean value. This has been found to be fairly constant for all the groups of stars.

Attention should be called to two points bearing on the results of Table I. The first is that of the effect of the selection of the stars. Reference has already been made to the omission of a number of stars of small proper motion in order to equalize the proportion of such stars. The effect of the selection of stars of large proper motion would no doubt have been very marked had all stars of the same spectral type been included in one group. The division according to absolute magnitude should, however, eliminate to a large extent the effect of selection, since most of the stars of large proper motion may be assumed to have been selected on account of their nearness and hence their low intrinsic brightness. A slight excess of rapidly moving stars of high luminosity might, however, be expected from a selection of stars of large proper motion, and this would tend to increase slightly the mean values of the giant stars in Table I.

A second point has to do with the stars of the very highest luminosity. This group contains some stars which have erroneously been estimated as too bright, and as there is a tendency toward an accumulation of such errors, the mean space-velocity and the mean tangential velocity are too large. In order to reduce this effect a special computation has been made for the very brightest G and K stars, omitting a few of the largest space-velocities. This result is given in the second line of the G and K subdivisions of Table I.

From the results of Table I it appears that the values of r_1, although somewhat larger for the brighter stars, do not show any very great range. Accordingly we may with sufficient accuracy adopt its mean value for all absolute magnitudes and spectral types. This value is

$$r_1 = 0.171 \pm 0.0033.$$

As will be shown in connection with the discussion of the frequency-law, the arithmetical mean of the space-velocities $\bar{v}$ and the most frequent velocity v_p can be computed from the geometrical mean by aid of the equations

$$\bar{v} = 10^{2.530 r_1^2}\, \underline{v}, \quad v_p = 10^{-5.061 r_1^2}\, \underline{v}.$$

Hence

$$\bar{v} = 1.186\, \underline{v}, \qquad v_p = 0.7113\, \underline{v}.$$

The values of $\overline{T}$ and $\underline{T}$ have been computed because of their importance in the derivation of mean parallaxes. Since

$$\overline{T} = k\left(\frac{\overline{\mu}}{\pi}\right),$$

we have approximately

$$\bar{\pi} = k\frac{\bar{\mu}}{\overline{T}}.$$

Furthermore

$$\underline{T} = k\left(\frac{\mu}{\pi}\right) = k\frac{\mu}{\pi},$$

or

$$\underline{\pi} = k\frac{\mu}{\underline{T}} = 10^{0.2(M-\bar{m})-1}.$$

With the aid of the data given in Table I we can now compute the general relationship between absolute magnitude and velocity. The geometrical means of the space-velocities and the tangential velocities have been used, since these can be obtained with a higher degree of accuracy than the arithmetical means, but the average radial velocity has been used directly. The tangential velocities are not corrected for the solar motion.

Two different solutions have been made. In the first solution we assume for each type the relationship

$$\log \underline{v} = a + bM,$$

with similar expressions for $\log \underline{T}$ and $\log \theta$, and use these equations under the assumption that they are constant for each spectral

TABLE II

EQUATIONS CONNECTING ABSOLUTE MAGNITUDE WITH VELOCITY
FIRST SOLUTION: CONTINUOUS VARIATION

Type	$\log \underline{v}$	$\log \underline{T}$	$\log \theta$
F.....	$1.356+0.0553\,M$ $\pm 0.032 \pm 0.0111$	$1.248+0.0690\,M$ $\pm 0.033 \pm 0.0113$	$1.149+0.0257\,M$ $\pm 0.044 \pm 0.0154$
G.....	$1.415+0.0605\,M$ $\pm 0.008 \pm 0.0021$	$1.313+0.0768\,M$ $\pm 0.016 \pm 0.0043$	$1.214+0.0412\,M$ $\pm 0.021 \pm 0.0067$
K.....	$1.428+0.0410\,M$ $\pm 0.018 \pm 0.0038$	$1.224+0.0649\,M$ $\pm 0.030 \pm 0.0063$	$1.232+0.0338\,M$ $\pm 0.017 \pm 0.0036$
M.....	$1.456+0.0302\,M$ $\pm 0.013 \pm 0.0026$	$1.300+0.0402\,M$ $\pm 0.019 \pm 0.0037$	$1.306+0.0282\,M$ $\pm 0.025 \pm 0.0049$

ALL TYPES

Space-Velocity	$\log \underline{v} = +1.408+0.0632M-0.00240M^2$	$\pm 0.011 \pm 0.0067 \quad \pm 0.00085$
Tangential Velocity	$\log \underline{T} = +1.256+0.0870M-0.00303M^2$	$\pm 0.017 \pm 0.0098 \quad \pm 0.00124$
Average Radial Velocity	$\log \theta = +1.219+0.0321M+0.00020M^2$	$\pm 0.017 \pm 0.0103 \quad \pm 0.00131$

type over the entire range of absolute magnitude. In the second solution a discontinuity is assumed for the K and M stars at the point of division between the giants and dwarfs. The evidence

afforded by Table I appears on the whole to be favorable to such a discontinuity, since the velocities of the dwarf stars of these types show little if any variation with absolute magnitude.

TABLE III

SECOND SOLUTION: SEPARATE EQUATIONS FOR GIANTS AND DWARFS OF TYPES K AND M

Type	log v	log T	log θ
	$M<2.5$		
K.....	$1.398+0.0531\,M$ $\pm 0.024 \pm 0.0206$	$1.232+0.0281\,M$ $\pm 0.052 \pm 0.0446$	$1.164+0.1062\,M$ $\pm 0.028 \pm 0.0239$
M.....	$1.455+0.0320\,M$ $\pm 0.016 \pm 0.0213$	$1.298+0.0440\,M$ $\pm 0.014 \pm 0.0191$	$1.304+0.1480\,M$ $\pm 0.012 \pm 0.0165$
All (F to M)	$1.422+0.0282\,M$ $\pm 0.010 \pm 0.0062$	$1.275+0.0417\,M$ $\pm 0.013 \pm 0.0082$	$1.232+0.0113\,M$ $\pm 0.022 \pm 0.0135$
	$M>2.5$		
K.....	1.710 ± 0.012	1.700 ± 0.012	1.431 ± 0.014
M.....	1.734 ± 0.031	1.645 ± 0.040	1.578 ± 0.012
All (F to M)	$1.640+0.0126\,M$ $\pm 0.024 \pm 0.0042$	$1.549+0.0234\,M$ $\pm 0.053 \pm 0.0089$	$1.271+0.0271\,M$ $\pm 0.030 \pm 0.0051$

Tables II and III give the values of the coefficients and their probable errors in the equations of the form

$$\log v = a + bM$$

for the two solutions. Further, all the types are discussed together, and a term involving the square of M has then been included in the first solution, the form being

$$\log v = a + bM + cM^2$$

with similar expressions for the tangential and radial velocities.

From the equations of Tables II and III we obtain the values given in Table IV. The columns marked 1 and 2 under K, M,

TABLE IV

ABSOLUTE MAGNITUDE AND VELOCITY: COMPUTED VALUES

M	F	G	K		M		All Types	
			1	2	1	2	1	2
	v = GEOMETRICAL MEAN OF SPACE-VELOCITIES							
− 2	17.6	19.7	22.2	19.6	24.9	24.6	18.7	23.2
− 1	20.0	22.6	24.4	22.1	26.7	26.5	22.0	24.8
0	22.7	26.0	26.8	25.0	28.6	28.5	25.6	26.4
+ 1	25.8	29.9	29.4	28.2	30.6	30.7	29.4	28.2
2	29.3	34.4	32.4	31.9	32.8	33.0	33.5	30.1
3	33.3	39.4	35.6				37.7	47.6
4	37.8	45.4	39.1				41.9	49.0
5	42.8	52.2	43.0	51.3			46.1	50.5
6		60.0	47.2				50.2	52.0
7			51.9				54.1	53.5
8			57.0		49.9		57.5	55.1
9					53.5	54.2	60.5	56.6
+10					57.3		63.1	58.3
	T = GEOMETRICAL MEAN OF TANGENTIAL VELOCITIES							
− 2	12.9	14.4	12.4	15.0	16.6	16.2	11.8	15.6
− 1	15.1	17.2	14.4	16.0	18.2	18.0	14.7	17.1
0	17.7	20.6	16.8	17.1	20.0	19.9	18.0	18.8
+ 1	20.8	24.6	19.4	18.2	21.9	22.0	21.9	20.8
2	24.3	29.3	22.6	18.4	24.0	24.3	26.2	22.8
3	28.5	34.9	26.2				30.9	41.6
4	33.4	41.7	30.5				36.0	44.0
5	39.2	49.8	35.3	50.1			41.2	46.3
6		59.4	41.0				46.7	48.9
7			47.6				52.0	51.6
8			55.3		41.9		57.3	54.4
9					45.9	44.2	62.2	57.5
+10					50.4		66.5	60.7
	θ = AVERAGE RADIAL VELOCITY							
− 2	12.5	13.6	14.6	9.0	17.8	10.2	14.3	16.2
− 1	13.3	14.9	15.8	11.4	19.0	14.3	15.4	16.6
0	14.1	16.4	17.1	14.6	20.2	20.1	16.6	17.1
+ 1	15.0	18.0	18.4	18.6	21.6	28.3	17.8	17.5
2	15.8	19.8	20.0	23.8	23.0	39.8	19.2	18.0
3	16.8	21.8	21.5				20.8	22.5
4	17.9	23.9	23.3				22.4	23.9
5	19.0	26.3	25.2	27.0			24.2	25.5
6		28.9	27.2				26.2	27.2
7			29.4				28.4	28.9
8			31.8		34.0		30.8	30.8
9					36.3	37.8	33.4	32.7
+10					38.7		36.3	34.8

and All Types give the results derived from the two solutions, the first representing a continuous and the second a discontinuous variation.

The geometrical means of the space-velocities may be converted into arithmetical means by multiplication with the factor 1.186. The results are given in Table V, the values used being those derived from the first solution, based on the assumption of a continuous variation with absolute magnitude.

TABLE V

ARITHMETICAL MEAN OF SPACE-VELOCITY AND CORRECTED AVERAGE RADIAL VELOCITY

M	$\bar{v}$					θ				
	F	G	K	M	All	F	G	K	M	All
− 2.....	20.9	23.4	26.3	29.5	22.2	11.9	12.9	13.9	16.9	13.6
− 1.....	23.7	26.8	28.9	31.7	26.1	12.6	14.2	15.0	18.0	14.6
0.....	26.9	30.8	31.9	33.9	30.4	13.4	15.6	16.2	19.2	15.8
+ 1.....	30.6	35.5	34.9	36.3	34.9	14.2	17.1	17.5	20.5	16.9
2.....	34.7	40.8	38.4	38.9	39.7	15.0	18.8	19.0	21.8	18.2
3.....	39.5	46.8	42.2		44.7	16.0	20.7	20.4		19.8
4.....	44.8	53.8	46.4		49.7	17.0	22.7	22.1		21.3
5.....	50.8	61.9	51.0		54.7	18.0	25.0	23.9		23.0
6.....		71.2	56.0		59.5		27.5	25.8		24.9
7.....			61.6		64.2			27.9		27.0
8.....			67.6	59.2	68.2			30.2	32.3	29.3
9.....				63.5	71.8				34.5	31.7
+10.....				68.0	74.8				36.8	34.5

The average radial velocities θ are derived from stars north of $-30°$ declination with absolute magnitudes determined at Mount Wilson. Consequently, on account of the effect of stream-motion, the values of θ require a slight systematic correction if they are to be compared with values obtained from stars distributed over the whole sky. Allowance is made for the omission of stars in the area south of $-30°$ by multiplication with a factor 0.95 and the results of θ corrected in this way are also given in Table V.

The mean velocities for the giants and dwarfs separately have been computed for each spectral type and are given in Table VI.

It is of interest to compare the results for θ, the average radial velocity corrected for stream-motion, with those given by Campbell.[1] His values are:

F	G	K	M
14.4	15.9	16.9	17.1 km/sec.

The agreement is excellent if we assume the following mean absolute magnitudes for the stars of Campbell's list:

F, +1; G, 0; K, 0 to +1; M, −2.

These values of the mean absolute magnitudes for the stars observed by Campbell appear quite reasonable, except perhaps in

TABLE VI

SUMMARY OF RESULTS

		F	G	K	M
Giants	No.	152	216	320	114
$M<2.5$	$\overline{M}$	0.1	0.3	0.8	0.1
	$\underline{v}$	21.7	27.0	27.9	29.0
	$\bar{v}$	25.7	32.0	33.1	34.4
	$\underline{T}$	18.0	21.7	18.2	20.0
	θ	14.1	17.4	18.2	21.4
Corrected	θ	13.4	16.5	17.3	20.3
Dwarfs	No.	191	184	148	18
$M>2.5$	$\overline{M}$	3.5	4.8	6.2	10.3
	$\underline{v}$	37.0	51.5	51.3	54.2
	$\bar{v}$	43.9	61.1	60.8	64.3
	$\underline{T}$	33.6	49.3	50.1	44.2
	θ	18.7	25.8	27.0	37.8
Corrected	θ	17.8	24.5	25.6	35.9

the case of the stars of the M type. For these stars it seems probable that the systematic motions differ somewhat from those of other types, and hence our values of θ need a special correction in order to make them comparable with those obtained from stars distributed over the whole sky.

[1] *Lick Observatory Bulletin*, **6**, 125 (No. 196), 1911.

It has been shown by Campbell[1] that, if equal numbers of stars move in all directions, the average radial velocity should be exactly half the average space-velocity. This is strictly true only if stream-motion is neglected. A comparison of the results in Table V shows a remarkably close approach to this ratio among the giant stars. Thus for absolute magnitudes < 2 we find for the ratio of space-velocity to radial velocity the values:

F	G	K	M	All Types
2.02	1.98	1.96	1.77	1.92

In view of the uncertainties introduced by possible differences in the systematic motions not allowed for in the determination of the average radial velocity, these results are rather surprising.

For the dwarf stars the relationship holds much less closely, especially in types F and G. These stars in general have very high space-velocities, and, as will be shown in connection with an investigation of the directions of stellar motions, they exhibit very marked differences from the giants in their systematic motions.

The variation of velocity with spectral type among the giant stars is fully confirmed by these results, the space-velocities showing it quite as well as the radial motions. The latter values, as already noted, are in good agreement with those of Campbell, except possibly for the M-type stars where the difference from those of type K is somewhat larger. Among the dwarf stars, the existence of such a relationship is very doubtful and there even appears to be a tendency toward a reversal of the effect found for the giants, the F and G stars moving more rapidly than the K and M stars. As already stated, the largest space-velocities are found among the F and G types. In view of the peculiar character of the motions of the rapidly moving dwarf stars it seems very doubtful if we can distinguish a relationship dependent upon absolute magnitude without a further great addition to our observational material.

The values of the radial velocities shown in Table I among the very brightest stars of spectral types F and K and the Cepheid variables are quite comparable with those of stars of type B, and suggest that there is little variation with spectral type among

[1] *Stellar Motions*, p. 215, 1914.

such stars. The material, however, is insufficient for a definite conclusion. The space-velocities of these stars cannot well be compared, since they are affected systematically by any accumulation of errors in their parallaxes or proper motions.

It is clear from the results of this investigation that the giant stars as a whole are much more homogeneous in character than the dwarf stars and show the effects of variation of velocity with absolute magnitude and spectral type more clearly. The latter show a much wider dispersion of velocities and are subject to systematic motions differing from those of the giant stars. This is perhaps to be expected if the masses of the giant and dwarf stars differ to any considerable extent.

THE FREQUENCY-LAW OF SPACE-VELOCITIES

It is of interest to compare the observed distribution of these space-velocities with that given by Maxwell's law. This assumes a

TABLE VII

COMPARISON OF FREQUENCY OF SPACE-VELOCITIES WITH THAT GIVEN BY MAXWELL'S LAW

v	F Type $M=2.5$ to 5.7		G Type $M=-1.5$ to $+2.5$		G Type $M=3.5$ to 6.6		K Type $M=-4.0$ to $+2.5$		K Type $M=5.5$ to 9.7		M Type $M=-3.8$ to $+1.5$	
	N_o	N_c	N_o	N_c	N_o	N_c	N_o	N_c	N_o	N_c	N_o	N_c
km/sec.												
0–20....	33	33	55	55	14	14	107	107	7	7	30	30
20–40....	90	90	101	101	39	39	154	154	28	28	57	57
40–60....	41	39	30	20	45	17	58	19	43	27	23	13
60–80....	16	5	17	1	33	2	30	0	24	11	7	1
>80....	47	0	12	0	49	0	16	0	29	2	6	0
Total..	227	167	215	177	180	72	365	280	131	75	123	101
h.....	0.0352		0.0428		0.0351		0.0472		0.0263		0.0417	
Excess in per cent..	36		22		151		30		76		·22	

random distribution in direction and contains a single constant, the modulus h, in the equation

$$F(v)dv=\frac{4h^3}{\sqrt{\pi}}e^{-h^2v^2}v^2\,dv\,.$$

Determining the value of h from the numbers of velocities between 0 and 20 km and 20 and 40 km, we obtain the results shown in Table VII. N_o and N_c denote the numbers of observed and computed velocities within the limits given.

This comparison at once shows a large excess in the number of observed high velocities over that required by Maxwell's law. It is especially marked among the dwarf stars and is probably due to the fact that a strong correlation exists among the three components of space-velocities, a large component along one axis being in general related to large components along the other two axes. Maxwell's function is based upon the assumption that the three components are independent of one another.

A type of frequency-function which represents much better the observed distribution of space-velocities is one based upon the assumption of a normal error-distribution of the logarithms of the velocities.[1] If we transform such a function into one expressing the frequencies of the velocities themselves instead of their logarithms, we obtain the form

$$F(v)dv = \frac{h \operatorname{Mod}}{\sqrt{\pi} v} e^{-h^2 (\log v - A)^2} dv ,$$

the logarithms here having the base 10.

This function contains two constants, h and A, the former of which is related to the probable error in the difference $\log v - A$ by the equation

$$r = \frac{0.6745}{\sqrt{2}\, h} .$$

The quantity A is the algebraic mean of the logarithms of the space-velocities, or,

$$A = \overline{\log v} = \log \underline{v} ,$$

where $\underline{v}$ represents the geometrical mean of the velocities.

[1] Another type of frequency-function, involving only one constant, which represents the distribution nearly as well as the logarithmic one, is

$$F(v)dv = \frac{h^3}{2} v^2 e^{-hv} dv .$$

This gives

$$\bar{v} = \frac{3}{h}, \quad v_p = \frac{2}{h} .$$

The arithmetical mean $\bar{v}$ and the most probable value v_p are related to v, h, and r by the expressions

$$\log \bar{v} = \log v + \frac{1}{4h^2 \operatorname{Mod}} = \log v + 2.530\, r^2,$$

$$\log v_p = \log v - \frac{1}{2h^2 \operatorname{Mod}} = \log v - 5.061\, r^2.$$

Hence

$$v_p < v < \bar{v}.$$

Table VIII shows how this frequency-function represents the observed velocities. The stars have been grouped according to

TABLE VIII

FREQUENCY OF SPACE-VELOCITIES ACCORDING TO LOGARITHMIC FUNCTION

v	F Type $M=2.5$ to 5.7		G Type $M=-1.5$ to $+2.5$		G Type $M=3.5$ to 6.6		K Type $M=-3.5$ to $+2.5$		K Type $M=5.5$ to 9.7		M Type $M=-3.8$ to $+1.5$	
	N_o	N_c	N_o	N_c	N_o	N_c	N_o	N_c	N_o	N_c	N_o	N_c
km												
0– 10.....	3	3.7	16	8.4	3	0.7	25	18.6	0	0.1	6	3.8
10– 20.....	30	31.7	39	49.2	11	9.9	82	88.7	7	3.8	23.5	26.8
20– 30.....	53	44.9	59	54.0	17	20.7	89	89.4	7	13.5	37.0	31.8
30– 40.....	37	38.7	42	38.7	21.5	24.9	65	62.5	21	19.9	20.5	23.1
40– 50.....	29	28.2	17	24.5	22.5	23.4	41	39.4	21	20.5	14	14.6
50– 60.....	12	19.2	13	15.0	23	20.1	17	24.1	22	17.8	9	8.9
60– 70.....	10	12.9	7	9.1	18.5	16.6	24	14.9	11	14.3	5	5.3
70– 80.....	6	8.7	10	5.8	14.5	13.1	6	9.2	13	10.8	2	3.2
80– 90.....	9	5.8	1	3.4	16	10.6	4	6.2	8	8.2	1	1.9
90–100.....	8	3.9	1	2.4	10	8.1	3	3.6	8	5.9	2	1.3
100–110.....	2	2.7	2	1.5	7	6.3	2	2.6	1	4.3	0	0.7
110–120.....	2	1.8	0	0.8	4	5.1	0	1.8	3	3.1	0	0.6
120–130.....	1	1.3	2	0.7	3	4.1	0	1.1	3	2.4	0	0.3
130–140.....	1	1.1	1	0.4	2	3.1	1	0.7	2	1.6	0	0.2
140–150.....	2	0.7	4	0.2	1.5	2.5	1	0.7	1	1.3	1	0.1
150–200.....	9	2.5										
200–250.....	0	2.6										
250–300.....	2	3.4										
300–350.....	2.5	3.4	1	0.9	5.5	10.8	5	1.5	3	3.5	2	0.4
350–400.....	2.5	3.0										
400–450.....	2	2.2										
450–500.....	1	1.7										
>500.....	3	2.9										
Totals....	227	227.0	215	215.0	180	180.0	365	365.0	131	131.0	123	123.0

spectral type and absolute magnitude. In the case of the F-type stars it was found necessary to use the sum of two frequency-functions, since there exists in this type a special group of stars of absolute magnitudes between 3 and 5 with velocities ranging from 160 to nearly 1000 km.

The constants of the frequency-function v and r, together with the arithmetical mean $\bar{v}$ and the most probable velocity v_p, are given in Table IX.

TABLE IX

CONSTANTS OF LOGARITHMIC FREQUENCY-FUNCTION

Type	m	v	r	v_p	$\bar{v}$	No.
		km		km	km	
F.....	+2.5 to +5.7	35.6	0.178	24.6	42.8	207
F.....	+2.5 to +5.7	346.0	0.104	306.0	368.0	20
G.....	−1.5 to +2.5	29.1	0.178	20.1	35.0	215
G.....	+3.5 to +6.6	55.0	0.190	36.2	67.7	180
K.....	−3.5 to +2.5	28.2	0.185	18.8	34.4	365
K.....	+5.5 to +9.7	54.1	0.156	40.8	62.3	131
M.....	−3.8 to +1.5	29.7	0.171	21.1	35.2	123

The marked difference in space-velocity between the giant and dwarf stars is shown clearly in the results of Table IX.

The principal results of this investigation may be summarized as follows:

1. The average space-velocities of the stars of types F, G, K, and M vary with absolute magnitude to a marked degree. The increase of velocity with decreasing brightness is most regular among the giant stars. Among the fainter dwarf stars, if the effect is present it is concealed in large measure by the individual peculiarities of motion.

2. The tangential and radial velocities show results similar to those obtained from the space-velocities.

3. The increase in average space-velocity is about 3 km/sec. for a decrease of one magnitude in brightness. In the radial velocity the increase is 1.2 km/sec.

4. The average space-velocity of the giant stars is very nearly twice the average radial velocity, a result which would follow strictly if equal numbers of stars moved in all directions.

5. The variation of velocity with spectral type is well marked among the giant stars, but is much less certain among the dwarfs.

6. The very brightest stars intrinsically of all the spectral types appear to have nearly equal radial velocities.

7. The greater homogeneity of the giant stars as a class and their pamocrative freedom from large individual motions are

indicated by these results. The dwarf stars show a very wide dispersion in motions.

8. The frequency of the space-velocities cannot be represented adequately by a distribution according to Maxwell's law, there being a large excess of high velocities. A type of frequency-function based upon the assumption of a normal error-distribution in the logarithms of the velocities is found to satisfy the observations in a much better way.

Mount Wilson Observatory
April 1921

THE ELECTRIC FURNACE SPECTRUM OF SCANDIUM[1]

By ARTHUR S. KING

ABSTRACT

Spectrum of scandium in arc and in electric furnace, λ *3015 to 6559* A.—A highly purified sample of scandia, prepared by Sir William Crookes, was placed in a graphite boat in the tube-resistance furnace operated as usual at low pressures. The relative *intensities* of 257 lines on grating spectrograms, some obtained with the furnace at a temperature of 2000, 2250, or 2600° C. and others with a carbon arc containing scandia, are recorded in Table I, together with the *classification* of each according to its behavior in furnace and arc. About 25 lines enhanced in the arc and 150 lines enhanced in the furnace are indicated by E and A respectively. The 29 arc-flame lines are all A lines but are scattered through temperature classes I to III; they cannot be due to oxidation, since none took place in the furnace. On the other hand, since the band lines are practically absent from furnace spectra, they are probably due to the oxide. These results are of great interest in *relation to solar and sun-spot spectra*. The A lines and low temperature furnace lines are absent or very weak in the solar spectrum but are prominent in the sun-spot spectrum.

Zeeman effect for scandium lines in sun-spot spectra is large and apparently uniform. Laboratory observations are lacking at present.

Observations as to chemical properties of scandium.—The scandia fused in the furnace seemed to form a carbide with the graphite boat. The shining black residue turned to a gray-brown powder after exposure to the air, presumably from the reabsorption of oxygen.

Scandium occurs in small amounts in a number of the rare-earth minerals, but its extraction in a fair degree of purity is an exceedingly difficult matter, and, as its separation has not been stimulated by any commercial application, the substance is extremely scarce. The late Sir William Crookes[2] described his examination of a large number of minerals in a search for those containing scandium. Wiikite, found in Finland, proved to contain over 1 per cent of scandium oxide (scandia) and was used by him to furnish pure scandia. The final difficulty in the tedious process of separation was the elimination of the closely related elements yttrium and ytterbium.

The spectrum of scandium is especially interesting on account of the peculiar intensity relations, to be discussed presently, among the scandium lines in the solar spectrum. An examination of the behavior of the lines at various temperatures of the electric

[1] *Contributions from the Mount Wilson Observatory*, No. 211.

[2] *Philosophical Transactions*, A, **209**, 15, 1909.

furnace was therefore desirable, in order to determine the part which temperature may play in bringing about the peculiarities observed.

Through the good offices of Professor Fowler, I have been able recently to obtain a sufficient amount of highly purified scandia to carry out the examination of the furnace spectrum. This scandia was prepared by Sir William Crookes. His former assistant, Mr. J. H. Gardiner, very kindly placed the material at my disposal through Professor Fowler.

In the earlier solar investigations in which the spot spectrum was studied it was noted that certain lines intensified in the spot coincided with lines in the scandium arc, while other strong arc lines were absent in the spot though present in the solar spectrum and prominent in the chromosphere. Fowler[1] explained this phenomenon by producing, besides the regular arc spectrum, the spectrum of the arc in hydrogen, which approaches that of the spark, and the spectrum of the flame of the arc, in which certain lines are given a high intensity. His results showed clearly that the lines prominent in the spot spectrum are those given by the flame of the arc and probably result from a reduced temperature in the spot, whi'e the scandium lines missing from the spot spectrum are enhanced lines, though present often with considerable intensity in the arc. The occurrence of three distinct types, enhanced, arc, and flame lines, in the scandium arc is a feature shown by some other elements, notably titanium, the low-temperature lines of which have been selected by the furnace,[2] while many lines prominent in the arc are much enhanced in the spark.

EXPERIMENTAL METHOD

The tube-resistance furnace was operated as usual, the chamber being pumped out to a few millimeters' pressure. To avoid scattering of the scandia in the tube, the powder was put in a small combustion boat of graphite, which was placed at the middle of the furnace-tube. The image of the space above this boat was focused on the slit of the spectrograph. The scandia fused in the boat,

[1] *Ibid.*, A, **209**, 47, 1909.

[2] *Mt. Wilson Contr.*, No. 76; *Astrophysical Journal*, **39**, 139, 1914.

entering to some extent into the graphite as if a carbide were formed. The fused residue was a shining black when removed from the tube, but after exposure to the air for some time turned to a gray-brown powder, presumably from the reabsorption of oxygen.

The spectrograms were made with a 15-foot concave-grating spectrograph, the second order with a dispersion of 1 mm = 1.86 A being used for the ultra-violet, and the first order for the region from λ 3800 into the red.

EXPLANATION OF THE TABLE

The method followed in the study of the furnace spectrum of scandium was the usual one of selecting three temperature stages, the lowest of which gives a small number of distinctive lines. These lines are of two kinds, some remaining practically unchanged or even losing in strength as the temperature is increased, while others strengthen with rising temperature and frequently show wide reversals. These two kinds of lines are given in Table I as belonging to Class I and Class II respectively.

A higher stage, designated as medium temperature, brings out a large number of lines, placed as a rule in Class III, while a still higher temperature gives the lines of Class IV. Still other lines, which are absent or very faint in the high-temperature furnace, go into Class V. The furnace temperatures required to bring out lines of these various classes differ with different elements. For scandium the three stages selected were 1900° to 2000° C. for the low, 2250° for the medium, and 2600° for the high temperature.

In Table I, the wave-lengths in the first column are those of Exner and Haschek[1] for the arc spectrum. The arc wave-lengths measured by Fowler[2] cover the visible spectrum beginning at λ 3934 and include some lines not measured by Exner and Haschek. The wave-lengths, according to Fowler, of such lines are denoted by a dagger. The enhanced lines of scandium form an important class. I have taken Fowler's selection of these and designated them by "E" after the class-number. Finally, a large proportion

[1] *Spektren der Elemente bei normalem Druck*, Leipzig, 1911.

[2] *Loc. cit.*

TABLE I

TEMPERATURE CLASSIFICATION OF SCANDIUM LINES

λ EXNER AND HASCHEK	ARC INTENSITY	FURNACE INTENSITIES			CLASS
		High Temperature	Medium Temperature	Low Temperature	
3015.50*....	8	5r	3	2	II
3019.48*....	10	5r	3	2	II
3030.87*....	3	2	2	1	II
3040.03*....		1	1		III A
3056.37.....	1	1			IV
3251.43.....	1	1			IV
3255.81.....	6	15r	10r	10	I A
3270.08.....	15	40R	30R	15	II A
3273.79.....	20	50R	50R	20	II A
3333.67.....	1	5	2		III A
3343.42*....	1	4	1		III A
3349.36.....	1	4	1		III A
3351.34.....	1	3			IV A
3352.19.....	2	1			IV
3353.90.....	10	8	8	1	III
3359.84.....	6	6	4		III
3361.48.....	6	6	4		III
3362.12.....	6	6	4		III
3365.01.....	1	5	2		III A
3369.13.....	8	8	6		III
3372.33.....	12	10	10	1	III
3386.02.....	1	2	tr		IV A
3416.80.....	2	4	2		III A
3429.34.....	3	8	5		III A
3429.61.....	3	8	5		III A
3431.50.....	3	8	6		III A
3435.68.....	5	12	10		III A
3439.55.....	1	3	1		III A
3440.31.....	1	5	2		III A
3444.13.....	1	4	1		III A
3448.62.....	1	4	1		III A
3457.56.....	3	8	5		III A
3462.30.....	2	5	3		III A
3469.76.....	1	4	2		III A
3469.84.....	1	3	1		III A
3499.05.....	2	6	4		III A
3535.89.....	6	7	6		III
3558.69*....	7	8	8	3	II
3567.89.....	6	6	4	2	II
3572.73.....	20	20	20	10	II
3576.53.....	8	10	10	4	II
3581.11.....	7	8	10	4	II
3589.81.....	6	6	5	2	II
3590.67.....	6	6	5	2	II
3614.00.....	30	25	25	15	II
3630.93.....	12	12	15	8	II
3635.45*....	1	?	1		III
3642.99.....	25	20	20	7	II
3645.50.....	10	15	8	2	III
3647.05.....	1	4	1		III A

TABLE I—*Continued*

λ Exner and Haschek	Arc Intensity	Furnace Intensities			Class
		High Temperature	Medium Temperature	Low Temperature	
3652.01	7	8	6	2	III
3657.75	tr	3	1		III A
3666.68	2	3	1		III
3895.11	1	2	tr		IV A
3907.69	75	75R	60	15	II
3912.03	100	100R	80	15	II
3915.09	tr	1			IV A
3933.59	20	25r	15	10	II
3952.43	1	2			IV A
3996.79	30	30r	20	20	I
4014.68	5	3	tr		IV E
4020.60	75	75R	60	40	II
4023.36*	2	5?	1		III A
4023.88	100	100R	80	40	II
4031.51	2	5	3		III A
4034.35	2	4	1		III A
4036.98	2	1			IV
4043.97	2	6	3		III A
4046.64	2	7	3		III A
4047.98	25	25r	25	20	I
4050.09	2	5	2		III A
4052.00	1	2	tr		IV A
4054.71	35	40R	40	40	I
4056.72	4	8	4		III A
4067.15	2	6	3		III A
4075.13	2	7	3		III A
4078.70	2	6	3		III A
4082.60	40	30R	40	50	I
4086.15	1	3	1		III A
4086.80	4	5	3		III
4087.28	8	7	5		III
4095.03	1	4	1		III A
4133.10	8	8	7		III
4140.42	10	8	7		III
4152.51	12	10	8		III
4165.39	12	10	10		III
4171.92	1	3	2		III A
4218.43	2	6	2		III A
4219.90	2	7	2		III A
4222.07†	1	3	tr		IV A
4225.76*	2	5?	2		III A
4232.13	2	5	1		IV A
4233.83	3	8	2		III A
4237.96	2	3	tr		IV
4238.21	6	10	5		III
4239.72	2	5	1		IV A
4240.27	1	5	1		IV A
4247.02	75	10	10		III E
4259.86†	1	1			IV
4283.71	2	6	1		IV A
4286.71	1	5	tr		IV A
4294.94	10	2			IV E

TABLE I—*Continued*

λ Exner and Haschek	Arc Intensity	Furnace Intensities			Class
		High Temperature	Medium Temperature	Low Temperature	
4305.89	10	2			IV E
4314.31	100	10	5		III E
4320.98	75	9	4		III E
4325.22	50	8	3		III E
4348.67	tr	2			IV A
4352.28	tr	2			IV A
4354.79	8				V E
4358.85	4	10	3		III A
4359.25	2	4	1		III A
4359.81	1	2	tr		IV A
4365.08	1	3	2		III A
4374.69	60	8	3		III E
4375.32	1	4	1		III A
4381.41	tr	3	1		III A
4384.98*	8	?	?		IV E?
4389.76	2	6	1		IV A
4400.63	50	7	2		III E
4415.78	40	7	2		III E
4431.52	4				V E
4542.74	2	8	3		III A
4544.86*	5	10	4		III A
4557.45	5	7	2		III
4574.20	6	8	3		III
4579.13	1	6	1		IV A
4593.15	3	3	tr		IV
4598.32	1	3	tr		IV A
4598.63	3	5	1		IV
4604.89	(1)	6	1		IV A
4609.69	(0)	6	2		III A
4610.15	(0)	4	1		III A
4670.60*	15	?			IV E
4709.51	5	4	2		III
4721.00	(0)	6	3		III A
4728.98	5	8	8	tr	III
4729.40	30	20	25	3	III
4732.48*	2	5?	?		IV A
4734.30	15	15	20	4	III
4737.83	20	18	20	6	III
4741.23	30	30	30	8	III
4744.03	40	40	40	10	III
4746.31	(1)	3	tr		IV A
4749.15	(1)	2			IV A
4753.34	15	20	60	150	I A
4759.15	(1)	4	1		III A
4763.30	(3)	7	1		IV A
4771.67	(1)	2			IV A
4779.59	20	25	80	200	I A
4791.74	4	20	20	20	I A
4793.10	(0)	tr			IV
4827.48	4	12	3		III A
4833.86	2	10	3		III A
4839.63	10	20	8		III A

TABLE I—*Continued*

λ Exner and Haschek	Arc Intensity	Furnace Intensities			Class
		High Temperature	Medium Temperature	Low Temperature	
4840.65.....	2	6	tr		IV A
4841.04*....	tr	4	2?		III A
4847.88.....	3	10	3		III A
4852.88.....	2	10	3		III A
4859.35†....	(0)	2			IV A
4878.32.....	(2)	4	tr		IV
4880.93.....	(1)	5	tr		IV A
4890.54.....	(1)	3			IV A
4893.20.....	(1)	4	tr		IV A
4906.87.....	(2)	15	3		III A
4909.95.....	3	25	6		III A
4923.03.....	(2)	20	5		III A
4934.30*....	(1)	5?	1		IV A
4935.95.....	(1)	4	1		III A
4941.51.....	2	10	3		III A
4951.46†....	(1)	7	1		IV A
4951.84.....	(1)	6	1		IV A
4954.22.....	5	30	7		III A
4973.84.....	3	12	4		III A
4980.51.....	4	15	4		III A
4983.60*....	2	20	3		III A
4992.14.....	5	15	3		III A
4995.24.....	(1)	7	1		IV A
5018.56.....	(2)	8	2		III A
5020.31.....	(2)	3			IV
5021.70.....	(2)	5			IV A
5031.23.....	10	1			V E
5032.90.....	(1)	2			IV
5064.51.....	10	15	5	tr	III
5069.05.....	2	2	1		III
5070.42.....	40	30	10	1	III
5076.00.....	10	10	4	tr	III
5081.80.....	125	40	40	20	II
5083.93.....	80	30	30	12	II
5085.75.....	40	15	15	6	II
5087.18*....	40	?	15	6	II
5087.32*....	10	?	1		IV?
5090.10.....	8	5	1		IV
5092.63*....	1	3?			IV A?
5096.92.....	30	15	4	1	III
5099.41*....	40	30?	8	2	III
5101.30*....	20	25?	5	1	III
5109.25*....	3	?	1		III
5113.05*....	4	?	1		III
5116.89*....	10	?	2		III
5210.70.....	20	15	1		IV
5211.50.....	(0)	2			IV A
5219.06†....	(0)	1			IV
5219.79.....	10	10	1		IV
5240.00.....	2	1			IV E
5258.51.....	15	15	1		IV
5285.15.....	tr	2			IV A

TABLE I—*Continued*

λ Exner and Haschek	Arc Intensity	Furnace Intensities			Class
		High Temperature	Medium Temperature	Low Temperature	
5285.91.....	10	10	1		IV
5302.15.....	2	60	20	12	II A
5314.91†....	tr	2			IV A
5315.77†....	tr	2			IV A
5318.53.....	1	tr			IV E
5323.26†....	tr	3			IV A
5323.94†....	(0)	tr			IV
5331.95.....	3	10	1		IV A
5334.40.....	tr	1			IV A
5339.56.....	8	12	2		IV
5341.20.....	8	12	2		IV
5343.13.....	10	50	40	30	II A
5349.49.....	50	20	5		III
5349.88.....	15	70	50	40	II A
5350.45.....	4	10	1		IV A
5355.92.....	8	10	2		III
5356.26.....	60	30	6	1	III
5375.52.....	20	20	4		III
5392.28.....	30	30	5	tr	III
5416.32.....	2	2	1		III
5425.76.....	2	3	1		III
5429.65.....	2	3	1		III
5433.45.....	2	2	1		III
5438.50.....	1	2	1		III A
5439.24.....	2	3	1		III
5442.80.....	2	3	1		III
5446.41.....	20	20	4		III
5447.66†....	1	1			IV
5451.55.....	6	12	2		III A
5455.50.....	1	2	1		III A
5465.44.....	tr	1			IV A
5468.63.....	2	2	1		III
5472.42.....	3	3	1		III
5482.20.....	100	40	15	3	III
5484.80.....	80	30	10	2	III
5514.41.....	80	30	10	2	III
5520.71.....	100	40	15	3	III
5527.04.....	10				V E
5541.19.....	3	3			IV
5546.63†....	1	1			IV
5565.10.....	4	10	2		III A
5591.55.....	15	30	3		IV A
5604.35.....	1	1			IV
5624.08†....	1	1			IV
5631.23*....	1	3?			IV A?
5641.18.....	2				V E
5646.58.....	4	5	1		IV
5647.78†....	1	2			IV A
5649.75.....	6	10	1		IV
5658.13.....	15	tr			V E
5658.56.....	2				V E
5661.86†....	tr	1			IV A

TABLE I—*Continued*

λ Exner and Haschek	Arc Intensity	Furnace Intensities			Class
		High Temperature	Medium Temperature	Low Temperature	
5667.38.....	2				V E
5669.26.....	2	2			IV E
5672.05.....	200	200	200	60	II
5684.41.....	8	tr			V E
5687.06.....	150	125	125	40	II
5691.55†....	(0)	tr			IV
5700.35.....	100	100	100	30	II
5708.81.....	15	100	10	3	III A
5711.99.....	100	200	150	20	III A
5717.51.....	15	100	10	3	III A
5721.20†....	tr	tr			IV
5724.30.....	15	100	10	3	III A
5739.53†....	2	4	tr		IV A
5741.56†....	1	5	1		IV A
5894.83†....	(2)	3	tr		IV
5919.21†....	tr	5	tr		IV A
5961.65†....	4	4	tr		IV
5969.37†....	3	3	tr		IV
5988.71.....	20	30	3		IV
6021.92†....	(0)	1			IV
6026.37.....	15	20	2		IV
6146.50†....	(3)	20	2		IV A
6193.94†....	(3)	100	100	40	II A
6198.69.....	(2)	10	1		IV A
6210.85.....	200	500	500	800	I A
6239.64*....	20	500	500	200	II A
6240.00.....	100	200	200	500	I A
6245.83.....	8	tr			V E
6250.15.....	15	20	1		IV
6259.20.....	100	300	300	400	I A
6262.50.....	10	15	1		IV
6273.37†....	(0)	tr			IV
6276.52.....	15	300	200	100	II A
6284.66†....	5	5	tr		IV
6293.30.....	(2)	4	tr		IV
6298.00†....	(0)	tr			IV
6305.94.....	400	500	600	1500	I A
6306.26*....	20	100	100	100	I A
6332.48.....	(1)	2	tr		IV
6345.06.....	5	100	75	50	II A
6379.07.....	40	300	300	300	I A
6396.62.....	2	2	tr		IV
6403.35.....	2	2			IV
6408.67.....	(1)	1			IV
6413.57.....	50	400	400	400	I A
6448.42†....	1	100	50	20	II A
6486.56†*...	(0)	2?			IV A?
6525.84†*....	(3)	1?			IV?
6558.28†*....	15	3?	tr		IV

λ	Remarks
3015–3040.	Weakened at high temperature through incipient absorption and appear readily in absorption when continuous ground is present. λ 3040 is faint in arc, given intensity 1 by Exner and Haschek.
3343.	Probably double.
3559.	Blend Ti. Probable intensity of Ti line subtracted.
3635.	Blend with impurity line at high temperature.
4023.36.	Blend with λ 4023.88 at high temperature.
4226.	Blend with impurity line at high temperature.
4385.	Blend V. Very faint in furnace.
4545.	Blend Ti. Probable intensity of Ti line subtracted.
4671.	Blend V. Faint if present in furnace.
4732.	Disturbed by carbon.
4841.	Blend Ti at medium temperature.
4934.	Slightly affected by Ba blend
4984.	Probably double.
5087–5117.	Disturbed by carbon.
5631.	Disturbed by carbon.
6239.64.	Measured in low-temperature furnace.
6306.26.	Measured in low-temperature furnace.
6487, 6526, 6558.	Disturbed at high temperature by band lines probably due to carbon.

of the scandium lines are found to be relatively strong in the furnace, at least at high temperatures, as compared with the arc. These are indicated by "A" after the class-number. The large number of these lines results in a measure from the choice of standard intensities in the arc and furnace spectra, but is chiefly due to the fact that there is less contrast among the scandium lines in the furnace than in the arc. Consequently faint lines often come out distinctly in the furnace, and if such lines were given the same intensity in arc and furnace very high values would have to be assigned to the stronger lines in the arc. The general meaning of "A" after the class-number then is that the furnace conditions are relatively favorable for the line in question

The arc intensities entered in the second column were estimated from photographs taken with scandia in the carbon arc. Not desiring to use much scandia for a minor part of the investigation, I made but one set of arc spectrograms, consequently there was no variation of the arc conditions. Some of the fainter arc lines measured by Exner and Haschek and by Fowler did not show in my arc spectra, usually on account of disturbance by the prominent

flutings. In such cases the arc values, usually from Fowler's list, are entered in parentheses.

An asterisk adjacent to the wave-length in Table I refers to a note among the "Remarks" at the end of the table. When a trace only of a line is to be seen, the intensity is denoted by "tr."

DISCUSSION

1. *Noteworthy lines of scandium.*—The temperature of approximately 2000°, designated as "low" for scandium, is about the same as has been employed as a medium temperature for several elements previously studied, so that the occurrence of low-temperature lines at wave-lengths as short as λ 3000 presents no anomaly. λ 2980.87 is probably to be classed with λλ 3015.50 and 3019.48, as it appeared at 2000°, but it is too near the end of the plates to show on those taken at higher temperature. λλ 3255.81, 3270.08, 3273.79 are strong and easily reversible lines. They maintain about the same relative strength except at low temperature, when the persistence of the first of the group justifies placing it in Class I. In this region, and throughout the spectrum, many lines remain about as strong at 2300° as at 2600°. Plates taken at 2100° showed lines of this type just appearing. Their absence in most cases at 2000° causes them to be placed in Class III.

Several strong lines occur in the violet, from λ 3908 to λ 4083. These are strong in the arc and reverse in the furnace at high temperature, retaining a considerable intensity at lower temperatures. From λ 4100 to λ 4700, the furnace gives no strong lines, and such lines as appear do not show at low temperature. The strong lines given in this region by the arc are uniformly classed as enhanced lines. Near λ 4750 a prominent group occurs, including the remarkable Class I lines λλ 4753.34 and 4779.59. These are not notably strong at high temperature, though their low density is caused partly by the beginning of reversal. At low temperature, however, they are much the strongest lines of the region, indeed, of the whole visible spectrum, with the exception of the very strong lines in the red.

Through the green and yellow the prominent lines are mostly arc lines which diminish gradually in strength with decreasing furnace temperature.

The region from λ 6146 to λ 6448 contains some very noteworthy lines. The stronger ones are relatively stronger in the furnace than in the arc. Two of them, λλ 6240 and 6306, have faint companions in the arc which have not been previously measured. These weak companions attain high intensities in the furnace and were measured on low-temperature furnace plates as λ 6239.64 and λ 6306.26. The lines in this red group are of three types, Class II and two varieties of Class I lines. some of the latter having about equal strength at all temperatures, and others being very strong at low temperature. A contrast between these two kinds of Class I lines is offered in the close pair λ 6305.94 and λ 6306.26, the former becoming three times as strong at low temperature as at high, while the latter retains the same strength at all the three temperatures. Especially notable is λ 6448.42. This has been measured in the arc only by Fowler. I have found it as a very faint line on a strong arc spectrum. In the furnace it is strong at all temperatures, but shows the behavior usually associated with strong arc lines, falling off rapidly with decreasing temperature. Fowler does not include it among the lines strong in the flame of the arc. It is difficult to account for a line of this type on the basis of dependence on intensity of excitation, as the arc conditions are distinctly unfavorable for it and it is relatively weak also at the low furnace temperatures. There being no reason to ascribe the line to an impurity, it must for the present be regarded as especially sensitive to some feature peculiar to the furnace radiation. λ 6345.06 shows a similar, though less pronounced, behavior in arc and furnace.

In addition to this type we have all gradations of intensity at different furnace temperatures for lines which are faint in the arc. Those of Class I A may be regarded as responding especially to low temperature. The many lines belonging to Class IV A, which, while faint in the arc, are strong at high furnace temperature, appear to respond only to a limited range of excitation.

2. *Enhanced lines.*—In the scandium spectrum we find the furnace able to produce with considerable intensity a number of enhanced lines. Of those given by Fowler in the visible region, and sufficiently strong in the arc to be entered in my list, 10 are in Class V, 8 in Class IV, and 7 in Class III. This means that at 2250°

some enhanced lines are given distinctly by the furnace. In most cases these are much stronger at 2600°, though λ 4247 is an exceptional line showing about the same strength at both temperatures. In every case the relative intensity in the arc as compared with the furnace is much greater than that of the regular arc lines.

In the furnace data given here, and previously, we have a confirmation of the view regarding enhanced lines expressed by Fowler in his paper on the scandium spectrum.[1] He called attention to the fact that in the spectra of titanium, calcium, strontium, and barium, as well as of scandium, the arc gives strong lines which have all the characteristics of enhanced lines. The furnace results show the relation among the enhanced lines of these several elements. Those of titanium[2] are just visible in the high-temperature furnace and are placed in Class V. Some of the scandium enhanced lines appear at medium temperature and go into Class III, while the H and K lines of calcium and the homologous pairs of strontium and barium[3] persist with considerable strength at temperatures as low as 1650°, and on account of their rapid increase at higher temperatures and in the arc are assigned to Class II.

Enhanced lines of different elements thus differ greatly as to the excitation required for their initial appearance. When given at all by the furnace, they agree in their rapid strengthening with increase of temperature and in the arc and finally in the great intensification shown in the spark. The last feature distinguishes them from the large group of high-temperature lines which in laboratory sources reach their maximum intensity in the arc and are unaffected or even weakened in the spark.

3. *Comparison of arc-flame and low-temperature furnace lines.*— By proper manipulation of the arc, a spectrum from the outer vapors can often be obtained which differs materially from that of the vapor in the direct path between the electrodes. The lines relatively strong in this "arc flame" are usually considered as the low-temperature lines, though in the arc the action of temperature

[1] *Op. cit.*, p. 52.

[2] *Mt. Wilson Contr.*, No. 76; *Astrophysical Journal*, 39, 139, 1914.

[3] *Mt. Wilson Contr.*, No. 150; *Astrophysical Journal*, 48, 13, 1918.

may be complicated by the vigorous oxidation taking place in the enveloping vapor.

Fowler[1] lists 29 of the principal arc-flame lines of scandium for the visible region and compares them with the corresponding sun-spot lines. All of these are strong in the furnace, usually at low temperature, though some belong in Class III. These lines, however, are strong also in the regular spectrum of the arc, in which the radiation of flame and core are superposed. In the same region the furnace gives 13 strong furnace lines not in Fowler's list. These are often stronger at low temperature than some of the arc-flame lines. All of them, however, are relatively weak in the arc, being lines with "A" after the class-number. This comparison shows how far the arc flame may be used to select low-temperature lines and also its limitation in this respect, in that it does not bring out with any notable intensity those lines which are faint in the core of the arc and, for some reason at present obscure, are strong in the furnace spectrum.

In the iron spectrum, the degree of extension into the flame of the arc of the various classes of furnace lines was studied by the write [2] and it was then remarked that lines of Class I A appear to be radiated almost entirely by the outer vapors but are inherently very faint. For the study of such lines the furnace conditions are very advantageous.

The fact that the low-temperature furnace in a partial vacuum gives all of the lines prominent in the scandium arc flame and a number besides, is evidence that the oxidation in the arc flame is not influential in producing the lines observed, but that they are due to the reduced temperature in this region of the arc.

4. *Band spectrum.*—The flutings prominent in the scandium arc burning in air were usually entirely absent in the furnace photographs. Only on some long exposures at low temperature was the head of the orange band at λ 6036 visible, and but one of these showed any development of structure. This evidence, as far as it goes, favors the view that the bands are due to the oxide, since, although the material was initially in the oxide form, it

[1] *Op. cit.*, p. 69.

[2] *Mt. Wilson Contr.*, No. 66; *Astrophysical Journal*, **37**, 239, 1913.

appeared to be reduced at once with the formation of a carbide, in which case the oxygen would unite with the carbon of the tube. The prolonged exposures in some cases may have allowed a little oxygen from the residue of air in the chamber to combine sufficiently with the scandium vapor to show the one band observed. If the flutings were due to scandium itself they should have appeared at one of the temperatures used, since in general the vacuum furnace is very effective in producing a banded spectum when this is due to the metal being vaporized.

5. *Comparison with solar and sun-spot spectra.*—The data now available furnish an extension of the observations of Fowler in regard to the scandium lines occurring in solar and spot spectra. In the first place a comparison of the lines in Table I with Rowland's "Table of Solar Spectrum Wave-Lengths" shows that, though only a few are identified by Rowland as belonging to scandium, and these in almost all cases enhanced lines, a large proportion of the scandium wave-lengths agree closely with those of solar lines. A number of these probable coincidences are listed by Lockyer and Baxendall.[1] The strength of scandium lines in the sun bears a rather close relation to the degree of electrical excitation in the laboratory, the strongest, graded 3, 4, or 5 on the Rowland scale, being enhanced lines or those strong in both arc and spark. Those showing no marked response to electrical excitation, but often strong in both furnace and arc, are faint in the sun, usually below intensity 1; while lines relatively strong in the furnace, designated by "A" after the class-number, are uniformly either of intensity 000 or 0000 in the sun, or entirely absent from Rowland's table. In this latter class the pronounced low-temperature lines λλ 4753 and 4780 have no counterparts in the solar spectrum and such powerful furnace lines as λλ 6194, 6259, 6306, 6379, 6413 are either lacking or just at the limit of visibility.

A comparison with the sun-spot spectrum showed a decided prominence of the lines which are strong in the furnace. For this purpose the lines in Table I of intensity 10 or higher in the furnace spectrum were selected. While some of them are indistinct or disturbed by blends, there is little question that these lines are

[1] *Proceedings of the Royal Society*, **74**, 538, 1905.

very generally present in the spot spectrum, and a striking increase appears regularly over the intensities in the solar disk.

The material available was used in two ways. First, a comparison was made with a list of spot lines compiled several years ago from spectrograms of moderate dispersion. In these the effect of the magnetic field in the spot was usually simply to widen the line, so that intensity estimates were more easily made than when the lines are resolved into magnetic doublets. In this list low-temperature scandium lines not visible in the solar spectrum often appeared in the spot with a value of at least oo on the Rowland scale, while λ 6413.57 of this type reaches an intensity of 2 in the spot. Lines with a solar strength of oooo or oo usually strengthen to 2 or higher in the spot.

The second comparison was with the more recent large-scale spectra in which, by means of a nicol prism and compound quarter-wave plate, the intensity of the line and also its response to the magnetic field is recorded across the spot and over a portion of the disk on each side. In these spectrograms the relatively high intensity in the spot of the scandium furnace lines is very pronounced, and many fine cases of magnetic separation occur. Lines faint or invisible in the solar spectrum appear with considerable strength in the spot, even when resolved into two components. Some of these magnetic doublets are very wide, notable among them being the strong furnace lines λλ 5717, 6194, 6240, 6259, 6276, 6306.26, 6345, 6414. As is usual with magnetic resolutions, the average width decreases as we proceed toward shorter wavelengths, though low-temperature lines such as λλ 4753 and 4780 are notable both for strength in the spot and for sensitiveness to the magnetic field. Judging from the spot spectrum, since there are no laboratory observations of the Zeeman effect for scandium, a uniformly strong response to the magnetic field characterizes this spectrum.

CONCLUSION

The varying response of spectrum lines to temperature change, observed in the study at different temperatures of the furnace spectrum of scandium, has concerned itself especially with the conditions of appearance and development of the three main types—

enhanced, arc, and low-temperature lines—which make up the spectrum. The scandium enhanced lines, as regards degree of excitation required, stand between the enhanced lines of titanium and those of the type of H and K of calcium. For the lines appearing in the arc spectrum the regular temperature classification is carried out. The group of arc lines given by the arc flame consists of prominent low-temperature lines, but, since many lines strong in the furnace are relatively weak in all parts of the arc, additional data on this type of line are supplied by the furnace spectrum.

The explanation advanced by Fowler as to the relative strength of the different types of scandium lines in the solar and sun-spot spectra is fully confirmed by their varying response to the furnace excitation. The strong low-temperature lines, faint or lacking in the disk, are distinctly brought out in the spot, and, especially in the red, show high sensitiveness to the magnetic field. A comparison of the Zeeman effect for scandium in the laboratory with that shown in spot spectra and a fuller listing of the scandium lines present in the sun are needed to give this element its due place among those on which solar studies are based.

Mount Wilson Observatory
May 1921

MAGNETIC ROTARY DISPERSION IN TRANSPARENT LIQUIDS

By R. A. CASTLEMAN, Jr., and E. O. HULBURT

ABSTRACT

Magnetic rotary dispersion of isotropic transparent media.—The electron theory as given by H. A. Lorentz is extended, and a formula for the rotation in a range of spectrum in which electrons of only a single type, with critical frequency c/λ_1, need be considered, is developed:

$$\theta = \pi(C_1 h_1) \cdot Hl \cdot \frac{[1+\sigma(\mu^2-1)]^2}{\mu} \cdot \frac{\lambda_1^4 \quad \lambda^2}{(\lambda^2-\lambda_1^2)^2}; \text{ where } C_1 h_1 = \frac{Ne^4}{2\pi^2 c m^2},$$

H is field strength, l is length, μ is refractive index, c is velocity of light, and σ is a constant which Lorentz puts equal to about $\frac{1}{3}$ and Voigt puts equal to zero. To test this theory, substances were chosen whose dispersion was known to conform to the theory of Lorentz, and the *magnetic rotations for carbon disulphide, α-monobromnaphthalene, benzene, nitrobenzene and ethyl iodide* for six wave-lengths from 436 to 620 $\mu\mu$ were determined with a cell 2 cm long in a field of 6480 gauss. The angles could be measured to $\frac{1}{10}°$ and were found to vary from 4° to 28°, increasing rapidly for each liquid with decreasing wave-length. Theoretical curves were computed, taking the values of C_1, λ_1 and μ from measurements by others. Below 590 $\mu\mu$ the experimental curves lie below the theoretical curves, the divergence increasing as the wave-length diminishes until the difference at 423 $\mu\mu$ is from 4 to 20 per cent. It is suggested that this discrepancy is due to the absorption of the violet end of the spectrum which was neglected in the theory. The results do not decide between the values 0 and $\frac{1}{3}$ for σ. The *values of e/m for the active electrons* may be computed from h_1 and vary from 0.5 to 1.78×10^7 e.m.u. according to the liquid and to the value of σ assumed.

1. *Introductory.*—In 1845 Faraday discovered that isotropic substances when placed in a strong longitudinal magnetic field rotate the plane of polarization of plane-polarized light. The obvious explanation of this, confirmed later by Brace, was the same as that offered by Fresnel for the rotation observed in certain crystals, viz., to consider the plane-polarized beam to be composed of two circularly polarized components which travel through the medium with different velocities, one greater and the other less than the velocity of the beam in the medium when unmagnetized. The variation of the angle of magnetic rotation with the wave-length of the light has been considered theoretically by several writers, and the theoretical relations have been applied to the experimental data available. Such data appear, however, to be rather meager, and it seemed desirable to pursue the subject afresh both theoretically and experimentally.

We do not presume to attempt a historical summary of the researches on the many aspects of this subject. For a summary of the earlier work we make reference to an article by P. Joubin.[1] Among the more important theoretical formulae for the magnetic-rotation angle in terms of the wave-length, magnetic field, etc. were those obtained by Joubin, Voigt,[2] and Drude.[3] For a summary of the experimental measurements of the magnetic-rotation angles we turn to the Landoldt-Börnstein *Physical Tables*. There the data have been tabulated in many cases as the *Verdet Constant*, which is defined to be the angle of rotation of plane-polarized light of specified wave-length produced by a medium 1 cm in length when magnetized by a longitudinal magnetic field of strength 1 gauss. These measurements were applied by Joubin and Drude to a dispersion theory of isotropic media, although for such a purpose the experimental data were hardly sufficiently numerous. With the exception of a few transparent liquids and solids the Verdet Constant was found either for unresolved light or for a single wave-length of monochromatic light. In the cases of those substances whose Verdet constant has been determined for a number of wave-lengths throughout the spectrum, one could introduce the values into a suitable dispersion formula to test a dispersion theory. Unfortunately, however, the refractive indices of most of these substances do not conform to any of the simpler dispersion formulae whose constants have a physical interpretation, and so these data are, from this standpoint, uninteresting.

In the present work transparent liquids were chosen whose dispersion conformed approximately to the electronic dispersion theory of H. A. Lorentz.[4] The angles of magnetic rotation of plane-polarized light for a series of wave-lengths of light in the visible spectrum were measured. A formula of Lorentz giving the relation between the refractive index and the strength of the magnetic field was modified to express the magnetic-rotation angle in terms of the wave-length, the field strength, and other quantities. The formula was found to agree approximately with experiment in

[1] *Thèses*, Faculté des Sciences, Paris, 1888.

[2] *Magneto- und Elektrooptik*, 1908.

[3] *Lehrbuch der Optik*, 1906.

[4] *Theory of Electrons*, 1909.

those regions of the spectrum wherein the assumptions upon which it was based were valid.

2. *Theoretical.*—Suppose plane-polarized light of wave-length λ *in vacuo* traverses a length l of a medium of refractive index μ for the wave-length in question with a velocity v. If the medium is placed in a magnetic field of strength H, such that the lines of magnetic force are parallel to the direction of propagation of the light, the medium becomes doubly refracting. The two circularly polarized components, which compose the plane-polarized beam, now pass through the medium with velocities v_1 and v_2, and the medium has the corresponding refractive indices μ_1 and μ_2, respectively.

Eddy, Morley, and Miller,[1] followed by Mills,[2] have shown by an interferometer method that

$$\frac{v_1+v_2}{2}=v, \tag{1}$$

or

$$\frac{1}{\mu_1}+\frac{1}{\mu_2}=\frac{2}{\mu}. \tag{2}$$

This was determined by measurements on carbon disulphide. The accuracy of the work was none too great, because the experiment was a difficult one; but, within the error of observation, the foregoing relation was true. It may be noticed that from general considerations one would not expect (1) to be exactly true, and further that one would expect the difference between (1) and the exact truth to be small. However, we now assume that (1) is true for all the substances and throughout the wave-length range used in this investigation.

Let θ be the observed angle in radians of the rotation of the plane of polarization produced by the magnetized medium. It is easily shown[3] that

$$\mu_2-\mu_1=\frac{\lambda\theta}{\pi l}. \tag{3}$$

where λ is the wave-length of the light *in vacuo*.

[1] *Physical Review*, 7, 283, 1898.

[2] *Ibid.*, 18, 65, 1904.

[3] Drude, *loc. cit.*, p. 396.

Solving (2) and (3) for μ_1 and μ_2, and considering $\frac{\lambda\theta}{\pi l}$ small compared with μ, we obtain

$$\left.\begin{aligned}\mu_1 &= \mu - \frac{\lambda\theta}{2\pi l},\\ \mu_2 &= \mu + \frac{\lambda\theta}{2\pi l}.\end{aligned}\right\} \quad (4)$$

Let us turn to a consideration of the dispersion theory in this connection. We restrict the discussion to isotropic, transparent media in which the temperature remains constant. We use the electron theory of dispersion as given by H. A. Lorentz (*loc. cit.*). Let ξ and E_x be the X components of the displacement of the electron from its equilibrium position and the electric force, respectively. η, ζ, E_y and E_z are the Y and Z components of these quantities; they are all expressed in c.g.s. electromagnetic units. The components of the "restoring force" with which the medium acts upon the electron are $f\xi$, $f\eta$, and $f\zeta$. The charge on the electron in c.g.s. electromagnetic units is e, its mass is m. N is the number of such electrons per unit volume. σ is a constant which Lorentz has shown to be approximately one-third for isotropic media. The external magnetic field is denoted by H in c.g.s. electromagnetic units. We shall suppose H to have the direction of the axis of Z, which is also the direction of the propagation of the light. The magnetic permeability of the medium is taken as unity.

We find for the equations of motion of the dispersion electron of a single type

$$\left.\begin{aligned} m\frac{d^2\xi}{dt^2} &= e(E_x + 4\pi c^2\sigma N e\xi) - f\xi + eH\frac{d\eta}{dt},\\ m\frac{d^2\eta}{dt^2} &= e(E_y + 4\pi c^2\sigma N e\eta) - f\eta - eH\frac{d\xi}{dt},\\ m\frac{d^2\zeta}{dt^2} &= e(E_z + 4\pi c^2\sigma N e\zeta) - f\zeta.\end{aligned}\right\} \quad (5)$$

Let ϵ be the base of natural logarithms, and let all dependent variables of (5) contain the time only in the factor $\epsilon^{i\frac{2\pi c}{\lambda}t}$ where $\frac{c}{\lambda}$

is the frequency, λ the wave-length of the vibration *in vacuo*, and c the velocity of light *in vacuo*. The solution of (5) gives the refractive index μ as determined by the relation

$$\frac{1}{\sigma+\frac{1}{\mu^2-1}}=\frac{C_s}{\frac{1}{\lambda_s^2}-\frac{1}{\lambda^2}\pm\frac{H}{\lambda}h_s}, \tag{6}$$

where

$$C_s=\frac{N_s e_s^2}{\pi m_s},$$

$$h_s=\frac{e_s}{2\pi c m_s}.$$

The subscript s is used to denote the sth type of electron. $\frac{c}{\lambda_s}$ is the frequency of the natural undamped vibration of this electron. When the plus sign in equation (6) is used, μ is the μ_2 of (4), and when the minus sign is used μ is the μ_1 of (4).

Equation (6) describes μ in terms of the constants of a single type of dispersion electron. There may be other types of dispersion electrons in the medium with constants peculiar to the type, so that in the more general case the right-hand member of (6) becomes a summation of similar terms, one term for each type. For this case the complete dispersion formula is

$$\frac{1}{\sigma+\frac{1}{\mu^2-1}}=\sum\frac{C_s}{\frac{1}{\lambda_s^2}-\frac{1}{\lambda^2}\pm\frac{H}{\lambda}h_s}. \tag{7}$$

We assume we are dealing with a region of the spectrum in which the change of the refractive index with wave-length is determined by the electrons of a single type, so that in the summation of (7) all the terms except one may be replaced by a quantity q_1 which is independent of λ and H. Then (7) becomes

$$\frac{1}{\sigma+\frac{1}{\mu^2-1}}=q_1+\frac{C_1}{\frac{1}{\lambda_1^2}-\frac{1}{\lambda^2}\pm\frac{H}{\lambda}h_1}, \tag{8}$$

where

$$\left.\begin{aligned} C_1 &= \frac{Ne^2}{\pi m}, \\ h_1 &= \frac{e}{2\pi cm}. \end{aligned}\right\} \tag{9}$$

A special case occurs when H is zero. For this (8) becomes equivalent to the well-known dispersion formula of Lorentz:

$$\frac{1}{\sigma+\dfrac{1}{\mu^2-1}} = q_1 + \frac{C_1}{\dfrac{1}{\lambda_1^2}-\dfrac{1}{\lambda^2}}. \tag{10}$$

Introducing (4) into (8) gives:

$$\frac{1}{\sigma+\dfrac{1}{\left(\mu \pm \dfrac{\lambda\theta}{2\pi l}\right)^2-1}} = q_1 + \frac{C_1}{\dfrac{1}{\lambda_1^2}-\dfrac{1}{\lambda^2} \pm \dfrac{H}{\lambda}h_1}. \tag{11}$$

It was expedient to transform this relation to one more amenable to arithmetical computation. This was readily done because $\dfrac{\lambda\theta}{2\pi l}$ and $\dfrac{H}{\lambda}h_1$ were smaller than the other quantities appearing with them in the denominators by a different order of magnitude.

Equation (11) becomes to a close approximation

$$\theta = \pi C_1 h_1 H l \frac{[\sigma(\mu^2-1)+1]^2}{\mu} \frac{\lambda_1^4\lambda^2}{(\lambda^2-\lambda_1^2)^2}. \tag{12}$$

θ is in radians.

We notice that if we use either the two plus signs of (11) or the two minus signs, we arrive at the same equation for (12). This shows that equation (8) is in close agreement with (4). We notice also that, other quantities remaining constant, θ is proportional to l and H in turn. This agrees with the experimental measurements of Rodger and Watson[1] and Dubois.[2]

[1] *Phil. Trans. Roy. Soc.*, A **186**, 621, 1896. This paper contains further references.

[2] *Wied. Ann.*, **35**, 137, 1888.

If σ is given the value $\frac{1}{3}$, equation (12) becomes

$$\theta = \pi C_1 h_1 H l \frac{(\mu^2+2)^2}{9\mu} \frac{\lambda_1^4 \lambda^2}{(\lambda^2-\lambda_1^2)^2}. \tag{13}$$

When σ is placed equal to 0, equation (12) becomes

$$\theta = \frac{\pi C_1 h_1 H l}{\mu} \frac{\lambda_1^4 \lambda^2}{(\lambda^2-\lambda_1^2)^2}. \tag{14}$$

Formula (14) agrees with one given by Voigt[1] when his quantities are expressed in c.g.s. electromagnetic units.

To compare the experimental measurements with the theory the following procedure was used. Values of the refractive index of the liquid under investigation for wave-lengths in the visible spectrum were taken from data published by others. Three values of μ and the corresponding three values of λ were substituted in equation (10), and the three constants q_1, C_1, and λ_1 were computed. Using these three constants, a fourth value of λ was substituted in (10) and the value of μ calculated. If this value of μ agreed approximately with the observed value, the substance was considered to conform to the Lorentz dispersion equation (10) for the region of the spectrum in question. The values of θ for a number of wave-lengths in the visible spectrum were measured for a known length l of the liquid subjected to a known magnetic field H. The constant h_1 was then determined by substituting in equation (13) the values of H, l, C_1, λ_1, and the values of λ, θ, and μ for a specified wave-length. θ was then computed by means of (13) for the other wave-lengths, and the computed value was compared with the observed value.

3. *Experimental arrangements.*—The arrangement of the apparatus is shown in plan in Figure 1. A gas-filled lamp with a spiral tungsten filament and a mercury-vapor lamp served as sources of light. The mercury-vapor lamp was used for observations at wave-lengths 435.9 $\mu\mu$ and 546.1 $\mu\mu$; the tungsten lamp was used for observations from the green to the red end of the spectrum.

[1] *Loc. cit.*, p. 130.

The source of light, shown by A, Figure 1, was focused on the slit s_1 of the spectrograph by a lens l_1, 3 cm in diameter and of focal length 22 cm.

The spectrograph consisted of the Littrow mounting of a plane grating. The grating had a ruled area 6 cm by 7.5 cm and was ruled 15,000 lines to the inch. The cone of light from slit s_1 was reflected by a right-angle glass prism through the large lens l_2, 10 cm in diameter and with a focal length of 75 cm. The spectrum was brought to a focus at slit s_2. The grating was mounted on a turntable which could be rotated from the outside of the case containing the spectrograph, so that various wave-lengths of light could be made to pass through the second slit. The grating possessed a bright first order, and this first-order spectrum was

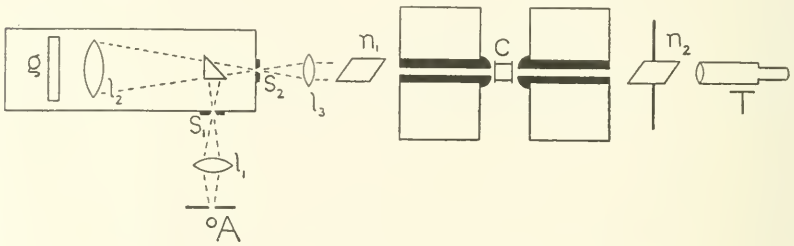


FIG. 1

used throughout the present work. The dispersion was such that with slit s_2 0.25 mm wide a beam of light containing a wave-length range of 5 A, or 0.5 $\mu\mu$, passed through. Both slit s_1 and slit s_2 were always 0.25 mm in width.

The monochromatic beam of light emerging from slit s_2, after being rendered parallel by a lens l_3, 2.5 cm in diameter and of focal length 12.5 cm, passed through the polarizing nicol n_1 and through the pierced pole pieces of a Ruhmkorff magnet between which the cell C containing the liquid under investigation was placed. The light then traversed the analyzing nicol prism n_2 and finally entered the telescope T. The lenses l_1, l_2, and l_3 were achromatic doublets.

The cell which contained the liquid was made of glass. A short length, about 2 cm, of glass tubing of internal diameter 1 cm, to which had been sealed a small side tube, was ground until the

ends were plane-parallel to within 0.003 cm. Glass plates with optically plane surfaces were cemented to this. Rubber cement, a mixture of lead oxide and glycerine, and LePage's liquid glue, were found useful as cements in various cases. The cell was filled through the side tube. The length of the column of liquid was found by subtracting the thickness of the end plates from the external length of the cell. The liquids used were obtained from the Chemical Laboratory and were of a high degree of purity.

The pole pieces of the Ruhmkorff magnet were elliptical in shape to give a uniform magnetic field; they were adjusted to be 2.5 cm apart. To calibrate the magnet, the angle of rotation θ for sodium light was observed for a known length of carbon disulphide for a current of 26.0 amperes through the magnet. From θ and from the value of the Verdet constant of carbon disulphide for sodium light, which has been carefully determined by Rodger and Watson (*loc. cit.*), the average strength of the magnetic field between the pole pieces was calculated, and was found to be 6480 gauss. This field strength was used for all the rotation measurements of this paper. It was found by tests that the rotation angle θ had the same absolute value for the magnetic field direct and reversed. This indicated that hysteresis effects in the magnet were negligible.

The mounting of the analyzing nicol carried a circular scale which measured the rotation angles to one-tenth of a degree of arc. It was found that the analyzer could be set for extinction for all the wave-lengths with a precision of two-tenths of a degree. The values of the rotation angle were in all cases the means of at least four measurements, two taken with the field direct and two with the field reversed. It was considered that the mean angle was correct to one-tenth of a degree of arc.

4. *Errors and corrections.*—No correction was made for the error due to scattered light. There were two ways in which scattered light might introduce systematic error into the rotation measurement, the first arising from light scattered by the grating, and the second from multiple reflections by the surfaces at the ends of the cell which held the liquid. To determine the effect of the light scattered by the grating, the beam issuing from slit s_2 was examined with a transmission grating. When the tungsten lamp

was used as the source of light, it was found that the beam contained light of foreign wave-lengths of rather feeble intensity; in the case of the mercury lamp this foreign light appeared still weaker. Upon looking into the telescope and setting the analyzer for extinction it was found that the image of slit s_1 did not fade out against an absolutely black background. Very faint light was seen in the field, due no doubt to the light scattered by the grating and to imperfections throughout the optical system. The settings for extinction could, however, be made with precision, and it was deemed that the extraneous light introduced no appreciable systematic errors. Any error due to multiple reflections from the surfaces of the ends of the glass cell was avoided by rotating the cell slightly until these surfaces were not perpendicular to the beam of light. The error which this caused in the determination of l was negligible.

TABLE I

λ	θ
436 $\mu\mu$	1.7°
503	1.3
546	0.9
579	0.85
589	0.85
620	0.8

It had been feared that errors due to temperature would be troublesome, but it was found that these fears were needless. To carry out a complete series of measurements of the rotation angle for five wave-lengths in the visible spectrum required about an hour. During this time the magnet heated up, and the temperature of the liquid in the cell increased. The increase was never more than 3° C. In the case of carbon disulphide the temperature coefficient of the Verdet constant for sodium light has been determined.[1] A three-degree change in temperature changed the Verdet constant by about 0.5 per cent. In the present case it was considered that errors due to temperature changes were for the most part less than 0.5 per cent, and that it was unnecessary to arrange a more accurate control of the temperature of the liquid in the cell.

[1] Rodger and Watson, *loc. cit.*

The rotation angle θ due to the liquid alone was obtained from the observed rotation angle produced by the liquid in the cell by subtracting from this observed angle the angle of rotation produced by the empty cell for the wave-length in question. Table I shows θ for the two glass plates on the ends of the cell. The thickness of the two plates together was 0.315 cm, the field strength was 6480 gauss. The magnetic-rotation angles plotted in the figure have in all cases been corrected for the effect of the glass ends of the cell.

5. *Carbon disulphide.*—The data for this substance and the results of the calculations are given in Table II and Figure 2. We shall discuss these in some detail, and shall avoid a repetition of the discussion for the other substances. The observed values of θ, shown by circles in Figure 2, have been plotted as ordinates against wave-lengths as abscissae; a smooth line, curve 1, has been drawn through them. The strength of the magnetic field, the length of the layer of liquid, and the temperature at the beginning and the end of the experiment are shown in the first two lines of Table II.

Verdet[1] has recorded relative values of θ for carbon disulphide for a number of wave-lengths in the visible spectrum. The magnetic field used was not mentioned. For the sake of comparison the values given by Verdet have been reduced to agree with curve 1 for λ 589.3 $\mu\mu$ and are shown by crosses in Figure 2. Joubin (*loc. cit.*) also carried out measurements on carbon disulphide. Neither the magnetic field, nor the length of the liquid, nor the temperature were recorded. By a coincidence his value for θ at λ 589.3 $\mu\mu$ was the same as that of curve 1, namely 10°.3. His values have been plotted as dots in Figure 2. We think that the measurements of curve 1 were correct, for they were repeated with precision a few weeks later.

In order to introduce these experimental results into the dispersion formula (10) we assume that the absorption of carbon disulphide is inappreciable for the visible wave-lengths in question. Such an assumption is manifestly not accurate, because this substance absorbs the blue end of the spectrum to a certain extent.

[1] Verdet, *Oeuvres complètes.*

We take the values of the refractive index found at 20°.0 C. by Flatow. These and the corresponding wave-lengths are shown in the third and fourth lines of Table II. Substituting these values into formula (10), the values of the constants C_1, q_1, λ_1 were computed and are tabulated in the fifth line of Table II. The agreement between (10) and observations was tested by using the foregoing values of the constants and computing μ for λ 394 $\mu\mu$ to be 1.7043. The observed value was 1.70226, and

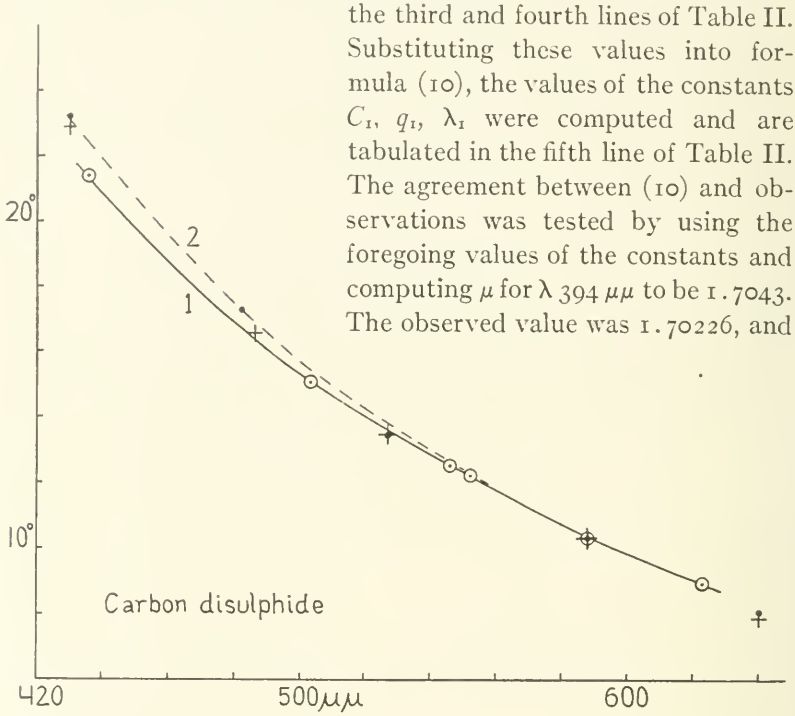


FIG. 2

TABLE II

CARBON DISULPHIDE

H = 6480 gauss			Temp. 21°.2 to 22°.0 C.	l = 2.272 cm
λ 441.6 $\mu\mu$	508.6	589.3		
μ 1.67180	1.64586	1.62806		at 20°.0 C.
Observed by Flatow, *Ann. d. Phys.*, 12, 85, 1903.				
C_1 = 10.381 × 10^8		q_1 = 0.57272		λ_1 = 204.2 $\mu\mu$
λ 394 $\mu\mu$		observed μ = 1.70226		
		calculated μ = 1.7043		
h_1 = 3.95 × 10^{-5} for λ 589.3 $\mu\mu$				

the agreement was considered sufficiently close. These numbers are given in lines 7 and 8 of Table II. The dispersion of carbon disulphide and α-monobromnapthalene has been more fully discussed in a former paper.[1]

The constant h_1 was then determined by substituting in equation (12) the values of H, l, C_1, and λ_1 given in Table II, and the values of λ, θ, and μ for the wave-length 589.3 $\mu\mu$. This gave 3.95×10^{-5} for h_1, as shown in the last line of Table II, when all the quantities were expressed in c.g.s. and c.g.s. electromagnetic units.

The constants of (13) were now completely known, and (13) was then used to compute the values of θ for the range of the spectrum under investigation. The computed curve is shown by the dotted line, curve 2, of Figure 2. It is seen that the agreement between the observed and calculated values of θ was fairly close for the longer wave-lengths, but that for the shorter wave-lengths the theoretical value was greater than the observed value, the difference between the two values increasing as the wave-length decreases. This difference between theory and experiment may be attributed, in part at least, to the neglect of the effect of absorption in the theory. The discrepancy was in the right direction to be attributed to this effect, for the introduction into the theoretical formula of terms denoting absorption will produce a decrease in the computed values of θ for the shorter wave-lengths.

In his treatise on optics Drude[2] has derived two theoretical expressions for the magnetic rotatory dispersion of isotropic media, one based on the "molecular stream" hypothesis, and the other on the "Hall effect" hypothesis. When written in a form to show the connection between θ and λ, neglecting absorption, the two formulae were, respectively,

$$\theta = \frac{\mu}{\lambda^2}\left(a_1 + \frac{a_2\lambda^2}{(\lambda^2 - \lambda_1^2)}\right) \tag{15}$$

and

$$\theta = \frac{1}{\mu\lambda^2}\left\{a_3 + \frac{a_4\lambda^4}{(\lambda^2 - \lambda_1^2)^2}\right\}. \tag{16}$$

[1] *Astrophysical Journal*, **46**, 1, 1917.

[2] *Loc. cit.*, p. 406.

a_1, a_2, a_3, and a_4 were quantities which involved the masses, the charges, and the numbers of the "bound" and "free" electrons, the strength of the magnetic field, the length of the medium, etc. The refractive index wave-length relation in this connection was

$$\mu^2 = a_5 + \frac{a_6}{\lambda^2 - \lambda_1^2}. \qquad (17)$$

Drude applied these equations to Verdet's magnetic-rotation measurements on carbon disulphide and creosote in the following manner. Using the value of λ_1 obtained from (17) and two known values each of θ and λ, the remaining two constants of (15) or (16) were determined. The θ-λ curve from either formula, which thus traversed two of the observed points, was found to pass closely to the remaining observed points. We do not believe, however, that the agreement found in this way between theory and experiment possesses great significance. One would not expect a theory which neglected absorption to portray the observations with great exactness.

Joubin (*loc. cit.*) has also derived a formula for the dispersion of magnetic rotation of somewhat the same type as (15). He applied this to the observations of rotations of carbon disulphide and creosote, which were measured for the purpose, in much the same manner as done by Drude.

6. *α-monobromnaphthalene.*—This substance was investigated in a manner similar to that described in the case of carbon disulphide. Table III shows a portion of the data and the results of the calculations. This table has been compiled exactly as was Table II for carbon disulphide, and therefore requires no further explanation. The observed values of θ have been plotted as circles in Figure 3, and a smooth line, curve 1, has been drawn through them. The computed values of θ from equation (13), using the constants of Table III, are shown by the dotted line, curve 2, of Figure 3. The differences between the observed and theoretical values are similar to those noted for carbon disulphide.

7. *Benzene.*—The values of θ for this substance were determined throughout the visible spectrum. These are shown by circles in Figure 4, through which a smooth line, curve 1, has been

passed. The Verdet constant of benzene was found by Jahn[1] to be 0.0297 minutes of arc for sodium light. From the data of Figure 4 and Table IV we obtain 0.0291 minutes of arc for the same wave-length. Jahn's value is not far different from this.

The computed values of θ from equation (13) are shown by the dotted line, curve 2, of Figure 4. It is seen that the differences between the observed and theoretical values are of the same character as those of the previous cases.

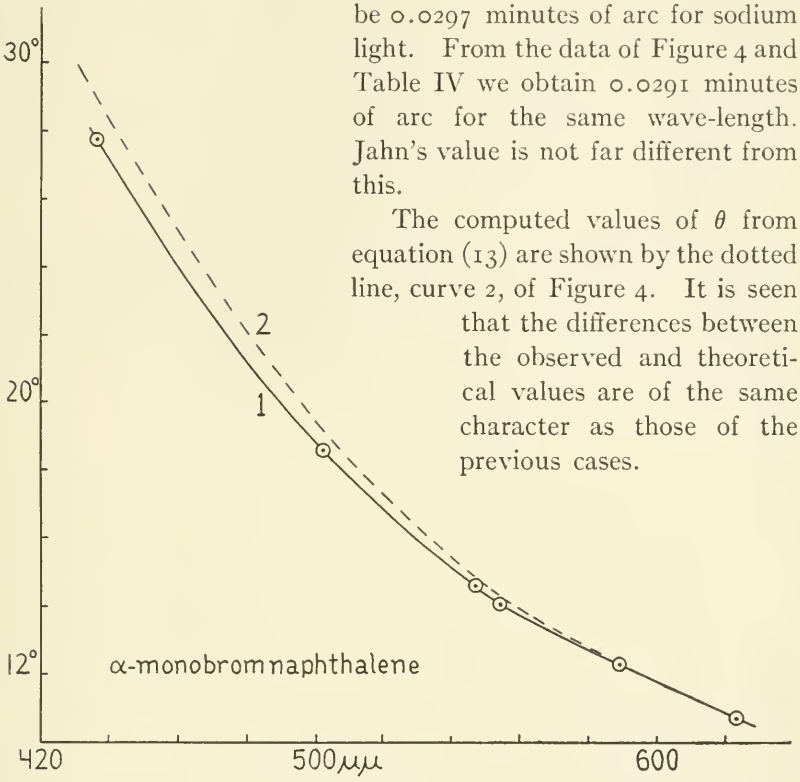


FIG. 3

TABLE III

α-MONOBROMNAPHTHALENE

$H = 6480$ gauss			$l = 2.272$ cm	
Temp. 23°.5 to 20°.7 C.				
λ 434 μμ	486	589		
μ 1.70433	1.68245	1.65876	at 19°.4 C.	
Observed by Brühl, *Ber. Chem. Ges.*, **22**, 388, 1897.				
$C_1 = 7.398 \times 10^8$	$q_1 = 0.70889$		$\lambda_1 = 215.6$ μμ	
λ 656 μμ	observed $\mu = 1.64995$			
	calculated $\mu = 1.6500$			
$h_1 = 5.02 \times 10^{-5}$ for λ 589.3 μμ				

[1] *Wied. Ann.*, **43**, 280, 1891.

8. *Nitrobenzene.*—The results of the work on this substance are shown in Table V and Figure 5. The observed values of θ were plotted as circles in Figure 5, and a smooth line, curve 1, has been drawn through them. The computed values of θ from equation (13) are shown by the dotted line, curve 2.

Discrepancies of the same character exist between the observed and theoretical values of θ as were noticed in the preceding cases, but perhaps greater in magnitude.

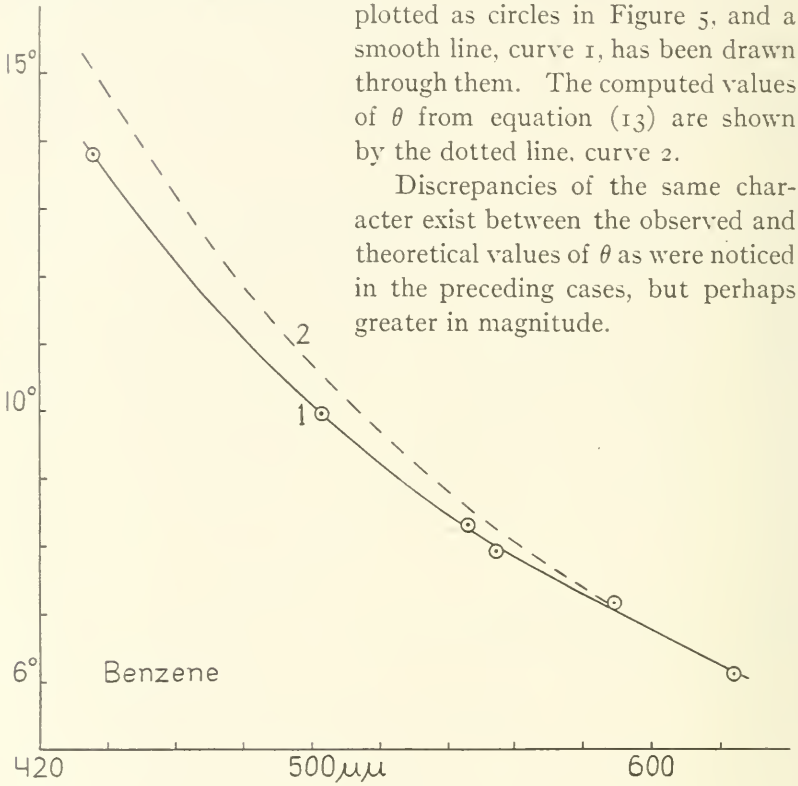


FIG. 4

TABLE IV

BENZENE

$H = 6480$ gauss			$l = 2.280$ cm
Temp. 22°.9 to 24°.6 C.			
λ 434 μμ	486	589	
μ 1.52380	1.51323	1.50111	at 20°.0 C.
Landoldt-Börnstein Tables.			
$C_1 = 11.643 \times 10^8$		$q_1 = 0.49898$	$\lambda_1 = 173.8$ μμ
λ 656 μμ	observed $\mu = 1.49646$		
	calculated $\mu = 1.4964$		
$h_1 = 5.34 \times 10^{-5}$ for λ 589.3 μμ			

9. *Ethyl iodide.*—The circles of Figure 6 show the observations on this substance; a smooth line, curve 1, has been drawn through the observed points. Other data are given in Table VI. Perkin[1] had determined the Verdet constant of ethyl iodide to be 0.0296 minutes of arc for sodium light. From the present data we find 0.0300 for this wavelength. The two values are not greatly at variance. The computed values of θ from equation (12) are shown by the dotted line, curve 2,

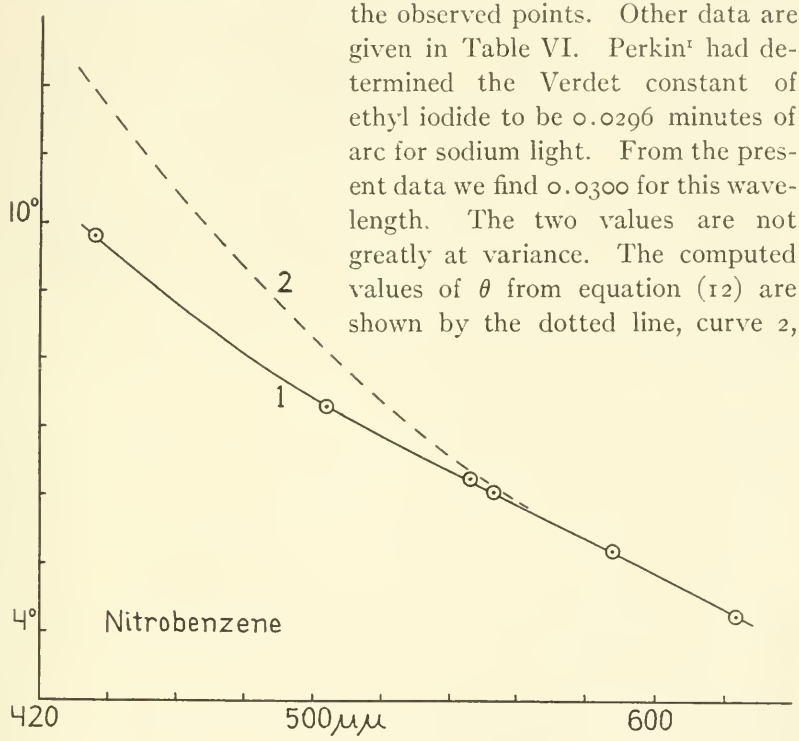


FIG. 5

TABLE V

NITROBENZENE

$H=6480$ gauss			$l=2.272$ cm
Temp. 21°.4 to 22°.6 C.			
λ 486.2 μμ	589.3	656.3	
μ 1.57165	1.55319	1.54641	at 20°.0 C.
Landoldt Börnstein Tables.			
$C_1=6.066\times10^8$	$q_1=0.62924$		$\lambda_1=217.13$ μμ
λ 434.1 μμ	observed $\mu=1.5895$		
	calculated $\mu=1.5888$		
$h_1=2.56\times10^{-5}$ for λ 589.3 μμ			

[1] Smithsonian Physical Tables, 1920.

Figure 6. It is seen that the discrepancies between the observed and theoretical values are similar to those of the preceding cases.

10. *Discussion of results.*—It has been demonstrated that the formula (13), which has been developed from the electron theory of Lorentz, served to express with a certain exactitude the dispersion of the magnetic rotation of certain liquids throughout the visible spectrum. For the longer

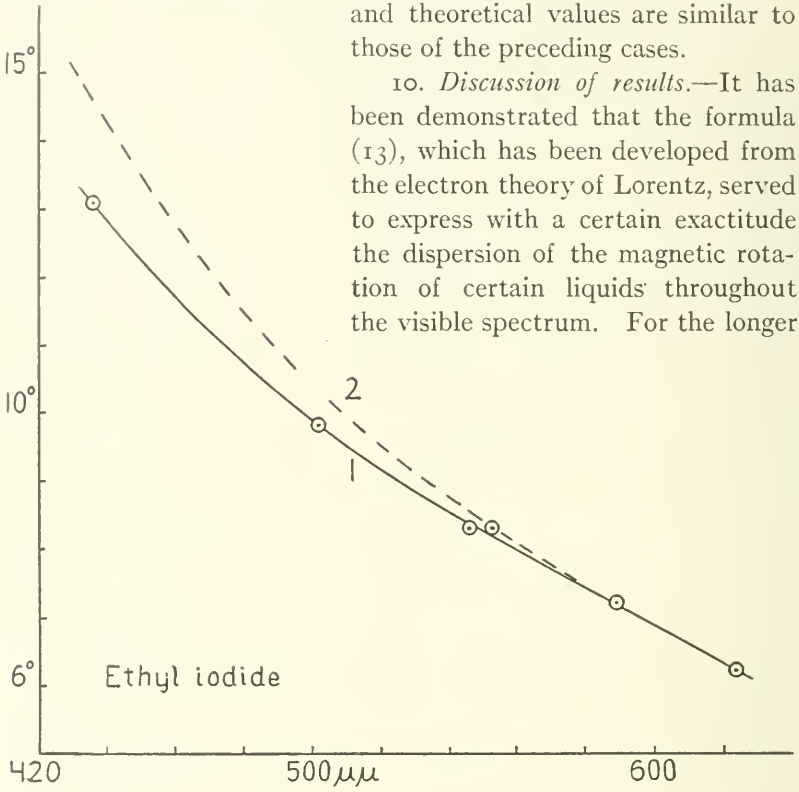


FIG. 6

TABLE VI

ETHYL IODIDE

$H=6480$ gauss			$l=2.220$ cm
Temp. 22°.7 to 24°.3 C.			
λ 486.2 μμ	589.3	656.3	
μ 1.52356	1.51203	1.50738	at 20°.0 C.
Observed by Lorentz, *Wied. Ann.*, **11**, 70, 1880.			
$C_1=12.782\times10^8$	$q_1=0.50762$		$\lambda_1=168.0$ μμ
λ 434.1 μμ	observed $\mu=1.53437$*		
	calculated $\mu=1.5336$		
$h_1=5.90\times10^{-5}$ for λ 589.3 μμ			

* Haagen, *Pogg. Ann.*, **131**, 117, 1866.

wave-lengths of the visible spectrum the agreement between theory and experiment is quite close. For the shorter wave-lengths discrepancies occur which increase as the wave-length decreases. The liquids investigated above possess strong absorption in the ultra-violet and appreciable absorption in the blue end of the spectrum. We may therefore reasonably attribute the discrepancy between theory and experiment in large part to the neglect of absorption. If absorption is taken into account in our equations, λ_1 is increased, and in general the modification which the constants of the equations undergo is such as to bring the theoretical values of θ into closer agreement with the observed ones. The absorption of these substances for light has, however, not been measured accurately, and it seems unprofitable at this time to consider its effect numerically.

11. *The values of* e/m.—From the known value of h_1, the ratio of the charge to the mass of the electron may be calculated by

TABLE VII

	h_1	e/m
Carbon disulphide	3.95×10^{-5}	0.74×10^{7}
α—monobromnaphthalene	5.02	0.95
Benzene	5.34	1.01
Nitrobenzene	2.56	0.49
Ethyl iodide	5.90	1.12

means of formula (9). This has been done and the results are shown in Table VII; e/m is expressed in c.g.s. electromagnetic units.

Becquerel[1], Voigt,[2] and Siertsema[3] have derived formulae for the dispersion of the magnetic rotation, by means of which e/m can be found as soon as the Verdet constant and the dispersion $d\mu/d\lambda$ of a substance for the same wave-length λ are known. These three formulae reduce to the same one, namely

$$\frac{e}{m}=\frac{2c}{\lambda}\frac{\theta}{lH}\div\frac{d\mu}{d\lambda}. \qquad (18)$$

[1] *Comptes rendus*, **125**, 679, 1899.

[2] *Wied. Ann.*, **67**, 351, 1899.

[3] *Comm. Lab. Leiden*, No. 82, 1902.

Using (18), Siertsema computed e/m for air, carbon dioxide, hydrogen, water, carbon disulphide, and quartz. The numbers varied from 0.75×10^7 to 1.77×10^7.

12. *The effect of σ upon the calculations.*—The value of the quantity σ has no very critical effect upon the variation of θ with wave-length. The calculated curves of the diagrams have been obtained by the use of $\frac{1}{3}$ for σ in formula (12). If σ is put equal to 0 in (12), we arrive at Voigt's formula (14), and if this is used to calculate the change of θ with λ we find values of θ which are a trifle less than those obtained from (13). They are about 1 per cent less at λ 434 $\mu\mu$, but are practically the same for wave-lengths greater than 500 $\mu\mu$. If σ is given values greater than $\frac{1}{3}$, the computed values of θ are found to be somewhat greater than the values given by (13), and therefore in greater discordance with the observed values. For example, in the case of carbon disulphide, if $\sigma=\frac{2}{3}$, θ is 25°.1 at 434 $\mu\mu$.

The values of e/m change to some extent when σ is given different values. This is shown for carbon disulphide in Table VIII. We conclude that, as far as the present data are concerned,

TABLE VIII

σ	e/m
0	1.78×10^7
$\frac{1}{3}$	0.74
$\frac{2}{3}$	0.30
1	0.25

it makes little difference whether σ is 0 or $\frac{1}{3}$. If, however, σ is increased above $\frac{1}{3}$, the discrepancies between the theory and the observations become greater.

In conclusion the authors take pleasure in expressing their thanks to Dr. J. S. Ames for valuable and constructive criticism.

JOHNS HOPKINS UNIVERSITY
February 1921

A STUDY OF ARC-CATHODE SPECTRA

By ARTHUR ST. C. DUNSTAN and BENJAMIN A. WOOTEN

ABSTRACT

Arc spectra; relative intensity of metallic lines at anode and cathode.—A series of experiments were performed to *test various suggested explanations* for the fact, amply verified by the authors, that metallic lines are always stronger at the cathode when the metal is introduced symmetrically. A horizontal arc inclosed in a furnace was fed with metallic vapor (Sr, Ba, Li, Cu or Pb) supplied by an alternating current arc 5 cm below. Water-cooling either electrode had no effect, and attempts to obtain separation of the vapors electrolytically or by electrostatic action failed. The spectrum of a 60-cycle alternating current arc taken through a rotating sector synchronized to transmit light during only half of each cycle, was the same as that of a direct current arc. This proves that the phenomenon is fully developed in 1/120 second and makes it unlikely that it is due to the transference of the vapor from one electrode to the other either thermally or electrically. When small pellets of metallic salt were dropped through the arc, the spectrum lines were fish-shaped with the heads toward the cathode. The evidence as a whole indicates that the light is due chiefly to bombardment of the metallic vapor by electrons from the cathode.

Variations with atomic weight.—In general the ratio of cathode to anode intensity was found to decrease as the atomic weight increased.

The fact that in the spectra from the anode of an electric arc the carbon bands are strongest, while in those from the cathode the metallic lines are strongest, was first shown by Lockyer's discovery of the long and short lines.

The subject has been investigated by Thomas,[1] Miss Baldwin,[2] Foley,[3] Beckmann,[4] Humphreys,[5] Oellers,[6] and Konneman.[7]

In general the explanations offered may be divided into two classes, (1) thermal, (2) electrical. In the first class are included such processes as convection, distillation, differences of temperature, etc., all of which ultimately depend upon heat. In the second class may be grouped electrolysis, electronic action (as suggested by Humphreys), and possibly a direct action of the difference of potential between the electrodes of the ionized gases surrounding the arc. An attempt has been made to study the question under as definite, reproducible conditions as possible, and efforts have been made to vary one factor at a time.

[1] *Comptes rendus*, **119**, 728, 1894.

[2] *Physical Review*, **3**, 370 and 448, 1896. [3] *Ibid.*, **5**, 129, 1897.

[4] *Zeitschrift für wissenschaftliche Photographie*, **4**, 335, 1906.

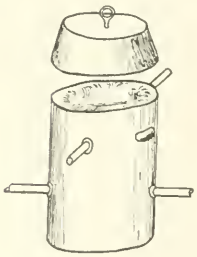
[5] *Astrophysical Journal*, **27**, 200, 1908.

[6] *Zeitschrift für wissenschaftliche Photographie*, **10**, 374–392, 1912.

[7] *Ibid.*, **12**, 65–76 and 123–124, 1913–1914.

In order to avoid the influence of convection currents in the air surrounding the arc, a horizontal arc inclosed in a refractory vessel was used, and in order to be independent of the fortuitous distribution of substances occurring as impurities in the carbons, elements were used which either did not occur as impurities, or occurred in the carbons in such small quantities that their spectral lines did not appear with the exposures given. It was found that Sr, Ba, Li, Cu, and Pb either did not occur in the carbons used, or occurred in very small quantities, and hence these elements were most often used, though for the sake of comparison others were occasionally employed. Strontium was the element generally used, in the form of sulphate.

The arc was surrounded by a nearly homogeneous atmosphere of the vapor of the metal, this vapor being supplied by another arc. The arrangement used is shown in the accompanying figure.



The lower carbons, forming what may be called the vaporizing arc, were bored out and packed with a salt of the metal studied. This arc vaporized the metal which diffused through the furnace. The temperature of the furnace was sufficiently high to prevent any considerable condensation of the metallic vapor on its walls or upon the upper carbons. In order to avoid any difference in temperature at the poles of the vaporizing arc, or different electrical condition in the vapor rising from it, alternating currents of from 15 to 30 amperes were used. The vertical planes passing through each pair of carbons were at right angles to each other. The holes through which the carbons pass were packed with asbestos wicking.

The upper carbons, which were situated approximately 5 cm above the vaporizing arc, were supplied with direct current of from 20 to 60 amperes. The light from the upper arc passed out through an elliptical hole in the wall of the furnace. The image of the arc was cast on the slit of the spectrograph by a quartz lens, the image being linearly magnified approximately six times. After the furnace reached a high temperature its operation was very regular and free from trouble. However, when steam was admitted

to the furnace the carbons were used up rapidly and constant attention was necessary.

Most of the plates were taken on a concave-grating spectrograph of 2 m radius, Rowland mounting, though some were obtained with a small spectrograph using either two prisms or a flat grating. On account of the astigmatism of the concave grating it was necessary to give two exposures to get photographs of spectra from two different portions of the arc. In order to eliminate any linearly progressive change in the arc during the time of exposure, one half the time of the first exposure was given, then all of the second, then the last half of the first, the camera shutter being turned between exposures; the arc itself and not the projection lens being shifted to bring the desired portion of the image on the slit at each exposure. That this process was successful was proved by photographing the same portion of the arc during the two exposures and by photographing the spectrum of an alternating-current arc near each electrode. The plates obtained were in both cases identical. With the magnification used, the breadth of the narrowest part of the image was considerably greate than the length of the slit of the spectrograph; hence the small unavoidable wandering of the arc had little or no influence. To decrease this wandering, cored carbons were generally used.

When the small prism spectrograph was used, it was turned over until the slit was horizontal, thus lying along the axis of the image of the arc. The size of the image was adjusted until its total length was smaller than the length of the slit, so that not only light from the arc stream but that from the tips of the electrodes entered the collimator. Thus the entire arc inclusive of the electrodes could be seen at one time.

In most of the work with the concave grating, spectra of the first order were used. In the blue and violet regions exposures of six minutes were sufficient, but in the red region, λ 6000 to λ 7000, exposures of fifteen to thirty minutes on Eastman Panchromatic films were necessary.

RESULTS

Relative intensities of lines at anode and cathode.—On the several hundred plates secured *there is not a single instance in which a*

metallic line is stronger at the anode than at the cathode, provided that the metal used is not an impurity in the carbons; and even when the metal is found as an impurity, *usually* its cathode lines are stronger than those at the anode.

If instead of surrounding the arc with a uniform atmosphere of metallic vapor, as is done here, the metal is introduced into the arc by loading the carbons, or by saturating them with solutions of the metallic salts, it is possible to have the lines strongest at either pole, depending upon which carbon has the greater supply of the element. In such cases it is probable that the vapor-density or the thickness of the vapor is greater near the more heavily loaded carbon. Several investigators have reported finding that certain metallic lines were stronger at the anode than at the cathode. So far as the writers are aware, in all such cases the metals were introduced by loading the carbons, by saturating them with solutions of the salts of the metals, or by depending upon the occurrence of the metal as impurities in the carbons. It may be that the difference between the results obtained by these investigators and that obtained in the present work is due to the fact that in the work of these investigators there may have been differences in the amount of the metals in the two electrodes.

As bearing upon this point, the following may be of interest. Using rods of wrought iron 12.5 mm in diameter for the upper electrodes and carbons loaded with $SrSO_4$ for the vaporizing arc, the plates show the *iron* lines of equal intensity at the anode and cathode, while the *strontium* lines were stronger at the cathode than at the anode.

The fact that the anode is hotter than the cathode has led several investigators to ascribe the stronger cathode lines to a process of distillation from the anode to the cathode with consequently greater vapor-density at the cathode. In order to investigate this matter, one of the upper carbons in the furnace was replaced by a water-cooled brass electrode. If there is a process of distillation in the arc whereby the vapors distil over from the hotter anode to the relatively cooler cathode, thus increasing the vapor-density in the vicinity of the latter, it ought to be possible to reverse the direction of the process by using an anode cooler

than the cathode. When the water-cooled electrode above mentioned is used as anode, the lines of the metals forming the vapor are as before, stronger at the cathode. In fact, the phenomenon is not interfered with in the least. Near the anode, however, the lines of the Cu and Zn of the electrode are stronger than they are at the cathode, though showing at both poles.

In order to determine whether or not the *gas of the arc stream* is cooler at the anode than at the cathode, two small thermopiles of the Rubens pattern were arranged so that they could be slid along a rail and either one could be placed at any desired point in the image of the arc. They were connected in opposition to each other and to a heavily damped galvanometer. The sensitiveness of the arrangement was tested by placing one thermopile near the image of the cathode while the other was moved to any desired portion of the arc. The difference of radiation from the different sheaths of the arc was easily shown.

The thermopiles showed plainly that with carbon electrodes the gas in the vicinity of the anode was hotter than that near the cathode. With the water-cooled electrode, however, the thermopile showed definitely and clearly that no matter whether this electrode formed the anode or cathode of the arc, the gas in its vicinity was cooler than the gas surrounding the carbon electrode.

Carbons bored out axially, the inner end of the boring not quite coming to the inner end of the carbon, and having the other end connected to the water supply, were also employed. The results were the same as with the brass tube.

The fact that the water-cooled electrode always lowers the temperature of the arc stream in its vicinity below that prevailing at the other electrode, taken in connection with the fact stated above that this electrode when used as an anode does not affect the greater intensity of the metallic lines near the cathode, seems to be evidence of considerable weight against the idea of distillation.

Blowing a gentle current of steam through a bored carbon in an attempt either to blow the metallic vapors away from the carbons or at least dilute them considerably resulted in a very badly burning arc, but no matter which electrode the steam-feeding carbon formed, the lines were stronger at the cathode.

Electrolysis.—The fact that when the vaporizing carbons are loaded with a mixture of elements standing as far apart in the electrochemical series as Li, K, Ba, Sr on the one hand, and Cu and Pb on the other, the lines of all of them are found to be stronger at the cathode, would seem to speak against the electrolytic theory. If there is electrolysis, it would seem that some of the elements mentioned should be found at one pole and some at the other. Experiment shows, however, that there is no separation of the elements in the arc.

If a third carbon loaded with these elements is pushed from the side into the arc, thus introducing the elements into the midst of the arc stream, there is no separation, the lines of all the metals being stronger near the cathode. This is true when the third electrode is connected to either of the electrodes through a moderate resistance, thereby changing the potential of the electrode with respect to the others.

If a fire-clay diaphragm with a small hole at its center is inserted in the furnace between the upper and lower carbons, thus making two chambers in the lower of which the vapor is formed, the vapor rises through the hole and crosses the arc stream as a jet of small diameter. It is found that still the metallic lines are strongest at the cathode, or rather between the cathode and the point where the jet impinges on the arc stream. As in the other arrangements just mentioned there is no separation of the elements. Owing to the somewhat indefinite outlines of the jet where it crosses or mingles with the arc stream, it could not be determined whether the lines were strongest at the cathode or at the boundary of the jet nearest the cathode.

Direct electrostatic action on the ionized gases surrounding the arc stream.—The term electrolysis was used above in the sense of implying an electrolytic transport of materials in the stream of the arc itself and by the action of the arc current. The term "direct electrostatic action on the ionized gases" is intended to convey the idea of an electrostatic action of the oppositely electrified electrodes upon the masses of vapor which surround the arc stream, but do not take part in conveying the arc current. It is possible at least that the ions coming from the lower arc, and

also to a certain extent from the upper one, would be attracted directly to the upper-arc electrodes, and, reaching them, would there give the spectral lines of the ionized elements.

To test this point, the lower arc was allowed to burn, furnishing a continuous supply of vapor, while the upper arc was extinguished and to its electrodes was connected a source of direct current of high potential. One electrode was thus at a high positive potential and the other negative, and both were immersed in the ionized vapors. After a run of from fifteen to twenty minutes, the source of high potential was disconnected, one of the deposition carbons was removed and a fresh carbon substituted for it. The arc current was now switched on, the new carbon being made the anode. A spectrum photograph was taken, the slit being located near the image of the deposition carbon. This carbon was now removed and the other deposition carbon substituted for it, and a second spectrum was photographed on the same plate. Using potential gradients of 200 to 5000 volts per cm of distance between the ends of the deposition carbons during the deposition, the spectrum plates were identical in lines and in the intensities of the same.

As a variation, the vapors from the arc are allowed to pass through an iron tube about 3.5 cm in diameter and about 40 cm long, in the axis of which was a brass rod 0.5 cm in diameter insulated from the iron tube by a porcelain bushing tube. A difference of potential of from 1000 to 2000 volts between the rod and the tube was applied, and after a suitable interval for deposition the rod and tube were removed, separated, and each wiped off with a wad of absorbent cotton. The wads of cotton were placed in separate beakers and each treated with hot dilute HCl in order to dissolve whatever had been deposited on the tube or rod and removed by the wads of cotton. New carbons were boiled in the solutions. These carbons formed in succession the cathodes of an arc whose cathode spectrum was photographed, the anode being a new carbon. The result of these photographs was that the spectrum lines of the metal used in the vaporizing arc were absolutely identical in the photographs. The spectral reaction was delicate enough to show the iron lines in the material deposited

on the iron tube, and the copper lines in the material deposited on the brass rod, these being due to the exceedingly small particles of the oxides wiped off by the wads of cotton. Using a mixture of elements in the vaporizing carbon, there was in no case any separation of these elements in this process, the materials deposited of the high potential anode and cathode being identical.

It is the opinion of the writers that the facts above given constitute a considerable body of evidence against any of the thermal processes and also against electrolysis and direct electrostatic action, and consequently of the various explanations offered there remains only the electronic one offered by Humphreys.

It can be said at once that although the work described above cannot be considered a proof of the electronic theory, yet there is nothing in its results in conflict with this theory. The following appears to be stronger and more direct evidence than that just given. An inclined carbon tube was arranged so that small pellets of the metallic salts from 1 to 2 mm in diameter could be fed into the upper end, gain considerable speed in the descent, and finally plunge through the arc stream at high speed. The time that these pellets were in the arc stream was too short for any perceptible diffusion, convection, or electrolysis, and further, since their diameters were so small there could not have been much difference of potential or difference of temperature between the side turned toward the cathode and that turned toward the anode. A plane-grating spectroscope with its slit horizontal was used to study visually the spectrum given by these pellets. Under the conditions mentioned, the lines of the metals were distinctly *fish-shaped*, the *head or thickest part of the fish being turned toward the cathode*. This suggests that the electrons, flying from the cathode, strike the vapor surrounding the pellet on the side turned toward the cathode, produce the light, and then, most of them being stopped by collision either with the vapor or the solid body of the pellet itself, there are only comparatively few left to produce light on the anode side. It seems that it would be difficult to explain this result on any other theory than that of ionization by impact.

Explanations based on convection, diffusion, distillation, or electrolysis are alike in that they postulate an accumulation of

metallic vapors in the vicinity of the cathode. In accordance with any of these explanations, if the polarity of a direct-current arc is reversed, the metallic lines from the new cathode cannot be more intense than those from the new anode until sufficient time has elapsed for the accumulation left around the new anode to diminish and for a new accumulation of vapor to build itself up around the new cathode. It is evident that such a process requires a finite time, since it requires a transfer of ordinary matter. On the other hand, on account of the high velocity of electrons electronic processes are almost instantaneous, and reversing the arc merely means reversing the direction of electron flow. Very little time is required for this, evidently far less than for the accumulation of metallic vapor around one of the poles of the arc. Hence the time required after the reversal of the arc for the lines to become more intense at the new cathode may be used as a means of deciding between the electronic and rival theories above mentioned.

In order to apply this method of discrimination, the following scheme was used. Sixty-cycle alternating current was used to operate the upper arc in the furnace, the "vaporizing carbons" as usual furnishing the metallic vapor. Each upper carbon was consequently the anode for 1/120 of a second, followed by an equal interval of time during which it was the cathode, and so on. Between the projection lens and the slit of the spectrograph was placed a small synchronous motor of 1800 r.p.m. on whose shaft was mounted a sectored metallic disk. The disk had two open and two opaque sectors. A contact device on the shaft of the motor insured that the beam of light traversed the center of one of the open sectors at the instant that one carbon was at its highest position potential and the other at its maximum negative potential. When the current through the arc reversed, an opaque sector had taken the place of the open one, thus shutting off the light. Since the open sectors were appreciably smaller than the opaque ones, there could be no overlapping.

Under these conditions the image of the alternating-current arc and the sheaths were in all respects precisely the same as those of a direct-current arc.

Spectrum photographs showed the familiar phenomenon of the increased intensity of the metallic lines at the cathode *precisely as if the arc had been produced by a direct current.* With the vaporizing carbons loaded with a mixture of the salts of Li, K, Sr, Ba, and Pb, the lines of all of these elements were stronger at the cathode. This shows without doubt that 1/120 of a second is ample time for the phenomenon to develop, and hence seems to exclude any possibility of there having been any bodily transference of metallic vapors from one pole to the other. It would probably be possible, by the use of narrower open sectors and by revolving the field frame of the motor to such a position as to allow the light to pass at an instant very nearly that at which the current passes through zero, to obtain a more definite value for the time limit required for the establishment of the phenomenon, but it would seem that a maximum limit of 1/120 of a second is sufficient to show that there could be little or no actual transference of metallic vapors from one side of the arc to the other.

The fact that elements of such widely different atomic weights, ranging from 7 to 208, all gave the same result under these conditions of rapid alternations of polarity, appears to furnish additional evidence against any explanation or theory involving the idea of transference of material across the arc, and to strengthen the supposition that the light emitted by the arc stream is due to vibration caused by the collision of electrons emitted by the cathode with the particles of the vapors surrounding the arc.

Relative intensities.—The different lines of a given element show considerable differences in their relative intensities at the two poles. Thus some Sr lines may have an intensity of 10 at the cathode and 8 at the anode, while others may have intensities of 20 and 1, and in some cases no trace whatever of the line could be seen at the anode. An attempt has been made to see whether there is any connection between this change of intensity in the line at the two poles and the Kayser and Runge series to which the line might belong. It has not, however, been possible to reach any definite decision on this point.

A similar question is that of correlating the behavior of the lines with the atomic weight of the element. While the number

of elements used was too small to allow any definite statement to be safely made, yet, so far as the results go, they indicate that the cathode strengthening is greater the lower the atomic weight of the element.

Conclusion.—All attempts to separate vapors of the arc by methods involving difference of temperature and by methods based on electrolysis and electrostatic action gave negative results. Results obtained with the alternating-current arc seem to show that the light from the arc stream is due to electronic collision, and they indicated that the phenomenon is completely established in 1/120 of a second or less.

Alabama Polytechnic Institute
Auburn, Alabama
January 12, 1921

Minor Contributions and Notes

IDENTIFICATION OF AIR LINES IN SPARK SPECTRA FROM λ 5927 TO λ 8683[1]

ABSTRACT

Spectrum of condensed spark in air and in oxygen, λ 5927 to λ 8683.—By operating the spark alternately in oxygen and in air, the lines due to oxygen have been identified. The remaining air lines, except a few *argon* lines, are ascribed to *nitrogen*. The work confirms numerous identifications made by other observers using vacuum tubes, and adds some identifications not previously available.

Experiments in continuation of those previously performed by one of the authors[2] have been carried out to determine the chemical identifications of the air lines from λ 5927 to λ 8683 in spark spectra.

The spark chamber, consisting of a glass bulb, was connected with an air pump and an oxygen apparatus in such a way that it could be filled either with air or with oxygen. The oxygen was generated by heating potassium permanganate and was purified by passage through caustic potash, calcium chloride, and phosphorus pentoxide. The photographic exposures were so arranged that the spectrum of the spark in air appeared on the negative close beside that of the same spark in oxygen, thus facilitating a comparison of the relative intensities of the lines. The pressure in the spark chamber was equal to one atmosphere in all cases. Several sets of comparisons were made with copper electrodes, and one with carbon (Acheson graphite) electrodes. All gave accordant indications of the identification of the air lines.

The second column in Table I gives our observations of the changes in relative intensities of the lines produced by the spark in oxygen as compared with the spark in air, *w* and *s* indicating weakened and strengthened, respectively. Of lines for which other identifications are available, those due to argon and nitrogen are weakened, while those due to oxygen are strengthened. Among the remaining lines, those weakened are believed to be due to nitrogen, and those strengthened to oxygen.

[1] *Contributions from the Mount Wilson Observatory*, No. 207.

[2] *Ibid.*, No. 183; *Astrophysical Journal*, **51**, 211, 1920.

One line, λ 6370.92, should be removed from the previous list,[1] as it is probably due to silicon, while a nitrogen line at about 6341.5 A should be added, as it is observable in air. It undoubtedly corresponds to a line observed at 6340.84 A by Porlezza in a nitrogen tube.

TABLE I

RELATIVE INTENSITIES OF SPARK LINES IN AIR AND IN OXYGEN

λ in Air, I A	Oxygen	Vacuum Tubes	λ in Air, I A	Oxygen	Vacuum Tubes
5927.83.....	*w*	N*	7424.04.....	*w*	
5931.78.....	*w*	N*	7442.70.....	*w*	
5941.54.....	*w*	N*	7468.72.....	*w*	
5952.33.....	*w*	N*		*s*	O 7476.58‡
6158.	*s*	O†		*s*	O 7479.23‡
6171.0	*w*				O 7481.27‡
6284.22.....	*w*	N*	7635.70.....	*w*	A
(6341.5).....	*w*	N 6340.84*	7772.07.....	*s*	O
6358.13.....	*w*	N*	7774.33.....	*s*	O
(6370.92)....		See note	7775.60.....	*s*	O
6379.52.....	*w*	N*	7947.83.....	*s*	O 7947.58‡
6456.	*s*	O†	7951.10.....	*s*	O 7950.84‡
6482.054....	*w*	N*	7952.3	*s*	O 7952.22‡
6610.39.....	*w*	N*	8185.26.....	*w*	
6640.7	*s*		8188.42.....	*w*	
6654.78.....	*s*		8200.72.....	*w*	
6721.25.....	*s*		8211.12.....	*w*?	
6887.61.....	*w*		8216.72.....	*w*	
6950.	*w*?			*s*	O 8221.84‡
6965.95.....	*w*	A	8223.48.....	*w*	
(7007)	*s*	O 7002†	8230.20.....	*s*	O 8230.05‡
7067.6	*w*	A		*s*	O 8233.05‡
7157.36.....	*s*	O?†	8242.80.....	*w*	
.....	*s*	O 7254†	8446.84.....	*s*	O
7384.53.....	*w*	A	8630.02.....	*w*?	
			8680.63.....	*w*	
			8683.70.....	*w*?	

* Porlezza, *Atti R. Accademia dei Lincei*, Serie 5. **20**, 584, 1911.
† Runge and Paschen, *Annalen der Physik*, **61**, 641, 1897; **27**, 562, 1908.
‡ Kiess, *Popular Astronomy*, **29**, 18, 1921.

NOTES

λ 6158 Very broad, probably double or triple; includes λ 6160.72.
6171.0 Broad, probably double or triple.
6370.92 Not an air line; probably Si.
7007 Very, very hazy.

PAUL W. MERRILL
F. L. HOPPER
CLYDE R. KEITH

MOUNT WILSON OBSERVATORY
February 1921

[1] *Loc. cit.*

AVOIDANCE OF ATMOSPHERIC DISPERSION IN MEASURES WITH THE STELLAR INTERFEROMETER

ABSTRACT

Stellar interferometer.—A direct-vision prism has been used with the stellar interferometer to avoid the disturbing effects of atmospheric dispersion.

Since Professor Michelson's tests here and at Mount Wilson have shown that the interference method for measuring close double stars is little affected by atmospheric conditions, we have applied this method to some of the known bright pairs with the 40-inch refractor. An experimental apparatus was built in 1920 by Mr. O. J. Lee and myself, with the use of wood and paper, because of lack of help in our shop at that time. It was placed in front of the 40-inch objective and consisted of two rectangular openings in cardboard that could be changed in position angle and varied in distance by means of cords held by the observer. This crude instrument showed the expected phenomena very plainly, but was only good enough to make a better one desirable. From a sketch by myself a small apparatus was made of iron and brass in which the movable slits were in the cone of light only one meter inside the focus. This instrument was mainly made by Dr. George S. Isham, of Chicago, who voluntarily proposed to undertake the construction in his private shop. His hearty co-operation is very cordially acknowledged here. Adapted to the 40–inch refractor by our instrument-maker, with the necessary adjustments for centering the apparatus in the cone of light, the instrument proved satisfactory. Between March 21 and June 25, 1921, Capella has been followed in position angle over nearly a complete revolution by observations during the day, some of them when Capella was culminating at noon.

From the very beginning, however, a difficulty was encountered in atmospheric dispersion. J. A. Anderson[1] has clearly explained the effect of this disturbing factor. When the interferometer is set on a star at low altitude the fringes appear fan-shaped if the slits are vertical, while in a direction normal to this the fringes would be completely blurred. Without going that far, it is evident that even at higher altitudes atmospheric dispersion will affect the change in

[1] *Astrophysical Journal*, 51, 268, 1920.

visibility of the fringes for varying position angles. The effect would be an apparent shift of the position angle toward the vertical. These deviations were quite evident on Capella. This star is too close to be measured in distance with the 40-inch refractor combined with the interferometer; yet the change of visibility of the fringes when the instrument is turned in position angle is such that, although the distance could not be measured, the position angle can be established fairly well. But the measures on a given day showed marked changes with the hour angle.

Anderson compensates for the atmospheric dispersion by putting plates of plane-parallel glass, one of them being slightly tilted, in front of each slit; but this appeared difficult, since the adjustment had to be modified for each change in the position angle. The alternative of using a prism of variable angle, kept in the required position by gravity, will probably be found too difficult in actual application.

Another method was devised by myself, which is simple and practical. It consists in mounting a direct-vision prism on the eyepiece, the edge of the prism being parallel to the line joining the centers of the slits, so that the dispersion is parallel to the slits. Since the eyepiece turns with the slits, the prism becomes part of the interferometer and does not require repeated adjustment. Direct-vision prisms of the Zöllner type, consisting of two crown prisms with the flint prism in between, were used for that purpose, the cylindrical lens being discarded. Dispersions of 3°, 4°, and 5° respectively, between the Fraunhofer lines B and G (λ 6868 and λ 4308) proved to be amply sufficient.

Atmospheric dispersion is represented by $0''.83 \tan z$ for zenith distances smaller than 70° if the limits of the spectrum are taken at λ 6500 and λ 4500.[1] The corresponding value between B and G is $1''.06 \tan z$. Since the observations are made with a power of about 2000, the atmospheric dispersion would appear to the eye under an angle of $2000 \times 1.06 \tan z$ or roughly $0''.7 \tan z$, as against a dispersion of 3° to 5° with the prism. The combination of the two dispersions will be a spectrum at a slight angle with the length of the slits. By adjusting the prism so that the resulting spectrum is

[1] Anderson, *loc. cit.*

parallel to the slits, the vertical dispersion is compensated and the fringes will be seen again over the whole length of the successive colors of the narrow spectrum, especially well in the red part for the prism used. Laboratory tests in which the light of a slit-source was dispersed through a 60° prism showed that even for such a high dispersion the lost fringes could be brought back and made so plain by the direct-vision prism oriented in the proper way that the width of the slit could be measured as if there was no dispersion, and since the settings could be made in the various colors, there is no uncertainty as to the wave-length to be used in the computations.

This method was used on Capella for the first time on June 16 and was found to work very well even when the star is as close to the sun as at present. On fainter stars the loss of light would reduce the number of objects that can be reached. Observations on stars as faint as $7^{M}.0$ were found possible under fair conditions, without the direct-vision prism. The dispersion introduced by this auxiliary apparatus would put the limit somewhere near $5^{M}.0$ with the actual arrangement of the instrument.

G. Van Biesbroeck

Yerkes Observatory
June 26, 1921

ERRATA

Vol. 53, January, 1921, "The Parallaxes of 1646 Stars Derived by the Spectroscopic Method," by W. S. Adams, A. H. Joy, G. Strömberg, and Cora G. Burwell:

Page 23, equation (19), *for* $\bar{A}^2$ *read* $\bar{A}^{-2}$.

Page 26, second line, *for* below *read* above.

Page 39, Boss 451: *for* 47 Cassiop. *read* 57 Ceti.

Page 44, the trigonometric π and authorities given for Boss 1074 refer to C594.

Page 60, first line, the Boss No. for Bu. 5695C should be deleted.

Page 75, Boss 4470: under "Authorities," *for* M *read* S.

Page 84, X Cygni: in the sixth column, insert ‖ after 0.018.

Page 87, C2797: in the sixth column, *for* 0″.056 *read* 0″.56.

THE
ASTROPHYSICAL JOURNAL
AN INTERNATIONAL REVIEW OF SPECTROSCOPY
AND ASTRONOMICAL PHYSICS

VOLUME LIV SEPTEMBER 1921 NUMBER 2

THE ECLIPSING VARIABLE 1 H. CASSIOPEIAE, WITH EVIDENCE ON THE DARKENING AT THE LIMB OF A STELLAR DISK

By JOEL STEBBINS

ABSTRACT

Variable star 1 H. Cassiopeiae; photometric study.—Observations during 1917–1921 with a photo-electric photometer show that this star is an *eclipsing variable.* The primary and secondary minima have ranges of $0^{M}.132$ and $0^{M}.032$ respectively, each with an interval of constant light showing that the eclipses are annular or total. From the *light-curve* are derived the *elements of the binary system* (Table IV, Fig. 3), which are in good agreement with the Allegheny spectroscopic results. There is, however, a discrepancy in the phase and duration of the secondary minimum which points to a *motion of the line of apsides*, and which in view of the *high eccentricity*, $e=0.25$, could be readily verified by a new determination of the spectroscopic elements. The *density* of the smaller and fainter body is probably seven times that of the primary.

Darkening at the limb of a star of spectrum B3.—This star furnishes an unusually favorable test for darkening at the limb, as there is an annular eclipse by a small companion; but the results indicate that there can at most be only a small fraction of the amount of darkening which is present in the case of the sun.

Comparison stars, 1 and σ Cassiopeiae.—These have been found to be constant in light, within perhaps $0^{M}.01$.

Photo-electric photometer for stars.—The *precision* which may be reached is indicated by the residuals for seventy-five normal magnitudes, which give the probable error of one normal $= \pm 0^{M}.0036$.

The variation of 1 H. Cassiopeiae (B.D. 57°.2748, H.R. 8926, magnitude 4.89, spectrum B3), was detected with the photo-electric photometer in 1918.[1] The spectroscopic orbit by Baker[2] depends upon plates taken in 1908 and 1909, and the period,

[1] *Publications of the American Astronomical Society*, **4**, 115, 1919.

[2] *Publications of the Allegheny Observatory*, **2**, 28, 1910.

6.067 days, was derived by comparison with several Yerkes observations in 1903. In our searching for an eclipse some ten years after the spectroscopic measures it was not surprising to find the star faint at a phase nearly half a day before the prediction, which difference after more than six hundred revolutions could be due to a small error in the assumed period. The photometric observations of this star have been continued at times during four seasons, and it is found that there are primary and secondary eclipses of $0^{M}.13$ and $0^{M}.03$ respectively, also that the eclipses are annular and total, which facilitate the derivation of the elements even though the light-range is so small.

1 H. Cassiopeiae, No. 12405 in Burnham's *General Catalogue*, is listed as a wide multiple star with no fewer than eight components, but of these the combination AB is all that is measured through a diaphragm of the photometer which limits the field to 72″ diameter. As B is more than four magnitudes fainter than A, the effect of the former is almost negligible.

There are two good comparison stars available:

H.R. 8797, 1 Cassiopeiae, magnitude 4.93, spectrum Bo
H.R. 9071, σ Cassiopeiae, magnitude 4.93, spectrum B2

As these are on either side of the variable, it is found that the differential visual extinction between 1 H. and the mean of the two stars is less than $0^{M}.004$ from $20^{h}.0$ to $4^{h}.0$ sidereal time. Thus for eight hours the stars are in good observing position, and there has been no suspicion of variability of either 1 or σ. From favorable measures of the comparison stars it is found that the photo-electric difference, 1 brighter than σ, is $0^{M}.010 \pm 0^{M}.002$.

In Table I are given the photo-electric observations of 1 H. Cassiopeiae. The first date is September 10, 1917. The times were reduced to the sun and the phases computed from the elements:

$$\text{Minimum} = \text{J.D. } 2422586.492 + 6^{d}.06630 \cdot E.$$

The difference of magnitude is in the sense 1 − 1 H., a positive sign meaning that 1 H. was brighter than 1. Unless otherwise noted, each difference is the mean of three sets of four readings each on the variable and comparison star, the latter being 1 Cassiopeiae unless σ is in the last column. The designation (1, σ) is given to the few sets where the mean of 1 and σ was used.

TABLE I

OBSERVATIONS OF 1 H. CASSIOPEIAE

Date, G.M.T.	Phase	1−1 H.	Remarks	Date, G.M.T.	Phase	1−1 H.	Remarks
2421482.812...	$0^d.390$	$+0^M.029$		2422525.888...	$0^d.059$	$-0^M.096$	
1483.805...	1.383	.036		2528.859...	3.030	+ .028	2 sets
1837.733...	3.464	.003	Rejected	2530.828...	4.999	.030	(1, σ)
1845.683...	5.349	.006		2531.710...	−0.185	.028	
1924.657...	5.461	.010		.725...	−0.170	.018	
1927.631...	2.368	.036		.739...	−0.156	− .009	
1928.567...	3.304	.020	2 sets	.749...	−0.146	− .020	
1932.615...	1.285	.034		.766...	−0.129	− .042	
1939.538...	2.142	.036		.776...	−0.119	− .070	
1943.512...	0.050	− .106		.792...	−0.103	− .086	
.535...	0.073	− .095		.803...	−0.092	− .095	
.549...	0.087	− .089		.829...	−0.066	− .100	(1, σ)
573...	0.111	− .072		.842...	−0.053	− .102	1 set
.587...	0.125	− .048		2533.765...	+1.870	+ .043	
.601...	0.139	− .026		2534.774...	2.880	.037	
.615...	0.153	− .020		2539.778...	1.817	.031	
.629...	0.167	− .003		2540.768...	2.807	.037	4 sets
.642...	0.180	+ .023		2553.799...	3.707	.011	
.659...	0.197	.010		.809...	3.717	.000	
.674...	0.212	.024		.849...	3.757	− .003	
1967.498...	−0.230	.026		.861...	3.769	+ .005	
.522...	−0.206	.005		.886...	3.794	− .014	(1, σ)
.537...	−0.191	.013	2 sets	2554.733...	4.641	+ .030	
.551...	−0.177	.013		.743...	4.651	.030	
.588...	−0.140	− .028		2558.810...	2.652	.021	
.604...	−0.124	− .058		2561.756...	5.598	.022	
1976.572...	+2.776	+ .016		.767...	5.609	.036	
1979.556...	5.760	.010		2566.766...	4.541	.039	
1983.517...	3.655	.009		.781...	4.556	.036	
.530...	3.668	− .003		2567.772...	5.547	.056	
1988.553...	2.624	+ .025		2573.749...	5.458	.032	2 sets
1990.537...	4.608	.032		2580.640...	0.217	.030	
.568...	4.639	.035		.651...	0.228	.034	
2307.493...	0.053	− .100		.671...	0.248	.038	
.511...	0.071	− .095		2583.754...	3.331	.035	
.535...	0.095	− .081		.769...	3.346	.033	
.547...	0.107	− .070		2584.719...	4.296	.038	
.586...	0.146	− .023		.735...	4.312	.021	
.599...	0.159	+ .013		2585.766...	5.343	.025	
.621...	0.181	.012		.785...	5.362	.023	
.637...	0.197	.032		2586.578...	0.089	− .105	
2313.494...	−0.012	− .088		.622...	0.133	− .016	
.501...	−0.005	− .083	σ	.662...	0.173	+ .014	
.542...	+0.036	− .083		.710...	0.221	.040	
.551...	0.045	− .095	σ	.764...	0.275	.030	
2517.792...	4.096	+ .015		.798...	0.309	.021	
2524.828...	5.065	.036		2589.659...	3.170	.033	
2525.730...	−0.099	− .091		2592.578...	0.023	− .076	
.744...	−0.085	− .105		.593...	0.038	− .092	
.785...	−0.044	− .107	2 sets	.636...	0.081	− .097	
.797...	−0.032	− .103		.706...	0.151	− .032	
.814...	−0.015	− .102		.728...	0.173	+ .023	
.825...	−0.004	− .116		.739...	0.184	.023	
.836...	+0.007	− .085		2593.692...	1.137	.057	
.853...	0.024	− .094	(1, σ)	.708...	1.153	.037	
.876...	0.047	− .100		2595.685...	3.130	.032	

TABLE I—*Continued*

Date, G.M.T.	Phase	1−1 H.	Remarks	Date, G.M.T.	Phase	1−1 H.	Remarks
2422595.722...	3^{d}167	+0^{M}040		2422613.737...	2^{d}983	+0^{M}027	
2596.646...	4.091	.053		740...	2.986	.043	σ
.657...	4.102	.039		2614.572 .	3.818	.034	
2598.672...	0.050	− .114		.577...	3.823	.000	σ
.700...	0.078	− .084		2616.578...	−0.243	.029	
2599.683...	1.061	+ .028		.582...	−0.239	.030	σ
.694...	1.072	.036		.601...	−0.220	.028	
2601.685...	3.063	.034		.604...	−0.217	.031	σ
.698...	3.076	.031		.624...	−0.197	.025	
2603.634...	5.012	.038		.626...	−0.195	.038	σ
.644...	5.022	.036		.647...	−0.174	.013	
2604.537...	−0.151	.002		.650...	−0.171	.006	σ
.551...	−0.137	− .022		.685...	−0.136	− .029	
.564...	−0.124	− .052		.687...	−0.134	− .031	σ
.576...	−0.112	− .070		.704...	−0.117	− .051	
.596...	−0.092	− .074		.708...	−0.113	− .073	σ
.608...	−0.080	− .096		.725...	−0.096	− .084	
.658...	−0.030	− .085		.729...	−0.092	− .088	σ
.669...	−0.019	− .088		.753...	−0.068	− .092	
.691...	+0.003	− .119		.758...	−0.063	− .093	σ
.701...	0.013	− .103		.776...	−0.045	− .085	
.722...	0.034	− .105		.781...	−0.040	− .100	σ
.733...	0.045	− .088		2618.640...	+1.819	+ .013	
.753...	0.065	− .120		.644...	1.823	.030	σ
.766...	0.078	− .111		2619.578...	2.757	.051	
2605.621...	0.933	+ .028		.582...	2.761	.047	σ
.630...	0.942	.040		2626.579...	3.692	.020	2 sets
2606.709...	2.021	.039		.583...	3.696	− .007	σ, 2 sets
.723...	2.035	.036		.599...	3.712	+ .001	2 sets
2607.628...	2.940	.043		.606...	3.719	− .005	σ, 2 sets
.644...	2.956	.039		2627.586...	4.699	+ .052	
2608.524...	3.836	.001		.590...	4.703	.045	σ
.563...	3.875	− .008		2628.592...	5.705	.032	2 sets
.572...	3.884	− .028		.596...	5.709	.029	σ, 2 sets
.610...	3.922	.000		2632.592...	3.639	.032	
.619...	3.931	− .013		.598...	3.645	.013	σ
.645...	3.957	+ .008		2633.600...	4.647	.062	
.654...	3.966	.019		.603...	4.650	.047	σ
.667...	3.979	.013		2640.693...	5.674	.019	
.678...	3.990	.018		.698...	5.679	.045	σ
.694...	4.006	.023	(1, σ)	2641.563...	0.477	.054	
.708...	4.020	.032		.567...	0.481	.042	σ
.718...	4.030	.021		2642.558...	1.472	.047	
.727...	4.039	.039		.562...	1.476	.051	σ
.751...	4.063	.027		2647.541...	0.389	.058	
.753...	4.065	.045	σ	.547...	0.395	.031	σ
.770...	4.082	.032		2648.615...	1.463	.019	
.773...	4.085	.042	σ	.620...	1.468	.063	σ
.795...	4.107	.042		2656.637...	3.417	.009	
.799...	4.111	.048	σ	.642...	3.422	.047	σ
2609.608...	4.920	.030		2699.521...	3.836	.012	
.612...	4.924	.048	σ	.524...	3.839	.000	σ
2610.723...	−0.031	− .092		.551...	3.866	− .005	
.730...	−0.024	− .118	σ	.556...	3.871	+ .015	σ
.754...	0.000	− .097		.578...	3.893	− .006	
.765...	+0.011	− .103	σ	.582...	3.897	+ .037	σ
.781...	0.027	− .091		.601...	3.916	− .001	
.785...	0.031	− .092	σ	.604...	3.919	+ .027	σ

The normal magnitudes in Table II were formed in the usual way, each normal being ordinarily the mean of three observations from Table I. The residuals give a comparison with the computed

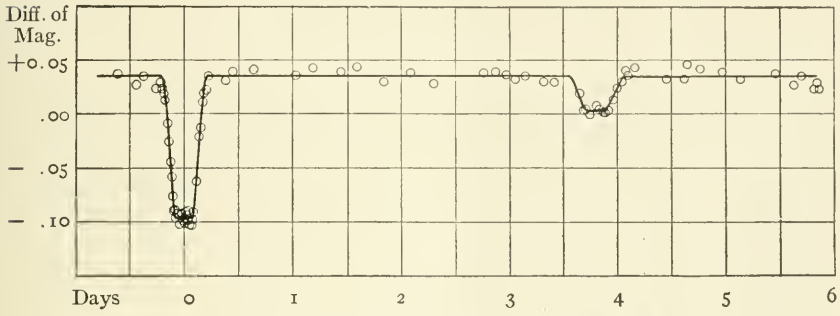


FIG. 1.—The light-curve of 1 H. Cassiopeiae

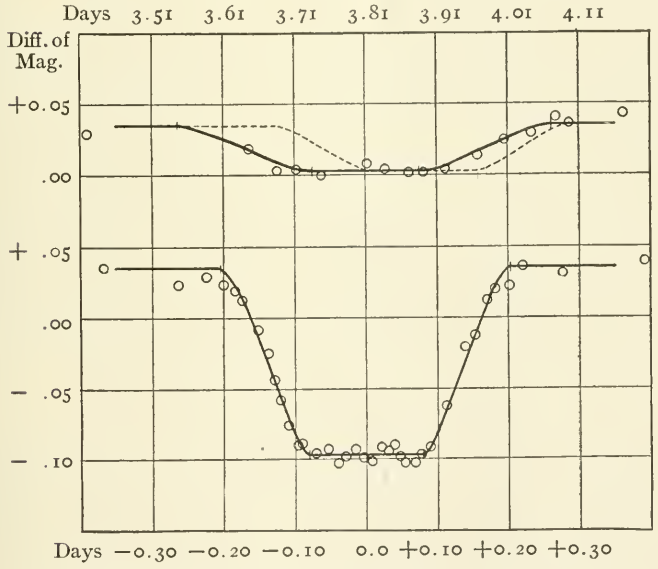


FIG. 2.—Primary and secondary minima of 1 H. Cassiopeiae. Broken line for secondary is computed from spectroscopic elements.

light-curve which is shown in Figures 1 and 2. From all the residuals is derived

Probable error of one normal magnitude = $\pm 0^{M}.0036$.

The constant light at each minimum shows that each eclipse must be either annular or total. As there is little variation between minima the bodies are presumably too far apart to show the effects of radiation and ellipticity of figure which are often observed in

TABLE II

NORMAL MAGNITUDES

Phase	I−I H.	Residual	Phase	I−I H.	Residual
−0.263	+0.023	−0.012	1.192	+0.043	+0.008
−0.222	.028	− .007	1.438	.039	+ .004
−0.199	.023	− .010	1.588	.043	+ .008
−0.184	.018	− .005	1.837	.029	− .006
−0.172	.012	+ .001	2.066	.037	+ .002
−0.151	− .009	+ .005	2.548	.027	− .008
−0.138	− .026	+ .005	2.765	.038	+ .003
−0.129	− .044	.000	2.876	.039	+ .004
−0.120	− .058	− .002	2.975	.036	+ .001
−0.109	− .076	− .005	3.056	.031	− .004
−0.096	− .090	− .005	3.156	.035	.000
−0.090	− .089	+ .001	3.327	.029	− .006
−0.071	− .096	+ .001	3.420	.028	− .007
−0.054	− .093	+ .004	3.646	.018	+ .001
−0.039	− .103	− .006	3.685	.003	− .005
−0.028	− .098	− .001	3.712	.004	+ .001
−0.015	− .093	+ .004	3.748	− .001	− .004
−0.003	− .099	− .002	3.812	+ .007	+ .004
+0.007	− .102	− .005	3.837	.004	+ .001
0.020	− .091	+ .006	3.871	.001	− .002
0.031	− .094	+ .003	3.891	.001	− .002
0.040	− .090	+ .007	3.922	.003	− .003
0.047	− .098	− .001	3.967	.013	− .002
0.054	− .103	− .006	4.005	.024	.000
0.070	− .103	− .006	4.044	.029	− .003
0.079	− .097	.000	4.078	.040	+ .005
0.090	− .092	− .002	4.096	.036	+ .001
0.114	− .063	+ .002	4.171	.043	+ .008
0.139	− .022	+ .008	4.470	.032	− .003
0.154	− .013	− .003	4.629	.032	− .003
0.171	+ .011	+ .001	4.649	.046	+ .011
0.182	.019	− .003	4.774	.042	+ .007
0.202	.022	− .013	4.978	.039	+ .004
0.222	.035	.000	5.143	.032	− .003
0.277	.030	− .005	5.456	.037	+ .002
0.391	.039	+ .004	5.627	.026	− .009
0.630	.041	+ .006	5.698	.035	.000
1.025	.035	.000			

close binaries. From the observations between minima we have the constants in Table III. It is to be remembered that these constants are the actual observed quantities, and include the light of the visual component B, which is assumed to be 4.4 magnitudes

fainter than A, and hence gives 1/60 of the light of the eclipsing system. In the further work this extra light has been duly allowed for.

Preliminary circular elements were found by Russell's method, and then the transition to an elliptical orbit was accomplished in

TABLE III

	Magnitude	Range	Light	Loss
Maximum	$+0^{M}.035$		1.000	
Primary minimum	-0.097	$0^{M}.132$	0.886	0.114
Secondary minimum	$+0.003$	0.032	0.971	0.029

TABLE IV

ELEMENTS OF 1 H. CASSIOPEIAE

		Photometric	Spectroscopic
Minimum, J.D. 242		8224.822	8224.798
Period	P	$6^{d}.06630$	$6^{d}.067 \pm 0^{d}.0005$
Phase of secondary minimum		$3^{d}.81$	$3^{d}.89$
Time of periastron	T	$-0^{d}.5454$	$-1^{d}.036$
Longitude of periastron	w	$37^{\circ}.25$	$3^{\circ}.35 \pm 8^{\circ}.17$
Eccentricity	e	0.25	0.224 ± 0.025
Compound of eccentricity	$e \cos w$	0.199	0.224
Ratio of radii of bodies	k	0.346	
Light of first body	L_1	0.970	
Light of second body	L_2	0.030	
Ratio of surface brightnesses	J_1/J_2	3.9	
Radius of first body	a_1	0.192	
Radius of second body	a_2	0.066	
Cosine of inclination	$\cos i$	0.096	
Mean density of system	ρ_0	0.049	

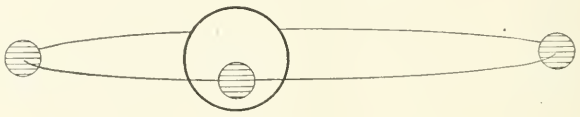
Assumption, $m_1 + m_2 = 10\odot$

		Sun = 1	
Mass of first body	m_1	7.7	
Mass of second body	m_2	2.3	
Radius of first body	a_1	5.8	
Radius of second body	a_2	2.0	
Density of first body	ρ_1	0.039	
Density of second body	ρ_2	0.28	

the manner indicated by him, except that the square of the eccentricity, $e = 0.25$, may not be neglected. However, only a couple of trials were necessary to secure a satisfactory approximation. Complete elements were derived from the light-curve so as to

have an independent set for comparison with the spectroscopic results.

From the light measures alone there are two solutions, one with a small faint star, $k=0.346$, in front at primary minimum, and the other with much greater difference in size, $k=0.18$, and with total eclipse of the smaller and brighter star at primary. The greatest difference between the corresponding light-curves is only $0^{M}003$, and we must depend upon the spectroscopic evidence for a decision. This is quite definite, for there is only one spectrum visible on the plates, and it is that of the component which is eclipsed at primary minimum, when only one-ninth of the combined light is lost. The second solution is therefore impossible, and we have a system in which the large star is the more intense,



○ The Sun

FIG. 3.—The system of 1 H. Cassiopeiae

while the companion has about one-third the diameter and one-fourth the surface-brightness of the main body. The photometric elements, together with a comparison with the corresponding spectroscopic results, are in Table IV.

The light elements in Table IV are represented by the system in Figure 3, and the final light-curve was computed rigorously from the positions in the elliptical orbit and the geometrical relations of overlapping disks.

In comparing the photometric and spectroscopic results we must remember that in the nature of the case the two methods are of different relative advantage, depending upon which element is concerned. Taking up first the time of minimum, the difference of 0.024 day corresponds to less than 2 km/sec. in the velocity-curve, a very good agreement. The period is much the better determined by the light measures, as the change during increasing or decreasing light at primary is quite rapid. In the phase of secondary minimum there is a large discrepancy, shown in Figure 3, and it is quite impossible to bring the two results into agreement.

The time of periastron T depends upon the adopted value of ω, and need not be discussed further.

The elements e and ω are fixed by the phase and duration of the secondary minimum; in particular $e \cos \omega$ is very accurately determined by the light-curve, and the photometric result is here of much greater weight, though it differs from the spectroscopic value by just the probable error of the latter. For the other component, $e \sin \omega$, we should expect the spectroscopic measure

TABLE V

LIGHT-CURVE

Phase	1 − 1 H.	Phase	1 − 1 H.
±0d00.....	−0M097	3d62.....	+0M023
±0.080.....	− .097	3.66.....	.014
±0.10.....	− .082	3.70.....	.006
±0.12.....	− .056	3.734.....	.003
±0.14.....	− .029	3.884.....	.003
±0.16.....	− .003	3.92.....	.006
±0.18.....	+ .020	3.96.....	.014
±0.20.....	.034	4.00.....	.023
±0.204.....	.035	4.04.....	.031
+3.546.....	.035	4.073.....	.035
3.58.....	.031	5.986.....	.035

to be superior, but for $\omega = 3°.35$ the secondary minimum should be almost of the same duration as the primary, whereas this seems quite impossible in the light-curve. I have computed a velocity-curve using the photometric values $e = 0.25$, $\omega = 37°$, together with the semi-amplitude $K = 58.5$ km/sec. found by Baker. This curve differs on the average from his by about 5 km/sec. and increases the sum of the squares of the residuals to about threefold the value in the original. Consequently, unless there is some unknown source of error in the velocity measures this alternative orbit must be ruled out.

We therefore seem forced to the conclusion which perhaps we should have assumed as true in the first place, namely, that the line of apsides is rotating. This explanation has been overworked to account for changes in the periods of other variable stars like Algol, but, as has been said, it would be more surprising if the major axis of the orbit were stationary than if it were in motion. Fortunately there is no particular difficulty in the case of this star.

The eccentricity of 0.25 is the largest of any eclipsing system that has come to my attention, and a new series of spectrograms should easily determine whether or not there is any change in the orbit.

The remaining elements of Table IV down to the masses were found in the usual way. The spectroscopic mass-function,

$$\frac{m_2^3 \sin^3 i}{(m_1+m_2)^2}=0.12,$$

combined with a reasonable assumption for the total mass, m_1+m_2, gives the actual masses and dimensions of the system. It is well known that the average star of spectrum B3 is more massive than the sun. Russell[1] found for the total mass of systems where the brighter component is of spectrum Bo–B5 the following averages:

	Number of Stars	Mass
Spectroscopic binaries	13	17.5⊙
Physical pairs	8	10.4⊙
From parallactic motions	36	7.1⊙

He made an allowance for the probable average inclination of the orbits. In Ludendorff's list[2] of spectroscopic binaries with two measurable components, nine stars give

$$(m_1+m_2) \sin^3 i=10.5 \odot .$$

It therefore does not seem much of an exaggeration to assume that the system of 1 H. Cassiopeiae has the round figure of ten times the mass of the sun. If it be objected that there is an observational preference for spectroscopic binaries of large velocity-variation and hence of large mass, it is still true that 1 H. Cassiopeiae is simply one of these stars for which there is such preference. In any event, since the hypothetical dimensions vary as the cube root of the assumed mass, we have a good approximation as to the scale of this system.

It is to be noted that the companion is much more dense than the primary; in fact, the formerly used assumption of equal density for the components of a close binary would give with the spectroscopic mass-function a total for the system of nearly two thousand times the mass of the sun.

[1] *Publications of the American Astronomical Society*, 3, 327, 1917.

[2] *Astronomische Nachrichten*, 211, 105, 1920.

DARKENING AT THE LIMB

The observations furnish a very good test of the darkening at the limb of the brighter star. It is evident from Figure 2 that there is no measurable variation during the annular eclipse at primary minimum, whereas by close approximation it is found that for a completely darkened star the difference would be $0^{M}.033$ between internal contact and conjunction. For the sun Abbot gives the intensity at the edge about one-fourth that at the center, measured in light of 4560 A, which is close to the maximum sensitivity of the potassium cell. For a star of this degree of darkening the variation during the annular eclipse would be $0^{M}.026$. Either of these amounts of variation should be easily detected, as there are fourteen normal magnitudes during the constant light, with a probable error of one normal equal to $\pm 0^{M}.0023$, or more than ten times smaller than the quantity to be observed.

It seems therefore that there is no evidence whatever of darkening at the limb in this star of spectrum class B3. Since the darkening effect is conspicuous for the sun, it seems plausible from this result and from other considerations to expect that there is progressive darkening in the spectral types, ranging from almost nothing in the B stars to extreme effects in classes K and M. For a number of years I have been trying to find an eclipsing red star, but as is well known there are very few spectroscopic binaries of short period and "late" types of spectrum. Somewhere in space there must be such a star which as viewed from the earth has a companion which will conveniently move across the disk of the primary, but the probability of the early discovery of such a case by present methods seems small indeed.

I am indebted to Messrs. Elmer Dershem and C. C. Wylie for some of the observations described in this paper, and to Miss Iva Hamlin for many of the reductions; while any communication on photo-electric photometry should be ascribed in part to my colleague, Dr. Jakob Kunz, whose long collaboration in the physics laboratory was the preliminary to all of our work at the telescope. I also return my thanks to the Draper Committee of the National Academy of Sciences for grants in support of this and other similar investigations.

UNIVERSITY OF ILLINOIS OBSERVATORY
June 1920

MUTUAL INFLUENCE OF FRAUNHOFER LINES

By W. H. JULIUS

ABSTRACT

Dispersion theory of Fraunhofer lines.—This theory, which assumes that the lines are almost entirely the effect of anomalous refraction and scattering, was developed by the author some years ago and led to the prediction and discovery of the mutual influence of neighboring Fraunhofer lines for which conclusive *evidence* is presented in the paper. The existence of this effect, not otherwise explained as yet, is considered by the author to powerfully support this theory. He concludes that anomalous dispersion is a most effective, perhaps the only, cause of the entire *limb-center shifts* and must, therefore, also produce *center-arc shifts*. If so the *gravitational shift* required by the general relativity theory may not exist.

Mutual influence of neighboring Fraunhofer lines.—Of the 866 lines for which the limb-center shifts were measured at Mt. Wilson in 1910 or at Kokaikanal Observatory in 1914–16, 128 have close companions which may be expected on theoretical grounds to influence their position. A study of the observations shows that there is, without doubt, a mutual influence equal, on the average, to 2/5 of the normal limb-center shift, a companion on the violet side causing an increase, a companion on the red side a decrease, of the shift.

1. REMARKS ON THE INTERPRETATION OF THE SPECTRA OF CELESTIAL BODIES

Since Kirchhoff's brilliant discovery we have known that the dark and bright lines in the spectra of heavenly bodies reveal to us the presence in them of those elements which on earth are characterized by the same lines. The overwhelming number of coincidences of Fraunhofer lines with lines of spectra produced in the laboratory leaves no doubt as to the validity of this inference.

By no means equally safe is the conception, tacitly admitted at the same time and accepted as a fundamental truth in astrophysics, that the bright lines of cosmical spectra are entirely due to specific emission, the dark lines to selective absorption, of light by the gases we recognize in the spectra. It was shown, indeed, in 1900[1] that bright as well as dark lines may also appear as a result of anomalous dispersion by refracting media, not only in laboratory experiments, but also under conditions very likely to obtain in large gaseous bodies. In 1904[2] we proposed the name *dispersion*

[1] W. H. Julius, *Proceedings of the Royal Academy of Amsterdam*, **2**, 580, 1900; *Astrophysical Journal*, **12**, 191, 1900.

[2] *Proceedings of the Royal Academy of Amsterdam*, **7**, 134, 140, 323, 1904; *Astrophysical Journal*, **21**, 271, 278, 286, 1905.

bands or *dispersion lines* for this new type of spectral phenomena, and have since made them the subject of extensive investigations in the Physical Laboratory of the University of Utrecht.[1]

The wave-lengths involved in the production of dispersion lines do not in general coincide with those corresponding to the free periods characteristic of the elements constituting the refracting medium, but often differ so little from them that dispersion lines may easily be mistaken for emission or absorption lines, the more so as several causes are known by which *real* emission or absorption lines appear widened and slightly displaced.

Various considerations concerning a great number of solar phenomena have led us to introduce the hypothesis that the irregular distribution of the different kinds of light on and around the solar disk is chiefly dependent on anomalous refraction and scattering, and that the darkness of the lines in the solar spectrum is almost entirely due to the same occurrence, so that we may presuppose that *Fraunhofer lines are mainly dispersion lines.*

This hypothesis has of course met with severe criticism and opposition, for, if it should prove to be inevitable, many problems of astrophysics would appear under a new light and require remodeling.[2] It was quite reasonable that these somewhat revolutionary ideas should be looked upon with skepticism so long as the observed phenomena could also be accounted for by current theories.

As, however, the above-stated hypothesis recommended itself from many points of view, we have been in search of such phenomena as might easily be explained by it and would leave the old interpretation of the solar spectrum hopelessly inadequate.[3]

[1] *Astrophysical Journal*, **25**, 95, 1907; *Proceedings of the Royal Academy of Amsterdam*, **12**, 266, 1909; *Astrophysical Journal*, **31**, 419, 1910; *Le Radium*, **7**, October, 1910; *Proceedings of the Royal Academy of Amsterdam*, **13**, 881, 1263, 1911; *The Observatory*, **37**, 252, 1914; *Astrophysical Journal*, **40**, 1, 1914; **43**, 43, 1916; *Archives neerlandaises* (III A), **4**, 51, 150, 1917; **5**, 116, 1918. Cf. also the inaugural dissertations by Dr. B. J. van der Plaats, Utrecht, 1917 (also published in *Archives neerlandaises* [III A], **5**, 132), and by Dr. P. H. van Cittert, Utrecht, 1919.

[2] In the *Astrophysical Journal*, **43**, 43, 1916, we have discussed the principal objections made, up to that time, against an extended application of anomalous dispersion in astrophysics.

[3] It may here be remembered that the general displacements of Fraunhofer lines toward the red exhibit certain features for which neither pressure nor motion can

Thus we were led to the discovery of mutual influence of neighboring Fraunhofer lines, a phenomenon required by the anomalous dispersion theory, but not explainable if Fraunhofer lines are assumed to be mere absorption lines.

2. PREVIOUS WORK ON MUTUAL INFLUENCE

The predicted effect depends on the degree of distortion which the dispersion-curve around a line suffers when another line is near.[1] If such a distortion really gives rise to a sensible change in the distribution of the light in a line (manifesting itself as a small variation of the displacement of its "center of gravity"), we may conclude that anomalous dispersion is the dominating factor in the production of the entire width of the line. The other assumption, indeed, that in the production of the lines anomalous dispersion should only be insignificant, or of secondary importance, would exclude the perceptibility of a universal effect caused by a mere distortion of the dispersion curve. We shall revert to this inference at a later stage.

Considering the way in which, according to our theory, dispersion lines originate and influence each other (as illustrated by the diagram in *Astrophysical Journal*, **43**, 51, 1916), it is easily realized that we shall be dealing with displacements amounting to only small fractions of the widths of the lines. In a search after mutual influence the very best measurements made with the most powerful instruments had therefore to be examined.

The result of our first attempt to detect the phenomenon in St. John's measurements of the Evershed effect in sun-spots, although positive,[2] was not sufficiently convincing, owing to the difficulty of correctly estimating "normal" displacements. St. John,[3] indeed,

account, and only the dispersion theory affords a direct explanation free from additional hypotheses. Such features are: the great disparity of the displacements on the one hand, and, on the other hand, the simple law connecting the displacement with the intensity of the lines when *mean* values of the displacement for each intensity class are compared (*Astrophysical Journal*, **40**, 27–29, 1914; *Archives neerlandaises* [III A], **4**, 59, 1917).

[1] Julius, *Astrophysical Journal*, **40**, 11, 1914; **43**, 50, 1916.

[2] *Ibid.*, **40**, 1, 1914; *Archives neerlandaises* (III A), **4**, 51, 1917.

[3] *Astrophysical Journal*, **41**, 28, 1915; *Mt. Wilson Contr.*, No. 93.

concluded from his own measurements (supplemented for the purpose) that there was not the slightest indication of mutual influence of Fraunhofer lines.

Then followed two papers on the subject by S. Albrecht,[1] in which it was shown that, in the general solar spectrum, iron lines, having close companions, are systematically displaced, in perfect accordance with the requirements of the theory of anomalous dispersion.

We have called attention to the fact that this positive result was compatible with St. John's above-mentioned negative conclusion (which may prove untenable in future) because in the Evershed effect mutual influence is of a somewhat different nature[2] and generally will produce smaller variations of the displacements there than in the case studied by Albrecht, where wave-lengths of Rowland's tables are compared with wave-lengths derived from international standards.

In a paper entitled "Observational Evidence That the Relative Positions of Fraunhofer Lines Are Not Systematically Affected by Anomalous Dispersion,"[3] St. John again vigorously defended the old standpoint. Controlling and supplementing by new measurements the work of Albrecht, he found the principal facts mentioned by that author generally confirmed,[4] but rejected their interpretation on the basis of anomalous dispersion. He substituted an explanation according to which the apparent repulsion was considered to be due to systematic "errors" in Rowland's wave-length determinations, occurring wherever close pairs of lines had been measured, and probably caused by inequality of contrast on the two sides of either line. This view he founded on the following observation. When remeasuring such pairs on negatives, specially prepared on Mount Wilson so as to give the clearest possible separation of the components, St. John found the alleged repulsions to be smaller or even absent.

In our opinion this result furnishes no proof whatsoever against the real existence of mutual influence, because the method by which

[1] *Astrophysical Journal*, 41, 333, 1915; 44, 1, 1916.

[2] Julius, *Astrophysical Journal*, 43, 40, 1916.

[3] *Astrophysical Journal*, 44, 311, 1916; *Mt. Wilson Contr.*, No. 123.

[4] *Ibid.*, p. 23.

those "most suitable" plates have been obtained has very likely led to a partial effacement of the asymmetrical dispersion lines leaving mainly their cores visible, which are not displaced (the Larmor effect[1] being imperceptible). That an overestimation of the distance of the components of narrow pairs by Rowland should only be an "error," an effect of contrast, and not a consequence of real asymmetry of the Fraunhofer lines, has not been proved by St. John. We have amply discussed these points in a paper on displacement of dispersion lines, communicated to the Amsterdam Academy at the meeting of March 31, 1917.[2]

Royds[3] objected to Albrecht's method that the wave-lengths compared by that author for determining the displacements had been measured on different plates. He himself, therefore, used the measurements of Evershed and Royds concerning plates on which terrestrial and Fraunhofer lines could be directly compared, and found that 17 lines with companion on the red side gave a mean sun-arc displacement toward the red of only 0.0032 A, whereas 30 lines with a companion on the violet side gave a mean displacement toward the red of 0.0079 A. This result confirms substantially Albrecht's conclusions; Royds nevertheless rejects the explanation, considering the differences too small, but offers no other solution.

In *Kodaikanal Bulletin* No. 49, 155, 1916, Evershed and Royds allude with some reluctance to the possible utility of taking anomalous dispersion into account; yet they assert that principle to be ruled out as an effective agent in displacing solar lines, because they believe that a close agreement in the separations of arc and solar double lines has been sufficiently proved.

A. S. King[4] went still farther in the negation of anomalous dispersion as a cause of line displacement. He concluded, from a study with the electric furnace under conditions which he believed

[1] J. Larmor, *The Observatory*, **39**, 103 and 230, 1916.

[2] Julius, *Archives neerlandaises* (III A), **5**, 116, 1918.

[3] *Bulletin of Kodaikanal Observatory*, No. 48.

[4] *Proceedings of the National Academy of Science*, **2**, 461, 1916; *Communications from the Mount Wilson Observatory*, No. 31; *Astrophysical Journal*, **45**, 254–268, 1917; *Mt. Wilson Contr.*, No. 130.

to be very favorable for the appearance of mutual influence if there were any, that even then no trace of such an effect was found. I have shown,[1] however, that King misunderstood the nature of the expected effect. His experiments and conclusions did not bear on "dispersion lines." If he had first produced true dispersion lines, he would have found—as I did in 1906, and B. J. van der Plaats, using an improved method, in 1917—that displacements and mutual influence of such lines may be demonstrated at will.

It remained, nevertheless, desirable to establish the existence of mutual influence of Fraunhofer lines in cases where neither personal error nor photographic effects nor complication with possible errors in the determination of terrestrial wave-lengths could have systematically distorted the result of the measurements.

3. MUTUAL INFLUENCE OF FRAUNHOFER LINES AS APPEARING IN THE LIMB-CENTER DISPLACEMENT.

Adequate material for our purpose is to be found in W. S. Adams' measurements, made on Mount Wilson, of the displacements of 467 lines in the spectrum of the sun's limb as compared with the spectrum of the center of the disk,[2] and in similar data concerning 399 lines obtained at the Kodaikanal Observatory by J. Evershed, T. Royds, and A. A. Narayana Ayyar.[3]

With very few exceptions these lines are, in the limb spectrum, shifted toward the red with respect to their positions in the central spectrum. Limb-center shifts are of the same order as center-arc shifts; on the average, they are a little larger. Evershed has convincingly shown that these displacements cannot be due to pressure, while the explanation proposed by himself, based on Doppler effect and requiring the existence of a specific repulsive force exerted by the earth on the solar gases, appears inacceptable. As it is also inconceivable that difference of gravitational potential should play any perceptible part in this limb-center phenomenon, we have anomalous dispersion left as the only basis on which to explain it.

[1] *Archives neerlandaises* (III A), **5**, 116, 1918.

[2] *Astrophysical Journal*, **31**, 30, 1910; *Mt. Wilson Contr.*, No. 43.

[3] Evershed and Royds, *Bulletin of Kodaikanal Observatory*, No. 39, 1914; Narayana Ayyar, *ibid.*, No. 44, 1914; Royds, *ibid.*, No. 53, 1916.

Assuming Fraunhofer lines to be dispersion lines which in general are more developed on their side facing toward the red[1] (owing to n_0 being, as a rule, >1), we have shown elsewhere that the apparent displacements of those lines with respect to the positions of their cores must increase from the center of the solar disk toward the limb. (The opportunity, indeed, for the light that comes from an incandescent solar core to be irregularly refracted and scattered by the gaseous envelope increases as we approach the limb.) The difference between the spectrum of the limb and the spectrum of the center may therefore be an almost pure dispersion-effect, all other causes of line-displacements at present known failing to require a systematic increase from the center of the disk outward.

It was an important and a delicate question how to select from the Mount Wilson and Kodaikanal tables those lines for which, from the point of view of the dispersion theory, an excess or a deficiency of displacement toward the red was to be expected. In collaboration with Dr. P. H. van Cittert, chief assistant at the physical laboratory, and Dr. M. Minnaert, principal observer in the heliophysical department, we agreed on the following procedure.

The columns containing the observed displacements were covered with strips of paper, in order to avoid that the choice might be influenced by a previous knowledge of the results of the measurements. Then the region surrounding every line occurring in the original tables was inspected on the atlases of Rowland and of Higgs in order to ascertain whether the line might be presumed to have an "effective" companion. The criteria for effectiveness employed by us will be mentioned on page 106.

In the first column of our Tables I and II we entered the wavelengths and elements, in the second column the intensities[2] of those lines of the original lists which we suspected to be appreciably influenced by neighboring lines. The Mount Wilson and the Kodiakanal data have been kept separate because it was inter-

[1] For a systematic deduction of the properties of Fraunhofer lines from the dispersion theory we must especially refer to *Proceedings of the Royal Academy of Amsterdam*, 12, 279, 1909; *Astrophysical Journal*, 31, 419, 1910; *Le Radium*, 7, October, 1911; *Proceedings of the Royal Academy of Amsterdam*, 13, 881, 1911.

[2] The intensities apply to the spectrum of the *center* of the disk, as given by Rowland.

esting to compare the results given by two entirely independent series of observations. The next four columns contain the data concerning neighboring lines, the third and fourth referring to companions on the violet side, the fifth and sixth to companions on the red side; the distances $\lambda - \lambda_v$ and $\lambda_r - \lambda$ of these companions from the lines of the first column, and their intensities, are taken from Rowland's wave-length tables. The figures of the seventh column refer to the criteria and considerations used to decide on the probable effectiveness of the companions; the resulting

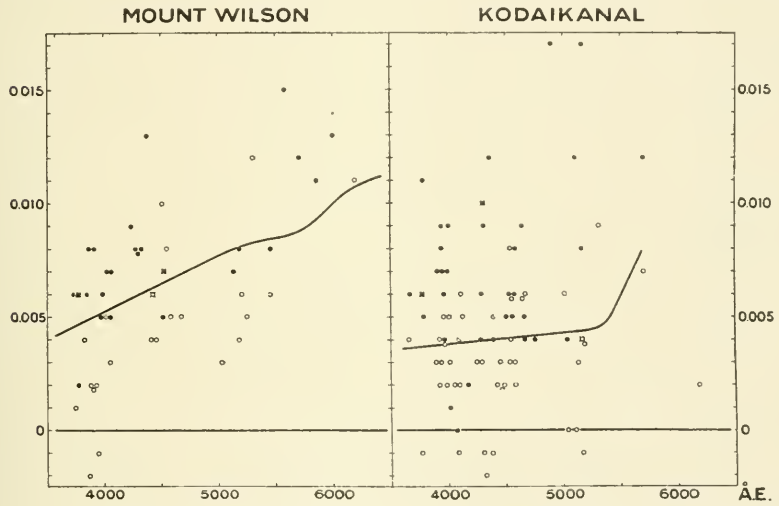


FIG. 1.—Diagram showing displacements of 128 lines having a close companion on the violet side (full dots) or on the red side (circles).

forecast is indicated by *V*, or *R*, or — in the eighth column, meaning that we expect a repulsion from the violet side, or from the red side, or no effect. In the ninth and tenth columns are given the observed displacements δ_v and δ_r, expressed in 0.001 A, for the cases *V* and *R* separately. They are plotted in Fig. 1, where full dots represent the displacements of lines with companion on the violet side, circles those of lines with companion on the red side.[1]

That *the full dots average higher than the circles* is obvious at a glance.

[1] Four dots and two circles, distinguished by a cross (×), would fall out if criteria 7 and 9 were not applied.

TABLE I

MUTUAL INFLUENCE OF FRAUNHOFER LINES AS APPEARING IN LIMB-CENTER DISPLACEMENTS OBSERVED ON MOUNT WILSON, 1910

Probably Influenced Lines			Companions				Criteria Used	Expected Repulsion From Violet or Red Side	Displacement (in 0.001 A)			$D_v=\frac{\delta_v-\delta_m}{\delta_m}$		$D_r=\frac{\delta_r-\delta_m}{\delta_m}$	
			Violet Side		Red Side				Observed		Average				
λ	El.	i	$\lambda-\lambda_v$	i	$\lambda_r-\lambda$	i			δ_v	δ_r	δ_m	+	−	+	−
3741.791	Ti	4	0.090	0				V	6		4.4	0.32			
3748.144	Ti	1			0.088 0.264	0 10	6	R		1	4.4				0.77
3778.203	Ni	2	0.128	0	0.098	0	3,4	—							
3778.939	C	1	0.098	3				V	2		4.6		0.57		
3783.674	Ni	6	0.191	2			7,9	V	6		4.6	0.30			
3792.824		2	0.036	0	0.145	2	4	—							
3801.511	C	1	0.072	0	0.168 0.309	0 3	4	—							
3829.501	Mg	10			0.116	2	9	R		−2	4.8				1.42
3834.364	Fe	10			0.142	4		R		4	4.8				0.17
3855.989	V	4	0.123 0.240	3 5	(0.018)	(00)	6	V	6		4.8	0.25			
3871.963	Fe	2	Blend				6	V	8		4.9	0.63			
3882.650	C	1	0.120	1	0.083	1	4	—							
3895.119	Co	3			0.105	1	3	R		2	4.9				0.59
3904.926	Ti	3			0.091 Blend	1	6	R		2	5.0				0.60
3916.545		3	0.162	2				V	8		5.0	0.60			
3921.563	Ti	1			0.132	4		R		2	5.0				0.60
3948.818	Ti, V	4			0.07	4		R		−1	5.0				1.20
3956.819	Fe	6	0.216	4	0.358	7	4	—							
3958.073	Co	2			0.282	5	3,(9)	—							
3984.294	Mn	2	0.181	4	(0.185)	(2)	10	V	5		5.2		0.04		
3995.463	Co	5	0.111	2				V	6		5.2	0.16			
3997.258	Cr?	1	0.143	2	0.289	4	4	—							
4012.541	Ti, Ce	4	0.142	1	0.090	0	3,4	—							
4014.420	Fe	1	0.456	5	0.257	5	3,4	—							
4024.726	Ti	3			0.155	4		R		5	5.2				0.04
4035.883		4	0.131	2			8,(c)	V	7		5.3	0.32			
4044.294	K	0	0.153	2			9	V	5		5.3		0.06		
4058 748	Ce	0			0.167	3		R		3	5.3				0.43

4059.081	Mn	3	0.166	3				*V*	7		5.3	0.32		
4167.884	C	1	0.147 0.446	1 8	0.141 0.249	2 2	4	—						
4238.970	Fe	1	0.050	0				*V*	9		5.7	0.58		
4288.310	Ti Fe	1	0.161 0.272	1 2			5, 6	*V*	8		5.9	0.35		
4299.149	Ca	3	0.182	2	0.147 0.261	1 4	4	—						
4300.211	Ti	3	0.076	0				*V*	8		5.9	0.35		
4315.262	Fe	4	0.124	3			5	*V*	8		6.0	0.33		
4385.548		2	Blend				5, 6	*V*	13		6.1	1.12		
4427.266	Ti	2			0.216	5	5	*R*		4	6.2			0.35
4435.129	Ca	5			0.192	2	7, 9	*R*		6	6.2			0.03
4469.316	Ti	1			0.229	4		*R*		4	6.3			0.36
4522.802		3			0.172	2		*R*		10	6.4		0.56	
4522.974	Ti	2	0.172	3				*V*	5		6.4	0.23		
4531.327	Fe	5	0.204	2			7	*V*	7		6.4	0.09		
4536.094	Ti	2	0.185 0.215	0 1	0.128	2	4, 6	—						
4549.642	Fe	2			0.166	6		*R*		8	6.5		0.22	
4592.707	Ni	2			0.133	4		*R*		5	6.6			0.24
4680.317	Zn	1			0.163	1	5, 6	*R*		5	6.9			0.28
4991.247	Ti	3			0.205	2	3	—						
5041.795	Ca	2			0.141	4		*R*		3	7.7			0.61
5139.644	Fe	4	0.217	4			3, 5, 9	*V*	7		7.9	0.11		
5167.497	Mg	15	0.043	3	0.181	5	2	—						
5188.863	Ti	2			0.155	3	5, 9	*R*		4	8.0			0.50
5189.018	Ca	3	0.155	2			5, 9	*V*	8		8.1	0.01		
5208.596	Cr	5			0.180	2		*R*		6	8.2			0.26
5265.729	Ca	3			0.164	2		*R*		5	8.2			0.38
5316.790	Fe	4			0.116 0.168	0 2	5, 6, 9	*R*		12	8.3		0.44	
5455.671	Fe?	2			0.163	4		*R*		6	8.4			0.29
5455.834	Fe	4	0.163	2				*V*	8		8.4	0.05		
5514.753	Ti	2	0.190	2			3	—						
5594.884	Fe	1	0.193	4				*V*	15		8.6	0.74		
5709.775	Ni	5	0.174	5			9	*V*	12		8.8	0.36		
5857.976	Ni	3	0.302	8			3	*V*	11		9.2	0.19		
6020.401	Fe	4	0.169	2				*V*	13		10.1	0.30		
6191.393	Ni	6			0.386	9	7, 9	*R*		11	10.8		0.02	
Total.....												7.31—1.08	1.24—9.12	

TABLE II

MUTUAL INFLUENCE OF FRAUNHOFER LINES AS APPEARING IN LIMB-CENTER DISPLACEMENTS OBSERVED AT KODAIKANAL OBSERVATORY, 1914–1916

PROBABLY INFLUENCED LINES			COMPANIONS				CRITERIA USED	EXPECTED REPULSION FROM VIOLET OR RED SIDE	DISPLACEMENT (in 0.001 A)			$D_v=\frac{\delta_v-\delta_m}{\delta_m}$		$D_r=\frac{\delta_r-\delta_m}{\delta_m}$	
			Violet Side		Red Side				Observed		Average				
λ	El.	i	$\lambda-\lambda_v$	i	$\lambda_r-\lambda$	i			δ_v	δ_r	δ_m	+	−	+	−
Kodaikanal Bulletin, No. 39															
3928.075	Fe	8			0.156	2	9, 7	R		2	3.7^s				0.47
3935.965	Fe	2	(0.178)	(0)	0.156	2		R		4	3.7^s			0.07	
3948.925	Fe	4	0.107	4	(0.114)	(1)		V	8		3.7^s	1.13			
3966.212	Fe	3	0.143	2				V	4		3.8	0.05			
3998.205	Fe	4	0.152	4				V	7		3.8	0.84			
4009.864	Fe	3	0.057	1				V	9		3.8	1.37			
4076.792	Fe	4	0.148	2	0.167	2	4	—							
4118.708	Fe	5			0.226 0.342	4 2	6, 7	R(?)		6	3.8^s			0.56	
4127.767	Fe	4			0.190	4		R		5	3.8^s			0.30	
4308.081	Fe	6	0.174	3			7, 9	V	10		3.9^s	1.53			
4315.262	Fe	4	0.124	3			5	V	9		3.9^s	1.28			
4369.941	Fe	4	0.068	0			9	V	12		4.0	2.00			
4592.840	Fe	4	0.133	2				V	6		4.1	0.46			
4654.672	Fe	4			0.128	5		R		6	4.1^s			0.45	
4654.800	Fe	5	0.128	4				V	9		4.1^s	1.17			
4667.626	Fe	4	(0.202)	(0)	0.124	3		R		6	4.1^s			0.45	
4903.502	Fe	5	0.058	0			5, 7, 9	V	17		4.2^s	3.00			
5107.619	Fe	4			0.204	4	3, 5	R		0	4.4				1.00

5107.823	Fe	4	0.204	4			3, 5	*V*	12		4.4	1.73	
5139.427	Fe	4			0.217	4	3,5, 9	*R*		3	4.4		0.32
5167.678	Fe	5	0.181	15			7, 9	*V*	17		4.4	2.86	
5169.069	Fe	3			0.151	4	9	*R*		−1	4.4		1.23
5169.220	Fe	4	0.151	3			9	*V*	8		4.4	0.82	
5316.790	Fe	4			0.168 0.116	2 0	5, 6, 9	*R*		9	4.6		0.98
Kodaikanal Bulletin, No. 44													
3949.039	Ca	1	0.221 0.114	4 4			6, 9	*V*	7		3.8	0.84	
4076.792	Fe	4	0.148	2	0.167	2	4	—					
4096.129	Fe	3			0.133	2		*R*		4	3.8^5		0.04
4098.689		4			0.057	2		*R*		2	3.8^5		0.48
4549.642	Fe	2			0.166	6		*R*		6	4.1		0.46
4581.575	Ca	4			0.118	4		*R*		3	4.1		0.27
4592.840	Fe	4	0.133	2				*V*	8		4.1	0.95	
5709.601	Fe	5			0.174	5	9	*R*		7	8.0^5		0.13
5709.775	Ni	5	0.174	5			9	*V*	12		8.0^5	0.49	
6191.393	Ni	6			0.386	9	7, 9	*R*		2	?		
Kodaikanal Bulletin, No. 53													
3662.096	Ni	3			0.212 0.283	1 5	6	*R*		4	3.6		0.11
3669.381	Ni	4	0.089	2				*V*	6		3.6^5	0.64	
3739.370	Ni	3	0.110	2	0.097	1	4	—					
3772.673	Ni	2			0.057	1		*R*		−1	3.6^5		1.27
3778.203	Ni	2	0.128	0	0.098	0	3, 4	—					
3783.674	Ni	6	0.191	2			7, 9	*V*	6		3.7	0.62	
3792.482	Ni	1	0.188	3				*V*	5		3.7	0.35	
3793.745	Ni	4	0.083	2				*V*	11		3.7	1.97	
3909.064*	Ni	1	0.164	4				*V*	7		3.7^5	0.87	
3970.631	Ni	1	0.091	2				*V*	6		3.7^5	0.60	
3972.313	Ni	2			0.094	1		*R*		4	3.8		0.05

* Not ascribed to nickel by Rowland.

TABLE II—*Continued*

Probably Influenced Lines			Companions				Criteria Used	Expected Repulsion from Violet or Red Side	Displacement (in 0.001 A)			$E_v=\frac{\delta_v-\delta_m}{\delta_m}$		$D_r=\frac{\delta_r-\delta_m}{\delta_m}$	
			Violet Side		Red Side				Observed		Average				
λ	El.	i	$\lambda-\lambda_v$	i	$\lambda_r-\lambda$	i			δ_v	δ_r	δ_m	+	−	+	−
3972.702	Ni, Zr	3			0.094 0.162	1 2	5, 9	R		5	3.8			0.32	
3974.774	Ni	2	0.137 0.238	2 3	0.130	6	4	—							
4006.304	Ni	1			0.160	2		R		5	3.8			0.32	
4017.724	Ni?	1	0.104	2				V	1		3.8		0.74		
4064.515	Ni	1			0.092	2		R		2	3.8^5				0.48
4086.283*	Ni	0			0.186	3		R		−1	3.8^5				1.26
4142.465*	Ni	2	0.135	2	0.164	2	4	—							
4184.641*	Ni	0	0.169	2				V	2		3.9		0.49		
4195.684*	Ni	1	0.192	5	0.101	2	4	—							
4288.149	Ni	1	0.111	2	(0.161)	(1)		V	4		3.9^5	0.01			
4296.044	Ni	1	0.130	2				V	6		3.9^5	0.52			
4325.777*	Ni	1			0.162	8	9	R		−2	3.9^5				1.51
4384.698	Ni	0	(0.221)	(1)	0.175	3		R		−1	4.0				1.25
4399.776	Ni	0			0.161	3		R		5	4.0			0.25	
4401.709	Ni	2	0.253 0.096	2 1			5	V	4		4.0	0.00			
4459.199	Ni	2			0.102	3		R		3	4.0^5				0.26
4466.548	Ni	0			0.181	5		R		2	4.0^5				0.51
4547.101	Ni	1			0.091	2	5	R		4	4.1				0.02
4592.707	Ni	2			0.133	4		R		2	4.1				0.51
4667.941	Ni	1	0.173	3				V	5		4.1^5	0.20			
4762.820	Ni	1	0.253	5				V	4		4.2		0.05		
5018.463	Ni	1			0.166	4		R		6	4.3^5			0.38	
5038.774	Ni?	2	0.195	2			5	V	4		4.3^5		0.08		
5142.958	Ni	2	0.265	4	0.253	3	4	—							

5168.832	Ni	1			{0.388 / 0.237}	{4 / 3}	5, 6, 9	*R*		4	4.4		0.09
3904.926	Ti	3	(0.159)	(0)	0.091	1	6	*R*		3	3.7^5	1.40	
3947.918	Ti	2	{0.088 / 0.243}	{1 / 4}			6	*V*	9		3.7^5		0.20
3948.818	{Ti / V}	4			0.107	4		*R*		3	3.7^5		0.20
3964.416	Ti	2	0.090	1	0.247	3	4	—					
3989.912	Ti	4			0.099	3		*R*		2	3.8		0.47
4024.726	Ti	3			0.155	4		*R*		3	3.8		0.21
4078.631	Ti	3	0.116	4			5	*V*	0		3.8^5	1.00	
4274.746	Ti	2			0.212	7	9	*R*		3	3.9^5		0.24
4298.828	Ti	2			{0.139 / 0.321}	{2 / 3}	6	*R*		3	3.9^5		0.24
4314.964	Ti	1			{0.174 / 0.293}	{3 / 4}	6	*R*		−1	3.9^5		1.25
4427.266	Ti	2			0.216	5	5	*R*		2	4.0		0.50
4489.262	Ti	0			0.089	2		*R*		2	4.0		0.50
4522.974	Ti	2	0.172	3				*V*	5		4.0^5	0.23	
4535.741	Ti	3			0.138	1	5, 6	*R*		3	4.0^5		0.26
4536.094	Ti	2	{0.185 / 0.215}	{0 / 1}	0.228	2	4, 6	—					
4536.222	Ti	2	0.128	2			5	*V*	5		4.1	0.22	
4544.864	Ti	3	0.076	1				*V*	6		4.1	0.46	
4552.632	Ti	2			0.093	1		*R*		8	4.1		0.95
4667.768	Ti	3	0.142	4				*V*	4		4.2	0.05	
5038.579	Ti	2			0.195	2	5	*R*		0	4.3^5		1.00
5188.863	Ti	2			0.155	3	5	*R*		4	4.4		0.09
Total.....												28.61—2.41	5.69—16.22

It should be remembered that, theoretically, for each individual dispersion line the magnitude of the displacement is not completely determined by the positions and intensities of its closest companions, but depends also on n_0 (the value which the refractive index of the medium would have for the examined region of the spectrum, if that special pair or group of lines were absent). As n_0 fluctuates along the spectrum, there will be a corresponding variation of the magnitude of the displacements, on which the effects of mutual influence of neighbors are superposed.[1] This explains the mutual penetration of the swarms of full dots and circles in Fig. 1.

Before proceeding to a numerical discussion of the result embodied in the diagram, we have still to mention the criteria used in selecting the lines.

1. By way of initial sifting we considered a line to be probably influenced if it had a companion of intensity i (Rowland scale) at a distance d or less, corresponding values of i and d being as in Table III:

TABLE III

i	d
0 and 1	0.1 A
2, 3, 4	0.2
5, 6, 7, 8	0.3
9 and higher	0.4

These limits served only as a general guide; we departed from them whenever one or more of the following cases were in evidence. (Criterion 1 having been applied to every line of Tables I and II, it was unnecessary to mention it in the seventh column.)

2. Lines of intensity >10 were omitted from the list of influenced lines, because they are only little subject to the general limb-center displacement ascribed by us to anomalous dispersion (cf. *Astrophysical Journal*, **40**, 28, 1914), and because from our point of view we cannot expect their degree of asymmetry to be sensibly changed by close neighboring lines.—Example: λ 5167.497, intensity 15, was not considered to be influenced by λ 5167.678, intensity 5.

[1] Cf. B. J. van der Plaats, *Dispersielijnen* (thesis, Utrecht, 1917), where the process is elucidated by experiments.

3. Deviation from the rigid limits of Table III was admitted when justified or demanded by special conditions. A companion, e.g., of intensity 5 at a distance of 0.30 A from the line under examination was considered effective only if other favorable circumstances could be indicated (cf. criteria 5, 6, 9); whereas a companion of intensity 8 was included even though its distance might be 0.31 or 0.32 A.—Example: λ 3958.073, intensity 2, was not considered to be influenced by λ 3958.355, intensity 5.

4. Lines presumed to be subject to nearly equal repulsions from opposite sides were canceled.—Example: λ 4076.792, intensity 4, influenced by λ 4076.644, intensity 2, and λ 4076.959, intensity 2, was excluded from the list.

5. If, on the other hand, a line is remarkably free from neighbors on one side, a companion on the other side may be expected to show a somewhat greater effect.—Example: λ 4469.316, intensity 1, is considered to be influenced by λ 4469.545, intensity 4, although the distance be >0.2 A.

6. Two or more companions on the same side of a line were supposed to join their effects; such a group might be considered effective even if the individual members were not.—Example: λ 4385.548, intensity 2, is included because influenced by a group of companions on the violet side, whereas its companions on the red side are few and much weaker.

7. Both the Mount Wilson and the Kodaikanal observations show that the limb-center displacements are greatest for lines of medium intensity. We therefore considered it also a favorable circumstance for a line to be sensibly repelled by a neighboring line, if the intensity of the influenced line is around 5 or 6.—Example: λ 4531.327, intensity 5, was taken to be influenced by λ 4531.123, intensity 2, though the distance is a little greater than 0.2 A.

8. Scarcely separable double lines were excluded from the list of influenced lines on account of the difficulties involved in determining their positions. Such double lines are: (*a*) lines resolved by Rowland, but treated as a whole by Adams (e.g., λ 4482.3, intensity 8, =λ 4482.338, intensity 5, +λ 4482.438, intensity 3); (*b*) lines with affix *d* in Rowland's table; (*c*) lines affixed by Rowland

with *d?*, which means "very difficult to separate"; among these, however, the line λ 4035.883 was included in the list because Rowland, in a footnote, doubted its duplicity; (*d*) lines to which correspond, according to Rowland, two terrestrial lines belonging to different elements, but of scarcely different wave-lengths (indicated, e.g., thus: Ni–Fe). There are, however, *exactly* coinciding lines due to different elements (denoted, e.g., Ni, Fe by Rowland); these were of course not excluded if they had effective companions. The corrections and additions, published by Rowland in *Astrophysical Journal*, **2**, 384, 1897, were taken into consideration.

9. The influence exerted by slightly nebulous lines (indicated by *s* in Rowland's table) was supposed to a be little greater than that of sharp lines of the same intensity.—Example: λ 4435.129, intensity 5, was considered to be influenced by λ 4435.321, intensity 2, *s*, in spite of criterion 3 (but also on account of criterion 7).

10. As illustrated by the last example, one had to balance and compromise whenever more than one of the foregoing considerations were applicable.

The selection of the lines was first made independently by Dr. van Cittert and Dr. Minnaert, who thereupon compared their lists and deliberated on difficult or dubious cases. In the final checking of the tables I took part.

4. NUMERICAL DISCUSSION OF THE RESULTS

Even a superficial study of the diagram suffices to produce the conviction that mutual influence of Fraunhofer lines is a reality. Meanwhile it will be interesting to investigate how far the conclusions are corroborated on closer examination of the result. We shall therefore compare numerically the average influence of neighboring lines on the displacements with the mean limb-center shifts observed in the successive regions of the spectrum.

The two curves in our diagram show those mean displacements. To obtain these, we have plotted, at intervals of 100 A, the mean values of all limb-center shifts[1] measured by Adams and by the

[1] Lines of intensity > 10 have been omitted.

Kodaikanal observers, respectively, and drawn smooth curves through the points.[1]

In the eleventh columns of our Tables I and II are given the values δ_m of the ordinates of the curves at the places corresponding to the wave-lengths of the first column. The twelfth and thirteenth columns contain the values of the expressions

$$D_v = \frac{\delta_v - \delta_m}{\delta_m} \quad \text{and} \quad D_r = \frac{\delta_r - \delta_m}{\delta_m}.$$

These expressions were considered preferable to $\delta_v - \delta_m$ and $\delta_r - \delta_m$ as a measure of influence, since the gradual progressing of dispersion-effects with wave-length was thus eliminated. D_v and D_r are "relative departures" from the curve; we shall refer to them as "departures" simply.[2]

Addition of the numbers in columns 12 and 13 gives, for the Mount Wilson observations:

$$\Sigma D_v = +7.31 \text{ (18 lines)} - 1.08 \text{ (7 lines)} = +6.23 \text{ (25 lines)},$$
$$\Sigma D_r = +1.24 \text{ (4 lines)} - 9.12 \text{ (19 lines)} = -7.88 \text{ (23 lines)},$$
$$\Sigma D_v + \Sigma D_r = -1.65 \text{ (48 lines)},$$

which indicates that the group of influenced lines, as a whole, had a small negative departure:

$$-\frac{1.65}{48} = -0.0344.$$

[1] The rather great difference between the two curves is perhaps partly due to the different selection of the lines. Among the Kodaikanal lines more than 94 per cent belong to Fe, Ni, and Ti, the rest to Ca, Na, Si, Mg; whereas the Mount Wilson lines are taken from a greater variety of elements. The proportion of very weak lines (intensity 00, 0, and 1, showing as a rule small displacements) is 21.9% in the Kodaikanal, and only 12.4% in the Mount Wilson number of measured lines. It is also possible that the average magnitude of the displacements varies from year to year, following the spot-cycle.

[2] In a recent paper on "The General Relativity Theory and the Solar Spectrum" by W. H. Julius and P. H. van Cittert (*Proceedings of the Royal Academy of Amsterdam*, **23**, 522, 1921), in which a preliminary account was given of some of the results mentioned in this paper, we denoted the differences themselves as "departures." Our present procedure (in which, moreover, still greater care has been given to the selection of the lines) leads to somewhat improved numerical results, without, however, altering the character of the conclusions there attained.

Referring the individual departures to the average position of the *group*, we therefore have to apply the correction +0.0344 to each of them. This brings two of the negative values of D_v over to the positive side, and we obtain:

corrected $\Sigma D_v = +7.96$ (20 lines) -0.87 (5 lines) $= +7.09$ (25 lines),
corrected $\Sigma D_r = +1.38$ (4 lines) -8.47 (19 lines) $= -7.09$ (23 lines),

whence the mean departure for a line with violet companion is:

$$\bar{D}_v = \frac{+7.09}{25} = +0.284,$$

and the mean departure for a line with red companion:

$$\bar{D}_r = \frac{-7.09}{23} = -0.308.$$

We are now in a position to answer the following question: Suppose there were no systematic influence involved in the origin of these departures, what would be the probability for 25 lines, taken at random out of our group of 48 lines, to give a mean departure as great as 0.284, or for 23 lines to give -0.308?

The average value of the 48 corrected departures, irrespective of signs, is

$$\eta = \frac{18.68}{48} = 0.389;$$

the probable value, therefore, of a single departure is

$$r = \rho\sqrt{\pi}\cdot\eta = 0.8453 \times 0.389 = 0.329,$$

by which the "precision $h = \frac{\rho}{r} = \frac{0.47694}{r}$ of the group" is characterized.

Now, taking at random 25 cases out of our group, the measure of precision of their arithmetical mean is $h\sqrt{25}$, hence the probable departure of that mean will be $r_0 = \frac{r}{\sqrt{25}} = 0.066$.

Our actual selection, however, was not at random; we took 25 lines with companion on the violet side and found a mean departure

$$\bar{D}_v = +0.284 = 4.30\, r_0 .$$

Applying the same reasoning to the 23 lines with red companion, for which $r'_0 = \frac{r}{\sqrt{23}} = 0.068$, we obtain

$$\bar{D}_r = -0.308 = -4.50\, r'_0 .$$

Since r_0 and r'_0 differ very little, the probability for a departure to lie between $+4.30\, r_0$ and $-4.50\, r'_0$ will be nearly expressed by

$$\frac{2}{\sqrt{\pi}} \int_0^{4.4\rho} e^{-t^2} dt$$

(in which $\rho = hr_0 = 0.477$), the value[1] of this integral being 0.997. So there is only 0.003 left for the probability that, by mere chance, the two selected groups should be so widely separated as they really are.

The Kodaikanal observations, treated similarly, lead to the following equations:

$$\Sigma D_v = +28.61 \text{ (30 lines)} - 2.41 \text{ (6 lines)} = +26.20 \text{ (36 lines)},$$
$$\Sigma D_r = +\ 5.69 \text{ (15 lines)} - 16.22 \text{ (29 lines)} = -10.53 \text{ (44 lines)},$$
$$\Sigma D_v + \Sigma D_r = +15.67 \text{ (80 lines)},$$

whence correction: -0.1961.

$$\text{corrected } \Sigma D_v = +23.26 \text{ (27 lines)} - 4.11 \text{ (9 lines)} = +19.15 \text{ (36 lines)},$$
$$\text{corrected } \Sigma D_r = +\ 3.26 \text{ (11 lines)} - 22.42 \text{ (33 lines)} = -19.16 \text{ (44 lines)},$$

$$\bar{D}_v = +0.532 \qquad \bar{D}_r = -0.435$$

$$\eta = \frac{53.05}{80} = 0.564$$

$$r = \rho\sqrt{\pi}\cdot\eta = 0.477$$

$$r_0 = \frac{r}{\sqrt{36}} = 0.0795 \qquad r'_0 = \frac{r}{\sqrt{44}} = 0.0719$$

$$\bar{D}_v = +6.68\, r_0 \qquad \bar{D}_r = -6.05\, r'_0$$

$$\frac{2}{\sqrt{\pi}} \int_0^{6.36\rho} e^{-t^2} dt = 0.999990,$$

[1] Chauvenet, *Spherical and Practical Astronomy*, 2, Table IX A.

from which follows that in this series of observations there is left no more than 0.00001 for the probability of a purely accidental separation, as great as observed, between the two selected groups.

Since the Mount Wilson and Kodaikanal sets of data are mutually independent, the probability that they should both have given such a striking separation by mere chance is 0.003×0.00001.

We may therefore conclude that the actual existence of mutual influence of Fraunhofer lines has been proved with a probability of more than 10^7 to 1.

5. CONSIDERATIONS REGARDING POSSIBLE ERRORS

A few remarks may be added concerning the degree of certainty that our result reveals a real phenomenon and does not rest on errors of any kind.

Bias on the part of the observers on Mount Wilson and at Kodaikanal Observatory is excluded because, when writing down the displacements, they were not aware of a possible mutual influence of neighboring lines. The data used by us have the full authority of the best Mount Wilson and Kodaikanal observations.

There was of course some arbitrariness in the fixation of the criteria to be used for selecting the probably influenced lines, and in some cases differences of opinion on the application of the criteria will subsist; but reasonable alterations in the sifting process are not likely to alter materially the character of the result.

Uncertainties in the wave-lengths of arc lines (by which, e.g., Albrecht's results might have been influenced) are not involved in the limb-center displacements.

In earlier work on mutual influence the result depended on the accuracy obtainable in measuring the separation of close solar lines. Two opposite effects may affect the estimation of the distance between the centers of the components of the pair: the maxima approach each other by the partial superposition of the intensity-curves, whereas, on the other hand, inequality of contrast on the two sides of either component may lead to overestimation of the distance.

Evidently these errors do not enter to any appreciable degree in the limb-center shifts.

Indeed, let us assume that in the spectrum of the sun's center the distance between the components of a certain pair of lines appears exaggerated owing to an error of estimation. The distance may be, say, 0.3 A, and the apparent exaggeration caused by this nearness 0.003 A.

Let us next consider the same pair in the spectrum of the sun's limb. There both components are perhaps slightly shifted with respect to their positions in the spectrum of the center; but as these shifts are of the order of 0.005 A, the separation of the lines can scarcely be altered thereby more than, say, 1 or 2 per cent of its original value of 0.3 A. Consequently the influence which the proximity of the lines may have on the estimation of their distance must be practically identical in the two spectra: the exaggeration of the distance in the spectrum of the limb would also be 0.003 A. A mutual influence depending on errors of estimation will not appear in the limb-center differences.

Any photographic effect that might perhaps influence the measured distance between close solar lines would also be very similar in both cases, since the operators have always taken care to give equal average intensities to the spectra of the center and the limb by regulating the exposure times.

The well-established observation that neighboring lines are nevertheless more distant from each other in the spectrum of the limb than in the spectrum of the center must therefore represent a real phenomenon.

6. CONCLUSION

It appears from the preceding discussion that, in the process which causes the limb-center shift of a line, the presence of a close neighboring line must be very momentous. Indeed, taking the general mean, irrespective of signs, of the relative departures ΣD_v and ΣD_r for Mount Wilson, and ΣD_v and ΣD_r for Kodaikanal (relating to 128 influenced lines in all) we find:

$$\bar{D}=\frac{7.09+7.09+19.15+19.16}{128}=0.410.$$

This signifies that, on the average, the limb-center displacement of a line increases or decreases by two-fifths of its normal

amount if another line is very near. And since such dependence can only be explained as the result of a modification which the neighboring line produces in the refracting power of the medium, the phenomenon of mutual influence gives strong evidence in favor of the view that anomalous dispersion really is the dominating factor in determining the distribution of the light in a Fraunhofer line, and also, therefore, in causing the entire limb-center displacement.

We have shown in former papers how, by irregular refraction and scattering, dispersion lines originate, and under which conditions they may be asymmetrical.[1] The fact that the asymmetry of Fraunhofer lines is, as a rule, such as to represent a displacement toward the red would prove that the mean refractive index of the visible layers of the sun is greater than unity—as might indeed have been anticipated.

If we take it for granted that the limb-center shifts can have no other cause than anomalous dispersion, we are obliged to assign a displacement of similar origin to the Fraunhofer lines of the spectrum of the center with respect to the positions belonging to the free periods on the sun, for the radiation coming from the central parts of the disk has also traveled over long distances through gaseous layers, although not such long distances as has the light coming from the limb.

Now, the average magnitude of the measured center-arc displacements is very nearly what we should expect it to be in comparison with the average magnitude of the limb-center displacements (considering the distances which the light from the center and the light from the limb have traveled through dispersing media), provided we admit that there is no difference between the free periods *on the sun* and those in the arc *on the earth*. Our results, therefore, furnish a strong argument against the real existence of the effect, derived by Einstein from the general relativity theory, viz., that the cores of the solar lines should be displaced with respect to the cores of the terrestrial lines by as much as 0.01 A.

[1] Cf. also, P. H. van Cittert, *Spectraalverschijnselen veroorzaakt door onregelmatige Lichtbreking en hun Beteekenis voor de Physica der Zon*, thesis, Utrecht, 1919, a French translation of which has appeared in the *Archives neerlandaises* [III A], **5**, 243, 1921.

This subject has been amply discussed in a recent paper published in common with Dr. van Cittert (cf. p. 109, n. 2).

The main conclusion to be derived from the establishment of mutual influence of Fraunhofer lines as a general phenomenon is that it seems impossible now to maintain the current interpretation of the solar spectrum. When trying to explain solar and stellar phenomena we are henceforth obliged to consider that anomalous dispersion may be a most effective agent in determining the observed distribution of the light in cosmical spectra.

I desire to express my sincere thanks to Dr. van Cittert and Dr. Minnaert for their valuable assistance in sifting the material used in this investigation and in discussing the problems to which it gave rise.

Heliophysical Observatory, Utrecht
January 1921

NATURAL AND MAGNETIC ROTATORY DISPERSION OF OPTICALLY ACTIVE TRANSPARENT LIQUIDS

By E. O. HULBURT

ABSTRACT

Natural and magnetic rotatory dispersion of transparent liquids.—From the electron theory of H. A. Lorentz a *theoretical formula* is derived for the rotatory power of an optically active medium placed in a magnetic field, neglecting the effect of absorption of light in the medium. To test the theory, *measurements of the angles* of rotation were made for *limonene* and for solutions of *cane sugar* in water, of *tartaric acid* in water, and of *camphor* in ethyl alcohol, using plane polarized monochromatic light of *from 436 to 620 μμ* and a field strength of 6480 gauss. The formula was found to agree with the results for natural rotation in each case. It could be compared with magnetic rotation measurements only in the case of the sugar solution, and then agreement was found for the longer wave-lengths but for the shorter ones the theoretical values are somewhat too great. The discrepancy is attributed to the neglect by the theory of the effect of absorption.

Refractive indices for limonene and for one to one solutions of cane sugar and tartaric acid in water and of camphor in ethyl alcohol, 436–620 μμ, were determined.

1. INTRODUCTORY

In 1815 Biot discovered that certain liquids possess the power of rotating the plane of polarization of transmitted plane-polarized light. Such media are said to be *optically active*, and the rotation which they produce is termed the *natural* rotation. Connected with this from the point of view of experiment is the effect discovered by Faraday that an optically inactive medium, when subjected to a longitudinal magnetic field, also rotates the plane of polarization of transmitted plane-polarized light. Each of these two phenomena has been the subject of many theoretical and experimental investigations. The magnetic rotation of optically active substances has, however, received less attention.[1] No attempt is here made to summarize the work upon the varied phases of these problems, but reference is made to a publication by H. Landolt[2] and to one by W. Voigt[3] in which are discussed many

[1] L. R. Ingersoll, *Physical Review*, **9**, 257, 1917. See references contained in this paper.

[2] *Das optische Drehungsvermögen*, 1898.

[3] L. Graetz (ed.), *Handbuch der Elektrizität und des Magnetismus*, Band IV, Lieferung 2, 1915.

of the more important researches. We shall have occasion to refer at times to certain reports which have special bearing upon various parts of this paper.

In the present work the magnetic rotation in optically active liquids has been considered. To this end four optically active transparent liquids were selected which differed markedly in their chemical and optical characteristics. The refractive indices and the angles of natural and magnetic rotation of the plane of polarization of plane-polarized monochromatic light were measured for a series of wave-lengths throughout the visible spectrum. Theoretical formulas based on the electronic theory of dispersion of H. A. Lorentz[1] have been derived, and as far as possible have been tested by the foregoing data.

2. THEORETICAL

We solve the problem theoretically by obtaining first an expression for the natural rotation alone, and secondly an expression for the natural and magnetic rotations together.

a) The natural rotation.—To explain the Biot phenomenon, Fresnel advanced the hypothesis, which was subsequently verified by experiment, that the effect of the optically active medium was to resolve the plane-polarized beam into two components, circularly polarized in opposite directions, which traveled with unequal velocities through the medium. Drude[2] developed the idea that the electrons in such a medium, when activated by a plane-polarized light-wave, move in circular orbits, and obtained an expression for the propagation of light through the medium which was in accord with experiment in certain cases. P. G. Nutting[3] obtained the same equation of motion for the electron as did Drude by a somewhat different argument. Instead of stating that a linear force produced a circular displacement of an electron, Nutting found it simpler to set up an equation which said that a linear force plus

[1] *Theory of Electrons*, 1909.

[2] *Lehrbuch der Optik*, p. 388, 1906.

[3] *Physical Review*, **17**, 1, 1903.

a solenoidal component is necessary to produce a linear displacement of the electron. In the present work we apply the idea of Nutting to the electron theory of H. A. Lorentz.

We restrict the discussion to transparent media in which the temperature remains constant; no external magnetic field. Let ξ, η, and ζ be the components of the displacement of the electron from its equilibrium position. The components of the restoring force with which the medium acts upon the electron are $f\xi$, $f\eta$, and $f\zeta$. According to our plan we write the electric force acting upon the electron

$$e(\bar{E}+\beta \operatorname{curl} \bar{E}).$$

β is a constant which depends upon the anisotropy of the medium, and may be positive or negative. The charge on the electron is e, its mass is m. N is the number of such electrons per unit volume. All quantities are expressed in c.g.s. electromagnetic units. The constant σ, which Lorentz has shown to be approximately $1/3$ for isotropic media, should in the present case be replaced by σ_x, σ_y, and σ_z. This would increase the complexity of the equations and would introduce an almost prohibitive number of unknown quantities. We content ourselves, therefore, as a first approximation, with letting σ be independent of the direction.

If the axis of Z be the direction of the propagation of the light, we find for the equations of motion of the dispersion electron of a single type,

$$\left.\begin{aligned} m\frac{d^2\xi}{dt^2} &= e\left[E_x+\sigma 4\pi c^2 Ne\xi+\beta\left(\frac{\delta E_z}{\delta y}-\frac{\delta E_y}{\delta z}\right)\right]-f\xi\,, \\ m\frac{d^2\eta}{dt^2} &= e\left[E_y+\sigma 4\pi c^2 Ne\eta+\beta\left(\frac{\delta E_x}{\delta z}-\frac{\delta E_z}{\delta x}\right)\right]-f\eta\,, \\ m\frac{d^2\zeta}{dt^2} &= e\left[E_z+\sigma 4\pi c^2 Ne\zeta+\beta\left(\frac{\delta E_y}{\delta x}-\frac{\delta E_x}{\delta y}\right)\right]-f\zeta\,. \end{aligned}\right\} \qquad (1)$$

Let ϵ be the base of natural logarithms, and let all dependent variables of (1) contain the time only in the factor $\epsilon^{i\frac{2\pi c}{\lambda}t}$ where $\frac{c}{\lambda}$ is the frequency, λ the wave-length of the vibration *in vacuo*, and

c the velocity of light *in vacuo*. The solution of (1) yields two vibrations, circularly polarized in opposite directions, whose refractive indices μ_1 and μ_2 are given by the relation

$$\frac{1}{\sigma + \dfrac{1 \pm \dfrac{2\pi\beta}{\lambda}\mu}{\mu^2 - 1}} = \frac{\dfrac{Ne^2}{\pi m_s}}{\dfrac{1}{\lambda_s^2} - \dfrac{1}{\lambda^2}}. \tag{2}$$

The subscript s denotes the sth type of electron. $\dfrac{c}{\lambda_s}$ is the frequency of the natural undamped vibration of this electron. When the plus sign of (2) is used, μ is μ_1; when the minus sign is used, μ is μ_2.

Equation (2) describes the refractive indices in terms of the constants of a single type of dispersion electrons. There may be other types of dispersion electrons in the medium with constants peculiar to the type, so that in the more general case the right-hand member of (2) may be assumed to be a summation of similar terms, one term for each type. For this case the complete dispersion formula is

$$\frac{1}{\sigma + \dfrac{1 \pm \dfrac{2\pi\beta}{\lambda}\mu}{\mu^2 - 1}} = \sum \frac{\dfrac{Ne^2}{\pi m_s}}{\dfrac{1}{\lambda_s^2} - \dfrac{1}{\lambda^2}}. \tag{3}$$

We assume we are dealing with a region of the spectrum in which the change of the refractive index with wave-length is determined by the electrons of a single type, so that in the summation of (3) all the terms except one may be replaced by a quantity q_1 which is independent of λ. Then (3) becomes, when the two formulas are written separately,

$$\frac{1}{\sigma + \dfrac{1 + \dfrac{2\pi\beta}{\lambda}\mu_1}{\mu_1^2 - 1}} = q_1 + \frac{\dfrac{Ne^2}{\pi m}}{\dfrac{1}{\lambda_1^2} - \dfrac{1}{\lambda^2}}, \tag{4}$$

$$\frac{1}{\sigma+\dfrac{1-\dfrac{2\pi\beta}{\lambda}\mu_2}{\mu_2^2-1}}=q_1+\frac{\dfrac{Ne^2}{\pi m}}{\dfrac{1}{\lambda_1^2}-\dfrac{1}{\lambda^2}}. \tag{5}$$

If $\beta=0$ in (4) or (5), we obtain a quantity μ_0 defined by the expression

$$\frac{1}{\sigma+\dfrac{1}{\mu_0^2-1}}=q_1+\frac{\dfrac{Ne^2}{\pi m}}{\dfrac{1}{\lambda_0^2}-\dfrac{1}{\lambda^2}}. \tag{6}$$

Comparing (4), (5), and (6) we find

$$\mu_0=\sqrt{1+\mu_1\mu_2}, \tag{7}$$

which shows that μ_0 is the geometrical mean of μ_1 and μ_2. If the refractive index of the optically active liquid is determined directly by a refractometer, the numbers obtained may be interpreted to be almost exactly μ_0.

Let θ_n be the angle in radians of the rotation of the plane of polarization produced by a length l cm of the active liquid. It may be shown[1] that

$$\frac{\lambda\theta_n}{\pi l}=\mu_2-\mu_1. \tag{8}$$

Substituting (4) and (5) in (8), and making use of (7), we obtain

$$\theta_n=\frac{2\pi^2\beta l}{\lambda^2}(\mu_0^2-1). \tag{9}$$

By the same reasoning as before we note that several types of electrons may contribute to the rotation, and therefore (9) may be written in the general case,

$$\theta_n=\sum\frac{2\pi\beta l}{\lambda^2}(\mu_0^2-1). \tag{10}$$

This formula is in agreement with those of Drude and Nutting. Again, considering that only a single type of electron is important

[1] Drude, *loc. cit.*, p. 396.

in determining the variation of θ_n with λ for the region of the spectrum under investigation, (10) simplifies to

$$\theta_n = b_1 l + 2\pi\beta_1 l \frac{\mu_0^2 - 1}{\lambda^2}. \tag{11}$$

We write $b_1 l$ in order that the quantity b_1 may refer to a unit length of the substance. b_1 is independent of λ, and may be positive or negative. This formula is in agreement with certain known facts concerning the rotatory dispersion of optically active substances. Far from the critical frequency, determined by λ_1, the formula expresses the fact that θ_n varies inversely as the square of the wave-length. As the critical frequency is approached the rotation increases more rapidly than the inverse square law. This is in accord with fact. To be more complete, formula (11) should include the effect of absorption. It is interesting to note that although formula (11) has been derived on the Lorentz electron-dispersion theory there is no theoretical reason why the same formula may not be applied to media whose refractive index does not satisfy the Lorentz dispersion equation (6). This is due to the fact that the refractive index μ_0 occurs explicitly in (11) and the constants of the dispersion equation do not occur therein.

b) The natural rotation combined with the magnetic rotation.— Suppose that the optically active medium is subjected to an external magnetic field of strength H in c.g.s. electromagnetic units, and suppose that H is in the direction of the axis of Z, which is also the direction of the propagation of the light. The magnetic permeability of the medium is taken as unity.

The equations of motion of the dispersion electron of a single type become in this case,

$$\left.\begin{aligned} m\frac{d^2\xi}{dt^2} &= e\left[E_x + \sigma 4\pi c^2 N e\xi + \beta\left(\frac{\delta E_z}{\delta y} - \frac{\delta E_y}{\delta z}\right)\right] - f\xi + He\frac{\delta\eta}{\delta t}, \\ m\frac{d^2\eta}{dt^2} &= e\left[E_y + \sigma 4\pi c^2 N e\eta + \beta\left(\frac{\delta E_x}{\delta z} - \frac{\delta E_z}{\delta y}\right)\right] - f\eta - He\frac{\delta\xi}{\delta t}, \\ m\frac{d^2\zeta}{dt^2} &= e\left[E_z + \sigma 4\pi c^2 N e\zeta + \beta\left(\frac{\delta E_y}{\delta x} - \frac{\delta E_x}{\delta y}\right)\right] - f\zeta. \end{aligned}\right\} \tag{12}$$

These equations are solved in a manner similar to that outlined in (*a*). When the squares of small quantities are neglected, the angle of rotation θ, expressed in radians, is found to be

$$\theta = b_1 l + 2\pi^2 \beta_1 l \frac{\mu_o^2 - 1}{\lambda^2} + Hl \frac{Ne^3}{2\pi c m^2} \frac{[\sigma(\mu_o^2 - 1) + 1]^2}{\mu_o} \frac{\lambda_1^4 \lambda^2}{(\lambda^2 - \lambda_1^2)^2}. \qquad (13)$$

The first two terms of the right-hand side of (13) are seen to be the contribution to θ due to the natural rotation θ_n (see formula [11]). The last term is the contribution to θ due to the magnetic rotation which we shall call θ_m. This same expression for θ_m has been derived in a former paper.[1] We may then write

$$\theta = \theta_n + \theta_m , \qquad (14)$$

where θ_n is given by formula (11), and θ_m is expressed by

$$\theta_m = Hl \frac{Ne^3}{2\pi c m^2} \frac{[\sigma(\mu_o^2 - 1) + 1]^2}{\mu_o} \frac{\lambda_1^4 \lambda^2}{(\lambda^2 - \lambda_1^2)^2}. \qquad (15)$$

We note that in formula (13), for wave-lengths far removed from the region of critical frequency, θ_n and θ_m are each roughly proportional inversely to λ^2, and hence their ratio is approximately constant for various wave-lengths. This is in agreement with an empirical relation, first enunciated by Wiedemann,[2] as the result of experiments on turpentine. It is seen from the formula that such relation is, in general, not true and at best only an approximation, as was shown by later investigations.

3. EXPERIMENTAL

The determination of the natural and magnetic rotation angles was carried out by means of the apparatus described in the former paper (*loc. cit.*). This consisted briefly of a grating spectrograph, two nicol prisms, and a Ruhmkorff magnet between whose poles was placed a cell containing the liquid under examination. The refractive indices of the liquids were measured for the wave-

[1] R. A. Castleman, Jr., and E. O. Hulburt, "Magnetic Rotatory Dispersion in Transparent Liquids," *Astrophysical Journal*, **54**, 45, 1921.

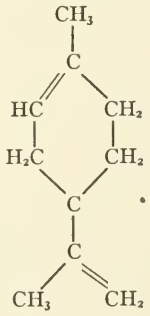
[2] *Pogg. Ann.*, **82**, 215, 1851.

lengths 436, 546, 578, and 620 $\mu\mu$ by an Abbé refractometer especially arranged for the purpose. A mercury-vapor lamp with filters served as the source of light for the three shorter wave-lengths, a tungsten gas-filled lamp with a red filter served for the wave-length 620 $\mu\mu$.

Four optically active liquids were investigated, one being an organic liquid limonene[1] and the others being solutions of cane sugar in water, tartaric acid in water, and camphor in ethyl alcohol. The solutions were prepared by dissolving 50 gm of the material in 50 gm of the pure solvent. The three solutions were practically colorless, but the limonene showed appreciable absorption in the blue. The values of the natural rotation angles θ_n, which have been reduced to refer to a length of 1 cm of the liquid, are shown by the curves 1 in Figures 1, 2, 3, and 4. The small circles are plotted from the observations, and smooth curves have been drawn through them. The natural rotation angles of these liquids, but for different concentrations in the case of the solutions, were measured by Nutting and by Ingersoll (*loc. cit.*). In the case of limonene Nutting's values, reduced to the scale of Figure 1 by multiplying one-tenth of the specific rotations given in his paper by the density 0.846, are plotted for comparison as small triangles in Figure 1. Ingersoll's values, also reduced to the scale of Figure 1, are shown by small squares. The difference between the observations may perhaps be ascribed to impurities in the liquid.

The magnetic rotation angles θ_m for a field strength of 6480 gauss, shown by the curves 3 in Figures 1, 2, 3, and 4, have been

[1] Also called "carven." The structural formula is:



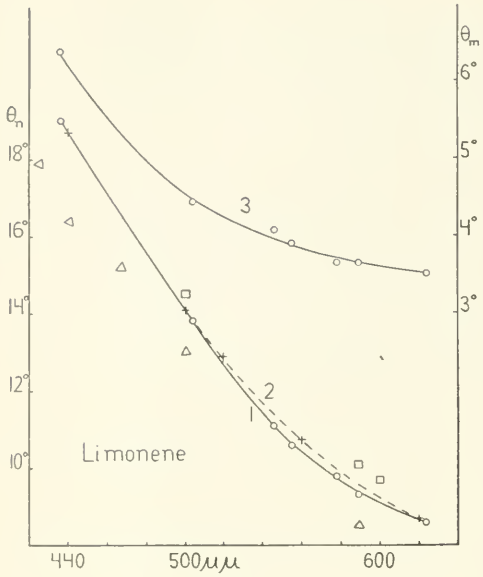


FIG. 1

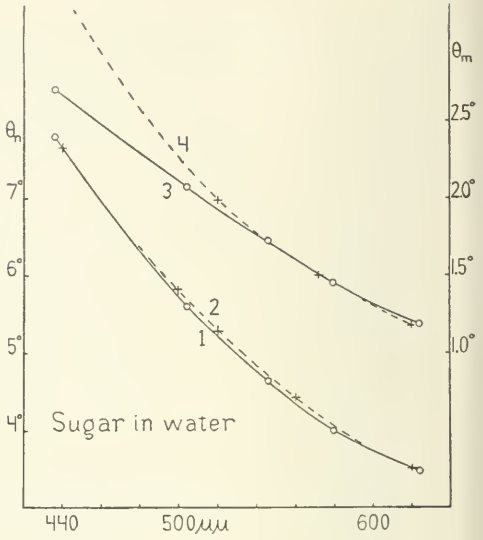


FIG. 2

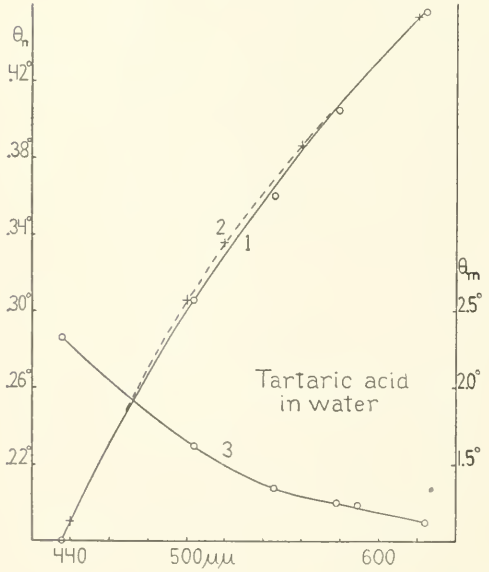


FIG. 3

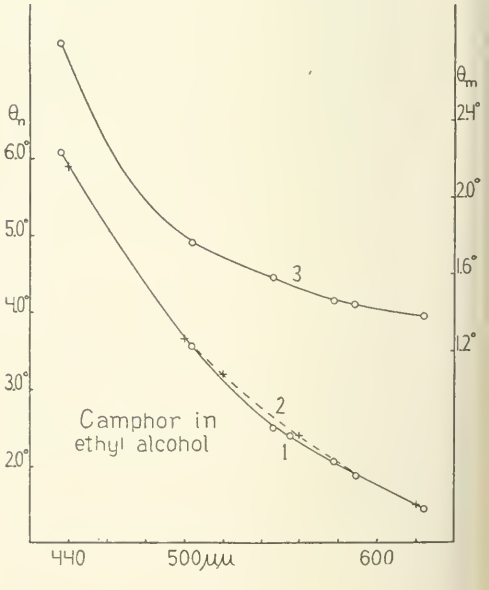


FIG. 4

obtained by taking the means of the magnetic rotations produced by the field direct and reversed. It was found that within the error of experiment the direct and reversed magnetic rotations were equal for all the liquids throughout the range of wave-lengths investigated. The observed values of θ_m, reduced to refer to 1 cm length of liquid, are shown by the circles of curves 3.

The values of the refractive indices, in our notation μ_0, obtained from the refractometer measurements at 20° C., are given in Table I. The error in these numbers was probably not greater than ± 0.0002.

TABLE I

REFRACTIVE INDEX μ_0

λ	Limonene	Sugar	Tartaric Acid	Camphor
$\mu\mu$				
620	1.4749	1.4200	1.4059	1.4108
578	1.4771	1.4211	1.4076	1.4126
546	1.4797	1.4222	1.4086	1.4136
436	1.4902	1.4288	1.4145	1.4207

4. TEST OF THE THEORETICAL FORMULAE

The two constants of formula (11) were calculated for each liquid by the use of two observed values of θ_n, and are given in Table II. The curves for the natural rotations computed from formula (11) are shown in the figures by the curves 2 which are indicated by crosses and a dotted line. It is seen that the formula expresses the observations with fair accuracy.

TABLE II

	b_1	β_1
Limonene	$-1°.50$	28.9×10^{-12},
Sugar	$0°$	11.7
Tartaric acid	$+0°.674$	-9.45
Camphor	$-2°.52$	13.7

To calculate the magnetic rotations from formula (15), λ_1 must be first determined from the dispersion equation (6). This is possible only for those substances whose relation of refractive index and wave-length corresponds to equation (6). In the present

instance the solution of sugar in water was the only liquid of the four whose refractive index satisfied this relation. The constants of (6) for this liquid were found to be

$$q_1 = 0.3154, \quad \lambda_1 = 251.6\ \mu\mu, \quad \frac{Ne^2}{\pi m} = 2.8587 \times 10^7.$$

Using 1/3 for σ and introducing the observed value of θ_m at λ 589 $\mu\mu$ into equation (15) gave $\frac{e}{m} = 3.30 \times 10^7$. With the constants of (15) thus determined, the magnetic rotations were computed throughout the visible spectrum and are shown by the dotted curve 4 of Figure 2. The discrepancy between theory and experiment for the shorter wave-lengths may be attributed rather to the neglect of absorption in the theory than to the inclusion of too few terms in the summations.

In the cases of limonene, tartaric acid in water, and camphor in ethyl alcohol, one might test a magnetic-rotation equation given by Siertsema,[1] namely,

$$\theta_m = lH \frac{e}{m} \frac{\lambda}{2c} \frac{d\mu}{d\lambda}. \tag{16}$$

This formula requires that the refractive-index-wave-length curve be determined with sufficient precision to enable one to compute the first derivative. The data of Table I were not numerous enough for such a purpose.

To conclude, the author takes pleasure in expressing his hearty thanks to Dr. J. F. King for valuable assistance in the experimental work.

Johns Hopkins University
April 1921

[1] *Comm. Lab. Leiden*, No. 82, 1902.

THE ORBIT OF 49 δ CAPRICORNI

By CLIFFORD C. CRUMP

ABSTRACT

Elements of the orbit of 49 δ Capricorni have been determined with considerable accuracy from 74 spectrograms taken with the Bruce spectrograph at Yerkes Observatory. The period is 1.02275 days and K is 65.7 km/sec.

The variable radial velocity of 49 δ Capricorni ($\alpha = 20^h\ 41^m.5$; $\delta = -16°35'$; visual magnitude 2.98) was announced by Dr. V. M. Slipher of the Lowell Observatory in the *Astrophysical Journal*, **24**, 361, December, 1906. Observations of the star were begun at Yerkes Observatory on June 21, 1915, and continued until August 18, 1919. During this interval 74 spectrograms were made with the one-prism arrangement of the Bruce spectrograph attached to the 40-inch refractor. Of the total number of spectrograms made, 69 were used in the determination of the radial

TABLE I

Element	Wave-Length	Element	Wave-Length
Fe	4045.975	*H*	4340.634
Fe	4063.759	*Ti*	4395.201
Fe	4071.908	*Mg*	4481.400
Si	4143.047	*Fe, Ti-Co*	4549.767
Fe	4271.325	*H*	4861.527
Ti	4326.527		

velocities. Seed 23 and Seed 30 plates were used. The times of the exposures are given in column 4 of Table II. Suspecting that the period was about a day, I took 7 plates during the night of August 9, 1917. This confirmed the belief, and on several nights plates were secured in as rapid succession as possible throughout the entire night.

The spectrum of 49 δ Capricorni is designated in the *Harvard Annals*, **50**, by A5, and in Miss Maury's classification in the *Harvard Annals*, **28**, by X*a*, *b*. For a spectrum of this type the lines are of perhaps average quality. Although there are many lines on some of the plates, only the best were used in this investigation.

The region used extended from λ 4045 to λ 4861. The comparison spectrum was that of titanium and iron. The lines used and the wave-lengths adopted are given in Table I. All the spectrograms were measured by the writer with the exception of Plates No. 4192, 4197, 4198, 4199, 4232, 4246, 4261, and 4630, which were measured by Julius Lemkowitz, formerly computer at Yerkes Observatory.

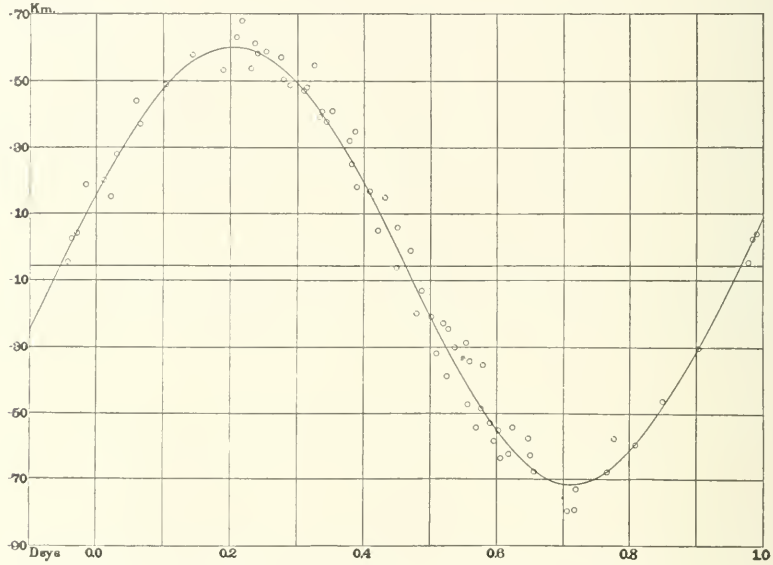


FIG. 1.—Velocity-curve of 49 δ Capricorni with observed values

The velocities were determined from the measurements in the usual manner, corrections being applied for the orbital velocity of the earth, the earth's rotation, and for curvature of the lines. Table II contains the observed data.

The period was determined by successive approximations as 1.02275 days, and since 1467 cycles were completed during the time of observation this may be considered as definitive.

The observed radial velocities of Table II were combined into normal places with phase as a basis for grouping. The weight of each normal place was determined on the basis of the weights of the plates combined to make the normal place. The largest of

TABLE II

Plate	Date	G.M.T.	Phase	Exp.	Obs.	No. L.	Wt.	Vel.	O−C
								km/sec.	km/sec.
IB4192.....	1915 July	9^{d}.847	0^{d}.582	20^{m}	B	5	5	−35.90	+13.66
4197.....		12.853	.521	20	My	3	3	−23.02	+ 5.00
4198.....		12.872	.539	20		7	7	−30.40	+ 4.44
4199.....		12.890	.558	25		2	2	−47.50	− 5.96
4202.....		16.778	.355	18	B	6	6	+40.42	+ 4.74
4232.....	Sept.	6.615	.031	40	My	7	7	+27.52	+ 1.72
4246.....		20.658	.779	26	B	5	5	−57.68	+ 8.82
4261.....	Oct.	11.571	.213	36	B	5	5	+62.90	+ 3.05
4512.....	1916 May	29.888	.388	26	B	11	14	+34.30	+ 9.98
4515.....	June	30.812	.608	30	C	9	9	−63.82	− 6.84
4520.....	July	7.875	.512	26	C	9	9	−32.36	− 7.96
4565.....	Aug.	11.735	.598	35	C	8	15	−58.66	− 4.51
4571.....		18.688	.391	35	C	8	12	+17.81	− 5.33
4578.....		21.700	.336	35	C	7	8	+38.55	− 2.80
4589.....		27.735	.234	35	C	9	9	+53.06	− 6.00
4630.....	Sept.	15.633	.722	50	B	4	4	−72.88	− 1.39
4668.....	Oct.	16.587	.994	60	Mk	8	14	+ 3.80	+ 0.30
4710.....	Dec.	13.469	.579	40	B	7	10	−48.76	− 0.12
4960.....	1917 July	20.745	.987	62	C	8	8	+ 2.07	+ 1.26
4961.....		20.794	.013	63	C	9	11	+19.86	+ 0.46
4962.....		20.842	0.061	55	C	9	10	+43.52	+ 7.71
4966.....		23.835	1.008	82	B	5	5	+18.35	+ 9.20
4990.....	Aug.	9.717	0.504	60	C	11	12	−21.03	+ 0.42
4991.....		9.769	.556	74	C	10	10	−29.17	+11.91
4992.....		9.818	.605	55	C	11	11	−55.24	+ 0.88
4993.....		9.863	.650	50	C	10	10	−57.61	+ 8.30
4997.....		10.687	.451	50	C	11	12	− 6.45	− 6.80
4998.....		10.726	.490	50	C	11	11	−13.24	+ 2.43
4999.....		10.765	.529	42	C	11	11	−24.98	+ 6.06
5000.....		10.797	.561	40	C	11	11	−34.59	+ 8.20
5001.....		10.828	.592	40	C	12	12	−53.04	− 0.53
5002.....		10.862	.626	30	C	10	10	−54.30	+ 7.08
5003.....		10.889	.653	35	C	9	9	−62.80	+ 3.63
5007.....		17.639	.244	45	C	11	11	+57.89	− 0.51
5008.....		17.674	.278	45	C	10	10	+56.73	+ 2.66
5009.....		17.708	.313	45	C	10	10	+46.84	− 0.34
5010.....		17.742	.346	45	C	11	11	+37.19	− 0.99
5011.....		17.775	.380	40	C	11	11	+31.48	+ 4.07
5012.....		17.806	.410	40	C	10	10	+16.11	− 0.13
5013.....		17.848	.453	57	C	11	11	+ 5.47	+ 5.77
5016.....		19.641	.193	60	C	3	3	+52.72	− 6.87
5017.....		19.697	.256	92	C	10	10	+58.15	+ 0.99
5018.....		19.769	.328	105	C	9	9	+54.04	+10.61
5022.....		24.774	.220	40	C	8	8	+67.98	+ 8.28
5023.....		24.837	.282	60	C	7	7	+50.00	− 3.41
5097.....	Nov.	5.487	.317	50	B, Wk	11	11	+47.68	+ 1.49
5540.....	1919 July	14.847	.981	68	Wk	11	11	− 4.70	− 3.21
5546.....		18.862	.906	70	C	10	10	−30.34	− 0.09
5549.....		21.744	.720	70	Wk	10	14	−79.00	− 7.51
5550.....		21.794	.769	60	Wk	10	13	−67.56	+ 0.32

TABLE II—*Continued*

Plate	Date	G.M.T.	Phase	Exp.	Obs.	No. L.	Wt.	Vel.	O−C
								km/sec.	km/sec.
IB5551	1919 July	21d836	0d812	50m	Wk	11	17	−59.49	− 0.18
5552		21.876	.852	53	Wk	10	13	−46.29	+ 2.35
5554		25.774	.658	72	C	9	15	−67.52	− 0.30
5555		25.833	.718	95	C	9	11	−79.28	− 7.79
5558	Aug.	1.708	.433	60	C	9	10	+14.69	+ 7.31
5559		1.757	.482	60	C	10	10	−20.04	− 7.39
5560		1.802	.527	60	C	8	11	−39.10	− 8.59
5561		1.847	.572	60	C	10	10	−54.65	− 8.11
5562		1.894	.620	64	C	11	12	−62.23	− 2.36
5564		8.674	.240	75	C	11	12	+60.99	+ 2.32
5565		8.726	.292	70	C	11	11	+48.14	− 3.57
5566		8.773	.339	60	C	11	13	+40.19	− 0.22
5567		8.818	.384	60	C	10	10	+24.27	− 1.63
5568		8.858	.424	48	C	11	13	+ 4.69	− 6.10
5569		8.906	.472	55	C	10	10	− 1.52	+ 6.80
5571		18.683	.022	69	Wk	9	9	+14.71	− 8.23
5572		18.728	.067	48	Wk	11	11	+36.48	− 0.98
5573		18.767	.105	53	Wk	10	11	+48.46	+ 0.89
5574		18.808	.146	54	Wk	9	9	+57.16	+ 1.91

NOTE.—Under observer the following letters are used: B = Barrett; C = Crump; Mk = G. S. Monk; My = C. A. Maney; Wk = Miss E. W. Wickham. Mr. F. R. Sullivan assisted at nearly all the exposures.

these sums was taken as unity and the rest reduced to this basis. Table III contains the data for the normal places.

TABLE III

No.	Phase	Limits of Phase	Vel.	O−C	Wt.	No. of Plates
			km/sec.	km/sec.		
1	0d020	0d00–0d05	+20.13	−2.55	0.360	3
2	.064	0.05–0.10	+39.83	+2.90	.280	2
3	.133	0.10–0.20	+52.42	−0.67	.307	3
4	.233	0.20–0.25	+60.10	+0.91	.600	5
5	.277	0.25–0.30	+53.38	−1.22	.507	4
6	.330	0.30–0.35	+43.86	+0.43	.827	6
7	.383	0.35–0.40	+28.78	+1.57	.707	5
8	.423	0.40–0.45	+11.18	−1.12	.440	3
9	.469	0.45–0.50	− 7.01	−0.70	.720	5
10	.521	0.50–0.55	−28.87	−1.38	0.707	6
11	.578	0.55–0.60	−46.63	+1.42	1.000	8
12	.622	0.60–0.65	−58.61	+1.65	0.693	5
13	.656	0.65–0.70	−65.75	+1.21	.320	2
14	.719	0.70–0.75	−78.26	−6.77	.387	3
15	.772	0.75–0.80	−64.82	+2.47	.240	2
16	.812	0.80–0.85	−59.49	+0.18	.227	1
17	.852	0.85–0.90	−46.29	+2.35	.173	1
18	.906	0.90–0.95	−30.34	−0.09	.133	1
19	.991	0.95–1.05	+ 2.89	+1.03	0.507	4

From the preliminary curve which was drawn to represent the observed velocities it was found from a Lehmann-Filhés solution that the eccentricity was very small. Since the most probable values of ω and T cannot easily be found from the least-squares solution, a study of the observations was made after the normal places had been formed. Different values of ω were assumed and

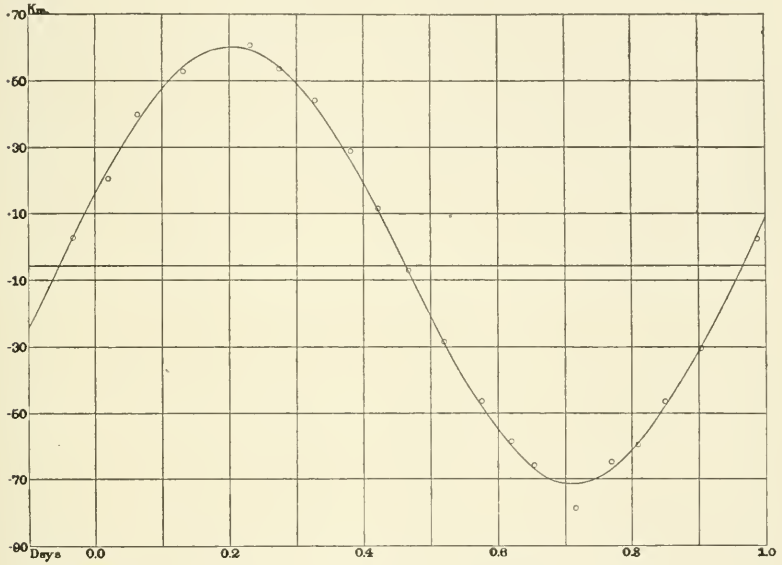


FIG. 2.—Velocity-curve of 49 δ Capricorni with the normal values

the corresponding values of T were computed by the method of least squares. The preliminary elements given below were adopted for the final least-squares solution.

ELEMENTS

Preliminary	Final
$P=1.02275$ days	$P=1.02275$ days
$T=0.63$ phase	$T=0.63$ phase
$e=0.026$	$e=0.019\pm0.008$
$\omega=149^\circ06$	$\omega=149^\circ057\pm0^\circ46$
$K=65.66$ km/sec.	$K=65.667\pm0.510$ km/sec.
$\gamma'=-5.69$ km/sec.	$\gamma'=-5.817\pm0.563$ km/sec.
	$a\sin i=925{,}940$ km

Assuming the constancy of the period and the epoch of periastron and using $d\gamma'$ instead of Γ as an unknown, the normal equations

were formed, and the method of solution was essentially that outlined by Dr. Schlesinger in Volume I of the *Publications of the Allegheny Observatory*. Thus the final elements were derived, as given above.

A second ephemeris was computed on the basis of the corrected elements. The sum of the weighted squares of the residuals was reduced from 382.82 to 35.305. The probable error of a normal place of weight unity was determined as ± 1.03 km. The probable error of a single plate determined from the column O−C in Table II was found to be ± 2.75 km.

It is with pleasure that I acknowledge my indebtedness to Professor E. B. Frost, through whose kindness this investigation was made possible.

Perkins Observatory
March 19, 1921

THE SPECTRUM OF FLUORINE

By WILLIAM R. SMYTHE

ABSTRACT

Preparation of fluorine gas by electrolysis of fused potassium acid fluoride.—The method due to Mather and others of the Chemical Warfare Service is described, together with the necessary apparatus. The gas was purified by passing through sodium fluoride and a freezing trap. To protect the pump a charcoal trap was inserted.

Visible and ultra-violet spectrum of fluorine and carbon tetrafluoride.—A dozen previous researches had failed to determine definitely the lines due to fluorine because of impurities in the gas used. In this research a spectrum with foreign lines absent or very weak was obtained by flowing practically pure fluorine gas at atmospheric pressure continuously through a discharge tube with gold electrodes. Although the tube had a fluorite window, put on in optical contact without cement yet practically air-tight, and both a quartz spectrograph and a 50 cm concave grating were used, the only fluorine lines found were ten between λ 6239 and λ 7034. The *wave-lengths* of these lines, determined to about 0.1 A, are given and also the approximate positions of the heads of nine bands presumably due to CF_4, between λ 4829 and λ 6525.

In 1910 Kayser, in his *Handbuch der Spectroscopie*, made the statement, "Das Spectrum des Fluor ist noch so gut wie unbekannt." Before that time Böttger[1] (1864) and Liveing[2] (1878), working with calcium fluoride; Mitscherlich[3] (1864), Ditte[4] (1871) and Demarçay[5] (1895), working with hydrofluoric acid; Salet[6] (1875), Ciamician[7] (1880) and Lunt[8] (1906), working with silicon tetrafluoride; Exner and Haschek[9] (1901), working with ammonium fluoride; and Moissan[10] (1889–1891), working with fluorine, had described lines which they assigned to fluorine. The most reliable of these were Lunt, who worked in the violet, and Moissan, who worked in the red.

[1] *Jahrbuch für practische Chemie*, **65**, 392–394, 1862.

[2] *Proceedings Cambridge Philosophical Society* (3), **3**, 96–98, 1878.

[3] *Poggendorffs Annalen*, **121**, 459–488, 1864.

[4] *Comptes Rendus*, **73**, 738–742, 1871. [5] *Spectres Electriques*, 1895.

[6] *Annales de Chimie et de Physique* (4), **28**, 34, 1873.

[7] *Sitzungsberichte der Kaiserlichen Akademie der Wissenschaften*, Wien (82), **2**, 425–457, 1880.

[8] *Annals of the Cape Observatory*, **10** (2), 5B, 1906; and *Proceedings of the Royal Society*, **75**, 118, 1905.

[9] *Sitzungsberichte der Kaiserlichen Akademie der Wissenschaften*, Wien (100), **20**, 964–987, 1901.

[10] *Comptes Rendus*, **109**, 937–940, 1889; and *Annales de Chimie et de Physique* (6), **35**, 125, 1891.

Since that time Exner and Haschek[1] (1912), working with potassium fluoride on charcoal, have assigned 69 lines to fluorine; and Porlezza[2] (1912), working with silicon tetrafluoride, has assigned 78 lines to fluorine. A comparison of their results shows only 19 lines in common, within one angstrom of each other.

It is evident that the spectrum of fluorine is not yet settled and further measurements are desirable. Apparently, since Moissan's time, no one has worked with the element itself, due probably to the great difficulty of preparing and keeping it. We are indebted to Dr. Mather and others of the Chemical Warfare Service for a practicable method for the preparation of fluorine.

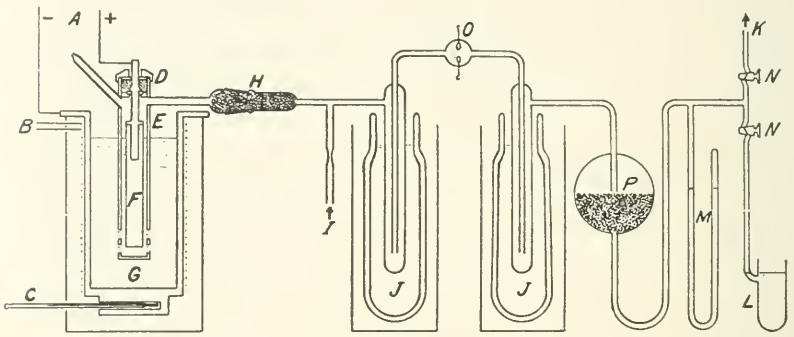


FIG. 1

The fluorine is generated by the electrolysis of fused potassium acid fluoride. A heavy copper vessel, on the outside of which is wound a nichrome heating coil, contains the electrolyte and serves as the cathode. Soldered to the base of this is a block of brass, having a hole in which a thermometer is inserted. The whole is insulated with asbestos to prevent loss of heat by radiation. The anode is of hard electrode carbon and is inclosed in a heavy copper "bell" which collects the fluorine. It is insulated from the bell and kept in position by powdered calcium fluoride packed

[1] *Die Spectren der Elemente bei normalem Druck*, 3, 85.

[2] *Gazetta chimica Italiana*, 42, 42, 1912.

between a fluorite and a glass washer, which is held in place by a brass cap.

A 5 mm copper tube on one side of the bell is open to the air and is annealed so that it can be pinched shut. A second copper tube supports the bell and carries off the fluorine, which passes through a copper-in-glass ground joint and a glass tube filled with sodium fluoride, into the purifying trap and discharge tube.

Potassium bifluoride is placed in the generator, melted at 230° C. and electrolyzed with about half an ampere for several hours to remove the last traces of water, while a current of nitrogen passes from a tank through the apparatus and bell into the air. When fluorine is detected by its odor, the nitrogen is turned off, the copper tube leading to the air pinched shut, and the electrolyzing current increased to an ampere and a quarter. The fluorine stream now enters the apparatus.

Besides being mixed with oxygen and nitrogen, this fluorine contains hydrofluoric acid given off by the electrolyte. This is largely removed by sodium fluoride to protect the glass parts. Since fluorine combines with every element except oxygen, nitrogen, and the noble gases, and since most of these compounds are solid at the temperature of frozen alcohol, while fluorine itself is still gaseous, the obvious way to purify the gas was to place a trap surrounded by frozen alcohol on each side of the discharge tube. Fluorine does not affect clean, cool, dry glass; so by passing a stream through the discharge tube for several hours, all spectroscopic impurities except nitrogen will be removed.

To prevent corrosion of the pump and contamination of the air in the room, the fluorine passed from a second trap into a bulb half-filled with charcoal, with which it combined violently, forming carbon tetrafluoride. In this reaction the charcoal glowed, shot off sparks, and generated so much heat that it was necessary to keep the point of combustion away from the walls of the bulb, as shown in the diagram; otherwise the carbon tetrafluoride reacted with the glass, forming carbon dioxide and silicon tetrafluoride.

Three types of discharge tubes were used. All were provided with a fluorite window. We could find no cement which was not attacked by fluorine. Hence the window was put on in optical

contact without cement. Mr. Pearson polished the fluorite plate and glass flange until the usual tests showed them to be flat within .00001 cm. They were then cleaned, placed in contact and pressed together until there was no light reflected from the junction surface. Tests showed that it required two weeks for the pressure in such a tube to rise from an X-ray vacuum to one millimeter. The outside of the joint was painted with shellac to prevent it from slipping and to stop inward leakage. Absolutely no trouble was experienced due to the negligible amount of fluorine which reached and attacked the shellac.

The first tube tried was of the electrodeless type shown in Figure 2. Working at a pressure of about 5 mm we could obtain only

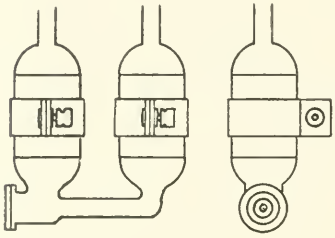


FIG. 2

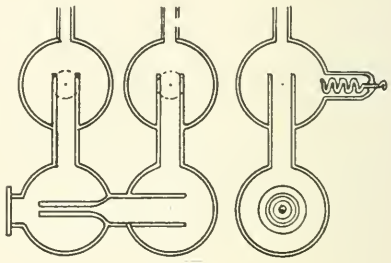


FIG. 3

band spectra in this tube without heating it to the point where the fluorine attacked it. The charcoal used in this run flared back into the alcohol trap, thus contaminating the contents with carbon tetrafluoride. The photograph on the quartz spectrograph showed a continuous spectrum from 2400 A to 2900 A, nitrogen bands from 2900 A to 4400 A, a set of nine bands, sharp on the violet side, between 4500 A and 6500 A, and five of the fluorine lines. The bands are listed in Table III as carbon tetrafluoride bands.

The second tube, shown in Figure 3, contained electrodes of a gold-palladium alloy. The heavy metals, which resist fluorine, sputter badly, so that a tube of ordinary pattern soon becomes short-circuited across the sputtered walls. The second tube was designed to avoid this, but, in so doing, its resistance was made so high that the energy required to operate it heated the capillary beyond the safety point. This resulted in the contamination of

the spectrum by lines due to most of the elements in the glass, especially silicon. The pressure in the tube was about 5 mm. At lower pressures the fluorine disappeared rapidly; at higher pressures the resistance increased. The photographs of this tube show about 500 lines, including most of those due to fluorine.

The third tube, shown in Figure 4, was designed to operate with a steady stream of fluorine at atmospheric pressure. The electrodes are of gold on platinum wires. By avoiding self-induction and capacity it was found possible nearly to eliminate metal lines and to obtain the gas lines fairly narrow. A tube of distilled water of 1 square cm cross-section and 60 cm long served as a resistance in the spark circuit. With this arrangement it was found possible to run the tube for eight hours without perceptibly heating it. The absence of a capillary reduced the action on the glass, and such impurities as were formed were carried out by the stream of fluorine at once. Spectra from this tube show only slight traces of silicon lines in the extreme ultra-violet, or none at all.

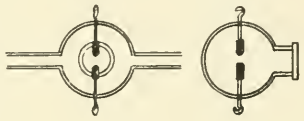


FIG. 4

A large transformer, operating on a 110-volt A.C. circuit, furnished the discharge current for the first two tubes. The third tube was operated by an induction coil giving a 6-inch spark on a 15-volt storage battery circuit.

Two spectroscopes were used. The first was an Adam Hilger quartz spectrograph of the standard type, and the second a grating instrument having a 4-inch concave grating of 50 cm focal length, with a dispersion of 24.88 A per mm. This grating, ruled for vacuum work in the extreme ultra-violet, throws practically all the light into the first order and is faster than any other grating in the laboratory. This is important, as the source of light is quite weak and the plates were slow in the red.

We used Wratten and Wainwright Panchromatic Plates, treated with a solution of 3.5 cc NH_4OH in 100 cc H_2O to increase the speed and sensitiveness in the red. For the grating we used Wratten and Wainright Panchromatic Films, treated in the same way. The quartz exposure was two hours and the grating exposure six

hours. All the lines in Table I except the longest were obtained on both instruments. The longest line appeared only on the quartz plate when heavily exposed. Its wave-length is computed by the Hartman interpolation formula and is accurate to about 1 A. The line at λ 6772.3 is very broad, perhaps double, and is

TABLE I

Porlezza		Smythe		Moissan	
	Int.		Int.		Int.
6239.75	10	6239.4	10	623	Strong
6348.73	10	6348.8	9	634	Strong
6413.95	10	6414.1	8	6405	Strong
6691.24	2				
6775.38	6	6772.3d?	2	677	Strong
		6834.1	2	6835	Medium
		6855.3	6	6855	Medium
		6868.8	2	6875	Medium
		6901.6	2		
		6909.1	1	691	Medium
		7034.	1	704	Medium

accurate to about 0.5 A. The other lines are accurate to 0.1 A. The copper and zinc lines from a brass arc photographed on each side of the fluorine lines served for comparison. No lines whatever appeared in the violet, but weak lines might have been present and covered up by the nitrogen bands. The lines in the red follow in international units.

As previously mentioned, a set of bands shading toward the red and supposed to be due to carbon tetrafluoride was photographed in the first tube. The approximate position of the heads of these bands is as follows:

TABLE II

	Int.		Int.
6525	10	5745	8
6500	5	5411	5
6209?	0	5105	3
6108	10	4829	1
5860	1		

In conclusion it may be said that fluorine has a characteristic spectrum in the red which is well established but that in the violet

the situation is still confused. Apparently it has no spectrum in the green and yellow. Our plates, showing only fluorine and nitrogen, were blank in this region. It may be that a more powerful discharge than was possible with our tubes will bring out the violet lines.

Thanks are due Mr. Bowen and Dr. Aronberg, who assisted in manipulating the apparatus and in computing, and special thanks are due Dr. Gale, who supervised these investigations and whose suggestions have been invaluable.

University of Chicago

ON THE ACCURACY WITH WHICH MEAN PARALLAXES CAN BE DETERMINED FROM PARALLACTIC AND PECULIAR MOTIONS[1]

By HENRY NORRIS RUSSELL[2]

ABSTRACT

Accuracy of mean parallaxes determined from parallactic and peculiar motions.—Assuming that the stars in the group are all at practically the same distance and that the velocities are distributed according to Maxwell's law, it is shown theoretically that the probable errors in the mean parallaxes determined by the two methods are, respectively, $\pm 1.035\ \bar{V}\pi/V_0\sqrt{n}$ and $\pm 0.721\ \pi/\sqrt{n}$. The ratio is 1.44 $\bar{V}/V_0$ and depends only upon the average value of the peculiar velocities, $\bar{V}$, since V_0 is the velocity of the sun. It follows that for Cepheids, stars of types A and B and others with peculiar velocities less than 14 km. the parallactic motions give the better result, while for stars moving faster the peculiar motions should be used. The formulae also show that results of value may be obtained from rather small groups.

Statistical study of 180 stars of types Bo to B5.—The *mean peculiar velocities*, radial and tangential, are 6.5 km and 0".0076; the *mean parallax* computed from parallactic motions is 0".0083 (π_1), and from peculiar motions 0".0058 (π_2). From π_1 and the *mean visual magnitude*, 4.08, the *mean absolute magnitude* comes out −1.38. The probable errors for the determinations of parallax agree closely with those to be expected from the foregoing theory. The lower value of π_2 compared with π_1 is probably due to the inclusion of unknown binaries for which the observed peculiar motions are too large.

If the proper motions and radial velocities are known for a group of stars the mean parallax may be found in two ways. Resolving the proper motions into two components, v toward the solar apex, and τ at right angles to this, and clearing the radial velocities of the solar motion so as to get the peculiar velocities V, we have the familiar equations

$$\bar{\pi}_1 = -\frac{\overline{v \sin\lambda}}{V_0\,\overline{\sin^2\lambda}}, \qquad \bar{\pi}_2 = \frac{\bar{\tau}}{\bar{V}} \tag{1}$$

where as usual the horizontal bars denote mean values, and where the means for τ and V are taken regardless of sign while V_0 is the velocity of the sun's motion in space, and, like V, is expressed in astronomical units per year.

To examine the accuracy of the two methods we may suppose that we are dealing with a group of stars which are all at substantially the same distance (so that we have to consider only the statistical errors resulting from the fact that the "law of

[1] *Contributions from the Mount Wilson Observatory*, No. 215.

[2] Research Associate of the Mount Wilson Observatory.

averages" does not apply exactly to small groups) and that the velocities of the stars are distributed according to Maxwell's law, so that the components in the directions of v, τ, and V obey the Gaussian law of errors, the probable errors defining the distribution being 0.845 $\overline{V}$ for the velocities and 0.845 $\overline{V}\,\overline{\pi}$ for the proper motions. Let n be the number of stars. The ordinary formula gives for the probable error of $\overline{\pi}$ as derived from the first equation

$$r_1 = \pm \frac{0.845\,\overline{\pi}\,\overline{V}}{V_0\sqrt{n\,\overline{\sin^2\lambda}}}$$

If the stars are distributed uniformly over the celestial sphere the value of $\overline{\sin^2\lambda}$ is $\frac{2}{3}$; if they are close to the Galaxy, it will be approximately $\frac{1}{2}$. Taking the former value, we have

$$r_1 = \pm \frac{1.035}{\sqrt{n}} \frac{\overline{V}}{V_0} \pi_1 \qquad (2)$$

For the second equation, the statistical error arises from the fact that the individual average values of τ or V, for groups of n stars, will not be identical with the averages for an indefinitely large number of cases.

The formula in this case is long established, but hardly familiar, and the proof is so simple that it is worth giving. Let $v_1, v_2, \ldots . v_n$ be any set of n quantities (all positive), selected at random from a great number, distributed according to the law of errors, whose arithmetical mean is η and whose mean square value is ϵ. It is well known that

$$\epsilon^2 = \frac{\pi}{2}\eta^2.$$

The square of the deviation between the mean of these particular quantities and the mean for an infinite number is

$$\frac{1}{n^2}(v_1 + v_2 \ldots . + v_n - n\eta)^2.$$

In the individual case this may have any value; but suppose we take the means for a great number of trials. The result may be obtained by expanding, substituting ϵ^2 for each squared term in the result, such as v_1^2; η for v in each term of the first degree, and η^2 for each product such as $v_1 v_2$ (since in these terms large and small values of v occur indiscriminately and the large ones do not multiply

themselves as in the case of v^2). We thus find for the mean of the squares of the deviations:

$$\epsilon_n^2 = \frac{1}{n^2}(n\epsilon^2 + n(n-1)\eta^2 - 2n^2\eta^2 + n^2\eta^2) = \frac{1}{n}(\epsilon^2 - \eta^2) = \frac{\pi - 2}{2n}\eta^2$$

Although the distribution of these deviations for individual stars does not at all follow the Gaussian law, that of the means of a group of six or more will probably do so very closely.[1] We may, therefore, use the ordinary formulae for computing the probable error of deviation of an individual mean of n quantities from the standard value η.

$$r = \pm 0.675\sqrt{\frac{\pi - 2}{2n}}\eta = \pm\frac{0.510}{\sqrt{n}}\eta \qquad (3)$$

The statistical probable error of $\bar{\tau}$ will therefore be $\pm\frac{0.510}{\sqrt{n}}\bar{\tau}$, while that of $\bar{V}$ will be $\pm\frac{0.510}{\sqrt{n}}\bar{V}$. Since the errors are independent of one another and proportional to the whole quantities concerned, the probable error of their quotient, $\bar{\pi}_2$, will be

$$r_2 = \pm\frac{0.721}{\sqrt{n}}\bar{\pi}_2 \qquad (4)$$

Comparing this with (2), we have

$$\frac{r_1}{r_2} = 1.44\frac{\bar{V}}{\bar{V}_0} \qquad (5)$$

The relative precision of the two methods depends only upon the average magnitude of the peculiar velocities (assuming, to be sure, that the sun's motion relative to the stars under consideration is accurately known). If the average peculiar velocity of the stars is less than 14 km, the parallactic motion gives the better result; otherwise the peculiar motions do so.

The actual law of distribution of velocities is not Gaussian, large velocities being in excess. This will operate to increase somewhat the numerical coefficients in (1) and (2) but should not greatly affect their ratio.

Similarly, in any actual group of stars, there will be real differences in parallax between the members, which will also introduce a statistical error into the determination of the typical mean from small samples, even though the individual parallaxes are exactly

[1] Compare Schlesinger, *Astron. Journal*, **30**, 185, 1917.

known; but this again operates to increase the probable errors given by both methods without much effect on their relative accuracy.

It follows that the parallactic motion affords the best means of determining the mean parallaxes of stars of spectra A and B, of Cepheids, and of other slow-moving stars. For the general run of naked-eye stars of the "later" types the two methods are about equally good, while for planetary nebulae, long-period variables, and other rapidly moving objects, the peculiar velocities afford the best solution. Results of value should be obtainable from rather small groups; thus the peculiar motions of ten stars give the mean parallax with a probable error of 23 per cent of its own value (so far as the statistical errors go); and the parallactic motions for slow-moving stars should give a considerably better value. It should further be noticed that the accidental errors of observation of both radial velocities and proper motions will increase the arithmetical mean values $\bar{V}$ and $\bar{\tau}$, while their influence upon the algebraic mean used in finding $\bar{\pi}$ will be much diminished. This is not, however, a serious matter, for, if the magnitude of the errors of observation is known, their effect may be removed from both $\bar{V}$ and $\bar{\tau}$ by well-known methods, and, in any case, both are increased, and the errors tend to compensate one another in their quotient $\bar{\pi}_2$.

As an example of these principles, the 180 stars of spectra Bo to B5 for which the quantities V and τ are given by Campbell[1] were divided into equal groups of ten stars each. To secure a random distribution, the first, nineteenth, and thirty-seventh stars, etc., were combined to form one group, the second, twentieth, and thirty-eighth were in the next, and so on. The results are given in Table I.

Each line of this table (except the last three) gives mean values for one of the eighteen groups of ten stars. The first column gives the mean of the visual magnitudes; the second, that of the spectral classes; the third, that of the peculiar radial velocities (corrected for the solar motion and K-term according to Campbell's solution III); and the fourth, that of the τ components. In the fifth column are the mean parallaxes $\bar{\pi}_2$ computed from the peculiar motions by equation (1); in the sixth, the values $\bar{\pi}_1$ found from

[1] *Lick Observatory Bulletin*, **6**, 101–124, 1911.

the parallactic motions; and in the last column, the absolute magnitudes corresponding to the parallaxes in the preceding column and the apparent magnitudes in the first.

The last three lines of the table give, respectively, the means of the quantities in the columns above, the probable error of one of those quantities computed in the usual way from the deviations from the mean, and the ratio of the probable error to the general mean in the cases where this is significant.

TABLE I

Mean Magnitude	Mean Spectrum	$\bar{V}$	$\bar{\tau}$	$\bar{\pi}_2$	π_1	Abs. Mag.
4.19.....	B3.5	5.0	0".0096	0".0091	0".0087	−1.1
4.38.....	3.4	6.2	43	33	66	−1.5
4.24.....	2.1	7.4	49	31	69	−1.6
3.98.....	2.8	10.4	68	31	94	−1.1
4.00.....	2.2	6.8	122	92	93	−1.2
3.22.....	2.7	6.4	55	41	90	−2.1
3.83.....	2.4	4.6	84	87	103	−1.1
4.71.....	3.6	9.0	73	38	71	−1.0
3.76.....	2.4	6.9	52	36	72	−1.9
4.09.....	3.2	4.6	72	74	51	−2.4
4.09.....	3.7	6.4	68	50	65	−1.8
4.19.....	3.9	5.0	77	74	101	−0.8
4.05.....	3.0	7.0	105	71	93	−1.1
4.35.....	3.9	7.3	94	61	96	−0.8
4.11.....	2.0	6.1	56	43	62	−1.9
4.41.....	3.4	5.8	79	65	88	−0.9
3.75.....	3.0	5.9	97	78	100	−1.3
4.01.....	3.3	6.6	64	46	90	−1.2
Means.....4.08	B3.0	6.5	0".0076	0".0058	0".0083	−1.38
P.E. one entry ±0.22	±0.41	±1.0	±0.00155	±0.00144	±0.00105	±0.32
Ratio.....		±0.15	±0.20	±0.25	±0.13	

The "probable errors" for the mean magnitude and spectral type indicate only the degree of statistical similarity between the various groups, which is fairly high; but those for the next four quantities afford a practical test of the applicability of the theory developed above. From equation (3) the ratio of the probable error of one of the tabular values of $\bar{V}$ or $\bar{\tau}$ to the average value of these quantities should be ±0.16. This is substantially the case for $\bar{V}$. The greater variability found for τ may reasonably be attributed to real differences in the mean parallaxes of the various groups (which were assumed to be the same in deriving the formulae). Equation (4) gives ±0.23 as the value to be expected for

$\bar{\pi}_2$ and equation (2) ± 0.11 as the expectation for $\bar{\pi}_1$. The agreement in both cases is remarkably close.

There is, however, a remarkable difference between the means of $\bar{\pi}_1$ and $\bar{\pi}_2$, the latter being only 70 per cent of the former. Only three of the twenty values of $\bar{\pi}_2$ are greater than the mean for $\bar{\pi}_1$, and only one value of $\bar{\pi}_1$ is smaller than the mean for $\bar{\pi}_2$. The discordance must therefore arise from some real cause, and there can hardly be a doubt regarding its origin. Campbell calls attention[1] to the fact that the observed values of $\bar{V}$ must be systematically too great on account of the inclusion in the lists of some undetected spectroscopic binaries for which the greater part of the observed velocity is due to orbital and not to systematic motion,[2] and of the probable variability of the K-term from one star to another; and Kapteyn[3] has pointed out that the accidental error of observation, which he finds to correspond to a probable error of ± 2.1 km for the well-observed stars, must also operate to increase them.

Campbell adopts the value 6 km instead of 6.5 for $\bar{V}$, which would raise $\bar{\pi}_2$ to $0''.0063$.

To obtain full accordance with $\bar{\pi}_1$, it would be necessary to reduce $\bar{V}$ to 4.5 km, which seems too large an allowance for these corrections, especially when it is considered that Boss,[4] from more than twice as many stars of the same spectral class, finds that the τ components correspond to a peculiar velocity of 6.3 km.

It is obvious, however, that the parallactic motions give much the better result in the case of the B-stars, irrespective of this uncertainty; and Kapteyn has based his classical work almost entirely upon them.

For rapidly moving stars, however, the peculiar motions are relatively much less influenced by such minor sources of error as have just been described, and by their use reliable values for the mean parallax can be obtained from groups of stars of moderate number.

MOUNT WILSON OBSERVATORY
July 2, 1921

[1] *Op. cit.*, p. 121.

[2] There are 53 of Campbell's 180 stars for which his notes indicate that the radial velocities are of inferior accuracy. The mean $\bar{V}$ for these is 7.5 km; for the remainder, 6.1 km. Hence the effect of this correction is small.

[3] *Astrophysical Journal*, **40**, 71, 1914. [4] *Astronomical Journal*, **26**, 198, 1911.

Reviews

Tables du mouvement képlérien, première partie. By F. Boquet. Paris: A. Herman et fils, 1920. 8vo. pp. vi+205.

These tables, published with the aid of a grant from the *Académie des sciences*, contain the true anomaly and the logarithm of the radius vector in elliptic orbits whose eccentricities do not exceed 0.49. These are the third tables for the true anomaly and the second for the radii vectores that have been published within eight years. The first of these, by Schlesinger and Udick, appeared in the *Publications of the Allegheny Observatory* in 1912; they give v (the true anomaly) for each degree in M (the mean anomaly) and each 0.01 in e (the eccentricity). They go as far as $e=0.77$. The second tables are by J. Peters of the Berlin Rechen-Institut (also published in 1912); they give the values of $v-M$ to 0°.01 and the logarithm of r (the radius vector) to 0.0001 for each degree of M and each 10′ in ϕ, sin ϕ being equal to e. They extend as far as $\phi=24°$, equivalent to $e=0.407$. The present tables use the *true anomaly* as one of the arguments, and give M to 0°.001 and log r to 0.00001 for each degree in v and each 0.01 in e. The use of the true anomaly as an argument instead of the mean anomaly is no real inconvenience, although it may appear to be so at first sight. To be sure, we almost always enter such tables with M (which depends directly upon the time), and we must therefore subtract the fractional part of the nearest M in the table from the given M in order to obtain the interpolating factor, or the fraction by which it is necessary to multiply the tabular difference; we then add this product to, or subtract it from the tabular v. In the present tables this last operation is really eliminated since the v's are all given to whole degrees, so that what this arrangement does is merely to substitute a subtraction in M for an addition or subtraction in v.

The Allegheny tables were primarily intended for spectroscopic binaries, and the Institut tables for asteroids; both of them, as well as the present tables, however, can be used for either purpose and for visual binaries in addition. Computers who deal extensively with any of these classes of objects will do well to have all three tables within reach.

In connection with each value of the mean anomaly, M. Boquet prints two tabular differences; the first is for two successive values of

v and the same value of e; the second is for two successive values of e and the same value of v. The Allegheny tables give only the former difference, the Institut tables give neither; but in both cases the tables are printed in such a way as to make these differences less indispensable. Thus, in the Allegheny tables, seven values of e can be put on a page with the corresponding v's in close juxtaposition; in the Institut tables, as no differences at all are given, it is found possible to put thirteen values of e on each page. In M. Boquet's tables only two values of e are on a page.

These tables were calculated in an interesting way that seems to be well known to the computers of perturbations, but which may be new to some readers. The differential coefficient of the mean anomaly with respect to the true anomaly is

$$(1-e^2)^{\frac{3}{2}} \div (1+e\cos v)^2.$$

This can be very easily computed for a fixed value of e, and with $v=0^\circ.5$, $1^\circ.5$, $2^\circ.5$, etc. Adding up these coefficients in succession it is obvious that we thus obtain approximations to the values of M for successive values of v that differ by 1°; these approximations may be made accurate by allowing for differences of the second and higher orders; or we may avoid calculating the higher differences by computing v for frequent values of M, say every tenth degree, and using the differences only over these shorter spans. M. Boquet has pursued a middle course by allowing for second-order differences only, and by checking his additions at intervals of 45°. This method is obviously of general application (and helps greatly to avoid errors) whenever the differential coefficients are easy to calculate, and when in addition the differences of higher order are not too great. This is the reason why the present tables use v as the argument instead of M.

The differential coefficient of the logarithm of the radius vector with respect to the true anomaly is

$$\text{a constant} \times \sin v \div \left(\frac{1}{e}+\cos v\right),$$

which is likewise easy to compute for fixed values of e or for fixed values of v.

In order to give additional accuracy, M. Boquet has put a + or a − after some of his tabular numbers; the former when the two neglected decimals are between 20 and 49, the latter when the tabular number has been increased from any decimal between 50 and 79. In the reviewer's opinion it would have been better to print instead an additional decimal.

Doubtless the objection that M. Boquet (and others who have used this device) would urge against the additional decimal is that it would entail considerable labor to make sure that this decimal is always the nearest one. But this same objection partly applies to putting + or − after a number, as it must sometimes be doubtful whether such a sign should be added or left off. Besides, computers should not fear to publish tables in which, if need be, the tabular numbers are occasionally in error by a little more than half a unit in the last printed place, though there seems to be a tradition against doing this that few tables have had the courage to disregard. But if in any set of tables the last printed place is not always the very nearest, a general statement to that effect should be made. The use of + and −, with occasional blanks, spoils the looks of the page, and does not save any expense.

It is a great pleasure to welcome after an absence of five or six years the return of the good quality of paper to which we are accustomed in French publications.

FRANK SCHLESINGER

February 21, 1921

THE
ASTROPHYSICAL JOURNAL
AN INTERNATIONAL REVIEW OF SPECTROSCOPY
AND ASTRONOMICAL PHYSICS

VOLUME LIV OCTOBER 1921 NUMBER 3

THE FLUORESCENCE OF MERCURY VAPOR

By J. S. VAN DER LINGEN and R. W. WOOD

ABSTRACT

The Fluorescent spectrum of mercury vapor cannot be excited in quiescent vapor, but only in vapor which is being distilled from the metal at a temperature of 150° or more. This proves that the *active molecules* are not neutral monatomic molecules but others present only during distillation, perhaps diatomic molecules. The spectrum consists of three lines—λ 2536, 2539, and 2346 A—and four structureless bands with maxima at 2346, 2540, 3300, and 4850 A. While the complete spectrum is excited by light from a zinc spark, single lines excite only part. *The relation of the spectrum to the exciting light* is of great interest. The broad bands with maxima at 3300 and 4850 may be excited, with varying relative intensity, by λ 1854–62, 2346, or 2536–40 A; whereas the band λ 2346–2100 A is excited only by λ 2000–2150 A, the position of the maximum depending on the particular wave-length used. All the effective exciting lines lie, of course, in the absorption spectrum of mercury vapor.

The fluorescence of mercury vapor was first observed by Hartley while he was carrying out experiments on the absorption spectra of the elements and their compounds.[1]

He found that the hot vapor, which was contained in an unexhausted quartz vessel, showed an absorption band which extended from 2526.8 A to 2571.67 A and that it fluoresced when it was excited by either a lead-cadmium or a tin-cadmium spark, the color of the fluorescent light being bluish green. He observed that the fluorescent light was most brilliant when the mercury was boiling briskly and that the fluorescence ceased when all the mercury had been converted into vapor above the boiling-point of the metal.

[1] *Proceedings of the Royal Society*, **76**, 428, 1905.

From these observations he concluded, (*a*) that the phenomenon was not due to oxidation, because of the expulsion of the air during the brisk boiling of the metal, and (*b*) that there must be an upper and a lower limit of temperature between which fluorescence occurs.

Subsequently Professor R. W. Wood proved that mercury vapor *in vacuo*, at room temperature, shows two absorption lines, viz., 2536.7 A and a fainter one at 2539.3 A, and that these fuse together when the temperature is increased, while a band develops asymmetrically toward the red end of the spectrum, the head of the band remaining fixed at 2536.7 A.[1] If air be introduced into the bulb, the head first grows symmetrically for about 8 angstrom units on either side of 2536 A, and then extends toward the red end only. It was thus due to the presence of air that Hartley found the absorption band extending to 2526.8 A. Wood also found that there are absorption lines at 2346.1, 2339, 2334.4, and 2331.2 A and that these lines shaded off toward the violet end of the spectrum. If the density of the vapor be increased, these lines fuse together and form a band. The development of this band is difficult to trace because it is blotted out by the absorption band which heads from the absorption line 1849 A to the visible spectrum. He found that the fluorescent spectrum of the vapor *in vacuo* is continuous and extends "roughly from the yellow down to wave-length 3000 with a very pronounced minimum at wave-length 3600," and that these bands show very little change, if any, when the vapor is excited by isolated lines of a spark spectrum. In addition to these fluorescent bands Wood found an emission line at 2536.7 A, and a fainter companion line 2539.4 A when the vapor is excited by an aluminum or cadmium spark, the emission being due to the last aluminum line and a group of cadmium lines which lie near the head of the 1849 absorption band. In the latter case, however, the emission line is much weaker than in the case of aluminum excitation. "This line appears strongest when the vapor density is such that the visible fluorescence does not quite appear. As the temperature is raised and the visible fluorescence grows stronger, the 2536 line fades away." Furthermore he showed that the fluores-

[1] *Philosophical Magazine* (6), **18**, 240, 1909.

cence disappears when the vapor is superheated, and also when air is introduced into the bulb.

Immediately after the appearance of Wood's results Steubing published his observations on the fluorescence of mercury vapor, and he showed that not only is the mercury line 2536 A emitted, but also the mercury line 2346 A, when the vapor is excited by an aluminum spark. He also found a fluted band, which extends from this latter line to about 2100 A. Furthermore he found that the ionization of the vapor was increased when it was excited by radiations lying within an absorption band of short wave-length. These results, he maintains, are in conformity with Stark's theory of absorption and fluorescence.[1]

In 1914 Phillips[2] examined the resonance phenomenon of this vapor, which was discovered by Wood, i.e., the emission of 2536 A when the vapor at room temperature is excited by 2536 A of a water-cooled quartz-mercury arc. In order to determine the percentage of secondary resonance radiation, he allowed the vapor to distil past a horizontal slit and discovered that the vapor emitted 2536 A as well as the fluorescent bands after it had passed out of the tract of the exciting light. He maintains that there are four fluorescent bands which from their position on his spectrum appear to be at the following positions approximately: (1) a diffused band at about 2700 A; (2) heads on 3132 A and ends at 3650 A; (3) at 4360 A; (4) a narrow band on the side of this region toward long wave-lengths. From what has been said it appears that mercury has absorption lines at 1849, 2346, and 2536 A and three absorption bands: (1) heads from 1849 A to the visible spectrum; (2) consists of the fused lines at 2346 A which develop into a band; (3) extends asymmetrically from 2536 A to the visible spectrum as the temperature is increased.

With regard to the work on the fluorescent bands and lines the results of the different observers do not agree.

OBJECT OF RESEARCH

The object of the following work was to find, as far as possible, the exact conditions under which mercury vapor fluoresces, and

[1] *Physikalische Zeitschrift*, **10**, 787, 1909.

[2] *Proceedings of the Royal Society*, **89**, 39, 1914.

also to determine the correlation between excitation in the various absorption bands and the emitted fluorescent lines and bands.

In the course of a somewhat extended study of the fluorescence of the vapor made by one of us, phenomena have from time to time been noticed which indicate that the fluorescence is not due to the monatomic mercury molecule. The evidence was thus summarized in a monograph on fluorescence not yet in print:

A thin-walled bulb, highly exhausted and containing a drop of mercury was heated in an Heraeus electric furnace and illuminated by an aluminum spark placed close to the bulb. The temperature of the furnace was determined by a nitrogen-filled mercury thermometer, placed close to the quartz bulb. With the temperature rising very gradually a very feeble fluorescence was observed at 150° C. while at 170° C. it was very bright. The density of the mercury vapor is increased less than twofold by this temperature increase, whereas the intensity of the fluorescence was certainly tenfold, if not more. On cooling the furnace, fluorescence disappeared entirely as soon as the temperature had fallen three or four degrees, though the density was much greater than that at which good fluorescence had been obtained with a rising temperature.

This makes it appear probable that something, diatomic molecules perhaps, commenced to come off the mercury at a temperature of 150°, the percentage of these fluorescing bodies increasing with rising temperature. As the temperature falls these bodies are no longer given off, and those already present disappear, probably by conversion into ordinary monatomic vapor.

The present investigation started out with a more careful study of this phenomenon. The experiment was repeated by using a similar quartz bulb which was placed over an asbestos chimney and gently heated by means of a Bunsen burner while a thermometer was placed over the bulb. On exciting the vapor by means of an aluminum spark placed near the bulb, it was found that the vapor exhibited faint fluorescence at 160° C., the intensity increasing rapidly with a rise of temperature.

On allowing it to cool, the fluorescence would cease at about 200°, and would only appear again on reheating up to 220° C. Very variable results were obtained by this method of heating, as was perhaps to be expected, but they verified completely the result of the earlier investigation, namely, that *the intensity of the fluorescence is a function of something other than the vapor-density.*

To secure a better control of temperature, an electric furnace was constructed of galvanized iron, lined with asbestos, the interior

being divided into two compartments by a vertical sheet of asbestos board. Two quartz bulbs joined by a short tube formed the mercury-vapor chamber, the tube passing through the asbestos partition. On either side of this partition an equal number of heating spirals were connected in series, and at the same time compensating spirals, having independent circuits, were fixed radially in each compartment. In this way the two connected bulbs could be kept at the same temperature, or a given difference of temperature between them could be established and held indefinitely. The exciting light entered the furnace as a parallel beam through a lateral hole, passing through the two bulbs and their connecting tube. In some cases the bulbs were illuminated one at a time by a beam entering the furnace at right angles to the axis of the bulb system. At constant temperature visible fluorescence could not be obtained; in other words, it was apparent that distillation must be going on in order to secure fluorescence. To settle this point definitely, the following very conclusive experiment was performed:

Two bulbs of very thin quartz, each about 1 cm in diameter, were joined by a short tube of quartz of about 1.5 mm bore. The two bulbs were mounted over a tall asbestos chimney, with a Bunsen burner at its base. The bulbs of two thermometers were placed immediately above the quartz bulbs. Operating under conditions avoiding air currents in the room, the two bulbs could be held at nearly the same temperature. One was always a little cooler than the other (about 5°) and in this one the liquid mercury of course collected.

When things had reached a steady state, say with one bulb at 200° and the other at 205°, both bulbs being illuminated by the light of an aluminum spark placed close to them, *no* fluorescence was observed. A blast of cold air, delivered through a small tube, was now directed against the hotter of the two bulbs, reducing its temperature enormously. The other bulb instantly flashed into a bright green fluorescence, which persisted until the last drop of mercury in it had disappeared, vanishing at the moment when distillation ceased.

The mercury was found now deposited as a dew on the cooled spot of the wall of the other bulb. The air current was now stopped and presently this bulb commenced to fluoresce as its temperature soon rose to its original value (205°) and the mercury began to distil back. No fluorescence was shown in either case in the bulb in which condensation was taking place. This was to be expected, as the pressure was lower in this part of the system.

However we interpret the results of this experiment, the fact is definitely established that only freshly formed mercury vapor is capable of exhibiting fluorescence.

This is not true of the resonance radiation described in previous papers by one of us, since mercury vapor in an exhausted tube at room temperature emits powerfully monochromatic light of wavelength 2536 A when illuminated by light of this same frequency obtained from a water-cooled quartz-mercury arc. Now it is known from the previous investigation just alluded to that the same radiation is also emitted by comparatively dense mercury vapor (say 4 mm pressure) when it is illuminated by the spark lines in the region 1860–1870 A.

It seems therefore desirable to ascertain whether this emission depended also upon distillation. This radiation appears first at much lower vapor-densities than any at which visible fluorescence does, which suggests that it very probably results from the stimulation of monatomic mercury molecules, and does not depend upon the presence of diatomic molecules or other unique entities.

The presence of this radiation can of course be detected only by the quartz spectrograph. The double bulb just described was used as before, the spectrograph being directed at the hotter bulb (250°). An exposure of 2 minutes was given, the bulb being illuminated with the light of the aluminum spark. A faint trace only of the 2536 Hg line appeared on the plate: no visible fluorescence was observed. This experiment was now repeated, and after an exposure of 2 minutes had been given, the spectrograph was screened off and the mercury brought over into the hotter bulb by an air blast. On removing the blast, the mercury commenced to distil back, and visible fluorescence occurred. Exposures were now made on the same plate of 2, 4, 6, and 8 seconds' duration.

On developing the plate it was found that the exposure of 2 seconds with the vapor distilling recorded the 2536 line with the same density as the 2 minutes' exposure of the stagnant vapor. This indicates that the 2536 emission line, excited by the short-wave-length spark lines, results in all probability from the stimulation of the entities which give rise to the visible fluorescence, but that a few of them are present even in the stagnant vapor, distillation increasing their number about sixty fold.

We will now consider the relation which exists between the wave-length of the exciting light, and the distribution of intensity among the various fluorescent bands and lines.

The absorption of mercury vapor is rather complex, and as one or two points in regard to it were still somewhat obscure, the investigation commenced with a study of this phenomenon. Combining previous work with our supplementary observations we arrive at the conclusion that the absorption spectrum is as represented in Figure 1*a*, viz.:

1. A strong absorption line at 2536 A, and a weaker one at 2539 A.

2. Four lines at 2346, 2339, 2334, 2331 A which fuse together with rise of temperature, forming a band which gradually pushes toward the side of short wave-lengths with increasing vapor-density.

3. There is in addition a strong absorption line at 1849 A corresponding to the powerful emission line at the same point.

4. Two strong and very asymmetrical absorption bands, one with its head in close proximity to the 2539 line and the other with its head near 1849 A. These bands creep out gradually, with increasing vapor-density toward the region of longer wave-lengths.

The complete fluorescence spectrum, which, for reasons which will be explained presently, is given by excitation with the zinc spark, is shown diagrammatically in Figure 1*b*.

It consists of: (1) a symmetrical structureless band, extending from the red down to wave-length 3700, with its maximum at 4850 A; (2) a similar broad band with a maximum at 3300 A, the two fusing together with long exposure; (3) an asymmetrical faint band coinciding with the absorption band just above 2539; and (4) a somewhat asymmetrical band extending from 2349 to 2100 A.

There are in addition the lines 2536 A and 2539 A, which, however, are not very strongly developed with the zinc spark.

It is of the utmost importance to find out how the absorption bands and lines are related to the fluorescent emissions.

For the examination of this point it is necessary to excite the vapor with monochromatic radiation or groups of such radiations lying in different regions of the absorption bands.

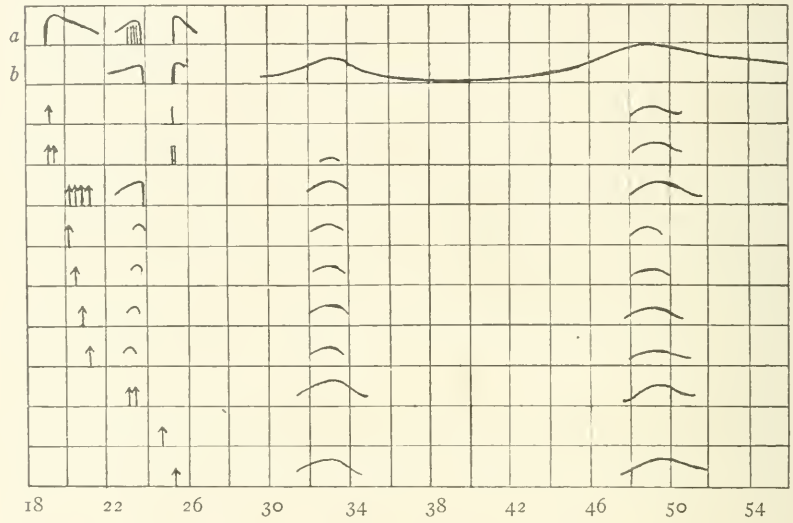


FIG. 1

a, absorption spectrum
b, fluorescent spectrum due to excitation by zinc spark
↑, exciting lines |, emission lines

Two methods have been employed for the isolation of such radiations, viz., prismatic decomposition of the light of the spark by means of two large quartz lenses with a quartz prism, and the method of focal isolation employed by Rubens and Wood for the isolation of very long heat waves.

In the former case two quartz lenses of 8 cm aperture and 50 cm focus were used in conjunction with two Cornu prisms, mounted on top of one another. In this case the bulb was placed immediately behind a tin screen, perforated with a slit and coated with

Willemite, on which the spark lines were focused. This screen rested on the funnel beneath which the Bunsen burner was placed, and the bulb was placed immediately behind the slit. By moving the quartz lens any desired spectrum line could be passed through the slit to the bulb.

In the second case the central portions of each lens were screened off by means of a black paper disk. The axes of the lenses and the spark were placed in line with a small, circular hole in a metal screen, coated with Willemite, behind which the bulb was placed. The desired groups of rays were then focused so as to pass through this hole on to the bulb. The object of the disk was of course to cut out the central beam of light.

This second method gives greater intensity of illumination, as the absorption of the prism is avoided, the full aperture of the lenses is utilized, and the greater transparency of the thin edges of the lenses for the very short wave-lengths comes into play. It suffers from the disadvantage that only a rather wide group of radiations can be isolated. Focal isolation with mercury fluorescence clearly shows the presence of the group of weak zinc lines between 1900 A and 1860 A. These lines are absorbed by the monochromator to such an extent that they have no effect on either the Willemite screen or the mercury vapor. To avoid the possible absorption of the fluorescent light by the vapor, the quartz spectrograph was directed toward the face of the bulb where the light entered in such a direction that little of the exciting light was reflected into the spectroscope. This condition was obtained by reducing the diaphragm of the spectroscope and observing the bulb through the instrument (eye placed at the focus) and arranging matters in such a way that none of the spark images seen reflected from the bulb walls fell within the aperture of the diaphragm.

EXCITATION IN THE 1849 ABSORPTION BAND

This absorption band begins at wave-length 1849 A and extends toward the visible spectrum with increase of vapor-density, reaching 2200 A at about 280° C., with a column of vapor 10 cm in length.

On separating the aluminum lines by means of the monochromator and allowing Al 1854 to excite the vapor, it was found that visible fluorescence first appeared at 210° C. and that the slightest increase in the temperature caused the fluorescent beam to recede to the face of the bulb.

On photographing the emission spectrum it was found that the excitation caused the emission of the 2536 line, and the continuous band in the green-violet (maximum at 4850). On increasing the density and photographing the emission spectrum again, it was found that the 2536 line was weaker, the green-violet band was more intense, and the ultra-violet band (maximum intensity at 3300 A) now appeared and grew stronger as 2536 A decreased in intensity. No trace of the 2539 line appeared, though this may have been due to insufficient exposure.

From this it appears that excitation at low vapor-density, with radiation at the head of the extreme ultra-violet band, causes a concentration of the emitted energy in the green-violet band; at higher vapor-density, however, the ultra-violet band appears and the 2536 line fades away. The same thing was observed if the excitation was caused by the Al lines in the region 1854–1862, though in this case there was a trace of the ultra-violet band, even at the low density, while at the higher density it was nearly as strong as the green-violet band. The development of the ultra-violet band is thus seen to be favored by excitation in a region a little removed from the head of the band.

It must be understood, however, that the wide ultra-violet absorption band may be a complex of several bands, each one associated with an emission band. If this were the case, we should then have the green-violet band associated with the component of the ultra-violet absorption band which falls just above the 1849 line, the ultra-violet emission band with a component of the absorption of somewhat longer wave-length, and if there were a third component of still longer wave-length, and we excited in this region, we should expect a third fluorescent band still farther down in the spectrum.

This is, in fact, the case, because on excitation by the group of zinc lines in the region 2000–2150 A we find a new fluorescent band,

not previously described, in the region 2349 to 2100. This band occupies approximately the position of Steubing's fluted band, of which we have never been able to find any trace. In addition, we find a trace of 2536 A and 2539 A and a faint band with its head at 2539 A which corresponds to the absorption band shown in Figure 1*a*.

The newly discovered fluorescent band at 2346 A behaves in a manner quite different from that of the bands in the green-violet and upper ultra-violet.

This band is excited in its entirety by the group of four zinc lines 2024, 2061, 2909, and 2138 A. If these are separated by the monochromator and the excitation is produced by each in turn, it is found that the region of maximum intensity in the new ultra-violet band moves to the violet end of the spectrum as the exciting line moves toward the visible end of the spectrum, i.e., excitation by the zinc line of shortest wave-length gives us only the portion of the emission band of longer wave-lengths, while excitation by the zinc line of longest wave-length gives only the short-wave-length portion of the band. Expressing this in other words, when we excite by the zinc lines in succession (increasing wave-length), the emission band moves down toward the excited region. If now we move the exciting wave-length still farther up the spectrum, utilizing a group of cobalt lines in the region of the group of absorption lines at 2346 A, we obtain the green-violet band and the next ultra-violet band (3300) of uniform intensity. The same is true if we excite with the monochromatic radiation of the 2536 Hg line obtained from the water-cooled mercury arc.

There is left now only the absorption band just above 2539 A. If we form an image of the two strong zinc lines (one of which lies to the right and the other to the left of the 2536 Hg line) on the surface of the quartz bulb, we find on heating the bulb that the zinc line of longer wave-length causes fluorescence. This line falls within the absorption band above referred to. The spectroscope shows that in this case we have also the green-violet and ultra-violet bands of uniform intensity.

On exciting the vapor by all the aluminum lines lying below 2360 a faint line appeared at 2346 A when the vapor was distilling

slowly. On increasing the vapor-density this line increases in intensity, but is soon blotted out by the extreme ultra-violet band which increases relatively faster in intensity than the line. In addition to the emission of 2346 A, first observed by Steubing, and the band in this region, 2536 A, 2539 A and the green-violet and ultra-violet bands are emitted.

Physical Laboratory
Johns Hopkins University
Baltimore, Maryland
June 1, 1921

WAVE-LENGTHS AND PERIODIC CHANGES OF SPECTRAL TYPE IN THE VARIABLE STAR *l* CARINAE

By SEBASTIAN ALBRECHT

ABSTRACT

Cepheid variable l Carinae; periodic variations in wave-lengths and spectral type.—Since the wave-lengths of many lines in stellar spectra change progressively with spectral type it might be expected that in the case of a variable star periodic changes of wave-length might occur. A detailed study of *l* Carinae shows this to be true. The results of measurements of 178 lines between λλ 4236 A and 4495 A, made on 17 three-prism spectrograms obtained at Lick Observatory, are given in Table I. In general, those lines which vary in wave-length with stellar type vary progressively from light-maximum to light-minimum, shifting by about 0.05 to 0.2A. The spectrum may not correspond to a pure type at any phase, but by taking the average of the types indicated by the different lines for each phase, it is found that the mean type varies from F 8 near light-maximum to G 9 near light-minimum. From this change of type a change of color-index may be inferred which agrees with the changes observed or inferred for other Cepheids, showing that color is correlated not only to the hydrogen spectrum, as others have found, but also to the general spectrum. Discrepancies between these results, based on changes of wave-length, and those of Adams and Joy, based on changes of relative intensity and width of lines, are discussed.

Relation of the spectral types of Cepheids to their periods.—By tabulating the available data it is shown (1) that Cepheids are progressively of "later" type as the length of the period of light-variation increases; and (2) that the *range of variation of type* is about one type-interval and is independent of the period.

INTRODUCTION

In my first paper[1] on the determination of wave-lengths in stellar spectra of known types it was found that for many lines the wave-lengths remain substantially the same in all of the spectral types in which these lines are present. For numerous other lines, however, the wave-lengths change progressively[2] from type to type, so that for any particular line a smooth curve can be drawn through points plotted with $\Delta\lambda$ as ordinates and types as abscissae. In my early experience this was found to hold so rigidly that it was possible to estimate the stellar type—which had not previously been looked up—from the residuals of radial velocity, or of equivalent $\Delta\lambda$,

[1] *Lick Observatory Bulletin*, 4, 90, 1906, and *Astrophysical Journal*, 24, 333, 1906.

[2] Progressive in the sense of not having discontinuities, but with no restrictions as to direction of change.

for a few of the lines which are subject to the most pronounced changes in position. Subsequently this inversion of the process was employed for developing a method[1] whereby the spectral type can be quantitatively determined from the spectrograms of the star by a direct comparison of the measured wave-lengths with the curves representing the variations in the regular series of types.

At the time when the progressive changes in wave-length as a function of stellar type were discovered, it was pointed out[2] that similar changes of wave-length which would be progressive with the phase of light-variation might be found in the spectra of individual variable stars. Such periodic changes of wave-length, if found, would offer a quantitative method for the determination of actual changes in spectral type synchronously with the changes in light. The very limited amount of material then available, principally for the star η Aquilae, ". . . . showed very strong indications of just such variations in the positions of certain lines."[3] At my suggestion Director Campbell kindly asked Dr. Curtis, then in charge of the Mills Observatory in Chile, to secure for this study series of spectrograms of the fourth-class variable stars l Carinae and κ Pavonis. The present paper discusses the measures of the spectrograms of l Carinae, $\alpha = 9^h42^m$; $\delta = -62°3'$ (1900); magnitudes 3.6–5.0; period 35.5 days, which were secured at that time.

PART I. WAVE-LENGTHS FROM 4236 A TO 4495 A, OBSERVED WITH THREE PRISMS

Seventeen three-prism spectrograms of l Carinae are available. Three of these (Nos. 299, 311, and 312) were taken with the short (16-inch) camera, and fourteen with the long ($21\frac{1}{4}$-inch) camera.[4] Hγ is central on the plates, and the Fe spark was used as source of light for the comparison spectra. All of the plates were measured

[1] *Astrophysical Journal*, **33**, 130, 1911.

[2] *Ibid.*, **24**, 335, 1906.

[3] *Lick Observatory Bulletin*, **4**, 131, 1907; and *Astrophysical Journal*, **25**, 334, 1907, footnote.

[4] *Publications of the Lick Observatory*, **9**, 56, 1907.

by the writer before leaving Mount Hamilton, except Nos. 1149, 1150, and 1201, which were measured by Dr. Olivier, and No. 312, which was measured by Dr. Palmer and the writer. Miss Hobe, Dr. Glancy, and Dr. Merrill assisted in the preliminary reductions. The methods of measurement and reduction employed are similar to those described in *Publications of the Lick Observatory*, 9, and no large errors would be introduced by assuming the system to be the

TABLE I

λ for Radial Velocity	Number of Long-Camera Plates	λ for Radial Velocity	Number of Long-Camera Plates
4245.438	8	4379.383	7
50.296	13	83.720	13
50.955	13	87.007	14
54.502	9	91.147	14
74.955	9	95.255	14
88.143	14	99.917	14
92.304	13	4400.615	14
93.224	6	01.613	14
94.277	14	04.932	13
4306.921	14	07.853	13
13.043	13	08.579	8
15.178	11	17.863	13
18.870	14	20.686	14
20.975	14	27.444	14
25.195	14	28.715	12
28.104	14	41.875	13
34.075	14	42.529	14
37.227	10	47.915	13
39.713	4	50.654	13
52.018	13	59.317	14
52.949	14	66.749	14
71.363	14	68.663	13
4376.104	14	4476.211	13

same as for plates with numbers 500+ in that volume. However, in order to define the system more accurately for future use, the stellar wave-lengths employed in the reductions for radial velocity are given in Table I, together with the number of long-camera plates on which these lines were used. Half of these lines are of constant wave-length, both in *l* Carinae and in the corresponding types in the stellar series. The remaining lines vary in wave-length. Logically, only the stellar lines of constant wave-length should have been used in defining the system, and the reductions might

TABLE II

OBSERVED WAVE-LENGTHS FOR THE PRINCIPAL LINES WHICH WERE FOUND TO VARY IN *l* CARINAE

λ	312 2.1	1115 2.6	1120 3.6	1124 6.7	1147 11.6	1149 12.5	1040 17.1	299 17.6	1201 21.0	1209 21.9	1212 23.0	1220 24.0	1150 24.5	311 29.6	1079 30.1	1090 32.2	1098 33.2	Rowland λ in Sun	Rowland Inten. in Sun	Adams Inten. in Sun-Spots	Lockyer Enhanced El.	Lockyer Enhanced Spark	Lockyer Enhanced Arc
4258.4...	.427	.377	.387	.403	.428					.458	.489	.467			.460	.433	.377	.201	Zr 0		Zr	2–3	1
																		.219	1N	0–1			
																		.477	Fe 2	4			
																		.639	0N				
																		.774	Fe 2				
4262.0...		.120	.060	.096	.110					.043		.043		.010	.099	.032	.056	.891	2		Zn	1	0
																		.086	1	0	Cr	5–6	0
																		.142	1				
4268.0...	.985	.009	.044	.047	.057					.033	.064	.043			.025	.005	.962	.900	1				
																		.985	Fe 3				
																		.138	Zr 0				
																		.266	1N				
4278.3...	.357	.371	340	.366	.351					.326	.401	.366			.363	.333	.289	.308	0				
																		.390	Fe-Ti 3	3–4			
4288.1...	.102	.127	.120	.163	.170	.149	.184	.179	.200	.162	.167	.147	.080	.039	.130	.122	.105	.038	Ti 2				
																		.149	Ni 1		Ru	1	0
																		.310	Ti, Fe 1	2			
4313.0...	.001	.014	.029	.040	.022	.009		.024	.017	.070	.992	.030	.062		.047	.067	.077	.871	0				
																		.034	Ti 3	2	Ti	7	1–2
																		.193	1N				
4320.9...	.924	.979	.977	.967	.975	.927	.954	.968	.968	.934	.948	.957	.839	.000	.973	.983	.010	.661	0	1–2			
																		.756	00				
																		.907	Sc 3	3			
																		.119	2	1	Ti	3	1
4331.8...	.853	.827	.829	.840	.815	.844	.822	.868	.824	.795	.811	.795	.802	.702	.801	.771	.779	.614	0N				
																		.811	Ni 2	2			
4334.0...	.056	.062	.072	.075	.078	.104	.092	.128	.086	.097	.071	.076	.081	.062	.065	.013	.035	.925	La 1N				
																		.063	00				
																		.174	00				
4344.5...	.561	.565	.563	.572	.582	.615	.624	.670	.630	.625	.662	.639	.692	.607	.581	.585	.566	.451	Ti– 2	n.c.	Ti	3	1
																		.670	Cr 4	6			
4352.9...	.954	.966	.958	.926	.943	.971	.921	.940	.969	.940	.959	.955	.020	.913	.945	.940	.919	.718	0N				
																		.908s	Fe 4	5			
																		.044	V 0	7			

4371.3...	.324	.334	.325	.344	.325	.356	.346	.392	.340	.347	.360	.332	.353	.289	.309	.286	.282	.144	Zr 1	1–2	Zr	3	1
																		.221	1				
																		.320	oo				
																		.442	Cr 2	3–4			
																		.588	on d?				
4390.1...		.185	.144	.128	.141		.137	.170		*.165*	*.175*	.162			.102	.052	*.175*	.801	o				
																		.930	Mn, Ni? o				
																		.034	oo				
																		.149	V 2	4			
4391.9...	.998	.886	.902	.897	.912		.916	*.848*		.953	.949	.919		.858	.908	.858	.857	.824	Co o	3			
																		.924	Cr 1				
																		.034	Co o				
4395.2...	.214	.176	.196	.199	.189	.220	.242	.264	.261	.254	.261	.280	.217	.372	.242	.293	*.309*	.943	oo	o–1	Mg	1	0
																		.020	Zr o				
																		.201	Ti 3	2	Ti	9	5
																		.413	V, Zr 2	3			
4398.2...	.325	.297	.299	.279	.265		.271	.297		.277	.291	.278		.339	.258	.298	.249	.178	1		Yt	5–6	4
																		.338	oo				
																		.460	o				
4399.9...	.934	.906	.916	.910	.913	.887	.849	.846	.925	.915	.777	.882	.874		.923	.907	.976	.776	Ni o				
4400.6...	.702	.685	.697	.659	.713	.638	.618	*.656*	.691	.726	.726	.713	.729		.656	.644	.627	.935	Ti, Cr 3	2	Ti	7	3
																		.343	Zr on d?				
																		.555	Sc 3	3–4			
																		.738	V 1	3			
4403.4...	.420	.478	.496	.458	.445		.433	.435		.448	.445	.412			.441	.441		.347	1	o–1			
																		.532	Cr, Zr o		Zr	1–2	o
4407.8...	.807	.844	.844	.844	.846	.852	.871		.797	.860	.802	.806	.854	.918	.834	.794		.810	V 2	8			
																		.871	s Fe 4				
4412.2...	.169	.206	.216	.195	.224	.258	.286	.323	.230	.219	.241	.247	.238	.232	.182	.147	.126	.092	1	o			
																		.297	V oo				
																		.415	Cr o	1:0	Mo	2	o
4416.9...	.947	.978	.958	.951	.988	.767	.833	.883	.802	.805	.807	.818	.771	*.927*	.850	.951	.967	.636	V o	1:1			
																		.811	oon				
																		.985	2	1			
4417.8...	.891	.857	.854	.872	.847	.823	.819	.846	.789	.835	.862	.853	.919	.787	.866	.928	.938	.450	Ti o	1–2			
																		.577	Co oo				
																		.740	oo				
																		.884	Ti– 3	n.c.	Ti	6	2
4422.0...	.065	.139	.109	.094	.030	*.854*	*.983*		*.912*	*.777*	.873	.844	.810		.921	.036		.733	V o	1:1			
																		.928	Ti oo	o	Ti	3	2
																		.104	1	oo–o			
																		.226	o				
4425.6...	.733	.652	.682	.654	.651		*.676*	.881		.807	.855	.799			*.690*	.657	.605	.608	s Ca 4	5–6			
																		.827	oo				
																		.931	oon				
																		.121	ooo				
																		.201	Ti on d?	2			

TABLE II—*Continued*

λ	312 2.1	1115 2.6	1120 3.6	1124 6.7	1147 11.6	1149 12.5	1040 17.1	299 17.6	1201 21.0	1209 21.9	1212 23.0	1220 24.0	1150 24.5	311 29.6	1079 30.1	1090 32.2	1098 33.2	Rowland λ in Sun	Rowland Inten. in Sun	Adams Inten. in Sun-Spots	Lockyer Enhanced El.	Lockyer Enhanced Spark	Lockyer Enhanced Arc
4427.4...	.465	.469	.453	.440	.437	.454	.450	.487	.488	.426	.481	.454	.518	.572	.505	.465	.484	.266	Ti 2	3			
																		.482	Fe 5	7			
4428.7...	.514		.664	.701	.621	.648	.660	.727	.629	.646	.674	.623	.661	.583	.649	.603		.711	V-Cr 1 d?	0:2			
4429.3...		.387	.425	.377	.400		.375			.393	.391	.384		.334	.403	.475	.328	.366	oo				
																		.456	oo				
4435.2...	.291	.194	.232	.237	.243		.258			.283	.276			.284	.249	.207	.177	.1298	Ca 5	7			
																		.321	Fe 2	3			
4441.8...	.890	.834	.904	.844	.864	.850	.830	.849		.825	.861	.864	.865		.914	.875	.843	.881	V 3N d?	5			
4444.7...	.720		.706		.676					.667	.689	.620		.659				.728	Fe, Ti 2	1–2			
4461.7...	.764	.682	.727	.745	.744	.768	.785	.826	.804	.769	.792	.765	.779	.711	.736	.711	.705	.617	Ti? 2	n.c.	Ti	3	1
																		.844	Mn 2	3–4			
																		.938	Fe 1				
4466.7...	.801	.705	.802	.758	.788	.779	.788	.797	.783	.771	.786	.756	.805	.790	.752	.749	.745	.548	Ni 0				
																		.727	Fe 5	7	K	1	0
4468.6...	.693	.604	.642	.638	.648	.654	.690	.644	.669	.682	.741	.690	.704	.764	.702	.761		.663	Ti– 5	4	Ti	9	4
4469.4...	.467	.461	.514	.502	.513		.545	.559		.581	.534	.499			.480	.447		.316	Ti 1	0–1			
																		.441	oooo				
																		.545	Fe 4	4			
																		.731	Co 0 d?				
																		.873	V oo	0			
4472.9...	.035	.010	.027	.010	.966		.966	.986		.927	.953	.920		.969	.950	.953	982	.884	Fe 1	2			
																		.967	Mn 0				
																		.095	Ni? 0	oo			

NOTES

λ 4258.4 Broad and fuzzy. Curve weak for types F to K.

4262.0 Wave-length seems smaller near minimum, in conformity with sun-spot data.

4268.0 Increase published wave-lengths for types by +.091 A.

4278.39 Narrow in sun-spots.

4288.1 Blend according to intensities in sun, .134.

4320.9 Quite broad. Blend of .907 and .119, according to intensities in sun, .992.

4331.81 Very narrow line in sun-spots.

4344.5 Blend according to intensities in sun, .597.

4352.9 Stronger at minimum. Blend of .9 and .0 is widened to red in sun-spots.

4371.36 Broad blend. The increase in wave-length toward light minimum is to be expected from sun-spot data. This effect seems not to be shown in my measures in types.

4390.1 Curve of variation systematically higher than in types, as though the weaker components had been neglected in the measures.

4391.9 Weak on violet edge in sun-spots. No measures in types earlier than G is also significant.

4395.2 Possibly the enhanced Ti component is relatively much stronger at maximum than in types? Blend according to intensities in sun, .286.

4407.8 Only slight variation to be expected. Blend according to intensities in sun .851.

λ 4412.2 .415 is given as doublet in sun-spots.

4416.9 V given as doublet in sun-spots. The relative intensities of .636 and .985 change in *l* Carinae.

4417.8 Are the strengthened companions to the violet included in blend near minimum? Or, personality in settings on close pairs (toward minimum) only?

4422.0 Near minimum broad and fuzzy. These components exhibit well the changes of type with change of light phase.

4425.6 Broad, double, rather unsatisfactory; measured single at times; fuzzy field on side toward red. Ca is winged in sun-spots.

4427.4 Partly discordant. Fe winged in sun-spots. Blend according to intensities in sun, .420.

4428.7 Doublet in sun-spots.

4429.3 In G and K the range of variation is small.

4435.2 Ca is winged in sun-spots. Solar blend, .184.

4441.8 Very broad in sun-spots. Small range and weakly determined in types.

4464.7 Wave-length is systematically smaller in *l* Carinae. Is enhanced Ti relatively stronger in *l* Carinae than in types? Solar blend, .772.

4466.7 Fe "widened, hazy" in sun-spots.

4472.9 Adams, "widened to red. Rowland inten. too low: 2 better for total."

have been repeated, a posteriori, for this purpose. However, a detailed examination of the lines of variable wave-length shows that the increases and decreases of wave-length for the various phases of the star pretty closely balance each other, so that no appreciable gain would result in this case from a re-reduction. The details for the wave-lengths of the Fe comparison lines, the dispersion formula, and the correcting curve used with the formula, being the same for my more extensive measures of Southern Mills spectrograms with numbers 500+, more appropriately belong with those results and need not be duplicated here. Other data in regard to the spectrograms are available, if desired by anyone.

The observed wave-lengths (on the Rowland system, defined), obtained from the individual spectrograms, correct relatively to each other within errors of measurement and reduction, are given in Tables II and III, columns 2 to 18. With the exception of the double measures for Plate 312, each tabulated value was derived from a single complete measure, i.e., from two settings of the micrometer thread in the direct and two in the reversed positions of the plate. The arrangement of the spectrograms in a sequence according to phase of velocity and of light variation of the star, as well as the additional columns, are for purposes to be discussed in Part II. The figures directly below the plate numbers[1] in the headings give the phase-interval to the nearest tenth of a day, after maximum of light.[2] Italics signify that the line is especially poor in appearance. The means in the "remarks" column and footnotes refer to the long-camera plates only, except when it is apparent from the subscript that short-camera plates have also been included. The wave-lengths for the lines in stellar types are taken in part from *Boletin No. 1* of the Córdoba Observatory and in part from unpublished data. As these contain small systematic corrections which may be somewhat altered in a definitive discussion to be made later, they should not be employed at present to derive systematic corrections to the wave-lengths in *l* Carinae.

[1] The Roman numerals, which refer to the plate-holders, have been omitted in the plate numbers.

[2] No recent or good early light-curve is available.

TABLE III

SUPPLEMENTARY LIST OF WAVE-LENGTHS OBSERVED IN THE SPECTRUM OF *l* CARINAE

λ in Types	312 2.1	1115 2.6	1120 3.6	1124 6.7	1147 11.6	1149 12.5	1040 17.1	299 17.6	1201 21.0	1209 21.9	1212 23.0	1220 24.0	1150 24.5	311 29.6	1079 30.1	1090 32.2	1098 33.2
4236.079	.061																
4239.970		.969	.964	.968	.964						.884	.944					.909
4241.2								.258									
4242.6	*.601*							*.512*									
4245.438	.360	.417	.409		.440		.471	.366		.379	.393	.382				.370	
4246.163	.100	.154	.160	.141	.148		.142			.132	.152	.139			.175	.147	.103
4246.9	.978		.934														
4247.583	.648		.607		.624					.559		.637					
4250.2	.289	.286	.299	.293	.280	.314			.330	.297	.271	.334	.241		.331	.273	.248
4250.9	.962	.930	.952	.939	.986	.986			.986	.956	.958	.990	.969		.985	.963	.972
4254.5	.491	.471	.508	.477	.461					.498	.533	.533		.530	.594	.557	
4256.3	.338																
4266.0		.126	.097	.061	.063		.065			.053	.052	.053			.081	.048	
4267.0	*.007*	*.030*	.064	.065	.006					.026	.040	.064			.051	.022	.902
4268.8			.889	.907	.896					.924	.857	.897			.883		
4271.322	.139															.122	
4271.9	.885																
4273.5			.541														
4274.9	.885	.934	.910	.956	.931			.832		*.934*	.978	.971			.992	.975	
4275.7	.674	.752	.749	.760	.735					*.875*	.744	.770			.734	.761	
4276.84		.908	*.808*	.864	.859					.847	.792	*.853*					
4277.62	.516	.633	.637	.644	.606		.557			.586	.568	.576			.544		
4279.04					.075						.037						
4282.580	.449	.615	.536	.594	.583												
4283.160		.160	.169	.189	.135									.142		.200	
4284.5	.510				*.511*												
4285.617		.599	.595	.632	.616												
4287.0	.042																
4287.596					.598												
4290.2	.238																
4292.307	.364	.377	.324	.364	.335	.348			.352	.395	.372	.354	.385		.355	.350	.335
4293.2	.185				.295					.158	.200				.170	.143	.214
4294.277	.198	.234	.226	.241	.248	.227	.238	.183	.220	.162	.236	.213	.110	.154	.271	.264	*.294*
4295.0			.053		.098					.120	.082	.085		.120	.079		
4296.02	.088		.102		.040	.091		.081	.053	.052	.048	.053	.095	.052	.091		
4296.8		.842	.813								.951	.897			.869	.823	
4298.1	.078	.149	.086					.097		.088	.102	.070			.102	.103	
4304.6	.666														.630	.702	
4306.924	.918	.951	.907	.955	.920	.941	.921		.944	.942	.904	.941	.984		.898	.867	.885
4308.041	.005	.058	.995													.085	

4309.7		.725	.765															
4314.3	.317	.330	.264		.312						.378	*.324*	.345		.357		.341	
4315.1	.156	.214	.198	*.238*	.202		*.244*				.198	.254	.231		.160	*.222*	.218	*.273*
4316.2	.282										*.222*							
4317.1		.010										.030						
	.150				.255			*.235*		.157					.163			
4317.4					.494							.467						
4318.8	.954	.957	.921	.938	.888	.916	.921	.959	.901	.895	.908	.905	.878	.866	.855	.868	.872	
4319.7					.718		.759	.728		.689	.721			.877				
4321.9		.017	.004	.980	.928	.907				.922	.933	.915			.926	.922		
4322.6		.727	.654	.669	.680		.660			.686	.701	.671				.639		
4323.5		.500																
4325.1	.173	.138	.143	.142	.175	.175	.152		*.204*	*.168*	.171	.198	.166	.224	.138	.166	.212	
4325.9	.905	.996	.992	.966	.969		*.028*		.020	*.993*	.046	.019			.967	.985	.025	
4327.16	.093	.127	.108	.099	.151		.139	*.141*		.126	.125	.122		.112	.122	.072	.171	
4328.104	.151	.113	.087	.110	.097	.170	.086	.094	.113	.110	.092	.108	.101	.151	.080	.124	.091	
4329.1	.171							.334		.227	.200	.180			.217			
4330.7	.718	.703	.717	.709	.697					.629	.629	.659		.780	.664	.752		
4332.9	.884	.942	.922	.896	.895		.886	.949		.874	.917	.906		.882	.887	.914		
4335.00							.950			.942	.993			.029				
4336.4	.436										.387							
4337.227	.312	.274	.289	*.259*	.212		.204	.291			*.243*	*.256*			.207	.232	.219	
4338.0	.126																	
4339.713											.717			.630	.652	.712	.651	
4340.6											*.624*							
4341.0														.024				
4341.5											.456							
4342.3		.341		.356	*.350*		.330	.362		.337	.337	.341			.376	.302		
4346.0								.081										
4346.8	.872				.762													
4347.46					.405									.461				
4348.0	*.940*				.023									.164				
4349.14	.124	.120	.192	.121	.170		.126	.132		.129	.141	.134			.116	.088		
4349.9	.982	.998	.958	.980	.980		.978	.080		.918	.926	.912			.967	.966		
4351.1		*.163*	.228	.180	.162						.207				.177	.145		
4352.0	.950	.006	.946	.022	.014	.024		.980	.041	.109	.038	.017	.031		.902	.021	*.004*	
4354.7	.708	.745	.734	.710	.710		.743	.898							.862	.790		
4355.29			.311	.240														
4356.12			.119	.136			.146									.105		
4358.3																.370		
4358.8	.726		.804		*.766*			.791		.678	.748	.656			.638	.872		
4359.8	.830	.833	.837	.791	.797		.822	.838		.798	.767	.774		.700	.771	.822	.779	
4360.9			.972											.853				
4362.2	.157		.176				.240	.187		.087	.111							
4363.4	.423		.412					.402			.430							
4364.8			.820															
4366.3	*.349*																	

TABLE III—*Continued*

λ in Types	312 2.1	1115 2.6	1120 3.6	1124 6.7	1147 11.6	1149 12.5	1040 17.1	299 17.6	1201 21.0	1209 21.9	1212 23.0	1220 24.0	1150 24.5	311 29.6	1079 30.1	1090 32.2	1098 33.2
4367.9	.033	.990	.928	*.970*	*.952*						.983					*.922*	.922
4369.9	.900	.812	.807				.888	.938		.856	.858	.850			.834	.815	
4373.7	.760																
4376.1	.104	.108	.096	.098	.111	.105	.131	.066	.096	.108	.117	.117	.134	.094	.115	.121	.093
4379.3	*.420*				.382		.388	.385		.362	.373	.402		.494	.382	.383	
4382.1					.169		.219							.209			
4383.721	.660	.702	.708	.717	.724	.701			.764		*.689*	*.634*	*.793*		.745	.755	.776
4385.0					*.040*												
4385.3								.338									
4385.6					*.646*												
4387.0	.962	.982	.957	.963	.962	.957	.962	.041	.975	.909	.953	.962	.917	.938	.937	.960	.979
4388.0					.035												
4389.4	.450	.400	.406	.407	.403		.415	.434		.414	.454	.406			.390	.406	.336
4391.14	.116	.129	.100	.110	.148	.077	.156	.105	.118	.169	*.099*	.113	.115	.986	.138	.115	.091
4393.4					.418												
4394.2	.197	.200	.214	.200	.217		.191	.287		.190	.188	.185		.200	.166	.218	.203
4396.01		.050	.053	.043	.053		.049			.998	.087	.032		.984	.985	.971	
4401.613	.648	.634	.622	.628	.632	.642	.657	*.634*	.616	.614	.598	.606	.626	.635	.601	.565	.562
4404.932	.942	.922	.950	.958	.958	.917		.907	.911	.900	.901	.923	*.811*	.023	.947	.928	.991
4406.81					.767		.769	.833		.781	.817	.782			.769		
4408.579	.648	.601	.620		.601					.654	.646	.614		*.679*	*.629*	.610	
4409.5		.558	.548		.533					.575	.525	.526		.505	.519	.525	
4411.0	.057		.099					.028		.983	.994	.962			.995		
4413.7	.874	.812	.834		.851					.807		.814		.780		.781	
4415.4	.443		.456							.375	.374	.371			.361	.410	.452
4418.5					.510												
4420.694	.789	.758	.730	.726	.695	.683	.710	.718	.677	.680	.676	.671	.634		.670	.718	.682
4422.7			.797		.778										.782	.817	
4423.0								.045$_n$		.928	.905						
4424.3	.527							*.342*		.361	.360	.327		.257	*.417*		
4430.1					.162												
4430.7					.741			.714									
4431.5					.525												
4433.3	*.393*				.365												
4434.0	.043				.020												
4435.4												.440				.411	
4435.7		.719	.753	.790	.750		.805			.787	*.759*			.839	.830		
4437.1					.152		.102							.051			
4437.9					.935												
4442.529	.548	.556	.531	.529	.506	.532	.528		.531	.538	.531	.531	.594		.544	.594	.500
4443.2	.254	.251	.237	.207	.209	.252	.182		.224	.212	.240	.185	.203		.212	.194	
4443.9	.975	.935	.949	.998	.966	.148	.977		.139	.060	.052	.059	.181	.058	*.066*	.048	

4445.6							.668	.734		.654	.684			.593				
4447.2					.214		.161				.189							
4447.915	.950	.936	.971	.911	.919	.952	.928	.881	.959	.897	.892	.874	.930	.897	.879	.908	.881	
4450.7	.724	.722	.743	.749	.746	.746	.810	.749	.713	.767	.763	.716	.752	.750	.731	.720	.715	
4451.8			.901							.878						.827		
4454.9			.923					.964						.955		.851		
4457.6			.659					.625										
4458.3	.443															.300		
4459.3	.348	.342	.370	.356	.339	.351	.356	.323	.320	.314	.332	.324	.360	.290	.280	.281	.307	
4460.4	.468	.392	.369		.430		.466	.397		.420	.318	.428		.446		.345	.345	
4471.1																.182		
4476.2	.226	.216	.208	.200	.211	.208	.227	.214	.176	.164	.184	.133	.182	.178	.191	.158	.182	
4481.4	.425																	
4482.4	.470													.456				

NOTES

λ 4250.2 Mean, .29213.
4250.9 Mean, .96713.
4271.322 λ is 0.2 A lower than in types.
4276.84 A rather poor line.
4282.580 Mean, .5824.
4284.5 Very broad blend.
4285.617 Mean, .6104.
4292.307 Mean, .35713.
4295.0 Broad.
4296.02 A slight variation indicated.
4296.8 Blend.
4298.1 λ slightly smaller near minimum?
4306.924 Mean, .9264.
4308.041 Mean, .0364.
4316.2 Narrow.
4319.7 .877 error? "v. faint and narrow."
4322.6 Narrow, faint. Mean, .6769.
4325.1 Fuzzy.
4325.9 Fuzzy field to red.
4327.16 Mean, .12411.
4328.104 Mean, .10614.
4329.1 Faint, broad.
4330.7 Very broad, double, resolved. On Plate 1220 the two lines are of about equal intensity; on 1090 the component toward the red is the stronger, as it is also in the sun.
4332.9 Mean, .90410.
4336.4 Faint.
4337.2 Red edge fuzzy. Faint companion included in measure near maximum?
4339.713 Mean, .6834.
4341.5 Corresponds to G5.
4342.3 Mean, 3419.
4349.14 Mean, 13410.
4349.9 Faint. Mean, .9579.
4352.0 Mean, .02013, corresponds to G4.4.
λ 4356.12 Mean, .1264.
4358.8 Broad, double. Possibly not always same components included in measure.
4360.9 .853 is blend with Ti.
4366.3 Very broad blend.
4367.9 Red edge fuzzy.
4369.9 Double, violet component weaker.
4376.1 Mean, .11114.
4379.3 Mean, .3827.
4387.0 Constant? Mean, .95514.
4389.4 Mean, .40311.
4391.14 Mean, .12014.
4396.01 Mean, .03210.
4401.613 Mean, .61414.
4404.932 Mean, .92413.
4406.81 Mean, .7816.
4408.579 Much stronger at minimum and in sun-spots.
4409.5 Mean, .5398.
4411.0 Mean, .0075. "Broad; Double?"
4413.7 λ may diminish toward minimum.
4415.4 Strong, broad (double). Variation may be real.
4420.694 Varies? Mean, .69414 corresponds to G4.6.
4423.0 Broad.
4424.3 Not always same components measured.
4430.1 Corresponds to Ko type.
4430.7 Correspond to G8 and K2 respectively.
4435.4 For mean of 35.2 and 35.7.
4437.9 Broad and strong at minimum. At maximum very faint.
4445.6 Mean, .6693.
4447.915 May vary. "Winged" in spots.
4450.7 Broad? Mean, .74214.
4460.4 Varies? Mean, .3909.
4471.1 Broad; fades off on edges.
4476.2 λ varies in *l* Carinae and in types.
4482.4 Much stronger at minimum. "Much widened" in spots.

PART II. CHANGES OF SPECTRAL TYPE IN l CARINAE

My early measures and reductions, in 1908, showed quite clearly changes of spectral type from maximum to minimum light. This change of type is at once evident by comparing under a microscope a plate taken near maximum with one taken near minimum. Unfortunately the spectrograms are not at hand, so that I shall have to be content with reproducing some of my notes from such a comparison made rather hastily in 1908:

The absorption is greater at light-minimum. The spectrum has a somewhat knotted appearance, giving the impression of the presence of bright lines. Probably on account of the increased absorption this appearance becomes more prominent at minimum. A direct comparison of plates 1115 II and 1220 IV, at 2.6 and 24.0 days respectively after maximum, shows:

4351 stronger at minimum.
4352.9 stronger at minimum.
4358.9 widened toward the violet and stronger at minimum.
4376.1 faint at maximum; strong at minimum.
4404.9 stronger and widened at minimum—thus resembling late type.
4408.5 becomes very much stronger at minimum. Compare appearance with 4409.5.
4413.7 good and sharp at maximum; becomes somewhat weaker and fuzzy at minimum.
4422.0 widens toward violet at minimum; violet edge fuzzy at minimum.
4325.6 red edge fuzzy at maximum; line broad, strong, and sharp at minimum; very marked.
4437.9 broad and fairly strong at minimum; at maximum very faint.
4445.7 strong and sharp at minimum; very faint (not measurable) at maximum.
4471.0 has edge toward red fuzzy at maximum; sharp at minimum; very decided difference.
4481.4 Mg and Ti much weaker at minimum.
4482.3 much stronger at minimum.
4490 much stronger at minimum.

The last line is a blend of 4489.91 Fe 4, in sun-spots 6, and 4490.25 Mn–Fe 3 N, in spots 3–4. These notes are especially interesting when compared with the data for the same lines in Tables II and III, most of which were subsequently obtained and which they supplement as far as they go. The changes of intensities from near light-maximum (type F9.4) to near minimum

(type G8.6)[1] run parallel with the changes from sun (type G) to sun-spots (type K). Note also, for example, that 4445.7, marked "very faint (not measurable) at maximum," later received no measures near maximum.

Although the wave-lengths resulting from my early reductions were at the time compared for type with my first curves of variation in the stellar series, publication of the results was delayed because this comparison lacked the quantitative accuracy which was readily foreseen to be possible. The improvement of the curves for the stellar types and my method for determining stellar types[2] resulted largely from a desire to determine accurately the changes of spectral type in variable stars in a way which would be strictly quantitative and be as free as possible from the personal element. The results given below for *l* Carinae still do not represent the greatest accuracy attainable by these methods, for the reason that the measures are not all by one observer, and, from the experience gained, a somewhat improved list of lines could be selected for measurement. I hope that observers with adequate instrumental equipment may extend this work to other variables and to other regions of the spectrum, as we may confidently expect very profitable results. If desired, I would gladly suggest a suitable list of lines to anyone who wishes to take up a similar study. The dispersion of three prisms should be employed in order to have the scale sufficiently large. The effects noted below were first looked for on the one-prism spectrograms of Y Ophiuchi and T Vulpeculae, but the dispersion was inadequate. For best results all the different factors entering into the problem, such as slit-width, general intensities of exposure, development, etc., should be maintained as constant as possible. Except for very short light-periods, the exposure time may more safely be varied than the slit-width to allow for the changing intensities of the light. For the present, in order to avoid certain systematic effects, discussed in a report to the Solar Conference in 1913, the curves of variation of wave-length upon which determinations of type are to be based

[1] See Table IV, Plates 1115 and 1220.

[2] *Astrophysical Journal*, 33, 130, 1911.

Lines of Varying Wave-Lengths

Spectrograms arranged according to phase of light variation

Continuous lines for *l* Carinae; dashed lines for types

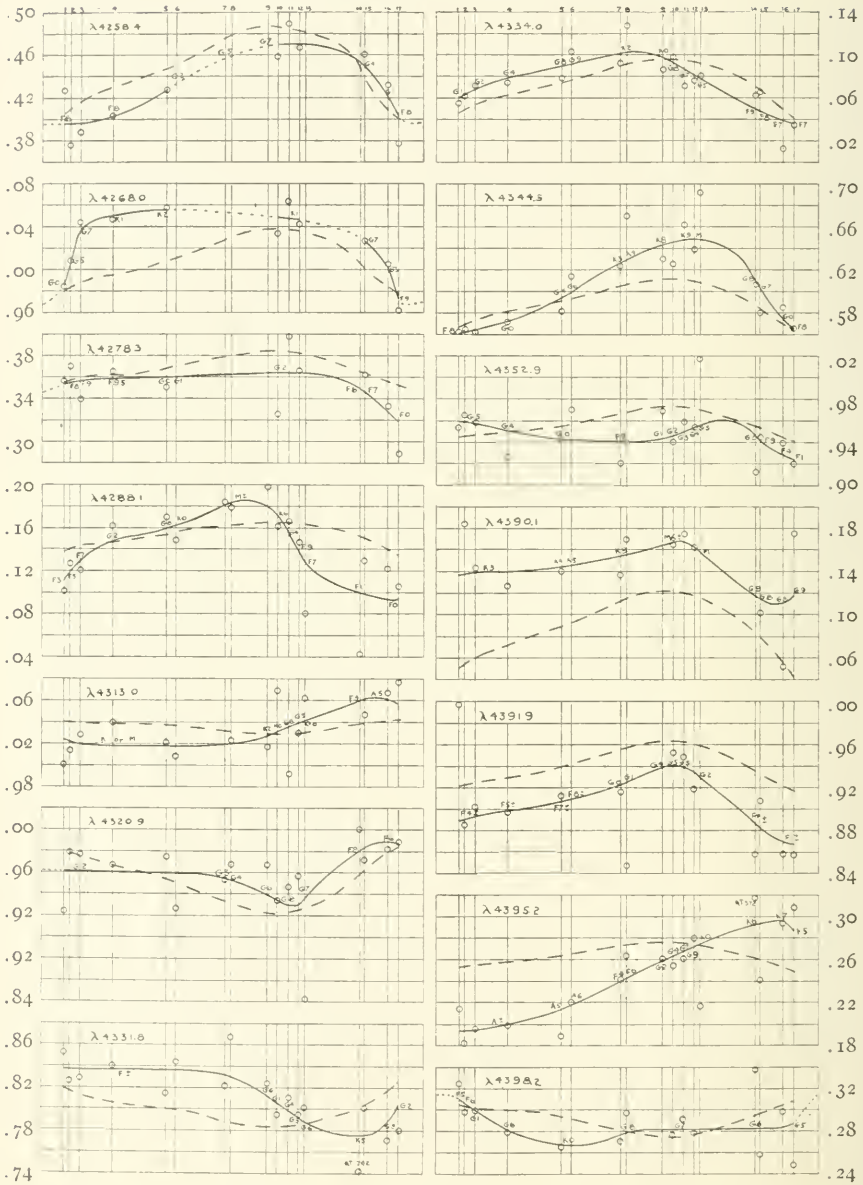


FIG. 1

Lines of Varying Wave-Lengths—*Continued*

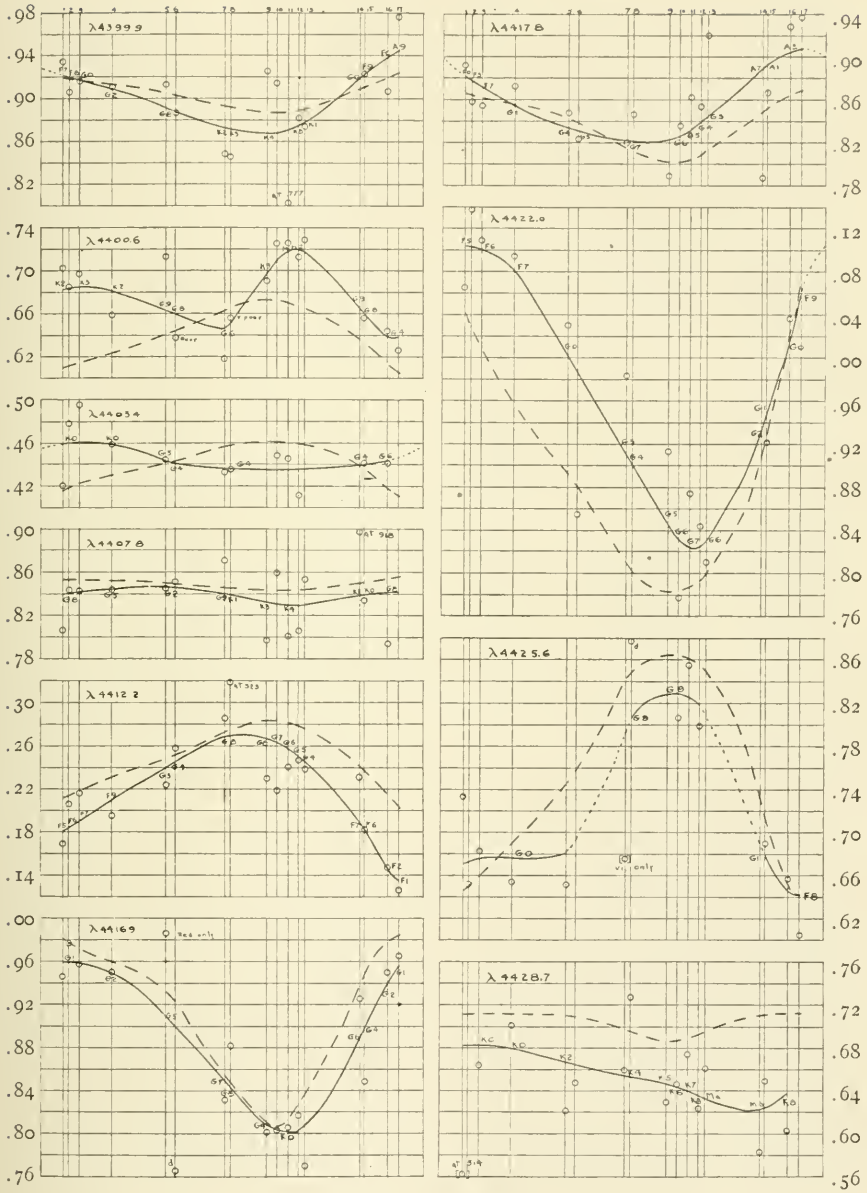


FIG. 1—*Continued*

Lines of Varying Wave-Lengths—*Continued*

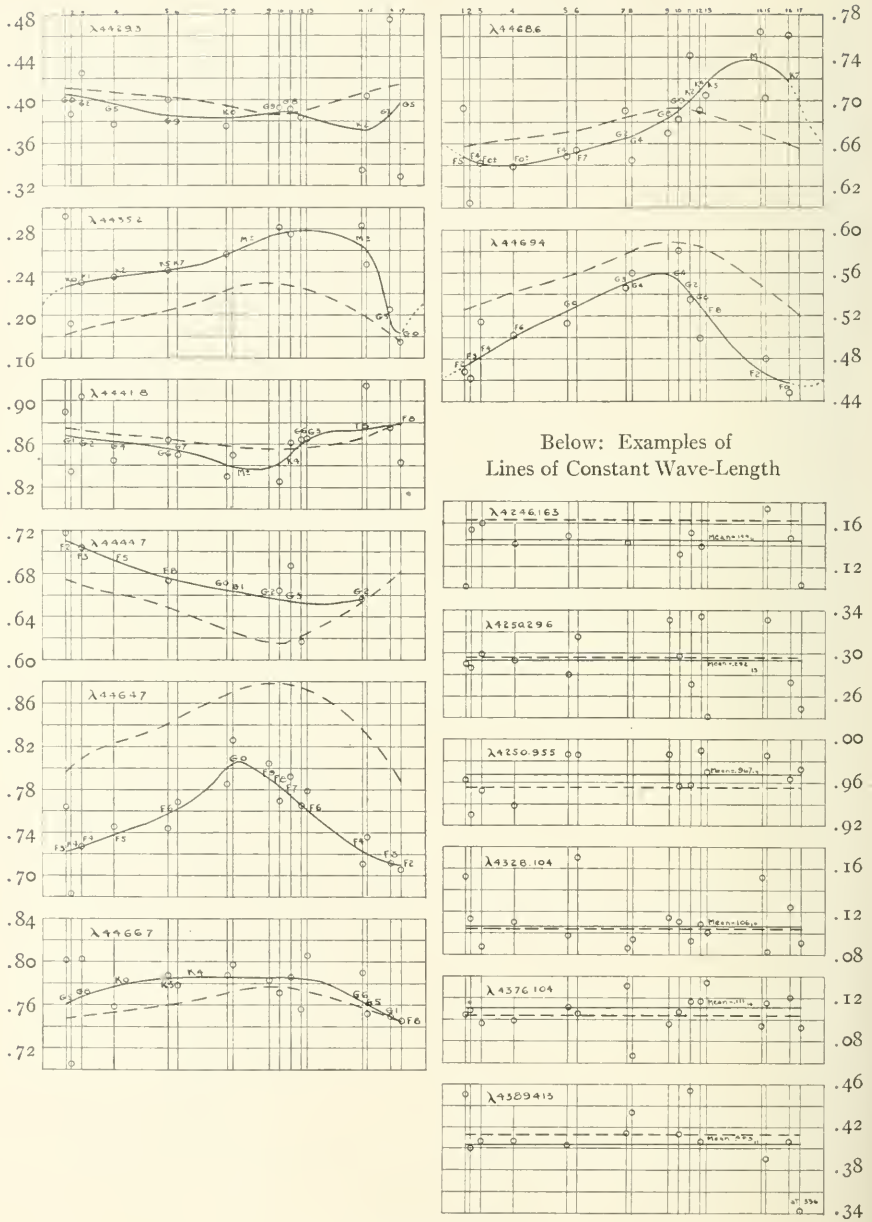


FIG. 1—*Continued*

should be determined from plates taken with the same instrumental equipment which was used to obtain the plates for the star under consideration.

The wave-lengths in Tables II and III furnish the data for a quantitative determination of the spectral type of *l* Carinae corresponding to each spectrogram. The individual lines give separate determinations of type by comparison of the observed wave-lengths with the curves of variation found for the lines in the general series of stellar types. With but two exceptions only curves published in *Boletin No. 1* of the Córdoba Observatory (1911) were used. The results of this comparison are collected in

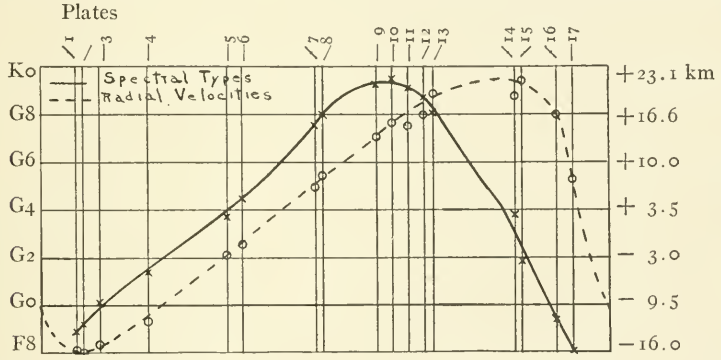


FIG. 2.—Simultaneous variations of spectral type and of radial velocity in *l* Carinae.

Tables IV and V, which are self-explanatory, and in the figures. The weights in the third column of Table IV were formed according to (*a*) the range of variation of wave-length from types F to K in the stellar types, and (*b*) the definiteness of the curve showing the change of wave-length with change of phase in *l* Carinae, taking into account also the number of observations upon which the curve is based. The means at the bottom of Table IV, which may be regarded as fairly representing the actual changes of type in this star, are compared in Figure 2 with the simultaneous changes of radial velocity. The curves for spectral type and for radial velocity in the figure synchronize with each other about as closely as other variations in Cepheids have been found to synchronize with each other.

TABLE IV

THE TYPES INDICATED BY THE INDIVIDUAL LINES FOR EACH SPECTROGRAM OF *l* CARINAE

λ	No. of Obs.	Weight	312 1	1115 2	1120 3	1124 4	1147 5	1149 6	1040 7	299 8	1201 9	1209 10	1212 11	1220 12	1150 13	311 14	1079 15	1090 16	1098 17
4258.4	11	.50	F8	F8	F8	F8	G1.5	G2	G5	G5.5	G7	G7.5	G7.5	G7.5	G7.5	G5	G4	G1	F8
68.0	11	.50	G0	G5	G7	K1	K2	K2	K1.5	K1.5	K1	K1	K1	K1	K1	G8	G7	G3	F9
78.3	11	.34	F7.5	F8	F9	F9.5	G0	G1	G1	G2	G2	G2	G2	G2	G1	F8	F7	F0	F0
88.1	17	.45	F3	F5	F7	G2	G8	K0	M±	M±	M±	K6	G4	F9	F7	F1	F0	F0	F0
4313.0	15	.0	(K or M)								K2	K0	G8	G5	G0	F9	A5	A5	A5
20.9	17	.45	G2	G2	G2	G2	G2	G3	G3	G4	G6	G8	G8	G8	G7	F8	F8	F6	F6
31.8	17	.0	(F±)								G0	G1	G4	G5	G6	K5	K5	G7.5	G2.5
34.0	17	.50	G1	G1	G2.5	G4	G7.5	G9	K2	K2	K0	G8	G7	G5	G5	F9	F8.5	F7	F7
44.5	17	.50	F8	F8	F8	F9.5	G4	G6	K3	K4.5	K8	K8.5	K9	M0	M0	G8.5	G7	G0	F8
52.9	17	.38	G5	G5	G5	G4	G0	G0	F9	F9	G1	G2	G3	G4	G5	G2	F9	F4	F1
90.1	12	.38	K3	K3	K3	K3	K4	K5	K9	Ma	Mb	Mb±	Mb±	Mb±	M0	G9	G8	G8	G9
91.9	14	.30	F4±	F4±	F4±	F5±	F7±	F8±	G0	G1	G4.5	G5	G5	G2.5	G2	F4±	F4±	F±	F ±
95.2	17	.34	A±	A±	A±	A±	A5	A6	F4.5	F6	G2	G3.5	G7	G9	K0	K6	K6	K7	K5
98.2	14	.38	F5	F6	G1	G6.5	K0	K0	G8	G8	G8	G7	G7	G7	G7	G6	G6	G6	G5
99.9	16	.42	F7	F7.5	G0	G2	G7.5	G8	K2	K3	K3.5	K4	K3.5	K3	K1	G0	F9	F0	A9
4400.6	16	.29	K2.5	K2.5	K3	K2	G9	G8	G5.5	G5.5	K9	Mb±	Mb±	Mb±	Mb±	G9	G8	G3.5	G3.5
03.4	12	.40	K0	K0	K0	G9.5	G5	G3.5	G3.5	G3.5	G3.5	G3.5	G3.5	G3.5	G3.5	G4	G4	G5.5	G6
07.8	15	.16	G8	G8	G8	G5	G2	G2	G9	K1	K3	K3.5	K3.5	K3.5	K3.5	K1	K0	G8	G8
12.2	17	.50	F5	F6	F7	F9	G3	G4	G8	G8	G8	G7	G6	G5	G4	F7	F6	F2	F1
16.9	17	.45	G1	G1	G1	G2	G5	G5	G7.5	G8	G9	G9.5	G9.5	G9.5	G9.5	G6.5	G4.5	G2	G1
17.8	17	.45	F0	F3	F7	G1	G4.5	G5	G7	G7	G7	G6	G5	G4	G3	A7	A1	A0±	A0±
22.0	14	.50	F5	F5	F6	F7	G0	G0.5	G3	G3.5	G5	G6	G7	G7	G6	G2.5	G1.5	G0	F9
25.6	13	.33	G0	G0	G0	G0	G0	G5	G9	G9	G9	G9	G9	G9	G6	G3	G1	G0	F8
28.7	14	.27	K0±	K0±	K0	K0.5	K2	K2.5	K3.5	K4	K5	K6	K7	K8	Ma	Mb	Mb	K8	K5±
29.3	12	.27	G0	G0	G1.5	G5	G9	G9	G9.5	G9.5	G9	G8	G8	G8	G8	K2	K2	G7	G5
35.2	12	.45	K0	K0	K1	K2	K5	K7	M±	M±	M±	M±	M±	M±	M±	M±	M±	G3	G0
41.8	15	.10	G1	G1	G2	G4	G6	G7	M±	M±	M±	M±	K4	G6	G3	F8.5	F8	F8	F8
44.7	7	.41	F2.5	F2.5	F3	F5	F8	F8.5	G0	G1	G2	G2	G3	G3	G3	G2	G2	G0	F7
64.7	17	.50	F3.5	F3.5	F4	F4.5	F6	F6	F9.5	G0	F8.5	F8	F7	F7	F6	F4	F3.5	F3	F2.5
66.7	17	.38	G5	G5	G7.5	K0	K3	K4	K4	K4	K4	K4	K4	K4	K4	G6	G5	G1	F8
68.6	16	.38	F5	F4	F0±	F0±	F4	F7	G2	G4	G8	G9	K2	K4	K5	Mb	Mo	K7	K0±
69.4	12	.50	F2.5	F3	F4	F6	F9.5	G0.5	G3	G4	G4	G4	G1.5	G0.5	F8	F2	F1.5	F0	F0
72.9	14	.41	F6	F6	F6	F7	G1	G1	G5	G5	K4	K5	K6	K6	K6	K3±	G7±	G6±	F9
Weighted means			F9.0	F9.4	G0.2	G1.5	G3.7	G4.4	G7.5	G8.1	G9.3	G9.4	G9.0	G8.6	G8.1	G3.8	G1.8	F9.5	F8.0
Sum of weights			12.2	12.2	12.2	12.2	12.2	12.0	12.0	12.0	12.2	12.2	12.2	12.2	12.2	12.0	1.20	12.0	12.2
Probable error for the mean			±0.9	±0.9	±0.9	±0.9	±0.8	±0.8	±0.8	±0.8	±0.8	±0.8	±0.8	±0.8	±0.8	±1.1	±1.1	±1.1	±1.0
Probable error of an observation of weight 1			±3.1	±3.0	±3.0	±3.0	±2.9	±2.7	±2.8	±2.7	±2.7	±2.7	±2.7	±2.9	±3.1	±3.7	±3.9	±3.8	±3.4

NOTES

λ 4313.0 Partly indeterminate—range from F to K only .020 A.
4331.8 Partly indeterminate.
4390.1 Questionable whether this line should be used here.
4391.9 Partly extrapolated. Weight too high?
4403.4 Direction of variation seems opposite to that in types.

λ 4422.0 Compared with unpublished curve.
4428.7 Curve systematically too low by .03A ±.
4435.2 Curve systematically too high.
4441.8 Compared with unpublished curve.
4472.9 1149, 1040, 299, 311, 1079, and 1090 have weight 0.16.

NOTE.—In Table IV, the seventeen vertical columns show a range of types one and three-fourths times as great as the horizontal lines. On account of the preliminary status of the method some lines were included in the determinations of type for which slight changes of wave-length correspond to large changes of type. The inevitable result is that not only will moderate accidental errors of measurement increase both the horizontal and the vertical ranges greatly, but small bodily displacements of wave-length for such a line in the spectrum of the star will shift the corresponding changes of type to a very different level, directly affecting the range in the vertical columns. To illustrate: One line may show a range of variation from, let us say, A to G while another line may indicate variations between G and K or M, the variations for the two lines synchronizing with each other and with the light- and velocity-variations of the star. For these reasons the probable errors accompanying Table IV, which were computed from the vertical ranges actually listed, do not represent the limit of accuracy which is inherent in the method. The means at the bottom of the columns may nevertheless be regarded as representing fairly well the actual changes of type of the star, because the errors referred to above, which are systematic for individual lines, partake of the nature of accidental errors for purposes of the means.

In order that the reader may not carry away the erroneous impression that an enormous amount of time will be involved in practical applications of the method employed above for the determination of spectral type, it may be well to call attention to the fact that the method is still in the preliminary stages of development. The aim has been to include as large a number of lines as the nature of the spectra and other limitations would permit, for the simple reason that the behavior of all lines was unknown and could not be safely determined by inference. As was pointed out in the article, a considerable amount of exploratory work is still urgently needed. Eventually measurement for type will be restricted to a very limited list of most suitable lines, probably not more than from eight to twelve per plate in addition to those used for radial velocity.

TABLE V

ADDITIONAL LINES GIVEN AS VARIABLE IN *Córdoba Observatory Boletin No. 1*

λ 4254.5	Partly indeterminate and partly discordant.
4267.1	Curve for stellar types is too weak—only six observations.
4274.9	Unsatisfactory. Not entirely accordant, nor is it especially discordant.
4293.2	Too few observations in *l* Carinae.
4314.3	Partly in accord in *l* Carinae, but the small range, together with the oscillations in stellar types, render this line unsuited for determinations of spectral type.

4315.1 Wave-lengths in *l* Carinae are nearly all above the highest parts of the curve for stellar types. This is one of the few lines which seem to be discordant.

4318.8 Partly accordant and partly indeterminate. The range of variation is apparently greater in *l* Carinae than in stellar types.

4321.9 Partly indeterminate—range from G to K2 is only .016 A.

4325.1 Wave-length changes by approximately the same amount as in types G to K, but the curve for types is systematically higher by .035 A±.

4325.9 More or less accordant, aside from being systematically higher by .035 A±.

4340.6 Hγ. One measure for Plate 1212 corresponds to type K2.

4351.1 Weakly determined both in types and in *l* Carinae.

4352.0 Not suitable for this purpose with present data—variation only .011 A from F to K.

4354.7 Data weak in *l* Carinae and in types.

4359.8 More or less indeterminate in types F to K except with a large number of observations.

4362.2 Data weak.

4394.2 In types later than G the measured line is a blend of λ .225 with two weak companions to the violet. The former gradually becomes weaker and the latter stronger. In *l* Carinae the faint companions were not included in the measures, as is indicated by a note for measure on Plate 1220.

4427.4 Omitted because too much of results had to be extrapolated.

4443.9 The measure sometimes includes the companion to the red, λ 4444.385. The displacement toward the red in the later types and in *l* Carinae near light-minimum may be largely due to personality in the settings on close pairs; the companion at λ .385 is then moderately strong, whereas it is quite weak in early types and in *l* Carinae near maximum light. With the additional data which I have for stellar spectra taken with several different dispersions, it should be possible to separate the personality effects from the true displacements.

4459.3 Not suited for this purpose, because in stellar types the variation of the wave-length is confined almost entirely to types earlier than G.

The Figures 1, in which the observed wave-lengths on individual spectrograms are represented by circles, give three things for each line: (*a*) the curve showing the variation of wave-length in *l* Carinae with change in phase of velocity and variation of the light; (*b*) the spectral type for each plate obtained by comparing the wave-length taken from the curve in (*a*) with the curve for the stellar series;

and (*c*) that portion of the curve for the stellar series which corresponds to the means of the types for the individual spectrograms of *l* Carinae, i.e., from F9 to G9.4 and back to F8.

The two curves in the graphs generally rise or fall together toward light-minimum, even when widely separated by systematic differences, thus illustrating how the individual lines show the progressive change of the star to the so-called later types. Note especially the lines with a large range of variation, such as 4412.2, 4416.9, 4422.0, 4425.6, 4464.7, and 4469.4. For only one line, 4403.4, the main tendencies of the two curves indicate opposite directions of change of wave-length. Minor or secondary deviations between the two curves are to be expected, first, because the present data are not ideal in every way, as explained above, and second, because of the fair possibility—and even perhaps probability—that the changes of type with changes of phase in the light and variations of velocity do not coincide in every detail with the corresponding stellar types as classified at present, and, moreover, may not always repeat themselves exactly in different periods. Also in the variable star where the surface conditions—i.e., in the comparatively shallow layer in which all of the light that reaches us originates—are undergoing constant and apparently violent changes, it would seem that a considerable overlapping of the distinguishing characteristics of types almost certainly takes place. An exact correspondence would perhaps be more surprising than the presence of moderate differences.

An interesting comparison is to follow in detail (for the components of lines) the changes of intensity from sun to sun-spots and from spark to arc and to compare these with the observed changes of wave-length in the series of stellar types and in *l* Carinae. The last five columns in Table II aid in showing the remarkable extent to which all of these changes run parallel. Some of these have been collected in Table VI in order to bring out, in a way in which verbal description cannot, how some of the shifts are produced by a weakening of an enhanced component as the star approaches light-minimum, while other shifts are due to a marked strengthening of arc or of sun-spot lines. "Str" stands for a strengthening and "wk" for a weakening of the component.

TABLE VI

λ_{Rowland}	Sun	Sun Spots	Spark	Arc	Near Minimum: Violet Comp.	Near Minimum: Red Comp.	Near Minimum: Shift of Blend in Star
	a) Enhanced Lines or Weakened in Spots						
4261.891	2						
.086	1	o	Cr 5–6	o		wk	to violet
.142	1						
4314.248	Sc 3	2			wk		to red
.381	1						
.479	Ti 1						
.673	ON						
4320.661	o	1–2					
.756	oo						
.907	Sc 3	3					
.119	2	1	Ti 3	1		wk	to violet
4371.3					wk		to red
4395.201	Ti 3	2	Ti 9	5	wk		to red
4399.776	Ni o						
.935	Ti, Cr 3	2	Ti 7	3		wk	to violet
4412.092	1	o			wk		to red
4416.636	V o	1:1					
.811	ooN						
.985	2	1				wk	to violet
4469.316	Ti 1	o–1			wk		to red
.441	oooo						
.545	Fe 4	4					
4472.884	Fe 1	2					
.967	Mn o						
.096	Ni? o	oo				wk	to violet
	b) Spot Lines or Arc Lines						
4258.219	1N	o–1					
.477	Fe 2	4				str	to red
4265.832	Ti o	o–1			str		to violet
.081	Mn 2	2–3					
4278.308	o						
.390	Fe-Ti 3	3–4				str	to red
4288.038	Ti 2						
.149	Ni 1		Ru 1	1			
.310	Ti, Fe 1	2				str	to red
4321.813	Ti o	1			str		to violet
.961	Fe 2						
.204	ON						
4344.451	Ti 2	n.c.	Ti 3	1			
.670	Cr 4	6				str	to red
4351.000	Ti 1	n.c.	Ti 2	o			
.216	Cr 3	5				str	*
4371.144	Zr 1	1–2	Zr 3	1			
.221	1						
.320	oo						
.442	Cr 2	3–4				str	to red

* To red in late types.

TABLE VI—*Continued*

λ_{Rowland}	Sun	Sun Spots	Spark	Arc	Near Minimum		
					Violet Comp.	Red Comp.	Shift of Blend in Star
	b) Spot Lines or Arc Lines						
4389.801	o						
.930	Mn, Ni? o						
.034	oo						
.149	V 2	4				str	to red
4395.201	Ti 3	2	Ti 9	5			
.413	V, Zr 2	3				str	to red
4400.343	Zr ond?						
.555	Sc 3	3–4					
.738	V 1	3				str	to red
4407.810 s	V 2	8			str†		to violet
.871	Fe 4						
4412.092	1	o					
.297	V oo						
.415	Cr o	1:0	Mo 2	o		str	to red
4416.636	V o	1:1			str		to violet
.811	oon						
.985	2	1					
4421.733	V o	1:1			str		to violet
.928	Ti oo	o	Ti 3	2			
.104	1	oo–o					
.226	o						
4464.617	Ti? 2	n.c.	Ti 3	1			
.844	Mn 2	3–4				str	to red
.938	Fe 1						

† Probably V is strengthened relatively more than Fe.

For numerous lines where the observed changes are clearly in the direction accordant with changes from sun to sun-spots, no application could be made to the determination of type because of inadequate data in stellar types. Nevertheless these lines also serve to confirm the fact that changes occur in the spectrum of *l* Carinae which are in many ways similar to consecutive changes of spectral type.

PART III

Recently Adams and Joy[1] have noted a marked distinction in the spectral types of Cepheids as obtained from the hydrogen lines alone or from the general spectrum. For nine stars they find in the mean a spectrum of F1 at maximum and F7 at minimum of light, based on the hydrogen lines alone. From the general

[1] *Proceedings of the National Academy of Sciences*, 4, 129–132, 1918.

spectrum they obtain for the same stars F9 at maximum and G0 at minimum. The mean variation of type indicated by the hydrogen lines is 0.6 of the interval between F and G, whereas the general spectrum shows a variation of only 0.1. That is, according to Adams and Joy, the general spectrum shows very little change of type during the period of light-variation. These observers note, however, in addition to the changes in the hydrogen lines, certain other differences in the spectra of Cepheids at maximum and minimum, the three most important of which, also previously observed, are: (1) a shift of the maximum of the continuous spectrum toward shorter wave-lengths at maximum of light; (2) a general, slight widening of the spectral lines at minimum; (3) an increase in the intensity of the so-called "enhanced" lines at maximum. The first of these can influence the positions of the lines only indirectly and in a minor way, and need not be especially dwelt upon here. The second and third will be referred to again later.

The main result of Adams and Joy, namely, that the indications of changes of spectral type in the Cepheids are confined chiefly to the hydrogen lines, appears to be completely at variance with my observed changes of spectral type in *l* Carinae, as determined from the general spectrum and given in detail above. In view of these contradictory results it may be well to discuss the data in Part II in somewhat greater detail, with special reference to their bearing upon this question.

The methods employed in Part II for the determinations of spectral type are essentially different from those employed by Adams, Shapley, and Joy. The latter are based upon differential relative changes in the intensities and widths of lines, partly estimated and partly measured. The former were intentionally freed as much as possible from qualitative estimations by placing the entire weight in the determinations of type upon the measured positions of the lines. Each of these methods has its limitations as well as its advantages, and I am inclined to the view that the best results will be attained by combining the two methods. To me it seems quite unsafe to neglect the measured positions of the lines, as these furnish the best means of identifying with a fair degree of certainty the components involved in observed changes of intensity and width.

As, unfortunately, the *l* Carinae spectrograms are in Santiago, they cannot be referred to at this time with the special aim of directly bridging the gap between the general spectrum and the hydrogen spectrum. My notes state that "in κ Pavonis and *l* Carinae (F5 and G types) the Hγ region looks very fuzzy and diffuse, Hγ being v v broad"; and they also contain the suggestion to "see if Hγ gets narrower and sharper toward light-minimum" than at maximum. This suggestion was not followed up because of other demands upon my time. Evidently the failure to measure Hγ on sixteen of the seventeen spectrograms is attributable to poor quality of the line, possibly in part due also to interference of close neighboring lines and to underexposure of the Hγ region on some of the spectrograms.

The lines observed, given in Tables II and III, belong to and are among the most characteristic and important lines in the general spectrum. Their measured positions identify them, on the whole I believe without any serious outstanding uncertainties, with corresponding lines in the spectra of the sun and of sun-spots, and these in turn have been identified with corresponding lines in stellar spectra. The lines having constant wave-lengths in the stellar types also have constant wave-lengths in *l* Carinae. The lines which vary progressively during the period of variation of light (Table IV), and upon which the changes of spectral type are based, are among the most important lines showing progressive changes of wave-length in the series of stellar types. Among the identified components of these lines are Cr, Fe, Mn, Sc, Ti, and V, elements of which the spectral lines exhibit marked and progressive changes of intensity in types A to M.

Nor are the observed changes in *l* Carinae covered by the general widening of spectral lines at minimum and by the increased intensity of the "enhanced" lines at maximum, effects (*b*) and (*c*) referred to by Adams and Joy. Table II shows numerous lines for which the position of the blend is progressively shifted in *l* Carinae from maximum to minimum light and in stars from early to late types, in the direction indicated by the changes in the intensities of the components from sun to sun-spots. Note, for example, the lines 4266.0, 4296.0, 4320.9, 4416.9, and 4422.0, for which both the shift indicated by sun-spot data and the observed shift in *l* Carinae

and in the later stellar types are to the violet; and the lines 4278.3, 4288.1, 4390.1, 4391.9, 4412.2, and 4469.4, for which the indicated and observed displacements are to the red. For most of these lines no enhanced components are involved. Several lines, 4292.3, 4298.1, 4391.1, and 4408.5, for which the sun-spot data indicate balanced changes for the intensities of the components, have practically constant wave-lengths in stellar types. Some lines, like 4334.0, show clearly accordant variations in *l* Carinae and in types, with no spot data given. Perhaps corresponding changes will be found in spot spectra. The wholly or partly discordant lines are few. Thus, for 4277.6 the observed displacement is toward the violet both in types and in *l* Carinae, contrary to the expected shift. For 4420.6 a slight shift toward the red might possibly be expected; the observed shift in the variable star is to the violet; in types the data are weak. Such apparent discordances may later be removed in part by additional data from spots and Cepheids. On the whole, the agreement between the expected or inferred and the observed changes of wave-length of the blends is remarkably close.

The "general slight widening of the spectral lines at minimum," additional effect (2) of Adams and Joy (above), seems also brought out in my notes of 1908, reproduced in Part II—unless I misconstrue the intent of these observers. Can the greater part of the apparent widening be explained as a widening of blends due to a considerable increase in intensity of one or more of the components rather than as a genuine widening of single lines? As in later types, so also in *l* Carinae toward minimum of light, the selective absorption increases, many more components being strengthened than weakened, with the result that numerous blends are apparently widened and a small number perhaps narrowed. This, however, does not explain all increases in width, as, for example, for 4468.6, which is apparently a single line in the sun.

My data also contain partial evidence bearing upon Adams and Joy's effect (3)—"an increase in the intensity of the so-called enhanced lines at maximum"—which seems in part confirmatory and in part suggests the changed statement "a greater relative intensity of the so-called 'enhanced' lines in *l* Carinae than in the corresponding types in the stellar series." For the former state-

ment the two curves in Figures 1 for the lines having enhanced components should diverge more and more as maximum of light is approached, the relative shift in *l* Carinae being in the direction of the enhanced component of the blend. This seems actually to occur for one or two lines (see 4395.2). For other lines (see 4464.7) the two curves remain parallel throughout their entire length, the systematic displacement between them being in the direction required for greater strength of the enhanced component in the variable star than in the corresponding stellar types. However, the evidence is not clear-cut either way. And, besides, for several lines for which the two curves are parallel and separated no enhanced components are given.

As one of the results of the foregoing investigation it is possible to outline roughly an extensive field of research which can profitably be followed. In order to be able to distinguish the characteristics shared by all Cepheids from those peculiar to individual stars, the spectra of a number of Cepheids should be studied in greater detail. The digressions from a strictly parallel behavior of the lines in Cepheids and in the series of stellar types may lead to results more interesting and far-reaching than the accordances. Also the emissions, the "knotted appearance" referred to in my notes, deserve further study. It may be to the point to recall that the one fact which more than any other led to serious questioning of the binary-star explanation for Cepheids was the discovery of the apparent relation between the light- and the velocity-variations. With dispersions equal to and greater than that of the three-prism Mills spectrographs, it should be possible to follow the simultaneous changes of the lines for the different elements through the cycle of changes of light and velocity.[1] Such results for a number of Cepheids would provide the necessary data for correlating any effects found with such factors as (1) the length of the period; (2) the limiting types between which the variations take place; (3) and (4) the types and the range of variation indicated by the different classes of lines (i.e., spark, arc, spot, etc.), and by the lines of individual elements or groups of elements; and (5) more

[1] The data in Part I are not sufficiently complete to permit of doing this in ample detail for *l* Carinae.

exact relationships of the curves representing variations of visual light, photographic light, velocity, color-index, and type.

Thus even the meager data at present available seem sufficient to establish a relation with the length of the period of light-variation. This seems to have been observed by Campbell[1] and later by Shapley[2] to apply to Cepheids as well as to the general list of variable stars as found, I believe, first at Harvard. However, the exact relationship noted below seems not to have been brought out. Table VII, taken in part from Shapley[3] and Seares and Shapley,[4] with *l* Carinae added, shows a fairly definite progression of the Cepheids toward "later" types, see columns "Shapley" and "Albrecht," with increasing length of the period. This effect seems more clearly and definitely shown in the means of groups of two or three consecutive stars, as given at the bottom of the table. Apparently it is much more strongly marked for very short periods and diminishes to slight changes for periods greater than five days. The poorly marked, slow increase in the length of the period with spectral type, found by Campbell, is thus readily accounted for by the poor representation of very short periods in Campbell's tables. The effect seems absent for the hydrogen spectrum in Adams and Joy's list of nine stars (*loc. cit.*) and to be indicated only slightly in their results from the general spectrum. Here also its apparent absence or small value seems to lie in part in the small number of stars used and in part in the absence from their list of stars with very short periods.

In Table VII my types for *l* Carinae should perhaps be somewhat reduced to make them strictly comparable with the types found by Shapley, due to the presence of a second effect, namely, that the hydrogen lines yield somewhat "earlier" types than the general spectrum. This second effect, which is apparently shown in the tables of Adams and Joy (*loc. cit.*) and somewhat strengthened by my results from the general spectrum of *l* Carinae, seems to

[1] *Lick Observatory Bulletin*, 6, 51, 1910.

[2] *Astrophysical Journal*, 40, 451, 1914, and *Contributions of the Mount Wilson Observatory*, No. 92.

[3] *Ibid.*, 44, 274, 1916, and *Contributions of the Mount Wilson Observatory*, No. 124.

[4] *Ibid.*, 48, 238, 1918, and *Contributions of the Mount Wilson Observatory*, No. 159.

TABLE VII

Star	App. Mag. at Max.	Period (Days)	Change in Color-Index				Types (at Max.—at Min.)				Type Range (Shapley, Albrecht)
			Observed Photometrically	From Spectrum			From Hydrogen		From General		
				Hydrogen		General					
				Adams and Joy	Shapley	Adams and Joy or Albrecht	Adams and Joy	Shapley	Albrecht	Adams and Joy	
RS Boötis	9.2	0.38						B8–F0			1.2
XZ Cygni	8.7	0.47	.58	(.32)			A0–A8	A0–A6			0.6
RR Lyrae	6.8	0.57						B9–F2			1.3
SU Cassiopeiae	5.9	1.95	.14	.12	.20	.04	F3–F6	A9–F4		F7–F8	0.5
TU Cassiopeiae	7.2	2.14						F1–F8			0.7
SZ Tauri	7.2	3.15						A9–F7			0.8
RT Aurigae	5.1	3.73	.35	.32	.40	.12	F0–F8	A9–F9		F7–G0	1.0
SU Cygni	6.2	3.85	.35		.36			A7–F6			0.9
T Vulpeculae	5.5	4.44	.40		.44			A9–G0			1.1
δ Cephei	3.5	5.37	.49	.40	.48	.00	F0–G0	F0–G2		G0–G0	1.2
Y Sagittarii	5.4	5.77						F4–G4			1.0
X Sagittarii	4.4	7.01						F1–G5			1.4
U Aquilae	6.2	7.02						F6–G2			0.6
η Aquilae	3.7	7.18	.42	.32	.44	{.08 .40	F1–F9	F0–G1		F9–G1	1.1
									F6–G6		1.0
W Sagittarii	4.3	7.60						A8–G2			1.4
W Geminorum	6.7	7.92						F2–G1			0.9
U Vulpeculae	6.5	7.99	.4		(.24)			F8–G4			0.6
S Sagittae	5.5	8.38	.53		.32			F4–G2			0.8
ζ Geminorum	3.7	10.1	.38	(.04)		(.04)	F2–F3			F9–G0	
Y Ophiuchi	6.1	17.11						F5–G3			0.8
T Monocerotis	5.7	27.01						F5–G2			0.7
l Carinae	3.6	35.5				.46			F8–G9		1.1
	Means for Groups										
3 stars		0.47						B9–A9			1.0
3 stars		2.41						F0–F6			0.7
3 stars		4.01						A8–F8			1.0
2 stars		5.57						F2–G3			1.1
3 stars		7.07						F2–G3			1.0
3 stars		7.84						F3–G2			1.0
1 star		8.38						F4–G2			0.8
2 stars		22.1						F5–G2			0.8
1 star		35.5						(F3–G4)*			1.1

* Estimated correction of −0.5 applied to make it systematically comparable with the values from the hydrogen spectrum. This correction, based on data of Adams and Joy and extrapolated beyond their limits of type, is quite uncertain.

have its source in the relatively greater strength of the hydrogen lines than of the lines of the general spectrum. In this connection it may be well to bear in mind also, as pointed out above, that the changes in the spectra of Cepheids are more complex than can be accounted for by pure and complete changes of type.

The range through which the type varies in Cepheids (see last column of Table VII) seems to be independent of the period, and to be nearly constant, averaging a little less than one type-interval (10.0 tenths).

Seares and Shapley (*loc. cit.*) have pointed out that the color changes in Cepheids inferred from the hydrogen spectrum (from the relation that the change in color equals 0.4 change in spectrum) agree with the color changes observed photometrically for these stars. On the other hand, the changes of color inferred from the general spectrum are nearly zero and thus discordant. These results are reproduced in my Table VII, columns 3, 4, 5, and 6. It should be noted that the change in color-index, inferred from my observed change of type in l Carinae from the general spectrum, is closely of the same magnitude as the changes of color-index obtained for the other Cepheids, both photometrically and inferred from the changes in the hydrogen spectrum. Very weak results for changes of type in η Aquilae, from measures of the general spectrum made by Campbell and Wright for other purposes, give an inferred change of color-index of 0.4. Thus my results seem to show practically the same correlation between the color of Cepheids and the general spectrum as was found for the hydrogen spectrum.

The foregoing investigation, begun a dozen years ago, has been interrupted a number of times. Aside from the part of the work completed at the Lick Observatory, portions of the final reductions were made at the Córdoba and University of Michigan observatories. The definitive discussion and preparation of the manuscript for the printer should be accredited to the Department of Meridian Astrometry of the Carnegie Institution of Washington (Albany). It is a great pleasure to acknowledge my indebtedness to these observatories for the time allowed toward this problem.

Dudley Observatory, Albany, New York
August 1919

EXCITATION STAGES IN OPEN ARC-LIGHT SPECTRA

PART I. SODIUM, POTASSIUM, CALCIUM, STRONTIUM, BARIUM, AND MAGNESIUM

By B. E. MOORE

ABSTRACT

Excitation stages in low-current arc spectra of Na, K, Ca, Sr, Ba, and Mg.—By using high potentials it is possible to lengthen the arc so that the middle region is well separated from the poles, and to reduce the current until few or none of the fundamental spectrum lines of the substance under observation are emitted. Evidently this arc affords a valuable means of studying the relative behavior of spectrum lines. Using currents of from 0.03 to 0.3 ampere from a 2000-volt D.C. dynamo, the author made visual observations of the *variation of spectrum with current*, supplemented by measurements of the intensities of many lines. The results for each of the above-mentioned elements are reported in detail. *Five stages of excitation* were distinguished. Stage I: Lowest-current lines, which extend across the arc; generally resonance lines; including the first member of the principal doublet series of Na and K and of the principal singlet series of Ca, Sr, and Ba. Stage II: Coming in with slightly higher currents; relatively weaker in the middle of the arc; generally ionization lines; including the diffuse and sharp subordinate series of Na, K, Ca, Sr, and Mg and the *p*-series of Ba. Stages III and IV each require a considerably greater current and each has considerably higher ratios of intensity at negative pole to that at positive pole and to middle intensity than the preceding stage. Stage V includes lines which failed to appear at all in the arc. Some bands were also observed coming in at early stages. It was found that the *ionization lines of impurities* such as Na appeared only when the ionization potential of the main element in the arc was greater than that of the impurity. These results will be summarized and discussed in Part II, to follow.

INTRODUCTION

The recent investigations upon low-potential discharge in vacuum[1] have led to some important distinctions which have a bearing upon the formation of spectral lines under all conditions. From these low-voltage experiments there appear to be two early stages of excitation of spectral lines. The first is designated the resonance and the second the ionization stage. The resonance stage contains one or two fundamental lines. The ionization stage contains a *rich* spectrum, which rather inadvertently has been designated the *complete* line spectrum. In these experiments

[1] Tate and Foote, *Philosophical Magazine*, **36**, 64, 1918; *Bureau of Standards, Scientific Papers*, No. 317. Foote and Mohler, *Philosophical Magazine*, **37**, 33, 1919; *Journal of Washington Academy of Sciences*, **8**, 513, 1918; Foote, Rognley, and Mohler, *Physical Review*, **13**, 59, 1919; Mohler, Foote, and Stimson, *Bureau of Standards, Scientific Papers*, No. 368; Davis and Goucher, *Physical Review*, **10**, 101, 1917; and numerous others.

it is further made clear that radiation is produced by recombination of electrons and ions after the force which displaced the electrons has ceased to act. Moreover, the displacing force has its origin in a potential which drives the electrons across the vacuum. These electrons may collide with an atom and will ionize it if the velocity of the electrons is adequate. When one considers the kinetic possibilities it is evident that velocities will be distributed over a wide range of values. But so far as the excitation of a line is concerned, all velocities below a certain limit will be ineffective, and all above the same limit will be effective. This critical velocity will define the beginning of a stage of excitation for that line. As the number of electrons which have a velocity above the critical value increases, the line increases in intensity. In a general way this number of ions will increase with the current. The current may therefore become an index of the development, and may be used instead of the potential and velocity, particularly when the latter are not available.

When one passes from the vacuum to an arc working under atmospheric pressure, one must make one essential distinction. The restraint of the gaseous particles is now such that there can be no free movement over an extended distance. There is also a great difference in the freedom of motion in different parts of the arc. This is due to the great inequalities of temperature in the arc. A large part of the difference in spectra in different parts of the arc have long been attributed to temperature differences and to chemical changes. The new concept does not invalidate the conclusions upon the effect of temperature and chemical action, for doubtless these effects are concurrent. It only shifts the point of view and seeks to analyze the radiation in terms of an electron disturbance produced by an effective potential.

From this standpoint let us take a view of the cross-section of the arc midway between the poles. Where the temperature is lowest in the outer mantle, the electrons have their lowest velocity, and the outside limits of the spectral lines are determined by their critical velocity in that region. Outside this region the electrons may be moving at a lower velocity. Lines which require a higher velocity of the electrons for excitation will not be found in the

outer region. In the hotter interior of this cross-section there is greater kinetic freedom, a more rapidly flowing current, and electrons of higher velocity. Consequently, in passing from the exterior to the interior of the discharge, there is a progressive increase in the velocity of the electrons. Hence one may arrive at a second critical excitation velocity characteristic of other lines upon passing from the exterior toward the interior of the discharge. When this critical velocity is reached, the line or lines to which the critical velocity belongs will show an incipient radiation. There will be an increase in radiation for this line or lines as one progresses farther toward the center of the section. This same argument holds as one passes from the middle along the axis of the discharge until one reaches the poles, near which there is probably a great increase in velocity. Therefore, one might expect to obtain in the pole discharge one or more critical velocities which would produce spectral lines of corresponding stages. The outer mantle, according to this view, would correspond to a low excitation stage, the middle of the arc to a medium excitation stage, and finally the poles would show higher excitation stages. The wide range of velocities in any given position certainly makes the problem more complex. One could go over the literature of arc spectra and make a fair selection of stages for lines with no further distinction than is made here.

The object of the experiments described in this article is to follow the production of lines a little more definitely. To accomplish this, it was necessary to obtain a larger separation of the different stages than is obtained in the usual high-current arc. First, the arc was spread out by deflecting it with a magnet.[1] This was very helpful, but it was soon found that reducing the current and raising the arc potential would isolate the parts of the arc better. The higher-potential arc could be longer, and hence the middle area (rather volume) would be more extended. With the lower currents, the polar illumination retreats toward the pole. With this retreat came another very decisive factor, viz., the disappearance of many lines. Out of this fact arose the determination of stages by determining the current at which the inception of the line occurs. This

[1] Referred to again in Part II (subsequent paper).

method will yield reasonable results unless the line is overlapped by a continuous or band spectrum. But it could not answer one question, viz., Do the lines have definite beginning-points as they appear to, or do they continue in a very weak state to a common excitation point characteristic of all lines? For this reason a method was devised for measuring roughly the development of the intensity of the lines with increase in current. This method shows that certain groups of lines have common beginning-currents, and instead of continuing in a weak state, they frequently disappear and reappear very suddenly and have a very rapid and decisive development after their inception. Knowing this, one could feel perfectly free to use the first course of investigation wherein the lines were followed to their beginning-current. This can be done at either pole or in the middle of the arc or in all of these positions.

THE ARC

As stated above, in the usual arc operated at high current it is difficult to separate the different degrees of excitation. The illumination herein designated "polar" does not appear *on* but just *off* the electrodes. Lines which usually have been designated "short" belong in the polar illumination. They vanish as the current decreases. Many lines which extend across the arc for high currents become short lines for lower currents. This feature helps to distinguish them. These high-potential arcs, according to Simon,[1] may act along two characteristic curves. The first curve is the glow characteristic and belongs to the glow arc. This curve depends only upon the medium and is independent of the electrodes. The second characteristic is the true-arc curve. In the true arc the material of the electrodes affects the electrode drop, and the gaseous products or ions therefrom affect the conduction of the medium. The middle of the low-current arcs under discussion often assumed a glow appearance, but there was at no time any clear evidence that the arc discharge had passed over into the glow form.

[1] Under investigation by Mr. V. L. Chrisler; Simon, *Physikalische Zeitschrift*, 6, 297, 1905; Simon and Malcolm, *ibid.*, 8, 471, 1907.

POWER

A dynamo rated at 2000 volts and 0.25 ampere was used. It stands an overload of 20 per cent for brief intervals. The current was adjusted by means of resistance in series.

SPECTROSCOPES

Five spectroscopes have been used. (1) A small student's spectroscope has been used for preliminary investigation. It could be turned with its slit perpendicular or parallel to the discharge. It thus served to observe the variation of intensity in cross-section as well as in length. It was particularly serviceable when the analysis reduced to a few visible lines. (2) A Hilger wave-length spectroscope has given most results. It just separates the D lines, but one could not rely upon its measurements to closer than 6 angstroms. This seldom interfered with identification. The field was usually diaphragmed to about 60 angstroms, which was a great help in determining luminosity. (3) A Steinheil plane-grating spectroscope gave more than double the dispersion of the Hilger spectroscope in the red, and helped particularly in this region. This instrument could be used either visually or photographically. (4) A quartz spectrograph was in good focus from λ 2800 to λ 4000 and gave a spectrum about 18 mm long. When there are but few lines in the ultra-violet, they may be recognized by this instrument.

MEASUREMENT OF INTENSITY

The reasons for following the changes of intensity in the lines as the current changes have been given in the introduction. Two convex lenses with a crossed-nicol system between them focused the light from the arc upon the slit of the spectroscope. Before the eye was placed a Wratten light-filter. After selecting a spectral line for observation a filter was introduced which would nearly extinguish the visibility of the line. The angle between the nicols was then adjusted until only the last trace of the line was visible. The reciprocal of the relative amount of light transmitted by the crossed-nicol filter system is designated the intensity of the

line. This method is open to three large sources of error: (1) personal judgment upon threshold intensities is quite variable; (2) the optical adjustments are subject to some variation; (3) the arc is inclined to migrate. This makes the measurements very rough, but they will serve the purpose of defining the starting-current of spectral lines and of showing their relative development.

DETERMINATION OF STAGES

In an attempt to distinguish stages of excitation the first step is to fix the general features of the spectrum. The last, but more concise, determination will be the growth of the lines themselves.

Stage I.—To recognize this stage, choose a minute current, then look for lines which extend across the whole arc from pole to pole. If these lines are but little stronger at the poles than in the center of the arc, they belong either to Stage I or Stage II. Next see if they can be traced to the last limit of the current. Those lines which hold out longest belong to Stage I. Next examine the rate of intensity development. Lines belonging to Stage I will fairly leap into brilliance at the negative pole and follow but little later at the positive pole. For later currents they will show very slow development. In the middle of the arc they will develop rapidly, but more uniformly. As far as experience with different substances has gone, the current may be reduced until these lines, small diffuse bands, and a low continuous radiation are in complete possession of the spectral radiation.

Stage II.—This stage usually represents a *rich* spectrum. The lines at the negative pole may persist to nearly the same limit as lines of Stage I. When the positive-pole radiation is not too confined, they separate better there than at the negative pole. In the middle of the arc, a line of Stage II must be intrinsically very brilliant to contest with lines of Stage I for first rights. When the intensities of these lines are studied, some of the stronger lines may show a growth very similar to lines of Stage I. But when the current-intensity curves are plotted, they will be seen to lie in a position which indicates stronger exciting currents and stronger inception currents (intercepts upon the current axis) than is required for lines of Stage I. There is furthermore a reluctance

upon the part of these lines to appear in the middle of the arc. This is best shown by the increased ratio of polar to middle intensities.

Stage III.—These lines will not generally show until the inception current of lines of Stage II has been doubled or trebled. When the current is large enough to indicate their decided presence at the negative pole, lines of Stage II will be reaching out far from the poles trying to become true long lines, while lines of Stage III will be cut off sharp and short in a region restricted to the very core of the pole illumination. So far as these experiments have progressed, experience has shown that lines of Stage III require four to five times as much current at the positive pole as at the negative to produce a first visible impression. Within the limits of the present experiments, a line of this stage must be very intense to show any trace in the middle of the arc. Necessarily, therefore, the ratio of their polar to middle intensities is very large.

Stage IV.—It requires a large increase in current over that required for lines of Stage III to bring out the lines of Stage IV. When once they appear, they are very similar to lines of Stage III. There is a decided continuous spectrum associated with most of these lines, which suggests a formation within a dense vapor. None of the lines have been seen outside the pole illumination.

Stage V.—In this class one may place all other known lines of the stronger-current arcs. There has been no attempt to analyze these lines, and, of course, there may be many stages present.

GRAPHS

Logarithms of intensities are plotted as ordinates, and logarithms of one hundred times the current are plotted as abscissae. Logarithms to the base 10 are used. The lines are designated upon the graphs and in the legends.

SODIUM

Lines D_1 and D_2 are predominant. They appear throughout the whole of the arc. With the slit normal to the current they are seen to be longer than the weak continuous background. In this position they fade off at the ends with no defined external

limits. These lines have a very low excitation. The other lines observed were members of the first and second subordinate series and the principal series pair, λ 3303. All of these lines appear in the middle of the arc at 0.25 ampere. With the slit normal to the current they fade off very quickly, but not abruptly, as one proceeds from the center toward the outer mantle. The lines appear to be one-third to one-half the length of D_2. Now Foote and Mohler[1] give an excitation potential for D_2 equal to 2.12 volts, and for the other lines a potential of 5.13 volts. The effective velocity for the latter is 2.4 times the velocity for the former. This means

TABLE I

INTENSITIES FOR D_2

CURRENT	$NaCl_2$		$SrCl_2$		$CaCl_2$	CARBON
	Negative Pole	Middle	Middle	Positive Pole	Middle	Middle
Ampere						
0.25			38	520	8–16	18
.2	7080	2220	24			
.15		1280	10	240–180		4.8
.1	2220	532		72		
.08		304				
.075	1332			28		
.067	396	176				
.....	(180)					
.048	(100)	96				

that with a current of 0.25 ampere one must pass from the outer effective excitation of the line D_2 halfway to the center of the current stream to reach a point where the velocity of flow has been doubled. In general, the "fading-off" of lines upon passing from the center to the outer mantle is not sufficiently abrupt to make sharp distinction in stages. As the current decreases, the subordinate-series lines fade out in the center of the arc. The yellow-green members can easily be seen to retreat toward the poles and to shorten. The red and blue members are not visible at the poles below 0.075 ampere, and the yellow-green members not below 0.05 ampere, except during intermittent flaring of the light. The sharp series was not recognized in the preliminary trial

[1] *Loc. cit.*

with the small spectroscope, but was readily found with the Hilger instrument. A cross-sectional view at the poles is interesting. The subordinate series (diffuse and sharp) essentially belong to this region for the lower currents. The D_1 and D_2 lines flash out with great brilliancy and are quite wide. Much of this is doubtless an irradiation effect. With the Rowland grating the D lines show reversal at 0.25 ampere in the pole illumination.

With the crossed-nicol filter system, the data given in Table I were obtained for D_2. Different salts, as represented in the table, were used upon the electrodes, but only this one line was studied.

In passing from the poles toward the middle, the easier lines, particularly lines of Stage I and Stage II, fade off slowly as above noted. This necessitates a little precaution as to what part of the middle one may use to determine middle intensity. Usually the position of weakest intensity is a little above the center of the arc toward the upper pole.

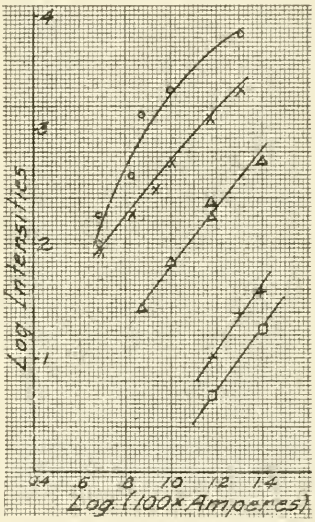


FIG. 1

⊙ $NaCl_2$, −pole
× $NaCl_2$, middle
△ $SrCl_2$, −pole
+ $SrCl_2$, middle
□ $CaCl_2$, middle

A graph, Figure 1, was plotted from the D_2 readings. It will be noticed that the line found in sodium shows two distinct slopes. When the line shows as an impurity in strontium, calcium, and carbon electrodes, its intensity proves to be surprisingly low. With carbon electrodes without salts added, the potential takes a decided increase. This increase in potential actually brings out the D lines stronger in the carbon arc than in the arc containing calcium salt. The slightly greater intensity of the line in the strontium salt suggests the presence of a trace of sodium in the substance.

The D lines belong to Stage I, and the other lines not earlier than to Stage II. The diffuse series certainly fall into this classification.

The decision upon the fainter sharp series was less certain. All other series have not been realized. With substances which follow it is easier to assign the missing lines to later stages. In sodium the writer has more reluctance to do so, because the relative intensity of the continuous background was a burden. With the Rowland grating this background could be dispersed so that it was unimportant, but 0.25 ampere would scarcely produce a trace of the *d* series. Hence there is real need of tracing the growth of the weaker lines at higher currents to determine their excitation stages.

POTASSIUM

The red lines λλ 7699, 7666 (the first term of the principal series of doublets) would naturally be expected to play the same rôle as D_1 and D_2, and the blue lines λλ 4047, 4044 the rôle of the λ 3303 pair, i.e., the former should be a resonance and the latter an ionization pair. Along with the latter would be expected the subordinate series. Although all these types may be seen in the visual spectrum, the red and blue pairs are at the extreme ends, where the sensitivity of the eye is very low. For the author's eyes the sensitivity is much better for the blue lines. But this fact ought not to account for his ability *always* to see the blue lines whenever the red lines are visible. There was no definite answer as to whether or not the blue excitation could be separated from the excitation of the subordinate series. They certainly occur together, but one cannot decide whether they may occur separately, for the subordinate series as well as the blue lines become quite intermittent at even 0.1 ampere. To make any comparison of the intensities, it would be necessary to know the relative sensitivity of the eye for the wide difference in radiations. The crossed-nicol system was not applicable. Evidently the blue pair had a high intensity in comparison to the subordinate lines. Photographically the blue pair are the only lines which show. The latter pair is the second member of the principal series. There are many other lines of conspicuous intensities, but none of them appear under the present excitation currents. This blue doublet λλ 4047, 4044 comes out as an impurity in other substances and with the carbon electrodes.

The D lines show in potassium both as middle and pole lines, but the ionization lines of sodium do not show. According to Foote and Mohler,[1] the ionization potential for potassium is 4.1 volts and for sodium 5.13 volts. It is possible to argue that we have here an effective ionization potential greater than 4.1 volts which produces the potassium lines and less than 5.33 volts which fails to produce the ionization of sodium. The existence of such a narrow range of effective potential seems, prima facie, improbable. Rather, the sodium ionization lines would appear to be absent because of their inherent weak luminosity. However, the following consideration confirms this rather unexpected result. The calcium doublet pair λλ 3969, 3934, the potassium doublet λλ 4047, 4044, the sodium doublet λλ 3303, 3302, and the sodium yellow doublet of the diffuse series, all of which are ionization lines, show prominently in the carbon arc. The ionization potential in this carbon arc is nearly doubled, as is apparent when one considers the potential fall in the different arcs. The ionization value for calcium as given by Foote and Mohler is 6.01 volts. Since the above-mentioned calcium lines appear, we have an effective ionization greater than 6.01 volts. Therefore the sodium ionization lines, which require only 5.13 volts, also appear; whereas sodium did not appear in the potassium arc where the required potential needed to reach only 4.01 volts. The amount of sodium actually present in the two cases could not have been appreciably different.

The red lines which would be expected to belong to Stage I could not be satisfactorily observed. The violet double which is the second member of the same series belongs in Stage II. The same is true of the yellow lines of the diffuse series. The observations could be carried no farther.

CALCIUM

A large number of lines in calcium as well as in strontium and barium were easy to realize. From the intensities which have been observed and the intensities which are recorded in the table for calcium in Kayser's *Handbuch der Spectroscopie* (**5**, 246) it was easy to infer which lines could have been reasonably expected. These lines are given in Table II. The first column indicates the

[1] *Philosophical Magazine*, **37**, 33, 1919.

TABLE II

CALCIUM

	Wave-Length λ	I	Current 0.25 Ampere		Limit of Visibility in Amperes		Stage
			Positive Pole I	Middle I	Positive Pole	Middle	
A	6500	4	18	1—			
	6494	4	15	2	0.045	0.12	II
	72	4	8	1—	.07		
	63	6R	15	2	.045	.12	II
	49*¶¶	4	5	0			
	6439†	10R	20	5	.033	.05	II
B	6170*	6	0				
	69	4	0				
	67	4	0				
	64†	4	8	0			
	62‡	10R	15	5	.04	.08	II
	61***	5					
	22	10R	8	2	.06	.15	II
	03	8R	8	1			?
C	5868§	6	0	0			V
	58	10	15	—	.035		III
D	5603***	8					
	02‖	8	4	0	.045		II
	5599	8	8	1	.045		II
	95	10	10	2	.045		II
	90	8	25		.035	.045	II
	89***	10		5			II
	82¶¶	8	6	0			
	5513‖‖	4					III
	5350¶‖	10	0	0	.1	.3	V
E	5270**	10	8	4	.035	.045	II
	64	8	6	2	.04	.055	II
	5162	6					
	60	4	4	2	.04	.055	II
	5042	3			.095	.3	III
F	4878	10	5		.08	.2	III
	47	4	0				
	34	1	0				
	23	1	0				V
	11.6		0				
	07	1	0				
G	4685‡‡	4	0	0			V
	25	1	8	3			

TABLE II—*Continued*

CALCIUM

	Wave-Length λ	*I*	Current 0.25 Ampere		Limit of Visibility in Amperes		Stage
			Positive Pole *I*	Middle *I*	Positive Pole	Middle	
H	4607§§		20	5	0.035	0.055	I
	4586	30	25	1.+	.038	.1	
	82	30	20	1.+	.04	.1	II
	79‡‡	20	10	1	.045	.15	
	4527	20	2	0	.12	—	III
I	4455††	200	60	5	.033	.055	
	35.1	100	50	5	.033	.055	II
	25.6	100	30	3	.033	.055	
	4355	3	2	0	.045	.15	III
J	4319	8	25	1.—			
	308	5	20	1.—			
	303	9	30	2	.045	.15	III
	299	8	20	1			
	90	0	25	1			
	83‡‡	8					
	4227	1000	200	50	.028	.033	I
	3967						II
	3933						

* Bands overlap the group.

† An easy middle line, while the rest of the group are difficult.

‡ First line of the first member of the sharp series. Strong like λ 6439, but not so persistent at low currents. Also an easy middle line, λ 6161, not resolved. Term 3 of this member overlapped by a band.

§ An easy position for observation with very unexpected results.

|| In comparison with other lines equally strong, Group "D" should be stronger in the middle, like λλ 5590, 5589. They are therefore difficult middle lines and may belong to Stage III.

¶ Unexpectedly missing.

** Uncommonly *relatively* strong lines at middle. Easy middle line.

†† Fade off through a distance as large as the pole bead, but are very weak toward the center, and intermittent across the center for low currents. Diffuse-series group, $2p_1$—*md*.

‡‡ This pair are the inverse of the expected result. Thalen gives four lines, and the one actually present he records as the weakest. Strong background interferes.

§§ A strontium impurity recorded for the sake of comparison.

|| || Lost in band.

¶¶ Exceptionally short line.

*** Unresolved.

anticipated lines and the second column the intensities of the lines taken from Kayser's table. The subsequent columns represent the observations with the Hilger spectroscope. The indexes pertain to some condensed statements in the footnotes in regard to the behavior of the lines. The lines are given in groups "A"

to "J." These are quite arbitrary groups. They represent aggregates of lines, not series grouping. It is largely a convenient method of making comparisons. However, many of these groups behave very similarly and doubtless have much in common. Group "C," for example, belongs to the Ritz combination, $3d_j - 3p_i$[1] There are also certain groups, or aggregates, which fail to appear at all.

Line λ 4227 corresponds to requirements of Stage I. There are numerous lines distinctly belonging to Stage II. Many of these have been examined in a preliminary way with the crossed-nicol filter system. With some lines there is considerable uncertainty; there are many late lines.

With carbon electrodes without calcium chloride the potential takes a big jump. The three leading lines which show in the pole illumination at the carbon are then λ 3934, λ 3968, and λ 4227, and in the order named. At 0.1 ampere, electrode λ 3934 is about three times as bright as λ 4227. These three lines occur as an impurity in barium, but a good share of the calcium there doubtless comes out of the electrodes. Again we find at the poles with 0.1 ampere an intensity about 50 for λ 3934 and about 20 for λ 4227, while in the center λ 3934 does not show and λ 4227 has an intensity of about 8. It will be noticed here that there is both a higher temperature and a larger potential fall at the poles; and that both of these factors will contribute to the production of higher-velocity electrons. This is the essential requirement of Stage II, while the middle of the arc for the lowest currents corresponds rather closely to Stage I. Therefore, with the increased velocity of the electrons, the lines λ 3969 and λ 3934 of Stage II replace the lower-excitation line λ 4227 of Stage I. If this consideration has merit, it is suggestive as to solar conditions, where these lines are of predominant interest, and where the doublet pair are not only the brightest, but also the most conspicuous lines in the entire solar spectrum.

From the results of Mohler, Foote, and Stimson,[2] it is shown that λ 6573 is the first and λ 4227 the second resonance line in calcium. It appears that resonance has been observed in three

[1] Popow, *Annalen der Physik*, **45**, 154, 1914.

[2] *Bureau of Standards*, Paper No. 368.

types of series, $1S-mP$, $1s-mp_2$, and a cross of these systems, $1S-mp_2$. Lines λ 3934 and λ 3968 represent the second type, clearly pole lines in the arc, and λ 4227 represent the first type, which is an extremely easy line in the middle of the arc. Line λ 6573 has always been unimportant in the arc. It represents the cross-system. King[1] finds it brilliant in the furnace spectrum of calcium. It seems therefore to deserve close attention. In the present arc the conditions almost baffle investigation. The line at the pole is doubtful even at 0.25 ampere. In the middle it intermittently comes out of a halo or narrow band, when it is brighter than its near neighbor λ 6500. (See λ 4571, magnesium.) Lines λ 5042, type $1D-2P$, and λ 4527, Type $1D-3P$, are lines which are just traceable under the experimental conditions in the middle of the arc at 0.3 ampere. They clearly belong to Stage III. Careful search for λ 5513, Type $1P-3S$, and for λ 4847, Type $1P-4S$, failed to discover them. Hence they must be assigned to a later stage.

The calcium spectrum nearly fades out to the blue of λ 3934. The lines of the second member of the sharp series of triplets are near neighbors of λ 3934. These lines are λλ 3974, 3957, and 3949. The first two lines have about 1/200 of the intensity of λ 3934, and the third line is invisible. Lines λ 3737 and λ 3734 have the same frequency differences as λ 3939 and λ 3934. The intensities for these two lines are respectively about 1/50 and 1/200 of λ 3934. These five lines belong essentially to Stage III, while the diffuse-series' first and second members are found in Stage II. The head of the so-called cyanogen band at λ 3883 is traceable.

The details of the crossed-nicol measurements are very similar to those found with barium lines and are not given here. The readings for a few prominent lines at 0.25 ampere only will be given. It is interesting to compare these values with the estimate of the unaided eye in Table II. The lines are given in angstrom

[1] *Astrophysical Journal*, 28, 389, 1908. King gives the literature concerning these three lines and an examination of them in the electric furnace with different quantities of calcium and at different temperatures. Our results are very similar. He attributes the growth of λ 3969 and λ 3934 to increase in temperature. In the present discussion temperature is recognized as a contributing cause and the participating cause is held to be the state of excitation.

units, with the measured intensities in parentheses following the lines: λ 5589 (30–50), λ 5485 (370), λ 5270 (133), λ 4878 (133), λ 4586 (40), D_2 (21), λ 5934 (370).

BANDS

Line λ 5485 is approximately the blue edge of a band, which contracts in width as the crossed angle of the nicol system increases. Another band, λ 5934, adjoining D_2 (sodium), seems more like a line in the midst of a broad radiation. As the crossed-nicol angle increases, the band contracts toward the line, but fades out more rapidly upon the less refrangible side. Judgment upon the lines was made at the poles and upon the bands in the middle of the spectrum. Band λ 5934 is much stronger at the pole than in the middle. It is, however, very fickle at the pole and some readings showed twice the intensity of others. Hence they were discarded. Band λ 5485 is different. It is weaker at the poles; its appearance, which was observed with a 20 per cent crossed-nicol, is shown in Figure 2. Adjoining the band on the red is Group *d*, of pole lines. In the pole region the band fades off upon its weaker side. It is strongest just above the limit of the pole lines. Another line or narrow band, about λ 6080 to the blue of λ 6103, behaves in the same manner as λ 5480. It requires no nicol to observe it. Opposite the pole line λ 6103 it is very weak. Line λ 6103 shows weakly as a middle line, and opposite its middle λ 6080 is much stronger than opposite the pole. Some bands of the chloride group are given in Kayser's tables in the region of λ 5480, and λ 5934 is there assigned to the metallic group. This suggests that the chloride molecule does not exist in the position of the pole excitation, and that there is a large recombination of metal and chlorine after passing beyond the pole excitation into the region of lower excitation. The metallic (molecular) excitations are just as persistent in the middle of the arc as the leading lines. They can be traced to the last limit with λ 4227, the resonance vibrator. Unfortunately the writer could not use the crossed-nicol with the latter line. Its behavior, in general, is like D_2. The band λ 5934

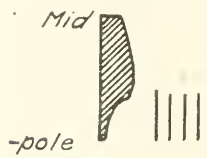


FIG. 2

grows in intensity with the current at the middle, not in two well-defined branches like resonance lines, but more like other lines, with moderate and progressive changes in the slope.

Some lines have been added to Table II since the receipt of an important contribution by Dr. F. A. Saunders.[1] His article gives one enough types to make some comparisons, which one may safely make and reserve the discussion of the matter to the subsequent contribution. The line of Stage I has Type $1S-1P$, while Type $1S-1p_2$ is missing. When ionization occurs and Stage II appears, Types $1p-1s$, $1p_i-2d$, $1p_i-3d$, and $1p_i-2s$ appear. Stage III is represented by Types $1P-3D$, $1D-2P$, $1D-3D$, $1D-1F$, $1D-2F$. Observe here an expansion of the atomic action as represented by the first term of the types and of the electron displacement as represented by the second term of the types in passing from Stage I to Stage III. A spectroscopic observation may also be added. Lines of Stage III come out of the very core of the polar illumination where there is a great vapor density, strong, continuous spectrum, greatest current density, and a *sustained* action upon the ions.

STRONTIUM

There will be no particular advantage in tabulating the observed lines as in calcium. Using Kayser's *Handbuch der Spectroscopie*, **6,** 539, as a guide, all strong lines given by Exner and Haschek for the arc are obtainable in the visible spectrum. Their lines of intensities 1 and 2 only are uniformly missing. Besides representatives of this weaker class of lines, there are seven lines missing between λ 5971 and λ 5599 inclusive.

These missing lines are not appreciably disturbed by continuous or band radiation, they therefore belong to late excitation stages. Lines λ 4338, λ 4319, and λ 4308, a triplet group, are overlapped by band or continuous radiation, and only the first line of the group is visible. These lines at the poles show no conspicuous variation from the values of relative intensity given by Exner and Haschek. The stronger the pole line, the more easily it is in general to trace it toward the middle of the arc. But

[1] *Astrophysical Journal*, **52**, 265, 1920.

strong pole lines do not always come out with the same ease at the middle. Some lines relatively weaker tend to come out at the middle much sooner than stronger lines. Because of this characteristic, it seemed desirable to tabulate the lines as in calcium. But there is too much diversity in this variation to reduce it to any system. In trying to trace the lines to the lowest current limit, the weaker lines go out first, invariably, in strontium. There are a number which vanish about 0.045–0.05 ampere at the negative pole. But many of these lines are still distinct at the negative pole at 0.032 ampere. Just off the center of the negative glow, either toward the pole or toward the center, there are only three lines, λ 4607, λ 4216, and λ 4078. On the outer mantle of the negative pole, and in the center much of the time, λ 4607 only is found. At the positive pole there are only the three lines at 0.05–0.055 ampere. Here, there is the first trace of a richer spectrum at about 0.07–0.08 ampere. It requires a current of 0.1 ampere at the positive pole to produce a many-lined spectrum as rich and strong as is found at the negative pole at 0.035 ampere. Later, by using 3000 volts, the current was carried down to 0.025 ampere. The three lines listed above are still visible at the negative pole, but the "*p*" pair of lines is very weak. At the positive pole and in the middle of the arc, λ 4607 alone is visible. Evidently the positive pole separates the excitations better. There is now only a low, wavelike illumination in the red-band region.

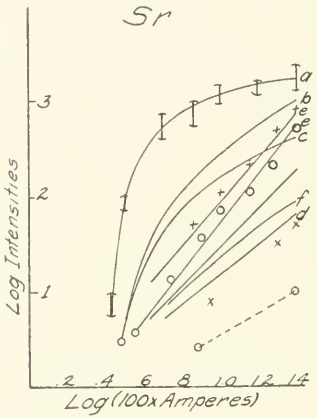


FIG. 3

a=λ 4607, −pole
b=λ 4607, middle
c=λ 4962, −pole
d=λ 4962, middle
e=λ 6025, band−pole
f=λ 6025, middle
+, λ 4873, −pole
×, λ 4873, middle
○, λ 5950, pole

A few of the lines have been studied with the crossed-nicol and filter combination. They are given in Figure 3. Line λ 4607 shows two distinct slopes. In the second slope, it was quite

impossible to secure readings which did not overlap. The slope is here less steep than for the other substances. The prime cause lies in the strong self-reversal of the line. It was found that reversal was evident at 0.1 ampere and became more pronounced as the current increased. This is the most conspicuous line in the strontium spectrum. Its series type is $1S-mP$, and the leading term of this series. Line λ 4227, in calcium, has been identified with this type, but it could not be followed. Lines D_1 and D_2 in sodium show the same characteristics as this line, but are represented by the series Type $1s-mp_2$. In strontium the latter type is represented by λ 4126 and λ 4078, as is clearly proved by the Zeeman effect. These cannot be followed satisfactorily in a quantitative way. It is clear from photographs with low currents that λ 4607 is predominant, and for larger currents that the lines λ 4216 and λ 4078 are overtaking the former. But even at 0.25 ampere it could not be said that they intrinsically equal λ 4607. The latter is a very wide line with strong self-reversal. As a middle-arc line, λ 4607 has no lower slope at 0.25 ampere than the same line at the pole with 0.05 ampere. The change in the line at the middle of the arc is more progressive. Even at the middle of the arc at low current it is more prominent than any polar line. Up to 0.25 ampere, no polar line, unless it be λ 5481, has equaled the intensity of this middle line.

Line λ 4962 is a second member representative of the diffuse series, while the first member lies in the extreme infra-red, at λ 2735–6, and cannot be studied. Line λ 4962 is a relatively easy middle line. Its characteristics show a development more like λ 4607 than had been expected. The development is slower. As a pole line it follows λ 4607 as a middle line for a short distance and then progressively falls off in intensity more than that line. Now too much stress may be laid upon these appearances. But realizing the apparently easy interpretation which could be placed upon it, the readings for the line were repeated three times by varying nicol at constant current, and by varying the current with constant nicol. This gave a *promiscuous lot* of readings along the line, but did not change the feature of a rapid early, and slow later, growth in intensity with increasing current.

Line λ 4968 is the stronger of the two satellites of λ 4962. It increases both at the pole and at the middle very uniformly. It is so very weak at the middle that there appears a great tint difference between it and its near companion λ 4962. At 0.25 ampere it is noted that the intensity of λ 4962 at the pole is twenty times as strong as at the middle, whereas λ 4962 pole is fifty times as strong as λ 4968 middle, i.e., we have here intensity ratios 50, 20, 1. The unobserved satellite λ 4972, according to Exner and Haschek, has an intensity of 3, and for the three lines they give ratios for intensity of 50, 20, and 3. Considerable allowance must be made in the methods of determining intensities. This is scarcely adequate to cover the difference observable. For, easily, 1/150 of the stronger line would have been observed in the clear field at λ 4972. This is nine times the ratio of values required from the Exner and Haschek values. It seems rather reasonable to conclude, therefore, that λ 4972 has not been excited at all. The same method of examination may be applied to missing lines whose intensity is about two, but it does not have quite as much force. Prolonged photographic exposure also failed to bring out these lines. It therefore seems probable that these lines are not excited in the low-current arc. The lines of the second subordinate or sharp triplet series are much less pronounced than those of the diffuse series. The first member lies in a band region, but lines can be recognized at the pole. There is a trace only of two lines, λ 4438 and λ 4362, of the second member. This is out of all proportion to the corresponding member of the diffuse series. For the two respective members Kayser's *Handbuch* gives very similar intensities. Within the first member of the sharp series lies λ 6892, which, the author strongly suspects from King's[1] results, belongs to $1S-m_2$,[2] mixed-series type, just as the calcium line λ 6573. When the pole illumination is accurately upon the slit, there is sufficient intensity here for visual observation. The diffuseness is even more pronounced than for λ 6573, and although having looked diligently, it is not possible to say there is a line in this diffuseness.

[1] *Astrophysical Journal*, 51, 184, 1920.

[2] Saunders confirms this classification.

The two red bands studied are doubtless each overlapping bands. The wave-lengths assigned represent approximately positions of maximum intensity. Band λ 6025 is more than twice as wide as λ 5950. Both at the pole and the middle these bands increase uniformly with the current.

As seen from the graph, Figure 3, pole line λ 5481, band λ 6025, and band λ 5950 are remarkably alike in their development and growth. After they are definitely established they grow uniformly with the current. They can be expressed by the equation[1]

$$\log I = k\,(\log i - \log i_0), \qquad I = \left(\frac{i}{i_0}\right)^k,$$

where I is the intensity, t the current, i_0 and k constants. Now i_0, the intercept upon the current axis, would be the inception current provided we may extrapolate along the curve below the lowest readings. After inception the intensity is proportioned to some power of the current. The apparent effect is that lines go out a little more rapidly down in this low-current region, but the whole effect is then masked by the hiding of the pole behind some small particle of salt or electrode material. Taking this feature into consideration, the graphs suggest a common origin for all lines studied except for λ 4607. The violet p series λ 4216 and λ 4078 could not be studied by the crossed-nicol method.

Basing conclusions upon the foregoing analysis, λ 4607 is the last limiting line upon reducing the current and belongs to Stage I. It is believed there is clear evidence at the positive pole that the "p" pair does not hold out as long as λ 4607; but whether or not its appearance slightly earlier than the many-lined spectrum was due to its intrinsic brightness could not be settled. If we make a separate stage for this pair, then the many-lined group would fall in Stage III. But these lines correspond very closely to the requirements of Stage II and are like the lines of this stage in other substances. Forty-six lines were counted in Stage II off the positive pole at 0.1 ampere. Lines of Stage III do not isolate well, as the analysis shows. Following the outline of stages, the unobserved lines would fall in Stage V, the unclassified stage.

[1] See Part II (subsequent paper).

BARIUM

The barium lines do not in general push as rapidly toward the middle of the arc as calcium or strontium. Nearly every line of intensity 3 or greater given in Kayser's *Handbuch* (5) is present in the pole illumination at 0.3 ampere. The following lines were missed (the parentheses show intensities by Hoeller): λ 6451 (6), λ 6175 (3), λ 5908 (4), λ 5819 (3), λ 5784 (3), λ 5714 (3), λ 5680 (5), λ 5594 (3), λ 4283 (8). The ultra-violet shuts off very rapidly. Line λ 3892, Stage II, is the most pronounced. Evidence for its similarity to λ 5536 was sought but not found. It is followed by a triplet of Stage II, λ 3545, λ 3525, λ 3501, the last of which is the strongest. These lines are not a true triplet according to Saunders.[1] The last line he classifies as the first member of the singlet series, $1S-mF$. The second member of Saunders' singlet series, $1S-mP$, of which λ 5536 is the leading member and the fundamental of the whole spectrum, is λ 3072. Air bands interfere in its observation. The Zeeman effect postulated for this series is the normal triple "*a*." The writer's observations[2] confirm this result for λ 5536, but show a value (12/11) *a* for the second member. The latter is a difficult line, and an error of 1/11 is not excluded. Members 2 and 3 of the *d* series are in evidence at the poles in the ultra-violet. Stage III seems to fit them just as it does the first member (see below). The first term of the first member of the *d* series is missing in barium, just as it was missing in calcium and strontium. Therefore it appears that the satellite types may arise as later excitations than the lines with which they are usually associated.

Increasing the potential in later experiments to 3000 volts, the current was carried down to 0.022 ampere by shortening the arc a little. The pole excitation may then conceal itself between the salt particles, or it may seize upon a salt particle and stand out prominently. In the latter case the spectrum is a beautiful green glow. Bands and the last trace of λ 4554 disappear. Line λ 5536 stands out definitely in the middle of this green spectrum. (Chloride bands are said to overlap this point.) This spectrum, growing

[1] *Astrophysical Journal*, 51, 23, 1920.

[2] *Ibid.*, 28, 1, 1908.

continuously weaker, extends far toward λ 4934. Toward the red it extends as far as, or farther than, the position of the D line, but the D lines are absent. In the red there is a succession of weak ripples—presumably a residue of the red bands.

In barium, some lines of the prominent types of series are very favorably located for study by the crossed-nicol filter combination. The lines also lie very advantageously with respect to each other for comparison. The leading singlet member λ 5536 lies close to λ 5519, the strongest line of the first member of the diffuse series. Now if λ 5519 were alone, its sudden appearance with change in current could be attributed to a drift to and fro of the image upon the slit of the spectroscope. But with λ 5536 pole illumination strongly in the field of view at the time of the current change, a sudden appearance has its origin in an outburst of the line. Now these lines are shown in the graph, Figure 4. It appears that line λ 5519 at its inception leaps very quickly to quite a distinct intensity. But it appears later than lines of Stage II, and reluctantly appears at the middle. It is therefore assigned to Stage III, which is a rather unexpected thing for a leading member of the *d* series. Likewise λ 4934 of the *p* series and λ 4900 of the *s* series are adjacent. Line λ 4900 makes a late appearance and is a rigid pole line. The same is true of its companion line λ 4525 which cannot be separated from λ 4523 for the crossed-nicol study. Both these lines are short lines. These series lines cannot therefore get into Stage III, much less get into Stage II, where there is the first appearance of the many-lined spectrum. The earliest assignable stage for this *s* series pair is therefore Stage IV. The pair λ 4934, λ 4554, *p* series, are contenders with λ 5536 for first place.

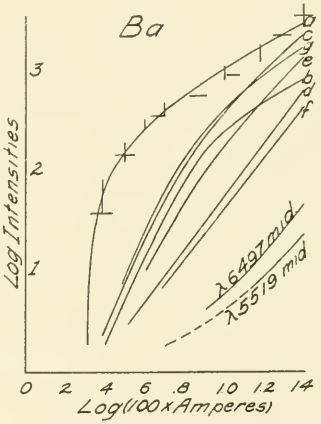


FIG. 4

a=λ 5536, −pole
b=λ 5536, middle
c=λ 4554, −pole
d=λ 4554, middle
e=λ 4934, −pole
f=λ 4934, middle
g=λ 5519, −pole

Following the current down to its lowest limits, they drop out. Along the graphs they have another characteristic. They are therefore assigned to Stage II. Another much weaker pair, λ 6497 and λ 5853, are assignable to Stage II. Line λ 6142 also belongs in this stage. It is generally recognized as a leading line of the barium arc.[1] From Table III it is the sixth line in brightness,

TABLE III

Wave-Length λ	Intensities at 0.2 Ampere		Stage
	Negative Pole	Middle	
6497	276	40	II
6142	268	14	II
D_2, Na		530	I
5853	364	24	II
5778	1150		III
5536	2500	(560)	I
5519	1460	(—)	III
4934	1080	250	II
4900	220	0	IV
4727	660	0	IV
4700	104	0	IV
4691	660	0	IV
4628	355	0	IV
4620	436	—	IV
4580	272	—	IV
4574	288	—	IV
4554	1720	316	II

instead of the fifth,[1] in the middle of the arc; and at the poles it stands much lower than several pole lines of Stage IV. In Figure 4, graph "*f*" represents equally well λ 4934 middle, λ 4900 pole, and λ 6497 pole.

As designated above, there were numerous other lines which are not recorded in Table III. If any of these belong to Stage II, they have escaped the writer's notice. There has been no attempt to separate them into Stages III and IV, where they all belong. Certain unobserved prominent lines noted above may be provisionally placed in a later stage.

MAGNESIUM

First, magnesium chloride was tried upon carbon in the same manner as with the other salts. The salt rapidly disappeared and

[1] Kayser, *Handbuch der Spectroscopie*, 5, 144–146.

the potential climbed toward the carbon electrode characteristic. For low currents it then assumed the distinct glow arc characteristics. The first member of the sharp series occurred at the negative pole in the glow discharge. Whether or not this member may continue to the lowest limits of the current is uncertain. Much seemed to depend upon the presence of the salt and whether it was participating in the action of the arc. The same holds with reference to the first term of the diffuse series in the ultra-violet, but this was more difficult because photography had to be applied. Neither set of lines appear in the middle of the arc below 0.07 ampere, and probably not below 0.09 ampere. Three leading lines of the oxide group beginning at λ 5007 can be seen for at least as low a current as 0.09 ampere. There are other groups close to the electrode surface also in the ultra-violet which were not identified. Particular interest centers in the line λ 4571. It is the fundamental resonance line of the substance,[1] $1S-2p_2$, mixed-series type. This type was not observed in strontium and very doubtfully observed in calcium. The line was not observed for any current either in the middle or at the poles with the chloride of magnesium. The metal magnesium was next tried. A small piece of the metal was used in a shallow crater of copper, and copper was used for the upper electrode. With a current of 0.07 ampere or less one could sustain the current without flaming for a short time and make a good inspection. The oxide group λ 5007 could be easily traced, and λ 5183 flares, but this line did not show until flaming ensued. This was not a flaming arc, but a combustion which would continue after the arc circuit was broken. The line may be observed in the arc for very large currents, if the salt is plentifully supplied. It then occurs in the middle of the arc, and after watching it some time, it was decided that it occurred by reason of a certain amount of *spraying* of the salt by the hot arc. The same thing could be happening in the larger-current calcium and strontium arcs. It is suggested that this is the solution of the question and that the type of line is foreign to the operation of these arcs. Another resonance line occurs at λ 2852. This line was

[1] *Loc. cit.*

found in the chloride spectrum, but it was not found without the presence of the *d* member λ 3838 and three or four other lines, not well separated, at λλ 2803–2790. The stage of these lines was not settled. They show well at 0.12 ampere. Only the first members of the *d* and *s* series could be safely classified, and then reliance must be made largely upon the ratio of polar to middle intensities. They are assigned to Stage II. Two other polar lines are found which were observed at both poles. These lines λ 5528 and λ 4703 are not earlier than the third stage.

Discussions and the conclusions will follow in Part II, which will deal with metals.

Brace Laboratory of Physics
University of Nebraska
March 1921

A PHOTOMETRIC STUDY OF Y CAMELOPARDALIS

By RAYMOND SMITH DUGAN

ABSTRACT

Eclipsing variable Y Camelopardalis.—The 1035 *photometric observations*, in which B.D.+76°.285 was used as comparison star are given in a table of 210 normals. The probable error of a single observation is $\pm 0^{M}.044$. The *light-elements* derived from the observations are in good agreement with Miss Harwood's conclusions concerning variation of the period. The *light-curve* shows the effects of ellipticity and reflection. A secondary minimum has been detected. The eclipses are partial and last about $12\frac{1}{2}$ hours each. The range of variation is $1^{M}.73$ in primary minimum and $0^{M}.05$ in secondary minimum. "Uniform" and "darkened" *orbital elements* are collected at the end of the paper. In order to get a satisfactory "darkened" solution, it was necessary to assume that one side of the fainter star was entirely dark.

The variability of Y Camelopardalis (B.D.+76°.286) was discovered by Mme Ceraski in 1903. According to Miss Cannon, the spectrum is between A and F. The faintness of the star—Wendell[1] makes it $10^{M}.6$ at maximum—makes impossible a precise classification. The star has been observed—with the usual concentration on the primary minimum portion of the light-curve—by Blajko,[2] Nijland,[3] Wendell,[4] and Lehnert.[5] Miss Harwood[6] has utilized the Harvard plates to form a photographic mean curve and has studied the variation of the period. Mean curves have been discussed and orbital elements derived by Dr.[7] and Mrs.[8] Shapley. My own observations were begun in 1906, but the bulk of the 16,560 measures were made in 1908–1909 and 1916–1917. The observations and discussion will appear in detail in *Contributions from the Princeton University Observatory*.

With the addition of the visual observations the plot of the difference between the time predicted with Miss Harwood's

[1] Wendell, *Harvard Annals*, 69, Part II.

[2] *Astronomische Nachrichten*, 163, 91, 1903; 177, 119, 1908.

[3] *Astronomische Nachrichten*, 176, 165, 1907; 183, 281, 1910.

[4] *Harvard Annals*, 69, Part II.

[5] *Astronomische Nachrichten*, 200, 163, 1915.

[6] *Harvard Annals*, 84, No. 2.

[7] H. Shapley, *Contributions from the Princeton University Observatory*, No. 3.

[8] M. B. Shapley, *Astrophysical Journal*, 46, 56, 1917.

constant period and the observed time retains the general character of her diagram. The residual which apparently increased to a maximum of $+50^m$ in J.D. 2416300 decreased steadily to -2^h24^m in J.D. 2421300. My own observations are best represented by a straight line which makes a slight angle with the contemporary portion of Miss Harwood's curve, and which corresponds to the elements:

$$\text{Min.} = \text{J.D. } 2418306.23526 + 3.3054517\,E$$

The mean epoch of these elements is J.D. 2418521. B.D.+76°.285 was used as comparison star and gave no indications of being a

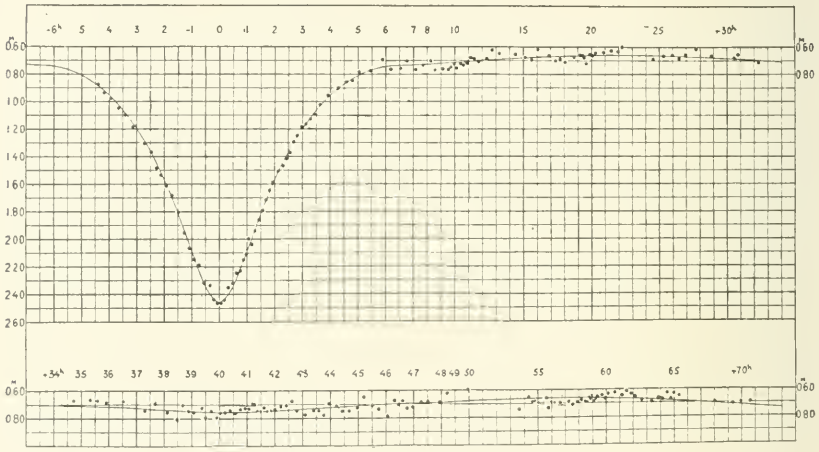


FIG. 1.—Y Camelopardalis

variable. A probable error of $\pm 0^M.044$ of a single observation (16 measures) is indicated by the residuals of the normals of observation from the theoretical curve.

The curve of primary minimum is sensibly symmetrical, results from a partial eclipse, is about $12\frac{1}{2}$ hours in length, and involves a loss of $1^M.73$. A secondary minimum of the same duration and involving a loss of but $0^M.05$ has been found. An apparent displacement of secondary minimum nearly an hour toward the following primary minimum is the only indication of orbital eccentricity.

TABLE I

TABLE OF NORMALS

Normal Number	Phase	Weight	$v-b$		O−C
			O	C	
1	$-0^d4^h24^m20$	4	$+0^M872$	$+0^M883$	-0^M011
2	4 11.90	4	0.936	0.919	+ 17
3	3 56.88	3	0.978	0.962	+ 16
4	39.50	4	1.049	1.022	+ 27
5	25.19	3	1.098	1.083	+ 15
6	3 8.28	3	1.183	1.158	+ 25
7	2 42.94	3	1.306	1.287	+ 19
8	28.00	5	1.366	1.372	− 6
9	16.40	5	1.485	1.450	+ 35
10	2 6.80	5	1.536	1.520	+ 16
11	1 56.33	4	1.613	1.599	+ 14
12	43.50	4	1.682	1.695	− 13
13	29.56	5	1.803	1.820	− 17
14	16.78	4	1.953	1.935	+ 18
15	1 5.94	4	2.064	2.039	+ 25
16	0 54.50	4	2.148	2.131	+ 17
17	44.56	4	2.189	2.225	− 36
18	33.50	4	2.318	2.318	± 0
19	20.56	4	2.335	2.399	− 64
20	12.17	5	2.438	2.430	+ 8
21	−0 0 4.39	5	2.464	2.451	+ 13
22	+0 0 3.94	4	2.463	2.452	+ 11
23	11.10	5	2.440	2.432	+ 8
24	19.10	5	2.350	2.402	− 52
25	29.06	5	2.319	2.347	− 28
26	36.67	5	2.244	2.290	− 46
27	45.80	5	2.230	2.215	+ 15
28	52.63	4	2.150	2.151	− 1
29	0 58.50	4	2.109	2.100	+ 9
30	1 3.38	4	1.998	2.056	− 58
31	10.28	5	2.038	2.000	+ 38
32	17.50	5	1.940	1.931	+ 9
33	26.00	5	1.860	1.850	+ 10
34	34.00	5	1.792	1.778	+ 14
35	41.20	5	1.713	1.715	− 2
36	48.22	4	1.644	1.658	− 14
37	1 55.50	4	1.586	1.609	− 23
38	2 7.33	4	1.507	1.510	− 5
39	18.11	5	1.469	1.437	+ 32
40	25.50	5	1.417	1.390	+ 27
41	33.11	4	1.371	1.340	+ 31
42	40.67	4	1.294	1.299	− 5
43	48.40	5	1.249	1.252	− 3
44	2 58.10	5	1.182	1.206	− 24
45	+0 3 7.13	4	+1.163	+1.163	±0.000

TABLE I—*Continued*

Normal Number	Phase	Weight	$v-b$		O−C
			O	C	
46	+0d 3h16m56	4	+1M127	+1M120	+0M007
47	25.29	3	1.091	1.081	+ 10
48	37.56	4	1.021	1.030	− 9
49	3 54.70	4	0.953	0.969	− 16
50	4 16.80	4	0.900	0.902	− 2
51	34.10	4	0.857	0.860	− 3
52	4 47.50	4	0.846	0.832	+ 14
53	5 2.20	4	0.782	0.804	− 22
54	26.70	4	0.773	0.769	+ 4
55	5 53.00	4	0.695	0.748	− 53
56	6 11.43	2	0.762	0.738	+ 24
57	32.50	4	0.758	0.735	+ 23
58	6 48.40	4	0.703	0.733	− 30
59	7 10.70	4	0.764	0.730	+ 34
60	7 41.60	3	0.733	0.728	+ 5
61	8 8.50	3	0.701	0.726	− 25
62	8 33.30	3	0.768	0.722	+ 46
63	9 8.70	3	0.760	0.719	+ 41
64	31.20	5	0.766	0.717	+ 49
65	42.20	5	0.747	0.714	+ 33
66	9 57.80	5	0.724	0.713	+ 11
67	10 9.90	5	0.754	0.711	+ 43
68	24.30	5	0.723	0.710	+ 13
69	36.90	4	0.734	0.708	+ 26
70	10 51.50	4	0.720	0.707	+ 13
71	11 9.40	5	0.678	0.704	− 26
72	24.50	4	0.687	0.702	− 15
73	11 43.00	4	0.709	0.700	+ 9
74	12 19.00	3	0.684	0.696	− 12
75	12 42.10	4	0.622	0.693	− 71
76	13 13.30	3	0.648	0.690	− 42
77	14 23.90	3	0.654	0.683	− 29
78	15 7.20	3	0.678	0.680	− 2
79	15 36.00	4	0.695	0.678	+ 17
80	16 4.30	3	0.618	0.674	− 56
81	16 51.90	3	0.662	0.671	− 9
82	17 22.40	4	0.700	0.670	+ 30
83	17 41.90	4	0.687	0.669	+ 18
84	18 2.90	3	0.711	0.667	+ 44
85	18 42.70	3	0.675	0.666	+ 9
86	19 9.70	4	0.660	0.664	− 4
87	18.90	5	0.663	0.664	− 1
88	28.50	5	0.680	0.663	+ 17
89	36.80	4	0.720	0.663	+ 57
90	+0 19 51.30	4	+0.653	+0.662	−0.009

TABLE I—*Continued*

Normal Number	Phase	Weight	*v–b*		O–C
			O	C	
91	+0d20h 4m60	4	+0M663	+0M661	+0M002
92	23.90	3	0.642	0.661	− 19
93	20 53.20	3	0.640	0.660	− 20
94	21 32.90	3	0.628	0.660	− 32
95	21 57.31	3	0.632	0.660	− 28
96	0 22 15.10	2	0.600	0.660	− 60
97	1 0 31.00	3	0.688	0.661	+ 27
98	1 18.20	3	0.666	0.664	+ 2
99	1 58.25	3	0.659	0.666	− 7
100	2 26.57	2	0.684	0.668	+ 16
101	2 55.22	3	0.656	0.670	− 14
102	3 42.80	3	0.616	0.672	− 56
103	4 50.25	1	0.665	0.677	− 12
104	6 30.69	3	0.680	0.687	− 7
105	6 48.00	2	0.653	0.689	− 36
106	8 18.63	1	0.713	0.697	+ 16
107	9 21.33	1	0.698	0.701	− 3
108	10 43.50	3	0.672	0.710	− 38
109	11 19.10	4	0.664	0.712	− 48
110	35.90	4	0.672	0.713	− 41
111	11 55.00	4	0.686	0.716	− 30
112	12 31.61	4	0.675	0.719	− 44
113	13 18.71	2	0.746	0.729	+ 17
114	13 41.11	3	0.693	0.734	− 41
115	14 7.20	3	0.754	0.738	+ 16
116	28.70	4	0.804	0.742	+ 62
117	41.10	4	0.702	0.745	− 43
118	14 52.90	4	0.746	0.747	− 1
119	15 4.50	4	0.766	0.750	+ 16
120	21.81	3	0.725	0.752	− 27
121	30.22	4	0.792	0.753	+ 39
122	42.44	5	0.746	0.755	− 9
123	15 54.00	4	0.791	0.756	+ 35
124	16 2.20	5	0.759	0.756	+ 3
125	12.60	4	0.758	0.756	+ 2
126	23.50	4	0.741	0.756	− 15
127	34.30	4	0.763	0.756	+ 7
128	45.40	4	0.735	0.756	− 21
129	16 56.10	5	0.729	0.755	− 26
130	17 4.00	5	0.730	0.755	− 25
131	10.90	5	0.691	0.754	− 63
132	16.50	5	0.697	0.753	− 56
133	22.20	4	0.746	0.752	− 6
134	29.70	5	0.747	0.752	− 5
135	+1 17 36.70	5	+0.721	+0.750	−0.029

TABLE I—*Continued*

Normal Number	Phase	Weight	$v-b$		O−C
			O	C	
136	+1d 17h44m20	5	+0M747	+0M749	−0M002
137	17 52.00	5	0.741	0.748	− 7
138	18 0.20	4	0.734	0.747	− 13
139	12.60	4	0.713	0.744	− 31
140	24.20	4	0.708	0.741	− 33
141	36.60	4	0.678	0.740	− 62
142	18 47.60	5	0.744	0.738	+ 6
143	19 5.80	4	0.774	0.732	+ 42
144	24.00	4	0.743	0.729	+ 14
145	35.80	5	0.746	0.727	+ 19
146	46.00	5	0.778	0.725	+ 53
147	19 56.40	4	0.694	0.722	− 28
148	20 13.20	4	0.710	0.720	− 10
149	25.20	4	0.748	0.717	+ 31
150	40.60	4	0.748	0.713	+ 35
151	1 20 58.50	4	0.724	0.710	+ 14
152	21 12.39	3	0.647	0.707	− 60
153	30.06	3	0.708	0.703	+ 5
154	21 44.30	3	0.736	0.702	+ 34
155	22 3.94	3	0.786	0.700	+ 86
156	18.39	4	0.674	0.697	− 23
157	27.44	4	0.703	0.696	+ 7
158	36.50	3	0.676	0.695	− 19
159	45.60	4	0.729	0.694	+ 35
160	22 58.25	3	0.722	0.693	+ 29
161	23 16.28	4	0.685	0.692	− 7
162	30.50	4	0.681	0.691	− 10
163	1 23 56.44	3	0.686	0.690	− 4
164	2 0 26.13	2	0.623	0.687	− 64
165	1 55.63	2	0.598	0.679	− 81
166	5 39.70	3	0.741	0.665	+ 76
167	6 20.60	4	0.652	0.664	− 12
168	35.20	4	0.686	0.663	+ 23
169	6 47.20	4	0.681	0.662	+ 19
170	7 1.50	4	0.696	0.662	+ 34
171	15.00	5	0.702	0.661	+ 41
172	27.00	4	0.705	0.661	+ 44
173	36.30	5	0.660	0.661	− 1
174	45.60	4	0.733	0.661	+ 72
175	7 59.90	4	0.689	0.661	+ 28
176	8 12.89	4	0.696	0.660	+ 36
177	8 37.08	2	0.694	0.660	+ 34
178	9 15.78	3	0.689	0.660	+ 29
179	32.30	4	0.711	0.660	+ 51
180	+2 9 52.10	4	+0.692	+0.660	+0.032

TABLE I—*Continued*

Normal Number	Phase	Weight	*v–b*		O–C
			O	C	
181	+2d 10h 11m 30	4	+0M679	+0M660	+0M019
182	26.50	4	0.689	0.660	+ 29
183	36.42	4	0.693	0.660	+ 33
184	45.17	5	0.656	0.660	+ 4
185	50.90	5	0.672	0.660	+ 12
186	10 58.60	5	0.645	0.661	− 16
187	11 6.30	5	0.686	0.661	+ 25
188	13.20	5	0.672	0.661	+ 11
189	20.94	4	0.653	0.662	− 9
190	41.30	4	0.641	0.663	− 22
191	11 54.90	4	0.667	0.664	+ 3
192	12 8.33	3	0.633	0.665	− 32
193	12 37.10	4	0.624	0.667	− 43
194	13 11.30	3	0.637	0.668	− 31
195	30.90	4	0.617	0.669	− 52
196	13 49.10	4	0.634	0.670	− 36
197	14 8.81	2	0.653	0.670	− 17
198	14 36.90	3	0.681	0.672	+ 9
199	15 19.70	3	0.692	0.674	+ 18
200	15 50.90	3	0.666	0.678	− 12
201	16 9.10	4	0.675	0.680	− 5
202	29.40	4	0.630	0.682	− 52
203	45.50	4	0.673	0.687	− 11
204	16 59.20	4	0.633	0.686	− 53
205	17 22.00	3	0.650	0.688	− 38
206	20 1.70	4	0.699	0.699	− 5
207	20 36.56	4	0.739	0.739	+ 31
208	21 20.70	4	0.709	0.713	− 4
209	21 56.50	4	0.699	0.718	− 19
210	+2 22 37.64	2	+0.694	+0.722	−0.028

The influences of ellipticity of figure and of reflection are apparent in the curve. Values of these constants, as well as for the intensity at quadrature, and the depth and the phase of secondary minimum were found by a least-squares solution. Assuming the brightness of the comparison star as 9M94, we have the following magnitudes of Y Camelopardalis: at maximum brightness 10M60; at primary minimum, 12M41; at secondary minimum, 10M68.

The solution of the curve on assumptions of uniform illumination and total darkening at the limb were carried through on the usual lines. The difference in luminosity of the two stars according

to the uniform solution is large. It was impossible to make a satisfactory darkened solution with the retention of all the values found from the least-squares solution. In order to retain the value 0.041 for the difference in brightness of the two sides of the fainter star, it was necessary to increase the depth of secondary minimum by 0.0065, thereby reducing the luminosity of the dark side to zero.

It is interesting to note also that we cannot tell which component is the larger until we know to what degree the disks are darkened

TABLE II

		Uniform	Darkened
Maximum radius of dark star	af	0.2451	0.2308
Minimum radius of dark star	bf	0.2287	0.2152
Maximum radius of bright star	ab	0.2228	0.2664
Minimum radius of bright star	bb	0.2079	0.2488
Ratio of radii of each star	b/a	0.934	0.934
Ratio of radii of two stars	k	1.100	0.866
Inclination of orbit plane	i	84°38′	86° 7′
Component of orbital eccentricity	$e\cos\omega$	+0.018	+0.018
Difference of light of sides of dark star	$2c$	0.041	0.041
Light of bright star	L_b	0.9498	0.9590
Light of brighter side of dark star	L_f	0.0502	0.0410
Light of darker side of dark star	L_f-2c	0.0092	0
Ratio of surface brightness:			
Of the bright star to brighter side of dark star	J_b/J_f	23	17.5
Of the bright star to darker side of dark star		125	∞
Equal-mass densities:			
Of the bright star		0.0418	0.0500
Of the dark star		0.0556	0.0325

at the limb. If the stars present uniformly illuminated disks, then the darker star is slightly the larger. The darkened solution, on the other hand, makes the brighter star considerably the larger.

The curve drawn out in the diagram and given also under "C" in the Table of Normals is the one computed on the assumption of total darkening.

The visual and photographic ranges in primary minimum are practically identical. As the dark star supplies but a small fraction of the light remaining at primary minimum, no conclusions in regard to difference in spectral type of the components can be drawn from this fact.

Other results of interest are summarized in Table II. The unit of length is the radius of the relative orbit. The unit of light is the combined light of the brighter sides of the two stars at maximum area. The mass of each component is assumed equal to that of the sun and the unit of density is the density of the sun.

PRINCETON UNIVERSITY OBSERVATORY
June 1921

THE SPECTROSCOPIC BINARY BOSS 3644, VIRGINIS[1]

By JOHN C. DUNCAN

ABSTRACT

Spectroscopic binary Boss 3644, Virginis.—The elements of the orbit of this sixth-magnitude star of type F2 have been determined from eighteen spectrograms. P is 2.6960 days, K is 24.3 km/sec., γ is 17.6 km/sec., and e is 0.00. A velocity-curve is given.

The radial velocity of the star Boss 3644 ($\alpha = 14^h 8^m.5$, $\delta = -22°25'$; 1900.0) was found to be variable by Miss A. M. Brayton from her measures of three spectrograms made with the 60-inch reflector and single-prism spectrograph early in 1920. During the current

TABLE I

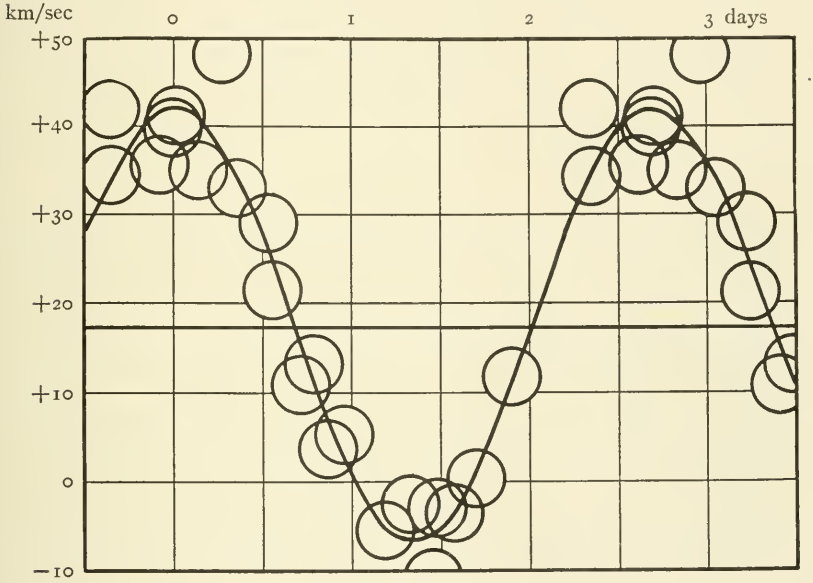
OBSERVATIONS OF BOSS 3644

Plate	Date, G.M.T.	J.D. 2422000+	Days after Maximum Velocity	Observed Velocity	O−C
8990.....	1920 Feb. 5 1h 06m	360.046	1.471	− 3.2	+ 2.6
9092.....	Mar. 31 21 57	415.915	0.724	+10.6	− 4.2
9239.....	May 31 20 20	476.847	2.344	+34.2	0.0
9881.....	1921 Jan. 29 1 02	719.043	1.900	+11.7	+ 0.9
9903.....	Feb. 17 23 18	738.971	0.260	+48.0	+10.4
9912.....	Feb. 19 1 14	740.051	1.340	− 2.7	+ 4.0
9925.....	Feb. 20 1 07	741.047	2.336	+41.8	+ 7.9
9930.....	Feb. 20 22 23	741.933	0.526	+28.8	+ 3.0
9943.....	Feb. 23 23 11	744.966	0.863	+ 3.6	− 3.7
9959.....	Feb. 25 22 31	746.938	0.139	+34.9	− 5.8
9972.....	Feb. 26 23 35	747.983	1.184	− 5.6	− 0.6
10017.....	Mar. 19 21 55	768.913	0.546	+21.4	− 3.3
10025.....	Mar. 20 19 38	769.818	1.451	−11.0	− 5.0
10027.....	Mar. 20 22 09	769.923	1.556	− 3.8	+ 0.1
10030.....	Mar. 22 20 17	771.845	0.782	+13.2	+ 1.7
10034.....	Mar. 23 0 30	772.014	0.951	+ 5.2	+ 2.2
10062.....	Mar. 27 19 16	776.803	0.348	+32.8	− 1.6
10096.....	Apr. 17 22 43	797.947	2.620	+35.5	− 6.1
10134.....	Apr. 27 19 31	807.813	1.702	+ 0.2	− 0.9
10142.....	Apr. 28 19 12	808.800	2.689	+39.9	− 2.0
10143.....	Apr. 28 19 36	808.817	0.010	+41.0	− 0.9

[1] *Contributions from the Mount Wilson Observatory*, No. 212.

year, eighteen additional plates have been secured by various observers with the same equipment. All the plates are listed in Table I, in which the column headed "Observed Velocity" gives for each plate the mean result of Miss Brayton's measures and mine. The numbers in the fourth and last columns are derived from the circular elements given below.

The star is of the sixth magnitude and of spectral type F2. From eight to twelve lines were measured on each plate, those



Velocity-curve of Boss 3644

chosen being of iron and occasionally of hydrogen. Preliminary elements were derived by the method of Lehmann-Filhés as follows:

$P = 2.6960$ days
$K = 25.0$ km/sec.
$\omega = 320°$
$e = 0.08$
T = J.D. 2422746.45
$\gamma = +17.47$ km/sec.

A least-squares solution was based on these elements, using only the eighteen plates of 1921 and omitting the period. As the

resulting correction to the eccentricity was -0.11 ± 0.06, this element was assumed to be 0.00 and a second solution was made with T, K, and γ as the only variables. By the first solution Σvv was reduced from 443 to 338, and by the second it was further diminished to 333. The circular elements from the second solution and the period originally found are:

$$P = 2.6960 \text{ days}$$
$$K = 24.34 \pm 1.08 \text{ km/sec.}$$
$$e = 0.00$$
$$T_\Omega = \text{J.D. } 2422744.103 \pm 0.023$$
$$\gamma = +17.60 \pm 0.85 \text{ km/sec.}$$
$$a \sin i = 902{,}300 \text{ km}$$
$$\frac{m_1^3 \sin^3 i}{(m+m_1)^2} = 0.00404 \odot$$

T_Ω indicates the epoch of maximum positive velocity. In the accompanying velocity-curve the radius of the circles representing the observations is equal to the probable error of a single plate, ± 3.18 km/sec.

Mount Wilson Observatory
June 1921

THE
ASTROPHYSICAL JOURNAL
AN INTERNATIONAL REVIEW OF SPECTROSCOPY
AND ASTRONOMICAL PHYSICS

VOLUME LIV NOVEMBER 1921 NUMBER 4

THE DEFINITION OF A NOVA

By J. G. HAGEN, S.J.

ABSTRACT

Collision theory of the origin of novae, irregular variables, O stars, planetary nebulae and δ Cephei variables.—Seeliger's suggestion that temporary stars originate from *encounters between stars and cosmic nebulae* is made more specific by assuming that the nebulae are cometary—that is, become luminous at the approach of the stars, and the possible results of four types of such encounters are discussed. (1) Transit without contact might produce a nova with a relatively small range of variation (type T Boötis ?). (2) Grazing the nebula, if repeated occasionally, might result in an irregular variable such as T Pyxidis. (3) Passage through the nebula on a hyperbolic path might result in a nova of the ordinary type (T Aurigae) and in a star with a nebulous envelope, an O star. (4) Capture of the star by the nebula might give a δ Cephei variable or a planetary nebula. The theory is shown to account for nearly all the facts of observation relating to ordinary novae, particularly the range of light, shape of the light-curve, character of the spectrum, their rarity, and their physical similarity to O stars and planetary nebulae.

Definition of a nova suggested by the above theory is "a cometary nebula brought temporarily into close proximity or contact with a bright star." This definition does not include novae in spiral nebulae, but fits the four types enumerated.

That the definition of new stars, so called, will have to be revised has been repeatedly expressed in recent publications. It is quite natural that Newton's definition should have held its own for two hundred years, because only the spectroscope could reveal new facts about these stars.

In his *Principia mathematica* (ed. 1760), III, last proposition, Newton defines the novae as "fixed stars that suddenly appear, at first shine brilliantly and then gradually fade away." Later

definitions, like those of Newcomb[1] and Miss Clerke,[2] are but expansions of that given by Newton.

I

In formulating a definition that takes account of what we now know about nebulae surrounding the novae, about stars of Class O and planetaries, it will be convenient, if not necessary, to start from certain assumptions that may yet be disputed. The resulting theory, although not definite, can for the present at least serve as a working hypothesis.

One of these assumptions is that temporary stars originate from encounters between stars and cosmic clouds, an opinion proposed and elaborated by Seeliger, in *Astronomische Nachrichten*, **181**, 81, 1909, and in other communications as far back as 1886. Another assumption consists in the views expressed by the writer in an article on the "Astrophysical Problem of Variable Stars"[3] and, in particular, in the view on the δ Cephei problem. We shall only recall from that article, that a δ Cephei variable may be considered as a binary system, one component of which is a star like our sun and the other a cosmic nebula of cometary qualities. A nebula is said to have "cometary qualities" when it becomes luminous by the mere approach to a star like our sun.

Seeliger's assumptions regarding star and cloud are quite general and exclude no special case. We now specify his "cloud" as a cometary nebula that will develop eruptions of light by the mere approach of a radioactive star similar to our sun. A clear basis is thus obtained for further conclusions on the nature of temporary stars.

II

To begin with, it seems necessary to exclude from our consideration the new stars found in spiral nebulae because, judging from the continuous spectrum of S Andromedae, the nova of 1885, they form a class of their own.

The light-curves of the novae are so much like those of the δ Cephei type that the comparison will be suggestive in many

[1] *The Stars*, p. 127.

[2] *Problems in Astrophysics*, p. 375.

[3] *Monthly Notices of the Royal Astronomical Society*, **81**, 226, 1921.

ways; there are only two differences: the light-curves of the novae have a larger range, amounting sometimes to fifteen magnitudes, and have no periodic repetition.

The range of variation in the δ Cephei stars is confined to about one magnitude, and yet they are known to be giant stars. What, then, must be the dimensions of a nova? Campbell and Moore have found evidence that planetary nebulae, which we hope to show to be a special class of novae, contain sufficient material to form systems more extensive than our solar system.[1]

The periodic variation of the δ Cephei stars consists essentially, as we have assumed, in the elliptic motion of two components. Now substituting other kinds of orbits, regular or disturbed, we may get temporary variables. Divers hypotheses can be made.

1. If a star passes by the nebula in a relatively hyperbolic orbit, without contact, one maximum brightness is produced, exactly similar to that of a δ Cephei variable, but without repetition. Temporary stars of this class easily escape observation, even when the eruption of light takes place on our side of the nebula, because of the small range of variation and the short-lived eruption.

May not Baxendell's T Boötis (1860) or Pogson's U Scorpii (1863), which reached the tenth and ninth magnitudes respectively, and other merely telescopic novae, belong to this class?

2. What will happen when the star just grazes the cosmic nebula may perhaps be learned from irregular variables like P Cygni, T Tauri, and T Pyxidis. The first of these had reached the third magnitude in 1600 and a second time in 1657–1659; since then it has remained a star of fifth magnitude. T Tauri was of the ninth magnitude in 1852 and again in the years 1877–1881 and 1902; according to the *Annual Report* for 1915 of the Mount Wilson Observatory (No. 61, p. 291) the star is surrounded by an extensive atmosphere which shows the emission lines of the O spectrum. Of T Pyxidis only three outbursts were noticed in thirty years, viz., in 1890, 1902, and 1920. The last one was observed spectroscopically with the 100-inch reflector by Adams and Joy, who found numerous relationships to the spectrum of novae.[2]

[1] *Publications of the American Astronomical Society*, 3, 195, 1918, and *Publications of the Lick Observatory*, 13, 177, 1918.

[2] *Popular Astronomy*, 28, 514, 1920.

Stars of this kind form a transition from the δ Cephei type to the novae properly so called.

3. Elliptic motion between star and nebula may become impossible when the star's mass, relative to that of the nebula, exceeds the limits compatible with the δ Cephei type. Indeed, mutual attraction may then become so strong that the star gets enveloped in the nebula. If its velocity relative to the nebula is sufficiently large to overcome the resisting medium and the two bodies separate in a hyperbolic orbit, we have a temporary star of the ordinary type, B Cassiopeiae, T Aurigae, and others.

This theory is put to the severe test of having to account for the range of light, for the character of the spectrum, and for the shape of the curve, but it seems to stand it.

a) The range has been explained by Professor Seeliger and the spectrum by Dr. Halm, both on the hypothesis of a (dark) celestial body entering a cosmic cloud. Now their explanations of the general case seem to be even facilitated when the body entering the cloud is specified as a star possessing all the radiant energy of our sun and the cloud as a nebula endowed with the cometary quality of becoming luminous by the mere approach to the radiating star.

While in a δ Cephei star, at periastron passage, the intensity of light is about doubled, that of a nova may be increased a million fold. According to Seeliger the mechanical impact alone, between star and cloud, is amply sufficient to account for a range like this. So much the more will, in our case, the combined effect of radiation and friction account for it. Examples worked out numerically are given by Veronnet in *Comptes Rendus*, **172**, 666, 1921. He calculates the surface temperature of a nova on various suppositions regarding the orbits, masses, densities, radii of star and nebula, and he shows how the mechanical theory is by itself apt to satisfy the observations. If we ever had the opportunity of observing a comet falling into the sun, we might be able to estimate the other factor of the process also, the radiation within the nova.

b) About the spectrum and its variations in temporary stars Dr. Halm has written an extensive treatise[1] in which he shows at

[1] *Proceedings of the Royal Society of Edinburgh*, **25**, 513–552, 1905; see especially p. 519.

least the possibility of explaining all the facts, provided the additional hypothesis is made that the star, in leaving the cloud, carries with it a quantity of nebulous matter. For a cosmic cloud specified as a cometary nebula this additional assumption is not only natural but apparently inevitable. There are thus two stages to be distinguished in a nova of this class: the initial stage of a giant nebula with a brilliant stellar nucleus, and the subsequent stage of a star surrounded by a nebulous atmosphere. The star has become an O star, entirely separate from the large cloud, and the latter will gradually fall back into its former obscurity. The O star remains, but the nova has disappeared.

Without entering into details, we quote a suggestion of Adams and Pease,[1] "that the disappearance of the chief nebular lines is coincident with the emergence of the star from the nebula."

c) The light-curve of a nova presents no difficulty to the theory. The varieties among some of the curves in the ascending branch may in part be due to the direction from which the star enters the cloud, relative to the line of sight. Suppose the star enters the nebula from our side, the process of illumination, preceding actual contact, becomes visible. It will, on the contrary, be partly hidden when the approach is from the averted side.

The passing of the star through the cloud must disturb the surface equilibrium of the nebula, which can only be restored through a series of oscillations. The descending branch of the light-curve discloses the disturbance by its undulating shape. It is for this stage of a nova that the pulsation theory would seem to find its full application.

4. If the star, after entering the nebula, does not leave it in a hyperbolic orbit, it is bound to become permanently captured by it. Even if it should escape and begin to describe an elliptic arc, it must re-enter the cloud and, in a spiral-shaped path, reach the center of gravity. When the two celestial bodies move in directions that form an acute angle, their relative velocity is partly the difference of their proper motions and may be so small that the star cannot overcome the resisting medium of the nebula; it has become its permanent nucleus.

[1] *Astrophysical Journal*, 40, 297, 1914.

Professor Campbell asks the question[1] whether planetaries and novae are "results of catastrophes" and suggests "a common or closely related origin of the two classes of objects." Why not say directly that the planetary nebula originated as a nova of the kind here considered?

According to this theory the difference between O stars and planetary nebulae is mainly one of quantity. The O star carries with it a portion of the nebula, the planetary is the entire nebula enveloping the star. The similarity was first recognized by E. C. Pickering[2] in 1891, when he combined the spectra of O stars and of planetary nebulae into Class V of Secchi's series. Twelve years later W. H. Wright found that the nuclei of some planetary nebulae are O stars, and, vice versa, that the envelopes of some O stars are planetary nebulae,[3] a discovery verified soon after by Bosler[4] and others.

III

The physical connection between novae, planetary nebulae, and O stars maintained in this theory thus accounts satisfactorily for nearly all the facts of observation, but a number of questions remain to be answered.

1. The salient feature of these celestial bodies is their rare occurrence. The number of known planetary nebulae is less than 150 and that of the O stars smaller yet. The ordinary novae are fully as uncommon relatively to the total number of stars. This circumstance has long since led to the view that the three classes of objects do not fit into the general path of natural evolution and must be considered as products of exceptional events. The fact that all of them are galactic phenomena lends support to this view.

The "exceptional events" must be the encounters between stars and nebulae, as explained above.

2. If a planetary originates from a star like our sun entering a giant nebula, the question may be raised as to the mass of a plane-

[1] *Publications of the Lick Observatory*, **13**, 173, 1918.

[2] *Astronomische Nachrichten*, **127**, 5, 1891.

[3] *Astrophysical Journal*, **40**, 466, 1914.

[4] *Comptes Rendus*, **160**, 124, 1915.

tary. Fortunately, the question has been answered by Professor Campbell. From the interior rotations of the larger and brighter nebulae he deduced that their minimum probable masses are several fold the sun's mass, while smaller planetaries may be comparable with, or even smaller than, our solar system.[1]

More serious perhaps is the question of color. No yellow light reaches us from the nucleus of a planetary, either visually or photographically, in contrast to spiral nebulae, whose nuclei are of the solar type and the branches intensely blue.[2] However, a conclusion from one of these essentially different classes of objects to the other is not warranted. Nor do we know what transformations a radioactive star undergoes when permanently imbedded in a cometary nebula.

The radial velocity of planetary nebulae, though in general of the same order of magnitude as that of the stars, is on the average more than twice as large.[3] The conclusion that cometary nebulae, as a class, move faster than stars would seem premature, because the five δ Cephei stars, contained in Voûte's *First Catalogue of Radial Velocities* (1920), have a mean velocity of only 13.4 km. The explanation is rather this, that the chances for collision are the greater, the greater the speed of individual stars and nebulae.

This view is not contradicted by the fact that the novae so far examined have small angular proper motions,[4] because stars that encounter nebulae with nearly opposite velocities and work their way through a resisting medium must necessarily lose part of their proper speed, angular or radial. The case is different from that of planetaries, in which the initial velocities of star and nebula are more or less parallel and are fused into one common motion.

IV

Recapitulating, we have the following classes of so-called new stars. First, the novae in spiral nebulae, excluded from our theory (type S Andromedae). Regarding those within our stellar

[1] *Publications of the Lick Observatory*, 13, 178, 1918.

[2] F. H. Seares, *Publications of the American Astronomical Society*, 3, 220, 1918.

[3] *Publications of the Lick Observatory*, 13, 72.

[4] *Popular Astronomy*, 29, 221, 1921.

system, some originate without actual contact between star and nebula and are rarely noticed (type T Boötis?). Others burst out through the occasional grazing of a star and a nebula which, at least for a time, are both physically connected (type T Pyxidis?). Still others, perhaps most of them, become O stars (type T Aurigae). Finally, some will turn into planetary nebulae (no type assignable because the transformation has not yet been directly observed).

Considering these various possibilities, we can understand why an unequivocal definition of temporary stars has hitherto been impossible. Restricting the concept of a new star to the outburst of light, and not comprising in it the permanent stages of planetaries and of O stars, the following definition would seem to cover all the cases within our stellar system: *A nova is a cometary nebula brought temporarily into close proximity or contact with a bright star.*

Vatican Observatory, Rome
June 1921

INVESTIGATIONS ON PROPER MOTION

FOURTH PAPER: INTERNAL MOTION IN THE SPIRAL NEBULA MESSIER 51[1]

By ADRIAAN VAN MAANEN

ABSTRACT

Spiral nebula Messier 51.—A comparison of a plate taken by Mr. Duncan on April 8, 1921, with one taken by Mr. Ritchey on February 7–8, 1910, both at the 25-foot focus of the 60-inch reflector, enabled the *proper motion of the nebula* and the relative motion of its parts to be determined. Measurements of 80 points of the nebula compared with those of 20 stars give for the nebula an annual proper motion of +0".006 in right ascension and +0".001 in declination. The *internal proper motion* is not a pure rotation since the mean radial component is outward and is 42 per cent of the mean tangential component which is 0".019 ENWS; rather it is a spiral motion out along the arms at the rate of 0".021 per year together with a slight outward radial motion of 0".003.

Two sixteenth magnitude stars with large proper motions, about 0".15 per year, were found *near Messier 51*. They are called *f* and *r*.

Five years have elapsed since the first evidence of internal motion in a spiral nebula, as derived from direct photographs, was announced in this *Journal*.[2] The time interval between the old and new plates taken at the 25-foot focus of the 60-inch reflector has now been doubled, thus quadrupling the weight of the annual motions derived from them; it was accordingly thought worth while to investigate several objects of this class.

The first spiral nebula for which two plates with a ten-years' interval became available was M 33. A note concerning the preliminary measures for 51 points of this nebula has appeared elsewhere.[3] These results show a decided internal motion, which, as in the case of M 101,[2] can be explained either as a rotation combined with a radial motion outward, or as an outward motion along the streamers of the nebula. More elaborate measures of this object await the securing of another plate. If, as is hoped, we can measure several hundred points in this object, some light may be thrown on the laws that govern the motions.

[1] *Contributions from the Mount Wilson Observatory*, No. 213.

[2] *Astrophysical Journal*, 44, 210, 1916.

[3] *Proceedings of the National Academy of Sciences*, 7, 1, 1921.

In the meantime Mr. Duncan secured a plate of the spiral nebula M 51, of which Mr. Ritchey had previously taken several photographs. Duncan's plate, taken April 8, 1921, compares most favorably with one secured by Ritchey on February 7 and 8, 1910. Both plates were exposed 3 hours and 55 minutes and are of good quality. Eighty points, presumably belonging to the nebula, were measured, while for comparison purposes 23 stars were selected. Further, two photographs taken by Mr. Seares, one with and one without a yellow color-screen, enabled me to see if objects were included in either category which probably did not belong there. Of the 80 nebulous points only one, No. 27, was decidedly red, and may therefore not be a part of the nebula. In the discussion of the internal motions this point was on this account excluded. Among the comparison stars, on the other hand, one object, *j*, was found to be decidedly blue. As for this reason it may be a part of the nebula, it was excluded for comparison purposes. A rough reduction of the measures showed, moreover, that two of the comparison stars, *f* and *r*, have large proper motions. These were also excluded, leaving 20 comparison stars in all.

The plates were measured with the new stereocomparator—which will be described in another article—in four positions, with the directions east, west, north, and south successively coinciding with that of increasing readings of the micrometer screw.

In order to deal with smaller values in the computations, the mean measured displacements in right ascension and declination, expressed in parts of the micrometer screw, were reduced to displacements in 0″.001 per year by multiplication of the factor

$$q=\frac{27200}{31890\times 11.16}=0.0764,$$

in which 27200 is the number of thousandths of a second of arc per millimeter on the plates, 31890 the number of the parts of the micrometer screw per millimeter on the plates, and 11.16 the interval in years between the two plates. The resulting values, m_α and m_δ, may be reduced to annual proper motion by

$$\left.\begin{aligned} m_\alpha &= a+bx+cy+dx^2+exy+fy^2+\mu_\alpha, \\ m_\delta &= a'+b'x+c'y+d'x^2+e'xy+f'y^2+\mu_\delta, \end{aligned}\right\} \qquad (1)$$

TABLE I

CO-ORDINATES AND MEASURED ANNUAL DISPLACEMENTS

No.	x	y	μ_α	μ_δ
a	+0′.4	+1′.6	−0″.036	−0″.006
b	+3.4	+4.3	+ 22	− 4
c	+4.9	+2.7	− 6	+ 8
d	+3.4	+1.3	− 14	− 14
e	+3.7	−3.1	+ 9	+ 15
f	+3.6	−8.1	− 140	+ 38
g	−0.3	−7.3	− 9	− 7
h	+0.6	−3.1	+ 9	− 5
i	+1.2	−2.2	0	− 9
j	+0.5	−2.2	+ 17	0
k	−3.1	−2.4	+ 6	+ 30
l	−2.4	−1.9	+ 10	+ 6
m	−3.9	−0.5	− 32	− 28
n	−1.9	−0.2	+ 28	+ 4
o	−1.1	+0.3	+ 19	− 2
p	−1.2	+0.9	− 14	+ 10
q	−1.5	+2.4	− 8	0
r	−2.5	+2.5	− 159	− 34
s	−4.3	+2.2	+ 12	− 4
t	−0.8	+3.0	+ 9	+ 4
u	−0.8	+4.0	− 3	+ 11
v	+3.7	+1.3	0	− 1
w	+2.5	+0.4	0	− 5
1	+0.5	0.0	+ 28	+ 10
2	+0.6	−0.2	− 21	+ 6
3	+0.5	−0.7	− 13	+ 6
4	+0.6	−0.9	− 12	+ 14
5	0.0	−0.9	+ 4	+ 9
6	0.0	−1.0	+ 9	+ 3
7	−0.1	−1.2	− 25	+ 9
8	−1.0	−0.9	− 1	− 1
9	−1.5	+0.3	− 3	− 19
10	−1.5	+1.3	− 16	− 22
11	−1.3	+1.7	+ 36	− 18
12	−1.0	+2.1	− 8	− 24
13	−0.5	+2.0	+ 16	− 9
14	−0.3	+1.6	+ 23	− 7
15	−0.5	+1.0	+ 23	− 28
16	0.0	+1.0	+ 8	− 9
17	+1.2	+0.5	+ 11	+ 10
18	+1.5	+0.5	+ 22	+ 17
19	+1.4	0.0	+ 28	+ 19
20	+1.9	−0.6	+ 24	+ 16
21	+2.1	−0.7	+ 43	+ 29
22	+1.6	−1.6	− 6	+ 17
23	+1.6	−2.1	− 11	+ 28
24	+1.2	−1.9	− 26	+ 7
25	+1.0	−2.1	− 20	+ 23
26	+1.1	−2.1	− 25	+ 24
27	−2.1	+0.9	+ 8	− 45
28	−2.2	+0.9	− 7	− 21
29	+0′.9	+2′.5	+0″.025	−0″.003

TABLE I—*Continued*

No.	x	y	μ_a	μ_δ
30	+1′.3	+2′.2	+ 0″.14	+0″.008
31	+1.6	+1.9	+ 12	+ 24
32	+1.6	+1.8	− 10	+ 3
33	+1.8	+1.5	+ 21	+ 23
34	+2.5	+0.3	+ 7	+ 23
35	+2.4	+0.2	+ 18	+ 30
36	+2.7	−1.1	+ 19	+ 18
37	+2.4	−2.5	− 8	+ 22
38	+2.1	−3.8	− 1	+ 34
39	+1.9	−4.0	− 9	+ 21
40	+2.0	−4.2	− 6	+ 18
41	+1.6	−5.2	− 25	+ 26
42	+0.6	−0.9	+ 20	+ 5
43	−0.8	−0.9	− 10	− 21
44	−0.9	−0.9	− 5	− 13
45	−1.2	−0.7	+ 5	− 28
46	−2.1	−0.2	+ 16	− 6
47	−1.8	0.0	+ 3	− 33
48	−2.5	+0.6	+ 3	− 17
49	−2.7	+0.3	+ 10	− 24
50	−1.8	+0.5	+ 6	− 29
51	−2.8	+2.4	+ 8	− 25
52	−3.1	+2.1	+ 9	− 16
53	−0.6	+2.4	+ 23	− 25
54	−0.6	+2.4	+ 38	+ 3
55	−0.3	+2.4	+ 34	− 8
56	−0.2	+2.5	+ 40	− 14
57	0.0	+3.1	− 9	− 5
58	0.0	+3.0	+ 18	− 17
59	−0.8	+1.2	+ 22	− 33
60	+1.5	+0.6	+ 11	+ 10
61	+2.0	−0.5	+ 12	+ 34
62	+1.9	−0.8	+ 31	+ 23
63	+1.8	−0.9	+ 6	+ 15
64	+1.7	−2.4	+ 4	+ 39
65	+0.8	−2.2	− 19	+ 9
66	+0.2	−1.9	− 31	− 2
67	0.0	−2.2	− 34	+ 9
68	−2.0	−1.3	− 24	− 12
69	+0.6	+2.8	+ 30	− 17
70	+1.8	+1.9	+ 8	+ 12
71	+2.1	+2.0	+ 14	+ 15
72	+2.1	+1.9	+ 29	+ 15
73	+2.4	+1.8	+ 17	+ 4
74	+2.4	+0.8	+ 44	+ 21
75	+2.4	−0.6	+ 32	+ 27
76	+2.5	−0.6	+ 10	+ 33
77	+2.2	−1.1	+ 4	+ 13
78	+2.5	−2.4	− 27	+ 9
79	+2.4	−2.7	− 11	+ 25
80	+1′.6	−3′.8	0″.000	+0″.020

in which a, b, ... f' are the plate-constants, x and y the coordinates of the objects measured, and μ_a and μ_δ the annual proper motions, expressed in thousandths of a second of arc.

The plate-constants were derived by a least-squares solution from the twenty pairs of equations of the form (1) for the 20 comparison stars. For these objects the usual supposition was made that μ_α and μ_δ are in the mean zero and are not functions of x and y. The constants a, b, ... f' thus found were substituted in the equations of condition (1) of all the objects measured. The resulting annual proper motions are given in the fourth and fifth columns of Table I. The second and third columns of this table contain the co-ordinates in x and y, expressed in minutes of arc with a precision sufficient for identification.

The motions thus derived for the nebular points include the motion of the nebula as a whole with respect to the 20 comparison stars as well as the internal motions of the individual points. To derive the motion of the nebula as a whole, the same process was followed as for M 101.

a) The mean for all of the 79 points gives:

$$\mu_\alpha = +0''.006 \quad \mu_\delta = +0''.004.$$

b) Dividing the points into four groups, corresponding to the four quadrants, the means of the two groups in opposite quadrants should give a good agreement. We find:

$$\text{Means for I and III} \begin{cases} \mu_\alpha = +0''.004 \\ \mu_\delta = 0''.001 \end{cases}$$

$$\text{Means for II and IV} \begin{cases} \mu_\alpha = +0''.006^5 \\ \mu_\delta = 0''.000 \end{cases}$$

The four quadrants combined give:

$$\mu_\alpha = +0''.005 \quad \mu_\delta = +0''.000^5.$$

c) In order to avoid points far from the center on account of their asymmetrical distribution, we may use only those within a radius of 3′. We then find:

$$\text{Means for I and III} \begin{cases} \mu_\alpha = +0''.004^5 \\ \mu_\delta = +0''.001^5 \end{cases}$$

$$\text{Means for II and IV} \begin{cases} \mu_\alpha = +0''.008^5 \\ \mu_\delta = -0''.001 \end{cases}$$

The four quadrants combined give:

$$\mu_a = +0''.006^5 \quad \mu_\delta = 0''.000.$$

Giving equal weight to each of the three methods used, we derive as the final motion of the nebula as a whole

$$\mu_a = +0''.006 \quad \mu_\delta = +0''.001.$$

If now we subtract these quantities from the values of μ_a and μ_δ for the nebular points, we obtain results which represent the internal motions. These are given in the second and third columns of Table II and are plotted in Plate II. The plate also shows the motions of the 23 stars as given in Table I. The 20 comparison stars are surrounded by a circle, while for the stars *f*, *j*, and *r*, which, for the reasons mentioned on page 238, were excluded for comparison purposes, the motions are represented by broken lines. The scale of the motions is indicated in the lower left-hand corner. The arrows represent the motions in about 1100 years.

The plate indicates motions analogous to those found for M 101 and M 33. They may be interpreted either as a rotation combined with a radial motion outward, or as a motion along the streamers outward. Both possibilities are briefly discussed.

a) *Rotational motion.*—In order to discuss the results from the standpoint of rotation, the internal motions of the 79 points (excluding No. 27) were analyzed into components perpendicular to and along the radius. The values are given in the fourth and fifth columns of Table II, the positive sign being used for rotation in the direction ENWS and for outward radial motion. For the rotational component we find 74 positive and 5 negative values; for the radial component 59 positive and 19 negative values, while one is zero. The mean rotational component is $+0''.019$; the mean radial component, $+0''.008$. As the mean distance from the center is $2'.3$, the rotational motion of $0''.019$ annually would indicate a rotation period of about 45,000 years. The radial component is so large, however, that we can hardly believe the motion to be one of rotation only. Similar results have been found in all three cases discussed so far. For M 101 the radial component is 32 per cent of the rotational component; for M 33, 48 per cent; for M 51,

242



INTERNAL MOTIONS IN MESSIER 51

The arrows indicate the direction and magnitude of the mean annual motions. Their scale (0".1) is indicated on the illustration. The scale of the nebula is 1 mm = 6".2. The comparison stars are inclosed in circles.

TABLE II

ANNUAL INTERNAL MOTIONS

No.	μ_α	μ_δ	Rotational	Radial	Stream	Transverse
1	+0″.022	+0″.009	+0″.007	+0″.022	+0″.011	+0″.019
2	− 27	+ 5	+ 12	− 24	+ 1	− 27
3	− 19	+ 5	+ 18	− 7	+ 16	− 9
4	− 18	+ 13	+ 21	+ 2	+ 21	+ 2
5	− 2	+ 8	+ 3	+ 8	+ 4	+ 7
6	+ 3	+ 2	− 3	+ 2	− 2	+ 3
7	− 31	+ 8	+ 30	+ 12	+ 31	+ 7
8	− 7	− 2	+ 6	+ 4	+ 7	+ 2
9	− 9	− 20	+ 17	+ 14	+ 20	+ 8
10	− 22	− 23	+ 3	+ 31	+ 14	+ 28
11	+ 30	− 19	+ 34	− 4	+ 33	+ 9
12	− 14	− 25	− 1	+ 28	+ 5	+ 28
13	+ 10	− 10	+ 12	+ 8	+ 14	+ 4
14	+ 17	− 8	+ 19	+ 3	+ 19	+ 1
15	+ 17	− 29	+ 27	+ 20	+ 32	+ 10
16	+ 2	− 10	+ 2	+ 10	+ 5	+ 9
17	+ 5	+ 9	+ 10	+ 1	+ 10	− 2
18	+ 16	+ 16	+ 20	+ 11	+ 21	+ 8
19	+ 22	+ 18	+ 20	+ 21	+ 20	+ 21
20	+ 18	+ 15	+ 7	+ 22	+ 21	+ 9
21	+ 37	+ 28	+ 13	+ 44	+ 41	+ 19
22	− 12	+ 16	+ 20	+ 4	+ 20	− 1
23	− 17	+ 27	+ 30	+ 10	+ 31	+ 7
24	− 32	+ 6	+ 30	− 11	+ 26	− 19
25	− 26	+ 22	+ 33	+ 8	+ 34	+ 3
26	− 31	+ 23	+ 38	+ 6	+ 38	0
27	+ 2	− 46				
28	− 13	− 22	+ 14	+ 20	+ 25	+ 3
29	+ 19	− 4	+ 16	+ 10	+ 16	+ 11
30	+ 8	+ 7	+ 10	− 2	+ 11	0
31	+ 6	+ 23	+ 20	− 14	+ 21	− 11
32	− 16	+ 2	− 12	− 11	− 8	− 13
33	+ 15	+ 22	+ 27	− 3	+ 26	+ 5
34	+ 1	+ 22	+ 22	− 2	+ 22	− 4
35	+ 12	+ 29	+ 29	+ 10	+ 31	+ 5
36	+ 13	+ 17	+ 11	+ 18	+ 18	+ 12
37	− 14	+ 21	+ 26	+ 7	+ 25	− 7
38	− 7	+ 33	+ 22	+ 27	+ 33	+ 6
39	− 15	+ 20	+ 20	+ 14	+ 24	− 7
40	− 12	+ 17	+ 18	+ 10	+ 20	− 4
41	− 31	+ 25	+ 38	+ 14	+ 35	− 20
42	+ 14	+ 4	− 10	+ 11	− 9	+ 12
43	− 16	− 22	+ 27	− 5	+ 25	− 10
44	− 11	− 14	+ 17	− 2	+ 17	− 2
45	− 1	− 29	+ 25	− 13	+ 23	− 16
46	+ 10	− 7	+ 6	− 10	+ 3	− 12
47	− 3	− 34	+ 34	+ 5	+ 34	− 3
48	+ 3	− 18	+ 19	+ 1	+ 17	− 8
49	+ 4	− 25	+ 25	− 1	+ 24	− 7
50	0	− 30	+ 29	+ 8	+ 30	− 1
51	+ 2	− 26	+ 21	+ 16	+ 26	0
52	+0″.003	−0″.017	+0″.016	+0″.007	+0″.017	−0″.003

TABLE II—*Continued*

No.	μ_α	μ_δ	Rotational	Radial	Stream	Transverse
53	+0″.017	−0″.026	+0″.024	+0″.020	+0″.026	+0″.018
54	+ 32	+ 2	+ 30	− 10	+ 28	− 13
55	+ 28	− 9	+ 30	+ 5	+ 30	0
56	+ 34	− 15	+ 35	+ 12	+ 37	+ 3
57	− 15	− 6	− 14	+ 7	− 11	+ 12
58	+ 12	− 18	+ 11	+ 19	+ 16	+ 14
59	+ 16	− 34	+ 32	+ 18	+ 34	+ 14
60	+ 5	+ 9	+ 10	+ 1	+ 10	− 1
61	+ 6	+ 33	+ 30	+ 14	+ 32	− 8
62	+ 25	+ 22	+ 9	+ 31	+ 31	+ 9
63	0	+ 14	+ 12	+ 6	+ 14	− 1
64	− 2	+ 38	+ 23	+ 30	+ 32	+ 18
65	− 25	+ 8	+ 26	0	+ 25	+ 2
66	− 37	− 3	+ 36	− 7	+ 37	0
67	− 40	+ 8	+ 40	+ 7	+ 36	+ 18
68	− 30	− 13	+ 29	+ 17	+ 29	+ 16
69	+ 24	− 18	+ 19	+ 24	+ 23	+ 20
70	+ 2	+ 11	+ 9	− 5	+ 10	− 3
71	+ 8	+ 14	+ 16	− 4	+ 16	+ 1
72	+ 23	+ 14	+ 26	+ 7	+ 24	+ 13
73	+ 11	+ 3	+ 10	+ 7	+ 7	+ 10
74	+ 38	+ 20	+ 32	+ 30	+ 25	+ 34
75	+ 26	+ 26	+ 18	+ 32	+ 27	+ 24
76	+ 4	+ 32	+ 30	+ 14	+ 32	+ 6
77	− 2	+ 12	+ 12	+ 3	+ 11	− 6
78	− 33	+ 8	+ 29	− 16	+ 18	− 28
79	− 17	+ 24	+ 29	+ 7	+ 28	− 8
80	−0″.006	+0″.019	+0″.013	+0″.015	+0″.020	+0″.002

42 per cent. It is on the basis of this continuous evidence against a purely rotatory motion that we feel more inclined to believe that the motions are in general along the arms.

b) *Motion along the arms of the spirals.*—Considering the motion as following the arms of the spiral, we find the mean motion to be +0″.021, with an additional perpendicular component outward of +0″.003. In the case of M 101, we found a small additional motion inward. In M 33 there is a slight indication of motion outward. But in all cases the mean deviations from the direction of the arms are very small. Definite conclusions as to the real meaning of these motions must, however, await further measurements. The best evidence may be expected from several hundred points to be measured in M 33, as soon as another plate can be secured.

Among the stars selected originally for comparison purposes, *f* and *r* require comment. Although their photographic magnitudes cannot be brighter than 16, they show annual proper motions of 0".145 and 0".163, respectively.

I wish to express my thanks to Mrs. Marsh of the computing division, who has performed all the duplicate computations necessary for the derivation of the present results.

Mount Wilson Observatory
June 1921

EXCITATION STAGES IN OPEN ARC-LIGHT SPECTRA

PART II. SILVER, BISMUTH, CADMIUM, ZINC, AIR, AND COPPER[1]

By B. E. MOORE

ABSTRACT

Excitation stages in low-current arc spectra of Ag, Bi, Cd, Zn, and Cu.—By a study of the *variation of the spectrum with current* for from 0.02 to 1 ampere, about *90 lines have been classified* in one or other of the five stages described in Part I. All lines appear first at the negative pole, then at the positive, and later still in the middle of the arc. Lines of Stage I come in first, usually resonance lines, the first terms of principal series. As the current is increased, the arc suddenly flares up and the lines of Stage II appear, the lowest ionization lines, including diffuse subordinate series and terms of the principal series. Lines of higher stages are distinguished chiefly by their inception currents, which are often three times greater for one stage than for the preceding stage; whether they are due to successive ionization is unknown. When lines first come in they are often intermittent and in any case have an appreciable and sometimes a considerable intensity. Before the lines of Stage I appear, the glow shows a continuous spectrum and also bands, probably due to molecules, elementary or compound. In fact most bands require only low excitation, some ceasing with Stage I; but others develop like Stage II lines. *Intensity-current curves for 18 lines* are given. They vary considerably in form, including three different types. Intensity growth *of* the positive pole is similar to that at the negative, as a rule, but later. *The relation* at *these results to the Bohr theory and to the Ritz equations* is briefly discussed. When the ring positions corresponding to the types of spectral lines are represented graphically, it appears that lines of a given stage are associated with rings lying within certain limits and that both these limits are larger in radius the later the stage; but the ranges for the various stages overlap. In a *discussion of Fowler's classes of enhanced lines*, it is pointed out that classification by excitation stages permits a more precise definition of enhancement, since the lines of each stage are evidently enhanced with reference to those of all earlier stages. A *comparison with King's temperature classification* in the case of Cu lines shows no correlation, some of his Class III lines falling in each excitation stage from I to IV.

Arc spectrum of cadmium.—A new resonance line at λ 3779 belonging to Stage I was discovered. Hitherto it had probably been supposed to be an iron line.

Arc spectrum of air.—With low excitation two new lines appear at λ 3064 and λ 3068, which may belong to the positive nitrogen bands.

SILVER

Table I gives a complete list and classification of all lines observed under 1 ampere. Lines of Stage I fulfil the requirements that they develop rapidly at the outset and are easily obtained in the middle of the arc. Stage III lines adhere rigidly to the pole position up to 1 ampere, while Stage II lines are then becoming

[1] The experimental method employed in Part II was the same as in Part I, except that a rotating sector was substituted for the crossed nicol system. This facilitated the readings very much.

long and are decidedly present in the middle of the arc. The line λ 5472 has a later origin than the other d_1 lines. This happens for the same type of line with some other substances.

TABLE I

CURRENT LIMITS IN AMPERES

λ	−Pole	+Pole	Stage
$3383p$	0.035*a*	0.05*a*	I
$3281p$	.035*a*	.05*a*	I
$5472d_1$	.09		II
$5466d_1$	.05	.02	II
$5209d_1$	.05	.02	II
$4212d_2$	.062	.18	II
$4056d_2$	.062	.18	II
5090		.7	III
4888		.6	III
4874		.6	III
$4669s_2$	.2	.6	III
4616		.7	III
$4476s_2$	.2	.6	III
4396		0.7	III

a, lower current not tried; *p*, *d*, *s*, principal, diffuse, and sharp series, respectively.

BISMUTH

The arc consisted of bismuth in a shallow brass crater at the lower electrode and platinum at the upper electrode. For the weakest currents the arc shows the above-described air features and one bismuth line at λ 4722. This one bismuth line was traceable at the negative pole to 0.015 ampere and was visible at the positive pole to at least as low as 0.035 ampere. The double slope characteristic of the line is shown in Figure 1. A similar characteristic is observed for line λ 5552, although it is later in its origin. The difference between positive and negative pole is a later origin of the lines at the positive pole. Graphically the positive-pole growth of the lines is like the negative-pole growth except that the curves are displaced toward higher currents.

Kayser's table, *Handbuch der Spectroscopie*, 5, shows a number of bright lines, some of which are marked "enhanced." In this list λλ 5078, 4803, 4798, 4391 (double), and 4308 (double) show intermittently at the positive pole when the current reaches 1 ampere. It does not seem possible, therefore, to place these lines in a class with Stage III, which are quite brilliant but very short

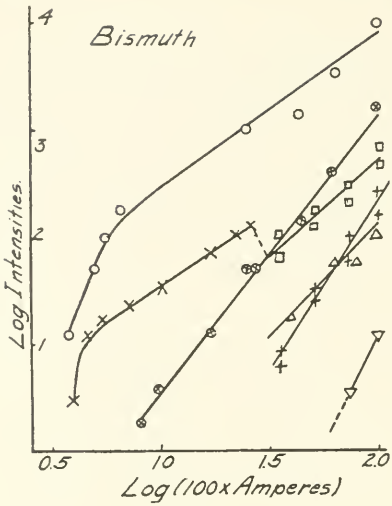


FIG. 1

○ = λ4720, upper −pole
⊕ = λ4720, lower middle
× = λ5552, −pole
□ = λ5552, +pole
+ = λ5552, middle
△ = λ5742, +pole
▽ = λ5742, middle

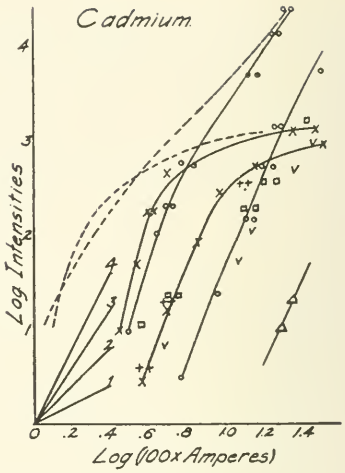


FIG. 2

○ = λ5086, −pole and middle
× = λ5378, −pole and middle
+ = λ6438, −pole
△ = λ6438, middle
□ = λ4800, −pole
▽ = λ5154, −pole

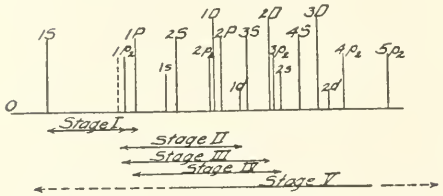


FIG. 3

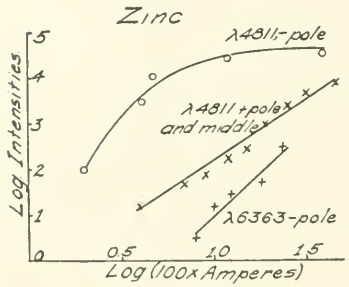


FIG. 4

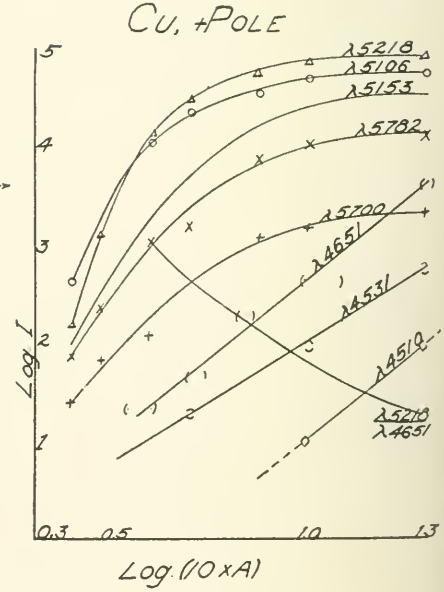


FIG. 5

polar lines at 1 ampere. Lines λλ 4803, 4798, one or both, are present. Kayser does not assign them to the arc and λ 4803 is designated "enhanced." There are two arc lines at λ 4308; one is designated "enhanced." No other enhanced lines or bright arc lines are traceable.

A Stage I line was sought in the ultra-violet at the strong line λ 3067, but the air band interfered precisely. With 0.06 ampere at the negative pole λλ 3596, 3511, and 3397 were present, using the quartz spectrograph, with a five-second exposure, while a three-minute exposure at 0.03 ampere failed to reveal anything but air and λ 4722. These three lines are therefore assignable to Stage II.

Table II shows the lines assembled in stages.

TABLE II

Stage I λ	Stage II λ	Stage III λ	Stage IV λ
4722	5552	5742	4803
	3596	5298	4798
	3511	4122	4308
	3397		

CADMIUM

In the visible spectrum, the ascendancy of λ 5378 both at the pole and in the middle of the arc is readily recognized for very low currents. The development of a few lines is shown in Figure 2. Note the relative position of λλ 5378, 5086, and 6438, Stage I, II, III lines respectively. It might appear that these lines could be extrapolated to a common origin. The difficulty is that the lines suddenly go out at about the positions shown in the graph. The stages are not separated as far as in most substances, but λ 5086 is a decidedly bright line when λ 6438 begins to show intermittently as a faint line. The line λ 5154 has a common origin with λ 6438, although it takes a different slope after its inception.

The real aspirants for Stage I lie in the ultra-violet at λ 3261, Type $1S-1p_2$, and at λ 2289, Type $1S-1P$. The former was easily realized, but along with it came an unknown line, which at first was supposed to be a line given by Morse,[1] found with the Wehnelt

[1] *Astrophysical Journal*, 21, 223, 1905.

interruptor at λ 3776. A spectrogram, with iron as comparison, with the Rowland grating, showed it to be nearly a duplicate of the iron line λ 3779.4. Hence the natural assumption that this line had been discarded from cadmium as an impurity due to iron. But a spectrogram of iron, at the low currents at which the line may be realized, showed that all lines of iron between the limits of λ 3000 and λ 6000 may be banished from the middle of the arc. As the

TABLE III

λλ	Amperes at		Condensed Spark Intensity	Stage	Type
	− Pole	+ Pole			
5154	0.05	0.19	745	III	$1P-3S$
6438	.04	.16		III	$1P-1D$
4662	.065	.30		III	$1P-2D$
3500	.1*p*	.35		III	$1p_2-1D$
3252	.12	*m*		IV	$1p_2-2S$
4413	.14	.5*a*		IV	
4511	.12	.35		IV	
6333	.16	.45		IV	$1P-1d$
25	*k*			IV	$1P-4S$
4307	.3	.85	*d*	V	
6116	.35	1.		V	$1S-4p_2$
12	*k*		450	V	$1S-4p_3$
6099	.35	1.		V	
4614		1.	300	V	
5607				V	$1S-5p_1$
04					$1S-5p_2$
5598			300	V	$1S-5p_3$
5298			33	V	
5637			11	V	
5784			11	V	

a, the substance is passing to the molten state.
d, surrounding field disturbs visibility.
k, not separated from the adjacent line.
m, requires five times the exposure of λ 3500 at 0.1 ampere.
p, lower current not studied.

current increases, this new line disappears. This behavior suggests Type $1S-1p_2$ in calcium, strontium, and magnesium. But the line λ 3261 has good claims to represent this type. The line conforms to the requirements of Stage I and for the present must be included in the cadmium list.

Table III gives some observations pertaining to Stages III and IV. In so far as the types of the lines were known, they are also included.

There seems to be some doubt concerning the arc line λ 5378.6. Kayser gives it as an arc line, and λ 5379.6 as a spark line. Steinhausen (see Kayser's tables) gives the latter as an enhanced line. This might imply that there was only one line. Watts's table gives only a spark line. It seems to the writer that there are two lines. Now in the spark λ 5379 is a brilliant companion of λ 5339, which occurs in the spark only. It was thought worth while to investigate these lines and the relations existing in the spark, although it might be said to transcend the scope of studies of the open arc light. Some of the observations upon spark lines are recorded in Table III. They represent well-known arc lines but they were not visible below 1 ampere. The spark produced by the induction coil was giving a spectrum more like the arc spectrum of Kayser's

TABLE IV

λ	Middle Arc		Spark	
	0.14 Ampere	0.25 Ampere	No Capacity	Capacity and Self-Induction
5378.6.....	500	800	0	0
5379.6.....	0	0	3–5	3100
5339.....	0	0	10	2600
5086.....	145	3000	100	1950

tables than the spark spectrum therein recorded. It reduced the intensity of the leading line λ 5086 to one-fourteenth of its value at the negative pole at 0.25 ampere and at the same time brought out subsequent lines of the same series which could not be observed below 1 ampere with the direct-current arc. The principal point which the writer wishes to emphasize is the disappearance of the line λ 5378 in the spark. This is shown in Table IV, which is a composite of observations of arc and spark upon four lines, or upon three lines if there be someone to insist that the first two are only one line. If there are two lines, λ 5378 is extinguished upon passing to the spark. If there be but one line, it suffers a practical extinction upon passing to the spark with no capacity and then a renewal by adding self-induction. This seems less plausible than the two-line assumption.

Table V shows the lines assembled in stages. Stage VI represents a departure in that spark lines are assigned to it. How late these lines occur in the development is not known.

TABLE V

Stage I λ	Stage II λ	Stage III λ	Stage IV λ	Stage IV λ	Stage V λ	Stage VI λ
5378	5086	5154	3252	6116	5784	5379
3779	4800	6438	6333	112	5637	5339
3261	4678	4662	6325	099	5298	Many
	3611	3500	4511	5607	4614	others
	3466		4413	604		
	3299			598		

ZINC

The resonance line λ 3076, Type $1S-1p_2$, was the first line investigated. No really satisfactory results were obtained, as the air lines are just in the way. What was called λ 3076 was a line which grew more rapidly than the adjacent lines. The line of Stage II at λ 4811 on graph and leading line of the principal series of triplets behaves at the negative pole exactly like a line of Stage I. At the positive pole it has the characteristics of a line of Stage II. The *d* triplet in the ultra-violet also belongs to Stage II. The current steps make Stages II and III necessary.

Figure 4 shows the development of λ 4811, Stage II, Type $1s-mp$, and of λ 6563, Stage III, Type $1D-mS$. There is a rich list of lines in Stage III; generally there is a rich Stage II list.

The lines are assembled in Table VI according to stages.

TABLE VI

Stage I λ	Stage II λ	Stage II λ	Stage III λ	Stage IV λ
3076	4811	3345	6563*a*	
	4722	3303	(3072)*b*	4924
	4680	3282	3036*b*	4912
			3018	

Lines λλ 4924 and 4912 are true spark lines. They are brighter in the spark spectrum with the small inductor than the triplets of Stage II. Stage IV only represents here the next stage as

observed. The lines are doubtless of the same origin as Stage VI in cadmium, Table V. In the spark λ 4811 receives the same setback as λ 5086 in cadmium.

AIR AND ITS COMPOUNDS

The spectra of air are more or less disturbing with all substances, as has already been noted in Part I. The purpose is now to specify the air spectra more definitely. These spectra show best with copper electrodes, and they are most easily followed in the glow arc.[1] As shown in Part I, there is first a low continuous spectrum in the middle of the arc and at the poles. There are two well-defined lines at λλ 3064, 3068, which have not been traced to any definite metal, and which, on account of their persistence, are assigned to air. They should be looked for in gas free from oxygen and nitrogen. These lines are overlapped by a fluting system and do not seem to be connected with the doublet, but may be connected with a fluting system which has a distinct head at λ 3805. If this is true the whole fluting system is probably connected with the second positive nitrogen spectrum. Certainly the latter is easily identified in the visible spectrum and is present at both electrodes just outside and never inside the polar illumination. It therefore has a low excitation. The oxides of the metals have very rich and strong spectra. For the metals these spectra rigidly pertain to radiation coming from the surfaces of the electrode. (Magnesium and aluminum are exceptions.) When the poles become definitely established upon passing from the glow to the true arc,[1] these oxide spectra disappear from the part of the electrode adjacent to the polar illumination, but they still persist outside of this limit. Hence it is apparent that the new ionization products at the instant of the pole "flare" are formed at the expense of the oxides. These ionization products which are first produced in the "flare" certainly represent the first well-defined ionization lines. They occur at low current and the potential required for the excitation is not high.[2] The flutings, therefore, correspond to a lower excitation.

[1] Simon and Malcomb, *Physikalische Zeitschrift*, 8, 471, 1908.

[2] Ionization potential of cadmium 8.92 volts. Tate and Foote, *Bulletin of the Bureau of Standards*, 14, 485.

COPPER

Since the principal series doublet lines λλ 3274, 3247 may be photographed outside the visible limits of the arc and at very low currents, and since the ratio of intensity at pole to middle differs but little from unity, these lines may be taken as typical lines of Stage I. Three other lines have been placed in this stage: λλ 5106, 5782, and 5700. It did not appear that they could be placed in Stage II, but the analysis may be at fault. Consider the five upper lines in Figure 5. This figure represents a study of the positive pole with an arc operated upon a 750-volt circuit. For a one-centimeter arc the current will go out between 0.25 ampere and 0.3 ampere. When attempting to operate upon a higher potential the arc shifts from the glow to the true arc form and makes quantitative readings practically impossible. From this curve one can readily see that λ 5106 may exist after λ 5218 has disappeared. But one could not approximate the course of λ 5782 and λ 5700 from the figure. Hence it was necessary to get some evidence from the glow discharge and from the flare when the glow goes over into the true arc form. In the glow, line λ 5106 is still very distinct in the absence of the "*d*" doublet λλ 5218, 5153. Some of the time λ 5106 was seen to the exclusion of λ 5782 and much of the time to the exclusion of λ 5700. But the latter lines are inherently weaker than λ 5106. Generally they were traceable, too, when the "*d*" doublet was absent. But more importance was attached to the behavior when the "flare" occurred. It has been repeatedly suggested that this flare indicates the appearance of an essentially ionization stage. Now in this flare there is an outburst of the doublet, λλ 5218, 5153 and its companion doublet λλ 4063, 4023. There can be no mistakes in assigning these two doublets to Stage II. Then if there is an error in the other three green lines it probably lies in the assignment of the pair of λλ 5782, 5700 to Stage I, instead of Stage II. The type of this pair of lines is unknown. Line λ 5782 has the Zeeman pattern[1] corresponding to the shorter wave in the "*d*" doublet and λ 5700 the same pattern as the longer wave of the doublet. Such a pair of lines in Stage I is certainly unprecedented.

[1] Runge and Paschen, *Astrophysical Journal*, 16, 131, 1902.

Line λ 4631 is a representative of the sharp series (see Fig. 5). At an intensity of about ten or a little greater, λ 4651 and λ 4531 have the habit of becoming very intermittent. They seem to insist upon shining distinctly or not at all. When these lines are in that intermittent state the "*d*" doublets are brilliant and extending far toward the middle of the arc. Hence it appeared that these two lines could not be traced to the same limits as λ 5218. They are accordingly placed in Stage III. The position of λ 4510 (see Fig. 5) is typical of the eleven lines in Stage IV.

The photographic density of λ 4651 was taken by King as a standard of reference.[1] It is strictly a short line for small currents.

TABLE VII

Stage I		Stage II		Stage III		Stage IV	
λ	King	λ	King	λ	King	λ	King
3247	II	5218	II	4531	III	5732	
3274	II	5153	II	4481	III	5646	III
5106	II	4063	II	4651	III	5408	
5783	III	4023	III			5392	
5700	III					5360	
						5355	
						5293	
						5017	
						4705	III
						4587	II
						4510	II

Hence for short lengths of arc King's exposure may be regarded as exposures on the pole. Furthermore, it appears that the intensity of the line grows very uniformly with the current. But when the density of this line is chosen as a unit of reference, the line λ 5218 should at first increase and then later decrease over threefold before 2 amperes is reached. This is shown in Figure 5 by the curve of the ratio λ 5218 divided by λ 4651. In general, King's method of study is adequate when there is a progressive change in the rate of development of the lines. It ought to succeed very well with such cases as are given in Table IV under cadmium, particularly in the ultra-violet.

[1] *Astrophysical Journal*, 20, 21, 1904.

The lines are assembled in stages in Table VII. There were a number of other lines observed between 1 and 2 amperes but observations were very indefinite. King's Groups II and III behave differently under self-induction. They are shown in Table VII and are distributed indiscriminately through the successive stages of excitation.

DISCUSSION

The discussion will be taken up under the following topics: "Preliminary Statement," "Thermionic Processes," "Resonance and Ionization," "Spectral Types," "Lowest Excitations," "Excitations of Molecules and Compounds," "The Second Stage in Excitation," "Subsequent Stages in Excitation," "Line Limits," "The Spark Discharge and Excitation Limits," "The Rate at Which Lines Develop," "Enhancement in the Arc and Spark Discharge," "Solar Enhancement."

Preliminary statement.—The basis of this discussion is a few well-established facts in gaseous conduction and in the emission of electricity from hot bodies. There is need to mention two simple equations:

$$(1)\ \tfrac{1}{2}mv^2 = eV \quad \text{and} \quad (2)\ eV = h\nu.$$

Equation 1 asserts the equivalence of the kinetic energy of an impact and the electrical energization, i.e., excitation, arising therefrom. Equation 2 states that the potential V, in an electrical energization, is directly proportional to the frequency of a luminous vibration, when the energy of electrical excitation disappears as radiation. Equation 1 represents an excitation and equation 2 represents a recovery after excitation has ceased. If one recognizes these two conditions as parts of a reversible process it should lead to no confusion if the radiation is spoken of as an excitation.

Thermionic processes.—The emission of electricity from hot bodies has had an extensive investigation in the last score of years.[1] It is natural to designate these processes as thermionic. This

[1] *The Emission of Electricity from Hot Bodies*, by O. W. Richardson, F.R.S., published by Longmans, Green & Co., gives a most lucid treatment of the subject and contains a very complete reference list to the literature.

implies a mechanical process, for the kinetic nature of heat is always taken for granted. Some subtleties have arisen concerning the nature of excitation during the process of chemical action. In so far as the present paper is concerned it need only be stated that chemical changes are accompanied by thermal changes; and any thermal loss by radiation may be accompanied by either line, band, or continuous spectrum radiation. Simon[1] and his students have developed the thermionic conception of the arc very carefully and have been able to explain a great many features in both the direct- and in the alternate-current arc. The arc must produce enough energy at the electrodes both to free the surface electrons and material from the adjacent matter and to impart a motion to the electrons and ions. After this condition is attained the electrons and ions are subjected to an accelerating force or fall of potential across the arc. Since the fall is practically constant there is a uniform equality between the accelerating force and the retarding force of the medium. Just off the electrode surface the electrons are subjected to the accelerating force of the *medium fall* and at the same time are in motion due to a velocity arising from repulsion from the electrodes. This action and the radiation from the adjacent electrode surface produce greater heat in the immediate neighborhood of the electrode than in the middle of the arc. This in turn permits greater freedom of motion, greater acceleration, and greater velocity of electrons and ions. This results in greater excitation and a richer spectrum in the pole illumination just off the electrode surface than is found in the middle of the arc.

Resonance and ionization.—Numerous recent experiments upon the emission of electrons from hot bodies have shown that there are two stages in the electrical excitations at low potentials.[2] The potential for the latter is considerably larger than for the former stage. When the spectral emission is examined it is found that the lower excitations correspond to the fundamental line of some

[1] *Physikalische Zeitschrift*, **8**, 471, 1907. Also his references and subsequent contributions in the same journal.

[2] A grasp of the resonance and ionization concepts may be obtained from the following contributions: Tate, *Physical Review*, **7**, 686, 1916; *ibid.*, **10**, 81, 1917; Tate and Foote, *Bureau of Standards*, **14**, 479, 1918. For magnitudes of resonance and ionization potentials, see Foote and Mohler, *Philosophical Magazine*, **37**, 46, 1919.

definite series of lines, while the latter corresponds to the last line or limit of the series. Hypothetically the theory has been advanced that the ionization releases the whole series of lines and all related series. Evidently from equation 2 all these lines cannot be represented by eV. In fact, none of the lines could be represented by this product except the final line of the series, which has never been observed.

Spectral types.—The Bohr[1] treatment of spectral series is very easy to visualize, although it does not afford as accurate a formula for the determination of the spectral lines as the theory of Ritz.[2] According to the Bohr theory the sequence arises because there exists a sequence of ring positions about a central ionic nucleus in which an electron may vibrate and be in a state of unstable equilibrium. The return of an electron from an outer to an inner ring produces radiation. The electron may then be free to return to another more stable ring position nearer the nucleus and emit another radiation. Each radiation represents a potential fall according to formula 2. When the electron has returned to its stable condition the sum of all the potential "falls" is equal to the ionization potential. If the return to the stable condition may take place in an entirely promiscuous fashion, it is possible to realize a very rich spectrum from an ionization. Bohr pointed out, in his first contribution upon this subject,[3] that the outer extension of the ring system would be interfered with by the material in the gaseous medium. He computed the number of rings, or the equivalent number of spectral lines which could be realized in the Balmer series for hydrogen at different pressures. To realize more lines one needed to have a more attenuated gas and greater volume excitation for increased intensity. In any finite medium an electron cannot expend all the energy of its excitation upon a single return. It must impart a portion of its energy to the surrounding medium, and the returns to the stable ring positions will be mostly

[1] *Philosophical Magazine*, **26**, 1, 1913.

[2] *Annalen der Physik*, **12**, 264, 1903. In the Ritz theory the lines may be expressed by $f(m, A, a), f(n, B, b)$ (see types throughout the experiments), where m and n represent a sequence of numbers and each value of m and n determine a term. The function signs, f, a, and b are usually suppressed for brevity in notation.

[3] *Ibid.*, **12**, 9, 1903.

made up of returns from rings nearest the stable position. Hence the first lines of the series are invariably the strongest. It ought to be possible, therefore, to realize more lines of a series from the emission of hot bodies in a vacuum than from an arc operating at atmospheric pressure. To this point we shall later return.

Low and high excitations.—High excitations belong with high velocity electrons, like those required to produce the X-rays. The term may be used relatively. It is known that an excitation lower than resonance may be secured. The fall from one ring position to another represents a loss of potential energy and has an excitation equivalent. One may designate these conditions and the accompanying spectral lines *ad libitum*, as produced by lower and higher velocities, lower and higher currents, lower and higher potentials, or lower and higher excitations, according to which of these features one wishes to emphasize.

Lowest excitations.—From the progressive appearance of the first spectral lines in the polar illumination, then in the middle of the arc, and then upon the outer mantle of the arc to the exclusion of other lines; then from the great displacement of these lines when the magnet acts upon the arc; and lastly from the analogy of these lines to proven resonance lines, it is concluded that these lines appear at the very lowest potential which will excite spectral lines. If there has been no error in the observations, *all lines in Stage I represent the lowest line excitation.*

Excitations of molecules and compounds.—It is now proper to state that when the current is reduced to the last limit of line excitation there is still present a weak continuous spectrum, narrow bands are often decidedly conspicuous, and fluting spectra at the poles are often observed. If one considers the total radiation, these features are more important than the initial lines. Clearly the energy expended in the lines is only a small portion of the total radiation; and, indeed, the line radiation would be an entirely insignificant portion if all the energy which goes into heat were considered. From the discussion of the preceding topic it appears that these radiations must all be classed as low excitations.

The second stage in excitation.—As the current increases new lines appear in the polar illumination. Sometimes this increase

in current occurs in a discontinuous manner; the sudden outburst or "flare" in the illumination arises. In this "flare" there is a new list of lines. Such an outburst in the current points either to a first or to another ionization of the electrode material. When these experiments were nearing completion the writer checked up Stage II lines with the appearance of lines which came out in the "flare." In every case of "flare," Stage II lines and the "flare" lines were identical. Consequently with some degree of confidence one may designate Stage II lines as the beginning of ionization in the arc. Before a "flare" takes place there is often observed a series of flutings coming from the face of the electrodes. This is particularly noticeable with copper. Just as soon as the "flare" occurs, the flutings cease at the electrode base adjoining the "flare." When a carefully cleaned copper surface is used as an electrode, the discharge is very migratory until some oxidation ensues. The flutings come from this product. When the "flare" ensues, flutings no longer come from the adjacent electrode base; but if the arc is stopped it will be found that this very electrode base is the portion most thickly covered with the oxide. It was clear that the oxide was forming previous to the "flare," and one may safely say that the flutings resulted from this combination. Thermionically considered, such a chemical process takes place with loss of heat which has partly disappeared as radiation, and which according to equation 2 is accompanied by a readjustment of the electrons. It is also apparent that these flutings belong with the low excitations which precede the "flare." In the "flare" stage the electrons emitted from the electrode base arise to a potential value greater than that represented in the fluting combination, and there is now a profuse outpouring of electrons from this identical oxide. It would appear that this process would either stop the formation of the oxide at the base of the "flare" or reverse the process and decompose it. The latter effect certainly does not take place. The amount of oxide has at least remained as large as it was before the "flare" and it seemed that it had quite possibly increased. In the latter case is it possible for the oxygen ions from the air to combine with the copper without producing the flutings? It becomes not only a subtlety of chemical action but also of ionization energy which is

not answered here. The compounds of the chloride salts in Part I in a few cases were found not to withstand an excitation as great as that required for Stage II lines. They broke up in the polar illumination and recombined in the middle of the arc where the excitation was lower. Hence the spectrum of these products also belongs to the lowest excitation. On the other hand, accepting the molecular identification of certain band lines by other spectroscopists as correct, it appeared that some radiations which belonged to the molecules of the elements did not diminish in the polar illumination but that they progressed in their development very similarly to other lines and, more particularly, similarly to the development of Stage II lines. This makes it clear that the elements in molecular combination represent a stronger energy bond than the chloride compounds.

Subsequent stages in the excitation of lines.—As just shown, lines of Stage II originate in an ionization. The question arises whether the subsequent stages have their origin in farther ionizations. That would be the easiest but not the only possible explanation. There is no "flare" accompanying them as in the case of lines of Stage II. The electrical examination of high-potential arcs has not been carried to the low currents of the third-stage lines, and in some cases not as far as the fourth-stage lines. It was this fact which led to the investigation by Mr. V. L. Chrisler in the following contribution.[1] There is another reason which may be assigned for the appearance of these subsequent stages in the arc. Under the topic "Thermionic Processes" the change in the degree of freedom in motion with temperature has been noted. Under "Spectral Types" the restriction of the outer rings has been mentioned. As the current in the arc increases there is an increase in temperature, and, by reason of the expansion, a greater degree of freedom between the molecules, and greater possibility of acceleration between the molecules, and a greater impact energy in the moving electrons. Increasing the current, then, would bring about ultimately another ionization if such an ionization is possible. But before reaching such a stage, the excess in potential over that required to produce the earlier ionization goes into other forms of energy, and principally or entirely heat energy. Now this heated

[1] Page 273 of this number.

or expanded medium will make it possible to realize a greater number of the external electronic rings (see the discussion upon "Spectral Types") about the ionic nucleus. Since it is these ring positions which determine the lines, the lines may be used to define them, and the current which causes the inception of the lines may be used to determine the stage at which these lines begin. Now the spectral types and the corresponding ring positions about the nucleus may be represented graphically by using the sequence values of the terms as computed from the Ritz equation. This method is followed for some of the lines in cadmium in Figure 3. The position of the nucleus is shown at "*O*" in this figure. The cologarithms of the values of the terms are then plotted from this point as origin. The positions of the lines then represent tangents to the rings whose centers are at "*O*." (The meaning of the letters is given with the types in the text.) The arrows represent the stages and ring limits for the lines in the stage. Stage V represents lines obtained in the spark. It is therefore not a continuity with the previous arc stages. If the restraint of the medium determines the outer ring limit it might seem that there should be a stage to mark each successive outer ring limit. It is doubtful if the measurements are capable of adequate refinement to test this possibility. But as one looks at the figure and notes the slight outward extension of the rings between Stage III and Stage IV, the existence of intermediate stages seems rather improbable. In fact the inquiry would be rather, "How is it possible to distinguish such slight difference in ring limits as that represented between Stage III and Stage IV?" The answer is in the current value required to cause an inception of the stage. In passing from Stage II to Stage III and thence to Stage IV the inception current is nearly trebled in each case. The stage limits seemed to be determined by a group of related rings rather than by each successive ring. The infra-red and ultra-violet possibilities in the ring system did not come under observation, and this interferes somewhat with the realization of some possible stages, if they are defined in terms of ring limits.

Line limits.—The outermost ring which can be realized for a given current is designated the "excitation limit" for that current.

According to the Bohr ring theory (see discussion of "Spectral Types") the return of an electron from an outer to the innermost ring position may take place in any number of accidental steps. Such a condition would make all steps equally probable, and therefore all possible lines equally probable. This is not strictly the case. Some types of lines, whose rings are intermediate, practically fail. It seems as if there is a possibility that the return of an electron to an intermediate position is not entirely a matter of chance but that there are conditions which predetermine the stopping place of the electron before it starts upon its journey from one ring to another. This question has been kept constantly in mind during the experiments. The effort was made to see if there was any evidence of definite selection in the formation of lines in the different stages. Nothing very conclusive was observed; but there was a *little* evidence bearing upon the question, as will be seen from the following analysis.

As the current increases, the new stage lines begin in the core of the polar illumination. The earlier lines are pushed outward and toward the middle of the arc. Now one may examine the old lines in a position which collimates with the new ones or in the outer mantle just outside of the position of the new lines. It is then seen that the old lines are increasing at a relatively slow rate in the central position but at a comparatively rapid rate outside. This is particularly true with reference to the growth of Stage I lines. The new slope for these lines when the new lines appear is shown in the figures. Now those figures represent the central growth, and it is apparent that when new stages begin part of the earlier radiations go to the radiation in the new stages. Now if the intensity determinations were accurate enough to justify the process, one could reduce the intensity in the collimating position by the intensity in the outer mantle and leave an intensity equal to that which arises from the excitation of these lines in the core of the illumination. This rather hazardous process would in some cases leave an unimportant development for some of the earlier stage lines in the core where the later stages are appearing. Reversals show that one is not warranted in completely removing the earlier stage lines from the core excitation. Now the inner core is

a position of high temperature and highest ionic velocities. If we assume that Maxwell's law of distribution holds, the average velocity will be increasing with the current, and the lower velocities will be progressively less important. There will be an "effective" velocity in the direction in which the current flows. The slow-moving ions will have the same amount of "effective" energy as the rapid-moving electrons. Now a moving electron might come into the range of an ion that had a velocity which represents a kinetic energy equivalent to a fall from some inner ring position to the stable position. In this condition the electron might not be able to return to a ring position inside of the one which represents the kinetic energy of the ion with which it combines. Furthermore, if an electron may make an incomplete return, it may be driven off again (re-ionized) from the recovered position. If this may be true, then also the ion may be subjected to a force sufficient to prevent a complete return. Goldstein was able to suppress the series lines of the alkalies and to bring out other groups of lines alone by passing a high potential discharge through a constricted space. There was here a relatively large density of electrons and low density of atoms. The conditions are somewhat similar within the small space of the core illumination, where also the number of ions which could have a low velocity might be very insignificant. Hence it might be that there is a "restraint" in the ionic system which determines the degree of the recovery of an electron. If one designates the outer limit of line production in the series of lines as the "excitation limit," it might be possible to designate the inner ring to which the electron returns as the "restraining limit." An "excitation limit" and a "restraining limit" would fix definitely the limits of radiation before the radiation ensues. The evidence for the former limit in the pressure exerted by the medium is fairly definite. The attempts to follow the latter have been rather illusive. The Sommerfeld[1] quantum theory of spectral radiation is expressed in terms of two limiting conditions, which are called the azimuthal and radial quantum conditions respectively. Lines

[1] W. Kossel and A. Sommerfeld, *Berichte der Deutschen Physikalischen Gesellschaft*, 21, 240, 1919.

are produced by a diminution of the radial term by any number of quantum units and by a change in the azimuthal value by -1, 0, or 1 units. As the writer interprets this paper, the physical conditions which determine the azimuthal term is the state of ionization. If one were to apply this to Stages II, III, IV of these experiments it would seem that the arrow files for those stages in Figure 3 ought in all cases to extend to the term p_2, wherein it would appear that ionization takes place from particles which are first thrown into a stage of resonance, and that they return to the limits of the resonance stage before recovery from ionization. An ionization from the p ring is accompanied by a loss of two electrons for bivalent atoms, as is shown by two methods of analysis. The series beginning with the ring position $1S$ are supposed to be due to the loss of one electron. The difficulty here is that $1S-1p_2$ and $1S-1P$ represent resonance, and the subsequent members of the same series represented by $1S-mp_2$ and $1S-mP$ are ionization lines. Two ionization potentials have not been observed for these substances. One can escape the dilemma by supposing that there is only one ionization, the one which carries off two electons for bivalent atoms, and that the recovery takes place by single electrons. The first recovery would take place from exterior rings to the azimuthal position p_2, and the second to the position $1S$. It will require much further analysis to see whether the above-suggested "restraining limits" can be best expressed in terms of the degree of ionization present at the time the radiation ensues.[1]

The spark discharge and excitation limits.—The presumption is usually made that the spark discharge first ruptures the gaseous medium, producing thereby the air spectrum; and second, that this discharge is followed by a discharge of ions and electrons from the electrodes along the rarified, highly heated path.[2] Herein the displacements occur at a higher velocity than in the arc and also in a rarified medium. Further, the spark discharge is both alternating and intermittent. Hence, if there were forces built up within

[1] J. Stark and students have zealously maintained that successive ionizations are present in spectra. For literature see *Annalen der Physik*, 64, 376, 1921.

[2] A. Schuster and G. Hemsalech, *Philosophical Transactions* (A), 139, 189, 1899.

the atom by the electric action to produce the foregoing internal restraining limits they would not be sustained in the spark except for the very briefest interval of time.

The rarified medium would permit of wider limits for the outer rings, and as a result there would be a larger possibility of lines. When, in the restricted conditions of the arc, a great amount of energy is going into one type of radiation, upon passing into the spark, the energy in the expanded, higher excited medium may pass to the other types or farther outlying rings in the same type of lines. This action is shown conclusively by the intensities in the composite table, Table VIII. The first two lines in each substance are the first and fifth lines of a definite series type, and the remaining two lines are found only in the spark discharge.

TABLE VIII

λ	Cadmium		λ	Zinc	
	0.25 Ampere Arc	Spark		0.25 Ampere Arc	Spark
5086*b*	27000*a*	1950	4810*b*	25000	2800
5604*c*	0	300	5310*c*	15	450
5339*d*	0	2600	4912*d*	0	3300

a, extrapolated from 0.22 amperes; *b*, Type $1p_1-1s$; *c*, $1s-5p_2$; *d*, leading spark lines.

The leading series line λ 5086 in the spark of cadmium is only one-fourteenth as bright as the same line at 0.25 ampere in the negative polar illumination of the arc. The fifth member, line *c*, Table VIII, of the same series was not observed in cadmium, and was only just beginning in zinc, where it had but one-sixteen-hundredth of the intensity of its leading member. In the spark each of these two lines has an intensity nearly equal to one-sixth of their respective leading lines. It would require an extended investigation to show how much of this change has been brought about by each of the factors, expansion of the medium and velocity of impact.

The rate at which lines develop in intensity.—Lines have a minimum value at which they first become visible. This current is called their inception value. After their inception, lines progressively increase in intensity in very different ways. In Figure 2 the

straight lines 1, 2, 3, 4 represent developments proportional to the first, second, third, and fourth power respectively of the current. The curves, for a few lines, might be characterized as having two rates of development, with a progressive change through a short range from one rate to another. These lines are generally limited to Stage I. The leading line of the zinc triplets seems to be an important exception. There are a number of lines which show nearly a uniform growth in intensity after their inception. Many lines develop most rapidly just after their inception. In the graphs the total current is plotted against intensity. It might appear that the effective current is the amount added to the current after the inception of the lines. If this were true, the abscissae in the graphs should have been represented by $\log (i-i_0)$ instead of by $\log i$, where i is the observed current and i_0 the inception current. Two broken lines in Figure 2 were plotted, using $\log (i-i_0)$ as abscissae. The curves to which they are tangent are the original curves. If all curves were plotted upon this plan there would be greater variation shown than when plotted against total current as abscissae. Some of the lines would even begin slowly and then for greater currents increase more rapidly. In the visible spectrum, the effect upon the eye is that of a sudden beginning of the lines, the variation consisting of an intermittent radiation. For this reason the graphs with logarithms of total current are given greater credence.

Enhancement in the arc and spark discharge.—The term "enhancement" covers the relative increase of a line or lines with respect to another line or lines when the conditions under which the lines are produced change.

Fowler[1] distinguishes three classes of enhancement, viz., (1) enhanced lines like the H and K lines of calcium, which are well developed in the ordinary arc; (2) lines which only appear with small intensities in the arc, such as the enhanced lines of iron; (3) lines which do not appear in the ordinary arc (except very locally at the poles) but are strongly developed under spark conditions—as in the well-known magnesium line at λ 4481.

[1] Fowler, *Phil. Trans. 214*, 259, 1914.

Fowler designates the p, s, and d lines of the bivalent elements herein discussed as enhanced. He includes also the narrow doublets of the same type, which certainly did not come out below Stage V. He lists also the f type and combination lines of the narrow doublets, all of which arise at excitation beyond the limits of present experiments. Fowler states that these lines are enhanced with respect to a few types of lines which he selects from the arc list of lines, and designates these as arc lines. These are the D and S singlets and the d and s triplets. It is not clear how many lines of these four series are used for comparison. From the observations here discussed, it appears that $1S-1p_2$, the first member of the s series, comes in Stage I while the next member is decidedly of the ionization type; it appears in Stage II or later and is therefore enhanced with respect to the earlier stage. In Stage I there are never more than a few lines and often only one, or a doublet pair of lines. They are always the *first* members of some definite type of series and never the *whole* series. The latter members of the series to which the Stage I lines belong show enhancement just as distinctly as members of other series. Particular attention was directed to this feature in barium, where the Stage I line λ 5536 was separated from the leading member of the p series with difficulty. The type of this line is $1S-1P$. The next member of the series is found at λ 3072. There are troublesome air bands in this region when the small quartz spectrograph is used. But if this line belonged to the class of lines which are not enhanced according to Fowler, one ought to have realized it with the Rowland grating for weak currents. In fact it was not as easily realized either at the pole or in the middle of the arc as the p_1 doublet pair. Evidently it is not "vibrating system," i.e., type, which determines enhancement. If one compares the later stages with Stage I, and if one accepts the reasonable conclusion that Stage I corresponds closely to a resonance condition, the conclusion would be that enhancement arises from an ionization. Mr. Megh Nad Saha[1] makes the statement, "Modern theories of atomic structure and radiation leave little doubt that the 'enhanced lines' are due to the ionized atom of the element." He then proceeds to compare H and K, two ionization lines, with g, the resonance line

[1] *Philosophical Magazine*, Oct. 1920.

of calcium. This freedom would sweep almost the complete spectrum of substances into the enhanced class. Different ionizations, i.e., the removal of a different number of electrons from the atom, have been evoked to explain enhancement. That the removal of more than one electron is necessary to explain the *p* and *d* series for bivalent elements was shown first by Lorenser.[1] He found the universal constant, *N*, in the Ritz equation, four times too small. This change is brought about in the Bohr equation by changing from the univalent condition, e^2, to the bivalent condition $(2e)^2$, where *e* is the charge of an electron. Now the determination of ionization potentials does not decide how many electrons are emitted; but more than one ionization potential would clearly point to different ionizations unless the potential values are multiples. This has not been realized.[2] To say that one electron and then the other is removed at one and the same ionization potential is purely a gratuitous assumption. The possiblity of successive ionizations in the arc as a cause of lines appearing in stages, was pointed out to Mr. V. L. Chrisler by the writer, and Mr. Chrisler proceeded to study the very low-current arcs particularly in reference to this point. In the following paper Mr. Chrisler shows that stages in ionization have *not* been realized within the limits of these experiments. Hence enhancement as a result of ionization is an incomplete explanation.[3]

Fowler does not define his Class (2) lines definitely enough for comparison. As the current increases, a rich list of Stage II lines appear.[4] One cannot prophecy how far the comparison of the weaker later lines with the second-stage lines can be carried. But the point which should be emphasized here is that such a comparison would be of one ionization line with another, and of lines enhanced, as some of the foregoing writers have indicated, due to ionization. Upon the basis of inception stages,

[1] Reference by Kossel and Sommerfeld, *Berichte der Deutchsen Physikalischen Gesellschaft*, **21**, 252, 1919. These authors show the bivalency of the *p* series from the term difference $2p_2 - 2p_1$.

[2] Tate and Foote, *loc. cit.*, and many subsequent experiments.

[3] See the closing remarks upon "line limits," p. 265.

[4] October 1921. Many iron lines of Fowler's Class (2) appear in Stage II.

all later stages are, of course, enhanced with reference to earlier stages. But stages may or may not be due to successive ionizations. So far as the writer can see Fowler's Classes (1) and (2) are representatives of one kind of enhancement. Fowler's Class (3) represents lines either nearly or completely absent in the arc. These lines are generally attributed to high velocity, high potential excitations, which ionize an inner ring of electrons. In this class are Fowler's magnesium lines λ 4481, *p* narrow doublet, and possibly the whole *p* narrow doublet series as well. The writer has seen only the member λ 4481 in the spark. It had the same dominance in the spark spectrum of magnesium that the cadmium lines λ 5579 and λ 5539, and the zinc lines λλ 4924, 4912 have in the spark spectrum of these elements. (See Table VIII, and pp. 264–266 and reasons there given for considering both expansion and higher excitation to be active causes of the enhancement.)

Solar enhancement.—One may consider an excitation to arise (1) from low-velocity impacts of the magnitude which is usually seen in the arc; (2) from the high velocity impacts which appear in the spark and vacuum discharges and which correspond to removal of internal electrons; (3) from a thermionic ionization. There can be no doubt about (1), and very little doubt about the analysis of (3). That there are high velocity electrons in solar disturbances is made evident by Hale's experiments upon the Zeeman effect in solar vortices. One would confidently expect high velocities and intense ionizations wherever they may occur, to bring out such lines as cadmium λλ 5579, 5539, zinc λλ 4924, 4912, and magnesium λ 4481. The conspicuous enhancements in the sun are not these high ionization lines, but the prominent lines of the Stage II group which appear at the earliest ionization.

Let us take the most conspicuous solar enhancement, known as the calcium pair λλ 3968, 3933, *p* series leading lines, which are enhanced with respect to the line λ 4227, *S* series leading line, as one advances to higher levels in the solar atmosphere. Now λ 4227 is the resonance line of calcium, and the change in the arc with increasing current conforms to the conception of an ionization arising at the expense of the neutral atomic excitation. As one passes to the solar conditions, one must recognize that the thermal

rather than the electrical action causes the thermionic process. Recently Mr. Megh Nad Saha[1] has made some very excellent and opportune computations upon the degree of dissociation of calcium, strontium, and barium for different pressures and temperatures, and has applied the results to hypothetical temperatures and pressures for different levels in the chromosphere. The treatment substantially follows the method of Eggert,[2] who discusses thermionic dissociation in fixed stars. The postulate is made of a reaction of the form

$$R \leftrightharpoons R_+ + e - U$$

where e is the electron and U the energy change. A resonance radiation is concerned with a radical R, or with its atoms, while ionizations are concerned with nuclear types R_+, R_{++}. Ionization potentials do not determine the valency of these nuclear types, but there is spectroscopic evidence to show that valency does enter into the radiation, and furthermore it is generally conceded that the radiation accompanies return from a nuclear type to an antecedent type. Now let us note again the Eggert-Saha theory. By dissociation we arrive at a condition which obliterates R and leaves R_+ in the attenuated solar atmosphere. In this process the inner ring, $1S$, is wiped out and along with it all lines which converge to this limit. The dissociation was computed from the potential which gives complete ionization, and this is a condition which would obliterate all lines. To get the radiation of the p series it is necessary to allow the electrons to return to the $1s$ ring, which becomes a new "restraining limit" for the electrons; a position, which, according to Sommerfeld, will represent a new azimuthal velocity but with a zero radial velocity. The process could be better understood if someone could make it clear how it is possible to have the fixed ionization potential and still to leave the electron in a ring position which is removed only one step from the normal ring, and in this position be ready to receive ionization impacts from moving electrons. There are some other things which will need examination. If the ring $1S$ is wiped out, so also are all lines of the series. The

[1] *Philosophical Magazine*, July, Oct., and Nov. 1920; Feb. 1921.

[2] *Physikalische Zeitschrift*, 20, 570, 1919.

first line appears in Stage I but the subsequent lines appear with ionization. If complete dissociation can remove entirely this ring, then the subsequent lines ought to be realized along with the first line, but in the arc the subsequent lines are realized in Stage II. In the solar chromosphere most of these lines would be unfavorably located because of the ultra-violet absorption of our atmosphere. But the second line of the series for barium might be investigated. It lies at λ 3072. In sodium the leading term of the *p* series is the resonating type. According to the dissociation theory the whole series should vanish in the solar chromosphere. If subsequent lines of the series are ionization lines one might expect to find λ 3303 in the chromosphere[1] just as it is realized in Stage II.

Brace Laboratory
University of Nebraska
May 1921

[1] Observations by S. A. Mitchell in 1905 begin just to the red of this position. Mr. Mitchell informs the writer that the plates used in the flash spectrum of the 1905 eclipse were weak in the ultra-violet region λ 3303. See *Astrophysical Journal*, **38**, 407, 1913.

THE LOW-CURRENT ARC

PART I. THE ARC IN AIR AT ATMOSPHERIC PRESSURE

By V. L. CHRISLER

ABSTRACT

Low-current arc in air.—Potential-current curves up to 0.5 ampere were obtained *for electrodes of various materials* (C, Ag, Cd, Cu, Fe, Sn, Zn, and salts of Ba, Ca, Cs, Na, and Sr); also the *cathode and anode falls and the gradients in the center* were measured with the help of probing platinum wires. As the current is increased the glow form of the arc changes suddenly to the true-arc form and at the same time the cathode fall drops sharply, in the cases of Ag, Cu, and Fe changing from 214 to 28 volts, from 290 to 16 volts, and from 205 to 24 volts respectively. Ag, Cu, Fe, and Pt all gave the glow discharge up to 0.1 ampere. The true-arc form probably begins with the volatilization of the electrode material and the ionization of the vapor. The gradient in the center of the arc is proportional to the length of the arc, decreases with increasing current, and varies in step with the ionization potential of the metal vapor from the electrode.

Extensive investigations have been made of the arc, and the theory of its action has been much discussed. Mrs. Ayrton[1] has shown that the relation between the current i flowing through the arc and the potential-difference v across the arc can be expressed by the equation

$$v = \alpha + \frac{\beta}{i} + \left(\gamma + \frac{\delta}{i}\right)^2,$$

where α, β, γ, δ, are constants.

Child[2] has made a study of the arc at different gas pressures, determining the anode and cathode fall and the potential gradient through the arc. He also pointed out that a hot anode is not necessary for an arc discharge, but it is essential that the cathode be hot if the arc is maintained.

J. Stark[3] found that at constant pressure, the potential fall, across the arc, for a given current, decreases when the density of the gaseous medium increases. This he showed was due to the conservation of heat by the heavier gases, an accompanying

[1] *The Electric Arc.*

[2] *Physical Review*, **19**, 117, 1904.

[3] *Annalen der Physik*, **18**, 213, 1905.

rise in temperature, and a greater free path for the electron movement. He also found that the anode fall depended upon the material and the density of the medium adjacent to the electrode. He found, further, that cooling the electrode raised the potential.

The thermionic conception of electrode and gaseous action has been a subject of extensive and elaborate investigation.[1] H. Simon[2] has applied this conception to the action of the arc. He states that, due to the electrodes being hot, they are emitting electrons. At the cathode this is in the direction of the current and therefore lowers the cathode fall, but at the anode it is against the current and increases the anode fall. He also considers that the ionization in the arc increases with increasing current, but not in proportion to the current, as the volume of the arc also increases and thus limits the ionization. His students have made extended studies confirming his theory.

Simon's students[3] carried the study of the arc to low currents for some electrode materials. For 0.5 ampere and less, they found that there was a negative crater formed, but no positive crater. They also found when the discharge passed from the glow to the arc form, that the character of the discharge at the anode remained the same until a greater current strength was reached. Simon states for these small currents that the evaporation from the negative crater does not suffice to fill the whole arc with electrode gas, and that the discharge from the arc light is partly carried by the surrounding gas. For larger currents with metallic electrodes he concludes that the discharge is very largely carried by the metallic vapor or gases, and that this metallic vapor has a vanishingly small resistance.

The spectroscopic experiments by B. E. Moore[4] reveal very important changes at low currents where the observations of the previous experimenters were far from complete. It was therefore

[1] Richardson, *The Emission of Electricity from Hot Bodies.*

[2] *Physikalische Zeitschrift*, 8, 471, 1907, and subsequent contributions in the same journal.

[3] Malcolm, *Physikalische Zeitschrift*, 8, 471, 1907; Grotrain, *Annalen der Physik*, 47, 141, 1915.

[4] *Astrophysical Journal*, 54, 191 and 246, 1921.

desirable to redetermine some of these low values. Since there was not a continuity of the spectroscopic changes, it appeared possible that some discontinuities in the electric action had been overlooked. Furthermore, the observations of Simon's students did not cover all of the substances which Moore had studied, or many others which Moore has not investigated. A priori, one has no right to say that an untried substance will act like other substances. Besides, even when the form of the equation, for different substances, is the same, the constants of the equation have individual values.

Spectroscopically there is a difference between the portion of the arc near the pole and that at the center, a difference between the central core and the surrounding mantle. These all need to be viewed in the light of the electrical behavior of the arc. Lastly, electrical action may be of special significance in the "pole effect" or the shift of spectral lines at the poles.

In these experiments it is necessary to call attention to the following features of the electrode fall. The potential at the electrodes possesses two components, viz., (1) a part of the energy is used to heat the electrodes, (2) another part is used to impart velocity to the ions. The electrodes will lose heat both by conduction and by evaporation in case vapors are given off. As the electrodes heat, less energy will be required for heating purposes and more will be available to impart velocity to the electrons and ions. Ultimately one reaches a point by increasing the current where the discharge surface is heated sufficiently to produce self-ionization. The energy required in this process might be called a "latent heat" of ionization.[1] In this condition only enough drop at the electrodes is necessary to sustain the action. For increased current the ionization surface thereafter broadens.

METHOD OF MEASUREMENT

As a source of potential three 1000-volt generators were used which could be operated in series or in parallel, depending upon the potential and current desired. The total potential across the arc was measured with a Weston voltmeter, and the current

[1] The gas laws apply to ionization processes, Richardson, *op. cit.*

through the arc with a Weston ammeter. The cathode and anode falls were measured with a Thompson electrometer. The cathode and anode falls were taken as the difference in potential between the electrode and a fine platinum wire inserted in the arc as close to the electrode as possible. The platinum wire was coated almost to the tip with cement.

RESULTS AND DISCUSSION

It was found very difficult to obtain accurate measurements for the anode and cathode falls, as the small point of light from which most of the discharge passed was continuously changing its position, and the values obtained for the anode and cathode falls were very much greater when the platinum wire was outside this point of light. It was often necessary to wait a considerable time for this point of light to become stationary long enough, where the probe wire was placed, to obtain a reading of the electrometer. These values were taken as the anode and cathode falls. In a few cases it was impossible to obtain any reading, as the point of light was shifting so rapidly that the electrometer needle did not come near enough to rest to give any approximate indication of the potential to be determined.

Electrodes of copper, silver, zinc, cadmium, iron, and tin, as well as carbon with salts of sodium, calcium, strontium, barium, and caesium have been used. The usual type of curve showing variation of potential fall across the arc, with the current flowing, was obtained, Figure 1 being that for copper. These results are similar to those of Simon, Malcomb, and others (*op. cit.*). With copper in particular, the discharge apparently takes place under two conditions, one of which has been designated by Simon and others as the glow current, and the other as the arc. From the curves it will be noticed that the glow form requires nearly 300 volts more potential than is required in the arc form for the same current. The discharge is very unstable through this region, as it tends to change constantly from one form to the other. The glow current was obtained with other metals, but not to such a marked degree as when copper electrodes were used.

An attempt was made to apply the Ayrton equation to the potential-current curves for low currents, but without much

success. For an arc of 1 cm length this equation reduces to the form

$$e=\frac{a}{i}+b$$

where a and b are constants. It was found that this equation fitted the curves very well in all cases where the current was over 0.5 ampere and for some electrode materials for currents as low as 0.25 ampere. For smaller currents, the curve deviates decidedly from that of the hyperbola which the Ayrton equation gives. An attempt was made to represent the data by an empirical equation,

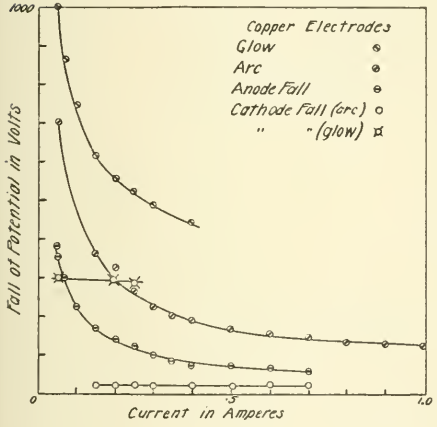


FIG. 1

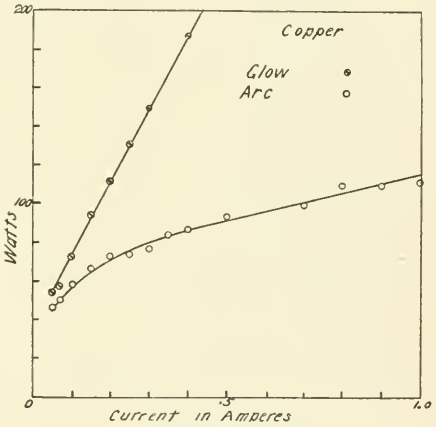


FIG. 2

but no equation containing a few constants seemed to express the conditions adequately.

The total energy was also plotted. Figure 2 shows the results for copper, and from these curves it is evident that the energy consumed in the glow current is much greater than that consumed in the arc for the same current. For larger currents the curve approaches a straight line, as required by the Ayrton equation. For smaller currents, however, the curves deviate decidedly from straight lines for all of the metals tested when the discharge was in the arc form. For the results obtained with the other metals which were tested see Figure 3. The results obtained with salts on carbon are shown in Figure 4.

After obtaining these curves, the anode and cathode falls were determined by the method previously mentioned. For the smaller currents there was only a point of light at the electrodes, and the anode or cathode fall was measured when the wire was inside this point of light or "polar illumination." For larger currents

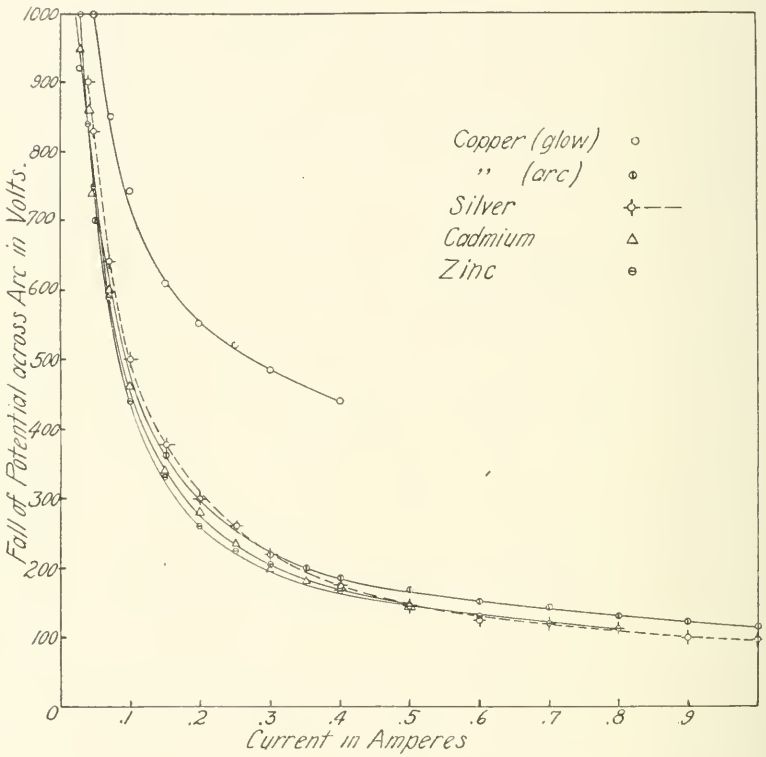


FIG. 3

this polar illumination increases in size and gradually extends across the arc.

In the glow current the point of light at the cathode disappears and in its place is found a diffuse glow. Just beyond the latter is a Crooke's dark space. In this case the cathode fall was found to be much higher. Table II gives the cathode fall for copper, iron, and silver.

The anode fall is the same for either form of discharge. From the curves of Figure 1 it will be seen that the change in the cathode fall for copper electrodes accounts approximately for the increased voltage required for the glow current.

For the arc discharge the cathode fall is almost independent of the current strength. With some electrode materials it increases slightly for smaller currents.[1] The anode fall is not constant and always increases for smaller currents and at about the same rate as the total potential. Figures 5 and 6 show curves of the anode and cathode falls for the various materials tested as electrodes.

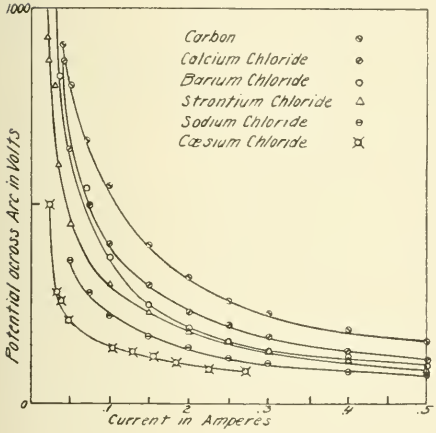


FIG. 4

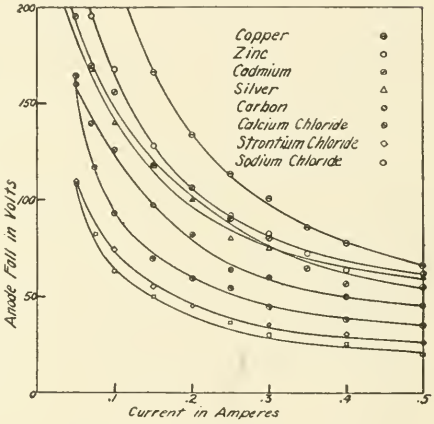


FIG. 5

The general form of the curves are the same as Grotrain found for the materials which he tested.

A few measurements were also made of the potential fall along the center of the arc. This potential fall was found to be directly proportional to the length of the arc, which agrees with the results obtained by Grotrain and Child. This potential fall through the center of the arc decreases at first very rapidly with increasing current. Stark states that an increase in the density of the gas in the arc decreases the fall of potential due to the conservation of heat by the heavier gases, and an accompanying rise in temperature, hence a greater free path for the electron movement. If

[1] Grotrain, *op. cit.*

this statement is accepted, the amount of metallic vapor in the arc, for very small currents, must increase quite rapidly as the current increases to account for the decreased fall in potential. Another factor which probably affects this potential fall is the ease with which this metallic vapor is ionized. If the potential-current curves across the center of the arc are plotted for these different metals and salts, it is found that the curves do not coincide, but fall one below the other (see Fig. 7). For elements of which the ionization potentials have been determined, the writer finds that

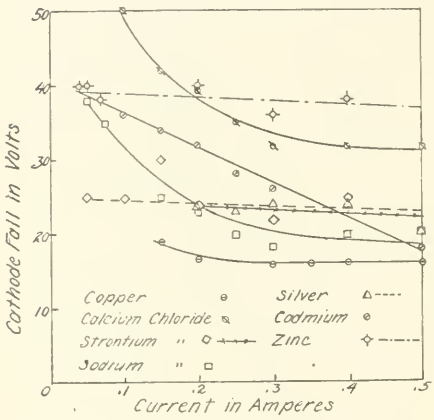


Fig. 6

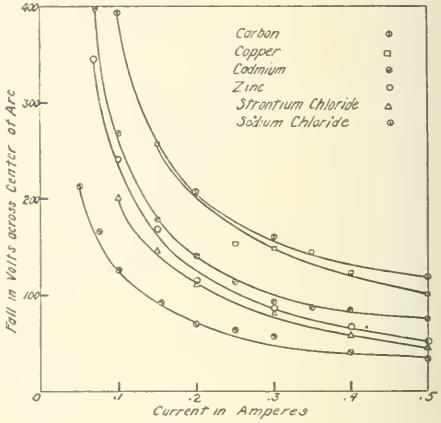


Fig. 7

in general the relative position of the curves is the same as the ionization potentials, in so far as these ionization values are known.

Energy-current curves were also plotted for the center of the arc. The results are shown in Figure 8. Simon, Malcolm, and others state that the glow-current discharge is carried by air, and that its characteristics are the same for all electrode materials. The total potential fall across the center of the arc when it is in the glow form is the same for silver and copper electrodes, but the anode and cathode falls are both smaller when silver electrodes are used. The cathode fall for silver is 75 volts smaller than for copper electrodes. This shows that the energy consumed in the center of the glow arc is greater for silver than for copper electrodes. From this it is quite evident that the air is not an exclusive carrier for the glow discharge when copper and silver electrodes are used. At

the present time this behavior has been investigated carefully for only two substances, copper and silver, but it is hoped to carry the investigation to other electrode materials.

As would be expected, the energy-current curves for the glow arc have a different slope from that for the true-arc form, but according to Simon there should be but one slope for the glow, whereas, as above noted, there has been one observed for copper and another for silver. Whether there are one or more slopes here, it can be seen that the curve for each substance in the true-arc form must intersect the glow curve. Above the point of intersection the true arc is stable, and below the intersection the glow is the more stable form. Provisionally, the term "latent heat" has been used. Just as water may be carried below the freezing-point, so the true arc, upon diminishing the current, may be carried into the region of the glow discharge. The point of intersection of these curves conforms very closely to the beginning of lines of Stage II as found by Moore. The slope in the true-arc form, then, is due to the ease with which the vapor passes from the electrode into the arc and also to the ease with which it is ionized. The vapors conserve the heat, and make possible a greater free path. At a given current, also, the distances of the curves above the x axis have a degree of parallelism to the ionization potentials (see Table I). Zinc appears out of order in this arrangement, but the zinc oxidizes badly when the arc is burning in air, with the result that the arc is full of vapor of zinc oxide which would undoubtedly lower the potential fall in the arc.

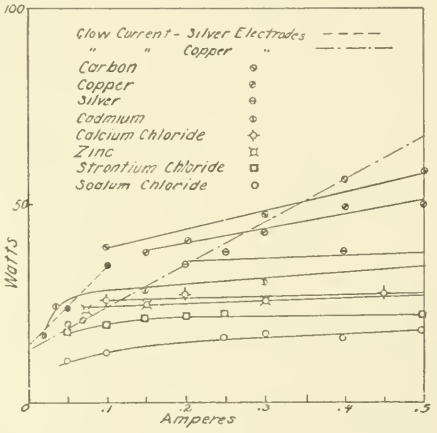


FIG. 8

One of the most interesting questions that has arisen in the study of the arc is, What are the conditions that cause the glow

discharge instead of the arc? Simon states that the glow discharge depends upon the oxides of the metal present and upon the melting-point. From the present investigation it is quite evident that the glow current is independent of the melting-point, as a glow current was easily obtained with tin and lead which have low melting-points but high boiling-points. A glow current was not easily obtained with zinc and cadmium. Zinc and cadmium

TABLE I

Electrodes	Watts	Ionization Potential
Carbon	44	
Copper	41	
Silver	35	
Cadmium	30	9.0
Calcium	26	6.01
Zinc	25	9.3
Strontium	22	5.67
Sodium	16	5.13

have low boiling-points as well as low melting-points. Copper, iron, silver, and platinum were also tested as electrodes and all gave the glow-current discharge up to one-tenth of an ampere. One of the most important features observed was the discontinuity in the cathode fall when the discharge changes from the glow to the true-arc form or vice versa. This has been observed for all cases of change in the form of discharge. Table II shows the discontinuity in the cathode fall for three substances, copper, iron, and silver. For copper electrodes the cathode fall in the glow is eighteen times as large as in the arc discharge.

TABLE II

Electrodes	Cathode Fall in Volts	
	Arc Form	Glow Form
Copper	16	290
Iron	24	205
Silver	28	214

The energy consumed at the cathode was much greater in case of the glow current, due to the increased cathode fall (see Table II),

but the discharge was spread over considerable area, so it is probable that the surface temperature was lower than it was at the point on the negative pole to which the discharge passed when it took the arc form. From the metals tested it would seem that the glow current appeared when the cathode was not heated sufficiently to cause the metals to be volatilized readily, or possibly sprayed out into the arc. Richardson speaks of the electrons being evaporated from a hot surface and of their having a latent heat of evaporation. From these observations it would appear that the temperature at which the electrons evaporate readily into the arc must be closely connected with the boiling-point of the metal. After the discharge passes to the arc form it is generally considered that the temperature at the point of discharge remains about constant; that is, an increase in current simply increases the area of discharge and the greater evaporation keeps the temperature constant. This effect of evaporation was especially noticed with silver electrodes. The surfaces were polished before using, and after using a very short time even with small currents the cathode had small pits 0.5 mm deep; small globules of silver also appeared on the surface. After the surface became pitted in this manner it was very difficult to get a glow current, as the discharge would seize on one of the small points and remain in the arc form. As soon as the surface of the electrodes became oxidized it was also more difficult to get a glow discharge. This latter action agrees with the results found by Simon.

When the discharge passed from the glow to the arc form there was a sudden increase of the current, indicating that there must have been a large increase in the number of electrons which were leaving the negative pole. This points clearly to an ionization of the electrode material. If there were a previous ionization and evaporation of the electrodes, then this is the second stage in the process. Spectroscopically, Moore finds this discontinuity accompanied by an outburst of lines of Stage II (see previous contribution). The works of Tate, of Tate and Foote, and of Foote and Mohler[1] indicate that the earlier spectrum lines are due to the resonance, and not to the ionization. It would seem justifiable, therefore, to

[1] Bureau of Standards, *Scientific Papers*, Nos. 400 and 403; Tate and Foote, *Philosophical Magazine*, **36**, 64, 1918.

regard this discontinuity in the pole fall as the true beginning of ionization of the electrode material.

A few potential measurements were also made in the outer mantle of the arc. It was found when the discharge was in the arc form, for very small currents, that for points outside the polar illumination near the cathode the potential drop between them and the cathode was almost as large as the cathode drop for the glow-current discharge. As the current was increased, this drop decreased, but was still large compared to the potential drop between the cathode and the point inside the polar illumination. At this outer surface Moore found the fluting spectrum to continue in the arc form of discharge, and in the outer mantle adjacent to the pole discharge he found the nitrogen excitations. This would indicate that in the outer mantle of the arc there was practically none of the electrode material which was ionized. It must also be a region of small ionic velocity compared to the center or core of the arc.

Successive ionizations have been postulated to explain spectral lines of different types, and very high ionizations to explain X-ray emissions. The first inference one would naturally make in reference to the sequence of lines found by Moore is that there existed a sequence of ionizations.[1] It has been found that only one ionization makes itself conspicuous in the arc at very low currents. In fact, the current is so low in some cases that it was impossible to realize its beginning point. This is particularly true for the alkalies. Successive ionizations might be of less importance than the first. They would, therefore, manifest themselves in a less pronounced way; but it seemed, if such ionizations were present, that they should become manifest in a change in the slope of the energy curve. No inflection has been found, however, although careful attention was given to this possibility. It is therefore not safe to conclude that ionizations subsequent to the initial flare are present within the range of these experiments.

Brace Laboratory of Physics
University of Nebraska
May 1921

[1] Stark and students, *op. cit.*

THE SPECTRUM OF RADIUM EMANATION

By R. E. NYSWANDER, S. C. LIND, and R. B. MOORE

ABSTRACT

Spectrum of RaEm, λλ 3982 to 7450.—Two capillary discharge tubes were filled with 0.2 and 1 curie of carefully purified emanation, respectively, and both visual and photographic *measurements* were made with a 4-prism spectrometer. The relative intensities of the lines differed markedly, as a rule, from the previous observations of Watson and Royds and Rutherford; many strong lines of the 120 previously measured were not found and yet of the 44 lines obtained, 9 are *new lines*. *Changes of intensity with duration of the discharge* were noticed, some lines decreasing, some increasing in strength, while the color of the discharge changed from a bright glow to violet. λ 5483 and some other *lines flashed out on reversing the current* after a thirty-minute run and then quickly disappeared.

Occlusion of RaEm in discharge tube.—After a discharge had passed through the glass capillary tube containing 0.2 curie for 5 hours, 35 per cent of the emanation had been occluded, most of it in the platinum mirror surrounding the cathode. The other tube became quite hard after a four-hour run.

Modification of Duane's apparatus for purifying RaEm.—The copper wire used to remove oxygen and hydrogen is spirally wound on a silica tube and is heated indirectly by an electrically heated Pt wire passing through the tube, instead of directly by a current through the Cu wire. This arrangement requires less current and less attention.

The spectrum of radium emanation has been determined by Ramsay and Collie;[1] Cameron and Ramsay;[2] Rutherford and Royds;[3] Royds,[4] and Watson.[5] The observations of Ramsay and Collie were entirely visual and showed a bright spectrum which rapidly disappeared and was replaced by the secondary spectrum of hydrogen. The first photographs of the emanation spectrum were those of Cameron and Ramsay, whose results showed a strong resemblance to xenon;[6] hydrogen also made its appearance in the spectrum. Rutherford and Royds photographed the emanation lines with a single (glass) prism spectrograph, using the emanation from 130 mg of radium. Hydrogen lines were also observed, but to separate these from the emanation lines a side tube attached to the spectrum tube was immersed in liquid air, and at the point of condensation of the emanation its lines disappeared, leaving

[1] *Proceedings of the Royal Society*, A, **73**, 470, 1904.

[2] *Ibid.*, **81**, 210, 1908.

[3] *Philosophical Magazine* (6), **16**, 313, 1908.

[4] *Ibid.*, **17**, 202, 1909.

[5] *Proceedings of the Royal Society*, A, **83**, 50, 1910.

[6] *Ibid.*, A, **82**, 22, 1909.

those due to hydrogen. Royds repeated the work, using a concave grating of a dispersive power, of 16.8 A per millimeter, and was able to photograph about thirty-five of the more intense lines already obtained by Rutherford and Royds with good agreement and extended the observations farther into the ultra-violet. Watson's investigation was undertaken with a view of accounting for the discrepancies between former observations and his own results; he employed both a prism spectrograph and a grating. His results are in very good agreement with those of Rutherford and Royds.

For the photographic work of the present experiments a Browning spectrometer with a train of four prisms and photographic attachment was employed, at the University of Denver. The results extended from λ 3982 to λ 7449, being limited in the violet end of the spectrum by the opacity of the glass system. The spectrum of helium was used as a comparison standard. To avoid relative displacement of the two spectra on the plate, a lens was fixed in front of the collimator slit, and the images of the two sources were focused alternately on the slit. By means of a small shutter, adjoining portions of the slit could be illuminated separately. The wave-lengths of the emanation lines were computed by the aid of Hartmann's dispersion formula. The dispersion of the instrument is 13 A per millimeter at λ 4000, and 136 A at λ 7000. The total length of the spectrum between these limits is about 6.8 cm. All measurements of wave-lengths were made with a Gaertner comparator of 200 mm range fitted with a screw of 1 mm pitch. Individual measurements of a line as read on the comparator seldom differed by as much as 0.005 mm, which will give an estimate of the accuracy of the results. The wave-lengths recorded in the table were determined from six photographs, and where a line appeared on more than one plate the mean value is recorded. The more intense lines were found on each of the six photographs. Two types of dry plates were employed, the Standard Orthonon and the Wratten Panchromatic. In addition to the spectrograph, a Hilger constant-deviation spectrometer was arranged so that visual observations could be made simultaneously with the photographic.

The method of purification of the emanation was developed by Lind and is a modification of Duane's apparatus. In addition to the process of purification as described in the note,[1] the emanation was frozen down in liquid air for removal of the residual gases by pumping. After purification the gas was collected in small glass vacuum tubes of capillary bore with platinum electrodes sealed in very small bulbs at the ends. Before the liquid air was removed from the vacuum tube in which the emanation was condensed, the tube was sealed off and the photographic exposure was then started as soon as the tube could be adjusted in front of the slit of the spectrograph. The photographs were obtained almost entirely from two spectrum tubes. The first of these contained 208 millicuries of emanation. Two exposures of two and three hours duration respectively were secured from this tube. It was then broken into small pieces along its length and each piece measured for occluded emanation. The total occlusion in the tube was 35.1 per cent, this being the largest amount of occluded gas measured in any case. This occluded emanation was found to be confined largely to the platinum mirror surrounding the negative electrode. The color of the tube changed from the characteristic bright glow at the beginning of the exposure to a violet color after about one hour's excitation. The second vacuum tube contained approximately 1000 millicuries of radium emanation. Four photographs were secured from this tube with almost continuous excitation for nearly four hours, when the tube became quite hard. After the conclusion of our photographic work with this tube, unfortunately it cracked, leaving us without exact measurements of both occlusion and total quantity of emanation. Small, fused, silica, electrodeless, vacuum tubes of capillary size were also tried. They were excited inductively by means of copper coverings deposited electrolytically on platinum coatings on the ends of the tubes. No effect on the photographic plate could be detected after more than one hour's exposure with these tubes.

It was not possible to photograph the entire spectrum on the plate at one exposure. Accordingly the plates were adjusted to receive the violet and red ends of the spectrum alternately. The greater portion of the spectrum appeared on each plate, leaving

[1] See note at the end of this article.

TABLE I

Photographic Plate	Wave-length	Int.	Watson	Int.	Royds	Int.	Rutherford and Royds	Int.
4	7449.5	1						
4	7269.6	1						
2, 4, 6	7054.0	3	7057	3				
			6749	0				
			6627	0				
			6605	0				
2, 4	6562.2†	1						
			6361	1				
			6309	5				
			6270	0				
			6224	2				
			6204	0				
			6079.3	0			6079*	0
			5977.4	3			5976*	1
			5944.9	2			5945*	1
4	5894.4	4						
4	5888.6	6						
			5838.8	0			5829*	1
			5765.2	1			5765*	1
			5716.1	6			5715.0	1
			5683.0	0				
			5608.4	0				
			5582.60	8			5582.2	8
			5546.6	0				
	5483*							
			5394.4	3				
							5392.4	0
			5386.3	2				
			5371.5	2			5372*	0
			5363.0	2				
			5255.0	1			5257*	1
			5238.0	0				
			5194.9	0				
			5119.5	3			5120*	2
			5084.66	10	5084.45	1	5084.5	4
	5058*							
							5060*	2
			5045.0	4				
			5038.3	1				
			4991.7	0				
			4978.87	10	4979.02	3	4979.0	4
							4965.6	0
			4958.0	2				
			4950.2	4			4949.4	00
			4915.7	4			4914.6	00
			4891.3	4			4889.5	0
2, 4, 5	4860.9†	1			4861.55	10	4861.3	
			4856.4	4				
	4826*		4829.4	4	4828.46	1	4827.8	1
			4817.78	7	4817.33	5	4817.2	4
			4797.3	2	4796.73	1	4796.7	1
			4793.2	2				

*Visual observations.

† H 6563.0, 4861.5.

TABLE I—*Continued*

Photographic Plate	Wave-length	Int.	Watson	Int.	Royds	Int.	Rutherford and Royds	Int.
			4785.8	0				
			4768.77	7	4768.16	5	4767.9	3
			4752.4	1				
	4735*		4732.2	1				
1, 2, 3, 4, 5, 6..	4721.2	3	4721.8	5	4721.70	2	4721.5	5
			4702.33	5	4701.88	3	4701.7	2
4, 5.....	4680.9	1	4681.01	9	4680.92	10	4681.1	10
					4671.58	1	4671.8	1
			4658.8	0			4659.3	1
4, 5.....	4644.0	2	4644.36	9	4644.29	15	4644.7	10
					4634.13†	3		
2.....	4631.4	1			4631.89	2		
					4628.08	1		
2, 4, 5.....	4625.3	2	4625.66	10	4625.58	15	4625.9	8
2.....	4617.8	1						
1, 2, 3, 4, 5, 6..	4609.2	9	4609.70	7	4609.40	10	4609.9	7
5.....	4603.7	1	4604.58	9	4604.46	6	4604.7	4
			4586.2	1				
					4580.03†	3		
1, 2, 3, 4, 5, 6..	4577.6	8	4578.0	8	4577.77	8	4578.7	7
2.....	4572.5	1			4572.66	0		
2.....	4567.4	1			4568.24	2		
			4547.0	4			4549.9	1
			4527.87	2				
			4513.4	1				
1.....	4510.2	2						
1, 2, 3, 4, 5, 6..	4508.5	8	4508.00	6	4508.68	7	4509.0	9
			4503.52	3	4503.89	2	4504.0	2
6.....	4497.8	1						
1.....	4492.7	1						
1, 6.....	4489.8	1						
1.....	4487.8	1						
1.....	4485.2	1						
1.....	4482.4	1						
1.....	4473.6	1						
1.....	4470.8	1						
1.....	4467.1	1						
1.....	4463.3	1						
1, 2, 3, 4, 5, 6..	4459.4	7	4459.3	7			4460.0	10
			4439.6	3	4439.88	1	4440.6	2
1, 2, 3, 4, 5, 6..	4435.1	6	4434.4	5	4435.25	3	4435.7	8
			4402.9	1				
			4392.6	1				
			4383.47	4			4384.0	3
			4371.69	5	4371.70	1	4372.1	4
1, 2, 3, 4, 5, 6..	4349.4	10	4349.91	10	4349.81	15	4350.3	15
5.....	4336.1	2	4335.0	1				
					4340.69†	4	4340.9	7
1, 2, 3, 4, 5, 6..	4307.9	9	4307.57	10			4308.3	10
			4296.7	1				
			4280.5	1				
			4236.4	0				

* Visual observations.

† H 4634.20, 4580.2, 4340.60.

TABLE I—*Continued*

Photographic Plate	Wave-length	Int.	Watson	Int.	Royds	Int.	Rutherford and Royds	Int.
5	4226.7	1	4224.2	4			4225.8	2
			4207.4	0				
1, 5	4203.5	2	4203.27	10	4203.39	10	4203.7	10
			4193.1	2				
			4187.97	4			4188.2	5
			4170.08	3				
1, 5	4166.9	3	4166.48	10	4166.59	20	4166.6	20
5	4165.5	1						
			4160.57	1				
			4114.62	6	4114.71	6	4114.9	7
							4102.2*	6
			4094.4	2				
			4088.1	2			4088.4	2
			4073.9	1				
			4055.4	2			4055.7	1
			4051.1	2			4051.1	2
							4045.4	4
			4039.5	2			4040.2	1
			4033.9	0				
			4017.92	7	4017.90	6	4018.0	10
5	3982.3	2	3981.75	9	3981.83	15	3982.0	12
			3971.82	7	3971.71	8	3971.9	9
			3965.0	2				
			3957.32	3	3957.30	8	3957.5	7
			3951.6	2			3952.7	3
			3931.97	2			3933.3	3
			3930.9	0				
			3927.1	0			3927.7	1
			3904.9	0			3905.7	2
			3867.68	2			3867.6	4
							3818.0	2
							3811.2	0
							3753.6	10
							3748.6	1
							3739.9	7
							3690.4	2
							3679.2	1
					3664.96	5	3664.6	10
							3650.0	0
							3626.6	2
							3615.4	1
					3612.76	3	3612.2	6
					3122.02	0		
					3100.31	1		
					3089.15	0		
					3005.84	1		

* H 4101.9.

only the extreme ends to be photographed alternately. In the first column of the table are given the plates on which each line appears, numbered from 1 to 6. Plates 1 and 2 were obtained from the first spectrum tube, and 3, 4, 5, and 6 from the second tube.

In the table of wave-lengths there have also been recorded, for comparison, along with our results the values determined by Watson and by Rutherford and Royds, since the results of these observers are most trustworthy. Wherever there is coincidence in the lines, the results of the present observations are in excellent agreement with those of the other observers; however, they have recorded many lines which do not appear on our plates. For example, the region between λ 6361 to λ 4732 contains a large number of lines, especially as recorded by Watson, yet our plates show only a few lines in this region and none that could be considered to coincide. It is noteworthy that lines of such great intensity as λ 5582 and λ 5084 should produce no trace on our photographs, nor were these lines observed visually by us.

Among the lines which we observed visually there were several which did not appear on the photographic plates; two of these were broad, faint lines at λ 5058 and λ 4826 respectively, and also a line of low intensity at λ 4735. During the visual observations it was noticed that upon reversal of the current through the induction coil certain lines would appear suddenly and then fade away rapidly. This effect could be produced only after operating the coil as much as 30 minutes in one direction and then reversing the current. The most prominent of these was λ 5483, which appeared very brightly at the moment of reversing the current, but after a few minutes became invisible. It could not be reproduced by later reversals of the current. Other lines appeared brightly at the instant of reversal, but vanished before their wave-lengths could be measured.

Watson has called attention to the differences observed in the intensities of emanation lines; he has also denoted the relative degree of persistence of certain lines in the spectrum. The results of the present experiments have shown that the lines of greatest intensity are the most persistent, and that the intensities of these strong lines change very little on successive plates obtained from the same tube. The group of faint lines between λ 4463 and λ 4492 with one exception were recorded only on the first plate of one tube. On the other hand, there are a number of lines which seem to develop as the time of excitation of the tube advances. For

example, the line λ 4721.2 has an intensity of 1 on the first plate, 4 on the second plate, and 5 on the third plate. The line λ 4625.3 does not appear in the first exposure of either tube, but appears on the second and third plates with increasing intensity. The line λ 4644.0 also belongs to this class. The lines λ 4577, λ 4460, and λ 4307, which Watson has observed to be fugitive lines, for us are quite persistent.

The emanation for these experiments was derived from a supply of radium belonging to the United States Bureau of Mines' Experimental Station at Golden, Colorado.

UNIVERSITY OF DENVER
September 1921

NOTE ON THE MODIFICATION OF DUANE'S APPARATUS FOR PURIFICATION OF RADIUM EMANATION

In 1915, Professor Duane[1] published a method for the purification of radium as collected from aqueous solution, without the use of liquid air. Collection was effected by mercury displacement by means of a system of glass bulbs which acted as an internal pump. In order to remove oxygen and hydrogen from the gaseous mixture, the gases were passed over an electrically heated, partially oxidized copper wire. The glowing wire causes the hydrogen and oxygen to unite, and the excess of hydrogen is reduced by the copper oxide. The water-vapor formed is removed by a side tube containing P_2O_5. The disadvantage in using an oxidized copper wire as the heating body is twofold. On account of the low resistance of copper, a rather high current, 10 to 15 amperes, must be used initially. As the gas pressure diminishes, the current must be correspondingly diminished in order to avoid overheating of the copper wire.

The modification in the furnace consisted in utilizing a platinum wire instead of copper. This has a double advantage in the high melting-point of platinum, and its high resistance. About 5 feet of No. 32 wire was wound on a small rod of silica 5 mm in diameter and 15 cm long. This was then incased in a thin tube of transparent silica fitting snugly over the spiral coil. It was found that sufficient heat was conducted through the quartz tube to raise an oxidized copper ribbon, wrapped spirally outside of the quartz tube, to a sufficient temperature to cause hydrogen to be reduced. By this indirect heating of oxidized copper the temperature was controlled so that there was no danger of overheating the copper, and a very low current, 1 to 3 amperes, was sufficient. Such a furnace was satisfactory for a period of nearly a year without renewal. The copper had to be reoxidized from time to time, as in the original Duane apparatus.

[1] *Physical Review* (2), **5**, 311–314, 1915.

NOTE ON COOLING BY EXPANSION IN SUN-SPOTS[1]

By HENRY NORRIS RUSSELL[2]

ABSTRACT

Cooling by expansion in sun-spots.—Assuming that the low temperature of sun-spots to be due to the expansion of the rapidly rising gases, it is shown that the base of the spot vortex must be a region of very high temperature, probably over 20,000°, and the increase of volume on ascending must be large, probably over 30 times. But only rough estimates can be made.

It is generally accepted that the relatively low temperatures of sun-spots are due to the cooling of the gases by expansion in the upper part of the vortex. The temperature of the spots is probably 2000° to 2500° C., lower than that of the photosphere, so that they may be regarded as the most powerful refrigerating engines known to science.

To estimate the degree of expansion which is necessary to produce this cooling, consider a mass of gas rising in the vortex. It cannot cool faster than the rate given by adiabatic expansion; nor, indeed, nearly as fast, for great quantities of heat are flowing into it by radiation from the hotter regions surrounding the vortex, and, within the gases of the vortex, processes of recombination of electrons with ionized atoms and of formation of chemical compounds are at work on a large scale, and these liberate great quantities of heat. (Formation of TiO_2, 3000 calories per gram of reacting material; neutralization of singly ionized calcium, 3500 calories per gram; most neutralizations give off more heat.)

Meanwhile, the temperature of the surrounding solar gases, through which the vortex column rises, must diminish upward; and this temperature gradient cannot be less than that of radiative equilibrium, for otherwise the observed outward flow of heat from the sun's interior could not be maintained.

In radiative equilibrium, we have

$$T \propto P^{1/4} \propto \rho^{1/3}$$

[1] *Contributions from the Mount Wilson Observatory*, No. 217.

[2] Research Associate of the Mount Wilson Observatory.

where T, P, and ρ represent the temperature, pressure, and density, respectively. In adiabatic expansion:

$$T \propto \rho^{\gamma-1} \propto P^{\frac{\gamma-1}{\gamma}},$$

γ being the ratio of specific heats. The effect of ionization in altering the mean molecular weight of the gases is here ignored.

Suppose that the vortex starts at a depth where the temperature, pressure, and density are T_0, P_0, and ρ_0, and rises to the surface where, outside the spots, these quantities are T_1, P_1, and ρ_1. In the spots, at the visible surface, the temperature will have the lower value T_2. The pressure will be about the same as P_1, for it is probable that we look down through about the same amount of matter per square centimeter, before being stopped by atmospheric scattering, in the spots and in the photosphere; and, of course, the solar gravity is the same.

Hence:

$$P_2 = P_1; \qquad \rho_2 = \frac{T_1}{T_2}\rho_1.$$

We have then for radiative equilibrium:

$$\frac{T_1}{T_0} = \left(\frac{P_1}{P_0}\right)^{1/4},$$

and for adiabatic equilibrium:

$$\frac{T_2}{T_0} = \left(\frac{P_1}{P_0}\right)^{\frac{\gamma-1}{\gamma}};$$

whence:

$$\frac{T_2}{T_1} = \left(\frac{P_1}{P_0}\right)^{\frac{3\gamma-4}{4\gamma}} = \left(\frac{T_1}{T_0}\right)^{\frac{3\gamma-4}{\gamma}},$$

$$\frac{T_0}{T_1} = \left(\frac{T_1}{T_2}\right)^{\frac{\gamma}{3\gamma-4}}; \quad \frac{P_0}{P_1} = \left(\frac{T_0}{T_1}\right)^4; \quad \frac{\rho_0}{\rho_1} = \left(\frac{T_0}{T_1}\right)^3.$$

Now in the actual case T_1 is about 6000°, T_2 3500° to 4000° C., and T_1/T_2 1.5 or more. The greatest possible value of γ is 5/3 (monatomic gas). This would give:

$$T_0 = 2.0T_1 = 12{,}000°; \qquad P_0 = 16P_1; \qquad \rho_0 = 8\rho_1 = 5.3\rho_2.$$

But, for reasons already stated, this must greatly underestimate the amount of expansion. If, as a rough allowance for the effects of radiation and recombination in the ascending vapor, we assume that, on the average, γ equals $7/5$, as for a diatomic gas, we would find:

$$T_0 = 17T_1 = 100{,}000^\circ; \quad P_0 = 80{,}000P_1; \quad \rho_0 = 5000\rho_1 = 3300\rho_2.$$

Assuming $\gamma = 3/2$, we have:

$$T_0 = 3.7T_1 = 22{,}000^\circ; \quad P_0 = 190P_1; \quad \rho_0 = 51\rho_1 = 34\rho_2.$$

It is evident, therefore, that the base of the spot vortex must be in a region of high temperature, and that the increase of volume in ascending must be great; but no numerical estimates can be made.

It may be noticed in conclusion that the very existence of cooling by expansion in sun-spots shows that any general vertical convection in the outer layers of the sun must either reach only to a depth which is small compared with that from which the ascending spot vortex comes, or else be so slow that the cooling by expansion as the gases rise is continuously made up by heating by radiation. Otherwise the temperature gradient would be so nearly adiabatic that no important differential cooling could occur in the spots.

MOUNT WILSON OBSERVATORY
July 27, 1921

NOTICE TO CONTRIBUTORS

There is occasionally published in the *Astrophysical Journal* a Standing Notice (for instance, on pages 179–80 of the number for September 1917). This is principally intended to guide contributors regarding the manuscript, illustrations, and reprints. This notice contains the following paragraph:

> Where unusual expense is involved in the publication of an article, on account of length, tabular matter, or illustrations, arrangements are made whereby the expense is shared by the author or by the institution which he represents, according to a uniform system.

The present sheet has been printed for amplifying further that paragraph.

The "uniform system" according to which "arrangements are made" is as follows: The cost of composition in excess of $50, and of stock, presswork, and binding of pages in excess of 40 pages, for any one article shall be paid by the author or by the institution which he represents at the current rates of the University of Chicago Press. When four articles from one institution or author have appeared in any one volume, on which the cost of composition has amounted to $50 each, or when the total cost of composition incurred by the *Astrophysical Journal* on articles for one institution has reached the sum of $200, the entire cost of the composition, stock, presswork, and binding of any additional articles appearing in that volume shall be paid by the author or by the institution which he represents.

As to illustrations, the arrangement cannot be quite as specific, but it may be generally assumed that not more than three half-tone inserts can be allowed without payment by the author. The cost of paper, presswork, and binding for each full-page insert is about $8.00, aside from the cost of the half-tone itself. In the matter of zinc etchings, considerable latitude has to be allowed, as in many cases diagrams take the place of more expensive tables. It may be assumed, however, that it will seldom be possible for the *Journal* to bear an expense of over $25 for diagrams and text illustrations in any one article.

Contributors should notice that since January, 1917, it has been impossible to supply any free reprints of articles.

Reprints of articles, with or without covers, will be supplied to authors at cost. No reprints can be furnished unless a request for them is received before the *Journal* goes to press.

Every article in the *Astrophysical Journal*, however short, is to be preceded by an abstract prepared by the author and submitted by him with the manuscript. The abstract is intended to serve as an aid to the reader by furnishing an index and brief summary or preliminary survey of the contents of the article; it should also be suitable for reprinting in an abstract journal so as to make a reabstracting of the article unnecessary. For details concerning the preparation of abstracts, see page 231 in the April, 1920, number of the *Journal*.

THE EDITORS

THE
ASTROPHYSICAL JOURNAL
AN INTERNATIONAL REVIEW OF SPECTROSCOPY
AND ASTRONOMICAL PHYSICS

VOLUME LIV DECEMBER 1921 NUMBER 5

A STUDY OF THE ULTRA-VIOLET END OF THE SOLAR SPECTRUM

By CHARLES FABRY and H. BUISSON

ABSTRACT

Solar spectrum from λ *3150 to* λ *2900A*.—To obtain photographs of this region it is necessary to eliminate diffuse light of longer wave-length. This was done by using a *double spectrograph* consisting of two quartz spectrographs in series arranged with their dispersion planes at right angles. The intensity of the spectrum falls off very rapidly, being only one-millionth as great at λ 2900 as at λ 3150; therefore, to enable the whole region to be photographed at once for measurements of absorption, *two absorption screens* made by intensifying photographic films with $HgCl_2$ were used in echelon to reduce the intensity above λ 2990. To obtain a *photographic map* with uniform normal exposure throughout, two plates, each covering half the region, were exposed by moving a shutter by hand at proper predetermined rates across each spectrum (see Plate III). The wave-lengths will be published soon.

Absorption of the atmosphere for λ *3150 to* λ *2900 A*.—By comparing the intensities of spectrograms taken for various zenith angles, the *coefficients* for various wave-lengths were determined. The effect of molecular diffusion was corrected for by using the Rayleigh formula, and the effect of haze was eliminated by assuming it independent of wave-length. A comparison with the corresponding coefficients for ozone, previously determined by the authors, shows remarkable agreement, leaving no doubt that this absorption is due to ozone.

Ozone in the atmosphere is found to be equivalent to a layer about 3 mm thick at atmospheric pressure. The *daily values* for May and June, 1920, vary irregularly from 0.29 to 0.34 cm. It would be interesting to follow these *variations* through a solar period. It is shown that the *location of this ozone* must be in the outer layers of the atmosphere, above 40 km, and in *explanation of its origin* it is suggested that the ozone is produced by solar rays of wave-length shorter than λ 2000 which penetrate only the outer layers and that longer rays dissociate the ozone and prevent its accumulation beyond the amount for equilibrium.

Distribution of energy in the solar spectrum outside our atmosphere for λ *3150 to* λ *2900 A* was determined by correcting the observed intensities for the absorption by the atmosphere and then reducing to units of energy by the use of a calibration-curve obtained by comparing the intensity-curve of an arc with the radiation from a black body at 3750° Abs. The energy-curve thus obtained shows only a gradual slope

toward the shorter wave-lengths. For λλ 3143, 2997, 2922, and 2898 the relative energies for the sun outside the earth's atmosphere come out 155,000, 218,000, 145,000, and 45,000 respectively, while at the surface of the earth when the sun is at the zenith the corresponding values are about 22,400, 1320, 2.2, and 0.02.

1. *Introduction.*—The very rapid falling off in the intensity of the solar spectrum in the ultra-violet region, which is without any doubt due to the absorption by the earth's atmosphere, has been attributed to one of the constituents of that atmosphere, ozone.[1] This seems in fact to be the only gas having absorptive properties which would permit of an explanation of the observed phenomena. Quantitative determinations of the intensity in this spectral region are completely lacking, however, although they are very numerous in the visible and in the infra-red spectrum. In the absence of such measures, the explanation of this cutting off of the spectrum as an effect of ozone is a trifle hypothetical, and we do not know the amount of that gas which intervenes between the sun and us. Further, we have no information as to the intensity of the solar radiations of that short wave-length prior to their entry into our atmosphere.

We have undertaken to make numerical determinations of the intensity, to measure the coefficients of absorption of the atmosphere for each wave-length, and to see if those coefficients accord with those of ozone. If so, we shall then be able to determine the quantity of ozone which produces the absorption. Finally, on correcting each radiation for the absorption which it has suffered, we shall be able to learn the intensity outside the atmosphere and to see if the spectrum thus freed from terrestrial absorption still shows a marked weakening in that region. Should this be the case, it would be necessary to conclude that solar phenomena have a part in this limitation of the spectrum.

Our measures were undertaken long ago, beginning with the study of the absorption of ozone in 1912.[2] It was necessary to make this study because its absorption was little known, whence it was impossible to compare it with that of the atmosphere.

[1] The presence of ozone in the atmosphere has recently been established beyond doubt by Fowler and Strutt, who have shown the existence of absorption bands of this gas in the region λ 3300, in the light of the sun and of the stars. *Proceedings of the Royal Society*, A, **93**, 577, 1917.

[2] *Journal de Physique* (5), **3**, 196, 1913.

The first attempts to measure the atmospheric absorption were made at that time and were continued in the course of the following years until interrupted by the war; they were resumed during the last two years. It is unnecessary to describe the succession of improvements, and we limit ourselves to describing the actual arrangement of apparatus and methods of calculation which we finally adopted.

Our experiments were made at the Faculty of Sciences, of the University of Marseille (latitude 43°17′, altitude 25 meters), under conditions which are not the most favorable, in the center of an industrial city where the air is seldom pure.

2. *Methods.*—The region of spectrum which we have studied is of shorter wave-length than λ 3150, and we have employed solely the photographic method for the measures of intensity. We could not dream of using a thermopile or a bolometer, which would have had the advantage of giving intensities directly in energy; but the region to be measured is greatly weakened by absorption, so that the radiation at λ 2900 is reduced, even for the sun at the zenith, to at least 10^{-5} of its value outside of the atmosphere.

The problem to be solved, then, is the comparison of the intensity of one and the same radiation at different hours of the day, which is relatively easy because it is free from all the difficulties due to the selective effect on different rays. On the same plate and with the same length of exposure, exposures are made at different hours. When the plate is developed, the blackening is more intense as the intensity of the effective radiation is greater. It is possible to graduate the plate as to intensity, that is to say, to establish the relation existing between the blackening and the intensity by taking two exposures which should be of known ratio. The difference of density of those two exposures, divided by the logarithm of the ratio of the intensities, gives the ratio γ which defines, for that plate, the relation sought in the region of normal exposure.

To make two exposures in known ratios of intensity, we employed two different procedures: in the first, we placed in the path of the luminous beam a polarizer and an analyzer, the latter being fixed while the polarizer was mounted on a graduated circle so that it

could be differently oriented. The beam was thus weakened in any desired ratio. The polarizers employed were Foucault prisms with an air space. It was in fact necessary to avoid apparatus with a layer of balsam, which is opaque to ultra-violet rays. This procedure grades the light in a direct manner, but it causes a somewhat complicated arrangement of apparatus; further, in our regular measures we have preferred to work with absorption. Filters, the construction and use of which will be described below, may be interposed in the beam. Their opacity having been measured once for all for each radiation by a polarimetric method, they then furnish a simple and convenient means of graduating the light.

All of the preceding applies to the intensity of one and the same ray. We may then go farther, and give, in the short spectral region which we have studied (λ 3150 to λ 2900), values of the photographic intensities of the different radiations expressed in the same unit. Such a plan would be meaningless if we wished to apply it to the whole of the spectrum. The law of opacity always keeping the same general form, is then very different from one ray to another in consequence of the great variation of the ratio γ, which may increase from one to two in passing from the region λ 3000 to the visible region. Two rays which give identical opacities will cease to do so, if their intensities are increased tenfold. This difficulty does not exist in our case, at least with the plates which we have employed. The factor γ remains constant during the interval studied, and consequently the ratios of photographic intensities have a value as well defined for two different rays as for the same ray. It is true that these photographic intensities thus measured for neighboring radiations should not be confused with the true intensities expressed in energy: they differ according to the law of dispersion of the spectroscopic apparatus and according to the variable sensitiveness of the plate. The essential thing is that they have a definite significance. We shall see farther on how we may pass from photographic intensities to intensities of energy.

All these determinations depend on the measures of density at different parts of the photographic plates. These densities

ought to be measured on regions of very small extent, limited by the very narrow intervals which separate the solar lines. It was with such measures in view that we have constructed our microphotometer, which is particularly well adapted to this class of work.[1]

We have employed almost solely the photographic plates of Jougla, bromo-iodide of silver (mauve label), which have great sensitiveness and a normal range of exposure.

3. *Spectroscope.*—In photographing the extreme end of the solar spectrum with an ordinary spectroscope, it is immediately evident that it becomes lost in an intense veil which limits the observable region. This veil is produced by the diffused light due to the more intense radiations of the spectrum, the diffusion itself being due to the passage of the light through the different transparent media of the dispersive apparatus. It is absolutely necessary to eliminate this foreign light of longer wave-length from the region to be studied. The use of absorbing filters serves this problem only very incompletely; a preferable arrangement is to employ a second dispersion which throws to one side of the spectral band the foreign light which contaminates it. This procedure has already been employed in an imperfect way by Miethe and Lehmann,[2] who interposed, at some distance from the principal prism, a second prism having its edge perpendicular to the first.

Our arrangement is as follows. The first spectroscope, having prisms and lenses of quartz, produces a real spectrum, one portion of which, limited in length and height, is isolated from the rest by a slit placed at a convenient place. A second quartz spectroscope disperses, in a plane perpendicular to the plane of dispersion of the first spectroscope, the light which has passed through that slit; thus the diaphragm, which has limited the first spectrum, forms the slit of the second spectroscope. The whole apparatus is shown in perspective in Figure 1; the collimator and tube of the first spectroscope are in a horizontal plane with the edges of the prisms P and P' vertical. The quartz objectives L and L' are each of focal length 1 meter and diameter 58 mm. The two quartz prisms

[1] *Journal de Physique* (5), **9**, 37, 1919.

[2] *Sitzungsberichte der preussische Akademie der Wissenschaften*, **1**, 268, 1909.

are traversed by the beam along their optical axes; the one is right-handed, the other left-handed. They have a height of 50 mm, and their base is an equilateral triangle of 57 mm side. We allow an amount of light that is strictly necessary to enter the apparatus, by limiting the height utilized of the slit F by means of a screen having an opening 1 mm in height. The spectrum produced at S is spread out horizontally and it is received on a diaphragm which limits it to the region between λ 3200 and λ 2800. The aperture of that diaphragm is about 40 mm long and 1 mm high. The second

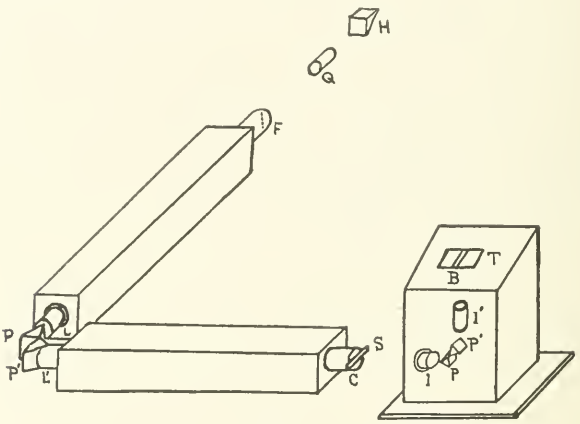


FIG. 1

spectroscope, which is arranged to disperse the light in a vertical plane, used that aperture as its slit, and is produced by two equilateral prisms of quartz p and p', the edges of which are horizontal, together with two lenses l and l', of focal lengths 25 and 17 cm. Another lens, C, of focal length 30 cm, placed in the plane of the slit S, plays the rôle of field lens, projecting an image of the prisms P of the first spectroscope upon those of the prisms p of the second spectroscope, so that all the useful light which has passed through the first apparatus may be gathered by the second.

If the slit S of the diaphragm was illuminated by a monochromatic light, the second spectroscope would give a straight line as an image; but since the different parts of that slit correspond to different wave-lengths, there is produced by dispersion an image

of which the points are unequally deviated, or, in other words, a curved image is produced. The foreign rays of less refrangibility, which form the diffuse light, are deviated completely beyond that image, which then is seen on a background entirely free from veil.

As neither of these two spectroscopes is achromatic, the final spectrum must occupy a complicated position in space. The position and the inclination which must be given to the photographic plate *T* have been determined by a series of preliminary experiments; but in spite of the complication of the optical path, the spectrum is sufficiently sharp. The scale of the spectrum is about 1 mm for 10 angstroms, and thus it is possible to separate two rays having wave-lengths differing by at least half an angstrom. We have thus obtained completely the object sought, and it is possible to make exposures of a quarter of an hour on the solar spectrum without having the extremity of the spectrum limited by the fog, and thus it is possible to push the study of the spectrum out to its actual limit.

This whole arrangement, formed by the two spectroscopes thus placed in tandem, forms an entirely rigid system, each part of which has been placed in its definitive position. The quartz parts were cut by M. Jobin and the remainder of the equipment was assembled in the workshop of the laboratory.

A heliostat, having a totally reflecting prism *H*, sends the solar beam into the apparatus with but a single reflection, and an achromatic lens *Q*, of quartz and fluorite, of 30 cm focal length, projects an image of the sun on the slit.

4. *Filters.*—The variation in the intensity in the region of the spectrum studied is so great that a single exposure of a given length does not furnish a plate that can be used over more than an extremely short interval. The regions of long wave-length are overexposed, while those of shorter wave-length need an excessive increase of exposure. In order to make the photographic impression more uniform from one exposure and thus to be able to extend the measures made on a single plate, we have greatly reduced the intensity for longer wave-lengths by the following device. Over a portion of the slit *S*, where the horizontal spectrum from the first spectroscope is projected, we place absorbing

screens of measured opacity, which reduce in a known ratio the intensity of the rays which pass through them. Thus we weaken the rays that are too intense, while allowing the others to pass freely, and we thus obtain on the plate a spectrum covering several regions which have all received a suitable exposure. With the judicious choice of filters, we thus obtain a spectrum throughout the whole length of which measures of intensity are possible.

After several attempts, we made these filters by taking gelatine films from photographic plates which had been developed and fixed and had been separated from the glass. Thus we had absorbers of very small thickness, of which the opacity could be selected at will. The coatings of ordinary photographic plates have one very serious inconvenience, for they are made by grains of silver scattered through the gelatine, and also have the anomaly of the transparence of the metallic silver in the region of λ 3100, so that they have there very slight opacity. Thus we should have filters of which the opacity would be very variable with the wave-length, and this in just the region which interests us.

We have gotten entirely rid of this disturbing property by intensifying the plate with mercuric chloride and ammonia before removing the gelatine. The layers thus obtained have an absorption without anomalies, which increases gently and uniformly as the wave-length decreases, but so that this variation is not disturbing to our measures. With these filters, we made the following arrangement: a sheet of cardboard contains an aperture on which was placed a strip of gelatine, detached from a plate, so that it should cover only a part of the aperture; then a second strip of gelatine was placed over a part of the first one, thus giving two successive echelons. The supporting cardboard is always placed in the same way before the slit S upon which the first spectrum is projected. Under this condition the region beyond λ 2990 does not suffer any absorption, while that between λ 2990 and λ 3040 undergoes absorption from a single strip of gelatine, and finally the region of wave-lengths greater than λ 3040 suffers absorption from two superposed strips.

We have determined the absorption of these screens under the conditions under which we use them, namely, in the apparatus

where they are to be used and not by measurements made under other conditions. The passage of light through these photographic films is accompanied by a slight amount of diffusion and the impression produced on the plate varies with the proportion of the diffused light used in forming the image. It is therefore necessary to make the measures of absorption upon the filter when in the place where it is going to be used and without any modification of the aperture of the luminous beams.

The transmission of the filters was measured by the polarimetric method described further on and was made separately on each of

TABLE I

LOGARITHMS OF OPACITIES OF FILTERS

λ	Filters		
	A	*E*	*C+E*
2946	1.12		
2956	1.11		
2963	1.10		
2997	1.08	2.08	
3022	1.06	2.01	
3052	1.04		3.35
3104	1.02		3.33
3143	1.01		3.31

the two filters which were used on the spectrum. One of these transmits about 1/100 of the incident light in the region of λ 3000, while the other transmits about 4 per cent; when they are superposed, the transparence is not over 0.0004.

It was further necessary to calibrate each plate on which the solar spectrum was photographed. This was accomplished by interposing for the whole of the beam, before its entry into the apparatus, a filter of the same sort as those described above, which weakened all the radiations in a known ratio.

The results of these measures are given in Table I, containing the logarithms of the opacities of the different filters. Filter *A* is the one which weakened the spectrum for calibrating the plate. Filters *C* and *E* are the ones placed over the slit *S* in the focal plane of the first spectroscope; *E* is introduced only in the region λ 3000; for wave-lengths greater than λ 3040 the light traverses the two filters *C* and *E*.

5. *Determination of the coefficient of absorption of the atmosphere for the different rays.*—We have followed the method proposed in principle by Bouguer two centuries ago, which has been correctly applied to monochromatic radiations from the sun by Langley and afterward by Abbot. This consists in studying the decrease of intensity of a definite ray when the zenith distance of the sun is increasing. If we let I_0 be the intensity of a ray before its entry into our atmosphere, the sun being at the zenith, it will arrive at the surface of the earth with a reduced intensity I_1 and we may define the coefficient of absorption of the atmosphere for that ray by the equation

$$m = \log_{10} (I_0/I_1). \tag{1}$$

Now if the sun is at zenith distance z, the path traversed by the light in each stratum is multiplied by sec z, and the intensity I which reaches the earth's surface is given by the formula

$$\log I = \log I_0 - m \sec z. \tag{2}$$

For determining the coefficient m we measure the intensity at different hours of the day and then trace a curve having for abscissas the values of sec z and for ordinates the values of log I. If the transparence of the air has not undergone any change during the course of the observation, this curve will be a straight line, the slope of which gives us the value of m. The solar spectrum is photographed at different hours of the day, on the same plate, with equal times of exposure, the filters C and E, mentioned above, being interposed to weaken the portions that are too strong. An identical exposure is further made at noon through the filter A to obtain the necessary data as to the calibration of the plate. We then measure with the microphotometer the density of the plate on the two spectra for rays conveniently chosen. In this choice we are limited by the great number of dark lines which occur in the solar spectrum in that region. Among these rays we have selected eleven intervals where the spectrum has a very uniform appearance, from λ 2922 to λ 3143. All of our measures refer to the points thus determined.

Thanks to the precaution taken in rendering the spectrum uniform by means of the absorbing filters, we have been able to keep

the blackening of the plate in the region of normal exposure, which is that where the curve connecting the photographic densities with the logarithm of the intensity acting is a straight line. The slope of that right line (coefficient γ) independent of the wave-length in the short spectral region studied here, is obtained by two exposures made at noon, one under general conditions and the other with a known reduction of brightness. We then obtain for every ray the intensity at different hours and further the photographic intensities of the different radiations.

TABLE II

Local Solar Time	λ 2922	λ 2931	λ 2936	λ 2946	λ 2956	λ 2963	λ 2997	λ 3022	λ 3052	λ 3104	λ 3143
$8^h 22^m$					0.66	1.23	0.67	1.56	0.96	1.77	2.14
8 39				0.28	1.10	1.61	0.96	1.85	1.12	1.91	2.24
8 56				0.63	1.44	2.01	1.17	2.05	1.25	2.04	2.35
9 16			0.38	1.05	1.86	2.28	1.47	2.22	1.46	2.09	2.45
9 38		0.35	0.74	1.44	2.20	2.64	1.72	2.41	1.58	2.18	2.59
10 2		0.65	1.05	1.72	2.46	2.95	1.87	2.54	1.64	2.27	2.63
10 31	0.28	0.84	1.28	1.91	2.64	3.10	1.94	2.64	1.70	2.31	2.65
11 25	0.52	1.10	1.55	2.15	2.92	3.27	2.10	2.78	1.78	2.37	2.68
13 22	0.37	0.97	1.39	2.03	2.77	3.23	2.03	2.71	1.76	2.39	2.68
13 52		0.68	1.06	1.75	2.50	2.95	1.89	2.57	1.67	2.28	2.60
14 24		0.37	0.72	1.43	2.20	2.72	1.72	2.45	1.62	2.27	2.56
14 44			0.46	1.12	1.92	2.52	1.52	2.27	1.50	2.17	2.47
15 4				0.79	1.64	2.07	1.35	2.13	1.37	2.13	2.41
15 20				0.44	1.28	1.83	1.13	2.01	1.25	2.01	2.34
15 46					0.71	1.19	0.76	1.68	1.03	1.86	2.16
11 23*				0.62	1.33	1.69	0.58	1.22		0.98	1.29

* With filter *A*.

6. *Example of a day's observations.*—We shall give as an example the measures made on June 7, 1920. Fifteen exposures, each of one minute, were spread over a total time of seven and one-half hours; an exposure of the same duration through the filter *A* was taken for the purpose of calibrating the plate. The densities of the plate for each exposure and for each of the selected rays are given in the Table II where the first column contains the hour of the different exposures in local solar time, while each of the others refers to one of the rays measured. A mere examination of Table II shows how the intensity decreases rapidly when the sun departs from the zenith, and how the effect is more marked for the short wave-lengths. We further see the useful effect of the

absorbing filters placed in the spectra; the measures would be impossible on account of the overexposure involved for wavelengths longer than 2963 if the intensity had not been reduced to a convenient value by the presence of the filters. The last line of the table refers to the exposure made at 11^h23^m through the filter *A;* from that comparison with the exposure made without absorption at 11^h25^m, for determining the calibration of the plate, we have adopted the number 1.40 as the value of the coefficient γ, this being the mean of values differing very slightly for different radiations. On dividing the densities given in the preceding table by that figure, we obtain the intensities of the different rays which have produced the blackening. For those which have been weakened by the interposition of the filter in the spectrum, it is necessary to take account of that absorption by adding the densities of the filter given in Table I. We thus obtain Table III, which gives in logarithms the values of the photographic intensity of each ray at different hours. The first column of that table contains the hours and the second the secant of the zenith distance of the sun. These measures must be corrected for two causes of weakening, from which all radiations suffer, in addition to the very selective absorption for which we are here seeking the origin. These two causes are the diffusion by the molecules of the air and the extinction produced by the haze or other foreign bodies in suspension in the air. The molecular diffusion obeys laws which are known, and its effect may be calculated a priori; it is enough to know its effect on each ray when the sun is at the zenith. Table IV gives the values of the coefficient β defined by

$$\beta = \log (I_0/I_1),$$

in which I_0 is the intensity outside the atmosphere and I_1 is the intensity which would be found at the earth's surface if diffusion by the molecules was the only effect existing. These data have been calculated by Lord Rayleigh's formula.

We have eliminated the effect of absorption by foreign particles, which may be very variable from moment to moment, in assuming that this action was subject to little variation as a function of the

wave-length in the narrow spectral region covered by our measures. The method of computation is as follows.

Let m be the coefficient of absorption of the atmosphere for vertical transmission, due to that unknown substance which acts selectively, and let β be the coefficient of extinction due to molecular diffusion under the same conditions. These two quantities depend

TABLE III

Time	Sec z	λ 2922	λ 2931	λ 2936	λ 2946	λ 2956	λ 2963	λ 2997	λ 3022	λ 3052	λ 3104	λ 3143
8^h22^m....	1.526					0.47	0.88	2.56	3.12	4.04	4.59	4.84
8 39	1.440				0.20	0.78	1.15	2.76	3.33	4.15	4.69	4.91
8 56	1.367				0.45	1.03	1.43	2.91	3.47	4.24	4.79	4.99
9 16	1.295			0.27	0.75	1.33	1.63	3.13	3.60	4.39	4.82	5.06
9 38	1.232		0.25	0.53	1.03	1.57	1.88	3.31	3.73	4.48	4.89	5.16
10 2	1.177		0.46	0.75	1.23	1.76	2.11	3.41	3.82	4.52	4.95	5.19
10 31	1.128	0.20	0.60	0.91	1.36	1.88	2.21	3.46	3.90	4.56	4.98	5.20
11 25	1.077	0.37	0.78	1.11	1.53	2.08	2.33	3.58	4.00	4.62	5.02	5.22
13 22	1.118	0.26	0.69	0.99	1.45	1.98	2.31	3.53	3.95	4.61	5.04	5.22
13 52	1.165		0.48	0.76	1.25	1.78	2.11	3.43	3.85	4.54	4.96	5.17
14 24	1.237		0.26	0.51	1.02	1.57	1.94	3.31	3.76	4.51	4.95	5.14
14 44	1.295			0.33	0.80	1.37	1.80	3.16	3.63	4.42	4.88	5.07
15 4	1.367				0.56	1.17	1.48	3.04	3.53	4.33	4.85	5.03
15 20	1.435				0.31	0.91	1.31	2.89	3.45	4.24	4.77	4.98
15 46	1.573					0.51	0.85	2.62	3.21	4.08	4.66	4.85

TABLE IV

λ.....	2922	2931	2936	2946	2956	2963	2997	3022	3052	3104	3143
β.....	0.48	0.47	0.46	0.46	0.45	0.45	0.43	0.42	0.40	0.38	0.36

only on the wave-length. If I_0 is the intensity outside the atmosphere, the intensity I at the surface of the earth will be given by the equation

$$\log I = \log I_0 - (m+\beta)\sec z - \delta, \qquad (3)$$

in which z is the zenith distance of the sun and δ represents the effect of the haze, irregularly variable from moment to moment, but independent of the wave-length. At the same moment for another ray, we have the analogous relation

$$\log I' = \log I'_0 - (m'+\beta')\sec z - \delta, \qquad (3')$$

whence we have

$$\log I - \log I' = K - (m - m' + \beta - \beta')\sec z, \qquad (4)$$

in which K is a quantity independent of the time. If we compare each of the rays with one of them, for example with λ 3143, the difference of the logarithms of the intensities of the radiations λ and 3143 should vary linearly as a function of sec z, and the slope of the right line which represents that variation gives for each ray the value of

$$m-m'+\beta-\beta'.$$

Let us now form the table of the differences log I − log I', understanding that I' refers to λ 3143. To avoid negative numbers,

TABLE V

Sec z	λ 2922	λ 2931	λ 2936	λ 2946	λ 2956	λ 2963	λ 2997	λ 3022	λ 3052	λ 3104	λ 3143
1.526					0.85	1.26	2.94	3.50	4.42	4.97	5.22
1.440				0.51	1.09	1.46	3.07	3.64	4.46	5.00	5.22
1.367				0.68	1.26	1.66	3.14	3.70	4.47	5.02	5.22
1.295			0.43	0.91	1.49	1.79	3.29	3.76	4.55	4.98	5.22
1.232		0.31	0.59	1.09	1.63	1.94	3.37	3.79	4.54	4.95	5.22
1.177		0.49	0.78	1.26	1.79	2.14	3.44	3.85	4.55	4.98	5.22
1.128	0.22	0.62	0.93	1.38	1.90	2.23	3.48	3.92	4.58	5.00	5.22
1.077	0.37	0.78	1.11	1.53	2.08	2.33	3.58	4.00	4.62	5.02	5.22
1.118	0.26	0.69	0.99	1.45	1.98	2.31	3.53	3.95	4.61	5.04	5.22
1.165		0.53	0.81	1.30	1.83	2.16	3.48	3.90	4.59	5.01	5.22
1.237		0.34	0.59	1.10	1.65	2.02	3.39	3.84	4.59	5.03	5.22
1.295			0.48	0.95	1.52	1.95	3.31	3.78	4.57	5.03	5.22
1.367				0.75	1.36	1.67	3.23	3.72	4.52	5.04	5.22
1.435				0.55	1.15	1.55	3.13	3.69	4.48	5.01	5.22
1.573					0.88	1.22	2.99	3.58	4.45	5.03	5.22

all the differences have been increased by the constant quantity 5.22, which amounts to making an arbitrary choice of the value K in the preceding formula. Thus we obtain Table V, which gives the logarithms of the intensities of the different rays at different hours referred to what they would be if λ 3143 did not suffer any absorption. If we trace for each ray the curve of the numbers given in each column as a function of sec z, we obtain the graph in Figure 2, on which the + sign represents the points referring to measures in the morning, and the symbol × to measures in the afternoon. The slope of each of these straight lines gives the values of

$$m-m'+\beta-\beta'.$$

In correcting for the values $\beta-\beta'$, known from Table IV, there remain the values of $m-m'$, which are the differences of the

coefficient of absorption of the atmosphere for the ray λ and the ray 3143.

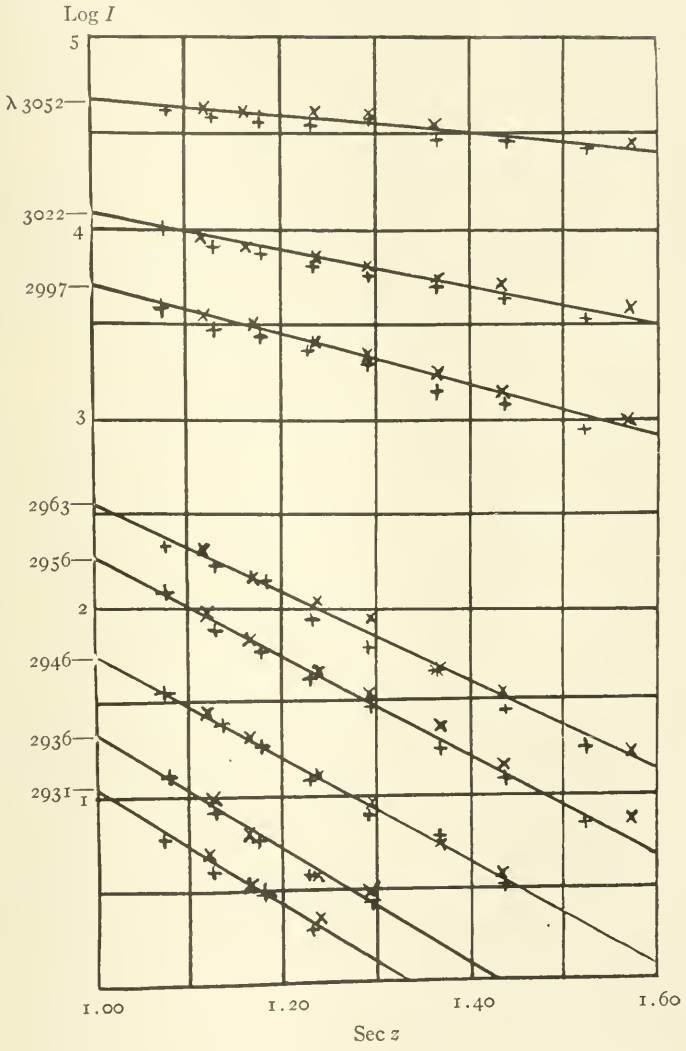


FIG. 2

It is necessary to compare these values with the coefficients of absorption of substances which are supposed to cause that absorption. If they are functions of wave-length, according to the same

law of variation as these coefficients, we may affirm that the substance in question is the one present in the atmosphere and which limits the solar spectrum. If a is the coefficient of absorption of the substance considered, and x its thickness, we ought to have

$$m = ax,$$
$$m' = a'x,$$
$$m - m' = (a - a')x.$$

Table VI gives for the wave-lengths selected the values of the coefficient β, the differences $\beta - \beta'$, the coefficient a of the ozone, the differences $a - a'$, the slopes P measured on the graph, the values of $m - m'$, and finally the quotients respectively of $m - m'$ divided by $a - a'$, which ought to yield the value of x, which is the

TABLE VI

λ	β	$\beta-\beta'$	a	$a-a'$	P	$m-m'$	x
2931	0.47	0.11	11.2	10.5	3.15	3.04	0.290
2936	0.46	0.10	10.5	9.8	3.16	3.06	0.312
2946	0.46	0.10	9.3	8.6	2.78	2.68	0.312
2956	0.45	0.09	8.1	7.4	2.66	2.57	0.347
2963	0.45	0.09	7.4	6.7	2.37	2.28	0.340
2997	0.43	0.07	4.7	4.0	1.32	1.25	0.309
3022	0.42	0.06	3.4	2.7	0.96	0.90	0.333
3052	0.40	0.04	2.3	1.6	0.44	0.40	0.250
3143	0.36	0.00	0.7	0	0	0	

thickness in cm of the stratum of ozone. The rays λ 2922 and λ 3104 have not been utilized, the first because the corresponding measures have not been sufficiently accurate, and the second because its slope is too small. Finally, it should be recalled that λ 3143 is the comparison ray. We see that the values of x obtained for the different rays are sensibly equal; the agreement is still better if we except the two extremes, which are less accurate than the others. The conclusion is forced upon us that it is the ozone which limits the solar spectrum by its absorption.

The adopted mean of the values in the last column, 0.325, gives for June 7, 1920, the thickness of pure ozone expressed in cm, at atmospheric pressure, which would be traversed by the solar rays were the sun at the zenith. Table VII summarizes the measures made by the same method on three different days. We see that the accordance between the different values of x for

each day is satisfactory, whence it follows that the quantity of ozone present in the atmosphere was sensibly the same for these three days. But this is not always the case, and we have established beyond doubt the existence of considerable variation in the amount of ozone from one day to another. We shall return to this question farther on.

7. *Mode of calculation.*—The method of computation which we have employed was necessary to eliminate the irregularities of absorption caused by the dust, the haze and the smoke, varying from one moment to the next, but affecting in the same manner all the rays in the short region which we have measured. If

TABLE VII

λ	May 13	May 26	June 7
2931		0.34	0.29
2936	0.30	0.34	0.31
2946	0.33	0.32	0.31
2956	0.33	0.33	0.35
2963	0.35	0.35	0.34
2997	0.33	0.36	0.31
3022	0.38	0.34	0.33
3052	0.30	0.33	0.25
Adopted value...	0.33	0.34	0.32

the purity of the atmosphere was constant during the whole day, one could immediately apply the method of secants to each ray and thus obtain the total absorption of the atmosphere. This is the case for the very beautiful days when the sky is exceptionally pure. This may be recognized on the diagram giving the intensity as a function of sec z, by the fact that the points then fall on a straight line. This happened on June 7, 1920, as shown by the graph for the ray 3143 (Fig. 3). The slope of the right line on which fall all the points both of the morning and of the afternoon, gives the value 0.84 for the logarithm of the opacity for that ray of the atmosphere traversed vertically. In subtracting from that number the part referring to the ozone, 0.23, and the part due to the molecular diffusion, 0.36, we may deduce the effect of the haze alone; we thus find that the logarithm of its opacity is 0.25 for vertical rays.

We do not find the same regularity for most of the days of observation. The points do not fall on a straight line and in particular the observations made in the morning do not accord with those made in the afternoon. This renders impossible any precise determination of the total opacity, which is so variable in the course of the day; but the method of calculation which we have employed is general and causes these irregularities to disappear.

8. *The solar spectrum freed from atmospheric absorption.*—It is now possible to calculate the intensities which the solar rays would have if they were not weakened by our atmosphere. Equation 3, solved with respect to I_0, gives, without the necessity of

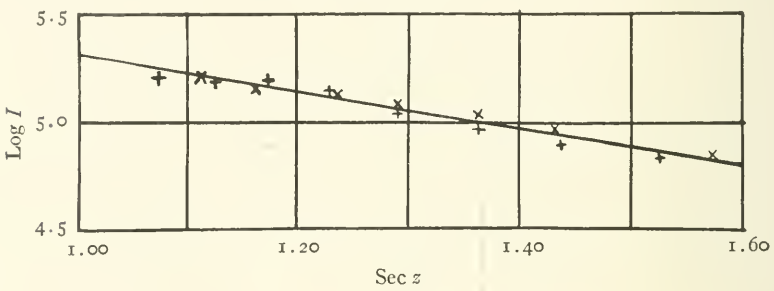


FIG. 3

introducing the value δ, the logarithms of the photographic intensities of the different rays expressed in a single arbitrary unit.

This computation has been made for those days of observation referred to above, by utilizing solely the exposure made near noon for which the term in sec z is the smallest. The results obtained are summarized in Table VIII. The measures stop at wavelength 2922, the shortest which we could obtain with an exposure of one minute. It is possible to extend the spectrum by increasing the length of exposure, at least when the sun is near the zenith, but the direct measures of the coefficient of absorption become impossible. These coefficients may be computed if a determination of the quantity of ozone has been made on the same day by the method which we will now indicate. We may then calculate the intensity before entrance into the atmosphere. This measurement has been made with exposures of 7^m and of 75^m on a plate to which had also

been given the usual exposure of one minute.[1] This time we have the necessary elements for determining the law of blackening as a function of the exposure time, and to refer to what we should have

TABLE VIII

LOGARITHMS OF THE PHOTOGRAPHIC INTENSITIES OUTSIDE THE ATMOSPHERE

	2922	2931	2936	2946	2956	2963	2997	3022	3052	3104	3143
May 13.....			5.35	5.36	5.41	5.47	5.69	5.55	5.86	5.64	5.71
May 26.....		5.30	5.31	5.31	5.44	5.52	5.64	5.52	5.86	5.70	5.77
June 7.....	5.30	5.21	5.28	5.28	5.39	5.30	5.60	5.63	5.85	5.85	5.85
Mean.....	5.30	5.25	5.31	5.31	5.41	5.43	5.64	5.57	5.85	5.73	5.78

TABLE IX

	λ 2898	λ 2906	λ 2912	λ 2917
Log I.....	−1.57	−1.20	−0.45	+0.03
Log I_0.....	4.76	4.52	5.00	5.16

with the same length of exposure. Thus we arrive at a measurement of the intensity out as far as wave-length 2898. Table IX, based on the preceding one, gives the values of log I, the photographic intensity at the surface of the earth when the sun is at the zenith, and of log I_0, the photographic intensity outside the atmosphere. All of these measures were made on June 20, 1920.

9. *Calculation of the intensity expressed as energy.*—All the preceding numbers are relative to the photographic intensities which we have defined above. They differ from the true values of the intensity expressed in units of energy because the dispersive apparatus, not having a constant dispersion, decreases the blackening for the shorter wave-lengths and also because the sensitiveness of the plate is not the same for all the rays studied.

We have eliminated at one stroke the effect of the two causes by studying, with the same spectroscope and the same plates, the law of blackening in the spectrum of a source giving a continuous spectrum with a known distribution of energy. For this purpose

[1] On the exposure of 75 minutes, the last trace of photographic impression corresponds to the wave-length 2885.

we used the light from a carbon arc, the image of which was projected on the slit of the spectroscope, and we interposed a polarizer and an analyzer so that we could vary all the rays at the same time in any desired proportion. Operating as in the case of the sun, we constructed the curve of photographic intensity with the spectra of the arc. The curve A of the graph (Fig. 4) was thus obtained, the abscissas being the wave-lengths, and the ordinates the logarithms of the photographic intensities.

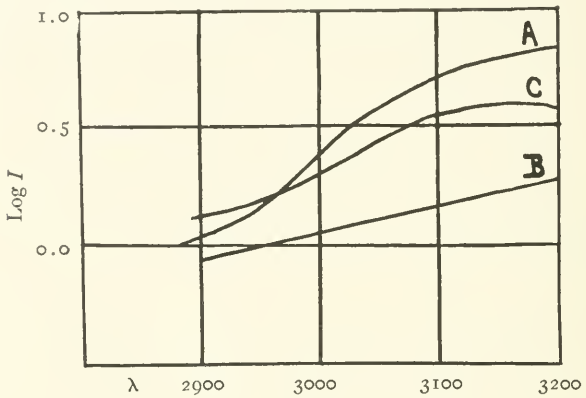


FIG. 4

Furthermore, the radiation of the crater of the arc is that of a black body at 3750° Abs. Its energy-curve as a function of the wave-length is known, being given by the equation

$$\log I = -5 \log \lambda - \frac{1.673}{\lambda}.$$

It is shown by the curve B of Figure 4. The difference of the ordinates of the curves A and B gives the value of the logarithm of the photographic intensity, for equal energy, for each wave-length; it is shown by curve C. If we now subtract the ordinates of curve C from the logarithms of the solar photographic intensities obtained before, we find for each ray the intensity that it would have in a normal spectrum expressed in units of energy. All of our results are summarized in Table X, which contains the values, already given, of the logarithms of the photographic intensities

of the rays before entering into the atmosphere, and then in logarithms and in numbers the intensity in energy of the same rays outside the atmosphere; furthermore, the logarithms of the total opacity of the atmosphere on the seventh of June for vertical rays; and finally the values as logarithms and numbers of the intensity in energy at the surface of the earth. The numbers in the last column show the extraordinary decrease of the intensity of the solar spectrum toward short wave-length at the base of our atmosphere:

TABLE X

λ	Outside the Atmosphere			Log. of Total Opacity of Atmosphere June 7	At the Surface of the Earth	
	Log. of Photo. Int.	Intensity in Energy			Intensity in Energy	
		Log I_0	$I_0\,10^{-4}$		Log I_1	I_1
3143	5.78	5.19	15.5	0.84	4.35	22400
3104	5.73	5.17	14.7	0.99	4.18	15100
3052	5.85	5.41	25.6	1.40	4.01	10200
3022	5.57	5.20	15.8	1.77	3.43	2700
2997	5.64	5.34	21.8	2.22	3.12	1320
2963	5.43	5.22	16.6	3.10	2.12	132
2956	5.41	5.21	16.2	3.33	1.88	76
2946	5.31	5.13	13.5	3.73	1.40	25
2936	5.31	5.15	14.1	4.12	1.03	11
2931	5.25	5.10	12.6	4.36	0.74	5.5
2922	5.30	5.16	14.5	4.82	0.34	2.2
2917	5.16	5.02	10.5	5.08	9.94	0.87
2912	5.00	4.87	7.4	5.39	9.48	0.30
2906	4.52	4.40	2.5	5.78	8.62	0.04
2898	4.76	4.65	4.5	6.36	8.29	0.02

between λ 3143 and λ 2898 the ratio of the intensities is about a million for the sun at the zenith. This great fall in intensity is not due to a diminution in the emission of the sun, but to the almost complete opacity for the short wave-length of our atmosphere, which does not permit the passage of more than one part in two millions of the radiation at λ 2898.

We see that aside from certain irregularities due to the presence of very many lines of solar origin, there is no evidence of any low point in the intensity in the region the best studied from λ 3143 to λ 2922. Beyond, from λ 2917 to λ 2898, the measures are less sure and they only show that it is not a very rapid falling off. Hence it is certain that the limitation of the spectrum does not

exist outside our atmosphere and that it is not due to an absorption having its origin in the solar atmosphere.

A comparison of the intensities of the radiations emitted by the center and the edge of the solar disk tends to confirm this conclusion. We have established the fact that the spectrum of the limb is about two times less intense than that of the center, without any appreciable difference from one end to the other of the spectral region studied; there should be a weakening more and more marked toward short wave-lengths, if the strata of the solar atmosphere were responsible for the limitation of the spectrum.

10. *Daily variation in the quantity of ozone.*—The method explained above gives the quantity of ozone in absolute units. It has the inconvenience of requiring a long series of exposures

TABLE XI

	λ 3143	λ 3104	λ 3052	λ 3022	λ 2997	λ 2956	λ 2946	λ 2936	λ 2931	λ 2922
Log I June 10.....	5.30	5.13	4.72	4.04	3.55	1.93	1.51	0.97	0.74	0.30
Log I June 21.....	5.35	5.17	4.84	4.15	3.80	2.24	1.94	1.54	1.31	0.84
Difference.....	0.05	0.04	0.12	0.11	0.25	0.31	0.43	0.57	0.57	0.54

in the course of a day, where the measures and computations are complicated. A method of comparison permits the study of the variation of the quantity of ozone by a single exposure made at noon each day.

An exposure is made under identical conditions on one and the same plate each day; once we also make a further exposure through a filter in order to have the necessary data for calibrating the plate. We thus obtain on a single plate the data relative to a score of different days. Thus we may deduce the values of the photographic intensities of the different rays for corresponding days. If the quantity of ozone should remain constant from one day to another, all the radiations would be modified in the same ratio by the effect of a change in the haziness. It is not so, however, for the distribution of intensities in the spectrum undergoes great changes from one day to the other. We give as an example those of June 10 and 21, 1920. Table XI gives for noon of these two days the logarithms of the photographic intensities of the different rays.

We see that the intensities are almost the same for λ 3143 and that the differences increase regularly so that at λ 2922 the spectrum is nearly three times weaker on June 10 than on June 21. The thickness of ozone traversed is thus notably greater on the tenth than on the twenty-first; as the zenith distance is almost the same, it is necessary to conclude that a greater quantity of ozone was present in the atmosphere.

We may further calculate for each day the quantity of ozone. Let I and I' be the intensities of the two radiations measured on the plate. We know further their intensities outside the atmosphere, I_0 and I_0, as given in Table X. The coefficients of absorption of the ozone are α and α' and those of the weakening by molecular diffusion are β and β'; finally the haze produces the same weakening, δ, on the two rays. We may write the two relations:

$$\log I = \log I_0 - (\alpha x + \beta) \sec z - \delta$$

and

$$\log I' = \log I_0' - (\alpha x + \beta') \sec z - \delta.$$

In order to eliminate δ we subtract member from member, whence we obtain:

$$x = \frac{(\log I' - \log I) - \log I_0' - \log I_0) - (\beta - \beta') \sec z}{(\alpha - \alpha') \sec z}.$$

We may thus combine any two rays whatever, but it is evidently desirable to choose two separate radiations among those measured under good conditions. For λ 2931 and λ 3104 the preceding formula becomes:

$$x = \frac{\log I' - \log I - 0.64}{10.1 \sec z} - 0.01.$$

Table XII gives for some of the days of May and June, 1920, values of x, the thickness of pure ozone, reckoned along the vertical in cm and at normal pressure:

These variations are evident. The other determinations made in the summer of 1919 led to the same result with variations of the same order. These changes appear irregular and of short period; in so short an interval as we have been able to follow them, we have not been able to notice any relation between them and the atmospheric conditions. It would be interesting to observe them

in a continuous manner, a task which would not present any difficulty but could be undertaken only by an institution having a sufficiently large personnel.

11. *Localization and origin of the atmospheric ozone.*—We now know the quantity of ozone to be found in our atmosphere, but we do not know where it is situated. If distributed uniformly, its proportion by volume would be 4×10^{-7} or 0.4 cubic cm per cubic meter. This is much more than the amount found in the

TABLE XII

May 1920	Thickness cm of Ozone	June 1920	Thickness cm of Ozone
21.....	0.304	4.....	0.293
25.....	0.310	5.....	0.297
27.....	0.298	7.....	0.325
28.....	0.290	9.....	0.321
29.....	0.275	10.....	0.335
31.....	0.306	11.....	0.314
		21.....	0.286
		23.....	0.289

air near the surface of the earth and in the regions of the atmosphere which we can reach. The best determinations by the chemists give a very much smaller quantity. When we gave a brief summary of our first results in 1913[1] we suggested a method for studying the presence of ozone in the lower atmosphere. In 1918 R. J. Strutt[2] made the experiment, which consisted in studying the absorption of ultra-violet radiation of an artificial source between two stations separated by several kilometers. Strutt found that the mercury ray λ 2536 is transmitted to an appreciable extent through 6.45 km of air. If in that distance the air contained the proportion of ozone given above (0.4 cubic cm per cubic meter) the intensity of the ray would be reduced in proportion of $10^{33}:1$, so that it would have been absolutely unobservable. Hence it is perfectly certain that ozone is not distributed uniformly in the atmosphere.

It is furthermore highly improbable that the necessary quantity of ozone is situated in the stratum of air accessible to man. Observations of the solar spectrum made at very high altitudes have

[1] *Journal de Physique* (5), **3**, 196, 1913.

[2] *Proceedings of the Royal Society*, A, **94**, 260, 1918.

shown that its limits undergo only very small variations with altitude. Therefore it is necessary for us to locate the great part of the ozone in the most elevated strata, possibly above 50 km. It is easy to explain its presence in this region, because we know that oxygen is transformed into ozone by radiation from the very short waves, shorter than λ 2000. The presence of these rays in the radiation emitted by the sun is very probable, because we do not see any limitation of the spectrum in the region we have studied. These rays should therefore ozonize the atmosphere, but being strongly absorbed by oxygen, are not able to penetrate very far and act only upon the very first strata. The ray λ 1800 is completely absorbed by a dozen meters of air at ordinary pressure; it is therefore incapable of penetrating at an altitude of less than 40 km. Hence it is not astonishing that the ozone should not be formed in the strata accessible to us. Furthermore, the rays between λ 2000 and λ 3000 decompose ozone. A state of equilibrium is established between these opposing actions, and the quantity of ozone which exists depends upon the relative proportion of the intensities of these two spectral regions. The variations observed in the quantity of ozone may have as their principal cause the variations in the solar radiation and in particular the region of exceedingly short rays, which unfortunately is not observable.

It would be interesting to follow the variations of the ozone through the solar period and further, in a set of daily observations, to compare them with measures of the solar constant which has been found by Abbot to vary. If an extensive collaboration was possible, as has been undertaken for other phenomena, it would be interesting to follow these observations at different points on the surface of the earth.

We might be able to obtain some idea as to the altitude of the stratum of the ozone by the following method. In consequence of the curvature of the earth, the law for sec z, which gives the thickness traversed, is no longer exact when the zenith distance is large. The complete law involves the altitude of the absorbing strata. By comparing the theoretical law with the results of observation, it might be possible to get an idea of the altitude at which absorption takes place. It would be necessary for that to make measures almost to the horizon; here it would not be possible

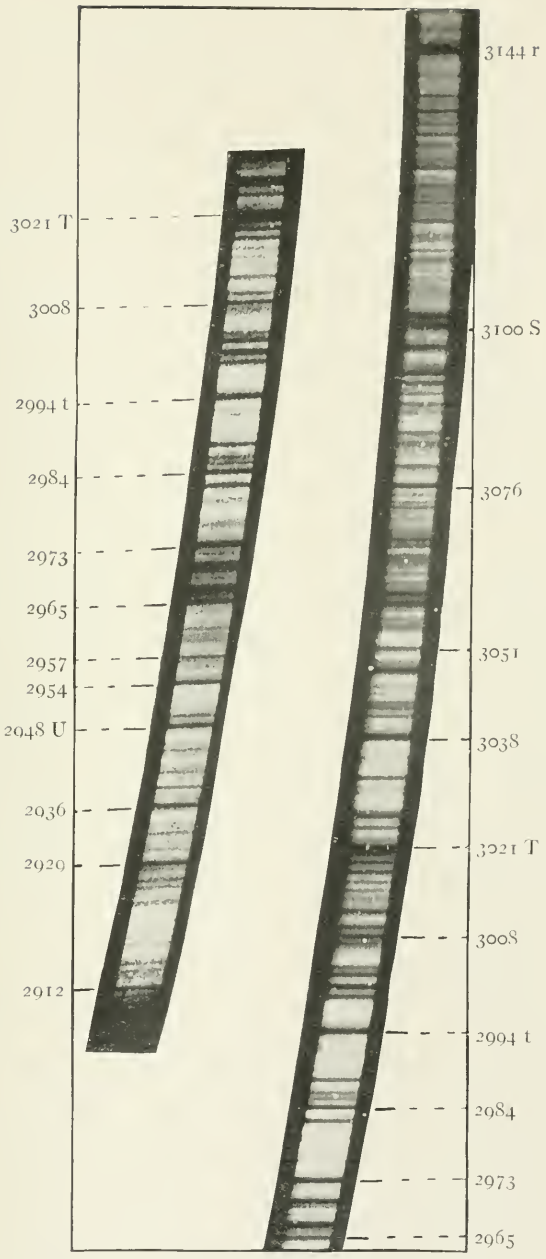
to use the region at λ 3000, which is totally suppressed before the sun has reached the horizon. We might employ the weak bands of ozone in the region λ 3300, the presence of which has been brought out by Fowler and Strutt in the spectrum of the stars and of the sun when near the horizon.

12. *Photographic map of the extremity of the solar spectrum.*— It seemed to us to be desirable to obtain a photographic map of the extremity of the solar spectrum. We do not know enough about this. Rowland's map stops at λ 3075, but that region is much disturbed by the superposition of the spectrum of another order. The map by Higgs, which is better in that region, does not go beyond λ 3000. Cornu published a drawing which extended to λ 2920, based on the photographs made by Simony at the Pic of Teneriffe, but such a drawing does not have the same authentic value as a direct reproduction. We have succeeded in obtaining a plate which has in all that part of the spectrum a suitable exposure in spite of the great variation in the intensity, by varying the exposure time along the region of the spectrum. For this purpose a shutter, movable by hand by a micrometer screw, was displaced in the focal plane of the first spectroscope in accordance with a law experimentally determined for making the impression almost uniform through the whole spectrum. This shutter was moved toward short wave-lengths, so as to occult successively the different regions of the spectrum; in this way, in going from λ 3020 to λ 2930, the time of exposure varied in the ratio of from 1:1000. We made thus two plates, one containing the region from wave-lengths shorter than λ 3022, the other extending from λ 3000 to λ 3150. Plate III gives a positive reproduction of these two spectra, enlarged about 10 times. The original plates have been measured, and with the use of the iron lines in the solar spectrum as standards, we have obtained a table of wave-lengths between λ 2898 and λ 3050. This table will soon be published in the *Journal de Physique.*

University of Marseille
Faculty of Sciences
December 1920

322

PLATE III



Map of Ultra-Violet End of Solar Spectrum

STUDIES BASED ON THE COLORS AND MAGNITUDES IN STELLAR CLUSTERS

NINETEENTH PAPER: A PHOTOMETRIC SURVEY OF THE PLEIADES[1]

By HARLOW SHAPLEY and MYRTLE L. RICHMOND

ABSTRACT

Survey of photographic and photo-visual magnitudes of 821 stars in four square degrees in the Pleiades.—The photometric study of a region two degrees square, with Alcyone in the center, was undertaken to supplement Trumpler's study of the proper motions. The results of measurement of 30 photographs made with the 60-inch reflector, comprising a total of 290 exposures, are given in Table II. There are no abnormally large color-indices. This is the first star cluster for which *comprehensive data for dwarf stars* have been secured.

A detailed study of the proper motions of over a thousand stars in the neighborhood of the Pleiades by Dr. Trumpler has shown that the cluster contains in the central field of 4 square degrees about 200 members brighter than the fourteenth magnitude. The parallax of the Pleiades is of the order of 0".01; hence the absolute magnitudes of the main bulk of the cluster stars lie between +5 and +9. As this is one of the few stellar groups in which the color, frequency, distribution, and motions of dwarf stars can be investigated successfully, a study of the photographic and photovisual magnitudes was begun at Mount Wilson three years ago in order to supplement Dr. Trumpler's work on proper motion.

The comparison of the Mount Wilson magnitudes and colors with the work of other observers will be made in Trumpler's monograph, which will also include a full discussion of the structure of the system of the Pleiades.

For each catalogued magnitude the average number of images measured is approximately four, and the average probable error is of the order of 0.06 mag. Only the final results of the photometric work are given in the present paper. Information relating

[1] *Contributions from the Mount Wilson Observatory*, No. 218.

to the photographs, measures, and reduction for any individual star can be obtained by communicating with the Mount Wilson Observatory.

In order to cover with the 60-inch reflector a region 2 degrees square (Alcyone at the center), it was necessary to divide the area

TABLE I

PHOTOGRAPHS OF THE PLEIADES

Plate Number	Kind	Date	Fields
4072	S 27	1917 Oct. 12	19, 20, 21, 22, 23, 24
4073	S 27	Oct. 12	25, 26, 27, 28, 29, 30
4183	Iso	Nov. 11	20, 23, N. P.
4184	S 27	Nov. 11	20, 23, N. P.
4185	S 27	Nov. 11	23, 24, N. P.
4300	Iso	Dec. 20	13, 14, 15, 16, 17, 18
4301	S 27	Dec. 20	13, 14, 15, 16, 17, 18
4680	S 27	1918 Sept. 1	31, 32, 33, 34, 35, 36
4681	Iso	Sept. 1	31, 32, 33, 34, 35, 36
4682	S 27	Sept. 1	1, 7, 13, 19, 25, 31
4765	Iso	Nov. 1	12, 10, N. P.
4766	S 27	Nov. 1	12, 10, N. P.
4767	S 27	Nov. 1	10, 7, N. P.
4768	Iso	Nov. 1	7, 8, 9, 10, 11, 12
4769	S 27	Nov. 1	7, 8, 9, 10, 11, 12
4849	Iso	1919 Feb. 25	19, 20, 21, 22, 23, 24
4850	S 27	Feb. 25	1, 2, 3, 4, 5, 6, N. P.
4851	Iso	Feb. 25	6, 3, N. P.
4852	S 27	Feb. 25	6, 3, N. P.
5026	S 30	July 23	6, 12, 18, 24, 30, 36, N. P.
5027	S 30	July 23	36, 33, N. P.
5043	Iso	Aug. 22	25, 26, 27, 28, 29, 30
5056	Iso	Sept. 21	1, 2, 3, 4, 5, 6
5118	Iso	Oct. 31	6, 12, 18, 24, 30, 36
5154	S 30	Dec. 18	15, 16, 22, N. P.
5155	S 30	Dec. 18	21, 22, 27, 28, N. P.
5607	Iso	1920 Sept. 14	28, 22, 21, N. P.
5608	S 30	Sept. 14	22, 21, N. P.
5609	S 30	Sept. 14	21, 15, 16, 22
5610	Iso	Sept. 14	22, 16, 8, 2, 20, 26

into 36 equal fields, the centers of adjacent fields being separated by about 20′.

The scales of the photographic and photovisual magnitudes were determined by comparison of these fields with the North Polar standards[1] and with each other. The list of photographs in Table I shows how the various fields were intercompared and connected with the Pole. Each plate was given two separate exposures

[1] Seares, *Mt. Wilson Contr.*, No. 97; *Astrophysical Journal*, **41**, 206, 1915.

to each of three or more fields, with exposure times of one minute and five minutes, respectively, for photographic and photovisual magnitudes. Yellow filter C was used with the isochromatic plates (Cramer Instantaneous). The measures and reductions were made according to the methods generally used for photometry at Mount Wilson.

The photometric catalogue, Table II, contains in the first three columns the number in Trumpler's forthcoming catalogue and the abbreviated positions for 1900.0 from the same source. The fourth and fifth columns contain the photographic magnitude and color index determined at Mount Wilson. In the sixth column the first number for each star refers to photographic plates, the second to photovisual plates.

All stars brighter than 11.0 photographic, or 10.0 photovisual, are omitted from our catalogue. Those stars whose magnitudes are disqualified by the proximity of the photographic images of other stars are also omitted. A few of the stars catalogued are probably variable; the data relative to them will be published by Trumpler.

The color indices of 753 stars are given in Table II; five of them are negative; only two exceed +2.00. For 26 stars there are photographic magnitudes, but no color indices; for 42 stars there are photovisual magnitudes only. The total number of stars in our catalogue is 821.

TABLE II

Catalogue of 821 Stars in the Pleiades

Trumpler No.	R.A. 1900	Decl. 1900	Pg. Mag.	C.I.	No. of Plates
	3^h37^m				
1	6^s3	24°41′.3	14.54	0.35	3,3
3	7.9	24 29.3	11.89		1,.
4	8.5	24 47.7	13.17	1.61	1,1
5	11.0	24 33.0	14.00	0.49	4,1
9	12.6	23 1.4	14.14	0.63	2,1
10	16.0	22 50.4	13.61	1.06	2,1
11	16.8	23 36.8	14.30	0.72	2,2
12	16.9	23 17.2			1,1
13	17.1	23 51.4	13.02	1.07	1,1
14	17.8	24 46.5	13.73	0.73	3,3
16	20.1	23 16.0	13.04	1.94	1,1
17	20.3	24 29.6	14.72	0.47	4,1
18	21.0	23 14.7	13.67	0.59	1,1
19	22.7	23 56.1	14.43	1.71	1,1
20	22.8	24 5.8	12.52	0.38	1,1
21	23.0	22 55.7	13.24	1.53	2,1
22	23.2	24 39.9	14.39	0.85	3,3
23	23.7	23 32.5	14.29	0.54	3,3
24	24.2	24 22.2	14.55	1.15	1,1
25	25.3	23 16.7	14.09	0.39	1,2
26	25.5	24 10.1			.,1
27	25.7	23 42.8	13.94	0.54	2,2
28	26.5	24 31.1	14.27	1.05	4,3
29	27.5	22 56.8	13.68	0.73	2,1
31	28.7	24 18.0	14.03	1.01	4,4
32	28.9	22 58.3	12.12	1.62	2,1
33	29.7	23 21.2			.,1
34	30.4	22 54.5			2,1
35	34.2	24 38.6	14.42	0.64	4,3
36	34.3	24 20.1	12.23	0.47	1,1
37	36.8	23 21.4	11.04	0.34	1,2
38	37.4	24 27.8	14.90	1.37	4,4
39	37.5	24 16.5	14.49	0.62	1,1
40	37.7	24 16.2	14.52	0.80	1,1
41	39.0	23 26.7	11.94	0.65	3,3
42	39.1	24 36.1	12.66	1.26	4,3
43	40.6	22 52.3	14.63	1.68	1,1
44	42.0	24 25.4	14.03	0.23	1,1
45	42.1	24 32.4	12.58	0.43	4,3
46	42.9	23 13.1			.,2
48	44.9	22 56.8	13.15	0.39	2,1
49	45.1	23 28.3	14.40	0.50	3,3
52	46.9	24 45.7	14.18	1.80	3,3
54	49.0	24 39.0	12.18	0.87	4,3
55	49.5	24 38.4	13.43	0.36	4,3
56	50.0	24 41.2	12.34	0.67	3,3
57	52.0	23 43.3	12.16	0.72	2,2
58	53.3	22 53.7	11.42	1.26	2,1
59	53.6	24 44.7	14.14	0.45	3,3
60	54.2	23 55.8	11.76	0.36	1,1
61	56.5	23 14.6	15.12	1.14	1,2
62	57.0	22 56.3	13.61	1.56	2,1
63	57.2	23 2.8	11.70	0.87	2,1
66	58.2	24 44.4	14.71	0.74	3,3
67	58.3	23 22.8	13.46	0.54	1,2
68	58^s9	23°56′.0	11.09	0.99	1,1
69	59.3	23 26.1	13.24	0.61	3,4
71	59.8	24 12.9			.,1
	3^h38^m				
72	2.0	23 55.8	13.85	0.41	1,1
73	2.3	24 8.3	12.29	0.27	1,2
76	3.2	23 49.8	11.62	1.27	2,3
77	4.1	23 53.1	11.79	0.47	1,1
78	5.2	22 54.6	13.86	0.81	2,1
79	5.6	23 13.6	11.32	−0.08	1,2
82	7.0	23 48.9	14.18	0.54	3,3
83	7.0	23 55.6	13.07	0.31	1,1
84	7.1	23 17.0	13.07	0.74	1,2
85	7.5	23 52.3	13.07	−0.09	1,1
86	8.1	24 25.9	13.75	0.67	1,1
87	8.1	24 41.2	13.97	0.69	3,3
88	8.1	23 45.4	14.34	0.47	3,2
89	8.2	23 57.6	12.08	0.32	1,1
90	8.5	24 4.8	14.09	1.37	1,1
91	9.2	24 1.6	13.95	0.51	1,1
92	9.7	24 1.2	14.03	0.59	1,1
93	10.4	24 12.2			.,1
94	13.4	23 55.8			.,1
95	15.0	24 25.2	11.65	0.41	1,1
96	15.2	24 18.4	14.63		1,.
97	15.8	24 14.4			.,1
98	16.1	24 27.8			2,2
99	16.2	24 5.2	11.20	0.70	1,1
100	16.6	23 3.8	12.15	0.82	2,2
101	16.6	23 43.0	12.64	0.62	2,2
102	16.6	24 45.4	12.33	1.09	3,3
103	17.0	23 42.9	12.28	0.58	2,2
106	20.0	23 57.4			1,1
107	21.5	22 51.3	12.91	0.58	2,1
108	22.2	24 28.8	11.04	0.31	1,2
111	22.5	22 49.2	13.80	0.92	2,1
112	22.5	24 14.5			.,1
113	22.7	24 27.4	11.55	0.93	2,2
114	22.9	23 56.7	12.26	0.06	1,1
115	24.1	24 27.2	14.14	0.87	2,2
117	25.6	23 12.1	13.88	1.07	1,1
119	27.4	24 6.6	13.53	1.39	1,1
120	28.4	23 21.1	12.13	0.85	1,1
122	28.9	24 16.4			1,2
123	32.0	24 23.9	13.85	0.37	1,1
124	34.8	23 3.8	14.09	0.17	1,1
124a	34.9	23 3.9	14.89	0.49	1,1
125	38.4	23 22.4	13.71	0.84	1,2
126	38.5	24 43.4	14.21	0.49	5,5
127	39.0	24 38.8	14.41	0.71	5,5
128	39.1	23 24.4	13.64	0.57	1,1
129	39.1	23 44.8	13.22	1.80	2,2
129a	39.3	23 41.2	15.68	1.48	2,1
130	42.2	24 11.7	11.89	0.76	1,1

TABLE II—*Continued*

Trumpler No.	R.A. 1900	Decl. 1900	Pg. Mag.	C.I.	No. of Plates
	3^h38^m				
131....	42.8	24°30'.2			.,1
132....	44.7	24 5.0	12.42	0.62	2,2
133....	44.9	23 2.9	14.02	0.62	2,1
134....	45.2	23 58.2	13.81	0.55	4,3
135....	45.8	24 35.3	14.64	0.49	5,3
136....	46.2	24 44.6	13.90	0.58	4,3
137....	47.3	23 55.0	12.11	0.64	4,3
138....	48.6	24 24.9	13.41	1.29	2,1
140....	51.9	24 35.8	14.50	1.14	4,3
141....	52.6	24 34.4	14.12	0.62	3,3
142....	52.7	23 50.8	13.24	1.78	3,2
143....	52.9	23 44.3	13.28		1,.
144....	53.2	24 6.1	14.95	0.84	3,2
145....	53.3	23 16.4	11.13		1,.
146....	55.0	23 4.5	14.11	0.75	2,1
147....	55.7	24 37.7	14.20	0.63	3,3
150....	57.0	24 24.9	14.03	0.91	1,1
151....	57.9	23 36.4	11.62	0.71	2,1
152....	58.7	24 28.4	13.04	1.12	1,3
153....	59.3	24 7.1	11.02	0.60	3,3
154....	59.9	23 3.2	13.95	0.64	3,1
	3^h39^m				
154a....	0.7	23 46.5	14.90	1.33	4,2
155....	2.4	23 38.0	14.84	1.11	1,1
156....	3.7	24 16.2	13.52	1.80	1,1
157....	5.3	23 46.6	14.12	0.56	4,2
157a....	6.9	23 9.4	14.94	1.26	1,2
158....	7.5	23 31.5	13.11	1.30	1,1
159....	8.4	24 40.3	14.61	0.79	2,2
160....	8.5	23 4.8	13.98	0.53	4,2
161....	9.0	24 43.0	12.82	0.40	2,2
164....	10.4	24 27.4	14.00	0.36	2,3
165....	10.9	24 21.6	13.98	0.54	1,1
167....	12.7	24 10.2	11.56	0.43	2,1
167a....	12.8	24 28.9	15.60	1.26	3,2
168....	14.8	24 46.4	14.49	0.74	2,2
169....	15.1	23 34.8	13.44	0.92	1,1
170a....	16.0	24 30.7	15.74	1.16	2,2
171....	16.1	23 48.6	12.86	1.26	3,2
172....	16.9	24 43.1	14.36	0.62	2,2
173....	17.1	24 37.2	13.25	0.62	2,2
174....	18.2	22 58.9	13.03	0.85	3,1
175....	18.4	24 9.7	15.00	1.42	2,3
176....	19.3	24 34.4	12.45	0.38	2,2
178....	19.8	24 24.6	12.20	0.36	1,1
179....	22.0	24 33.4	14.02	0.49	2,2
181....	22.6	23 50.3	13.68	0.49	3,2
182....	22.8	24 40.5	14.64	0.69	2,2
183....	23.1	23 51.9	11.23	0.39	3,2
184....	23.5	24 18.4	14.60	0.65	1,1
185....	24.1	23 47.6	14.42	0.71	4,2
186....	25.6	23 24.8	13.22	0.70	2,3
187....	3^h39^m 25.9	24°34'.3			2,2
188....	26.1	24 25.1	14.81	0.84	1,1
189....	27.2	24 24.8	14.66	1.00	1,1
190....	27.2	23 9.5	13.15	0.67	1,2
192....	29.5	23 45.3	14.05	0.59	4,2
193....	29.5	23 10.3	12.58	0.67	1,2
194....	29.7	24 12.6	14.32	0.79	1,1
196....	30.4	24 18.0	14.12	0.72	1,1
197....	31.1	23 7.0	12.90	0.82	4,3
199....	32.5	23 55.8	13.80	1.46	3,2
200....	33.0	22 48.0	13.12	0.94	3,1
201....	33.0	22 56.6	13.82	0.98	3,1
202....	33.2	23 5.1	13.00	0.64	4,3
203....	33.9	23 26.8	14.80	1.22	2,3
204....	35.1	24 42.2	14.09	0.69	2,2
205....	35.8	23 33.4	13.98	1.06	1,1
206....	36.0	23 59.4	14.02	0.96	3,2
207....	36.0	23 18.4	13.83	0.80	1,2
207a....	37.0	23 41.5	15.98	1.38	1,1
209....	38.1	22 57.2	13.98	0.58	3,1
210....	38.4	24 35.3	11.84	1.07	2,2
211....	38.8	24 11.2	12.54	0.48	1,1
212....	38.8	23 36.8	13.92	0.64	1,1
213....	39.0	23 46.2			4,2
214....	39.8	23 2.5	14.18	0.78	3,1
216....	41.2	23 36.0	13.98	0.83	1,1
217....	42.5	24 18.8			1,1
218....	43.7	24 36.3	14.16	0.63	2,1
220....	43.7	23 26.5	13.38	1.18	2,3
221....	43.8	24 35.6			2,2
222....	43.8	24 44.6	14.32	1.07	2,2
223.....	44.5	23 58.5			2,2
224....	44.6	24 7.1	12.12	0.82	4,3
225....	46.5	23 57.4	12.64	0.68	3,2
226....	46.7	24 24.0	12.48	1.45	1,1
227....	47.1	24 40.4	12.84	0.86	3,2
228....	47.7	23 54.4	11.46	0.48	3,2
228a....	47.7	23 45.7	15.20	0.69	2,1
229....	50.3	24 33.9	13.59	0.64	2,2
230....	51.2	23 11.2			1,1
232....	52.5	24 6.8	12.12	1.18	4,2
236....	55.3	23 18.4	13.44	1.14	1,2
237....	56.2	24 41.2	14.94	0.64	3,3
238....	56.3	24 29.3	12.93	0.68	1,2
239....	56.7	23 7.1	12.44	0.24	1,2
241....	57.8	23 56.3	13.75	1.84	3,2
241a....	59.9	23 8.6	14.70	1.20	1,2
	3^h40^m				
242....	0.1	22 49.8	13.85	1.01	4,1
243....	0.5	24 3.8	14.11	0.61	3,2
244....	0.7	24 44.3			2,2
244a....	1.8	24 12.8	15.04	0.80	1,1
245....	4.0	24 31.6	12.84	0.50	3,2
246....	4.1	24 6.6	14.29	0.66	1,1
248....	7.7	23 43.9	12.52		2,.
249....	7.1	23 25.5			.,2
250....	7.3	24 40.8	11.10	0.64	2,3
251....	7.6	24 42.3	11.02	0.12	3,3

TABLE II—*Continued*

Trumpler No.	R.A. 1900	Decl. 1900	Pg. Mag.	C.I.	No. of Plates	Trumpler No.	R.A. 1900	Decl. 1900	Pg. Mag.	C.I.	No. of Plates
	3^h40^m						3^h40^m				
252....	7.9	24°26.0	14.40	1.25	2,1	317....	40.0	22°48.1	14.35	0.44	2,1
253....	8.9	24 15.3	14.03	1.41	1,1	318....	40.1	24 1.9	12.89	0.71	2,2
254....	9.0	24 34.2	14.30	0.89	3,3	319....	40.1	24 38.9	11.12	0.69	1,2
255....	9.1	24 31.7	13.96	0.78	2,2	321....	40.4	24 37.7	14.20	1.08	2,2
257....	9.3	24 15.0	14.66	1.19	1,1	322....	41.3	24 12.6	14.52	0.96	1,1
258....	9.4	22 59.8	14.11	0.99	4,1	323....	41.7	24 30.5	13.76	0.61	2,3
259....	9.4	24 33.3	12.88	0.74	2,3	324....	41.8	23 28.6			2,2
260....	9.9	22 47.8	14.08	1.04	2,1	325....	42.0	24 35.4	14.04	0.51	2,2
261....	10.9	24 36.3	13.98	1.12	3,3	326....	42.3	23 41.0	13.58	0.95	2,1
262....	10.9	24 37.1	13.85	0.53	3,3	328....	42.7	24 2.4	13.77	0.26	2,2
263....	11.4	24 35.8	14.46	1.08	3,3	329....	42.9	23 43.1	12.80	0.43	2,1
264....	11.4	24 19.3	14.07	0.73	1,2	330....	45.0	23 11.2	12.83	0.52	1,1
265....	11.6	23 44.9	11.28		2,.	332....	46.5	24 37.1	13.75	0.63	2,2
266....	11.6	22 54.4	11.25	0.88	4,1	333....	46.6	23 56.7	14.20	0.79	2,2
267....	12.9	22 49.2	13.20	1.59	2,1	333*a*....	46.7	23 56.7	15.29	1.07	2,2
268....	14.0	24 18.6	12.51	0.70	2,2	334....	47.2	24 0.1	10.92	0.28	2,2
269....	15.0	22 59.4	14.64	1.17	2,1	335....	47.3	23 1.8	14.06	0.30	2,1
271....	15.7	22 49.4	13.96		2,.	336....	47.5	24 19.0	14.17	0.18	1,1
272....	16.3	24 43.8	13.74	0.70	3,3	339....	49.0	24 17.5	14.47	0.74	1,1
274....	17.2	23 53.3	13.85	0.65	2,4	340....	49.3	24 35.3	14.28	0.55	2,2
275....	17.5	24 18.7	14.75	1.28	2,1	341....	49.6	23 30.9	13.47	0.32	2,1
276....	17.7	24 45.0	14.19	0.63	3,2	342....	50.5	24 14.9	13.41	0.19	1,1
277....	17.8	22 53.8	14.03	0.88	3,1	343....	52.3	22 50.5	12.48	0.89	2,1
278....	18.4	22 49.0			.,1	344....	54.5	24 39.2	13.85	0.41	1,2
280....	19.2	23 40.4	13.79	0.61	2,1	344*a*....	55.2	24 13.3	14.84	0.42	1,1
282....	20.4	24 33.5	12.30	0.66	1,1	345....	55.6	23 51.7	14.43	0.53	2,2
283....	20.7	24 30.6	13.35	0.39	1,1	347....	56.6	24 36.6	11.90	0.71	2,2
283*a*....	21.0	23 36.4	15.35		3,.	348....	56.6	24 29.2			.3
283*b*....	21.9	24 1.2	14.55	0.73	2,2	349....	57.7	22 53.9	11.52	0.99	2,1
285....	22.8	23 10.5	11.55	0.65	1,1	350....	58.3	23 16.4	11.00	0.22	1,1
							3^h41^m				
287....	23.5	23 43.4	13.58	0.30	2,1	350*a*....	0.3	24 10.5	15.18	0.88	3,3
287*a*....	23.5	23 36.3	14.87	0.51	2,1	351....	0.5	23 30.4	13.66	0.51	2,1
288....	24.5	23 12.5	13.17	0.76	1,2	352....	1.3	24 46.6	13.45	1.29	1,1
289....	25.0	24 15.5	11.00	0.36	1,1	353....	1.6	22 59.8	13.98	0.76	2,1
290....	25.1	24 38.4	14.05	0.37	2,2	355....	2.4	23 46.7	12.60	0.34	4,3
291....	27.0	24 3.0	13.52	0.71	2,2	356....	2.4	24 4.4	11.30	0.40	2,2
292....	27.2	24 42.3	11.80	1.62	2,2	357....	2.6	24 1.2	12.68	1.36	2,2
293....	27.5	24 38.1	13.58	0.40	2,2	358....	4.0	23 40.3	12.69	0.85	2,1
294....	29.5	23 0.6	11.62	1.20	2,1	359*a*....	5.5	23 33.8	14.41	0.02	2,1
296....	31.0	24 7.4	11.51	0.33	1,2	360....	5.8	24 19.5	12.29	1.90	1,1
297....	32.4	23 16.9	13.56	0.90	1,2	361....	6.1	23 11.1	12.39	0.96	1,1
298....	32.8	23 3.8	14.15	0.59	2,1	362....	6.7	22 57.5	14.12	0.70	2,1
299....	33.3	24 44.8	13.68	0.70	2,2	363....	7.0	22 49.6	13.86	0.58	2,1
300....	33.7	23 4.0	14.34	0.68	2,1	364....	7.1	23 23.8	14.12	0.32	1,1
302....	34.4	22 47.6	14.06	0.54	2,1	366....	10.2	24 33.6	12.67	0.39	1,2
303....	34.5	24 1.3	13.74	0.26	2,2	367....	10.4	23 7.4	13.92	0.44	2,2
304....	34.7	24 0.7	13.93	0.27	2,2	368....	10.6	24 12.9	14.01	1.07	1,1
305....	34.9	24 36.9	14.38	0.06	2,2	369....	11.0	23 24.3	12.87	0.56	1,1
305*a*....	35.4	23 58.2	15.36	0.90	2,2	370....	11.9	23 10.2	13.79	0.41	1,1
306....	35.6	22 52.3	12.32	0.55	2,1	370*a*....	12.8	23 24.0	14.32	1.10	1,1
306*a*....	35.6	23 40.3	14.59	1.03	2,1	371....	12.9	24 46.3	14.79	0.77	1,1
307....	36.1	23 33.0	11.41	0.08	2,1	373....	13.2	24 48.4	11.52	0.30	1,2
308....	36.4	24 16.6	14.21	0.41	1,1	374....	13.3	24 7.5	14.07	0.56	3,3
309....	37.4	23 49.6	12.23	0.32	3,2	375*a* ...	14.3	23 44.0	14.59	0.34	2,2
310....	37.5	23 32.1	13.41	1.07	2,1	376....	14.3	23 53.6	14.16	0.34	2,2
312....	38.7	24 27.5	13.86	0.10	1,2	377....	16.0	24 29.4	14.75	0.77	2,1
313....	38.8	23 39.0	11.90	−0.06	2,1	378....	17.7	23 24.2	13.17	0.68	1,1
314....	38.8	23 29.3	13.78	0.58	2,2	379....	18.0	23 48.4	13.86	0.48	4,3
315....	38.8	23 40.7	13.37	0.62	2,1	380....	18.3	23 53.0	13.03	0.59	2,2
316....	39.7	24 26.2	12.70	0.52	1,1	382....	20.4	23 30.5	11.50	0.83	2,1

TABLE II—*Continued*

Trumpler No.	R.A. 1900	Decl. 1900	Pg. Mag.	C.I.	No. of Plates	Trumpler No.	R.A. 1900	Decl. 1900	Pg Mag.	C.I.	No. of Plates
	3^h41^m						3^h41^m				
383....	20.7	24° 4′.8	13.62	0.86	2,2	451....	57.0	23°29′.0	13.85	0.50	3,2
384....	20.9	23 36.2	12.44	1.42	3,2	452....	58.0	23 30.8	13.80	0.78	2,2
385....	21.2	24 8.6	12.96	1.06	3,3	453....	58.3	23 59.6	13.96	0.42	4,5
385*a*....	21.2	23 47.4	15.17	0.83	3,3	454....	58.8	24 42.2	11.77	1.01	4,3
386....	21.4	24 19.9	13.93	0.25	3,2	455....	59.0	22 54.2	14.26	0.40	3,2
388....	21.8	22 56.5	13.99	0.71	4,1	456....	59.0	24 27.2	13.34	0.74	4,3
389....	22.4	24 33.8	13.39	0.68	4,2	457....	59.2	23 22.8	13.72	1.05	2,3
390*a*....	22.6	23 38.4	14.66	0.62	3,1	458....	59.8	23 7.7			.,4
392....	23.2	23 41.5	13.92	0.72	3,2						
393....	23.5	24 39.3	14.82	0.75	5,3		3^h42^m				
394....	24.1	23 0.2	13.87	1.35	4,1	459....	0.0	23 23.2	11.96	0.23	2,3
396....	24.3	23 46.2	13.75	0.73	3,3	460....	0.1	24 1.2	14.25	0.49	4,5
398....	26.1	24 44.6	13.98	1.15	5,3	461....	0.1	23 26.0	14.13	0.25	3,4
400....	27.5	23 14.6	11.18	0.24	3,3	462....	0.3	23 9.4	11.56	0.17	2,3
401....	27.7	23 36.3			.,1	463....	0.7	23 17.0	13.43	0.37	3,4
401*a*....	28.1	23 46.8	15.08	1.46	3,3	464....	0.7	24 25.8	13.88	0.67	4,2
403....	28.4	24 21.0	11.40	0.18	2,3	465....	0.8	24 26.0	13.90	0.22	4,2
404*a*....	28.5	23 35.3	14.83	0.81	1,3	466....	1.4	24 25.4	14.51	0.93	3,2
405*a*....	28.7	24 16.6	15.28	0.49	4,1	467....	1.5	23 7.5	12.76	0.28	4.4
406....	29.3	24 37.0	15.06	1.39	5,4	468....	1.5	22 53.0	11.58		2,.
407....	29.4	24 11.9	13.82	0.48	3,2	469....	1.6	23 40.8	13.85	0.46	3,3
408....	29.8	23 19.2	13.43	1.24	3,2	470....	1.8	23 16.7	13.94	1.05	3,4
409....	30.4	23 13.9	11.92	1.22	3,3	471....	2.1	22 53.2	13.96	0.73	3,1
411....	31.2	24 14.8	12.30	1.70	4,3	473....	2.7	23 7.0	14.31	0.42	4,4
415....	33.5	23 38.6	13.89	0.96	4,3	475....	4.6	23 34.2	12.49	1.14	2,2
416....	34.0	24 14.9	14.56	0.60	4,2	476....	5.1	23 46.7	13.51	1.53	5,5
417....	34.2	24 46.2	14.32	0.76	4,4	477....	5.6	23 20.1	11.94	0.26	2,3
417*a*....	34.5	24 0.2	15.62	0.96	2,3	478....	6.0	24 17.4	14.60	0.36	4,2
418....	34.7	24 29.1			1,1	479....	7.0	24 33.4	11.28	−0.12	3,2
419....	34.8	24 17.7	14.76	0.51	4,2	481....	8.1	24 36.0	14.90	0.52	3,2
420....	35.6	24 22.5	13.92	0.96	4,3	482....	8.4	23 45.8	13.52	1.24	3,5
421....	36.2	23 39.4	14.14	0.28	4,3	483....	9.4	24 9.9	12.67	0.59	6,5
422....	36.4	24 11.6	13.80	1.27	4,3	484....	9.5	23 4.4	11.04	0.88	1,2
423....	37.0	23 22.2	13.66	0.49	3,3	485....	9.5	24 8.6	14.54	0.21	6,5
424....	37.9	24 13.6	12.00	1.66	4,3	487....	11.0	24 34.7	13 28	0.36	3,2
425....	38.7	23 54.3	13.57	1.07	5,4	488....	11.2	23 33.4	12.56	0.24	2,2
426....	40.9	22 58.5	13.56	0.57	4,2	489....	11.2	23 25.7	14.21	0.25	3,5
428....	41.6	24 46.4	13.33	0.77	3,3	490....	12.1	23 56.3	13.05	0.45	3,3
428*a*....	42.7	23 9.5	14.42	1.10	3,3	490*a*....	14.2	23 8.1	14.53	0.57	2,4
429....	43.1	24 46.5	13.58	0.90	4,3	491....	14.3	24 47.4	12.99	0.31	3,2
430....	43.1	24 3.3	11.27	0.39	5,4	492....	16.1	23 41.4	13.78	1.88	2,2
431....	43.2	24 22.6	12.98	0.40	4,3	494....	18.6	22 56.6	12.42	0.40	2,1
432....	43.4	23 41.6	11.85	1.06	4,3	495....	18.6	24 44.4	11.22	0.04	3,2
433....	43.6	23 50.4	12.53	0.83	4,4	496....	19.2	23 20.6	12.94	0.99	2,3
434....	44.1	23 49.7	12.58	0.86	4,4	497....	19.5	23 59.1	13.39	0.53	3,3
435....	45.0	23 39.8	14.31	1.02	4,3	498....	19.7	22 51.7	14.12	0.03	2,1
436....	46.0	23 58.3	12.63	0.66	5,5	498*a*....	19.9	23 20.8	14.48	0.57	2,3
437....	46.3	24 21.7	14.56	0.33	4,2	499....	20.8	23 35.0	11.05	0.49	1,2
438....	46.5	22 48.2	12.88	0.22	3,2	500....	21.1	23 19.7			.,2
440....	46.9	24 22.3	13.38	0.17	4,3	501....	21.3	24 32.3	11.72	0.12	5,3
441....	52.8	24 22.2	14.15	0.32	4,3	502....	21.6	24 28.0	13.54	0.50	5,4
442....	52.9	24 15.7	13.60	0.36	4,3	503....	21.8	24 22.0	13.85	0.40	3,2
443....	53.2	24 33.4	14.68	0.57	3,2	504....	22.5	23 45.2	13.08	1.16	3,5
444....	53.4	22 54.6	11.64	0.28	3,2	505....	23.6	23 24.8	13.43	0.25	3,5
445....	53.7	24 3.4	12.47	1.01	4,5	507....	25.7	24 32.2	13.65	1.13	3,2
446....	55.5	23 6.0	13.48	0.64	4,3	508....	26.2	24 34.2	11.04	0.12	3,2
447....	55.5	24 27.8	14.20	0.59	5,3	509....	27.1	23 17.0	13.30	0.23	2,3
448....	56.1	23 38.0			1,2	510....	27.4	22 57.6	13.99	0.55	2,1
449....	56.7	24 47.7	13.45	0.39	3,2	511....	28.0	24 41.2	11.84	0.52	3,1
450....	56.9	24 16.0	14.30	0.60	4,3	512....	29.1	23 27.0	13.87	0.79	4.5

TABLE II—*Continued*

Trumpler No.	R.A. 1900	Decl. 1900	Pg. Mag.	C.I.	No. of Plates	Trumpler No.	R.A. 1900	Decl. 1900	Pg. Mag.	C.I.	No. of Plates
	3^h42^m						3^h43^m				
513....	$29^s.2$	24° 0′.0	12.34	0.11	3,3	575....	$0^s.4$	24°44′.9	14.41	0.58	4,3
514....	29.4	23 44.4			1,3	576....	0.9	23 21.6	13.98	0.38	2,4
515....	29.5	23 19.7	11.96	0.25	2,3	577....	1.7	23 57.6	14.35	0.85	4,5
516....	31.7	23 47.0	13.84	0.54	5,5	578....	3.1	23 34.7	13.18	1.39	4,3
517....	32.1	24 33.9	13.58	0.61	3,2	579....	3.3	24 24.4	13.74	1.05	2,1
519....	32.7	24 7.3	13.24	0.11	4,4	580....	3.6	22 53.7	12.40	0.76	4,2
520....	33.0	22 59.6	13.50	0.70	2,1	581....	4.0	23 39.0	14.63	1.11	3,3
521...	33.5	23 36.4	13.92	0.37	2,2	581*a*....	5.5	23 47.8	15.32	1.00	1,1
522....	33.8	23 58.0	12.39	0.94	3,3	582....	5.8	24 18.1	14.44	0.33	4,3
523....	34.8	24 21.0	13.18	0.22	3,2	583....	6.3	23 45.2	13.83	0.90	1,1
524....	35.6	24 45.5	11.24	0.10	3,2	584....	7.3	22 56.8	12.46	0.58	4,2
525....	35.7	23 18.5	13.94	0.99	2,3	585....	8.5	24 5.4	14.39	0.84	1,3
526....	36.6	23 36.1	13.42	1.04	2,2	586....	9.1	23 1.7	13.44	0.59	1,1
527....	37.2	23 46.3	14.25	0.97	3,5	586*a*....	9.8	23 43.9	14.49	0.00	1,1
529....	39.0	24 34.1	14.26	0.52	3,2	587....	9.8	24 10.3			.,1
530....	39.2	23 7.6			.,3	588....	9.9	23 28.5	11.03	0.70	1,1
531....	39.4	23 30.7	12.76	1.54	2,2	589....	10.0	23 20.8	13.89	0.97	1,3
532....	39.6	23 54.7	13.12	−0.03	3,3	590....	10.2	24 26.8			.,1
533....	39.6	24 28.4	14.47	0.99	4,3	591....	10.5	23 39.6	13.83	0.53	4,3
534....	41.4	24 22.5	11.96	0.08	3,2	592....	10.9	23 42.2	13.67	1.01	3,3
535....	42.7	24 8.8	12.34	0.45	4,4	592*b*....	11.2	24 1.0	14.49	0.05	1,2
536....	42.7	23 14.4	12.50	0.13	2,3	592*c*....	11.5	24 1.0	15.32	0.78	1,2
537....	42.8	24 27.9	13.66	0.40	4,3	593....	12.6	23 19.4	14.47	0.48	1,4
538....	43.2	23 0.7	13.40	0.63	2,1	595....	13.2	24 28.1			.,1
539....	43.4	24 37.4	14.12	0.43	3,2	596....	13.5	24 19.8			.,1
540....	43.4	23 28.2	13.18	1.30	3,5	597....	13.5	23 33.7	12.58	0.50	2,2
541....	44.8	22 59.5	12.54	0.27	2,1	598....	13.7	23 16.2	14.14	0.44	1,4
542....	45.2	24 1.4	12.26	0.99	3,3	600....	13.9	22 57.7	14.01	0.38	1,1
543....	45.2	23 28.4	13.76	0.50	3.5	601....	14.1	23 18.3	11.13	0.17	2,3
544....	45.6	24 10.5	13.96	0.18	3,2	603....	14.5	23 55.8	12.59	0.57	2,3
545....	45.9	23 31.6	14.27	0.37	2,2	604....	15.1	23 13.4	12.82	1.38	1,4
546....	46.0	24 0.9	14.08	0.97	3,3	605....	15.1	23 45.4	14.33	1.21	1,1
547....	46.8	24 23.7	14.15	0.33	3,2	606....	15.4	24 26.6			.,1
548....	47.7	23 34.8	13.40	0.26	2,2	608....	15.8	22 57.6	11.06		2,.
549....	48.6	24 1.2	13.29	0.36	3,3	609....	16.5	23 8.8	14.44	0.60	1,2
550....	48.7	22 52.9	14.24	1.01	2,1	610....	16.8	24 10.3	13.20	0.60	1,1
552....	49.1	23 50.4	14.18	0.46	3,3	612....	17.1	23 11.0	14.26	0.28	1,3
553....	49.4	24 27.4	14.52	0.50	3,2	612*a*....	18.2	24 2.2	15.51	0.87	1,2
554....	49.5	23 20.0	14.28	0.94	2,3	613*a*....	20.2	23 45.7	14.83	1.02	1,1
555....	49.6	22 53.2	14.23	0.30	3,1	614....	20.4	24 6.5	12.37	0.59	2,3
556....	50.0	24 14.2	14.35	0.49	3,2	614*a*....	21.1	23 50.2	14.90	0.40	1,2
557....	50.3	23 1.9	14.56	1.12	2,1	615....	21.9	23 56.8	12.96	0.82	2,3
558....	50.4	23 13.1	11.22	1.03	2,2	616....	22.0	24 28.2	13.47	0.89	2,3
559....	50.5	24 43.0	12.84	0.34	4,3	617....	23.3	24 43.4	13.88	0.35	2,2
560....	50.8	24 19.6			.,3	618....	23.3	23 43.2	12.87	0.25	2,1
561....	51.0	24 25.1	14.40	0.50	3,2	619....	23.4	23 57.5	14.01	0.44	2,3
562....	51.6	23 57.6	11.75	0.59	2,5	620....	23.5	22 59.0	13.97	1.01	2,1
563....	52.7	23 40.2	13.54	0.76	2,3	621....	23.5	24 38.1	14.92	0.24	2,2
564....	52.7	23 7.0	13.34	0.33	1,2	621*a*....	23.7	23 50.8	15.04		1,.
565....	53.0	24 28.1	14.37	0.63	2,1	623....	24.2	23 17.3	1..66	1.14	1,3
566....	53.2	24 44.2	14.88	1.00	4,3	624....	26.0	24 33.8	13.98	0.30	2,2
567....	54.2	23 59.0	13.86	0.44	3,5	625....	26.4	24 28.6	13.84	0.70	3,3
568....	55.5	24 28.0	14.65	0.75	2,1	626....	26.7	24 37.9	11.54	0.88	2,2
569....	56.4	24 24.3	12.85		3,.	627....	27.1	24 25.1	13.81	0.75	1,1
569*a*....	57.6	23 34.2	15.50	0.91	1,3	628....	27.6	23 32.0	12.07	1.02	2,1
570....	58.1	23 50.0	12.14	0.52	3,4	630....	28.7	23 10.2	13.66	0.84	1,3
571....	58.3	23 27.6	12.86	0.00	1,2	632....	28.9	23 29.3	14.14	2.19	2,1
572....	58.3	23 31.6	12.98	0.41	3,3	633....	29.4	23 30.2	12.76	1.22	2,1
572*a*....	58.7	23 29.1	15.02	0.66	1,2	634....	30.4	22 50.8	14.16	0.61	2,1
573....	59.4	23 59.0	12.55	1.19	2,2	635....	30.7	24 0.2	13.28	0.74	2,3

TABLE II—*Continued*

Trumpler No.	R.A. 1900	Decl. 1900	Pg. Mag.	C.I.	No. of Plates	Trumpler No.	R.A. 1900	Decl. 1900	Pg. Mag.	C.I.	No. of Plates
	3^h43^m						3^h44^m				
636....	$31^s.4$	22°48′.4	13.38	0.58	2,1	701....	$4^s.6$	23° 6′.7	14.00	0.94	2,3
637....	32.4	22 55.4	14.27	0.53	2,1	702....	5.2	24 23.6	13.60	0.67	1,1
638....	32.6	24 10.0	13.89	0.47	1,2	703....	6.0	24 22.0	12.41	0.46	1,1
639....	32.6	24 4.7	14.04	0.42	2,2	704....	6.2	24 19.2	13.47	0.63	1,1
640....	32.6	23 24.4	12.13	0.74	1,2	705....	8.8	23 54.6	11.98	0.48	2,2
641....	32.7	23 34.7	13.82	2.09	2,1	706....	10.0	23 59.6	14.42	0.55	2,3
642....	32.7	23 57.8	13.99	0.43	2,2	707....	10.1	23 42.8	13.52	1.03	2,1
643....	33.3	24 10.4	14.41	0.39	1,2	708....	11.1	23 40.1	12.30	1.20	3,2
644....	33.6	24 29.0	14.24	0.69	3,3	709....	12.6	23 50.4	14.33	0.85	2,2
645....	34.9	24 21.0	13.53	0.53	1,1	710....	12.8	23 55.4	12.49	1.28	3,3
646....	35.2	24 19.4	11.40		1,.	711....	13.3	24 36.3	13.90	0.67	4,3
647....	35.9	22 58.4	13.69	0.69	2,1	712....	14.2	24 13.7	14.28	1.12	2,1
648....	36.7	24 20.4	13.57	0.51	1,1	713....	14.4	23 59.5	14.46	1.10	3,3
649....	36.8	23 29.4	11.47	0.90	2,1	714....	14.7	24 19.4	11.32	0.04	2,2
650....	36.8	23 43.5	13.68	0.62	2,1	715....	14.7	24 9.9	13.78	0.35	1,1
650*a*....	36.9	24 3.6	14.66	0.05	2,2	716....	15.0	22 54.1	14.03	0.52	4,2
652....	38.2	23 40.4	13.74	0.53	4,3	717....	15.1	24 29.2	13.90	0.50	2,1
653....	38.6	24 35.3	14.58	1.38	2,2	718....	16.0	23 30.9	13.77	0.41	3,2
654....	38.7	24 11.9	13.75	0.23	1,1	719....	16.6	24 30.1	14.14	0.52	2,1
655....	38.8	24 44.6	14.64	0.48	2,2	720....	17.2	23 34.8	13.93	0.48	4,2
656....	38.9	23 57.2	13.59	0.36	2,2	722....	18.0	23 34.8	13.69	0.21	4,2
657....	39.0	23 59.4	12.52	0.98	2,3	723....	18.9	23 11.6	14.28	0.56	2,3
657*a*....	40.5	23 27.2	15.06	0.54	2,1	725....	19.9	24 46.7	14.40	0.22	5,2
658....	40.6	23 9.8	13.81	0.15	1,2	726....	22.8	24 10.2	12.92	0.15	2,1
659....	41.0	23 10.8	13.60	0.54	1,1	727....	22.9	24 9.8	11.74	0.86	2,2
660....	41.2	24 22.6	13.89	0.73	1,1	728....	23.4	24 0.2	14.54	0.48	3,3
661....	42.0	23 55.3	13.32	1.14	2,2	729....	23.4	23 36.1	14.48	0.58	4,2
662....	42.3	23 39.0	13.88	0.76	2,1	730....	23.5	23 34.6	13.12	0.24	4,2
663....	43.6	24 7.6	13.74	0.15	3,3	731....	23.5	23 38.9	13.02	1.40	4,2
664....	43.8	24 6.6	12.62	0.65	3,3	732....	23.6	24 17.8	14.44	0.34	1,2
665....	43.8	23 43.9	11.96	1.32	2,1	733....	23.7	23 30.2	14.08	0.48	3,2
666....	44.0	23 8.6	14.19	0.33	1,1	734....	24.8	23 55.0	14.22	1.00	3,3
667....	44.2	22 59.1	12.02	0.63	2,1	735....	25.2	22 50.6	14.24	0.56	4,2
668....	44.4	24 9.5	13.01	0.83	3,3	736....	26.6	23 52.6	14.47	0.72	3,3
669....	44.6	23 22.6	14.26	0.89	1,2	736*a*....	27.0	23 3.8	14.86	0.39	2,1
672....	47.9	24 2.6	12.96	0.88	2,2	737....	27.1	23 34.2	14.46	0.22	4,2
673....	48.1	24 13.3	14.00	0.29	1,1	738....	27.9	24 27.4	13.70	1.14	1,1
674....	48.6	22 58.0	12.28	0.18	2,1	739....	28.8	23 52.9	14.66	0.55	2,3
675....	48.6	23 56.4	11.11	1.04	2,1	740....	29.1	23 0.4	13.85	0.80	4,2
676....	49.2	24 41.4	13.94	1.08	2,2	741....	29.1	24 21.2	14.47	1.12	2,2
677....	49.5	23 28.5	11.70	0.35	2,3	742....	29.9	24 11.5			.,2
678....	50.0	23 26.4	11.93	0.67	3,3	743....	30.2	24 2.6	12.67	1.24	3,3
679....	50.7	23 49.6	13.88	0.40	4,2	744....	30.5	24 12.8	11.58	0.75	2,2
680....	54.2	23 24.0	12.30	0.57	2,2	745....	30.6	23 16.1	11.58	0.38	2,3
681....	54.4	24 12.2	13.05	0.41	1,1	746....	31.8	23 35.2	13.98	0.36	4,2
682....	54.6	23 59.8	13.44	0.39	2,2	747....	32.2	24 32.0	12.54	0.40	4,2
683....	55.5	23 25.3	14.98	0.50	2,2	748....	32.3	23 43.8	13.81		3,.
684....	56.6	23 43.4	13.16	0.56	2,1	749....	33.5	24 12.3	11.34	0.27	2,2
685....	57.0	24 2.2	13.23	0.69	2,2	750....	33.7	24 13.5	14.12	0.96	1,2
687....	57.6	23 13.5	11.50		1,1	752....	35.1	24 33.9	14.20	0.48	5,2
690....	58.9	24 17.0	13.20	0.24	1,1						
691....	59.8	23 32.6	14.67		1,.	753....	35.1	23 52.6	13.72	0.40	2,2
						755....	35.8	24 36.1	11.76	0.49	4,4
						757....	36.1	23 57.0	13.56	0.27	2,3
						758....	36.3	24 2.6	10.92	0.40	1,1
						759....	36.3	23 0.2	14.30	0.86	3,2
	3^h44^m										
692....	0.4	23 38.7	14.04	0.88	2,1	760....	36.4	24 12.3	13.96	1.00	2,1
696....	1.4	22 54.8			.,1	761....	37.9	22 57.1	13.84	0.54	3,1
698....	2.7	24 3.3	12.66	0.36	2,2	762....	39.3	23 58.0	14.08	0.63	2,3
699....	3.7	23 36.6	13.80	0.37	2,1	763....	39.3	23 29.2	14.75	0.50	2,1
700....	3.8	23 53.0	14.01	0.57	1,2	764....	39.9	24 14.4	14.04	0.31	2,1

TABLE II—*Continued*

Trumpler No.	R.A. 1900	Decl. 1900	Pg. Mag.	C.I.	No. of Plates	Trumpler No.	R.A. 1900	Decl. 1900	Pg. Mag.	C.I.	No. of Plates
	3^h44^m						3^h45^m				
765....	$40^s.0$	24°37′.1	15.01	0.89	4,2	827....	$15^s.4$	23°20′.8	13.17	0.14	1,1
766....	40.5	23 11.4	13.32	1.37	2,2	829....	15.6	24 13.0	12.54	0.15	1,1
767....	40.8	23 39.4	14.60	0.95	3,1	830....	17.1	22 59.1	14.27	0.46	2,1
768....	41.2	22 56.4	13.54	0.37	3,1	831....	17.3	23 12.7	13.14	0.45	1,1
769....	41.4	23 53.5	12.42	0.37	2,1	833....	20.2	23 31.5	13.27	0.64	2,1
770....	41.6	23 34.3	13.32	0.52	3,1	834....	20.3	24 17.2	13.41	0.38	1,1
771....	42.2	22 55.0	13.62	0.55	3,1	835....	21.5	23 55.1	14.44	0.54	1,1
772....	43.3	23 37.8	10.63		1,.	835a....	22.	23 22.6	14.74	1.38	1,1
773....	44.1	24 17.0	14.16	0.83	2,1	836....	22.3	24 4.8	11.43		1,1
774....	44.6	24 43.0	12.34	1.09	4,2	837....	22.3	24 32.0	14.48	0.90	3,2
775....	46.2	23 15.5	14.26	0.41	2,2	838....	25.0	24 33.6	12.11	0.86	3,2
776....	46.4	23 2.1	14.21	0.68	2,1	839....	25.0	24 32.0	14.80	0.88	3,2
777....	46.6	23 0.4	12.18	1.12	3,1	840....	25.3	24 13.4	14.19	0.83	1,1
778....	46.8	23 33.2	14.52	0.96	3,1	841....	25.7	24 21.8	13.45	0.49	1,1
780....	48.5	22 56.4	13.77	0.63	4,2	842....	25.9	24 33.5	14.10	0.66	3,2
781....	48.6	23 4.8	14.10	1.02	3,2						
782....	50.0	24 8.2	13.71	0.39	2,2	843....	27.1	23 23.6	13.69	0.39	1,1
783....	50.3	24 23.9	14.22	0.49	1,1	844....	27.1	23 47.2	14.38	1.02	3,1
783a....	50.4	23 12.0	15.20	0.51	1,1	845....	27.2	24 46.5	11.69	0.49	3,2
784....	51.0	24 7.6	11.42	1.06	2,2	846....	28.3	23 28.9	14.33	1.13	2,1
						847....	28.5	23 39.4	13.14	0.98	2,1
785....	51.4	24 16.8	13.41	0.34	1,1						
786....	51.8	23 33.1	13.20	0.24	2,1	849....	29.1	24 25.0	14.22	0.49	1,1
787....	53.6	24 24.3	14.03	1.12	1,1	850....	29.5	24 15.7	12.23	0.45	1,1
788....	53.8	23 7.2	11.77	0.35	2,2	851....	29.6	24 4.5	14.54	0.43	2,1
789....	54.5	23 25.4	13.46	0.32	2,2	853....	30.3	24 42.8	13.96	0.50	2,1
						854....	30.5	23 21.1	14.22		1,.
790....	54.6	23 26.3	14.62	0.86	3,2						
792....	55.7	24 29.1	14.34	0.53	4,3	855....	30.6	23 33.4	14.36	0.71	2,1
794....	57.0	23 1.3	14.44	0.68	2,1	856....	31.0	24 30.3	14.50	0.24	3,2
795....	57.6	23 53.7	12.26	0.58	1,1	857....	31.1	23 37.4	12.54	0.69	2,1
796....	57.7	23 31.9	12.20	0.73	2,1	859....	32.0	22 57.9	11.62	0.59	2,1
						861....	33.0	23 54.3	14.44	0.63	1,1
797....	57.9	23 19.2	13.65	0.31	1,2						
798....	58.7	23 10.7	13.69	0.46	1,1	862....	33.1	23 35.9	14.71	1.01	2,1
799....	59.0	24 21.8	14.52	0.76	1,1	863....	33.9	24 19.0	14.22	1.17	1,1
800....	59.1	24 32.6	12.70	0.52	3,2	865....	35.0	24 11.1	14.25	0.40	1,1
801....	59.1	24 14.7	13.35	0.39	1,1	866....	35.2	24 18.6	13.50	0.40	1,1
803....	59.3	23 56.9	14.07	0.71	1,1	867....	35.2	23 43.9	12.90		2,.
804....	59.9	24 8.8	13.92	0.52	2,2						
	3^h45^m					868....	35.4	23 20.1	13.69	0.33	1,1
805....	0.3	23 26.0	14.20	0.74	3,2	869....	35.5	23 5.8	14.69	0.96	2,2
806....	0.5	24 22.6	13.45	0.49	1,1	870....	35.6	23 36.6	12.66	0.64	2,1
807....	2.8	24 45.2	14.00	0.82	3,2	871....	35.7	23 49.8	13.73	0.37	1,1
808....	4.0	24 23.8	14.22	0.89	1,1	872....	35.9	24 41.9	14.05	0.65	3,2
809....	4.7	24 2.4	13.65	0.35	1,1						
						873....	37.2	23 42.8	14.68		2,.
810....	4.8	23 55.2	14.12	0.70	1,1	874....	39.2	24 43.6	14.24	0.48	3,1
811....	5.4	24 17.7	14.12	0.39	1,1	875....	39.5	23 44.7	14.55		2,.
812....	5.5	23 36.1	11.18		2,.	877....	40.2	24 46.1	14.66	0.62	3,2
813....	5.7	24 38.2	12.46	0.98	3,2	878....	40.6	24 10.5	14.22	0.57	1,1
814....	5.9	24 39.2	14.48	0.94	3,2						
815....	6.1	23 39.3	13.34	1.29	2,1	879....	40.9	24 14.9	12.73	0.49	1,1
816....	6.3	23 54.0	14.00	0.70	1,1	880....	41.0	24 40.9	11.61	0.57	3,2
817....	6.8	24 26.1	14.74	0.93	1,1	881....	41.7	23 27.5	14.59	0.68	2,2
819....	7.2	24 22.3	12.13	1.10	1,1	882....	42.1	23 42.6	14.64		2,.
820....	7.5	23 48.5	13.79	1.02	3,1	883....	42.2	24 22.0	12.73	0.60	1,1
821....	9.8	24 3.3	14.03	1.29	1,1	884....	42.5	23 20.4	14.22	0.61	1,1
822....	9.8	24 45.2	14.39	0.95	3,2	885....	42.8	24 40.2	12.45	0.43	3,2
823....	11.0	23 35.7	13.62	0.39	2,1	886....	42.8	22 52.9	14.26	0.93	2,1
824....	12.3	23 55.6	14.00	0.15	1,1	887....	44.0	24 40.4	13.68	0.34	3,2
825....	12.9	24 26.8	13.70	0.56	2,2	888....	44.9	24 15.0	12.90	0.10	1,1

TABLE II—*Continued*

Trumpler No.	R.A. 1900	Decl. 1900	Pg. Mag.	C.I.	No. of Plates	Trumpler No.	R.A. 1900	Decl. 1900	Pg. Mag.	C.I.	No. of Plates
	3^h45^m						3^h45^m				
890....	$46^s.8$	23°13′.4	14.52	0.76	1,1	903....	$51^s.2$	23°41′.1	14.33		2,.
892....	47.4	24 25.5	13.14	1.73	1,1	905....	52.1	24 25.7	14.00		1,.
894....	48.0	22 53.4	12.69	0.49	2,1	906....	52.7	24 41.2	13.90	0.28	3,2
895....	49.4	24 46.0	13.84	0.92	3,2	907....	53.2	24 36.5	11.41	0.06	3,2
896....	49.7	24 19.4	13.45	0.15	1,1	908....	53.4	23 19.4	14.12	0.44	1,1
897....	49.7	24 3.6	14.19	0.83	1,1	909....	54.4	24 44.2	11.47	0.21	3,2
898....	49.8	23 55.4	14.07	0.24	1,1	910....	55.0	23 56.0	12.85	0.01	1,1
899....	50.1	22 53.9	12.76	0.33	2,1	915....	57.3	24 23.0	14.22		1,.
901....	50.9	24 46.3	13.37	0.47	3,2						
902....	51.0	23 27.0			.,1						

Mount Wilson Observatory
March 1921

ON MAJORANA'S THEORY OF GRAVITATION[1]

By HENRY NORRIS RUSSELL[2]

ABSTRACT

Majorana's theory of gravitation.—As a result of some delicate pendulum experiments, Majorana has suggested that gravitational force is weakened by passing through matter. In this paper certain *astronomical consequences* of this assumption are presented. The true masses of the planets according to this theory are computed and it is shown (1) that the inertial masses cannot be equal to these true masses, and (2) that if we assume them equal to the apparent gravitational masses we are led to such discrepancies in the case of the tides that we are forced to conclude that the absorption of gravitational force cannot exceed 1/5000 of the value assigned by Majorana.

Possible influence of one body on the mass of another body.—The interpretation of Majorana's positive experimental result, assuming it to be real, must be that the mass of a body is actually changed by the presence of another body.

Professor Majorana, in a very interesting series of papers,[3] has proposed a new theory of gravitation, with experimental evidence supporting it. The present communication deals with certain astronomical consequences of the theory, in the form in which he presents it, and suggests a modification which will remove the resulting discrepancies.

1. The law which Majorana proposes[4] is that the force of attraction between any two material particles is directed along the line joining them, but that its intensity is less than that given by Newton's law whenever this line traverses matter, being diminished in accordance with the "law of progressive absorption" which holds good for radiation.

If M_1 and M_2 are the masses of the particles, r their distance apart, and k the ordinary constant of gravitation, the attractive force will be

$$f = k\frac{M_1 M_2}{r^2} e^{-\int h\theta dr}, \qquad (1)$$

[1] *Contributions from the Mount Wilson Observatory*, No. 216.

[2] Research Associate of the Mount Wilson Observatory.

[3] *Philosophical Magazine*, **39**, 488, 1920. *Atti della Reale Accademia dei Lincei*, **28**, 160, 221, 313, 416, and 480, 1919, and **29**, 23, 90, 163, and 235, 1920. Further citations refer to the detailed account in Italian.

[4] *Op. cit.*, p. 170.

where h is a second universal constant, that of absorption of gravitation, and θ the density of matter at any point on the line joining the particles, and the integral is taken over the whole length of this line.

In consequence of this absorption the attraction of any large body upon objects outside it will be diminished, and its "apparent mass," measured by means of its attraction, will be less than the true mass. For spherical bodies of uniform density Majorana shows[1] that the attraction will still be exactly proportional to the inverse square of the distance, while the apparent mass m will be connected with the true mass M by the equations

$$m=\psi M, \tag{2}$$

$$\psi=\tfrac{3}{4}\left[\frac{1}{p}-\frac{1}{2p^3}+e^{-2p}\left(\frac{1}{p^2}+\frac{1}{2p^3}\right)\right], \tag{3}$$

$$p=hR\theta, \tag{4}$$

where R is the radius of the mass, and θ the *true* density.

For small values of p we find, expanding in series,

$$\psi=1-\tfrac{3}{4}p+\tfrac{2}{5}p^2-\tfrac{1}{6}p^3+\ \ldots\ . \tag{5}$$

For large values of p, ψ approaches asymptotically to the value $3/4p$ and m to the value $\pi R^2/h$. The apparent mass of a homogeneous sphere has therefore, according to this theory, a superior limit, depending only upon its superficial area and the universal constant h. Majorana gives no calculations for bodies not of uniform density; but an easy calculation shows that the attraction of any spherical mass in which the density depends only upon the distance from the center, upon an external particle, is inversely proportional to the square of the distance from the center, as in the Newtonian case. The difference between the true and apparent masses will be greater, the greater the central condensation. For example, if the density at the distance r from the center is proportional to $(R^2-r^2)^n$, it is easy to show[2] that

$$\psi=1-\frac{(2n+3)^2}{12n+12}p+\ \ldots\ .$$

[1] *Op. cit.*, p. 420. The notation is slightly changed here.

[2] See the appendix to this paper.

(where the *true mean density* is to be used in calculating p). For $n=1$, $\psi = 1 - \frac{2}{2}\frac{5}{4}p$; for $n=2$, $\psi = 1 - \frac{4}{3}\frac{9}{6}p$. The former value corresponds to a central condensation greater than in the case of the earth, and the latter to a central density more than four times the mean density.

Majorana's conclusion, based upon qualitative reasoning, that condensation toward the center will not radically change the amount of absorption of gravitation, is therefore justified; but the numerical effects of such condensation appear to be somewhat greater than he has estimated.

2. We may now proceed to calculate the effects of absorption of gravitation in various bodies belonging to the solar system, using

TABLE I

GRAVITATIONAL ABSORPTION ACCORDING TO MAJORANA

	R	p	$p\psi$	ψ
Sun	6.95×10^{10} cm	1.41	0.660	0.33
Jupiter	7.23×10^{9}	1.33	0.065	0.951
Saturn	5.90×10^{9}	0.72	0.029	0.978
Earth	6.37×10^{8}	5.53	0.024	0.981
Mars	3.39×10^{8}	3.95	0.0090	0.993
Moon	1.74×10^{8}	3.40	0.0040	0.997
Eros	2×10^{6}	3	0.00004	1.0000

the value determined by Majorana[1] for the constant of absorption ($h=6.73\times10^{-12}$ in c.g.s. units) and assuming the bodies to be of uniform density. It must be remembered that, if ρ is the mean density derived from observation on the Newtonian theory, we will have $p=\psi\theta$, and hence $p\psi=hR\rho$. Knowing this, ψ may be determined by successive approximations, or, if p is small, by the equation

$$\psi = 1 - \tfrac{3}{4}p\psi - \tfrac{1}{8}\tfrac{3}{0}p^2\psi^2 - \tfrac{5}{4}\tfrac{3}{8}\tfrac{3}{0}p^3\psi^3 \ldots . \qquad (6)$$

obtained by "reversion" from (5).

The results are given in Table I. The data for the sun are from Majorana's paper. The diameter and density given for the asteroid Eros are rough estimates, but doubtless correct as regards order of magnitude.

[1] *Op. cit.*, 29, 236.

It is evident that the absorption of gravitation within the larger planets is by no means negligible.

3. The changes which such an absorption would introduce into the planetary theory are remarkable. The attraction between two spherical bodies of masses M_1 and M_2 at a distance r is kM_1M_2/r^2 according to Newton. According to Majorana, we must substitute $kM_1M_2\psi_1\psi_2/r^2$ (since the force is weakened in traversing both bodies).

Nothing in Majorana's discussion suggests that any change would occur in the inertial masses. If these remain the same, the acceleration of M_1 will be $kM_2\psi_1\psi_2/r^2$, or $km_2\psi_1/r^2$. Similarly that of M_2 will be $km_1\psi_2/r^2$, and the relative acceleration of the bodies toward one another will be $k(m_1\psi_2+m_2\psi_1)/r^2$.

The expression in parenthesis takes the place of the sum of the masses, M_1+M_2, in the Newtonian theory. Let M_1 represent the sun and M_2 the planet. We will have, by Kepler's Third Law,

$$\frac{a_2^3}{T_2^2}=\frac{k}{4\pi^2}(m_1\psi_2+m_2\psi_1), \tag{7}$$

where a_2 and T_2 are the mean distance and periodic time of the planet. Comparing this with another planet, M_3, we find:

$$\left(\frac{a_2}{a_3}\right)^3=\left(\frac{T_2}{T_3}\right)^2\frac{m_1\psi_2+m_2\psi_1}{m_1\psi_3+m_3\psi_1}.$$

The masses of the planets are all less than a thousandth part of the sun's, and the factor ψ_1 is also small. We may therefore write with high approximation:

$$\frac{a_2}{a_3}=\left(\frac{T_2}{T_3}\right)^{\frac{2}{3}}\left(\frac{\psi_2}{\psi_3}\right)^{\frac{1}{3}}.$$

The error committed by disregarding the planetary masses is at most one part in ten thousand. This equation differs from the ordinary form of Kepler's law by the presence of the factor involving ψ_1 and indicates that a massive planet should be considerably nearer the sun than a planet of small mass and identical period.

Applying it first to Jupiter and the earth, we have $\psi_2/\psi_3=0.969$, so that, taking the earth's mean distance as unit, the mean distance

of Jupiter should be less than that computed on the ordinary theory by 1.04 per cent.

This is utterly inadmissible. When Jupiter is in quadrature with the sun, its annual parallax (the angle at the planet between lines drawn to the sun and earth) is approximately 11° 5′, and the suggested change would increase this angle by 6′ 56″. The planet's longitude would then deviate from the ordinary ephemerides, which are computed on the Newtonian theory, by this amount every time that Jupiter was in quadrature, but in opposite directions according as it was east or west of the sun. Any actual deviation of this sort cannot at most exceed 1/500 of the predicted amount, and to avoid conflict with observation, Majorana's constant h would have to be correspondingly diminished.

The case of Eros is even more striking. Taking the earth again as standard, we find that $\psi_2/\psi_3 = 1.019$, and the distance of the asteroid should be greater by 0.63 per cent. When it is in perihelion and at the same time in quadrature, its distance from the sun is 1.13 astronomical units and from the earth 0.55. The suggested change in its mean distance would displace it by 39′ in geocentric longitude. With the planet in perihelion, but nearer to opposition (in about the position which it occupied in 1901, when it was very carefully observed), the discordance would exceed 1°—which is fully five thousand times as much as is allowable.

The most conspicuous case of all is provided by the moon. On Majorana's theory, the attraction of the sun should produce in the moon an acceleration greater by 1.6 per cent than that experienced by the earth at the same distance. This would be equivalent to a continually acting disturbing force, directed toward the sun, and amounting to 1/60 of its whole attraction on the moon, or 1/30 of the earth's attraction. This is three times the maximum disturbing force due to the sun on the Newtonian theory, and its introduction would play utter havoc with the whole lunar theory. The admissible magnitude of such an unrecognized disturbing force is probably less than one ten-thousandth as great.

Yet again, the tides on the earth's surface would be radically altered. In addition to the usual tidal forces depending on the

variations in the magnitude and direction of the attraction of the sun and moon, there would be a force depending on the difference of the screening action for the earth as a whole and for a water particle on its surface. Over the hemisphere facing the sun this force would be directed toward the sun and amount to 1.9 per cent of the sun's attraction. In the opposite hemisphere it would rapidly diminish, changing sign for points such that the absorption along the "gravitational ray" from the sun was equal to the average value for the earth as a whole. Beyond this the force would be directed away from the sun and reach a maximum at the point opposite it, where it would be 2.9 per cent of the sun's whole attraction (assuming, as elsewhere, a homogeneous earth).

The tides are produced by the horizontal component of this force, which will evidently be a maximum when the sun (or moon) is on the horizon, and amount to 0.019 times the whole attraction of the body. The ordinary tide-raising force vanishes when the sun is on the horizon, is greatest when it is 45° above or below it, and amounts to 0.025 of the moon's whole attraction and 0.000064 of the sun's.

The additional tide-raising force demanded by Majorana's theory is therefore about three-quarters of the recognized force due to the moon, but nearly three hundred times the recognized component in the case of the sun. This last term is more than eighty times the greatest tidal force that can occur on the Newtonian theory.

4. We are forced therefore to the conclusion that upon the hypothesis that there exists an absorption of gravitational force in matter, without change in its inertial mass, the coefficient of absorption cannot exceed one ten-thousandth of that derived by Majorana from his experiments, and must be hopelessly beyond the reach of investigation in the laboratory. There is nothing really new in this conclusion, or in the reasoning by which it has been reached. All depends upon the old and familiar proposition that the motions of the planets prove that their gravitational and inertial masses are strictly proportional to one another, at least within a few parts in a million. Any influence which modifies one must alter the other in the same proportion.

Accepting this, we must assume in section 3 that the accelerations are inversely proportional to the apparent masses, m, instead of the true masses, M. It would then follow that all astronomical motions will take place in accordance with the Newtonian law, but that the apparent masses will everywhere appear in the place of the true masses. The only exceptions occur when one body intervenes directly between two others. The resulting effects are negligible for the planets and small for the moon; but in the case of the tides they are important.

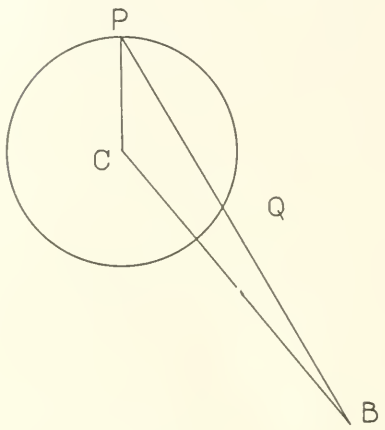


FIG. 1

Let the apparent mass of the earth be m_2 and the radius R, and let there be a body B (Fig. 1) of apparent mass m_1, at a distance D from the earth's center C, and D_1 from a point P on its surface. At this point there is a particle of apparent mass μ. The attraction of the earth upon it is

$$g = km_2\mu/R^2.$$

The horizontal tide-raising force acting upon P will be the sum of the components in this direction of the direct attraction of B and the inertial reaction arising from the acceleration of the system of axes, fixed in the earth, with respect to which the force is measured. (We may suppose that the earth does not rotate.) The force due to the attraction of B is:

$$f = \frac{km_1\mu}{D_1^2} \sin z_1 e^{-h\theta S},$$

where z_1 is the apparent zenith distance of B for an observer at P, S the distance PQ which the line PB traverses inside the earth, and θ the earth's true density (supposed as usual to be constant).

Since $S = -2R \cos z_1$, we have by (4):

$$f_1 = \frac{km_1\mu}{D_1^2} \sin z_1 e^{2p \cos z_1} = \frac{km_1\mu}{D_1^2} \sin z_1 (1 + 2p \cos z_1)$$

(since p is small).

If $\cos z_1$ is positive, the last factor is to be set equal to unity.

In this case, where the attraction between P and B varies with their direction as well as their distance, the apparent gravitational mass of P will vary according to whether we consider the attraction between it and B, or between it and the earth. (We obviously cannot suppose that the apparent masses of the earth or of B, whose attraction on one another is unaltered, are sensibly affected by the existence of the minute particle P.)

The inertial mass of P may be equal to either of these values of its gravitational mass, or, more probably, to some compromise between them. Let us set it equal to $\mu\ (1-\epsilon)$. The acceleration of the earth, due to the attraction of B, will be $km_1/D^2 \sin z$, where z is the angle PCB (the geocentric zenith distance). We have, rigorously,

$$D \sin z = D_1 \sin z_1 ,$$

and, neglecting R^2/D^2,

$$D = D_1 + R \cos z_1 .$$

The inertial reaction of the particle P, in the horizontal direction, will be, to the first order:

$$f' = \frac{km_1\mu}{D^2}(1-\epsilon) \sin z = \frac{km_1\mu}{D_1^2} \sin z_1 \left(1-\epsilon-\frac{3R}{D} \cos z_1 \ \ldots \ . \right) .$$

The deflection of the vertical by the tidal force will be given by

$$\tan \delta = \frac{f_1 - f'}{g} = \frac{m_1}{m_2}\frac{R^2}{D_1^2} \sin z_1 \left(3\frac{R}{D} \cos z_1 + 2p \cos z_1 + \epsilon \right) .$$

The first term in the parenthesis gives the effect on the Newtonian theory.

The quantity ϵ must be very small. If the inertial mass of the pendulum, swinging under the earth's attraction, were $1-\epsilon$ times its gravitational mass, its period would be $1-\epsilon/2$ times that derived from the ordinary theory. When the sun and moon are above the horizon, ϵ must be zero. If it were as great as 0.001 when both are below the horizon, all pendulum clocks would gain at the rate of nearly two seconds an hour. The greatest admissible value must be well below 0.0001. On the other hand, $3R/D$ is 0.050 in the case of the moon, and 0.00013 for the sun, while $2p$, for the earth, is 0.048.

The assumption of an absorption of gravitational force in passing through the earth leads therefore to discrepancies in the case of the tides which cannot be removed by any admissible assumption regarding changes in the inertial mass of the attracted water. The lunar tides should be twice as great, and the solar tides 370 times as great, when the attracting bodies are below the horizon as when they are at the same altitude above.

The most accurate observations of tidal force are undoubtedly those of Michelson and Gale, derived from observations of the displacements of the water level in underground pipes. From their curves[1] it is evident that the Newtonian theory represents the forms of the observed curves within a few per cent. The relative amplitudes of the solar and lunar tides, for a whole year, agree with theory within the probable errors (about 3 per cent for the larger oscillations). This indicates that any absorption of gravitation, in passing through the earth, cannot exceed 1/5000 of the value assigned by Majorana.

5. It appears therefore that the assumption that gravitational force is weakened in passing through matter must be definitely abandoned.

But what then becomes of Professor Majorana's long and careful series of experiments? If their result is accepted, it seems necessary to interpret it as showing that the *mass* of one body (his suspended sphere of lead) was diminished by the presence of another large mass (the surrounding mercury); that the effect was a true change in the mass (since inertial mass and gravitational mass are all the kinds of mass that we know of); and that it depended on the proximity of the larger mass, and not upon any screening action upon the earth's gravitation.

Strange as this notion may seem, it is not inherently absurd. Indeed, if the phenomena of gravitation and inertia may be accounted for by assuming that the four-dimensional "world" possesses certain non-Euclidean properties, or "curvature," both in the presence of matter and remote from it, it is not very surprising if the curvature induced by one mass of matter should be

[1] *Astrophysical Journal*, 50, 342, 1919.

modified to some degree by the superposition of the curvature due to another, so that the effects were not exactly additive.

A great variety of assumptions may be made regarding such an influence, and many of these might have the advantage of giving a conservative field of force, which Majorana's did not. Complications are still likely to arise. For example, consider a large spherical mass, alone in space and gradually contracting upon itself while it moves forward in a straight line. Its mass will presumably diminish as its various parts come closer together; but what will happen to its velocity? Presumably this would increase, but it seems obvious that either the conservation of momentum or the conservation of energy would have to be abandoned, if not both. Come next to a planet revolving in an eccentric orbit about the sun. Its mass will diminish at perihelion, and this will probably lead to changes in its orbital velocity. The resulting alterations in the orbit will depend on the law of change of velocity, and it might be possible to invent a law which would lead to conclusions consistent with observation.

Further speculation on such matters seems, however, to be premature, when it is considered that the whole structure would rest upon the observation of a change in weight amounting to one part in 1200 millions. Discussion of the possibility that some undetected systematic error has crept into the results, in spite of the great care taken to eliminate such errors, or to correct them, must be left to those better versed in experimental technique than the present writer; but it is to be hoped that the further experiments which Professor Majorana contemplates will provide the data regarding the reality, magnitude, and laws of variation of the suspected influence which are now evidently desirable.

APPENDIX

The proofs of certain statements made previously are collected here to avoid interruption of the course of the discussion.

Let P, Figure 2, be any point at which it is desired to find the gravitational attraction of a mass M. Draw through P an elementary cone, of solid angle $d\omega$, intersecting M between the points

A and B. Let Q be any point inside M at a distance r from P. The element of this cone between the distance r and $r+dr$ from P will have a volume $r^2 dr d\omega$ and a mass $\theta r^2 dr d\omega$, where θ is the true density. Its attraction upon a unit particle at P will be $k\theta dr d\omega$, according to Newton's law. If we set $\theta dr = dn$, n will be the total mass per unit section of a thin cylindrical column extending from Q to A, and the attraction at P will be $kd\omega dn$. Integrating, we find for the attraction of the conical frustum AB the value $kn_1 d\omega$ where n_1 is the value of $\int \theta dr$ between A and B.

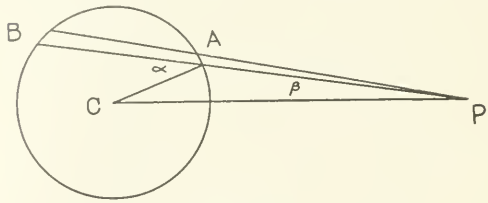


FIG. 2

According to Majorana, we must take the absorption of gravitation into account. In passing through a distance dr, this is $h\theta dr$ or hdn. Hence the transmission through the layer QA is e^{-hn}, and we find easily for the whole attraction at P, due to the frustum,

$$\frac{k}{h}(1-e^{-hn_1})d\omega.$$

Suppose now that M is spherical and that the density depends only on the distance from the center C. Let the angle CPB be β and CAB be α, also let $CP=R$, $CA=R_0$, then

$$\sin\beta = \frac{R}{R_0}\sin\alpha\,.$$

The whole attraction of the sphere at P must obviously be directed toward C. The component in this direction of the attraction of the frustum already considered is $kn_1 d\omega \cos\beta$. If ϕ is the position-angle about the axis CP, we have:

$$d\omega = \sin\beta\, d\beta\, d\phi = \frac{R_0^2}{R^2}\sin\alpha\cos\alpha\sec\beta\, d\alpha\, d\phi\,.$$

The whole attraction of the sphere at P will be

$$F = \frac{2\pi k R_0^2}{R^2}\int_0^{\frac{\pi}{2}} n_1 \sin\alpha\cos\alpha d\alpha, \qquad (1)$$

according to Newton, but

$$F' = \frac{2\pi k R_0^2}{hR^2} \int_0^{\frac{\pi}{2}} (1 - e^{-hn_1}) \sin \alpha \cos \alpha d\alpha, \qquad (2)$$

according to Majorana.

It is evident that n_1 depends only upon the length of the chord AB, that is, that it is a function of α, and hence that the definite integrals in (1) and (2) depend only upon the distribution of density within the sphere. Therefore the whole attraction of the sphere at an exterior point is inversely proportional to the square of the distance from the center, on Majorana's theory as well as Newton's.

When finally reduced, equation (1) goes over, of course, into the familiar form

$$F = kM/r^2.$$

If the density is uniform, $n_1 = 2R_0\theta \cos \alpha$, and equation (2) gives Majorana's formula for ψ. For other laws of density the integrals will in general be difficult or impracticable to reduce to known forms; but if the total absorption is small, we may write:

$$\frac{1}{h}(1 - e^{-hn_1}) = n_1 - \tfrac{1}{2}hn_1^2 \ldots\ldots$$

If the density θ is proportional to $(R_0^2 - S^2)$, where S is the distance from the center of the sphere, we find without difficulty that n_1 is proportional to $(R_0^2 - S_0)^{2n+\frac{1}{2}}$, where S_0 is the least distance of the chord from the center. But then $S_0 = R_0 \sin \alpha$. We may then write $n_1 = CR_0 \cos^{n+1} \alpha$ and find on Majorana's theory:

$$F' = \frac{2\pi kcR_0^3}{R^2}\left(\frac{1}{2n+3} - \frac{hcR_0}{8n+8} + \ldots\ldots\right).$$

The first term equals kM/R^2, or $4k\pi\theta_0 R_0^3/R^2$, if θ_0 is the true mean density. Hence

$$C = \frac{4N+6}{3}\theta_0,$$

and

$$F = \frac{kM}{R}\left(1 - \frac{(2n+3)^2}{12n+12} h\theta_0 R_0\right),$$

as stated in the text.

MOUNT WILSON OBSERVATORY
July 20, 1921

NOTE

Professor D. L. Webster, in a conversation with the writer, has pointed out that the supposition of a change in velocity of a spherical body which is contracting and hence diminishing in mass (according to the alternative theory suggested in section 5) is inconsistent with the principle of relativity, since, from the magnitude of such a change (no matter whether energy or momentum should be conserved) it would be possible to determine the absolute velocity of the body.

This difficulty makes the theory of an actual change of mass appear very improbable, and the trouble is not diminished when it is asked what becomes of the energy which, on relativistic principles, is equivalent to the mass which has disappeared. Further evidence regarding the reality of the experimental effect appears to be urgently called for.

PRINCETON UNIVERSITY OBSERVATORY
September 27, 1921

INVESTIGATIONS ON PROPER MOTION

FIFTH PAPER: THE INTERNAL MOTION IN THE SPIRAL NEBULA MESSIER 81[1]

By ADRIAAN VAN MAANEN

ABSTRACT

Spiral nebula Messier 81.—Two plates taken at Mount Wilson, one by Ritchey in 1910 and the other by Duncan in 1921, were measured with the new stereocomparator, and from the shifts of 104 points in the nebula with reference to 14 comparison stars, the *proper motion of the nebula* as a whole was found to be: $\mu_a = 0''.014$ and $\mu_\delta = -0''.005$. In addition, when the displacements of the points with reference to the nebula as a whole were corrected for the fact that the *inclination of the plane of the nebula* to the celestial sphere is about 49°, the *internal motion* was found to be, in general, a spiral motion out along the arms, of $0''.039$ per year NWSE, combined with a slight outward transverse motion of about $0''.007$ per year. The rotational component of the motion is $0''.038$ and corresponds to a period of rotation of 58,000 years.

Formation of spiral nebulae.—The four nebulae whose internal motions have been studied, M 33, 51, 81, and 101, all have internal spiral motions such as Jeans described in his *Problems of Cosmogony and Stellar Dynamics*. This fact *suggests* that the nebulous masses were rotating and had reached a lenticular shape when the arms began to be formed by matter being thrown off at antipodal points.

In a previous paper[2] it was mentioned that measures of two photographs of M 81 taken by Mr. Ritchey in 1910 and 1916 gave preliminary evidence of internal motion, similar to that revealed in the case of M 101. Another plate of M 81 was obtained in 1921 by Mr. Duncan which made it advisable to examine the additional evidence made available by the longer interval. The photographs used for the present paper are of 1910, February 5, and 1921, April 7; both received exposures of 4 hours and 15 minutes and are of good quality. Since no plates taken with a color screen were available, the choice of nebular points and comparison stars was necessarily based on the appearance of their images. Six of the 58 points included in the former discussion on account of their coincidence with the streamers of the nebula were excluded from the present discussion in advance of measurement because of their starlike appearance; they were, however, again included in the measures. Their numbers are 4, 28, 40, 42, 51, and 54.

[1] *Contributions from the Mount Wilson Observatory*, No. 214.

[2] *Mt. Wilson Contr.*, No. 118, 17, 1916; *Astrophysical Journal*, 44, 210, 1916.

Although the brighter stars were avoided, the comparison stars, as a whole, are somewhat brighter than the nebular points. For this reason a magnitude error may have vitiated the relative motions of the latter. While this may have affected the total motion of the nebula, it cannot have influenced the internal motion, since the magnitudes of the nebular points have a nearly symmetrical distribution around the center of the nebula. For the present investigation 14 comparison stars (the same as before) and 110 nebular points were selected for measurement.

As in the case of M 51,[1] the plates were measured with the new stereocomparator, with the directions east, west, north, and south coinciding successively with that of increasing reading of the micrometer screw.

The means of the two sets of measures in right ascension and in declination, which are expressed in parts of the micrometer screw for the interval of 11.17 years, were reduced to annual displacements in thousandths of a second of arc by multiplying them by the factor 0.0764. The resulting quantities m_α and m_δ were then reduced by the formulae:

$$\left.\begin{aligned} m_\alpha &= a+bx+cy+dx^2+cxy+fy^2+\mu_\alpha \\ m_\delta &= a'+b'x+c'y+d'x^2+c'xy+f'y^2+\mu_\delta \end{aligned}\right\} \qquad (1)$$

in which a, b, ... a', b', ... f' are the plate constants, x and y the co-ordinates of each point measured, and μ_α and μ_δ the annual proper motions, expressed in thousandths of a second of arc. For the derivation of the constants a f', the two sets of equations (1) for the comparison stars were solved by least squares, after making the usual supposition that the motions of the comparison stars are in the mean zero and are not functions of their position on the plates. Substitution of the constants thus determined into the equations (1) for all the objects measured yields the annual proper motions. These are given in the fourth and fifth columns of Table I; the second and third columns of this table give the co-ordinates of each object measured. The proper motions thus derived are relative to the group of comparison stars. To separate the motion of the nebula as a whole from the

[1] *Astrophysical Journal*, 54, 237, 1921; *Mt. Wilson Contr.*, No. 213, 1921.

TABLE I

CO-ORDINATES AND MEASURED ANNUAL DISPLACEMENTS

No.	x	y	μ_α	μ_δ
a	+1′.7	+0′.6	+0″.005	0″.007
b	+4.6	+2.0	+ 5	+ 14
c	+5.5	+3.9	+ 2	− 1
d	+4.0	+7.1	− 2	− 2
e	−2.9	+8.0	− 5	+ 1
f	−5.5	+2.1	+ 17	+ 3
g	−1.6	+1.3	− 2	− 6
h	−3.7	−0.2	− 12	+ 1
i	−1.5	−0.5	− 5	− 8
j	−0.9	−3.2	− 10	+ 10
k	−7.1	−6.0	− 4	− 1
l	+1.0	−6.6	+ 21	+ 2
m	+5.2	−6.3	− 11	− 3
n	+4.0	−1.3	0	− 3
1	+2.5	+0.3	+ 23	+ 20
2	+2.5	0.0	+ 22	+ 26
3	+2.8	−0.3	+ 11	+ 27
4	+3.1	−0.2	− 1	+ 15
5	+3.2	−2.5	+ 52	+ 11
6	+0.3	−4.0	+ 38	− 31
7	+0.6	−4.2	+ 32	− 37
8	+0.6	−4.3	+ 43	− 22
9	+1.2	−4.7	+ 42	− 21
10	+1.7	−4.6	+ 59	− 25
11	+1.9	−4.8	+ 53	− 19
12	+2.1	−5.0	+ 27	− 31
13	+2.2	−5.1	+ 62	− 39
14	+2.2	−4.9	+ 58	− 6
15	+2.3	−5.1	+ 51	− 12
16	+2.4	−4.7	+ 25	+ 20
17	+2.7	−4.9	+ 40	− 30
18	+3.0	−5.6	+ 45	0
19	+2.9	−5.9	+ 60	− 20
20	+3.4	−5.1	+ 51	+ 11
21	+4.5	−4.8	+ 52	+ 40
22	+3.9	−0.6	+ 20	+ 14
23	+4.0	−0.5	+ 52	+ 67
24	+4.1	+0.4	+ 43	+ 20
25	+3.1	+1.2	+ 16	+ 31
26	+3.9	+1.7	+ 12	+ 29
27	+3.9	+2.2	+ 20	+ 14
28	+4.3	+2.5	− 5	+ 5
29	+2.2	+5.0	− 4	+ 17
30	−0.2	+7.9	− 37	+ 12
31	−2.9	+9.0	− 28	+ 19
32	+1.2	+1.8	− 12	+ 19
33	+1.0	+3.3	− 7	+ 11
34	+0.3	+3.5	− 16	+ 14
35	+0.1	+3.6	− 34	+ 5
36	−0.3	+3.7	− 22	+ 15
37	−0.2	+3.8	− 35	+ 9
38	−0.8	+4.2	− 16	+ 10

TABLE I—*Continued*

No.	x	y	μ_a	μ_δ
39	−1.′6	+5.′0	−0.″016	+0.″015
40	−2.3	+5.8	− 4	− 2
41	−3.5	+5.5	− 15	− 22
42	−3.8	+5.2	0	+ 17
43	−3.7	+4.9	− 5	− 16
44	−3.3	+4.9	− 3	− 24
45	−3.2	+4.8	− 5	− 19
46	−4.0	+2.9	+ 5	− 24
47	−4.0	+2.0	− 2	− 28
48	−5.3	+1.9	+ 29	− 12
49	−4.9	+1.5	+ 19	− 19
50	−4.8	+1.3	+ 14	− 38
51	−4.7	+0.8	+ 16	+ 10
52	−4.8	+0.6	+ 13	− 25
53	−4.7	+0.1	+ 28	− 37
54	−4.6	−0.4	+ 30	− 11
55	−4.1	−0.6	+ 22	− 35
56	−1.7	−6.5	+ 36	− 22
57	−0.5	−5.2	+ 36	− 20
58	−1.6	−1.2	0	− 24
59	+2.2	+0.8	− 4	+ 39
60	+2.4	+0.6	+ 19	+ 8
61	+3.3	−0.7	+ 21	+ 27
62	+3.2	−0.8	+ 23	+ 34
63	+3.8	+1.7	+ 8	+ 17
64	+3.2	+3.3	+ 4	+ 35
65	+3.4	+3.9	− 7	+ 32
66	+2.3	+5.2	− 29	+ 4
67	+0.8	+6.3	− 11	+ 21
68	+0.6	+7.1	− 23	+ 44
69	−0.8	+8.3	− 30	+ 42
70	−0.8	+9.2	− 45	+ 52
71	−2.8	+6.9	− 21	+ 4
72	−2.1	+5.3	− 10	+ 1
73	−1.0	+5.9	− 27	+ 23
74	−1.7	+5.2	− 38	+ 8
75	−1.7	+5.0	− 14	− 18
76	−1.4	+4.5	− 30	+ 32
77	0.0	+4.0	− 17	+ 11
78	0.0	+4.5	− 23	+ 17
79	+1.0	+4.0	− 44	+ 11
80	+1.8	+3.4	0	+ 21
81	+1.7	+1.7	− 15	+ 25
82	−2.2	+3.2	− 9	− 19
83	−2.9	+3.1	− 4	− 36
84	−2.9	+3.4	− 8	− 32
85	−3.5	+3.7	− 1	− 42
86	−5.1	+2.7	0	− 22
87	−4.8	+1.0	+ 18	− 5
88	−4.9	+1.1	+ 25	− 11
89	−4.7	+0.4	+ 4	− 18
90	−4.6	+0.4	+ 30	− 11
91	−4.6	−0.5	+ 27	− 36
92	−4.0	−1.7	+ 12	− 36

350°

PLATE IV



INTERNAL MOTIONS IN MESSIER 81

The arrows indicate the direction and magnitude of the mean annual motions. Their scale (0".1) is indicated on the illustration. The scale of the nebula is 1 mm = 9".3. The comparison stars are inclosed in circles.

TABLE I—*Continued*

No.	x	y	μ_a	μ_δ
93	−2'.9	−2'.8	+0".051	−0".050
94	−2.7	−5.4	+ 47	− 73
95	−0.9	−6.5	+ 33	− 45
96	−1.2	−2.0	+ 14	− 32
97	+0.6	−4.3	+ 25	− 20
98	+0.7	−5.7	+ 29	− 24
99	+1.2	−4.6	+ 36	− 52
100	+1.3	−3.8	+ 30	− 23
101	+1.5	−5.7	+ 43	− 32
102	+2.9	−4.5	+ 44	+ 6
103	+4.6	−5.7	+ 74	+ 22
104	+3.4	−3.8	+ 39	+ 16
105	+3.2	−2.6	+ 44	+ 25
106	+3.7	−1.6	+ 18	+ 26
107	+4.5	−2.9	+ 66	+ 27
108	+3.1	−7.4	+ 57	0
109	+3.2	−7.3	+ 55	− 13
110	−1.7	+3.4	− 13	− 40

internal motion, the same process was used as previously in the case of M 101 and M 51, with the following results:

a) The mean motion of the 104 nebular points (excluding Nos. 4, 28, 40, 42, 51, and 54 for reasons given on page 347) is $\mu_a = +0''.014$, $\mu_\delta = -0''.002$.

b) Combining the mean motions in quadrants I and III, we have $\mu_a = +0''.017^5$, $\mu_\delta = -0''.005$; while for quadrants II and IV, $\mu_a = +0''.012^5$, $\mu_\delta = -0''.008$. All four quadrants combined give $\mu_a = +0''.015$, $\mu_\delta = -0''.006^5$.

c) Excluding points outside a circle with radius 5'.5, we find for quadrants I and III $\mu_a = +0''.017$, $\mu_\delta = -0''.006$; for quadrants II and IV $\mu_a = +0''.011^5$, $\mu_\delta = -0''.006$. For all four quadrants $\mu_a = +0''.014$, $\mu_\delta = -0''.006$.

For the motion of the nebula as a whole the mean result from the three methods is

$$\mu_a = +0''.014, \qquad \mu_\delta = -0''.005.$$

Subtracting these values from the annual motions given in Table I, we derive the internal motions, which are given in the second and third columns of Table II. These motions are plotted in Plate IV. For the comparison stars, which are surrounded by circles, the

TABLE II

ANNUAL INTERNAL MOTIONS

No.	μ_α	μ_δ	Rotational	Radial	Stream	Transverse
1	+0".009	+0".025	+0".024	+0".025	+0".017	+0".030
2	+ 8	+ 31	+ 32	+ 25	+ 25	+ 32
3	− 3	+ 32	+ 35	+ 6	+ 33	+ 12
4	− 15	+ 20				
5	+ 38	+ 16	+ 35	+ 31	+ 15	+ 45
6	+ 24	− 26	+ 30	+ 21	+ 36	+ 8
7	+ 18	− 32	+ 17	+ 34	+ 28	+ 26
8	+ 29	− 17	+ 35	+ 14	+ 38	+ 3
9	+ 28	− 16	+ 34	+ 15	+ 37	+ 6
10	+ 45	− 20	+ 57	+ 21	+ 57	+ 20
11	+ 39	− 14	+ 48	+ 20	+ 50	+ 14
12	+ 13	− 26	+ 2	+ 30	+ 4	+ 30
13	+ 48	− 34	+ 45	+ 45	+ 50	+ 40
14	+ 44	− 1	+ 59	+ 12	+ 60	+ 3
15	+ 37	− 7	+ 50	+ 13	+ 51	+ 2
16	+ 11	+ 25	+ 35	− 18	+ 33	− 20
17	+ 26	− 25	+ 16	+ 34	+ 14	+ 35
18	+ 31	+ 5	+ 45	+ 9	+ 45	+ 4
19	+ 46	− 15	+ 52	+ 31	+ 55	+ 22
20	+ 37	+ 16	+ 58	+ 10	+ 59	0
21	+ 38	+ 45	+ 85	+ 10	+ 85	+ 8
22	+ 6	+ 19	+ 22	+ 14	+ 25	+ 10
23	+ 38	+ 72	+ 82	+ 76	+ 91	+ 65
24	+ 29	+ 25	+ 23	+ 53	+ 30	+ 50
25	+ 2	+ 36	+ 33	+ 38	+ 32	+ 39
26	− 2	+ 34	+ 32	+ 21	+ 35	+ 14
27	+ 6	+ 19	+ 14	+ 23	+ 18	+ 19
28	− 19	+ 10				
29	− 18	+ 22	+ 28	+ 8	+ 29	+ 1
30	− 51	+ 17	+ 63	− 2	+ 55	− 31
31	− 42	+ 24	+ 46	+ 28	+ 54	− 6
32	− 26	+ 24	+ 35	+ 1	+ 35	− 3
33	− 21	+ 16	+ 27	+ 3	+ 27	− 4
34	− 30	+ 19	+ 38	+ 5	+ 37	− 13
35	− 48	+ 10	+ 61	− 11	+ 52	− 34
36	− 36	+ 20	+ 45	+ 10	+ 45	− 9
37	− 49	+ 14	+ 63	− 2	+ 58	− 25
38	− 30	+ 15	+ 36	+ 12	+ 37	− 7
39	− 30	+ 20	+ 32	+ 22	+ 39	0
40	− 18	+ 3				
41	− 29	− 17	+ 51	+ 1	+ 51	0
42	− 14	+ 22				
43	− 19	− 11	+ 33	+ 4	+ 33	+ 4
44	− 17	− 19	+ 36	− 6	+ 36	− 2
45	− 19	− 14	+ 36	+ 1	+ 36	0
46	− 9	− 19	+ 25	− 3	+ 25	− 4
47	− 16	− 23	+ 34	+ 16	+ 35	+ 13
48	+ 15	− 7	+ 2	− 19	0	− 19
49	+ 5	− 14	+ 14	− 6	+ 13	− 8

TABLE II—*Continued*

No.	μ_α	μ_δ	Rotational	Radial	Stream	Transverse
50	0″.000	−0″.033	+0″.036	+0″.002	+0″.036	−0″.002
51	+ 2	+ 15				
52	− 1	− 20	+ 24	+ 6	+ 24	+ 3
53	+ 14	− 32	+ 35	− 8	+ 32	− 15
54	+ 16	− 6				
55	+ 8	− 30	+ 35	+ 5	+ 35	− 4
56	+ 22	− 17	+ 30	+ 3	+ 30	− 3
57	+ 22	− 15	+ 29	+ 3	+ 29	− 2
58	− 14	− 19	+ 7	+ 31	+ 12	+ 30
59	− 18	+ 44	+ 45	+ 5	+ 44	+ 10
60	+ 5	+ 13	+ 11	+ 14	+ 8	+ 15
61	+ 7	+ 32	+ 44	+ 20	+ 33	+ 36
62	+ 9	+ 39	+ 39	+ 17	+ 29	+ 31
63	− 6	+ 22	+ 26	+ 8	+ 27	+ 5
64	− 10	+ 40	+ 35	+ 27	+ 38	+ 22
65	− 21	+ 37	+ 40	+ 13	+ 40	+ 11
66	− 43	+ 9	+ 48	− 28	+ 38	− 41
67	− 25	+ 26	+ 36	+ 19	+ 39	+ 7
68	− 37	+ 49	+ 49	+ 37	+ 60	+ 13
69	− 44	+ 47	+ 50	+ 41	+ 64	+ 6
70	− 59	+ 57	+ 68	+ 48	+ 82	+ 9
71	− 35	+ 9	+ 41	+ 15	+ 38	− 20
72	− 24	+ 6	+ 28	+ 9	+ 30	+ 4
73	− 41	+ 28	+ 48	+ 23	+ 50	− 17
74	− 52	+ 13	+ 64	+ 16	+ 65	− 3
75	− 28	− 13	+ 43	− 12	+ 38	− 25
76	− 44	+ 37	+ 44	+ 41	+ 55	+ 25
77	− 31	+ 16	+ 39	+ 7	+ 37	− 15
78	− 37	+ 22	+ 47	+ 8	+ 43	− 19
79	− 58	+ 16	+ 69	− 26	+ 62	− 40
80	− 14	+ 26	+ 26	+ 15	+ 28	+ 9
81	− 29	+ 30	+ 43	− 2	+ 42	− 8
82	− 23	− 14	+ 40	+ 4	+ 40	+ 1
83	− 18	− 31	+ 49	− 4	+ 49	− 7
84	− 22	− 27	+ 49	− 4	+ 49	− 6
85	− 15	− 37	+ 51	− 10	+ 52	− 5
86	− 14	− 17	+ 29	+ 13	+ 28	+ 15
87	+ 4	0	− 2	− 6	− 2	− 6
88	+ 11	− 6	+ 2	− 14	+ 1	− 14
89	− 10	− 13	+ 16	+ 16	+ 16	+ 16
90	+ 16	− 6	+ 5	− 21	+ 2	− 21
91	+ 13	− 31	+ 34	− 4	+ 32	− 13
92	− 2	− 31	+ 28	+ 23	+ 32	+ 17
93	+ 37	− 45	+ 58	− 4	+ 58	− 9
94	+ 33	− 68	+ 64	+ 40	+ 71	+ 25
95	+ 19	− 40	+ 31	+ 33	+ 34	+ 29
96	0	− 27	+ 16	+ 28	+ 25	+ 20
97	+ 11	− 15	+ 12	+ 17	+ 19	+ 7
98	+ 15	− 19	+ 17	+ 16	+ 18	+ 15
99	+ 22	− 47	+ 13	+ 51	+ 35	+ 40
100	+ 16	− 18	+ 13	+ 21	+ 20	+ 15

TABLE II—*Continued*

No.	μ_a	μ_δ	Rotational	Radial	Stream	Transverse
101	+0".029	−0".027	+0".032	+0".028	+0".033	+0".026
102	+ 30	+ 11	+ 46	+ 9	+ 45	+ 14
103	+ 60	+ 27	+ 94	+ 28	+ 95	+ 21
104	+ 25	+ 21	+ 48	+ 8	+ 39	+ 28
105	+ 30	+ 30	+ 59	+ 23	+ 45	+ 44
106	+ 4	+ 31	+ 36	+ 6	+ 34	+ 14
107	+ 52	+ 32	+ 70	+ 53	+ 62	+ 62
108	+ 43	+ 5	+ 62	+ 5	+ 62	− 6
109	+ 41	− 8	+ 50	+ 17	+ 51	+ 8
110	− 27	− 35	+ 57	− 30	+ 62	− 18

motions of Table I are used. The scale of the motions is indicated in the lower right-hand corner. The arrows represent the motions during an interval of about 1,300 years.

As in the case of M 101, 33, and 51, there is a question as to whether the displacements are best represented by a rotation or by a motion along the arms of the spiral. To investigate this, the motions were resolved into (*a*) rotational and radial components; (*b*) components along and perpendicular to the arms of the spirals (stream and transverse components). In order to do this, a diagram was made in which the foreshortening of the nebula was corrected. This was necessary because M 81 is decidedly elliptical in appearance, due undoubtedly to an inclination of the plane of the nebula to the tangential plane of the celestial sphere. It was estimated that the intersection of the two planes is in position angle 149° and that the inclination is 49°. Hence, the positions and components of the measured objects in the direction of position angles 149° and 329° were made the same in the diagram as on the photographs, while distances and components at right angles to this direction were increased in the ratio $1/\cos 49° = 1.5$. The results for individual points derived from the diagram are in the last four columns of Table II, where, as before, the positive sign is used for motions in the directions north, west, south, east, and outward.

The mean rotational component is +0".038; the mean radial component, +0".013, which is 34 per cent of the rotational vector. Since the mean distance of the nebular points from the center is

5!8, the rotational component would correspond to a hypothetical period of about 60,000 years. The mean stream component is +0".039, with a transverse component of +0".007.

The evidence on internal motions derived from the four nebulae which have been measured, viz., M 101, 33, 51, and 81, is summarized briefly in Table III, in which the second column gives the focal length used, the third column the interval in years. The next four columns give the mean rotational, radial, stream, and transverse components of the motions derived, while the last column gives the number of nebular points measured.

TABLE III

SUMMARY OF INTERNAL MOTIONS IN SPIRAL NEBULAE

(Unit for motions and their probable errors is 0".001)

Object	Focus in Feet	Interval in Years	Rotational	Radial	Stream	Transverse	*n*
M 101*.....	25	5	+21±1	+ 5±1	+21±1	0±1	87
M 101†.....	18	9	+20±2	+ 6±2	+22±2	− 3±2	69
M 101†.....	18	15	+12±2	+ 7±2	+14±2	+ 2±2	46
M 33.....	25	10	+20±3	+ 6±2	+24±3	− 2±2	30
M 33.....	80	5	+14±4	+12±3	+18±4	+ 4±3	21
M 51.....	25	11	+19±1	+ 8±1	+21±1	+ 3±1	79
M 81.....	25	6	+20±4	+17±3	+25±3	+16±3	52
M 81.....	25	11	+38±1	+13±1	+39±1	+ 7±1	104

* Including the measures by Mr. Nicholson, *Mt. Wilson Contr.*, No. 118, 18, 1916.
† Photographs taken with the Crossley reflector of the Lick Observatory. All others were taken with the 60-inch reflector at Mount Wilson.

All pairs of plates show the same type of motion, and when we keep in mind the different numbers of points measured, the agreement in the values of the motion for each nebula derived from different pairs of plates is as satisfactory as could be expected.

The rotational components would correspond to the following periods: for M 101, 85,000 years; for M 33, 160,000 years; for M 51, 45,000 years; for M 81, 58,000 years.

For M 101 there is no appreciable change in the measured rotational component with distance from the center, but for M 33, 51, and 81 there appears to be some increase of motion with distance.

All four nebulae show a large outward radial component, which for M 101 is 32 per cent of the rotational component; for M 33, 48 per cent; for M 51, 42 per cent; for M 81, 34 per cent.

The transverse components are in general very small and well within the limits of error, although the positive value for M 81 may be real. In all cases, however, the measured displacements agree better with the hypothesis of outward motion along the arms of the spiral than they do with an assumed rotation of the nebulae as a whole.

The close agreement of the displacements in direction with the spiral arms suggests that we have here a realization of the motions described by Jeans in *Problems of Cosmogony and Stellar Dynamics*, from which I quote freely.

If so, we must then suppose that before the formation of the spiral arms the nebular masses were rotating and had reached a lenticular shape. The formation of Laplace's ring requires perfect symmetry of mass about the axis of rotation. The distances of adjacent masses in space are in general so great that their gravitational influence will be extremely small, but even the slightest external gravitational field will be sufficient to preclude the formation of a ring; instead of this, the matter will be thrown off at two antipodal points. The masses first thrown off at the antipodal points form in themselves a tide-generating system which concentrates the region of ejection more and more at two points. The result is an extension farther and farther into the equatorial plane as the evolution of the nebula proceeds. The determination of the shape of the arms seems at present to be beyond the reach of mathematical analysis, but the long streams of gaseous matter must become longitudinally unstable and will tend to break up into condensations or nuclei.

Mount Wilson Observatory
July 1921

INDEX TO VOLUME LIV

SUBJECTS

PAGE

Air Lines in Spark Spectra from λ 5927 to λ 8683. *Paul W. Merrill, F. L. Hopper,* and *Clyde R. Keith* 76

Arc, The Low-Current. Part I. *V. L. Chrisler* 273

Boss 3644, Virginis, Spectroscopic Binary. *John C. Duncan* 226

Burnham, Sherburne Wesley, 1838–1921. *Edwin B. Frost.* 1

Y Camelopardalis, Photometric Study of. *Raymond Smith Dugan* . . 217

49 δ Capricorni, Orbit of. *Clifford C. Crump* 127

l Carinae, Wave-Lengths and Periodic Changes of Spectral Type in Variable. *Sebastian Albrecht* 161

1 H. Cassiopeiae, The Eclipsing Variable. *Joel Stebbins* 81

Clusters, Studies Based on Colors and Magnitudes in Stellar, XIX. Photometric Study of Pleiades. *Harlow Shapley* and *Myrtle Richmond* 323

Colors and Magnitudes in Stellar Clusters, Studies Based on, XIX. Photometric Study of Pleiades. *Harlow Shapley* and *Myrtle Richmond* 323

Contributors, Notice to 296

Darkening at Limb of Stellar Disk, Evidence on. *Joel Stebbins* . . . 81

Dispersion in Measures with Stellar Interferometer, Avoidance of. *G. Van Biesbroeck* 78

Dispersion of Optically Active Transparent Liquids, Natural and Magnetic Rotatory. *E. O. Hulburt* 116

Dispersion in Transparent Liquids, Magnetic Rotary. *R. A. Castleman, Jr.,* and *E. O. Hulburt* 45

Errata 80

Fluorescence of Mercury Vapor. *J. S. Van Der Lingen* and *R. W. Wood* 149

Fluorine, Spectrum of. *William R. Smythe* 133

Fraunhofer Lines, Mutual Influence of. *W. H. Julius* 92

Gravitation, Majorana's Theory of. *Henry Norris Russell* 334

Interferometer, Avoidance of Atmospheric Dispersion in Measures with Stellar. *G. Van Biesbroeck* 78

Liquids, Magnetic Rotary Dispersion in Transparent. *R. A. Castleman, Jr.,* and *E. O. Hulburt* 45

Liquids, Natural and Magnetic Rotatory Dispersion of Optically Active Transparent. *E. O. Hulburt* 116

PAGE

Magnitude to Space-Velocity, Relationship of Absolute. *W. S. Adams, G. Strömberg,* and *A. H. Joy* 9
Magnitudes in Stellar Clusters, Studies Based on Colors and, XIX. Photometric Study of the Pleiades. *Harlow Shapley* and *Myrtle Richmond* 323
Majorana's Theory of Gravitation. *Henry Norris Russell* 334
Mercury Vapor, Fluorescence of. *J. S. Van Der Lingen* and *R. W. Wood* 149
Motions, Accuracy with Which Mean Parallaxes Can Be Determined from Parallactic and Peculiar. *Henry Norris Russell* 140
Nebula Messier 51, Internal Motion in Spiral. *Adriaan van Maanen* . 237
Nebula Messier 81, Internal Motion in Spiral. *Adriaan van Maanen* . 347
Notice to Contributors 296
Nova, Definition of. *J. G. Hagen, S.J.* 229
Orbit of Spectroscopic Binary Boss 3644, Virginis. *John C. Duncan* . 226
Orbit of 49 δ Capricorni. *Clifford C. Crump* 127
Parallaxes Determined from Parallactic and Peculiar Motions. *Henry Norris Russell* 140
Photometric Study of Pleiades. *Harlow Shapley* and *Myrtle Richmond* 323
Photometric Study of Y Camelopardalis. *Raymond Smith Dugan* . . 217
Pleiades, Photometric Study of. *Harlow Shapley* and *Myrtle Richmond* 323
Proper Motion, Investigations on. Fourth Paper. Internal Motion in Spiral Nebula Messier 51. *Adriaan van Maanen* 237
Proper Motion, Investigations on. Fifth Paper. Internal Motion in Spiral Nebula Messier 81. *Adriaan van Maanen* 347
Radium Emanation, Spectrum of. *R. E. Nyswander, S. C. Lind,* and *R. B. Moore* 285
Review:
Boquet, F. *Tables du mouvement képlérien, première partie* (Frank Schlesinger) 146
Scandium, Electric Furnace Spectrum of. *Arthur S. King* 28
Solar Spectrum, Ultra-Violet End of. *Charles Fabry* and *H. Buisson* . 297
Space-Velocity, Relationship of Absolute Magnitude to. *W. S. Adams, G. Strömberg,* and *A. H. Joy* 9
Spectra, Excitation Stages in Open Arc-Light. *B. E. Moore* . . 191, 246
Spectra from λ 5927 to λ 8683, Air Lines in Spark. *Paul W. Merrill, F. L. Hopper,* and *Clyde R. Keith* 76
Spectra. Mutual Influence of Fraunhofer Lines. *W. H. Julius* . . 92
Spectra, Arc-Cathode. *Arthur St. C. Dunstan* and *Benjamin A. Wooten* 65
Spectral Type in Variable Star *l* Carinae, Wave-Lengths and Periodic Changes of. *Sebastian Albrecht* 161
Spectroscopic Binary Boss 3644, Virginis. *John C. Duncan* 226
Spectrum of Fluorine. *William R. Smythe* 133

PAGE
Spectrum of Radium Emanation. *R. E. Nyswander, S. C. Lind,* and *R. B. Moore* 285
Spectrum of Scandium, Electric Furnace. *Arthur S. King* 28
Spectrum, Ultra-Violet End of Solar. *Charles Fabry* and *H. Buisson* . 297
Sun-Spots, Cooling by Expansion in. *Henry Norris Russell* 293
Ultra-Violet End of Solar Spectrum. *Charles Fabry* and *H. Buisson* . 297
Variable 1 H. Cassiopeiae, Eclipsing, with Evidence on Darkening at Limb of Stellar Disk. *Joel Stebbins* 81
Variable Star *l* Carinae, Wave-Lengths and Periodic Changes of Spectral Type in. *Sebastian Albrecht* 161
Velocity, Relationship of Absolute Magnitude to Space-. *W. S. Adams, G. Strömberg,* and *A. H. Joy* 9
Virginis, Boss, 3644, Spectroscopic Binary *John C Duncan* 226

INDEX TO VOLUME LIV

AUTHORS

PAGE

Adams, W. S., G. Strömberg, and A. H. Joy. Relationship of Absolute Magnitude to Space-Velocity 9

Albrecht, Sebastian. Wave-Lengths and Periodic Changes of Spectral Type in the Variable Star *l* Carinae 161

Buisson, H., and Charles Fabry. Study of the Ultra-Violet End of the Solar Spectrum 297

Castleman, Jr., R. A., and E. O. Hulburt. Magnetic Rotary Dispersion in Transparent Liquids 45

Chrisler, V. L. The Low-Current Arc. Part I 273

Crump, Clifford C. Orbit of 49 δ Capricorni 127

Dugan, Raymond Smith. Photometric Study of Y Camelopardalis . 217

Duncan, John C. Spectroscopic Binary Boss 3644, Virginis . . . 226

Dunstan, Arthur St. C., and Benjamin A. Wooten. Study of Arc-Cathode Spectra 65

Fabry, Charles, and H. Buisson. Study of the Ultra-Violet End of the Solar Spectrum 297

Frost, Edwin B. Sherburne Wesley Burnham, 1838–1921 1

Hagen, J. G., S.J. Definition of a Nova 229

Hopper, F. L., Clyde R. Keith, and Paul W. Merrill. Identification of Air Lines in Spark Spectra from λ 5927 to λ 8683 76

Hulburt, E. O. Natural and Magnetic Rotatory Dispersion of Optically Active Transparent Liquids 116

Hulburt, E. O., and R. A. Castleman, Jr. Magnetic Rotary Dispersion in Transparent Liquids 45

Joy, A. H., W. S. Adams, and G. Strömberg. Relationship of Absolute Magnitude to Space-Velocity 9

Julius, W. H. Mutual Influence of Fraunhofer Lines 92

Keith, Clyde R., Paul W. Merrill, and F. L. Hopper. Identification of Air Lines in Spark Spectra from λ 5927 to λ 8683 76

Lind, S. C., R. E. Nyswander, and R. B. Moore. Spectrum of Radium Emanation 285

Merrill, Paul W., F. L. Hopper, and Clyde R. Keith. Identification of Air Lines in Spar Spectra from λ 5827 to λ 8683 76

Moore, B. E. Excitation Stages in Open Arc-Light Spectra. Part I. Sodium, Potassium, Calcium, Strontium, Barium, and Magnesium . 191

Excitation Stages in Open Arc-Light Spectra. Part II. Silver, Bismuth, Cadmium, Zinc, Air, and Copper 246

PAGE

Moore, R. B., R. E. Nyswander, and S. C. Lind. Spectrum of Radium Emanation 285

Nyswander, R. E., S. C. Lind, and R. B. Moore. Spectrum of Radium Emanation 285

Richmond, Myrtle, and Harlow Shapley. Studies Based on Colors and Magnitudes in Stellar Clusters, XIX 323

Russell, Henry Norris. Accuracy with Which Mean Parallaxes Can Be Determined from Parallactic and Peculiar Motions 140

Cooling by Expansion in Sun-Spots 293

On Majorana's Theory of Gravitation 334

Schlesinger, Frank. Review of: *Tables du mouvement képlérien, première partie*, F. Boquet 146

Shapley, Harlow, and Myrtle Richmond. Studies Based on Colors and Magnitudes in Stellar Clusters, XIX 323

Smythe, William R. Spectrum of Fluorine 133

Stebbins, Joel. The Eclipsing Variable 1 H. Cassiopeiae, with Evidence on the Darkening at the Limb of a Stellar Disk 81

Strömberg, G., A. H. Joy, and W. S. Adams. Relationship of Absolute Magnitude to Space-Velocity 9

Van Biesbroeck, G. Avoidance of Atmospheric Dispersion in Measures with the Stellar Interferometer 78

Van Der Lingen, J. S., and R. W. Wood. Fluorescence of Mercury Vapor 149

van Maanen, Adriaan. Investigations on Proper Motion, Fourth Paper. Internal Motion in the Spiral Nebula Messier 51 . . . 237

Investigations on Proper Motion, Fifth Paper. Internal Motion in the Spiral Nebula Messier 81 347

Wood, R. W., and J. S. Van Der Lingen. Fluorescence of Mercury Vapor 149

Wooten, Benjamin A., and Arthur St. C. Dunstan. Study of Arc-Cathode Spectra 65

INDEX TO VOLUMES 51–54

THE ASTROPHYSICAL JOURNAL

AN INTERNATIONAL REVIEW OF SPECTROSCOPY AND ASTRONOMICAL PHYSICS

EDITED BY

GEORGE E. HALE
Mount Wilson Observatory of the Carnegie Institution of Washington

EDWIN B. FROST
Yerkes Observatory of the University of Chicago

HENRY G. GALE
Ryerson Physical Laboratory of the University of Chicago

ANALYTIC INDEX OF VOLUMES 51–54 1920 AND 1921

BASED ON THE ANALYTIC ABSTRACTS

Prepared by

GORDON S. FULCHER

THE UNIVERSITY OF CHICAGO PRESS
CHICAGO, ILLINOIS, U.S.A.

THE CAMBRIDGE UNIVERSITY PRESS, London
THE MARUZEN-KABUSHIKI-KAISHA, Tokyo, Osaka, Kyoto, Fukuoka, Sendai
THE MISSION BOOK COMPANY, Shanghai

ANALYTIC INDEX OF *ASTROPHYSICAL JOURNAL* FOR 1920 AND 1921, VOLUMES 51–54, BASED ON THE ANALYTIC ABSTRACTS

INTRODUCTION

For two years analytic abstracts have been accompanying the articles in the *Astrophysical Journal*. The use of italicized subtitles has emphasized the fact that most titles do not describe the contents completely and precisely. Evidently an index of the titles, such as that provided by the *Journal*, however well made, cannot be a complete and precise index of the contents; and since in connection with the abstracts subtitles have been prepared which aim to be both complete and precise, why not form an index of them? This has in fact been done; and the index entries have been thoroughly classified so as to get all the references to each particular subject, like X-rays and Zeeman effect, together. It is hoped that the following analytic index made in this way will not only prove of value to the readers of the *Astrophysical Journal* but will also recommend itself so highly that other journals will provide such indexes and especially that our abstract journals will do so. The number of words in the following index is only twice the number in the corresponding title indexes, and while the labor of making it is of course considerably greater, it need not be excessive if properly organized, and no unusual ability is required on the part of the indexer.

INDEX

For references to spectra and spectroscopy of elements and compounds *see* Spectra.

Absorption of light
by atmosphere, 315–290 $\mu\mu$; coefficients, **54,** 297
by vapors in King's electric furnace; Kirchhoff's law applied to, **51,** 13

Aethylamine, preparation of; method, **52,** 129

Angles, extremely small; interferometer method of measurement, **51,** 257

Arc
low-current; anode fall, cathode fall, potential and potential gradient as functions of current, to 1 amp., for various cathode materials (Ag, C, Cd, Cu, Fe, Sn, Zn, and salts of Ba, Ca, Cs, Na, and Sr), **54,** 273

Atmosphere (*see also* Sky)
absorption of light, 315–290 $\mu\mu$; coefficients, **54,** 297
absorption spectrum (Fraunhofer lines) (*see* Sun, spectrum)
dispersion of light; measurement; stellar interferometer method suggested, **51,** 263
ozone in; amount, daily variations, location, and suggested origin, **54,** 297

Atomic theory, Bohr (*see* Spectra, theory)

Benzene; dispersion, rotary magnetic, 436–620 $\mu\mu$; **54,** 45

Benzene, nitro-; dispersion, rotary magnetic, 436–620 $\mu\mu$, **54,** 45

Binaries, spectroscopic (*see also* Variables)
- Boss 373, elements of both orbits, parallax, and proper motion, **53,** 201
- Boss 3644, Virginis, elements of orbit, **54,** 226
- Boss 5026, elements of both orbits, **51,** 187
- Boss 5591, elements of both orbits, parallax, and proper motion, **53,** 201
- +65°369 Camelopard, radial velocity, **52,** 198
- α Capella, elements determined by interferometer, **51,** 263
- 49 δ Capricorni, elements of orbit, **54,** 127
- 12, 15K, 42, and 50 Cassiopeiae, radial velocities, **52,** 198
- 19 Cephei, radial velocity variations, **51,** 252
- 13 Ceti, binary component; elements of orbit, **52,** 110
- Class Oe5: 19 Cephei, A Cygni, 9 Sagittae, and 4 more; radial velocity variations, **51,** 252
- A Cygni, radial velocity variations, **51,** 252
- X Cygni (Cepheid), spectroscopic orbit, **53,** 95
- 65 τ Cygni, binary component, elements of orbit, **53,** 144
- 34 ψ^2, 68, 71, +62°1637 Draconis, radial velocities, **52,** 198
- 205 Draconis, elements of both orbits, parallax and proper motion, **53,** 201
- dynamics; tides on sphere due to second sphere rotating around it, **51,** 309
- comp. α Hercules, elements of orbit, parallax and proper motion, **53,** 201
- Lalande 29330 and 46867, elements of orbit, parallax and proper motion, **53,** 201
- magnitudes, absolute (*see* parallax)
- measurement of relative brightness and position of components; interferometer method, **51,** 257, 263
- orbits; elements of, including periods, radial velocity curves, mass functions (*see* Boss 373, 3644, 5026, 5591; α Capella, 49 δ Capricorni, 13 Ceti; X and 65 τ Cygni, 205 Draconis, comp. α Hercules, Lalande 29330 and 46867, OΣ 82)
 - measurement of; interferometer method, **51,** 257
- origin, theory of, from nebulae, **51,** 309
- π^4 Orionis, photometric study, **51,** 218
- OΣ 82, elements of orbit, parallax, and proper motion, **53,** 201
- parallax and absolute magnitude (*see* Boss 373, 5591; 205 Draconis, comp. α Hercules, Lalande 29330 and 46867, OΣ 82, **53,** 201)
- proper motion (*see:* Boss 373, 5591; 205 Draconis, comp. α Hercules, Lalande 29330 and 46867, OΣ 82, **53,** 201)
- radial velocity (*see* orbits, *also* +65°369, Camelopard; 12, 15K, 42, and 50 Cassiopeiae, Class Oe5; 34 ψ^2, 68, 71, +62°1637 Draconis, 21 π Ursae Minoris)
- radiation pressure between components, theory, **53,** 1
- 9 Sagittae, radial velocity variations, **51,** 252
- spectrum of Boss 2830, comp. α Geminorum, and W Serpentis; notes, **53,** 13
- theory (*see* dynamics, origin, and radiation pressure)
- 21 π Ursae Minoris, radial velocity, **52,** 198

Binaries, visual (Double stars)
- 13 Ceti, orbit, **52,** 110 (*see* Triple systems)
- α Hercules and comp.; probably optical pair, **53,** 201
- measurement of separation, photographic; possible errors due to mutual action, **53,** 349

Brightness (*see* Clusters, Comet, Galaxy, Magnitudes, Nebulae, Novae, and Sky)

Brightness ratio, of palladium point to gold point, **51,** 244

Camphor
- dispersion, rotary; magnetic and natural; solution in ethyl alcohol, **54,** 116
- refractive indices for 1:1 solution in ethyl alcohol; 436–620 $\mu\mu$, **54,** 116

Carbon disulfide; dispersion, rotary, magnetic; 436–620 $\mu\mu$, **54,** 45

Cathode, for vacuum tube
- carbon, limed; preparation, **53,** 323
 - use as source of large current, **53,** 323

Cathode rays; excitation of light in air; intensity for 1500–3500 volts, **52,** 278

Cepheids (*see* Variables)

Cluster stars
- catalogue, photometric (colors and magnitudes)
 - in Messier 3, 848 stars, **51,** 140
 - in Messier 68, 56 giants, **51,** 49
- colors (*see* catalogue)
 - distribution (number) (*see* M3 and M68)
 - relation to magnitude (*see* M3 and M68)
 - variation with radial distance (*see* M3)
- giants (*see* M68)
 - color; relation to magnitude, general conclusions, **51,** 49
- magnitudes (*see* catalogue)
 - distribution (number) (*see* M3 and M68)
 - relation to color (*see* M3 and M68)
 - variation with radial distance (*see* M3)
- in Messier 3; photometric analysis, **51,** 140:
 - colors and magnitudes
 - catalogue of 848 stars
 - distribution (number of each color and magnitude)
 - distribution in space, variation with distance from center
 - relation between color and magnitude
 - position co-ordinates of 370 stars
 - variables, 17 probable
- in Messier 53 (N.G.C. 5024); variables positions of 23 shown in photograph, **52,** 73
- in Messier 56 (N.G.C. 6779); variables positions of 3 shown in photograph, **52,** 73

Cluster stars (*cont.*)
in Messier 68 (N.G.C. 4590); photometric analysis, **51,** 49:
giants, colors, and magnitudes
catalogue of 56
distribution (number of each color and magnitude)
relation between color and magnitude
variables; colors, magnitudes, positions, and ranges of variation of 28
in Messier 72 (N G.C. 6891)
comparison stars, magnitudes of 29, **52,** 232
variables; periods and light curves of 26 Cepheids, **52,** 232
position of 34, in photograph, **52,** 73
in Messier 75 (N.G.C. 6864); variables
position of 16, in photograph, **52,** 73
in N.G.C. 7006 and 7789; number, **52,** 73
number, in N.G.C. 7006 and 7789, **52,** 73
number of each color and magnitude (*see* M3, M68)
variables (*see* M3, 53, 56, 68, 72, 75; Variables)
Clusters (*see also* Cluster stars)
analysis, photometric (colors and magnitudes of the stars) (*see* Messier 3 and 68)
brightness of average cluster, **52,** 73
diameter, of N.G.C. 7006 and 7789, **52,** 73
form of Messier 68, **71,** 49
magnitude, absolute (*see* parallax)
Messier 3; photometric analysis, **51,** 140
Messier 8 (N.G.C. 6530), photograph, **51,** 4
Messier 16 (N.G.C. 6611), photograph, **51,** 4
Messier 22 (N.G.C. 6656), photograph, **51,** 4
Messier 53 (N.G.C. 5024), photograph, **52,** 73
Messier 56 (N.G.C. 6779), photograph, **52,** 73
Messier 68 (N.G.C. 4590); analysis, photometric; form; computed parallax; photograph, **51,** 49
Messier 72 (N.G.C. 6981); parallax, **52,** 232; photograph, **52,** 73
Messier 75 (N.G.C. 6864); photograph, **52,** 73
N.G.C. 7006; diameter, parallax and star counts, **52,** 73
N.G.C. 7492, photograph, **52,** 73
N.G.C. 7789; diameter; number of stars, **52,** 73
parallax and absolute magnitude (*see* Messier 68, 72; N.G.C. 7006)
average cluster, brightness, **52,** 73
computation, methods, **51,** 49
globular clusters, forty, **52,** 73
photographs, large scale (60-inch)
Messier 53, 56, 72, 75 and N.G.C. 7492, showing variable stars, **52,** 73
Messier 68, showing variables, **51,** 49
in Sagittarius and Scutum, including Messie 8, 16, and 22, **51,** 4
stars in (*see* Cluster stars)
Colors (*see* Cluster stars, Novae, Stars, Variables)
Comets
1919*b*: brightness, photographs, behavior of tail, **51,** 103
Morehouse's; rejection of tail, **51,** 103
tail, rejection of; instances and stages, **51,** 103
Constant stars (*see* Stars)
Córdoba Observatory Catalogue
correction for position of star 12431, **51,** 4
Corona (*see* Sun)

Dark markings (*see* Nebulae, dark)
Diameters, of planetoids, satellites and stars
measurement (*see* Interferometer, stellar)
Discharge through gases
occlusion of RaEm, **54,** 285
Dispersion
by atmosphere; measurement; interferometer method suggested, **51,** 263
theory, electron, modified to include variation with temperature, **51,** 223; note as to priority, **53,** 326
Dispersion, rotary (*see* Camphor, Limonene, Sugar, Tartaric acid, **54,** 116)
Dispersion, rotary, magnetic (*see* Benzene, nitro-Benzene, Camphor, Carbon disulfide, Ethyl iodide, Limonene, α-monobrom-Naphthalene, Sugar, Tartaric acid)
theory, electron, extended
isotropic transparent media, **54,** 45
optically active media, **54,** 116
Double stars (*see* Binaries, visual)
Dynamics
binary system (*see* Binaries, spectroscopic)
single mass, rotating; equilibrium, **51,** 309
potential of distorted ellipsoid, **51,** 309

Eclipse (*see* Sun)
Einstein effect (*see* Gravitation)
Electron theory (*see* Dispersion and Dispersion, rotary, magnetic)
Electrons; e/m for those active in magnetic rotary dispersion, computed, **54,** 45
Emission of light, in discharge tube
intensity as function of energy of exciting cathode rays, **52,** 278
Equilibrium (*see* Dynamics)
Ethyl iodide; dispersion, magnetic rotary, 436–620 $\mu\mu$, **54,** 45
Exploded wire, source of high temperature spectra (*see* Spectra)
appearance and mechanical effects (Plate), **51,** 37

Fluorine; preparation of gas by electrolysis, **54,** 133
Furnace
black body, double platinum wound, **51,** 244
electric (*see* Spectra)
vacuum, cathode ray, for high temperature, **53,** 323

Galaxy
brightness, surface, as viewed from distance, **52,** 162

Galaxy (*cont.*)
comparison with typical spiral nebulae, **52,** 162
distribution of stars in; section, **52,** 23
origin; theory, **51,** 309
radiation pressure exerted on nebulae, **53,** 1
Giant stars (*see* Cluster stars and Variables)
Gratings (*see* Spectra)
polarizing effect on reflected and transmitted light, **51,** 129
theory, Rayleigh-Voigt; evidence confirming, **51,** 129
Gravitation
attraction on nebulae due to Galaxy, **53,** 1
Einstein effect; photographic measurement; possible error due to mutual action of adjacent images, **52,** 98; **53,** 349
Majorana's theory; astronomical consequences, **54,** 334

Hydrogen; production by high potential sparks, apparent, **52,** 47

Integral, definite
table of values of $\int_0^1 (1-x^2)^{n+\frac{1}{2}} \cos kx \cdot dx$, **53,** 249
Interferometer, stellar (Michelson's)
description
100-inch; accuracy and limits, **51,** 263
20-foot; construction, adjustments, and photographs, **53,** 249
modification to compensate for atmospheric dispersion, **51,** 263; **54,** 78
effective wave-length, determination, **51,** 263
measurements
α Capella; separation and positions of components, and inclination of orbit, **51,** 263
theory and uses; to measure
angles, extremely small, and changes of angle, **51,** 257
diameters of planetoids, satellites, and stars, **51,** 257; *also* distribution of luminosity on the disks, **53,** 249
dispersion of the atmosphere, **51,** 263
parallaxes and relative motions of stars, **51,** 257
relative brightness, position, and separation of double stars (binaries), **51,** 257, 263

Jean's contributions to theory of cosmic origins, **51, 309**

Kirchhoff's law (*see* Absorption)

Light (*see* Absorption, Dispersion, Emission, Polarization, Radiation, Refraction, Spectra)
Limonene
dispersion, rotary, magnetic, and natural, 436–620 μμ, **54,** 116
refractive indices, 436–620 μμ, **54,** 116

Magnetic rotary dispersion (*see* Dispersion)
Magnitudes (*see* Binaries, Clusters, Cluster stars, Stars, Variables)
Markings, dark (*see* Nebulae)
Mass, constancy of; possible influence of one body on the mass of another, **54,** 334
Melting-point, of palladium, **51,** 244
Meteorites, falling into sun; light to be expected from, **51,** 37
Molecular models, Bohr type, of halogen acids, as basis for theory of band structure, **51,** 230

Naphthalene, α-monobrom-; dispersion, rotary, magnetic, 436–620 μμ, **54,** 45
N.G.C.; corrections to descriptions and positions of various nebulae, **51,** 276
Nebulae
attraction, gravitational, by Galaxy, **53,** 1
brightness, surface, of nebulous areas
measurement, photographic method, **52,** 162
spirals; results for well-known nebulae compared with value for Galaxy, **52,** 162
catalogue, descriptive, of 330, **51,** 276
changes in N.G.C. 1555 and 2245, **51,** 276
constant (unchanged); N.G.C. 995, 1186, 2024, and 7023, **51,** 276
dark clouds or markings; photographs
I.C. II, 5146, Cygnus; unique array, **51,** 276
N.G.C. 2146, Camelopard, **51,** 276
near ζ Orionis, including Barnard 33, **53,** 392
in Sagittarius and Scutum; N.G.C. 6523 (M8), 6611 (M16), and 6618 (M17), **51,** 4
forces acting on; electrostatic, gravitational, and radiative, **53,** 1
internal motion in spirals (*see* Messier 51, 81)
I.C. 431, 432, and 434; photographs, **53,** 392
I.C. II, 5146, Cygnus; dark markings; photograph, **51,** 276
Messier 8 (N.G.C. 6523); photograph, **51,** 4
Messier 16 (N.G.C. 6611); photograph and spectrum, **51,** 4
Messier 17 (N.G.C. 6618) (Swan); photograph, **51,** 4
Messier 51 (spiral); internal motion, photograph, and proper motion, **54,** 237
Messier 81 (spiral); internal motion, photograph, and proper motion, **54,** 347
N.G.C. 1555 and 2245; changes in, **51,** 276
N.G.C. 1700 and 3379; radial velocity and spectrum, **51,** 276
N.G.C. 2023 and 2024; photograph, **53,** 392
N.G.C. 2146; photograph, **51,** 276
N.G.C. 2261 (Hubble), theoretical explanation, **53,** 169
N.G.C.; corrections to descriptions and positions of various nebulae, **51,** 276
new; descriptive catalogue of 255, **51,** 276
origin, theory of
N.G.C. 2261, with fan-shaped appendage, **53,** 169

Nebulae (*cont.*)
origin, theory of (*cont.*)
planetary nebulae, by collision, **54,** 229
spirals, **54,** 347; Jeans' theory, **51,** 309
photographs, large scale (*see* I.C. 431, 432, 434; I C. II, 5146; M8, 16, 17, 51, 81; N.G.C. 2023, 2024, 2146; *also* dark clouds)
near ζ Orionis, **53,** 392
in Sagittarius and Scutum, **51,** 4
spirals; N.G.C. 2146 and 15 others, **51,** 276; M51, **54,** 237; M81, **54,** 347
misc.: I.C. I, 1470; N.G.C. 1491, 2245, 2247, 2294, 2359, 3379, 3384, and 6888, **51,** 276
planetary, origin; collision theory, **54,** 229
proper motion (*see* Messier 51 and 81)
radial velocity
explanations suggested; discussion, **53,** 1
N.G.C. 1700 and 3379, **51,** 276
radiation pressure on, due to Galaxy, **53,** 1
spectrum (*see* M16; N.G.C. 1700 and 3379)
nebulosity around six nebulous stars, **52,** 8
spirals (*see* brightness, catalogue, internal motion, new, origin, photographs, proper motion)
Swan (N.G.C. 6618); photograph, **51,** 4
theory (*see* N.G.C. 2261, origin, radial velocity)
effect of passage of a star near or through a nebula, **53,** 169; **54,** 229
types, four; examples, **53,** 392
variable (*see* changes)
Nebulous areas; brightness (*see* Nebulae)
Nebulous stars (*see* Stars)
Novae
brightness and color of Persei No. 2, **52,** 183
definition suggested, **54,** 229
Ophiuchi 1919; spectrum and radial velocity, **51,** 121
origin, collision theory, **54,** 229
spectrum
Ophiuchi 1919; shifts of lines and bands, **51,** 121
shifts, simple interpretation, **51,** 121
theory (*see* origin)

Occlusion, of RaEm in discharge tubes, **54,** 285
Origin; theory of (*see* Binaries, Galaxy, Nebulae, Novae, Solar system, Variables)
cosmic origins; Jeans' contributions, **51,** 309
Ozone, in atmosphere (*see* Atmosphere)

Palladium, melting-point, **51,** 244
Parallax (*see* Binaries, Clusters, Stars, Variables)
Photo-electric cells
alkali metals and hydrides; color sensitiveness curves, **52,** 129
fatigue tests for K and KH cells, **52,** 129
preparation of Li cell, **52,** 129
sensitiveness, color, for 30 cells, including all alkali metals and hydrides of Na, K, Rb, and Cs, **52,** 129
Photo-electric photometer, for stars
description, **51,** 193; precision, **53,** 105; **54,** 81
Photographic plates; properties
contrast functions γ and Γ; variation with wave-length; Purkinje effect, **52,** 86
drying, time of; effect of exposure on, **53,** 349
grain size; relation to sharpness, theoretical, **52,** 201
images
contraction and distortion during drying, **52,** 98
mutual action of adjacent spectrum lines and stars; analysis of effects involved; variation with exposure, **53,** 349
sections of star images, Plates, **52,** 86, 98
intensification; effect on resolving power, **52,** 201
penetration of light of different wave-lengths, **52,** 86
resolving power
effect of intensification, **52,** 201
relation to grain size and sharpness, theoretical, **52,** 201
variation with development and wave-length **52,** 201
sharpness
measurement; improved method, **52,** 201
relation to contrast and turbidity, **52,** 201
variation with development and wave-length **52,** 201
shifts of spectrum lines and star images due to mutual action of adjacent images (*see* images)
theoretical relations for resolving power and sharpness, **52,** 201
turbidity; variation with wave-length, **52,** 201
Photographs (*see* Clusters, Comets, Nebulae, Sun)
Photometer (*see* Photo-electric photometer)
Photometry, photographic, heterochromatic; discussion and warning, **52,** 86
Planetoids, diameter; measurement, interferometer method, **51,** 257
Polarization
measurement, using gratings; warning, **51,** 129
produced by gratings, reflected and transmitted light, **51,** 129
Prominences, solar (*see* Sun)
Proper motion (*see* Binaries, Nebulae, Stars)
Purkinje effect, photographic, **52,** 86

Quantum theory (*see* Spectra)

Radial velocity (*see* Binaries, Nebulae, Novae, Stars)
Radiation
constant c_2; computed from gold point to palladium point ratio, **51,** 244
pressure
on atoms and electrons; theory based on classical dynamics, **52,** 65
between binary stars, **53,** 1
on nebulae due to Galaxy, **53,** 1

Radium emanation (Niton)
occlusion in discharge tube, **54,** 285
purification; modification of Duane's apparatus, **54,** 285
Refractive indices (*see* Camphor, Limonene, Sugar, Tartaric acid)

Satellites, diameter; measurement; interferometer method, **51,** 257
Scandium, carbide; possible formation in electric furnace, **54,** 28
Sky, night; brightness; various determinations; discussion, **52,** 123
Solar corona and **prominences** (*see* Sun)
Solar system, origin; tidal theory, **51,** 309
Spectra and **spectroscopy**
absorption spectra
exploded wire, of Fe, λ 2270–5645 A, spectrogram, **51,** 37
furnace, electric, of Ba, Ca, Co, Fe, Ni, and Ti; variation of relative intensities with temperature, **51,** 13
production of
electric furnace spectra, **51,** 13
high temperature spectra, extreme; exploded wire method, **51,** 37
theory (*see* halogen acid gases)
Kirchhoff's law applied to electric furnace spectra, **51,** 13
Zeeman effect, inverse (*see* Fe and V)
air
arc spectrum; two new lines, **54,** 246
spark spectrum, condensed
effect of self-inductance on relative intensities, 590–872 μμ, **51,** 236
identification of Ar, N, and O lines, 590–872 μμ, **51,** 236; **54,** 76
shift with reference to vacuum tube lines, **51,** 236
wave-lengths, 590–872 μμ, **51,** 236; **54,** 76
ammonia bands, visible and ultra-violet; identification, **52,** 301
arc spectra (*see* air, Fe, pole-effect, pressure shift)
anode and cathode spectra; relative behavior of various metal lines; variation with atomic weight, **54,** 65
comparison with furnace spectra (*see* Ca, cyanogen, and Swan bands)
ionization lines; behavior, **54,** 191, 246
low-current; variation with current; excitation stages
for Ba, Ca, K, Mg, Na, Sr, **54,** 191
for Ag, Bi, Cd, Cu, and Zn, **54,** 246
relation of results to Bohr theory and Ritz equations, **54,** 246
standard lines, secondary; comparison of 12-mm 5-amp. with 6-mm 6-amp. arc, **53,** 260
argon; lines in condensed spark spectrum in air, 590–872 μμ, **51,** 236; **54,** 76; shift with reference to vacuum tube lines, **51,** 236
band spectra (*see* ammonia, cyanogen, halogen acids, Swan, water, C, CO, CO_2, CF_4, H_2S, N, SO_2)
arc and furnace spectra; comparison of intensity distribution; CN and Swan bands, **53,** 161
Deslandres' law; test with nitrogen positive bands, **52,** 301
theory of structure of infra-red bands (*see* halogen acids)
vacuum tube discharge through CO_2, H_2S, NH_4, N_2O, N_2O_4, and SO_2; bands excited in visible and ultra-violet, **52,** 301
barium
absorption spectrum, electric furnace; variation with temperature, **51,** 13
arc spectrum, low current; variation with current, **54,** 191
classification of lines
furnace excitation, infra-red, **51,** 179
low-current arc excitation, **54,** 191
infra-red furnace spectrum to 856 μμ, at various temperatures, **51,** 179
series of single lines and triplets; identification of terms; constants, **51,** 23
binaries (see Binaries)
bismuth
arc spectrum, low current; variation with current, **54,** 246
classification of lines, arc excitation, **54,** 246
structure
of λλ 4122, 4308, 4722; Plate, **53,** 323, 339
of λλ 3397, 3511, 3596; Plate only, **53,** 323
of λ 4722; changes in relative intensity of components, **53,** 339
cadmium
arc spectrum, low current; variation with current, **54,** 246
classification of lines, arc excitation, **54,** 246
new resonance line, λ 3779, **54,** 246
calcium
absorption spectrum, electric furnace, **51,** 13
arc spectrum, low current; variation with current, **54,** 191
classification of lines
furnace excitation, infra-red, **51,** 179
low-current arc excitation, **54,** 191
furnace spectra; absorption, emission and mixed, **51,** 13; infra-red, **51,** 179
infra-red furnace spectrum to 733 μμ, at various temperatures, **51,** 179
new lines, fifty, **52,** 265
pressure shifts to 1 atm., 315–650 μμ, **53,** 224
series of singlets and triplets; identification of terms; constants, **52,** 265
carbon
bands, negative; origin, **52,** 301
band, positive, fourth; wave-lengths, **52,** 301
ultra-violet vacuum spark spectrum; λ 1931–360 A; Plate, **52,** 47; wave-lengths, **53,** 150
X-ray spectrum, L-series; identification, **52,** 47

Spectra (*cont.*)
carbon dioxide; bands in visible and ultra-violet, including several new, **52,** 301
carbon monoxide; bands in visible and ultra-violet; identification, **52,** 301
carbon tetrafluoride; bands in visible and ultra-violet; wave-lengths, **54,** 133
cathode rays; intensity of N bands excited, as function of energy, **52,** 278
classification of lines
enhanced lines, Fowler's; discussion, **54,** 246
furnace excitation stages, King's electric;
for Ba, Ca, Co, Ni, and Sr; infra-red, **51,** 179
for Mn, λ 2795–6500 A, **53,** 133
for Sc, λ 3015–6559 A, **54,** 29
low-current arc excitation stages
for Ag, Bi, Cd, Cu, and Zn, **54,** 246
for Ba, Ca, K, Mg, Na, and Sr, **54,** 191
comparison with furnace classification, **54,** 246
cobalt
absorption spectrum, electric furnace; variation with temperature, **51,** 13
classification of lines; furnace stages; infra-red to 809 μμ, **51,** 179
infra-red furnace spectrum to 809 μμ, at various temperatures, **51,** 179
copper
arc spectrum, low current; variation with current, **54,** 246
classification of lines; low-current arc stages and comparison with furnace stages, **54,** 246
continuous background obtained with exploded wire source, **51,** 37
cyanogen bands
intensity distribution, in furnace and arc spectra, **53,** 161
λ 3883 in arc and furnace; Plate, **53,** 161
excitation of spectra; minimum voltage; helium spectra, **52,** 1;
variation with current density; helium, **52,** 1
exploded wire spectra (extremely high temperature absorption and emission spectra)
of Cu, Ni, Mn; continuous background, **51,** 37
of Fe; absorption spectrum, λ 2270–5645 A; Plate, **51,** 37
production, method, **51,** 37
use for study of pressure shift suggested, **51,** 37
fluorescence spectra (*see* mercury, **54,** 149)
fluorine; spark spectrum, visible and ultra-violet, of pure gas; wave-lengths, **54,** 133
Fraunhofer lines (*see* Sun, spectrum)
furnace spectra, electric
absorption spectra of metallic vapors
comparison with emission spectra, **51,** 13
production, method, **51,** 13
theory; Kirchhoff's law applied to, **51,** 13
variation with temperature; spectra of
Ba, Ca, Co, Fe, Ni, and Ti, **51,** 13
Ba, Ca, Co, Ni, Sr; infra-red, **51,** 179
Mn, 280–820 μμ, **53,** 133
Sc, 301–656 μμ, **54,** 28
comparison with arc spectra
intensity distribution in
cyanogen and Swan bands, **53,** 161
spectra of Ba, Ca, Co, Ni, Sr, **51,** 179; Sc, **54,** 28
comparison with solar spectrum; Sc, **54,** 28
effect of small potential gradient, **52,** 187
infra-red absorption spectra to 920 μμ, of Ba, Ca, Co, Ni, and Sr, **51,** 179
mixed absorption and emission spectra; production, method, **51,** 13
origin of radiation; discussion, **52,** 187
red fringe; explanation, **52,** 187
variation with temperature (*see* furnace absorption spectra)
Zeeman effect for iron lines, **51,** 107
grating spectrograph
comparison with interferometer, **53,** 260
ghosts and reversals; use of, in accurate measurements, **53,** 260
intensity effect on wave-length nil, **53,** 260
polarizing effect on reflected and transmitted light, **51,** 129
ultra-violet, extreme, **52,** 47, 286; **53,** 150
halogen acid gases (HBr, HCl, HF); bands
HCl band 3.7 μ; wave-lengths, law of spacing, evidence of satellites, **53,** 300
theory of structure of infra-red bands
isotopic theory of doublets, **52,** 248
quantum theory, based on simple molecular model of Bohr type, **51,** 230
helium
excitation of various spectra; minimum voltage, **52,** 1
intensity, relative, of series lines and bands in arc spectrum; variation with voltage, **52,** 1
ultra-violet, extreme, spark spectrum; identification of lines, **52,** 47
hydrogen, Balmer series
shift of H_α; condensed spark in air compared with vacuum spectrum, **51,** 236
variations in relative intensity of lines in spectrum of Class Md variable star, **53,** 185
hydrogen bromide, chloride, and fluoride (*see* halogen acid gases)
hydrogen sulfide; spectrum of discharge through, **52,** 301
infra-red spectra (*see* air, Ba, Ca, Co, Ni, Sr, halogen acid gases, sun, water)
elimination of scattered light of shorter wave-lengths, **53,** 121
screen for light to 7200 A, **53,** 121
interferometer spectrograph
comparison with grating, **53,** 260
ghosts and reversals; use of, for accurate measurements, **53,** 260
intensity effect on wave-length nil, **53,** 260
reduction of measurements, method, **53,** 260
ionization lines, in low-current arc; variation with current, **54,** 191

Spectra (*cont.*)
iron
absorption spectrum
furnace; variation with temperature, **51,** 13
exploded wire, λ 2270–5645 A; Plate, **51,** 37
arc lines, λ 3370–6750 A: wave-lengths of 1026 lines, measured with grating and interferometer, and compared with Bureau of Standards results, **53,** 260
intensity effect for arc lines nil, **53,** 260
pole-effect in Pfund arc
comparison of 12-mm 5-amp. with 6-mm 6-amp. arc, **53,** 260
relation to Zeeman effect nil, **53,** 329
ultra-violet spark spectrum to 200 A; Plate, **52,** 47; wave-lengths, **53,** 150
variations in relative intensity of lines in spectrum of Class Md variable stars, **53,** 185
Zeeman effect
furnace lines; direct and inverse effect for 100 lines; camparison with results for spark lines; Plates, **51,** 107
relation to pole-effect nil, **53,** 329
isotopes, components due to
measurement of separation; displaceable slit-method suggested, **53,** 329
theory, for case of bands of HBr, HCl, **52,** 248
magnesium
arc spectrum, low-current; variation with current, **54,** 191
classification of lines; low-current arc stages, **54,** 191
manganese
classification of lines, 280–650 μμ; furnace stages, **53,** 133
furnace spectrum, 280–820 μμ; variation with temperature, **53,** 133
measurements
errors, possible, due to mutual influence of adjacent photographic images, **52,** 98; **53,** 349
of shifts, minute; displaceable slit method, suggested, **53,** 329
of ultra-violet wave-lengths, extremely short, **53,** 150
mercury; fluorescence spectrum, excitation of; active molecules; relation to exciting spectrum, **54,** 149
mixed absorption and emission spectra; production in electric furnace, **51,** 13
nebulae; spectra (*see* Nebulae)
neon; low-voltage spectrum of trace of neon in helium, **52,** 1
nickel
absorption spectrum, electric furnace; variation with temperature, **51,** 13
classification of lines, furnace stages; infra-red to 780 μμ, **51,** 179
infra-red furnace spectrum to 920 μμ; at various temperatures, **51,** 179
ultra-violet spark spectrum to 731 A; Plate, **52,** 47; wave-lengths, **53,** 150
nitrogen; band spectrum
excitation by vacuum discharge through N_2O and N_2O_2, **52,** 301
intensity as function of energy of the exciting cathode rays, **52,** 278
new ultra-violet positive bands from low-current arc in air, possible, **54,** 246
structure; divergence from Deslandres' law, **52,** 301
wave-lengths of third positive, **52,** 301
nitrogen; line spectrum
identification of lines in condensed spark in air, 590–870 μμ, **51,** 236; **54,** 76
relative intensity; effect of self-inductance with spark, **51,** 236
shift of spark lines with reference to vacuum tube lines, **51,** 236
nitrogen peroxide; spectrum of discharge through, **52,** 301
nitrous oxide; spectrum of discharge through, **52,** 301
novae; spectrum (*see* Novae)
oxygen
identification of lines in spark in air and O_2, 590–870 μμ, **51,** 236; **54,** 76
shift of spark lines with reference to vacuum tube lines, **51,** 236
pole-effect
in iron arc, comparison of 6-mm 6-amp. and 12-mm 5-amp. arcs, **53,** 260
measurement, displaceable slit-method suggested, **53,** 329
relation to Zeeman effect, for iron, nil, **53,** 329
potassium
arc spectrum, low-current; variation with current, **54,** 191
classification of lines, low-current arc stages, **54,** 191
pressure shift
calcium arc lines, 315–650 μμ, **53,** 224
source for study; exploded wire suggested, **51,** 37
in stellar spectra, Arcturus, Procyon, **53,** 327
quantum theory (*see* theory)
radium emanation (niton)
new lines, 398–745 μμ, **54,** 285
relative intensity of lines; variation during discharge, **54,** 285
resonance lines in low-current arc spectra
intensity variation with current for
Ag, Bi, Cd, Cu, and Zn, **54,** 246
Ba, Ca, K, Mg, Na, and Sr, **54,** 191
Ritz equations (*see* series)
scandium
classification of lines, furnace stages, **54,** 28
furnace spectrum, 301–656 μμ; at various temperatures; comparison with arc, solar and sun-spot spectra, **54,** 28

Spectra (*cont.*)
scandium (*cont.*)
Zeeman effect for lines in sun-spot spectrum, **54,** 28
series
in Ba spectrum, singlets and triplets, **51,** 23
in Ca spectrum, singlets and triplets, **52,** 265
notation; explanation, **51,** 23
Ritz equations; relation of low-current arc results to, **54,** 246
shifts of lines (*see* spark spectra, Sun)
measurement; displaceable slit method suggested, **53,** 329
photographic, due to mutual action of adjacent images, **52,** 98; **53,** 349
silver
arc spectrum, low current; variation with current, **54,** 246
classification of lines; low-current arc stages, **54,** 246
sodium
arc spectrum, low current; variation with current, **54,** 191
classification of lines; low-current arc stages **54,** 191
Zeeman effect for D-lines; explanation of Woltjer's observations, **51,** 107
sources of light (*see* arc, exploded wire, spark, vacuum)
exploded wire; appearance and mechanical effects of explosion, **51,** 37
spark spectra (*see* air, argon, fluorine, hydrogen, nitrogen, oxygen)
relative intensity; effect of self-inductance on air and O lines, **51,** 236
shift with reference to vacuum tube lines; air, Ar, H, N, and O lines, **51,** 236
ultra-violet, extreme (*see* C, Fe, He, Ni, Zn, ultra-violet)
spark, condensed, in vacuum; as source for extreme ultra-violet, **52,** 286
spectrographs (*see* grating, interferometer)
standards, international secondary; questioned lines; comparison of 6-mm 6-amp. and 12-mm 5-amp. arcs; pole-effect, **53,** 260
stellar spectra (*see* Stars)
strontium
arc-spectrum, low-current; variation with current, **54,** 191
classification of lines
arc stages, low-current, **54,** 191
furnace stages, infra-red, **51,** 179
infra-red furnace spectrum to 920 $\mu\mu$; at various temperatures, **51,** 179
structure (*see* bands, bismuth)
sulfur dioxide bands
in visible and ultra-violet, including forty new; wave-lengths, **52,** 301
sun (*see* Sun)
Swan band
intensity distribution; 5165 A; arc and furnace spectra, **53,** 161
theory
Bohr; relation of low-current arc results to, **54,** 246
relation of minimum voltage results for helium to, **52,** 1
isotopic, of separation of doublets of HBr and HCl, **52,** 248
quantum, of structure of band spectra of halogens, based on simple molecular model of Bohr type, **51,** 230
titanium; absorption spectrum, electric furnace, at various temperatures, **51,** 13
ultra-violet spectra (*see* Ca, CO, CO_2, F, Mn, N, NH_4, N_2O, N_2O_2, SO_2, Sun)
extreme, to 200 A (*see* C, He, Fe, Ni, Zn)
measurements of wave-lengths, **53,** 150
source; condensed vacuum spark, **52,** 286
spectrograph, vacuum, **52,** 47, 286; **53,** 150
screens for region 290–315 $\mu\mu$, **54,** 297
spectrograph, special double, for solar spectrum, 290–315 $\mu\mu$, **54,** 297
vacuum discharge spectra (*see* CO, CO_2, CF_4, N, Ne, NH_4, RaEm, SO_2)
intensity of N bands as function of energy of cathode rays, **52,** 278
minimum voltage for excitation of He spectra, **52,** 1
spectra of discharge through CO_2, H_2S, NH_4, N_2O, N_2O_2, SO_2, **52,** 301
vacuum sources
cathode rays from treated carbon cathode, used to heat anode, **53,** 323
condensed spark, **52,** 286
vanadium; Zeeman effect, direct and inverse, for 90 furnace lines; comparison with effect for spark lines, **51,** 107
Venus; spectrum (*see* Venus)
water vapor; absorption band, 930–963 $\mu\mu$, **53,** 121
X-ray spectra
L-series of carbon; identification, **52,** 47
Zeeman effect (*see* Fe, Na, Sc, V)
furnace lines compared with spark lines, of Fe and V, **51,** 107
relation to pole-effect for Fe lines nil, **53,** 329
zinc
arc spectrum, low current; variation with current, **54,** 246
classification of lines, low-current arc stages, **54,** 246
ultra-violet spark spectrum to 316 A; Plates, **52,** 47, 286; wave-lengths, **52,** 286

Stars
atmospheres, pressure in; Arcturus and Procyon, **53,** 327
binaries (*see* Binaries and Variables)
brightness (*see* parallax)

Stars (*cont.*)
catalogue (*see* Cluster stars)
in Pleiades; magnitudes and colors of 821 stars in region 2° square, **54,** 323
spectroscopic parallaxes, magnitudes, type, and proper motion of 1646 stars, **53,** 13
Cepheids (*see* Variables)
Class Bo–B5; statistical study of 180 stars; mean magnitude, parallax and proper motion, **54,** 140
Class O; collision theory of origin, **54,** 229
Class Oe5 (*see* Binaries)
Class Md (*see* Variables)
cluster (*see* Cluster stars)
colors (*see* Cluster stars)
determination for nebulous stars, **52,** 8
nebulous stars, 47, including ρ Ophiuchi, σ and 22 Scorpii, **52,** 8
in Pleiades; 753 dwarfs, **54,** 323
comparison stars, for Messier 72; photographic magnitudes of 29, **52,** 232
constant stars, from photometric studies
Bond 624, **53,** 317
1 and σ Cassiopeiae, **54,** 81
Class B: π^4 Orionis, ξ, e, and μ Tauri, **51,** 193
π^4 Orionis, **51,** 193, 218
ξ, e, and μ Tauri, **51,** 193
l and π Persei, **53,** 105
radial velocity constant (*see* radial)
density of stars
in Gal. long. +32°, lat. −20°, **52,** 73
in Galaxy; distribution, **52,** 23
in space, as function of parallax and magnitude, **52,** 23
diameters
measurement with stellar interferometer, **51,** 257 (*see* Interferometer)
α Orionis, **53,** 249
disk (*see* diameter)
darkening of limb (*see* Variables)
distribution of luminosity; interferometer method of study, **53,** 249
distribution in space (*see* density)
number of each magnitude per unit volume, luminosity curve, **52,** 23
double stars (*see* Binaries, visible)
dwarf stars, in Pleiades (*see* catalogue)
Galaxy (*see* Galaxy)
giants (*see* Cluster stars, Variables)
magnitudes, absolute (*see* parallax)
magnitudes, photo-electric, of β, δ, *l*, π Persei, **53,** 105
magnitudes, photographic and photo-visual
catalogue, of 1646 stars, **53,** 13
Class Bo–B5, 180 stars, **54,** 140
comparison stars
for Messier 72, 29, photographic, **52,** 232
for Nova Persei No. 2, 36, **52,** 183
in Messier 3 and 68 (*see* Cluster stars)
in Orion, eight; photo-visual, **53,** 317
in Pleiades; statistical study of 821, **54,** 323
scales, photo-visual; comparison of Barnard's with Mount Wilson, **54,** 323
measurements from photographs; possible errors due to contraction effect, **52,** 98; and mutual action of images, **53,** 349
nebulous stars
colors of 47, including ρ Ophiuchi, σ and 22 Scorpii, **52,** 8
spectrum
R Aquarii, nebulous lines; Plate, **53,** 375
nebulosity around six stars, **52,** 8
novae (*see* Novae)
number of each absolute magnitude; luminosity curve, **52,** 23 (*see* density)
parallaxes and absolute magnitudes
catalogue for 1646 stars; spectroscopic and trigonometric results, **53,** 13
Class Bo–B5 stars; mean for 180, **54,** 140
Boss 1517, **51,** 254
determination; methods
accuracy, relative; discussion, **54,** 140
interferometer method suggested, **51,** 257
spectroscopic; description, **53,** 13
distribution of stars in space and number of each magnitude, **52,** 23
relation of magnitude to space velocity; statistical study of 1350 stars, **54,** 9
relation of parallax to apparent magnitude and proper motion, **52,** 23
pressure in atmospheres (*see* atmospheres)
proper motion
catalogue, for 1646 stars, **53,** 13
Class Bo–B5, mean for 180 stars, **54,** 140
large; two faint stars near M51, **54,** 237
measurement; interferometer method suggested, **51,** 257
radial velocity (*see* velocity, space)
binaries (*see* Binaries)
16, 19, +59°2395, +83°104 Cephei, **52,** 198
constant for δ Ophiuchi, η Serpentis, β Pegasi, **52,** 317
+73°835 Draconis, **52,** 198
α Hercules and comp., **53,** 201
25 θ Ursae Majoris, 23 δ Ursae Minoris, **52,** 198
spectra (*see* nebulous stars)
combined bright and dark line spectra; explanation, **51,** 13
variable (*see* Variables)
spectral type
catalogue for 1646 stars, **53,** 13
theory; effect of passage of a star near or through a nebula, **53,** 169; **54,** 229
origin of Class O stars, **54,** 229
variable stars (*see* Variables)
velocity; radial, tangential and space
distribution; frequency of each velocity; statistical study of 1350 stars, **54,** 9
relation to absolute magnitude, **54,** 9

Sugar, cane; aqueous solution
dispersion, rotary, magnetic and natural, 436–620 μμ, **54,** 116
refractive index, one to one solution, 436–620 μμ, **54,** 116
Sun
corona; May 29, 1919; photograph, **51,** 1
eclipse; May 29, 1919; Smithsonian expedition; brief report, **51,** 1 (*see* corona)
meteorites falling into; light expected from; theoretical discussion, **51,** 37
prominence; May 29, 1919; photograph, **51,** 1
October 8, 1920; very high; stages of growth; photographs with Ca line, **53,** 310
spectrum, including Fraunhofer lines
comparison with arc and furnace spectra; scandium lines, **54,** 28
energy distribution, corrected for atmospheric absorption, 315–290 μμ, **54,** 297
infra-red, 890–990 μμ; identification and origin of lines; wave-lengths of 563 lines, including 50 solar; also Plate, **53,** 121
shifts of lines
atmospheric refraction, **53,** 380
center-arc, predicted by anomalous dispersion theory, **54,** 92
mutual influence of adjacent lines; data from limb-center comparisons, **54,** 92 (*see* photographic)
photographic effect of adjacent lines, **52,** 98; **53,** 349
theory, anomalous dispersion; of gravitational shift, limb-center shift, and mutual influence shift, **54,** 92
spot spectra (*see* spots)
theory (*see* shifts)
ultra-violet (*see* energy distribution)
map, photographic; 315–290 μμ, **54,** 297
spots
spectrum
comparison with arc and furnace spectra; scandium lines, **54,** 28
Zeeman effect for scandium lines, **54,** 28
theory; cooling of rising gases, **54,** 293
theory (*see* spectrum, spots)

Tartaric acid; aqueous solution
dispersion, rotary, natural, and magnetic, 436–620 μμ, **54,** 116
refractive index, for one to one solution, 436–620 μμ, **54,** 116
Telescope objective; diffraction by; effect on image of disk and combination of disks, including lune; mathematical theory, **51,** 73
Temperature scale
brightness ratio, gold point to palladium point, **51,** 244
palladium melting-point, **51,** 244
Theory (*see* Binaries, Dynamics, Electron, Gratings, Gravitation, Interferometer, Nebulae, Novae, Origin, Photographic plates, Radiation pressure, Spectra, Stars, Sun, Variables
Transits; observation; effect of diffraction by telescope objective; theory, **51,** 73
Triple systems
65 τ Cygni; orbit of spectroscopic binary component, **53,** 144
13 Ceti; orbit of spectroscopic binary component and perturbations due to fainter visual component, **52,** 110
light curve of variable binary component of λ Tauri, **51,** 193
orbits; of binary components (*see* 65 τ Cygni, 13 Ceti, and λ Tauri)
perturbations due to third body (*see* 13 Ceti and λ Tauri)
λ Tauri; photometric study of variable binary component; orbit, light curve, effect of third body nil, **51,** 193

Variable nebulae (*see* Nebulae)
Variable stars
Algol; photometric study, elements of eclipsing system, light curve, color of satellite, **53,** 105
R Aquarii; spectrum, intensities and displacements of lines and nebular lines (Plate), **53,** 375
γ Argus; spectrum; temporary, shifting, absorption He lines, **52,** 39
γ Camelopardalis; photometric study; light curve and elements, **54,** 217
RS Canum Venaticorum; light curve, elements, computed parallax, **53,** 99
l Carinae; periodic variations of wave-length and spectral type, **54,** 161
1 H. Cassiopeiae; photometric study; light curve, elements, darkening of limb, **54,** 81
SX Cassiopeiae; light curve, elements, **53,** 165
T Cephei; periodic spectrum changes, **53,** 185
U Cephei; photometric study; light curve, elements, evidence of tidal evolution, **52,** 145
Cepheids (*see l* Carinae, X Cygni, Messier 72)
light curves of 26, in Messier 72, **52,** 232
light range, small; possibility of Cepheids with; suggestion, **51,** 62
orbit, spectroscopic, for X Cygni, **53,** 95
origin; collision theory of, **54,** 229
magnitude, mean, for 26 in M72, **52,** 232
periods; in M72, 26 variables, **52,** 232
relation to spectral type, **54,** 161
spectral type; range of variation and relation to period, **54,** 16
spectrum; periodic variations in wave-length and type; *l* Carinae, **54,** 161
theory (*see* origin)
general conclusions; mean atomic weight; ratio of mass to radius, **52,** 73
relation of period to brightness, **52,** 73
variation
binary theory; discussion, **51,** 62
condition of; ratio mass to radius, **52,** 73

Variable stars (*cont.*)
Class Md; spectrum; periodic changes in emission lines (see T Cephei, X Cygni, R Hydrae, R Leonis, X Ophiuchi, R Serpentis, **53,** 185; R Aquarii, **53,** 375)
classification of long-period variables, **53,** 179
cluster variables (*see* Cepheids)
color variation of typical, **51,** 49
colors and magnitudes of 28 in M68, **51,** 49
magnitude, absolute, of typical, **51,** 49
new; in M3; 17 probable, **51,** 140
in M53, 56, 72, and 75; positions of 80 shown on photographs, **52,** 73
in M68; 28, mostly typical, **51,** 49
colors (*see* cluster)
satellite of Algol, **53,** 105
X Cygni; spectroscopic orbit, **53,** 95
χ Cygni; periodic changes of spectrum, **53,** 185
darkening of limb; 1 H. Cassiopeiae, **54,** 81
205 Draconis, probable eclipsing variable, **53,** 201 (*see* Binaries)
eclipsing variables
light curve and elements (*see* Algol, γ Camelopardalis, RS Canum Venaticorum, SX and 1 H. Cassiopeiae, U Cephei, RT Lacertae, λ Tauri)
probable, 205 Draconis, **53,** 201
ellipsoidal variable (*see* π^5 Orionis)
evolution, tidal, of U Cephei; evidence, **52,** 145
giants (*see* Cepheids)
R Hydrae; variations in spectrum, **53,** 185
irregular variables; collision theory of origin, **54,** 229
RT Lacertae; light curve and elements, **52,** 257
R Leonis; variations in spectrum, **53,** 185
light curves (*see* Cepheids, eclipsing, ellipsoidal, and long-period variables)
long-period variables
classification, **53,** 169
light curves of 66; constants, **53,** 169
spectrum of R Aquarii, **53,** 375
magnitude (*see* Cepheids)
magnitude, absolute (*see* cluster, parallax)
Messier 3, 53, 56, 68, 72, 75; new variables (*see* cluster)
Messier 72; light curves of 26 Cepheids, **52,** 232
nebulous variable (*see* R Aquarii)
new variables (*see* cluster variables)
B.D. +81°27; +81°30, **52,** 145
orbits; elements (*see* eclipsing variables)
spectroscopic; X Cygni, **53,** 95
origin, of Cepheids and irregular variables; collision theory, **54,** 229
X Ophiuchi; variations in spectrum, **53,** 185
π^5 Orionis; photometric study; light curve and elements, **51,** 218
parallax and absolute magnitude, of RS Canum Venaticorum, **53,** 99
periods (*see* light curves, Cepheids)
photometric study (*see* Algol, γ Camelopard, 1 H. Cassiopeiae, U Cephei, λ Tauri)
π^4 Orionis, constant star, **51,** 193, 218
R Serpentis; variations in spectrum, **53,** 185
spectrum; periodic variations in emission lines (*see* R Aquarii, γ Argus, Cepheids, Class Md)
suspected variables
B.D. +10°1771, **52,** 9
Bond 624 in Orion; photometric study; Hartwig's elements incorrect, **53,** 317
205 Draconis, **53,** 201
δ Persei, **53,** 105
λ Tauri; photometric study; light curve and elements for binary, **51,** 193
theory (*see* origin)
tidal evolution; evidence of; U Cephei, **52,** 145
Wolf-Rayet star (see γ Argus)
Venus; spectrum; systematic shifts of solar lines; variation with zenith distance; explanation; Plate, **53,** 380

X-rays
L-series of carbon; identification, **52,** 47
source; condensed vacuum spark, **52,** 47

Zeeman effect (*see* Spectra)

GORDON S. FULCHER
CORNING GLASS WORKS
CORNING, NEW YORK

PRINTED IN THE U.S.A.

BINDING
MAY 1 1 1971

QB
1
A9
v.53-54
[redacted]
cop.3
Physical &
Applied Sci.
Serials

The Astrophysical journal

PLEASE DO NOT REMOVE
CARDS OR SLIPS FROM THIS POCKET

UNIVERSITY OF TORONTO LIBRARY

STORAGE